| **REPORT DOCUMENTATION PAGE** | Form Approved OMB No. 0704-0188 |
|---|---|

Public reporting burden for this collection of information is estimated to average 1 hour per response, including the time for reviewing instructions, searching existing data sources, gathering and maintaining the data needed, and completing and reviewing the collection of information. Send comments regarding this burden estimate or any other aspect of this collection of information, including suggestions for reducing the burden, to Department of Defense, Washington Headquarters Services, Directorate for Information Operations and Reports (0704-0188), 1215 Jefferson Davis Highway, Suite 1204, Arlington, VA 22202-4302. Respondents should be aware that notwithstanding any other provision of law, no person shall be subject to any penalty for failing to comply with a collection of information if it does not display a currently valid OMB control number.
**PLEASE DO NOT RETURN YOUR FORM TO THE ABOVE ADDRESS.**

| | | |
|---|---|---|
| **1. REPORT DATE *(DD-MM-YYYY)***<br>16-11-2004 | **2. REPORT TYPE**<br>Conference Proceedings | **3. DATES COVERED** *(From – To)*<br>13 September 2004 - 17 September 2004 |

**4. TITLE AND SUBTITLE**

Materials and Coatings for Extreme Performances: Investigations, Applications, Ecologically Safe Technologies for Their Production and Utilization

**5a. CONTRACT NUMBER**
FA8655-04-1-5008

**5b. GRANT NUMBER**

**5c. PROGRAM ELEMENT NUMBER**

**6. AUTHOR(S)**

Conference Committee

**5d. PROJECT NUMBER**

**5d. TASK NUMBER**

**5e. WORK UNIT NUMBER**

**7. PERFORMING ORGANIZATION NAME(S) AND ADDRESS(ES)**
Institute for Problems of Materials Science
3 Krzhyzhanovsky Str.
Kyiv 03142
Ukraine

**8. PERFORMING ORGANIZATION REPORT NUMBER**
N/A

**9. SPONSORING/MONITORING AGENCY NAME(S) AND ADDRESS(ES)**

EOARD
PSC 802 BOX 14
FPO 09499-0014

**10. SPONSOR/MONITOR'S ACRONYM(S)**

**11. SPONSOR/MONITOR'S REPORT NUMBER(S)**
CSP 04-5008

**12. DISTRIBUTION/AVAILABILITY STATEMENT**

Approved for public release; distribution is unlimited.

**13. SUPPLEMENTARY NOTES**
Page numbering is haphazard in places and page numbers are missing, but everything seems to be complete.

**14. ABSTRACT**

The Final Proceedings for Materials and Coatings for Extreme Performance: Investigations, Applications, Ecologically Safe Technologies for Their Production and Utilization, 13 September 2004 - 17 September 2004

Principles of designing materials and coatings for operation in hazard conditions; Scientific fundamentals and computer models for the processes of manufacturing materials and coatings for operation in hazard conditions; Advanced technologies for production and joining materials and products for operation in hazard conditions; Structure and properties of materials and coatings for operation in hazard conditions; Experimental data obtained from performance of materials and coatings in on location hazard conditions; Potential and contemporary technologies for recycling industrial waste aimed to production structural, heat-insulative, facing and other materials.

**15. SUBJECT TERMS**
EOARD, Coatings, Fluids & Lubrication, Materials

| **16. SECURITY CLASSIFICATION OF:** | | | **17. LIMITATION OF ABSTRACT** | **18, NUMBER OF PAGES** | **19a. NAME OF RESPONSIBLE PERSON** |
|---|---|---|---|---|---|
| **a. REPORT** | **b. ABSTRACT** | **c. THIS PAGE** | UL | 590 | KEVIN J LAROCHELLE, Maj, USAF |
| UNCLAS | UNCLAS | UNCLAS | | | **19b. TELEPHONE NUMBER** *(Include area code)*<br>+44 (0)20 7514 3154 |

**Standard Form 298** (Rev. 8/98)
Prescribed by ANSI Std. Z39-18

**National Academy of Sciences of Belarus (NASB)**
**Ukrainian Material Research Society**
**Frantsevich Institute for Problems of Materials Science of NASU**
**Institute for High Temperatures of RAS**
**Lykov Institute for Heat & Mass Exchange of NASB**
**Bauman Moscow State Technical University (Russia)**
**State Design Bureau “Yuzhnoe” (Ukraine)**
**INTEM LTD (Ukraine)**

**Under auspices of International Astronautical Federation (IAF)**

**MEE·2004**

# THIRD
# INTERNATIONAL CONFERENCE

## *«Materials and Coatings for Extreme Performances: Investigations, Applications, Ecologically Safe Technologies for Their Production and Utilization»*

# PROCEEDINGS OF CONFERENCE

**Under editing of NASU academician Valery V. Skorokhod**

**13—17 September, 2004**
**Katsiveli-town, Crimea, Ukraine**

# OUR SPONSORS:

***We wish to thank the following for their contribution to the success of this conference:***

- ***European Office of Airspace Research and Development, Air Force Office of Scientific Research, United States Air Force Research Laboratory***
- ***European Programme INTAS***
- ***Ukraine Ministry of Education and Science***
- ***Kiev State Administration***
- ***Frantsevich Institute for Problems of Materials Science, National Academy of Sciences, Kyiv, Ukraine***
- ***Bauman Moscow State Technical University, Moscow, Russia***
- ***Institute NIIGraphite, Moscow, Russia***
- ***Joint Stock Company “Ukranalit”***

# ABBREVIATIONS:

| | |
|---|---|
| **NASB** | **— National Academy of Sciences of Belarus** |
| **NASU** | **— National Academy of Sciences of Ukraine** |
| **RAS** | **— Russian Academy of Sciences** |
| **SB RAS** | **— Siberian Branch of Russian Academy of Sciences** |

**PROCEEDINGS ARE PUBLISHED IN ORIGINAL**
**PRESENTED BY THEIR AUTHORS**

**ORGANIZING COMMITTEE DOES NOT RESPONSIBILITY**
**FOR QUALITY AND CONTENT OF THESE MATERIALS**

**Scientific Secretary of Conference**
**L. Chernyshev**

# INTERNATIONAL ORGANIZING COMMITTEE

***SKOROKHOD V. (UKRAINE) — CHAIRMAN***

***BEGUIN Y. (FRANCE) — CO-CHAIRMAN, EXECUTIVE DIRECTOR OF IAF***

***PAVLYUKEVICH N. (BELARUS) — CO-CHAIRMAN***

***POLEZHAEV YU. (RUSSIA) — CO-CHAIRMAN***

***CHERNYSHEV L. (UKRAINE) — SCIENTIFIC SECRETARY***

# MEMBERS:

**Antsiferov V.**
*(Russia)*
**Borisov Yu.**
**(UKRAINE)**
**Bronovets M.**
**(RUSSIA)**
**Dariel M.**
*(Israel)*
**Frage N.**
*(Israel)*
**Froes S.**
*(USA)*
**Frolov G.**
*(Ukraine)*
**Fedorov O.**
*(Ukraine)*
**Gofin M.**
*(Russia)*
**Gamulya G.**
**(UKRAINE)**
**Ivanchev S.**
*(Russia)*
**Kostikov V.**
*(Russia)*
**Kostornov A.**
*(Ukraine)*
**Krukovskii P.**
*(Ukraine)*
**Krut'ko N.**
**(BELARUS)**
**Kuznetsov A.**
**(UKRAINE)**
**Matsevitui Yu.**
*(Ukraine)*
**Naidich Yu.**
*(Ukraine)*
**Nakamura T.**
*(Japan)*
**Nouri H.**
*(Great Britain)*
**Pokhil Y.**
*(Ukraine)*
**Reznik S.**
*(Russia)*
**Shafran M.**
*(Poland)*
**Sitalo V.**
*(Ukraine)*
**Suzdal’tsev E.**
*(Russia)*
**Timofeev A.**
*(Russia)*
**Timoshenko V.**
*(Ukraine)*
**Tsimbaliyuk M.**
*(Russia)*
**Turkevich V.**
*(Ukraine)*
**Van de Voorde M.**
*(Germany)*

# CONTENT

**Pages**

**PLENARY SESSION** **1–25**

**337 TOPICAL DIRECTIONS AND TASKS FOR RESEARCH IN THE FIELD OF CREATING MATERIALS FOR EXTREMAL PERFORMANCES**
Skorokhod V.V. **3**

**140 SOME PROBLEMS CONCERNING RESISTANCE OF SPACECRAFT MATERIALS AND COATINGS TO ENVIRONMENTAL FACTORS**
Timofeev A.N., Galygin A.N., Grigorevskiy A.V., Shvagirev V.M.(1) **5**

**316 INVESTIGATION OF EFFECTIVE THERMAL CONDUCTIVITY OF PERSPECTIVE HEAT-PROTECTION MATERIALS**
Reznik S.V., Paderin L.Ya., Prosuntsov P.V., Mikhalev A.M.,Shulakovsky A.V.,
Fisher W.P.P.(1), German M.L.(2), Grinchuk P.S.(2), Oznobishin A.N.(2),
Pavlyukevich N.V.(2), Toropov V.V.(2), Tretiak M.S.(2) **7**

**66 FUNDAMENTALS OF PRODUCTION TECHNOLOGY FOR CARBON-CAR-BON-SILICON CARBIDE COMPOSITES FOR ARTICLES TO EXPLOIT UNDER EXTREME CONDITIONS**
Kostikov V.I., Cherneko N.M., Sidorov I.I. **9**

**236 TEMPERATURE FIELD IN LOW-THERMAL CONDUCTIVITY MATERIALS UNDER INTENSIVE THERMAL INFLUENCE**
Skorokhod V., Frolov G., Baranov V.(1) **10**

**46 THERMOPHYSICAL PROPERTIES OF HEAT-SHIELDING MATERIALS WITH ORGANIC MATRIX**
Isayev K.B., Polezhayev Yu.V.(1) **12**

**112 COMPUTER SIMULATION OF THERMO-GASDYNAMIC PROCESSES OF WORKING IN EXTREME CONDITIONS MATERIALS TREATMENT**
Timoshenko V.I., Galinsky V.P., Belotserkovets I.S. **14**

**143 MATHEMATICAL METHODS OF CALCULATION AND OPTIMIZATION OF THE STRUCTURE OF COMPOSITE CONSTRUCTIONS OPERATED UNDER EXTREME CONDITIONS**
Gusev E.L., Bakulin V.N.(1), Markov V.G.(2) **16**

**118 USE OF ELASTOMER MATERIALS FOR PROTECTION OF DESIGNS FROM CORROSION AND EROSIVE WEAR**
Khorolsky M.S. **18**

**319 SCINTILLATORS FOR THE DETECTION OF IONIZING RADIATION UNDER EXTREME CONDITIONS: RADIATION AND MECHANICAL OVERLOADS, TEMPERATURE GRADIENTS, CHEMICALLY AGGRESSIVE MEDIA**
Globus M., Grinyov B., Lubinskiy V., Ratner M.(1) **19**

**144 DEVELOPMENT OF A SET OF FUNCTIONAL COATINGS FOR SATELLITE AND CABLE TELEVISION PARABOLIC AERIALS**
Borisov Yu.S., Borisova A.L., Kozyakov I.A., Dotsenko N.M. (1) **21**

**247 THE PROTECTION OF INTELLECTUAL PROPERTY IN THE FIELD OF MATERIAL SCIENCE**
Kossko T.G. **23**

**356 HIGH-DAMPING HARD METAL-CERAMIC COATINGS**
Movchan B.A., Ustinov A.I. **25**

**SECTION A. PRINCIPLES OF DESIGNING MATERIALS AND COATINGS FOR OPERATION IN HAZARD CONDITIONS** **25–57**

**A21 PROTECTIVE COATINGS BASED ON TRIFLUOROCHLOROETHYLENE-VINYL ETHER COPOLYMERS**
Ivanchev S.S., Konovalenko V.V.(1), Polozov B.V.(2) **29**

**A53 COMPOSOTION MATERILA THINWALLED FAIRING FRONTIERS**
Rusin M., Kurakin V. **30**

**A167 COMPOSITION MATERIALS ON BASE OF SILICIDES**
Dvorina L.A. **31**

**A329 FLUORO-CONTAINING MONOMERS AND POLYMERS FOR ION-EXCHANGE MEMBRANES**
Pazdersky Yu.A., Gida V.M., Ivanchev S.S.(1) **33**

**A314 STRENGTHENING MECHANISM OF REINFORCED CERAMIC COMPOSITES ON A BASE OF BORIDES**
Loboda P.I., Bogomol Yu.I. **34**

**A332 PROCESS ACTIVATION ENERGY AND KINETIC PARAMETERS AS QUALITY MEASURE OF DIAMOND-CONTAINING MATERIALS**
Novikov N.V., Bondarenko N.A., Zhukovskiy A.N.(1), Mechnik V.A. **36**

**A1 UNIVERSAL THERMAL PROTECTING COATING**
Galkin A.F **39**

**A24 OPTIMIZATION OF COMPOSITION AND STRUCTURE OF PLASMA COATINGS FOR INCREASING OF SERVICE LIFE OF STARTING DEVICES**
Voevodin V.P., Safronov A.V. (1), Saigin V.V., Zarubova N.I. **40**

**A312 THERMODYNAMICS OF LIQUID ALLOYS OF Ni—Al—Cr SYSTEM**
Vovkotrub N. E., Sudavtsova V. S., Kotova N. V. **42**

**A331 THE MODELING OF THERMODYNAMIC PROPERTIES OF BINARY AND Al-IVaMDM TERNARY SYSTEMS**
Sudavtsova V.S., Bieloborodova E.A., Zinevich T.N, Kotova N.V., Usenko N. I. **44**

**A36 CALCULATIONS FOR STRESS-STRAIN STATE OF SPACECRAFT SOLAR CELL-PANELS UNDER THERMAL LOADING CONDITIONS**
Gavrylov R.V., Pokhyl Yu.A., Koval K.V. **46**

**A177 THE FORMATION MODEL AND PROPERTIES OF ELECTRIC-SPARK CERAMIC COATINGS FOR VACUUM FRICTION UNITS**
Podchernyaeva I.A., Panasyuk A.D., Frolov G.A., Kostenko A.D., Yurechko D.V., Bloschanevich A.M. **47**

**A351 PHYSICAL MEANING OF THE CONCENTRATION COEFFICIENT FOR POLYMERIC COMPOSITES FILLED WITH SHORT FIBRES**
Burya A.L., Kozlov G.V., Rula L.V. **49**

**A32 COMPLEX DIFFUSIVE – CONDENSATION PROTECIVE COATINGS FOR BLADES OF TURBINES OF HEAT – STRUSSED TURBINE ENGINES (GTE)**
Kusnetsov V.P., Lesnikov V.P. **52**

**A353 ELECTROEROSION DISPERSION OF HARD ALLOY WC-8 wt. % Co IN WATER**
Fadejev V.S., Verkhaturov A.D., Ershova T.B., Dvornik M.I. **54**

**A352 PRINCIPLE OF CREATION OF SANDWICHED COMPOSITE MATERIALS WITH GRADIENT DISTRIBUTION OF PROPERTIES ON HARD ALLOY SURFACES**
Fadeev V.S., Verkhoturov A.D., Podchernyaeva I.A.(1), Pryadko L.F.(1) **56**

**SECTION B. SCIENTIFIC FUNDAMENTALS AND COMPUTER MODELS FOR THE PROCESSES OF MANUFACTURING MATERIALS AND COATINGS FOR OPERATION IN HAZARD CONDITIONS** **59–126**

**B333 MODELLING OF NUCLEATION, DIFFUSION AND CHEMICAL REACTIONS IN PRODUCING SUPERHARD MATERIALS BY POWDER METALLURGY METHODS**
Novikov N.V., Bondarenko N.A., Zhukovskiy A.N.(1), Mechnik V.A. **61**

**B125 MODELING OF PROCESSES OF CARBON COMPOSITE MATERIAL COCARBONIZATION WITH PORE AGENTS**
Skachcov V.A., Karpenko V.D.(1), Karpenko A.V., Ivanov V.I., Nesterenko T.N. **64**

**B4 EXPULSION OF $AL_2O_3$ COATING FROM STEEL SUBSTRATE THROUGH PULSED LASER IRRADIATION**
Daniel Leo, Oltra Roland (1) **65**

**B145 THE PHYSICAL MODEL OF THERMAL STABILIZATION OF COATINGS**
Kadyrzhanov K.K., Rusakov V.S. (1), Turkebaev T.E., Zhankadamova A.M., Plaksin D.A.(1) **68**

**B301 MECHANISM OF GROWTH OF DIFFUSION LAYER WHILE FORMATION OF COVERINGS**
Artemyev V.P., Sokolov E.G., Chalov A.A. **70**

**B54 PROBABILITY STATISTIC ANALYSIS OF GLASSCERAMIC MATERIAL APPLICABOLITY MATERIAL FAIRING CONSTRUCTIONS OF SUPERSPEED FLYING DEVICES**
Levshanov V., Rusin M., Kurakin V., Suzdel’tsev E. **72**

**B330 PHASE EQUILIBRIA IN SYSTEM Ni-B-C**
Kudin V.G., Makara V.A. **74**

**B94 DIAGNOSTICS AND FORECASTING OF POWDER DISPERSION - STRENGTHENED MATERIALS PROPERTIES BY "MIXTURE- RESPONSE” SIMPLEX DIAGRAMS**
Lyulko V., Jmajlov B., Artamonov I. (1), Ivanova A. **76**

**B84 ELABORATION OF CONJUGATE UNSTEADY HEAT AND MASS TRANSPORT IN THE VAPOUR-PHASE FABRICATION OF 3D COMPOSITE WITH SiC MATRIX**
Kulik A.V., Bogdanov M.V., Kulik V.I.(1), Ramm M.S.(2) **78**

**B83 MODELING OF SiC AND AlN CRYSTAL GROWTH BY SUBLIMATION**
Demina S.E., Bogdanov M.V., Kalinin D.S., Kulik A.V., Matukov I.D., Ramm M.S., Makarov Yu.N.(1) **80**

**B87 CONDITIONS FOR SELF-PROPAGATING HIGH-TEMPERATURE SYNTHESIS IN THIN FILMS**
Grinchuk P.S., Rabinovich O.S., Pavlyukevich N.V. **82**

**B344 INTERPHASE INTERACTION OF ZR-BASED ALLOY WITH REFRACTORY MATERIALS**
Verkhovluk A. M., Shcheretsky A. A., Shumikhin V. S., Bespalyy A. A., Apuhtin V.V. **84**

**B183 MATHEMATICAL SIMULATION OF STRUCTURE AND RESISTIVITY OF VACUUM DEPOSITS OF BINARY SYSTEMS WITH BOUNDED SOLID SOLUBILITY**
Kurochkin V.D., Kravchenko L.P., Minakova R.V. **85**

**B194 DESIGNING OF OPTIMUM CONSTRUCTIONS OF A LAYERED POWDER COMPOSITE BASED ON $ZrO_2$ AND Ni**
Tkachenko L.N., Maydanyuk A.P., Panichkina V.V., Shtern M.B. **87**

**B2 DEFECT FORMATION MECHANISMS AND MODIFICATION OF SEMICONDUCTOR FILMS OF THE COMPOUNDS $A_{IV}B_{VI}$**
Freik D.M., Galuschak M.A., Ruvinsky M.A., Mezhylovska L.Y. **89**

**B189 SOME PROPERTIES OF SOLID SOLUTIONS WITH THE FLUORITE-TYPE STRUCTURE IN THE $ZrO_2$-$HfO_2$-$Y_2O_3$ SYSTEM**
Lopato L., Shevchenko A., Red'ko V., Pasichny V. **90**

**B196 COMPUTER MODELING OF POWDER MATEPIALS BENDING**
Mikhailov O.V., Serdyuk G.G., Tkachenko L.N. **92**

**B9 KINETICS OF DISSOULUTION OF IRON-CHROMIUM ALLOYS IN LIQUID ALUMINIUM**
Dybkov V. I., Khoruzha V. G., Meleshevich K. A., Barmak K. (1) **94**

**B320 THERMOMECHANICAL STABILITY OF CONDUCTOR UNDER ACTION OF ELECTROMAGNETIC FORCES**
Chemerys V.T. **96**

**B10 KINETICS OF FORMATION OF INTERMETALLIC LAYERS BETWEEN IRON-CHROMIUM ALLOYS AND LIQUID ALUMINIUM**
Dybkov V. I., Sidorko V. R., Samelyuk A. V., Barmak K. (1) **98**

**B244 MATHEMATICAL FORMALISM OF THE PROCESSES IN THE ONE-PARTICLE MODELS IN THE MATERIALS SCIENCE AND THE ONCOLOGY**
Raychenko O.I. **100**

**B27 INSULATOR-METAL TRANSITION IN LOW-Z MATERIALS AT HIGH PRESSURES**
Morozov A.F., Eremeichenkova Yu.V. **103**

**B327 SELECTING THE MODE OF CONTINUOUS COIL COATING WITH ROLLS**
Mukhin I.A., Ivanenko A.A. **105**

**B227 INVESTIGATION OF THE INTERGROWTH FACTORS WHICH MAKE FOR AN MOLECULAR ADHESION MICROMECHANISM**
Uskova N.A., Grishchishyna L.N., Molyar A.G.(1) **108**

**B239 COMPUTER MODELING AND PREDICTION OF PHYSICAL-CHEMICAL PROPERTIES OF SiC-Me$^{IV-V}$C-MeB$_2$ COMPOSITES**
Unrod V.I., Ordaniyan S.S.(1), Udalov Yu.P.(1), Neshpor I.P.(2) **110**

**B246 PHASE INTERACTION IN THE SYSTEM $HfO_2$-$Y_2O_3$-$Eu_2O_3$ AT HIGH TEMPERATURES**
Andrievskaya E. R., Lopato L. M. **111**

**B138 PHYSICAL AND MATHEMATICAL MODELING OF BEMETAL MATERIALS HIGH SPEED WELDING**
Gul'bin V., Nikitin I., Kobelev A.(1), Kolesnikov F.(1) **113**

**B63 THE ELECTRONIC STRUCTURE AND PROPERTIES OF $Ni_{1-x}Li_xO_{1-y}$ $(0 \le x \le 1/4; 0 \le y \le 1/8)$**
Zainullina V.M., Korotin M.A. (1), Zaikov Yu.P. (2), Shurov N.I. (2) **115**

**B76 TUNGSTEN CARBIDE OBTAINING BY TREATMENT OF MELTS BY GASES**
Gab A.I., Malyshev V.V., Uskova N.N.(1), Glushakov V.G.(1) **117**

**B81 NUMERICAL SIMULATION OF THERMAL-GRADIENT CHEMICAL VAPOUR INFILTRATION OF 4D FIBROUS PREFORM BY CARBON** MATRIX
Kulik V.I., NiloA.S., Kulik A.V. (1), Ramm M.S. (2), **118**

**B350 RELATIVE TO INCREASE THE EFFICIENCY OF THERMO-PHYSICAL PROPERTIES MESURING FOR CERAMIC MATERIALS**
Sereda G.N., Rusin M.Ju., Reznik S.V.(1), Prosuntsov P.V.(1) **120**

**B82 STATE-ON-THE-ART IN THE MODELLING OF VAPOUR-PHASE FABRICATION OF CARBON AND CERAMIC MATRIX COMPOSITES**
Kulik V.I., Kulik A.V. (1), Bogdanov M.V. (1), Ramm M.S. (2) **122**

**B359 THE CONTROL OF BIMODAL DISTRIBUTION OF PORES IN MANUFACTURING OF SUPERLIGHT STRUCTURED MATERIALS**
Shtern M. B., Kuzmov A. V., Frolova E.G. **124**

**B346 PHASE EQUILIBRIA IN THE TERNARY SYSTEM $ZrO_2$-$HfO_2$-$CeO_2$ AT 1500 °C**
Andrievskaya Elena R., Gerasimyk Galina I., Lopato Lidiya M., Red'ko Victor P. **125**

**SECTION C. ADVANCED TECHNOLOGIES FOR PRODUCTION AND JOINING MATERIALS AND PRODUCTS FOR OPERATION IN HAZARD CONDITIONS** **127–213**

**C97 THE PHYSICAL ASPECTS OF THE HARDENING OF THE CUTTING HARDENING ALLOYS TOOL BY POWERFUL ION BEAMS OF CARBON**
Tsareva I.N., Ovsyannikov M.Ju., KutuzovV.L., Kutuzov A.V. **129**

**C20 PLASMA METHODS OF SOLID LUBRICANT FILMS FORMATION ON FRICTION UNITS, WORKING AT EXTREME CONDITIONS**
Lesnevsky L.N., Troshin A.E., Tyurin V.N., Ushakov A.M., Chernovsky M.N. **131**

**C28 EFFECTIVE CHARGED PARTICLE BEAMS TECHNOLOGY FOR DIAMOND-LIKE CARBON THIN FILMS PRODUCTION**
Semrnov A., Semenova I., Belyanin A.(1) **133**

**C123 THE PROCESS OF GETTING MICROPARTICLES OUT OF REFRACTORY MATERIALS**
Arinkin S.M. **135**

**C22 GAS-STATIC PRESSING IMPROVES QUALITY AND WORKABILITY OF BLADES OF GAS TURBINE ENGINES**
Tikhonov A.A., Logunov A.V., Golovanov V.I., Razumovsky I.M., Marinin S.F., Poklad V.A. (1), Frolov V.S. (1), Bykov Ju.G. (1) **137**

**C111 HIGH-PRESSURE SYNTHESIZED $MgB_2$-BASED MATERIALS WITH HIGH CRITICAL CURRENTS, INFLUENCE OF Ta, Ti, SiC AND Zr ADDITIONS**
Prikhna T.A., Savchuk Ju.A., Nagorny P.A., Sergienko I.V., Moschul V.E., Dub S.N., Gawalek V.(1), Vendt M.(1), Khabishreiter T.(1), Shmidt Ch.(1), Dellit Ju.(1), Mel'nikov V.S.(2) **140**

**C339 QUASISTATIONARY SOURCE OF CLUSTER BEAMS**
Nosachev L.V. **142**

**C187 MICROSTRUCTURE AND CHEMISTRY OF INTERGRANULAR PHASES IN SiC-BASED CERAMICS SINTERED IN THE PRESENCE OF A LIQUID PHASE**
Izhevsky V.A., Koval'chenko M.S. **143**

**C311 COMBINED HEAT RESISTANT COATING AND THEIR EFFICIENCY IMPROVEMENT METHODS**
Abraimov N.V., Shkretov Ju.P.(1), Poklad V.A.(1) **145**

**C321 FABRICATION OF SiC MATRIX COMPOSITE MATERIALS AND COATINGS BY CHEMICAL VAPOR DEPOSITION/INFILTRATION (CVD/CVI)**
Bogachev E.A., Lakhin A.V., Timofeev A.N., Manukhin A.V.(1) **146**

**C224 IRON POWDERS OF WARM COMPACTION**
Masljuk V.A., Sosnovsky L.A., Minitsky A.V., Gaiduchenko A.K. **148**

**C222 OPTIMUM PARAMETERS OF MILLING PROCESS OF CARBIDE-STEEL IN ATTRITOR**
Pavlygo T., Svistun L.(1), Plomodyalo R.(1), Plomodyalo L.(2) **150**

**C234 LASER IRRADIATION EFFECTS UPON OPTICAL PROPERTIES PRASEODYMIUM OXIDE FILMS**
Andreeva A.F., Paustovsky A.V., Sheludko V.E. **152**

**C195 CLADDING OF POWDERS AS A METHOD FOR PREPARATION OF COMPOSITE MATERIALS WITH CONTROLLED PROPERTIES**
Maslyuk V.A., Panasyuk O.A., Apininskaya L.M., Vergeles N.M., Minitsky A.V. **154**

**C199 PECULIARITIES OF PRODUCING, PRESSING AND SINTERING OF DISPERSE MOLYBDENUM CARBIDE**
Savyak M.P., Uvarova I.V. **155**

**C119 THE ELECTRIC - DISCHARGE TECHNOLOGY OF RESTORATION OF POROSITY AND PERMEABILITY IN THE SEDIMENTARY ROCKS - THE HIGHLY EFFECTIVE METHOD IN THE OIL PRODUCTION**
Sizonenko O.N. **157**

**C124 THE RESEARCH OF EFFICIENCY OF SHIELDING PROPERTIES OF A GAS-POWDERED MEDIUM, WHICH IS CREATED BY REDUCTION OF LOW-BOILING REFRACTORY ALLOYS**
Arinkin S.M. **159**

**C151 ADSORPTION-CHEMICAL ACTIVITY OF HIGHDISPERSITY AMORPHOUS BROWN AND BLACK BORON USED IN METAL BORIDE SYNTHESIS**
Zenkov V.S. **161**

**C152 NANO-STRUCTURED TiN BASED PECVD COATINGS**
Ivashchenko L.A., Porada O.K., Ivashchenko V.I., Rusakov G.V., Dub S.N., Timofeyeva I.I. **163**

**C3 DEPOSITION OF NICKEL ON HIGH-POROUS MATERIAL FROM PROCESS SOLUTION OF JSC «URALELEKTROMED»**
Antsiferov V. N., Zamaletdinov I. I., Egorova O. I. **165**

**C14 PROBLEMS OF FUSION ARC WELDING OF PARTICULATE REINFORCED ALUMINIUM MATRIX COMPOSITES**
Chernyshov G., Chernyshova T.(1) **166**

**C17 THE ATMOSPHERIC CORROSION INHIBITION OF METALS BY IMPLANTATION OF ALUMINIUM**
Belous V.A., Nosov G.I. **167**

**C25 EFFECTS ARISING FROM HIGH-SPEED PARTICLES INTERACTION WITH A TARGET**
Usherenko S.M., Sitalo V.G.(1), Y.P.Bunchuk(1), Gubenko S.I.(2) **169**

**C138 PTIMIZATION OF THE PROCESS TO PRODUCE HEATRESISTANT AND WAREPROOF OXIDE AND CARBIDE/CARBON DISPERSION STRENGTHENED MATERIALS OF DISCOM TRADE MARK BASED ON COPPER POWDER**
Shalunov E.P. **172**

**C230 THE FORMATION OF SURFACE LAYERS ON SiC-AlN-Si$_3$N$_4$ CERAMICS UNDER THE INFLUENCE OF CONCENTRATED SOLAR RADIATION**
Podcherniayeva I.A., Panasijuk A.D., Uvarova I.V., Lijudvinskaya T.A., Neshpor I.P., Mosina T.V., Derinovskaya N.A. **174**

**C231 PRODUCING OF THE WELDED JOINT OF TITANIUM ALLOYS BY THE METHOD OF ELECTRON-BEAM DISPERSING THE MELT**
Mayboroda V.P., Shevchenko O.M. **175**

**C233 FERROELECTRICS KNbO$_3$ FILMS**
Andreeva A.F., Kasumov A.M. **177**

**C249 CHEMICAL-HEAT TREATMENT OF COBALT**
Yamrozek J., Vajs E., Luchka M. (1) **178**

**C29 PECULIARITIES OF $\alpha$-$SI_3N_4$-(MGO, $Y_2O_3$) SYNTHESIS UNDER COMBUSTION MODE AND CERAMIC PROPERTIES**
Zakorzhevsky V.V., Borovinskaya I.P., Chevykalova L.A. (1), Kelina I.Yu.(1) **180**

**C33 CORE CERAMICS OBTAINED BY REACTION BONDING AT SIALON COMPOUNDS OXIDATION**
Smirnov K.L., Borovinskaya I.P., Ospennikova O.G.(1) **182**

**C34 FORMATION OF CORROSION- AND EROSION-RESISTANT COATINGS ON INTERNAL SURFACES**
Krokhmal S.A., Zueva T.N. **184**

**C35 NUCLEAR TRANSMUTATION DOPING OF PHOTOCATALYTIC TIO2 FILM COATINGS WITH TRANSITION 3D METALS**
Belous V.A., Neklyudov I.M., Holomeev M.G., Shiljaev B.A. **186**

**C38 PRODUCTION OF THIN CAST SHS-ELECTRODES BY SPUN CASTING**
Sanin V.N., Yukhvid V.I., Deev B.B., Ospennikova O.G.(1) **187**

**C40 ALKOXO METHOD IS DIRECT WAY OF INORGANIC CERAMIC MEMBRANES MODIFICATION**
Tsodikov. M.V., Teplyakov V.V., Uvarov V.I.(1), Borovinskaya I.P.(1) **188**

**C93 DEVELOPMENT OF IN-SITU TRIBOTECHNOLOGY OF OBTAINING SURFACE NANOCRYSTALLINE STRUCTURES BY FRICTION AT SHEAR UNDER PRESSURE**
Bilousov M.M. **190**

**C209 DEVELOPMENT OF NEW WAYS OF THE SOLDERING OF NON-METALLIC MATERIALS WITH METALS FOR SPACE ENGINEERING**
Naidich Yu.V., Zhuravlev V.S., Gab I.I., Kurkova D.I., Stetsyuk T.V., Chernigovtsev E.P. **192**

**C214 COVERINGS OF TYPE HYDROXYAPATITE-GLASS ON THE TITANIUM FOR WORK IN EXTREME CONDITIONS**
Ivanchenko L.A., Pinchuk N.D., Zyrin A.V., Kuzmenko L.N. **194**

**C217 DEVELOPMENT OF LIGHTENING-PROTECTION NETS FOR REINFORCING CARBON FIBER-REINFORCED PLASTICS**
Vishnyakov L.R., Kokhaniy V.O., Kokhana I.M., Neshpor O.V., Korol A.A. **196**

**C107 GLUING TOGETHER OF NITRIDE, CARBIDE AND CORUNDUM CERAMICS FOR EVALUATION OF GLUED ARTICLES ADAPTABILITY UNDER EXTREME CONDITIONS**
Baranova T.F, Vikulin V.V, D’jachenko O.P, Kelina I.Ju., Kurskaja I.N. **197**

**C172 PERSPECTIVE TECHNOLOGY OF OBTAINING NANOCOMPOSITE FERROMAGNETICS FOR MAKING MATERIALS WORKING IN EXTREME CONDITIONS**
Kuschevsky A.Ye., Oleshko A.I., Kuschevskaya N.F.(1) **198**

**C6 STUDY OF POSSIBILITY OF QUALITY EMPROVEMENT OF LARGE SIZED COMPLEX-SHAPED CERAMIC BLANKS MOLDED ON THE BASE OF SLIPS OF INORGANIC MATERIALS**
Kharitonov D.V., Suzdaltsev Ye.I. **199**

**C131 EFFECT OF CHEMICAL PURIFICATION METHODS ON STRUCTURE PARAMETERS OFNANOCARBON MATERIALS**
Len T., Ovsienko I, Kopan V., Matzui L., Brusilovets A., Sharff P.(1), Kapitanchuk L. (2) **201**

**C132 TECHNOLOGIES PRESSING OF THE CERAMIC POWDERS, BASED ON USE OF COMBINED AND CYCLIC DEFORMATIONS OF THE PRESSING MATERIALS**
Zubro S., Perelman V. **203**

**C133 SUPERLIGHT CARBON FIBER REINFORCED PLASTIC SHIELDS FOR ONBOARD WIDE-APERTURE RADIATORS AS STANDARD MEASURES FOR BRIGTNESS TEMPERATURES IN THE MICROWAVE RANGE**
Yurchuk E., Meleshko A., Demechev V.(1) **205**

**C213 SINTERING UNDER HIGH PRESSURES – AN EFFICIENT METHOD FOR PREPARATION OF CERAMIC NANOCOMPOSITES**
Bykov A.I., Ragulya A. V., Timofeeva I.I., Klochkov L.A., Gridneva I.V. **207**

**C146 THE MANUFACTURE OF VACUUM-TIGHT PRODUCTS FROM CARBON FIBER REINFORCED PLASTIC-BASE COMPOSITES**
Demichev V., Meleshko A., Soldatov A.(1) **209**

**C347 WATERPROOFING COATINGS FOR WORKING IN EXTREMAL CONDITIONS**
Rusin M.Ju., Pashutina T.A., Muzhanova L.P., Vasilenko V.V. **211**

**C357 FEATURES OF FORMATION OF PHASE STRUCTURE OF CERAMICS ON BASIS $TiB_2$ AND C**
Kazo I.F., Кogutyk P.P., Makara V.A., Trushkovskaja L.M **212**

**C358 NEW OPPORTUNITIES IN RECEPTION СПЕЧЕННЫХ OF MATERIALS ON BASIS ПОЛЫХ OF GLASS MICROSPHERES**
Kazymyrenko Y.A. **213**

**SECTION D. STRUCTURE AND PROPERTIES OF MATERIALS AND COATINGS FOR OPERATION IN HAZARD CONDITIONS** **215–470**

**D70 HOW TO FORECAST MATERIALS' PROPERTIES USING INDUCTIVE METHODS**
Nadiradze A.B., Ivakhnenko A.G.(1), Ivakhnenko G. A.(1), Savchenko E.A.(1) **217**

**D225 THE NANOLAERED FRAGMENTS IN AN AMORPHOUSED ALLOY $Ni_{82,3}Cr_{7,0}Si_{4,6}B_{3,1}Fe_{3,0}$**
Shpak A.P., Maiboroda V.P.(1), Molchanovskaya G.M.(1), Zukhina A.L.(1), Kunitskii Yu. A.(2) **219**

**D79 CAST COMPOSITE SHS-MATERIALS ON TITANIUM AND CHROMIUM CARBIDES AND BORIDES BASIS**
Gorshkov V.A. Yukhvid V.I. **221**

**D23 ALUMINUM CASTING ALLOYS FOR SERVICE AT CRYOGENIC TEMPERATURES**
Tikhonov A.A., Gavrilyuk V.V., Karpov V.N.(1) **223**

**D228 STRUCTURE AND PROPERTIES OF THE WC–40%Co COMPOSITE PREPARED FROM AN ULTRAFINE POWDER, WITHIN A BROAD TEMPERATURE RANGE**
Laptev A., Tolochyn O., Golovkova M. **225**

**D5 DISCONTINUOUSLY REINFORCED ALUMINIUM COMPOSITES FABRICATED BY REACTION CASTING PROCESS**
Chernyshova T.A.(1), Kobeleva L.I., Bolotova L.K., Panfilov A.A., Panfilov A.V. **227**

**D30 REFLECTANCE AND EMITTANCE OF POLYMER COMPOSITE MATERIALS AT NONSTATIONARY HEATING BY LASER RADIATION**
Dlugunovich V.A., Zhdanovskij V.A., Snopko V.N. **229**

**D237 DEVICE AND SOME OUTCOMES OF DEFINITION HEAT CONDUCTION LOW HEAT CONDUCTIVITY OF MATERIALS**
Borovik V.G., Frolov G.A., Borovik D.V., Sitalo V.G.(1), Tykhyy V.G.(1) **231**

**D215 STUDY OF STRUCTURE AND HIGH TEMPERATURE STRENGTH OF COMPOSITE MATERIALS BASED ON BORON NITRIDE**
Vishnyakov L.R., Pereselenceva L.N., Sinayskyi B.M., Mazna O.V., Barschevskya A.K. **233**

**D39 POLYMER COMPOSITES CONTAINING NATURAL ZEOLITES TO BE EXPLOITED UNDER EXTREME CONDITIONS***
Okhlopkova A.A., Petrova P.N. **235**

**D345 THE STUDY OF THE ENVIRONMENT HIGH TEMPERATURE EFFECTS ON THE OPTICAL PARAMETERS OF SILICON AND TITANIUM OXIDE THIN FILMS**
Prosovskii O.F., Kelina R.P. **237**

**D324 ABOUT NATURE OF POROSITY OF THE CAST REFRACTORY COMPOUNDS**
Stepanchuk A.N. **238**

**D104 RESEARCH INTO PHYSICOTECHNICAL PROPERTIES OF BORON NITRIDE AT HIGH TEMPERATURES. EXPERIMENTAL EVALUATION OF SINTERED BORON NITRIDE SERVICEABILITY IN THE ARTICLES FOR HIGH-TEMPERATURE EQUIPMENT**
Rusanova L.N., Gorchakova L.I., Kulikova G.I., Alexeev M.K. **240**

**D103 INVESTIGATION OF THE DEPENDENCE OF OXYGEN-ION CONDUCTIVITY OF SOLID ELECTROLYTES OPERATING IN LIQUID-METAL MEDIA ON STRUCTURAL AND PHASE CERAMIC COMPOSITION**
Yakushkina V.S., Korablyova Ye.A., D’jachenko O.P., Vikulin V.V. **241**

**D102 SOLID-PHASE PROCESSES AND THERMAL DIFFUSIVITY OF HEAT-INSULATING CARBIDE MATERIALS**
Ulyanova T.M., Krut’ko N.P. **242**

**D105 THE USE OF AERO-GEL $AL_2O_3{\cdot}H_2O$ FOR THE PRODUCTION OF SILICON NITRIDE CERAMICS**
Kelina I.Yu., Chevykalova L.A., Pljasunkova L.A., Peshchenko D.V., Martynov P.N.(1), Askhadullin R.Sh.(1), Yudintsev P.A.(1), Zakorzhevkij V.V.(2) **244**

**D116 FRICTION AND WEAR BEHAVIOUR OF MATERIALS AND COATINGS PROMISING FOR VACUUM AND LOW-TEMPERATURE CONDITIONS**
Vvedenskij Yu.V., Gavrylov R.V., Gamulya G.D., Ostrovskaya Ye.L., Yukhno T.P., Kostornov A.G. (1), Solntsev V.P. (1), Frolov G.A. (1) **246**

**D106 PERSPECTIVES OF THE DEVELOPMENT OF SILICON NITRIDE CERAMIC SHELLS**
Kelina R.P., Rusin M.Yu., Shkarupa I.L., Vikulin V.V. **248**

**D57 THE THIN-FILM TRANSDUCER OF LOW PRESSURE**
Karitskaya S.G. **250**

**D142 FEATURES OF MECHANICAL AND MICROSTRUCTURAL BEHAVIOR OF ECA PRESSED Al—Mg—Li—Zr ALLOY UNDER HIGH STRAIN RATE SUPERPLASTICITY**
Myshlyaeva M.M., Medvedev M.M., Zolotarev A.K., Isaev V.V., Travkin A.A., Myshlyaev M.M.(1), Mironov S.Yu.(2) **252**

**D135 STRUCTURE AND PROPERTIES OF AL-STEEL JOINTS FOR EXTREME PERFORMANCES**
Gul'bin V. **253**

**D68 PLASMA SYNTHESIS OF METAL-CARBON CLUSTERS AND CAPABILITIES OF THEIR USAGE IN HAZARD CONDITIONS**
Churilov G. **255**

**1D235 ACOUSTIC RESEARCH IN MATERIALS WITH DEVELOPED MESOSTRUCTURE**
Bezimyanniy Y.G. **257**

**2D326 DEFECT CREATION UNDER COATING AND THEIR INFLUENCE ON BORIDE LAYERS PROPERTIES**
Spiridonova I.M., Fedash V.P. **259**

**3D190 METHODOLOGY OF THE ANALYSIS OF CONSTRUCTION MATERIAL WITH MICRO- NANOCRYSTALLINE STRUCTURE**
Minakova A.V., Minakov V.N., Puchkova V.Y. **260**

**4D173 INFLUENCE OF LOADING RATE AND LOAD VALUE ON CREEP OF TITANIUM-SILICEOUS CARBIDE $Ti_3SiC_2$ AT THE MICROINDENTATION**
Gorban' V.F., Pechkovsky E.P., Samelyuk A.V, Firstov S.O. **262**

**5D176 ELECTRONIC STRUCTURE OF RHOMBOHEDRAL PHASES $\zeta$-$Ta_4C_{3-x}N_x$**
Khyzhun O.Yu., Kolyagin V.A.(1) **264**

**6D218 STRUCTURE AND MECHANICAL PROPERTIES OF SURFACE LAYER ON IRON UNDER FRICTION HEATYING**
Yurkova A.I., Belots`ky A.V., Byakova A.V.(1) **266**

**7D174 CREEP OF TITANIUM-SILICEOUS $Ti_3SiC_2$, TITANIUM, SILICON, GRAPHITE AND TITANIUM CARBIDE AT MICROINDENTATION**
Gorban' V.F., Pechkovsky E.P., Firstov S.O. **268**

**8D181 PERSPECTIVE MATERIALS FOR ELECTRODES OF ELECTROCHEMICAL GAS SENSORS**
Afanasyeva V.P., Sylenko P.M.(1) **270**

**9D128 STRUCTURAL CHARACTERISTIC OF NANOCARBON MATERIALS**
Ovsiyenko I.V., Len T.A., Babich N.G., Kapitanchuk L.M.(1), Sharff P.(2), **272**

**10D157 METALLMATRIX COMPOSITE ON $TIH_2$ BASE TO BE NOT DESTRUCTED DURING THE REVERSIBLE HYDROGENATION**
Bratanich T.I., Permyakova T.V., Skorokhod V.V. **274**

**11D219 INFLUENCE OF ELEMENTARY COMPOSITION ON PLASTICITY CHARACTERISTIC OF NANOSTRUCTURED $TIN_{1\pm X}$ COATINGS**
Byakova A.V., Milman Yu.V., Vlasov A.A.(1) **276**

**12D178 COALESCENCE PHENOMENON IN $CrSi_2$ AMORPHOUS-CRYSTALLINE THIN FILMS**
Dvorina L.A., Dranenko A.S. **278**

**13D191 PECULIARITIES OF SURFACE LAYER STRUCTURE FORMATION UNDER LAZ TREATMENT OF POWDERED COATINGS ON TITANIUM ALLOYS**
Bloschanevich A.M., Dan'ko S.V., Khomenko G.E., Popchuk R.I., Rogozinskaya A.A., Rudyk N.D. **280**

**14D245 RESEARCH INTO ANISOTROPY OF POWDER IRON PROPERTIES**
Bezimyanniy Y.G., Skorokhod V.V., Talko O.V., Glazkov E.E.(1), Frydman G.R.(2) **282**

**15D193 HEAT CAPACITY AND ENTHALPY OF $Mg_2Ni$ IN TEMPERATURE RANGE 59.43 – 947 K**
Gorbachuk N.P., Muratov V.B., Zakharov V.V. **284**

**16D197 OXIDATION BEHAVIOUR OF TITANIUM ALLOYS OF TI-B SYSTEM**
Poryadchenko N.E., Oryshich I.V., Khmeljuk N.D., Kalashnikova L.A., Kulak L.D., Kuzmenko N.N., Golovkova M.E. **286**

**17D198 NANOCOMPOSITES BASED ON THE POWDER (SiC-C)-$Si_3N_4$-$Si_2N_2O$, OBTAINED UNDER THE CONDITIONS SHS**
Davidchuk N.K., Gadzyra N.F., Gnesin G.G. **288**

**18D182 THE ELECTRICAL RESISTIVITY AND HALL EFFECT OF $La_3Se_4$, $Pr_3Se_4$ AND $Nd_3Se_4$ AT CRYOGENIC TEMPERATURES**
Kopan' A.R., Kopan' T.V.(1), Korablov D.S.(2) **290**

**19D179 UTILIZATION OF CONCENTRATED SOLAR IRRADIATION FOR PRODUCTION MODIFIED SPARK COATINGS OF TiN-Cr MATERIAL**
Paustovsky A.V., Novikova V.I., Tsyganenko V.S., Mordovets N.M., Timofeyeva I.I., Isayeva L.P., Sheludko V.E., Lityuga I.V. **292**

**20D175 HIGH-TEMPERATURE CREEP OF $Ti_3SiC_2$ – TiC COMPOSITES AT THE INDENTATION**
Burka M. P., Grigorjev O. N., Demidik A. N., Ivanova I. I., Kotenko V. A., Pechkovskii E. P., Firstov S. A. **294**

**21D150 RESEARCHES OF CAST STRUCTURE FORMATION AND MECHANICAL CHARACTERISTICS IN A TEMPERATURES INTERVAL OF 20-1300 $^{O}$C OF ZrCr$_2$ INTERMETALLIC**
Pisarenko V.A., Kusnetzova T.L., Zubets Yu.E, Kalashnikova L.I., Sameluk A.V. **296**

**22D229 ACOUSTIC IMAGING OF STRUCTURE OF CARBON COMPOSITES WITH A METAL MATRIX**
Bezymyanniy Y.G., Kasimov M. A. **298**

**23D232 TiSi$_2$ OXIDATION UNDER NONISOTHERMAL CONDITION**
Koshelev M.V., Dranenko A.S., Dvorina L.A. **300**

**24D226 STRUCTURE AND PHASE COMPOSITION OF QUASICRYSTALLINE SYNTHESIZED COVERINGS OF AN Al-Cu-Fe ALLOY**
Maiboroda V.P. Buzhenets E.I., Oliker V.E., Terentyev A.E., Frolov G.A., Golovkova M.E. **302**

**25D216 FORMATION OF NANO-CRYSTALLINE CARBON DURING THE SYNTHESIS PROCESS OF SiC FIBERS**
Vyshnyakova K.L., Oleinik G.S., Pereselentseva L.M. **304**

**26D212 RESEARCHES OF HEAT RESISTANCE STEEL 45 BY ELECTRIC SPARK ALLOYING WITH FERROCHROMIUM**
Paustovsky A.V., Brodnikovsky N.P., Kuznetsova T.L., Alfintseva R.A., Oryshich I.V., Rokitska E.A **305**

**27D153 STRAIN SENSITIVITY IN BaB$_6$–LaB$_6$ AND SnO$_2$–Sb THICK FILM RESISTORS**
Paustovsky A. V., Rud B. M., Sheludko V. E., Gonchar A. G., Telnikov E. Ya. **307**

**28D154 THE NEW SELF–LUBRICATING COMPOSITION MATERIALS FOR JOINTS OF FRICTION IN SPACE EQUIPMET**
Kostornov A.G., Fusshich O.I., Chevichelova T.M., Simeonova Yu.(1), Sotirov G(1) **309**

**29D155 STRUCTURE AND PHASE STATE OF COATINGS DEPOSITED BY HARD ALLOYS SPARK TREATMENT**
Paustovsky A.V., Gubin Yu.V. **311**

**30D156 RESEARCH OF 3D-METAL ATOMS CHARGE STATES IN ARC-MELTED ELECTROCONDUCTING OXIDE MATERIALS**
Zyrin A.V., Bondarenko T.N. **313**

**31D159 PROPERTIES OF MATERIALS OF THE BN-B$_4$C SYSTEM**
Grigorev O.N., Kotenko V.A., Lyashenko V.I., Rogozinskaya A.A., Dubovik T.V., Chernenko L.I., Panashenko V.M. **314**

**32D160 HEAT-RESISTANT TWO-PHASE EUTECTIC (Li$_2$+β) ALLOY OF Al-Ti-Cr SYSTEM**
Mordovets N.M., PoryadchenkoN.E., Korzhova N.P., Chmeljuk N.D., Legkaya T.N.(1), Vojnash V.Z.(1) **316**

**33D161 ELASTIC AND DAMPING PROPERTIES OF MICROSCALE MULTILAMINATED Cu(Y)/Mo COMPOSITES**
Vdovychenko O.V. **318**

**34D162 IMPACT OF THE HIGH-SPEED HEATING ON SHAPE MEMORY EFFECT IN ZrIr**
Kudryavtsev Yu.V., Semenova E. L.(1) **320**

**35D163 INVESTIGATION OF SINTERED TITANIUM ALLOY Ti–Cr–TiC HEAT RESISTANCE**
Petrova A. M. **322**

**36D164 CONSTITUTION OF THE AS–CAST ALLOYS OF THE Al–Cr–Fe SYSTEM IN THE RANGE OF COMPOSITIONS 50–100 at. % Al**
Khoruzhaya V.G., Pavlyuchkov D.V., Korniyenko K. Ye., Martsenyuk P.S., Velikanova T.Ya. **323**

**37D165 CREATION OF THE REGULAR MACROSTRUCTURE OF THE LAMINATE CERAMIC FOR THE HEAT RESISTANCE INCREASE**
Frolov A.A. **325**

**38D166 WEAR AND OXIDATION RESISTANCE SPRAY COATINGS BASED ON ALUMINIDE TITANIUM AND TIALITE**
Oliker V. E., Sirovatka V.L., Hrechyshkin Y.F., Timofeeva I.I., Gridasova T.Y.(1) **327**

**39D184 PHOSPHORUS DETERMINATION IN ALUMINUM-PHOSPHATE GAS-THERMAL COATINGS**
Kravchenko L.P., Kurochkin V.D., Romanenko O.M., Derenovska N.A., Kolomytcev M.V.(1) **328**

**40D186 OPTICAL PROPERTIES OF INN FILMS - BASIC MATERIAL FOR SOLAR CELLS**
Goryachev Yu.M., Malakhov V.Ya., Rud B.M. **330**

**41D169 EMISSION PROPERTIES OF SCANDATE CATHODES WITH Os-Tr-Al TOP-FILMS**
Getman O.I., Panichkina V.V. **332**

**42D171 ELECTRICAL CONDUCTIVITY OF POROUS MATERIALS FROM DISCRETE METAL FIBERS**
Kostornov A.G., Klimenko V.N. **334**

**43D336 METASTABLE AMORPHOUS METALLIC MATERIALS**
Hertsyk O.M., Kovbuz M.O., Bednarska L.M., Yezerska O.A.(1), Nosenko V.K.(2) **336**

**44D26 CAST INVAR AND SUPERINVAR ALLOYS FOR ELEVATED TEMPERATURES**
Rabinovitch S. V., Kharchuk M. D., Chermensky V. I., Rusin M. J.(1) **337**

**45D201 PRESSURE AND SCALE DEPENDENCES OF RESISTIVE PROPERTIES OF CERAMICS**
Goryachev Yu.M., Dekhteruk V.I., Rud B.M., Siman M.I., Fiyalka L.I. **339**

**46D205 SUPERCONDUCTING THICK FILMS AND POSSIBILITIES OF THEIR APPLICATIONS IN CRYOGENIC TECHNICS AS SENSOR MATERIALS**
Shulishova O.I. **341**

**D220 THE FEATURES OF NONEQUILIBRIUM STATE AND PROPERTIES OF W-NI-CU CONTACT WORKING LAYER UNDER COMMUTATION OF CURRENT IN THE OIL**
Minakova R.V., Golovkova M.E., Gorban' V.F., Popov S.M., Kizimenko F.A.(1) 343

**D210 ELECTRO- AND TRIBOTRCHNICAL PROPERTIES OF THE SILVER-BASED SLIDING CONTACTS IN VACUUM**
Zatovsky V.G., Kriachko L.A. 345

**D126 PYROLYTIC GRAPHITE, ITS STRUCTURE, PROPERTIES AND PRODUCTION PARAMETERS**
Skachkov V.A., Ivanov V.I., Karpenko V.D.(1) 347

**D137 THE INFLUENCE OF THERMAL STRESSES ON STRENGTH OF CARBON MATERIALS AT HIGH TEMPERATURES**
Gracheva L. I. 348

**D11 HEAT RESISTANCE AND THERMAL STABILITY OF COMPLEX COATINGS ON COMPOSITE CARBON MATERIALS UNDER HIGH-TEMPERATURE AND CORROSION MEDIA ACTION**
Zmij V.I., Kartmazov G.N., Kartsev N.F., Kovtun N.V. 350

**D18 TRIBOTECHNICAL PROPERTY OF SUBSTRUCTURE FROM ALLOYS VT3-1 AND SAP-2 WITH Ti-Al-N, Mo-Al-N COATS**
Beresnev V.M., Tolok V.T., Gritsenko V.I., Chunadra A.G. 352

**D139 STRUCTURE AND PROPERTIES COMBINED COATINGS OF HEAT RESISTANT ALLOYS**
Abraimov N.V., Shkretov Yu.P.(1), Tereokhina A.M.(1), Lukina V.V.(1), Borsch E.B.(1) 354

**D323 STRUCTURAL EVOLUTION OF Ti/TiC MULTILAYERED COATINGS**
Dahan I., Frage N., Frumin N., Goldberg M., Dariel M. 355

**D241 THE FEATURES OF COLLISION OF DEFORMABLE PARTICLE WITH A SURFACE OF DUCTILE SOLID BODY**
Uryukov B., Kadyrov V., Tkachenko G. 357

**D71 DEVELOPMENT AND EXPLORATION OF OVERLAYING WELDING MATERIAL PROOF IN REQUIREMENTS OF ABRASIVE OUTWEARING**
Marchenko S.V. 359

**D72 FIRE-PROOF COATING THERMOPHYSICAL CHARACTERISTIC DETERMATION ON BASE OF FIRE TESTING**
Krukovsky P., Novak S. (1), Cvirkun S. (2) 360

**D73 LIFE TIME AND OPERATION TEMPERATURE ESTIMATION FOR MCrAlY COATINGS FOR GAS TURBINE BLADES**
Krukovsky P., Tadlya K., Tadlya O., Rybnikov A. (1), Kryukov I. (1), Mojaiskaya N. (1), Kolarik V. (2), Stamm W. (3) 362

**D16 THE EXAMINATION AND SELECTION OF ORGANIC COATINGS FOR THE PROTECTION OF THE ABOVEGROUND STORAGE TANKS FROM CORROSION**
Groysman A. 364

**D13 TEMPERATURE DEPENDENCE STRENGTH OF ADHESION BOND EPOXY CAUCHUK GLUES WITH STEELS**
Kuksenko V.S., Vettegren V.I., Bashkarev A.Ja.(1), Sytov V.A.(2) **365**

**D56 THE TEMPERATURE SENSITIVE COATING**
Akylbaev Gh. S., Kusainov K.K., Karitskaya S.G. **367**

**D200 THE ANALYSIS OF DYNAMICS OF INCLUSIONS IN VISCOUS MEDIA UNDER THE THERMOCAPILLARITY EXERTION**
Raychenko O.I., Byakova A.V., Derev'yanko O.V., Nakamura T.(1), Gnyloskurenko S.V.(2) **369**

**D64 THE EFFECT OF STRUCTURE-TOPOLOGICAL TRANSFORMATIONS ON DYNAMIC CONSTANTS AND OPTICAL DAMAGES OF $AS_2S_3$ CHALCOGENIDE GLASSES AND FILMS**
May K.V., Fekeshgazi I.V., Klimenko A.P. (1), Mitsa V.M. (2) **371**

**D355 INVESTIGATION OF EFFECTIVE THERMAL CONDUCTIVITY OF THERMAL PROTECTION MATERIALS AT EXTREMUM TEMPERATURES**
Paderin L.Ya., FischerW.P.P. (1) **373**

**47D338 GAS THERMAL TREATMENT OF B-POWDERS AND COATING PROCESS**
Gabunia D.L., Tsagarcishvili O.A., DarchiashviliM.D., Gabunia L.D., Darsavelidze G.Sh. **375**

**48D206 PROPERTIES OF MATERIALS ON THE BASE OF ALUMINUM OXIDE AND ALUMINUM NITRIDE**
Tsyganenko V.S., Lityuga N.V., Dubovik T.V., Rogozinskaya A.A., Panashenko V.M. **377**

**49D207 FORMATION OF INTERMETALLIDES DURING ANNEALING CHROMIUM WITH EVAPORATED LAYER OF Nb AND Zr**
Brodnikovsky N.P., Dubicovsky L.F., Zykova E.V., Sameluk A.V. **379**

**50D208 KINETIC OF FORMATION OF SPARK COATINGS ON THE BASE OF NI–CR ALLOYS IN DEPENDENCE OF THEIR STRUCTURE**
Paustovsky A.V., Alfintseva R.A., Kurinnaya T.V., Pyatachuk S.A. **381**

**51D31 WEAR RESISTANCE OF THE COMPOSITE ELECTROCHEMICAL COATINGS WITH FILLER OUT OF FINEDISPERSED OXIDOCERAMIC**
Barykin N.P., Valeeva A.Kh., Valeev I.Sh. **383**

**52D37 CALCULATION OF OSCILLATORY SPECTRA DEUTERATING cis-1,4-POLYISOPRENES**
Egamov M.Kh., Karimov S.N. **385**

**53D41 INVESTIGATION OF THE MANUFACTURE PROCESS OF HEAT RESISTANT KAOLIN MATERIAL BY PLASMA METHOD**
Brinkiene K., Cesniene J., Kezelis R., Mecius V. **387**

**54D42 HIGH TEMPERATURE OXIDATION OF THE CONNECTION POINT OF THIN THERMOELEMENTS**
Kriukiene R., Cesniene J. **389**

**55D50 FORMING DIFFUSIONE COVERINGS ON THE BASIS OF TITAN ON WOLFRAMLESS HARD ALLOY TH20**
Khyzhnyak V.G., Dolgykh V.Y.(1), Sygova V.I.(1) **391**

**56D52 THE WETTABILITY OF DIMOND-LIKE CARBON FILMS BY SOLUTION OF DIFFERENT PHYSICO-CHEMICAL NATURE**
Kaplunenko O.I., Kutsay O.M., Loginova O.B., Perevertailo V.M., Gontar A.G. **392**

**57D58 OBTAINING OF DIAMONDLIKE a-C:N COATINGS UNDER ELECTRIC AND MAGNETIC IRRADIATION**
Shalaev R.V., Prudnikov A.M., Varyukhin V.N. **393**

**58D59 EFFECT OF HIGH-TEMPERATURE ANNEALING AND ULTRAVIOLET IRRADIATION ON CAPILLARY AND MECHANICAL PROPERTIES OF NANOSTRUCTURED TITANIA COATINGS**
Ostrovskaya L.Yu., Perevertailo V.M., Dub S. N., Shmegera R.S., Matveeva L.A.(1), Milani P. (2), Kholmanov I. N.(2) **395**

**59D62 THE FORMATION OF CRYSTALLINE PHASES UNDER HIGH-TEMPERATURE TREATMENT OF RAPIDLY QUENCHED CoSiB ALLOYS**
Zakharenko M.I., Babich M.G., Yeremenko G.V., Semen’ko M.P., Speka M.V. **397**
Shevchenko National University, Kyiv, Ukraine

**60D65 DEFORMATION AND FRACTURE OF CARBON-CARBON COMPOSITE MATERIALS AT HIGH TEMPERATURES**
Dzyuba V. S., Kravchuk L. V., Kuriat R. I., Oksiyuk S. V., Tokarsky V. A. **399**

**61D67 RESEARCH OF A REACTIONARY SINTERING OF A SYSTEM Al-CR**
Romanov G.N., Tarasov P.P. (1), Dyachkovskii P.K. (1) **401**

**63D74 INCREASE OF CORROSION STABILITY OF STEEL DETAILS BY DRAWING CHROMOSILICIDE COATINGS**
Iantsevitch C. V. **403**

**64D75 INFLUENCE OF ANNEALING ON STRUCTURE AND PROPERTIES OF COATINGS OF CARBIDES CHROME**
Khyzhniak V.G., Korol V.I. **405**

**65D80 MECHANOSYNTHESIS, STRUCTURE AND PROPERTIES OF TERNARY CARBIDE $Ti_3SiC_2$**
Antsiferov V. N., Smetkin A. A., Kachenyuk M. N. **407**

**66D88 MAGNETIC PROPERTIES OF AMORPHOUS ALLOYS Fe-Si-B IN A WIDE INTERVAL OF TEMPERATURES**
Hryhoryeva O.V., Belous M.V., Sidorenko S.I. **409**

**67D89 ELECTRIC PROPERTIES OF NANOCOMPOSITE MATERIALS GRAPHITE-COBALT**
Matzui L., Vovchenko L., Stelmakh O., Kapitanchuk L. **411**

**68D90 ANISOTROPY OF ELASTIC PROPERTIES OF COMPACTED SAMPLES BASED ON THERMOEXFOLIATED GRAPHITE**
Vovchenko L., Zhuravkov A., Samchuk A., Matzui V. **413**

**70D98 STRUCTURE AND THERMOMAGNETIC BEHAVIOR OF TEG-Co NANOCOMPOSITE MATERIALS SYNTHESIZED BY CHEMICAL DEPOSITION TECHNIQUE**
Babich M.G., Len’ T.A., Matzui L.Yu., Semen’ko M.P., Zakharenko M.I. **415**

**69D91 INFLUENCE OF IRRADIATION ON ELECTRICAL RESISTIVITY OF COMPOSITE MATERIAL THERMAL EXPANDED GRAPHITE - FLUOROPLASTIC**
Kopan V. S., Revo S. L., Karaman D. Yu., Ivanenko Ye. A., Sementssov Yu. I.(1) **417**

**71D109 INFLUENCE OF ANNEALING ON STRUCTURE AND COMPLEX OF MECHANICAL CHARACTERISTICS RIBBON SAMPLES OF METALLIC GLASSES 82К3ХСР**
Feodorov V.A., Permyakova I.J., Ushakov I.V. **419**

**72D110 HEALING OF MICROCRACKS IN ALKALI–HALIDE CRYSTALS AT INFLUENCE OF ULTRA-VIOLET RADIATION**
Fedorov V.A., Plushnikova T.N., Tjalin Yu.I., Chivanov A.V., Chemerkina M.V. **421**

**73D127 ZYRCONOLITE MATRIXES FOR HIGH-LEVEL WASTE ($CaZrTi_2O_7$) IMMOBILISATION**
Shabalin B.G. **423**

**74D129 EFFECT OF MECHANICAL DEFORMATION ON HYDROGEN TRANSPORT IN Al**
Lunarska E., Chernyayeva O., Ryumshyna T.A.(1) **425**

**75D130 INFLUENCE OF PHASE COMPOSITION ON DEFORMATION MECHANISMS IN Ti-5Al-5Mo-5V ALLOY**
Konsantinova T.E., Ryumshyna T.A., Volkova G.K. **247**

**77D149 OVERHEATING EFFECT ON STRUCTURE AND MECHANICAL PROPERTIES OF NICKEL-BASE HIGH-TEMPERATURE CASTING ALLOY ZHS6K**
Dashunin N.V., Manilova E.P., Masaleva E.N., Rybnikov A.I. **429**

**78D302 FEATURES OF STRUCTURE AND EVOLUTION OF PROPERTIES AMORPHOUS METALLIC ALLOY 82K3XCP AFTER IMPULSE LASER RADIATION**
Ushakov I.V., Feodorov V.A., Permyakova I.J. **431**

**80D306 HEAT RESISTANCE OF DETONATION COATINGS OF POWDERS PRODUCED BY THE SHS METHOD**
Borisova A.L., Borisov Yu.S., Astakhov E.A., Kaplina G.S., Mits I.V. **433**

**79D305 EFFECT OF HEAT TREATMENT ON STRUCTURAL TRANSFORMATIONS OF AMORPHOUS DETONATION COATINGS**
Astakhov E.A., Kaplina G.S., Adeeva L.I., Mits I.V., Golnik V.F. **435**

**81D307 GAS-ABRASIVE WEAR OF DETONATION COATINGS OF COMPOSITE POWDERS AT INCREASED TEMPERATURES**
Borisov Yu.S., Borisova A.L., Astakhov E.A., Revo S.L.(1), Kostyuchenko A.I.(1) **437**

**82D309 INFLUENCE OF PLASMA COATINGS ON MECHANICAL PROPERTIES OF COBALT-CROMIUM ALLOYS**
Besov A.V., Dolgov N.A.(1) **439**

**83D313 STRUCTURE AND MECHANICAL PROPERTIES OF Al—Cu—Fe QUASICRYSTALLINE ALLOYS**
Sidorenko S.I., Demchenko L.D., Makogon Yu.N., Pavlova E.P., Zakharov S.M.(1) **441**

**84D19 OPERABILITY OF INORGANIC COMPOSITE MATERIALS UNDER EXTREME CONDITIONS**
Podobeda L.G., Vasilenko V.V., Rusin M.Yu. **444**

**85D317 SPECIAL FEATURES OF THE THERMAL AND THERMOMECHANICAL BEHAVIOUR OF TiNi UNDER FORMATION OF MONOCLINIC AND RHOMBOHEDRAL MARTENSITES** **445**
Koval Yu.N., Kudryavtsev Yu.V., Semenova E. L.(1)

**87D328 THE INCREASING OF MECHANICAL PROPERTIES OF SILICICON NITRIDE BASED CERAMICS DURING HIGH TEMPERATURE DEFORMATION**
Gnylytsya.I.D., Kryl Ya.A. **446**

**88D55 PROPERTIES OF TITANIUM – FULLERENE COATINGS**
Shpilevsky M.E., Shpilevsky E.M., Matveeva L.A. (1) **448**

**89D340 STRUCTURAL DISTORTIONS IN $ZrB_{12}$ AND $LuB_{12}$ SINGLE CRYSTALS**
Werheit H., Paderno Yu.(1), Filippov V.(1), Paderno V.(1), Schwarz U.(2), Pietraszko A.(3) **450**

**90D341 EUTECTIC COMPOSITE MATERIALS BASED ON $B_4C$ - $Me^{V-VI}B_2$ SYSTEMS**
Paderno Yu.B.,Liashchenko A.B.,Paderno V.N.,Filippov V.B.,Martynenko A.N. **452**

**91D342 DIRECTIONAL SOLIDIFICATION OF WC – $MeB_2$ ALLOYS**
Paderno V.N., Liashchenko A.B., Paderno Yu.B., Filippov V.B. **454**

**92D134 THE STRUCTURE AND PROPERTIES OF THE COMPOSITES BASED ON IRON ALLOYS CONTAINING BORON AND CARBON DESIGNATED FOR SERVICE IN AGGRESSIVE MEDIA**
Spiridonova I.M., Sukhovaya E.V., Vashchenko A.P.(1) **456**

**93D108 MECHANICAL CHARACTERISTICS SOLAR CELL BATTERIES OF MAJOR STRUCTURE COMPONENTS**
Pokhil Yu.A., Gavrilov R.V., Yacovenko L.F., Alexenko E.N., Tarasov G.V.(1),
Rassamakin B.M.(2) **458**

**94D113 STUDY OF NANOSCALE HETEROSTRUCTURE MATERIALS BY DENSITY FUNCTIONAL TB AND PATH PROBABILITY METHODS**
Masuda-Jindo K., Kikuchi R.(1) **460**

**95D148 INVESTIGATION OF BORID COATING STRUCTURE AND PROPERTIES ON THE BORON-CHROMIUM-PLATED CARBON STEEL**
Spiridonova I.M., Pilyaeva S.B., Zdorovets N.A., Fedorenkova L.I. **461**

**96D348 DISLOCATION ANALYSIS OF FRACTURE PROCESS OF DEFORMATION ORIGIN NANOMATERILAS**
Borysovska K.M., Podrezov Yu. N., Verbylo D.G. **463**

**97D354 INVESTIGATION OF TOTAL EMISSIVITY OF TERMAL INSULATION MATERIALS AND COATINGS AT EXTREMAL TEMPERATURES**
Paderin L. **464**

**98D188 THE ROLE OF DISPERSED “QUASI-PARTICLES” OF CRYSTALLINE BODY IN STRENGTHENING OF TITANIUM AND HIGH-STRENGTH ALLOY VT-22**
Minakov V.N., Minakov N.V., Puchkova V.Y. **466**

**99D362 MECHANICAL PROPERTIES OF HIGH POROUS METALLIC MATERIALS WITH POROUS SPACE STRUCTURE CORRELATION**
Boitsov O., Chernyshev L.(1), Solonin S.(1) **468**

**100D365 TRIBOTECHNICAL PROPERTIES OF NANOCOMPOSITES AL-SIC, AL-SIC-MNS**
Antsiferov V.N., Gilev V.G.(1), Rabinovich A.I.(1) **470**

**SECTION E. EXPERIMENTAL DATA OBTAINED FROM PERFORMANCE OF MATERIALS AND COATINGS IN ON LOCATION HAZARD CONDITIONS** **471–544**

**E47 SOME ASPECTS OF APPLICATION OF COMPOSITE MATERIALS IN UNITS OF FRICTION SUBMERGED ELECTRIC MOTORS (SEM) WORKING IN EXTREME CONDITIONS**
Kurilov G.V., Kurilov A.G. **473**

**E15 STUDY ON FRICTION AND WEAR BEHAVIOR OF PARTICLES REINFORCED ALUMINUM ALLOY MATRIX COMPOSITES UNDER DRY SLIDING CONDITIONS**
Chernyshova T.A., Kobeleva L.I., Lemesheva T.V. **475**

**E315 INVESTIGATION OF STRENGTH CAPACITY OF CERAMIC SHELLS UNDER HIGH-TEMPERATURE HEATING**
Lipovtsev Yu.V., Rusin M.Yu.(1), Khamitsaev A.S.(1), Rabinovitch S.V.(2), Khartchuk M.D.(2), Chermenski V.I.(2), Golementsev L.M.(3) **477**

**E240 PHASE OPTICAL AND PROTECTIV SILICON CARBIDE FILMS**
Krupa M.M., Skirta Yu.B., Andreeva A.F.(1), Bondar Yu.V.(2) **479**

**E117 STUDY OF FRICTION-AND-WEAR CHARACTERISTICS OF STRUCTURAL MATERIALS IN TECHNOLOGICAL CRYOGENIC ENVIRONMENT**
Vvedenskij Yu.V., Volobuev F.I, Gamulya G.D., Ostrovskaya Ye.L., Yukhno T.P. **481**

**E120 NEW WC-Co HARDMETALS WITH REINFORCED Co-BASED BINDER FOR MINING AND CONSTRUCTION**
Konyashin I., Cooper R., Ries B. **482**

**E303 INFLUENCE OF ENVIRONMENTAL FACTORS ON OUTGASSING OF SPACECRAFT COATINGS**
Khassanchine R.H., Grigorevskiy A.V., Timofeev A.N., Rasskazov P.V.(1), Ivanova I.V. (1) **483**

**E185 DEVELOPMENT ANTIFRICTION COMPOSITION MATERIAL FOR OPERATION IN TETROXIDE OF NITROGEN**
Slys I.G., Brakhnov N.V., Berezanskaya V.I. **484**

**E147 PLANNING TEMPERATURE MEASURMENTS AT EXPLORING THERMOPHYSICAL PROPERTIES OF ANISOTROPIC MATERIALS**
Prosuntsov P.V. **486**

**E221 ESTIMATION OF METAL COVERING INFLUENCE ON RESISTANCE TO DESTRUCTION OF SILICON CARBID IN A BEND AND COMPRESSION CONDITIONS**
Dubikovsky L., Okhrimenko G. **488**

**E223 THE PROBLEMS OF MATERIALS AND COVERINGS USED IN HIGH PRESSURE AND TEMPERATURE AUTOCLAVES**
Denbsky Yu.V.(1), Schmidt C., Shtefan E.V.(1), Mikhailov O.V.(2) **490**

**E242 INVESTIGATION OF HIGH-TEMPERATURE CORROSION RESISTENCE OF STRUCTURUL STEEL ALUMINAZED WITH THE USE OF HIGH-SPEED FUEL-AIR SPRAYING**
Kotlyar A., Buchakov S., Kisil V., Yevdokimenko Yu., Kolotilo A. **491**

**E243 EXPERIMENTAL INVESTIGATION OF MATERIAL DAMAGES INDUCED BY HOT XENON PLASMA**
Hassanein A., Burtseva T.A., Minakova R.V.(1), Golovkova M.E.(1), Popov S.M.(1) **493**

**E43 INFLUENCE OF METHODS OF RECEIVING AND TECHNOLOGY OF SURFACING ON STRENGTH PROPERTIES OF SELICON CARBIDE CERAMICS**
Savorovskiy F. G., Maslov V. P. **495**

**E44 OPTICAL METHODS FOR NONDESTRUCTIVE CONTROL OF STRENGTH CHARACTERISTICS OF DETAILS MADE OF BRITTLE NON-METALLIC MATERIALS**
Maslov V. P. Sarsembaeva A. Z., Rodichev Yu. M.(1) **496**

**E170 CORROSION RESICTANCE OF Ti AND ITS ALLOYS IN SEA WATER**
Vyazovikina N.V., Kus'menko H.H., Kulak L.D., Vyazovikin I.V.(1) **498**

**E45 TECHNOLOGICAL SUPPORT OF OPTICAL - ELECTRONIC SENSOR DEVICES FUNCTIONABILITY UNDER EXTREME CONDITIONS**
Maslov V. P. **499**

**E60 THE FORMATION OF HARD SCALE COATINGS ON THE HEAT EXCHANGE SURFACES IN EXTREME CONDITIONS AND THE TECHNOLOGY OF THEIR REMOVAL**
Kusainov. K., Sakipova S., Nusupbekov B. **500**

**E77 INVESTIGATION OF INFLUENCE OF OIL MEDIUM ON THE PROPERTIES OF FROST RESISTANT SEALING RUBBERS UNDER NATURAL EXTREME CONDITIONS**
Petrova N.N., Fedorova A.F. **502**

**E85 WEAR RESISTANCE OF DIFFERENT MATERIALS IN BODY SIMULATED FLUID (BSF)**
Lashneva V.V., Dubok V.A., Tkachenko Ju.G., Matveeva L.A.(1) **504**

**E139 PECULIARITIES OF WELDING TOOL OPERATION MADE OF OXIDE AND CARBIDE/CARBON DISPERSION STRENGTHENED MATERIALS OF DISCOM® TRADE MARK IN RIGID WELDING MODE**
Shalunov E.P., Dovydenkov V.A.(1), Simonov V.S.(2) **505**

**E141 USE OF THE SOLAR BATTERY IN AUTONOMOUS REQUIREMENTS OF MAINTENANCE**
Tarasov V.K., Murzin L.M. **507**

**E192 GAS DETONATION COATINGS TO PREVENT "SELFBONDING" OF MACHINERY PARTS**
Kadyrov V., Remeslo V. **509**

**E203 STRUCTURAL ASPECTS OF HIGH-ENERGY INFLUENCE ON TITANIUM ALLOYS**
Dan’ko S.V., Minakov N. V., Popchuk R.I., Rudyk N.D. 512

**E204 INFLUENCE OF CORROSION IN SEA WATER ENVIRONMENT ON PHYSICO – MECHANICAL PROPERTIES OF GREEN BODIES FABRICATED FROM A COPPER BASED HETEROGENEOUS MATERIAL**
Epifantseva T. A., Martiukhin I. D., Scherbakova L. N., Kayuk V. G., Mikhailov O. V. 514

**E96 RADIATION RESISTANCE MAGNETO-RESISTIVE PERMALLOY FILMS**
Krupa M.M., Lezhnenko I.V., Matvienko A.I., Skirta Yu.B. 516

**E325 THE GETTING OF FLEXIBLE POWDER CORDS FOR DEPOSITION OF COMPOSITE COATINGS**
Stepanchuk A.M., Vdovichenko H.S., Polegeshko O.B 517

**E168 APPLICATION OF COMPOSITE SELFLUBRICATING MATERIALS FOR OPERATION AT INCREASED TEMPERATURES**
Shevchuk U.F., Roik T.A.(1) 519

**E101 IMPROVED HIGH TEMPERATURE SUPERCONDUCTOR MATERIAL FOR POWER APPLICATIONS**
Habisreuther, T., Zeisberger, M., Litzkendorf, D., Kracunovska, S.Gawalek. W.(1), Prikhna, T.A.(1), Oswald, B.(2), Kovalev, L.K.(3) 521

**E95 GOVERNING PARAMETERS THERMO-EROSION DESTRUCTION OF A MATERIALS IN A SUPERSONIC HETEROGENEOUS FLOW**
Ershova T.V., Mikhatulin D.S., Polezhaev Yu.V. 523

**E51 THE INVESTIGATION OF PROTECTIVE COATING INFLUENCE ON CORROSION RESISTANCE OF WELDED ZIRCONIUM COMPOUNDS**
Bushmin B.V., Gorchakov A.A., Dubrovsky Y.V., Hazov I.A., Dubinin G.V. (1), Nikitin I.A. (1), Plishevsky M.I. (1), Semenov A.N. (1), Tyurin V.N. (1) 525

**E61 INVESTIGATION OF HEAT RESISTANCE OF THIN LAYER COVERINGS**
Gladkov V.E., Kusainov K.K., Gladkova V.K. 526

**E248 NEW MATERIALS IN SPACE-ROCKET SYSTEMS OF AN UNLIMITED DISCRETIZATION**
Nerus M. 528

**E310 ELABORATION AND OPERATION OF THERMAL CONCRETE «BRAB30И15*» LINING ELEMENTS AND OXIDE-CERAMIC «M-1*» IN EXTREME CONDITIONS**
Tropinov A., Tropinova I., Vladimirov V.(1) 530

**E238 ENERGY CONSTANTS DETERMINING WARM-UP AND ABLATION OF HEAT-PROTECTIVE MATERIALS**
Frolov G., Solntsev V., Baranov V.(1) 532

**E318 HEAT TRANSFER IN RINGER CHANNAL BETWEEN INTERNAL HEATED AND EXTERNAL COOLED POROUS CILINDERS**
Karimova A.G., Dezider’yev S.G., Zubarev V.M.(1), Sattarov I.Kh.(1), Khabibullin M.G.(1) 534

**E360 MATERIALS FOR THE RELATIVE CONJUGATIONS OF SPACE ENGINEERING**
Bronovets M.(1), Kostornov A., Skorokhod V., Solntsev V., Frolov G., Fushich O. **535**

**E100 NEW TECHNICAL BRANCHES OF IRON POWDERS**
Mironov V. **537**

**E335 PERFORMANCE OF VARIOUS MATERIAL COATINGS IN AUTOMOTIVE 42 VDC SWITCHES**
Nouri H, Driscoll P, B. Miedziński(1), Ciric R **539**

**E334 LIGHT-WEIGHT SEAMLESS BOTTLES OF HIGH-STRENGTH STEEL FOR AUTOMOBILE TRANSPORT**
Sergeyev V, Ivanov A., Litvinsky I., Makatyora V., Jarko.V., Yelansky Y.(1) **541**

**E300 PERSPECTIVE REFRACTORY AND HEAT-INSULATED MATERIALS AND COATINGS FOR EXTREMAL OPERATION CONDITIONS**
Vladimirov V., Karpukhin I.(1), Ilyukhin M.(1), Maizis S.(1), Maizis E.(1) **543**

**SECTION F. POTENTIAL AND CONTEMPORARY TECHNOLOGIES FOR RECYCLING INDUSTRIAL WASTE AIMED TO PRODUCTION STRUCTURAL, HEAT-INSULATIVE, FACING AND OTHER MATERIALS** **545–573**

**F343 TO THE PROBLEM OF REFUSE RECLAMATION OF MACHINE MANUFACTURING**
Rud V. D., Halchuk T. N.(1) **547**

**F122 UTILIZATION OF NICKEL-CADMIUM STORAGE BATTERIES WITH OBTAINING OF CHARGES FOR PRODUCTION OF CERMET CONTACTS**
Sribniy V., Skydanovych N., Olynets(1) V., Tsupko F.(1) **548**

**F8 ELECTROCHEMICAL PRODUCTION OF THE NICKEL POWDERS FROM AMMONIUM SOLUTIONS OF THE LEACHING OF SECOND RAW MATERIALS AND THEIR MORPHOLOGY**
Kunty O.I. **550**

**F86 GAS GENERATOR AS A MEANS OF SOLID ORGANIC WASTE UTILIZATION**
Gavrylov R.V., Gladkiy V.V., Bescorsiy A.P. **552**

**F7 CERAMIC MATERIALS BASED ON INDUSTRIAL WASTES**
Suzdaltsev E.I., Tsvetkova M.M. **553**

**F12 HIGH TEMPERATURE PROCESSING OF SOLID DOMESTIC AND INDUSTRIAL WASTES**
Tovarovskiy I. G., Tovarovskaya G. I. **554**

**F92 ECOLOGICAL PURE PRESSED MATERIALS BASED ON OF SCRAPS OF BIORAW MATERIAL AND NEW ORGANIC-INORGANIC CONNECTING**
Ishchenko S.S., Budzinska V.L., Lebedev E.V. **556**

**F121 THE REFINEMENT OF LAMINATED MATERIALS**
Gul'bin V. **558**

**F158 FINVESTIGATION OF POSSIBILITY TO USE CONCENTRATED SOLAR RADIATION FOR REDUCTION OF TUNGSTEN OXIDE OBTAINED BY INDUSTRIAL WASTE REPROCESSING**
Pasichny V.V., Ostapenko V.S., Ostapenko S.A., Babutina T.E. **560**

**F180 CALORIMETRATION OF SOLAR FURNACES**
Loudanov K.I. **562**

**F211 DIELECTRIC COMPOSITES FOR APPLICATION UNDER CONDITIONS OF GLOWING DISCHARGE**
Zdolnik S.N., Petrovsky V.Ya. **564**

**F202 INVESTIGATION OF POSSIBILITY TO USE THE CONCENTRATED SOLAR RADIATION FOR SURFACE AND SOLID PARTIAL MELTING OF BASALT, OBTAINING FIBRES AND CUTTING ARTICLES OF THEM**
Pasichny V.V., Sergeev V.P., Lykhodid S.I., Yastchenko O.M. **566**

**F99 PERFORATED STEEL PROFILES ON THE BASE OF INDUSTRIAL WASTES**
Mironov V., Serdjuk D., Muktepavela F.(1) **568**

**F308 SURFACE STRUCTURE OF COPPER ELECTRODEPOSITED IN MAGNETIC FIELD**
Silantiev V.I., Bondar E.A., Bondarkova G.V. **570**

**F349 THE SYSTEMS OF THE TECHNOLOGICAL AND TECHNOLOGICAL MOHNITORING OF INDUSTRIAL WASTE UTILIZATION**
Primisky V.F., Bezruk Z.D. **572**

**C A PROCESS OF MANUFACTURING VOLUMINOUS PARTS AND RENOVATIVE-PROTECTIVE COATINGS**
Bizyuk V.V., Kolodyazhniy A.V., Melchakova N.V. **573A**

**LIST OF PARTICIPANTS** **575–582**

# TOPICAL DIRECTIONS AND TASKS FOR RESEARCH IN THE FIELD OF CREATING MATERIALS FOR EXTREMAL PERFORMANCE

**Skorokhod V.V.**
Frantsevich Institute for Problems of Materials Science of NASU, Kiyv, Ukraine
Krzhyzhanovsky Str. 3, Kyiv, 03142, Ukraine

Extremal conditions for operation structural and functional materials and articles are specific for many types of modern technique, specifically, the extremal conditions are determined by temperature and operating mechanical stresses, as well as another factors, e.g. chemical activity for external ambient; radiation, abrasion-erosion or electromagnetic effects, etc.

The heat insulating materials for aviation and rocket-space technique, electrical contacts in high-current switches of high voltage, electrodes for arc welding, nozzles of plasmatrons, work blades of high-temperature gas turbins, friction materials of aircraft brakes, materials for friction assemblies working in space vacuum etc., all these are classical examples of objects operating under extremal loads.

Traditionally, the main criterion in slecting materials for operation under high temperature and mechanical loads is considered to be the set of both kinetic and thermodynamic indices of material stability. However, the most often the system "material-medium that interacts with it" is opened by definition and obeys the laws of nonequilibrium thermodynamics. Moreover, the transfer processes in such systems are as a rule of not-steady state nature. Therefore, in selecting materials for operation under conditions of external extremal action the integral criterion of survivability becomes principal, which defines the maximum possible time interval for which material keeps its function.

In each specific case, this time internal depends on the nature of damage (failure or accumulation of internal defects) material structure and properties, operation regime, and it may be from tens of second to tens of hours.

The main types of surface or local catastrophic failure of material should be considered the following:

1) thermal failure under effect of supercritical heat fluxes due to change in aggregate state of material substance (melting, evaporation, sublimation);
2) mechanical fracture in frictional contacting or due to impact with making solids or dispersed particles (seizing, abrasive erosion, cutting);
3) chemical destruction in reaction with aggressive media (liquid or gaseous) accompanied by formation of fireable or volatile products of reaction.

The cause of accidental damage of articles may be also gradual accumulation of defects within the volume of material, which occurs upon:

1) cyclic mechanical loading (fatigue);
2) thermocycling, including transition over the temperature of polymorphic transformation, i.e, with cyclic variation of internal thermoelastic stresses by both magnitude and sign (thermal fatigue);
3) intense effect of radiation or bombardment by high-energy ions (radiation swelling);
4) chemical decomposition of compounds or metastable solid solution accompanied by formation and active release of gaseous products of reaction.

Under extremal conditions, such a critical accumulation of defects may occur for sufficiently short time period.

The combined action of thermal and mechanical effects, or chemical and mechanical, or radiation and thermal, or thermal and chemical etc., can be specifically danger from the viewpoint of material survivability.

In many cases, it is possible to find that help in considerable increase in material service capacity even such sever conditions.

For example, the rate of normal ablation damage of heat-protecting polymeric-matrix composite coating of increase sharply if crumbly carbomized layers are formed in destruction of polymeric matrix, which then are mechanically removed by gas flow.

This effect can be eliminated if the formation of solid refractory compounds can be assured due to reaction between the products of thermal destruction of polymeric binder and specially introduced filler. As a result, the mechanical removing of material decreases considerably and ablation of it occurs as far as aggregate state of material changes.

Another examples may be rapid failure at relatively low temperatures of a number of carbon materials (pyrocarbon, high-densegraphite) in uxidizing air ambient, which have high erosion resistance in neutral gaseous media even at extremely high temperatures.

An efficient means protecting graphite from oxidation is silicomizing that requires formation of silicon carbide not only on the surface, but also inside carbon material.

Similarly, the rate of high-temperature corrosion (oxidation) of heat-resistance alloys can increase sharply with simultaneous erosion effect of abrasive hard particles that damage protective oxide film. The directed alloying can be used as a means for protection of material from catastrophic corrosion-erosion damage, which increases hardness and wear resistance of the oxides formed in combination with dosed pre-oxidation of the alloy. The effect can be enhanced by small open porosity in material.

Electroerosion damage of contacts and electrodes under effect of arc discharge in real conditions occurs not only due to electrical transfer of metal ions in arc plasma, but also due to ejection of liquid metal from the both by ponderomotive force, which is formed in base spot, as well as due to formation and breaking of bridges. When using pceudo-alloys of tungsten-copper type, the directed alloying of fusible phase is an effective means to improve its adgesion properties, and therefore to enhance concervation of the meet in the both by capillary forces. Such alloying, as a rule, increases hardness of contact material and decreases probability for bridge formation.

Under dry friction of metal surfaces in vacuum or inert gas ambient, an increase in temperature in zone of frictional contact may result in formation of seizing areas, local surface tearing-out of metal, and finally total loss of the working function of friction assembly. The require of regular friction with stable friction coefficient and moderate foreseen wear can be realized through creation the conditions for structural adaptation of materials. Large effects have in this case the thribochemical processes of formation of non-equilibrium disperse phases in friction zone, which can be caused by either interaction with ambient (oxidation) or secondary reactions of base metal with specially introduced additions (dichalcogenides).

In all above cases, we have considered predominantly the means for prevention of surface failure. It is much more difficult to solve the problem of accumulation of damages within material volume, or what is even more tempting, of searching the mechanisms that govern defect “self-healing”, i.e. of creation of materials with self-regeneration effect.

Although there are the more or less successful approaches for solving above problem as regards some specific cases (e.g. suppression of radiation swelling due to introduction into material of fine (particles), on the whole this problem is one of the most complicated and urgent in contemporary materials science.

References

1. Францевич И.Н. и др. Вопросы порошковой металлургии и прочности материалов, вып.2. Изд. АН УССР, Киев (1955). Стр.5-15, 79-116.
2. Ц. Карролл-Порчинский. Материалы будущего. Москва, изд. «Химия» (1966). 239 с. Поверхностная прочность материалов при трении / Костецкий Б.И. и др.Киев, «Техніка» (1976).296 с.

# SOME PROBLEMS CONCERNING RESISTANCE OF SPACECRAFT MATERIALS AND COATINGS TO ENVIRONMENTAL FACTORS

**Timofeev A.N., Galygin A.N., Grigorevskiy A.V., Shvagirev V.M.(1)**
Joint-stock company "Kompozit"
4, Pionerskay str., 141070, Korolev, Moscow region, Russia, e-mail: Kompozit.Mat@g23.relcom.ru
(1)The Russian Aviation and Space Agency, 42, Shchepkina str., Moscow, Russia

*Requirements imposed on materials of external surfaces of long-term performance spacecraft under exposure to environmental factors are examined. Advanced paint thermal control coatings are presented.*

With the increase of spacecraft's service life up to 10—15 years, the Russian Federal Space Program on space systems, complexes, and scientific and civil means imposes more rigid requirements on reliability of spacecraft materials. Service life of a spacecraft, regardless of its type and purpose, is determined by retaining operational properties of materials within the admissible limits. Structurally new generations of spacecraft with 10—15 year and longer service life, that are able to solve a wide range of tasks, will have, as a rule, no pressurized equipment capsule that will cause for the requirements to become tougher.

As for the exposure to environmental factors, the operation conditions of spacecraft are varied widely. These are determined by orbits where the spacecraft operate, namely, low-earth orbit (LEO), high elliptical orbit (HEO), HEO with entering the Earth radiation belts, geostationary orbit (GSO), interplanetary transfer orbit, etc. Their common feature is an ionizing radiation effect that produces in outer skin of a spacecraft absorbed doses from $10^2$ to $10^9$ rad annually, and UV-radiation of the Sun. Vacuum and temperature changing from –150 °C to +150 °C are also common factors. When in service, due to design features of spacecraft and influence of environmental factors, there occur undesirable extraneous phenomena, such as electrostatic charging and generation of a spacecraft outer atmosphere.

In general, the only basic requirement imposed on spacecraft materials is not to change its operating properties in the course of service life that is unfeasible for most materials, especially polymeric. Therefore, specific requirements are imposed on each material in dependence on its purpose in the spacecraft structure.

These requirements can be summarized provided the spacecraft materials are grouped according to their functionality as follows:

- structural materials;
- lubricants;
- thermal control coatings.

This paper examines polymeric materials being the most degradable if exposed to environmental factors. The fundamental requirement imposed on structural materials is a radiation resistance, decrease in strength at the end of spacecraft service life by 15—20% with respect to initial value being permissible. Another requirement is their outgassing properties (or mass loss). This is general characteristic for all spacecraft materials. And much more rigid requirements are imposed on materials that are within the field of view of the contamination-sensitive optical systems. For instance, steady-state outgassing rate of a number of materials of the ISS should not exceed $10^{-14}$ g/sq.cm×s.

The essential characteristic of large-sized structural materials located on surface of spacecraft is a degree of electrostatic charging that is characterized by a specific surface resistance and should be $\leq 1\times10^6$ Ω/□. Under such conditions static electricity drains off without discharging.

Being located under and protected with material (metal) and friction assemblies, the lubricants employed are not generally exposed to intensive radiation. However, their radiation resistance must be at least $1\times10^6$ rad. Radiation resistance means keeping the endurance and friction factor to maintain specified lifetime of devices and mechanisms.

Evaporation of volatile products from lubricants deteriorates not only the spacecraft outer atmosphere, but also the properties of the lubricant itself, therefore requirements here are stringent enough.

External coatings of spacecraft are the elements of passive or active thermal control systems and are applied on external surfaces and structure members.

Mainly, the external coatings of spacecraft are fabrics for optical purposes (upper layer of EVTI mat), photovoltaic cells of solar arrays, thermal control coatings.

External coatings of spacecraft are intended to ensure the design values of external thermal loads caused by solar and planetary light (passive systems) and to remove heat into space.

In addition to standard process parameters like good spreading capacity, adhesion, etc. there are a number of other requirements imposing on external coatings of spacecraft with long-term lifetime,

- stability of As in operation conditions under exposure to damaging environmental factors and thermal cycling;
- low outgassing level with $\Delta m/m \leq 1{,}0\%$ and content of volatile condensable material $\leq 0{,}1\%$;
- low specific volume resistance ($\rho_v \leq 10^6$ $\Omega \times m$) for coatings of spacecraft that may enter the Earth radiation belts.

The advanced thermal control coatings of ECOM-1, ECOM-2, ECOM-1P type and new ones being developed on their basis meet the above specified requirements.

# INVESTIGATION OF EFFECTIVE THERMAL CONDUCTIVITY OF PERSPECTIVE HEAT-PROTECTION MATERIALS

**Reznik S.V., Prosuntsov P.V., Fisher W.P.P.(1), German M.L.(2), Grinchuk P.S.(2), Mikhalev A.M., Oznobishin A.N.(2), Pavlyukevich N.V.(2), Toropov V.V.(2), Tretiak M.S.(2), Shulakovsky A.V.**
Bauman Moscow State Technical University
5 Baumanskaya 2nd Str., Moscow, 105005, Russia, e-mail: sreznik@serv.bmstu.ru
(1)European Aeronautic Defence and Space Company,
Bremen, Germany, e-mail: wolfgang.fischer@space.eads.net
(2)A.V. Luikov Heat and Mass Transfer Institute of NASB
15 P. Brovka Str., 220072, Minsk, Belarus, e-mail: gps@hmti.ac.by

The reliable heat protection is one of primary factors ensuring successful operation of reusable transport space systems. It is obvious that a weight–efficiency ratio of heat protection is of special significance. Then on development of passive systems of heat shielding the preference is given to high-porous materials with a low thermal conductivity. These materials have great ability to dissipate heat radiation on optical inhomogeneities (pores, particles, and fibers). Despite of long-time research in this field, the problem of determination of thermophysical properties of heat-shielding materials at high temperatures remains actual.

The process of heat exchange in high-porous materials has a complicated combined character. For mathematical modeling of such a process it is necessary to solve a problem of radiation–conduction heat exchange with taking into account a dependence of material thermophysical properties on pressure and temperature of an external medium. However there is another way. This is based on the use of so-called effective coefficient of thermal conductivity describing total radiation–conduction heat transfer inside of material. Such an approach essentially simplifies mathematical models used for thermophysical computations. However the technique of determination of the effective coefficient requires experimental reproduction of the extreme conditions of a material operating.

The present work is dedicated to investigation of temperature dependence of effective thermal conductivity of three various materials provided by EADS Company: 1) silicon dioxide-based fibrous material ($SiO_2$) with a filament diameter of about 3 microns and density of $\rho$=90, 105, and 120 kg/m$^3$ (porosity of a material is 96,1, 95,4 and 94,8% respectively); 2) alumina-based fibrous material ($Al_2O_3$) with a filament diameter of about 3 microns and density of $\rho$=79 and 113 kg/m$^3$ (porosity of a material is 98% and 97% respectively); 3) molybdenum-based cellular material with density of 300 and 800 kg/m$^3$ (porosity of a material is 97% and 92% respectively).

The investigation technique is based on a solution of two-dimensional inverse coefficient problem of a heat conduction with the use of data of full-scale experiments.

Experimental samples were tested on radiation heating plant "Uran-1", which allows to generate a focussed beam with a radiation energy of a density up to $6 \cdot 10^6$ W/m$^2$ on a 12 mm diameter spot. Experimental samples of the cylindrical form are placed in the hollow graphite cylinder with a wall thickness of 5 mm. This cylinder is used for creation of a radial heat flow. Chromel-alumel or tungsten-rhenium thermocouples in amounts of 6-7 were installed in a sample. Before realization of each experiment, its duration and coordinates of thermocouples were determined from a solution of a two-dimensional problem of optimum planning of temperature measurements. The automatized system consisting of the computer and the industrial controller with a 16-channel analog-to-digital converter carried out the collection of the thermocouples indications during experiments. The frequency of channels inquiry is 77 Hz. The thermograms obtained in this way were used for calculation of effective thermal conductivity. For this purpose an inverse coefficient problem in extreme statement was solved numerically. In so doing were found the temperature dependences of thermal conductivity of investigated material which lead to a minimum of quadratic functional of discrepancy between experimental and calculated values of temperature.

**THE RESULTS OF RESEARCH ARE PRESENTED IN FIGURES 1—3.**

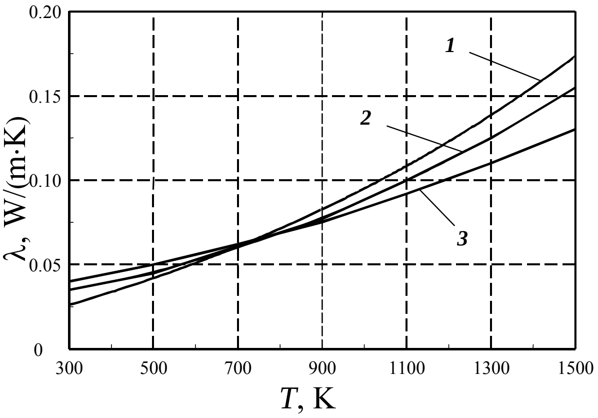

Fig. 1. Dependence of an effective thermal conductivity of high-porous fibrous $SiO_2$ based material on temperature: *1* – $\rho$ = 90 kg/m$^3$; *2* – 105; *3* – 120

As can be seen, for fibrous materials the effective thermal conductivity increases with temperature. It is reasonable that for such high-porous materials radiation component contributes significantly to effective thermal conductivity at high temperatures. This is confirmed indirectly by the possibility of good approximation of obtained dependencies by a cubic polynomial one on temperature. Of interest is the fact, that above 700 K a thermal conductivity $SiO_2$-based material with a smaller density grows faster (Fig. 1).

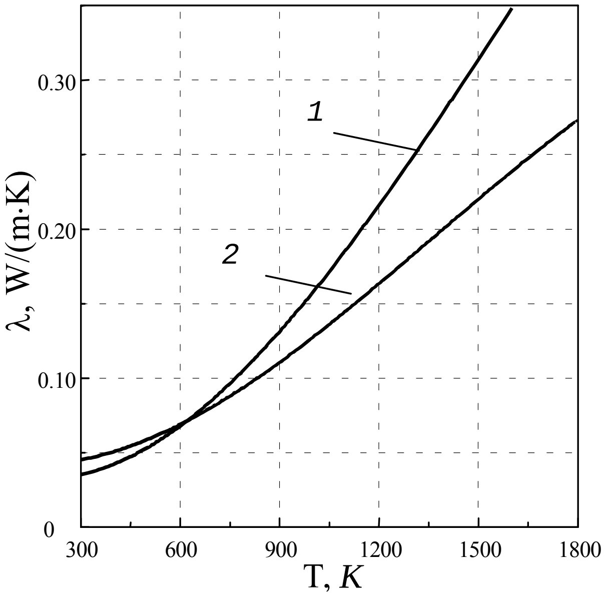

Fig. 2. Dependence of an effective thermal conductivity of high-porous fibrous $Al_2O_3$ based material on temperature: *1* – $\rho$ = 79 kg/m$^3$; *2* – 113

The effective thermal conductivity of a molybdenum cellular material has a non-monotonic behavior. It seems likely that such a behavior is a result of a competition of two processes: conductive heat transfer through a solid hull of material and radiation heat transfer over porous space.

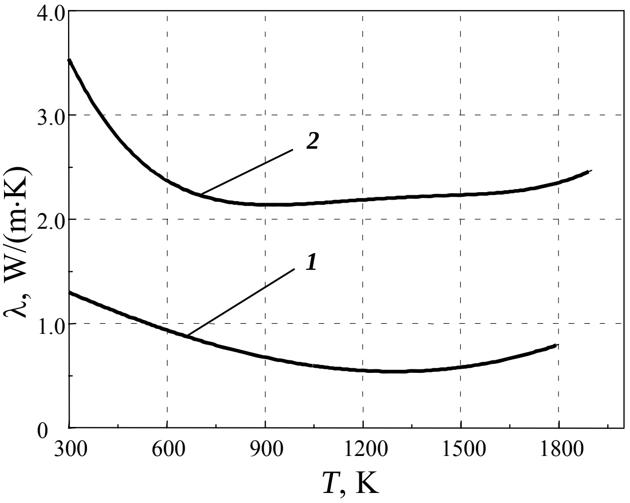

Fig. 3. Dependence of an effective thermal conductivity of cellular molybdenum material on temperature: *1* – $\rho$ = 300 kg/m$^3$; *2* – 800

The work was performed with the support of INTAS (grant N 00-0652).

# FUNDAMENTALS OF PRODUCTION TECHNOLOGY FOR CARBON-CAR-BON-SILICON CARBIDE COMPOSITES FOR ARTICLES TO EXPLOIT UNDER EXTREME CONDITIONS

**Kostikov V.I., Cherneko N.M., Sidorov I.I.**
FSUE Research Institute of Graphite-Based Structural Materials “NIIGrafit”
Moscow 111141, 2 Electrodnaya Str. E-mail: grafit@aha.ru

The improvement of present-day facilities exployed under extreme conditions is based on the development of novel structural materi-als which are to withstand thermomechanical loads in an oxidizing medium under heating up to 1700 $^{o}$C without strength losses.

The reinforcement of ceramics as the most heat- and oxidation-resistant material by car-bon fibers creates prerequisites for obtaining heat- and shock-resistant composites. Silicon carbide as a matrix material is characterized by an optimal thermal compatibility with carbon fibners. However when obtaining carbon-carbon-silicon carbide composites (CCSCC) a number of materials-science and technological problems arise. The direct combination of SiC with carbon fibers is impracticable insofar as SiC has actually no flowability when heating up to the temperature of active sublimation and dissociation.

The mathod of obtaining CCSCC developed by NIIGrafit consists in thermochemical con-version of carbon plastic into a carbon-carbon composite followed by conversion of its car-bon matrix into a silicon carbide one under di-rect interaction of liquid silicon with carbon (Fig. 1).

The specific feature of the production tech-nology for high-quality large-size articles from CCSCC is to ensure a uniform and stable im-pregnation of a carbon-fiber filler with a poly-mer coke-forming binder, infiltration of a car-bonized preform with pyrolytic carbon and impregnation with liquid silicon, while avoiding contact with the carbon fibers, as well as to en-sure the preform stable carbonization under si-liconizing without internal stresses, including preforms of thin-walled articles design exam-ples whereof are presented in Fig. 2.

The siliconizing process is most considerab- ly affected by the structure perfection, type and parameters of the carbon body porosity, as well as by the temperature of its interaction with liquid silicon.

The main provisions of CCSCC formation concept are based on the theory of carbon ma-terials siliconizing:

- Carbon fibers increase crack resistance and stability of strehgth indices of CCSCC, and a silicon carbide matrix protects carbon fibers against oxidation;
- Under siliconizing it is the carbon matrix of the carbonized carbon-carbon preform that will convert into SiC due to its higher thermodynamic activity as compared to the carbon fibers;
- The nonuniformity of the binder content and the number of locally nonresiinified areas of carbon fibers in the starting car-bon plastic are to be minimum;
- Under carbonization of the polymer ma-trix, coke with an open porosity of inter-communicating type will be formed;
- The carbonized preform internal surface will be coated with a film-barrier against carbon diffusion into the siliconmelt;
- The adhesive interaction between the car-bon filler and the silicon carbide matrix in CCSSCC will be of a mechanical cohesion type.

The solution of problems from the devel-oped concept standpoint at each of the produc-tion stages makes it possible to obtain high-quality articles from CCSCC.

Prof. Kostikov Valeriy Ivanovich, the director of FSUE “NIIGrafit”, a corresponding member of RAS, D.Sc. (technology), State prozes win-ner of USSR and RF, an honoured worker of science and technology, a specialist in the field ofcomposites and carbon materials.
Born in 1937, graduated from MISiS in 1959.
Address: Moscow 119331, Maria Ulyanova
Str., 9, buil. 2, apart. 12.
Chernenko Nikolai Michailovich
Chief of laboratory of FSUE “NIIGrafit”, Sen. Sc. Worker, D. Sc. (technology), a specialist in the field of polymer, carbon – carbon, and carbon – ceramic composites.
Born in 1941, graduated from MATI in 1966.
Adress: Moscow, 155409, Str. Of Koshkin, 12, ld. 1, apart. 256.
Sidorov Igor Igorevich, a scientific worker of FSUE “NIIGrafit”, a specialist in the field of polymer, carbon-carbon, and carbon-ceramic composites.
Borm in 1967, graduated from MATI in 1990.
Address: Moscow 111622, Oranzhereinaya Str., 14, apart. 14.

# TEMPERATURE FIELD IN LOW-THERMAL CONDUCTIVITY MATERIALS UNDER INTENSIVE THERMAL INFLUENCE

**Skorokhod V., Frolov G., Baranov V.**(1)
Frantsevich Institute for Problems of Materials Science, of NAS of Ukraine
3 Krzhizhanovsky St., Kiev, 03142, Ukraine, E-mail: frolov@alfacom.net
(1)G.E.Pukhov's Institute of Simulation Problems in Power Engineering of NAS of Ukraine

A linear equation of heat conductivity is usually used for calculation of warm-up of a material with constant thermal and physic properties:

$$\frac{\partial T}{\partial \tau} = a\frac{\partial^2 T}{\partial y^2}. \qquad (1)$$

At ablation of mass from material surface, it can be presented as:

$$\frac{\partial T}{\partial \tau} = a\frac{\partial^2 T}{\partial y^2} + V_\infty \frac{\partial T}{\partial y}. \qquad (2)$$

In accordance with Fourier hypothesis (law), the heat stream drifting to warm up internal layers of material looks like:

$$q_\lambda = -\lambda \frac{\partial T}{\partial y}. \qquad (3)$$

Here $T$ is the temperature, $\tau$ is the time of heating, $a$ is the temperature conductivity factor, $y$ is the coordinate, $V_\infty$ is the linear speed of ablation, $\lambda$ is the thermal conductivity factor.

As any type of the boundary conditions is finally reduced to (3), the temperature profile near the surface with the constant $\lambda$ (absence of radiating heat transmission etc.) may differ only in value of the temperature gradient $(\partial T/\partial y)$.

However the *S*-shaped temperature profile has been set up in a non-stationary warming-up mode for samples of opaque alloyed quartz glass ceramics (QGC) close to the rupturing surface. It exponentially changes in a stationary mode and is well described by the equation for a stationary warm layer following from (2) at $\tau \to \infty$. Thus it has been proved, that the establishment of a stationary warm-up mode practically up to any isotherm of the temperature field occurs at the moment when the thickness of the ablated layer is equal to the depth of occurrence of the isotherm limiting the warmed layer. It resulted in a solution which represents linear superposition of solutions for the linear equations (1) and (2):

at $S(\tau) < y < y_s$

$$T(y,\tau) = T_0 + (\bar{T}_w - T_0)\exp\left[-\frac{\bar{V}_\infty}{a}[y - S(\tau)]\right], \qquad (4)$$

at $y \geq y_s$

$$T(y,\tau) = T_0 + (\bar{T}_w - T_0)\exp\left(-\frac{\bar{V}_\infty}{a}[y - S(\tau)]\right) \times$$
$$\times\left[1 - \operatorname{erf}\left(\frac{y - y_s}{2\sqrt{a\tau}}\right)\right]. \qquad (5)$$

Here $y_s \approx S(\tau) + \delta_T \approx 2S(\tau)$ is the coordinate which is counted off from an initial surface and determines the bottom border of the stationary warmed layer; $S(\tau)$ is linear mass ablation; $\delta_T$ is the thickness of the stationary warm layer; $T_0$ and $\bar{T}_w$ is the temperature of a cold material and the established temperature of the surface; $\bar{V}_\infty$ is the stationary speed of the linear ablation.

The design-experiment investigation, for example, fig. 1, has discovered that the experimental data will be in harmony with the calculation on (4) and (5), while the S-shaped temperature profile appears owing to rather sharp differentiation of the stationary and non-stationary areas of the temperature field. The depth of the bottom border occurrence of a stationary warmed layer is equal to the thickness of a material layer ablated from the surface.

However, proceedings [1] presents experimental data that give grounds to assume that the S-shaped temperature profile is available in the alloyed QGC specimens in the case when ablation of a melting film from the material surface can be neglected. The conclusion that has been drawn above is not obviously the unique reason for occurrence of the S-shaped temperature profile.

Provided that in this variant of heating, occurrence of the S-shaped profile follows from any wave disturbance, the results obtained in fig. 2 may be apparently explicable.
Fig. 2 shows designed and experimental temperature profiles in the alloyed QGC, constructed for the time of heating $\tau \leq \tau_T$, where

$\tau_T$ is the time of achieving the established temperature for a rupturing surface.

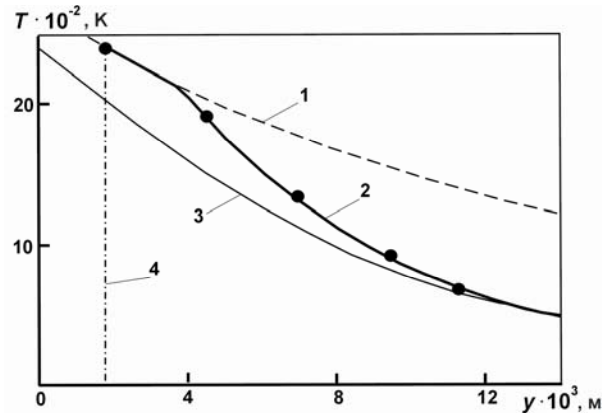

Fig. 1. Comparison of designed and experimental temperature profiles in the alloyed QGC for 50 second of heating at $\overline{V}_\infty = 0.05\cdot10^{-3}$ m/s, $T_w = 1400$ K, $a$=$0.65\cdot10^{-6}$ m$^2$ /s: 1 - calculation on (4), 2 - on (4) at $S(\tau) < y \le y_s$ and on (5) at $y \ge y_s$ , 3 - on (6), 4 - position of the surface being heated, point - experiment.

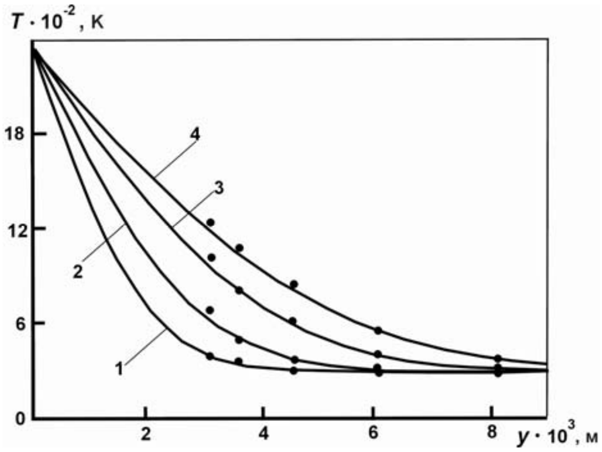

Fig. 2. Comparison of designed and experimental temperature profiles in the alloyed QGC at time of heating $\tau \le \tau_T$ and $T_w = \text{const}$ : 1 - 4 calculation on (6) on 2, 4, 8 and 13 seconds of heating, points - experiment ($\overline{T}_w = 1350$ K, $a$=$0.6\cdot10^{-6}$ m$^2$/s, $\tau_T$ =13 c).

All cases observe quite satisfactory congruence of experimental and calculated data designed for the established value of the temperature surface under the formula received from (1) for the half-space, at $T_w = \text{const}$ :

$$\theta^* = \frac{T^* - T_0}{\overline{T}_w - T_0} = \operatorname{erfc}\left(\frac{y}{2\sqrt{a\tau}}\right) = \operatorname{erfc}\left(\frac{K}{2}\right). \quad (6)$$

The depth of the warmed layer limited to an isotherm with the dimensionless temperature $\theta^*$ is subjected to an equation $y \approx K\sqrt{a\tau}$ . Hear $K$ is a coefficient that characterizes the moving rate for various isotherms and depends only on $\theta^*$ and the law of change $T_w$ . From here follows, as the coefficient $K$ at $T_w = \text{const}$ provides the highest moving rate for isotherms in comparison with other boundary conditions, the formation of the temperature field is not dependent on the heating process. It is immediately determined as an established (maximal) value of the surface temperature even at times of heating when this temperature has not been achieved at all. Apparently, the heat stream, which value exceeds a critical level of the acceptable thermal energy for non-destructive heating of this material, sets the depth of heat penetration that corresponds to a boundary condition $T_w = \text{const}$ since the moment of heating, i.e. immediately determines the highest rate of the isotherm motion.

The similar conclusion has been made in [1]. It is established that various conditions of heating and close values of an integral-average heat stream give almost equal mass ablation rates, though the evaporating share of the material ablated from the surface differed 8 times. The same proceedings takes an example of asbestos-reinforced laminate to show that at an identical calorimetric (initial) thermal stream position of the bottom border of the coked layer in a non-stationary mode warm-up is equally spaced from an initial surface. Tests of asbestos-reinforced laminate specimens were carried out in streams of air, nitrogen and radiating heating, and mass ablation rates differing thrice as much.

From here follows, that under the effect of the heat streams exceeding the critical level necessary for a non-destructive material heating, permit the existence of an additional heat transfer, for example, by wave mechanism.

## References

1. Frolov G.A. Heat Destruction Constant and Its Role in Warming-Up and Ablation Processes in Material // IFJ 2004. Vol. 77, № 2.

# THERMOPHYSICAL PROPERTIES OF HEAT-SHIELDING MATERIALS WITH ORGANIC MATRIX

**Isayev K.B. and Polezhayev Yu.V.**(1)
Francevich Institute for Problems of Materials Sciences of NASU,
3 Krzhizhanovsky str. Kyiv 03412, Ukraine, e-mail: isayev_k@gala.net
(1)Institute of High Temperatures RAS, 13/19 Izhorskya str. 125412 Moscow, Russia

The composites with an organic polymeric matrix find wide application in the most different areas of engineering. The most capacious customer of these materials is space-rocket engineering. On its portion it is necessary more than 50% from common consumption of these materials in the world.

The method of heat removal at the expense of physicochemical transformations is applied to products of space-rocket engineering in conditions of affecting of mean and high specific heat flows (0,5—30MW/m$^2$) already during several decades. For this purpose the ablative polymers and compositions on their basis are utilized. A broad applying these materials have received due to their capability to absorb, to disperse and to detain a thermal energy for the account of sacrificial carry-over of a part of material as a result of passing in it of the whole complex of physicochemical transformations during the heating. This complex of physicochemical transformations is called as ablation [1].

Using of these materials is impossible without of the reliable information about their different performances, including thermophysical, in a wide range of temperatures and heating rates.

The most important temperature range, from the point of view of exploitation of heat-shielding materials (HSM) is the range in which a process of resin destruction takes place. In this temperature range the strength and thermophysical properties of these materials are sharply changed [1—3].

Now there are a great many of the publications dedicated production process of composites with an organic matrix, choice of their optimal composition, structure, different properties at low temperatures etc. However, amount of works dedicated for study of HSM properties at high temperatures, and especially, at high heating rates, is calculated literally by units. In this connection, the comprehensive investigation for influence of different factors on the thermophysical properties (TPP) of heat-shielding materials (HSM) with an organic matrix in of high temperatures and heating rates was realized. These ones are modeling conditions of their exploitation.

The technology of determination both TPP HSM and temperatures of a beginning ($T_d$) and ending ($T_c$) of thermal destruction process of organic resin, included in composition of these materials, is proposed. This one is based on experimental temperature fields in samples of material and methods for solving of inverse heat conduction problems (IHCP).

The mathematical model (MM) of heatmasstransfer in HSM is designed. In this one the influence of heating rate ($b$) on process of resin thermal destruction is allowed at the account of this factor influence on temperatures of a beginning and ending of this process.

The effective thermal conductivity ($k(T)$) HSM at different heating rates has the minimum, which one with growth of heating rate is sheared in area of high temperatures. The minimum $k(T)$ is conditioned by maximal speed of resin destruction, which one is accompanied by formation of maximal second porosity in material at heating. The shear of the minimum $k(T)$ in area of high temperatures is connected with shear of resin thermal destruction in this area. Thus the values $k_{min}$ with growth of heating rate are decreased, and value of temperature $T_{kmin}$, at which this minimum $k(T)$ takes place, are increased.

The algorithm of determination TPP HSM and both $T_d$ and $T_c$ with the help of described above technology is introduced. It consists of following stages.

1. Testing of samples of materials, which have one type of organic resin, in different conditions of one-sided heating for determination of temperature fields. An estimation of maximal heating rate under the indication of the first thermocouple from a heating surface of the sample.

2. Determination of a thermal conductivity of investigated materials with the help of methods for solving of inverse heat conduction problem. At this stage the volumetric specific heat ($C_v$) is fixed and sinks (sources) of heat in a mathematical model of heat mass transfer are equal to zero. The

temperatures $T_{kmin}$, at which $k(T)$ has minimum value, are determined. From different $k(T)$ for different heating rates one is received the dependence $T_{kmin}(b)$. On nature of this dependence the limiting heating rate for the given type resin is estimated. This temperature with increase of heating rate increases and after reaching maximum value remains invariable at further growth of heating rate.

3. Determination of temperatures of a beginning and ending of resin destruction as functions of heating rate in the supposition, that they are equidistant $T_{kmin}(b)$. The temperatures of a beginning and ending of resin destruction at 0-th heating rate are determined under the method [4] or from thermogravimetric analysis of this resin.

4. Determination of specific heat for investigated materials as functions of temperature and heating rate. It is carried out with account of that circumstance, that up to temperature of a beginning of resin destruction (for each heating rate) the specific heat HSM is a linear function of temperature. If one known the composition of material coke that its specific heat at temperatures larger $T_c$ is calculated under the relationship of additivity. Since from the previous post $T_d$ and $T_c$ are known, one can connect values of specific heat at these temperatures and determine temperature dependence of specific heat HSM at particular heating rate. It is supposed that a density of material till $T_d$ and at $T>T_c$ is constant, and at $T_d \leq T \leq T_c$ it is a quadratic function of temperature [5].

5. Determination $k(T)$ of heat-shielding materials by IHCP with account in MM $C_v(T)$ and sinks (sources) of heat.

6. Analysis of influence of the different factors on $k(T)$ investigated HSM.

The above described know-how of study TPP is applied to materials with different polymer matrixes (phenolic, organosilicone, epoxy), filling agents of the different nature (asbestos, silica, carbon) and structure (filament, cloth). Samples of these materials were tested in conditions of convective (plasma, combustion products of kerosene in oxygen) and radiative (concentrated solar radiation) heatings. The experimental thermal fields in samples of these materials are obtained. This experimental information is treated with the help of two methods for solving of inverse heat conduction problems [5, 6].

Influence of different factors on a thermal conductivity HSM is shown. These factors are:

- Sort and rate of heating;
- Mathematical model of heatmasstransfer;
- Type and contents of resin;
- Nature and structure of filling agent etc.

The limiting rate of heating HSM with phenolic and epoxy matrixes in conditions, which are simulated a working conditions, is estimated. After reaching this heating rate the process of resin thermal destruction is not shifted any more in area of high temperatures.

On a particular example, it is quantitatively shown, that the basic source of errors at calculation of a temperature field in heat-shielding coating of a product is the mismatch of mathematical models of a solving of inverse (determination TPP) and direct heat conduction problems (calculation of a temperature field) [7]. This error can reach more than 200%.

### *References*

1. Polezhaev Yu.V. and Yurevich F.B. Heat Protection. Moscow, Energiya, 1976. 392p.

2. Goetzel C.G. High-temperature properties of reinforced phenolic composites // High Temp. - High Press. 1980. V.12, No 2. P.131—146.

3. Shashkov A.G. and Tyekaev V.I. Thermo-physical properties of decomposing at high temperatures materials. Minsk, Nauka & Technica, 1975. 80p.

4. Isayev K.B. Study of thermophysical properties of heat-shielding materials with an organic matrix. Part 1. The specific heat and temperature of begining resin of HSM destruction at zero heating rate. Indust. Heat Engin. 2003. V.25, No2. P.77—81.

5. Isayev K. B. Heat Transfer in composite materials disintegrating under high-rate one-sided heating. J. Engin. Physics and Thermophysics. 1993. Vol.65, No 6. P.1149—1155.

6. P.G.Krukovsky A universal approach to solution of inverse heat transfer problems (method and software) // 30th National Heat Transfer Conf. New York. ASME. Proc. V.10 (HTD-V.312), P.107—112 (1995).

7. Isayev K.B. and Polezhayev Yu.V. Thermal conductivity in a quasi-stationary material heating regime. J. Engineering Physics and Thermophysics. 1989. V.56, No3. P.368—373.

# COMPUTER SIMULATION OF THERMO-GAS-DYNAMIC PROCESSES OF WORKING IN EXTREME CONDITIONS MATERIALS TREATMENT

**Timoshenko V.I., Galinsky V.P., Belotserkovets I.S.**
Institute of technical mechanics of the NASU and NSAU,
15, Leshko-Popel str., Dnepropetrovsk 49005, Ukraine
Tel. (0562) 46 10 51, fax (0562) 47 34 13, E-mail: timoshenko@itm3.dp.ua

Development of many technologies of materials working in extreme conditions manufacturing and treatment, and also of products and materials utilization needs detail study of galloping high temperature processes accompanying gas mixture flows and their interaction with boundary surface materials. It is necessary to consider these flows with taking into account heterogeneous phases interaction, chemical transmutations, change of phases, etc. Experimental simulation of such flows is connected both with difficulties of high temperature flows getting and with problems of parameters measurement and test results interpretation. That’s why methods of mathematical mostly numerical simulation take an important place at high temperature technologies development. Mathematical modeling of processes in technological devices needs coordinated solution of rather big amount of separate problems. It leads to the necessity of rational choice of gas dynamic and heat mass exchange processes that should be taken into account and to the rational choice of mathematical models describing these processes. This work results from one side in formulation of physical and mathematical models allowing describing technological process with completeness enough for practical work and from the other side in development of algorithms and corresponding software allowing making calculations by existing PCs with acceptable machine time [1].

General principles of creation of unificated software, which can be used both at separate flows investigations and at computer simulation of technological processes in total, are under discussion in the report. Application of states proposed in the report for the investigation of the specific technologies is given by the separate examples.

Taking into account the fact that simulation software is as a rule used not by professional programmers, but by experts in the field of technological processes development and improvement special attention is given to the problems of insuring possibilities to work with the software in interactive regime with the use of terms and definitions from the specific field of the complex purpose. The tool for it is a specifically organized interface. This interface together with other auxiliary programs making service part of the complex allows to form and to memorize initial data, to carry out current calculations, to treat, to store, and to analyze obtained results. It allows to work with the software without any special preparations in programming field and without complex specifications study.

A methodical basis of the development of unificated algorithms for technological processes computer modeling is a consistent application of decomposition approach ideas according to physical processes and to features of mathematical equations describing these processes.

Models of various technological processes can be divided into three groups A, B and C depending on the mathematical features of equations. Models of A group are based on the systems of transcendental algebraic equations and allow determining equilibrium composition of chemically reacting multi-component gases and their mixture with suspended particles, and also the range of dust particles burnout, gas temperature and pressure in the given volume. Models of B group include systems of ordinary differential equations and describe non-stationary medium-volume processes or stationary one-dimensional flows of continuums. Such models describe not only equilibrium, but also kinematic processes. Models of C group include systems of differential equations in partial derivatives, which numerical solution features are determined by their type: parabolic, elliptic or hyperbolic.

Great class of problems connected with technological non-stationary processes is based on the parabolic type equations. Problems of temperature determination in structure elements and in gas phase, liquid and rigid working bodies; non-stationary problems of mixture components concentration determination with taking convective transfer, diffusion and chemical reactions into account; and also some stationary problems of simultaneous convective and diffusive components mass and energy transfer are concerned with this class.

Various applications of the technological problems solution total methodology are differed by the range of the physical medium parameters change, the kind of substance and gas mixture, the set of physical-chemical transformations, which take place in technological process, etc. All these facts are taken into account at software and algorithms development. Computer modeling effectiveness is illustrated by examples of specified problems solutions. They are problems connected with estimation of parameters of high speed aircrafts heating protection [2], of thermo-gas-dynamic parameters of carbons gasification and power-like iron-ore materials reduction [3], of problems of material particles acceleration and heating by gas flow, which are interesting for various technological applications (flame spraying, jet mills, abrasive surfaces cleaning, etc.) [4,5]. Problems of recrystallized sheet steel rolls annealing in bell-shaped furnace parameters estimation [6], gas-liquid system of technological devices thermo-stressed elements cooling [7], thermo-chemical and mass transfer processes of solid domestic waste utilization are also considered.

Examples of interactive software complexes for computer modeling of specific technological processes are given.

These programs work under Windows and use its objects maximally. Here programs realizing numerical algorithms determining data direction of the entire software complex are used by the service part as executing file (EXE-file) independently on the algorithm language, which was used at program code creation.

1. Timoshenko V.I., High temperature technological processes gas dynamics. - Dnepropetrovsk: Institute of Technical mechanics of NASU and NSAU, 2003.- 460pp.
2. Timoshenko V.I., Frolov G.A. Problems of insuring of guidance for development and operation of heat reflecting covering of rocket-space technique elements. I. Mathematical modeling of heat reflecting and coverings destruction processes //Space science and technology. – 2003. – V. 9, № 2/3. – Pp. 34—44.
3. Timoshenko V.I., Belotserkovets I.S., Tovarovskiy I.G., Lazuchenkov N.M. Numerical modeling of thermo-mass exchange processes of nature coal gasification and iron-ore materials reduction in cyclone type devices // Proceedings of the third Minsk international forum of thermo-mass exchange / V.X. Thermo-mass exchange in energetic devices and energy-saving. P1. – May 20–24, 1996. – Minsk: ANB publisher, ANK «A.V.Lykov's thermo-mass exchange institute», 1996. – Pp. 240—244.
4. Timoshenko V.I., Belotserkovets I.S., Galinsky V.P., Kadyrov V.H., Kisel' V.M., Jevdokimenko Ju..I. Investigation of acceleration, heating and melting processes for particles from refractory materials in gas dynamic sections of bumer devices for high speed gas-plasma evaporation // Technical-physical magazine. – 2002.– V.75, №2.– Pp. 36—41.
5. Timoshenko V.I., Belotserkovets I.S., Galinsky V.P., Zagny V.V Software for imitation modeling of acceleration, heating and melting processes of particles in gas dynamic sections of technological devices //Technical-physical magazine. – 2004. – V.77, №3.
6. About the mechanism of cold rolled strips rough surface influence on the conditions of roll turn adhesion at annealing and surface defects development /Prikhod'ko I.Ju., Timoshenko V.I., P.P.Chernov at al. //Metallurgy and mining industry.- 2002.- № 8—9.
7. Timoshenko V.I., Galinsky V.P. Motion of hot-air steam mixture with liquid in pipes // Technical mechanics.– 1994.– V.3.– Pp.19—25.

# MATHEMATICAL METHODS OF CALCULATION AND OPTIMIZATION OF THE STRUCTURE OF COMPOSITE CONSTRUCTIONS OPERATED UNDER EXTREME CONDITIONS

**Gusev E.L., Bakulin V.N.(1), Markov V.G.(2)**
The United Institute of Physical-Technical Problems of the North, SB RAS,
Oktyabrskaya St., 1, Yakutsk, Russia, e-mail e.l.gusev@ipng.ysn.ru
(1)Institute of Applied Mechanics, RAS, Russia, Moscow

Problems of optimum design of composite systems with the plane and curvilinear symmetry and with the required set of properties, interacting with the wave processes of different physical nature (electromagnetic, acoustic, temperature, elastic), are considered. In the variation statement the problems of optimum synthesis of composite systems with the given set of properties can be formulated as the problems of optimum control of composite systems described by the interdependent totality of the systems of differential equations. Besides, solutions of boundary-value problems have discontinuities on the interface of layers. The optimization criterion expresses closeness of functional characteristics of the structure synthesized to the required ones.

The formulated problems of optimum control have a number of peculiarities, such as discreteness of the range of control parameters, which are physical properties of layer materials (as a set of materials at designing is, as a rule, finite), discontinuity of solutions of the corresponding boundary-value problems describing the wave process in the composite system, essential multiextremality, property of incorrectness of the problems by A.N. Tykhonov, which substantially hamper the use of the known methods of optimum synthesis and numerical calculation.

Moreover, the above problems of optimum control over the composite systems have some specific peculiarities, which differ them from the traditional problems of optimum control considered in the theory of optimum control over dynamic systems. Phase variables undergo a break in the points of discontinuity of physical properties' distribution along the direction of medium stratification. Furthermore, the magnitude of discontinuity obviously depends on the control parameters, which are physical properties of layer materials on both sides of discontinuity. Due to finiteness of a given set of physical properties of structural materials, the range of control parameters is discrete. In this sense the problems considered can be referred to the problems of optimum control over the composite systems of a combinatorial type. Different physical properties of structural materials are related by the nonlinear dependence that causes nonlinearity of Hamiltonian by control and, consequently, complication of corresponding optimum solutions.

For the above problems of optimum control over the composite systems we have developed the necessary conditions of optimality related to the nonlocal variations of control parameters. On the basis of these necessary conditions of optimality the computational procedures of optimization are constructed. These procedures allow taking account of all the totality of parameters determining structure of an optimum construction: physical properties of layer materials, thickness of layers, number of layers, total thickness of the system of layers, as well as the order of reciprocal arrangement of layers with different physical properties in a construction. In addition, discreteness of the range of some control parameters, being the physical properties of layer materials, is effectively allowed for. Numerical experiments have shown high efficiency of the computational methods of optimum synthesis of composite systems with a given set of properties.

Now in many areas of engineering there is an actual task of creation of perfect designs possessing high weight efficiency on the one hand, both high reliability and long-lived service life on the other hand. The combination of these opposite requirements results in necessity of consideration of problems of fatigue and destruction. In preliminary designing the simplified approaches of the fatigue analysis (for example, such as installation of a limit of voltage ratings etc.) are used, as a rule. The tighter requirements have resulted in weight of a flight vehicle and its reliability to appearance of the concept of a safely damaged design. This concept admits safe growth of fatigue cracks before their visual acquisition. The optimization of such design is more composite task because of following reasons: it is necessary to determine residual strength after cracking and factor of intensity in tops of standard longitudinal and cross-sectional cracks. It is necessary to develop a method of a non-linear calculus permitting to decide this task in acceptable time with the greatest accuracy.

The considered method [5-8] allows to execute synthesis of optimum outlines of the shell with variation of a cross-section profile and simultaneous search of its optimum structurally - power scheme with variation of quantity of load-bearing elements and their sizes.

The cylindrical shells weighted with the bending moment, перерезывающей by force and internal pressure are considered. The shell consists of cylindrical panels. For definition normal and shearing stresses at absence of cracks the classical beam theory of thin-walled stiffened shells is used.

The optimum project is searched in the class of stiffened shells, for which any of segments of a skin has no local loss of stability at operation of computational loads. For definition of a residual crack strength and for definition of factors of intensity of stresses in tops of standard cracks the theoretical relations corrected on the basis of experiments are used.

According to a method of penal functions the task of minimization of weight of the shell at presence of limitations is reduced to the task of unconstrained minimization of supplementary object function. Minimization of supplementary object function is carried out by a method of coordinate of descent with cyclical exhaustive search of variables on each step and with variable pitch on each variable. The regulation of a step of variation on each variable implements with usage of sequence of the Fibonacci numbers. This method for the first time is applied in [8] for the non-linear task of optimization with many variables.

With the help of designed algorithms and computing program the calculations of baies of three types of fuselages (two passenger airplanes and one manoeuvrable airplane) are carried out. Weight of these baies has appeared less by 9-14% as compared to baies designed by the conventional methods.

References.

1. Gusev E.L. Qualitative regularities of the structure of optimum solutions in the problems of optimum synthesis of multilayer structures under the effect of elastic waves // Proc. RAS, 1998, v. 368, No. 1, p. 53-56.
2. Gusev E.L. Optimal synthesis methodology of nonhomogeneous structures under the influence of electromagnetic waves // J. of Applied Electromagnetics and Mechanics, 1999, No. 10, p. 405-416.
3. Gusev E.L. Property of periodicity of the structure of nonhomogeneous constructions realizing the limiting possibilities under the effect of elastic waves // Mechanics of Rigid Body, 2002, No. 1, p. 112-120.
4. Gusev E.L. Optimal Synthesis of Inhomogeneous Layered Structures // Acoustic, 2002, № 3.
5. Bakulin V.N., Gusev E.L, Markov V.G. // Mathematical simulation. 2000. № 5. pp. 28-32.
6. Gusev E.L., Bakulin V.N., Markov V.G. Optimum designing and numerical calculation of designs with application of composite and conventional materials. // The Eleventh international conference on a computing mechanics and modern applied software, Moscow - Istra, 2001 – pp. 164 - 165.
7. Bakulin V.N., Gusev E.L , Markov V.G.,. // Tenth anniversary international conference on a computing mechanics and modern applied software. Pereslavl-Zalessky - Moscow 1999. pp. 234-235.
8. Bakulin V.N., Gusev E.L. Markov V.G. Optimum designing of designs from conventional and composite materials. // International technological conference "Progressive technologies of engineering and modernity". Donetsk. 1997. p. 24.

# USE OF ELASTOMER MATERIALS FOR PROTECTION OF DESIGNS FROM CORROSION AND EROSIVE WEAR

**Khorolsky M.S.**
Ukrainian State Research, Design-
Technological Institute of Elastomer Materials and Products (URDTI "DINTEM")
Krotova Str. 24a, Dniepropetrovsk, 49033, Ukraine, E-mail: postmaster@dintem.dp.ua

It is known, that corrosion – one of the most widespread processes of destruction of materials (metal, concrete, ferroconcrete) owing to their interaction with an environment. Corrosion destruction of materials proceeds mainly by formation of the located damages which increase under influence of different external factors and result in negative consequences.

URDTI "DINTEM" has experience on protection from corrosion and erosive wear of elements of designs with the help of elastomer coverings. Rubberizing is widely applied to protection against corrosion of the chemical equipment. Recently many rubbers are developed in which such properties as corrosive medium resistance, elasticity, vibration resistance, ability to maintain the big hydrodynamic shocks, heat- and frost-resistance etc. are inherent. Features of elastomer's destruction under influence of various factors are studied. In institute two methods of rubber fastening to metals by glues of cold hardening and during vulcanization at the set temperature under pressure is developed. Elastomer coverings (on a basis of chloroprene rubber) of internal surfaces of metal capacities for transportation of a hydrochloric acid of different concentration are developed and introduced into manufacture.

A lot of shaft of different purpose is used in many branches of industries. The surface of a shaft from usual steels gives in to corrosion that frequently does not allow to receive a high quality product. Rubberizing is the most widespread means of protection of shaft from corrosion. In institute the technology of rubberizing more than twenty kinds of shaft for papermaking, cement-slate, printing productions etc. is developed. Rubberizing of these shafts is carried out by a method of vulcanization.

At the present stage rubber-armored carriage (RAC) in bridge engineering are even more often used for bridges spans. In RAC rubber functions as the following: protects metal elements from corrosion, compensates temperature and force deformations and protects from vibration. In institute new rubber is developed which surpasses serial rubbers on parameters of ozone ageing resistance in 35 times and has physical-mechanical properties considerably best. On researches, rubber provides reliable protection of RAC metal armature during not less than 25 years.

Also different designs of connections with a rubber covering with some functions are developed. Rubber protects working faces of connections from corrosion and erosive wear simultaneously. For example, it can be tracks of different purpose, seals of shafts, rubber-metal bushings, rubber-metal bearings for ship screws and circulating pumps of thermal and atomic power plants. In asphalt shoes for caterpillars rubber reduces contact stresses in a zone of contact with a hard surface and protects armature from corrosion.

The rubber covering allows to increase a resource of sliding joint more, than on the order, due to that the moisture and hard parts do not get on sliding joint.

As is obvious, rubber coverings can be used for protection from corrosion and erosive wear that considerably increases operation life of objects under influence of aggressive factors. Simultaneously rubber can be used for performance of other functions in view of its properties.

# SCINTILLATORS FOR THE DETECTION OF IONIZING RADIATION UNDER EXTREME CONDITIONS: RADIATION AND MECHANICAL OVERLOADS, TEMPERATURE GRADIENTS, CHEMICALLY AGGRESSIVE MEDIA

**Globus M., Grinyov B., Lubinskiy V., Ratner M.(1)**
Institute for Scintillation Materials of NASU
60 Lenin avenue, 61001 Kharkov, Ukraine, globus@isc.kharkov.com
(1)Institute for Single Crystals of NASU
60 Lenin avenue, 61001 Kharkov, Ukraine, ratner@isc.kharkov.com

There exists a broad class of scintillation materials (dielectrics and semiconductors) which transform ionizing radiation energy into light signals. During last decade, the applicability field of scintillators was intensively expanded, they broadly used in high energy physics, nuclear physics, in apparatus for space investigations and diagnostic medicine instruments, introscopy, geophysics, in manifold industrial measurement systems, in radioisotope environmental monitoring. Besides a usual general set of requirements to scintillation materials (a high light output and energy resolution, high density and effective atomic number, a short decay time of 10 to 100 ns), specific applications condition additional requirements. Below we consider rigid additional requirements to scintillation materials, intended for working under extreme operation conditions, and describe the methods for preparing scintillators meeting such requirements. We will give a brief review of the state of the problem and describe the most important results of the authors.

*Scintillation crystals for high energy physics working under strong irradiation.*

An electromagnetic calorimeter, used in high energy physics experiments as a main instrument, contains a very large number ($>10^4$) of scintillation crystals which must work under strong irradiation during at least ten years without noticeable variations of their scintillation characteristics. In particular, inadmissible are structure changes resulting in lowering count rate or in a spatial nonuniformity of light output.

The authors have shown that an increase of irradiation dose up to about 1 Mrad or more is accompanied by a change of the radiation damage mechanism as compared to the range of low doses. Since the dose range dictates the character of the irradiation-induced structure process, an adequate way to improve radiation hardness of scintillation crystals depends on dose range, which will be elucidated in more detail. There is a fast process of populating hole or electron traps already existing by photoproduced electrons or holes; as a result, color centers are formed which can reabsorb luminescence light thus lowering light output. This fast process is saturated at a small irradiation dose $D\sim 1$ krad. There exists also a slow process of creating new lattice defects that is not saturated even at a dose $D\sim 1$ Mrad. The existence of the fast and slow processes should be taken into account when defining the radiation stability of a crystal by a dose $D_{stab}$ causing in the crystal noticeable radiation changes. As applied to a large dose range $D>>1$ krad, only the slow process is essential so that $D_{stab} \sim 1$ Mrad; but for a small dose range $D \sim 1$ krad radiation stability is determined by the fast process, so that $D_{stab} \sim 1$ krad. In corresponding publications, this circumstance usually is not taken into account, which results in a large straggling in the radiation stability inferred from experiment.

For a crystal, used under irradiation with doses $D < 1$ krad, radiation hardness can be enhanced via decreasing the number of initial lattice defects through heightening structural perfection. But for $D\sim 1$ Mrad this way is inefficient since photoproduced defects much exceed in number initial defects. In this case radiation changes of a crystal can be diminished in an opposite way, via preliminary irradiation increasing the number of initial defects. The latter act as recombination centers for photoproduced vacancies and interstitials and impede their accumulation that results in the formation of defects (e.g., vacancy clusters).

*Scintillation detectors, resistant to heat and vibration, for nuclear geophysical well logging and space apparatus.*

Gamma-ray logging of wells is the most widespread method of the search and prospecting of uranium deposit and of the estimation of the mass portion of radionuclides in rock ore. This method is based on the high-sensitive registration of gamma-irradiation of natural radioactive elements, contained in rocks, with the use of scintillation crystals, whose operational characteristics must remain stable in a wide temperature region and mechanical loads. Single strokes with acceleration exceeding that of vibrations make the most dangerous action on crystals. Besides, mechanical stresses caused by a temperature gradient are also very dangerous. To enhance the region of thermal and mechanical stability of scintillators, experimental and theoretical investigations were carried out, which permitted one to optimize the detector construction. Some examples are given below.

The output window of a scintillation detector is most sensitive to temperature stresses and strokes. As a proper material for a window, sapphire single crystal was chosen. Along with durability, sapphire provides a good transmission for scintillation light (about 86 % at a wavelength of 415 nm and 90% at 540 nm for a window thickness of 3 to 4 mm). Crystals NaI(Tl) with sapphire window withstand a rigid testing regime at temperature varying from –60 to +100 °C with a rate of 2 °C/min and up to +210 °C with a rate of 5,5 ° C/min. Such crystals tolerate the action of single strokes in different directions with acceleration of 4000 m/sec$^2$ (20 strokes) as well as the relative air moisture up to 98% at a temperature of 35 °C during 48 hours. For joining the output window with a container, a modern technology of soldering together glass and metal was used instead glue connection. A convex or stepped shape of the crystal top provides its safe joining with the output window and a centering ring. The investigations and testing of scintillation materials, intended for space apparatus, were carry out. For such application, a scintillator and its hermetic encapsulation must meet especially rigid requirements to stability under conditions of strong vibrations and acceleration, thermal strokes, temperature changes and mechanical overloads.

*Stability of scintillation crystals and thin films intended for radiation monitoring under extreme conditions: high temperatures, action of chemically aggressive liquids and their vapors.*

For the detection and identification of radionuclide pollutions, scintillation crystals and films are used. For this purpose, new scintillation materials – oxide crystals and thin films were investigated. These materials, due to a high chemical and thermal resistance, can be applied for monitoring under extreme conditions which traditional alkali halide scintillators are incapable to sustain. A high chemical stability is inherent in luminescent oxide films grown by the liquid phase epitaxy method on a bulk luminescent substrate. Several film – bulk combinations were explored and proved high chemical and temperature stability along with good scintillation properties: the $Y_3Al_5O_{12}$:Ce film on the $Y_3Al_5O_{12}$:Sc substrate; the $\alpha$-$Al_2O_3$:Ce film on the $\alpha$-$Al_2O_3$:Ti,Ca substrate; the $\alpha$-$Al_{1.8}In_{0.2}O_3$:Pb film on the $\alpha$-$Al_2O_3$:Ti,Ca substrate [1]. The film, matched by thickness to the path length of short-range particles ($\alpha$-, $\beta$-particles), and the substrate, intended for detecting long-range particles ($\gamma$-photons), must have strongly different luminescence decay times in order to discriminate the photoreceiver signals from the film and substrate. Such combined scintillators are devoid of a most unstable constituent – an immersion or glue layer joining the film and substrate.

This work was supported by the Fundamental Research Foundation of the Education and Science Ministry of Ukraine (Project № 04.07/00399).

[1].M. Globus, B. Grinyov, M. Ratner, V. Tarasov et al., New Type of Scintillation Detectors for Biological, Medical and Radiation Monitoring Applications // IEEE Transactions on Nuclear Science, 2004, in press.

# DEVELOPMENT OF A SET OF FUNCTIONAL COATINGS FOR SATELLITE AND CABLE TELEVISION PARABOLIC AERIALS

**Borisov Yu.S., Borisova A.L., Kozyakov I.A., Dotsenko N.M.**(1)
E.O.Paton Electric Welding Institute
11 Bozhenko Street, 03150, Kiev, Ukraine, e-mail: borisov@pwi.ru.kiev.ua
(1)Factory "Quant", 2 Trutenko Street, 03030, Kiev, Ukraine

Wide application of satellite and cable television networks by different levels of customers is based on the quality of the information they receive and price of the involved hardware. One of the key elements of radio engineering systems responsible for the scope and quality processing of the information received is the aerial. If there is a loss or distortion of the signal at the air-aerial interface, this leads to an irremediable defect of the information received.

Main objective of this development was to make a new type of the cable television parabolic aerial with improved technical characteristics through using a set of functional coatings deposited on the surface of the aerial reflector by thermal spraying methods (electric-arc metallising, flame and plasma spraying). As to the functions performed, the applied coatings were subdivided into three groups: anticorrosive (to protect the aerial material from atmospheric corrosion), optical (to reflect infrared part of solar radiation) and with special electrophysical properties (to control the processes of absorption and reflection of electromagnetic radiation).

Principles of design of the parabolic aerials with functional coatings were worked out in the course of the development efforts on the basis of analysis of peculiarities of interaction of electromagnetic radiation with the reflector surface (Fig. 1). These principles consisted in local arrangement of different types of the coatings on the aerial reflector surface to control absorption of electromagnetic radiation. They were intended to decrease the level of side and rear lobes and reduce the amount of the electromagnetic energy flowing into the rear part of the reflector, which had to lead to reduction of the noise temperature and improvement of the quality of the received signal. Another method for improving the quality of reception consisted in the application of coatings dissipating infrared radiation and thus decreasing the degree of heating of the converter. The anticorrosive coating on the surface of the aerial reflector made from a steel sheet provides reliable protection from atmospheric effects for 30—50 years, combined with high mechanical strength of the aerial.

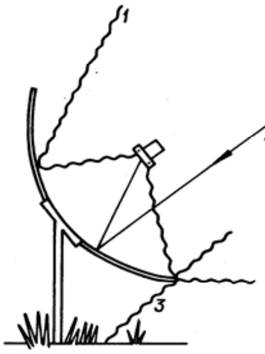

Fig. 1. Signals and noises received by the aerial:
1 – noises due to other satellites and air noise;
2 – valid signal from satellite; 3 – diffraction of Earth noise at the reflector edge

The above technological approach was implemented through selection of appropriate raw material to deposit coatings: mechanical mixtures of polymeric powders with different fillers for absorbing coatings; aluminium oxide for production of diffusely scattering and dielectric coatings, and aluminium alloy with 10% zinc for anticorrosive coatings.

Factory "Quant" developed a package of design documents for the parabolic aerial with functional coatings, made experimental samples of the coated aerials (Fig. 2), as well as developed and manufactured a measurement rig located in the Quant acoustic chamber. Measurements were conducted by the collimator method comprising elements of the aperture-probe method.

As shown by measurement of characteristics of the initial Al alloy prime-focus aerial with a diameter of 1.2 m without a coating at a frequency of 4 GHz, the gain is 31.7 dB, level of the first side lobes is –15,39/-15,07 dB, width of the beam is 3°, and deflection of the first side lobe from the main one is 12°.

As established by measurement of parameters of the coated aerial, the gain is 31,7 dB, level of the first side lobes is –16,5/-16,6 dB, and width of the beam is 3,2°.

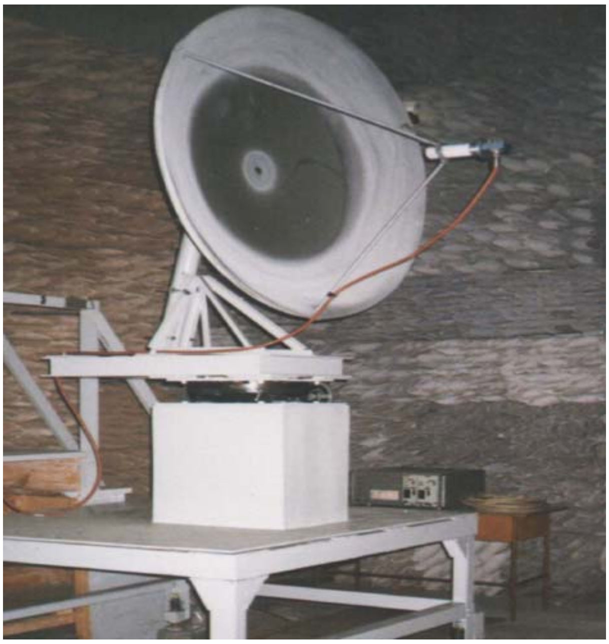

Fig. 2. Parabolic aerial with functional coatings

The following levels of side lobes with respect to the main one were obtained from the aerial beam value (see Table).

Table

| Side lobes | Level, dB, $\theta_{0+}$ | Level, dB, $\theta_{0-}$ | Difference in levels of side lobes between aerials with and without coating |
|---|---|---|---|
| 1 | -16,5 | -16,5 | 1,1+1,4 |
| 2 | -17,14 | -16,81 | 0,7+0,72 |
| 3 | -18,63 | -18,63 | 0,27+0,78 |
| 4 | -23,05 | -20,11 | 2,57+0,6 |
| 5 | -26,6 | -26,1 | 0,29+2,7 |
| 6 | -26,3 | -26,75 | 0,34-3,47 |

Deflection of the first side lobe from the main one is 11,5°.

Therefore, the following advantages of the aerial with functional thermal spray coatings can be noted on the basis of the results obtained:

1. The aerial beam is more symmetric about the main lobe.
2. The level of the side lobes is lower by 1.8 dB on the average.
3. The intensity field is redistributed from the side lobes to the main one.
4. Noise temperature of the aerial is decreased and the signal/noise ratio of the entire system is improved.

No impact of coatings on the gain and width of the side lobes was established.

In addition, in this case temperature of the reflector and risk of overheating of the converter under the effect of solar radiation decrease.

In general, this leads to improvement of the quality of operation of systems with the parabolic aerials.

The authors would like to thank the Science and Technology Center in Ukraine for the financial support it rendered to perform this work (Project 386).

# THE PROTECTION OF INTELLECTUAL PROPERTY IN THE FIELD OF MATERIAL SCIENCE

**Kossko T.G.**
Frantsevich Institute for Problems of Material Science, NASU,
Krzhizhanovsky str., 3, Kyiv, 03142, Ukraine, E-mail: Kossko@materials.kiev.ua

The report considers the problems connected with protection of rights for intellectual property objects, in particular, of industrial property objects and with protection of economical interests of patentees as well as inventors.

The questions of national legislation in the sphere of intellectual property, including the Civil Code [1], laws and legal acts [2] are discussed. The legislation questions in the sphere of intellectual property are examined in connection with obtaining and realizing the defense and protection of the rights for industrial property objects [3].

Nowadays the unification of national legislation is accomplished according to international standards, including, in particular, registration of TRIPS and other international treaties [4].

Specific problems of protection of new developments in the field of material science are considered. There are also described the peculiarities of detection, record and defence of inventions in concrete field.

The retrospective, up-to-date and perspective views are given in accordance with protection of rights of industrial property in the field of material science. There are exposed the most acute problems being difficult to solve, for example, the use of modern information technologies, in particular, applying data bases of Intellectual Property Department and UkrISTEI.

There are given concrete examples of protection of such industrial property objects as “materials”, i.e. new materials, in particular, materials working under extreme conditions and coatings, and methods for their obtaining and applying .

The consideration is given to commercial Significance of new material developments and protection of them with patents. The important step in this direction is transfer of rights for industrial property objects and transfer of technologies [5].

There are discussed the problems of transfer of technologies and vending of licenses for patented invention, useful models and know-hows.

There is proposed the scheme of patenting and commercial realization of industrial property objects in the field of material science and powder metallurgy.

Literature:

1.Гражданский кодекс Украины. Цивільний кодекс України. Книга четверта “Право інтелектуальної власності”;
2.Закон Украины “Про авторське право та суміжні прова “ Відомості Верховної Ради України (ВВР), 1994. - №13. – Ст. 64. (Із змінами, внесеними згідно із Законами №850 - IV від 25.05.2003, ВВР, 2003, № 35, ст. 271 № 1294 – IV (1294 – 15) від 20.11.2003);
3.Закон Украины “Про охорону прав на винаходи і корисні моделі”, Відомості Верховної ради України, 2000р. №37. Ст.307; 2001р. №8; ст. 37; 2002р. № 16, ст. 114, № 35, ст. 256;
4.Філіпенко А. Охорона інтелектуальної власності в Україні – справа державна. Інтелектуальна власність. – 2001. - №4. – Ст.9;
5.Капица Ю.М. Экспорт – импорт технологий: правовое регулирование. – К. – 2000. – 28с.

# HIGH-DAMPING HARD METAL-CERAMIC COATINGS

**Movchan B.A., Ustinov A.I.**
ICEBT of Paton Electric Welding Institute of NASU
68 Gorkii st., Kiev, 03150, Ukraine, ustinov@paton-icebt.kiev.ua

Durability of titanium compressor blades in a gas-turbine engine (GTE) drops significantly because of the abrasive particles damaging their surface and initiation of endurance cracks. Hard coatings have now been developed, which may ensure protection of their surface from damage, as well as damping coatings, which lower the probability of development of resonance vibrations in operation of blades under the conditions of cyclic loading with variable parameters. On the other hand, at deposition of hard coatings, the fatigue limit of the blades usually drops, and at deposition of damping coatings the erosion resistance of the blades is decreased. Therefore, an urgent issue is development of highly damping hard coatings, deposition of which would not change the fatigue limit of the blade material.

High-damping hard coatings and technology of their deposition by single-stage EBPVD process have been developed for the case of Sn-Cr-MgO systems.

As an example Fig. 1 shows the amplitude dependence of the logarithmic decrement of free vibrations in supported in cantilever flat samples of VT-6 titanium alloy (Ti-6Al-4V) with Sn-Cr-MgO based coating deposited on its surface at substrate temperature below 400 ºC. It should be noted that microhardness of the upper layers of the coating reaches 16 - 18 GPa. Such a combination of the mechanical properties, at a high adhesion strength of the coating and substrate, is provided for a smooth variation of element concentration at transition from the layers directly adjacent to the metal-based substrate to the ceramic-base upper layers of the coating with a high hardness.

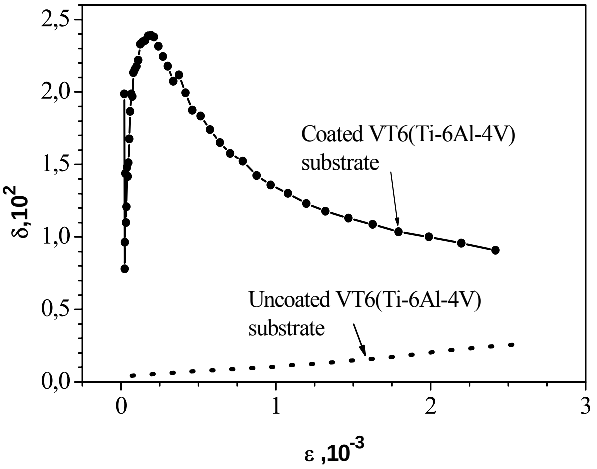

Fig.1. Amplitude dependence of the logarithmic decrement of vibrations of flat samples 2 mm thick of a sheet titanium alloy VT6 without coating and with 40 μm coating deposited on its surface.

The paper analyzes the results of studying the stability of damping properties of such graded metal-ceramic coatings at their thermomechanical loading in a wide temperature range.

The paper substantiates the possibility of practical use of the developed coatings for their deposition on compressor blades of GTE to protect them from erosion wear and vibration loads.

# PROTECTIVE COATINGS BASED ON TRIFLUOROCHLOROETHYLENE-VINYL ETHER COPOLYMERS

**UIvanchev S.S., Konovalenko V.V.(1), Polozov B.V.(2)**
St-Petersburg Department of the Boreskov Institute of Catalysis
of the Siberian Branch of the Russian Academy of Sciences
14, prospect Dobrolubova, St-Petersburg, 197198, Russia, email: ivanchev@SM2270.spb.edu
(1)Share Holding Company Plastpolymer, 32, Polyustrovsky prospect, St-Petersburg, Russia
(2)NPO Pigment, 18, Oktyabrskaya Naberezhnaya, St-Petersburg, Russia

Trifluorochloroethylene (TFCE) - alkylvinyl ether terpolymers are widely used as easily curable surface protective coatings featuring with high weather and corrosion stability. However, their preparation is complicated due to structuring in the course of synthesis caused by secondary reactions involving hydroxyalkylvinyl ether. So, at the preparation of TFCE - alkylvinyl ether - hydroxy-alkylvinyl ether terpolymer the crosslinked polymer content reaches 70% during the synthesis significantly reducing the efficiency of the polymer solution application.

This study presents the consideration of the approaches to copolymerization providing the elimination of structuring in the course of the process and affording efficient loss-free obtaining of trifluorochloroethylene (TFCE) terpolymers with alkylvinyl ethers, including alternating hydroxyalkylvinyl ethers.

The addition of various primary alcohols into the polymer system is found to prevent the polymer structuring in the course of copolymerization.

The application of amino-alcohols affords the simplification of the polymerizing system recipe due to the combination of tertiary amine and primary alcohol functions in one reactant.

The optimum contents of the used additives are determined.

The synthesized terpolymers were used to prepare coatings curable with toluylene-diisocyanate. The characterization of their properties indicated their high chemical stability (tolerance towards gasoline, sea water, acids and alkali), reduced flammability, low adhesion to dirtying substances. In addition, the obtained coatings are tolerant to deactivating agent solutions, which allows their effective application for the protection of rooms possibly subjected to radioactive pollution.

# LIMITING POSSIBILITIES OF COMPOSITE THIN-WALLED FAIRINGS

Rusin M.Yu., Kurakin V.I.
Federal State Unitary Enterprise
“Obninsk Research and Production Enterprise “TECHNOLOGIYA”, Obninsk, Russia
E-mail: info@technologiya.ru

Iteration methods are widely used in mechanics of a deformable solid body for solving applied problems. These methods are extensively laid down by the mathematicians and illustrated by solving classical problems of the theories of elasticity or plasticity, gas dynamics, heat and mass transfer. In this case method of division and alternate-triangular method have made the best use in solving multidimensional problems.

The use of the algorithms in question for the determination of stress-strain state of shells has not found a wide utility. It is connected with the use of nonconstructive (in terms of determinative equations structure) shell structure models which contain differential equations of high order or equation systems of various orders.

The equations mentioned are difficult to analyze for ellipticity and consequently for problem solving. It is obvious that in the process of numerical solving of these equations various inconveniences emerge which are associated with the approximation adequacy, choice of method for solving their algebraical analogs, analysis of computational process convergence and stability.

In this paper efficient algorithms are extended to the problems for the determination of shell stress-strain state and stability. A system of five differential equations uniform in order of differentiation of the functions being determined was obtained to evaluate the stress-strain state. In this case the problem was solved in displacements and a model of the Timoshenko type shell theory taking account of the lateral shear deformation was taken as the base.

Hereafter the equations were divided according to the coordinates and a number of standard one-dimensional boundary problems to be solved uniformly were obtained. However during the analysis of the characteristics of the operator designed major difficulties emerged and it was not very easy to obtain a uniformly converging process. A dummy viscosity had to be entered into physical equations and iteration parameters had to be selected according to Neyman criterion. This invited further investigations sometimes as difficult as the solution of the main problem but in this case the possibilities of the analysis were dramatically limited by the shell design features and by the type of the problems being solved.

A variational and differential method (VDM) appeared to be more suitable. It permitted the efficient iteration algorithms to be developed in a strictly mathematical way. The auxiliary theorems of convergence and stability of the computational processes built for solving the problems of strength, stability and orthotropic shell vibrations were proved.

With this algorithm the calculations for a great number of structures were performed and the efficiency of the calculations particularly for the problems of orthotropic composite fairing stability was proved. Ultimate load values for thin-walled structures working under asymmetrical loading and heating were obtained.

The results of the solution were compared with the results obtained by other methods with the use of application package and a satisfactory agreement was revealed.

The calculation results show that compared to Kirchhoff - Love model the results obtained are higher for displacements and lower for ultimate load. Besides they tend to improve with the decrease of the lateral shear.

The Timoshenko model is likely to introduce the effect of rigidity in shear into equations (from the viewpoint of mathematical quality of the problem - the availability of a boundary layer, asymptotical components in the solution).

In the course of realization the rigidity phenomenon causes a marked error in the solution and from the standpoint of quality this error differs from the behavior of the error governed by the order of digitization. This effect enhances with the increase of anisotropy.

Certain advances in the rigidity phenomenon control can be made by turning from the “primitive” approximation patterns (as in this case –VDM) to highly precise ones. The problem can be solved by combining asymptotic and numerical expansion though the results obtained with the use of the procedure mentioned above are acceptable in practice.

# COMPOSITION MATERIALS ON BASE OF SILICIDES

**Dvorina L.A.**
Frantsevich Institute for Problems of Materials Science of NASU,
3, Krzhizhanovsky St., 03142, Kiev, Ukraine, E-mail:dvorina@ipms.kiev.ua

Composites on base of silicides may be divide on three groups: a) materials for the heat accumulators, b) light constraction materials for spase aerospase technigues, rocketproductions and c) hightemperature heat resistance materials with high mechanical properties.

**Composite for heat accumulaters:**
For creating of heat accumulator materials the systems Mg-Si-Me (Me- Li, Al), Mg-Me-Si-O was employ[1-3]. The Li-Mg-Si system is more perspective to provide the high storage battery capacity. The amper-hour of 1370 and 1074 Mah/g (at charge and at discharge respectively) accumulator cell was realized by intercolation of Li-atoms into crystal lattice $Mg_2Si$.

The creep resistance of Mg-Li composites increase by reinforced $MgO/Mg_2Si$ particles[2]. The high thermal stability have the heat accumulators with MgO matrix , in which a granules of TAComposites Al-132%Si with protective $Al_2O_3$ coating are distributed. They holding > 540 cycles of heating -cooling in range 2--600-20 $^{o}C$ with speed of heating 300-1200 $^{o}C$ and cooling - 152-200 $^{o}C$ [3].

**The light constraction materials.**
Weigh reduction of constraction elements of flying vehicle provide the materials on the base of Al-Si-Me (Me-Cu,Zn, Mg, Ca, V, Fe et al.) reinforced and unreinforced with SiC, AlN, $Al_2O_3$ articles. Also they are perspective in new direction in aluminumbased materials for automotive application [4]. Al-Si alloys with Si, Mg, Zn, Cu, hypereutectic alloys Sl-Si, containing before 40%Si, and with Al-alloy matrix, $SiB_6$, $B_4C$, Al up to 40% have high elacomposites stic modules (>90 HPa). For coating of piston machine with cylindrical surfase used Al-Mg-Si-alloys with high machanical properties combined with plasticity, that is important in the case of the incompability of Cu and some fuel kinds. Among hopo- and hypereutectic alloys Al-Si. The Al-18Si alloy, which coating reinforced with SiC are the most wear reresistant [6]. High resistants to metal bath have composite with $Si_3N_4$- or $Si_{(6-z)}Al_zO_zN_{(8-z)}$, (z<3)-matrixs with distributed in it dispersed phase of double compounds of system Me-N( $ZrN_{1-x}$ or BN) or triple compounds system Me-Si-N(Zr-Si-Al-N)[7].

**Heat resistanc construction materials.** System Ti-Si-C was employ to create of materials with high elecrto- and heat physical, mechanical and heat resistance properties. Spesial attention was pay for triple compounds as $Ti_3SiC_2$ and many phase compositions (high electro- and heat-conductivity, high oxidation resistance), Cu-5% $Ti_3SiC_2$ ( preserve high conductivity, increasing $H_v$ up to 122 and yield limit up to 2911 Mpa), $Ti_3SiC_2/SiC$ (increasing of mechanical properties), $TiC/Ti_5Si_3/Ti_3SiC_2$ (combine of unique machanical and electrical properties). Modification of $Ti_5Si_3$ with B (0,3-3,3 %) C (0,3-3,6) has improved oxidation resistance at high temperatures (~ 1000 $^{o}C$)[8].

High breaking resistance have the composites reinforcedor with SiC [9]. The viscosity breaking of $TiSi_2/SiC$ composites make up - 4,2 $MPa \cdot m^{1/2}$, that is in 2 times more than $TiSi_2$, and hardness - 8,5-12 HPa[10].Temperature dependancesher stregth of composites with $TiSi_2$ interlayers have maximum (34-41 MPa) at 1164 $^{o}C$[11].

For aerospase systems and rocket production the composites on base of $MoSi_2$, that working at thetemperature range 1275-1975 K and have high oxidation resistance up to 2075 K are perspective. Composites on base of $MoSi_2$ with addition of SiC, $Si_3N_4$, TiC, ZrC, HfC, $TiB_2$, $ZrB_2$, $HfB_2$, $ZrO_2$, and $HfO_2$ have high stability< whereas C and $TiO_2$ in $MoSi_2$-matrix decrease it. The system $Al_2O_3$-$MoSi_2$ is stability at temperaturas < 1800 K [12].

Oxidant resistive $Mo_3Si_3B$ has metal conductivity, its hardness make up 120 Mpa, creap rate - $7{,}2 \cdot 10^{-7}$ $c^{-1}$ [13]. Us Dept. of Energy"s [14] $Mo_5Si_3B$ have used in fabrication of a heat exchangers, roller bearing and high temperatures nozzless.
Comparisson of composites $MoSi_2$ with addition of SiC, $Si_3N_4$, TiC, ZrC, HfC, $TiB_2$, $ZrB_2$, $HfB_2$, $ZrO_2$, and $HfO_2$ scale-resistannce on air, thermal resistant to "catastrophic" distruction at the 400-600 $^{o}C$ on $O_2$-Ar (20:80)gaseous medium [15] has

shown, that scale-resistance of $MoSi_2$- $ZrO_2C$ is higher than is another composites and $MoSi_2$. Heat resistance decrease in the rang $MoSi_2$-SiC, $MoSi_2$-$TiB_2$, $MoSi_2$-$HfB_2$, $MoSi_2$-$ZrB_2$, thermal resistant to "catastrophic" distruction in range rang $MoSi_2$-SiC, $MoSi_2$-$ZrB_2$,

$MoSi_2$-$HfB_2$, $MoSi_2$-$TiB_2$. has impact strength begger than is $MoSi_2$. Hihg oxidant resistive composite $MoSi_2$-SiC have preserved plasticity (in 29 times more plasticity than the best heat resistive alloys), have destruct resistance in 40 times bigger than is construction ctramics. $MoSi_2$-SiC is perspective material for production of shaft turbine engine . Composites $MoSi_2$-$Si_3N_4$ [16] are used in high temperature volume constructions. $Si_3N_4$ thai is necessary to correspond thermal efficiency of $MoSi_2$-$Si_3N_4$ and $MoSi_2$ at 1000-1500 $^{O}$C make up 30-35 % . Mo-Me-Si (Me-Ti, Nb, Mo, W et al.) have high mechanical and thermal resistive properties. $MoSi_2$-27 mol.% $Mo_5Si_3$, $MoSi_2$-50 mol.% $Mo_5Si_3$ $MoSi_2$-50 mol.% $WSi_2$ have Young's modulus at 20 $^{O}$C 387,5; 337,5; and 401,2 HPa respectively[17]

**References**

1. The insertion mechanism of lithium into $Mg_2Si$ anode material for Li-ion batteries. / H.Kim, J.Choi, H.-J. Sohn, T.Kang // J. Electrichem. Soc. - 1999. - 146, n. 12. - P. 4401-4405.
2. Creep resistance of MgO/$Mg_2Si$ particles reinforced Mg-Li matrix composites./Guanghui Min, Huashun Yu, Xichen Chen, Shengxu Zhag//Metal Phys.. and new. Technol. - 1999. - 21, № 10. - C. 65-68.
3. Bulitchev V.V., Slastilova S.V., Chelnocov V.S. Thermal resistivity of heat accumulator composite material on base aluminium-silicon alloy and magnesium Oxde. / Mosc. inst. steel and alloys (technol. univ.).- M., 2000. - 11 c.; bibliog. name dep. in VINITI 20.03.2000. №692-800.
4. Hunt Warren H. New direction in aluminumbased P/M materials for automotive application/(Jr) Int. J. Powder Met. - 2000. - 36, n. 6. - P. 51-56, 58-60.
5. Shakesheff A.J., Purdue G. Designing metal matrix composites to meet their target: gpaprticulate reinforced aluminium alloys for missible applications. // Mater. Sci. and Technol. - 1998.- 14, n. 9-10. - P. 581.
6. Patent № 19806203 DE. Composite ceramics material and method, it production. /Schober R./ Fraunhofer-Gesellschaft zur forderung der angewandten Forshung E.V. - Publ. 19.08.1999.
7. Zang Yi, Zhou Yanchun. CopperМедь with dipersion reinforced (phase) $Ti_3SiC_2$ - new disperse-reinforsed copper alloys. /(Ceramic and Composite Department, Institute of Metal Research, The Chinese Academy of Sciences, Shenyang 110015). Jinshu Xuebao=Acta Met. Sin. 2000. 36, n. 6. - P.662-666.
8. Synthesis of $Ti_3SiC_2$/SiC and $TiSi_2$/SiC composites using displacement reactions in the Ti-Si-C system./R.Radhakrishnan, C.H.Henager (JR), J.L.Brimhall, et all.//Scr.Mater. (Scr. Met. et Mater.). - 1996. - 34, n. 12. - 1809-1814.
9. Wen Jinhai, Vedula Krishna, Yellamanchili Kumar. $TiSi_2$ composites reinforced with *in situ* synthesized TiC and SiC. /Int. J. Powder Met. - 1996. - 32, n. 3. - P. 259-264.
10. Dadras P., Ngai T.T., Mehrotra G.M. Joining of carbon-carbon composites using boron and titanium disilicide interlayers. //J. Amer. Ceram. Soc. - 1997. - 80, n. 1. - P. 125-132.
11. This boron-dopped material combines the best of metal and ceramics.//Chem. Eng. (UAS). - 1994. - 102, n.6. - P. 21.
12. Processing, microstructure and mechanical properties of Mo silicides and their composites. / P.D.Eason, E.N. Ross, L.A.Dempere et. all.// Trans. NonFerrous Metals Soc. China. - 1999. - Spec. Issue. - C. 1-12.
13. The oxidation resistance of $MoSi_2$ composites. / E.Lee, J.Cook, A.Khan, et all.// Jom. - 1991. - 43, n. 3. - P. 54-57.
14. Fabrication of $MoSi_2$-SiC composites by a spark plasma sintering method./Kurokama Kazuya, Ube Makoto, Takahashi Hideaki, et. all./ J. Univ. Sci. and Technol. Beijing. - 1999. - 6, n. 82, - P. 116-118.
15. Srinivasan S.R., Schwarz R.B. Elastic moduli of $MoSi_2$-based materials. / J. Mater. Res. - 1992. - 7, n. 7. - P. 1610-1613.

# FLUORO-CONTAINING MONOMERS AND POLYMERS FOR ION-EXCHANGE MEMBRANES

**Pazdersky Yu.A., Gida V.M., Ivanchev S.S.**(1)
Borislav R&D Institute «Synthez», Borislav, Ukraine
(1) St-Petersburg Department of the Boreskov Institute of Catalysis, St-Petersburg, Russia
14, prospect Dobrolubova, St-Petersburg, 197198, Russia, email: ivanchev@SM2270.spb.edu

Ion-exchange polymeric materials with high chemical and thermal stability based on fluoro-containing monomers are widely applied for the production of ion-exchange membranes used in chlorine electrolysis and electrochemical power sources purposed for extreme exploration conditions.

The possibilities and optimum conditions are considered for the synthesis of three types of functionalized fluoro-monomer systems:

1. Perfluoro-4-methyl-3,6-dioxaoctene-7-sulfonylfluoride

$CF_2=CFOCF_2CF(CF_3)OCF_2CF_2SO_2F$

The main raw materials for its production are commercially available tetrafluoroethylene, hexafluoropropylene oxide and sulfuric anhydride.

2. Methylperfluoro-5-oxaheptene-6-ate

$CF_2=CFOCF_2CF_2CF_2COOCH_3$

produced from hexafluoropropylene oxide and perfluorosuccinic acid.

3. α,β,β-trifluorostyrene

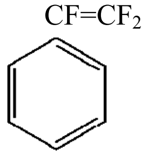

produced from benzene and trifluorochloro-ethylene.

The performed R&D activities provided an improved process for the synthesis, reduction of raw materials consumption levels, approaches to efficient utilization of wastes, enhanced economic performances, reduced monomer costs.

The obtained monomers were used for the preparation of copolymers and film membrane materials therefrom. The properties of the developed membrane systems correspond to the expected level and suggest the prospects for their effective application.

# STRENGTHENING MECHANISM OF REINFORCED CERAMIC COMPOSITES ON A BASE OF BORIDES

**Loboda P.I., Bogomol Yu.I.**
National Technical University of Ukraine "KPI"
Peremogy av., 37, Kyiv, Ukraine, PetrLoboda@yandex.ru

The reinforcement of friable ceramic materials by friable ceramic fibers allows to receive quasi-viscous condition and to increase a value of strength in borides systems $LaB_6$-$Me^{IV}B_2$, $B_4C$-$LaB_6$-$MeB_2$, $B_4C$-SiC up to 1500 MPa, hardness – 50—75 GPa, fracture toughness - $K_{1C} > 25$ MPa $m^{1/2}$. As in the nature there is a lot of systems on a base of refractory compounds, containing noninteracting components, the special interest introduces clarifying of a strengthening mechanism of directed reinforced boride materials, reception, structure and the properties which one for today are learnt fullestly [1—3].

For clearing up of a strengthening mechanism using computer simulation the theoretical analysis of influence of calorific and elastic properties, geometrical sizes of phase components on strength is carried out. The physical model of the composite structure was introduced by a lanthanum hexaboride single-crystal matrix with regularly arranged cylindrical diboride fibers by diameter 0,3—1,5 microns and length 20—500 microns. Coefficient of thermal expansion (CTE) of the matrix accept as $10*10^{-6}$ $K^{-1}$. Was considered, that the CTE of $LaB_6$ does not depend on a crystallographic orientation, as the experimental values for three main directions (001), (011) and (111) differ less than 10 %. The volume ratio of fibers varied from 10 up to 20 vol. %. On the ground of literary data on CTE anisotropy diborides [3], it is supposed, that the fibers of all three diborides are compressed by a matrix in a radial direction. In longitudinal direction the fibers of $ZrB_2$ and $HfB_2$ are compressed, and of $TiB_2$ - are stretched.

By fractography explorations of a surface of the composites fractures is shown, that during destruction the fibers of titanium diboride are predominantly destroyed, and of hafnium diboride are stretched out of matrix. Besides, by microindentation is fixed, that the crack always propagates on a matrix phase of the composite. Therefore, it is supposed, that the maximal strength will be had composites, at which one the binding force of fibers with matrix is maximum. When the strength of a fiber is less than binding force, the fibers are not pull out of matrix but failed. The binding force of fibers with matrix of a crystallized composite can has both physical, and chemical nature. Physical nature is involved with dominating action of elastic stresses. For count of elastic stresses, the frictional force was calculated on expression: $F_{mp} = \pi \times d \times l \times \sigma_{0m} \times \mu$, where $d$ and $l$ - a diameter and length of a fiber, $\sigma_{0m}$ - thermal stress, originating in perpendicular direction to filaments; $\mu$ - the friction coefficient of a fiber material with a surface of matrix (in calculation accepted equal 0,1-0,5). From a condition $F_{mp}$=Ff, determined the greatest possible stresses, which can arise in a fiber at the moment of composite destruction: $\sigma_f$=Ff/S, where S- cross sectional area of a fiber. The strength of composite calculated by the rule of mixes $\sigma_c = \sigma_f \times V_f + \sigma_m \times (1 - V_f)$, where $\sigma_m = \sigma_{mэ} \pm \sigma_{0m}$; $\sigma_{mэ}$ — experimental value of ultimate strength of a single-crystal matrix in three base crystallographic directions - (001), (011) and (111), received in the bend strength test data of $LaB_6$ single crystals; $V_f$ - volume ratio of fibers.

It is fixed, that the magnitude of frictional force rise in accordance to magnification of temperature range, in which there is a refrigeration of composite. The strength of composite is increased proportionally to frictional force and at 1000 °C reached of maximal experimental value – 1200—1600 MPa for filaments of a minimum diameter - 0,3 microns. The stress, experienced of fibers of composite in longitudinal direction, is increased with a diminution of their diameter and magnification of difference of magnitudes of the calorific and elastic characteristics of phase components. The maximal calculated values of fibers strength compose 0,04—0,03 of elastic modulus (E) of applicable diborides, that will be agreed evaluation calculations of theoretical strength of crystals of a different type of a chemical bond (0,03—0,17E) [4]. Both nature of association, and the predicted data of strength are satisfactorily coincided with experimental data at a value of a friction coefficient - 0,38 (fig. 1).

Evaluation calculations is shown, that independently of a fiber diameter, for a composite of identical chemical composition, the specific value of binding strength is constant magnitude and can characterize strength of a chemical bond between atoms of boride phases of a composite which generate close to the coherent boundary, as the interatomic spacing intervals of boric sublattices of lanthanum hexaboride and diborides are close.

In accordance to a diminution of a diameter and magnification of length of filaments the specific value of binding force and, accordingly, the part of load transferred during deformation from matrix to fibers are grown, as results in enhancement of strength of a composite at the invariable volumetric contents of a reinforcing phase.

Thus, the high mechanical strength of ceramical directed reinforced composites $LaB_6$-$MeB_2$ is satisfactorily explained by magnitude of frictional force, which depends on thermal stresses originating in fibers in a transversal and longitudinal direction, and also by strength of interatomic bond on the boundary of division a matrix – fiber, which depend on nature of phase component.

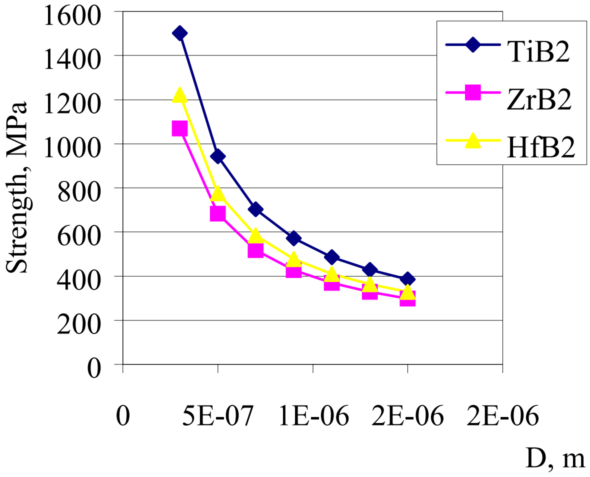

Fig.1 Influence of fiber diameter on strength of composite granting only binding forces.

# PROCESS ACTIVATION ENERGY AND KINETIC PARAMETERS AS QUALITY MEASURE OF DIAMOND-CONTAINING MATERIALS

**Novikov N.V., Bondarenko N.A., Zhukovskiy A.N.(1), Mechnik V.A.**
Institute for Superhard Materials of NASUkraine, Kiyv, Ukraine
2, Avtozavodskaya St. Kiev, 04074, Ukraine
(1)Institute of Mathematics of NASUkraine, Kiyv, Ukraine
3, Tereschenkovskaya St. Kiev, 01601, Ukraine

1. INTRODUCTION. Modern industry has sharply raised the requirements for superhard diamond-containing materials (SDCM), in connection with this the interest in physical phenomena and laws defining various properties of SDCM has grown. SDCM based on tungsten-cobalt alloys are used for manufacturing drilling bits which work under hard loading conditions and vibration. Such SDCM must possess high hardness, strength, high temperature counteraction, wear-resistance and reliability, must have self-sharpening ability and be chemically inert with regard to drilling mud reagents. We have established that in producing 94WC-6,0 Co-based SDCM by hot pressing method over the temperature range of 300-1800 K and the pressure range of 0,5-16 MPa in the first stage of sintering there take place viscous flow of material and nucleation. In parallel with these processes there begin cobalt diffusion into tungsten carbide and surface chemical reactions between the charge components. In the final stage of sintering three-dimensional diffusion with the increase of chemical reaction order predominates as the result of the composite internal structure change and mass transfer mechanism change. According to [1,2] if diffusion activation energy (in this case cobalt diffusion into tungsten carbide) and chemical reaction energy are less than the corresponding energetic barriers, the reaction system atoms easily overcome these barriers for diffusion processes and chemical reactions to occur. It becomes evident that the energies of diffusion activation and chemical reaction together with kinetic parameters characterize the physical-chemical behaviour of the material sintered. For such processes the conclusions of known theories are too general or, at the best, require deep knowledge about the process speeds, kinetic parameters, diffusion activation energy, nucleation, and chemical reaction which as a rule are not at the investigator's disposal when he begins selection of substances, synthesis and sintering of material. The above mentioned class of problems has chemical, physical, material-concerning and, of course, mathematical aspects.

The present work is devoted to the development of new methods of studying the physical-chemical behaviour of superhard diamond-containing materials in various stages of sintering and methods of estimating the final products quality.

2. MATERIALS AND METHODS OF STUDYING. As basic samples of SDCM there have been chosen the boring inserts of 10 mm in diameter and 10 mm in height produced by hot pressing $C_{diamond}$-(94 WC-6,0Co) mixture over the temperature range of 300-1800 K and the pressure range of 0,5-16 MPa (samples No.1). For deeper studying physical-chemical processes and their effect on the behaviour of the material sintered, its structure and properties there have been manufactured test samples (samples No.2) with chromium diboride ($CrB_2$) additives introduced in the charge. Sintering samples No.2 was carried out according to special technological conditions. To the work charge there were added natural diamonds of 800/630 μm granularity with relative concentration of 100%, corresponding to 4,4 carat per 1 $cm^3$. The dependences of relative shrinkage and shrinkage velocity upon temperature, pressure and sintering time were studied. The methods of X-ray phase analysis and metallographic analysis, standard methods of determining microhardness and wear were used for studying the microstructure on the surface of metallographic sections.

3. KINETIC EQUATIONS. For description of physical-chemical processes occurring during sample sintering in different stages three known kinetic equations and the model of shrinkage velocity [3] we've proposed were used. Thereto, there has been carried out the modification of Arrenius's classic ratios with the end of more correct consideration of compacting pressure effect on process activation energies and kinetic parameters.

In the stage of intensive shrinkage the process of sample No.2 shrinkage is characterized by instantaneous nucleation which fact is confirmed by Johanson-Mehl-Avrami-Erofeev-Kolmogorov generalized kinetic equation received on the basis of experimental data:

$$\ln(1-\alpha) = 0{,}000483\, t^{0{,}42} \times \\ \times \exp\left(-\frac{14642{,}16 - 0{,}014052 \cdot P}{RT}\right), \qquad (1)$$

where $E_{G1}$=14642,16 J/mole – activation energy of nucleation process; $V_1$=0,014052 $m^3$/mole – activation volume; $K_{0,1}$=0,000483 $sec^{-1}$ – pre-exponential multiplier (frequency factor); r=0,42 – kinetic parameter characterizing nucleation process; t – current time, sec.; R=8,31 J/(mole.K) – gas constsnt; P and T – current pressure, MPa and temperature, K, respectively.

At the same time there begins the process of cobalt diffusion into tungsten carbide according to the parabolic law:

$$(1-(1-\alpha)^{1/3})^2 / t = 1{,}0005 \cdot 10^{-8} \times \\ \times \exp\left(-\frac{27120{,}65 - 0{,}027589P}{RT}\right) \qquad (2)$$

Here $E_{G1}$=27120,65 J/mole is the activation energy of cobalt diffusion into tungsten carbide. It is approximately two times the activation energy of nucleation. Cobalt diffusion into tungsten carbide in this stage would be expected to become difficult because of insufficient compression of the composite structural components, and nucleation processes take preference over diffusive ones. In sintering standard sample No.1 the fact that $E_{G1}$=28501,66 J/mole testifies of $CrB_2$ use efficiency in diamond-containing charge even in the initial stage.

When analyzing the received equations (3)–(5) for the case when process speed is determined by chemical reaction, one can see that they are not adequate to actual process in the first stage of sintering ($F_{расч} < F_{кр}$):

$$(1-(1-\alpha)^{1/3})\ / t = 5{,}4975 \cdot 10^{-8} \times \\ \times \exp\left(-\frac{7431{,}036 - 0{,}013168P}{RT}\right), \qquad (3)$$

$$(1-(1-\alpha)^{1/2})\ / t = 8{,}2428 \cdot 10^{-8} \times \\ \times \exp\left(-\frac{7368{,}809 - 0{,}013092P}{RT}\right), \qquad (4)$$

$$\alpha / t = 1{,}6465 \cdot 10^{-5} \\ \times \exp\left(-\frac{7185{,}401 - 0{,}012867 \cdot P}{RT}\right), \qquad (5)$$

the role of chemical reactions may therefore be assumed to be not so important.

In the second stage of sintering the nucleation process slows down and moves up into the established regime that is ditectly linked with diffusion within the whole period of sintering and with surface chemical reactions in this stage:

$$\ln(1-\alpha) = 0{,}086558 t^{0{,}396} \times \\ \times \exp\left(-\frac{1635{,}002 - 0{,}00164P}{RT}\right). \qquad (6)$$

Here $E_{G2}$= 1635,002 J/mole that is far less than values of $E_{G1}$ in the first stage of sintering. At the same time the fact that in sintering samples No.1 $E_{G2}$, which equals approximately 5857,3 J/mole, is higher than $E_{G2}$ in sintering samples No.2 suggests that introduction of $CrB_2$ with simultaneous increase of compacting pressure improve SDCM structure and contribute to the formation of strong diamond-to-matrix contact.

As the result of the composite structure change due to compacting pressure increase and $CrB_2$ effect the activation energy of cobalt diffusion into tungsten carbide has decreased from 27120,65 to 1085,585 J/mole:

$$(1-(1-\alpha)^{1/3})^2 / t = 0{,}000194 \times \\ \times \exp\left(-\frac{1085{,}585 - 0{,}00011P}{RT}\right). \qquad (7)$$

Sharp drop in diffusion activation energy facilitates the formation of substitution reaction solid solutions and the increase of strength properties [4]. Introduction of $CrB_2$ with such a combination of charge and sintering conditions may therefore be assumed to form in metallic zone around diamond a new phase more strong than those of WC and Co. In the final stage of sintering together with diffusion processes surface chemical reactions proceed intensively:

$$(1-(1-\alpha)^{1/3} / t = 0{,}00127116\ \exp\left(-\frac{8040{,}669}{RT}\right), \\ (1-(1-\alpha)^{1/3} / t = 0{,}00018971 \times \\ \times \exp\left(-\frac{8375{,}018 - 0{,}000904\,P}{RT}\right), \qquad (8), (9)$$

$$\alpha / t = 0{,}00034633\ \exp\left(-\frac{8012{,}41 - 0{,}000853\,P}{RT}\right) \qquad (10)$$

For each of the equations $F_{расч} > F_{кр}$ but the highest $F_{расч}$ corresponds to chemical reactions in all three directions. In sintering samples No.2 $E_{R2}$ 1,6 times less $E_{R2}$ in sintering samples No.1 which testifies that introduction of $CrB_2$ in standard charge helps the reaction system atoms to overcome energetic barriers for chemical reactions to occur that is extremely important for formation of small-grained poreless structure with required physical-chemical properties of SDCM.

The detailed analysis of kinetic constants and parameters according to the proposed model of shrinkage velocity showed that in the first stage the values of kinetic parameters m and n testify that during sample sintering there take place viscous flow, nucleation and second-order chemical reactions. In the final stage of the process the kinetic parameters m and n indicate three-dimensional diffusion and the increase of chemical reaction order between the charge components in samples containing $CrB_2$ as compared to standard ones.

For each model the correlation coefficient values, actual and critical values of Fisher's criterion with significance level $\alpha=0{,}05$, $F_{фак}>F_{кр}$ which testifies of accuracy and adequacy of modelling physical-chemical processes in SDCM.

4. STRUCTURE AND PROPERTIES. Microstructural analysis revealed that in metallic zone around diamond in sample No.1 there are cracks and transcrystallite chips. In sample No.2 with $CrB_2$ additives sintered according to optimized technological conditions the surface of the metallic zone around diamond does not contain cracks and chips. The characteristic feature of these samples is that pores were not found either in cross- or longitudinal section of metallographic sections. The microstructure is small-grained with regular distribution of WC and Co phases. On the sample working surface after wear-resistance tests there were found 19 mounted diamonds and 1 diamond which had fallen out the matrix. At the same time the structure of samples No.1 is coarse-grained with irregular Co phase distribution, many aggregations are observed. 7 mounted diamonds and 15 diamonds which had fallen out have been found on the working surface. Introduction of $CrB_2$ in standard charge and optimization of sintering technological regimes facilitate Co migration from the composite working part to matrix and tungsten carbide migration from matrix to the working part.

Microstructure images of fracture surface showed that metallic zone around sample No.1 diamonds contained cracks, hollows and many diamond fall-outs from matrix. In contrast to samples No.1 samples No.2 have strong and tight diamond-to-matrix contact, the metallic zone around diamond does not contain either pores or hollows and cracks, diamond falling out has not been found, the matrix fracture takes place on diamond body. The characteristic feature of these samples is that they have wave fracture surface of diamonds and the developed relief structure of matrix that again corroborates high bond strength between diamond and matrix. The matrix microhardness of sample No.2 50 μm away from diamond-to-matrix contact boundary is 25,2 GPa, and 10 μm away from this boundary its value is 23,5 GPa. The matrix microhardness of sample No.1 in those zones were 21,5 and 13,0 GPa respectively. Wear-resistance tests showed that the intensity of samples No.2 wear-out two times less the similar parameter of samples No.1.

5. CONCLUSION. The combination of small-grained poreless structure, high hardness and strength of diamond-to-matrix contact, wear-resistance and reliable work of 94WC-6,0Co-based samples with $CrB_2$ additives sintered according to optimized technological regimes testifies that diffusion processes and chemical reactions play the most important role in improving the structure and properties of SDCM. Diffusion activation and chemical reactions energies along with kinetic parameters are the effectiveness measure of sintering processes and the quality measure of SDCM final products.

1. Smirnov A.A. Molecular-Kinetic Theory of Metals. – M.: Nauka, 1966. – p.488.
2. Murrel J., Kettle S., Tedder J. The Chemical Bond.- M., Mir, 1980. - p.382.
3. Novikov N.V., Mechnik V.A., Zhukovskiy A.N., Bondarenko N.A., Tkach V.N.// Enlarged, NAN Ukraine, - 2003, No.10. – pp. 102-104.
4. Herzriken S.D., Dekhtjar I.Ya. The Diffusion in Metals and Alloys in Solid Phases. – M., Phys.-Math.-Giz., 1968, p.564.

# UNIVERSAL THERMAL PROTECTING COATING

**Galkin A.F.**
Institute of Physical-Technical Problems of the North SB of RAS, Yakutsk, Russia
1, Oktyabrskaya St., Yakutsk, 677891, Russia, afgalkin@iptpn.ysn.ru

To provide safety operation of the objects, which are used in the permafrost area at changing in time above-zero and subzero temperatures of the internal medium and strength properties of rocks, that change at phase transitions, one should use thermal protection. Usually, synthetic materials on the polyether foam basis or light concretes are used for thermal insulation of rocks. The substantial shortcoming of most thermal insulating materials and protective structures made on their basis is a practically constant coefficient of thermal conductivity, which slightly changes with temperature. During operation of the object with the above-zero temperature thermal insulation provides the frozen state of rocks and, consequently, their stability, while at a temperature being lower of that of phase transitions of moisture and natural temperature of rocks thermal insulation prevents their cooling. The investigations have shown [1] that thickness of thermal insulation, that provides the safety regime of operation at the above-zero air temperature, must be the less and, consequently, more effective, the lower temperature of the surrounding rock is. Thus, it is evident that the conventional thermal insulation in the operation conditions considered produces both negative and positive effect. In practice it makes one significantly increase the thermal insulation thickness or use the strengthened types of support that causes the additional economic expenses. In this case the use of the universal thermal protective coatings with the variable thermal resistance is the most expedient. At subzero air temperature in a structure thermal resistance of the coating is minimum that provides the effective cooling of rocks, while at the above-zero temperature of the internal medium thermal resistance of the coating increases the more the higher air temperature is. At the inverse change of temperature from plus to minus thermal resistance of the protective coating decreases and attains its initial calculated value.

To realize the above idea the author suggests the original structure of the elementary cell of the coating. The cell consists of layer elements, connected to each other in a certain way, and elements with the linear expansion coefficient that significantly depends on temperature. At subzero temperature the coating cell presents a sufficiently dense material the number of layers of which is determined by a range of a possible change of the operating temperature. When temperature increases, delamination of the layer material takes place due to the formation of air gaps between layers. The higher the heat flows, affecting the coating, the larger air gaps are. Air gaps become smaller or larger in proportion to the transverse temperature gradient in the coating. Thus, the higher air temperature in the construction, the higher thermal resistance of a cell of such coating. At temperature drop the air gaps become smaller, and separate layers joint to each other causing sharp decrease of thermal resistance that provides effective cooling of rocks. The procedure of calculating the elementary cell of the universal coating is developed. The above procedure makes it possible to determine thermal resistance variation, depending on heat flow density and temperature in the construction, as well as find the optimum structural parameters of a coating cell.

## References.

1. A.F. Galkin. “Thermal regime of underground structures in the North”. Novosibirsk, “Nauka”, 2000. — 303 p.

# OPTIMIZATION OF COMPOSITION AND STRUCTURE OF PLASMA COATINGS FOR INCREASING OF SERVICE LIFE OF STARTING DEVICES

**Voevodin V.P., Safronov A.V.(1), Saigin V.V., Zarubova N.I.**
Public Joint Stock Company "KOMPOZIT",
4, Pionerskaya Strt., Korolev, 141070, Moscow Region, Russia, Kompozit.Mat@g23.relcom.ru
(1)Federal State Unitary Enterprise "Central Research Institute of Machine Building",
4, Pionerskaya Str., Korolev, 141070, Moscow Region, Russia, asteroid@ami.rospac.ru

Impact of high temperature gas flows of propulsion systems leads to considerable thermal erosion of individual structural elements of starting devices (SD) and conditions a necessity of special undertakings to protect SD from destruction. This problem takes on a special urgency on case of presence of condensed phase combustion products in a gas jet.

Plasma spraying application of special erosion resistant heat shielding coatings based on compositions of refractory compounds onto thermally loaded zones [1] can be a feasible solution of the problem of increasing of service life of SD elements.

In this work, results are given of theoretical and experimental investigations on estimation of non-stationary heat shielding coatings, optimization of their composition and structure.

Working conditions of the most thermally loaded elements of SD are characterized by the following numbers:

Jet pressure, $P_0$ ………………2.0 MPa.

Gas temperature, $T_0$ …………3600 K

Impact duration, $\tau$ …………..0.3 s

Maximum heat flux to the "cold" wall ($T_w$=300 K), $q_{\max}$ ................250 MW/m$^2$.

Total thermal load during impact time, $Q$ ……………………………$2.9{\cdot}10^4$ kJ/m$^2$.

Estimation of non-stationary temperature regimes of operation was performed in one-dimensional approximation basing on numeric solution of the problem of heat flux impact onto a multi-layer plate with thickness $h$.

Possibility of one-dimensional approach is conditioned by the fact that characteristic size of destroying elements of SD is considerably larger than depth of heat penetration during jet impact.

It was assumed that on reaching of a certain constant temperature $T_p$ at the surface, a material starts being taken off at a rate of $v$ absorbing at this energy $H_p$.

In a coordinate frame with origin continuously moving with the takeoff boundary, thermal conductivity equation appears as:

$$\rho c\frac{\partial T}{\partial t}=\rho c v\frac{\partial T}{\partial z}+\frac{\partial}{\partial z}\left(\lambda\frac{\partial T}{\partial z}\right),$$

where $T\ (z,t),\lambda,\rho,c$ are temperature, thermal conductivity coefficient, density and specific heat of materials respectively.

In case of takeoff, boundary conditions at the heated surface are:

$$T(0,t)=T_p=const\,,$$

and the heat-balance equation appears as:

$$-\lambda\frac{\partial T(0,t)}{\partial t}=(\alpha/c_p)\cdot(I_0-I_w)-\rho v H_p\,,$$

where $I_0, I_w, (\alpha/c_p)$ are gas enthalpy temperatures $T_0$ and $T_w=T(0,t)$, heat exchange coefficient respectively.

In absence of takeoff $(T_w \langle T_p)$, boundary conditions appear as:

$$-\lambda\frac{\partial T(0,t)}{\partial z}=(\alpha/c_p)\cdot(I_0-I_w).$$

It was assumed that continuity of heat flux and temperature at the boundaries of layers takes place, and the opposite surface of a multi-layer plate is thermally insulated, i.e. $\frac{\partial T}{\partial z}=0$ at $z=h-\delta$, where $\delta$ is the thickness of the material taken off.

Calculations of heating of an element of SD (steel X18H10T) without a heat shielding coating performed according to this model had demonstrated that already after 0.02 s, the surface temperature reached the melting temperature of steel, and the takeoff rate reached ~$15{\cdot}10^{-3}$m/s. At the same time, the total thermal erosion during jet impact time reached a value of ~$1.4{\cdot}10^{-3}$m fairly correlating with full scale testing results.

A series of parametric calculations had been carried out of heat penetration through heat shielding coating with fixed values of density and heat capacity and thermal conductivity value varying in a range of (1.0÷15) W/m·K. Dependence was determined of thickness and maximum temperature of a coating on its thermal conductivity at a given surface temperature, which could possess two values – the melting point and 300° below it.

Analysis of the obtained data had demonstrated that starting from the condition of limitary thickness of plasma sprayed layer (~500 μm), thermal conductivity of heat shielding coating must be not higher than (5÷8.5) W/m·K, and destruction temperature must be not lower than (3000÷3100) K. In conditions of impact of high temperature oxidizing medium, plasma coatings based on refractory oxides of zirconium, hafnium as well as their metal-ceramic compositions with tungsten as metallic constituent can fit the listed requirements.

Three-layered heat shielding packages were considered with metallic sublayer from Nichrome, intermediate cermet layers from mechanical mixtures of $ZrO_2$-W, $HfO_2$-W and external ceramic layers based on $ZrO_2$, $HfO_2$, as well as coatings without intermediate layers [2]. Dependencies were investigated of the heat shielding coating linear takeoff value and of the substrate temperature regime ($T_{max}$) on thickness of layers and package structure.

It was determined that due to high level of thermal loads the considered protective compositions worked in conditions close to extreme, i.e. there was takeoff of external ceramic layers. Decrement of initial thickness of ceramics decreased takeoff, however the temperature under the coating increased thus reaching melting point values. Introduction of intermediate metal-ceramic layers improves temperature regime of the substrate but leads to growing takeoff of ceramic layers.

Analysis of calculation results had shown that at total thickness of heat shielding package ~$(300÷400)\cdot 10^{-6}$m, optimizing composition and thickness of its structural constituents, it is possible to assure efficient protection of thermally loaded elements of SD in conditions of multiple (4÷5) starts.

Model bench testing and application of heat shielding packages in full-scale articles had confirmed the obtained characteristics.

References.

1. Сайгин В.В., Воеводин В.П., Зарубова Н.И. «Плазменные металлокерамические покрытия на основе композиции $HfO_2$-W», Сб. тр. 6-ой Междунар. конференции «Пленки и покрытия 2001» под ред. Клубникина В.С., с. 496-498.
2. Акопян Ю.А., Васильев В.Е., Сайгин В.В., Сафронов А.В., Степанов Г.Н. «Исследование ресурса работы плазменных покрытий на основе диоксидов циркония и гафния в условиях воздействия на них высокотемпературного газового потока», Космонавтика и ракетостроение, ЦНИИМашиностроения, №3, 1995, с. 83-86.

# THERMODYNAMICS OF LIQUID ALLOYS OF Ni—Al—Cr SYSTEM

**Vovkotrub N. E., Sudavtsova V. S., Kotova N. V.**
Shevchenko Kiev National University, Kiyv, Ukraine
60 Vladimirskaya Str., Kiev, 01033, Ukraine, vsudavtsova@univ.kiev.ua

Alloys on a nickel basis are widely used in technics as heat- and corrosionstability materials, which are frequently reinforced by refractory metals. In this connection it is expedient to investigate thermodynamic properties of multicomponent alloys of Ni—Al—Cr system, which till now are little investigated.

Thermochemical properties of the binary boundary systems Ni(Al)—Cr and of ternary Ni—Al—Cr system were investigated by calorimetric method at 1870-1960 K.

Thermochemical properties of liquid alloys of Ni-Cr system are investigated by different variants of calorimetry: earlier at 1960 K [1], in [2] - at 1830 K, [3] - at 1729 K and in the presented work at 2200 K. The hard Cr entered in researches [1—3] at 1728 - 1960 K into a calorimetric bath with liquid nickel. In calculations used the melting enthalpies of refractory metal chromium to receive the mixing enthalpies of alloys from liquid nickel and undercooled liquid chromium. As nickel-chromic alloys are characterized by weak interpartial interaction, we have improved a technique of researches - chromium samples were melted in the special device and liquid chromium poured out in the nickel at 2200 K. This has increased accuracy of measurements. We are compared the data received by us on mixing enthalpies of liquid alloys of Ni—Cr system with available in the literature determined by a method of calorimetry for liquid [1—3] and hard alloys at T=1514-1571 K [4]. It is established, that the data [1, 2, 4] will be coordinated among themselves though concern to different state of aggregation. Mixing enthalpies determined by us at 2200 K are negative in all an concentration interval, and minimal $\Delta H$ =-6,0 kJ/mol and fitted on $x_{Cr}$=0,45. According to [3] minimum of the mixing enthalpie of Ni-Cr alloys is -3 kJ/mol at $x_{Cr}$=0,6. These data indicate that the interpartial interactions in nickel - chromic alloys are slight and change with temperature insignificantly.

Thermochemical properties of liquid alloys of Ni-Al system are determined by a method of calorimetry at 1923 K in an interval of concentration $0,6<x_{Ni}<1$ in [5]. On the data [5] the first partial mixing enthalpie of Al in Ni amounts -147,5 kJ/mol. These data were well be coordinated with established by us at 1870 K in concentration interval $0,5<x_{Al}<1$ [7].

Thermochemical properties of Al—Cr system have been investigated by us earlier a method of calorimetry at 1870 K in [7] and at 1723 K in [3]. Values of partial and integral enthalpies of mixing are resulted in the table. It is shown, that they will be coordinated among themselves and characterized by medium interpartial interaction. Comparison of the first partial enthalpies of mixing of 3d-metals in liquid aluminium has shown, that the minimal interpartial interaction is typical for liquid alloys of Al—Cr system.

Own and literary data on the mixing enthalpies of liquid alloys of binary Ni (Cr)—Al systems have been critically analysed and determined the most authentic. In the table presented the most exact ΔH for Ni (Cr)—Al alloys.

The mixing enthalpies for liquid alloys of quasibinary (NiAl)—Cr systems are determined within the concentration interval of $0<x_{Cr}<0,3$ and resulted in the table. They are positive, that is caused by strong connection of nickel with aluminium in intermetallic NiAl.

Also in the table are resulted experimental ΔH for 4 sections of ternary Ni—Al—Cr system and quasibinary sections, values ΔH which are counted on process of alloy formation from pure components.

It is established, that introduction of chromium in Ni-Al alloys results in decrease of exothermal effects, which are observed in liquid alloys of Ni-Al systems. The similar behaviour is observed for other systems by type of Ni—Al-refractory metal.

Using experimentally established $\Delta H$ for binary systems and five sections, have constructed a surface of mixing enthalpie of liquid alloys of Ni—Cr—Al systems. It is established, that the minimum on this surface corresponds to area of the concentration to equiatomic alloy of nickel with aluminium. It is no wonder, as interaction between components in liquid binary alloys of boundary systems Cr—Ni (Al) is small.

Having extrapolated the mixing enthalpies of Al-Cr system received in an interval 0 <$x_{Cr}$ <0,3, on all concentration interval, it was possible to calculate the mixing enthalpies of ternary Ni-Al-Cr system on the equations by Bonnier. Comparison of the experimental and calculated data has shown, that they correlate among themselves. It has allowed to draw conclusions on an opportunity of correct calculation of thermochemical properties of ternary Ni—Al—M systems from the data for binary boundary systems. Clearly, that the mixing enthalpies of the investigated ternary system smoothly decrease from alloys of system Ni—Al to Cr. And mixing enthalpies are negative in all concentration interval, that it is possible to explain determining influence of properties of Ni-Al system on power of ternary Ni—Al—Cr system.

## Literature

1. Batalin G.I., Kurach V.P., Sudavtsova V.S. Mixing Enthalpies of liquid alooys Ni-Cr system // Ukr. Khim. Zhurn.-1983.-V.49, №5 - P. 547—548.
2. Chistyakov L.S., Stomakhin A.Ya., Grigorovich K.V. Investigation of enthalpies of formation of Fe-Si and Ni-Cr solutions with higt-temperature calorimetry / Metals. – 1993. - № 4. –P. 27—37.
3. Saltykov P., Witusievicz V.T., Arpshofen I., Seifert H.J., Aldinger F. Enthalpy of Mixing of Liquid Al-Cr and CCr-Ni Alloys // J. Mater. sci. Technol.. – 2002. – Vol. 18. – No.2. –P 167—170.
4. Kubashevski O., Olkkok S.B. Metallurgical Thermochemistry (trans. from eng.) // M,:Metallurgy.-1982, 391 p.
5. Geld P.V., Esin Yu.O., Petrushevski M.S., Sandakov V.M. The enthalpie of formation of alloys of Al-Ni system //In book. Proc. V All-Union. conf. on calorimetry.- M.:MGU.-1971.- P. 42—44.
6. Dyubanov V.G., Stomakhin A.Ya., Philippov A.Ph. The enthalpies of formation of dilute solutions on basis of iron, cobalt and nickel // Izv.VUZov. Black Metallurgy.-1975.-№3.- P. 5—7.
7. Sudavtsova V.S., Sharkina N.O., Shuvalov A.V. The thermodynamic properties of liquid binary Al-Cr(Ni) alloys // Rasplavi.-1990.-№1.-P. 97—99.
8. Saltykov P., Witusievicz V.T., Arpshofen I., Fabrichnaya O., Seifert H., Aldinger F. Thermodynamics of liquid and undercooled liquid Al-Cr-Ni alloys // Scand. J. Metallurgy. – 2001. – 30. – P. 297—301.

| | 0 | 0,1 | 0,2 | 0,3 | 0,4 | 0,5 | 0,6 | 0,7 | 0,8 | 0,9 |
|---|---|---|---|---|---|---|---|---|---|---|
| Ni—Al system, T=1870 K | | | | | | | | | | |
| -ΔH | 0 | 18 | 32 | 42 | 50 | 54 | 54 | 44 | 30 | 16 |
| Al—Cr system, T=1870 K | | | | | | | | | | |
| -ΔH | 0 | 2,9 | 5 | 6,6 | 7,6 | 7,4 | 6,7 | 5,5 | 4,0 | 2,0 |
| $-\Delta\overline{H}_{Cr}$ | 32 | 26 | 19 | 15 | — | — | — | — | — | — |
| (NiAl)-Cr quasibinary system, T=1942 K | | | | | | | | | | |
| -ΔH | 0 | 3,4 | 6,9 | 10,2 | — | — | — | — | — | — |
| $-\Delta\overline{H}_{Cr}$ | 30 | 24 | 19 | 15 | — | — | — | — | — | — |

# THE MODELING OF THERMODYNAMIC PROPERTIES OF BINARY AND Al-IVaM-TM TERNARY SYSTEMS

**Sudavtsova V.S., Bieloborodova E.A., Zinevich T.N, Кotova N.V., Usenko N.I.**
Shevchenko Kiev National University, Kiyv, Ukraine
60, Vladimirskaya Str. Kiev, 03033, Ukraine vsudavtsova@univ.kiev.ua

Scientific interest in alloys of silicon, germanium and other p-metals originates from their valuable physicochemical properties, resulting in numerous applications. For example, silicon- and gernamium based alloys are the well-known semiconducting materials. Tin based alloys are irreplacable soldering materials. P-metals are widely used for the purposes of alloys modification and deoxidization. In order to explain the properties of such alloys and to be able to make some predictions of physicochemical properties of multicomponent systems we need the thermodynamic data on corresponding liquid alloys.

Thermodynamic properties of ternary alloys of (Al-IVaMe-3dTM) systems and of boundary binary systems were determined for the first time by high temperature calorimetry and by various kinds of EMF techniques. Experimental temperatures lied between 1500 and 1900 K. The alloys were investigated in limited concentration range because of high melting points of 3d transition metals. In order to obtain the thermodynamic information through the whole concentration range the data on systems phase diagrams accepted as authentic ones were used and also the data on formation enthalpies of binary intermetallic solid compounds were used.

Calculated parameters were corrected taking into account experimentally established values obtained in limited concentration range. The resulting values are listed in table.

One can see that the strongest interparticle interaction between different kinds of atoms is observed for alloys with Sc, Co and Ni. This fact can be explained in the frameworks of donor-acceptor model. Similar $\Delta H$ behavior is observed for binary alloys of Al with 4d and 5d transition metals. As to the alloys of Al with IVa metals one can see that in silicon and germanium containing alloys there is only slight interparticle interaction due to the small contribution of both the electrochemical factor and the size difference one. On the contrary, in Al-Sn alloys interaction between the same kinds of atoms prevails because of large atomic size difference of Al and Sn.

For binary Si(Ge)-TM systems interparticle interaction is stronger than for Al-TM binary systems, that is confirmed by Fig. 1 on which dependence of $\Delta\overline{H}^{\infty}_{TM}$ values on atomic number is given. Fig. 1 also demonstrates that the wakest interaction between different atoms is observed for Sn-TM systems probably due to the great size difference contribution in these systems. Obtained in limited concentration range thermochemical data for ternary Al-Si-TM alloys are the significant exothermic values. Exothermic alloying effects have been established for ternary Al-IVaMe-TM systems. This depends on strong interaction between transition metals and p-metals. So, addition of 3d TM to Al-Si system which characterized by small interaction leads to great exothermic effects.

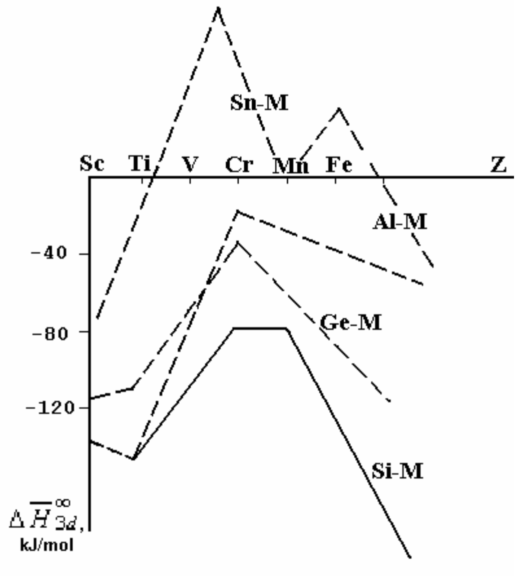

Fig. 1.

To estimate the thermochemical parameters in the whole concentration range we have used Bonnier-Caboz and Toop equations. Direct calorimetric data were used to verify the truth of estimated $\Delta H$ values. It have been found that Bonnier-Caboz equation can be used for thermodynamic description of Al-Si-3dTM alloys with satisfying accuracy. And Toop equation is better for Al-Si-4d(5d)TM systems.

Experimental and calculated $\Delta H$ values for ternary systems Al-Si-VbMe are given in Fig. 2. Interparticle interaction decreases from V to Nb and Ta. Minimum values of mixing enthalpies fall on boundary systems Si-TM.

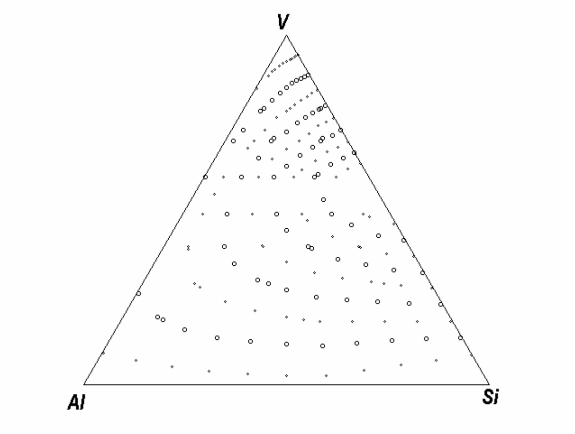

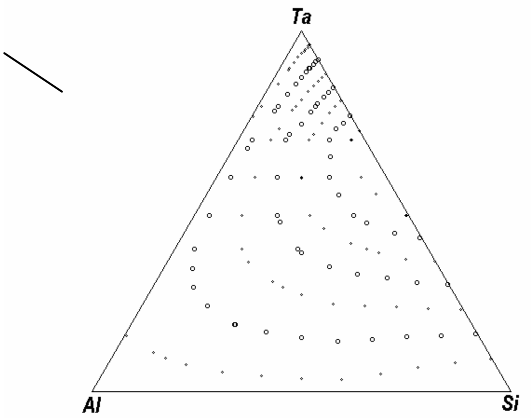

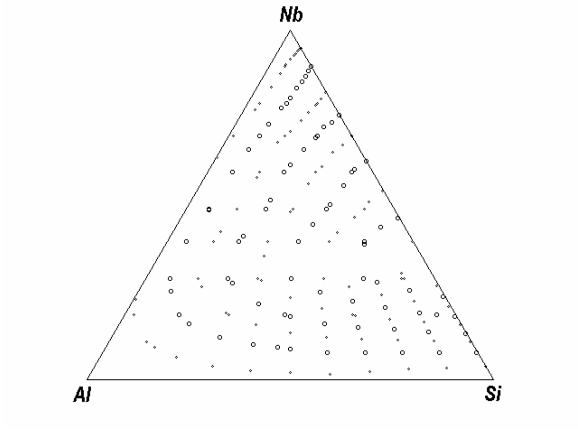

Fig. 2

Analysing obtained thermochemical data for Al-IVaMe-TM systems we can conclude that Al-Si(Ge)-TM alloys formation is accompanied by exothermic effects, and on contrary Al-Sn-TM alloys formation leads to endothermic effects.

| M | $-\Delta H$ , kJ/mol | | | | | | | | | | |
|---|---|---|---|---|---|---|---|---|---|---|---|
| $x_M$ | Sc | Ti | V | Cr | Mn | Fe | Co | Ni | Si | Ge | Sn |
| 0,1 | 15,6 | 11,2 | 5,0 | 3,5 | 6,0 | 8,5 | 22,0 | 16,0 | 0,9 | 1,0 | 1,9 |
| 0,2 | 23,7 | 20,1 | 8,0 | 5,2 | 12,0 | 15,0 | 29,6 | 30,0 | 1,7 | 1,8 | 3,1 |
| 0,3 | 41,4 | 27,0 | 10,4 | 6,6 | 15,3 | 18,9 | 35,2 | 44,0 | 2,7 | 2,5 | 3,8 |
| 0,4 | 42,8 | 29,8 | 11,6 | 7,6 | 16,1 | 20,6 | 36,0 | 54,0 | 3,6 | 3,1 | 4,1 |
| 0,5 | 43,6 | 29,8 | 11,2 | 7,4 | 16,8 | 20,5 | 29,6 | 54,0 | 3,5 | 3,5 | 4,11 |
| 0,6 | 43,1 | 25,8 | 10,0 | 6,7 | 15,4 | 19,2 | 22,8 | 50,0 | 3,2 | 3,5 | 3,8 |
| 0,7 | 33,8 | 20,1 | 9,4 | 5,5 | 13,0 | 15,9 | 12,4 | 42,0 | 2,8 | 3,3 | 3,2 |
| 0,8 | 23,1 | 15,5 | 6,4 | 4,0 | 10,0 | 11,4 | | 32,0 | 2,2 | 2,6 | 2,3 |
| 0,9 | 11,9 | 8,9 | 4,0 | 2,0 | 6,0 | 6,2 | | 18,0 | 1,2 | 1,8 | 1,2 |

# CALCULATIONS FOR STRESS-STRAIN STATE OF SPACECRAFT SOLAR CELL-PANELS UNDER THERMAL LOADING CONDITIONS

**Gavrylov R.V., Pokhyl Yu.A., Koval K.V.**
SDTB at Physical Technical Institute of Low Temperature of NASU, Kharkiv, Ukraine
Lenin Ave. 47, Kharkiv, 61103, Ukraine mail@cryocosmos.com

In present- day spacecraft engineering, tasks of structural design- optimization for solar cell panels (SCP), with purpose to dramatically minimize thermo- mechanical stresses imposed hereon are of actual importance. Analytical models elaborated per various computational schemes of different levels of trustworthiness appear to be key tools to meet these requirements successively.

This paper represents two unified techniques for determination of stress – deformation status (SDS) of Space vehicles' SC- panels subjected to thermo-mechanical loading: a single-dimensional model and a quasi- two- dimensional model of SC- panels glued – joints.

The major difference between both models is feasibility for the latter one to operate either of Poisson's constants. In presentation of both models, the SC- panels are structures compiled of five functional layers jointed together by aid of glue.

Since mathematical radicals of characteristic equation resulting from differential equation, are not always feasible to be solved analytically, reasonable efforts were undertaken to investigate the entire range of rigidity- characteristics of materials. It has been stated that in our case, radicals are really true. This advantage has enabled us to present the solution in analytical form.

Determination and analysis of model SCP-structure' SDS- parameter, as well as comparison of outcomes of these studies vs. outcomes from finite element- method calculations, have been carried out. Initial data for these researches were obtained in experimental provisions.

Calculations have shown that SCP- structure, as a unit, undergoes its maximum loading on shaded segment of orbit. Maximum number of normal stresses is observed in the middle of the SC- panel, whereas maximum of tangential stresses is characteristic at periphery of SC- panels.
The maximum tangential stresses occur in glue-joint inter- layers, adjacent to polyimide layers. However, such the tangential stresses are much less than ultimate strength of glue- joints against shifting force. Structural decomposition is here a debatable question; however, if glue- joints will ever fail, this may only occur due to alternation of shift- forces endlessly repeated under multi- cycle loading.

Results of testing the experimental Solar cell-panels by: thermo- cyclic loading, (rated as high as a virtual equivalent to one year of Space- vehicle's presence on geo- stationary orbit), and thermal shock, have shown that Solar cell- panels' structure did not ruin at all. Moreover, Solar cell- panels do not display any significant degradation of their properties, either.

These facts, as well as outcomes of mathematical modeling efforts, is another evidence of decent operational lifetime resource of SCP structures.

Parametric researches for influence of geometrical and rigidity characteristics of SCP- inherent materials, on their SDS- factor, have been implemented.

It was found that maximum influence on shift strength of SCP is rendered by geometrical and rigidity- characteristics of "sandwiches" construed of a polyimide layer and two glued inter- layers adjacent hereto.

These data make up ways to practical guidelines to selection of optimum SCP- structure, from viewpoint of its strength parameter. Thus, in order to minimize a level of shift stresses in glued inter-layers SCP- structures, it is recommended to employ carbon- plastic skins and polyimide films of minimum tolerable thickness and minimum allowed rigidity. At the same time, further preference should be focused to increase of shift – modulus, as well as ultimate strength of glued inter- layers vs. shift.

# THE FORMATION MODEL AND PROPERTIES OF ELECTRIC-SPARK CERAMIC COATINGS FOR VACUUM FRICTION UNITS

**Podchernyaeva I.A., Panasyuk A.D., Frolov G.A., Kostenko A.D., Yurechko D.V., Bloschanevich A.M.**
Frantsevich Institute for Problems of Materials Sciences of NASU,
03680, Kiev-142, 3 Krzuzhanovsky str., Ukraine, E-mail: lavrenko@ipms.kiev.ua

The development of composite wear-resistant coatings for friction units in the extreme exploatation conditions including cosmic apparatus is connected with the fabrication of coatings without lubrication. The peculiarity of their manufacturing is the necessity to introduce a solid lubricant into the material being deposited. Traditionally such lubricants are the molybdenum chalcogenides. Another way may be realized for the coatings being formed in the oxygen-containing environment (the different kinds of gas-thermal spraying, electric-spark and laser alloying, etc.). It consists of such choice of structural components of the material deposited which could be foresee the formation, during the coating deposition, of oxide phases and new compounds fulfilling the role of a solid lubricant. In the range of coating deposition methods pointed above the electric-spark alloying (ESA) is differed, together with the low energy capacity and simplicity of technology, by the complex of physical-chemical processes on electrodes surfaces and in an interelectrode gap. This allows to consider the ESA as a model method for the understanding of formation mechanism of coatings under high-temperature conditions of plasma thermal-mechanical effect. The goal of this study is to develop the model of formation of wear-resistant ceramic ESA-coatings on high-performance alloys using as alloying materials the advanced AlN-Ti(Zr)$B_2$, AlN-TiN composite ceramics based on aluminum nitride (ТБНА, ЦБСАН, ТАН, ТАНХ) and $ZrB_2$-$LaB_6$-$ZrSi_2$ (ЦЛАБ-2) ceramics based on zirconium diboride (ЦЛАБ-2) and β-sialon. These materials may be refered to the self-lubrication ones, because of a possibility of formation of $TiO_2$-$Al_2O_3$, $Al_2O_3$-$SiO_2$, $Fe_2O_3$-$TiO_2$, Fe(Ni)$_2O_3$-$Al_2O_3$, $Al_2O_3$-$B_2O_3$, $Al_2O_3$-$La_2O_3$, solid solutions and corresponding compounds of β-tialite ($Al_2TiO_5$), mullite ($Al_2SiO_5$), iron (nickel) aluminate etc. (fulfilling the role of solid lubricants) on a coating surface and in its volume due to high-temperature interaction between the components and their oxidation during a coating deposition.

The “Elitron-21” installation was used for the ESA. The alloying electrodes were manufactured by powder metallurgy. For laser treatment (LT) of a powder layer of the corresponding composition, the “Kvant-15” installation was used. The coating composition and structure were studied by XRD, EPMA and metallographic methods. The tribological tests under dry friction were carried out in the air and vacuum ($1.33 \cdot 10^{-2}$ Pa) using the IPMS NANU installations in the “shaft-inset” and butt-end friction regimes, correspondingly.

The model of formation of an wear-resistant ceramic coating at the ESA of Fe-C-, Ti- and Ni-Cr-alloys with the composite ceramics having the components with different wetting was proposed the base of the study of kinetic of ESA with the materials of AlN-Ti(Zr)$B_2$ systems as well as coating composition, structure and element distribution through a cross-section and on a surface [1-3] of the coating. The model consists of the formation of surface quasi-globules based on the component not wetted by the substrate metallic alloy. The quasi-globules have a gradient structure due to a substrate metal masstransfer into the coating. The globule outer layer not containing a metallic component or reinforced by substrate metallic insertions ensures high physical-mechanical properties peculiar to ceramics. The inner layer adjoing to the base contains a substrate metal ensuring adhesion and elastic properties. The interglobule space is a substrate metallic alloy modified mainly with the electroerosion products of an allioying electrode which are wetted by a substrate material. The intensity of formation of oxide solid solutions pointed out during the ESA-coatings tribooxidation increases with the growth of sliding velocity ensuring in low level of both friction *f* (0,15÷0,17) and wear intensity I (8÷13 μ/кm). As for tribological behavior, the ESA-coatings obtained at ESA with the traditional electrode materials of “refractory compound-metallic binder” are considerably less effective compared with the ceramic ones: the *f* and I magnitudes exceed the same by $50\div75$ % for the coatings developed.

The positive influence of oxide phases on an ESA-coating surface are also preserved under vacuum tests (Table). In all cases the coating wear intensity is lower by one-two order compared with an uncoated steel. The compositions of materials deposited favour the formation of β-tialite and $Al_2O_3$-$TiO_2$ solid solutions due to high-temperature oxidation during the coating deposition. This, probably, defines their low wear intensity and friction in vacuum.

So, for the construction of wear-resistant coatings (deposited in an oxygen-containing environment) for vacuum friction units without a lubricant, it is necessary to choose the material structural components which must foresee the possibility of formation in the coating material during its deposition of oxide solid solutions and oxide phases (β-tialite, mullites and etc.) playing a role of solid lubricant. In the range of alloying materials studied the materials of Al-Ti-B-N system in the most degree satisfy to this demand.

References
1. Подчерняева И.А., Панасюк А.Д., Лавренко В.А. и др. Структура и свойства композиционных электроискровых, лазерных и магнетронных покрытий из материала $AlN$-$TiB_2$ / Порошковая металлургия, 2001. — № 9/10. — С. 69—77.
2. Тепленко М.А., Подчерняева И.А., Панасюк А.Д. и др. Структура и износостойкость покрытий на титановом сплаве и сталях, получаемых при ЭИЛ материалом $AlN$-$ZrB_2$ / Порошковая металлургия, 2002. — № 3/4. — С. 48—57.
3. Подчерняева И.А., Панасюк А.Д., Тепленко М.А. и др. Триботехнические свойства тонкодисперсных покрытий при ЭИЛ материалами системы Ti-Al-N / Порошковая металлургия, 2002. — № 11/12. — С. 49—60.

Table

Tribotecnical parameters of ESA-coatings on steel 45 in vacuum

| Material of coating (method of deposition) | P=1.5 MPa; V=0.012 m/s; КТ – steel 45 | | | |
|---|---|---|---|---|
| | Δm specimen, g | I, $g/(cm^2\cdot km)$ | $f$ | Δm contr-body, g |
| ТБНА (LT) | 0 | 0 | 0.26 | -0.002 |
| Sialon +STB | $3.8\cdot10^{-4}$ | $1.15\cdot10^{-3}$ | 0.28 | — |
| ТБНА (ESA) | $5.0\cdot10^{-4}$<br>— | $1.50\cdot10^{-3}$<br>— | 0.28<br>0.26* | 0.720<br>— |
| ЦЛАБ-2 (LT) | $5.0\cdot10^{-4}$ | $1.50\cdot10^{-3}$ | 0.31 | -0.100 |
| ТБНА (ESA) | $2.2\cdot10^{-3}$ | $6.6\cdot10^{-3}$ | 0.34 | 0 |
| ТАНХ (ESA) | $2.9\cdot10^{-3}$ | $8.78\cdot10^{-4}$ | 0.34 | 0.620 |
| ТАН (ESA) | $1.0\cdot10^{-4}$ | $3.03\cdot10^{-4}$ | 0.38 | 0.75 |
| without coating | steel 45/ steel 45 (P=2.5 MPa; V=0.02 m/s) | | | |
| | $5.0\cdot10^{-4}$ | $1.34\cdot10^{-4}$ | 0.42 | — |

*) V=0.088 m/s

# PHYSICAL MEANING OF THE CONCENTRATION COEFFICIENT FOR POLYMERIC COMPOSITES FILLED WITH SHORT FIBRES

**Burya A. I., Kozlov G.V., Rula I. V.**
Dnepropetrovsk State Agrarian University
Voroshilov str. 25, 49027 Dniepropetrovsk, Ukraine, e-mail: university_burya@pisem.net

Mechanical properties of polymeric composites with good adhesion at polymer-filler interface boundary are described by the models considering a possibility of transfer of the impressed voltage over this boundary by means of shift mechanism. In the mentioned case the deformation stress $\sigma_p$ of the filled polymer will be the function of polymer matrix's shearing strength $\tau_м$ and stability of polymer-filler interface relation $\sigma_a$. The correlation of these parameters makes Ladner-Woodhams equation [1]:

$$\sigma_p = \left(\sigma_a + 0{,}83\tau_м\right) + \sigma_a K\left(1 - \varphi_н\right), \qquad (1)$$

where $K$ stands for the coefficient of stress concentration, $\varphi_н$ – volume content of filler.

Although the equation (1) is obtained for the filler's spherical particles, it was revealed on the basis of structural models for composites with short fibers, and as the authors [1] marked, it can be applied to such composites. The main disadvantage of this equation is the difficulty of independent experimental determination of $K$ value. That is why the aim of this work is to define the physical meaning of the coefficient of stress concentration in Ladner-Woodhams equation.

Aromatic polyamide phenilon was used as a polymeric binder, and carbon fibre (CF) with the diameter of 7 ÷ 9 mcm and the length of 3 mm – as the filler. CF content made 15 mass %. The composite was prepared by a dry method including mixing the components within the rotating electromagnetic field. In order to do this, powder-like polymer, CF and unequiaxial ferromagnetic particles 40 mm long were loaded into the reactor. Then, the reactor was put into the boring of electromagnetic apparatus' generator. Under the effect of rotating electromagnetic field the ferromagnetic particles start rotating and collide; as a result, CF are evenly (chaotically) distributed within the polymer matrix. As a result of collision the particles wear out and the wear products come to the composition. For eliminating ferromagnetic particles after mixing the methods of magnetic and mechanical separation were used.

The specimens for investigating mechanical properties were prepared by means of hot pressing at the temperature of 606 K and the pressure of 55 MPa. The tests for compression were executed at FP-100 machine at the temperature of 293 K.

Defining specific heat capacity was held at IT-C-400.

The value of the coefficient of stress concentration $K$ may be calculated from the equation (1) if the rest of the included parameters are estimated as follows. The interface layer's strength $\sigma_a$ may be evaluated by the following equation [2]:

$$\sigma_a = 1{,}4 \times 10^5 \left( \frac{\varphi_{мф}}{2N_A \cdot l_0 \cdot S \cdot C_\infty} \right)^{5/6}, \text{ Па}, \qquad (2)$$

where $\varphi_{мф}$ is relative share of interface areas, $N_A$ – Avogadro number, $l_0$ – the length of skeleton connection of the main chain, $S$ – area of macromolecule's cross-section, $C_\infty$ – characteristic relation which is the index of static flexibility of polymeric chain [3]. For phenilon $S$=17,6Å$^2$ [4], $l_0$= 1,25Å [5], and for macromolecules in interface areas the value $C_\infty$=9 [6]. Relative share of interface areas is determined by the equation [7]:

$$\varphi_{мф} = 1 - \frac{\Delta C_p^к}{\Delta C_p^п}, \qquad (3)$$

where $\Delta C_p^к$ and $\Delta C_p^п$ are the values of heat capacity jump at constant pressure by the vitrification temperature for the composite and matrix polymer, correspondently.

The tensile strength of polymer matrix $\sigma_p^м$ is connected to $\tau_м$ value by a simple correlation [8]:

$$\tau_м = \frac{\sigma_p^м}{\sqrt{3}}, \qquad (4)$$

where $\sigma_p^м$ value is defined from the equation (2), but with the exchange of $\varphi_{мф}$ for the relative share of local order areas (clasters) in the volume polymer matrix, and at $C_\infty=3$ [6]. The equation (1) drives at the fact that the increase of both $\sigma_p^{м}$ and $\sigma_a$ leads to the growth of macroscopic strength $\sigma_p$ of the composites.

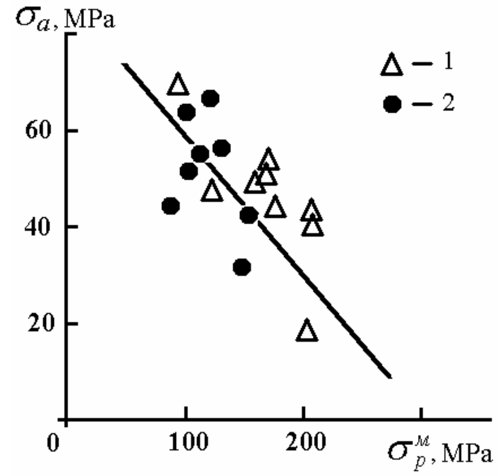

Fig. 1. Correlation between the stabilities of interface areas $\sigma_a$ and volume polymer matrix $\sigma_p^{м}$ for carbon plastics based on phenilon obtained with the application of magnetic (1) and mechanical (2) separation

However, as it follows from the data of fig. 1, the change of polymer matrix strength and interface layers are slope opposite, i.e. $\sigma_a$ value almost linearly decreases with the increase of $\sigma_p^{м}$. Such a dependence is conditioned by the presence of back coupling in the structure of carbon plastics based on phenilon; this structure is a synergetic system and the back coupling is analytically expressed as follows [6]:

$$\varphi_{кл} = 0{,}74 - \varphi_{мф}\,. \tag{5}$$

Consequently, $\sigma_p$ must have some optimal value at definite $\sigma_a$ and $\sigma_p^{м}$. As the experimental data showed, the maximum value of $\sigma_p$ equal to ~406MPa is achieved at high $\sigma_a$ (~70 MPa) and relatively low $\sigma_p^{м}$ (~120 MPa).

The calculation of $K$ according to the equation (1) showed its significant variation: $K$=0,96÷5,49. There arises a question about the reasons of such variation due to the fact that $\varphi_н$ = const, the fibres' geometry is unchanged and the absence of their aggregation is supposed. It was noted that $K$ value grows with the increase of $\sigma_p^{м}$ and the decrease of $\sigma_a$. That is why we can presuppose that $K$ is the function of $\sigma_p^{м}/\sigma_a$ relation [1].

Factually, the dependence of $K$ on $\sigma_p^{м}/\sigma_a$ given at fig. 2 allows approximating the coefficient of stress concentration in such a way:

$$K \approx \sigma_p^{м}\big/\sigma_a\,. \tag{6}$$

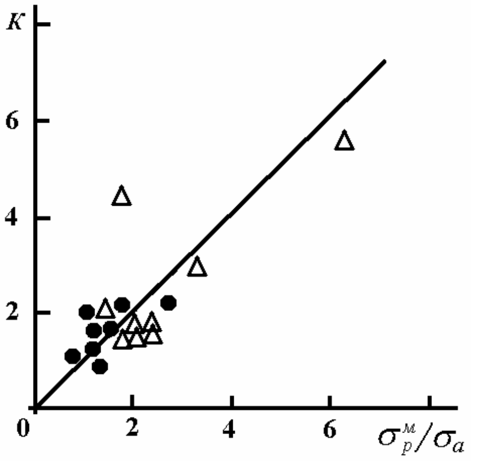

Fig. 2. Correlation between the coefficient of stress concentration $K$ and $\sigma_p^{м}/\sigma_a$ relation for carbon plastics based on phenilon. Marking is the same as at fig. 1

It follows from equation (1) that at constant $\sigma_a$, $\tau_н$ and $\varphi_н$ the growth of $K$ leads to the increase of the composites' macroscopic strength. That is why a question arises which structural parameter of carbon plastics controls $K$ value. As it is known [9], the governing parameter for carbon plastics' structure is the factor of fibres' orientation $\eta$. At fig. 3 the dependence of $K$ on the reciprocal value $\eta$ is cited, and it shows the decrease of $K$ with the increase of $\eta$. This presumes $\sigma_p$ decrease with $\eta$ increase.

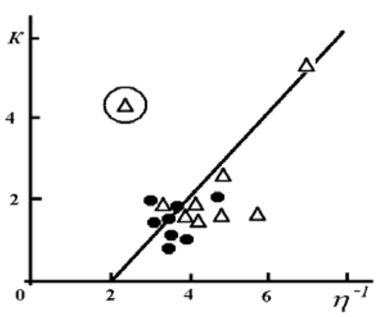

Fig. 3. Dependence of the coefficient of stress concentration $K$ on the reverse value of fibres' orientation factor $\eta$ for carbon plastics based on

phenilon. The result for t= 60 sec is circled (see text). Marking is the same as at fig. 1

However, drawing the plot $\sigma_p(\eta)$ of secondary tendency did not show the assumption of $\sigma_p^{м}$ decrease compensation by the increase of interface layer's strength $\sigma_a$ (see fig.1).

The combination of equations (1) and (6) allows to get the following approximation of Ladner-Woodhams equation for carbon plastics:

$$\sigma_p = \sigma_a + 1{,}48\sigma_p^{м}\left(1 - \varphi_н\right), \qquad (7)$$

Where stress $\sigma_p$ is given for the case of testing for tensility.

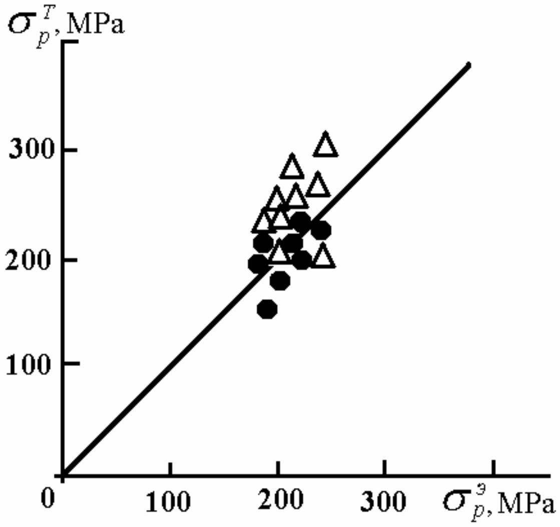

Fig. 4. Comparison of experimental $\sigma_p^э$ values of macroscopic strength for carbon plastics based on phenilon and those calculated from the equation (b) $\sigma_p^T$. Marking is the same as at fig. 1

Fig. 4 cites the comparison of experimental $\sigma_p^э$ and calculated from the equation (7) $\sigma_p^T$ values of macroscopic strength for carbon plastics based on phenilon. As it can be seen, there is obtained quite good correspondence between the experiment and the theory. This presupposes that *K* value cannot be regarded as the result of stress concentration by the filler's particles. For carbon plastics *K* value, like in the work [1], is represented by the relation of volume polymer matrix stabilities and interface layers. We should note that breaking this rule resulting in significant growth of *K* (fig.3) and $\sigma_p$ was obtained at the components' mixing duration of 60 sec where the negative back coupling is observed, and consequently the correlation is broken (5).

Thus, the results of this work showed the applicability of Ladner-Woodhams equation for the description of the strength of polymeric composites filled with short fibres. As it was presupposed, the coefficient of stress concentration is the relation of the stabilities of volume polymer matrix and interface layers. The value of this relation is defined by the governing parameter of the structure, which is the factor of carbon fibres' orientation.

Bibliography

1. Leidner Y., Woodhams R.T. The strength of polymeric composites containing spherical fillers. Y. Appl. Polymer Sci., 1974, v. 18, №8, p. 1639-1654.
2. Новиков В.У., Козлов Г.В., Липатов Ю.С. Исследование межфазного слоя в наполненных полимерах с использованием концепции фракталов. Пласт. массы, 2003, №10, с. 4-8.
3. Будтов В.П. Физическая химия растворов полимеров, СПб.: Химия, 1992, 384 с.
4. Aharoni S.M. Correlations between chain parameters and failure characteristics of polymers below their glass transition temperature. Macromolecules, 1985, v. 18, №12, p. 2624-2630.
5. Aharoni S.M. On entanglements of flexible and rodlike polymers. Macromolecules, 1983, v. 16, №9, p. 1922-1728.
6. Буря А.И., Козлов Г.В. Синергетика структуры полимерных композитов, формируемой во вращающемся электромагнитном поле: Материалы научно-практической конференции, Р-н/Д: Изд-во Рост. ун-та, 21-28 февраля 2004, с. 56-59.
7. Липатов Ю.С. Физическая химия наполненных полимеров. М.: Химия, 1997, 304 с.
8. Новиков В.У., Козлов Г.В., Бурьян О.Ю. Фрактальный подход к межфазному слою в наполненных полимерах. Механика композитных материалов, 2000, т. 36, №1, с. 3-32.
9. Буря А.И., Козлов Г.В. Описание формирования структуры углепластиков в рамках синергетики твердого тела. Матер. 24 ежегодной междунар. научно-практич. конфер. «Композиционные материалы в промышленности», 31 мая-4 июня 2004, Ялта – Киев: УИН «Наука. Техника. Технология», с. 246-248.

# COMPLEX DIFFUSIVE – CONDENSATION PROTECIVE COATINGS FOR BLADES OF TURBINES OF HEAT – STRUSSED TURBINE ENGINES (GTE)

**Kusnetsov V.P.**, **Lesnicov V.P.**
LTD “TURBOMET”, 19, Mira Str., Ekaterinburg, 620002, Russia, E-mail: walrus@r66.ru

For modern air gas turbine engines (GTE) 4—5 generations the rotor blades of the turbine are produced from heat resisting nickel alloys in a single – crystal, should have a temperature - resistant coatings on an outside surface of pen, ensuring a guard from a high – temperature gas stream, and also protective coating in shank bores and punched foramens.

Now it is possible to receive temperature - resistant protective coatings with given resource at heats and demanded properties, only by sequential alternation of different technologies: gas circulation method (GCC), ionic – plasma technology (IPT) and electron – beam precipitation from vapor (EBP).

The phase and structural stability of a protective coating at heats will determine its reliability and longevity at maintenance. With this purpose were developed and complex diffusive – condensation protective coatings having graded – index allocation of alloying elements on depth are constructed: shaping on a surface of an alloy of blades of a diffusive barrier layer, consequent deposition of multilayer condensate layers composed of doped layers on the basis NiCoCrAlY and an enveloping layer on the basis of a doped β-phase NiAl or ceramics $ZrO_2$: $Y_2O_3$.

In a fig. 1 are showed a microstructure and allocation of elements in a complex protective coatings (GCC CrAl+NiCrAlTaReY+AlNiCrY) on a single – crystal alloy HA36VI. The external zone of such coating consist of a β- phase NiAl, keeping 20 mass. % Al. The internal layer of coating consists of a mixture doped β, γ′, γ - phases, and on border with an alloy is doped β-phase NiAl, keeping 18 mass. % Al. The given β- phase is formed at deposition of a GCC CrAl and is natural diffusion barrier, ensures a good adhesion layers among themselves and alloy, has low parameters of diffusion of high – melting elements as from an alloy in coating, so from condensation coating in an alloy.

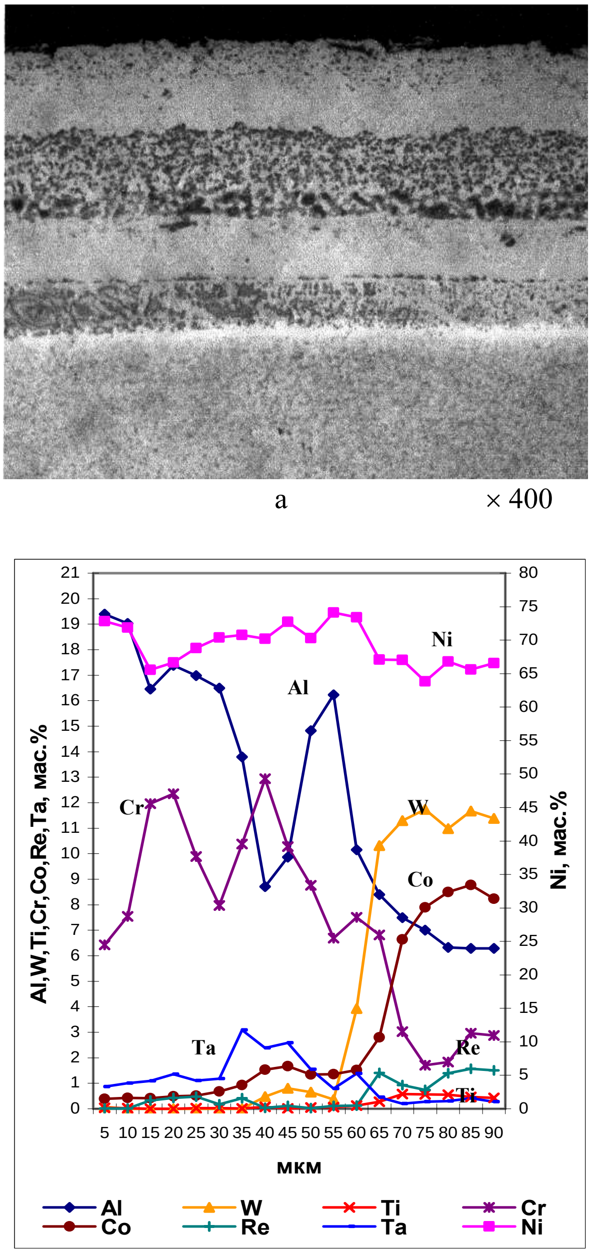

a × 400

b

Fig. 1 Microstructure (a) and allocation of elements (b) in complex coating GCC CrAl + NiCrAlTaReY+ AlNiCrY on an alloy HA36VI.

The realization of high-temperature tests at T=l 100 ... 1250 °C on air has shown very high fire resistance of the given protective coating. The lapse rate of concentration on Al on borders of GCC CrAl -NiCrAlTaReY - AlCrNiY stabilizes structural and phase states of coating and ensures its high capacity. The given complex coating is intended for a guard from oxidation of single-crystal cooled blades of GTE of a new generation with temperature of gas on a going into the turbine 1820 K.

For working turbine blades of a GTE working on heavy solar oil, oil casing-head gas or in marine and coastal areas, the corrosion-resistant complex protective coatings (fig. 2) are developed. Only usage of protective coatings composed of separate functionally interdependent layers, ensures a reliable guard of an outside surface of rotor blades THP with major resource of activity from corrosive attack of an aggressive gas stream.

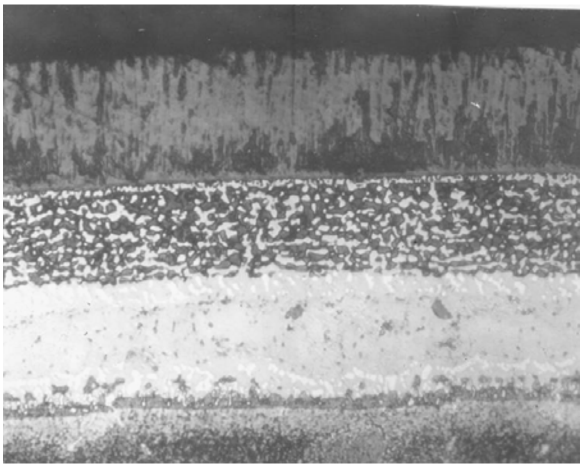

Fig. 2 Microstructure of complex corrosion coating of a GCC CoAl+CoNiCrAlY+$ZrO_2$: $Y_2O_3$ on an alloy ЧС-88УВИ × 500

At deposition of a GCC CoAl on a surface of an alloy the coating composed of phases $\beta$ (Ni, Co) Al+$\gamma$ (Co, Ni) will be derived. In aggressive gas media at heats the $\beta$-phase (Ni, Co) Al undergoes disintegration on depletion on aluminum $\beta$-NiAl and $\gamma$ (Co, Ni, Cr) solid solution, passing natural for want of Co transformation $\beta$-NiAl $\rightarrow \gamma'$ - $Ni_3Al$. In a number of phases $\beta$- (Ni, Co) Al, $\gamma$ (Co, Ni, Cr), $\gamma'$-$Ni_3Al$ the least corrosion resistance has $\gamma'$- phase. Availability on a external surface of complex coating of a ceramic layer $ZrO_2$: $Y_2O_3$ considerably augments an incubation interval of a beginning of corrosion destruction of a metal condensation layer.

The test data of capacity of protective coatings on gas dynamic bench are adduced in a fig. 3.

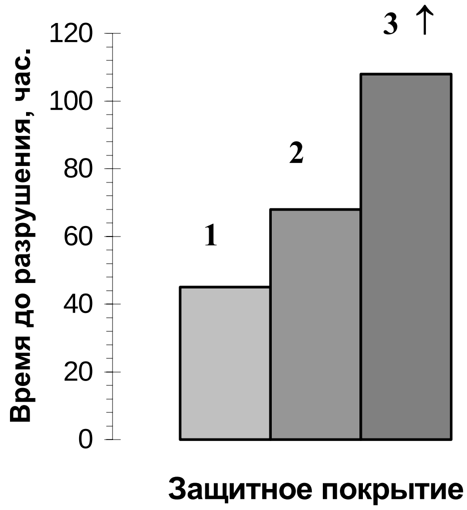

1 - AFC-1 (NiCoCrAlY)
2 - GCC CoAl + AFC-1
3 - GCC CoAl + AFC-1+ $ZrO_2$: $Y_2O_3$
(without destruction)

Fig. 3. Durability of complex protective coatings in products of combustion of solar oil with injection of ocean water.

Metal sub layer at availability having chopped off ceramics ZrO2: Y2O3 should ensure fire resistance of a blade in extreme conditions on all between repairs resource and should not reduce structural strengths of a blade.

Is showed, that the complex coating on blades THP for each engine should be constructed individually, that is a perspective problem for the designers and the investigations of metals. Specially it is actual for single-crystal blades with penetrate system of cooling: with a composite system of internal bore and developed system of thin foramens.

# ELECTROEROSION DISPERSION OF HARD ALLOY WC-8 wt.%Co IN WATER

**Fadeev V.S., Verhoturov A.D., Ershova T.B., Dvornik M.I.**
Institute of Materials, far eastern branch of RAS
Tihookeanskaya 153, Khabarovsk, Russia, E-mail: imdvo@imdvo.fe.ru

## Introduction

Modern industry cannot do without hard alloys. Reduction of raw materials stocks and its high cost generate a need to search a way of recycling of hard alloy and its scrap generated during production process and after its use.

The most difficult operation during recycling of hard alloy is disintegration. One of the methods of powder production from compact scrap is the method of electrospark dispersion which was offered for the first time in 1943 by Lazarenko, B. R. and Lazarenko, N. I [1]. The method has a number of advantages: production of powder in one operation, little cost of equipment and low equipment deterioration, harmlessness and appropriate technology, possibility of dispersion of any conducting materials, reception of the mainly spherical particles by size form several nm to 100 mkm [2].

Aim of this work is a study of granulometrical, morphological, phase and chemical compositions of particles produced by spark erosion of hard alloy WC-8wt.%Co in water.

## Routine or experiment

We designed installation to carry out experiments (fig. 1). It consists of vessel with sieve inside. All space is filled by dielectric liquid. Along the edges two electrodes are located at 40 mm length. Voltage impulse applied to the electrodes. Electric sparks appear between pieces of material and induce erosion of material. To maintenance spark gaps vessel must be shake by shaker. Eroded material is removed by liquid and next it is settled in vessel. As dielectric liquid is choused distilled water, because it is economical and does not pollute received powder.

Dispersion carried out in following mode: frequency 1000Hz, on-off time ratio 8, middle current I=10 A, middle voltage U=30 V. Hard alloy WC-8wt.%Co is choused as reduced material and electrode.

Gravimetric analysis carried out on analytical balance VLR-200, Phase analysis carried out on installation Dron-3. Carbon content in receipt powder was measured using analyzer AN 7520. Derivatographic analysis carried out on derivatoraph Q-1000 °C E. Paulik, J. Paulik, L. Erdey system.

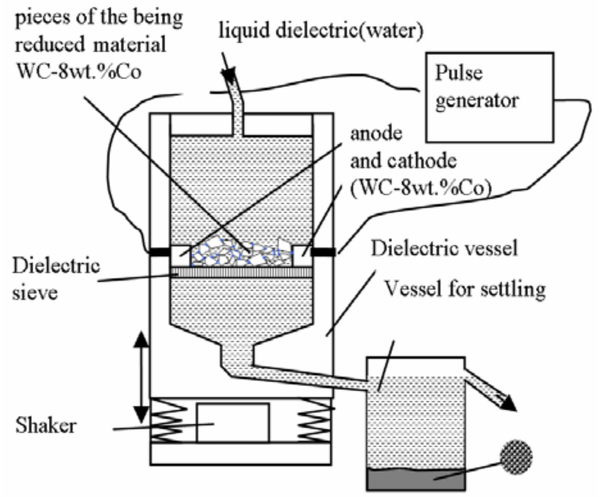

Fig. 1. Installation for electrospark dispersion.

The microscopic studies of the powder carried out on electronic microscope LEO-1420. Studies of granulometric composition of powder carried out on lazer analyzer of the sizes of the particles Analysette 22 Comfort.

## Results and discussion

Gravimetric analysis of samples has shown that erosion during several hours of dispersion did not change. Total erosion of anode, cathode and being reduced pieces of material is 10 g/hour. A power input on reception one kg powder is 30 kWh.

Powder dried under room temperature, contains 4,6 % adsorbed water, which could be removed by vacuum cleaning at temperature 250 - 300 °C. Phase composition of receipt powder: α - W and β - W, β - Co and $Co_x W_y C_z$. The chemical analysis has shown that 2,7 % carbon is kept in powder.

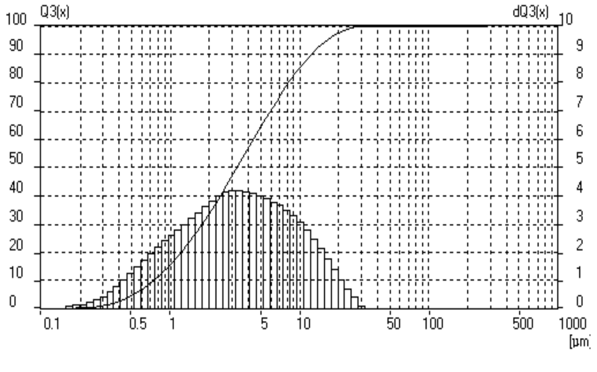

Fig 2. Granulometric composition of powder.

Granulometric composition of powder presented on fig 2. Powder has a wide particle size distribution range from nanometers to separate particles with size 20-30 mkm. Arithmetic mean size of particles is 5 mkm. Primary powder consists of spherical particles, some of which is coreless (Fig.3). Besides agglomeration of superdispersed particles are visible.

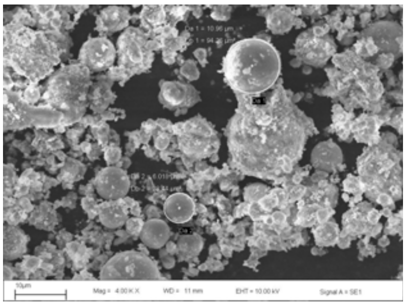

Fig. 3 Particles of receipt powder.

In spark discharge condition ($T \approx 10^4$ °K, $P \leq 280$ MPa) [2] this processes consecutively occur with hard alloy: $\alpha$- WC phase is heated higher melting point of tungsten (3410°C) and mixed with cobalt; drops of melted and boiling solid solution W+C mixed with cobalt eject from lune and being decarbonized under oxygen and hydrogen action; fast cooling in water with speed $10^6 - 10^9$ °K/sec [2,3] resulted in crystallizing with phase formation $\alpha$ , $\beta$ – W, $\beta$ - Co и $Co_x W_y C_z$.

Absence of big quantity of oxides could be explained by fast cooling of particles. Little quantity of oxides probably is holding on surfaces of spherical particles (fig 4.) and among superdispersed particles(fig.3). The most of spherical particles crystallized from melted metal (liquid phase). As a result of crystallizing of boiled material is a superdispersed particles(vapor phase).

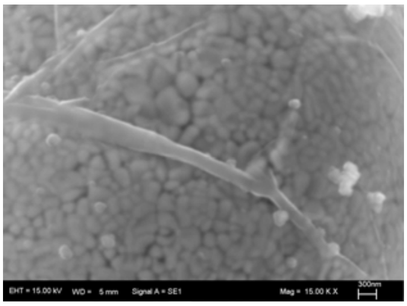

Fig 4. Surface of spherical particle.

## Conclusions:

Drowned results show that spark erosion of hard alloy is an economical method of production of spherical particles, primary consisting of tungsten with mid-size 5 mkm. Fast cooling prevents its oxidation. In future receipt powder could be use in production of different powder materials on the base of tungsten and cobalt including hard alloys.

This work has been made with support of grant RFFR № 04-03-97001.

**Список использованной литературы.**

1. Lazarenko, B. R. and Lazarenko, N. I., author's certificate 70000 USSR, Method of способ получения порошков и устройство для его осуществления. // Открытия. Изобретения. - 1964.-№22.- p.120

2. A.E.Berkowitz, M.F.Hansen, F.T.Parker, K.S.Vecchio, F.E.Spada, E.J.Lavernia, R.Rodriguez. Amorphous soft magnetic particles produced by spark erosion // Journal of Magnetism and Magnetic Materials – 2003 - № 1-6, c 254-255

3. Полубесов Ю. С., Дмитриев Г. Г., Фоминский Л. П. Расчет скорости охлаждения частиц сферической формы // Металлические порошковые материалы, их обработка и свойства.— М. : Металлургия, 1985.— С.7—11.

# PRINCIPLE OF CREATION OF SANDWICHED COMPOSITE MATERIALS WITH GRADIENT DISTRIBUTION OF PROPERTIES ON HARD ALLOY SURFACES

**Fadeev V.S., Verkhoturov A.D., Podchernyaeva I.A.(1), Pryadko L.F.(1)**
Institute of materials, far eastern branch of Russian academy of sciences
Tihookeanskaya 153, Khabarovsk, Russia, E-mail: imdvo@imdvo.fe.ru
(1)Frantsevich Institute for Problems of Materials Science of NASU
3 Krzhyzhanovsky Str., Kyiv, 03142, Ukraine

The constant expansion of the circle instrumental material rising by capacity to work pertains to firm trend of the industrial development. It is connected with increase the assortment of difficult-to-cut material, necessity of saving of tungsten-contained material, intensification of the cutting process and increasing of quality of handled materials. In this regard formation of protective coat with gradient properties distribution on surface of hard alloy that enables significantly raise its capacity for work is the main interest. However, systematical information about creation of sandwiched material with gradient properties distribution for extreme conditions of cutting has not been found not in literature[1,2].

Aim of the work is creation and research of sandwiched material for tool purpose on the hard alloy base with gradient properties distribution for extreme conditions of cutting.

Research has been made on VK and TK hard alloys. Formation of sandwiched material has been made by injection in solid phase composition of ductile metal, or in combination with its by two technology: 1) plasma spraying on hard alloys of alternate layers of titanium and titanium nitride 2) dispersion hardening of hard alloys by processing of hard alloy tools between preliminary and final sintering in titanium ion plasma. Thermodiffusion satiation and vapor deposition coatings have been researched for comparison.

Analysis of experimental data and mechanism of wear and destruction of different hard alloys with coatings under non-stationary cutting conditions and wide-ranging of temperature-power load allows to make conclusion that injection in coating composition of plastic matrix metal or formation in coating disperse particles with smooth variation of composition and properties in depth of layer is necessary formation of coatings with high relaxation properties of microvolume in order to inhibiting crack growth. It could be achieved by various methods.

According to stated above composition material with coating consisting of alternating titanium and titanium nitride layers has been made by plasma spraying. General scheme of the material is shown in fig. 1. Varying of soft layers thickness can change gradient of relaxation properties in depth of coating. Preparatory titanium coating allows achieving high adhesiveness of coating with substrate. Calculation of the thickness of the layers of laminated coatings has been found out from fracture mechanics equations. It shows coatication of multilayer coatings consisting of titanium and titanium nitride must be in the range: 0,05…0,1 mkm dimensions of titanium interlayer is 0,5…1,0 of thickness of titanium nitride layers. Relationship of thicknesses of hard and soft layers has been choused alternating in range from 1:1 to 1:5 (for substrate with TiC coatings). Coating with alternating layers of titanium and titanium nitride has $H_\mu$ 17500MPa, high microductility of volumes and enough adhesiveness with substrate in comparison with TiN coatings. Coating with alternating layers allows reducing a gradient of microductile and thermalphysic properties from surface to substrate [3]. Increase of a number of layers is resulted in increase of a number of stages of micro-cracks rising until critical size. A number of loading cycles until initialization of main crack is increased.

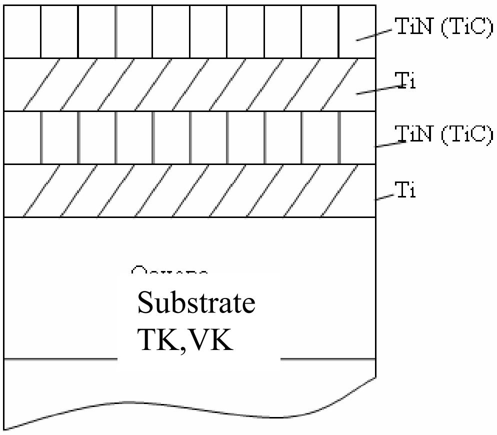

Fig 1. General scheme of sandwiched material consisting of alternating layers of refractory compounds and titanium.

The most effective variant of improving of crack-resistance and heat resistance of compositional material on metal matrix due to formation of extensive diffusion layer between coating and substrate with varying composition with improved yield point and microplastic properties is the dispersion hardening which has been offered by us. In conformity with WC-Co-alloys the most favorable reinforcing phase is carbides and intermetallics of fourth and six groups of periodic table. Since the most widespread substrate of hard alloy else tungsten carbide is titanium carbide a titanium has been offered as alloying constituent. Hard alloy with improved capacity for work has been made by processing of hard alloy substrate in ion plasma after preliminary sintering over liquid cobalt as binding material [4]. The result of liquid phase (solution Co (W, Ti, C)) migration of solution in volume of material and recrystallization through liquid phase of elements inside solution and diffusive interaction of titanium with tungsten carbide under high temperatures is redistribution of elements in surface layers with formation of extensive doped layer saturated by again formed compounds with alternated concentration from surface to volume.

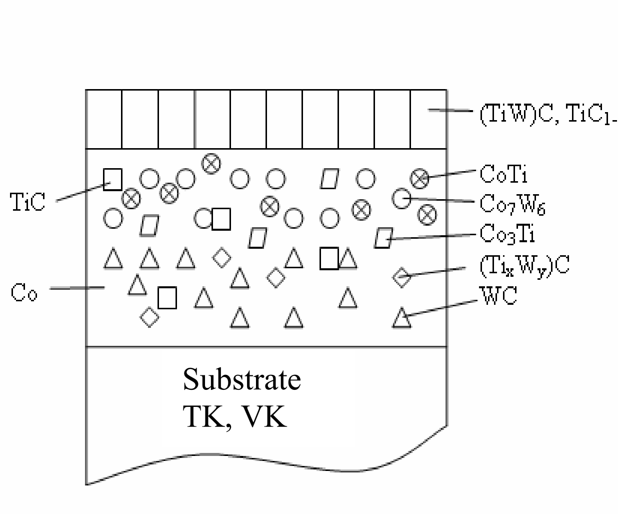

Fig.2. Formation of disperse impurities in surface layers by diffusion of titanium.

General scheme of the material is shown on fig. 2. Comparative test of tool resistant shows that wear resistant improved 1,52 times more as standard (VK6+TiN). At the same time cost of the tool is increased by 4-9%. Reliability level is improved by 34%. Wear resistant of sandwiched material in comparison with TTK6 is lowed by 20-25% with equal reliability level, but cost of sandwiched material below 3 times.

## Литература

1. Верещака А.С.. Работоспособность режущего инструмента с износостойкими покрытиями М.:Машиностроение,1993. 336с.

2. Кабалдин Ю.Г. Структура, прочность и износостойкость композиционных материалов. Владивосток: Дальнаука, 1996. 183с.

3. А.с. №1508602 4 С 23 С 14/06. Износостойкое покрытие.

Фадеев В.С., Паладин Н.М., Щитов Г.А., Котляков В.М.

4. А.с. №1730784 В22F 7/02, В23В 27/14. Способ получения твердосплавного м атериала с износостойким покрытием. Верхотуров А.Д., Фадеев В.С., Паладин Н.М., Чигрин Ю.Л. Котлярова Т.В.

# MODELLING OF NUCLEATION, DIFFUSION AND CHEMICAL REACTIONS IN PRODUCING SUPERHARD MATERIALS BY POWDER METALLURGY METHODS

**Novikov N.V., Bondarenko N.A., Zhukovskiy A.N.(1), Mechnik V.A.**
Institute for Superhard Materials of NASU
Avtozavodskaya St. 2, Kiev, 04074,Ukraine
(1)Institute of Mathematics of NAUkraine
Tereschenkovskaya St. 3, Kiev, 01601, Ukraine

1. INTRODUCTION. In connection with intensive use of superhard diamond-containing materials (SDCM) based on tungsten-cobalt alloys for oil and gas industry and mineral resource industry investigating the kinetics of physical-chemical processes which occur during producing SDCM is of great interest. Such SDCM are produced by powder metallurgy methods from mixture of natural diamond or especially strong and thermal-resistant synthetic diamond particles with less coarse particles of tungsten carbide and cobalt. High-melting temperature compounds of transition metals activating sintering process and ensuring the required properties of a composite are sometimes introduced into these mixtures. A number of complex processes such as plastic or viscous flow, cobalt diffusion into tungsten carbide, self-diffusion, chemical reactions between charge components, change of mass transfer mechanisms, formation of new phases, passive motion of diamonds and their interaction with matrix proceeds in such compounds during sintering under pressure. Under some conditions these processes can lead to unique structures and properties, new phenomena and effects. The experimental investigation of these processes is an expensive and labour-intensive matter requiring complex equipment. It is usually carried out for test samples in order to determine the main direction in improving SDCM structure and properties. The investigation is therefore complemented by mathematical modelling of sintering processes to find the dominant factors of sintering and to determine physical-chemical process quantitative parameters which are, in the long run, responsible for SDCM quality.

The present work proposes a method of description of physical-chemical processes taking place in producing SDCM by hot pressing in different stages of sintering. The method is based on kinetic analysis of nucleation, diffusion and chemical reactions according to a known model and the model we’ve proposed.

2. MATERIALS AND METHODS OF STUDYING. SDCM samples 10 mm in diameter and 10 mm in height were prepared by hot pressing in a graphite mold. As starting material there was used the mixture of powders 94WC-6,0Co (mas. %) with grain sizes from 3 to 5 μm (matrix). For the working part of samples to charge there were added natural diamonds of 800/630 μm granularity with relative concentration of 100% (which corresponds to 4,4 carats per 1 cm$^3$). The powders were being mixed in alcohol medium and stirred in a rotating container for 72 hours. The outfit of a cell for sintering was prepared in conformity with the requirements for producing boring inserts based on 94WC-6,0Co hard alloy. Sintering was carried out in a special unit. The samples were sintered over the temperature range of 300-1800 K and the pressure range of 1,5-16 MPa according to standard technological conditions after preliminary cold pressing of the mixture under P=0,5 MPa. The accuracy of temperature and pressure measurements were 1 degree and 100 Pa respectively. When studying the dependences of relative shrinkage and shrinkage velocity upon temperature, pressure and time over the whole sintering process it was assumed that the results were not affected by carbon-containing environment. For calculating shrinkage velocity on the base of experimental data of relative shrinkage cubic splines were used.

3. KINETIC MODELS. For solving a problem there were used three known models: Johanson-Mehl-Avrami-Erofeev-Kolmagorov generalized equation for describing nucleation processes:

$$\ln(1-\alpha) = \mathrm{K}_{\alpha} t^{r}, \tag{1}$$

The parabolic law for describing diffusion:

$$(1-(1-\alpha)^{1/3})^2 = \mathrm{AK}_{\alpha} t \,. \tag{2}$$

The equation when process velocity is determined by a chemical reaction:

$$1-(1-\alpha)^n = \mathrm{K}_\alpha t, \qquad (3)$$

Here $\alpha = (l-l_0)/l$ – standardized shrinkage or a relative parameter of compaction; $l$ and $l_0$ – linear dimensions at initial and current moments of time $t$, respecively, sec; $\mathrm{K}_\alpha$ - generalized constant of velocity, sec$^{-1}$; $r$ and $n$ – exponents which have the sense of kinetic parameters.

The mathematical description of SDCM sintering processes with using kinetic equations (1) – (3) is based on principles [2] of the work.

Within kinetic equation (1) in the stage of intensive shrinking the process of sintering SDCM samples is characterized by two-dimensional growth of nuclei:

$$\ln(1-\alpha) = 0.0005643 \cdot t^{1.06} \times$$
$$\times \exp\left(-\frac{7592.3 - 0.004996P}{RT}\right), \qquad (4)$$

where $E_{G1}$ = 7592,3 J/mole – activation energy of nucleation process; $V_1$ = 0,004996 m$^3$/mole – activation volume; $K_{0,1}$ = 0,0005643 sec$^{-1}$ – pre-exponential multiplier (frequency factor); $r$ = 1,06 – kinetic parameter characterizing nucleation process; $t$ – current time, sec; P – current compacting pressure, MPa; R = 8,31 J/(mole K) – gas constant; T – current temperature, K.

At the same time there begins the process of cobalt diffusion into tungsten carbide according to the parabolic law:

$$(1-(1-\alpha)^{1/3})^2 / t = 2{,}285 \cdot 10^{-5} \times$$
$$\times \exp(-\frac{28501{,}66 - 0{,}01104 \cdot P}{RT}) \qquad (5)$$

Here $E_{D1}$=28501,66 J/mole is the activation energy of cobalt diffusion into tungsten carbide. It is far high than the activation energy of nucleation. In this step nucleation processes are assumed to be stimulated, in the first place, by sintering conditions (high enough temperatures and pressure) and diffusion processes.

When analyzing a role of chemical reactions in the first stage it can be seen that the received mathematical models (6) – (8) for their description are not adequate to actual process ($F_{расч} < F_{кр}$):

$$(1-(1-\alpha)^{1/3} / t = 0{,}0002628 \times$$
$$\times \exp(-\frac{8121{,}538 - 0{,}004893P}{RT}), \qquad (6)$$

$$(1-(1-\alpha)^{1/2} / t = 0{,}0003872 \times$$
$$\times \exp(-\frac{7997{,}69 - 0{,}004804P}{RT}), \qquad (7)$$

$$\alpha / t = 0.0007348 \cdot \exp\left(-\frac{7636 - 0.00455P}{RT}\right), \qquad (8)$$

the role of chemical reactions may therefore be assumed to be not so important.

In the second stage of sintering the nucleation process slows down and moves up into the established regime and its increase is directly linked with diffusion over the whole period of sintering and with surface chemical reactions in the final stage of sintering:

$$-\ell n(1-\alpha) = 0{,}5268 t^{0{,}08} \times$$
$$\times \exp(-\frac{2600{,}76 - 8{,}55 \cdot 10^{-5} \cdot P}{RT}). \qquad (9)$$

Here $E_{G2}$ = 2600,76 J/mole is far less than the values of $E_{G1}$ in the first stage of sintering. As the result of the composite internal structure change the diffusion activation energy essentially changes, from 28502,67 to 2113 J/mole, which leads to diffusion proceeding actively. Diffusion processes in this step may be assumed to play an important role in formation of SDCM structure; cobalt diffusion into tungsten carbide predominates in this stage:

$$(1-(1-\alpha)^{1/3})^2 / t = 0{,}000254 \times$$
$$\times \exp(-\frac{2113{,}06 - 0{,}00019 \cdot P}{RT}) \qquad (10)$$

Such an approach allows to receive an expression for coefficients of element mutual diffusion in phases and to solve the problem of components diffusion which is in principle important for investigating physical effects and phenomena of ascending diffusion.

In the final stage in parallel with diffusion processes the influence of surface chemical reactions on sintering process increases:

$$(1-(1-\alpha)^{1/3})/t = 0.002031 \exp\left(-\frac{13507.46}{RT}\right), \qquad (11)$$

$$(1-(1-\alpha)^{1/2})/t = 0.0029137 \exp\left(-\frac{1367498}{RT}\right), \qquad (12)$$

$$\alpha / t = 0.00247973 \cdot \exp\left(-\frac{14126.82}{RT}\right), \qquad (13)$$

In the final stage the composite properties are assumed to be essentially affected by surface chemical reactions between charge components; the formation of chemical bonds on diamond-matrix boundary at high temperatures is also possible. The last circumstance plays the most important role in wear-resistance and reliable work of drilling bits because strong enough chemical bonds on diamond-to-matrix contact tens and more times exceed the strength of mechanical squeezing of diamond by cobalt (liquid phase wetting) which fact allows to use the potential possibilities of diamond. For the received models (11) – (13) $F_{расч} > F_{кр}$ but the highest value of $F_{засч}$ corresponds to chemical reactions in all three directions. The activation energy of chemical reactions $E_{R2}$ = 13507,46 J/mole ≈ $E_{D1}/2$. Since $E_{R2} < E_{D2}$, the surface chemical reactions exceed in intensity the diffusive ones and their role in improving the structure and bond strength of diamonds in matrix is difficult to overestimate.

More accurate calculation of kinetic constants and other process parameters which are not taken into consideration in models (4) – (13) may be made regarding sintering process velocity as product of two functions – velocity constant depending on temperature and pressure and model function which meets the condition of dependence between the two variables. In this case the equation of shrinkage velocity has the following form:

in the first stage

$$\frac{d\alpha}{dt} = 0,037447\alpha^{0,43}(1-\alpha)^{2,08} \times$$
$$\times \exp(-\frac{9755,19 - 0,000808 \cdot P}{RT}), \qquad (14)$$

in the final stage

$$\frac{d\alpha}{dt} = 0,0596\alpha^{0,59}(1-\alpha)^{3,51} \times$$
$$\times \exp(-\frac{7420,43 - 0,001105 \cdot P}{RT}), \qquad (15)$$

where the parameters of $\alpha^m(1-\alpha)^n$ relation characterize generalized processes. In the first stage $m$ = 0,43 ≈ 2/5 testifies that during sintering there take place viscous flow of material, nucleation and second-order chemical reactions. In the final stage of the process the exponent $m$ = 0,59 ≈ 2/3 indicates three-dimensional diffusion with the increase of chemical reaction order ($n$ = 3,51).

4. CONCLUSION. The method of finding kinetic constants defining the behaviour of diamond-containing composites based on 94WC-6,0Co hard alloy produced by hot pressing has been presented. It has been shown that the use of the known model and the model we've proposed allows to study deeper physical-chemical processes in various stages of sintering. Statistical authenticity of experimental and model calculations testifies of accuracy and adequacy of modelling physical-chemical processes of SDCM sintering.

1. Panchenko G.M., Lebedev V.P. Chemical Kinetics and Catalysis. M., Chemistry, 1974, p. 591.

2. Novikov N.V., Mechnik V.A., Zhukovskiy A.N., Bondarenko N.A., Tkach V.N. // Enlarged, NAN Ukraine, 2003, No. 10, - pp. 102-104.

# MODELING OF PROCESSES OF CARBON COMPOSITE MATERIAL COCARBONIZATION WITH PORE AGENTS

**Skachcov V.A.**, **Karpenko V.D.**(1), **Karpenko A.V.**, **Ivanov V.I.**, **Nesterenko T.N.**
Zaporozhye State Engineering Academy,
Lenin, 226, Zaporozhye, 69006, Ukraine colourmet@zgia.zp.ua
(1) State plant «Uglecompozit»,
GSP-982, Severnoye shosse, Zaporozhye, 69600, Ukraine kvd@vuglecomp.zp.ua

The problem of formation of carbide-formed carbon composite materials with predetermined structure and physic-mechanical properties is pressing, and the methods for calculation of technological conditions for such materials is undoubtedly of scientific interest.

One of the efficient methods of creation, in the volume of carbonized carbon materials, of predetermined porosity with adjustable shape and arrangement of pores is the introduction of pore agents. Pore agents must have low carbon residue, shape and arrangement in the volume of carbon composite materials corresponding to the required porosity. In the course of cocarbonization of carbon fibers, phenol-formaldehyde matrix and pore agents, the required structure of carbonized carbon composite materials are formed.

The modeling of cocarbonization process is based on representation of carbon composite materials as micronon-uniform medium of $B_2$ class. For the model medium the statistical boundary problem of micromechanics of structurally non-uniform media is set, in which physical equations are presented as

$$\xi_{ijj} = \sum_{k=1}^{N} Q^{k}_{ij\alpha\beta} \cdot (1-\omega^{k}) \cdot \lambda_{k} \cdot \left[ \varepsilon_{\alpha\beta} - \sum_{k=1}^{N} b^{k}_{\alpha\beta} \cdot (1-\varphi^{k}) \cdot \lambda_{k} \cdot \Delta T \right], \qquad (1)$$

where $\xi_{ij}$, $\varepsilon_{ij}$ - microstructural tensions and deformations, accordingly; $Q^{k}_{ijmn}$ - random modules of elasticity of k component of carbon composite material at temperature T; $\omega^{k}$ - random thermostructural functions, which establish dependence of elastic properties of composite material components on the degree of structural transformations at temperature T; $b^{k}_{ij}$ - random coefficients of thermal expansion of k component; $\varphi^{k}$ - random thermostructural functions, which establish dependence of thermal shrinkage of k component on the temperature of carbonization; T - temperature of the process; N - number of components in carbon composite material; $\lambda^{k}$ - random indicator function.

For equation (1) the procedure for construction of random thermostructural functions $\omega^{k}$ has been elaborated which is represented as product of two random functions, one of which characterizes the process of formation of defects, the second function characterizes the change in elasticity characteristics of carbon composite material components at the temperature of the process.

The determination of parameters of random thermostructural functions $\varphi^{k}$ is based on the method of calculations and experiments, for which it is necessary, by way of experiment, to determine thermochemical shrinkages of each carbon composite material component.

The statistical problem of micromechanics of carbon composite materials is solved by application of Green's function by the method of moments. The solution is obtained in correlational approximation, sufficient for conducting technological calculations.

The solution of the problem allows determining elastic and strength characteristics of carbonized carbon composite material at a predetermined temperature of the process, to assess the degree of crack formation in each component of composite material, to determine the coefficients of thermochemical shrinkage and coefficients of linear thermal expansion of carbon composite material being carbonized at temperature T.

The proposed approach has been tested on the examples of calculations of technological conditions for the processes of carbon composite material cocarbonization with several types of pore agents having various chemical nature.

# EXPULSION OF $AL_2O_3$ COATING FROM STEEL SUBSTRATE THROUGH PULSED LASER IRADIATION

**Daniel L. Oltra R.**(1)
European Space Agency,
ESTEC, TOS-MCS, P. O. Box 299, 2201 AZ Noordwijk, The Netherlands
(1)CNRS - University of Burgundy, LRRS, UMR 5613, BP 4787 21078 Dijon, FRANCE

## Introduction

Many research publications have shown that thermal stress can have significant effect in delamination process of coated ceramic-based materials using pulsed laser [1-3]. In this work, the delamination behavior of ceramic coatings on stainless steel substrates is studied based on the different stresses that developed in the differential medium. Finite element analysis is used to calculate the effect developed at the interface due to the build up of thermal condition during pulsed laser irradiation. It is shown that cracks of the ceramic coatings are likely to occur at a given time scale and at a given critical stress under a critical laser energy application. It has also been shown that thermal stresses are crucially dependent on material properties and the layer geometry and this can vary widely depending on parameters in a multi-layered system.

## Finite Element Description

The CASTEM software was used to run the finite element method (FEM) for the calculation of thermal stresses due to laser irradiation of the coating and the substrate. The calculation has involved three separate steps. The first step has involved the power density calculation, which is based on a methods of Mansuripur, Connell and Goodman [3] for the absorption of the energy through the ceramic absorbing layers, taking into account the density of the ceramic coating and the pores volume fraction. The power source is a typical nanosecond pulsed Nd:YAG laser (B.M. Industries); emitting at the IR ($\lambda$=1064 nm), with a pulse duration of 34 ns, was used for the irradiation of the ceramic coatings with energies from 5 mJ up to 50 mJ, which provides a mean energy densities from 0.3 to 2.8 Jcm$^{-2}$. The temporal profile of the laser pulse energy was approximated by a Gaussian fit with a Full Width at Half Maximum (FWHM) of 14 ns, whilst the spatial distribution of the energy was also gaussian. A disk diameter of 50 mm and a 5 mm thickness stainless steel was used as a substrate with various thicknesses (10-80 u.m) of coated alumina ($A1_2O_3$) for the model.

The power density is calculated at the centre of the finite element mesh and as the problem is axis-symmetric, a single two-dimensional cross section of the alumina-substrate medium was considered. This represents a one-half cross-section of the modeled rectangular materials with axis on the left, 2000 nm in radius and 1600 nm in depth, using a mesh comprising 800 quadrilateral, eight-noded elements as depicted in Figure 1.

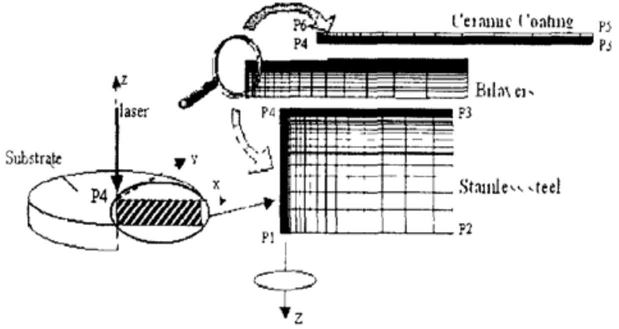

Figure 1: Construction of grids of metal coated with transparent alumina layer comprising of eight-noded elements [1].

The upper model rectangular coated material is free to expand in the z direction with the constraining effect of boundary condition at the bottom. The material may also expand to the left along the x direction with a boundary condition on the right. The pulsed laser energy profile obtained is variably dependent on the ceramic layer thickness and its refractive index.

The second step involves the time-dependent conduction equation, using Finite Element Methods (FEM), to calculate the change in temperature. The change in temperature is calculated at an interval of 1 ns for 20-40 'ns time duration. For each time interval, the thermal stresses are calculated, which determine the stress fields and the interfacial strength of the material. The propagation of longitudinal waves model, Figure 2 of the acoustic waves are subjected to multi-reflection at the coating/substrate interface, which appears in a waveform as successive normal displacements. This propagation has shown that delamination is likely to occur at different interfacial boundaries depending on the systems geometry.

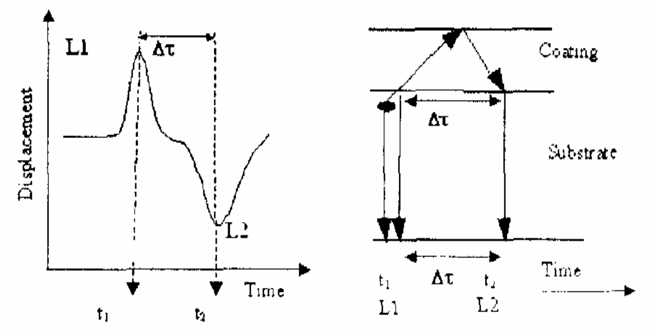

Figure 2: Details of acoustic waves with multi-reflection at the coating/substrate interface [1].

Two systems were examined. These are, 600 nm transparent absorbing ceramic materials on a stainless steel substrate and 800 nm thick transparent ceramic layer on the same substrate to see the effects of thickness geometry. The shape and mechanism for initiation of cracks and delamination is perhaps due to fracture process between substrate ceramic coating as a result of buckling instability generated by thermal stresses in the media. The laser energy absorbed is more in the ceramic layers with increase in thickness, as more number of interfaces cracks increases, creating a zone of distributed delaminations. The time for crack propagation of the width of the ceramic blister Figure 3 is assumed to be directly proportional to the optic fibre diameter of 1.5 mm between 1 and 1.5 ns for typical crack propagation rates of up to $10^3$ ms $^{-1}$.

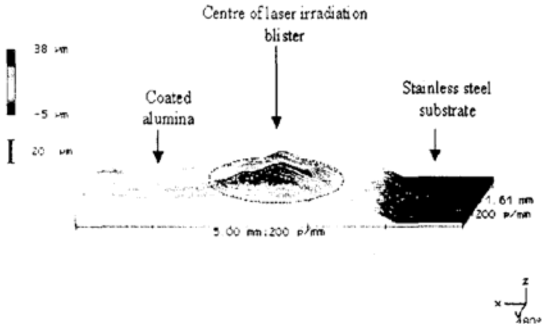
Centre of laser irradiation blister
Coated alumina
Stainless steel substrate
38 µm
-5 µm
20 µm
1.61 mm
200 p/mm
5.00 mm;200 p/mm

Figure 3: Profile of laser irradiation blister zone in 3D

This is comparable to the transient thermal conduction effect, which indirectly generates cracks along the interfaces and sometime on the through-thickness ceramic layers that lead to brittle fracturing of the ceramic coating. Considering that the ceramic-coated materials have many pores, an artificial pore zone or flaw is inserted into the mesh at the initiated boundary of delamination, which is assumed to be at the interfacial boundary between the ceramic coatings and metallic substrate. The stress calculation for the particular temperatures at this time interval are then repeated and a newly deformed mesh is obtained. Hence, the thermal distribution at the time interval is associated with the fundamental mode of thermal conductivity of the media with a peak value determined by conservation of heat energy absorbed especially in the metallic substrate. The procedure is sequentially repeated for the next time step. The new thermally deformed mesh ideally provides the fundamental approach for further calculation in the next time step.

**Results and Discussion**

The influence of a nanosecond pulsed laser irradiation on bi-layered systems transparent ceramic coating-metallic substrate is partially reflected at the coating surface and, partially absorbed by the substrate with much dependency on the optical properties of the material system. Figure 4 illustrates the variation in the absorbed temperature gradient along the axis of the laser irradiation volume at 20 ns with variable power density profile for the cases of no delamination at zero time. The absorption profile increases abruptly with in peak share profile.

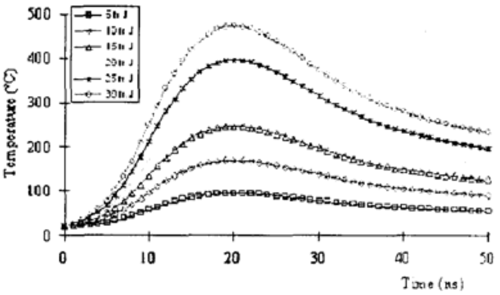

Figure 4: Axial plot of absorbed temperature gradient versus time measured from the air interface for 80 (im

The effect of these changing power density profiles with delamination will affect the resulting temperature profiles. This is depicted in Figure 5 showing axial through-thickness temperature profiles.

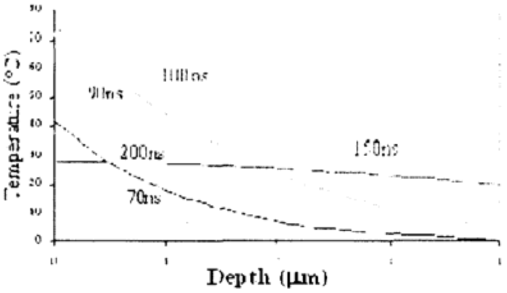

Figure 5: Axial temperature profiles versus depth at 70 - 200 ns

In figure 6 the resulting thermal stress contours plots at 20 ns are presented. The stresses shown are the radial components, which illustrate the general distribution of stress with the irradiation of pulsed laser.

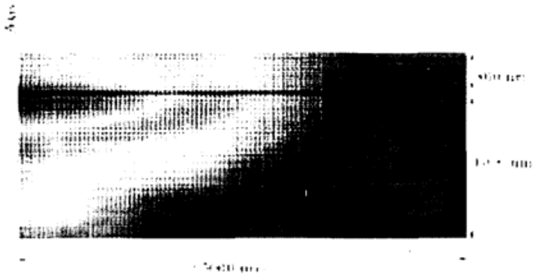

Figure 6: Contour plots of radial component stress produced after 20 ns

The stresses in both absorbing systems are primarily compressive and also reflect the axial temperature profiles. The values in the simulation were calculations using radial stress formula; $\sigma_r$ - $E\alpha\Delta T$ where E is the modulus, *a* the thermal expansion coefficient, and $\Delta T$ is the change in temperature. With this result Figure 7, the radial stress along the interfacial axis is plotted. As expected, the stresses are much less in the delaminated cases where deformation or fracturing of the ceramic layers causes stress relief at each successive iteration and point of interaction. The same is also true for the thinner ceramic layers, where the stress profiles are more symmetric about the center of the delaminated layers.

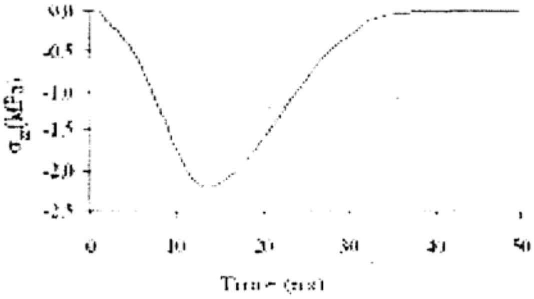

Figure 7: Axial plot of radial stress versus time

The principle result here is that the substrate experience an initial tensile stress as soon as delamination has occurred and is then instantly unstressed.

**Conclusions**

The Finite Element Modeling (FEM) simulations and calculations presented indicate that formation of crack initiation and delamination at the interface under the influence of pulsed laser irradiation having linear elastic effects is as a result of propagation of acoustic waves process. The calculations allow only for elastic behavior and do not use time or temperature-dependent properties. The mechanisms involved are interface failure due to axial tensile stress and elastic buckling due to high radial compressive stresses generated by axial thermal expansion and thermal gradient of the two dissimilar systems. This has significant effect in the delamination of the coating ceramic from the stainless steel substrate with a proportional effect of the temperature gradients generated across the interface.

**Reference:**

1. G. Rosa, Ph.D Thesis 'Etude de 1'adherence de revetements d'oxydes sur des substrats metallique' (2001).
2. M. A. Nkansah and K. E. Evans, 'Modeling delamination due to Thermal Stress in Optical Storage Media', J. Appl. Phys. 66, 50, 1989.
3. M. Mansuripur, G. A. N. Connell, and J. W. Goodman, Appl. Opt. 21, 1106 (1982).

# THE PHYSICAL MODEL OF THERMAL STABILIZATION OF COATINGS

**Kadyrzhanov K.K., Rusakov V.S.** (1)**,**
**Turkebaev T.E., Zhankadamova A.M., Plaksin D.A.**(1)
Institute of Nuclear Physics NNC RK, Almaty, Kazakhstan, turkebaev@inp.kz
(1)Moscow State University, Moscow, Russia, rusakov@moss.phys.msu.su

The progress in present-day techniques makes the construction of novel materials operating under extreme conditions of high temperatures, intensive mechanical loads, aggressive and contacting environments, external irradiation possible. Because of various requirement to surface and volume properties the employment of traditional technologies of production of the material with depth-homogeneous composition and structure are not perspective. For instance, a great amount of chromium atoms (5—10 at.%) are to be introduced into the high-temperature ($\gamma+\gamma'$) nickel superalloys to provide heat-resistance, however, their high-temperature strength and durability decreased in this case. The creation of protective coatings on industrial materials was the next stage in technology development. Nowadays the progress in the production of high-qualitative coatings is associated with ion-beam technologies.

Analyzing the numerous publications on ion-beam methods of surface layer modification we have come to the conclusion that only specific metastable surface states were the main subjects of interest for many investigators, whereas the principal aspects, such as thermal and chemical stabilities of surface layers were ignored. In this context it is not surprising that ion technologies could not find appropriate application for hardening of industrial products being exploited at high temperatures, when specific properties of ion-implanted surface due to inherent metastable phases are being lost.

In the present paper we developed a physical model that enables to describe diffusion processes in a laminar systems with formation of thermally stable phases on surface of metallic samples.

Let's one-component (1) coating is deposited on one-component (2) sample. For one-phase region the time dependence for concentration of the components $C_i$ is determined by the equation:

$$\frac{\partial C_i}{\partial t} = -\mathrm{div}\mathbf{J}_i \qquad (1)$$

where $\mathbf{J}_i$ – flow of atoms:

$$J_i = D_{12}(C(x))\frac{\partial C_i(x)}{\partial x} \qquad (2)$$

For binary system the coefficient of mutual diffusion is as follows:

$$D_{12}(C(x)) = C_1(x)D_2 + C_2(x)D_1, \qquad (3)$$

where $D_1$ and $D_2$ – diffusion coefficients of the component 1 into 2 and 2 into 1; $C_1$ and $C_2$ – atomic concentrations of the components 1 and 2. For a binary system $C_1+C_2=1$.

Temperature dependence of diffusion coefficients $D_1$ and $D_2$ in one-phase regions is determined by Arrhenius law:

$$D_i = D_{0i}\exp\left(-\frac{Q_{0i}}{RT}\right), \qquad (4)$$

where $D_{0i}$ – frequency factor, $Q_{0i}$ – activation energy for a corresponding atom, R – gas constant.

Combining (1) and (2) we have:

$$\frac{\partial C_i}{\partial t} = \frac{\partial D_{12}(x)}{\partial x}\frac{\partial C_i}{\partial x} + D_{12}(x)\frac{\partial^2 C_i}{\partial x^2} \qquad (5)$$

For each time step there was calculated change in profile of the components' concentration. If the concentration lies in two-phase region, then the relative concentration of $\alpha$-phase in a two-phase region at depth x was determined as (lever rule):

$$P_\alpha(x) = \frac{C_\alpha - C(x)}{(C_\beta - C_\alpha)}. \qquad (6)$$

In this context the rate of phase formation exceed significantly the diffusion rate.

Coefficient of mutual diffusion in two-phase region $D_i(x,\lambda)$ depends both on depth x and size of new phase inclusions $\lambda$:

$$D_i(x,\lambda) = D_{bound}W_i, \qquad (7)$$

where $D_{bound}$ corresponds to coefficient of mutual diffusion $D_{12}$ at interface of one- and two-phase regions; the probability $W_i$ of formation of diffusion channels at depth $x_i$:

$$W_i = \sum_{j=i}^{M}\Omega_j = \Omega_i + \Omega_{i+1} + \Omega_{i+2} + \ldots + \Omega_M, \qquad (8)$$

M – number of layers in two-phase zone, determined by the relation of thickness of a two-phase zone to the size of inclusion of a new phase. Probability of formation of diffusion channels at the depth $x_i$:

$$\Omega_i = (P_1 \cdot P_2 \cdot \ldots \cdot P_i \cdot (1-P_{i+1})) = \left(\prod_{j=1}^{i} P_j\right)(1-P_{i+1}) \qquad (9)$$

It was supposed that all inclusions are of the same size λ. From the above-presented one can see that wider two-phase region, stronger the attenuation of diffusion coefficients and the rate of phase formation decreases.

Initial condition was taken in the form:

$$C_1 = \begin{cases} 1 \quad \text{at} \quad 0 < x < d_1 \\ 0 \quad \text{at} \quad d_1 < x < d \end{cases}, \qquad (10)$$

where $d_1$ – thickness of the produced coating, d – thickness of the whole sample. Boundary conditions corresponded to absence of flows at the sample surface: $\left.\frac{\partial C}{\partial x}\right|_{x=0;d} = 0$.

The system of equations (5) can be numerically solved using a standard software package IVPAG/DIVPAG of the library DIGITAL.

In fig.1 are shown the calculation results of relative content of the phases formed at isothermal annealing for the systems Be(1.2 μm)-Fe(11μm) and Be(1μm)-Fe(11μm)-Be(1.2μm) (solids). The points are the results of treatment of Mossbauer spectrum at registration of conversion electrons (CEMS) in back scattering geometry from both sides of the samples. One can see that the results of calculations are in good agreement with experimental ones as the case of complete dissolution of beryllium with formation of beryllium solution in iron (α-Fe(Be)), and the case of observed stabilization of $FeBe_2$ phase on the surface.

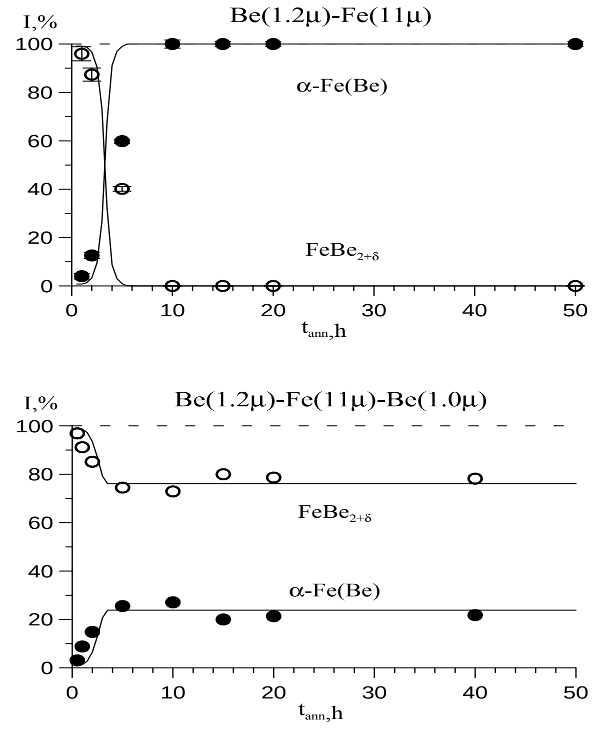

Fig.1. Relative intensities of formed phases on surface of Be-Fe samples depending on duration of the consequent isothermal annealing at $T_{ann}$=720 °C: ○,●-result of CEMS-experiment processing [1] (○ – from beryllium coating side, ● – from iron substrate); solid line - numerical calculations.

Variations of sizes of phase inclusions within reasonable limits influence only slightly the kinetics of phase formation (see fig. 2). It is possible to make a conclusion that the main reason for thermal stabilization is formation of well-formed two-phase region.

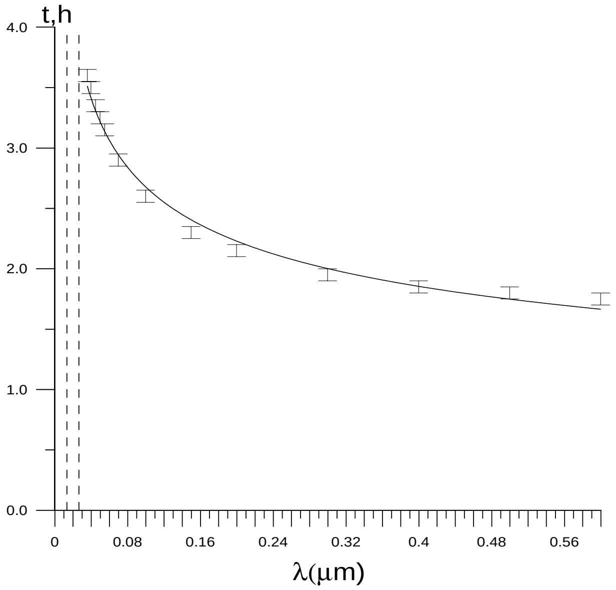

Fig.2. Time till the system becomes stable versus size of inclusions λ

Based on the obtained results one can make the following conclusions:

1. There was developed a physical model that enables to describe diffusion processes in a laminar system with formation of thermally stable phases on surface of metallic samples.
2. There were performed numerical calculations that describe the obtained experimental data.

## LITERATURE:

1. Kadyrzhanov K. K., Kerimov E. A., S. V.Kislitsin, A. N.Platov, Rusakov V. S., Turkebaev T. E. //Eurasia Nuckear Bulletin –2002 — №1 — p.82—87.

# MECHANISM OF GROWTH OF DIFFUSION LAYER WHILE FORMATION OF COVERINGS

**Artemyev V.P., Sokolov E.G., Chalov A.A.**
Kuban State Technological University, Krasnodar, Russia
2, Moskovskaya Str. Krasnodar, 350072, Russia, e-mail: artemyev@kubstu.ru

Thermochemical treatment by a method of diffusion saturation is based on elements transition through boundary of various phases, i.e. based on the phenomenon of interphase heterodiffusion. The surface of a product interacts with created external environment in temperature conditions during certain time. External environment, out of which the selection of an element is made for reception of a covering – is one of the major factors providing the received coverings. Many factors depend upon it: technology, temperature and time of process; distribution of components on thickness of diffusion layer, phase structure of a covering; ultimate attainable concentration of saturation element on a surface and, at last, structure of a covering. All these take place, if environment provides an opportunity of complex of processes occurring on interphase boundary, necessary for reception of a covering. On receiving one and the same covering the environmental influence is doubtless and it is confirmed by comparison of experimental data.

If the surface of saturating metal is in active condition, i.e. is free from oxide films, then the process of boundary interaction is determined by three consecutive interconnected stages: first - adsorption, second - heterodiffusion in contact zone, third - volume diffusion, resulting in formation of a solid solution and origin and growth of new phases. The determination of chemical connection between metal of a substrate and diffusing element is necessary for the course of heterodiffusion. It depends on thermodynamic requirements of reduction of free energy by interphase interaction.

In the case of diffusion metallizing in environment of fusible metals - lead, eutectic lead-bismuth - the role of external environment is played by this or that fusible metal containing diffusing element in dissolved condition, in this very case - titanium. By consideration of the diagram of condition "iron - titanium" the following covering structure is possible:
α - solid solution of titanium in iron with forming of intermetallic combinations of a type of Fe3Ti. The mechanism of diffusion layer formation in this case is as follows: superficial layer 1-1 is created (fig. 1), thickness of which is determined by parameters of superficial diffusion. It consists from adsorbate atoms of saturating element of titanium and atoms of basic metal. The speed of bringing of titanium atoms and atoms of the basic metal to the basis surface is equal to or a little bit more than the diffusion speed in a solid phase – this is typical for normal kinetics of the saturation process by diffusion metallizing, if the choice of external environment is made correctly. As a result of this in the superficial layer 1-1 during short period of time in comparison with the time of saturation process, the constant titanium concentration $Co^{TI}$ = const is established, which value is determined by difference of interphase titanium potentials. Further occurs mutual diffusion of titanium and components of the basis, therefore appears the diffusion zone consisting from continuous number of solid solutions $C=\phi(x)$ on all length of thickness of the covering. Growth character of diffusion zone depends on relation of speeds of titanium diffusion and components of the basis, in particular, of iron.

The special experiment for an estimation of Kirkendall effect (shift of marks) was made [1] to find out the mechanism of growth of diffusion titanium layer on armco iron and steel 08X18H10T and also to determine the speed of plane movement with the certain concentration in diffusion process.

In amount of basis metal (fig. 1) at the level of division surface 1-1 on two sides were put marks from inert material in form oftungsten wires with diameter 30 microns. With a help of microscope with precision up to 0,01 mm were made measurement of sample and of distance between inert marks. The sample thus prepared was exposed to diffusion saturation with titanium in melt of eutectic lead-bismuth at saturation temperature 1100 C° within 10 hours according to the technique stated in work [2]. After diffusion saturation a metallographic section was made and then sample dimensions, thickness of diffusion layer and distance between the marks were measured. Moving of marks was defined as difference:

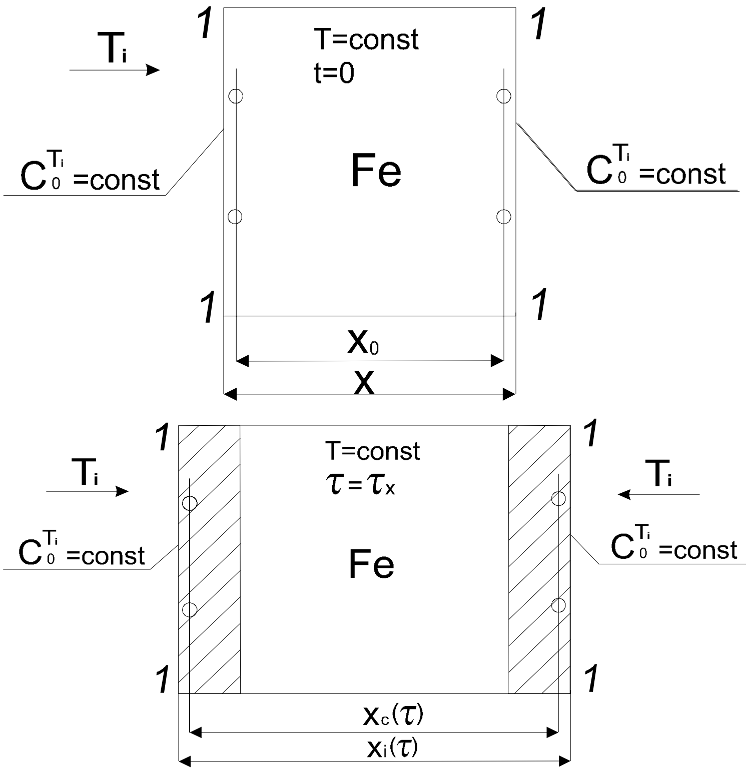

Fig.1. Scheme of growth of diffusion titanium covering at DTi>DFe

$$x_o(\tau)=x_c(\tau)-x_o, \quad (1)$$

value of which turned out to be positive and has made up 180 microns on one side for steel 08X18H10T and 310 microns for armco iron.

The difference in moving of sample dimension turned out to be also positive

$$X_i(\tau)=X(\tau)-X, \quad (2)$$

which equals to 200 microns and 350 microns on the side accordingly for steel 08X18H10T and armco iron.

On the grounds of the fact that Kirkendall effect can be explained only on basis of the mechanism providing an opportunity of uncompensated atoms flow, then diffusion processes can go according to one of two mechanisms - vacantional or diffusion on interstices. Taking into account that at vacantional mechanism of diffusion owing to isolation of vacancies on crystallographic planes, are formed the pores which are not found out at diffusion titanation, it is possible to think that the process of titanation is the titanium diffusion on interstices. Positive moving of datum marks and increase of the sample size can happen only in the case if the coefficient of titanium diffusion is more than the coefficient of diffusion of the basic steel component - iron (DTi>DFe), therefore arises a resulting flow of titanium atoms, directed behind the line of datum marks. These excessive atoms cause the appropriate displacement of crystallographic planes with datum marks to the left, since at the formation of solid solutions of replacement the periods of a lattice are increased because of the difference of nuclear diameters of the dissolved titanium element (1,45) and iron solvent (1,27). At the first approximation this displacement should be proportional to concentration of the dissolved component.

Thus, with the help of Kirkendall effect, the mechanism of growth of diffusion titanium layer on armco iron and on austenitic steel 08X18H10T is determined, which allows to predict the change of details sizes while titanium coating.

**References:**

1. Bokshtain B.S. Diffusion in metals. - M.: Metallurgy, 1978. – 247pg.

2. A.c.954502, USSR. MKI C23c 9/00. Method of thermochemical treatment of steel products / V.P. Artemyev, M.I. Chaevskiy.

# PROBABILISTIC AND STATISTICAL ANALYSIS OF GLASS-CERAMIC MATERIAL APPLICABILITY IN SUPERHIGH-SPEED AIRCRAFT FAIRINGS

**Levshanov V.S, Rusin M.Yu., Kurakin V.I., Suzdaltsev E.I**
Federal State Unitary Enterprise “Obninsk Research and Production Enterprise “TECHNOLOGIYA”, Obninsk, Russia
e-mail: info@technologiya.ru

The strength of β-spodumene glass-ceramic material used for the production of aerial fairing shells is under study. The bearing capacity of fairings is characterized by a safety factor η equal to the ratio of fairing material allowable strength $[\sigma_\partial]$ to maximum stress ($\sigma_{\max}$) resulting from the effect of heat and load on the fairing. The probability of trouble free operation (PTFO) of fairings is evaluated as

$P_1 = P(\eta = [\sigma_\partial] / \sigma_{max} > 1) = P(\sigma_{max} < [\sigma_\partial])$.

In this case the probability $P_2 = 1 - P_1 = P(\sigma_{max} > [\sigma_\partial])$ implies the risk of not providing the given bearing capacity.

The value of $\sigma_{max}$ is determined from the calculations of fairing stress-strain state. Its variability is controlled with the help of Monte Carlo method according to which the analysis of the fairing structure strength is carried out repeatedly. In every variant of fairing load calculations the random values defined by a normalized random value are used. As a result a function of maximum stress distribution $\sigma_{max}$ is obtained which in case of normal distribution is defined by the mathematical expectation $m(\sigma_{max})$ and the standard deviation $S(\sigma_{max})$.

The reliability with respect to the strength or PTFO is determined through Laplace function:

$$P_1 = P(\sigma_{\max} < [\sigma_\partial]) = \Phi(z) = \frac{1}{\sqrt{2\pi}} \int_{-\infty}^{z} \exp\left(-\frac{z^2}{2}\right) dz,$$

where $z = ([\sigma_\partial] - m(\sigma_{max})) / S(\sigma_{max})$.

The value of material allowable strength for a specific article depends on the potentialities of the technological process used for the production of this material and the potentialities depend on the spread of the material ultimate strength $(\sigma_u)$ or on its distribution. It is apparent that the choice of $[\sigma_\partial]$ value depends on the stability of the technological process used for the production of the preassigned quality material with the maximum value of probability $P_3 = P(\sigma_u > [\sigma_\partial])$ which makes possible the production of the material with the assured strength higher than the allowable. In this case the probability $P_4 = 1 - P_3 = P(\sigma_u < [\sigma_\partial])$ describes possible spoilage of the technological process. In case of normal distribution of $\sigma_u$ this probability is also calculated through Laplace function:

$$P_4 = P(\sigma_u < [\sigma_\partial]) = \Phi(z) = \frac{1}{\sqrt{2\pi}} \int_{-\infty}^{z} \exp\left(-\frac{z^2}{2}\right) dz,$$

where $z = (m(\sigma_u) - [\sigma_\partial]) / S(\sigma_u)$; $m(\sigma_u)$ and $S(\sigma_u)$ are mathematical expectation and standard deviation of the ultimate strength $\sigma_u$, respectively.

Fig. 1 shows possible frequency distribution functions of $\sigma_{max}$ and $\sigma_u$ and the values of allowable strength $[\sigma_\partial]$ defining the value of the probability $P_2$ and $P_4$ which on one hand must be minimized and on the other hand a compromise must be found between them as they are inconsistent with each other in nature.

The approach presented above was used to evaluate the probabilities $P_2$ and $P_4$ and to refine the minimum allowable strength of the OTM 357 material used for the manufacture of nose fairings for the PBB-AE type missiles.

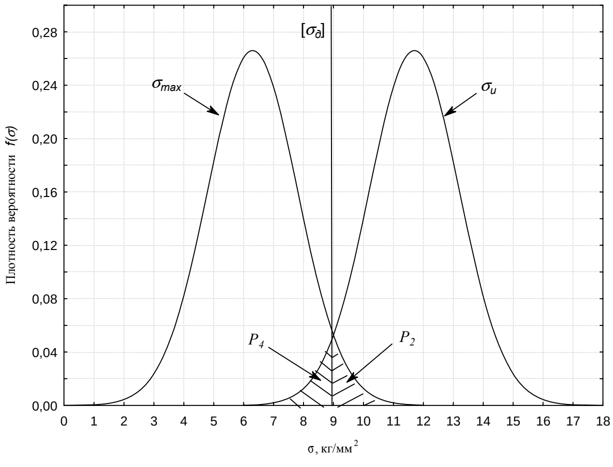

Fig.1 Distribution of strength and associated probabilities $P_2$ and $P_4$ for a given allowable strength $[\sigma_\partial]$

Calculation of the fairing strength was carried out using the model of the stress-strain state for the shell of revolution under random loading and heating with due regard for lateral shear. A thermal analysis was carried out by solving unidimensional nonstationary problem for the combined transfer of heat through a multilayer wall. The preassigned loads on fairings such as variations of maximum operational lateral forces along the fairing length and variations of temperature on the external surface in the reference section were used for the calculations.

Random variation of forces and temperatures was carried out by Monte Carlo method within ±20% of nominal values and at the number of realization equal to 100. The distribution of maximum stress $\sigma_{max}$ resulting from aerodynamic load effects is described by the normal distribution curve with $m(\sigma_{max}) = 4.4$ kg/mm$^2$ and $S(\sigma_{max}) = 0.3$ kg/mm$^2$ (Fig. 2).

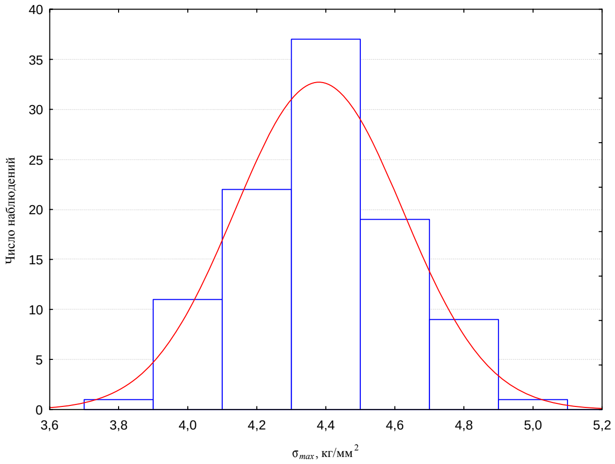

Fig.2. Distribution of maximum design stresses $\sigma_{max}$ in fairings

The results of $\sigma_u$ measurements in the material specimens made from shell stoke were analysed to evaluate the ultimate strength distribution functions. The distribution of $\sigma_u$ obtained (Fig. 3) is also described by the normal law with $m(\sigma_{max}) = 11.9$ kg/mm$^2$ and $S(\sigma_{max}) = 1.6$ kg/mm$^2$.

The distribution of maximum design stresses $\sigma_{max}$ in a fairing and ultimate strength $\sigma_u$ in the OTM 357 material plotted with the use of the parameters determined are given in Fig. 4. Both distributions do not practically intersect so the determination of the allowable strength value within [σ$_Д$] = 6–9 kg/mm$^2$ causes minimum risk both for the article itself and for the technological process.

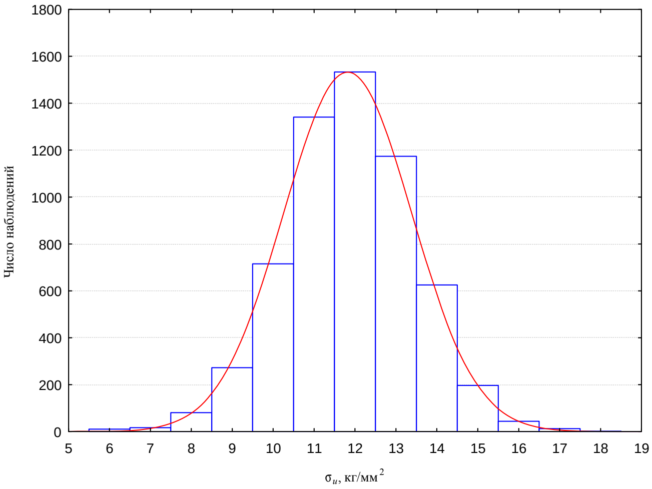

Fig.3. Distribution of ultimate strength $\sigma_u$ for the OTM 357 material

When the probability value $P_3$ equal to 95% is taken to produce an article with the assured strength higher than the allowable, the value of $[\sigma_\partial]$ equal to 9.3 kg/mm$^2$ is obtained.

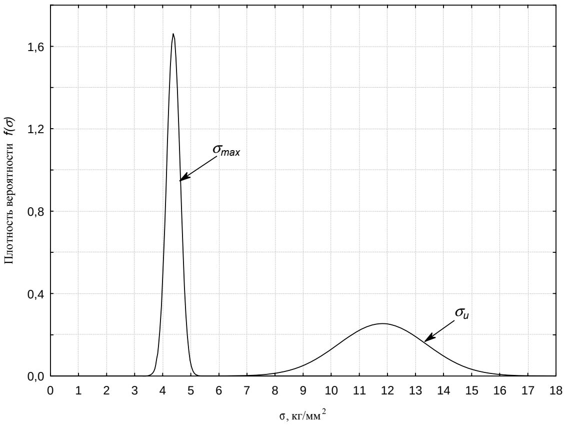

Fig.4. Distribution of maximum design stresses $\sigma_{max}$ in fairings and the ultimate strength $\sigma_u$ in the OTM 357 material

These estimates were supported in comprehensive studies of fairings which withstood the whole cycle of tests and retained their integrity.

# PHASE EQUILIBRIA IN SYSTEM NI-B-C

**Kudin V.G., Makara V.A.**
Shevchenko Kiev National University, Kiyv, Ukraine
Vladimirskaya st. 64, Kiev, 03033, Ukraine, kudin@univ.kiev.ua

Carbides, carbooxides, carbonitrides of metals and materials on their basis use widely in different regions of the industry as they have unique properties (refractory, highly rigid, electrowire).

The isothermal section of Ni-B-C system has been designed using software package Thermocalc. This program enables to calculate the phase equilibrium in system using known thermodynamic parameters of phases in this system. Temperature and concentration dependences for free energy of phases of our system have been calculated using model of subregular solutions. Values of parameters for this model have been taken from Kaufman database from program package Thermocalc. The calculation result of phase equilibrium presents on fig.1.

Certainly, this calculation is approached and cannot precisely agree with real form, but it allows to find the most complicated and interesting areas on the diagram. There is a intersection of two straight lines $Ni_3B$-$B_4C$ and $Ni_3B$-C on the calculated diagram that fits with phase equilibria between different chemical compounds. This area has been selected for experimental research (it marked on fig. 1 by dashed lines).

The alloys of quasibinary $Ni_3B$-$B_4C$(C) systems have been pressed from powders $Ni_3B$, $B_4C$ of quality "pure" and “spectral pure” graphite. The degassing of the charge has been realized in vacuum at 1000 °C for charge purification. Initial mixes of component powders of researched system weighed on analytical balance, carefully mixed and pressed at a tablet.The pressing in weight from 10 up to 15 g keeped up preliminary in vacuum at temperature 1000 °C. Research alloys have been received by melt of decontaminated tablets in the arc furnace, using a not consumable tungstic electrode on water-cooled copper bottom in the argon quality (pressure 50-80 kP), cleared by the previous fusion of titanic getter during 3 minutes. Speed of cooling of samples was approximately 100 °C/second.

The evaporation of more flying components (boron and graphite) has been observed on the melt process. A spitting of liquid alloy and allocation of slaggy float away mass took place also. It has the cause of the shade change of the alloy composition.

The samples weighing 1,5-2 g have been placed in corundum crucibles and heated up with speed of 80 °C/minute to the melt temperatures. Next they have been cooled from melt temperature with the same speed. Thermal curves for some investigated alloys presented on fig. 2, 3. The phase diagrams of quasibinary systems $Ni_3B$-$B_4C$(C) have been constructed on the basis of the received data. It was shown by fig. 4, 5.

It was established, that there are no the ternary connections in system Ni-B-C. It is coordinated with received by us the phase equilibria of our data for quasibinary sections $Ni_3B$-$B_4C$ (C). Nevertheless in [1] it was found, that the compound $Ni_{6,6}B_{2,7}C_{0,6}$ crystallize from liquid alloy of system Y-Ni-B-C as does not get on investigated by us the sections. Not clear, this compound can exist in systems without yttrium in a stable state. So in work [2] it was investigated that all borides of nickel do not interact with carbon at 1173-2273 K. On the other hand $Co_3B$ interactes with carbon at temperature above 1173 K with the formation of mixture $Co_2B$ and $Co_3C$. It was established, that it is possible to receive the boroncarbide of composition $Co_{11}B_2C$ from elements by synthesis at 2273 K. The composition of this compound is isomorphic by $Mn_8BC$ and $Fe_{23}B_3C_3$, received in [3-5]. There is evidence of necessity of the further research of alloys of Ni-B-C system for the purpose of an establishment of new ternary compounds and phases on their basis.

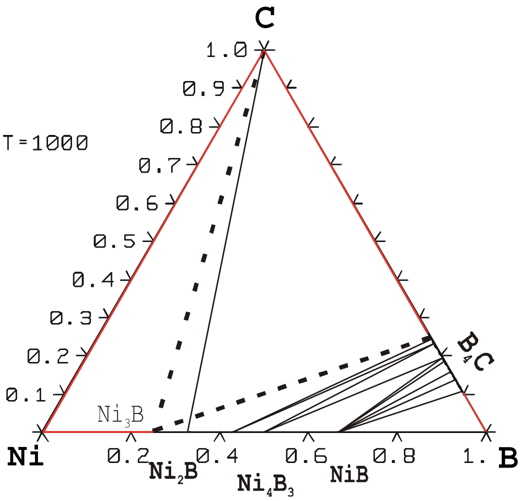

Fig. 1. Isothermal section of system Ni-B-C, calculated by program Thermocalc at T=1000 °C

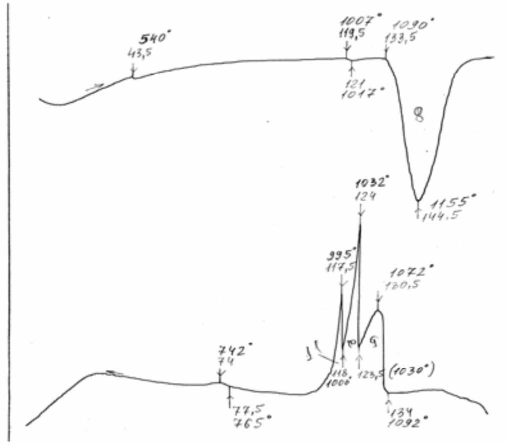

Fig. 2. Differential curves of heating and cooling for the alloy of composition NB$_2$ (speed of heating and cooling at 80 °C/minute)

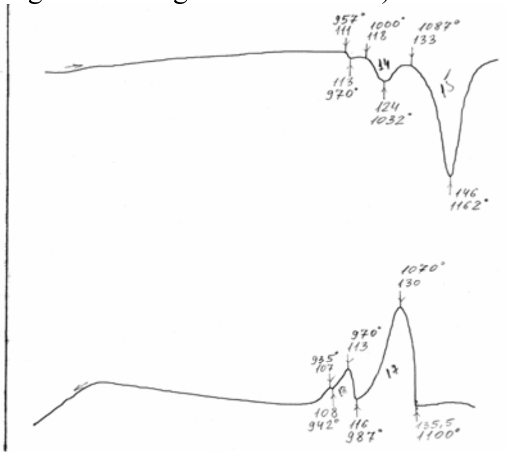

Fig. 3. Differential curves of heating and cooling for the alloy of composition NC$_1$ (speed of heating and cooling at 80 °C/minute)

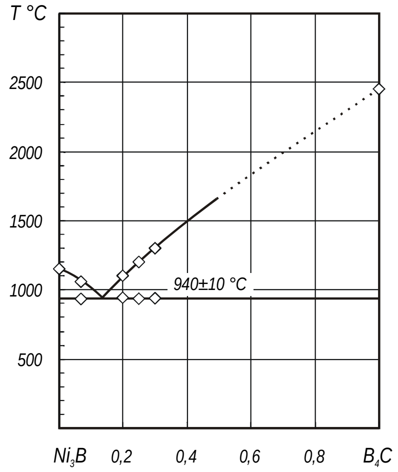

Fig. 4. The quasibinary section of Ni$_3$B-B$_4$C system constructed by results of the thermal analysis

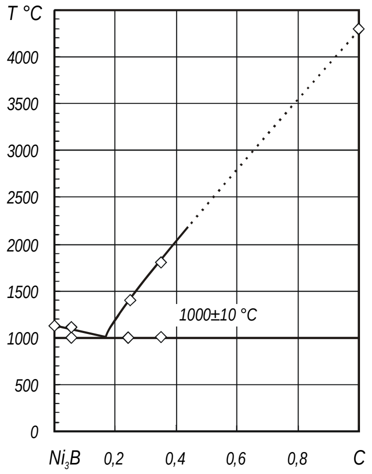

Fig. 5. The quasibinary section of Ni$_3$B-C constructed by results of the thermal analysis

## References

1. Szillat H., Majewski P., Aldinger F. Phase equilibria in system Y-Ni-B-C // J. Alloys and Comp. – 1997. – Is. 1-2. -Vol. 261. - P. 242-249.
2. Markovskij L.J., Bezruk N.T., Berkova G.E. About stability of borides of nickel and cobalt in relation to carbon // Izv. Acad. Sci. USSR. Inorganic materials. - 1971. – Vol. 7. - №1. - P. 56-58.
3. Markovskij L.J., Bezruk T.Z. // J. Appl. Chem. – 1966. - Vol. 39. – P. 258.
4. Fomichev O.I., Katkov V.F., Kushnereva A.K. Investigation of ternary diagram Fe-Fe$_2$B-Fe$_3$C // J. Phys. Chem. - 1978. - Vol. LII. - №9. - P. 2240-2243.
5. Fomichev O.I., Katkov V.F., Kushnereva A.K. The phase composition of Fe-B-C alloys // Inorganic materials. - 1976. - т. 12.

# DIAGNOSTICS AND FORECASTING OF POWDER DISPERSION - STRENGHTENED MATERIALS PROPERTIES BY “MIXTURE-RESPONSE” SIMPLEX DIAGRAMS

**Lyulko V.G., Jmajlov B.B., Artamonov И.E.** **(1)**, **Ivanova A.A.**
Don State Technical University, Rostov-on-Don, Russia
Sq. Gagarin 1, Rostov-on-Don, 344010, Russia, atm1@mail.ru, bjmailov@dstu.edu.ru,
(1)Ltd "Pharmacist", St. Ivanovskogo, 38, Rostov-on-Don, 344010, Russia, ilya@farmacevt.ru

Growth of intensity of operational loadings tokosyomnyh contact pairs - pantograph of the electric locomotive, sliding contact a train of underground, collector high-speed (6—8 tsd. T/min) the electric motor - defines a problem of selection and reliable operation of materials for such interfaces. One of opportunities is use of powder dispersion-strengthened composite materials (DUKM) and products on the basis of copper with strengthening phases oxides, nitrides, carbides etc. They are widely used in practice of plasma processing (plasma cathodes, atomizers of torches), for welding processes - electrodes of contact welding, electric supply , elektrokontaky etc. There is an extensive nomenclature of such products, for example, let out STF "Tehma", Cheboksary, NPP "Kermet", Ioshkar-Ola, joint-stock company "Uralelectromed” V.Pyshma, under trade mark "Diskom" manufacture, a beside of foreign manufacturers - Ekkart Werke (Germany), "Diskom - DisPal" (Austria), to use as erosions- and wear proof current supply inserts in current-collecting devices of units and electrotransport [1—3]. Perfection of such materials goes on a way distant distributions a strengthening phase up to shares of micrometers and nanosize, allowing to keep a matrix (copper) as high electric conductivity an electromaterial (operational conductivity not below 90% from pure copper).New reception of manufacturing techniques DUKM is two-phasic introduction of strengthening phase in basis structure - a copper powder. Namely, it is consistently precipitated by an ionic- plasma method on a copper powder high dispersiveness (the initial size ~0,5 microns) carbines - nitrides phase Ti (C, N) - is used technology of reception of polycomponental materials by thermo synthesis in a vibrating layer on disperse systems with introduction mikro- and macroadditives of alloying elements (Cu/CuO/Cu2O, Al, P, S, B, Ti (C, N), and about - environment of sublayer on particles base powder [4] . Then graphite is traditionally mixed before mechanical alloying a source oxides phases Al, Al2O3, and with, which then in regular intervals enough distribute in granulates after mechanic-chemical synthesis (mechanical alloying in attritore) as ultra disperse (0,02—0,05 microns) inclusions [1, 2]. Considering at the given stage technology of reception granulate and products from him (hot ekstruzija on core, machining by cutting,) enough fulfilled, there is a question on necessity and sufficiency of a dispersions-strengthening phase for maintenance of the certain ready material properties - wear proof by temperature constancy, hardness, conductivity. Wide enough interval concentration of dispersion-strengthening phases, namely: conditionally speaking "rough" Al2O3 from 2,3 up to 9,2%mas. and "fein" Ti (C, N) - from 2,0 up to 6,0 %vol. about give the most different effects - from high hardness, but falling conductivity, up to wear proof [1—3]. Saved up resultant can be systematized and interpreted by the some in the best way, that the today's condition of computing techniques and programming allows. Attempts such are constantly undertaken also methods of diagnostics and forecasting of functional properties of powder materials can yield effective results [3, 5]. In particular, for realization of estimations system for powder materials properties on simplex-trellised plans active and passive (virtual) the fulfilled algorithm of data processing after planned experiment on the equations of various degree regress of the complexity, connecting result (the response, in this case, conductivity, p, % from copper) with influencing factors (structure, coordinates on axes of 3 componential simplexes (fig.) and construction original a “planimetric card " can be used. The settlement system leans on the window interface (see fig.) where the basic objects and elements of management settle down: a choice of type a simplex of the diagram (cubic, the fourth degree - she on fig., the eighth degree), the table for gathering and processing’s of the information that it is possible to count adaptive system of gathering and processing of experimental data. Set of three parameters of coordinates x1-x2-x3 (relative coordinates on three parties of simplex, for example 50 % Al2O3 (tab.) correspond to his absolute maintenance of 4,6% mas) unequivocally defines a site experimental (or diagnosed) points on the simplex diagram, and the required result (y(p)-response) is a numerical method on equation-model of components system, which for considered factorial space of components concentration Cu-Al2O3-Ti (C, N ) it is designed on experimental data and it is resulted under the diagram. In the working table (on fig. - at the left) discrete values of responses in the central points, received by graphic constructions on the screen which accuracy is defined by accuracy of positioning of the cursor (at scaling- increase / reduction - are given - "picture" accuracy varies). Introduction of experimental data and their automated processing on the set algorithms allow the user to receive the discrete response of each point limited 2D- simplex of space on coordinates of initial mixture of composite, and to receive functional dependences, here p=f (x1-x2-x3). On it to a basis the library of powder materials with a guaranteed level of various service characteristics can be created.

1. Shalunov E.P., Matrosov A.L., Vendland S. Vysoeffektivnye tokos'jemnie ustroistva electropoezdov… // Proc. Conf. « Modern technology, materials and products of powder metallurgy », Rostov on-Don., 2002, PP. 22—24 Joint-stock company " Uralelectromed" // CD. 2001
2. Lyulko V.G, Shalunov E.P. et al. 3D/2D-Modell // Proc.of Plansee-Seminar. 2001, Vol.1. PP. 352—359
3. Lyulko V.G., etc. Technology of composite powders thermosyntesis in vibrating layer //Report of URGTU, Novotcherkassk - 2000, PP. 148—155.
4. Lyulko V.G., Jmajlov B.B., etc. Algorithm of construction for estimations system of powder materials properties \ Proc .Conf "The newest technologies in PM .Kiev, 2003, PP. 30—31

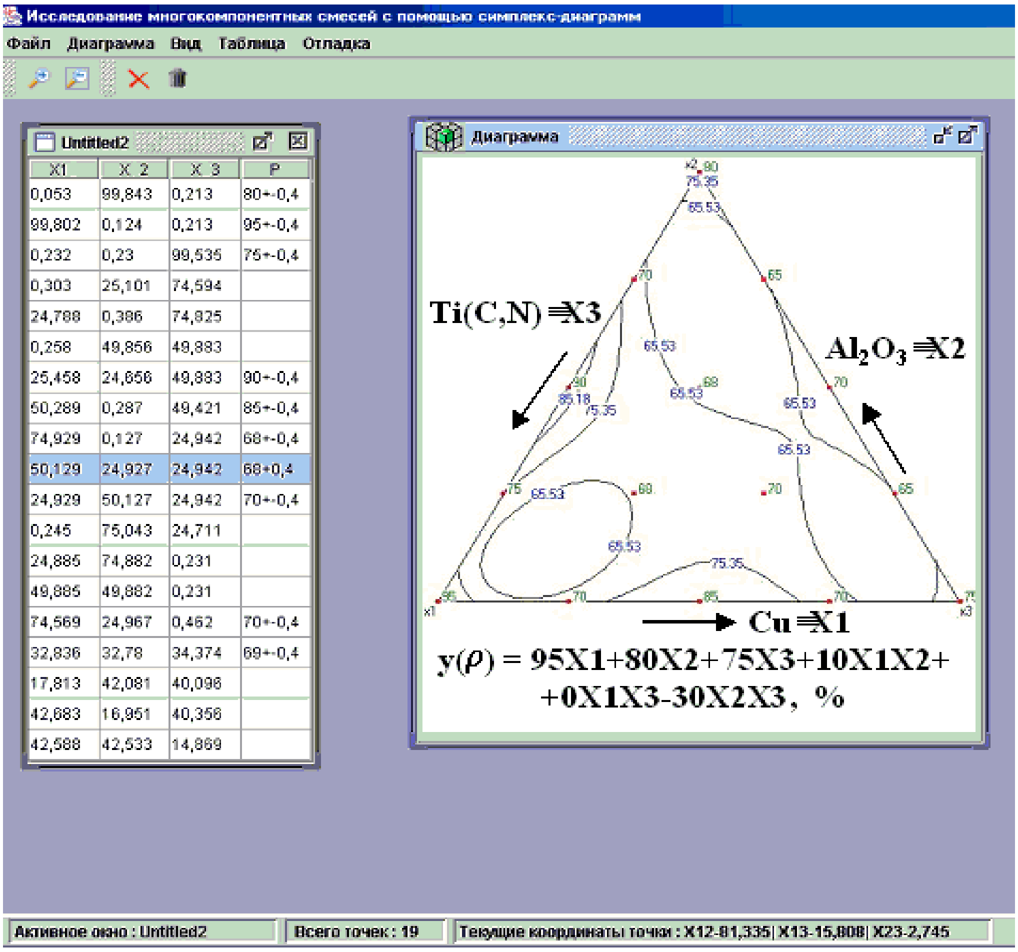

| X1 | X 2 | X 3 | P |
|---|---|---|---|
| 0,053 | 99,843 | 0,213 | 80+-0,4 |
| 99,802 | 0,124 | 0,213 | 95+-0,4 |
| 0,232 | 0,23 | 99,535 | 75+-0,4 |
| 0,303 | 25,101 | 74,594 | |
| 24,788 | 0,386 | 74,825 | |
| 0,258 | 49,856 | 49,883 | |
| 25,458 | 24,656 | 49,883 | 90+-0,4 |
| 50,289 | 0,287 | 49,421 | 85+-0,4 |
| 74,929 | 0,127 | 24,942 | 68+-0,4 |
| 50,129 | 24,927 | 24,942 | 68+0,4 |
| 24,929 | 50,127 | 24,942 | 70+-0,4 |
| 0,245 | 75,043 | 24,711 | |
| 24,885 | 74,882 | 0,231 | |
| 49,885 | 49,882 | 0,231 | |
| 74,569 | 24,967 | 0,462 | 70+-0,4 |
| 32,836 | 32,78 | 34,374 | 69+-0,4 |
| 17,813 | 42,081 | 40,096 | |
| 42,683 | 16,951 | 40,356 | |
| 42,588 | 42,533 | 14,869 | |

$$y(\rho) = 95X1+80X2+75X3+10X1X2+ +0X1X3-30X2X3,\ \%$$

Активное окно : Untitled2
Всего точек : 19
Текущие координаты точки : X12-81,335| X13-15,808| X23-2,745

Fig. The simplex – diagram, table and regress equation p =f (x1-x2-x3) "structure - response" of system Cu-Al2O3-Ti (C, N).

# CONJUGATE UNSTEADY HEAT AND MASS TRANSPORT IN THE VAPOUR-PHASE FABRICATION OF 3D COMPOSITE WITH SiC MATRIX

**Kulik A.V., Kulik V.I. (1), Bogdanov M.V., Ramm M.S. (2)**
Soft-Impact Ltd., St. Petersburg, Russia, E-mail: kulik@softimpact.ru
(1)Baltic State Technical University, St. Petersburg, Russia,
(2)Ioffe Physical Technical Institute, RAS, St. Petersburg, Russia

Many modern ceramic materials exhibit high melting temperature, high compression strength, thermal and chemical stability. Thus they are potentially advantageous for variety of applications, particularly at high temperatures and in aggressive environment where metals can not survive. The major problems with the monolithic ceramics, restricting their application, are low tensile strength and brittleness. Mechanical properties of the monolithic ceramics can be dramatically improved by embedding a reinforcement phase (particles, whiskers, or fibres), i.e. producing a Ceramic-Matrix Composite (CMC). Among all fibre-reinforced CMC, of great importance are composites with SiC matrix which can be reinforced by ceramic or carbon fibres. These materials possess heightened resistance to mechanical shock and thermoplegia, have high chemical stability, erosion resistance and specific mechanical characteristics and can operate at very high temperatures.

One of the most attractive methods for production of ceramic-matrix composites is Chemical Vapour Infiltration (CVI) [1—2]. This method is based on deposition of the ceramic matrix on the heated fibres by chemical decomposition of gaseous precursors infiltrating through a fibrous reinforcing substrate or "preform". The most widely used commercial process is isothermal CVI (ICVI) where the entire preform is kept at a constant temperature. The main drawbacks of the method are nonuniform densification of the preform and a high residual void fraction (porosity) of the material. To achieve relatively uniform infiltration, the mass transport rate must be high relative to the deposition rate. This leads to extremely long process duration, sometimes up to several weeks. Hence, one of the most important problems in ICVI research is finding the optimal values of technological parameters providing minimal infiltration time and required quality. Obviously, experimental research and optimization of the ICVI technology is very time consuming and expensive.

Lately, numerical modelling has become a helpful tool for the ICVI study and optimization. At present, there are a number of publications on the CVI modelling [3—5]. These works generally deal with one-dimensional models describing phenomena only in the preform ignoring transport processes in the whole reactor.

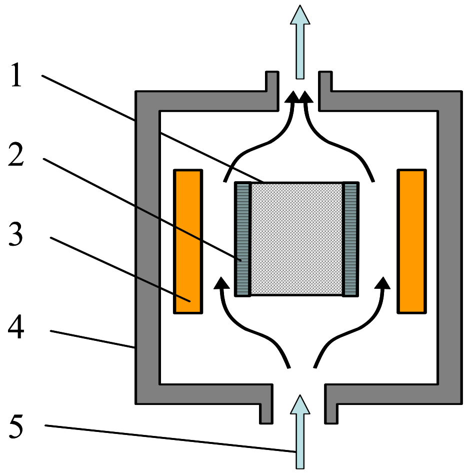

Fig. 1. Schematic ICVI reactor.
1 – graphite susceptor, 2 – fibrous preform, 3 – heater, 4 – chamber, 5 – gaseous precursors

In the present work, 2D model of the ICVI is developed. The model describes conjugate heat and mass transport in the whole reactor (schematically shown in Fig. 1). Thermal field in the reactor is computed accounting for conductive, convective and radiative heat transfer. Multicomponent gas mixture flow in the porous medium of the preform is conjugated with the flow in the chamber and is computed using Navier-Stokes equations and Darcy–Brinkman–Forchheimer flow model. Conditions of continuity of heat and mass fluxes are set at the interface between the porous preform and the gas region of the chamber. To allow for the preform densification, the quasi-steady state approach is employed. Within this approach, the overall simulation is carried out by solving a series of steady-state problems at various discrete moments of growth.

The preform is considered as a complex porous medium representing a bulk structure reinforced by fibre bundles in three orthogonal directions. Such multidirectional preform includes pore systems of various scale – between fibres in bundles (intra-bundle pores) and between bundles (inter-bundle pores). The evolution of the preform structure is computed basing on the rate of the heterogeneous chemical reaction of the matrix material deposition. Effective heat conductivity of the porous medium is evaluated from the local value of the porosity using the method of ref. [6].

We analyse production of SiC-matrix composite by ICVI from methyltrichlorosilane ($CH_3SiCl_3$) diluted by hydrogen. The chemical deposition of SiC is assumed to occur in the following reversible reaction of the MTS decomposition:

$$\mathrm{SiCl_3CH_3(g) \leftrightarrow SiC(s) + 3HCl(g)},$$

allowing for inhibitory effect of HCl.

We analysed the influence of the ICVI operating conditions, namely the MTS concentration in the ambient gas, the pressure in the reactor, the susceptor temperature, on the process duration (densification time) and the quality of the composite – the average residual porosity and distribution in the preform of the residual porosity.

## References

1. S.M. Gupte, J.A. Tsamopoulos. Densification of Porous Materials by Chemical Vapor Infiltration. – J. Electrochem. Soc., 136, 1989, pp. 555—561.
2. T.M. Besmann, B.W. Sheldon, R.A. Lowden, D.P. Stinton. Vapor-phase Fabrication and Properties of Continuous-filament Ceramic Composites. – Science, vol. 253, 1991, pp. 1104—1109.
3. H.-C. Chang, T.F. Morse, B.W. Sheldon. Minimizing Infiltration Times during Isothermal Chemical Vapor Infiltration with Methyltrichlorsilane. – J. Am. Ceram. Soc., 80(7), 1997, pp. 1805—1811.
4. V.I. Kulik, A.V. Kulik, M.S. Ramm, Yu.N. Makarov. Modeling of SiC-Matrix Composite Formation by Isothermal Chemical Vapour Infiltration. – Accepted for publication in J. Cryst. Growth (2004).
5. V.I. Kulik, A.V. Kulik, M.S. Ramm, Yu.N. Makarov. Modelling of SiC-matrix composite formation by thermal gradient chemical vapour infiltration. – Accepted for publication in Mater. Sci. Forum (2004).
6. В.И. Кулик, А.В. Кулик, М.С. Рамм. Определение коэффициентов теплопроводности многонаправленных пористых волокнистых каркасов. Тезисы 2-й международной научной конференции РКТ-2003, М., in press.

# MODELING OF SiC AND AlN CRYSTAL GROWTH BY SUBLIMATION

**Demina S.E., Bogdanov M.V., Kalinin D.S., Kulik A.V.,**
**Matukov I.D., Ramm M.S., Makarov Yu.N.(1)**
Soft-Impact Ltd., P.O. Box 83, St.Petersburg 194156, Russia, ramm@softimpact.ru
(1)Semiconductor Technology Research, Inc., Richmond, USA
P.O.Box 70604, Richmond, VA 23255-0604 USA, yuri.makarov@semitech.us

Silicon carbide (SiC) and Aluminum Nitride (AlN) are advanced materials widely used in high-power, high-frequency, high-temperature electronics and optoelectronics. The breakthrough in their applications in the middle of the 1990s was associated with the development of blue/green light emitting diodes and lasers [i], high-power high electron mobility transistors [ii], and the first commercially available high-voltage Schottky diodes [iii]. However, further progress in the wide-bandgap semiconductor technology is primarily hindered by the lack of homoepitaxial substrates suitable for the epitaxy of multi-layered high-quality device structures.

The conventional methods of bulk crystal growth, like Czochralski growth from the melt, are inapplicable to the fabrication of SiC and AlN crystals due to extremely high melting temperatures (2830 °C and ~2400 °C, respectively), a high volatility of the vapor species, and a high melt reactivity. Therefore, an alternative, sublimation technique, is world-wide spread for growing these materials. Increasingly larger crystals impose the increasingly stringent requirements on the choice and control of the operating conditions. Additionally, the cost of an individual growth run rises significantly with the crystal size. All this makes the growth modeling an important tool applicable to every stage of the technology devlopment, from the growth system design to the optimization of the growth conditions, including the materials utilization efficiency and other economical factors.

This paper reviews the advances in the modeling of SiC and AlN bulk crystal growth by sublimation with the focus on specific features of this growth technique. Here, we focus on the basic mechanisms underlying the sublimation growth and on the appropriate modeling approaches. We discuss the key aspects of sublimation growth of SiC and AlN and show how modeling can help to solve a number of practical problems [iv].

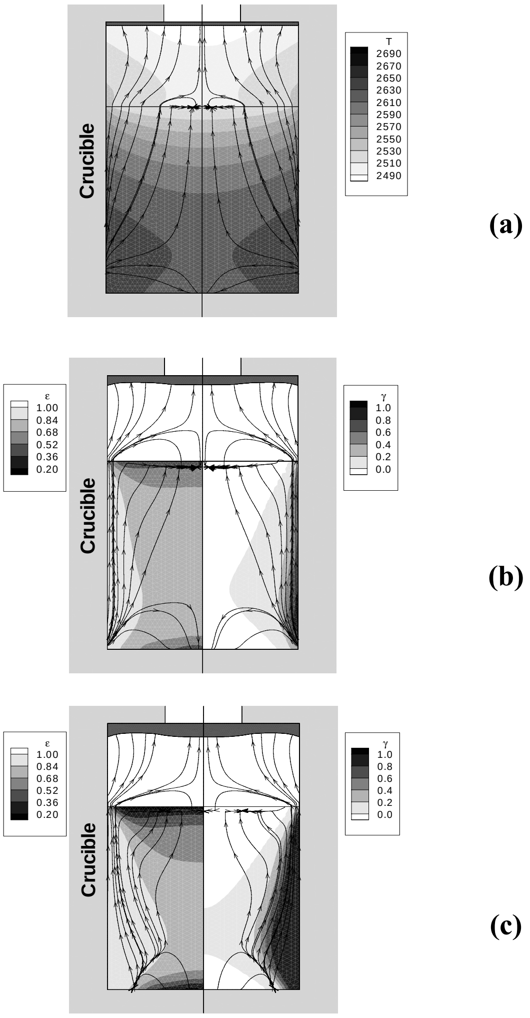

**Fig. 1**. Powder evolution in SiC growth. Streamlines and temperature (in Kelvin) distribution at the start of the growth (a). Streamlines, porosity $\varepsilon$ (left hand side) and graphitization degree $\gamma$ (right hand side) distribution after 10h (b) and after 20 h (c) of growth. Initial porosity is 0.8.

As the temperature distribution in the growth chamber is the most critical factor in the sublimation technology, we discuss in detail specific features of heat transfer with the focus on the porous materials normally involved in the growth system: powder source, thermal insulation, and graphite. In particular, we suggest an empiric formula estimating the heat conductivity of porous graphite $\lambda_{gr}$ [v]. The equation operates with parameters available from the supplier (room temperature heat conductivity and material porosity) and predicts $\lambda_{gr}$ at a high temperature. The species transport in porous source is simulated using advanced approach accounting for a heterogeneous chemical reactions occurring on the granule surface [vi]. A 2D model of mass transport in the powder charge accounting for evolution of the powder source during long-term growth of bulk SiC crystals is suggested. The model operates with such powder parameters as the local porosity, granule size and graphitization degree. In accordance with observations, intensive SiC evaporation accompanied by graphitization in the hot zones along crucible walls is predicted, as well as recrystallization on the top of the powder charge, resulting in formation of a dense material. Fig. 1 presents temporal variation of the powder parameters and flow pattern in the porous source.

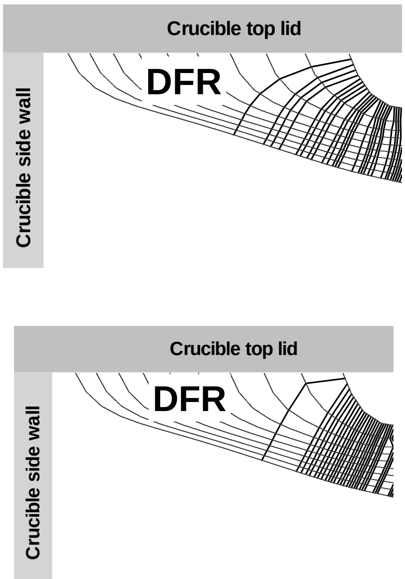

**Fig. 2**. Evolution of the crystal interface (fragment is shown) and threading dislocation traces in SiC crystal spreading. Top and bottom plots present behavior of screw and prismatic dislocations, respectively. Dislocation free region (DFR) arising from the dislocation bend on the crystal periphery is indicated.

A special analysis is made to find a correlation between the growth conditions and defect distribution in the grown crystal, with the focus on dislocations produced by temperature gradients. The high-temperature dynamics of gliding dislocations and consequent plastic stress relaxation in the material is examined. Dynamics of threading dislocations is analyzed in terms of energetic approach, successfully used for SiC thin films [vii] and generalized recently for bulk crystal growth (Fig. 2).

To optimize the growth system design and operating conditions, we suggest an inverse-problem approach instead of commonly used trial-and-error methods. This simulation procedure has proved quite efficient for getting design solutions, which could hardly be found by the conventional methods. In particular, we demonstrate high efficiency of the inverse modeling for finding the growth conditions that provide crystals of desired shapes.

In conclusion, the prospective of global modeling of crystal growth from the vapor and still open questions are discussed.

---

[i] S. Nakamura, G. Fasol, The Blue Laser Diode, Springer Verlag, Berlin 1997.
[ii] S.J. Pearton, F. Ren, A.P. Zhang, K.P. Lee, Mater. Sci. Engg. **30** (2000) 55.
[iii] D. Peters, K.O. Dohnke, C. Hecht, D. Stephani, Mater. Sci. Forum **353—356** (2001) 675.
[iv] M.V. Bogdanov, S.E. Demina, S.Yu. Karpov, A.V. Kulik, M.S. Ramm, and Yu.N. Makarov, Crystal Research and Technology **38**, 3—5 (2003) 237—249.
[v] E.L. Kitanin, V.V. Ris, A.A. Schmidt, S.E. Demina, S.Yu. Karpov, and M.S. Ramm, Abstracts: IV International Seminar on SiC and Related Materials (ISSCRM-2002) 30-31 May, 2002, Novgorod of Great, Russia, 24.
[vi] A.V. Kulik, M.V. Bogdanov, M.S. Ramm, S.Yu. Karpov, and Yu.N. Makarov, Accepted for publication in Mater. Sci. Forum (2004).
[vii] A.K. Semennikov, S.Yu. Karpov, M.S. Ramm, A.E. Romanov, and Yu.N. Makarov, Accepted for publication in Mater. Sci. Forum (2004).

# CONDITIONS FOR SELF-PROPAGATING HIGH-TEMPERATURE SYNTHESIS IN THIN FILMS

**Grinchuk P.S., Rabinovich O.S., Pavlyukevich N.V.**
Luikov Heat and Mass Transfer Institute NASB, Minsk, Belarus
15 P. Brovka Str., Minsk, 220072,Belarus, E-mail: gps@hmti.ac.by

The phenomenon of self-propagating high-temperature synthesis (SHS) was discovered about 40 years ago and since that it had been firmly implanted in practice. Today SHS is one of the most practically feasible and economically efficient methods for manufacturing various materials such as intermetallics, carbides, oxygen-free ceramics and functionally graded materials. SHS-technologies find their applications for the development of new nanostructured materials as well. The feasibility of SHS in multilayer nanofilms was shown in a number of experimental works. The films synthesized by this method have nanocrystalline structure and unique physical properties. These properties can be used for resolving a variety of practical problems. In particular, unique hardness of titanium-based multicomponent nanofilms (Ti—B—N, Ti—Al—N, Ti—Si—B, Ti—B—C—N) allows obtaining thin and durable protective coatings. The small size of ferromagnetic nanoclusters of Fe, Ni, Co in a dielectric matrix of $Al_2O_3$ or $SiO_2$ is a basis for designing devices with a high density of magnetic and magneto-optical information recording. Besides, a useful microelectronic application of SHS in nanofilms is microwelding and creation of microcontacts (Ni/Al, Fe/Al, Zr/Al, $CuO_x$/Al, Nb/Al, Cu/Zr, Co/Cu, Co/Si and some other systems). The advantages of SHS in multilayer nanofilms are (i) spatial separation of initial reactants before caring out the synthesis; (ii) accelerated diffusion ensuring a high rate of synthesis and cooling of the products; (iii) a possibility to control these processes and obtain a specified phase composition and size of nano-crystallites; (iv) a possibility of manufacturing functionally graded materials.

In the most practical applications, SHS is carried out in nanofilms deposited on relatively thick inert substrates as compared with the thickness of synthesized films. Preliminary estimations have shown that in this case the heat diffusion rate from a synthesized film to the substrate is very high. This circumstance does not allow the propagation of a self-sustaining synthesis wave without the use of an additional heater on which the substrate should be placed. The problem of determining the conditions when the synthesis of nanofilms in such systems is possible in the SHS mode (in other words, the determination of an allowable relationship between the thickness of the reactant films and substrate, their thermophysical properties, the synthesis rate and temperature of the heater), is of primary importance for the development of particular technological applications. With the purpose of a deeper investigation of the problem we developed a mathematical model of the process and performed numerical simulation of the synthesis wave propagation in nanofilms.

## 2. PROBLEM STATEMENT

To correctly formulate the problem of SHS in thin films it is necessary to consider a conjugate problem, i.e. perform self-consistent calculation of the temperature field in both the film and the substrate placed on the heater. The estimations show that the film is practically isothermal in the direction normal to the substrate due to its small thickness. Therefore, the temperature of the film depends only on the longitudinal coordinate. Thus, the energy equation for the film has the following form:

$$\frac{\partial T_{\mathrm{f}}}{\partial t} = a_{\mathrm{f}} \frac{\partial^2 T_{\mathrm{f}}}{\partial x^2} - \bar{\alpha}_{\mathrm{fs}} \left( T_{\mathrm{f}} - T_{\mathrm{s}}\big|_{y=0} \right) -$$

$$- \bar{\alpha}_{\mathrm{r}} \left( T_{\mathrm{f}}^4 - T_0^4 \right) + \frac{Q}{c_{\mathrm{f}}} W(T_{\mathrm{f}}, \eta) \cdot \qquad (1)$$

Here subscripts *f* and *s* designate the film and substrate, respectively. Factors $\bar{\alpha}_{\mathrm{fs}}$ and $\bar{\alpha}_{\mathrm{r}}$ describe heat exchange between the film and substrate and radiation heat exchange between the film and the reactor walls, correspondingly. The last summand in Eq. (1) describes heat release due to a chemical reaction in the film. The equation of chemical kinetics has the form:

$$\frac{d\eta}{dt} = W(T_{\mathrm{f}}, \eta) \qquad (2)$$

$$W = k_0\, exp\left(-\frac{E}{RT_f}\right) H(T_f - T_{in})(1-\eta) \qquad (3)$$

In equation (3), the reaction initiation temperature $T_{in}$ is present: reaction in the film begins only after attaining this temperature. The existence of such temperature barrier is a known fact in the SHS theory. The initial condition for the conversion degree in the film is $\eta(x)\big|_{t=0} = 0$.

The energy equation for the substrate has a form:

$$\frac{\partial T_s}{\partial t} = a_s\left(\frac{\partial^2 T_s}{\partial x^2} + \frac{\partial^2 T_s}{\partial y^2}\right) \qquad (4)$$

The boundary conditions for the substrate were set as follows. At the lower boundary, the temperature of the substrate is equal to that of the heater. At the upper boundary, heat exchange of the substrate with the film takes place (third kind boundary condition). Another heater placed at the left-hand side of the sample-performed initiation of combustion. At the right boundary of the system, adiabatic conditions were set. The system of equations was converted to a dimensionless form for numerical integration. The numerical integration and obtaining of a non-stationary solution of the dimensionless system was carried out with the use of a common finite-difference scheme.

## 3. SIMULATION RESULTS

The combustion of a two-layer Al/Ni film was modeled. The ratio of the layer thicknesses corresponds to the stoichiometry of product $NiAl_3$.

Numerical simulation of the process has confirmed the conclusion of the preliminary analysis about the existence of two modes of nanofilms synthesis. They are (i) the annealing mode when the reaction is slow and product formation occurs over the whole film length, and (ii) the SHS mode, for which a quasi-stationary self-sustaining wave of the chemical reaction propagates along the film. Also, simulations have allowed determining a parametric boundary between these modes and their characteristics. An example of simulation results is presented in the table.

A principal difference between these two modes of film synthesis consists in the values of the interaction completion time: SHS is a much faster process than annealing. For this reason, the properties of films obtained in these modes can be considerably different. As a result of a very high rate of synthesis and cooling in the SHS mode, metastable products are formed and fast quenching of these products occurs. The rate of synthesis and cooling determines a size of crystallites formed during the synthesis. An upper estimation of the crystallite size is the thickness of the reactant monolayer. However, its size can be determined more accurately using the residence time of a given film area in the combustion zone, when the temperature is sufficiently high for effective mutual diffusion of reactants. For example, for initial $Al/Fe_2O_3$ system the characteristic size of iron crystallites formed during interaction change from 3 up to 70 nm depending on the velocity of a synthesis wave. Eventually, the characteristic sizes of nanostructures formed by the synthesis determine unique physical properties of the films.

Table

Parameters and characteristics of SHS in a nanofilm for different film thickness h. The characteristic reaction time is $t_r = 10^{-4}$ s, the temperature of the heater is 450 $^0$C, the film length is 10 mm

| *h*, nm | *Mode* | U, cm/sec | t, s |
|---|---|---|---|
| 50 | annealing | 0 | 8,617 |
| 100 | annealing | 0 | 8,617 |
| 200 | annealing | 0 | 8,617 |
| 250 | SHS | 47,5 | 0,022 |
| 300 | SHS | 53,5 | 0,019 |
| 400 | SHS | 60,7 | 0,017 |
| 600 | SHS | 67,1 | 0,016 |
| 800 | SHS | 70,3 | 0,011 |

Comment: U is the propagation velocity of the combustion wave along a film, t is the time of synthesis.

*The work was supported by the Byelorussian State Research Program “Nanomaterials and Nanotechnologies” (project Nanotech 5,10).*

# INTERPHASE INTERACTION OF ZR-BASED ALLOY WITH REFRACTORY MATERIALS

**Verkhovluk A. M., Shcheretsky A. A., Shumikhin V. S., Bespalyy A. A., Apuhtin V.V.**
Physico-technological institute of metals and alloys of NASU, Kiyv, Ukraine
03680, Kiev -142, GSP, Ukraine; E-mail: metal@ptima.kiev.ua

Zr-Cu based alloys are interesting both for practical application and for theoretical aspect. They can be used as the superconductors, amorphous materials, solders and shape-memory materials. These alloys exhibit of high thermal resistance and mechanical properties. The malting of Zr-based alloys on air have some difficult: chemical composition of alloys can be changed, the materials of crucible can be destructed. The problem of selection of flux and refractory materials for the preparation of Zr-based alloys is actual.

That is why the wetting of some refractory materials with Zr-Cu-Ni-Al alloys have been studied. Iodic zirconium, copper of type M0 (99.95%), nickel of type N0 (99.985%), aluminium (99.99%) were used for the preparation of Zr-Cu-Ni-Al alloys.$Al_2O_3$, $Y_2O_3$, $SiO_2$, $Al_2O_3$-MgO-$Cr_2O_3$, $ZrO_2$-CaO-$SiO_2$, AlN, BCN were used as the refractory materials. The research of interphase properties of Zr-based alloys – refractory material system were studied by the method of sessile drop. It was done in vacuum ($2.266 \cdot 10^{-5}$ Pa.) within the range of temperature from 920 to 1200°C. The time of contact was 10 min. usually. For the some system time of contact under constant temperature was increase up to 40 min.

It was fixed that the dencity and the surface tension of liquid Zr-based alloy are described by next empirical equation:

$$\rho = 5.71 - 0.0013\ (t - 920) \qquad (1)$$

$$\sigma_{lg} = 1527 - 0.15\ (t - 920) \qquad (2)$$

where:

t – temperature, °C

It was fixed, also, that with increasing of temperature and time of contact the decrease of wetting angle is observed for all systems (Table)

Interphase properties between the Zr-based alloy and refractory materials under difference temperatures.

Only when temperature is 985 ˚C the wetting angles is less then 90grad. Heat time of liquid alloy on $ZrO_2$-CaO, $Al_2O_3$ refractory materials at this temperature during 10min. and 40min. leading to decrease of wetting angles down to 55grad. and 30 grad. consequently. The data of wetting of $Y_2O_3$ and $SiO_2$ by Zr-based alloy are differ from all others. The $Y_2O_3$ and $SiO_2$ refractory materials are wetted at 1100˚C and 1020˚C consequently. For the some systems besides decreasing of $\theta$ also impregnation of refractory materials is observed. That is why the color of refractory materials is change. Decreasing of interphase tension and increasing of chemical interaction on the interface liquid alloy – refractory materials are cause of increase the wetting when the temperature and time of contact are increase.

Zirconium is very chemically active element. That is why it reduces almost all oxides. Due to difference between diffusion velocity of oxygen and such elements as Al, Mg, Y etc oxygen desolves in crystallographic lattice of Zr, and reduced elements mainly concentrate in interaction zone, that is to say, on the interface solid – liquid. Also formation of chemical bond metal – oxygen in zone of contact with the help of surface oxidation is enable. After formation of this bond interaction of oxide's coatings of metal and oxides that is to say, with stabilized additives of investigated ceramics is observed. These coatings are bound with strong ionic bond with anion of solid oxide, building its lattice. Ions of oxygen from the liquid metal concentrate on these positive – charged points (cations of metal). It leads to formation of complex oxides of liquid phase. It was noted, that the BCN, AlN refractory materials were wetted with Zr-based alloy right after occurrence of liquid phase. It is possibly, the chemical interactions in this systems run in solid phase too and oxides, carbides and oxicarbides creates.

# MATHEMATICAL SIMULATION OF STRUCTURE AND RESISTIVITY OF VACUUM DEPOSITS OF BINARY SYSTEMS WITH BOUNDED SOLID SOLUBILITY

**Kurochkin V.D., Kravchenko L.P., Minakova R.V.**
Institute for Problems of Material Science, NAS of Ukraine, Krzhizhanovsky str. 3, 03142, Kyiv, Ukraine, vkur@ipms.kiev.ua

Composite materials, based on Cu and Cr(Mo) are finding expanding application as electric contact materials for medium-current vacuum switching units. For the last time such materials are produced by electron-beam evaporation technology. Deposits, produced by this technology, have sandwich-type structure with great concentration spread in each layer (1 – 99 % of Cr(Mo)) and thickness of intercalation (~1 – 500 μm). Each layer consists of colony of columnar grain with main axis directed along the condensation flux [1].

This work presents experimental study and geometric-probabilistic approach with Monte Carlo simulation to investigate structure formation of such systems. It is assumed that crystal grains grow on nucleus of crystallization with given concentration. Atom hitting onto crystalline surface consisting of the same atoms results in its growth. Since a system with bounded solid solubility is discussed, atoms of opposite sort may also fix on it, if on the surface there are nucleation centers. These atoms give rise to a daughter crystalline particle of another sort. Growing onto the parent crystalline surface it may partly cover it and diminish probability of atom hitting onto lower crystal and suppress its growth. But lower crystal also is growing and may outrun in growth daughter crystal and interlock it. Crystals of similar sort in result of diffusion may coalesce not interfere to each other but crystals of opposite sort compete for the free volume. Result of such competition depends on proportion of flux density of each component, nucleus concentration for Cu growth on Cr and respectively – Cr on Cu, i.e., on interstitial-producing jogs. The crystal grains supposed to have simplified shape as a cube or parallelepiped.

The model discussed is a typical stochastic process. Probability $P_\alpha$ of an atom hitting of a sort $\alpha$ onto a surface area S at the given flux density $J_\alpha$ in a time slice $\Delta t$ was calculated by means of stochastic Poisson process [2]:

$$P_\alpha = 1 - \exp(-SJ_\alpha\Delta t), \quad (1)$$

where parameter of distribution - $SJ_\alpha$ was calculated according to the statement of the problem. The probability of the onset of daughter crystalline growth is considered to be complex event - the probability of atom hitting onto a crystal and the probability of presence of nucleation center on it. This probability was calculated by means of binomial distribution [2].

This mechanism predicts essential instability of the process. Small fluctuation of flux densities, increase for instance, results in avalanche increase of surface of such crystal. Growing rapidly they interlock crystal of other sort. Typical structure of lateral section of Cu-Cr condensate is shown on the Fig.1. Metallographic specimen was ion-beam etched by argon ions in glow discharge.

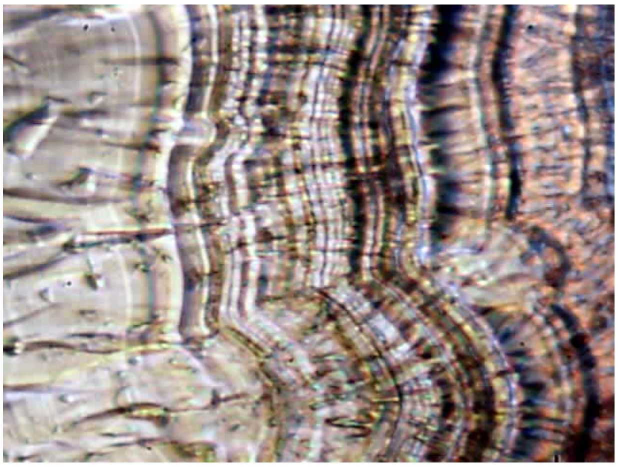

Fig.1. Structure of lateral section of Cu-Cr condensate. Light tone corresponds to the layers enriched by Cr, dark - by Cu.

Nucleating centers concentration significantly influence on condensate composition even at constant flux densities (Fig.2).

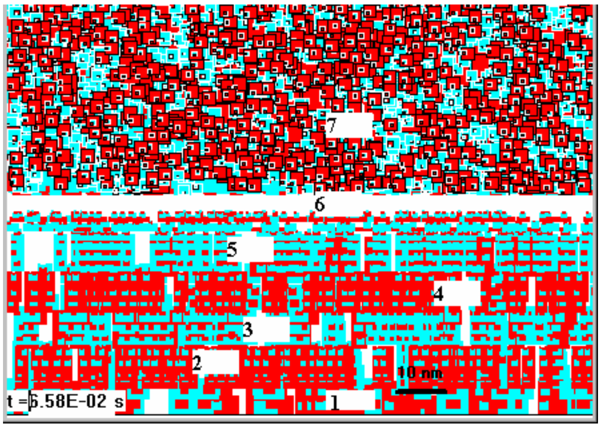

Fig. 2. Formation of sandwich-type structure of Cu-Cr condensate at variation of nucleation centers concentration. $J_{Cu}$, $J_{Cr}$ = $1 \cdot 10^{23}$ $1/m^2s$. 1 - $C_{nucl}$ = 0.001 $C_{Cr} \approx 50$ %; 2, 4, 6 - $C_{nucl}$ (Cu on Cr) = 0.007, $C_{nucl}$ (Cr on Cu) = 0.001, $C_{Cr} \approx 15 - 25$ %; 3, 5 - $C_{nucl}$ (Cu on Cr) = 0.001, $C_{nucl}$ (Cr on Cu) = 0.007, $C_{Cr} \approx 75 - 85$ %; 7 - top view of the surface of crystallization.

Competitive mechanism discussed results in formation nano-sized in cross-section Cu- and Cr-based columns directed along condensation flux. Cross-section of a column depends on nucleation centers concentrations and on Cu to Cr fluxes ratio. It ranging from several tens of nm to part of nm. Columns have entrapping of another phase having 1 - 1.5 nm (Fig.3).

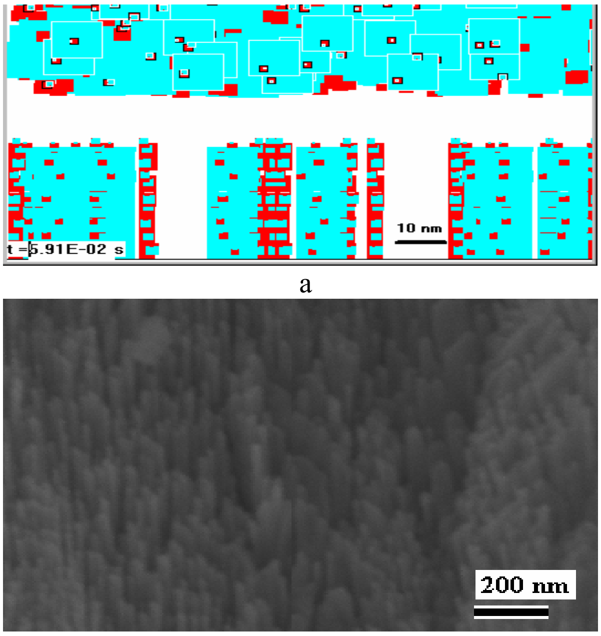

a

b

Fig. 3. Formation of columnar crystal grain; a - simulated structure; b- electron micrograph of a structure.

Decreasing in Cr flux density results in significant drop in Cr content compared with expected value. So at Cu to Cr ratio 1:0.4 a layer is formed containing 7 – 9 at % of Cr instead of expected 28.5 at %.

Calculation of resistivity was done on assumption that equivalent circuit consists of joining-up in parallel Cu-based and Cr-based columns of crystals having cross-section area and composition obtained from mathematical model .

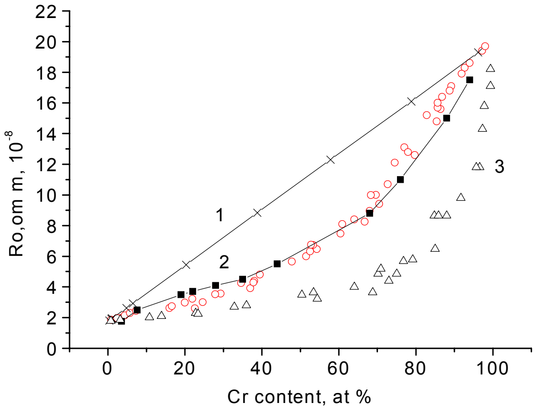

Fig.4. Dependence of resistivity on Cr content in condensate. $C_{nucl}$ = 0.001, $J_{Cu}$ = $1 \cdot 10^{23}$ $1/m^2s$. 1-additive low; 2 - experimental data (solid line), circle points - calculation by the model; 3 - calculation at assumption that columns consist of pure components.

Results obtained show that proposed model reasonably good describes real system. Process of competitive crystalline growth for system with bounded solid solubility is essentially unstable. This exhibits itself in significant variation of condensate composition at small fluctuations of ambient conditions. Taking into account stochastic nature of the process random fluctuations also contribute into sandwich-type structure formation.

## REFERENCES

1. Хоменко Е.В., Минакова Р.В., Осокин В.А., Гречанюк Н.И. Структура и свойства медно-хромовых конденсатов и перспективы их использования в качестве вакуумных контактов. - Сб. Электрические контакты и электроды. - Киев.: 2001. - С.12 - 22.
2. Смирнов Н.В., Дунин-Барковский И.В. Курс теории вероятностей и математической статистики. - М.: Наука, 1969. - 511 с.

# DESIGNING OF OPTIMUM CONSTRUCTIONS OF A LAYERED POWDER COMPOSITE BASED ON $ZrO_2$ AND Ni

**Tkachenko L.N., Maydanyuk A.P., Panichkina V.V., Shtern M.B.**
Frantsevich Institute for Problems of Materials Science of NASU
3, Krzhizhanovsky St., Kiev, 03142, Ukraine, E-mail: tkach@ipms.kiev.ua

The most effective approach to carrying out the optimization of rigidity and pliability of a layer structure due to the special layer's position and the determination of their sizes is the experimentally- analytical one. At that the model of layer structure behavior under the influence of mechanical or thermal loadings (or both at once) is developed at first, and then the reaction adequacy of the developed model on these loadings is established with help of experimental data. The researches of model's sensitivity to change of the input and structural data, which are included in the criterion of optimization of a layer construction, will be carried out after the specification of the model. Then the optimization of rigidity and pliability of a layer structure in the field of thermomechanical, constructive and technological parameters will be carried out.

According to the given approach the generalized thermomechanical model of the layered composite behavior under the action of thermal loadings was developed. The connection of the layers in this model was considered to be ideal. The model is completed by the ratio between the local pressure and deformations, which in contrast to the existing ones, allows considering the influence of the distant layers properties on the strained state and deformations within the limits of the given layer. Under the certain conditions (first of all connected with the structure of a temperature field) the given model assumes nonlinearity of dislocations within the single layer (considering the irreversible effects). It leads to the non-uniform distribution of pressure within the single layer. The model allows considering both the presence of restrictions on the dislocation of layers finite elements and their behavior in the presence of free side surfaces. Proposed ratio transform into the known Pagano′s model if the movement of the layers is coordinated.

The experimental specimen in the form of five layers cylinder, in which two layers of nickel are placed between the three layers of zirconium dioxide, was investigated (Fig. 1). The layers should be counted from the bottom up to the top. The cylinder is under the action of slow thermal loading, i.e., the top base is heating up to 700 K and on the bottom base the temperature is 300 K. There is no thermal flow through a side surface.

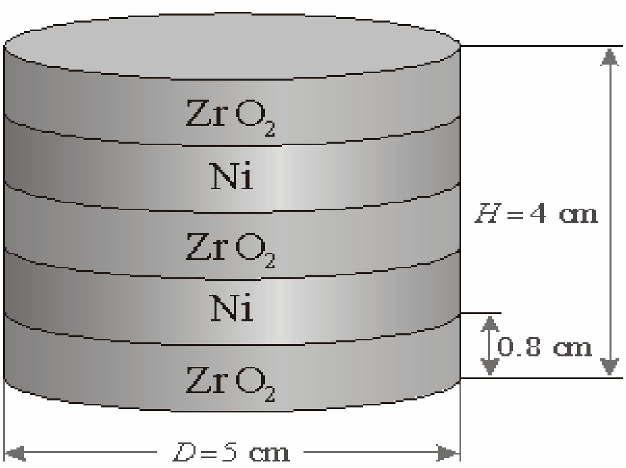

Fig.1. The experimental specimen.

It is provided, that the pressure of deformation equals to zero in an initial state at temperature 300K There is no external mechanical loading, and the only mechanical limit condition is the attaching of all units of finite-element grid with coordinate **r**=0 in cylindrical coordinate system along the radius **r**. These units are found on the **z** axis.

There is the non-uniform field of stressis formed in the sample under action of temperature. The sum of three composite deformations (elastic, temperature and plastic) fit with this field. Corresponding field of temperature deformations is defined by the field of temperatures the sample volume and by the temperature coefficient of expansion the $ZrO_2$ and Ni materials. According to this statement the problem put by was solved as untied, i.e. two more sub-problems were solved in series:

1) Permanent heat problem. Steady-state temperature field was defined according to this problem and fit with the temperature difference

(200 and 400 K) in the top and the bottom bases of the cylinder;

2) The definition of strain-stress state of the experimental sample under action of monotonous volumetric thermal deformation, which fit with the getting of necessary finite temperature field from the first subproblem. The second subproblem was being solved in two variants: elastic behavior of $ZrO_2$ and Ni layers was taken into account for the first variant and elastic behavior of $ZrO_2$ and plastic Ni layer for the second one.

The algorithm, similar to the finite elements method was developed for the solving the problem put by.

The reaction of a layered composite to thermal loading was being estimated relying on the analysis of temperature fields, loadings, displacements and strains in the sample. The last three fields were defined for both thermo-elastic model of composite behavior and thermo-elastic and plastic model.

The character of temperature field in the sample is linear change of temperature in $ZrO_2$ layers steady temperature and in Ni layers; i.e. it does not depend on Ni layer thickness.

The analysis of average stress and Misses stress were carried out for the estimaion of stress fields. The average stress is the highest in the fourth layer at the centre of the cylinder (they change far more in thermoelastic model composite material behavior and grow as the temperature raises). Intensity of Misses stress is the smallest at the bottom base of the cylinder, and then they increase from the first layer of the cylinder up to fourth and come down in the volume of the last layer, reaching a slight magnitude on the top base of the cylinder (Fig,2).

The radial strains fields increase nonlinearly from the bottom base up to the top of the cylinder in both models of a layered composite behavior. The strains also grow as the temperature raises, so does the axial strains.

The displacement fields are also nonlinear on the cylinder volume. The displacement are the highest on the top base of the cylinder around its side surface. They are also growing with the temperature increase.

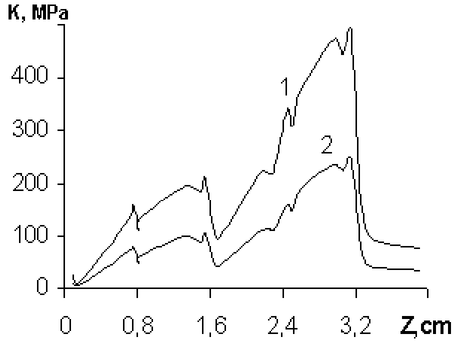

Fig.2. Intensity of Misses stress at ΔT, K:
1 – 400, 2 – 200.

The tentative recommendations relatively to the optimization of layer structure due to the optimal layers allocation and the choice of its geometrical sizes were made relying on the analysis of known results. The most important of them is the necessity of significant decrease of Ni layers thickness and non-uniformity of $ZrO_2$ layers thickness. In this case the temperature gradient of $ZrO_2$ layers will decrease if the cylinder altitude is constant, and also the opportunity of getting the given type of pressure on the cylinder height will appear.

More detailed recommendations can be received after the establishment of adequacy of the developed model of a layered composite behavior considering respective experimental data. After that the realization of a layer construction optimization (according to the criterion of optimization of this construction in real running conditions) is possible.

# DEFECT FORMATION MECHANISMS AND MODIFICATION OF SEMICONDUCTOR FILMS OF THE COMPOUNDS AIVBVI

**Freik D.M., Galuschak M.A., Ruvinsky M.A., Mezhylovska L.Y.**
Physical-Chemical Institute at the 'Vasyl Stefanyk' Prekarpathian University
57, Shevchenko Str., Ivano-Frankivsk, 76000, Ukraine, E-mail: fcss@pu.if.ua

At first for explanation of influencing technological factors on the electrical-physical properties of lead chalkogenides films PbX (X=S, Se, Te), grown from the vapour phase by "hot wall" method [1], offered the general model of disordering of metallic sublattice by Francle mechanism with the simultaneous formation of different charge states of point defects – from electrical-neutral to the double charged vacancies and interlattice atoms [2]. The offered models permit also to take into account the inlaying tensions in film and type of substrate, as it turned out necessary for the quantitative agreement with experience, and also optimize technological factors of growing films with the optimal values of thermo-electric parameters [3]. An experimental research of formation of metallic phase in case of films synthesis in "hot wall" method is conducted also and given the quasichemical explanation of mechanism of this phenomenon.

Heterogeneities of electric parameters are considered after thickness (their types) in the thin films of lead chalkogenides in case of their growing from the vapour phase, which related to the processes of factional of the hinge-plate, and also at annealing in vacuum and oxygen atmosphere. In the last cases take place processes of ambipolar diffusion both of chalkogen vacancies and electrons, and also oxygen on intergrain borders accordingly. For experimental results the theoretical explanation is given.

An experimental data and results of quasichemical and thermodynamics computations of dependence of the concentration current carriers (n) and atomic defects in films us substrate temperature ($T_S$) temperatures of additional source with lead ($T_{Pb}$), contain by thallium ($N_{Tl}$) for PbTe<Pb>:Tl, and PbSe<Pb>:Tl, temperatures of additional sources of tellurium ($T_{Te}$) and indium ($T_{In}$) for PbTe<Te>:In, grown by "hot walls" method analysis is executed. And by methods of quasichemical and on the basis of use of thermodynamics approaches models of defects formation the computation are offered, and the equilibrium concentration of current carriers and atomic defects depending on content of superstoichiometrical components (Pb) and alloying admixtures is executed (Tl, In). Power parameters, which characterize the defects of crystalline structure, are definite.

Processes, related to influencing electric an active gas (oxygen) on the chemical composition, structural and phase changes, imperfect and electronic films subsystems of lead chalkogenides are explored. Explanations on the basis of model with the complex spectrum of defects and conception of education and disintegration in films of neutral complexes of own defects and alloying admixture of oxygen are offered by us.

Is described the model of generational-recombinational mechanism of defects formation in films in case of alpha-irradiation.

1. Freik D.M., Galushcak M.A., Mezhylovska L.Y. Physics and technology of semiconductor films. — Lviv: Vyscha shcola, 1988. — 152 p.
2. Freik D.M., Prokopiv V.V., Galushcak M.A., Pyts M.V., Mateik G.D. Crystal-chemistry and defect thermodynamics on $A^{IV}B^{VI}$ compounds. — Ivano-Frankivsk: Plai, 1999. — 164 p.
3. Freik D.M., Ruvinski B.M., Ruvinski M.A., Galushcak M.A., Dovgiy O.Y. Influence of internal tension on defect formation on lead telluride films at the vpour phase epitaxy // Journa of the physical chemistry. — 2002. — V.76, — N 2. — P. 367—373.

# SOME PROPERTIES OF SOLID SOLUTIONS WITH THE FLUORITE-TYPE STRUCTURE IN THE $ZrO_2$-$HfO_2$-$Y_2O_3$ SYSTEM

**Lopato L., Shevchenko A., Red'ko V., Pasichny V.**
Frantsevich Institute for Problems of Materials Science of NASU
3 Krzhizhanovsky St., Kiev, 03142, Ukraine, E-mail: dep25@materials.kiev.ua

The last years great attention was paid to create materials based on $ZrO_2$. However, lesser attention was paid to the materials investigation based on $HfO_2$ and $ZrO_2$-$HfO_2$. It can be explained by the expensiveness of hafnium compounds that obstructs its wide use. Nevertheless hafnium oxide is a refractory oxide physical and chemical properties of which are similar to the properties of $ZrO_2$. But $HfO_2$ is characterized by the following specific properties in comparison with $ZrO_2$: higher temperatures polymorphic transformations, lower coefficient of thermal expansion and higher thermochemical stability. For example, the electrolytes based on $HfO_2$ are characterized by higher chemical stability and resistance to fast temperatures change and lower electronic conduction under temperatures above 1200 $^oC$. Moreover, $Zr_3Y_4O_{12}$ rhombohedral phase (δ-phase) can be formed at the temperature below 1400 $^oC$ in the $ZrO_2$-$Y_2O_3$ system in accordance with the system state diagram. This process leads to the disturbance of the materials homogeneity, and, consequently, to the change of materials properties. Compound $Hf_3Y_4O_{12}$ does not form in the $HfO_2$-$Y_2O_3$ system. That is why using the materials based on isomorphic cubic solid solutions $ZrO_2$ and $HfO_2$ with the fluorite type crystal structure it can be expected the absence of δ-transformation and the increase of work efficiency for such systems as oxygen sensors, high-temperature fuel cells, electrochemical oxygen pumps and heaters. A high cost hafnium compounds can be overcome by using the compositional materials including $HfO_2$ as a component.

The ternary $ZrO_2$-$HfO_2$-$Y_2O_3$ system practically is one of the interesting systems in which F-type solid solutions occupy extensive fields on the system liquidus surface, and in wide temperatures range within subsolidus region. Optimum composition of such solid solutions in dependence with their practical use can be selected only after through analysis and study of its properties within wide concentrations and temperatures range.

In the present work special attention was given to the samples preparation and formation, taking into account that the $ZrO_2$-$HfO_2$-$Y_2O_3$ system components have the high melting temperatures (2710, 2820, and 2440 $^oC$ accordingly). Diffusional processes in such systems run very slowly. The distinctive features of this work were using both solid state reaction and chemical (hydrothermal synthesis) methods of the samples preparing and concentrated solar radiation for samples synthesis and their investigation. For the solid-state reaction method of the samples preparation high purity powders of zirconia (99,9 %), hafnia (99,9 %) and yttria (99,99 %) were used as initial materials. Two techniques differed by using sintered or melted materials were developed for the formation of the samples. They permit to assure the samples with high and uniform density and sufficiently high heat resistance to withstand thermal stresses during rapid heating up to melting (several seconds) in the focus of a solar furnace or solar radiation simulators. The samples were prepared from powders of two fractions: a coarse fraction (100-300 μm) produced by screening the material preliminary synthesized at 1550 $^oC$ or the material premelted in a solar furnace and crushed, and fine fraction (1-10 μm) taken at weight ratio 4:1.The samples uniaxially pressed and finally heat treated at 1550 $^oC$ for 2 h. The process of melting of the samples produced in the optimum conditions is not accompanied by the generation of trapped gases and vapors that is important peculiarly carrying out thermal analysis. This fact results in the formation of a “still” surface of the oxide melt with approximately the same thickness over the entire area of the melt. After overlapping the flux of solar radiation, solidification of the melt and its further cooling take place in the entire volume because of the small thickness of the melt. This is recorded in the form distinctive phase transformations effects with a high resolving power.

The hydrothermal synthesis (the high-temperature hydrolysis of zirconium and hafnium oxychlorides in an acid medium and yttrium nitrate as stabilizer) has been found to be the effective method for the preparation of the samples in the quasi-static equilibrium conditions for subsequent comparison their properties with the properties of the samples melted and quenched in a solar furnace or solar radiation simulators. This method is described in detail in [1]. The samples with relative density above 99 % were produced out of nanocrystalline powders after usial uniaxial pressing or slip casting and consequent sintering of the samples in the furnace with heating elements based on $ZrO_2$ at 1200 °C (2 h), 1450 °C (2 h), 1570 °C (3 h) in air. The powder compositions were chosen in accordance with the phase state diagram of $ZrO_2$-$HfO_2$-$Y_2O_3$ system along the isoconcentrates at 5, 7 and 10 mol.% $Y_2O_3$.

Melting and thermal analysis of the samples were carried out in a 1,5 kW solar furnace with direct tracking Sun. The phase transformation temperatures and monochromatical radiating oxides capacity ($\varepsilon_\lambda$) were determined on the basis of the solidification process of the samples which were partially melted on the surface in the focus of a solar furnace. The cooling curves recorded using pyrometric system with a narrow-band light filter in the infrared ($\lambda$=1,39 μm) range of the spectrum. The change rate of the melted surface sample temperature being cooled was recorded. In this case the method of derivative thermal analysis (DTA) was used. In determining the phase transition temperatures in the ternary $ZrO_2$-$HfO_2$-$Y_2O_3$ system it was assumed that the $\varepsilon_\lambda$ value of the samples with intermediate compositions is governed by the additivity rule and is equal to the sum of the products of the molar fractions by the monochromatic radiation capacity of the initial oxide. This assumption has been verified by the determination of the $ZrO_2$-$Y_2O_3$ system liquidus as an example.

Phase composition of the samples was investigated by the X-ray diffraction and petrographical analyses. X-ray diffraction analysis was performed by the powder method at room temperature on the DRON-1,5 equipment in $Cu_{k\alpha}$ radiation at a scanning rate 1-4 deg/min over the angles $2\theta$=15-110 °. Lattice parameters of cubic phases were determined with an accuracy not larger than 0,0002 nm.

Phase analysis of the samples manufactured with the use of initial oxides mixtures has shown that the majority of the samples sintered at 1550 °C did not reach equilibrium state. Beside of F-phase formation it was observed formation of monoclinic phase the amount of which increased with the increase of $HfO_2$ content in sintered samples. After melting in a solar furnace the samples phase composition changed essentially. Solid solutions with the fluorite-type structure were found in the samples the compositions of which lay on the isoconcentrate 10 mol.% $Y_2O_3$. In the samples with 5 and 7 mol.% $Y_2O_3$ the solid solutions formed which were based on metastable tetragonal modification of (Zr, Hf)$O_2$ with M-phase traces.

Phase compositions of the samples manufactured with the use of hydrothermal method have shown that already after the samples annealing at 650 °C the phase with crystalline structure of F-type formed in the samples laying on the isoconcentrates 7 and 10 mol.% $Y_2O_3$. The formation of the mixture of F-, M- and T-phases was observed only on isoconcentrate with 5 mol.% $Y_2O_3$. But the phase of the fluorite type was metastable. It has been confirmed by the samples annealing at 1200 and 1450 °C. In these samples (10 mol.%$Y_2O_3$) along with the stable F-phase monoclinic phase has been found the amount of which decreased with annealing temperature increase and it disappeared after repeated samples annealing at 1570 °C. The results of the investigation of the samples containing 7 mol.% $Y_2O_3$ were similar to the results obtained for the samples containing 10 mol.% $Y_2O_3$ but the amount of M-phase in them was greater considerably and this phase remained after repeated samples annealings.

The conclusion can be drawn from the carried out investigations that the samples compositions laying on the isoconcentrate with 10 mol.% $Y_2O_3$ are the most proper for the development of high-temperature materials. In these samples a single phase of fluorite type forms under sintering and melting.

As a result of the measuring samples melting temperatures being on isoconcentration lines with 5, 7 and 10 mol.% $Y_2O_3$ content it was established that for all the isoconcentration lines melting temperature decreased steadily with the increase of $ZrO_2$ content.

1. Lopato L., Shevchenko A., Red'ko V., Ruban A., Dudnik E. Nanocrystalline powders bazed on $ZrO_2$ and $HfO_2$ in the $ZrO_2$-$HfO_2$-$Y_2O_3$ system. Theses of the reports at the International Conference "The Latest Achievements in Powder Metallurgy and Ceramics", September 8-12, 2003, Kyiv, p.306-307.

# COMPUTER MODELING OF POWDER MATEPIALS BENDING

**Mikhailov O.V., Serdyuk G.G., Tkachenko L.N.**
Frantsevitch Institute for Problems of Materials Science, NASU
3, Krzhyzhanovsky St., Kyiv, 03142, Ukraine, E-mail: olmi@alfacom.net

The technological action of bending is used while making the powder articles by forming (Fig.1). But insufficient knowledge in this sphere restrains industrial assimilation of the given technological process.

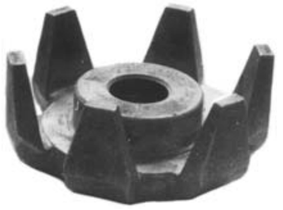

**Fig. 1. A powder detail, obtained with use of bending process**

The results of theoretical and experimental researches of plastic bending process of sintered powder billets were presented in the given article. The math's model of the process was based on the correlation the plasticity theory of porous body and finite elements method [1-4].

As a consequence of computer modeling the distribution of tension, density and cumulative plastic deformation of base material of porous body were obtained. The influence of the article's shape, its initial properties and deformation scheme were investigated.

Under the bending of rectangular cantilever the materials compaction in the area of concave free surface and decompaction in the area of convex one take place at the same time. At the bending of conical article the compaction and decompaction areas shift aside from the place of cantilever attaching. Similarly to this the maximum point of the cumulative plastic deformation magnitude of base material of porous body and tension.

The influence of a number of structural elements of the billet on the bending was studied by the example of spherical lug by the attached border of the cantilever. The structural elements were present in both top and bottom part of the article. It was found, that the extent of loosening in the presence of spherical lug is higher than at the rectangular cantilever deformation. At the same time the presence of spherical lugs leads to the decrease of the loosening extent in the most dangerous places of the billet (if the lug is in the bottom part of the article, decrease is prepotent).

The influence of backpressure in the extension zone was investigated. It was found that loosening extent of the material decreases in this case. One can see the metal transition to the extension field. This fact allows decrease the magnitude of finite article porosity in the pointed zone.

The process of simultaneous article bending and sintering was simulated (the correlation of continued sintering theory were used). There are two simultaneous processes in the extension zone: porosity growth under the action of bending and its decrease as a consequence of sintering (under the action of Laplas pressure). The finite density of the material and its ability of deformation without destruction depend on the correlation of the pointed processes intensity.

The peculiarities of multilayer powder materials were studied. Two loading scheme conditions have been considering: the bending of cantilever beam and the three-point bending. The layers differed either by solid phase material (Cu, Fe) or by the magnitude of initial porosity (0,1; 0,2). The loading of two-and three-layer samples was investigated. The more durable layer could be located both above and beneath the layer which durability is less in the two-layer sample. The two cases were also investigated in the three-layer sample: the inner layer was more durable than the outer ones and vice versa. Besides, the thickness of all layers could be the same or different (the inner layer was both thicker and thinner than the outer ones). It has been determined that the stress-strained condition of the flexible samples is non-uniformly and depends on the layers dislocation.

So, if at the three-point bending of the two-layer samples the less strong layer is located on the top, the zone of maximum compaction is located in the region of the loading; if it is located on the bottom part, the maximum compaction is in the bearing zone (Fig.2). In case when the three-layer sample is being bent and the less strong layer is located inside one can see an action of the stronger outer layers upon it. It is appears when the zones of compaction increase. The greatest stress magnitude arises within the stronger layers.

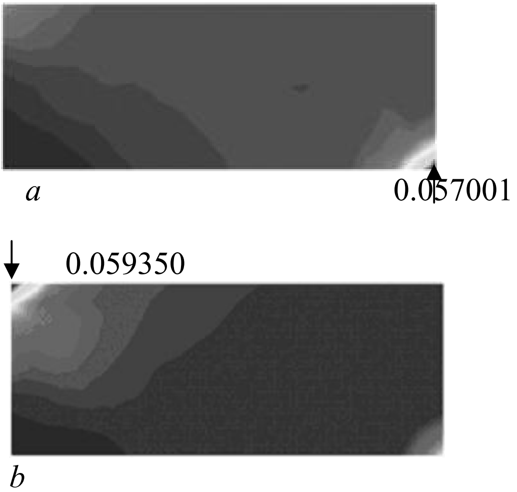

b

Fig. 2. The influence of layer material on the porosity distribution at a bending of a two-layer sample (the initial porosity magnitude was 0.1).

*a* – Fe top layer, Cu lower layer;
*b* – Cu top layer, Fe lower layer

The obtained data of computer modeling allow to estimate energy and power parameters of the process of multilayer powder billets plastic bending and to foresee the properties of derivable articles. The researches were realized with use of sintered samples, made of iron powder of PG4M3 GOST 9849-74 brand and brass powder of LN 65-5 brand (all-Union State Standard). This powder was obtained by dispersion method (Fig.3). The distribution of density and microhardness in different zones of bent samples were studied. Received results confirm the results of computer modeling.

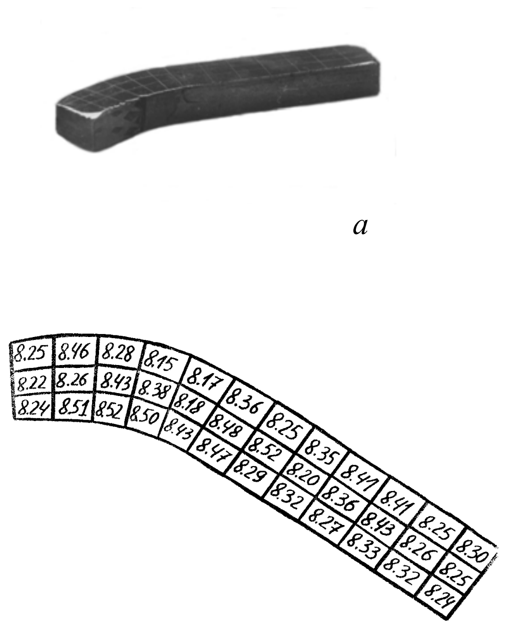

*a*
*b*

Fig. 3. The appearance of the bent sample (*a*) and the density distribution (*b*).

## REFERENCES

1. Mikhailov O.V., Shtern M.B. Allowance for a difference in resistance to extension and compression in theories of plasticity porous solids, *Powd. Metall. Metal Ceram., (translated from Russian), N 5, 11-17 (1984)*
2. Serdyuk G.G., Mikhailov O.V. The mathematical modelling of plastic deformation of PM materials in the presence of a free surface, *Powd. Metall. Metal Ceram., (translated from Russian), N 4, 18-22 (1986)*
3. Mikhailov O.V. Integrated scheme of computer simulating for PM articles pressure treatment *Powd. Metall. Metal Ceram., (translated from Russian), N 9/10, 99-104 (1995)*
4. Gorokhov V.M., Mikhailov O.V., Ustinova G.P., Shtefan E.V. Physical and geometrical modeling system of powder parts manufacturing processes with plastic deformation method application, *Powd. Metall. (Minsk), 1997, Vol.20, 5-10*

# KINETICS OF DISSOLUTION OF IRON-CHROMIUM ALLOYS IN LIQUID ALUMINIUM

**Dybkov V. I., Barmak K. (1), Khoruzha V. G., Meleshevich K. A.**
Frantsevich Institute for Problems of Materials Science of NASU, Kiyv, Ukraine
3, Krzhyzhanovsky Str., Kyiv, 03142, Ukraine, vdybkov@ukr.net, dep6@materials.kiev.ua
(1)Carnegie Mellon University, Pittsburgh
PA 15213, USA, E-mail: katayun@andrew.cmu.edu

To evaluate the thickness of the dissolved iron–chromium alloy material during its hot-dip aluminizing and the extent of saturation of the aluminium bath with the alloy constituents in the course of this procedure, experimental data on the kinetics of dissolution of the solid-alloy base in the aluminium melt are needed. The dissolution process is characterized by the saturation concentrations (solubilities), $c_s$, of the alloy components in the liquid phase and their dissolution rate constants, $k$.

In the case of a binary alloy, the dissolution rate constants can be either identical for both components (non-selective dissolution) or different (selective dissolution). The dissolution kinetics of Fe—Cr alloys containing up to 25 mass% of chromium in the aluminium melt is found by the rotating-disc technique to be non-selective, that is, iron and chromium atoms pass into the bulk of molten aluminium in that ratio in which they are present in an initial Fe—Cr alloy.

During dissolution, the concentration of the dissolved substance in the liquid increases with passing time and eventually reaches its limiting value, $c_s$, as was the case for Fe—Cr alloys investigated (Fig. 1). At 700 °C, this limiting value was found to be 2,5±0,2 mass% Fe and 0,28±0,03 mass% Cr for an Fe—10 mass% Cr alloy and 2,2±0,2 mass% Fe and 0,72±0,06 mass% Cr for an Fe—25 mass% Cr alloy. For comparison, the solubility limits of iron and chromium in liquid aluminium in the Al—Fe and Al—Cr binary systems at 700 °C are 2,5 mass% and 0,72 mass%, respectively. The former value coincides with the saturation concentration of iron for an Fe—10 mass% Cr alloy, while the latter corresponds to the saturation concentration of chromium for an Fe—25 mass% Cr alloy.

To determine the dissolution rate constant, $k$, initial parts of the dissolution curves such as those shown in Fig. 1 were investigated in detail (Fig. 2). As seen from Fig.3, a plot of ln $[c_s/(c_s - c)]$ against $st/v$ ($s$ is the surface area of the solid, $t$ is the time and $v$ is the volume of the liquid) is linear. It means that a value of the dissolution rate constant can be calculated using the equation $\ln [c_s/(c_s - c)] = kst/v$. At an angular disc rotation speed of 24.0 rad $s^{-1}$, the value of $k$ was found to be $(4{,}2\pm0{,}2)\times10^{-5}$ m $s^{-1}$ for an Fe–10 mass% Cr alloy and $(3{,}0\pm0{,}2)\times10^{-5}$ m $s^{-1}$ for an Fe—25 mass% Cr alloy.

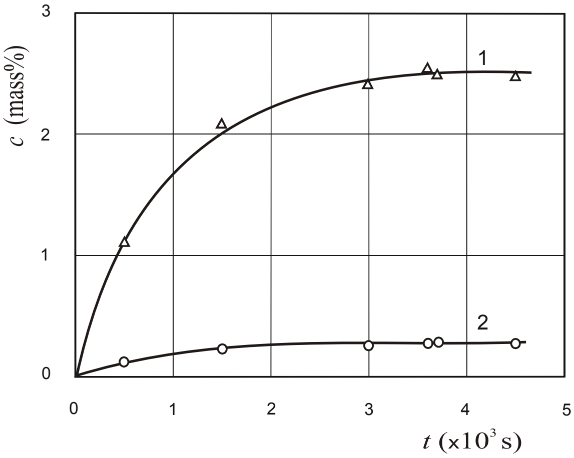

*Fig. 1.* Contents of iron and chromium, dissolved into liquid aluminium from an Fe–10 mass% Cr: alloy, are plotted against time to determine the saturation concentrations, $c_s$. Temperature=700 °C, rotational speed ω=54,0 rad $s^{-1}$, $s/v$=27.5 $m^{-1}$. 1, Fe; 2, Cr.

The analysis of these and previous data [1] shows that, for the same liquid-metal solvent, values of the dissolution rate constant rarely show a systematic change over the compositional range of a binary or multi-component alloy. This lack of systematic change is indicative of the complicated nature of the physicochemical interactions in the liquid state. Indeed, at a temperature of 700 °C and a rotational speed $\omega$=24,0 rad $s^{-1}$, $k=3{,}8\times10^{-5}$ m $s^{-1}$ for iron, $5{,}5\times10^{-5}$ m $s^{-1}$ for chromium and $6{,}5\times10^{-5}$ m $s^{-1}$ for nickel in their binary systems with aluminium. Under the same conditions, $k=5{,}9\times10^{-5}$ m $s^{-1}$ for an Fe—10 mass% Ni alloy and $6{,}0\times10^{-5}$ m $s^{-1}$ for an Fe—25 mass% Ni alloy. The dissolution rate constant of Fe—Ni alloys in liquid aluminium tends to decrease slightly with increasing time, while that of Fe—Cr alloys and an 18—10 stainless steel is indeed a constant, with a value of 4,8×10$^{-5}$ m s$^{-1}$ found for the latter.

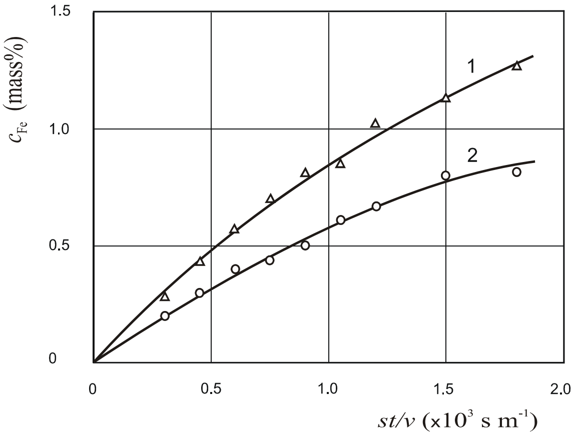

*Fig. 2.* A plot of the concentration of iron, dissolved into liquid aluminium from the Fe—Cr alloys, against $st/v$. Temperature=700 °C, rotational speed ω=24.0 rad s$^{-1}$, $s/v$ = 10,0 m$^{-1}$.

1, Fe—10 mass% Cr alloy; 2, Fe—25 mass % Cr alloy.

In view of the larger value of the dissolution rate constant for chromium than for iron in their respective Al binary systems, it may seem surprising that $k$ has a lower value for an Fe—25 mass % Cr alloy than for an Fe—10 mass % Cr alloy. The lower value for the former alloy is likely a result of the strong elemental interactions during their transition across the diffusion boundary layer into the bulk of liquid aluminium.

It is worth recalling that the concentration of the solute in the boundary layer in the vicinity of the surface of a solid phase is taken to be equal to its saturation concentration, $c_S$. For an Fe—25 mass % Cr alloy, $c_S$ is 2,2 mass% Fe and 0,72 mass% Cr. Comparing those with the values of 2,5 mass% Fe and 0,72 mass% Cr for the respective Al binary systems, it can be concluded that for an Fe—25 mass % Cr alloy the ternary liquid solution, Al—Fe—Cr, is saturated with respect to both components (Fe and Cr). Therefore, iron and chromium atoms for this alloy must overcome a higher barrier in their transition into the melt than in the case of an Fe—10 mass % Cr alloy, for which the ternary liquid solution, Al—Fe—Cr, being saturated with respect to iron, is under-saturated with respect to chromium. This appears to slow down the rate of dissolution of a Fe—25 mass % Cr alloy in liquid aluminium, compared to that of an Fe—10 mass % Cr alloy.

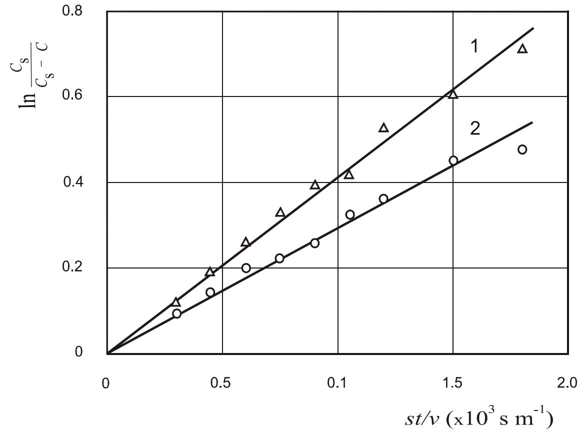

*Fig. 3.* A plot of ln [$c_S/(c_S - c)$] against $st/v$ for the data of Fig. 2.

For a rotating disc, the dissolution rate constant, $k$, is a function of the diffusion coefficient, $D$, of the solute atoms across the diffusion boundary layer at the solid-liquid interface into the bulk of the liquid, the melt viscosity, ν, and the angular speed of rotation, ω [2]. Therefore, experimental values of $k$ can be used to calculate the diffusion coefficients. At 700 °C, their values were found to be 1,4×10$^{-9}$ m$^2$ s$^{-1}$ for an Fe—10 mass % Cr alloy and 0,9×10$^{-9}$ m$^2$ s$^{-1}$ for an Fe—25 mass % Cr alloy. These are clearly averages for the concentration range 0 – $c_S$. However, in view of the relative narrowness of this range, the concentration dependence of the diffusion coefficient may reasonably be expected to be insignificant.

The diffusivities obtained characterize the rate of cooperative diffusion of iron and chromium atoms from the Fe—Cr alloys across the diffusion boundary layer into the bulk of the aluminium melt. For each Fe—Cr alloy, the iron and chromium diffusion coefficients thus found are identical in view of the non-selectivity of the dissolution process, even though in the respective binary systems Al—Fe and Al—Cr they differ considerably, being 1,2×10$^{-9}$ m$^2$ s$^{-1}$ for iron and 2,2×10$^{-9}$ m$^2$ s$^{-1}$ for chromium [1].

1. Dybkov V. I. Reaction diffusion and solid state chemical kinetics.- Kyiv: The IPMS Publications, 2002.- Ch. 5.

2. Kassner T. F. Rate of solution of rotating Ta disks in liquid tin // J.Electrochem.Soc.- 1967.- V.114, No.7. — P.689—694.

# THERMOMECHANICAL STABILITY OF CONDUCTOR UNDER ACTION OF ELECTROMAGNETIC FORCES

**Chemerys V.T.**
National Aviation University of Ukraine
1, Cosmonaut Komarov Ave., Kyiv, 03058, Ukraine, vchemer@uprotel.net.ua

The active conductor of elctromechanical devices, especially at non-ferrous homopolar rail accelerators or generators of the pulsed current, can be loaded by intensive thermomechanical actions whose duration consist since 1 up to 10 ms corresponding to the working regime. This range of duration covers the work conditions of the pulsed energy converters as well as extra-ordinary regimes of cyclic converters. The regimes of loading are very high in the launchers for acceleration of macrobodies. There are flowing currents up to 1 MA at non-uniform distribution along the conductor cross section. The local current density can reach up to $5{\cdot}10^3$A/mm$^2$, with corresponding heat sources up to $5{\cdot}10^{11}$W/m$^3$ and local super-heating on the 300...400° in result of restricted heat transfer due to short-time process. Like conditions can exist also at lower loading but at the multi-pulse operation. For analysis of thermal and mechanical stresses of conductor and for prediction its ability to stable work there is necessary to consider connected equations of electrodynamics, that give the distribution of electrodynamic forces and heat sources, and equations of thermo-mechanics with using of rheological models of conductor allowing transition from elastic deformation up to viscous flow. The model of viscous-elastic medium by Maxwell or the more late rheological models of body by Bingham and Shvedov can be used there. The goal of investigation is to find the marginal conditions preceding to plasticity creation and transition to the viscous flow at the most loaded layers. The same importance belongs to damage checking with respect to destruction stipulated by thermal stresses due to sharp non-uniformity of heat sources. At the short-time process is can cause the bursting of material. That is known that problems of such complex level present the not enough studied area of thermomechanics [1—3].

It seems significant to make analysis of what can be attracted to resolve the problem outlined in the wide field of the known results. There are the round works of many authors devoted to selected problems not connected with current-carrying materials behavior under high magnetic field conditions. So, in the work [4] the thermo-electromechanical behavior for piezoelectric crystals but not conductors. Data about cold deformation resistance of copper and aluminum is given in the work [5], but data about hot deformation resistance is given only for steels. The peculiarities of static and dynamic deformation and destruction are presented in the reference book [6], the most attention is taken here for cyclic creep of materials. The influence of quasi-stationary electromagnetic field of moderate intensity (including the field leakage) has been studied in the work [7]. The work [8] is most close to the problem under consideration, however these results are needed in some generalization by taking into account the presence of intensive heating caused by current passage.

In our work the attempt is undertaken to built the model of connected thermomechanical and electromagnetic processes at using of reasonable assumptions. Saving the main problematics, these assumption enable to estimate the conductor behavior and to define the marginal regimes with accuracy that is enough for qualitative or semi-quantitative description of mutual interconnection of phenomena. The method to reach this goal can be direct or undirect, using the known and new criteria of similarity and numerical analysis if needed. The conductor in the form of rectangular parallelepiped has been considered here, with magnetic pressure applied to the one of its sides. Orientation of electromagnetic field action relatively to possible direction of metal flow has been under variation. At the problem formulation sometimes the real skin distribution of current density in the conductor was replaced by the uniform current layer of equivalent thickness. It was possible to simplify the thermomechanical analysis due to this approach. The resolution of task wants the knowledge about the temperature dependence of material strength characteristics which are not always known reliable even for copper. Author's approach to the analysis of problem is based on the using of general theoretical model of connected processes as initial point for the following search of its possible partition with minimal loss of information. Preliminary study of problem was done at using of partial models with one of connected processes supposed known. By such a way the plastic flowing of conductor in the channel rail accelerator has been considered when moving through by electromagnetic forces. The plastic deformation of back front of accelerated body in railgun was studied too. The conditions of viscous flow of plastified metal on the surface of cylindrical conducting body accelerated by the field of pulsed solenoid has been analyzed also. It is useful to take into account that similar problems exists also in the practice of high field pulsed solenoids creation for magneto-pulsed forming or physical investigation in the strong fields (up to 50—60 T or more). The wide experimental material is stored here, its study gives a qualitative presentation of current-carrying conductor behavior under high loading. In this connection the problem of theoretical models creation for prognosis of margins for conductor workability is looking actual.

The final part of work contains the analysis of general model of connected electromagnetic and thermomechanical processes and discussion about the ways of its application to the performance of engineering estimation for stable operation of conductor at the intensive loading. The examples of conductor's behavior analysis is given for the rail accelerator with the field about 10—15 T taking into account the interconnection of processes.

[1] E.M.Kartashov. Analytical methods in the theory of heat transfer in the solid. - Moscow, High School Publ., 2001, 550p. (in Russian).

[2] A.M.Protsenko. Theory of elastic - ideally plastic systems. - Moscow, Science Publ., 1982. - 288p. (in Russian).

[3] V.P.Maiboroda, A.S.Kravchyuk, N.N.Holin. High-speed deformation of design materials. - Moscow, Machines Building Publ., 1986. - 262p. (in Russian).

[4] V.G.Karnauhov, I.K.Senchenkov, V.P.Gumeniuk. Thermomechanical behavior of viscous-elastic bodies at harmonic loading. - Kyiv, Naukova Dumka Publ., 1985. - 288p. (in Russian).

[5] V.A.Masterov, B.S.Borkovsky. Theory of plastic deformation and metal processing by pressure. - Moscow, Metallurgy Publ., 1989. - 400p. (in Russian).

[6] Resistance of materials against deformation and destruction // Reference book (in 2 vol.), edited by V.T.Troshchenko.- Kyiv, Naukova Dumka Publ., - Vol.1 -1993, 288p. Vol.2 - 1994, 702p. (in Russian).

[7] V.A.Stryzhalo, L.S.Novogrudsky, E.V.Vorobiev. Strength of metals and alloys for cryiogenics under electromagnetic actions. - Kyiv, Naukova Dumka Publ., 1990 - 160p. (in Russian).

[8] G.V.Stepanov. Elastic - plastic deformation of materials under pulsed loading action. - Kyiv, Naukova Dumka Publ., 1979. - 268p. (in Russian).

# KINETICS OF FORMATION OF INTERMETALLIC LAYERS BETWEEN IRON-CHROMIUM ALLOYS AND LIQUID ALUMINIUM

**Dybkov V. I., Barmak K. (1), Sidorko V. R., Samelyuk A. V.**
Frantsevich Institute for Problems of Materials Science of NASU, Kyiv, Ukraine
3, Krzhyzhanovsky Str., Kyiv, 03142, Ukraine, vdybkov@ukr.net, dep6@materials.kiev.ua
(1)Carnegie Mellon University, Pittsburgh
PA 15213, USA, E-mail: katayun@andrew.cmu.edu

Many technologically important processes such as hot-dip protective coating of solid material surfaces, soldering or welding of dissimilar metals and alloys, sintering in the presence of the liquid phase, etc., are based on the interaction of a solid metal or alloy with a liquid-metal melt. During the interaction, the solid base dissolves in the melt, while the intermetallic compounds are formed at or in the vicinity of phase interfaces. The formation of thick brittle intermetallic layers strongly deteriorates the mechanical strength of the transition zone between dissimilar metals or alloys. This is especially the case with the couples formed by iron or its alloys with aluminium. Amongst those, the Fe—Cr alloy-aluminium couple is known to be one of the most unfavourable with respect to the weakness of the joint, due to the occurrence of the intermetallics both at the phase interface in the form of a relatively thick continuous layer and in its vicinity in aluminium as the aggregation of coarse grains. The former occurs in the course of a chemical reaction, while the latter are formed during cooling-down the aluminium melt.

At 700 °C, two intermetallic layers were found to form at the interface of aluminium with iron–chromium alloys (10 and 25 mass% Cr), namely, a compact uniform layer adherent to the alloy base and a porous non-uniform layer adjacent to aluminium. In many cases, the latter actually consisted of separate grains weakly linked or not linked at all with each other. This means that, whenever present, its formation might be partly a result of a solid-state chemical reaction and partly a consequence of crystallization from the melt. On the contrary, the layer adherent to the alloy base was formed entirely in the course of another solid-state chemical reaction.

To identify the intermetallic phases, x-ray patterns were taken from different sections of the intermetallic layers. Experimental values of the interplanar distances were compared with those available in the literature for the intermetallics of the Al—Fe and Al—Cr systems. Two main constituent phases were $Fe_2Al_5$ and $FeAl_3$, with the compact layer being the $Fe_2Al_5$ phase, and the porous layer the $FeAl_3$ phase, also designated $Fe_2Al_7$. x-ray patterns of the porous layer also contained a number of unidentifiable, very weak diffraction peaks, indicative of the presence of other intermetallic compounds.

To reveal the phase compositions, electron probe microanalysis measurements were carried out across the transition zone up to a depth of 100 μm into the alloy bulk and 100 μm into the aluminium bulk. The composition of the compact layer was found to correspond to that of the $Fe_2Al_5$ phase (28,6 at.% Fe, 71,4 at.% Al). A change of elemental content across its thickness (69,0—72,9 at.% Al) agrees fairly well with the width (70,0—72,5 at.% Al) of the homogeneity range of this intermetallic compound in the equilibrium phase diagram of the Al—Fe binary system [1, 2]. The porous layer consisted of grains of $Fe_2Al_7$ or $FeAl_6$, with an aluminium solid solution between them. The layer also contained inclusions of $FeAl_3$ and occasionally $Fe_2Al_5$.

The coarse grains in the vicinity of the Fe–Cr alloy-aluminium interface are the $CrAl_7$ phase, also designated $Cr_2Al_{13}$ or $Cr_7Al_{45}$, with the homogeneity range 86,3—87,6 or 87,3—88,5 at.% Al. It is worth mentioning that, when formed under non-equilibrium conditions, this phase has a composition closer to $CrAl_6$ than to $CrAl_7$. In the presence of a third metal (Fe, Mn, etc.), the $CrAl_6$ phase is known to give rise to a few metastable phases of five-fold symmetry, whose composition corresponds to the chemical formula $Cr_{0.7}Fe_{0.3}Al_6$.

Fine grains near the $Fe_2Al_5$ layer had an approximate composition of $Cr_{0.67}Fe_{0.33}Al_{13}$. With increasing distance from this layer towards aluminium, their size increased, while the composition approached $CrAl_7$. The observed phase sequence and composition profile appears to be a result of transformations $Cr_{0.67}Fe_{0.33}Al_{13} \rightarrow Cr_{0.7}Fe_{0.3}Al_6 \rightarrow CrAl_6 \rightarrow CrAl_7$. The iron solubility in the latter phase reaches 4 at.%.

In the case of the aluminium melt saturated with the Fe–10 mass% Cr alloy constituents, the thickness of the compact layer increased in the 100—3600 s time range from 14 μm to 128 μm, while that of the porous layer from 8 μm to 13 μm. For an Fe–25 mass% Cr alloy, appropriate values were 12—60 μm and 4—12 μm.

Though the growth kinetics of two intermetallic layers are traditionally assumed to be parabolic, this is not the case with many systems, including the system under investigation. Instead, a few kinetic laws (linear, paralinear, asymptotic, etc.) may be observed for one and the same system at sufficiently long times of interaction, and only relatively small portions of the layer thickness-time dependence are close to a parabola. In the case under consideration, a parabolic relation did not produce a satisfactory agreement with the experimental data because the layer growth-rate constant proved to be time-dependent. Moreover, this relation could not be applied at all to the porous layer whose thickness quickly (in about 400 s) reaches a certain value and then remains practically unchanged during a considerable period of time. Such a dependence cannot be explained from purely diffusional imaginations predicting only parabolic kinetics for all growing layers but seems to be quite natural in the framework of physicochemical views giving a variety of growth laws [3].

Dissolution was found to cause a three-fold decrease in layer thickness compared to the case where the Fe-Cr alloy is in contact with a saturated melt and hence no dissolution occurs. Note that under conditions of simultaneous dissolution only the compact $Fe_2Al_5$ layer survives, whereas other intermetallic phases ($FeAl_6$, $Fe_2Al_7$, $FeAl_3$) exist as separate inclusions in the aluminium matrix.

Though a general mathematical equation describing the intermetallic layer-growth kinetics under conditions of its simultaneous dissolution in the liquid phase is rather complicated and difficult to solve [3], in the case under consideration it assumes a simpler form suitable for estimating the layer thickness: $x_t=k_1/b_t$ where $k_1$ is the layer growth-rate constant and $x_t$ is the maximum thickness that can be reached by the growing intermetallic layer in time $t$ if the rate of its dissolution remains constant and equal to $b_t$ in the time range $0 - t$.

When employing this equation, the main difficulty to overcome is evaluating the layer growth-rate constant, $k_1$. If a single-phase intermetallic layer occurs in the case of both saturated and undersaturated melts, its value is readily found from the experimental layer thickness-time dependence for the saturated melt. With the Fe–Cr alloys investigated here, however, this is not possible since the number of intermetallic layers growing from saturated and undersaturated melts is different (two, namely, $Fe_2Al_5$ and $Fe_2Al_7$ in the case of the saturated aluminium melt, and only one, $Fe_2Al_5$, from the undersaturated melt). Therefore, the layer-growth constant, $k_1$, can only be calculated using a few experimentally determined points of the layer thickness-time dependence for the undersaturated melt, preferably at short times. This makes the calculation of other points of that dependence possible.

As the dissolution rate diminishes exponentially from $b_0$ to $b_t$ in the time range $0 - t$, calculations were carried out twice for each point by putting in the denominator of the equation $x_t=k_1/b_t$ first equal to $(b_0+b_t)/2$ and then $b_t$. Thus, two sets of the $Fe_2Al_5$ layer thickness were obtained, namely, the underestimated values, $x_{\text{under}}$, and the overestimated ones, $x_{\text{over}}$. Experimental values, $x_{\text{exp}}$, must clearly lie somewhere in between. For both alloys, the layer growth-rate constant, $k_1$, was estimated using the first two points $t$=100 s and $t$=225 s, with $x_{\text{exp}}=9\times10^{-6}$ m and $x_{\text{exp}}=10\times10^{-6}$ m for an Fe–10 mass% Cr alloy and $x_{\text{exp}}=5{,}0\times10^{-6}$ m and $x_{\text{exp}}=5{,}2\times10^{-6}$ m for an Fe–25 mass% Cr alloy. Appropriate values of $k_1$ were found to be $14{,}1\times10^{-12}$ $m^2$ $s^{-1}$ and $5{,}5\times10^{-12}$ $m^2$ $s^{-1}$. These are the average of $b_0x_{100}$ and $b_{100}x_{225}$ (subscripts designate time). Calculations according to the proposed equation yielded a good fit to the experimental data.

The Fe—Cr alloy-to-aluminium transition joints were made and their uniaxial tensile tests were carried out on a P-500 tester. The rupture strength was typical of pure aluminium (70—80 MPa). If the gauge length exceeded the diameter, the rupture took place approximately in the middle of the aluminium part of the specimens after the plastic deformation of aluminium.

1. Hansen M. Constitution of binary alloys.- New York: McGraw-Hill, 1958.- P. 81, 90.

2. Ternary alloys: A comprehensive compendium of evaluated constitutional data and phase diagrams.- Vol. 4, Eds. G. Petzow and G. Effenberg., Weinheim: VCH, 1991.- P. 324—343.

3. Dybkov V. I. Reaction diffusion and solid state chemical kinetics.- Kyiv: The IPMS Publications, 2002.- Ch. 5.

# MATHEMATICAL FORMALISM OF THE PROCESSES IN THE ONE-PARTICLE MODELS IN THE MATERIALS SCIENCE AND THE ONCOLOGY

**Raychenko O.I.**
Frantsevich Institute for Problems of Materials Science of NASU,
3, Krzhyzhanivs'ky St., 03680, Kiev-142, Ukraine, e-mail: raitch@ipms.kiev.ua

One can see some similar peculiarities in the mathematical formalism of the models the medium-foreign spherical inclusion (in materials science) and the organism tissue-tumour (in oncology). The changes in models (by the means of diffusion, chemical and biological reactions, phase transformations) are analysed. Some of processes may proceed both directly and backwards. One of the typical processes, which happen in experiments with powders, in technology of metals or in nature, is the complex process including diffusion and chemical reaction. Sometimes such a process is attributed to the type of diffusion in the "active" medium. One proceeds often from the following thesis: the particles (atoms, molecules, ions) of the free admixture (diffusant) may move in the medium containing the acceptors ("snares") which are able to capture the diffusant particles. At the creating mathematical model of the process mentioned in case of immovable acceptors it is expedient to proceed from the system

$$\frac{\partial c_d}{\partial \tau} = D\Delta c_d + f_{d1}(c_d) + f_{d2}(c_s) + f_{d3}(\boldsymbol{r},\tau) + \\ + f_{d4}(c_d, c_s) \tag{1}$$

$$\frac{\partial c_s}{\partial \tau} = f_{s1}(c_d) + f_{s2}(c_s) + f_{s3}(c_s, c_d) \tag{2}$$

where $c_d$ is the free diffusant concentration, $c_s$ is the concentration of acceptors capturing the diffusant particles, $D$ is the diffusion coefficient, $f_{di}$ are the velocities of change of the free diffusant concentration $c_d$ depending on: $c_d$ $(f_{d1})$, concentration of acceptors which capture the diffusant particles $c_s$ $(f_{d2})$, arguments (geometric $\boldsymbol{r}$ and time $\tau$) $(f_{d3})$, the free diffusant and acceptors concentrations jointly $(f_{d4})$; $f_{si}$ are the velocities of change of the acceptors concentration depending on: $c_d$ $(f_{s1})$, $c_s$ $(f_{s2})$, $c_s$ and $c_d$ jointly $(f_{s3})$.

In the system (1), (2) the volume, mass or particles concentrations figure. The system of such a type is applied not in most general appearance usually. For example, if $f_{d1}=-kc_d$ (where $k$ is the "reaction " constant), $f_{d2,3,4}=0$, then there is the first order process [1, p.127]. It happens that (2) is solved without dependency on (1), and then the solution obtained $c_s$ may be used for solving (1). If $f_{d1}=-c_d^2$, $f_{d2,3,4}=0$, then such equations correspond to the second order process [2, p.118].The solution of the equations of such a type describes, for example, the diffusion under radiolysis of water [3]. At $f_{d1}=$ $=-k_1c_d$, $,f_{d2}=f_{d3}=0$, $f_{d4}=-k_4c_dc_s$ the system (1),(2) corresponds to the complex process including diffusion and reactions of the types diffusant particle-diffusant particle and diffusant particle-acceptor [2, p.118; 4].The solution of such a system describes some processes of the ion chemistry. When the diffusion area size is very small and changes of diffusion flows in its limits are small, the term $D\Delta c_d$ in (1) may be neglected and the structures of (1) and (2) became more similar. The processes proceed in the kinetic regime. At the bounded solubility of diffusant in inclusion's material the problems of transfer in peripheral layers of inclusion play the more important part [5-7]. The next step which complicates the process may be the superposition of some outer exertion, for example, the magnetic field. This may result in arising of superposition of the probability motion and drift [8].

Let us consider the transformations in a tumour surrounded by ordinary tissue of a living organism. The tumour cells are able to propagate itself by gemmation (proliferation). An organism containing a tumour has ability to counteract to tumour's existence and expansion by means of its immune system. The material carriers of the immune system function are the special cells – lymphocytes. They arise outside the tumour, move to it, encroach in it and capture ("eat up") the tomour cells. The lymphocytes are the analogues of the diffusant particles, the tomour cells are the analogues of the acceptors. Let us consider the model in which the access of lymphocytes to inner part of the tumour is impossible practically because of low permeability of the blood-vessels or some other causes. Therefore let us suppose that the events happen in the peripheral layer of the tomour [9], the magnetic field acting on it. The influence of magnetic field results in destruction of membranes and nuclei in cells, energetic deficit, dystrophia and necrosis of the tumour cells [11,12].The process of "struggle" of the lymphocytes and the tumour cells is described by the system (written in the reduced values)

$$\frac{dx}{dt} = -\lambda_L x + \alpha_L \frac{xy^{\frac{2}{3}}}{1+x}\left(1 - \frac{x}{x_c}\right) = X(x,y) \qquad (3)$$

$$\frac{dy}{dt} = \lambda_T y - \alpha_T \frac{xy^{\frac{2}{3}}}{1+x} - \beta = Y(x,y) \qquad (4)$$

where $x$ is the number of the free lymphocytes, $x_c$ is the maximum number of the free lymphocytes, $y$ is the total number of tumour cells, $t$ is the time expressed in intervals of mean "life time" of lymphocytes [10], $\lambda_L$ is the parameter which characterizes the dependency of decrease of the change number lymphocytes velocity on their number, $\lambda_T$ is the parameter which characterizes the process of tumour cell-division, $\alpha_{L,T}$ are the parameters which characterize the joint exertion of lymphocytes and tumour cells on increase of the velocity of change of lymphocytes number and on decrease of the velocity of change of tumour cells number accordingly, $\beta$ is the parameter which characterizes the destructive exertion of the magnetic field on the tumour cell of some types. The ratio of the left and right sides of equations (3) and (4) yields equation of trajectory (with exclusion of time).At making right sides of (3) and (4) vanish the routs $(x_0, y_0)$ of equations $X(x,y) = Y(x,y) = 0$ will be the singular points [13, p.37].If one consider the case $\frac{\beta \lambda_T^{\,2}}{\alpha_T^{\,3}} << 1$ then the singular points will be obtained by intersecting the curves

$$y_L = \left(\frac{\lambda_L}{\alpha_L} \frac{1+x}{1-\frac{x}{x_c}}\right)^{\frac{3}{2}} \qquad (5)$$

$$y_T = \frac{\alpha_T}{\lambda_T}\frac{x}{1+x} + \frac{3\lambda_T \beta}{\alpha_T^{\,2}}\left(\frac{1+x}{x}\right)^2 \qquad (6)$$

It is interesting to note that the appearance of the magnetic field parameter $\beta$ in (4) alters principally the character of the function $y_T(x)$ by comparison with the proper function at $\beta=0$ [9]. At approaching the value $x$ to zero the function (6) increases infinitely, whereas at $\beta=0$ $f_T(0) = 0$ (Fig.1).

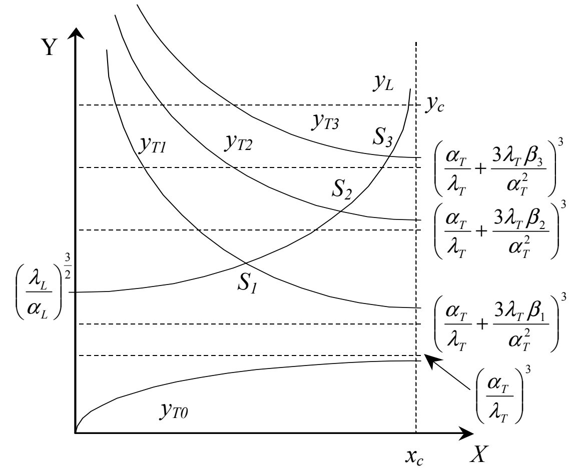

**Рис.1.** Dependencies of the reduced quantities of onco-cells $y_L$ (5) and $y_T$ (6) on the reduced quantity of lymphocytes $x$: $y_{T0}$ ($\beta=0$), $y_{T1,2,3}$ ($0<\beta_1<\beta_2<\beta_3$). $y_c$ is the critical value of the quantity of onco-cells. $S_{1,2,3}$ are the singular points at $\beta=\beta_{1,2,3}$ respectively.

The function (5) is the same one as in [9].The points of intersection of curves (5) and (6) move upwards, and the higher, the larger $\beta$. After the addition else one parameter ($\beta$) to five ones (in case without the magnetism, $\beta=0$ [9]) more wide possibilities arise in order to influence conditions which ensure more favorable dynamics of "struggle" between the immune system and the oncologic illness. For example, let us consider such a pair of the singular points: the saddle and the center. At the saddle the branches exist which lead to the unlimited increase of $y$ (Fig.2a), and this is baneful from the oncologic standpoint. At the center the trajectories are exclusive curves (Fig.2b). At elaboration of the strategy of the influence on the lymphocytes-tumour "struggle" it is desirable, by varying the parameters, to make the singular point the center but not the saddle. If the trajectory near the center does not intersect the critical level $y=y_c$, then its ordinates will change in a cyclic manner within some limited values. Such a situation corresponds to the dynamic stability of the system or, in other words, the successful "struggle" of lymphocytes against tumour.

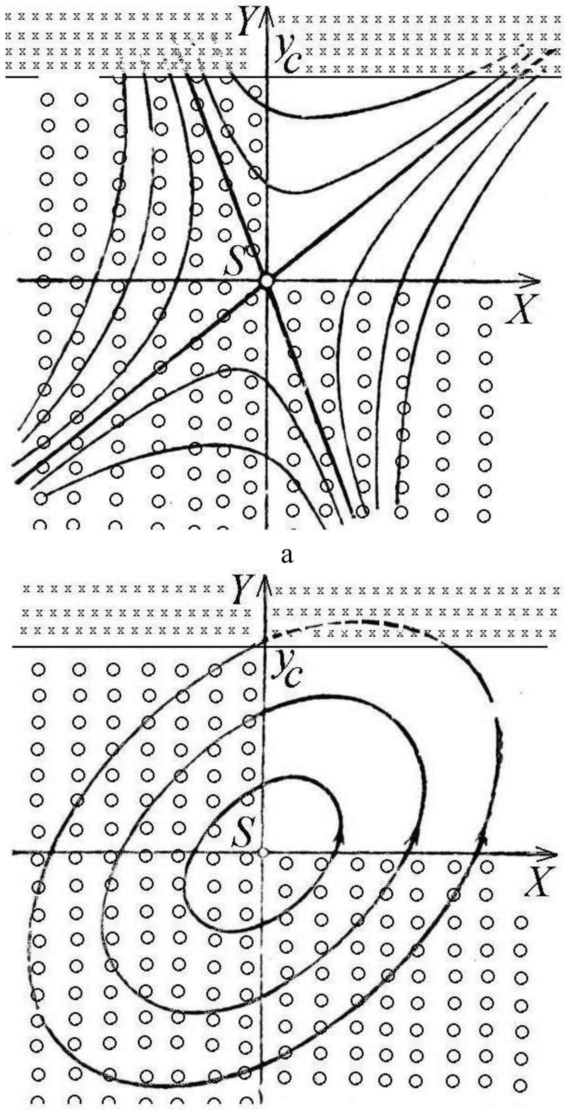

a

b

**Рис.2.** Trajectories near the singular points.
a – saddle, b - center.

However, at any type of the singular point the trajectory should not intersect the critical level as the situation $y>y_c$ is supposed one which is incompatible with life.

Most of the problems of the materials science now about behavior of the model medium-inclusion, contain the linear terms in the (1)-type equation.

As it is seen from the structure of system (3),(4) the equations in case of oncology may include the terms containing both functions: *x* and *y*. But in case of materials science the example of the process in "active" zone was adduced where there is the term with both functions ($c_d$ and $c_s$) [4]. The methods of the qualitative theory of differential equations (analogous to ones which are used in oncology) may turned out effective at analysis of the transfer and the transformations in the materials science

## References

1. J. Crank, *The Mathematics of Diffusion,* Clarendon Press, Oxford, 1956.
2. Д.А. Франк-Каменецкий, *Диффузия и теплопередача в химической кинетике*, Наука, Москва, 1967.
3. A. H. Samuel and J.L. Magee, *Journal of Chemical Physics*, **21***,* p.1080-1087, (1953).
4. H. Fricke, *Annals of the New-York Academy of Sciences,* **59**, p.567-573, (1955).
5. А.И. Райченко, *Порошковая металлургия*, №10, с.43-46, (1968).
6. А.И. Райченко, *Порошковая металлургия*, №8, с.19-22, (1980).
7. А.И. Райченко, *Диффузионные расчеты для порошковых смесей*, "Наукова думка", Киев, 1969.
8. А.И. Райченко, *Украинский физический журнал*, **32**, с.142-147, (1987).
9. C. DeLisi and A. Rescigno, *Bulletin of Mathematical Biology,* **39**, p.201-221, (1977).
10. А. Балаж, *Биология опухолей. Сомнения и надежды*, "Мир", Москва, 1987.
11. Л.Х. Гаркави, Е.Б. Квакина, М.А. Уколова и др., в кн. "*Нетрадиционные методы в онкологии, Материалы Всеросс. науч.-практ. конф. онкологов*", Ростов н/Д: Ростовский н.-и. институт, 1991. С.4-15.
12. А.К. Панков, Р.Н.Салатов и Н.М. Кузьмина, *там же*, с.68-75.
13. В.В. Немыцкий и В.В. Степанов, *Качественная теория дифференциальных уравнений*, ГИТТЛ, М.-Л., 1947.

# INSULATOR-METAL TRANSITION IN LOW-Z MATERIALS AT HIGH PRESSURES

**Morozov A.F., Eremeichenkova Yu.V.**
Galkin Donetsk Phys. & Tech. Institute of NASU, Donetsk, Ukraine
R.Luxemburg str., 72, Donetsk, 83114, Ukraine, E-mail: morozov@mail.fti.ac.donetsk.ua

When the pressure reaches megabar values pressure induced energy change in a crystal becomes comparable with its cohesive energy. Crucial modification of chemical bond type takes place in a crystal, namely, insulator-metal transition or metallization which is defined as forbidden gap closure in energy spectrum of insulator. One takes moderated interest in the materials with low atomic number (low-*Z* materials) since these substances possess high compressibility, with the pressure effects being essential. Rare gas crystal neon is one of the low-*Z* materials. Moreover, investigating the properties and the metallization of compressed rare gas crystals is a deal of special interest because rare gases are widely used as a media able to create almost perfect hydrostatic conditions in experiment.

Ab-initio band structure calculation of solid neon at megabar pressures is presented in this paper. Occupied bands are calculated as it is proposed in [1] in Hartree-Fock approximation using the basis of atomic orbitals orthogonalized exactly at different sites of a crystals. Cluster expansion for orthogonalizing matrix (CE) from [2] is applied. It was firstly proposed by prof. E.V.Zarochentsev in [3] to calculate band structure of a cryctal. To obtain the conduction bands of compressed crystal orthogonalized plane waves (OPW) method is modified by using occupied band wave functions calculated with the CE [3, 4]. Using the CE is equivalent to taking account for all the powers in overlap integrals *S* of neighbour atoms orbitals. It allows using no small parameters like to the overlap integrals, which constrain the applicability of used methods by low pressures only. Moreover, two-particle cluster approximation is estimated to be applicable for compressed neon up to metallization point. All further calculations are performed in this approximation.

At the fig. 1 band structure of solid neon is given.

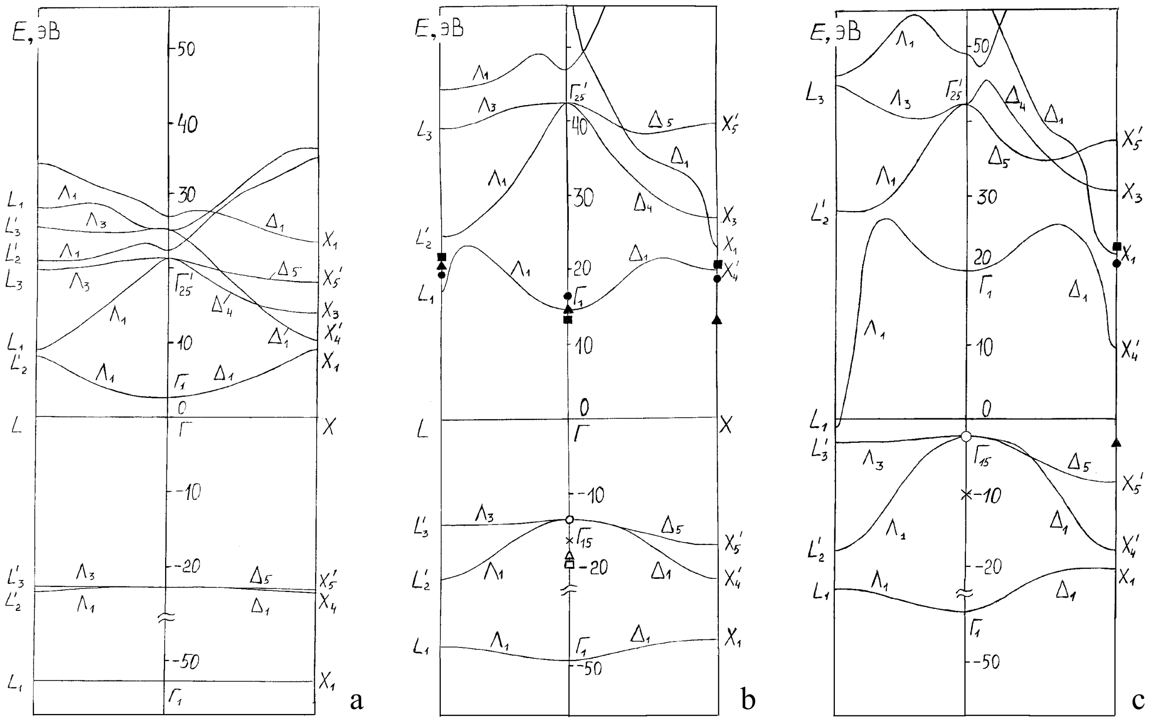

Fig. 1. Band structure of solid neon: a - $u$=$\Delta V/V_0$.=0, b - $u$=0,7, c - $u$=0,77. Solid lines - calculation with taking all the powers in overlap integrals $S$ into account. Full symbols - the lowest conduction band energies: - standard OPW method with $S$=0, Δ - OPW method with orthogonalization in the first order in $S$.

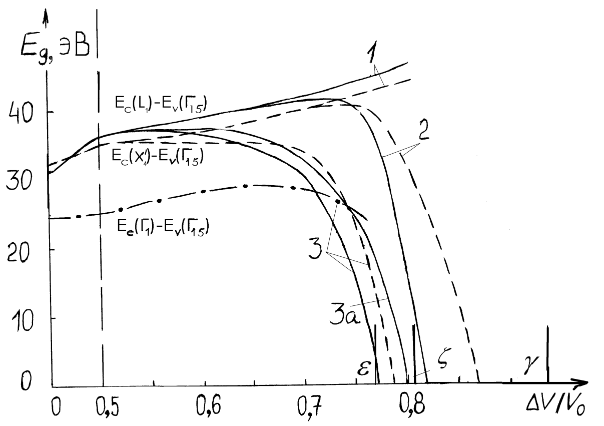

Fig. 2. Band gaps of solid neon. Indirect gaps are solid lines and dashed lines. Direct gap is dashed-dotted line. The models are denoted by the digits: 1 - $S$=0, 2 - orthogonalization in the first order in $S$, 3 and 3a - accounting for all the powers in $S$. Vertical short lines denote calculated metallization compression: γ - [6], ε - [7], ζ - [8].

Conduction bands $E_{\mathbf{kc}}$ and upper 2$p$- and 2$s$-occupied bands $E_{\mathbf{kv}}$ are plotted. We can see an ordinary picture of insulator for uncompressed crystal. As compression is being enhanced, the occupied bands are widening and rising up on the energy scale. Valence electrons effective mass $m^*$ decreases and some branches have $m^* \sim 1$ near the metallization (at the compression ratio $\Delta V/V_0$=0,77).

Direct band gap between the energies in the $\Gamma$ Brillouin zone (BZ) point increases as the pressure is being moderated. Indirect gaps between the top of occupied band in the $\Gamma$ point and the conduction bands energies in the $X$ and $L$ BZ points increases too (up to $\Delta V/V_0$=0,7). Then, the energy of the lowest conduction band begins to drop harshly at the $X$ and $L$ points while all the rest energies enhances. Finally, the lowest conduction band overlaps with the upper occupied band. It causes indirect gaps closure, i.e. metallization.

One can see that the Brillouin zone center energy is insensitive to the model choirs. It is the Birllouin zone boundary on that high powers in S contribution becomes essential.

Fig. 2 shows the neon band gaps behavior via the $u=\Delta V/V_0$. One can see no band gap closure in the model which take no overlap integrals into account (standard OPW method, the curve 1). The metallization is predicted at $u_m$=0,78±0,01 when all the powers in $S$ are taken into account, with the metallization pressure being $p_m$=3,5±0,7 Mbar according the equation of state calculated in [5] with the CE. Average value among all the models is $u_m$=0,80±0,03 with the pressure spread 2,9≤ $p_m$≤10,5 Mbar. However, the pressure spread obtained is not so large to give anomalous values $p_m$~ 1300 Mbar from [6]. All our models and a number of estimations [7,8] give $u_m$ about 0,8, with a pressure $p_m$≤10 Mbar.

1. V.G.Bar'yakhtar, E.V.Zarochentsev, E.P.Troitskaya, Yu.V.Eremeichenkova Fiz. Tv. Tela 40, 8, 1464 (1998) (translated from russian).

2.I.V.Abarenkov, I.M.Antonova Phys. Stat. Sol. 38, 783 (1970).

3.Yu.V.Eremeichenkova, E.V.Zarochentsev, E.P.Troitskaya Theoretical and Mathematical Physics 106, 408 (1996) (translated from Teoreticheskaya i Matematicheskaya Fizika).

4.E.V.Zarochentsev, E.P.Troitskaya, Yu.V.Eremeichenkova Metalofiz. Noveishie. Tekhnol. 21, 5, 3 (1999) (translated from russian).

5. E.V.Zarochentsev, E.P.Troitskaya, Yu.V.Ere-meichenkova, V.V.Chabanenko FTVD 10, 2, 7 (2000) (in russian).

6. J.C.Boettger Phys.Rev.B 33, 6788 (1986).

7. E.V.Zarochentsev, E.P.Troitskaya, Fiz. Tv. Tela 27, 2474 (1985).

8. N.H.March // in Advances in high pressure research. Ed. by Bradley R.S.-New York: Acad. Press., 1969.-Vol. 3.-p.241.

# SELECTING THE MODE OF CONTINUOUS COIL COATING WITH ROLLS

**Mukhin I.A., Ivanenko A.A.**
Lipetsk State Technical University, Lipetsk, Russia
Moscovskaya Str., 30, Lipetsk, 398600, Russia, iart@lcpi.ru

Roll application is a modern, highly effective method of coating both organic and inorganic materials on a continuously running strip. In 2004, Russia is expected to commission three lines with total performance exceeding the capacity of all such lines in this country in 2003.

One of the main targets affecting not only the products quality but technological and economic performance of the process as well, is the uniform coating layer of the desired thickness (e.g. painting). There are optimum thicknesses for each coating enabling to obtain the desired protective, decorative and special features [1].

The schematic diagram of the two-working roll coater is shown on Fig.1. The two-roll coaters are mostly used now. The three-roll coaters are used with highly viscous materials only; they are more complicated and are rarely used.

There are two methods of coil coating: with direct and reverse rotation. The direct rotation method (See Fig. 1) is used for thin coatings (up to 10 μm) with low requirements to appearance, as the application roll leaves stripes along the rolling direction. The reverse rotation method (See Fig. 2) is used for coatings more than 10 μm thick: mainly these are finishing layers.

The application roll is coated with elastic material (usually, polyurethane rubber).

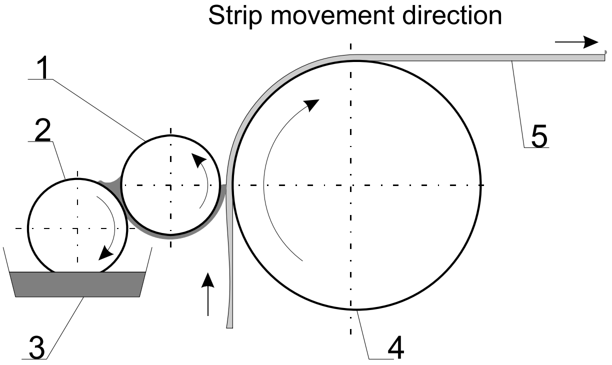

Fig. 1. Two-working roll coater scheme (direct rotation). 1 – application roll; 2 – pick-up roll; 3 – paint tray; 4 – backup roll; 5 – strip.

Let us consider the transmittal scheme of coating material (paint) from the tray to the strip by 2-roll reverse rotation method, and evaluate how each element of the roll application mode is affecting the thickness and the quality of the coating (See Fig. 2) [2].

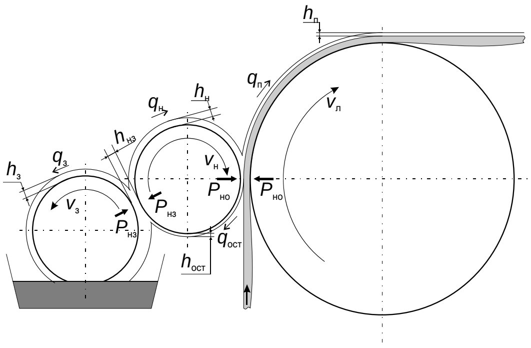

Fig. 2. Coating material circulation scheme in a two-roll coater (reverse rotation).

The wet coating layer is maid mainly in the gap which is generated by hydrodynamic forces between the application and the pick-up rolls, pressed with $P_{нз}$ stress, where the paint acts as lubricant. The paint movement in the gap between the rolls is described by the two differential equations: the solid body elastic deformation equation and the Reynolds equation [3]. The numerical solution of this system is given in works [4] and [5].

The main parameters affecting the lubricating film thickness between the rolls are: rolls radii *R,* their elasticity modules *E,* the circumferential speeds *v,* the pressing force between the rolls *P,* as well as the painting material viscosity *η*. In the work [4] it is shown how the solution depends on the dimensionless parameter

$$J = \sqrt{\frac{P^2}{\eta R(v_1 + v_2)\pi E^*}}$$

which characterizes the ratio of the hydrodynamic pressure within the film to the elastic deformations pressure (all the formulas are given for the rolls unit length). Here $R$ and $E^*$ are accordingly the radius and the elasticity module: $\frac{1}{R} = \frac{1}{R_1} + \frac{1}{R_2}$ and $\frac{1}{E^*} = \frac{1-\mu_H^2}{E_H} + \frac{1-\mu_3^2}{E_3}$.

The dependency of dimensionless film thickness $H = \frac{Ph_{\min}}{\eta R(v_1 + v_2)}$ from *J,* obtained by numerical methods is approximated by the equation [3]:

$$H = \gamma J^{\beta},$$

or, passing to the dimensional variables:

$$h_{\min} = \gamma \left( \frac{P}{l} \right)^{\beta - 1} (\pi E^*)^{-\frac{\beta}{2}} \left[ \eta R (v_1 + v_2) \right]^{1 - \frac{\beta}{2}},$$

where $h_{min}$ is the minimum film thickness, and, in all cases, $h_{min}$ *? 0,8h**.

Let us consider more in detail the $h^*$ value. Taking into account that liquid flow rate in any cross-section out of the Reinolds equation is equal to:

$$Q = h \frac{v_1 + v_2}{2} - \frac{h^3}{12 \eta} \frac{dp}{dx},$$

where *dp/dx* – is pressure gradient. Accordingly, in cross-section where the pressure gradient *dp/dx* = 0,

$$Q = h^* \frac{v_1 + v_2}{2}.$$

From the point of view of the coating thickness adjustment, the film thickness in “zero” cross-section $h^*$ is of more interest than the minimum thickness $h_{\text{min}}$.

Obviously, the painting material flow rate in the gap between the application and the pick-up rolls is equal to total flow rates on the rolls surface after they go out of contact $Q_{\text{нз}} = q_{\text{н}} + q_{\text{з}}$, i.e.

$$h^* \frac{v_{\text{Н}} + v_{\text{З}}}{2} = h_{\text{Н}} v_{\text{Н}} + h_{\text{З}} v_{\text{З}}.$$

Taking into account that $h_{\text{н}} \approx h_{\text{з}}$, we can put down $h^* = 2h_{\text{н}}$.

So, the speeds values of the application and pick-up rolls and the pressing force between them can be determined from the needed wet layer thickness on the application roll. Thus it should be noted that if the pick-up roll speed is too low, it can happen that the amount of painting material that comes from the roll to the entry zone of rolls deformation could be comparable with the painting material consumption. In this case one can observe the lack of painting material excess in the entry zone, which usually is uneven along the roll barrel length and results in the different coating thickness through the strip width, accordingly.

For roll application of the organic soluble painting materials, the typical values of *J* parameter are in the 5 to 12 range, with $\beta \approx 0{,}72 \div 0{,}8$.

The same calculations can be used for “the application roll – backup roll” pair, when coating is applied by direct rotation. With reverse rotation, the strip layer thickness is determined by the formula:

$$h_{\text{П}} = \frac{q_{\text{Н}} - q_{\text{ост}}}{v_{\text{Л}}} = \frac{v_{\text{Н}} (h_{\text{Н}} - h_{\text{ост}})}{v_{\text{Л}}}.$$

The paint material layer thickness $h_{\text{ост}}$ remaining on the application roll after it goes out of contact with the strip, can be calculated in the same way as for $h_{\text{н}}$, taking into account that one of the rolls speed should be with minus (it is more convenient to estimate the strip speed as a negative value). It should be noted also that when the strip speed, according to the module, exceeds the application roll speed, then $h_{\text{ост}}$ becomes negative. Physically, it means that the painting material layer which acts as lubricant is broken before the rolls go out of contact. This results in dry friction of the steel strip against rubberized application roll leading to roll surface damage and roll changing.

In order to avoid this and form lubricating layer, the application roll speed is set up a little higher than the strip speed. To provide the guaranteed carrying capability, the lubricating layer thickness should exceed the total height of the strip and roll roughness [6]. With less painting material lubricating capability as compared with oil, this difference should be higher, accordingly. Thus, the application roll circumferential speed value can reach: $1{,}05 \div 1{,}5 v_{\text{л}}$, but with lower strip or roll surface quality it can be up to $1{,}8 v_{\text{л}}$.

However, if one rewrites the strip coating layer thickness equation, where $q_{\text{ост}}$ is taken as a constant of $q_{\text{н}}$, as $q_{\text{н}} - q_{\text{ост}} = \alpha q_{\text{н}}$, it becomes obvious that increasing the application roll speed results in proportional increase of the coating thickness:

$$h_{\text{п}} = \alpha h_{\text{н}} \frac{v_{\text{Н}}}{v_{\text{Л}}}.$$

The main parameter which can adjust the thickness is the pressing force between the application and the pick-up roll.

Thus, in order to adjust the coater for relevant mode, it should be taken into account:

- the geometric (radii) and the mechanic (elasticity modules) rolls parameters;
- the rolls speeds and pressing forces;
- the coating material viscosity;
- the processed rolled products quality (roughness, defects).

References:

1. BASF-Handbuch. Lackiertecknik. Prof. Dr. Arthur Goldschmidt, Dr. Hans-Joachim Streitberger. Muenster, 1996.
2. Заявка $^1$05220441, Япония, МКИ B05D 1/28, B05D 3/00, B05D 7/14, B05C 1/08. Method for controlling thickness of coating film on strip-like material by roll coater. 1993
3. Джонсон К. Механика контактного взаимодействия: Пер. с англ./Под ред. Р.В. Гольдштейна – М.: Мир, 1989 – 509 с.
4. Dowson D., Higginson G.R., Whitaker A.V. Elastohydrodynamic lubrication: a survey of isothermal solutions. – J. Mech. Engng. Sci. 1962, 4, p.121.
5. Finite element analysis of fluid-solid interaction in the metering nip of a metering size press. E. Fourcade, F. Bertrand, O. Reglat, P.A. Tanguy. – Computer Methods in Appl. Mech. and Engng. Vol. 174 (1999), issue 1-2, p.235.
6. Гидродинамические опоры прокатных валков. Тодер И.А. и др. М.: Металлургия, 1968. – 398 с.

# INVESTIGATION OF THE INTERGROWTH FACTORS WHICH MAKE FOR AN MOLECULAR ADHESION MICROMECHANISM

**Uskova N.A., Moljar A.G.(1), Grishchishyna L.N.**
Frantsevich Institute for Problems of Materials Science of NASU
03680, Kiev-142, Krzyzanovski str. 3, Ukraine, E-mail: dep40@ipms.kiev.ua
(1)O.K. Antonov`s The Aero-Science-Technical Comlex
03062, Kiev, Tupolev str., 1, Ukraine

Investigations of the intergrowth factors from the manylaers coatings (having been mana-gemented by regulation of electronic and atomic parameters) is a present-day problem for the aero-spacing material science.

As a matter of experimental fact, that the coating with a high power of a column textured stand three times as much external loads.

The special chemical atmosphere aids in formation of a topology-bonding three-dimentional of the defect structure from clusters of d-metal atoms and admixtures.

It made framework for conjugative (by non-saturated bonds) difference phase states in process formation of manylayrs of a column textured coatings.

We will very briefly outline defectformatign by clustering in the d-metal atomic structure (Sc, Ti, V, Cr, Mn, Fe, Ni, and other). It is now that energy of primary clusters of the d-metal base defects are change free Gibb`s energy **G** (at temperature **T**) in proportion of local changes **g** .

Gibb`s energy and a local contribution from configuration enthropy for everyone microvolum of atomic lattice is in proportion to the stacking fault energy (SFE):

$$SFE \sim \sum g \sim \delta G \cong \delta U - T\delta S \qquad (1)$$

The **U** - internal energy as function of a lattice energy (**U** – is in proportion to microhardness).

$$\delta G = \sum \delta g = \sum_{\substack{i=1\\ j=1}}^{\substack{B\\ z}} \{dh - Td[(s_0 + s_k)^i - (s_0 + s)^j]\} = \sum_{\substack{i=1\\ j=1}} (\mu_i dc_i - \mu_j dc_j) \qquad (2)$$

b
z

It is now from equation (2), that change of free energy **dg** form by an individual atomic and electronic parameters by chemical potentisl $\mu$, charge density and local thermodynamical characteristics of microvolum.

Thus difference of chemical potentials $\mu_i$ and $\mu_j$ creates a premise for clastering and for an defect structure. Fermi`s energy of phases is analog of chemical potential one:

$$\mu \cong (\partial g/\partial n_i)_{P,T,nj} = -T\,(\partial s/\partial n_i)_{E,V,} \cong E_f \qquad (3)$$

It is to be noted, that the stacking fault energy (SFE ) has bond with density of electronic states on Fermi level $N(E_f)$ trough entalphy **h**.

It is a matter of common knowledge this $N(E_f)$ controls forming many physical-chemical and mecanical properties on level of the material atomic structure:

$$SFE \cong h - h_o \approx \Delta h^{i \to j} \sim \Delta N(E_f)^{i \to j} \qquad (4)$$

**h** - enthalpy of ideal lattice of solid solution, $\mathbf{h_0}$ – enthalpy of defectsaturated layer.

Thas, owing to $\Delta N(E_f)$ we will be made correc-tion in calculation.

The density of electron states on the Fermi`s level my be done experimental by means of X-ray photo electronic spectroscopy (or by Ultra-violet spectroscopy): the first – from nondefect surface, the second – from defect surface.

The end forms of equations for the stacking fault energy (SFE) for Gibb`s energy (5)

$$SFE = (dE/dQ_o)_{ni,V,T} = (dG^s/dQ_o)_{ni,V,T} \qquad (5)$$

and through Helmholz`s potencial (6):

$$SFE = ( dE/dQ_o)_{ni\,,\,V,\,T} = (dF^s/dQ_o)_{ni\,,\,V,\,T} \qquad (6)$$

has been written by local internal energy as function of a lattice energy:

$$\delta u = \sum_{n=1}^{\infty}[3n\xi(3nd)- (3n-1)]\xi(3nd-d)- \Delta N(E_f)^{\,i-j} \quad (7)$$

here **d** – lattice constant, **n** - dimentional order, ξ value, which depends from a valence electron charges and parameters Fermi`s surface, and from concentration of an free electrons per atom (1,14).

The intergrowth structure forms after the type micromechanism of selfdriving of trasfer charge between atoms components and admixture elements.

Report will be discussion the problem a motion defect of packing (a vacancies, a point atom defects) and defect of chemical nature (after the type d-metall complex with trasfer of charge).

It will be consider of the defect balance equation on Stoks`s theorem base and at athors approach too.

References.

1. Uskova N.A. Osobenosti formirovaniya struktury pokrytiy i ee vliyanie na phisico-mehanicheskie cvoistva // Adgeziya rasplavov i paika materialov. - Kiev: IPM. - 1997, S. 113.
2. Moljar A.G. Vliyanie ekspluatacionyh nagrevov na strukturu, svoistva i phazovyi sostav mnogosloynyh ionno-plazmenyh pokrytiy // Tam ge. – S. 98-100.
3. Grishchishyna L.N. Rol elektronnoy struktury v phazovyh prevrasheniyah splavov. – Disser. kand. phis.-mat. nauk. – Kiev, 1990, 157 s.
4. Grishchishyna L.N., Trefilov V.I. Svjaz electrokhimicheskikh svoystv s elektronnoy strukturoy vysokokhromistykh splavov // Dokl. AN SSSR. – 1991, 318, 1. – S. 96-101.
5. Grishchishyna L.N., Lysenko A.A., Trefilov V.I. Kompleksnoe issledovanie splavov titana s 3d-metallami // EMiPM. – Kiev: IPM NANU. – 2001. – S. 69-80.

# COMPUTER MODELING AND PREDICTION OF PHYSICAL-CHEMICAL PROPERTIES OF $SiC\text{-}Me^{IV\text{-}V}C\text{-}MeB_2$ COMPOSITES

**Unrod V.I, Ordaniyan S.S.(1), Udalov U.P.(1), Neshpor I.P.(2)**
Cherkasy State Technological University, E-mail: unrod@chity.uch.net
(1)Saint Peterburg's Institute of Technology, E-mail: udalov@peterlink.ru.
(2)Frantsevicn Institute for Problems of Materials Sciences, E-mail: cherm@materials.kiev.ua

Metal-like covalent compounds have unique physical-chemical and mechanical properties and are used as base for ceramics for different technical application. Alloys based on carbides, diborides, nitrides and diborides of d-transition metals of IV-V groups due to the investigation of quasi-binary section of Me-C-B, Me-N-B systems are used as heat-resistant, thermo stable, corrosion-proof, wear-resistant materials which have in case of fine differentiated eutectic structure formation high plastic properties at high temperatures. SiC high-temperature ceramics are of great interest at a high-temperature ceramics market due to their high corrosion resistance, thermo conductivity, low coefficient of thermal expansion.The character of interaction of wide range of SiC-MeC, $SiC\text{-}MeB_2$ state diagrams which differ with eutectic transformations has been determined. It extends technological possibilities of composite materials obtaining with high physical-mechanical characteristics, particularly for engines high temperature ceramics.

Due to the analysis of studied binary systems of $Me^{IV,V}C\text{-}MeB_2$, $SiC^{IV,V}\text{-}MeC$, $SiC^{IV,V}\text{-}MeB_2$ some of uninvestigated before state diagrams of $SiC\text{-}Me^{IV}C\text{-}Me^{IV}B_2$, $SiC\text{-}Me^{V}C\text{-}Me^{V}B_2$ (where Me $^{IV,V}$- d-transition metals (titanium, zirconium, gafnium, vanadium, niobium, tantalum) have been constructed. State diagram construction of binary and more complicated systems both by experimental and by the use of strict thermo dynamical calculations is rather labor-consuming and, in some cases, hard solving problem. For construction such diagrams calculation methods of state diagrams are used. The base of the calculations is the idea of alloy specific, power of structural units interaction at solid-alloy phase transformation. Using equations that express thermodynamics of models of ideal, regular, associated solutions the following equations which allow to describe many types of binary systems, including limited solid solution areas have been used:

$$RT = \frac{x^2 V_l + y^2 V_s + R S_f T_f}{S_f - \ln\left(\frac{1-x}{1-y}\right)}$$

Where: x - concentration of component in melt; y - concentration of component in co-existing solid solution at temperature T; $V_l$ – energy of interaction of component in melt; $V_s$ – energy of interaction of component in solid solution; $S_f$ – change of entropy at L – S phase transformation.

With the help of computer modeling and in line with calculation equations 6 state diagrams have been constructed and both eutectic temperature and eutectic composition in following triple systems have been determined:

1. In $SiC\text{-}TiC\text{-}TiB_2$ system: temperature of triple eutectic (Teut.) is 2047±40 °C, concentration of triple system components in eutectic point corresponds to: SiC=0.587; TiC=0.128; $TiB_2$=0.284 (mole fraction).
2. In $SiC\text{-}ZrC\text{-}ZrB_2$ system: Teut.=2074±40 °C, concentration of triple system components in eutectic point corresponds to: SiC=0.577; ZrC=0.171; $ZrB_2$=0.251 (mole fraction).
3. In $SiC\text{-}HfC\text{-}HfB_2$ system: Teut.=2280±40 °C, concentration of triple system components in eutectic point corresponds to: SiC=0.718; HfC=0.052; $HfB_2$=0.228 (mole fraction).
4. In $SiC\text{-}VC\text{-}VB_2$ system: Teut.=1825±40 °C, concentration of triple system components in eutectic point corresponds to: SiC=0.196; VC=0.415; $VB_2$=0.388 (mole fraction).
5. In $SiC\text{-}NbC\text{-}NbB_2$ system: Teut.=2156±40 °C, concentration of triple system components in eutectic point corresponds to: SiC=0.444; NbC=0.206; $NbB_2$=0.348 (mole fraction).
6. In $SiC\text{-}TaC\text{-}TaB_2$ system: Teut.=2195±40 °C, concentration of triple system components in eutectic point corresponds to: SiC=0.635; TaC=0.037; $TaB_2$=0.327 (mole fraction).

Experimental investigations of $SiC\text{-}Me^{IV,V}C\text{-}Me^{IV,V}B_2$ systems acknowledge both values of eutectic temperatures and composition of eutectic alloys.

# PHASE INTERACTION IN THE TERNARY SYSTEM $HfO_2$-$Y_2O_3$-$Eu_2O_3$ AT HIGH TEMPERATURES

**Andrievskaya Elena R.**, **Lopato Lidiya M.**
Frantsevich Institute for Problems of Materials Science, Ukraine NASU,
Krzhizhanovsky str. 3, 03680, Kiev 03142,Ukraine, E-mail: ragulya@materials.kiev.ua

## ABSTRACT

Phase equilibria in the binary $HfO_2$-$Eu_2O_3$, $Eu_2O_3$-$Y_2O_3$ and the ternary $HfO_2$-$Y_2O_3$-$Eu_2O_3$ systems were studied in the wide range of temperatures (2500-1250 °C) and concentrations (0-100 mol % $Eu_2O_3$) by thermal analysis in air, X-ray diffraction, microstructural and petrographic analyses, electron microscopy using melted and annealed samples. Phase diagrams of the $Eu_2O_3$-$Y_2O_3$, $HfO_2$-$Eu_2O_3$ and $HfO_2$-$Y_2O_3$-$Eu_2O_3$ systems are developed.

## INTRODUCTION

Europia as well as yttria is useful dopant to refractory oxide such as hafnia. Because of its high capture cross section in fast neutron fluxes and because this absorption worth is sustained by chains of high cross-section daughter isotopes, europia is attractive as a control and shutoff rod material in fast reactors. Europia is a suitable for these purposes since it is relatively stable chemically, has a high melting point (2320°C), can be fabricated easily into dense bodies with a high europia density, and is readily available. However, disadvantage associated with the use of pure europia is that when it is fabricated at temperatures above 1100°C the higher-temperature monoclinic B form is produced which exhibits undesirable swelling under fast neutron irradiation. The cubic structures can be stabilized at sintering temperatures by using suitable additives. Additions of hafnia and yttria to europia suppress grain growth and improve its elastic properties [1].

The main purpose of this work is to investigate the physics and chemistry of phase interactions in the ternary $HfO_2$-$Y_2O_3$-$Eu_2O_3$ system at high temperatures and wide concentration range. This system is perspective from the standpoint of creation high-refractory materials and ones with increased strength characteristics in which the composition of both matrix and strengthening phase is the same.

Phase relations in the boundary binary systems $Eu_2O_3$-$Y_2O_3$, $HfO_2$-$Eu_2O_3$ were studied in the wide range of temperatures (1250-2800°C) and concentrations (0-100 mol % $Eu_2O_3$). Phase diagrams of these systems were developed [2, 3].

Phase equilibria of the system $Eu_2O_3$-$Y_2O_3$ are characterized by the formation of the fields of solid solutions of various extent based on the hexagonal (A- and H-type), monoclinic (B), cubic (C- and X-type) modifications of the rare-earth oxides, that is known for the majority of cerium subgroup oxides. There are the peritectic-type transformation on the liquidus at 2370 °C, 58 mol % $Y_2O_3$ and point of minimal temperature at 2310 °C, 10 mol % $Y_2O_3$.

In the subsolidus region of the phase diagram $HfO_2$-$Eu_2O_3$ system the fields of solid solutions based on monoclinic (M), tetragonal (T) and cubic (fluorite-type, F) modifications of hafnia, pyrochlore-type compound $Eu_2Hf_2O_7$ as well as solid solutions on the basis B, A, H and X forms of $Eu_2O_3$ were found. The dopants of hafnia to europia have stabilized the C-phase at the higher temperatures, increasing the range of its existence. The liquidus of the system $HfO_2$-$Eu_2O_3$ is characterized by eutectic transformation at 2150°C, 25 mol % $HfO_2$. The compound $Eu_2Hf_2O_7$ is not observed on the liquidus surface but is formed in the solid phase at temperature ~ 2450 °C.

Solid solutions based on T, M and F modifications of hafnia as well as C and H modifications of yttria are known to form in the system $HfO_2$-$Y_2O_3$ at high temperatures [4]. The liquidus of this system is characterized by an eutectic transformation at 2400 ±25 °C and 84 ±2 mol % $Y_2O_3$ and a peritectic transformation at 2430 °C and 77±2 mol % $Y_2O_3$ [5].

## EXPERIMENTAL PROCEDURE

The samples for investigations of the phase equilibria in the ternary $HfO_2$-$Y_2O_3$-$Eu_2O_3$ system were prepared from 5 to 10 mol % by both mechanical mixing of oxides and coprecipitation of hydroxides. Part of these samples was used for the investigation in the as prepared form (melted specimens). Other samples were annealed at 1550 °C for 70 h in air. The boundaries of the phase fields were determined by thermal analysis in air up to 3000 °C using a solar furnace. The phase compositions were investigated by petrography, X-ray phase analysis, electron microprobe X-ray analysis, chemical and X-ray fluorescence spectrum analysis.

## RESULTS AND DISCUSSION

An investigation of interaction in the system $HfO_2$-$Y_2O_3$-$Eu_2O_3$ over the whole range of concentrations at temperatures above 2000 °C revealed no new phases. The results of this investigation showed that the liquidus surface of this system consists of four fields of phase-primary crystallization: namely, solid solutions based on $HfO_2$ phase with a fluorite-type structure F, H and C forms of $Y_2O_3$ as well as X- $Eu_2O_3$. There are two invariant points of incongruent-type four-phase equilibria on the liquidus with the coordinates 17 mol % $HfO_2$, 55.5 mol % $Y_2O_3$ at 2360 °C ($U_1$) and 19 mol % $HfO_2$, 36 mol % $Y_2O_3$ at 2310 °C ($U_2$).

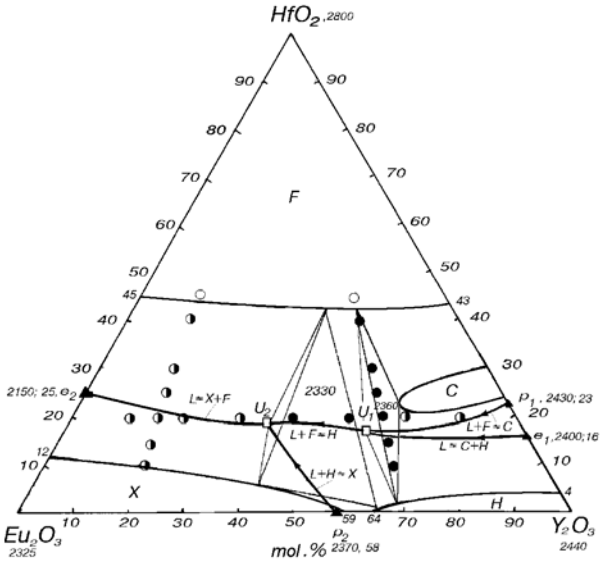

Fig. 1. Crystallization paths for the $HfO_2$-$Y_2O_3$-$Eu_2O_3$ system (○ -single phase, ◑ - binary phase, ● - ternary phase samples).

The minimal melting temperature for the $HfO_2$-$Y_2O_3$-$Eu_2O_3$ system is 2150 °C($e_2$), maximum temperature of the liquidus surface is equal to 2800 °C, which corresponds to the melting point of pure $HfO_2$. The liquidus surface of this system contains the same fields as do the solidus surface, and the most extended field is that of the fluorite based solid solutions. Solidus surface in the investigated system consists of 2 ternary-phase fields corresponding to the transformations L+H⇄X+F and L+C⇄H+F. The crystallization of the alloys was investigated using the data on structure of the liquidus and solidus surfaces. The crystallization paths for the alloys and the schematics of the reactions were constructed (Figs. 1, 2).

Fig. 2. Schematic of the reactions proceeding during equilibrium crystallization of melted samples in the $HfO_2$-$Y_2O_3$-$Eu_2O_3$ system.

The isothermal sections were developed at 1550 °C and 1250 °C. We identified single phase regions of solid solutions based on M- and F-$HfO_2$, B- and C-$Eu_2O_3$, C-$Y_2O_3$ and $Eu_2Hf_2O_7$ (Py).

## REFERENCES

[1] R.W. Scheidecker, D.R. Wilder, H. Moeller: J. Am. Ceram. Soc. Vol. 60 (1977), 501.

[2] E.R. Andrievskaya, Z.A. Zaitseva, A.V. Shevchenko, and L.M. Lopato: Inorganic Materials. Vol. 33, No. 4 (1997), 390.

[3] E.R. Andrievskaya, L.M. Lopato, A.V. Shevchenko, and V.P. Smirnov: Inorganic Materials. Vol. 33, No. 7 (1997), 835.

[4] M.F. Trubelja and V.S. Stubican: J. Am. Ceram. Soc. Vol. 71 (1988), 662.

[5] A.V. Shevchenko, L.M. Lopato, and I.E. Kiryakova: Inorganic Materials. Vol. 20, No. 12 (1984), 1991.

## ACKNOWLEDGEMENTS

Authors thanks A.V. Shevchenko, V.P. Red'ko, I.E. Kiryakova, Z.A. Zaitseva, and V.P. Smirnov for their helpful advices and assistance in experimetal study of presented phase diagram.

# HYSICAL-MATHEMATICAL MODEL OF HIGH-RATE WELDING OF BIMETAL MATERIALS

Gulbin V.N., Nikitin I.S., Kobelev A.G. (1), Kolesnikov F.V. (1)
Federal State Unitary Enterprise “Scientifical Research Technology” Moscow, Russia,
43, Altufievskoe sh., Moscow, 127410, Russia, E-mail: vngulbin@mtu-net.ru.
(1)Moscow State Institute of Steel and Alloys “Technical University”, Moscow, Russia
4, Leninsky prospect, Moscow, 119049, Russia

This paper presents a physical-mathematical model of high-rate impact of isotrope and homogeneous media’s layers, whose physical properties are independent from temperature and deformation. Basing on these results a methodic was developed for calculation of explosive welding parameters for bi-metal products.

Just after the moment of welded materials impact an elastic-viscose behavior model was applied for metals with plasticity point depending on deformation rate. In this case temperatural destrengthening and contact interaction in a “friction-connection” regime are depended on plastic deformation level. This methodic was tested by development of technology and manufacture of thermal-bimetal products made of titanium, corrosion-resistant steel, chrom-nickel alloys, aluminum with Бр.Б2 berillium bronze claddind, which were purposed as sensors for thermal instruments. Calculation of explosive welding parameters for bi-metal materials shall be performed with accounting of stress-deformation characteristics of welded materials, with use of a physical-mathematical model for their study.

A significant role in fast welded joint production have physical-mechanical processes, high-rate elastic- and plastic deformation and also contact friction. Joint forming is prevented by a volumar elasticity wave generated in the metal by detonation products pressure and by mechanical interaction forces between welded surfaces n process of their impact. This wave spreads in the welded materials’ thickness; its reflection from the contact surface causes separation of the joined maerials each from other.

Let us show a physical model of high-rate impact of two non-similar metal tubular parts placed co-axially, under detonation wave influence, which moves along the external wall surface of the movable part. Let it be $d_1$ and $d_2$ joined walls thicknes significantly lower then both their $R_1$ and $R_2$ radiuses and L length, but greater then $\Delta$ clearance between them. The $\Delta$ value shall define further inclination (dynamic) angle for the walls’ impact.

By explosive welding a detonation wave’s speed along the tube’s external surface is 2-4 km/s, that is near to elastic waves travel speed in metals and defines a preferable sub-sonic impact regime for explosive welding. For example, in titanium and steel: $C_{PTi}$~6 km/s, $C_{STi}$~3,5 km/s, $C_{PFe}$ ~5,55 km/s, $C_{SFe}$ ~3,25 km/s ($C_P$ and $C_S$ = travel speeds of longitudinal and transversal elastic waves). Pressure in detonation wave depends also on explosive charge’s characteristics and achieves $(0{,}3\text{-}1{,}0)*10^4$ MPa; that exceeds the static plasticity point of the metals and allows to apply a hydraulic-dynamical approach for rough evaluation. However, the dynamical plasticity point increases significantly as result of dynamical reinforcing. Ignoring of such strength effects can give a very wrong picture of SDC for welded metals. Actual width of a chemical reaction zone by charge detonation, which defines length of pressure pulse and loading rate, is h ~(1-2) mm, that is $h \le d_{1,2}$. That means the pressure pulse’s length is: $\Delta\tau = \dfrac{h}{v} = \dfrac{7\times10^{-3}}{2\times10^{6}} = 3{,}5\times10^{-9}$ s.

Thus level and period of pulsed loads define choose of elastic-plastic behavior model for metals with plastisity point depending on deformation rate. Because of a greater part of plastic deformation work is transformed into heat, it is possible to choose a competetive mechanism of dynamical dis-strengthening (regarding dynamical strengthening). It leads to decrease of plastisity point because of heating.

The model of contact interaction shall account a character and parameters of “friction-interaction” of impacting surfaces. Thus the model of Coulogn friction was choosen, which applied dependence on plastic deformation level with account welding criteria. This criteria does not contradict the known welding jet criteria, because of forming of “cleaning” cumulative jet being possible only in the case of developed plastic flows in near-impact front of welded walls.

A mathematical task setting within frames of modified elastic-plastic model (with account of heat disstrengthening) in a general tenzor form includes a system of evolution equations for travel, continuity, shear deformation and temperature change correspondently:

$$\rho\dot{\upsilon} = \nabla\sigma; \qquad (1); \qquad \rho + \rho\nabla\dot{\upsilon} = 0; \; (2)$$

$$S^R = 2\mu e' - \eta\langle F\rangle s; \quad (3); \qquad \rho CT = \frac{s}{e^P}. \; (4)$$

Also it is possible to apply final ratios of volumetric deformation, non-linear rlaxation, change of plastic deformation rate's tenzor and decreasing dependence of plasticity point upon temperature correspondently:

$$P = P(\rho); \qquad (5)$$

$$F = \sqrt{\frac{0{,}5s:s}{\tau_s - 1}}, \qquad \langle F\rangle = FH(F); (6)$$

$$e^P = \eta\langle F\rangle\frac{s}{2\mu}, \qquad \tau_s = \tau_s(T); \quad (7)$$

here:: ρ = density of movable wall's material; $\dot{\upsilon}$ = travel speed vector of the movable wall; σ = stress tenzor; ∇ = space nabla-operator; s = deviator of stress tenzor; μ = shear module; η = viscosity coefficient; F = non-linear relaxation function; e = tenzor of deformation rates; $\tau_s$ = statical plasticity point; C = thermal heat capacity; T = temperature.

As result of anlytic solving of the system of base equation it is possible to obtain a formula for a normal contact force ensuring non-penetration conditions:

$$P_n = \frac{[r_1 - (r_0 + \Delta r_0) - \Omega\Delta r_1]n}{[C_0 + C_1 + 2C_1\Omega + (C_1 + C_2)\Omega^2]\Delta t(\Delta r_1 \Delta r_2)}.$$

$$\Omega = -\frac{[r_1 - (r_0 + \Delta r_0)] \bullet \Delta r_1}{\Delta r_1 \bullet \Delta r_2}. \quad C_{0,1,2} = \frac{\Delta t}{\dfrac{\rho_{0,1,2}}{\Delta v_{0,1,2}}}.$$

The feature of the formula for $P_n$ is that it gives a wittingly necessary sign (–) of contact force by failure of the non-penetration condition for contact pair (component, part).

The similar "compensation approach" is applicable for definition of tangential contact forces $P_\tau$. First it is necessary to define $P_\tau$ basing on sliding condition:

$$\begin{aligned} &U_{\tau 0} + P_\tau \Delta t C_0 = \\ &(U_{\tau 1} - P_\tau \Delta t C_1)(1 - \Omega) + \Omega(U_{\tau 2} - P_\tau \Delta t C_2) \end{aligned} \qquad (8)$$

Then:

$$P_\tau = \frac{[(1-\Omega)U_1 + \Omega U_2 - U_0] \bullet \Delta r_1}{[C_0 + C_1 - 2\Omega C_1 + C_1 + C_2\Omega^2]\Delta t(\Delta r_1 \Delta r_1)}.$$

If defined value should not break interaction condition $|P_\tau| \le C_0 + q|P_n|$, the calculation of contact interaction could be completed. If such condition is broken, it is necessary to consider the tangential force as equal to a limit one: $|P_\tau| = C_0 + q|P_n|$. Tangential speeds of the cmponent and the part's edges shall be defined accounting this additional force. The third law of Newton shall be applied in this case by changing of directions of corresponding forces both in right and left parts of equation (1), where $P_n$ and $P_\tau$ have opposite signs.

The described algorythm of task solving for high-rate impact of metal walls is pealised in a working software package, whose structure repeats consequense of the procedures described in the paper. This software was tested by calculation of explosive welding parameters for tubular jionts,as wellas for explosive welding of plane thermal bi-metals.

# THE ELECTRONIC STRUCTURE AND PROPERTIES OF $Ni_{1-x}Li_xO_{1-y}$ ($0 \le x \le 1/4$; $0 \le y \le 1/8$)

**Zainullina V.M., Korotin M.A.**(1)**, Zaikov Yu.P.**(2)**, Shurov N.I.**(2)
Institute of Solid State Chemistry, Ural Branch RAS, Ekaterinburg, Russia
Pervomayskaya, 91, GSP-145, Ekaterinburg, 620219, Russia, e-mail: Veronika@ihim.uran.ru
(1)Institute of Metal Physics, Ural Branch RAS, Ekaterinburg, Russia
S.Kovalevskaya, 18, GSP-170, Ekaterinburg, 620219, Russia, e-mail: mkorotin@optics.imp.uran.ru
(2)Institute of High-Temperature Electrochemistry, Ural Branch RAS, Ekaterinburg, Russia
S.Kovalevskaya, 20, GSP-146, Ekaterinburg, 620219, Russia, e-mail: Zaikov@ihte.uran.ru

Nickel oxide with the NaCl-type structure refers to a wide class of Mott-Hubbard insulators. There are many results of calculations of the electronic structure and magnetic properties for stoichiometric NiO in the literature [1,2]. Nonstoichiometric nickel oxide (with structural defects) is poorly investigated [3]. Defects existed in NiO have a considerable effect on its transport properties. Pure nickel oxide, which is synthesized at a low partial pressure of oxygen, is a dielectric. NiO, which is prepared in air at T=1000 °C, becomes a semiconductor. The electrical conductivity for lithium-doped NiO reaches ~1 $(\text{Ohm}\cdot\text{cm})^{-1}$ at 10 at. % Li.

The effect of structural defects on the electronic spectrum and electrical conductivity of NiO has been investigated by means of the *ab initio* TB-LMTO method in the LSDA+U approximation [4]. The electronic structures NiO, $Ni_{0.875}O$, $NiO_{0.875}$, $Ni_{0.875}Li_{0.125}O$, $Ni_{0.875}Li_{0.125}O_{0.875}$ and $Ni_{0.75}Li_{0.25}O_{0.875}$ have been calculated using the cells: $Ni_8O_8$, $Ni_7VO_8$, $Ni_8O_7V$, $Ni_7LiO_8$, $Ni_7LiO_7V$ and $Ni_6Li_2O_7V$, where V is an empty sphere (vacancy) on a nickel or oxygen site.

The electronic spectrum of NiO in Fig. corresponds to the spectrum of an insulator with a charge transfer gap (calculated value is about 3.7 eV). A wide valence band consists from hybrid Ni3*d*-O2*p*-states and a narrow conduction band is formed mostly by 3*d*-states of nickel atoms. The shape, the location and the origin of the bands in the electronic energy spectrum of NiO agree well with the X-ray photoemission spectroscopic data.

The *ab initio* calculations of electronic structures for $Ni_{0.875}O$, $NiO_{0.875}$, $Ni_{0.875}Li_{0.125}O$, $Ni_{0.875}Li_{0.125}O_{0.875}$ and $Ni_{0.75}Li_{0.25}O_{0.875}$ have shown that the presence of defects in the cation and anion sublattices of nickel oxide leds to appearance of the bands in the region of the energy gap. The nature of the bands depended on the defect type.

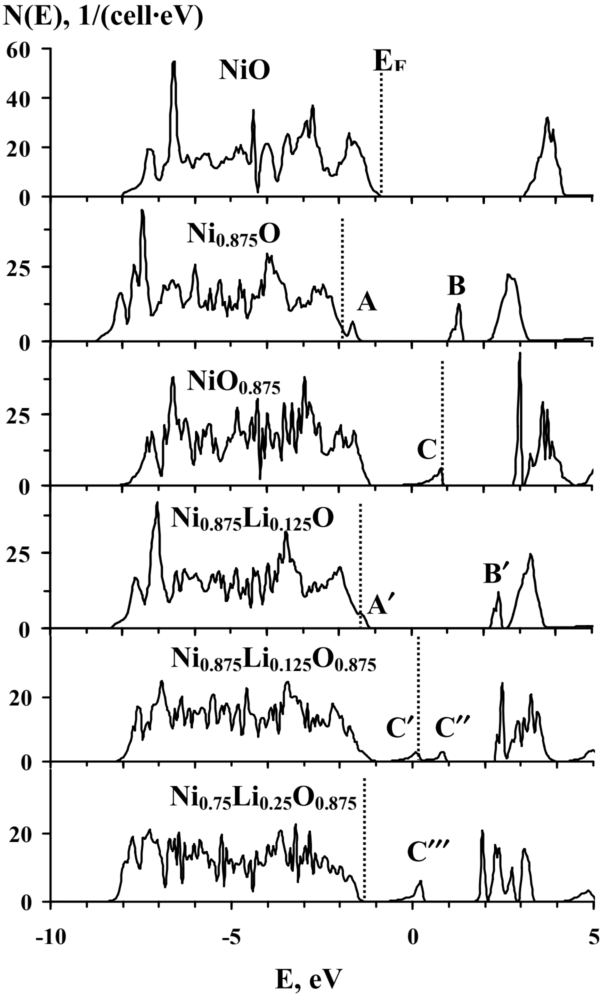

**Fig.** The total densities of states for NiO, $Ni_{0.875}O$, $NiO_{0.875}$, $Ni_{0.875}Li_{0.125}O$, $Ni_{0.875}Li_{0.125}O_{0.875}$ and $Ni_{0.75}Li_{0.25}O_{0.875}$.

In $Ni_{0.875}O$ two peaks (**A** and **B)** appear in the electronic spectra (Fig.). The empty **A** peak at the valence band top is determined by oxygen 2*p*-states of the nearest octahedral neighbours of nickel vacancies and 3*d*-states of nickel in the ratio of about 4:1, and small contributions of 1*s*-states of vacancies. The **B** peak located at the conduction band bottom consists mainly of 3*d*-states of nickel atoms. The hole conductivity in $Ni_{0.875}O$ is determined by the transition of an hole from the acceptor **A** subband to the valence band.

The main feature of the electronic structure of $NiO_{0.875}$ is the presence of the **C** band near the center of the gap (Fig.). This band consists of the *s*-states of oxygen vacancies ($V_O$), 3*d*-states of six nickel atoms from the nearest neighbours of vacancies. The semiconductor type of conductivity characterizes NiO0.875.

As is see from Fig. the $Ni_{0.875}Li_{0.125}O$ spectrum has the **A'** shoulder at the top of the valence band and the narrow **B'** band near the metallic conduction band. The Fermi level passes through the maximum of the **A'** shoulder, which is comprised mainly 2*p*-states of oxygen in the first coordination sphere of lithium atoms. The hole type of conductivity in $Ni_{0.875}Li_{0.125}O$ (the effective mass is negative along the symmetry directions in the Brillouin zone) is explained by the transfer of electrons from the valence band to the empty acceptor subband **A'**. When the concentration of lithium atoms is 12,5 at. % the acceptor band merges with the valence band and the electron transfer energy tends to zero.

In the case of $Ni_{0.875}Li_{0.125}O_{0.875}$ and $Ni_{0.75}Li_{0.25}O_{0.875}$ oxygen vacancies and lithium ions are mutually attracted and formed dipoles $Li–V_O$ and tripoles $Li–V_O–Li$ with the dissociation energy of 0,07 eV and 0,34 eV respectively. These defects formed wide band (**C'** or **C'''**) up to 1.7 eV in the energy gap of stoichiometric NiO (Fig.). The presence of defects like $Li–V_O$ and $Li–V_O–Li$ in $Ni_{0.875}Li_{0.125}O_{0.875}$ and $Ni_{0.75}Li_{0.25}O_{0.875}$ could be one of the reasons for the impairment their electrical conductivity.

Main characteristics of the electronic spectra of NiO, $Ni_{0.875}O$, $NiO_{0.875}$, $Ni_{0.875}Li_{0.125}O$, $Ni_{0.875}Li_{0.125}O_{0.875}$ and $Ni_{0.75}Li_{0.25}O_{0.875}$ have been summarized in the Table. The calculated values of the energy gap on nickel atoms in NiO approached the corresponding experimental values. The majority of phases based on nickel oxide are characterized by small densities of states at the Fermi level, $n(E_F)$, and the hole type of conduction. The exceptions are $NiO_{0.875}$ and $Ni_{0.75}Li_{0.25}O_{0.875}$ having the semiconductor gap.

The cohesive energy $E_{coh}$, which characterizes the stability of compounds, was calculated for NiO, $Ni_{0.875}O$, $NiO_{0.875}$, $Ni_{0.875}Li_{0.125}O$, $Ni_{0.875}Li_{0.125}O_{0.875}$ and $Ni_{0.75}Li_{0.25}O_{0.875}$ (see Table). The cohesive energy has maximum value for NiO and $Ni_{0.875}Li_{0.125}O$, and a minimum value for $Ni_{0.75}Li_{0.25}O_{0.875}$. The calculations of the cohesive energy show that NiO and $Ni_{0.875}Li_{0.125}O$ are most stable and $Ni_{0.75}Li_{0.25}O_{0.875}$ is the least stable. The concurrent presence of oxygen vacancies and lithium ions in nickel oxide impaired the stability of the crystalline structure of NiO-based phases.

**Table.** Characteristics of electronic spectra of NiO, $Ni_{0.875}O$, $NiO_{0.875}$, $Ni_{0.875}Li_{0.125}O$, $Ni_{0.875}Li_{0.125}O_{0.875}$ and $Ni_{0.75}Li_{0.25}O_{0.875}$ the energy gap $\Delta E_g$; the densities of states at the Fermi level, $n(E_F)$; the cohesive energy $E_{coh}$. Given in brackets are the corresponding experimental values.

| Compound | $\Delta E_g$, eV | $n(E_F)$, 1/eV | $-E_{coh}$, eV/f.u. |
|---|---|---|---|
| NiO | 3,70<br>(4,0) | — | 14,46 |
| $Ni_{0.875}O$ | — | 5,91 | 12,56 |
| $NiO_{0.875}$ | 2,04 | — | 13,16 |
| $Ni_{0.875}Li_{0.125}O$ | — | 4,77 | 13,86 |
| $Ni_{0.875}Li_{0.125}O_{0.875}$ (with dipole) | — | 2,84 | 12,79 |
| $Ni_{0.75}Li_{0.25}O_{0.875}$ (with tripole) | 0,36 | — | 12,39 |

## REFERENCES.

[1]. V.I. Anisimov, M.A. Korotin, E.Z. Kurmaev. J. Phys.: Condens. Matter, **2**, *17*, 3973 (1990).

[2]. A. Svane, O. Gunnarsson. Phys. Rev. Lett. **65**, *9*, 1148 (1990).

[3]. D. Ködderitzsch, W. Hergert, Z. Szotek, W.M. Temmerman. Phys. Rev. **B68**, 125114 (2003).

[4]. V.I. Anisimov, F. Aryasetiawan, A.I. Lichtenstein. J. Phys.: Condens. Matter, **9**, *4*, 767 (1997).

*The reseach has been supported by Russian Science Support Foundation grant and RFBR grant № 01-02-17063.*

# TUNGSTEN CARBIDE OBTAINING BY TREATMENT OF MELTS BY GASES

**Gab A.I., Uskova N.N.(1), Glushakov V.G.(1), Malyshev V.V.**
National Technical University of Ukraine "KPI", Kiyv, Ukraine
37, Peremoga ave, apt#4, Kyiv, 03056, Ukraine, lina_gab@ukr.net
(1)Vernadskii Institute of General and Inorganic Chemistry of NASU, Kiyv, Ukraine
32/34, Palladina ave., Kyiv, 03142, Ukraine, synthesis@ionc.kar.net

We developed the method of high-temperature selective extraction from ores and concentrates earlier [1, 2]. Tungsten compounds pass into chloride phase during melting of sodium chloride and metasilicate mixture with tungsten ores and concentrates. Experimentally established optimal compositions of the melts containing 25—35 wt.% of $WO_3$ correspond to the $WO_3$ extraction degree up to 99%.

Reducing gas treated the molten halide-tungstate phase. Tungsten carbide was isolated from reaction mass by excess salt decantation and carbide crystals leaching. Preliminary investigations of gas barbotage were carried out in crucibles made from gaphite, silicon carbide, diamond, inconel. Methane, natural gas, carbon monooxide, hydrogen and their mixtures were tried as reducing gases. Influence of additives of fine-dispersed carbon and calcium carbide was also investigated.

Preliminary experiments have shown that the best material for reactors and bubbling tubes is inconnel (since carbonizing gas does not break into carbon and hydrogen in contrast to the case of non-metallic materials). Methane was appeared the best gas for barbotage, and additives of carbon and calcium carbide did not improve the product quality and process conditions. The temperature range 1050—1070 °C was found to be optimal. At lower temperatures the yield of tungsten carbide amounts only to some %. At higher temperatures melt evaporation considerably increases. Optimal methane bubbling rate is 3—4 l/min. The further increase of bubbling speed did not result in essential increase of WC yield and caused increase of salts losses. Unreacted methane was incinerated at the top of the reactor.

Two types of reactors, open and closed, were used in apparatus design. Various operating conditions were also used: with single and multiple (up to 5 times) loading. Experiments have shown that in the open chamber up to 60 % of tungsten is extracted as WC and 2,6 % of carbon (methane) is also converted into WC. In the closed reactor up to 75 % of tungsten is extracted as WC and 2,5 % of carbon (methane) is also converted into WC. Losses of salts in the former case made 17—20 % and in the second case – less than 1 %. The overall content of carbon in WC was 6,1 %, and of free carbon — 0,06 wt. %. For 1 kg of WC the following reagents are consumed, in kg:

$Na_2WO_4$ – 2,1
NaCl – 3,1
$Na_2CO_3$ – 0,6
$SiO_2$ – 0,7
Natural gas (methane) – 2,2

This work was supported in part by the Ministry of science and education in the framework of the Ukrainian-France program "Dnipro", project №M/353—2003

[1] Gab A.I., Uskova N.N., Malyshev V.V. Tungsten extraction from ores and concentrates by method of high-temperature selective extraction // International Conference "Novel technologies in powder metallurgy and ceramics". Kyiv, September 8—12, 2003. Book of abstracts. — P. 79—80.

[2] Malyshev V.V., Butov S.A., Gab A.I., Uskova N.N., Gritsaj T.G. Processing of waste products of hard alloys "tunsten carbide - cobalt" in the phosphoric acid solutions. // Ecotechnologies and resources-economy. — 2003. — No. 3.–P. 33—36.

# NUMERICAL SIMULATION OF THERMAL-GRADIENT CHEMICAL VAPOUR INFILTRATION OF 4D FIBROUS PREFORM BY CARBON MATRIX

**Kulik V.I., Kulik A.V.** $^{(1)}$**, Ramm M.S.** $^{(2)}$**, NiloA.S.**
Baltic State Technical University, St.Petersburg, Russia, E-mail: kulik@softimpact.ru
$^{(1)}$Soft-Impact Ltd., St.Petersburg, Russia
$^{(2)}$A.F.Ioffe Physical Technical Institute, RAS, St.Petersburg, Russia

Among all fibre-reinforced composites, of great importance are composites with carbon matrix reinforced by carbon fibres (carbon-carbon composites – CCC). CCC were first produced as an alternative to composites with a polymer matrix, which had a low heat stability. As compared to non-reinforced graphite materials, CCC have higher strength and rigidity properties, low thermal expansion coefficient, high impact elasticity and thermal shock stability. CCC keep working efficiently at the temperatures up to 773 K in oxidative medium and up to 3273 K (for a short period, up to 3873 K) in an inert medium or in vacuum. Such composites are stable to radioactive radiation, have a high thermal conductivity and high erosion stability and can absorb high heat energy. Besides, porous composites have high adsorption capacity. Among CCM disadvantages, there are low oxidation stability at a temperature above 400 – 500 °C (in the absence of oxidation inhibitors and protective coatings) and corrosion in nitrogen at high temperature.

The major and potential areas of application of CCC are elements of brake devices of airplanes, construction elements of nuclear reactors, elements of nozzle blocks of solid-rocket and liquid-propellant engines, nose cones of rockets, protection attachments on the wings of space shuttles and inlets of hypersonic aircrafts, etc.

One of the most attractive methods for production of CCC is Chemical Vapour Infiltration (CVI) [1]. This method is based on deposition of the ceramic matrix on the heated fibres by chemical decomposition of gaseous precursors infiltrating through a fibrous reinforcing substrate or "preform". An advantage of this method is a possibility to obtain composites with matrices having very high melting temperatures under minimum thermal, mechanical and chemical impact on the reinforcing fibers.

To produce a carbon matrix, gaseous hydrocarbons (methane, propane, ethylene, benzene, acetylene, etc.) are normally used diluted by a carrier gas (hydrogen, nitrogen, argon, etc.).

A promising modification of this technique is Thermal-Gradient CVI (TG CVI). This method is characterized by a temperature gradient across the preform bulk, which is provided by placing the preform on a heated susceptor. The densification of the preform starts in the inner regions with higher temperature. During the process, the densification front moves to the cooler outer regions. Thus, the pores are not prematurely closed at the preform surface. The TG CVI method provides producing CCC of high density (1700—1800 kg/m$^3$) per a cycle and is characterized by a relatively high deposition rate and a possibility of bulk composite densification.

One of the most important problems in TG CVI research is finding the optimal values of technological parameters providing minimal infiltration time and required quality. Lately, numerical modelling has become a helpful tool for the TG CVI study and optimization. In the present work, we develop a model of TG CVI which describes one-dimensional (along the thickness preform) multicomponent heat and mass transport in the porous medium including heterogeneous chemical interaction between the gas and the preform.

In contrast to most previous works, our model of the TG CVI process considered the preform as a complex porous medium representing a bulk structure reinforced by fibre bundles in *n* directions. Such multidirectional preforms include pore systems of various scales – between fibres in bundles (intra-bundle pores) and between bundles (inter-bundle pores). The pore scale varies from microns within the bundle to hundreds of microns between bundles. The model accounts for the convective mass transport caused by the pressure variation due to the phase transitions and describes densification of the preform as a simultaneous saturation of multi-scale pore systems, allowing for diffusive and convective mass exchange between them [2].

The model also considers the evolution of the parameters of the complex porous medium during the preform densification. The method of the evolution computation is based on the data from ref. [3] on the multidirectional structure geometry.

To describer the heat transport, we have developed a method of evaluation of effective thermal conductivity of porous media with a bulk multidirectional structure reinforcing [4].

We analyse production of carbon matrix by TG CVI from methane ($CH_4$) diluted by hydrogen. The chemical deposition of carbon is assumed to occur in the following reaction of the methane decomposition:

$$CH_4\,(g) \rightarrow C(s) + 2H_2(g).$$

To describe the porous structure evolution due to material deposition, we use the quasi-steady state approach since characteristic time of mass transport is much less than time of the structure change.

Computations were made for a preform composed of bundles oriented along four cube diagonals (Fig. 1). Such structure, commonly known as 4D, allows producing an isotropic composite, which has a number of advantages compared to orthogonal 3D structure.

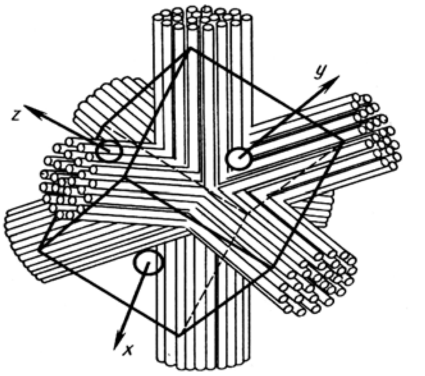

Fig. 1. Schematic of the 4D structure

This 4D preform includes two pore systems: 1) the inter-bundle pores, 2) the pores in the bundles oriented at the angle relative to the preform surface. Mass transport in these pore systems is considered to occur along the pore axis accounting for the mass exchange between the pore systems.

We analysed the influence of the TG CVI operating conditions, namely the methane concentration ($C_{CH4}$) in the ambient gas, the pressure in the reactor ($p$), the maximum temperature ($T_{max}$), and the temperature gradient ($\Delta T^0$) in the preform, on the process duration (densification time) and the quality of the composite – the average residual porosity and distributions along the preform thickness of the residual porosity in the different pore systems and in the whole material.

Fig. 2 shows an example of the average porosity distribution along the preform thickness at various stages of the densification process.

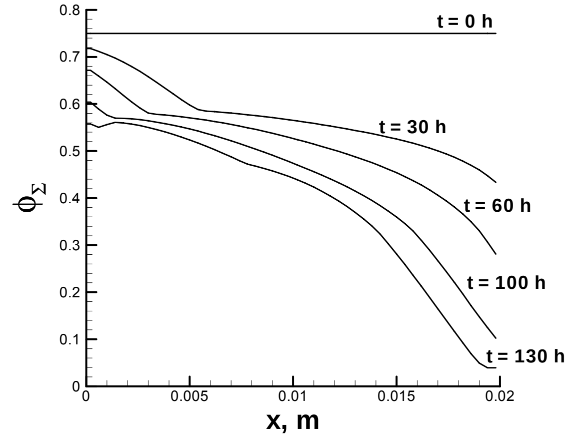

Fig. 2. The average porosity distribution along the preform thickness at various stages of the TG CVI

($T_{max}$=1300 K; $\Delta T^0 = 250\,\mathrm{K}$; $p$=30 kPa; $C_{CH4}$=0,6)

The computations have revealed that the densification time and residual porosity considerably vary in different pore systems. Thus, the optimal values of the TG CVI operating conditions are different in the pore systems. So, the densification should be performed in two stages with the individual operating condition values for each stage.

**References**

1. T.M. Besmann, B.W. Sheldon, R.A. Lowden, D.P. Stinton. Vapor-phase Fabrication and Properties of Continuous-filament Ceramic Composites. – Science, vol. 253, 1991, pp. 1104—1109.

2. V.I. Kulik, A.V. Kulik, M.S. Ramm, Yu.N. Makarov. Modeling of SiC-Matrix Composite Formation by Isothermal Chemical Vapour Infiltration. – J. Crystal Growth, in press.

3. Малько Д.Б., Островский В.С. Особенности пористой структуры углерод-углеродных композиционных материалов. Механика композиционных материалов и конструкций. т.3, №4, 1997, с. 29—35.

4. В.И. Кулик, А.В. Кулик, М.С. Рамм Определение коэффициентов теплопроводности многонаправленных пористых волокнистых каркасов.

Тезисы 2-й международной научной конференции РКТ-2003, М., in press.

# ON THE INCREASE OF EFFICIENCY OF THE PROCESS FOR THE DETERMINATION OF STRUCTURAL CERAMIC MATERIAL THERMAL AND PHYSICAL PROPERTIES

**Sereda G.N., Reznik S.V. (1), Rusin M.Yu., Prosuntsov P.V. (1)**
Federal State Unitary Enterprise
"Obninsk Research and Production Enterprise "Technologiya",
Obninsk, Kaluga region, 249035, Russia, onpptechn@kaluga.ru
(1)Bauman Moscow State Technical University, Moscow, 107005, Russia
E-mail: sreznik@serv.bmstu.ru, copyserv@mtu-net.ru

The investigations into thermal and physical properties (TPP) of aluminooxide, quartz ceramics and glass ceramic materials in a wide range of temperatures are urgent nowadays. The procedure and the results of the investigations into the TPP temperature dependences for a number of structural ceramic materials for the case of unidirectional radiant heating of the specimens and the use of heat exchange inverse problems are described in this paper. The problems of the specimen dimensions and test model choice, quantity and temperature sensor installation coordinates determination, TPP determination error assessment have been solved in the context of this paper.

A special-purpose plant for the material specimen radiant heating with the halogen incandescent lamps unit controlled by the regulator "Minitherm" was used in the experiments. The plant allows the variation of the specimen heat exchange conditions (maximum temperature up to 1500 K, heating rate up to 50 K/s) providing the high homogeneity of the temperature field in a plane parallel to a frontal surface at high (up to 100 K/mm) gradients through the thickness owing to the use of forced cooling of the sample back surface with the measurement of the heat flow absorbed by the refrigerator.

The following heat diagnostics means were used: chromel-alumel thermocouples 0.2 mm in diameter manufactured by butt welding of electrodes and heat flow transducer the sensing element of which is a plate from aluminooxide ceramics with thermocouples fastened on its frontal and back surfaces.

It is suggested that the measurements, collection, storage, preprocessing of the converter output signals and the preparation of the original file for the following determination of the specimen TPP should be carried out with the help of information – measurement system "MIC" and the software which make it possible to perform tests in accordance with the predetermined modes.

The specimens of two types were tested. The specimens of the first type were prepared from the round plates of different thickness which were stacked vertically. Thermocouples were dropped in plate slots of a given section to provide a tight contact of the thermocouples and the material. The specimens of the second type were prepared from the rectangular bars collected in a horizontal plane by pressing them to each other with lateral surfaces with the help of thermoinsulating shroud. In this case thermocouples were dropped in horizontal slots of different depth made on bar lateral surfaces.

The analysis of the TPP determination error included the assessment of temperature measurement errors in a "thermocouples – specimen" system. With the aim of planning the experiments (justification of specimen dimensions, temperature sensor installation coordinates, program of heating unit power variation) a two-dimensional mathematical model of specimen heat exchange was developed which reproduced test conditions including the work of a heating unit and a refrigerator and which predicted the specimen temperature and stress-strain state. Mathematical modelling was carried out with the use of the approximate data on the TPP of the similar materials. The signs of the semiconductive (from the viewpoint of electrical conductivity) effect were observed in some specimens of the materials being studied at high temperatures.

The experimental data were processed with the help of the program ICP-3 for solving one-dimensional nonlinear coefficient inverse problem of nonstationary thermal conductivity (IPTC). An extreme statement implying a search of the TPP temperature dependences providing a minimum of a quadratic functional of a residual of the experimental and design temperatures at the points of the sensor installation during the whole experiment was used in solving IPTC. The design temperature values at the points of temperature sensors installation used to calculate a functional are determined by a finite difference method. An algorithm for temperature calculations implies an iterative refinement of the TPP values and the boundary conditions within the current time interval. The closeness of the calculated temperature values corresponding to the preassigned relative accuracy is a necessary condition for turning to the following time interval. The TPTC is solved by the iterative regularization method. An iterative process of the functional minimization is modeled by the gradient method. The temperature dependences of the thermal conductivity and/or the heat capacity being determined are represented in the form of discontinuous linear dependences. The gradients of the closing error functional according to the parameters being evaluated are determined by solving a conjugate problem. The ICP-3 program only works on a personal computer with the operational system not lower than Microsoft Windows 95/98.

The solution of primal thermal conductivity problems and the restored (with the help of the calculated temperatures) TPP dependences over the region of the hypothetical values characterizing the TPP of the ceramics being studied showed that a satisfactory accuracy is achieved when 4 or 5 thermocouples mounted at a different distance from a frontal surface are used. When the first temperature sensor is mounted on a frontal surface, it is worthwhile to locate the second sensor within 1–2 mm from the surface being heated. A satisfactory accuracy of the TPP values over the whole temperature range from the starting to the maximum specimen temperature is achieved at random alternating errors distributed according to a normal law with the amplitude of 1% and at preassigned starting values, for example heat capacity with the error of no more than 5%.

This procedure makes it possible to expand the temperature range of the TPP of some materials by more than 300 K as compared to the publicated data with the error of no more than 10%.

# STATE OF THE ART IN THE MODELLING OF VAPOUR-PHASE FABRICATION OF CARBON AND CERAMIC MATRIX COMPOSITES

**Kulik V.I., Kulik A.V. (1), Bogdanov M.V. (1), Ramm M.S. (2)**
Baltic State Technical University, St.Petersburg, Russia, E-mail: kulik@softimpact.ru
(1)Soft-Impact Ltd., St.Petersburg, Russia
(2)A.F.Ioffe Physical Technical Institute, RAS, St.Petersburg, Russia

Present stage of industrial development is characterized by an increasing application of new constructive materials whose functional characteristics were unavailable in materials of previous generations. Development of materials based on carbon and various ceramics appears to be particularly promising. Of special interest among such materials are composites with carbon or ceramic matrix reinforced by fibres (Carbon-Carbon Composites – CCC; Ceramic Matrix Composites – CMC). These materials possess unique mechanical, electrophysical and magnetic properties, being able to operate at high temperature in corrosive or radiation media. The major aspect preventing effective industrial application of such materials is a high cost and long duration of production cycle.

At present, vapour methods are the most preferable for manufacturing of CCC and CMC. These methods are grounded on porous medium densification during filtration of gaseous chemical reactants (precursors), their decomposition at high temperatures, and matrix material deposition on the surface of heated reinforcing material. Such method is named CVI (Chemical Vapour Infiltration). An advantage of this method is a possibility to obtain composites with matrices having very high melting temperatures with minimum thermal, mechanical and chemical impact on the reinforcing fibres.

An analysis shows that CVI methods have obvious advantages, while CVI-produced materials are very promising for production in many areas of today industry. However, the present experience reveals a number of following problems faced in industrial implementation of CVI methods: a very long process duration required for producing high-quality composites; difficulties in determining optimal technological parameters providing a minimum densification time and the desired characteristics of the composite quality; complexity of estimation of characteristics of the produced composites as a function of structural and technological parameters, etc. Generally, one can state that the problem of increasing the technical and economical CVI characteristics and quality of the produced materials still remains unsolved.

An analysis of data available in the literature has shown that a possible way of solving these problems involves development of numerical models of CVI processes. Applicability and validity of the modelling results essentially depends on the accuracy of the description of realistic fibrous preform structure, specific features of the heat- and mass transport in porous media (in the general case, transport in the overall volume of the processing setup), deposition kinetics, relationship between the material characteristics and the structural and technological parameters.

In the present study, the analysis of the history of the CVI modelling has been made, which shows that major efforts of researchers carrying out simulation of the CVI technology are focused on development of mathematical models and studying the processes occurring in the porous reinforcing structures (preforms). One can distinguish three major aspects of the problem: (1) modelling of the porous media structure and its evolution during the preform densification; (2) simulation of the heat and mass transport in porous media; (3) modelling of the kinetics of deposition of the matrix material.

Construction of a model usually employs a number of assumptions and simplifications. Thus, in most theoretical studies, only one-dimensional problem is considered. Also, convective mass transport through the fibrous preform is usually ignored in the isobaric CVI modelling. However, the gas flow along the preform thickness can arise due to phase transitions during matrix material deposition. Generally, existing CVI models either neglect the complex porous structure of preforms, describing the densification of pores of a single scale, or ignore the mass transport between the pore systems. Real reinforcing preforms have a complex structure comprising several pore systems with significantly different transversal dimensions. It is obvious that process of deposition of the matrix material and transport properties in the above pore systems also differ considerably. Besides, the parameters of the gas phase have their own profiles in the different pore systems. This leads to arising of the convective and diffusive mass exchange between the pore systems. It should be noted that optimization problems are normally solved analytically for reduced primitive models.

In this study, basic problems and directions of development of the CVI modelling are formulated. The major problems are:

1. Construction of a model of porous medium structure, which should allow description of a preform based both on disperse (powder-like) filling materials and on fibrous filling materials of a regular (square, hexagonal) or irregular (chaotic) arrangement of the reinforcing elements, including spatial multi-directional structures, as well as structures with curved fibrous reinforcing elements (for example, in woven or wicker preforms). The model should describe the principal geometrical parameters of the porous medium during its evolution. Development of methods of evaluation of the medium permeability and thermal conductivity, which generally can be anisotropic. Eventually, the model should be applicable to solving the problems of synthesis of porous media of any structural complexity from structural elements of various levels.

2. Construction of 1D, 2D and 3D models of unsteady multicomponent heat and mass transport in reactive porous media of a complex structure, accounting for convection and mass exchange between different pore systems for various CVI modifications – isothermal, thermal gradient, non-isobaric.

3. Construction of models of the chemical kinetic involving a series of basic homogeneous and heterogeneous reactions, including homogeneous nucleation (i.e. a possible formation and deposition of parasitic condensed phases on the preform). Estimation of constants of homogeneous reactions is evaluated using the Arrhenius formula. The heterogeneous reaction rates can be either found by evaluating the reaction constants from the Arrhenuis law or calculated assuming the thermodynamic equilibrium on the phase interfaces. If necessary, the model may include an analysis of the condensed phase composition.

4. Elaboration of 2D and 3D models of conjugate unsteady heat and mass exchange in processing setups for various CVI modifications. The model should provide solution to the following key problems: evaluation of the thermal field inside the reactor; computation of the species fraction and gas velocity distribution in the reaction space, in particular, in the zone adjacent to the preform surfaces. Solving these problems will enable precise assignment of initial and boundary conditions for the CVI model at the preform level, including account of their variation along the length and/or width of the preform.

5. Development of methods and procedures of multiparametric optimal design of CVI technologies, preferring the approaches employing coupled solution of materials science, constructional and technological problems.

6. Development of a method of evaluating (predicting) the characteristics of CVI-produced materials. These methods should be based on composite models predicting a complex of mechanical, thermophysical, electrical and other materials parameters as a function of composite composition, composite structure and technological parameters. The models should maximally account for the effect of porosity of CVI-produced composites and non-uniformity of its distribution over the bulk.

7. Construction of an effective numerical methods and algorithms for solution of these problems and their implementation as a software package.

8. Numerical study of CVI processes and analysis of the results obtained, with recommendations on the optimization of CVI technology, setup, composite and product construction.

The basic results obtained during solution of the formulated above problems are presented in this paper. Examples of the CVI numerical modelling are considered for reinforcing preforms of different structure and for production of various composites with carbon, silicon carbide (SiC) and alumina ($Al_2O_3$) matrices.

# THE CONTROL OF BIMODAL DISTRIBUTION OF PORES IN MANUFACTURING OF SUPERLIGHT STRUCTURED MATERIALS

**Shtern M. B., Kuzmov A. V., Frolova E.G.**
Frantsevich Institute for Problems of Materials Science of NASU
3 Krzhizhanovsky St., Kiev, 03142, Ukraine, E-mail: stern@materials.kiev.ua

The purpose of the given work is the theoretical bases of a numerical modeling of mechanical properties and technology of manufacture of porous structural materials containing two types of pores, which have great difference in size. The matter is that obtaining of highly porous structures with minimal changes in volume at sintering and provision the high quality of interpartical contacts at the same time are two alternative tasks, as this quality can be achieved during active sintering of dispersible powders and is accompanied by a significant volumetric shrinkage, which leads to high final density. The use of compacts with bimodal structure will help to solve this matter (to achieve an optimum ratio of quality of sintering and high porosity of obtained material). Biporous structure, which is an extreme case of inhomogeneous pore-size distribution, is ensured by the presence of two types of pores in compacts with great difference in size. Biporous structure can be obtained at pressing the powder mixtures with the special filler, which is removed in the process of sintering.

For numerical modeling of technology of obtaining of articles made from biporous material it is necessary to know the constitutive rheological relationships for such kind of materials. Such relationships is formulated in this report for sintering of materials with bimodal pores-size distribution. Contrary to works of Sherer [1,2], where the material with anarchical biporous structure was considered, here we examine the material with double matrix structure including none-porous matrix for small pores and porous matrix for large pores.

It's supposed, that as well as for a usual porous material, at sintering the behaviour of biporous material is controlled by linearly - viscous constitutive relationships:

$$\sigma_{ij} = 2\eta_{eff}(e_{ij} - \frac{1}{3}e\delta_{ij}) + \zeta_{eff}e\delta_{ij} + P_{Leff}\delta_{ij} \text{,(1)}$$

where $\eta_{eff}$ and $\zeta_{eff}$ are effective viscous modules and $P_{Leff}$ effective Sintering stress depending on two parameters $\Pi_1$ and $\Pi_2$. Where $\Pi_1$ - is the contents of small pores in porous matrix and $\Pi_2$ - general contents of large pores in material. With help of the method of a representative cell effective viscous modules and effective sintering stress was found. As one can see from (1), biporous material was considered to be isotropic, the spherical representative cell with a spherical cavity in the middle was used. The material filling the space between two spheres was considered to be small-porous, and the internal cavity was identified with large pore.

It should be noticed, that in our model the condition of material is described by two parameters of condition - the contents of large and small pores, therefore to retrace their evolution and to close the constitutive relationships, it is not enough to use only one equation of mass reservation. So the additional kinetic equation for the contents of large pores was formulated with the help of the same representative cell. Thus, the system of two kinetic equations for determination of the concentration of small and large pores was obtained. Contrary to the similar equations for determination of pores concentration which were obtained in work [3], these equations take into account the influence of the stress-strained condition on the kinetics of both types of pores.

The analysis of obtained kinetic equations for $\Pi_1$ and $\Pi_2$ leads to the conclusion, that the absence of changes in volume at sintering in material is possible only when large pores grow at the expense of small ones. That means, the coalescence at sintering can be described within the framework of obtained model.

1. George W. *Sherer* Viscouse sintering of a bimodal pore-size distribution. // Journal of American Ceramic Society. Vol. 67. No. 11 (1984). Pp. 709-715
2. George W. Sherer, Viscouse sintering with a pore-size distribution and rigid inclusions. // Journal of American Ceramic Society. Vol. 71. No. 10 (1988). C447.
3. E. Olevsky, R.Rein, Kinetics of sintering for powder systems with bimodal pores distribution, Int. J.High Temp.-High Pressures 27/28 (1995) 81-90.

# PHASE INTERACTION IN THE TERNARY SYSTEM $HfO_2$-$Y_2O_3$-$Eu_2O_3$ AT HIGH TEMPERATURES

**Andrievskaya Elena R., Lopato Lidiya M.**
Frantsevich Institute for Problems of Materials Science, Ukraine NASU,
Krzhizhanovsky str. 3, 03680, Kiev 03142,Ukraine, E-mail: ragulya@materials.kiev.ua

## ABSTRACT

Phase equilibria in the binary $HfO_2$-$Eu_2O_3$, $Eu_2O_3$-$Y_2O_3$ and the ternary $HfO_2$-$Y_2O_3$-$Eu_2O_3$ systems were studied in the wide range of temperatures (2500-1250 °C) and concentrations (0-100 mol % $Eu_2O_3$) by thermal analysis in air, X-ray diffraction, microstructural and petrographic analyses, electron microscopy using melted and annealed samples. Phase diagrams of the $Eu_2O_3$-$Y_2O_3$, $HfO_2$-$Eu_2O_3$ and $HfO_2$-$Y_2O_3$-$Eu_2O_3$ systems are developed.

## INTRODUCTION

Europia as well as yttria is useful dopant to refractory oxide such as hafnia. Because of its high capture cross section in fast neutron fluxes and because this absorption worth is sustained by chains of high cross-section daughter isotopes, europia is attractive as a control and shutoff rod material in fast reactors. Europia is a suitable for these purposes since it is relatively stable chemically, has a high melting point (2320°C), can be fabricated easily into dense bodies with a high europia density, and is readily available. However, disadvantage associated with the use of pure europia is that when it is fabricated at temperatures above 1100°C the higher-temperature monoclinic B form is produced which exhibits undesirable swelling under fast neutron irradiation. The cubic structures can be stabilized at sintering temperatures by using suitable additives. Additions of hafnia and yttria to europia suppress grain growth and improve its elastic properties [1].

The main purpose of this work is to investigate the physics and chemistry of phase interactions in the ternary $HfO_2$-$Y_2O_3$-$Eu_2O_3$ system at high temperatures and wide concentration range. This system is perspective from the standpoint of creation high-refractory materials and ones with increased strength characteristics in which the composition of both matrix and strengthening phase is the same.

Phase relations in the boundary binary systems $Eu_2O_3$-$Y_2O_3$, $HfO_2$-$Eu_2O_3$ were studied in the wide range of temperatures (1250-2800°C) and concentrations (0-100 mol % $Eu_2O_3$). Phase diagrams of these systems were developed [2, 3].

Phase equilibria of the system $Eu_2O_3$-$Y_2O_3$ are characterized by the formation of the fields of solid solutions of various extent based on the hexagonal (A- and H-type), monoclinic (B), cubic (C- and X-type) modifications of the rare-earth oxides, that is known for the majority of cerium subgroup oxides. There are the peritectic-type transformation on the liquidus at 2370 °C, 58 mol % $Y_2O_3$ and point of minimal temperature at 2310 °C, 10 mol % $Y_2O_3$.

In the subsolidus region of the phase diagram $HfO_2$-$Eu_2O_3$ system the fields of solid solutions based on monoclinic (M), tetragonal (T) and cubic (fluorite-type, F) modifications of hafnia, pyrochlore-type compound $Eu_2Hf_2O_7$ as well as solid solutions on the basis B, A, H and X forms of $Eu_2O_3$ were found. The dopants of hafnia to europia have stabilized the C-phase at the higher temperatures, increasing the range of its existence. The liquidus of the system $HfO_2$-$Eu_2O_3$ is characterized by eutectic transformation at 2150°C, 25 mol % $HfO_2$. The compound $Eu_2Hf_2O_7$ is not observed on the liquidus surface but is formed in the solid phase at temperature ~ 2450 °C.

Solid solutions based on T, M and F modifications of hafnia as well as C and H modifications of yttria are known to form in the system $HfO_2$-$Y_2O_3$ at high temperatures [4]. The liquidus of this system is characterized by an eutectic transformation at 2400 ±25 °C and 84 ±2 mol % $Y_2O_3$ and a peritectic transformation at 2430 °C and 77±2 mol % $Y_2O_3$ [5].

## EXPERIMENTAL PROCEDURE

The samples for investigations of the phase equilibria in the ternary $HfO_2$-$Y_2O_3$-$Eu_2O_3$ system were prepared from 5 to 10 mol % by both mechanical mixing of oxides and coprecipitation of hydroxides. Part of these samples was used for the investigation in the as prepared form (melted specimens). Other samples were annealed at 1550 ° C for 70 h in air. The boundaries of the phase fields were determined by thermal analysis in air up to 3000 °C using a solar furnace. The phase compositions were investigated by petrography, X-ray phase analysis, electron microprobe X-ray analysis, chemical and X-ray fluorescence spectrum analysis.

RESULTS AND DISCUSSION

An investigation of interaction in the system $HfO_2$-$Y_2O_3$-$Eu_2O_3$ over the whole range of concentrations at temperatures above 2000 °C revealed no new phases. The results of this investigation showed that the liquidus surface of this system consists of four fields of phase-primary crystallization: namely, solid solutions based on $HfO_2$ phase with a fluorite-type structure F, H and C forms of $Y_2O_3$ as well as X- $Eu_2O_3$. There are two invariant points of incongruent-type four-phase equilibria on the liquidus with the coordinates 17 mol % $HfO_2$, 55.5 mol % $Y_2O_3$ at 2360 °C ($U_1$) and 19 mol % $HfO_2$, 36 mol % $Y_2O_3$ at 2310 °C ($U_2$).

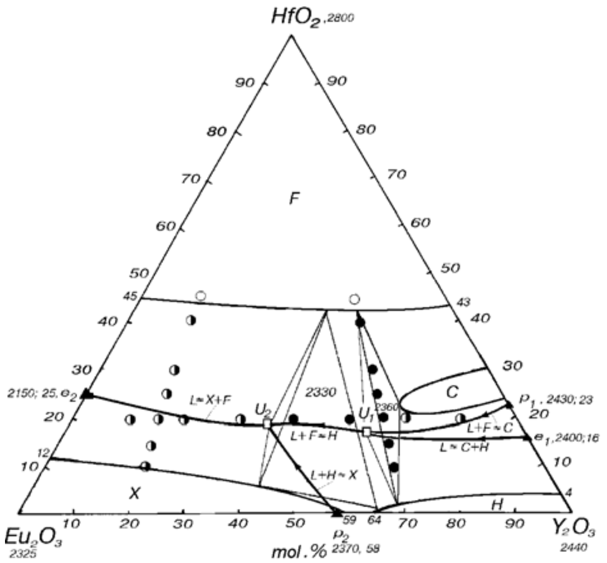
HfO2, 2800
90
80
70
60
50
45
40
30
20
10
12
90
80
70
60
50
43
40
30
20
10
4
F
C
X
H
2150; 25, e2
L⇌X+F
U2
2330
U1
2360
L+F⇌H
L+H⇌X
L+F⇌C
L⇌C+H
P1, 2430; 23
e1, 2400; 16
Eu2O3
2325
10
20
30
40
50
59
64
70
80
90
Y2O3
2440
p2
2370, 58
mol.%

Fig. 1. Crystallization paths for the $HfO_2$-$Y_2O_3$-$Eu_2O_3$ system (○ -single phase, ◑ - binary phase, ● - ternary phase samples).

The minimal melting temperature for the $HfO_2$-$Y_2O_3$-$Eu_2O_3$ system is 2150 °C($e_2$), maximum temperature of the liquidus surface is equal to 2800 °C, which corresponds to the melting point of pure $HfO_2$. The liquidus surface of this system contains the same fields as do the solidus surface, and the most extended field is that of the fluorite based solid solutions. Solidus surface in the investigated system consists of 2 ternary-phase fields corresponding to the transformations L+H⇄X+F and L+C⇄H+F. The crystallization of the alloys was investigated using the data on structure of the liquidus and solidus surfaces. The crystallization paths for the alloys and the schematics of the reactions were constructed (Figs. 1, 2).

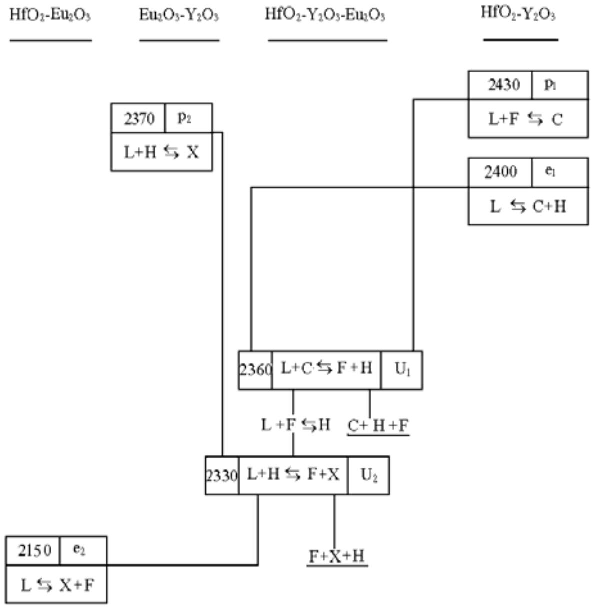
HfO2-Eu2O3
Eu2O3-Y2O3
HfO2-Y2O3-Eu2O3
HfO2-Y2O3
2430
P1
L+F ⇆ C
2370
P2
L+H ⇆ X
2400
e1
L ⇆ C+H
2360
L+C ⇆ F+H
U1
L+F ⇆H
C+H+F
2330
L+H ⇆ F+X
U2
2150
e2
L ⇆ X+F
F+X+H

Fig. 2. Schematic of the reactions proceeding during equilibrium crystallization of melted samples in the $HfO_2$-$Y_2O_3$-$Eu_2O_3$ system.

The isothermal sections were developed at 1550 °C and 1250 °C. We identified single phase regions of solid solutions based on M- and F-$HfO_2$, B- and C-$Eu_2O_3$, C-$Y_2O_3$ and $Eu_2Hf_2O_7$ (Py).

REFERENCES

[1] R.W. Scheidecker, D.R. Wilder, H. Moeller: J. Am. Ceram. Soc. Vol. 60 (1977), 501.

[2] E.R. Andrievskaya, Z.A. Zaitseva, A.V. Shevchenko, and L.M. Lopato: Inorganic Materials. Vol. 33, No. 4 (1997), 390.

[3] E.R. Andrievskaya, L.M. Lopato, A.V. Shevchenko, and V.P. Smirnov: Inorganic Materials. Vol. 33, No. 7 (1997), 835.

[4] M.F. Trubelja and V.S. Stubican: J. Am. Ceram. Soc. Vol. 71 (1988), 662.

[5] A.V. Shevchenko, L.M. Lopato, and I.E. Kiryakova: Inorganic Materials. Vol. 20, No. 12 (1984), 1991.

ACKNOWLEDGEMENTS

Authors thanks A.V. Shevchenko, V.P. Red'ko, I.E. Kiryakova, Z.A. Zaitseva, and V.P. Smirnov for their helpful advices and assistance in experimetal study of presented phase diagram.

# THE PHYSICAL ASPECTS OF THE HARDENING OF THE CUTTING HARDENING ALLOYS TOOL BY POWERFUL ION BEAMS OF CARBON

**Tsareva I.N., Ovsiannickov M.U., Kutusov V.L., Kutusov A.V.**
SPE "Linetron-Nizhni Novgorod", Nizhni Novgorod, Russia
7, Larina Str., Nizhni Novgorod, 603107, Russia, e-mail: linetron@nn.ru

The processing by powerful ion beams (PIB) differs from other ion-beam methods of hardening of a surface of firm bodies by pulse character of influence, by high power consumption of process and intensity of an ion flow (density of a flow of capacity entered into a material achieves $10^7$-$10^9$ Vt/cm$^2$). The updating of materials is achieved due to three cooperating processes: to the amorfization of a surface at the expense of super fast crystallization of a heated up layer; to influence of a shock wave accompanying an irradiation; and to the легированию of a superficial layer by the ions of carbon resulting to carbide formation in these layers.

The purpose of the present work is:
- the research of influence of processing by the powerful ion beams of carbon with different intensity on thin structure and phisical-mechanical properties of superficial layers of the firm alloy T14C8 ( chemical structure: WC - 78 %, TiC - 14 %, Co - 8 %);
- the development of physical criteria ion-beam hardening resulting to increase of operational properties of the cutting твердосплавного tool.

The researches are carried out on твердосплавных cutting plates from the alloy T14C8. The processing PIB $C^+$ was carried out by pulses (quantity n=2-4) duration t=60 ns (frequency of following 5-10 c) on the accelerator "Rate - 5" with energy E=300 кэВ at density of an ion current j=100-200 A/cm$^2$. The samples were exposed отжигу on air at 300°C within 1 hour after an irradiation. For the analysis of a structure of a firm alloy before and after of an ion influence were used the methods of X-ray diffraction analyses, metalografic. While researching phisical-mechanical properties were used methods of measurement of a microhardness ($H_\mu$) on the device PMH-3, the roughness of a surface on parameter $R_a$ and factor of friction (f). The resistance of the cutting PIB-hardening tool was determined at operation draft polishment of carload wheels from an item S 20 on the machine tool "Raphamet" (in a standard mode of processing).

After processing PIB $C^+$ the phase structure of a firm alloy T14C8 does not vary (WC + TiC + α-Co). With increase quantity of pulses more than 3 was marked the change of relative intensity of diffraction maxima (reduction of intensity of lines (100), (200), (101) WC and (220) TiC, and also increase of intensity of lines (010) WC (200) TiC), caused by occurrence of a texture in a thin superficial layer is marked only at course of processes of plastic deformation under the action of shock waves. The extreme character of dependences of parameters of substructure (size grans of blocks and size of microdeformations in them) of a carbide phase WC from number ion of pulses is established. The processing by two or three of pulses beams $C^+$ results to decreasing of grains blocks in 1,5-2,5 times in a researched interval of density of an ion current. On estimated accounts the density of subboundary dislocations after an irradiation in case of maximal decreasing of thin structure of the grains WC (for j=120 A/ cm$^2$, n=2) grows by the order, is reaching size $2 \cdot 10^{10}$ cm$^{-2}$ (at a reference value ~ $2 \cdot 10^9$ cm$^{-2}$). The increase quantity of pulses up to 4 is accompanied by integration of blocks of a mosaic owing to of the recrystallizational processes at high-temperature heating of a surface under action of the ion beams. The processing by 2-3 pulses PIB $C^+$ results to increase of a level of micro deformations in карбидных grains because of increase of density chaotically allocated inside subgrains of dislocations. While increasing of quantity of pulses up to 4 the tendency of decrease of micro pressure is found out.

For all investigated modes of processing PIB the increase of micro hardness of a surface of an alloy T14C8 is achieved. The greatest stronger effect is marked for a mode with j=120 A/ cm$^2$, n=3. For the indentation depth ~ 1 micron the relative gain of micro hardness achieves 60 %. With increase of distance from the irradiated surface the stronger effect is reduced up to 20 %. The depth of the modified zone at different modes of processing reaches 140-200 microns. The basic mechanism of PIB-hardening is dislocational, connected with increasing of density dislocations inside and on borders of grains blocks of a carbide phase WC.

The processing by powerful ion beams in the investigated modes results, as a rule, in increaseing parameter of a roughness of a surface. $R_a$, caused by processes of dispersion or evaporation of a material of a surface under the action of high-energy ion beams.

The behaviour of the factor of friction contact " the irradiated alloy T14C8 - sapphire " is ambiguous for different modes of an irradiation. The decrease (reduction) of the factor of friction under action PIB is established at presence of a positive gradient of mechanical properties (on depth h~0,8-1,5 mcm - for different modes of processing) irradiated surface at the expense of the plastification effect, creating a favorable condition for realization of shift at friction.

Thermal processing results in integration blocks of a mosaic, relaxation of micro pressure inside of carbide grains, and as a consequence, to reduction of micro hardness. After the thermal processing smoothing a micro relief is observed at the expense of formation of an oxygen film and additional decrease of factor of friction on 10-20 %.

As a result of the spent researches the optimum modes of processing PIB are determined from the point of view of hardening: n=2, j=120-180 A/cm$^2$. In the specified interval of density of an ion current the changes of microstructure of a surface increase with the increase j. If at j=120 A/cm$^2$ appreciable changes of microstructure it is not revealed, at j=180 A/cm$^2$ under action PIB the recrystallization occurs to crushing of sub grains of a carbide phase. The plates with the recrystallizational structure of a surface have shown maximal hardening effect and greatest resistance in naturale tests at polishment of wheel pairs. The laws of formation of substructure of a material of superficial layers for maintenance of optimum operational properties of the cutting hardening alloys tool are determined.

For the normal work of the cutting tool working in conditions of shock and high-temperature loadings, the combination of high hardness and sufficient plasticity is necessary. On a technique offered in work [1], the factors of plasticity for alloys T14C8, MC 221, GC 11 etc., widely used are designed at manufacturing of твердосплавных plates of railway assignment. The diagrams of a condition " hardness - plasticity " are constructed and as the much as possible allowable meanings of micro hardness of a surface of these firm alloys are determined at PIB-hardening. The further hardening is inexpedient because of decreasing factor of plasticity and increasing probability of fragile destruction. The given approach is applied for hardening cutting plates of a different configuration (from alloys T14C8, MC 221, T5C10, MM2, GC 11 etc.).

On the basis of the carried out researches the technology of PIB-processing of the hardening alloys tool is developed and optimized. The technology is introduced in carload depot of the Горьковской railway, Saratov railway. The small-scale The characteristic of plasticity received at measurement of hardnessmanufacture of PIB-hardening is organized, the quality of let out production is confirmed by the certificate of quality.

Literature:

1 – Milman Yu.V., Galanov B.A.The characteristic of plasticity received at measurement of hardness, Kiev, 1992, P.25.

# PLASMA METHODS OF SOLID LUBRICANT FILMS FORMATION ON FRICTION UNITS, WORKING AT EXTREME CONDITIONS

**Lesnevsky L.N., Troshin A.E., Tyurin V.N., Oushakov A.M., Tchernovsky M.N.**
Moscow Aviation Institute (State Technical University), Moscow, Russia
Volokolamskoe shosse, 4, Moscow, 125993, Russia, E-mail: kaf205@mai.ru

One of the major tendency of modern engineering development is continuous toughening of operation conditions of different modern machine friction units.

The required efficiency and reliability of such units working in conditions of extremely high and low temperatures, aggressive environments, deep vacuum, weightlessness, rigid radiation, is provided with a number of the factors, including at the expense of improvement of the tribotechnical characteristics of contacting surfaces.

One of the most effective ways of achievement of the necessary tribotechnical characteristics is use of plasma and vacuum-plasma methods of formation of solid lubricant films (SLF).

The carried out analysis [1] has allowed is proved to choose the following methods of formation SLF and to formulate their basic opportunities:

-deposition in magnetron sputtering system – magnetron sputter deposition;

-deposition with use of the pulse plasma accelerator;

-micro arc oxidation.

Deposition in Magnetron Sputtering Deposition (MSD) system. For researches the reactionary method of formation SLF on a basis TiN was chosen. The experimental dependence of microhardness TiN from ratio of reactionary gas $N_2$ and working gas Ar was obtained and in view of choice of more viscous film the working range of flow these gases $ØN_2/ØAr_2$=0,55—0,63 was used.

To the same range there corresponded also minimal meanings of preliminary estimations of friction coefficient. The thickness of the generated film from TiN did not exceed 3,8 microns. Temperature of substrate at formation TiN was 200 °C.

Results of the chemical structure analysis of films received on electronic spectrometer XSAM - 800 «Kratos» and x-ray diffractometer «RIGACU» has shown, that generated of a TiNx films are superstochiometric, i.e. X=1,09—1,14. The comparison of obtained TiN films, with films, generated by Ion Beam Assisted Deposition (IBAD) and Cathode Arc Deposition (CAD) methods has shown, that of TiN films, received in MSD system within the framework of the present paper had the maximal volumetric contents TiN in the structure (89%) and had the best tribological properties [2].

Tribological tests were carried out for films generated on steel and alloys, on the ceramics $Si_3N_4$ and in the compositions with the soft metal – Pb on the steel substrait.

Test of samples carried out at normal temperature by the friction machine under the «pin – disk» diagram (disk Ø78x10 mm and pin Ø8 mm with the spherical head) in pair of friction TiN - steel 440 °C have shown, that only forming of TiN film on both details of pair friction guarantees of satisfactory results obtaining on friction coefficient and wear resistant.

On base of TiN on ceramics $Si_3N_4$ were generated SLF on the developed technology and are tested by the five-ball friction machine in a spin mode at pressure 1 and 1,75 GPa at temperature 20—200 °C and speed of a ball Ø9,6 mm rotation - 280 rpm.

Was established that wear of samples from $Si_3N_4$ grows at increase of working temperature from 20 °C up to 200 °C. Use of TiN film results in essential decrease of volumetric wear of samples from $Si_3N_4$ approximately on the order at temperature 20 °C and on two order at temperature 200 °C.

The obtained TiN+Pb films by a method of joint sputtering TiN and lead Pb were subjected to tribological tests by the friction machine under the «pin - disk» diagram (pressure 15 MPa, speed 2,5 m/c). This composition at normal test specifications has allowed to obtain for TiN film the lowest friction coefficient ~0,1. Wear resistance of this film in comparison with TiN film obtained on SEP (France) [2] technology, has appeared much above.

Test of TiN+Pb composition on fretting of wear in environment of liquid nitrogen have shown, that it continued successfully to work and after development of the given resource in $10^6$ of cycles.

Deposition with use Pulse Plasma Accelerator (PPA). With the purpose of an effective utilization PPA in technological processes of formation of metal SLF (Sn, Bi, Cd, In, Ga) [3] was experimentally established, that by selection of energy at the second stage $W_2$ it is possible to obtain of nondropping modes of PPA operations.

The estimation of metal condensate adhesion has shown high efficiency developed by PPA. They were tested by development of the next technological processes of films forming: solders on a basis Sn; films on a basis Cd for protection against corrosion; and SLF films, obtained together with magnetron deposition TiN films as a composition TiN+Pb films for use its in friction units.

Microarc oxidation (MAO). Researches of MAO coatings on an AU4G alloy at dry alternating friction were carried out on the specialized friction machine at reciprocating (with frequency 10 Hz) moving of two samples with a coating from each other with amplitude up to 2 mm, at force of pressing 80 H and temperature 20 °C.

It was disclosed, that speeds of MAO coating wear, received on a mode 1, after the small period of wear-in, monotonously grows, reaching of meaning $650\cdot10^{-3}$ $mm^3$/hour after 4 hours of continuous tests.

MAO coating obtained on a mode 2 (in structure of electrolyte was present the special additives), very quickly wore out in the wear-in up period to the meaning $586\cdot10^{-3}$ $mm^3$, but in the further wear is stopped, and the wear speed is remained constant within 5 hours of continuous tests.

Such law has allowed making a conclusion that, operating with structure of electrolyte, it is possible to obtain of SLF coating with inessential wear.

The researches, which have been carried out on an aluminum alloy 6061 on formation of MAO coatings, have allowed receiving new results on use of this alloy with a coating for manufacturing of cylinder liner of internal-combustion engine [4].

The sample represented the aluminum cylinder Ø90 mm and length 180 mm, on which internal surface with use of the additional central cathode was generated of MAO coating and it is processed by honing up to 50...70 microns thickness.

Test for friction and wear was carried out on special research installation. MAO coating, in pores of which there was a graphite greasing or viscous oil SAE SW 30) have shown much lower meanings of friction coefficient up to 0,02, as against pig-iron - 0,14 at higher microhardness and lower wear in identical test specifications (speed 100...600 rpm, loading 0...35kg).

Thus, as a result of the carried out researches the physical bases of technological processes of formation SLF by plasma and vacuum-plasma methods are developed, and the pilot (-scale) technological processes are offered:

- magnetron deposition of high-temperature SLF (up to 10000C) on base TiN and composite SLF on base TiN and lead Pb for protection against fretting of wear;
- deposition by pulse plasma accelerator of metal SLF from Pb, Sn, Ga, In, Cd etc. with high adhesion properties;
- microarc oxidation of aluminum alloys with the purpose to form of high wear resistance SLF and combined SLF with impregnation.

## References:

1. Lesnevsky L.N. Plasma technology of SLF for Aircraft Engine Lifetime Providing. SNECMA-Russia Technical Center: Lifetime Management Seminar. Moscow, 2000. 16p.
2. Colligon J.S., Kheyrandish H., Lesnevsky L.N., Naumkin A., Rogozin A., Shkarban I.I., Vasiliev L., Yurasova V.E. Composition and chemical state of titanium nitride films by different methods. Surface and Coating Technology, 70, 1994, p.9—17.
3. Lesnevsky L.N., Tyurin V.N. A Study of Pulsed Plasma Accelerator with Metal Propellant for Space and Technology Application. Proceeding of 26th IEPC, Kitakiushy, Japan, 1999. 8p.
4. Rao V.D.N., Cikanek H.A., Boyer B.A., Lesnevsky L.N., Tchernovsky M.N., Tyurin V.N. Friction and Wear Characteristics of Micro-Arc Oxidation Coating for Light Weight, Wear Resistant, Powertrain Application. SAE Paper #970022, 1997, p.91—105.

# EFFECTIVE CHARGED PARTICLE BEAMS TECHNOLOGY FOR DIAMOND-LIKE CARBON THIN FILMS PRODUCTION

**Semenov A., Semenova I., Belyanin A.**(1)
Physical Problems Department at the Presidium of
Buryat Scientific Center of SB of RAS, Ulan-Ude, Russia,
8, Sakhyanovoy Str., Ulan-Ude, 670047, Russia, semenov@pres.bsc.buryatia.ru
(1)Central Research Technological Institute "TECHNOMASH", Moscow, Russia,
4, Ivan Franko Str., Moscow, 121355, Russia, belyanin@orc.ru

Technology of charge particle beams generated in discharges with cold cathode based on sputtering of graphite and processing of carbon film by ion or electron beam allows growing diamond and diamond-like carbon thin films at low temperatures and pressures [1]. Creation of high-temperature radiation-stable devices with the element base providing a level of characteristics, close to critical, wider including extreme conditions of application is the purpose of introduction of diamond materials in the modern electronics. Production of high heat conducting substrates for electronic devices is one of the fundamental directions of diamond technology. Diamond is an ideal material for the devices using plasma of charge carriers, generated by optical radiation and an electric field. Diamond has the highest dissemination speed of surface acoustic waves (~9 km/s) that does his perspective for acoustoelectronics [2]. The opportunity of diamond materials application as a source of electrons is based on property of negative electronic affinity that enables to lower emission threshold at manufacturing not heated cathodes of emission electronic devices. Thin diamond-like carbon films are perspective as protective, anticorrosive, strengthening coverings.

The development of equipment for thin film deposition is connected with creation of effective, reliable electron and ion sources, among which the constructions on the base of cold hollow cathodes are more technological [3]. The conventional profit of discharge with cold cathode using for reception spraying ion and electron beams is caused by an extreme high resource >100 h of burning on chemically active gases, high mechanical reliability and profitability of designs, simplicity and convenience of service. These advantages allow expanding opportunities of thin film deposition processes. Charged particle beams sources on the base of glow discharges with hollow cold cathodes generate electron beams with power efficiency (up to ~15 mA/W), discharge burning voltage is of 85—180 V, discharge current 2 A, ion beam current 0,1—0,15 A, electron beam current 1 A [4]. Such device was entered into a design of a vacuum post VUP-4, reconstructed for thin films deposition (Fig. 1, 2).

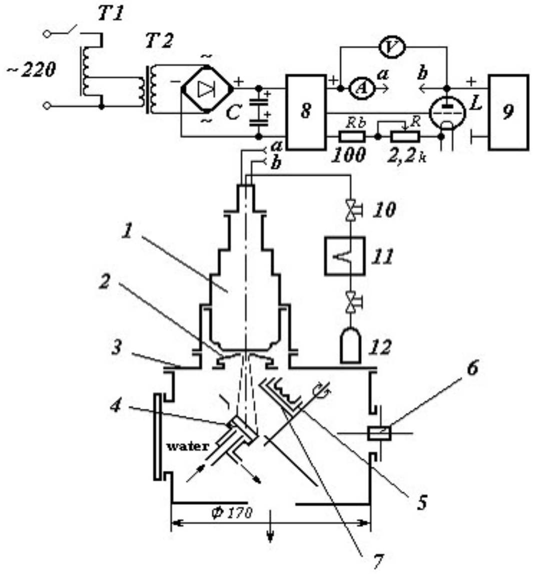

Figure 1. Scheme of the ion beam sputter deposition system. 1. plasma ion source; 2. acceleration electrode; 3. working chamber; 4. holder of graphite target; 5. heater; 6. shutter drive; 7. shutter; 8, 9. high-voltage rectifiers; 10. gas entry; 11. consumption gauge; 12. gas cylinder

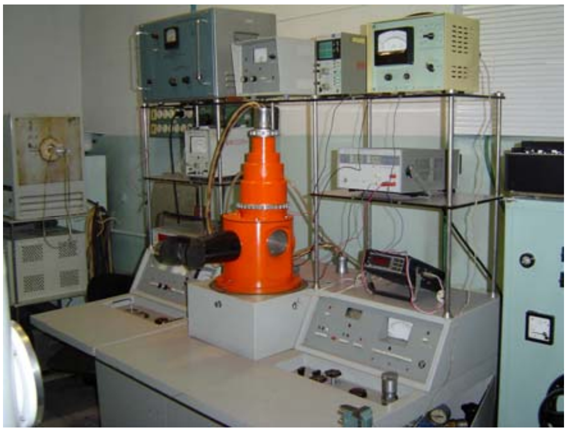

Figure 2. General view of the installation

The growing processes of carbon thin films can be classified into two types. The first type is two stage formations of diamond-like carbon thin films by ion beam sputtering of graphite target and electron beam treatment of carbon film. The processes of diamond thin films growing by low energy ion beam are the second. The deposited thin films are studied by X-Ray diffraction, Raman spectroscopy and Atomic Force Microscopy. It is determined that in varying the ion sputtering parameters and the electron beam annealing regime, it is possible to control the diamond content in carbon thin film. Diamond-like carbon materials are perspective as a basis for creation of effective cathodes using the phenomenon of field electron emission. Such emission occurs without additional heating of the cathode that allows receiving electron flow with low initial speeds and as a result essentially to simplify a design of electro vacuum devices [5, 6]. One of the most attractive applications of such "cold" field cathodes is expected in flat cathode luminescence displays. Emission properties of carbon thin films were investigated by the method of measurement of emission current dependence on voltage of electrical field. The sharp growth of an electron current, so-called threshold of emission, is observed at ~$3 \cdot 10^5$ V/cm, though the initial emission is already appreciable at smaller value of a field ~$1{,}5 \cdot 10^5$ V/cm, emission current density of $1{,}2 \cdot 10^{-5}$ A/cm$^2$ (Fig. 3).

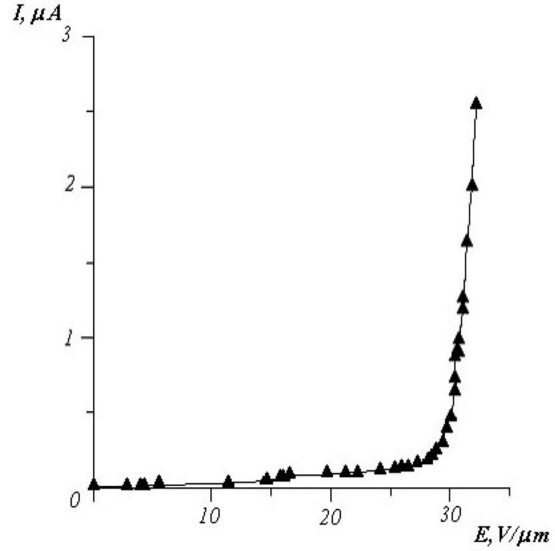

Figure 3. Volt-Ampere characteristic of the cold cathode

In summary, we have presented the low-temperature and pressure technology growing of diamond, carbine and diamond-like carbon thin films using charge particle beams generated in discharges with cold cathode. Perspective of ion beam sputtering and electron beam treatment are connected with high precision of regulation of substrate temperature, voltage displacement, density, energy, incidence angle and composition of particles.

**Acknowledgments**

This work was supported by grant INTAS-2001—2399 and Lavrentyev grant of young scientists.

**References:**

[1] Semyonov A.P. Sputtering ion beams: generation and application. Ulan-Ude, 1999. p. 132.

[2] Vecherin P.P., Zhuravlyov V.V., Kvaskov V.B., Klyuev U.A., Krasilnikov A.V., Samoilovich M.I., Sukhodolskaya O.V. Natural diamonds of Russia. Moscow,1997. p. 184.

[3] Semyonova I.A., Semyonov A.P., Belyanin A.F. Proc. 1th International congress on radiation physics, high current electronics and modification of materials. 5 Conference on modification of Materials with particle beams and plasma flows (Tomsk) 2000; 3:411.

[4] Belyanin A.F., Semyonov A.P., Semyonova I.A. Effective charged and neutral particle beams source on the base of discharge with hollow cathode // Abstracts of The 10th International conference on ion sources. Dubna: 2003. P.200.

[5] Himpsel F.J., Knapp J.A., Van Vechten J.A., Eastman D.E. Phys. Rev. B. 1979; 20: 624—630.

[6] Armatunga G.A.J., Silva S.R.P. Appl. Phys. Lett. 1996; 68: 2529—2531.

# THE PROCESS OF GETTING MICROPARTICLES OUT OF REFRACTORY MATERIALS

**Arinkin S.M.**
Lykov Heat And Mass Transfer Institute of NASB, Minsk, Belarus
15, P.Brovki Str., Minsk, Belarus, E-mail:SergeyArinkin@tut.by

The creation of high-powered plants (gas-core reactors and plasma reactors, rocket engines and aeroengines) requires the construction of walls of combustion chambers from the materials that help to stand thermal action up to dozens of $kW/cm_2$

Out of certain wall's types of combustion chambers in a work described in [1] was examined the condition of a hollow cylindric wall made of a porous refractory metal. Sintering of tungsten and molybdenum microparticles makes such walls.

In this report is introduced the complex of equipment for getting microparticles out of metals by reducing their low-boiling compounds, such as $WCl_6$, $MoCl_6$, $WF_6$,$MoF_6$,$SiCl_4$ When heating up to 350 °C these compounds sequentially turn from crystalline state into liquid and then into gaseous state. At the temperature over 1200 °C in a hydrogen medium they are reduced with microparticles' formation that have the size of Angstroem Units. In the process of moving along the path of the channel the particles conglomerate up to the size of dozens and thousands of A.U.

As shown in the works [2, 3] the greatest influence on the amalgamation process of the particles has their contact with the walls of the channel, along which the gas-powdered flux is moved. In a work [4] is taken up a combustion chamber's wall, made of a porous metal, transpiration cooling is used here.

The reduction of low-boiling alloys and non-metal compounds in high-temperature hydrogen, conglomeration of reduced hot particles in the process of staying in a high-temperature gas-powdered medium caused the technical proposal of the equipment complex based on electrolyzers, that were created at the Welding Institute of the Ukrainian Academy of Science.

The fundamental scheme is represented in the pic. 1

It includes a hydrolyzer 1 GVK – 1,5, 2 a jar for heating low-boiling compounds, a chamber for reduction of low-boiling compounds 3 with a cylindric wall 4, a jar 5 for cooling that is partially filled with water 8, gate 6, a detonating gas burner 7.

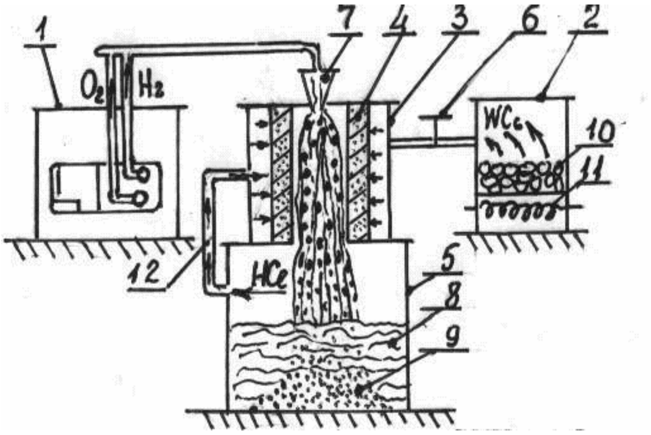

The complex works in the following way: the jar 2 is filled with salt of the low-boiling compound 10, then power supply of the heater 11 of the jar and of the electrolyzer is switched on.

In the process of heating low-boiling compounds turn into liquid and then into gaseous state. In the electrolyzer 1 as a result of water decomposition hydrogen and oxygen are formed, they are mixed and afterwards enter the burner 7. The mixture is set on fire. The jet of the over-hydrogened fire-damp heats the porous wall up to (1200—1700) °C. Then the gate opens and the gasoues low-boiling compounds under the gauge pressure pass through the porous wall to the jet of the over-hydrogened fire-damp. The low-boiling compounds when passing through a porous wall cool it, however, are heated themselves. In the jet's volume under the influence of hydrogen takes place the process of compounds' reduction when metal microparticles are generated.

The generated dust flux comes in the jar 5. Microparticles of the metal 9 come into contact with water, then they are cooled and sink. Burned gaseous products move through the drainage canal 12 into the jar 3. Along the whole way from the reduction chamber 3 to water surface 8 in the jar 5 hot gas-powdered flux do not touch walls of the path, and as a result microparticles slightly conglomerate.

The generated and conglomerated microparticles of refractory metals in gaseous flux have the sizes from A.U. to hundreds of A.U. This gives an opportunity to use them for making effective gas-powdered screens in front of the walls of high-powered plants, and also for making porous walls.

**Bibliography**:

1. Arinkin S.M. The Method of Protection and Diagnostics of Combustion Chamber's walls.IFG,volume 74, № 6, 2001.
2. Polezhaev U.V., Urevich F.B. Thermal Protection.M.Energy, 1976.
3. Arinkin S.M. The Loss of Radiant Energy by Gaseous Flux.M.Sb.<< Heat Exchange - 98>>,Soviet Researches.M.,1980.
4. Heberlain V., Pfender E. Porous Cooling of Combustion Chamber's walls.Heat Exchange, №2, 1971.

# GAS-STATIC PRESSING IMPROVES QUALITY AND WORKABILITY OF BLADES OF GAS TURBINE ENGINES

**Logunov A.V., Golovanov V.I, Razumovsky I.M., Marinin S.F., Tikhonov A.A., Poklad V.A.(1), Frolov V.S.(1), Bykov Yu.G.(1)**
Public Joint Stock Company "KOMPOZIT", Korolev, Russia
ul. Pionerskaya 4, Korolev, Moscow Region, 141070, Russia, Kompozit.Mat@g23.relcom.ru
(1)Federal State Unitary Enterprise MMPP "Salut", Moscow, Russia
prosp. Budennogo 16, Moscow, 105118, Russia

Molded pieces, including blades from refractory nickel alloys for gas turbine engines, cannot be obtained without occurring discontinuities in them such as shrinkage cavities, macro- and microporosity, even when using state-of-the-art casting technologies.

Besides that, a creep strain occurs and develops in blades under impact of high temperatures, loads and environment during exploitation or bench tests, which is followed not only by changes in material structural state of blades but also by occurring there some micro-discontinuities – micro-tears, micropores and microcracks.

Material "damage" degree of the blades during the operation time (exploitation or testing) depends on loading regime as well as on chemical composition, structural status and other factors.

A cause of formation of discontinuities during operation timee is mainly traveling of dislocations under the affect of stresses, their arrest and accumulation near obstacles – phase particles, precipitation of particles of the second phase and carbides, interfaces and grain boundaries, etc. As much as creep strain is developed, a degeneration occurs of dislocation agglomerations into micro-tears, wedge-shaped cracks and micropores.

Primary (casting) discontinuities and the same obtained during the operation time decrease workability of blades and finally lead to their destruction.

The most efficient elimination method of internal pores and cavities in molded pieces from various alloys is hot isostatic pressing (HIP), which is used for years on our country and abroad for treatment of responsible destination castings.

HIP of castings consists in overall unicorm compressing them in special installatioms (barostats) at certain values of temperature and pressure of the working medium, which in most cases is argon.

At HIP, closing and diffusion welding of walls of internal cavities takes place as a result of plastic deformation of material of castings.

In this work, results are given of feasibility study of HIP application not only for elimination of primary casting) discontinuities in blades from the alloy ЖС6У-ВИ, but also for removal of discontinuities occurred during the bench operation time of blades.

In investigations, effect of HIP was estimated on size and quantity of micropores in blades after the long operation time (956 hours) on their endurance limit and thermocyclic fatigue. HIP of blades after casting was not performed.

Gas-static treatment of blades was performed in a barostat HIRP10/26 (Switzerland) according to the following regime: temperature of heating – 1210$^0$C, argon pressure – 160MPa, holding time in operation conditions – 3 hours.

Metallographic sections for investigation were prepared from blades of two states (operation time 956 hours and operation time 956 hours + HIP) and then subjected to metallographic analysis with optical microscope.

At the section of the blade with the operation time 956 hours, 8 fields with porosity were investigated at magnification factor of 100. At the section of the blade being in the state "operation time 956 hours + HIP", 3 fields were investigated at magnification factor of 500 due to small quantity and size of pores. Number and size of pores in the investigated samples are given in Table 1.

Table 1.

| Subject of analysis | Results of analysis | |
|---|---|---|
| | A blade with operation time 956 hours | A blade with operation time 956 hours + HIP |
| Number of fields investigated, pcs. | 8 | 3 |
| Total area of analysis, sq. mm | 5.165 | 0.078 |
| Average pore size, µm | 21.2 | 2.7 |
| Maximal pore size, µm | 87.6 | 4.0 |

As a result of metallographic analysis of porosity, a positive effect was ascertained of HIP on decreasing of size and quantity of pores in blades with a long operation time: maximal pore size decreased more that by 20 times.

A certain amount of residual pores in blades after HIP seem to be linked with insufficient value of argon pressure in a barostat or holding time at the working regime.

Decrement of quantity if of internal discontinuities in blades of initial (cast) state and with a long operation time by HIP was confirmed also by autoradiograph investigations.

The basis of this method is a phenomenon of boosted diffusion of atoms of radioactive elements over structural defects in alloys: grain and subgrain boundaries, interfaces, dislocation agglomerations, individual lattice vacancies, micro-tears, microcracks, etc. [1].

Besides a general pattern of distribution of defects in the alloy microstructure, this method allows estimation of diffusive permeability of a material over structure imperfections.

For performing these investigations, metallographic sections were prepared from the blades, and a thin layer of radioactive isotope $^{63}$Ni was applied to their surface by electrolytic plating technique. Then section were subjected to vacuum annealing at a temperature $900^0$C for 10 hours, whereas atoms of radioactive isotope diffused into the depth of samples and accumulated in defective sites of microstructure.

After that, a layer of fine-grain photoemulsion was applied to the prepared surface of samples and its exposure was performed during 2 weeks. During exposure, β-radiation of radioactive isotope atoms affects photoemulsion similarly to usual light. On completion of exposure, photoemulsion on a sample was subjected to standard stages of photoprocess – development, fixing, rinsing.

A "photograph" (autoradiograph-structure) of radioactive atoms distribution over the section plane obtained as a result of all these operations can be studied by means of usual optical metallographic microscope.

Analysis of autoradiograph-microstructures revealed the following:

- In initial state blades (casting + TVT), main structural defects with boosted diffusion were grain boundaries. At that, diffusive permeability (as can be seen by width of boundaries) in longitudinal and transversal directions with respect to the blade axis was practically equal and uniform. Diffusive non-uniformity in volume of grains was feebly marked and connected with defects of interfaces carbide/matrix and $\gamma'$-phase/$\gamma$-phase.
- A long bench operation time lead to considerable changes of diffusion flows in microstructure of blades. Comparing to the initial state, considerable increasing of diffusion flows was marked for grain boundaries transversal to the blade axis (widening and "blackening" of boundaries). In the volume of grains, sites of new defects formation occurred carachterized by boosted diffusion (black rash), i.e. micro-discontinuities (micro-tears) were formed not only in transversal boundaries but also in the volume of grains.
- Diffusion permeability of grain boundaries and in volume of grains in microstructure of blades with a long operation time decreased after performing HIP and became similar to permeability of initial state. Grain boundaries (including transversal ones) became thin and "pale", quantity of black rush in volume of grains decreased and it became pale.

Besides such estimation of "damages" of the blade structure during the operation time and its "correction" during HIP, radionuclide method allowed measurement of effective diffusive permeability of blades in various states (Table 2).

Table 2.

| Name | Values for the blades in the state… | | |
|---|---|---|---|
| | Initial | Operation time | Operati on time +HIP |
| Effective diffusive permeability, $D_{eff}$, cm$^2$/s | $1.2\times10^{-12}$ | $1.0\times10^{-11}$ | $1.9\times 10^{-12}$ |

From the data of the table it issues that the value of effective diffusive permeability of samples with a large operation time grows up almost by an order of magnitude comparing to the initial state. It means that a long operation time initiates formation in the microstructure of numerous defects with boosted diffusion. Usage of HIP after operation time restores almost completely initial diffusive permeability of heterogeneous microstructure of the alloy, i. e. liquidates structural defects in the form of various micro-discontinuities occurring during operating time.

Hence, application of HIP to blades with a long operation time promoted elimination of structural damages obtained during the operation time and restoring the structure to the state close to the initial one.

It should be noted that HIP removing primary and adopted discontinuities such as cavities, micropores, micro-tears and microcracks cannot "correct" changes of the blade structure itself, which occurred during exploitation or bench testing (though some changes of structure occur as a result of heating during this operation). Therefore, for structure reconditioning of blades with some operation time, they must be subjected to compulsory thermal vacuum treatment (TVT)after HIP treatment.

According to the existing technology, on the expiry of a certain operation time, the blades can be subjected to a reconditioning repairing to increase their service life. Reconditioning repair of blades consists in removal of the old protective coating, performing TVT and applying a new protective coating.

Introduction of HIP into technological line-up before TVT considerably increased mechanical properties of blades.

In case of using a new technology, the endurance limit of blades with the operation time of 646 hours at a room temperature basing on $2\times10^7$ cycles and the reference stress level of 150MPa increases by 40MPa comparing to the blades without repair and by 20MPa comparing to the blades repaired using the old technology.

Thermal fatigue testing of blades with a run of 1100 hours also had shown beneficial effect of HIP on their serviceability. These tests were performed at cyclic changing of the temperature by the scheme 475↔950$^0$C before the first crack ~0.5mm in length occurs at the exit edge in the central section of the blade. Test results (3 blades of each state) are given in Table 3.

Data of the table indicate that application of HIP in technological line-up of the reconditioning repair of blades with a long operation time increased their thermocycling fatigue resistance on average by 3 times for blades without repair and by 2.5 times for blades repaired by the old technology.

Table 3.

| State of blades | Number of cycles before the first crack occurs | |
|---|---|---|
| | Maximal value | Average value |
| Operation time 1100 hours without repair | 3000 | 1831 |
| Operation time 1100 hours with repair by old technology | 4048 | 2082 |
| Operation time 1100 hours with repair by new technology | 7500 | 5500 |

Thus, efficiency was established of application of hot isostatic pressing in combination with subsequent thermal vacuum treatment in reconditioning repair of exploited blades from the alloy ЖС6У. At that, internal discontinuities occurred during operation are practically completely eliminated, and microstructure and service characteristics of the blades approach to the initial state.

Similar reconditioning repair can be also applied to blades or other molded pieces from other refractory nickel alloys, steels and titanium alloys.

References

1. С.З. Бокштейн, С.С. Гинзбург, С.Т. Кишкин, И.М. Разумовский, Г.Б. Строганов. Авторадиография поверхностей раздела и структурная стабильность сплавов. М. Металлургия. 1987

# HIGH-PRESSURE SYNTHESIZED MGB$_2$-BASED MATERIALS WITH HIGH CRITICAL CURRENTS, INFLUENCE OF TA, TI, SIC AND ZR ADDITIONS

**Prikhna T.A., Savchuk Y.A., Gawalek W. (1), Sergienko N.V., Moshchil V.E., Wendt M. (1), Melnikov V.S. (2), Dub S.N., Habisreuther T. (1), Schmidt Ch. (1), Dellith Jh. (1), Nagorny P.A.**
Institute for Superhard Materials of NASU, Kyiv, Ukraine
2, Avtozavodskaya Str., Kiev, 04074, Ukraine, prikhna@iptelecom.net.ua
(1)Institut für Physikalische Hochtechnologie, Jena, Germany
Albert-Einstein-Strasse 9, Jena, D-07745, Germany, gawalek@ipht-jena.de
(2)Institute of Geochemistry, Mineralogy and Ore-Formation, Kyiv, Ukraine
34, Palladin Pr., Kiev, 02142, Ukraine

Soon after the discovery of superconductivity close to 40K in $MgB_2$ by the team of Akimitsu, an intense research effort was launched to use this material in industrial applications, including strong currents conduction. In order to reach high transport characteristics superconducting materials should have optimal pinning character, which strongly depends on the synthesis process. High pressure- high temperature synthesis has been shown to produce $MgB_2$ bulk material with the best critical current density ($j_c$) and fields of ireversibility [1—3].

The structure of magnesium diboride samples high-pressure synthesized (HPS) from Mg and B that in accordance with XRD analysis contained mainly well-crystallized $MgB_2$ phase turned out to be more complicated as showed by SEM and microprobe examination [1]. In parallel with Mg and B the nanostructure of main ”matrix” phase of the samples contains oxygen (Mg—B—O) and is superconducting and Mg-B (or most likely monocrystalline $MgB_2$) inclusions of size from 10 μm down to 200 nm or even smaller are distributed throughout the “matrix”. The suggestion that Mg-B inclusions are $MgB_2$ single crystals is supported by the following facts: (1) EDX analysis shows that the amounts of Mg and B contained in such an inclusion are very close to the $MgB_2$ stoichiometry and (2) nanohardness (estimated by a nanoindenter) at 60 mN-load of these inclusions is 35,6±0,9 GPa, which is higher than that of sapphire (31,1±2,0 GPa), while nanohardness of the “matrix” is 17,4±1,1 GPa only. The Young moduli are 213±18 GPa of “matrix”, 385±14 GPa of the Mg-B inclusion and 416± 22 GPa of sapphire.

Usually a higher amount of Mg-B inclusions in the structure corresponds to a higher critical current density and irreversibility field at 30-10 K, in the so-called range of working parameters for $MgB_2$ [1—3]. Samples, which are better from the point of view of superconductive (SC) characteristics contain some amount of pure Mg and lesser amount of $MgH_2$ impurity or this phase is absent at all. With increase in the synthesis temperature from 750—800 $^oC$ to 950 $^oC$, the reduction of the amount of Mg-B inclusions and $MgH_2$ impurity phase is observed. But the reduction of Mg-B inclusions affects more drastically the decrease of $j_c$ than the reduction of $MgH_2$ promotes its increase. In addition, we may assume that impurity hydrogen may enter into the material structure decreasing the superconductive characteristics. Our previous findings have proved that hydrogen is harmful for critical current density in high-pressure synthesized $MgB_2$ [1]. The structure of all high-pressure synthesized samples contains MgO in small amount, which does not practically vary with synthesis conditions.

A number of investigations have been performed to study a possibility to produce additional pinning centers in the $MgB_2$ structure by chemical doping. Promising results have been obtained by adding Ti, Zr and SiC. It has been found that the grain size of a SiC powder added to a Mg and B mixture affects the SC characteristics of $MgB_2$ synthesized at ambient pressure, the optimal size being about 20 nm [4].

Additions of Ta, Ti, Zr and nano-SiC can increase critical current density of high-pressure synthesized (HPS) $MgB_2$ (Fig.1) The main effect of Ta, Ti and Zr seems to be due to the absorption of impurity hydrogen at low synthesis temperatures to form TaH, $Ta_2H$, $TiH_2$, $ZrH_2$, which prevents harmful $MgH_2$ impurity phase from appearing and may prevent impurity hydrogen from being introduced into the material structure. Additions of Ti and Zr to $MgB_2$ synthesized under high pressure provoke the highest increase of $j_c$. In the case with Zr the higher synthesis temperature (950 $^oC$) give rise to $ZrB_2$ phase, but the presence of $ZrB_2$ does not improve the SC characteristics of HPS $MgB_2$. Ti and Zr absorb impurity hydrogen at low synthesis temperature. Ta adsorbs hydrogen as well but the more pronounced effects of Ti and Zr as compared to that of Ta might be attributed to their higher absorptivity.

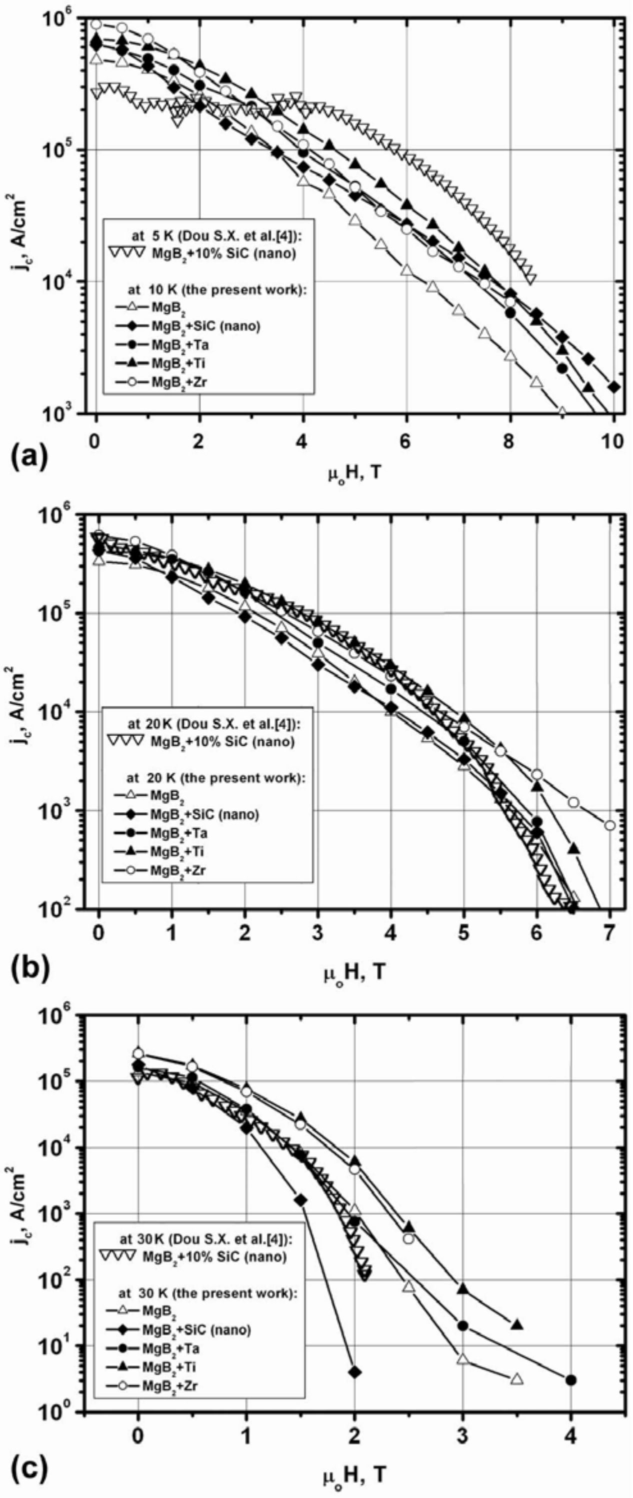

Fig. 1 General dependences of critical current density ($j_c$) vs. magnetic field ($\mu_0H$, T) of $MgB_2$ with and without additions at different temperatures (a) 10 K, (b) 20 K, (c) 30 K. For comparison the data on $MgB_2$ with 10% of SiC (20 nm) addition at (a) 5 K, (b) 20 K, (c) 30 K synthesized at ambient pressure [4] are given. We took the best data on $j_c$ for each field for the samples synthesized in all ranges of temperatures and amounts of additions (2 or 10 wt%) being studied.

Nano-SiC (20-30 nm) addition provokes the highest $j_c$ in the fields above 8 T at 10 K. When nano-SiC have been used, grains of SiC and/or $Mg_2Si$ may serve as additional pinning centers in $MgB_2$ obtained at 900 °C. A decrease in the amount of Mg-B inclusions in the samples with nano-SiC added that have been synthesized at higher temperatures seems to be replenished by the presence of SiC nanograins that may act as additional pinning centers. It is also possible that formation of $MgB_2(SiC)_x$ takes place. As it was shown in [5], only a small reduction of the crystal lattice parameters observed up to high level of SiC doping ($x$ =0.34). Such co-substitution may induce defects (dislocations) and local composition change within superconducting grains that can act as effective intra-granular pinning centers. It is likely that further increase in the synthesis temperature will lead to a further increase of $j_c$ of HPS $MgB_2$ with nano-SiC additions and more investigations should be conducted to ascertain the optimal synthesis temperature.

High-pressure synthesized $MgB_2$–based material shows at 20 K up to 3 T $j_c \geq 100$ kA/cm$^2$ and up to 5 T $j_c \geq 10$ kA/cm$^2$.

## References

1. Prikhna T.A. et al., High-pressure synthesis of $MgB_2$ with addition of Ti, Physica C 402 (2004) 223—233.

2. Prikhna T.A. et al., High-pressure synthesis of a bulk superconductive $MgB_2$-based material, Physica C 386 (2003) 565—568.

3. Prikhna T.A. et al., High-pressure synthesized $MgB_2$ with high critical current density and irreversible field, positive influence of Ta on superconductive characteristics, Proc. Int. Conf. on Science for Material in the Frontier of Centuries: Advantages and Challenges, 4–8 November 2002 Kyiv Ukraine, 406—407.

4. Soltanian S et al., Effect of grain size and doping level of SiC on the superconductivity and critical current density in $MgB_2$ superconductor, IEEE Trans. Appl. Supercond. **13** (2003) 3273.

5. S X Dou et al., Substitution-induced pinning in $MgB_2$ superconductor doped with SiC nano-particles, Supercond. Sci. Technol. **15** (2002) 1587—1591.

# QUASISTATIONARY SOURCE OF CLUSTER BEAMS

**Nosachev L.V.**
Zhukovsky, Central Aerohydrodynamic Institute, Zhukovsky, Russia
Zhukovsky, 140180, Moscow reg., Russia, E-mail: cfd@tsagi.ru

In a basis of modern know-hows of deriving of materials collected from clusters, with special properties usage of cluster beams and cluster plasma [1,2]. Clusters as against macroscopic fragments is not monotonic functions of number of atoms and have extremums of the arguments at magic numbers of atoms in them. The magic numbers answer closures of clusters and higher values of bond energy of atoms, of energy of an electron attachment etc. [3]. By photoionization of neutral clusters it is possible to receive a stream positively of charged clusters controlled electric and a magnetic fields and having high reactivity.

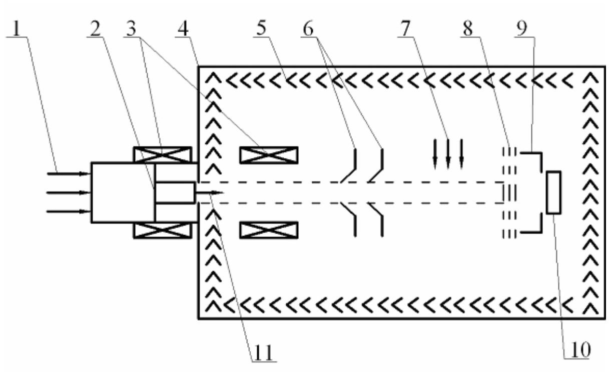

Fig. 1 Quasistationary source of cluster beam.
1 - working gas, 2 - jet resonator, 3 - solenoid, 4 - vacuum chamber, 5 - cryopanel, 6 - skimer, 7 - UF-radiating, 8 - ion - optical system, 9 - electrostatic trap, 10 - sample, 11- baffer gas.

Reviewed possibilities of creation of optimal conditions for forming multishell nanostructures from carbon cluster plasma synthesized with the help of a quasistationary source of cluster beams of high intensity are reviewed.

1 the schema of a quasistationary source of cluster beams is rotined. Here stream of clusters is generated in output stream of a high frequency jet resonator 2 such as Гартмана-Шпренгера [4], with composite pattern of shock and detonation wave originating at the hypersonic expiration from a slotted nozzle and detonation combustion of a working mixture from hydrocarbons, soot and cushion gas 11. The stream is entered in an vacuum chamber 4 with cryopump [5] from cryopanel 7 on pool azote and gaseous helium with temperature about 10°K. The facilitiess of diagnostic are designed, in particular, high frequency pitot tube with built-in subextrasmall (O1,8 mm) the sensor of pressure oscillation, explains the method of application prob of measurings and the observed datas in output stream of an jet resonator of pressure oscillations in frequency band up to 10 kHz are.

1. Nefedov A.P., Petrov O.F., Fortov O.V., UFN 167 (11), 1997.
2. Smirnov B.M. UFN 170 (5), 2000.
3. Harris I.A., Kidwell R.S., Northby J.A. Phys. Rev. Lett. 53 2380 1984.
4. Puchkin R.M., Tarasov A.I., Patent USSR $^1$1672933 1991.
5. Johov V.A., Kexvaianc V.G., Potapov Y.F., Sidorov S.S., Prusov B.V., Patent of Russian Federation $^1$2140568 1998.

# MICROSTRUCTURE AND CHEMISTRY OF INTERGRANULAR PHASES IN SIC-BASED CERAMICS SINTERED IN THE PRESENCE OF A LIQUID PHASE

**Izhevskyi V. A., Kovalchenko M. S.**
Frantsevich Institute for Problems of Materials Science of NASU
Krzhizhanovskogo st. 3, Kiev 03142, Ukraine, e-mail: izhevsky@ipms.kiev.ua

Silicon carbide (SiC) is characterized by a unique combination of properties such as high strength retained up to high temperatures, high corrosion resistance, high wear resistance, high thermal conductivity, good thermal shock resistance, high oxidation resistance which makes SiC-based ceramics a promising candidate for high temperature applications under extreme mechanical loading. However, densification of SiC-based ceramics presents certain difficulties and for sintering it to near-theoretical densities the use of sintering aids is necessary. For liquid-phase sintering (LPS) of SiC various oxides are used, the most common ones being $Al_2O_3$ and rare-earth (RE) oxides, and lately oxynitride sintering aids, in particular RE – AlN, are closely scrutinized.

Although the observed as-sintered microstructures largely depend on the preparation route and processing parameters utilized there are a number of features which are common to all liquid-phase sintered SiC-based ceramics. Typically, the microstructure is composed of SiC grains, amorphous grain-boundary films between adjacent SiC grains, and phases at triple junctions of SiC grains which can be present either in an amorphous or partly crystalline form. The presence and stability of intergranular phases in ceramic materials is of great importance. The liquid condition of intergranular phases at sintering temperatures determines the densification processes. When solidified, in as-sintered material they largely influence the mechanical properties of structural ceramics, in particular fracture toughness and creep resistance [4-6].

Intergranular phases in SiC-based ceramics are investigated far less than in the $Si_3N_4$-based ones. The liquid condition of amorphous intergranular $SiO_2$-based films in SiC-based ceramics was particularly studied by Clarke [7] when he was developing his model based on an intricate balance of attractive and repulsive forces that determine the stability of such films. He suggested that SiC-based ceramics is the only material where attractive Van der Waals force is larger at all distances than the repulsive steric force, as it is indicated by the high refractive index of SiC. Therefore it was concluded that the liquid silica film would not be stable between SiC grains. However, the existing by now experimental data on the microstructure of sintered SiC-based ceramics are rather contradictory. While the results of some studies indicate that there are no amorphous films between the adjacent SiC grains [8], other authors claim the presence of such films with the equilibrium thickness of 1-2 nm [9].

The goal of the present work is the detailed microstructural investigation by means of transmission electron microscopy (TEM), scanning TEM (STEM), high-resolution TEM (HRTEM) and precise compositional identification by a number of analytical methods and techniques (XRD, WDS, EELS, PEELS) of intergranular phases in LPS SiC-based ceramics. This will enable to determine the equilibrium conditions of such phases and provide new knowledge for better LPS-SiC structure-sensitive properties tailoring.

Investigations were carried out in two systems: SiC – $SiO_2$ and SiC – AlN – $Y_2O_3$. In the latter system SiC powders with varying grain size were used. The composition of the first system was consistent with the one used by Clarke for devising of his model, while the composition of the second one was chosen as the most interesting from the commercial point of view. The use of a coarse-grained SiC powder (32-160 μm) for the preparation of the second composition was necessary for the microstructure of the LPS samples to be coarse enough for precise and reliable analyses of the intergranular phases. Dense samples of of ceramics were obtained by means of liquid-phase sintering in the atmosphere of nitrogen or argon at the temperature of 1950°C. Samples for TEM investigations were prepared according to a standard ceramographic procedure.

Investigations carried out in the SiC-$SiO_2$ system showed that after sintering in the nitrogen atmosphere secondary phases consisting of oxycarbide or oxynitride glasses are formed in the material. Calculations carried out according to the model developed by Clarke [7] showed that incorporation of C and N into the structure of silicate glasses changes the structural correlation length of the intergranular phases, increasing the steric repulsive force and finally stabilizing the intergranular amorphous films. Moreover, if the influence of incorporated C and N on the properties of the glassy phase is taken into consideration the values of the equilibrium thickness of the intergranular amorphous films calculated in terms of the Clarkes's model are in good agreement with the experimental values measured by HRTEM.

Stable amorphous films were shown to be present at all the grain boundaries in the liquid-phase sintered SiC-AlN-$Y_2O_3$ materials. The equilibrium thickness was measured by HRTEM to be 0.8 to 2 nm. EELS analyses show that Si, Al, C, O and N are present in the grain-boundary films. When $N_2$ instead of Ar is used as sintering atmosphere, N segregartion at grain boundaries is largely increased, while O content remains constant. Segregated carbon at grain-boundary films was proved by energy-loss near-edge structure (ELNES) analyses to be bonded to silicon. Crystallization processes in intergranular phases during sintering and post-sintering heat treatment in different sintering atmospheres were also thoroughly studied.

**References**

1. M. A. Mulla and V. D. Krstic. Mechanical Properties of β−SiC Pressureless Sintered with $Al_2O_3$ Additions, Acta Metall. Mater., **42** [1] 303-308 (1994).
2. Y –W. Kim and M. Mitomo. Fine-Grained Silicon Carbide Ceramics with Oxynitride Glass, J. Am. Ceram. Soc., **82** [10] 2731-2736 (1999).
3. V. A. Izhevskyi, L. A. Genova, J. C. Bressiani and A. H. A. Bressiani. Liquid-phase sintering of SiC-based ceramics. Key. Eng. Mat., **181-191** (2001) 173-180.
4. R. Raj. Fundamental Research in Structural Ceramics for Service Near $2000^0$C, J. Am. Ceram. Soc., **76** [9] 2147-2174 (1993).
5. S. M. Wiederhorn, B. J. Hockey and J. D. French. Mechanisms of Deformation of Silicon Nitride and Silicon Carbide at High Temperature, J. Eur. Ceram. Soc., **19** 2273-2284 (1999).
6. J. J. Cao, W. J. Moberlychan, L. C. DeYonghe, C. J. Gilbert and R. O. Ritchie. In Situ Toughened Silicon Carbide with Al-B-C Additions, J. Am. Ceram. Soc., **79** [2] 461-469 (1996).
7. D. R. Clarke. On the Equilibrium Thickness of Intergranular Glass phases in Ceramic Materials, J. Am. Ceram. Soc., **70** [1] 15-22 (1987).
8. R. W. Carpenter, W. Braue and R. A. Cutler, "Transmission Electron Microscopy of Liquid Phase Densified SiC", J. Mater. Res., **6** [9] 1937-1949 (1991).
9. L. K. L. Falk. Microstructural deve-lopment during Liquid Phase Sintering of Silicon Carbide Ceramics, J. Eur. Ceram. Soc., **17** 983-994 (1997).

# COMBINED HEATRESISTANT COATINGS AND METHODS OF GROWING THEIR EFFICIENCY

**Abrahimov N.V., Poklad V.A. (1), Shkretov Y.P. (1).**
Zhoukovsky Air Force Engineering Academy
Planetnaya street, 3, Moscow, 125190, Russia, OGMet@ salut.ru
(1) Federal State Unitary Enterprise, Moscow Machinbuilding Production Plant "Saluit",
Budienovsky avenue, 16, Moscow, 105118, Russia, OGMet @salut.ru

Most important function of alloy high temperature strength actual implementing is belong to heat resistant coatings by the way of protecting part upper layers of high temperature assemblies from chemical destructions operated under extreme conditions of speedy gas flow and intensive temperature changes. Besides chemical destructions by gas atmosphere thermo fatigue cracks are created at the surface layer that substantially cut durability life of parts. Due high thermo mechanical forces gas turbine blades have low specified life that's why it's important new coating creating owned at the same time with higher corrosion resistance much better mechanical performances the extremely importance has a sharp problem solution of machine durability life prolongation.

Two methods of coating deposition are carried out widely in turbine manufacturing. They are diffusion and condensation. Coatings are produced by contact and non-contact methods with a forced halogen supply that are responsible for either substances transferring on the part surfaces. A positive effect gets two stage processing carry out when at the first stage cobalt, chromium, platinum, palladium, nickel- based alloys, doped with high-melting (rhenium, wolfram, tantalum) and easy oxidized (yttrium, silicon, Gaffney, ytterbium, erbium, etc.) elements are deposited, and at the second stage diffusion aluminizing or chromo-aluminizing are carried out. Such processes provide implementing of surface layers and coatings complex doping, getting better durability life of parts in extremely conditions operated [1].

Substantial improving durability life was got under depositing alloy as a first layer with weight proportions, %: nickel – a base; chromium 12-30; aluminum 2-15; tantalum – 0.2-20; wolfram 0.5-10; Gaffney 0.2-6.0; silicon 0.1-5; yttrium 0.01-5 [2]. High-melting coating elements improve noticeable features of phase and structural stability, but easy oxidizing elements suppress speed of oxidation film spalling under a cyclic oxidation. The second coating layer is produced by aluminizing or chromo-aluminizing in gas medium contained aluminum and chromium halogens, correspondently [3]. Such processes are allowed to solve successfully problems of surface layers protective performances improving for such parts as turbine cooled blades with simultaness forming of protective layers on inner cavities and passes. Tantalum and wolfram provide better durability of coating layers by the way of strengthening inter-atomic bonds in coating structure, inhibiting elements diffusion and improving structure stability. Coincident inserting yttrium, Gaffney and silicon influence mach efficiently than separate one, on better bonding an oxidation film with metal coatings as due known "pin" mechanism and bonding sulphur additives as well into high – melting sulphides and preventing this way creation cavities with gas substances of sulphur oxidances that are cause film spalling in oxidizing processes.

Normally forming of condensate and diffusion coatings are accompanied with more or less developed micro-porosity as processing types and due non- compensated elements diffusion in surface alloy layers as well. In this connection it's highly actual the problem of compression thin hard coating films. Thermal treating of coatings with compressing stresses super positioning in temperature fields excided over aluminized coating thermal transitions from embrittlement to a plastic condition allows substantially improve resistance features to thermo- fatigue cracking and cyclic durability life of parts [4].

References:

1. N.V. Abrahimov, Y.S. Eliseev. Thermo-chemical treating of heat resistant steal and alloys, M., Intermet engineering, 2001, 622 p.
2. RF Patent # 2213807, 2002.
3. RF Patent # 2212473, 2003.
4. RF Patent # 2213801, 2003.

# FABRICATION OF SIC MATRIX COMPOSITE MATERIALS AND COATINGS BY CHEMICAL VAPOR DEPOSITION/INFILTRATION (CVD/CVI)

**Bogatchev E.A., Lakhin A.V., Manukhin A.V. (1), Timofeev A.N.**
JSC "Kompozit", Korolev, Russia
4, Pionerskaya st., Moscow region, 141070, Korolev, Russia, pyrocarbide@mail.ru,
(1)Moscow State Institute of Steel and Alloys (Technological University)
4, Leninsky prospekt, Moscow, 117936, Russia, B-49, GSP-1, manukhinmisa@list.ru

Aerospace and aeronautical engineering continues to stay the only area of science where the application of the Ceramic Matrix Composites (CMC) is economically feasible. It is necessary to reduce the costs and the price of CMC, because the using of ceramic composites has very good prospects for national economy and civilian life in the view of efficiency and competitiveness on the market.

According to this fact the world practice found a way named Cost Effectiveness Concept (CEC) [1] to bring together scientific and technological purposes in the area of CMC production, taking in consideration reduction of costs and optimization of these new materials. This Concept proposes a long-term strategy of development and perfection of the CMC and coating technology. CEC is enabling to control the achievement of the strategy on different levels: within scientific groups or separate researchers. The strategy is based on exchange relations. We meet different problems trying to realize the strategy: on the one hand – research activities – i. e. achievement of high-level properties and efficiency of the materials; on the other hand – reduction of costs with the respect to the science, engineering and production; development of new engineering processes; analysis and upgrading of the technological stages of the CMC productions with the aim to improve their properties; bringing together scientific and technical purposes.

The aim of the present work is the consideration of the results, achieved during several years dedicated to the CMC and coating production development on basis of silicon carbide by CVD/CVI from methylsilane (MMS) under the condition of relatively low temperatures and pressures without use of chlorine containing reagents and diluent gas [2] according to the clauses of CEC.

The use of MMS for CMC and coatings production on basis of SiC has obtained a large application in the technology of silicon carbide processing for high-temperature semiconductor devices for the last 10—15 years. CVD/CVI permits to position a new way as a hi-tech method today. It also permits to lead the process at the temperatures 650—800 °C, which is quite lower than using chlorine containing silicon compounds, organic and inorganic. That fact corresponds very well with the clauses of CEC concerning the reductions of costs for CMC articles (saving on loss of power).

Advanced researches, thermodynamic calculation and physical model definition permitted to explain the process of geterogeneous SiC coatings creation from MMS at low temperatures, which conformed to the contemporary scientific ideas of complicated geterogeneous chemical processes. The results of the experiments (kinetic mechanism research), permitted to confirm our assumption: an opportunity to refuse from hydrogen and inert gas dilution; it also allowed to improve the properties of carbide, to divide distinctly the methods of matrix and coating processing. So, the researches of SiC properties, obtained by CVD/CVI methods, confirmed that according to such methods the geterogeneous polycrystalline deposits could be formed. These deposits consist of silicon carbide and do not contain free phases of silicon and carbon [3]. The kinetic researches of densification process of porous and fibrous preforms, used for composites, at the temperature interval mentioned, confirmed that when we lowered the temperature at the constant capacity we could achieve higher level of densification of the preforms and more uniform filling of the preforms with silicon carbide matrix. This fact improves homogeneity of the composite material and its physical, mechanical, constitutive properties.

The method is characterized by the following technological advantages:

-processing temperature reduction;

-opportunity to use non-oxidation-resistant and non-heat-resistant preforms;

-simple equipment for the processing control;

- simplification of gas-phase silicon carbide coating and composite matrix fabrication;

-opportunity to reduce the costs for energy, diluent gases, refinment and utilization of reagents.

We developed the schematic flow chart that was advantageously distinguished from the traditional ones. There is no necessity to prepare any special reagents for our process and to utilize the unreacted reagent — that is the simplification of the process and the reduction of costs. The setup does not equipped with devices corresponding to such operations. Our schematic flow chart has also many advantages over the others, where the dangerous and toxic reagents, hydrogen dilution are used. The process is nonpolluting and has a high level of fire safety.

There is also one more advantage of the technology proposed, which could make easier the manufacturing application: there is a tendency of mounting simplification and equipment unification that could help to realize the method of CMC and coatings obtaining on basis of SiC.

Development of the schematic flow chart due to the methods of in situ rate control processes CVD/CVI (the optical mode has been used before in the area of raising the epitaxial semi-conducting films by the MOCVD method [4], and weight mode, developed by us) could complicate the process itself and rise the costs for production on the one hand, but on the other hand it could permit to reduce the costs for technology development later.

We have developed the outstanding science that brought together researches and technology. By experience we know how to develop new materials and technologies, how to reduce their cost, to accelerate the stages of execution and production.

The manufacturing application of in situ control of CMC and coating obtaining process has very good prospects from the point of view of automation of these processes and it cold be applied in computer techniques.

The automation perspectives open large opportunities for information technologies application, which in theirs turn could provide fast communication, facilitate the technological stages control and accelerate the development of the process.

## References

1. Drissi-Habti M., Suzuki K. e.a.//Adv.Composite Mater.-1999.-V.8.-N1.-P.87-96.
2. Pathent FR 2130509 C1 published 20.5.99.
3. Lakhin A.V., Manukhin A.V., Timofeev A.N., Bogatchev E.A., Gabov A.V.// Composite Materials Structures. -2002.-N2.-Moscow.-P.8-14.
4. Kuznetsov P.I., Zakharov L.U., Zhitov V.N., Shemet V.V.// Gallium, indium and aluminium nitrides – structures and apparatus: thesis of the report. II All-Russian Conference.-St.Petersburg.-2001.-P.95-96.

# WARM COMPACTION OF POWDERS OF IRON

**Maslyuk V.A., Sosnovsky L.A., Minitsky A.V., Gayduchenko A.K.**
Frantsevich Institute for Problems of Materials Sciences of NASU
Krzhizhanovskii St., 3, Kiev 03142, E-mail: maslyuk@materials.kiev.ua

The warm compaction of metal powders researched still since 30th years of the last century, now is in details used and successfully realized abroad with reference to products from a powder of iron. The purpose of the present work was comparison of compactibility at pressing at 800 МПа powders: SC-200.26 (manufacture of firm Hoganes in a condition of delivery) and ПЖР3-200.28 (manufacture БКЗПМ) as in a condition of delivery, and the ambassador anneal in hydrogen (750 $^0$C, 1 hour). As the greasings entered into these powders amount 0,6 wt % used zinc stearatum and animal fat. The following basic results have been received.

Transition from pressing a mix of powder SC-200.26 with zinc stearatum at room temperature to warm (150 ± 10 $^0$C) to pressing provides a gain of density of 0,2 g/sm$^3$ (7,2 and 7,4 g/sm$^3$ accordingly), that coincides with the known data. Addition of 0,3 % thermally widen graphite in this mix practically has not changed its compactibility at the specified temperatures. On the contrary, addition 1 мас. % of aluminium powder or 30 wt % of powders chroum or iron of mark ПЖР3-200.28 has resulted in elimination of a gain of density at warm compaction. Replacement zinc animal fat practically does not change compactibility at room temperature. However, at warm pressing the gain of density is not realized; expression of less viscous, than стеарат zinc stearatum, animal fat from volume of a pressed powder takes place. Thus, it has been established, that the gain of density at warm compaction powder SC-200.26 is sensitive to handicapes and is realized only at presence of the certain properties of used greasing.

In a condition of delivery powder ПЖР3-200.28 has rather low compactibility (6,9 g/sm$^3$), raised up to 7,1 g/sm$^3$ carrying out anneal in hydrogen. Thus, values of compactibility at room temperature of powders SC-200.26 (a condition of delivery) and ПЖР3-200.28 (the ambassador anneal) are relatives. However, warm compaction of powder ПЖР3-200.28 as annealed, and in a condition of delivery, has not given a gain of density at use of each of the specified greasings, that, can be consequence tolerance of a limit of fluidity of this powder to heating.

The carried out experiments have allowed to draw a conclusion that warm compaction is process dependent from reological the properties of greasing in turn determining a range of pressure in which is realized mechanically and thermally caused reorganization particles. Greasing should be enough viscous to not be squeezed out from contacts between particles but thus to not prevent their mutual sliding. The known data also testify that results of warm compaction depend on properties of greasing. However, this process is dependent also from plasticity of particles of a powder of iron, which alongside with action of greasing settling down in interpartial contacts (including thermally active) promotes sliding the particles divided by greasing. Presumably, beneficial effect of increase of plasticity can be caused and that crushing particles in contact zones reduces specific pressure upon greasing and by that prevents its expression from them. Therefore more rigid particles render the greater resistance as them reorganization, caused by imposing of pressure, and to the further condensation, realized at plastic deformation at a final stage of pressing.

Such treatment of process of condensation at warm compaction provides necessity of search of the greasings having sufficient viscosity at certain temperature of heating and plasticity of the pressed powder, and allowing thus it is reliable to provide a gain of density.

# OPTIMUM PARAMETERS OF MILLING PROCESS OF CARBIDE-STEEL IN ATTRITOR

**Pavligo T., Svistun L.(1), Plomodyalo R.(1), Plomodyalo L.(2)**
Frantsevich Institute for Problems of Materials Science of NASU,
3, Krzhizhanovsky St., Kiev, 03142, Ukraine, E- mail: serdyuk@materials.kiev.ua
(1)Kuban State Technological University, 2, Moskovska St., Krasnodar, 350072, Russia
(2)Industrial enterprise "Technical rigging-tool", 18, Kozhevenna St., Krasnodar, 350004, Russia

Initial powder mixture for carbide-steel contains particles of the refractory component (TiC, TiNC etc.) with the size of 1 … 2 microns and less and steel particles (or their components) with the size of 5 … 10 microns [1]. Vertical or horizontal type attritors are advisable for milling of powders up to the dispersity condition. The attritors are the high-energy mills with grinding bodies (balls) which are actuated by one or several mixers (cores with cross blades) rotating with high speed. The speed of rotation of mixers of industrial attritors by firm Gebryuder Netzsch Mashinenfabrik (Germany) reaches 400 rev/min. There is information about attritors with number of revolutions of a mixer more than 1000 [ 2 ].

Efficiency of the milling in attritors depends not only on energy characteristics, but also on design parameter - the sizes of the chamber, amount and weight of balls, quantity of mixers and their blades (up to three or four), technological possibilities - volume of the chamber, the volume occupied with balls, volume of the loaded material, and also on ratio of the listed volumes. The important factors are the material (hard alloy, steel) and size of balls.

The present work concerning the milling of carbide-steel powders is executed on the experimental vertical type attritor having the chamber with diameter of 10,4 sm and volume of $1 \cdot 10^3$ $sm^3$, a mixer with three blades and speed of rotation of a mixer of 980 rev/min. There are studied following technological parameters effecting on milling efficiency: ratio of volumes of loading of balls and attritor, ratio of volumes of loaded material and balls, the size (diameter) of the balls.

Mixture contained the sprayed powder of high speed steel P6M5Φ3 (80 mas. %) and carboterm titanium carbide TiC (20 mas. %) was ground. The milling was carried out in isopropil spirit with steel balls. Time of milling was 3 hours. Efficiency of milling was estimated according to percentage of fractions up to 10 microns in finished mixture.

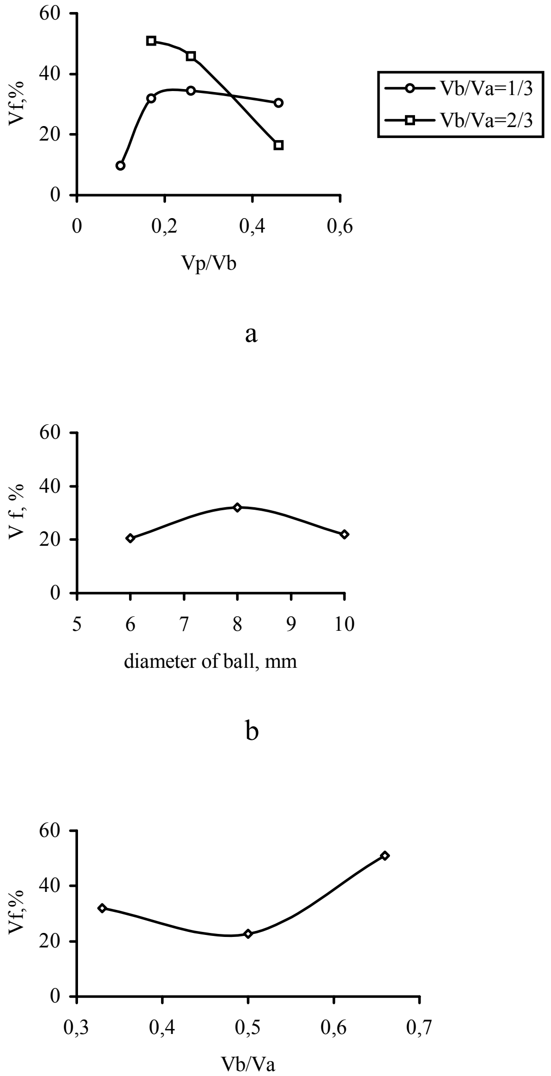

Fig. Dependencies of the volume contents of fractions of milled mixture P6M5Φ3-TiC on parameters of milling process: a – on relation $V_p/V_b$ - initial volumes occupied by powder and balls (at $V_b/V_a$= 1/3 and 2/3) where $V_a$ – attritor chamber volume and with balls diameter 8 mm; b – on diameter of balls (at $V_p/V_b$=0,17 and $V_b/V_a$=1/3); c - on relation $V_b$/Va (at $V_p/V_b$= 0,17 and diameter of balls 8 mm).

Granulometric composition (according to the size of particles) was defined by analyzer SIAMS-600 [ 3 ], the volume contents of fractions was defined with accordance with state standard 23402-78.
The results of investigation are submitted in figure.

In accordance with presented dependencies the optimum parameters of milling process of carbide-steel are $V_p/V_b$ - 0,17, diameter of balls - 8 mm, $V_b/V_a$ - 0,66 (2/3).

## LITERATURE

1. Ю.Г.Гуревич, В.К.Нарва, Н.Р.Фраге. Карбидостали.-М:Металлургия, 1988.-144 с.
2. Я.Кюбарсепп. Твердые сплавы со стальной связкой.- Таллин: Валгус-ТТУ, 1991.-164 с.
3. Промышленная система анализа изображений SIAMS-600.-Екатеринбург, 1992.-73 с.

# LASER IRRADIATION EFFECTS UPON OPTICAL PROPERTIES PRASEODYMIUM OXIDE FILMS

**Andreeva A.F., Paustovsky A.V., Sheludko V.E.**
Frantsevich Institute for Problems of Materials Science NASUkraine,
3 Krzhyzhanovsky Str., Kiev - 142, 03680,Ukraine, andreeva@ipms.kiev.ua

Praseodymium is classified among rare-earth elements, which have various valent states in its different compounds. In combination with oxygen, praseodymium comparatively easily changes its valency, forming a number of oxides of intermediate composition (from $Pr_2O_3$ to $PrO_2$).

The physical properties of praseodymium oxides of intermediate composition considerably differ from those ones of one-and-a-half oxides. Thus, for example, in comparison with praseodymium one-and-a-half oxide, the $Pr_6O_{11}$ specific resistivity is essential less, the absorption coefficient is changing by a factor of 2 (Fig.1)

In addition, praseodymium oxides have excellent operating characteristics inherent all rare-earth oxides - high thermal, chemical and radiation stability and their films offer good adhesion to a substrate.

In this paper the character of phase transitions in praseodymium oxide $Pr_6O_{11}$ films under the effect of laser irradiation is researched.

Praseodymium oxide films were obtained by electron-ray evaporation of metal praseodymium in oxygen medium. In accordance with the x-ray phase analysis data, polycrystal layers of body-centered cubic lattice - the structure with the lattice parameter really agreeing with the massive $Pr_6O_{11}$ tabular data - were condensed on the substrates. The deposition with a rate of 0,02 mkm/s was conducted on a quartz glass K-8 substrates. The film thickness is amounted to 0,2-0,3 mkm.

The film irradiation was conducted by the “Kvant-15” solid state laser with a λ=1,06 mkm wave length and a τ=4 ms pulse duration. The spot diameter was 2 mm; the focus shift was conducted perpendicularly to the film surface within a 18-20 mm range.

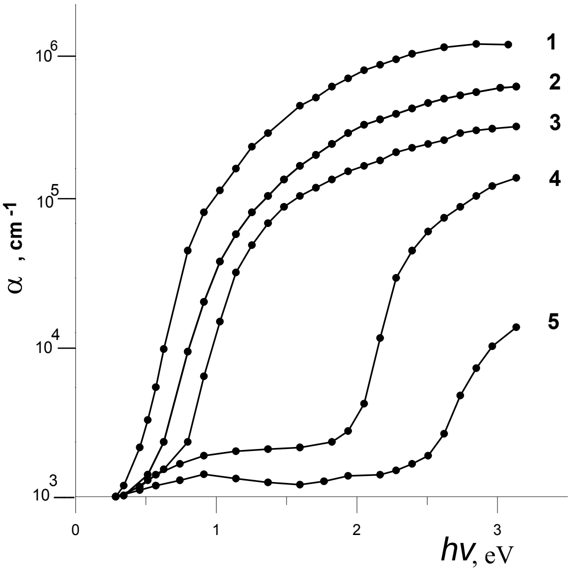

Fig. 1. The spectral dependence of optical absorption coefficient α for the films of the praseodymium oxide with different compositions: 1 - $PrO_2$; 2 - $Pr_6O_{11}$; 3 - $Pr_4O_7$; 4 - $Pr_5O_8$; 5 - $Pr_2O_3$.

Figure 2 shows the praseodymium oxide film optical density as a function of irradiated power. The layer transparency began to change at a 30 V/mm$^2$ irradiated power density, at ≥ 75,6 V/mm$^2$ one the density of the glass substrate surface was beginning to fail. A roughness of the spot edge made up 0,1mm.

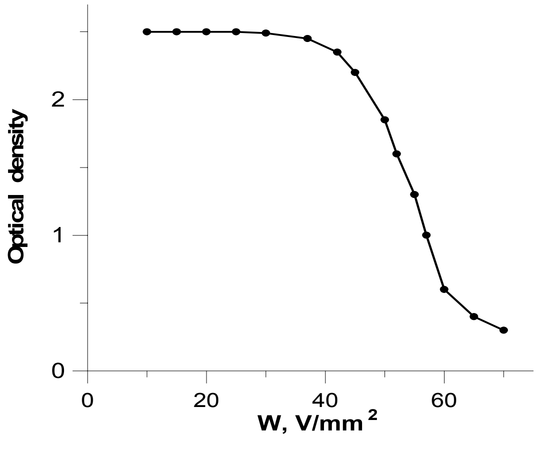

Fig.2. The variation of the optical density of praseodymium oxide as a function of the irradiated energy

In accordance with the x-ray analysis data the phase transition from $Pr_6O_{11}$ intermediate oxide to $Pr_2O_3$ one-and-a-half oxide took place. Under further annealing at $350^0C$ in the open air the $Pr_2O_3 \rightarrow Pr_6O_{11}$ reverse transition took place, the layer optical density was restoring.

Using of change of the praseodymium oxide film optical density under the laser irradiated effect is very promising for high resolution optical recording of information.

The high resistance to strong magnetic and radiated fluxes and high thermal and chemical stability of praseodymium oxides will allow preparing stable operating devices for information recording on their basis.

References

1. Kushkov V.D., Zaslavskiy A. M., Melnikov A.V. Strukturnye prevrashenija v plionkach oksida prazeodima // Zhurn. neorgan. chimii. - 1991. -36 . №6. -C. 1400-1401 (in Russian).
2. Andreeva A.F., Gilman I.Y. Nekotorije svojstva plionok $Pr_6O_{11}$ i $Tb_4O_7$. // Poluchenije i svojstva tonkich plionok. Kiev: IPM AN USSR, - 1977. C.107 - 111 (in Russian).
3. Andreeva A.F., Gil`man I.Y., Gamarnik M.Y., Struktura i nekotorije opticheskie svojstva plionok $Pr_6O_{11}$ // Izv. AN SSSR. Neorgan. Material. - 1986. -22, №9. - C.1475 -1479 (in Russian).

# CLADDING OF POWDERS AS A METHOD FOR PREPARATION OF COMPOSITE MATERIALS WITH CONTROLLED PROPERTIES

**Maslyuk V.A., Panasyuk O.A., Apininskaya L.M., Vergeles N.M., Minitsky A.V.**
Frantsevich Institute for Problems of Materials Sciences of the NASU
Krzhizhanovskii St., 3, Kiev 03142, E-mail: maslyuk@materials.kiev.ua

Coatings on iron powder particles were obtained by electrochemical reduction of metals (copper, nickel, and tin) from solutions of their salts using different reducers and complexing agents. Composite materials prepared from powders cladded by copper, nickel, and tin possess controlled magnetic characteristics and an increased corrosion resistance. The indicated properties can be controlled by varying the cladding conditions. Chemical nickel coatings are obtained from acid and basic solutions, which provides different phosphorous contents in them, and this, in turn, affects the magnetic and corrosion-resisting properties of the studied powder material. In the work, both types of solution were investigated with the aim of using them for cladding of iron powder. Composite powder materials with an increased electric conductivity, achieved by using powder cladded by Cu, were prepared. Copper coatings were obtained by contact deposition, chemical reduction, and electrochemical deposition. By varying the thickness and the quality of copper coatings deposited by different methods and the annealing temperature of such powder, we managed to prepare powder with a copper coating, the use of which in composite materials allows to change the anisotropy of the magnetic properties of magnetic cores. To improve the magnetic characteristics of powder materials, the tinning of iron powder particles was performed. The composition of the solution and its operation conditions were investigated. It was established that the quality and density of the tin coating on preliminarily coppered iron powder increased The deposition of tin proceeds on the catalytically active coppered surface of iron powder at a rate of 8 μm/h. The coating is a dense crystalline β-tin deposit. The magnetic characteristics of the powder soft magnetic material are improved with using preliminarily phosphated iron powder. The phosphating conditions and the compositions of the solutions influence on the phosphorous content in the phosphate film, which, in turn, favors changes in the properties of the powder materials

Table. Chemical compositions and coercive forces of cladded iron powders

| No. | Powder type | Chemical composition, % | | | | Coercive force $H_c$, Oe |
|---|---|---|---|---|---|---|
| | | P | Ni | Cu | Sn | |
| 1 | Initial ПЖР3 iron powder | 0.015 | - | - | - | 6.75 |
| 2 | ПЖР3 cladded by Ni from acid solution after annealing at 400ºC for 60 min in hydrogen | 0.39 | 3.6 | - | - | 6.05 |
| 3 | ПЖР3 cladded by Ni from basic solution after annealing at 400ºC for 60 min in hydrogen | 0.25 | 2.5 | - | - | 6.1 |
| 4 | ПЖР3 cladded by Cu (contact deposition) | | | | | 6.9 |
| 5 | ПЖР3 cladded by Cu (chem. reduction) after annealing at 800ºC for 60 min in hydrogen | - | - | 4.3 | - | - |
| 6 | ПЖР3 cladded by P | 1.4 | - | - | | 5.8 |
| 7 | ПЖР3 cladded by Sn | - | - | - | 1.4 | 5.6 |

# PECULIARITIES OF PRODUCING, PRESSING AND SINTERING OF DISPERSE MOLYBDENUM CARBIDE

**Savyak M.P. Uvarova I.V.**
Frantzevich Institute for Problems of Materials Science, Ukraine,
03680 Krzhizhanovsky str. 3, Kiev, Ukraine E-mail: saviak@materials.kiev.ua

## Introduction

Particles of crystalline bodies sized under 100 nm are know to have unique physical, thermodynamic and structural properties. In such particles there may occur a change in crystalline lattice parameters, decrease in the temperature of transition into a liquid state and phase transitions. All these changes are connected with peculiarities of atom-atom interaction, mainly with increasing the number of surface atoms in the total quantity of particle atoms [1].

This work deals with processes of production of nanosized molybdenum carbide powders by reducing oxides both in the presence of solid carbon and in various gaseous carbon containing media. The influence of the molybdenum carbide dispersity on subsequent forming and sintering of samples has also been investigated.

## Processes of low-temperature reduction and molybdenum carbidization in the presence of solid carbon

Thermodynamic calculations have shown that reduction processes in the $MoO_3$-$H_2$ system can start at room temperature.

Catalytic additives and using atomic hydrogen permit one to solve the problem of chemical interaction acceleration and to lower the temperatures of the initial and final stages of reduction. Low-temperature reduction in the presence of palladium additives proceeds in accordance with the scheme $MoO_3 \rightarrow H_{1,63}MoO_3 \rightarrow$ nonstoichiometric oxide→ $Mo_{1-x}O \rightarrow Mo$. Comparison of processes of surface development during molybdenum reduction from trioxide under low- and high-temperature conditions showed that the specific surface of the intermediate reaction products under low-temperature conditions promotes development of the specific surface up to S= 200 м$^2$/г, whereas the surface of products under high-temperature conditions is lower by an order of magnitude. Carbon was introduced in the reaction zone in a solid state in the form of carbon black. A great excess of the free surface energy, which in the first approximation is equal to the free surface area S of the disperse system multiplied by the surface tension $\sigma_s$: $\Delta G_s = \sigma_s x\ S$ [1], transforms the system into a nonequilibrium state. In such thermodynamically nonequlibrium systems with an excess of free surface energy, energy relaxation takes place due to phase transitions and ultrafine $Mo_2C$ formation. Quantity of the general carbon of 6.0 %, free 0.1%

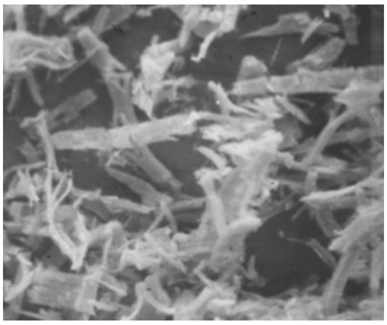

Fig.1. SEM photo of $Mo_2C$

Processes of reduction and carbidization in gaseous media

The results of calculation of the change in the isobaric-isothermal potential for processes of hydrocarbon decomposition and molybdenum dioxide decomposition showed that probability of carbide formation in atmosphere of saturated hydrocarbons increases with increasing the number of carbon atoms in the homologous row of saturated hydrocarbons. Hydrocarbons were introduced in the reaction zone at the intermediate stage of low-temperature molybdenum reduction with hydrogen from molybdenum trioxide, namely at a reduction degree of 84 %.

X-Ray analysis established that molybdenum suboxide obtained through low-temperature reduction at 650 °C in the presence of mixtures of natural gas, propane-butane, and acetylene transforms into molybdenum oxycarbide with the cubic type of lattice. Under further holding in these gaseous mixtures or with increasing temperature, process of transformation of the cubic oxycarbide phase into hexagonal molybdenum carbide $Mo_2C$ takes place. By structure and lattice parameters, oxycarbide is close to molybdenum suboxide and can be interpreted from the viewpoint of carbon atom introduction in the suboxide lattice. In other words, oxycardide formation takes place during saturation of molybdenum suboxide with carbon contained in the gaseous phase. In paper [2], the oxycarbide phase with a lattice parameter of 4.15-4.18 A, isostructural with g-$Mo_2N$, was detected while investigating the decomposition of molybdenum hexacarbonils The existence of this phase was confirmed by Yu.Solonin [3]. The data of the chemical analysis evidence that under carbidization in a propane-butane atmosphere, the amount of bound oxygen in the oxycarbide phase varies from 6.5 to 10.5 %, with the oxygen content changing from 5.8 to 3.5 %. A general formula for oxycarbide obtained in propane-butane mixture can be written as $Mo_3C_{2-x}O_x$, where x=1.2. Annealing of oxycarbide at 800 $^oC$ in a hydrogen atmosphere promotes transition of the cubic phase with a lattice parameter of 4.15-4.18A into the hexagonal molybdenum carbide $Mo_2C$. The specific surface area of carbide obtained attains 40 $m^2/g$; in air such powder absorbs oxygen.

## Forming and sintering of ultrafine molybdenum carbide

Densification of ultrafine molybdenum carbide is substantially worse compared to that of commercial molybdenum carbide powder with a specific surface area of 0.1 $m^2/g$.

Ultrafine powders have a developed surface, which makes densification difficult whereas more loose commercial powders are compacted much better.

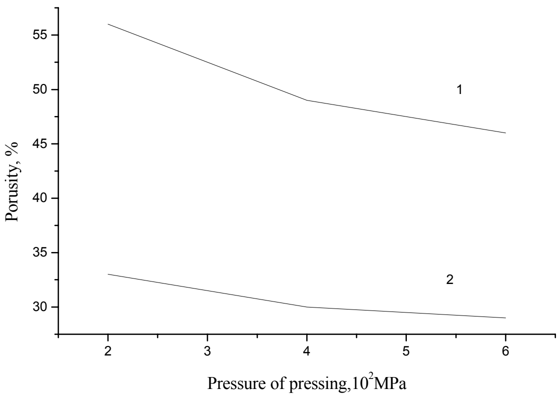

Fig.2. The pressure dependence of the porosity of $Mo_2C$ powders with different dispersion:
1- 0.1 $м^2/г$; 2 - 4 $м^2/г$.

In this work the temperature dependence of porosity was studied in the course of sintering molybdenum carbide of various dispersity.

Table Sintering of molybdenum carbide with different dispersity

| $S_{Mo2C}$ $м^2/г$ | Porosity % | | | |
|---|---|---|---|---|
| | Starting samples | Sintering $^oC$ | | |
| | | in vacuum | | in Taman's furnace |
| | | 1700 | 1850 | 1300 |
| 4 | 57 | 8 | 3 | 18 |
| | 55 | 7 | 8 | 13 |
| 0,1 | 49 | 7 | 7 | 11 |
| | 30 | 18 | 17 | 25 |

## Conclusions

It has been established that the structure of powders produced can be changed by controlling reduction processes. Low-temperature molybdenum reduction in the presence of a carbide-forming agent promotes formation of nanosized carbides and oxycarbides. It was also shown that densification processes change under pressing and sintering molybdenum carbide powders when the specific surface area increases from 0.1 to 4 $m^2/g$, that is, when the particle size changes from several micron to 0.1 μ. Such technological properties as ability for pressing and sintering have been established to markedly depend on carbide dispersity. Molybdenum carbide with a specific surface area of 4 $m^2/g$ sinters to a porosity of 3 %.

## References

1. В.В.Скороход, И.В. Уварова, А.В.Рагуля. Фізико-хімічна кінетика в наноструктурних системах, Київ, “Академперіодика”, 2001.
2. Б.А.Вишняков, К.А.Осипов. О получении пленок карбида молибдена из гексакарбонила молибдена под воздействием электронного луча. ФГТ.,т.9, вып.5,1967г., 1545-1547
3. В.В.Скороход, Ю.М.Солонин, И.В. Уварова. Химические, диффузионные и реологические процессы, Киев, «Наукова думка», 1990.

# THE ELECTRIC - DISCHARGE TECHNOLOGY OF RESTORATION OF POROSITY AND PERMEABILITY IN THE SEDIMENTARY ROCKS - THE HIGHLY EFFECTIVE METHOD IN THE OIL PRODUCTION

**Sizonenko O.N.**
Institute for Impuls processes and Technologies of NASU, Nikolaev, Ukraine
pr. October 43A, Nikolaev, Ukraine, e-mail:ipre@iipt.aip.mk.ua

The electric - discharge technology of processing of a near zone of a layer (NZL) is intended for restoration of permeability and porosity of the sedimentary rocks, collector composing a oil, gas and water, with the purpose of increase of productivity of extraction and acceleration characteristics of delivery chinks. At electrodigit pulse influence on NZL there is an increase in its permeability and clearing of filtering surfaces the chinks, achievable for the account: destructions of firm adjournment in a zone of punching; developments of existing cracks and creations new channels; removals and carrying out of polluting substances.

However, as have shown results of works in various geologic-specifications of the operation of chinks and the carried out laboratory researches, the electric - discharge technology does not always provide a necessary positive effect, in particular, it concerns to breeds having low permeability with the reduced permeability due to fall asfalt - and resinous and paraffin accumulations (ARPA) in them that is caused by viscous - plastic properties of ARPA.

To remove ARPA from a near zone of a layer in world practice are widely applied various surface-active substances (SAS). However, in collectors having low permeability it is possible to clear from ARPA only tubing string pipes and the trade equipment and only the small layer of the punched surface as solutionas a reagent cannot deeply penetrate into a near zone of a layer because of its insufficient permeability.

Therefore researches of physical features and principles of management by change of filtrational characteristics (porosity and permeability) various on the structure of the porous saturated environments (sandstones and carbonates) have been executed at electrodigit influence and improvement on this basis of the electric - discharge technology of processing of near zones of chinks.

The work was carried out at the experimental stand modelling conditions of a chink. The power part of the stand includes a control panel and the generator of pulse currents. The technological part includes the chamber of a high pressure with the built - in holder of a core in whom all-round compression of a core is created, and the electrode system entered inside of the chamber intended for energy transfer of the capacitor store in a working environment and accordingly forming discharge. The stand is supplied with the hydrosystem including installation IIPC which allows to carry out the filtration of a liquid through the core with the constant discharge, independently of work of an electric - discharge source. The stand allows to realize various combinations of geostatic, seam and hydrostatic pressure.

In experiments cores of sandstones and the carbonates, cut out perpendicularly the axes from cores lifted of a chink (direct circular cylinders) are used. Cores vere extacted, and then their porosity and permeability were determined, then they were saturated with oil and dried up at the temperature t =70 °C up to constant weight then porosity and permeability of the "polluted" core were determined.

For researches cores of sandstones and carbonates with identical initial porosity
$m \cong 15\%$ and permeability $\kappa \cong 3\bullet 10^{-14}$ m$^2$ have been selected, after pollution ARPA porosity has decreased up to ~2%, and permeability up to $\sim 0,2\bullet 10^{-15}$ m$^2$.

As a working environment filling the chamber of a high pressure liquids for muffling chinks at their stop for underground or major overhaul were used: water electrolit with $\sigma_0$=0,066 Om$^{-1}$m$^{-1}$ and water-in-oil emulsion (WOE), containing 30% of water. As filtrational characteristics of cores of rocks - collectors are reduced due to pollution ARPA for which removal basically surface-active substance (SAS) are used, in the base solutions the water electrolit (water) and WOE, was added the surfactant- multipurpose water-soluble composition NMK-21 which represents the multicomponent mix of anionic and non-ionic surfactants of the various chemical structure and target additives and possesses the best washing and inhibitory properties in comparison with reagents of similar action.

It is established, that opportunities of the high-voltage electric discharge in water in change of permeability absolutely insignificantly (~on 35%) exceed opportunities of processing of reagents. Use as working environment WOE allows essentially (in 2 times for sandstones and 1,5 times for carbonates) to raise efficiency of electric - discharge influence, in comparison with water. Use as a working environment at the electric discharge of water solution NMK-21 results to the synergetic effect in increase of permeability of rocks, the effect from complex influence in 2 times exceeds the sum of effects for the each component. The effect of synergism is kept also at the additive NMK-21 in WOE, and absolute values of permeability and speed of its growth in this case are higher, than in water solutions NMK-21, WOE and the more so to water.

The most essential changes of porosity at sandstones (up to 3 times) and carbonates (up to 2,5 times) are observed at the additive of SAS in WOE, efficiency of restoration of porosity reaches 95%.

Synergism from complex processing can be caused by the following factors.

1. Activation of the solution of SAS at the high-voltage electric discharges as a result of generation of gas and the subsequent foaming as a result of hashing at presence of the foaming agent (non-ionics SAS). After electrodigit processing 0,3 % solution NMK-21 practically completely deletes ARPA (reaches 95%), that confirm the data on restoration of porosity of cores. Washing of ARPA is (being) improved as a result of the best adsorption of SAS on a firm surface to that promote blisters foams.

Molecules of the foaming agent being adsorbed on gas blisters strengthen hydratedis layers at their environments. It results in increase of mechanical resistance of blisters and interferes with their destruction at collision.

2. Variable pressure (compression - extension) in solutions SAS, filtered in a layer that stimulates the effect of washing up pore from adjournment (up to 95%) and promotes increase in a cover zone by influence.
3. Adsorption of activated SAS on firm surfaces that (walls of filtrational channels) promotes decrease in a superficial tension on border of the separation of phases the liquid - a firm body and increases penetrating filtrational ability of the solution of SAS.
4. By adsorption of activated SAS on washed from ARPA rock that interferes with the subsequent growth of crystals ARPA and their sticking to a surface (inhibition ability is increased in 2 times), promoting increase in time of effect of influence.
5. Adsorption of activated SAS on crystals ARPA in the oil taking place in pores that results in destruction of its structural skeleton, improving its mobility at the filtration (the limiting pressure of shift is reduced on 40 %, in 2 times the pressure of shift and dynamic viscosity).
6. Adsorption of activated SAS in pores and microcracks that promotes creation of the wedged out effect due to pulse saturation by the filtered environment and dilatantion seal failure rock due to reorganization of its structure at formation of additional porosity (porosity has increased in 2,5—3 times).

The executed work has allowed to develop main principles for management of filtrational characteristics of the porous environments saturated with a liquid, consisting in a choice of a working liquid which should be chemically active to a kind of adjournment in the rock, and an establishment of a time mode of selective complex cyclic influence depending on type of the rock and its porosity.

Use of the received results allows to expand opportunities of the electric - discharge technology in change of structural - rheologying and filtrational properties of natural, technogenics and the synthetic structured disperse systems.

Legitimacy of the stated results has been confirmed with check of their use in various geologic-specifications of collectors of oil.

# THE RESEARCH OF EFFICIENCY OF SHIELDING PROPERTIES OF A GAS-POWDERED MEDIUM, WHICH IS CREATED BY REDUCTION OF LOW-BOILING REFRACTORY ALLOYS

**Arinkin S.M.**
Lykov Heat And Mass Transfer Institute of NASB, Minks, Belarus
15, P.Brovki Str., Minsk, Belarus, E-mail:SergeyArinkin@tut.by

We examined the efficiency of heat protection of the walls of high-powered plants with a temperature of active capacity running into thousand and dozens of thousands degrees [1, 2]. They are plasma reactors [3], gas-core nuclear engines [4], combustion chambers of aeroengines and rocket engines made from porous refractory materials with transpiration cooling [5].

In a work [6] it is suggested that in energy installations with a hydrogen working medium low-boiling refractory alloys should be used, the alloys turn from solid state into gaseous state at the temperature of 15—350 °C. Passing through a hot porous wall the alloys cool it and at the outlet they are reduced at the temperature of 1200—1700 °C. The gas-powdered screen of metal particles is formed in the parietal layer. It absorbs and scatters thermal radiation in the wide wave band. In a work [7] it was found that such a medium strongly extands while moving through the channel. At that time absorbing and scattering properties vary continuously. In a work [8] it was found that in the wave band of thermal radiation $0{,}005<\lambda<1$ μm the particles with a radius of $0{,}03\leq r\leq 0{,}1$ μm provide the largest value of the mass coefficient of radiation attenuation.

When the process of particles' downsizing takes place the maximum of radiation loss moves to the UV region, for which a gas-powdered medium with a size of particles $0.005\leq r\leq 0{,}03$ μm provides the highest shielding. The particle distribution function is given in [9].

At the temperature $10000\leq T\leq 100000$ °C most of radiation is connected with the wave band of $0{,}005<\lambda<004$ μm. The particles that are of that size appear only during the direct reduction of such compound as $WCl_6$,$WF_6$, $SiCl_4$ on the way out of a porous wall when their size amounts to Angstroem Units. These particles form a screen against X-ray radiation and a vacuum ultraviolet wave band.

With the purpose of analysing the protective properties of a gas-powdered screen numeric calculations of characteristics of arc hydrogen plasma in a plasma generator of a linear circuit were done according to the procedure described in [10]. The presence of tungsten particles became available due to the special density distribution and the distribution of thermophysical properties over the radius of a channel. For the registration of radiation transfer the method of partial characteristics was used [11]. The adiation flux coming from hydrogen plasma is reflected and then is partially absorbed by tungten particles. The proportion of the reflected to the absorbed flux depends on the size of the particles. The calculations for 2 radiuses of the channel of 0,5 and 1 cm were done at the atmos-heric pressure.The current turndown varied from 100 to 300 A, the hydrogen rate $G_{H2}$ varied from 0,1 to 1 g/s. Taking into account that in a reducing reaction the part of tungsten accounts 94% consuming $WCl_6$=2,5 g/s [12], $G_w$ corresponded to the range of 2,35 – 1,5 g/s. The boundary condition of the enphalpy transfer equation was chosen on account of temperature constancy of a channel's wall. For registration of heat scattering by tungsten particles was used the table [8]. In the picture you can see the loss of heat into the wall of the channel of the plasma generator in the presence of the gas-powdered screen with tungsten particles that have the size of 1;0.1;0.01 μm.

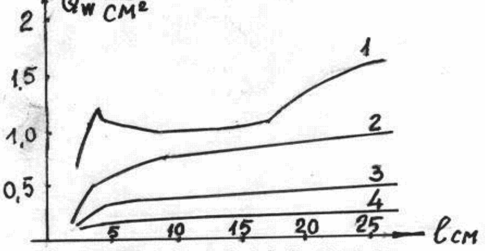

Pic. I=200A,$G_{H2}$=0.1 lg/s, R=0.5 cm.
1 – without a screen, 2 – $r_w$ = 1 μm, 3 – $r_w$ = 0.1 μm,
4 – $r_w$ = 0.01 μm.

Pic. I=200A,$G_{H2}$=0.1 lg/s, R=0.5 cm. 1 – without a screen, 2 – $r_w$ = 1 μm, 3 – $r_w$ = 0.1 μm, 4 – $r_w$ = 0.01 μm.

The introduced method of thermal protection of the walls of high-powered plants and the method of calculation of thermal state prove their effeciency and a possibility of their practical use.

High-powered protection in combination with transpiration cooling gives a possibility to make the heat load on a wall of the high-powered plant chamber two times less.

**Bibliography:**

1. Arinkin S.M. The Method of Protection and Diagnostics of Combustion Chamber's walls.IFG,volume 74, № 6, 2001.
2. Heberlain V., Pfender E. Porous Cooling of Combustion Chamber's Walls.Heat Exchange,№2,1971.
3. Dresvin S.V. and others.Physics and Technics of Low-temperature Plasma. M.Atomizdat,1972.
4. Tom G.K., Shvenk F.K. The Systems Based on Gas-core Nuclear Fuel.RTK,volume 16, № 1,1972.
5. Gas Cooling High-temperature Reactors.M. Atomizdat,1975.
6. Arinkin S.M.,Tretiyak M.S. The Method of Protection of High-powered Plant Wall. № 130724,1992.
7. Arinkin S.M. The Loss of Radiant Energy by Gaseous Flux.M.Sb.<< Heat Exchange - 78>>,Minsk,HMTI,1978.
8. Hewst G. Light Scattering by Small Particles.Moscow,1961.
9. The Research on the Coefficients of Radiation Attenuation and Indicatrix of Gas-powered Medium Diffusion. Report № 1298,HMTI – The New York University,1976.
10. Panasenko L.N. The Influence of Reabsorption on the Characteristics and Thermal State of Arc Plasma. The Fourth International Symposium in Radiation Plasma Dynamics. Moscow,1997.
11. Stepanov K.L., Panasenko L.N. Total Radiation Transfer of Real Spectrum in Problem of Radiation Plasma Dynamics.IFG,volume 72,№6,1999.
12. Suris A.L., Plasmachemical Processes and Systems.M.Chemistry,1989.

S.M.Arinkin, The Academic Scientific Comlex "A.V. Lykov Heat And Mass Transfer Institute" of the National Academy of Sciences of Belarus.

//The Research of Efficiency of Shielding Properties of a Gas-powdered medium, which is Created by Reduction of Low-boiling Refractory Alloys.

This article touches on the following subject: the efficiency of heat protection of the walls of high-powered plants with a temperature of active capacity running into thousand, created by reduction of low-boiling refractory alloys. This method provides high polydispersity and shielding properties of a gas-powdered screen.

# ADSORPTION-CHEMICAL ACTIVITY OF HIGH-DISPERSITY AMORPHOUS BROWN AND BLACK BORON USED IN METAL BORIDE SYNTHESIS

**Zenkov V.S.**
Frantsevich Institute for Problems of Material Science of NASU,
3 Krzizanovsky St, Kiev, 03142, Ukraine, e-mail: uvarova@materifld.kiev. ua

Using high-dispersity nanocrystalline powder materials in powder metallurgy needs additional information on the condition and properties of reactive surface. Initial powder particles may change their physicochemical properties during adsorption- hemisorption processes which take place in the course of production and keeping powders. To avoid undesirable accompanying chemical processes which influence the phase composition and quality of the product, all these factors should be taken into account. Processes in closed systems especially undergo such influence. Gases desorbed from surface can change the composition of the initial medium used. In synthesis. There is also possibility of primary chemical interaction of the adsorbed gases with the highly developed surface of particles acting in the synthesis with poisoning them. The chemical activity of commercial high-dispersity amorphous brown ad black boron powder, contacting with titanium, towards oxidizing gaseous components and the powder ability for adsorption-desorption have been studied in this work. Titanium powder used for production of titanium boron nitride is very sensitive to oxidizing components($O_2$, $H_2O$, $N_2$), which can change physicochemical properties of the initial surface. Under normal conditions boron is rather inert towards these components. From the thermodynamics view-point, these exothermal reactions of the interaction are highly-energetic .On attaining an activation barrier, they are capable for self-development near the boundary between a solid and adsorption layer with local or integral energy transfer to the surface reactive volume. In this case, a change in powder properties, including powder reactivity in solid-phase systems, may occur.

The gravimetric study of desorption processes revealed the presence of adsorbate on commercial powders of amorphous brown boron up to 10 mass % and up to 5.1 mass % on black boron powder. Desorption started at 50-60 °C. Most of the adsorbate moved off before attaining 110 °C. Increasing temperature to 170 C promoted removal of adsorbate remains. With decreasing temperature adsorption practically did not observed up to 90 °C. The adsorption rate increased in the temperature range 60-30 °C with subsequent attenuation of the process due to filling up adsorption layers. Within 24 h, adsorption from dried gaseous mixture (21 mass % O2, 79% N2) achieved 30 % of the initial mass of desorbed adsorbate of brown boron and 40 mass % in case of using black boron.

Also was carried out investigation of the process kinetics aimed at determination of chemical activity of the surface of initial brown and black boron towards oxygen and nitrogen. Oxidation of brown boron started about 450 °C. Black boron surface showed up higher activity towards oxygen in the gaseous mixture and began actively interact with it at 360 °C. Interaction with dried nitrogen also started near 360 °C. The process, however, attenuated when the degree of nitration reached 2%, owing to blockade of particle surface with a boron nitride film.

It is of interest to get some information on mass exchange on both the initial surface and acidified surface of amorphous brown boron ( up to =4.76 and 20%, respectively). The adsorption rate of the dry gaseous mixture on the acidified surface doubled. Despite the mass gain of adsorbed gases, oxidation depth does not much influence the adsorption rate of dry gas. The degree of surface layer filling up increased from 3.61 to 12.75. The adsorption rate from wetted gas increased by an order of magnitude and was equal to $4.21.10^{-4}$ mol/m2h (as compared to $4.86.10^{-5}$ mol/m2h). At $P_{H20}$=0.025 adsorbent from unoxidized surface gained the initial absorption mass, and the process practically ceased within 0.5 h.

The adsorption-chemical properties of boron substantially depend on product purity and degree of its amorphism.or crystallization. The intensities of reactions of boron with $O_2$ $H_2O$ and $N_2$ were shown correspond to termodinamic parameters: both the value LnK of the reactions and interaction rate decreases from oxygen to nitrogen. In accordance with these data, boron interacts rather with oxygen from gaseous mixture than with nitrogen: traces of BN are not detected. At temperatures near 400 °C the interaction with both oxygen and nitrogen attenuates owing to blockade of reactive surface with oxidized or nitrated film. Above 400 °C the rate of interaction between oxygen and active surface of black boron increases by an order of magnitude from $6.04.\cdot10^{-4}$ mol/m$^2$h to $1.22.10^{-3}$ mol/m$^2$h. Self-accelaration of the reaction is observed at the expense of its exothermal character and accumulation of internal energy of the reaction system. Interaction of amorphous boron with oxygen in the gaseous mixture begins at 430 °C and achieves the self-development stage at about 500 °C. The lower chemical activity of amorphous boron surface should be attributed to surface passivation while producing and keeping. Interaction of black boron with dried nitrogen is less active than that with oxygen and achieves diffusion region at =8% and T>500 °C.

Surface oxidation up to =4.76% leads to a sharp increase in adsorption characteristics in wetted gaseous medium. Adsorption of moisture begins at 170 °C. At the stage of filling up the first adsorption layer, at T<110 °C, a stepwise character of the process is observed, however, at T<90 °C the rate of water molecule adsorption increases as a result of polyadsorption and possible formation of chemical bonds with boron oxide surface. Within 24 h the process stabilizes at $\theta=28,9$ The increase in the degree of oxidation does not change the adsorption mechanism, but $\theta \to \infty$. The adsorption processes are limited by the oxide phase. The adsorption rate from wetted gaseous medium with $P_{H2O}=0.025$ is five times that from dry gas ($5.4.\cdot 10^{-4}$ mol/m$^2$h). The process starts at the temperature at which dry gas is not adsorbed. It follows therefrom that mainly water molecules fill surface.

Based on the results obtained, different absorption-chemical activities of commercial amorphous brown and black boron were established. In addition to solid impurities, initial boron may have on the surface absorbed gaseous components up to 10 mass %, which can change physicochemical parameters of the system and influence the phase composition and quality of products. Therefore necessity of taking into account of absorption-chemical activity of high-dispersity powders while using and keeping them is evident.

# NANO-STRUCTURED TiN BASED PECVD COATINGS

**Ivashchenko L.A., Porada O.K., Ivashchenko V.I., Rusakov G.V., Dub S.N., Timofeyeva I.I.**
Frantsevich Institute for Problems of Material Science, NAN of Ukraine,
Krzhyzhanovsky str. 3, Kiev-142, 03680, Ukraine, e-mail: ivash@materials.kiev.ua

Titanium nitride is widely used for surface hardening of tools due to high hardness, good corrosion stability and low friction coefficient [1]. This material is basic in producing the mono-layer, multi-layer and nano-composite coatings [2,3]. Besides, in the majority of cases, TiN mono-layer coatings exhibit the best tribological properties [1]. This work is devoted to the further development of TiN based wear resistant coatings. We have obtained and investigated nano-crystalline titanium nitride (nc-TiN) based coatings. For this purpose, a remote plasma – enhanced – chemical – vapor - deposition (RPECVD) 40.68 MHz technique has been used [4]. A new in our approach as applied to TiN coatings is the use of the two-generator scheme of RPECVD: an additional bias at substrates was provided by a r.f. generator of 5.27 MHz. To identify the obtained structures, X-ray investigations were carried out by using a difractometer DRON-2 (USSR). Chemical composition was determined with an Auger spectrometer JAMP-10S. The mechanical properties of the films (nanohardness, elastic module) were investigated with the help of a tester Nano Indenter-II, MTS Systems Corporation, Oak Ridge, TN, USA at loadings 50 mN and 120 mN using the Berkovich indenter. Coating adhesion was estimated by using several approaches: during nanoindentation, from the ball-on-plane tests in the presence of diamond paste and from the scratch tests carried out at constantly increased loading on the Vickers indenter that moves on the film surface with constant speed. Film thicknesses were determined from the ball-on-plane tests. The coatings were deposited on different substrates: silicon crystalline wafers, WC-Co (BK-8) alloys, Ti-W-Co-C (T15K6) alloys, steel (40X13) and high speed steel (P6M5D) from tetrachloride titanium $TiCl_4$, $N_2$, $H_2$ as precursors. So, the properties of the coatings were controlled by means of varying deposition parameters: substrate temperature, bias voltage, gas pressure and gas flow rate. The gas pressure of about 0.9-1.0 Torr and the substrate temperature of about 550-600 $^0$C were kept constant during deposition. The substrate bias was varied around –150 V. The depositions during 30-40 min provided the film thickness in the range of 0.3-0.9 μm depending on the deposition parameters.

According to the Auger data, the coatings contain on average 40-45 at% of Ti, 40-45 at% of N, up to 10 at% of C, 5-15 at% of O and up to 0.8 at% of Cl. Oxygen and carbon were detected in the films and are due to unwanted oxygen and carbon present in the chamber during deposition. Their content was controlled by means of changing the evacuation rate and by varying the deposition parameters.

The results of the X-ray investigations show that the coatings consist of TiN islets that are strong grain-oriented in the (h00) direction. Two main reflection lines from the (200) and (400) planes are observed. Reflection angles of $\theta$ =21.4° and 46.75° correspond to stoichiometric titanium nitride. For some films, the weak line associated with TiNC was detected. The grain texture in such films is less developed than in TiN coatings. The interplaner distances in TiNC coatings are larger as compared with those in TiN films.

The X-ray pattern that is typical for TiN coatings is shown in Fig. 1. There are two main peaks. The first broad peak is associated with a halo at $2\theta \approx 19\div20^\circ$, and the second peak around 42.8˚ is caused by the TiN (200) reflection. Taking into account these results and the data of the calculations of the X-ray patterns for a series of the samples with different compositions, we deduce that the obtained coatings are formed from the TiN or TiCN grains. The size of such grains, evaluated from the integral widths of all Bragg reflections using the Scherrer formula, is lower than 15 nm. The oxygen mainly is introduced into grain boundaries forming a strongly disordered Ti-O-C tissue. It is the disordered tissue that gives rise to the broaden peak shown in Fig. 1. The TiN nano-scaled grains are responsible for the second peak. Thus, one can conclude that, at the chosen deposition parameters, we succeeded in obtaining the TiN based films with the nano-crystalline structure. The application of the –150 V bias in RPECVD enabled us to prepare nc-TiN coatings that have the smaller grain sizes (up to 15 nm) as compared with those of the TiN films prepared by using other PECVD procedures (above 30 nm) [5].

The nanoindantation of the coatings was carried out at loadings of 5 mN and 120 mN. The results of nanoindentation at the 5 mN load are given in Fig. 2. The two regimes of the nanoindentation give the indentation depths of 0.09-0.1 μm and 0.58-1 μm, respectively. So, in the first case we investigate the coatings, while the second regime of the nanoindentation gives mostly the information about the substrates. The nanohardness (H) and elastic modulus (E) of the coated substrates, extracted from the loading-unloading curves (Fig. 2) [6], are presented in Fig. 3. We note that the nanohardness of all the covered substrates is higher than the one of the clean substrates. The highest hardening is observed for the steel materials, silicon wafer and BK8 hard alloy. The coated substrate of T15K6 hard alloy exhibits nanohardess that higher one of the clean substrate on average by 6%. (The best coated samples show H ~35 GPa). This prompts us to deduce that the nanohardness of the TiN coating is close to the H value of the T15K6 alloy, i.e., it amounts about 25 GPa. For the Young's modulus, the similar picture is observed, although this value is more sensitive to a substrate material. The coated T15K6 substrate turned out to have lower the Young's modulus than the uncovered substrate. Based on this finding and allowing for the fact that the Young's modules of the covered and uncovered BK8 samples are close, we deduce that the E value of the TiN coating does not exceed 500 GPa. Here, we have to stress that the values of H ~25 GPa and E ~500 GPa are close to the limit values of 26 GPa and 600 GPa for TiN coatings, respectively [1].

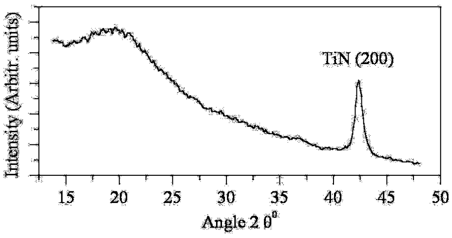

Fig. 1. X-ray pattern of the nc-TiN coating on a silicon substrate.

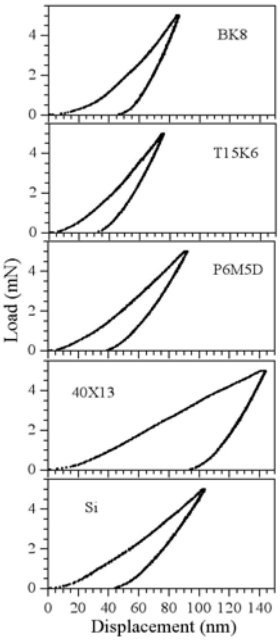

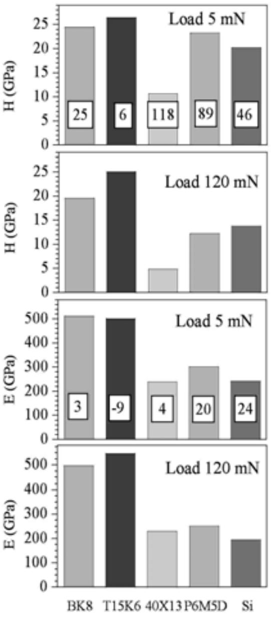

Fig. 2. Results of the nanoindentation tests of TiN films deposited on various substrates.

Fig. 3. Nanohardness H and elastic modulus E of TiN coatings on various substrates. Numerals denote the H(E)[5 mN]/H(E)[120 mN] ratios in %.

The coatings exhibit the good adhesion to various substrates, which was determined from the nanoindentations, ball-on plane tests and scratch tests. Particularly, the films were not destroyed under the nanoindentation at the 120 mN loading. The ball-on plane tests show that the substrate-coating zone is homogenous and does not contain micro-voids. It follows from the results of the scratch tests that the adhesion of the films to the substrates of the steel materials and silicon slightly decreases with increasing film thickness.

The abrasive wear-resistance of the TiN coatings on silicon wafers evaluated from the ball-on-plane tests was found to be several times higher than that of the clean substrates.

In summary we note that the application of the RPECVD apparatus enabled us to obtained the nano-structured dense TiN based coatings that exhibit the high hardness and Young's modulus, good adhesion and high wear resistance. The good mechanical properties of nc-TiN based coatings are supposed to be due to the comparatively small grain sizes and to the stoichiometric composition of the TiN or TiNC nano-scaled grains.

This work was supported in part by STCU Contracts No. 1590-C and 1591.

References

[1] A. Matthews, A. Leyland, Key Engineer. Mater. 206-213 (2002) 459-463.

[2] D.N. Allsopp and I.M. Hutchings, Wear, 251 (2001) 1308-1314.

[3] S. Veprek, J. Vac. Sci. Technol., A 17(5) (1999) 2401-2420.

[4] O.K. Porada, V.I. Ivashchenko, L.A. Ivashchenko, G.V. Rusakov, S.N. Dub, A.I. Stegnij Surf. Coat. Tech., 181-182C (2004) 121-125.

[5] O.R. Shojaei, A. Karimi, Thin Solid Films, 332 (1998) 202-208.

[6] W.C. Oliver, G.M. Pharr, J. Mater. Res. 7 (1992) 1564-1583.

# DEPOSITION OF NICKEL ON HIGH-POROUS MATERIAL FROM PROCESS SOLUTION OF JSC «URALELEKTROMED»

**Antsiferov V. N., Zamaletdinov I. I., Egorova O. I.**
Center of Powder Material Science of Perm State Technical University, Perm, Russia
6, Professora Pozdeeva Str., Perm, 614013, Russia, E-mail: patent@pm.pstu.ac.ru.

Under investigation there was possibility of electrolytic nickel deposition on high-porous material (HPM) from JSC "Uralelektromed" process solution of the following composition (g/l): 120—130 $Ni^{2+}$, 3—4 $NH_4^+$, 0,95—1,10 $Mg^{2+}$, 0,68 $Na^+$, 0,6—0,7 $Ca^{2+}$, 0,24 $K^+$, ≤0,1 $Zn^{2+}$, ≤0,02 $Cu^{2+}$, ≤$Fe^{3+}$, 2—5 of free $H_2SO_4$, pH 1,7. Deposition of high-quality sediment at initial value of pH=1,7 solution is impossible. Current efficiency (CE) at this pH amounted to 50% only. CE increases from pH value nearly linearly and reaches maximum value of 95—98% at pH=5,5—6,0 (Fig. 1).

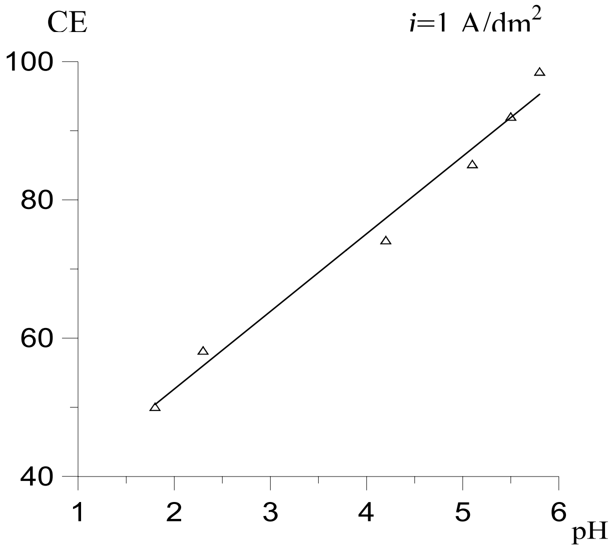

Figure 1. Dependence of Current Efficiency on Solution pH.

Within the range of change of nickel concentration from 120—130 to 95 g/l, CE decreases linearly. Change of initial pH of the solution should be done not by means of adding dry NaOH, but its solution with titre of 0,3 g/ml with thorough agitation during 30—40 minutes for dissolution of greenish amorphous residue of nickel hydroxide. During the electrolysis, pH value decreases very fast, thus it is necessary to adjust it every 3 or 4 hours of electrolysis.

Dependence of CE on current density is extremal: increase of current density from 0,75 to 1.0 A/dm² results in increase of CE from 80 to 95—98 %; further increase of current density to 2 and 3 A/dm² promotes decrease of CE to 85 and 62 % correspondingly (Fig. 2).

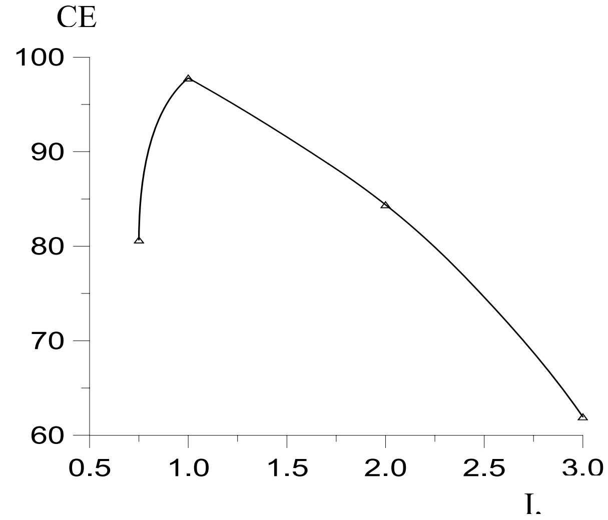

Figure 2. Dependence of Current Efficiency on Current Density.

Dissipating property of electrolyte was studied using composite cathode consisting of 5 pressed together HPM plates (5 mm thick each). Deposit mass percentage distribution decreases significantly from 34—41 to 10—13% at the first outer plates, and in the middle it changes insignificantly from 8—13% depending on current density. Dissipating property of electrolyte is the highest at current density of 0,8 and 1,0 A/dm².

# PROBLEMS OF FUSION ARC WELDING OF PARTICULATE REINFORCED ALUMINIUM MATRIX COMPOSITES

**Chernyshov G., Chernyshova T.**$^{(1)}$,
Bauman Moscow State Technical University, Moscow, Russia
2nd Baumanskaya, 5, Moscow 107005, Russia, e-mail: aleshin@bmstu.ru
(1)Baikov Institute of Metallurgy and Materials Science of RAS, Moscow, Russia
Leninsky prospect, 49, Moscow, 119991, Russia, e-mail: chern@ultra.imet.ac.ru

Metal matrix composites (MMCs) based on aluminium alloys reinforced with discrete refractory fillers are promising materials for operation in brakes, sliding bearings, components of cylinder-piston systems and other sections of machines. However, the extensive application of MMCs in industry depends on possibilities of welding them together or with material not containing fillers. Principal problems at welding of MMCs consist in obtaining flawless permanent joints with satisfactory shaping of welds, without notches and pores, preservation in a zone of joints an initial composition of MMCs, volume fraction and uniform distribution of reinforcing fillers. Preference should be given to the solid-phase methods of joining (diffusion bonding, friction welding). But there are an examples of successfully fusion joining of the particulate reinforced MMCs. Main goal into these processes is limitation of chemical reactions at the particle/matrix interface which result in the formation of brittle phases. In the present work the fusion arc welding of cast aluminium matrix MMCs containing diverse discrete fillers, such as SiC, $Al_2O_3$, $Si_3N_4$, $B_4C$, C, intermetallic compounds $Al_3Ti$ or combination of these fillers are investigated. Samples of MMCs arc welded by a tungsten electrode in argon atmosphere. From weld joints are produced macro- and microsections for microstructural observations and x-ray analysis of the reaction products. The uniformity of particle distribution in matrix is evaluated on Dirichlet tessellation-based method. Hardness and strength by three point bending tests are determined. It is established, that the equiaxed crystals of intermetallic compounds transform into needles as result of dissolution in the overheated weld pool and solidification in the conditions of quench cooling. The ceramic and graphite particles generally do not melt or dissolve in the pool, however near to a line of fusion and on an axes close to weld surface the zones free from particles may be observed. The formation of the first of them is associated with the start of the solidification of the weld pool when the cells and dendrites of α-Al growing mainly in normal direction to the fusion line, push the particle to the central part of the pool. Second zone free from particles may form in the final stage of solidification as a result of adsorption of the gases dissolved in the pool on the particle surface and their flotation. The size of these zones depend on welding conditions and composition of the MMCs. At minimum power density of welding and good wetting of the particles by the Al-melt it is possible to receive more homogeneous macrostructure of a weld, best particle distribution in matrix, major dispersity of matrix structure. Increase of the strength and hardness of a weld in comparison with both the strength and hardness of initial MMCs can be also stipulated by a modification of the interfacial bonding between the particles and the matrix.

# THE ATMOSPHERIC CORROSION INHIBITION OF METALS BY IMPLANTATION OF ALUMINIUM

**Belous V.A., Nosov G.I.**
National Science Center “Kharkov Institute of Physics and Technology”, Kharkov, Ukraine
1, Akademicheskaya St., Kharkov, 61108, Ukraine, E-mail: belous@kipt.kharkov.ua

Recently for protection against corrosion, erosive and mechanical wear the development receives a method of creation in a surface of materials modified nanolayers with the help of ion irradiation [1, 2]. In the given work the results of research of corrosion firmness Fe and U in a humid atmosphere after implantation of aluminium are set out. Iron and uranium are chosen as model materials owing to behavior similarity of oxide films. The oxide layer on iron, uranium and their some alloys in conditions of an environmental atmosphere, as is known, does not create an acceptable protective barrier, that is caused, basically, its porosity, unsoundness of structure, and also tendency to self-flaking from a surface.

At a choice of a material entered as an impurity into a surface Fe and U, such circumstance was taken into account, that the corrosion of metals in a humid atmosphere has electrochemical character. For inhibition of corrosion speed at ion implantation of metals it is necessary to create on an irradiated surface of a conditions promoting to reduction of speeds of cathode or anode reactions or else to creation of passivating films of sparingly soluble secondary products with high protective properties on a surface [3]. From the analysis of the literary data follows, that at a choice of a alloying impurity material for atmospheric corrosion inhibition of an alloy it is necessary to be guided by the following requirements [4]:

– the allowing component should have greater affinity with oxygen in comparison with the basic metal;
– the alloying element should form oxide with high electrical resistance making difficulties for movement of ions and electrons in him;
– at the given degree alloyage alloying and basic components should create a solid solution ensuring an opportunity of formation of a continuous and uniform film of alloying component oxide on all surface of an alloy.

It is necessary also to take into account, that for reception of the maximal concentration of an entered impurity it is necessary to choose a material for introduction at implantation, having low sputtering coefficient. It, first of all, easy metals (aluminum, titanium etc.). Taking into account the stated requirements, as a material entered in Fe and U at ion implantation for inhibition of corrosion in a humid atmosphere, the aluminium was chosen.

The irradiation by ions of aluminium carried out on installation with an electroarc source of separated metal plasma [5]. Acceleration and extraction of ions of aluminium from a plasma source was carried out by application of negative potential to specimens.

The irradiation of specimens spent at potential -10 kV, operation of clearing of a surface by ions $Ar^+$ with energy ≤ 200 eV was preceded this. Temperature of irradiated specimens did not exceed 200 °C. Pumping out the chamber was realized by the sorption titanium pump. Specimens from iron of purity 99,95 % and natural uranium of purity 99,5 % were used in experiments.

The corrosion tests carried out in vapor of distilled water at temperature +60 °C and humidity of an atmosphere 98 %. The control carried out by a weight method by periodic comparison of weight of the irradiated specimens with weight of the not irradiated specimens - witnesses. The cycle of tests lasted 3500 hours.

Besides uranium specimens sustained corrosion tests, were exposed to influence of thermocyclic loading at change of temperature from -20°C up to +60 °C.

The method of X-ray photoelectronic spectroscopy (XPES) in a combination to level-by-level moving of a material at sputtering by xenon ions was applied for definition of element composition of a surface and distribution of implanted aluminium in a uranium surface at implantation.

Kinetic curves of the accelerated corrosion tests specimens from iron and uranium irradiated by aluminium ions and also not irradiated specimens - witnesses are given on fig. 1.

From figure follows, that implantation of aluminium ions results in increase in some times corrosion firmness of iron and uranium. As it is visible from figure, the growth of an ion irradiation doze from $10^{17}$ up to $10^{18}$ ion/cm$^2$ conducts to increase of corrosion firmness of uranium. The effect of increase of corrosion firmness implanted metals was kept during all term of corrosion tests (3500 hours).

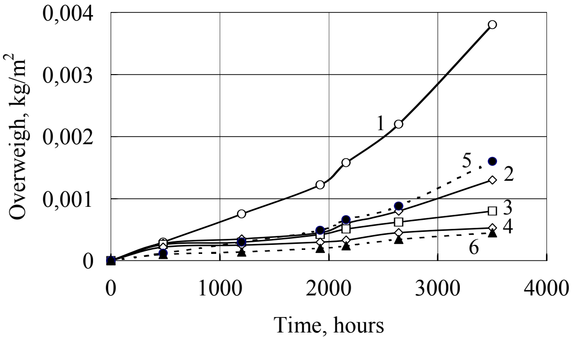

Fig. 1. Dependence of specimens overweigh from uranium (1, 2, 3, 4) and iron (5, 6) from duration of corrosion tests. 1,5 - not irradiated specimens; 2,6 - doze of ion irradiation $10^{17}$ ion/cm$^2$; 3 - $5\cdot10^{17}$ ion/cm$^2$; 4 - $10^{18}$ ion/cm$^2$.

Specimens from uranium exposed to influence of thermocyclic loading, have sustained more than 30 thermocycles, while the not irradiated samples have sustained only some thermocycles and were removed from tests because of flaking-of oxide films and appearance of corrosion traces as cracks and blisters.

The analysis of a chemical state of elements with the help of the XPES method has shown, that in starting state both aluminium and uranium were in oxidated state. In a fig. 2 the concentration of implanted aluminium into the surface of the uranium in dependence from depth of a layer is presented.

The maximal concentration of aluminum in surface of uranium at a doze of an ion irradiation $10^{17}$ ion/cm$^2$ reaches 12% at. The maximal depth of layer, on which the aluminum is found out, makes 45…50 nm.

It is necessary to note, that the aluminum in comparison with Fe and U has more negative standard equilibrium electrode potential and will provide catode protection of irradiated metals. At such way of protection thickness and the uniformity of a implanted layer will not have the large significance, that is very important, as the depth of the modified layers of a surface does not exceed 50 nm.

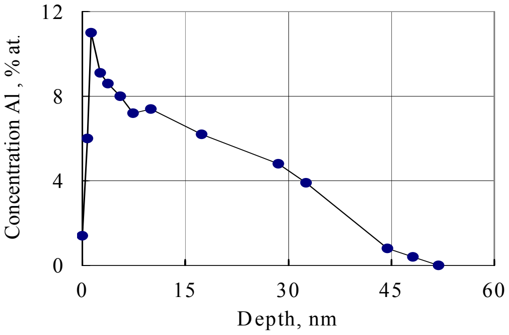

Fig. 2. The dependence of concentration Al in implanted uranium from depth of a layer at a doze of an ion irradiation $10^{17}$ ion/cm$^2$.

Positive quality of aluminium is as well that circumstance, that on it at interaction with corrosion environment the stable, continuous film of aluminum oxide promoting formation of an inert material and inhibition of corrosion is easily formed.

## LITERATURE

1. Калин Б.А. Радиационно-пучковые технологии обработки конструкционных материалов // ФизХОМ. — 2001. — №5. — С.5—16.
2. Белоус В.А. Ионно-плазменная обработка материалов в высокоплотных потоках плазмы // Нові матеріали в металургії та машинобудуванні. — Запоріжжя. — 2001. — №1.- С.80—84.
3. Эшворт В., Проктер Р.П., Грант У.А. Ионная имплантация и водная коррозия. В кн. Ионная имплантация. Под ред. Дж. К. Хирвонена. Пер. с англ. — М.: Металлургия, 1985. — С.139—202.
4. Дернели Г. Термическое окисление. В кн. Ионная имплантация. Под ред. Дж. К. Хирвонена. Пер. с англ.- М.: Металлургия, 1985. — С.139—202.
5. Аксенов И.И., Белоус В.А., Падалка В.Г., Хороших В.М. Устройство для очистки плазмы вакуумной дуги от макрочастиц // ПТЭ.- 1978. — №5. — С.236—237.

# EFFECTS ARISING FROM HIGH-SPEED PARTICLES INTERACTION WITH A TARGET

**UsherenkoS.M., SitaloV.G.(1), GubenkoS.I.(2), BunchukY.P.(1)**
Institute of Professional Development, Minsk, Belarus, impuls@BN.BY
(1)Yuzhnoye State Design Office, Dniepropetrovsk, Ukraine, kbu@public.ua.net
(2)National Metallurgical Academy of Ukraine, Dniepropetrovsk, Ukraine, sgubenko@email.dp.ua

A phenomenon of super deep penetration of a high-energy stream composed of solid particles into a metal target is used for obtaining new composite materials used for manufacturing the tools.

Metallographic examinations of this phenomenon allowed to establish laws of hardening the metals and alloys with a stream of high-speed particles. Particles penetration at high speed causes piercing a target bound with overcoming the forces of intermolecular strength of a metal (Fig. 1). The particles interact with walls of a channel, which is being created, that proves to be true by a local X-ray spectral analysis of samples. As particles travel in a metal matrix, they excite ahead of themselves the plastic waves and move area of high pressure. The waves generated have as though «short-range and long-range» effect. In the areas adjacent to trajectories of particles motion atoms drift from crystalline lattice points of a target and the energy-permitted strongly excited states of a material (so-called atom-vacant state) are created. Distinctive feature of this state lies in the extremely high mobility of atoms, what the anomalous high speed of mass transfer testifies to. The shock waves, moving ahead of particles, transform more and more new volumes of a metal target into disordered state.

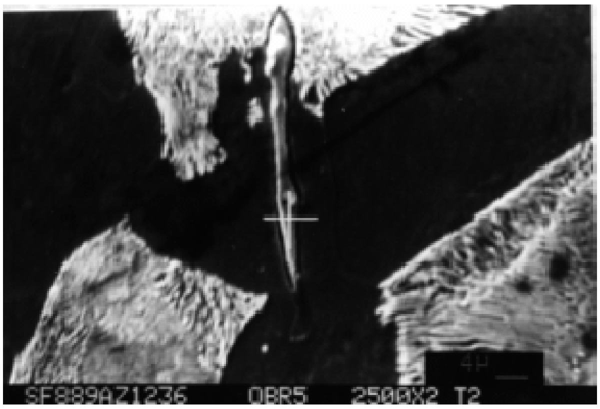

Fig. 1. A particle in a metal target

The metal behind particles flows around them and fills in channels that results in channels collapse. This effect is stimulated also by an elastoplastic relaxation in metal and increase of its volume at a disordering. Thus, particles travel in an extremely movable medium with disordered atomic structure, which renders very small resistance to their motion, whereas the channels collapsed behind the particles as though push them. Disordered state of a metal target near to walls of channels and particles is recorded after removal of a loading owing to small time of process ($10^{-7}$-$10^{-8}$ s) [1], and also as a result of good heat release from these areas into volume of a metal target.

The shock waves under their propagation in a target cause a vast plastic deformation along the whole trajectory of particles motion and in places of their braking. Plastic shears and turns occur not in a homogeneous stress field, and at their concentrations, which continuously arise and relax thus creating strongly excited states in a bulk of a metal target [2]. At explosive action the plastic deformation has the features consisting in sharp increase of number of dislocation sources and sliding systems, increase of dislocations motion velocity, developed non-conservative motion of dislocations with steps, giving to magnification of point defects density [3]. Dislocations interaction at high speed causes dynamic surges of stress.

Deformation is gradually reduced in proportion as moving off channels and particles. As a result the structures relevant to a wide range of rates of deformation (Figs. 2a, b) are formed along channels and near to particles.

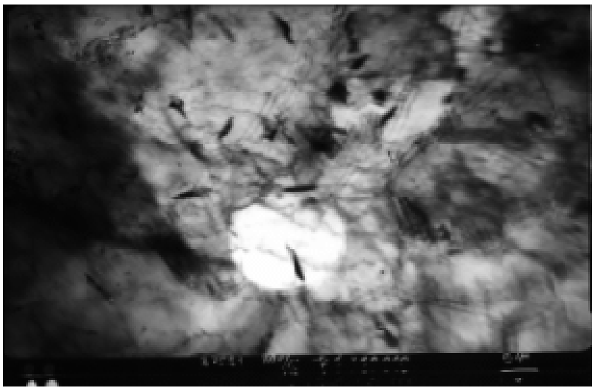

a

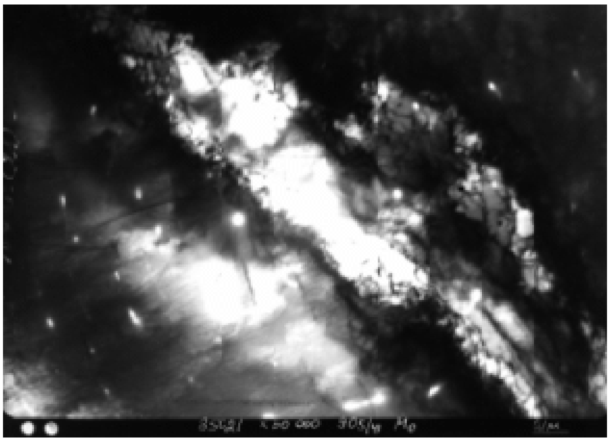

b

Fig. 2. Dislocation substructure of treated materials; magnification x20,000

Transition from one deformation zone to another zone is as though phase transition from one dislocation phase (structure) to another. Directly near the channels walls there is a zone with disordered (amorphous) state, then strongly fragmented dislocation structure follows, then cellular structure, then zone with intersecting dislocations and, at last, initial structure with disordered distribution of dislocations. The plastic deformation is of local character and high-speed.

All the above described processes acts simultaneously, their superimposition calls integrated complex processes of metal material structure reorganization at different structural levels (atomic, mesoscopic, fragmentary, microstructural). Whereas the last three levels has been studied by us quite thoroughly, new approaches are required for an atomic level investigation. With the help of X-ray spectral analysis abnormal local increase of elements concentration was detected, average quantity of which in a material is much less, or birth of certain quantity of any element missing in an initial state of a material was found. It is natural, that even small quantity of any element is present in an initial state of (sometimes at a level of traces), its atoms travel to particular sites within so small period of time of explosive action is impossible. Occurrence of a new element in an alloy directly testifies to running the nuclear reactions that was confirmed by a film exposure contacted with a sample at the moment of treatment.

Phenomena under exploration are of interest for flying vehicles encountering with streams of fine high-speed particles in outer space, parameters of which are close to parameters obtained in our experiments.

Experiments were conducted in which changes of electrical parameters of electronic devices (microcircuits of high-speed CMOS) were recorded; the devices were placed behind a steel heavy-wall barrier (200 mm thick), which the stream of high-speed explosion energy -generated SiC particles (particles velocity - 1 km/s, stream density - 1 g/cm$^3$, sizes of particles 10-40 micron) impacted on [4]. It was found that the extent of the electronic devices damage was equal to 80 %, i.e. practically they failed. During testing microcircuit were placed inside cermet and plastic containers behind a barrier in such a manner to prevent from impact with container walls [4, 5]. For the option where cermet container was used the upper and lower lids were made of metal. Microcircuits were arranged inside containers so either the microchip faced a stream of high-speed particles or, on the contrary, with its back side to the stream. Stream of high-speed particles was generated by compression of mixture composed of nickel, aluminum and copper particles with an explosion according to a procedure described in work [5]; the mixture was placed inside aluminium shaped lens.

After treatment by a particles stream microcircuits were inspected visually and by X-rays to check-up their integrity, lack of mechanical damages and separation of pinouts (legs). Then microchips were opened and explored with the help of an optical microscope and scanning electronic microscope “Hitachi” with an X-ray microanalyzer.

Single and multiple intrusions (Fig. 3) identified as particles from a high-speed stream were detected in extracted microchips.

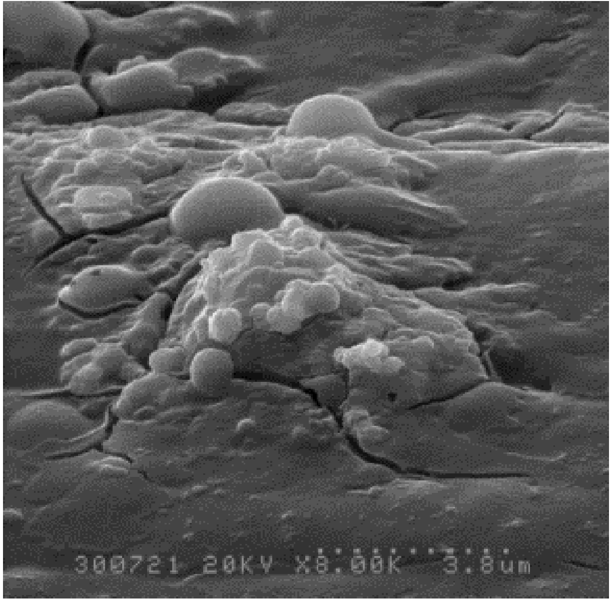

Fig. 3. Particles in a microcrystal

Numerous damages of electronic microcircuits and pinouts (legs) in form of flaws (Fig. 4) were found.

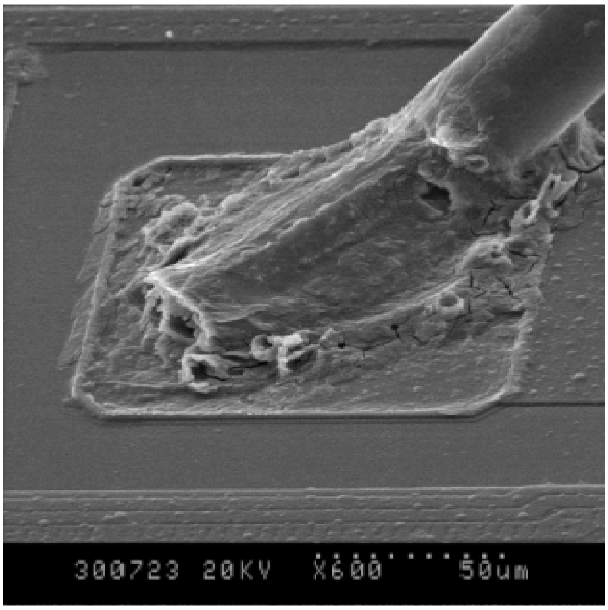

Fig. 4. Defective pinout (leg) of a microcircuit

In case particles impact according to the first option the upper lid was pierced and microchips with elements on their surfaces were exposed to mechanical effect. In the second variant piercing of the lower lid of a container and microcircuit substrate was less effective, and microchips were less damaged. It was confirmed by results of testing of microcircuits parameters. Apparently, energy of traveling particles was insufficient for piercing more thick lower lid (as contrasted to the upper lid) and substrate. It is necessary to take into account not only effect of lid thickness but also it strength properties.

So, it was established that the stream of high-speed particles generated by energy of explosion, pierce thick metal barrier (200 mm) and interacts with an electronic microcircuit body resulting in its piercing and microchip damage. Character of this interaction depends on type of particles and arrangement of electronic microcircuits in relation to a stream. The detected phenomenon has prospects for development and needs further consideration.

References

1. Andilevko S.K., Roman O.V., Romanov G.S., Usherenko S.M. Super deep penetration of powder particles into a barrier // Powder metallurgy. Vol.9. Minsk, Vysshaya shkola., 1985, pp. 3—13

2. Panin V.E., Yegorushkin V.E., Khon Y.A., Elsukova T.N. Atom - vacant state in crystals // Proceedings of IHEs, Physics, 1982, №12, pp. 5—29

3. Epstein G.N. Structure of explosion-deformed metals.- M.: Metallurgy, 1980.- p. 256

4. Usherenko S.M., Romanov G.S., Dybov O.A., Belous A.I., Shwedov S.V. Effect of superdeep penetration, barrier piercing of and its impact on operation of electronic devices // IFZh, 2002, Vol.75, №6. pp. 7—9

5. Dybov O.A., Romanov G.S., Usherenko S.M. About penetration to large depth of particles material from high-speed jet under collision with steel barrier // IFZh, 2003, vol.76, №5. pp. 8—9.

# OPTIMIZATION OF THE PROCESS TO PRODUCE HEATRESISTANT AND WAREPROOF OXIDE AND CARBIDE/CARBON DISPERSION STRENGTHENED MATERIALS OF DISCOM TRADE MARK BASED ON COPPER POWDER

**Shalunov E.P.**
Innovation Scientific & Technological Center DISCOM Co., Ltd, Cheboksary, Russia
8, Afanasyev St., Cheboksary, 428018 Russia, e-mail: discom@inbox.ru

In recent years Oxide and Carbide Dispersion Strengthened Copper (OCDS-Copper) bearing a DISCOM® trade mark, produced by means of mechanical alloying technology [1], has proved to be a highly-effective substitute for generally used copper alloys operating under high loads especially at high temperature, and even under extreme conditions in numerous technological fields [2, 3, 4, 5] (welding apparatus, propulsion engineering, current-collection device of electric trains, electric apparatus contacts etc.) both in Russia and abroad.

However, the unwillingness of the consumers to pay for the products made of these materials (and equally of many other new and promising materials at that) prevents them from wide application and distribution at a price taking into account an excess of life time of the products produced from more effective materials as compared with the life time of the products produced from generally used materials. In this connection the most radical measure to promote OCDS-Copper of DISCOM® trade mark onto the market has been unfortunately and is likely to be all possible reduction of costs when producing these materials.

Reduction of costs can be carried out in two directions that can coexist both separately and in interaction. As the first and the main direction there has been chosen the optimization of technological production process of these materials.

The basis of this direction, apart from the introduction of all possible necessary and sufficient measures to reduce the percentage of the production defects and amount of technological wastes [6], is still made up by the decrease in the number of technological process operations aiming at the production of the accomplished semi-finished products (rods, tubes, stripes etc.).

The research and experimental work held in this direction at pilot and industrial production of OCDS-Copper of DISCOM® trade mark made it possible to substantially reduce the number of technological process operations without deterioration of their physical and mechanical properties. In particular, for most types of OCDS-Copper of DISCOM® trade mark me managed to do without remilling of the sintered stuff made of reduced granulated material, cold compacting of the granulates into the briquette, heating of the briquette, its additional hot compacting up to the press-blank of the relative density equal to 95…98% and turning of this blank to remove the defective layers. By means of specially developed technological capsules filled with carbonizer, the granulated material obtained as a result of mechanical alloying, during its thermal processing in these capsules is not only reduced but also sintered having shape and size of the future press-blank.

As a rule, relative density of such a blank is equal to 65…70%. That is why its further heating before hot extrusion to get a semi-finished product is also conducted in the capsule with carbonizer placed either into an open gas furnace or an electric resistance furnace.

Before hot extrusion a heated capsule with the press-blank inside is moved to the extrusion zone, the blank is evacuated from it directly into hydraulic press container. If the hydraulic press has special facilities of High Frequency Current to heat blanks, then in this case the heating of the porous blank is carried out without any capsule directly in the inductor where shielding gas is applied. As the experiments showed the above mentioned ways to heat porous blanks made of OCDS-Copper prevent them from oxidation during the heating before hot extrusion.

The availability of porosity with such blanks enables the producer to considerably reduce the required force of hot extrusion and loads to extrusion toolage, to increase the rate of the material draw at hot extrusion by 30…60% and thereby to apply the standard set of extrusion toolage and not to make a new one of a smaller diameter.

Applying definite ratios of hot extrusion pressure and the draw rate it is possible to get a semi-finished product made by means of hot extrusion (e.g. a rod) having no porous structure in the end. But for a number of application cases (e.g. for further production of electrodes from rod by means of cold forming) rod are specially produces with residual porosity up to 3…5%. Firstly, it facilitates cold forming of electrodes, secondly, during the forming the electrode material is additionally consolidated and acquires nonporous structure.

But for those types of OCDS-Copper of DISCOM® trade mark which are supposed to have a higher conductivity and the least content of any gases (e.g. for electric apparatus contacts, a vacuum arc chute, electronics and cable engineering), sintered press-blanks are produced having higher relative density- up to 90…95%. To achieve it degassing of the granulated material placed in the capsule (container) is held, and the process of its gradual compacting is overlaid on the process of the reduction and simultaneous sintering of the granulated material.

The second direction of the cost reduction of accomplished semi-finished products made of OCDS-Copper of DISCOM® trade mark is of a more organizational than technical character and reduction of costs is achieved due to the production of these semi-finished products of maximal possible length and sometimes they are even coiled. To produce them powerful horizontal hydraulic presses are required of drawing force not less than 3.000 to. Such powerful hydraulic presses can be found mainly at the plants where non-ferrous metals are processed.

However, at such plants producing hot extruded semi-finished products from ingots, as a rule there is no equipment to make press-blanks (e.g. cold compacted briquettes) directly from granulated OCDS-Copper. So, to use the potential of powerful hydraulic presses it is necessary to supply there either hot extruded and later turned granulated briquettes or above mentioned sintered press-blanks. In this case non-ferrous metal processing plants fulfill only functions of hot extrusion of semi-finished products, their straitening, smooth finishing, for example by means of calibration by drawing.

Realization of these two above mentioned directions provides the cost reduction when producing OCDS-Copper of DISCOM® trade mark by 20…40% depending on the type of OCDS-Copper and dimention-type of the accomplished semi-finished products made of it.

As it is shown by the work held at a number of domestic and foreign plants processing non-ferrous metals, the best result of the cost reduction is achieved in case when both directions are applied not separately but combined.

The information mentioned above let us give an account of the production of the accomplished semi-finished products made of OCDS-Copper of DISCOM® trade mark at the least possible cost. The technical side of the matter does not only look real but is also approved in many cases. However, to get the stable output of the products made of these materials for the market, and what is more important, using the facilities of non-ferrous metal processing plants, it is necessary to unite business with these plants or to establish a new specialized plant to produce OCDS-Copper of DISCOM® trade mark.

## References

1. Патент РФ 2116370. Способ получения дисперсно-упрочненных материалов на основе меди / Е.П. Шалунов. Заявл. 27.03.1997. Опубл. 10.08.1998. – 24 с.
2. Шалунов Е.П. Высокоресурсный сварочный инструмент из дисперсно-упрочненных композиционных материалов на основе порошковой меди. – Чебоксары: ИНТЦ «ДИСКОМ», 2003. – 257 с.
3. Shalunov E.P., Dovydenkov V.A., Simonov V.S. Anwendung der hocheffizienten dispersionsgehärteten Werkstoffe auf Pulverkupferbasis in der Teilen von Motoren und Kraftanlagen der Transportmittel // Powder metallurgical high performance materials: Proc. of the 15th Int. Plansee seminar, Reutte, Tirol, May 28 – June 1, 2001. – Vol. 4. – P. 126 – 149.
4. Шалунов Е.П., Берент В.Я., Вендланд С. Жаро- и износостойкие дисперсно-упрочненные композиционные материалы на основе порошковой меди для сильноточных скользящих и разрывных контактов // Электрические контакты и электроды: Тез. докл. Междунар. конф. «ЭК-2003», Кацивели, Крым, 15 – 21 сент. 2003 г. / ИПМ НАНУ, Киев, 2003. – С. 23 – 26.
5. Shalunov E.P., Lipatov J.M., Golubyatnikov D.A. Experience of producing semi-finished items and ready-mady articles made of oxide and carbide dispersion strengthened powder copper in Russia // Deformation and fracture in structural PM-materials: Proc. of the Int. conf. «DF PM-99», Piešťany, Slovak Republic, Sept. 19 – 22, 1999. – Vol. 1. – P. 365 – 373.
6. Dovydenkov V., Shalunov E. Experience of production and use of precipitation strengthened copper-based materials made mechanical alloying // 1998 Powder Metallurgy: Proc. of the World Congress, Granada, Spain, Okt. 18 – 22, 1998. – Vol. 1. – P. 372 – 377.

# THE FORMATION OF SURFACE LAYERS ON SiC-AlN-$Si_3N_4$ CERAMICS UNDER THE INFLUENCE OF CONCENTRATED SOLAR RADIATION

**Podcherniayeva I.A., Panasijuk A.D., Uvarova I.V., Lijudvinskaya T.A., Neshpor I.P., Mosina T.V., Derinovskaya N.A.**
Frantsevich Institute for Problems of Materials Sciences of NASU,
3 Krzhizanovsky, 03680, Kiev-142, Ukraine, E-mail: cherm@materials.kiev.ua

SiC-AlN-$Si_3N_4$ composite ceramics have high level of physical-chemical properties and can be used as high temperature wear-resistant materials.

The results of phase transformations and formation of gradient structures on the surface of SiC-AlN-$Si_3N_4$ composite ceramics during the process of layer by layer modification by titanium and zirconium borides as well as by alloys based on oxides formed during the process of heating under the conditions of concentrated solar radiation effect have been represented.

To carry out the experiment SGU-2 technique, 155D/65 antinometer, 7052 microampermeter have been used. Concentrator of solar rays was 4-8 mm in diameter. Heat flow has been measured. Duration of radiation was 15 sec. Structure and surface layer compositions have been investigated by metallographic, X-Ray and MRSA methods.

To create gradient structure on specimens surface $TiB_2$ and $ZrB_2$ powder layers with (Fe-Cr-Al) sublayer on nitrocellulose base have been put. Coverings on specimens surface have been put immediately before solar radiation influence and were about 150-200 μm.

Previous investigations carried out on specimens of SiC-AlN-$Si_3N_4$ system without coverings under solar radiation conditions showed that formation of silicium and aluminium oxides took place and during their interaction dense oxide layer of mullitum was formed. The layer had high adhesion to composite surface and was the barrier for oxygen diffusion into the composite.

After the influence of concentrated solar radiation on composite surface with $TiB_2$ covering surface layer contained oxides of $SiO_2$, $Al_2O_3$, $Al_2SiO_5$, $TiO_2$ and underlayer contained of the base phases of β-SiC, AlN, $TiB_2$ according to X-Ray data have been formed.

X-Ray investigation of composite surface layer with $ZrB_2$ covering and (Fe-Cr-Al) sublayer showed that the last consists of mainly oxides of $SiO_2$, $Al_2O_3$, $ZrO_2$ and formed solid solutions of $Al_2O_3$-$SiO_2$, $Fe_2O_3$-$Al_2O_3$ ($FeAl_2O_4$), Fe $Cr_2O_4$ on their base.

Investigations which have been carried out showed that composite materials both with covering and without it have high resistance to high temperature oxidation under the conditions of concentrated solar radiation by formation of protecting dense oxygen films which prevent oxygen diffusion into the composite.

LITERATURE

1. Lyudvinskaya T.A., Panasiyuk A.D., Neshpor I.P., Subbotin V.I. / SiC-AlN-$Si_3N_4$ and SiC-AlN based composite materials at extremal solar energy affect. // Second International Conference «Materials and coatings for exstreme performances. 16-20 Sept. 2002, Katsively, Crimea, Ukraine.

# PRODUCING OF THE WELDED JOINT OF TITANIUM ALLOYS BY THE METHOD OF ELECTRON-BEAM DISPERSING THE MELT

**Mayboroda V.P., Shevchenko O.M.**
I.Franzevich Institute of Materials Sciense Problems of NASU, Kiev, Ukraine
Krshishanovskii Street 3, Kiev, 03142, Ukraine, E-mail:maiborod@ipms.kiev.ua

Titanium and its alloys are successfully employed in aerospace technique, during work in aggressive environments and at low temperatures. But the large affinity of titanium to gases at high temperatures requires for its welding the defence of all areas of the metal, heated higher then 673 K. New possibilities are revealed by the electron-beam technology using the dispersing melts, the features of which are deep vacuum ($P < 0{,}05$ Pa) in the technological chamber and high speed of cooling of the dispersed layer ($10^4$ K/s).

The method to spray a coat by dispersing the melt on the surface shaped has been developed, which combines the advantages of the refining electron-beam melting and the technology of speed solidification. In the vacuum chamber one of the electron cannons heats up the surface of a consumed workpiece, and the second – the surface shaped. At suitable technological parameters the directed stream of small drops of the melt is generated, which are spraying on the surface of a back, spreading and solidifying with the formation of a thin layer. By the layer spraying of dispersed melt the coat of the controlled geometrical sizes and shape is formed. During the process of «freezing» the melt on the surface of a backing a constant temperature near the solidus of dispersing material is holding, that is sufficient to produce the reliable adhesive bonding between the separate layers of spreading drops of the melt [1].

Aluminium is the basic alloying element (α-stabilizer) of titanium alloys. Making small alloying additions of β-stabilizers to the Ti-Al alloys does not result in fixing of β-phase, but prevents the formation of hyperstructures, that allows to increase possible concentrations of aluminium in the alloys without their embrittlement.

The experiments upon the producing of small ingots as the welded joint of titanium alloys by electron-beam dispersing the melt with the method, described in [1,2], were conducted. For welding the titanium alloy with 2% Al was taken, and the alloy containing 4% Al and 2% V was used as the consumed workpiece. The spectral analysis of the produced weld showed a presence of 3,7 % Al and 1,7 % V in the joint material. The studying of the joint produced on the raster electron microanalizer Superprobe was conducted, and the X-ray analysis and measuring of microhardness were also made.

In titanium alloys at the rapid cooling or supercooling of the high temperature β-phase in the definite temperature range there can be martensite structure of the two kinds: martensite with the hexagonal close- packed lattice α′and martensite with the rhombohedral lattice α″. The α′-phase appearing in the few alloyed titanium alloys has the needle-shaped structure, and its presence increases hardness of the alloys. The difference of α″ -phase from α′ -phase consists in the lowering of symmetry from hexagonal to rhombic because of the greater oversaturation of α -solid solution by an alloying element. As a result there must be the splitting of some lines of the martensitic phase on sciagraphs. The hardness of alloys with α″- phase is considerably below the hardness of alloys with α′-phase.

From the data of X-ray analysis the calculations of plane-to-plane spaces of parent metal and «freezed» as a welded joint ingot were conducted. The sciagraphying of a sample, consisting of two areas, was performed without a rotation in Cu $K_{\alpha}$-emission.

At small content of alloying elements in the explored alloys there is also less the oversaturation of α-solid solution. As a result the substantial displacement of α′-phase lines on a sciagram comparing to lines of α-phase will not be, however the lines of α′-phase are somewhat smeared because of considerable internal stresses. Measuring of the sciagraphs, their computation and comparison of the results obtained with the data of metallography studying, fig. 1, show that on sciagraphs of the alloys in question the only lines of hexagonal lattice are present. A displacement of lines does not take place, and some their widening can be supposed to have only the lines of weak intensity.

Measuring of microhardness has shown that hardness of the weld ($H_\mu$ = 3240 MPa) slightly differs from hardness of the parent metal ($H_\mu$ = 3300 MPa). The alloys under study in the initial state have the plate structure, in some areas there are needles (fig. 1a). The presence of needles and some rise of microhardness to 3600 MPa in these areas evidences to the insignificant presence of α′ -phase.

Material with the dense dispersing structure is formed in the weld area (fig. 1a). The presence of micropores is noted with shapes following the counters of flattened solidifying drops of the dispersed melt. Overweld thermal affected zone (the area of overheat or complete recrystallization of the parent metal), characterized by the presence of large grains with needle-shaped martensite crystals inside, the total width of which at the ordinary methods of welding achieves 3,5 mm, in this case is absent.

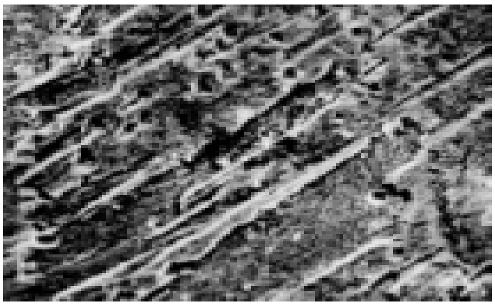

*a*

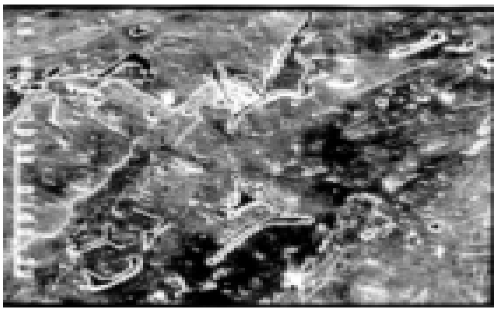

*b*

Figure 1. Microstructure of the parent metal (*a*) and the welded joint (*b*) of titanium alloys.

Thus, it is ascertained, that both the parent metal and the area of joint have the structure of α-solid solution of titanium. And the type of structure is determined by the alloying and intensity of cooling. The conducted experiments upon the producing of the welded joint of titanium alloys by the method of electron-beam dispersing the melt have shown, that this method provides forming the weld with a fine-grained structure, chemical composition of which practically does not differ from composition of the consumed workpiece. The insignificant losses of alloying additions are explained by time of staying metal in liquid state (about $10^{-4}$ sec) and small surface of molten metal ($10^{-3}$ $m^2$). The presence of pores requires the further working of the technological conditions to improve reliability of the adhesive bonding between separate spreading drops of the melt. High output of the process (100-150 kg/h), small losses of metal (coefficient of the use of material 75-85 %), and also producing joints of the required configurations with chemically homogeneous fine-grained structure make the method of electron-beam dispersing the melts promising for use in the welding of titanium alloys.

1. Тихоновский А.Л. и др. Способ электронно-лучевого литья из диспергированного расплава // Проблемы СЭМ. – 1993. – № 3. – С. 35–39.
2. Жук Г.В., Тригуб Н.П., Пап П.А. Соединение титана со сталью методом электронно-лучевого диспергирования расплава // Там же. – 1997. – № 3. – С.18–21.

# FERROELECTRICS $KNbO_3$ FILMS

**Andreeva A.F., Kasumov A.M.**
Frantsevich Institute for Problems of Materials Science NAS Ukraine,
3 Krzhyzhanovsky Str., Kiev - 142, 03680, Ukraine, andreeva@ipms.kiev.ua

The distinction of the ferroelectrics of $KNbO_3$ , $KTaO_3$ and their solid solutions is ability to spontaneous polarization at low temperatures.

The potassium niobate and potassium tantalate ferroelectrics are close to each other in composition, crystal structure and chemical and physical properties. At the same time, the temperature ranges, where they show their ferroelectric properties, contrast sharply.

In contrast with $KNbO_3$, the Curie temperature of which is 708K, the Curie temperature of $KTaO_3$ is near 4K. Having chosen the component ratio of $KNbO_3$ and $KTaO_3$ in their solid solution, it is possible to create ferroelectrics with Curie temperatures in a wide temperature range. The published date on a preparation and properties of films of $KNbO_3$, $KTaO_3$ and their solid solutions are limited.

The present paper proposes a procedure of preparation of $KNbO_3$, $KTaO_3$ and their solid solution thin films, consisting in a deposition and further annealing of a multilayer system on the Nb and Ta oxides and KOH basis.

The films were deposited on glass ceramic, quartz and NaCl substrates (for electron diffraction study) in vacuum $1\cdot10^{-3}$ Pa. For study of electric properties the films were deposited on a Ti substrate. Aluminum point contacts were used as upper electrodes.

Non-annealed films were amorphous. At temperature of ~$300^0$C an interaction between the oxide layers and KOH began.

At temperature of ~$500^0$C a potassium niobate (tantalate) polycrystal structure formation was observed. The diffraction patterns, presented in the Figure, show that the diffraction maxima have been becoming sharper with increasing of the $KNbO_3$ film annealing temperature that certificates an raising of the grain size in condensates. The interplain distances calculated by means of the electron diffraction patterns were close to the $KNbO_3$ monoclinic structure tabular data showing ferroelectric properties.

The film surface morphology was characterized by the presence of blocks ~10 mkm in size constituting a mosaic structure. These blocks were similar to the formations, whicht appeared as a result of a solid crystals etching, their origin is explained by the domain structure presence [1].

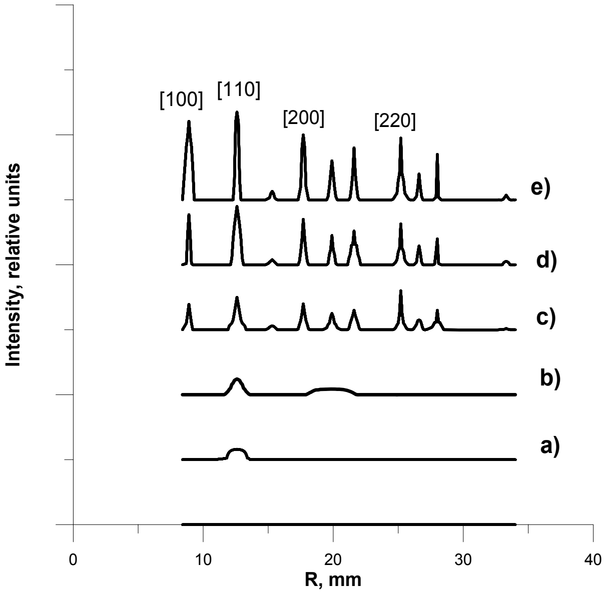

Fig. Diffraction patterns of $KNbO_3$ films after annealing at different temperatures: a - $100^0$C; b - $300^0$C; c - $500^0$C; d - $700^0$C; e - $900\,^0$C

When an alternating electric field with an intensity of $10^3$V/cm and a frequency of 5 kHz was applied perpendicularly to the $KNbO_3$ film surface the dielectric permittivity $\varepsilon$ was 30, no hysteresis was seen on the oscillogram.

When the field intensity was raised up to $10^5$ - $10^6$ V/cm, on the oscillogram one could observe the appearance of a hysteresis loop and the sharp rise $\varepsilon$ up to 30000 that can be explained by the polarization vector switch in strong electric fields known for potassium niobates solid crystals [1].

References

1. Kuzminov Ju.S. Segnetoelectricheskije crystally dlja uprawlenija lasernim islucheniem. - M.: Nauka, 1982. -400p (in Russian).

# CHEMICAL-HEAT TREATMENT OF COBALT

**Yamrozek J., Vajs E., Luchka M.** (1)
Polytechnic Sventokrinska in Kielce,
al. 1000 l. P.P., 7, 25-314 Kielce, Poland, wajs@tu.kielce.pl
(1)Frantsevich Institute for Problems of Materials Science of NASU
st. Krizhizhanovski, 3, Kyiv, 03142, Ukraine, miron@ipms.kiev.ua

The process of diffusive borating is promising as a method for chemical heat treatment providing a significant increase in the wear of machine elements. Steel borating is known over hundred years. In Poland study of cobalt borating was initiated by I. Feschenko-Chopivsky in the 1920 th [1]. Nevertheless, at present there is little information available on borating of cobalt and its alloys.

Cobalt is the nearest iron neighbor and is characterized by much lower affinity for oxygen compared to that of iron but some higher one than that of nickel, which results in the high resistance of cobalt and its alloys to action of atmosphere, humidity, and some salts [2].

Borated layers are characterized by high wear resistance and high friction coefficient and are used in friction centers where lubrication is slight or absent. The high hardness of borated layers and their corrosion resistance in solutions of HCI, $H_2SO_4$, $H_3PO_4$, HF, and organic acids, in which corrosion resistance increases by a factor of 15, as well as in solutions of alkalis and salts have made their application in engineering successful [3].

In accordance with the equilibrium phase diagram, the cobalt melting temperature is 1495 $^0$C, the Curie temperature 1121 $^0$C. The allotropic transition of the hexagonal lattice into cubic face-centered one, $\varepsilon \rightarrow \alpha$, occurs at about 417 $^0$C [4]. Borides contained in the layer have the peculiarities of daltonides. The cobalt borides $Co_2B$, CoB, and $Co_3B$ contain 8,4%, 15.5%, and 7.8% boron, respectively.

Cobalt is a valuable component in many steels and alloys, for example, in high-strength stainless steels and alloys with specific physical properties such as alloys for soldering with glass. It is a component of special ferromagnetic alloys for permanent magnets. For example, alnico alloy contains Co alongside with Al, Ni, and Fe. It is promising to use cobalt in heat-resistant alloys where it either partly replaces nickel or is a basic component (in stellite, vitalium, containing 50-70% Co). Cobalt is also irreplaceable in hard alloys as a binding phase. Of new applications of cobalt, maraging-type steels should be noticed. They contain about 18% Ni, 8% Co+Mo+Ti and up to 0.02% C and permit one to achieve high strength through martempering and subsequent age hardening [5]. The application of cobalt as a basic material in composite diamond-metal cutting tools to be used in sawing natural stone [6] is also new and perspective.

The review above points to the necessity of further investigation into cobalt abilities. The aim of the work is to strengthen cobalt and its alloys by using diffusive borating and studying the influence of saturating mixture composition and saturation conditions as well as of the borating method itself on the composition, structure, microhardness, and thickness of coatings obtained.

For the investigation, we used alloys produced from the following powders: Co Extrafine and mixture 50%Co Extrafine + 50% sprayed nickel powder containing 0.75% C, 4.3% Si, 3.1% B, 3.5% Fe, 14.8% Cr.

Two methods for borating were used: Aluminothermal method based on using $B_2O_3$ which contained additives of aluminum as a reducer; NaF + $NH_4CI$ as an activator, and $AI_2O_3$ as a filler. The composition of this mixture was 25% $B_2O_3$, 25% Al, 2%(NaF+$NH_4Cl$), and $Al_2O_3$.

Method based on using mixture containing $B_4C$ as a basic component and a source of boron: 15% $B_4C$, 2% ($NH_4Cl$+NaF) as an activator, and calcinated $Al_2O_3$ as a filler.

Both processes took place at 950 $^0$C for 6 h. To seal the containers, kaolin clay diluted with liquid glass was used. The samples were cut with a diamond disk at small turnovers; sample sections were examined on metallographic microsections.

To study microstrucrure, samples were etched with a solution of 2.5 g picric acid and 25 g NaOH in 75 g water at 30 $^{0}$C for 30 sec. Then photographs of the structure were taken, and microhardness was determined with the help of a microhardnessmeter "Hanemanna" under loading 100 g. After that, the boride layer rigidity was measured on the basis of examining Vickers prints and using a microscope "Neophot 2" with magnification x1000.

In Fig. 1 a photograph of V- Co hard alloy microstructure taken after borating in accordance with the procedure above. The samples fabricated from cobalt only were marked with "Co" and from mixture of nickel and cobalt powders - with 'Co+Ni".

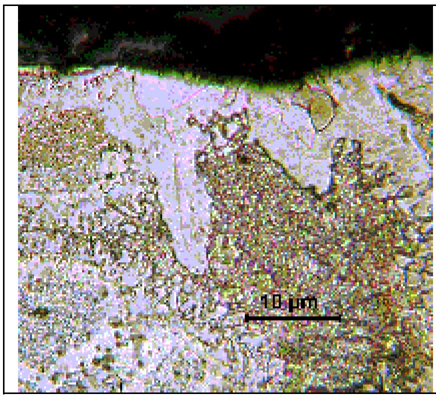

Fig. Micro-structure of boride layer. Magnification x340. Method based on using B$_4$C.

The microhardness of the boride layers obtained through the aluminothermal method reached 1500 mkHV100 except for the "Co+Ni" alloy. The microhardness of the substrate material was about 270 mkHV100. No undesirable changes in the substrate after high temperature borating was detected. The layer thickness was up to 15 mkm after using the aluminothermal method and up to 25 mkm in the case of using B$_4$C.

No needle-like structure of the boride layer was identified on the "Co-Ni" sample fabricated using the aluminothermal method..

1. Metallographic analysis showed that under the given conditions (time and temperature) two-phase cobalt boride layers are obtained, which are characterized by high hardness and microhardness distribution.
2. The microhardness obtained is within the values specific for boride layers and is equal to about 1500 mkHV100. The absence of microcracks in the corners of Vickers prints evidences to high plasticity of the boride layer obtained.
3. On the sample 50% Co+50% Ni made under spraying nickel-containing powder and borated using the aluminothermal method, no needle-like structure, specific for boride layers, was detected as well as no high hardness, expected for boride layers, was obtained.

References

1 Przybyłowicz K. Badania procesu dyfuzji w metalach w okresie 70 - lecia AGH // Zeszyt naukowy AGH: Met. – Odl.-1986.- N 130.- S. 47 – 60.
2 Heslop R.B, Robinson P.L. Chemia nieorganiczna, Krakov: Wyd Naukowo-Techniczne, 1964.- 384 p.
3 Ляхович Л.С.: Борирование стали. Изд. Металлургия, Москва, 1978.- c.
4 Metals Handbook. :Properties and Selection: Nonferrous Alloys and Special-Purpose Materials, V 2.ASM International, 1998, s 616
5 Malkiewicz T. Metaloznawstwo stopów żelaza, PWN, Kraków: AGN.- 1976.- 123 s.
8 Konstanty J. Cobalt as a Matrix in Diamond Impregnated Tools for Stone Sawing Applications, Kraków: Uczelniane Wydawnictwa Naukowo-Techniczne.- 2002.- 123 S..

# PECULIARITIES OF $\alpha$-$SI_3N_4$-(MGO, $Y_2O_3$) SYNTHESIS UNDER COMBUSTION MODE AND CERAMIC PROPERTIES

**Zakorzhevsky V.V., Borovinskaya I.P., Chevykalova L.A.(1), Kelina I.Yu.(1)**
Institute of Structural Macrokinetics and Materials Science, RAS, Chernogolovka, Russia
Chernogolovka, 142432, Moscow, Russia, e-mail: Zakvl@ism.ac.ru
(1)State Unitary Federal Enterprise "Tekhnologiya", Obninsk, Russia
Obninsk, Kaluga region, Russia, e-mail: Kelinai@ mx1.technologiya.ru

Silicon nitride is distinguished by its excellent operation properties such as strength, hardness, and crack resistance. However, in order to extend the application fields of silicon nitride, it is necessary to improve high-temperature and strength characteristics. For this purpose it is necessary to develop silicon microstructure. At present, there are to ways to do it: 1) to develop composite materials when SiC, $\beta$-$Si_3N_4$ whiskers or TiN, TiC and some other nanopowders are introduced into $Si_3N_4$ matrix [1]; 2) to use nanopowders for obtaining fine structure ceramics [2]. One of the possible ways to affect the ceramic microstructure is to use metastable composite powders based on $\alpha$-$Si_3N_4$ and obtained by the method of self-propagating high-temperature synthesis (SHS) [3].

SHS silicon nitride is synthesized by silicon powder combustion in nitrogen atmosphere with ammonium halides. Use of salt and other additives allowed affecting synthesis parameters and characteristics of the final products. During the synthesis process silicon nitride is formed through the gas phase in nonequilibrium thermal conditions.

Two conventional mixtures $Si_3N_4$+5 mass % MgO and $Si_3N_4$+10 mass % $Y_2O_3$ were chosen for obtaining $Si_3N_4$-based ceramics. The oxides were introduced into the green mixture compositions on the stage of dosing, and then everything was mixed. $\alpha$-$Si_3N_4$-based composites with oxide sintering additives were synthesized in one stage in the SHS-30 reactor.

Synthesis of $\alpha$-$Si_3N_4$-(MgO, $Y_2O_3$) based on the optimum green mixture composition was followed by a significant increase in the combustion velocity from 0,12—0,13 mm/s (without oxides) up to 0,32—0,4 mm/s (with oxides) and in the combustion temperature up to 2070K. When the green mixture was burnt under such terms, the synthesis product was characterized by a low content (30—40%) of alpha phase and its nonuniform distribution in the cake cross section. After the synthesis mode optimization, the maximum combustion temperature was decreased to 1920K while alpha phase content grew up to 70—82 mass%.

Since magnesia and yttria provide $\alpha\to\beta$ phase transition, we studied influence of magnesia and yttria on formation of silicon nitride phase composition during the synthesis of $\alpha$-$Si_3N_4$-based composites under the combustion mode. In such experiments it was observed that phase transition started at the temperatures lower than the melting points of the corresponding eutectics ($MgSiO_3$ $T_{melt}$=1825K, $Y_2Si_2O_7$ $T_{melt}$=1933K), Fig.1. Time of $\alpha\to\beta$ phase transition was 3-5 minutes.

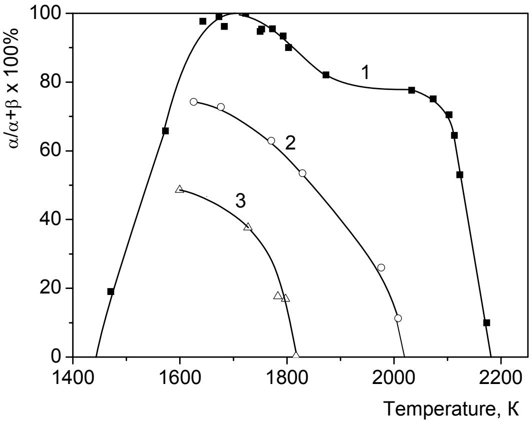

Fig.1. Dependence of $Si_3N_4$ phase composition on combustion temperature in presence of oxides.
1 – No oxides; 2 – 5%mass. MgO;
3 – 10%mass. $Y_2O_3$.

The low temperature of the beginning of phase transition in the case of magnesia and yttria introduction proves that the oxides begin participating in the process of phase formation on the stage of $\alpha$-$Si_3N_4$ synthesis. Gas phase reactions are obvious to be also important for formation of such properties.

Use of oxide additives in silicon nitride synthesis affected the particle morphology. The powders synthesized are characterized by a low specific surface (1,6—1,7 $m^2/g$) but by a finer structure. The particles of equiaxial shape of 1 μm in size prevail in the composites. They are united in oxide conglomerates, Fig.2.

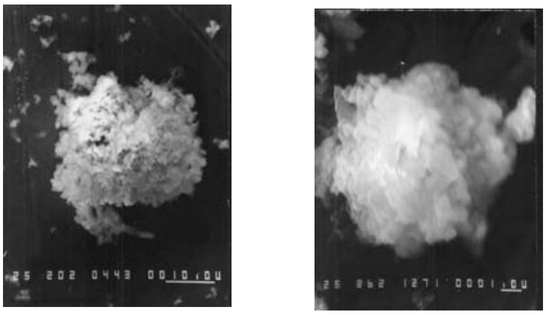

a b

Fig.2. Morphology of composites particles after synthesis.
a) $\alpha$-$Si_3N_4$-5%MgO; b) $\alpha$-$Si_3N_4$-10%$Y_2O_3$.

The particles of 100% $\beta$-$Si_3N_4$-oxide powder are characterized by a columnar shape but a finer microstructure (diameter – 0,3—0,5 μm, length – up to 10 μm) in comparison with the conventional whiskers of $\beta$-$Si_3N_4$ (d=1—2 μm, L=5—10 μm) regardless of the oxide type (Fig.3).

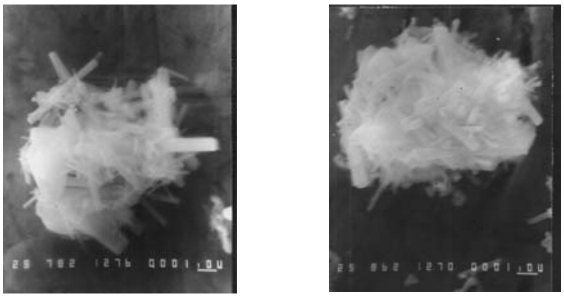

a b

Fig.3. Morphology of composites particles.
a) $\beta$-$Si_3N_4$-MgO; b) $\beta$-$Si_3N_4$-$Y_2O_3$.

The composites obtained were milled in a ball mill in a liquid medium. After milling, the powders' specific surface area was 8 $m^2$/g, the average particle diameter was 0,9 μm.

The ceramic samples obtained from metastable powder composites of $\alpha$-$Si_3N_4$-$Y_2O_3$, $\alpha$-$Si_3N_4$-MgO by hot pressing are characterized by uniform self-reinforced microstructure containing particles of a columnar shape, of 0,5—1 μm in diameter and 10 μm in length (Fig. 4). The grain size of the obtained ceramic microstructure is comparable with the average diameter of the initial powder particles.

Therefore, due to the short times of phase transition it became possible to dense the initial billet and prevent growth of β-phase grains.

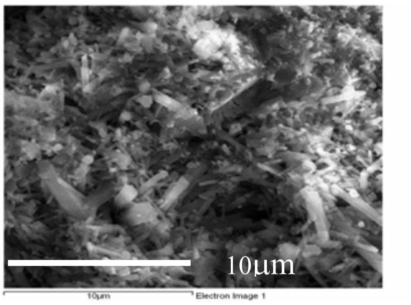

Fig.4. Microstructure of ceramics obtained from $\alpha$-$Si_3N_4$-$Y_2O_3$ composite.

**Conclusions:**

Composite powders of $\alpha$-$Si_3N_4$-$Y_2O_3$, $\alpha$-$Si_3N_4$-MgO, which are unstable at 1823K, were obtained. Their instability consists in a very high rate of phase transition which lasts several minutes.

Use of the novel composite powders of silicon nitride with new characteristics allowed producing poreless ceramics. The grain size of its microstructure is comparable with the particle size of initial silicon nitride powder. This material with fine microstructure will be characterized by excellent strength and high-temperature properties in comparison with those of the available ceramics based on silicon nitride.

**References.**

1. Young-Hang Koh, Hae-Won Kim, and Hyoun-Ee Kim, Microstructural evolution and mechanical properties of $Si_3N_4$-SiC (nanoparticle)-$Si_3N_4$(whisker) composites.// J. Mater. Res., V.15. №2. P. 364—368. 2000.

2.S. Veprek, P. Nesladek, A. Niederhofer, F. Glatz, Search for superhard materials: nanocrystalline composites with hardness exceeding 50 GPa. Nanostructured Material,V.10. №5. P.679—689. 1998.

3. V.V. Zakorzhevsky I.P. Borovinskaya. Some Regularities of $\alpha$-$Si_3N_4$ Synthesis in a Commercial SHS Reactor. Int. J. SHS.V.9. №2. 171—191 (2000).

# CORE CERAMICS OBTAINED BY REACTION BONDING AT SIALON COMPOUNDS OXIDATION

**Smirnov K.L., Borovinskaya I.P., Ospennikova O.G.**$^{(1)}$
Institute of Structural Macrokinetics and Materials Science RAS, Chernogolovka, Russia
Moscow region, 142432, Russia, E-mail: kosm@ism.ac.ru
$^{(1)}$Federal State Unitary Enterprise MMPP «SALUT», Moscow, Russia,
16, Budionny Avenue, Moscow, 105118, Russia. E-mail: mlvm@salut.ru

## Introduction

The method of reaction bonding at oxidation is efficient for producing near net-shaped ceramic items [1—3]. The aim of the present work is to study the possibility of the method for obtaining ceramic cores used for formation internal cooling channels in the items made of nickel-based superalloys. Powders of solid solutions formed in Si—Al—O—N (sialon) system were used as initial components. At present, these compounds are successfully used for development of advanced structural ceramics with excellent strength characteristics, thermal and corrosion resistance [4].

## Experimental procedure

Filtration combustion of reactive mixtures of aluminum and silicon powders and their oxides in high-pressure gaseous nitrogen was used to synthesize sialons [5]. The average particle size of the synthesized powders after milling depended on the type of sialon compound and ranged from 3 up to 10 μm. The experimental procedure included the following operations: preparation of a thermoplastic slip with a paraffin-based plasticizer; pressure molding of initial billets; two stage thermal treatment in the air in the compartment electric furnaces. The treatment included a slow increase in the temperature up to 800 °C for removing an organic binder and exposure at 950÷1550 °C during 7—10 hours for realizing the oxidation process. The materials obtained were subjected to analysis: their phase composition, solubility in 30 % water solution of KOH at 100÷110 °C, flexural strength under conventional conditions, and linear sample shrinkage during firing were examined.

## Results and Discussion

Influence of the firing temperature was studied. At T≤1200 °C, the oxidation rate of sialon compounds is insignificant, a small amount of aluminosilicate phase is formed; it provides low strength of the ceramics obtained. At T≥1500 °C, the oxide phase becomes soft, nitrogen bubbles appear in it. Besides, in the case of sialon compounds with a high content of silicon as the result of the intensive interaction between initial and oxidized components, volatile silicon monoxide $SiO_g$ is formed. It causes a significant mass loss of the sample and formation of a burn-on which is difficult to remove. A high level of the ceramics strength ($\sigma_f$ ~16,0÷18,0 MPa) is achieved at 1300÷1400 °C. At such temperatures aluminum nitride polytypes are completely oxidized to mullite and $\alpha$-$Al_2O_3$, and solid solutions based on silicon oxinitride and silicon nitride are partially oxidized to cristobalite and mullite. In each case the ratio between the oxide phases is determined by the ratio of Si and Al in the initial sialon compound (Fig. 1).

The ceramics obtained due to oxidation of sialon with Si/Al≥4 and containing cristobalite as the main phase is characterized by high solubility in 30 % water solution of alkali. However, due to a significant volume effect of the oxidation reaction of the mentioned compounds ($\Delta V_{\beta\text{-SiAlON}}$ ~76%, $\Delta V_{o\text{-SiAlON}}$ ~44%), a remarkable swelling of the samples occurs during the firing process. No changes in geometry are observed only when these materials are formed due to oxidation of sialon compounds with a high content of aluminum (Fig. 2).

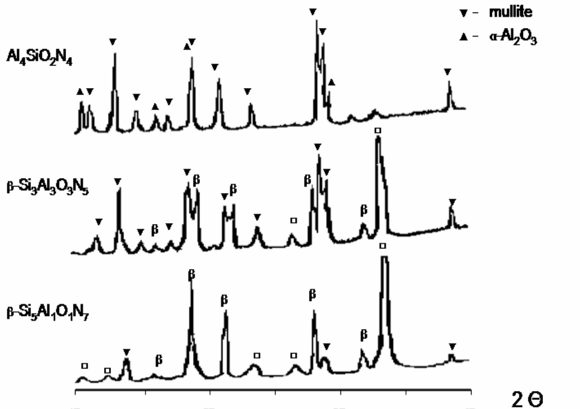

Fig. 1. X-ray pattern of sialons oxidized at 1350°C. It is possible to suppress swelling of sialon compounds with a high content of Si, if $ZrO_2$, $Al_2O_3$, $SiO_2$ are introduced into the initial mixture. In these composites it is possible to achieve an acceptable linear sample shrinkage ($\delta \leq 1.0$ %) if the total amount of the introduced oxides is 50 mass % minimum (Fig. 3). When $SiO_2$ is used as the main additive, it provides an excellent solubility of the obtained ceramics in 30 % water solution of KOH. If $ZrO_2$ is introduced, the ceramics is distinguished by better strength characteristics ($\sigma_f$ ~20,0÷22,0 MPa).

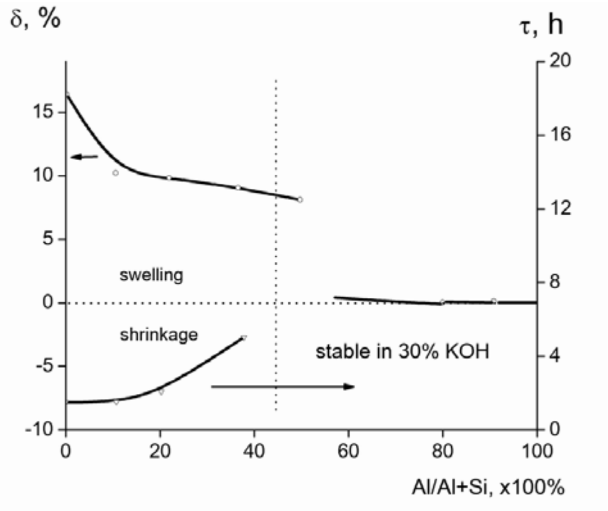

Fig. 2 Linear sample shrinkage at firing and solubility time in 30% solution of KOH at 100÷110 °C in dependence on Si/Al ratio in the initial sialon.

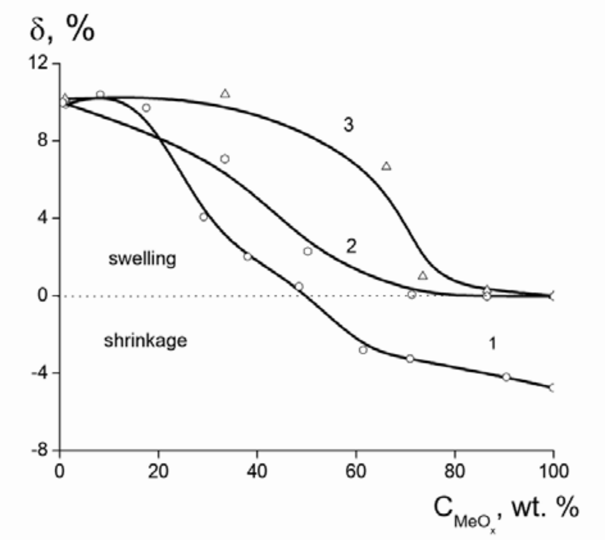

Fig. 3. Linear sample shrinkage at firing as a function of oxide content in green mixture: β-$Si_5Al_1O_1N_7$—$ZrO_2$ (1), β-$Si_5Al_1O_1N_7$—$SiO_2$ (2), β-$Si_5Al_1O_1N_7$—$Al_2O_3$ (3).

## References

1. D. Holz, S. Wu, S. Scheppokat, and N. Claussen. Effect of Processing Parameters on Phase and Microstructure Evolution in RBAO Ceramics // J. Am. Ceram. Soc., 77 [10] 2509—17 (1994).

2. D. Holz, S. Pagel, C. Bowen, S. Wu, and N. Claussen. Fabrication of Low-to-Zero Shrinkage Reaction-Bonded Mullite Composites // J. Eur. Ceram. Soc., 16, 255—60 (1996).

3. K.H.Sandhage, P.Kumar, K.A.Rogers. Near net-shaped, alkaline-earth-bearing ceramics and composites by oxidation metal-infiltrated performs // 5th International Symposium on Self-propagating High-temperature Synthesis, Moscow, Russia, Abstracts, p. 91—92 (1999).

4. T.Ekström, M.Nygren. SiAlON ceramics // J. Am. Ceram. Soc., 75 (2), 259—276 (1992).

5. I.P.Borovinskaya, K.L.Smirnov. Self-propagating High-temperature Synthesis of SiAlON ceramics // Nauka – proizvodstvu (in Russian), 10 (8), p. 70—7.

# FORMATION OF CORROSION- AND EROSION-RESISTANT COATINGS ON INTERNAL SURFACES

**Krokhmal S.A., Zueva T.N.**
National Centre of Science "Kharkov Institute of Physical and Technology" Kharkov, Ukraine
Academic Str., Kharkov, 161108, Ukraine, shirokov@kipt.kharkov.ua

One of most composite problems in technology of obtaining of coatings is the maintenance of their uniformity on internal surfaces of narrow extended channels. The given problem can be decided by a method of gas phase deposition from metalloorganic compounds. To such connections concerns chromium-organic liquid (KHOZH) "BARKHOS" [1, 2], representing mixture of homologues of the large-scale integrated bis-aren chromiumorganic connections.

Thus receive coating on the basis of carbides of a chromium having following properties:

- Corrosion and erosion resistance;
- By absence of balling even at enough heats;
- Hydrophobic for the majority of liquids;
- By high antifriction properties, and also high stability to grasping at friction;
- By absence of a through porosity already at small depth of cover(coating) (1—10μm).

Such coatings represent a bivariate composite material arising during growth at the expense of self-oscillations, both temperature, and pressure in a zone of a deposition. The data of oscillation result in formation of interleaving layers of coating consisting from rather clean (and plastic) of a chromium and a mix of his carbides with microchips of a chromium [3]. The depth of these layers varies within the limits from 0,01 up to 2μm and is determined in technological parameters of a precipitation process. In activities [3, 4] the capability of regulation of depth of these layers is rotined, that allows to operate mechanical properties of received coatings.

Absence of a through porosity, which one together with a corrosion stability of coating determines his protective attributes, is provided at thicknesses 1—15μm [5, 6, 7]. Such dispersion of the data is conditioned by difference as parameters of process, so by methods of combat training of a surface before a deposition of coating. The decrease of a threshold of a through porosity will allow to lower minimumly indispensable depth of coating for reliable protection against corrosion destruction, having increased thus his stability to flexural pressure. In tendered activity the factors influential in stability of properties of coatings received deposition from a vapour phase, received by a deposition, (KHOZH) "BARKHOS" are studied. The process was conducted at the temperature of with job surfaces 400—500°C During experiments were obtained carbidecromium of coating on internal surfaces a diameter from 45 up to 0,8mm. The time-average settling rate reached 15μm/mines, and productivity of a reactant 80—90%. The frame of coatings obtained on internal surfaces, is similar to frames of coatings received at a deposition on outside surfaces (fig. 1)

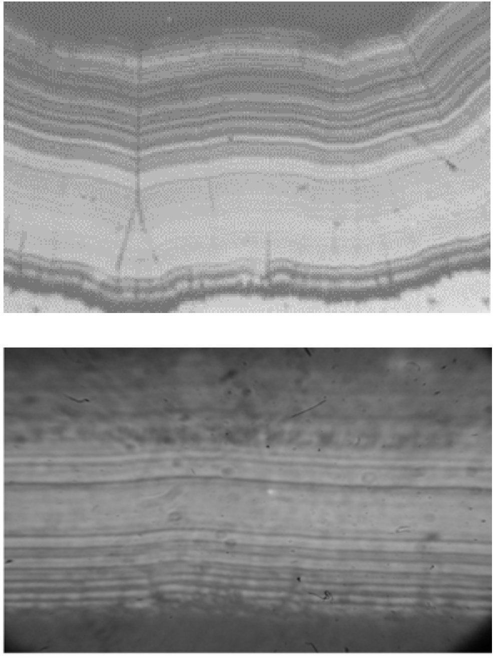

a)

б)

Fig. 1. Frame of coatings:
a) - on an internal surface (×200),
б) - on an outside surface (×1000).

At research of a corrosion stability of coatings, dissolution of their surface, at exposure within 360 hours in HCl (conc.)., at room temperature is not detected. The depth of coating 10μm provided absence of a through porosity in coating deposited on a surface with an initial roughness $R_a$=0,1—0,3μm.

At a deposition carbidechromium of coatings on a surface with a hardly developed relief the effect of smoothing (fig. 2) was watched.

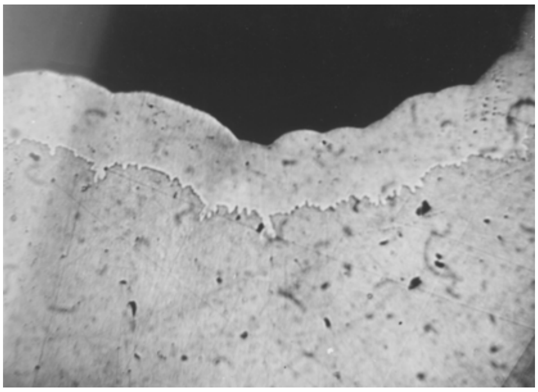

Fig. 2. A cushioning effect

The non-uniformity of depth of coating lengthwise of channel depend on accuracy of dosage of a reactant and in conditions of the present activity did not exceed 13% for a passage diameter 3mm. At a decrease of a passage diameter in 3 times up to values not exceeding 40—45 % were augmented.

**Conclusions.**

By method of a pyrolysis KHOZH "BARKHOS" the obtaining corrosion - and erosion-resistant coatings on internal surfaces of channels a dia less 1mm is possible.

The productivity of a reactant on an offered technique of a deposition reaches 80-90 %.

The increase of uniformity of depth of coating in the given method demands increase of uniformity dosing of a reactant in a zone of a deposition.

**List of the literature:**

1. Kogan Ya. D. " The gas-thermal methods of obtaining of tear-proof and rustproof coatings ".- In col. Scientific works MADI, M., 1988, p.4—12 : " Modern technological methods of a reliability augmentation both durability of machines and tool ".

2. Shurov A.F., Kotkis A.M. Etc. " Frame and destruction of a contact layer " pyrolytic carbidechromium cover - steel " ". -In book: A strength of materials in hostile environments. Krasnodar, 1986, p. 63—76.

3. Lakhtin Yu. M., Kogan Ya. D , Gorovoy A.P.,Strulev V.M.. " Vapour-phase technology of obtaining of protective coatings thermal dissociation of organometallic compounds ". - In col: Engineering, economics, information, technology. Moscow, 1988, p. 3—12.

4. Gorovoy A.P., Karavaeva L.V., PotapovM.A., Malinin S.G. " Modification of an elemental composition of pyrolytic chromiums and their properties ". - In col. Scientific works MADI: technological methods of a reliability augmentation both durability of machines and tool, Moscow, 1988, p. 13—16.

5. Kostenkov V.A. Etc. " Definition of technological parameters and creation of the reactor for a deposition of pyrolytic coatings of a chromium on small-sized items of the composite forms": - In book: II All-Union conference on organometallic compounds for obtaining metallical and oxide coatings, (Gorkiy, 1977): Thesis of reports, M.: Science, 1977, p. 70.

6. Luzin A.S, Polycarpov V.B. Etc. " Research of frame and porosity pyrolytic carbidechromium of covers on shells fuel element from an aluminum alloy ". – In book: Application of organometallic coatings and stuffs. (Gorkiy, 1987):Thesis of reports of 5-th All-Union. conference, Moscow, Science, 1987, p. 76—77.

7. Kostenkov V.A. Research of processes of a chemical deposition of coatings of carbide of a chromium from a vapour phase of the large-scale integrated circuit - arenchromorganic of connections:Ph. D. thesis techn. sciences. L.: Leningr. technol. Ins-t, 1978.

# NUCLEAR TRANSMUTATION DOPING OF PHOTOCATALYTIC TIO2 FILM COATINGS WITH TRANSITION 3D METALS

**Belous V.A., Neklyudov I.M., Holomeev M.G., Shiljaev B.A.**
Institute of solid state physics of National Science center
"Kharkov Institute of Physics and Technology", Kharkov, Ukraine
1, Academicheskaya St., Kharkov, 61108, Ukraine, belous@kipt.kharkov.ua

After detecting 30 years ago of photocatalytic properties in $TiO_2$ compounds, this dioxide was largely used as catalyst, in a film's kind also [1]. However wide use of this catalyst is appreciably restrained by the fact that the photocatalytic properties of the dioxide are manifested to the largest degree only under irradiation with wavelength less than 380 nm (ultraviolet region) that makes 3% of solar radiation spectrum. Revealing of photocatalytic properties under ultraviolet irradiation determines by high width of this semiconductor band gap (~ 3…3,2 eV). To prepare $TiO_2$ photocatalysts which can work under visible light irradiation this compound is doped by transition metals such as V, Cr, Ni, Co to form donor or acceptor impurity site. Doping is carried out by chemical process or by ion implantation [2, 3].

In the present paper a method of nuclear-transmutation doping of $TiO_2$ films produced by ion-plasma deposition is proposed. As a transmutation products in nuclear reactions with braking radiation photons of electrons with energy of ≥ 20 MeV, with protons with energy of 15-20 MeV, with fast and thermal neutrons Ti forms atoms of all transition 3d elements from Sc to Zn. The proposed method advantage is the localization of atom-products in crystalline grains but not in the intergranular space as on chemical alloying [4] because $TiO_2$ nanocrystallites and intergranular space has comparable volumes [5]. Transition 3d atoms implantation into the structure of nanocrystallytes forms donor or acceptor impurity site, changes Fermi level position into the band gap, shifts photosensitivity of $TiO_2$ into visible light region. All this decrease a chemical energy of activation of degradation reactions of organic and inorganic compounds on the surface of $TiO_2$ film coatings that causes the environmental contamination.

During present investigation, the processes of successive transmutation of titanium and oxygen isotopes are developed for photons, protons and 1neutrons reactions. Concentration of nuclei-products was received by solving a system of Bateman differential equations describing these processes [6]. A $TiO_2$ irradiation conditions, density of particle fluxes, irradiation time and conditions for each transition element production were determined.

**References:**

1. V.A.Belous, I.V.Zalivadnaja, Proceedings of Kharkov scientific Assembly "Functional coatings on glasses", p.148—152.
2. H.Yamasshita, Y.Ichihashi, V Taakeeuchi, S.Kisshigusshi, M.Anpo,- J.Syncchrotron Rad., 6 (1999) 451—452.
3. J.M.Herrman, J.Disdier, P.Pichat, Effect of cchromium dopping on the electrical and catalyticc properties of powder titania render UV and visible illumination.- Chem.Phys.Lett., 108 (1984) 618—622
4. L.N.Larikov, Physics of metals and the newest technologies, v.17, N1 (1995), p. 3—9
5. N.P.Lyakishev, Nanocrystalline structures- recent trendsin development off sstructure materials. Bulletin of RAS, 73, N 5 (2003), p.422—425

H.Bateman. The ssolution of system of differential equations occuring in the theory of radio-active transformation. — Proc. Cambridge Phil. Soc., 15 (1910) 423—435

# PRODUCTION OF THIN CAST SHS-ELECTRODES BY SPUN CASTING

**Sanin V.N., Yukhvid V.I., Deev B.B, Ospennikova O.G.**(1)
Institute of Structural Macrokinetics and Materials Science of RAS, Chernogolovka, Moscow
Chernogolovka, Moscow region, 142432, Russia
(1)Federal State Unitary Enterprise "MMPP SALUT", Moscow, Russia
Moscow, 105118, Budenov avenue 16, Russia, svn@ism.ac.ru

The method SHS-metallurgy [1—3] was used for solution tasks during production of air engines.
The work consists of two parts:

- The possibility of obtaining of thin cast electrodes by SHS under high gravity created by centrifuge (Fig. 1) has been for the first time studied. The obtained results are illustrated on an example of synthesis and use of electrodes of nickel aluminide ($Ni_3Al$), which is a basis of industrial heat resisting alloy. The mixture NiO+Ni+Al have been used. In the part a greater attention has been paid to the selection of optimal green composition for obtaining cast final products, influence of gravity on combustion process, phase separation and the depth of form infilling. Depending on the key parameters (gravity, ratio of initial components, weight of green mixture, form diameters etc.) three areas (full, partly filling and non filling) of form infilling for various diameters of synthesis of electrodes were found. The optimal regime for selective forms infilling (metal phase only) was revealed.
- Second part of the present study devoted investigation of practical application of obtained thin cast SHS electrodes (Fig. 2). The research is directed on depreciation of expenses in aeronautical engineering. The new technique for hermetic sealing of technological holes during manufacture of turbine blades was investigated. The technique includes following stages:
  (*1*)-production of thin (diameter 1—4 mm) electrodes from heat resistant alloys by SHS spun casting. The
  (*2*)-manufacture of plugs for technology holes from the electrodes
  (*3*)- welding of the technological holes by the SHS electrodes by method arc argon welding.

  Fig.3 shows a blade before and after sealing of technological holes.

The parameters of welding were determined. The microstructure of a welded seam was investigated. The researches have shown good compatibility of a blade material and SHS electrode.

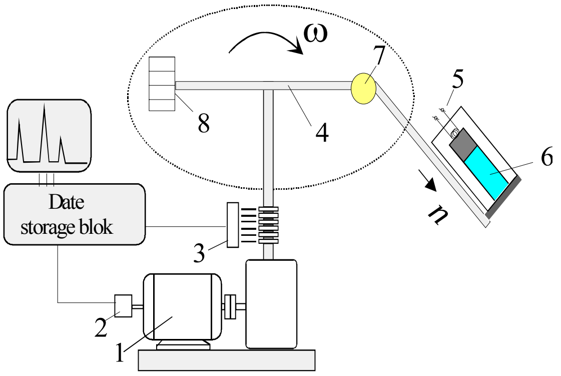

Fig. 1. Sketch of centrifuge.
(1)-electric motor, (2)-tachometer, (3)-collector , (4)-rotor of centrifuge, (5)-ignitor, (6)-mould, (7)-hinge, (8)-counterbalance.

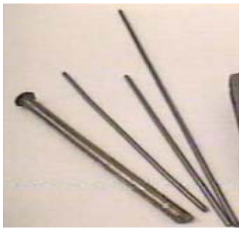

Fig. 2. SHS-electrodes

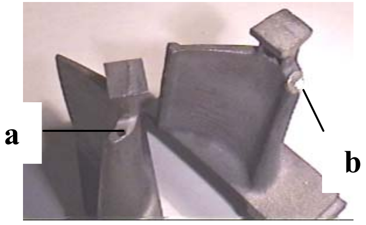

Fig. 3. Turbine blades before (a) and after (b) sealing of technological holes

List of references
1. Yukhvid V.I.,G.A. Vishnyakova, Silyakov S.L.Sanin V.N. and A.R. Kachin. Structural Macrokinetics of Alumothermic SHS Processes. *International Journal SHS.* 1996, Vol. 5, Number 1, pp. 93—105.
2. Yukhvid V.I. Modifications of SHS processes. *Pure and Appl. Chem.*, 1992, v.64, N 7, p.977—988.
3. V.I. Yukhvid, V.N. Sanin, and A.G. Merzhanov. The Influence of High Artificial Gravity on SHS Processes. Processing by Centrifugation. Edited by L.L. Regel and W.R. Wilcox. Kluwer Academic, 2001, ISBN 0—306—46654—6, p.185.

# ALKOXO METHOD IS DIRECT WAY OF INORGANIC CERAMIC MEMBRANES MODIFICATION

**Tsodikov. M.V., Teplyakov V.V., Uvarov V.I.⁽¹⁾, Borovinskaya I.P.⁽¹⁾**
Topchiev Institute of Petrochemical Synthesis RAS, Moscow, Russia
Moscow, 117912, Russia, E-mail: tsodikov@ips.as.ru
⁽¹⁾Institut of Structural Macrokinetics and Materials Science RAS, Chernogolovka, Russia
Chernogolovka, Moscov region, 142432, Russia. E-mail: kosm@ism.as.ru

Alkoxo methods based on alkoxide and another elementorganic complexes are recognized as perspective approach for direct formation of mixed oxide catalysts and materials of a new generation [1, 2]. The main feature of these methods is the structure formation of the final oxide systems realizing even at the early stages of colloidal mother solution preparation [3, 4]. The latter provides a satisfactory reproducibility of product properties relates to elemental and phase composition, structure, morphology and dispersity.

In this work presented results of this approach application for ceramic and metal ceramic membranes modification and preparation of functional gibrid systems. The goals of this study were follows:
formation of the catalytic coatings inside of membrane channels and study its catalytic activity in model reactions of methanol decomposition into syngas; oxidation of CO contained in a poor air mixings (exhaust gas) and oxidative methane condensation.

## Experimental

It was used two types of the pore membranes: ductile with mark "Trumem" [1] and ceramic with mark "BUM" [2]. Ductile membrane is double layer system consists of pore stain-less support with ceramic layer - thick – 20 mkm and average pores size – 0,13 mkm. Ceramic membrane was prepared from titanium carbide have thick – 4-5 mm and it contained the pores with average size — d=4—5 mkm.

Catalytic activity and permeability studied with use original laboratory flow set-up. Gasouses components contained in the started mixing and in the products were analyzed on-line with use gas chromatograph "Biochrom" and gas analisator Reken-Kaken equipped by IR-spectrometer sell.

The tests relating with wear-resistance of ductile membrane determined as mass loss during abrasion with use standarted method.

The metal oxide meso pore membrane was formatted by dropped of mother solution on the surface of rotating ductile membrane.

## Results and discussion

60% ZnO×20% $Cr_2O_3$×20% $Al_2O_3$ system having spinel structure similar to commercial catalyst with element compositions [5] was formed inside of the ductile membrane channels. For comparison purposes intensity of the reaction carrying out this reaction also originating in the traditional reactor with fixed bed of the catalyst. The volume of the flow reactor was equal to membrane tube.

As follows from the table at 300 °C the rate of the metanol decomposition was more than 1,5 order higher comparison with traditional reactor. The selectivity into syn-gas formation was a little smaller (87% against to 92%). The velocity of the gas diffusion from pores of the wool membrane was $10^{-2}$ c.

For reaction of CO oxidation were formed inside of the membrane channels two type of metal oxide catalytic systems such as $Cu_{0,03}Ti_{0,97}O_2$ and 5% NiO×95% $Al_2O_3$ with anatase and spinel structure subsequently has been shown high catalytic activity in this reaction early as powder systems loaded in the flow reactor [6, 7]. As it is seen in the fig. 1 the cupper titania system possesses more high activity comparison with nickel alumina system. Practically full conversion of CO, contained up to 1% vol in air reach at 250 °C at the time of gas diffusion through membrane pore – $10^{-3}$ c.

Study of the kinetic regularities shown that the rate constant increase with increase of the catalytic system quantity as result of pre-exponential parameter amplification. This result indicates that with the increasing of the catalytic system formed inside of the membrane channels rises number of the active collisions of the substrate with active catalytic surface.

Recently it was shown that conversion of oxidative methane condensation into the light hydrocarbons $C_2$—$C_4$ reach to 20% in the presence of La+Ce/MgO system at 720 °C [8]. Over ceramic membrane modified by this system inside of pore space the same conversion at the 80% selectivity relates to light alkanes was reach at 550 °C.

Thereby the results presented in this work permit to conclude that alkoxo methods can be recognize as perspective for pore membrane modification by metal oxide coatings in order to membrane fictionalize. Moreover results relate to catalytic tests shown that the random of catalytic reactions can be intensificated when reaction carrying out inside of membranes micro channels modified by metal oxide catalytic systems. In this case the pore membrane as some self-serving as support. The preliminary data of kinetic study permit to propose that emplification of the catalytic reactions is conditioned by increasing of active collisions of the substrates molecules with active metal oxide surface distributed inside of the membrane micro channels. This proposition is need in the carrying our of more spacious investigations consist of as in kinetic regularities and structural specific of the oxide coatings studies.

## Reference

1. L.I.Trusov, Patent USA
2. I.P.Borovinskaya, A.G.Merdganov, V.I.Uvarov Russian Patent №2175904 25.02.2000.
3. Y.Abe, T.Gunji, Y.Kimata, M.Kuzamator, A.Kasaor, and T.Misono, J.Non-Cryst.Sol.,1990, 121, 21.
4. N.Ya.Turova E.P.Turevskaya, M.I. Yanovskaya, The Chemistry of Metal Alkoxides, 2001, KLUWER ACADEMIC PUB-LISHERS, 384 p.
5. R.C.Mehrotra, J.Non-Cryst. Sol., 1990, 121 1.
6. O.G.Ellert, I.A.Petrunenko, M.V. Tsodikov et al, J.Sol-Gel Sci and Tech., 1997, 8, 213.
7. V.V.Sakulin, R.A.Aronovich, E.V. Slivinskii et al, Osnovnoy organicheskii sintez I neftechimiya, 1993, 28, 7.
8. . Yu.V.Maksimov, M.V.Tsodikov, E.A. Trusova, I.P.Suzdalev, And J.A.Navio, Catalysis Letters, V.72, N1—2, 11—15, 2001.
9. M.V.Tsodikov, Ye.A.Trusova, Ye.V. Slivinskii et al, Studies in Surface and Catalysis, V 118, (Eds:B.Delmon and J.T.Yates) p 679—689, 1998, Lonvain-la-Neuve, Belgium, September 1-4, p 679—689.
10. A.G.Dedov, A.S.Loctev, I.I.Moiseev et al, Doklady Academii Nayk, 2001, 380, 6, 791.
11. F.Sanchez-Bajo, F.L.Cumbrera, A. Domingez-Rodrigez, et al, Mater. Lett., 1992, 15, 39.
12. F.Sanchez-Bajo, F.L.Cumbrera, M.V. Tsodikov et al, Mater.Lett., 1998, 33, 283.
13. R.A.Kozlovskii, V.V.Yuschenko, M.V. Tsodikov et al, Russ.Chem.Bull., Intern.Edit., 2002, 51, 6, 967.

# DEVELOPMENT OF IN-SITU TRIBOTECHNOLOGY OF OBTAINING SURFACE NANOCRYSTALLINE STRUCTURES BY FRICTION AT SHEAR UNDER PRESSURE

**Bilousov M.M.**
Galkin Donetsk Phys.&Tech. Institute of NASU, Donetsk, Ukraine
72, R. Luxemburg Str. Donetsk, 83114, Ukraine, E-mail: slobodina_vera@mail.ru

The development of in-situ formation of surface structures in extreme conditions of frictional-contact interaction (at the maximal contact pressure) is a necessary condition of severe surface hardening of materials and alloys capable of working in extreme operating conditions [1, 2]. The idea of in-situ technology of structural hardening of a surface at severe frictional interaction of contacting bodies consists in the establishment of functional dependence between tribomechanical structure forming parameters and microstructural changes in a superficial layer.

The purpose of research: development of in-situ tribotechnology of surface hardening of materials, by a purposeful formation of surface structures of extreme friction, at severe shearing strain under high pressure.

## Material and experimental procedure

The bases of technology of volumetric shear under pressure are stated in [3]. For realization of severe torsional strain under pressure a special chamber has been designed and made allowing to deform directly in devices of the standard breaking machine with simultaneous registration by methods of introscopy of microstructural surface changes. The produced structure and the properties of a surface were investigated by methods of XRD analysis, kinetic microindentation, dynamic sclerometry and profilometry. Disk of a given thickness were used which were firat exposed to normal compression. At the fixed value of compressive stresses, severe torsional deformation at a given speed was used. The dependence of a rotation angle on torgue value for various value of compression pressure was established. From the moments of rotation the shear stress was calculated and coefficient of friction of contacting surfaces was estimated. The machine 2167-P50 (diameter and thickness of samples of about 5—10mm) with computer registration of external tribomechanical parameters was used. The velocity at torcional deformation varied within the limits of 0.01-1 rad/s; speed of compression was constant and equal to $10^{-3}$ $c^{-1}$.

For realization of contact friction the anvils [3] were used as truncated cones from alloy ВК-6 past special thermal processing.

The basic material of research was high-nitrogen steel such as Х18АГ10Н16 with $C_N$=0,06-0,57%N in austenite condition, as it is the most promising for use in extreme conditions of operation.

## The basic results of research

The in-situ technology of surface structural hardening of materials has been developed and realized. The technology is a complex usage of methods extreme-friction surface structure formation and of in-situ methods of continuous registration structure-sensitive parameters, such as: temperature, electroresistance, acoustic emission.

Surface sudmicro- and nanocrystalline structures of extreme dry friction in ausnenite of high-nitrogen steel at severe turn plastic deformation under high pressure have been for the first tiuce formed. The results of tribological researches have shown, that: the curve of dependence of shear stress on value of surface torsional deformation has a stage-like character, it is marked: a) a stage of elastic behaviour at friction-contact interaction; b) a stage of surface plastic deformation with fragmentation of structure of extreme friction c) a stage of surface structural - phase hardening at frictional interaction of contacting bodies. It is revealed, that a broadening and intensity of x-ray lines were unmonotonously changong with the increase in shear-stress, that correlated with non-monotonous change of temperature, electroresistance and increase of intensity of acoustic emission. For P< 1GPa rotation through an angle of severel radians resulted in a significant incrising diffuse scattering at the x-ray diffraction from the extremely deformed surface layer. The quantitative processing of x-ray diffraction patteerns in the field of the large and small angles of reflection has shown presence nanodimentional elements of surface structure of friction of about 80—20nm ([n value of coherent scattering region) occupying more than 60% of the tota quantity l of structural elements of a surface layer. It is shown, that the process of formation of nanocrystalline structures of friction depending on nitrogen concentration there occurs a transition from the mechanism of sliding (for $C_N$=0,06%N) to twinning and rotational mechanism of plastic deformation in the material of a surface layer of contacting bodies (for $C_N$=0,3—0,57%N). It is revealed, that depending on nitrogen concentration in local zones of the actual area of contact a surface layer of the increased nitrogen concentration (secondary austenite of friction) is formed, that results in a substantial growth of hardening of the surface layer connected with direct and inverse martensite transformation (nitrogen-phase hardenong) and the beginning of the nitride phase precipitation in the surface layer. It is revealed, that for steel with $C_N$=0,3—0,57%N surface naclep is lager then at small deformation while situation is opposite for steel with $C_N$=0,06%N. It is shown, that for the given concentration of nitrogen in austenite of high-nitrogen steel there is an optimum torsional strain at which the hardening of the surface is maximum. The concentration dependence of the factor of friction high-nitrogen steel austenite.

By in-situ methods of kinetic microindentation and dynamic sclerometry it is shown that the physical-mechanical properties of surface layers are non-uniform on thickness of the formed structure.

The kinetics of changes in the yield strength in temperature range of the maximal diffusion mobility of nitrogen atoms during isothermal and isochronous annealing of surface structure. Three stages of physical-mechanical properties recovery and stabilization of surface structure are revealed. Essential relaxation of internal elastic stresses, small change of the yield strength and absence of grain growth characterize the first stage. At the second stage a significant reduction of yield strength and insignificant uniform growth of the grain sizes is observed. The third stage is characterized by further weaker reduction of yield strength and significant non-uniform grain growth with the increase in dispersivity with the size. The values of the energy of activation at the first and third stages are equal to 40 and 90 kJ/m$^2$ accordingly, that is satisfactorily agree with the energy of activation of dynamic recovery and thermal recrystallisation.

## References

1. Пшибыльский In. Technology of superficial plastic processing. M, Metallurgy, 1991.
2. Любарский И.М., Палатник h.p. Металлофизика of friction. M, Metallurgy, 1976.
3. Бриджмен П., In the Newest works in the field of high pressure (пер. With англ.) m. OR, 1948.

# DEVELOPMENT OF NEW WAYS OF THE SOLDERING OF NON-METALLIC MATERIALS WITH METALS FOR SPACE ENGINEERING

**Naidich Yu.V., Zhuravlev V.S., Gab I.I., Kurkova D.I., Stetsyuk T.V., Chernigovtsev E.P.**
Frantsevich's Institute for Problems of Materials Science of NASU
03680, Kiev - 142, 3 Krzhyzhanovsky St., 3, naidich@ipms.kiev.ua

During the brazing of non-metallic materials both at the Earth and in space conditions there is a number of technical difficulties. For example, results of the performed theoretical analysis of the liquid menisci form in the conditions of microgravitation bring us to a conclusion that during the brazing of units with wide ring-type soldering gaps under conditions of space and perfect wetting (interfacial wetting angle Θ=0) cutouts and cavities in the gap since it will be filled with solder only parttially. If the greater gap filling is necessary, special alloys need to be used or special conditions for realization of large (within the reasonable limits) values of interfacial angle should be created (Fig. 1). During performance brazing operations in weightlessness there are also some other problems, e.g. solder feeding in the gap (in terrestrial conditions gravitation are frequently used for this purpose). In this connection methods of solder feeding through the special conductors, which wettability is high (the positive spreading coefficient: $S = W_A - W_K$, where $W_A$ and $W_K$ are work of adhesion of a liquid to a solid and work of cohesion in the liquid, correspondingly), were developed. On these conductors solder goes, or "creeps", in the necessary direction (even reverse to the gravitation direction) (Fig. 2).

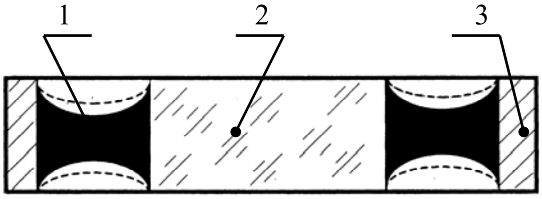

Fig.1. The form of molten meniscus in the ring-form wide gap during the soldering at weightlessness (Θ~0°). The dotted curve for Θ=60°: 1 – molten solder; 2 – quartz glass; 3 – metal holder block.

For manufacturing of a number of brazed non-metal/metal units necessary for space engineering, in particular, of quartz-metal windows with high optical characteristics it is necessary to use wide brazed junctions in order to decrease the heat stresses caused by different thermal expansion of non-metallic and metal details. Under the terrestrial conditions solder will outflow from such gaps under action of gravitational forces. In this connection the researches of filling and retention of solder in wide (up to 10 mm) and high (up to 50 mm) brazing gap were carried out and the appropriate technological methods were developed.

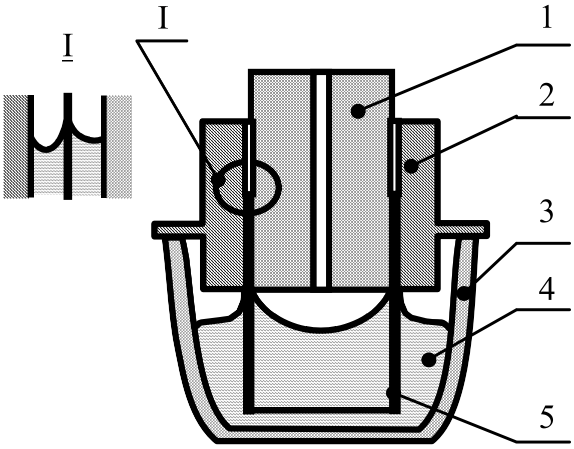

Fig. 2. The schema of the assembly unit: 1 - glass or ceramics; 2 - metal holder block; 3 - ceramic auxiliary crucible; 4 - solder; 5 - metal conductors by which solder is transported.

One of the studied methods of solder retention in the brazing gap is tight lock-out of solder in the gap. For this purpose it is necessary to provide close fit of nonmetallic disk to the supporting part of metal frame. For warping prevention it is necessary for metal detail to be made with a small allowance within the dimensions of supporting flange, to be annealed at more severe conditions than conditions of the brazing, and also it is necessary to level the supporting flange. For large-sized products such operation can be repeated for some times until preservation of support planeness. For prevention of solder leakage from brazing gap the following measures are taken:

1 – the method of more tight junction of quartz glass and metal details during assembly of

details before the soldering with the help of special sealing pastes has been developed. It has allowed us to made, in particular, the joint of the quartz window 50 mm in diameter and 50 mm thick (brazing gap height);

2 – it was recommended in some cases to use alloys with less density as solders. Thus, the density of molten lead (typical solder for connection of a quartz glass) amounts to about 11 g/cm$^3$, but this value for indium is equal to ~ 7 g/cm$^3$. It means that hydrostatic pressure in brazing gap will be ~1,7 times less, i.e. it is easier to retent such metal liquid in the high non-capillary gap. Certainly, it would be possible to use more light-weighted metals (for example, aluminium with density equal to ~2,5 g/cm$^3$), in which case the situation should become even more favorable, but aluminium does not fit for the brazing of glasses for some other reasons.

The other studied method of solder retention in the wide and high non-capillary gap is its artificial division into a number of capillary gaps by means of placing of capillary structures and diaphragms into the gap. It can be the capillary cells made from thin tin-plate of various configuration or powder spongy fillers. In the present work filling of the gap with capillary foil structures is considered.

In order to determine the capillaries sizes which were technologically suitable for such type brazed joints manufacturing the sample with flat capillaries of various width (capillaries are made from titanic foil and annealed in vacuo at T ~ 700°C) is produced. Results of researches have shown that lead is kept in gaps no more than 0,15 – 0,20 mm wide.

With the use of these data, two models of brazed windows was made from quartz glass 65 mm in diameter and 10 mm thick with the average (calculated) size of flat (circumferential) capillaries of 0,15 mm (one model – with thin foil support for capillaries and another – without a support). As a result of models examination it turned out that the joint is well formed but there are individual chips in glass that is evidence of significant tension existence in the brazing zone.

For improvement of system capillarity and reductions of tension the two-layer capillary structure with the 1,5×2,5 mm capillaries sizes was produced and all details in the brazing zone are metallized with tin - titanic (1,5 % Ti) paste. The procedure is as following: T = 750°C, $\tau$ = 5 minutes, coating thickness– not less than 0,15 mm. Such system provides good wetting at melting temperature of lead which comes from additional feeder.

Except for the described capillary structures, for solder retention in brazing gap the ring metal diaphragms representing a set of hollow thin-walled metal cylinders with diameters increased by fixed step from value of diameter of quartz glass being brazed. These cylinders were located concentrically in the brazing gap 10 mm wide and 40 mm high and intervals between them were filled by solder. The other mode of the diaphragm application was its spiral-shaped placement together with the solder tape in the brazing gap. Copper foil 0,1 - 0,15 mm thick was used as a material of the metal diaphragm. Application of foils made from more hard metals is unwanted since residual thermomechanical stresses would increase in such a case.

Thus, using the developed methods and techniques it became possible to made large-sized (up to 250 mm in diameter) brazed metal-quartz windows with high optical characteristics for use in space instrumentation.

Also recommendations and methods of carrying out of process of the soldering of non-metals with metals immediately in the space environment (aboard the orbital station) were developed.

The present study was carried out under the STCU project NN-35.

# COVERINGS OF TYPE HYDROXYAPATITE-GLASS ON THE TITANIUM FOR WORK IN EXTREME CONDITIONS

**Ivanchenko L.A., Pinchuk N.D., Zyrin A.V., Kuzmenko L.N.**
Frantsevich Institute for Problems of Materials Science of NASU,
3 Krzhyzhanovsky St., Kyiv, 03142, Ukraine, E-mail: osteo@ipms.kiev.ua

Glassceramics on a basis of silicate-phosphates of calcium represent rarefied dispersed environment such as "sphere-cluster-series". The new composite materials consisting of a structural combination silicate and phosphates clusters incorporated by chains, and possessing the advanced surface, show low heat conductivity and thereof are of interest as heat-insulating coverings [1].

The combination of physic-mechanical features of substrates from the titan and layers silicate-phosphates of calcium ceramics on their surface will allow to expand opportunities of reception of new kinds of heat-insulating protection for electrical engineers and some kinds of instrument making. One of the important applications of such coverings is reception metal implants which surface is protected by biologically active material for the fastest implantation and safety of long existence in extreme conditions of an alive organism.

The purpose of this work is creation and research of new coverings with low heat conductivity on substrates from the titan or its alloys possessing wide prospects of practical use.

Hydroxyapatite-glass composite materials were developed by us, investigated for application as biomaterials earlier and described in [2-4]. The structure of one of composites is specified on fig. 1. Other structures of composites differ a ratio of hydroxyapatite-glassphase, thus the amount of the glassphase changes within the limits of 15-70 mass % (table 1). The manufactured specimens were tested the composition and the structure of by X-ray, chemical and IR-spectroscopy analyses.

The investigated comparative physical and chemical characteristics of glass ceramics on the basis of silicates of sodium and phosphates of calcium with a various ratio of the phases, including picnometric density, porosity, mechanical strength, factor of thermal expansion etc. have shown perspectivity of their further use as biomaterials [5].

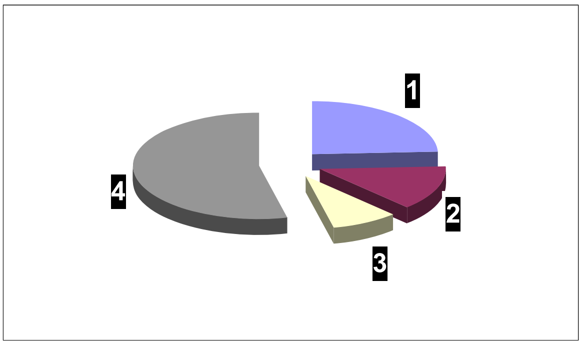

Fig. 1. Structure of a ready hydroxyapatite-glass composite , mass %:
1, 2, 3 - glassphase (oxides of silicon, sodium and boron, accordingly); 4 - hydroxyapatite.

Table 1
Some parameters of composites hydroxyapatite-glass

| Composite | Hydroxyapatite, mass % | Ave-rage porosity, ±5 % | Picnometric density, ± 0,01g/cm$^3$ | The maximal strength, ± 5 MPa | |
|---|---|---|---|---|---|
| | | | | On compression | On a bend |
| 1 | 32,809 | 18 | 2,75 | 184 | 34 |
| 2 | 50,274 | 23 | 2,86 | 131 | 25 |
| 3 | 68,508 | 25 | 2,87 | 91 | 12 |
| 4 | 85,103 | 40 | 2,89 | 51 | 5,6 |

High-speed heating of the above-stated powder mixes on air with the help of radiant energy allows to determine the high-temperature behaviour of materials, enables to study their interaction with titanic substrates and to exclude thus possible negative factors of heat treatments at different ways.

Researching the factor of thermal expansion of composites have shown, that they are in limits $(1{,}307\text{-}1{,}444)\cdot 10^{-5}$ degree $^{-1}$ in a temperature range 30-630 ºC. This parameter is $(0{,}8\text{-}1{,}5)\ 10^{-5}$ degree $^{-1}$ for the titan oxide which practically exists on a surface of titanic substrates and $(1{,}1\text{-}1{,}4)\cdot 10^{-5}$ degree $^{-1}$ for composites of type the titan oxide - hydroxyapatite approximately in the same temperature range [6]. Hence, these materials are compatible on the factor of thermal expansion that excludes an infringement of a covering integrity at high-speed changes of temperatures of heating and cooling of samples.

Preliminary tests of change of structural characteristics of the specified glass ceramics under action of the concentrated streams of radiant energy are carried out. For carrying out of experiment arrangements "СГУ-2 "and "СГУ-4" have been used. The concentrator of a solar beam is 4 mm in diameter. Heat treatment of composites as powders and ready compact samples has been carried out in alumina ceramics crucibles and as free poured powders on titanic substrates. Various modes of heating are used: a corner of disclosing jalousie from 10 º up to 50 º, speed of opening jalousie 2,5 º/min, exposure of 10 minutes at the maximal corner of disclosing.

It has been established, that partial melting a composite occurs under action of the concentrated sunlight. The melting intensity depends on a ratio of hydroxyapatite-glassphase in a material. Superficial interaction of titanic substrates with a free poured composite powder is observed. Formed coverings are non-uniform on the area and on depth.

In this connection, row mixes of samples with blowing agents have been used in the further researches for reception of more homogeneous coverings on the titanic substrates. It was supposed that synthesis of composites and their simultaneous interaction with a surface of substrates should be carried out under action of a sunlight. The mode of heating was similar above-stated, but the exposures made 20 seconds at the maximal corner of disclosing.

The visual analysis of the received coverings has established, that the coverings were the most homogeneous on colour and a macrostructure when they were based on the row mixes of the composites containing ~50 mass % of the glassphase.

Adhesion of such coverings appeared the highest in comparison with coverings on the basis of composites with the smaller glassphase contents. Adhesion can be improved, if the sublayer of the glassphase is put on titanic substrates which further becomes covered by a layer of a composite. Thus composites with the smaller glassphase contents can be used for reception of coverings with a gradient structure and necessary physical and chemical characteristics.

The possibility of obtaining composite coverings of type hydroxyapatite-glass is investigated on the surface of specimens made from spongy titanium of complex configuration by the method of thermal burning in the muffle furnace. The adhesion of such coatings also depends on a quantity of glass phase in the composites. The physical chemistry properties of coatings are studied.

### References:

1. Т.Каназава. Неорганические фосфатные материалы: Пер. с англ. – Киев: «Наукова думка», 1998. – 297 с.
2. Ivanchenko L.A., Falkovska T.I., Danilenko N.V., Zyrin A.V., Kobilochna L.G., Pinchuk N.D., Vorobey V.V. (1999) Structure and properties of a high-porosity glass ceramic containing biological hydroxyapatite, Powder Metallurgy and Metal Ceramics **38**, P. 418-453.
3. Иванченко Л.А., Фальковская Т.И., Пинчук Н.Д., Лаврентьева О.В., Логунова И.А. Получение и свойства упрочненного стеклофазой гидроксиапатита // Порошковая металлургия. – 2003, № 1-2, - С. 62-68.
4. Иванченко Л.А., Пинчук Н.Д., Крупа А.А., Фальковская Т.И. Структура и свойства композиционного материала на основе гидроксилапатита // Стекло и керамика. - № 6, - С. 30-31.
5. Пинчук Н.Д., Иванченко Л.А. Технологические процессы получения кальцийфосфатных биоматериалов // Порошковая металлургия. – 2003, № 7, - С.36-52.
6. E. Fidancevska, G. Ruseska, S. Zafirovski, B. Pavlovski Thermal-expansion and Mechanical Properties of the $Ca_{10}(PO_4)_6(OH)_2$–$TiO_2$ Composite. Science of Sintering, 34 (2002) 241-246.

# DEVELOPMENT OF LIGHTENING-PROTECTION NETS FOR

# REINFORCING CARBON FIBER-REINFORCED PLASTICS

**Vishnyakov L.R., Kokhaniy V.O., Кokhana I.M., Neshpor O.V., Korol A.A.**
Frantsevich Institute for Problems of Materials Science of NASU,
3 Krzhizhanovsky str. 03142, Kyiv, Ukraine, E-mail: vish@i.com.ua

Constructions made of reinforced polymer composite materials (PCM) are being widely used in modern engineering. The use of PCM in aircrafts causes a problem in view of an ability of PCM to accumulate charges of static electricity and destroy when stroke by a lightning. Therefore, the design of a protection system able to protect aircrafts against static electricity and lightning is of great importance.

We suggested to use knitted metallic nets made of copper wire of 0.07-0.12 mm in diameter covered with tin-lead solder to produce lightening protection, current-sinking systems for PCM based on carbon-fiber reinforced plastics (Patent of Ukraine No.6198, 1994). These nets performed well as reinforcing elements for lightning-protection covering during a long period of operation in a lot of airplanes. However, a high electric resistance due to the loss of electrical conductive capacity in mobile contacts of loops because of a loose adjacency between the loop wires is a shortage of a knitted net. Besides, binder may penetrate into the interstices between the contacting wires of a net while formation of a covering upon the polymer composite panel. This also reduces electric conductivity of the net fabric and the PCM resistance to lightning strike.

Accounting for the above features of the knitted net structure, the development was aimed at the design of a lighting-protection covering having a conductive layer made of knitted metallic fabric, the wires of which form fixed joints at their contacting sites. Soldering of such contacts by a tin-lead solder was choose as a method of making such joints. It was found that soldered joints provided a substantial increase of electrical conductivity of the knitted fabric in the loop column direction due to a reliable contact established between the loops, and prevents penetration of the binder into the wire interstices.

The knitted net fabric retains its high resistance to stretching being its main advantage, without the rupture of the net.

Description is offered how the lightning-protection net operates in a PCM during a complex destruction of carbon fiber reinforced plastics, under the lightning strike. In particular, it was established an improvement of the soldered knitted net resistance to the mechanical factor accompanying the lightning strike, i.e. the loosen loops take a part of mechanical load through deformation due to a lower strength of the solder material and the process of its evaporation:. This is favoring for decreasing of the pulling the wires out of the covering and thus the damage occurence due to reduction of the cleavage of the panel.

The metallic knitted fabric can be prepared by interweaving techniques such as «Eraser».

Various knitted metal fabrics were tested to select the nets knitted by «eraser» mode as most useful because their weight, electrical and strength characteristics.

Processing conditions for making material with desired characteristics were determined on a proper specialized machine for net soldering. The quality of soldered net fabric was characterized using our proper methods through measurement of specific resistivity.

The nets and other current-sinking patterns including copper foils of Astrostrike type (USA) were comparatively tested.

The studies permitted amelioration of the structure and composition of lighting-protection elements. Initial requirements useful for the development of pilot or industrial technology of making lightning-protection materials were developed, which are now implementing into the aeronautical industry.

# GLUING TOGETHER OF NITRIDE, CARBIDE AND CORUNDUM CERAMICS FOR EVALUATION OF GLUED ARTICLES ADAPTABILITY UNDER EXTREME CONDITIONS

**Baranova T.F, Vikulin V.V, D'jachenko O.P, Kelina I.Ju., Kurskaja I.N**
Federal State Unitary Enterprise
"Obninsk Scientific Industrial Enterprise "Technolodiya", Obninsk, Russia
15, Kyiv high road, Obninsk, 249035, Russia

The process of glued joint formation has been investigated using the samples and articles from silicon nitride, silicon carbide and sintered corundum. Ceramic glue presents a two-component composition: filler – binder (of the silicate and phosphate types). One of the components – $Si_3N_4$, SiC, $Al_2O_3$, along with non-oxide and oxide additives including aerogels, was used as a filler.

The structure and strength properties of glue joints have been examined depending on materials porosity and oxidation level at various firing temperatures.

The open porosity of the materials based on non-oxide compounds and of corundum materials measured 14-24 % and 0.05 % respectively. Shear strength values were in the range from 4 to 18 MPa. Heat resistance of the silicon nitride samples depended on the firing temperature, which determined their oxidation level.

All samples were fired at 1000, 1300 and 1400°C in oxidizing atmosphere. Then the samples were subjected to thermocycling with the temperature difference 1000-20 °C (air). The samples, which were oxidized after gluing, are broken up, while unoxidized samples are broken in amounts of 30 %.

Gluing together technique was applied in the production of long-sized thermocouple sheaths used in the measurement of ceramics firing temperatures in gas furnaces (sheaths from $Al_2O_3$), temperatures of molten metals in the melting plants (sheaths from silicon nitride).

Service life of glued corundum sheaths at a temperature of 1500-1550°C in the firing furnaces measured 1.5 year, of the $Si_3N_4$-based sheaths – 1-2 months and when employing these sheaths as chlorine supply tubes – up to 1 month.

# PERSPECTIVE TECHNOLOGY OF OBTAINING NANOCOMPOSITE FERROMAGNETICS FOR MAKING MATERIALS WORKING IN EXTREME CONDITIONS

**Kuschevskaya N.F.** ⁽¹⁾**, Kuschevsky A.Ye., Oleshko A.I.**
Institute for Problems of Materials Science of I.N. Frantsevich NAS of Ukraine,
Krzhizhanovsky str., 3, Kiev 03142, Ukraine
(1)Institute of Colloid Chemistry and Water Chemistry of A.V.Dumansky NAS of Ukraine,
Vernadsky str., 42, Kiev 03142, Ukraine

Now explorations intensively develop in the field of obtaining and practical using of nanosized ferromagnetic powders. For the theory and practice of obtaining of metal magnetic powders the great significance is given to problems of dispersity, corrosion resistance, phase composition and structure of particles. The solution of these problems allows to create new modern materials of technical assigning, usable in extreme requirements.

Today we have resolved a problem of obtaining nanocomposite ferromagnetic powders by a thermochemical method with the surface of particles protected from oxidizing on air and given complex of properties, which are implemented simultaneously in practice. The physicochemical principle of their synthesis on the basis of metals is requested for exploration and operations on making technology of obtaining of powders by a method of a chemical deposition of salt of metal, obtaining of its precipitate in nanodispersive state with the subsequent reduction in the of hydrogen flow. As a result, nanocomposite powders of iron were synthesized and iron – cobalt - nickel in stable chemically inert state, not pyrophoric, corrosion-resistant and with a given complex of properties [1]. On the basis of properties of obtained powders the attempt to solve the following practical problems was undertaken:

-making composites with nanostructural components on the basis of epoxide oligomers (glues, glues - potting compounds, potting compounds etc.);

-working methods and materials for potting of flaws, fistulas etc. defects on effective main gas-pipelines operating in extreme conditions of environment, under collateral action of temperature, water, its vapours, oxygen, ultraviolet radiation, salts dissolved in water, biological factors etc.

The used compositions not always are up to quality, presented by such operations. The special difficulty is repair works, in particular, welding to eliminate gas escape from the different kinds of discontinuity flaws (fistulas, flaws, microcracks etc.) rormed in operating pipelines. Therefore, application of composites with nanostructural components, which trusty operate in extreme conditions proved to be rather perspective in such operating.

The results of full-scale investigations of our of materials with usage of nanocomposite ferromagnetic powders as filler, plastifiers to rise frost resistance etc. guarantee adhesion of linkings metal - metal in the temperature range from minus 50 $^{o}$C up to plus 50 $^{o}$C at pressure 65 MPa within 5 years. Thus, utilised glues, the potting compounds have heightened toughness, temperature capability, resistance to formation of crack and its growth, corrosion resistance.

Thus, the practical results, obtained by us, testify to prospects of technology of obtaining nanocomposite powders of ferromagnetics and actuality of making on their basis or with their application of new composites working in extreme requirements.

References

1. Kuschevskaya N.F. Physico-chemical conditions of syntesis of Nanocomposite ferromagnetic powders for biomedical application. Avtoref. dis. for drs techn. sciences / K.: Sciences world, 2003. –39p.

# STUDY OF POSSIBILITY OF QUALITY IMPROVEMENT OF LARGE-SIZED COMPLEX-SHAPED CERAMIC BLANKS MOLDED ON THE BASE OF SLIPS OF INORGANIC MATERIALS

**Kharitonov D.V., Suzdaltsev Ye.I.**
Federal State Unitary Enterprise
"Obninsk Research and Production Enterprise "Technologiya", Obninsk, Russia
15 Kiev. Str., Obninsk, 249035, Kaluga Region, Russia,
onpptechn@kaluga.ru, info@technologiya.ru

The process of ceramics manufacture consists of such main stages as preparation of starting material (powder, slip), putting it into a necessary shape (molding), firing (formation of the structure and determination of ceramics physical/technical properties). Blank molding stage occupies particularly important place because it determines the properties, shape and dimensions of the articles. Many different methods of ceramic blanks molding are known, but only slip-cast molding enables one to make complex-shaped large-sised articles.

Slip-cast molding is a blank molding method which involves filling the aqueous slip into the cavity of a porous mold made of hygroscopic material and holding there for some time. The articles are molded due to the capillary forces of the mold material suction; these forces cause the movement of liquid phase towards the mold wall. Slip solid particles also move towards the mold walls along with the liquid. The liquid accumulates in the mold pores, and solid particles deposit and they are being packed on the mold walls forming the gradually increasing layer.

However, there is one essential shortcoming in the method of slip-cast molding of large-sized complex-shaped blanks, namely long duration of blank molding process with the result that the blank body formation takes place not only due to the capillary forces of the mold material suction but as a result of thedeposition of larger particles [1].

The researches carried out into the molding of large blanks of various shape confirmed the assertions of the authors of paper [1] that the gradual filling of the mold cavity with solid sediment from lower part of the cavity to its upper part takes place in the course of formation of the walls of a large-sized blank on the base of aqueous slips. In so doing the blank walls formation was stated to be slowed down in the blank upper part by a factor of 1.5-2.0 as compared with the lower part. This causes difference in the grain composition and blank density in height and thickness. Such difference in density results in different degree of blank sintering which causes the geometry distortion, cracks arising, deterioration of article physical/mechanical properties. Thus, from the above reasoning, increase in blank formation speed and decrease in gradient of wall formation speed throughout the height of the blank can become one of the ways to improve the quality of large-sised complen-shaped ceramic blanks molded on the base of the slips of inorganic materials.

In paper [2] the authors have studied the various factors (parameters of the slip, material of the molds, pressure difference on the mold walls and others) which affect the ceramic articles molding speed, ft is stated that the elecrtrophoretic molding method appears to have the most promise in solving the arised problem. This method consists in directional movement of charged particles of ceramic mass under electric field and also in deposition of these particles on the oppositely charged electrode. On the base of the further researches the authors [3] have developed the kit for electrophoretic molding of large-sised complex-shaped ceramic articles. The present work was carried out just with the use of this kit.

Large-sized complex-shaped ceramic blanks have been made as a result of researches carried out by the method of electrophoretic molding on the base of aqueous slips prepared with the use of aluminosilicate glass. The duration of the present blanks molding is only 1.5 - 2.0 hours, which is 10 times, less than it was in the traditional slip-cast molding. Such acceleration enables one to assume that there is no delamination in height, which is typical for slip-cast molding. The further researches confirmed completelythis assertion.

Besides, the authors have investigated the influence of various factors (value of applied voltage, slip parameters) on the quality of the blanks. The optimal values of applied voltage have been set as a result of researches carried out; it is found that the slip parameters do not have considerable influence on the blank molding process in ceramics electrophoretic molding, which widens essentially the possibilities of the technology.

Thus, the possibility of manufacturing the large-sized complex-shaped ceramic blanks with improved quality has been established as a result of researches carried out.

## BIBLIOGRAPHY

1. Ye.l. Suzdaltsev, V.I.Kurakin. Account-theoretical model of the formation of ceramic blank wall thickness in slip-cast molding in porous molds. // Refractories and technical ceramics (OrHeynopw H TexHHMecKaa KepaMHKa), 2001, N°10, p.8-11.
2. Ye.l. Suzdaltsev, D.V.Kharitonov. The present state and perspectives of the blank molding on the base of aqueous slips of inorganic materials. // Refractories and technical ceramics, 2002, N° 12, p. 4-7.
3. Ye.l. Suzdaltsev, D.V.Kharitonov. The researches and development of the kit for electrophoretic molding of the ceramic articles. // Refractories and technical ceramics, 2003, *N*° 10, p. 12-20.

# EFFECT OF CHEMICAL PURIFICATION METHODS ON STRUCTURE PARAMETERS OFNANOCARBON MATERIALS

**Len T., Ovsienko I, Kopan V., Matzui L., Brusilovets A., Sharff P.(1), Kapitanchuk L. (2)**
Shevchenko Kyiv National University, Kiyv, Ukraine
Glushkov ave. 2, Kiyv, 03680, Ukraine, Ukrainetalen@univ.kiev.ua
(1)TU Ilmenau, Institute of Physics, D-95684 Ilmenau, Germany
(2)Paton Institute for Electric Welding of NASU, Kyiv, Ukraine, 3 Bozhenko Str., 01006, Ukraine

Carbon nanotubes is the novel carbon form with unique physical and chemical properties. As known while the nanotubes are obtained by he arc discharge method, the produced on the elelctrode surface deposition contains the nanotubes beside a lot of inpurities including as metal particles such particles of amorphous carbon. That is why the development of purification methods and investigation of influence of these methods on the structure of obtained nanocarbon materials are urgent tasks.

The presented work investigates the changes of structural parameters of nanocarbon materials during purification process.The carbon depositions formed on the different regions of electrode were used as initial material. The following scheme was proposed for purification of carbon deposition. The main stages of this scheme are:

1. Heating of raw material in nitric acid solution (2,5 M) for removing catalysts particles.
2. Sequential material washing with distilled water, caustic soda solution (pH 10—11) and ethanol.
3. Vacuum dehydration at temperature T=110—120 °C during 5,5 hours. This stage is necessary for partial nanotubes structure recovery, which was possible damaged during acid treatment of nanocarbon material.
4. Open air oxidation at T=550 °C during 30 minutes for removing amorphous carbon particles.

The structure parameters of purified material are investigated by methods of X-Ray diffractometry (diffractometer ДРОН- 4 07 in filtered Co Kα radiation) and scanning electron microscopy (SEM, JSM–840, JEOL, Japan).

The Fig.1 shows diffractograms raw and purified samples obtained from different regions of cathode surface.

As can be seen from figures 002-lines of graphite are found in diffragtograms obtained for all samples.

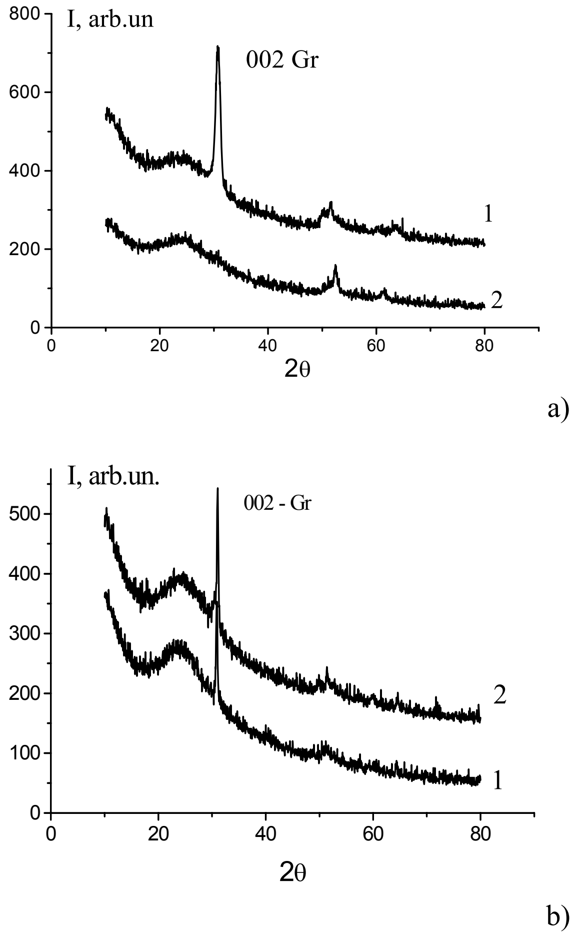

Fig.1. Diffractograms of the samples obtained from different regions of cathode surface: a) from the top of cathode; b) from the surface of cathode; 1- the raw samples; 2 – purified samples.

Difractogram for sample obtained from the top of cathode also exposes the 004-line and weak 101-line of graphite. According to the date of SEM the material obtained from the top of cathode is solid carbon mass with included single nanotubes with diameter up to 30 nm. The sample obtained from cathode surface is dendritic structure with single nanotubes with diameter up to 6 nm [1]. Thus 002-lines of graphite corresponds either CNT or nanocarbon particles. After purification 002-line of graphite in the sample from cathode surface is remained, although it becomes non symmetric. For sample obtained from the top of cathode, lines corresponded to reflexes from graphite layers are disappeared. It can be caused by effect of acid treatment on the initial material that makes to formation of fine amorphous phase or single nanographite shifts.

The Fig. 2 presents SEM images of purified samples surface from different electrodes.

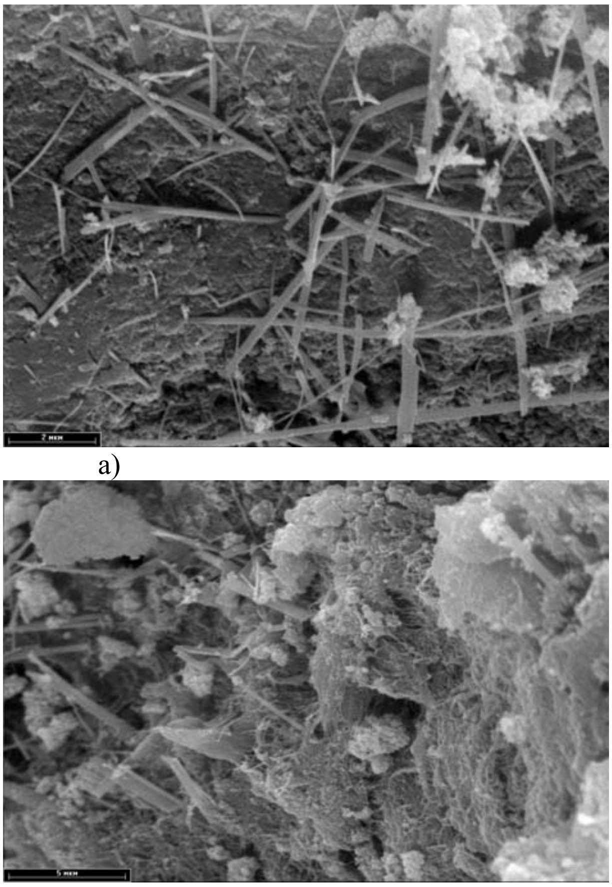

a)

b)

Fig.2. The SEM images of surface of purified samples obtained from different electrodes: a) from anode; b) from the top of cathode.

In the sample from anode (Fig. 2, a) after purification a lot of new structures are formed. These new formations are similar to “nanoscrolls”. The average diameter of these “nanoscrolls” (up to 300 nm) is essentially greater than diameter of multiwall nanotubes presenting in raw material. The sample obtained from the top of cathode after purification (Fig. 2, b) presents single “nanoscrolls” with diameter up to 500 nm and single nanoshifts.
As it is shown from (Fig. 1) diffractograms for raw samples also demonstrate the lines of catalysts presented in raw materials. These are nickel, cobalt, and iron. After purification these lines remained although their intensity is changed.

In order to clarify what catalysts is remained in samples after purification the investigations of temperature dependence of magnetic susceptibility by Faraday method were carried out. For samples obtained from anode and surface of cathode the behavior of temperature dependence of magnetic susceptibility for raw and purified samples practically isn’t changed.

The result of investigations of temperature dependence of magnetic susceptibility for sample from the top of cathode is presented on the Fig. 3.

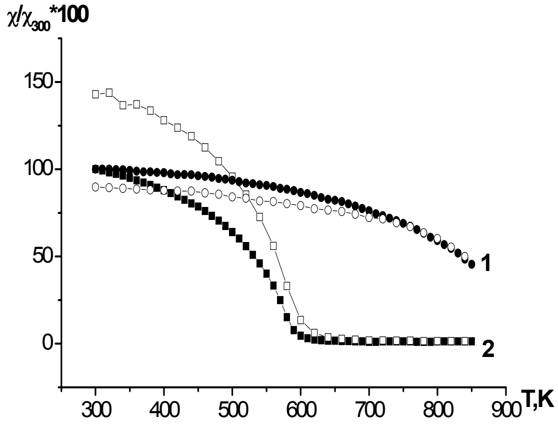

Fig.3. The temperature dependence of magnetic susceptibility for sample obtained from the top of cathode: 1- raw material, 2 – purified material.

As it is shown from Figure in this material after purification the curve of temperature dependence of magnetic susceptibility presents the transition, which is typical for pure nickel, although the temperature of this transition is decreased in comparison with pure nickel. This evidences that relative contain of nickel after purification was increased in comparison with contain of cobalt and iron.

Thus, proposed scheme of purification of raw nanocarbon material results in the change of contain and structural characteristics initial material. These changes are determined by such purification procedure as position of initial material on the electrode surface.

1. Ovsienko I., Len T., Babich N., et al. Structural characteristics of nanocarbon materials. In these tes.

# TECHNOLOGIES PRESSING OF THE CERAMIC POWDERS, BASED ON USE OF COMBINED AND CYCLIC DEFORMATIONS OF THE PRESSING MATERIALS

**Zubro Svetlana, Perelman Vladimir**
Lomonosov Moscow Institute of Fine Chemical Technology, Moscow, Russia
pr. Vernadsky, 86, Moscow, 117571, Russia, perelman@mtu-net.ru

The offered technology is base on following cardinal principles.

Any remaining changing density reformatted powdered material without fall is kept a primary phase - a ruining of available structure of material, but efforts, required for realization of this phase, are in each concrete scheme pressing limiting value. So rational schemes pressing are that, in which stage of destroying a material goes under minimum power influences.

Increase of density samples is a function of two arguments: pressures pressing and degrees to deformation, received by the material. Intensity of changing density when increasing any factors depends, in turn, from the current value of corner of internal friction of material, which is a complex evaluation of amount and values of breaks on surfaces of shift an samples. Beside material, having smooth of surface of slide, corner of internal friction is a zero and their density under power and reformatted influences stays constant.

All power characteristic under pressing powdered systems are formed, mainly, on surfaces of shift in material, but projection of these power characteristics on planes, parallel and orthogonal to the direction of main compression, close to the value of shift toughness of material on these planes. This rule is executed more exactly under pressing ceramic powder, as well as powders with particles an even the form.

When changing a direction pressing deformation goes along new surfaces of shift, on stage of shaping which corner of internal friction of ambience has a greater value. Herewith molded material does not become isotropic, as far as realignment of structure is accompany by destroying the relationships between particles on formed earlier surfaces of shift, but since relative displacing the particles go when changing a direction of deforming in directions, cross these surfaces of shift, this leads to the growing of corner of internal friction along these directions. Thereby, under each change of power and deformed influences will be reconstruct usual anisotropy structure of material. Note that in initial stage of this process, to which shaping of new and ruining of old structure only begins, structure of material close to isotropic. Required For the packed realignment of structure, value deformed influences depends on source parameters of powder, from density of material and from the value of current average voltages in the material.

Optimum is such changing a direction deformed influences, under which new surfaces of shift will develop along the most weak on shift toughness of surfaces in the material, formed on the preceding stage of power and deformed influences. These surfaces, naturally, have the most values of corner of internal friction and are direct parallel and orthogonal direction pressing.

Under pressing ceramic material already on early stages pressing under big relative porosity dog-legs on surfaces of shift disappear and corners of internal friction in the material take values close zero. Essential reduction of porosity of such structure to the account of increase as pressures pressing, so and degrees by the get material to deformation at the conservation of scheme pressing, at the conservation of direction of power and deformed influences, difficult for realizing.

Phased frequentative changing a direction of deforming an sample, including and recurrent using one or another directions of deforming leads to shaping on each stage of new surfaces of shift, which will pass along surfaces, to which values of corner of internal friction will differ from the zero. Under the sufficient value of average voltages in the material such relative shifts of particles in different directions will be accompany also by their destroying and such changing a factious composition, which allows to realize more thick packing the particles.

These principles lie in the base of two technologies, passed experienced and is experienced-industrial stage of realization.

For getting on band presses of big stocking up from ceramic masses under small degrees an drawing (less than 2) was used method frequentative phased precipitation (draft) of stocking up in directions, orthogonal direction an drawing. Directions a precipitation (draft) in planes, orthogonal current of material, on each stage were displace comparatively each other. Amount such sediment varied from 4 before 6 once. Minimum degrees to deformation on each stage a precipitation (draft) depending on characteristics of masses were select individually. Except this to the account of round-robin changing an area of transverse sections of material was select one or another degree a precipitation (draft) of material toward, complying with the direction an drawing. Such total deformed influence on molding material has allow get stocking up with high parameters of texture and with even sharing density of mechanical characteristics on the volume of stocking up. This has allow also practically to avoid peculiar to band presses a marriage on S-figurative rifts in central areas samples, which, as a rule, exist at degrees an drawing less than 6. Amounts is experienced industrial party of products by the diameter 240 and 210мм, received on the new technology, form groups of ten thousand pieces.

Developing technology pressing is captive from powder carbide silicon comprises of itself phased shift deformation an samples in planes, orthogonal direction pressing. On each stage a direction to deformation is displace comparatively each other on the corner from 30 before 45 degrees. At, material is subjected to an additional round-robin compression in directions, orthogonal guideline pressing. Depending on amounts of cycles of processing and from values of used pressures pressing remaining porosity of material falls within 15—10%. Technology passes a stage is experienced-industrial mastering on square bars with the side 50 mms.

# SUPERLIGHT CARBON FIBER REINFORCED PLASTIC SHIELDS FOR ONBOARD WIDE-APERTURE RADIATORS AS STANDARD MEASURES FOR BRIGTNESS TEMPERATURES IN THE MICROWAVE RANGE

**Yurchuk E. Meleshko A., Demichev V.**(1)
**FSUE UNIIFTRI Mendeleevo, Moscow region, Russia E-мail: Yurchuk@uniiftri.ru**
(1)Kompozit Corp., Korolev, Russia, 4 Pionerskaya st., Korolev 141070, Moscow region, Russia
Tel. (095) 513-23-26, fax (095) 516-07-00, E-mail: Kompozit.Mat@g23.relcom.ru

Outer space remote measurements of the Earth parameters (land, atmosphere, ocean) by means of microwave radiometers are the efficient method to obtain land, atmosphere and ocean data. A slight relationship between radiometers of microwave range and cloudiness conditions is the advantage over those of visual and infrared ranges.

Required accuracy of determining geophysical Earth parameters makes severe demands to accuracy of measuring brightness temperatures of the radiation objects (within wide frequency band of 0,5…2 K). Such strict characteristics require producing up-date highly sensitive microwave radiometers and precision devices to calibrate them both on ground and in flight.

Thermal wide-aperture radiators [1,2] being similar by characteristics to the ideal black body parameters are most experienced instruments for ground and flight calibration. Onboard wide-aperture radiators (OWAR) make possible the periodic calibration of radiators at their antenna systems outlets, which allows the exclusion of errors due to changes both in the parameters of a receiver and an antenna system depending on the changes in the temperature instrument conditions.

In collaboration with KOMPOZIT Corp. FSUE UNIIFTRI has produced a superlight onboard standard wide-aperture radiator designed for calibrating satellite radiometric modules for Earth remote probing.

The main requirements to OWAR features when designed are that they be of low masses and provide minimum changes in OWAR temperatures since a satellite periodically passes anti-face and sunward sides. So, measurements have revealed that the variation in thermodynamic OWAR temperatures in Meteor-3 from revolution to revolution were about 30 K.

An OWAR radiating element is made of bonded together square (7 x 7 mm$^2$) monocrystalline silicon pins with one end tapered off with apex of 16°. The radiating element is 150 mm in diameter (Fig. 1).

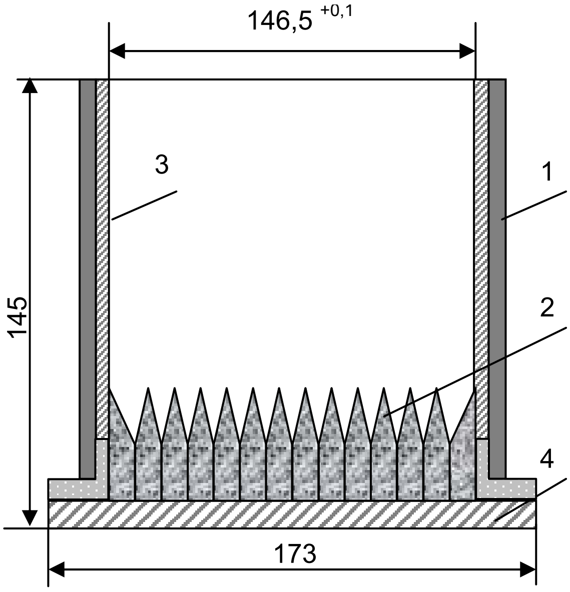

Fig.1 Schematic of the onboard wide-aperture radiator: 1 – carbon fiber-reinforced plastic casing of the shield; 2 – radiating element; 3 – mirror surface; 4 - master board.

The total OWAR mass should not be more than 1500 g. Since OWAR mass could not be reduced through the radiating element, mass should be decreased at the cost of the shield.

OWAR shields are to be of minimum masses, possess good stiffness (better than that of aluminum alloy D16T), high mechanical and heat stabilities that comply with requirements to products operated in outer space, as well as satisfied all ground mechanical and thermovacuum tests. Therefore, to manufacture a shield casing the material of choice that meets the purpose set should be an engineering highly rigid carbon fiber-reinforced plastic.

The OWAR shield (blende) is a thin-walled cylinder of a ~0,4 mm-wall in thickness. The cylinder is 145 mm in height, inner diameter is $146{,}5^{+0{,}1}$mm. A thin-walled flange the cylindrical section of which is an integral structure with a carbon fiber-reinforced shield fixes the shield to the OWAR radiating element. The interior of the shielding cylinder is a mirror surface to reduce noise electromagnetic radiation losses.

A unidirectional LUP-0.1 carbon tape with a 0.11 mm-thick monolayer is chosen as a reinforcing filler for carbon plastics, an epoxy-phenol binder (ENFB) outer space-proven is as a matrix [3]. Physical and stress-strain properties of the chosen carbon plastic along the length of the fiber were as follows: density is 1,5 g/cm$^3$, tensile strength is 0,8 GPa, Young's modulus is 150 GPa, compressive strength is 0,7 GPa. The mirror surface is due to the carbon plastic combined with aluminum-metalized lavsan film of 20 micrometers in thickness.

The steps of manufacturing technique were as follows.

A polished shaping mandrel with a turning for a flange at one end was coated with a thermostable antiadhesion lubricant and heated for four hours at 160 $^0$C, then another lubricant layer was applied. Upon antiadhesion protection a thin-walled flange with its external cylindrical section to be applied by a thin layer of the epoxy binder ED-20 with a hardener PEPA was mounted on the mandrell.

The metalized lavsan film with the end to be fixed on the cylinder flange surface by the epoxy binder was wounded overlapped to some extent on the mandrel. A perform was held for an hour at 60 °C to harden the epoxy binder.

The preform was wound with three layers of the prepreg (LUP-0.1 impregnated with alcohol-acetone solution ENFB and dried to volatile-matter content of about 3%) with further rolling-on by means of a warm roller (50 °C), then coated with fluoro-varnished fabric, and the preform obtained was placed into a metallic cylinder providing an exterior of the blende.

The hardening was in an oven for three hours at 170 °C.

The shields manufactured met requirements imposed to them, and successfully satisfied mechanical and thermovacuum tests and were included into OWARs of FSUE UNIIFTRI development, intended to calibrate satellite radiometers ranging from 140 GHz to 240 GHz.

Bibliograpphy

1. Yurchuk E.F., Arsaev I.E., Zhuravlev A.V.. "Metrological provision of brightness temperature measurement method in the microwave range" – 6 th Specialist meeting on microwave radiometry and remote sensing of the environment, 15-18 March 1999 – Firenze, Italy, Abstract, p.150-151.

2. Saunders R.W. at all "The Radiometric Characterization of AMSU – IEEE Trans on micro-wave theory and Techniques", v.43, 4, 1995, p.760-771.

3. V.Demichev, A.Meleshko. Materials and coatings in extreme cases, V.2, § 3,1 – M.: Bauman MSTS Publisher.

# SINTERING UNDER HIGH PRESSURES – AN EFFICIENT METHOD FOR PREPARATION OF CERAMIC NANOCOMPOSITES

**Bykov A.I., Ragulya A. V., Timofeeva I.I., Klochkov L.A., Gridneva I.V.**
Frantsevich Institute for Problems of Materials Science of NAS of Ukraine
3, Krzhyzhanovsky St., Kiev, 03142, Ukraine E-mail: abykov@materials.kiev.ua

Sintering of powders of refractory covalent compounds is a difficult problem requiring the use of rather high temperatures. It has been shown that high pressures provide conditions for the consolidation of powder by intensive compaction of a powder briquette. The use of high pressures is of particular importance in the preparation of nanocrystalline materials, since a force action intensifies the contact interaction of particles, which accelerates sintering, proceeding at lower temperatures. In this case, high compression stresses provide the retardation of recrystallization processes.

In the work, high pressures were used in the preparation of ceramic nanocomposites with the compositions TiN-$TiB_2$ and $TiB_2$-$B_4C$. A method for evaluating optimal compression stresses, providing the efficient sintering of nanopowders with consideration for their high strength properties, is proposed.

The consolidation of refractory high-modulus composites is considered on the base of an analysis of deformation processes in a porous body. They can be realized by using three major variants of loading of materials with compression stresses: (1) the multiplication of mean compression stresses ($\sigma_{mean}$) in a high-pressure cell at the sites of point contact of particles; in this case, the deformation of the compressed powder body takes place under the condition $\sigma_{mean} << \sigma_0$, where $\sigma_0$ is the compression strength of the material; (2) the material is in the state of uniaxial compression when there exist free surfaces and the condition of deformation can be written as $\sigma_{mean} \geq \sigma_0$; (3) the volume of the material is compressed in three directions and has a limited free surface (the surface of an isolated pore) where it is pressed out; in this case, the deformation condition can be written using the Huber-Mises equation, in which principal stresses attain the values of mean compression stresses in two directions, while in the third direction they cannot exceed the strength of the material and, hence, the equation takes the form $\sigma_{mean} = 2\sigma_0$ and the deformation condition takes the form $\sigma_{mean} \geq \sigma_0$. All indicated variants take place as the density of a powder briquette increases. In the last-mentioned case, the material, being under conditions of large hydrostatic compression stresses ($\sigma_{mean} \geq 1.5$ GPa), deforms in a plastic manner. Such deformation causes the hardening of the material and $\sigma_0$ must be written as $\sigma_t$ (the ultimate strength after hardening under certain plastic deformation). To evaluate $\sigma_t$, hardening curves were constructed from the results of hardness tests of sintered polycrystals with using Meyer pyramids [1]. In the figure, we present a complete strain – ultimate strength curve of titanium nitride:

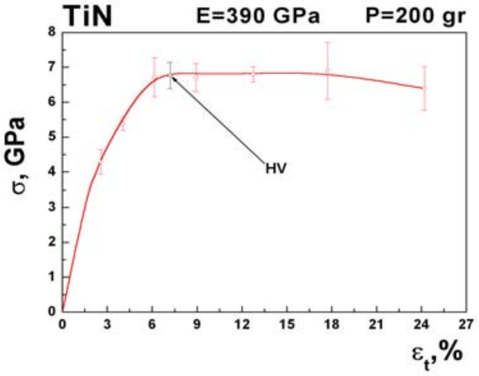

As can be seen from the figure, for titanium nitride, $\sigma_t$ can attain 6-7 GPa.

The joint effect of pressure and temperature on the sintered objects was considered. As the investigated ceramic materials were heated to temperatures above 1000°C, their strength decreased to 0.2-0.3 GPa [2]. As a result, the next stage of deformation of the sintered briquette is realized. An experimental corroborating of processes of hot deformation was obtained by X-ray analysis. . An analysis of the broadening of the diffraction lines of sintered titanium nitride nanosized powders show that the increase in the sintering temperature from 1200 to 1400°C under a pressure of 2 GPa leads to a certain decrease in residual microdistortions of the crystal lattice. Their value in the indicated temperature range decreases from $3.36 \cdot 10^3$ to $3.15 \cdot 10^3$.

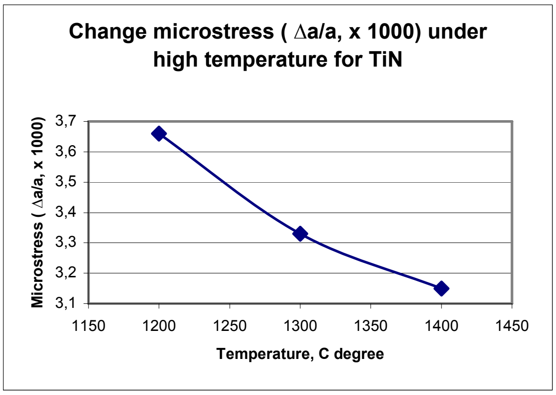

Moreover, coherent scattering fields (CSF) decrease in size.

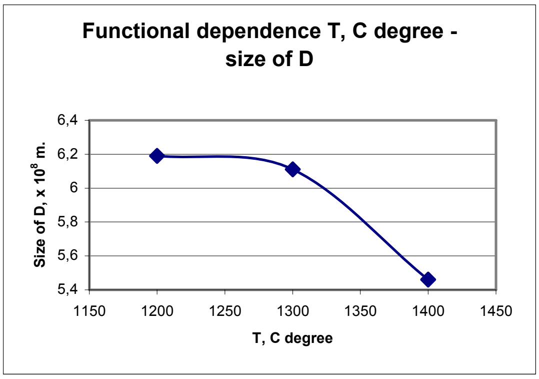

This indicates features of the behavior of the nano-sized material under conditions of deformation under high pressures and at high temperatures, which cause the formation of improved properties of the material.

To obtain highly dense nano-sized polycrystals on the base of the TiN-$TiB_2$ and $TiB_2$-$B_4C$ compositions by sintering under high pressures, the optimal values of pressure were used. According to the presented estimates of the optimal pressures, they must not be smaller than 2.5 GPa and 3 GPa for the TiN-$TiB_2$ and $TiB_2$-$B_4C$ system, respectively.

The polycrystalline materials were sintered under optimal pressures in the temperature range 1500-1600°C. The porosity of the materials was not higher than 2%. The structure of the nanocrystalline material on the base of titanium nitride is shown below.

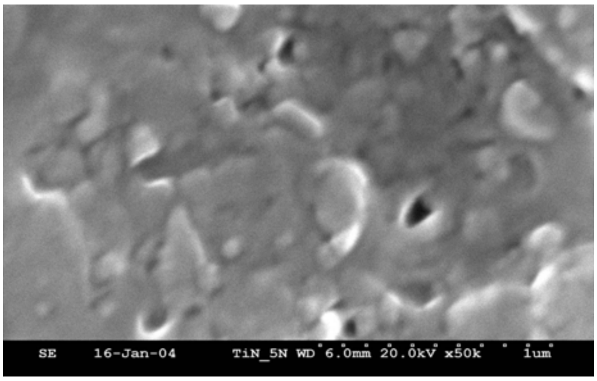

The microhardness of the sintered nanocrystalline titanium nitride compacts is 24-26 GPa (the microhardness of micron-sized grains of the compacts is 20), while the microhardness of the composites with the composition $TiB_2$-$B_4C$ is ≥30 GPa.

It is evident that the use of high pressures in the manufacture of nanoceramics can increase their physicomechanical properties up to a qualitatively new level and extend significantly the fields of their application.

## References

1. В.И.Трефилов, Ю.В.Мильман, Д.В.Лоцко и др. Изучение механических свойств квази-кристаллической фазы Al-Cu-Fe методом индентирования. Доклады АН, 2002, т.373, №4, с. 470-473.
2. Properties, Preparation, and Application of Refractory Compounds. Handbook [in Russian], Ed. Kosolapova T.Ya., Metallurgiya, Moscow (1986).

# THE MANUFACTURE OF VACUUM-TIGHT PRODUCTS FROM CARBON FIBER REINFORCED PLASTIC-BASE COMPOSITES

**Demichev V., Meleshko A., Soldatov A.(1)**
Kompozit Corp., Korolov, Russia
4 Pionerskaya Str., Korolev, 141070, Moscow region, Russia, Kompozit.Mat@g23.relcom.ru
(1)GNTs EFV IFBE, Protvino, Russia
1 Pobeda Str., Protvino, Moscow region, 142284, Russia, Soldatov_a@mx.ihep.su

Manufacturing vacuum-tight products from carbon fiber reinforced plastic-base composites requires the solution of two problems: the choice of a reinforcing filler and a matrix material.

While choosing filler the close filament laying and the adhesion to a polymer matrix should be taken into account.

The analysis of the carbon-fiber filler properties and structures reveals that the unidirectional ~ 0,1мм-thick carbon tapes (LU-P-0.1) can be most acceptable fillers for vacuum-tight products made from carbon fiber-reinforced plastics. Since filaments are highly closed in these tapes, it makes possible the using prepreg techniques, and high pressures and temperatures (e.g vacuum-autoclave molding) when molded. This molding allows a significant increase in density of the material molded. Adhesion in carbon tape-reinforced carbon plastics determined by shearing strength using a short-beam method is in the direct relation to Young's modulus and decreases as it increases. LU-P has rigidity reqired for a structure, and adhesion as well (E=260 GPa, $\tau$=0.07 GPa).

The analysis of the matrix material by workability, physicochemical properties, shrinkage, porosity and permeability has put thermosetting plastics in the forefront. These are thermosetting plastics hardened according to the polymerization mechanism, as they do not release by-products typical for polycondensation and, thus, have a denser structure that hold the greatest interest. Epoxies to the advantages of which can be attributed low shrinkage when cured and relatively low pressure when molded, fit these requirements most of all. Such characteristics allow using epoxy as a base for sealing compounds. (Sealing Compounds, Encyclopaedia of Polymers, v.1, Moscow 1972.).

Thus, to produce vacuum-tight materials and structures out of them prepregs reinforced with unidirectional LUP-0.1-type epoxy compound-base carbon tape, and compression molding should be used (acceptable density is 1,50—1,55 g/sm$^3$) .

For more sealing an external surface can be after-treated with vacuum-tight Anaterm-1-type-anaerobic sealant.

The material chosen makes it possible to produce spacial structures of vacuum of $10^{-7}$ torr kept, e.g. to produce a vacuum subsystem of Fig.1.

Strength and stability of cylinder and sphere shells were calculated by unidirectional material properties using formulas determined structure material characteristics along principle axis of symmetry (X, Y). Calculations revealed that 11 layers of longitudinal-transverse laying-up, where a central layer was longitudinal, and external ones were transverse, margin of safety of the structure for stable, static and dynamic losses was more than 3.

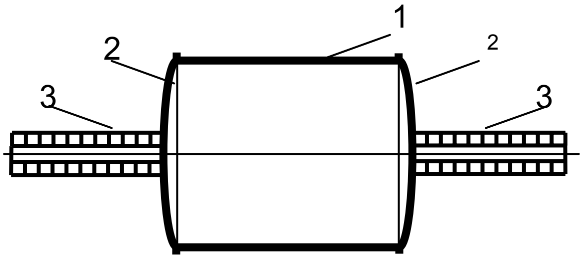

Fig.1. The vacuum subsystem: 1- decay vacuum chamber casing, 2- cups, 3-ion-pipings.

From the above, a decay vacuum chamber casing can be manufactured with prepreg wound on a molding mandrel in longitudinal and transverse directions. Prepregs are made from unidirectional carbon LUP-0.1-type tape machine-impregnated with epoxy compound (binder applied is 36 %, volatile solvent residue is 2 %). These are autoclave-molded.

According to the reinforcement pattern chosen a member "cup" is made with prepregs laid-up on a shaping surface using templates. The laying-up pattern and the number of layer are calculated using the requirements imposed to the structure as a base.

The vacuum-autoclave molding, temperature-time conditions, pressure and vacuum are determined on the basis of binder properties chosen and pack thickness molded. When hardened a stack molded is under a vacuum membrane that provides good seal both under heat and pressure. Temperature interval (100—120 °C) when volatiles are most released should be kept till vacuum is significantly increased. At the maximum hardening temperature of 170 °C the pressure should be up to 8 atm.

An “ion-piping” casing should be formed as follows: according to the reinforcement pattern chosen a mat of 4...6 layers should be butt laid up on a shaping cylinder surface. A joint of each following laying-up is displaced. A perform assembled should be autoclave molded under set conditions.

Longitudinal and transverse functional parts should be molded separately.

“Ion-pipings” should be assembled as follows: with marks, rings are fitted on the “ion-piping” casing and fixed with epoxy binder. On hardening, longitudinal functional parts are placed into slots.

A final operation is to put the “ion-piping” and the “cup” together such that the “ion-piping” casing should be push fitted into the “cup” casing at the set depth, with abutting members to be first epoxy coated.

# MOISTURE – RESISTANT COATINGS WORKING UNDER EXTREME CONDITIONS

**Rusin M.Yu., Pashutina T.A., Muzhanova L.P, Vasilenko V.V.**
Federal State Unitary Enterprise
“Obninsk Research and Production Enterprise “TECHNOLOGIYA”, Obninsk, Russia
E-mail: info@Technologiya.ru

Quartz ceramic materials with a number of valuable properties are porous materials and therefore the use of these materials for aerial fairings is limited. One of the methods of moisture proofing is the impregnation of quartz ceramics with acetone solutions followed by the polymerization.

The process of moisture-resistant coating application with the use of the TMΦT and MΦCC-8 oligomers as the impregnation agents has been developed to solve this problem.

The following peculiarities are typical for the TMΦT and MΦCC-8 oligomers. There is a central bifurcating atom in the molecules of both oligomers. In case of the TMΦT oligomers it is titanium and in case of the MΦCC-8 it is silicon. It is well known that silicone polymers of these classes are characterized by the enhanced flexibility of molecule chains owing to which they retain their main physicomechanical and first of all dielectric characteristics over a wide range of temperatures.

High resistance to thermal-oxidation destruction is a characteristic feature of the TMΦT and MΦCC-8 – based coatings. Thus the quartz ceramic materials with the TMΦT- based coatings work for a long time at 400°C and for a short time – at 700°C without the loss of radio-frequency transmissivity and strength. Quartz ceramic materials with the coatings based on MΦCC-8 have higher thermal resistance. They work for a long time at 450°C and for a short time – at 950°C.

The procedure of applying moisture-resistant coatings by the impregnation of quartz ceramics to a minimum depth has been tried out. It is profitably used for the development of fairings of different types.

The investigations of the process of moisture-resistant coating application by the impregnation of silicone resins with acetone solutions followed by the polymerization show that besides moisture proofing the polymer “heals” the defects occurring on the surface during ceramics machining.

The impregnation of the above mentioned oligomers surfaces with acetone solutions to a design depth followed by the polymerization makes a fairing hermetically sealed and resistant to moisture absorption.

Silicone polymers with spirocyclic and crosslike structure used as moister-resistant coatings are very promising for the development of new components working under more severe conditions.

# FEATURES OF FORMATION OF PHASE STRUCTURE OF CERAMICS ON BASIS $TiB_2$ AND C

**Kazo I.F., Кogutyk P.P., Makara V.A., Trushkovskaja L.M.**

Shevchenko Kyiv National University,
6 Acad.Glushkov Ave., Kiev, 03022, Ukrain, E-mail: kazo@ukr.net; makara@univ.kiev.ua.

The purpose of researches was studying laws of formation of crystal and phase structure of ceramic materials on basis $TiB_2$ and C with the raised contents of carbon (up to 33 % at.). Ceramics received methods high-temperature solid phase synthesis at hot pressing or high-temperature heat hardening in inert gas.

**Manufacturing of samples.**

Initial materials for reception of compact samples were powders TiC and $B_4C$. The content of free carbon in powders agree to ТУ: TiC there are more 0,5 %, $B_4C$ than 5 % there are less.

The order of carrying out of experiments was such. A mix of initial powders TiC, $B_4C$ in different parities used for preparation homogeneous mixture. Preparation homogeneous mixture and manufacturing of samples were carried out by the standard technique of reception of products by methods of powder metallurgy.

Samples were two categories.

For the first category of samples hot pressing made with induction heating without a protective atmosphere at temperature from 1800 $^0$C up to 2150 $^0$C and pressure 30 MPa in many-placed graphite pressforms.

The second category of samples subjected preliminary izostatics to compression at 2000 °C and pressure 5 GPa during 30 sec. After such processing in samples change of phase structure has not been noticed. Then made high-temperature heat hardening in differential thermoanalizator in an atmosphere of helium. After carrying out of processes high-temperature solid phase synthesis samples were exposed to machining and then were investigated.

The microstructure was studied by methods of optical microscopy.

The phase analysis of the made samples, and also mixes of initial powders was made with the help DRON-3M (copper radiation), roentgenograms removed in a step-by-step mode.

**Results of researches.**

After hot pressing in samples of a double mix $0{,}57TiB_2+0{,}43TiC$ it is not revealed significant (more than 1 % on weight) quantities of carbon. However, there is a sharp change of parameters of a crystal lattice as $TiB_2$.

For phase $TiB_2$ (type of structure $AlB_2$) and = 3,0290, with = 3,2274 - for a reference powder and after hot pressing and = 3,0241, with = 3,2307 - for the pressed sample.

After hot pressing in samples on the basis of a double mix $0{,}667TiC + 0{,}333B_4C$ it is not revealed phases TiC and $B_4C$, only phases $TiB_2$ and free carbon.

Carbon in the received samples is as a firm solution in crystal lattice $TiB_2$ and as separate phases. The condition of carbon substantially depends on time of endurance of samples under pressure at high temperature.

During hot pressing mixes at which there are chemically incompatible connections TiC and $B_4C$, occur exetermical reactions high-temperature solid phase synthesis borons of titan to allocation of carbon. The chemical equation of process can be written down so:

$2TiC + B_4C = 2TiB_2 + 3C$

The opportunity of course of such reaction is obviously connected to chemical activity of particles $B_4C$. Surplus of any component after hot pressing remains in samples as an independent phase and is shown metallographic as separate grains. Their sizes it is much less, than the sizes of grains in an initial mix.

Carrying out high-temperature heat hardening in differential thermoanalizer has shown, that process of synthesis begins at temperature 1790 °C. After 25 minute endurances of an initial mix at temperature 1900 °C process of synthesis comes to the end. In samples phase $TiB_2$ with the changed parameter crystal lattice comes to light only. Carbon as a separate phase is not shown. Synthesized phase $TiB_2$ under a microscope looks as continuous weight without presence of crystal grains or blocks.

Carbon in the received samples is only as a firm solution in crystal lattice $TiB_2$.

# NEW OPPORTUNITIES IN RECEPTION СПЕЧЕННЫХ OF MATERIALS ON BASIS ПОЛЫХ OF GLASS MICROSPHERES

**Kazymyrenko Y.A.**
National university of shipbuilding of Ukraine,
pr. Gerojev Stalingrada 9, Nikolaev, 54025, Ukraine, uakazi@mksat.net

Hollow glass microspheres (HGM) represent finely divided gas-filled powders and are perspective initial raw material for filling composite materials (CM). The basic assignment HGM consists in reduction in density of materials. Except for it other purposes are pursued: increase damped abilities, downturn of heat conductivity and dielectric permeability, increase of buoyancy and durability at all-round hydrostatic compression. Technologies of reception of KM on basis ПСМ are various also: them add in melt metals, mix with epoxy pitches, varnishes and paints.

The author offers the special class of KM received as a result of sintering HGM in various combinations:

- The first group is represented with the materials received as a result of sintering HGM of one structure of different dispersiveness among themselves without binding additives;
- The second group - the glass-to-metal materials received as a result of sintering HGM of same structure and dispersiveness with powders of metals: bronze, babbitt metal, aluminium.

Unites these technologies the following: hollow microspheres conglomerate in an oxidizing atmosphere with application of hot pressing in a temperature range of their softening. The basic technological parameters of their reception is the temperature of sintering, pressure of pressing and time of isothermal quotation. As a result of a variation in these parameters it is possible to receive CM with various properties. The main task at reception of necessary structure of these materials - to not allow destruction of microspheres under action of pressure and temperatures [1].

The material concerning to the first group, has received the name «cyntactic celluar glass», is characterized by the combined porosity, its operational density makes 270...450 kg / m3. This material chemically proofand be non-corrodible, is capable to be applied up to temperature 490 °C, but its main feature consists in a combination heat-insulating properties with properties of a material of buoyancy. Besides it is characterized by stable factor of heat conductivity at rise in temperature and water absorption. So, for example, the factor of heat conductivity of a material with optimum density (360 kg / m3) at temperature 25 °C makes 0,035 W (m·K), at temperature 400 °C - 0,043 W (m·K), and at 10 %-s' water absorption it reaches 0,11 W (m·K). Due to a combination of these properties cyntactic celluar glass the application has found as thermal isolation for the courts transporting hot bulk cargoes, heat-insulating coverings of underwater pipelines, and also in structure of the combined blocks of buoyancy of underwater means with small depth of immersing.

Application of materials which concern to the second group, has received absolutely other direction. These are the new antifrictional materials used in aggressive and corrosion environments with temperature of operation about 300 °C. The additive of powders of each of the offered metals: bronze, babbit metal, aluminium bearsa new combination of properties. Besides application ПСМ as a glass component in structure glass-to-metal materials will allow to give to these compositions damped properties. The main technological difficulty at reception glass-to-metal materials on basis ПСМ is stratification of components, so-called "streak" which results from the big difference in density of used powders and microspheres.

Thus, expanding ranges sintered with hollow glass microspheres of components, it is possible to create various KMS with unlike properties and different scopes.

# HOW TO FORECAST MATERIALS' PROPERTIES USING INDUCTIVE METHODS

**Nadiradze A.B.**, **Ivakhnenko A.G.**(1), **Ivakhnenko G. A.**(1), **Savchenko E.A.**(1)
Moscow Aviation Institute (Technical University)
Volokolamskoe shosse, 4, Moscow, 125993, Russia, MAI,
(095)158-4674, nadiradze@mai.ru
(1)International Scientific and Educational Center of
Information Technologies and Systems of NASU
Pr. Glushkova, 40, Kiev, 03187, Ukraine, (044)266 30 28, koleso@i.kiev.ua

Nowadays the tasks to forecast materials' properties such as sputtering and accommodation coefficients and so on can be solved with the help of the two main methods. It is used either relatively simple semi-empirical (regression) models or complex computer models [1]. In the first case an error in forecasting occurs due to the fact that interaction between bombarding particles and a substance is described with an inaccuracy and this error can be 200%. [2]. In the second case the situation is principally differ. Modern computing facilities and scientific experience permit to take into account the majority of processes determining a value of sputtering coefficient and, if there is needed input information, modern computer models permit to have a forecast with high accuracy. But in the majority of cases there is poor data about new materials and this fact complicates greatly computer model usage. So, it is necessary to develop the models with medium level of complexity, which permit to forecast sputtering coefficients under different data level. In presented work it is suggested to use so-called self-organizing models, which is built by inductive method.

The idea to use a concept of self-organization belongs to Prof. A.G.Ivakhnenko [3]. Optimal model's structure is selected using so-called external criteria, including additional information, according to which a resolution about approximation quality is made. As the criterion – a criterion of consistency is used. The criterion requires the following: models made on two different samples should give close results. Nowadays the following form of criterion of consistency, called a criterion of minimum drift, is commonly used:

$$n_{\tilde{n}\grave{\imath}}^{2} = \frac{\sum_{i=1}^{N} (x_A - x_B)_i^2}{\sum_{i=1}^{N} x_{\hat{o}i}^2} \rightarrow \min \, , \qquad (1)$$

where $x_A$— model's output quantity, coefficient estimation, obtained on a sub-sample A; $x_B$ – the same but on a sub-sample B, $A \cap B = \varnothing$ and $A \cup B = W$, where W- total sample; N- a number of points; $x_{\hat{o}}$ - sample real data.

An idea to separate a sample on to two sub-samples is used in combinatorial GMDH (COMBI), which is widely used for a lot of tasks [4]. The GMDH permits to choose excellent forecasting models. It is very suitable to use such models in the case when data sample is small and a number of parameters is great.

As an example, lets examine the task how to obtain sputtering coefficient for an elementary substance. Lets assume that ion's type, its energy and incidental angle are invariable. So, it is necessary to determine a sputtering coefficient for one material using sputtering coefficients and physical properties for other ones.

A sample of initial data standardized over maximum value for every variable is represented in table 1 (all data is taken from [2,5]). In the table: $x_1$ – sputtering coefficient for Xe ions with energy 300eV and normal incidental angle, mg/C; $x_2$ – mass density, g/cm$^3$; $x_3$ – molecular weight, atom units; $x_4$ – sublimation temperature, K; $x_5$ – heat capacity J/mol/degree; $x_6$ - binding energy, eV, MCC - modules of correlation coefficients (between every variable and output value).

The model is created as a function ($y=x_1$) on initial parameters and their pair covariations:

$$y = f(x_2, x_3, x_4, x_5, x_6, x_2^2, x_2x_3, x_2x_4, x_2x_5,$$
$$x_2x_6, x_3^2, ..., x_6^2) \qquad (2)$$

*Table 1. – Initial data for calculation*

| | $x_1$ | $x_2$ | $x_3$ | $x_4$ | $x_5$ | $x_6$ |
|---|---|---|---|---|---|---|
| **Material** | **Y** | **$R_o$** | **$M_w$** | **$T_{sub}$** | **$C_p$** | **$U_o$** |
| **Be** | 0,0228 | 1,848 | 9,01 | 2744 | 16,440 | 3,480 |
| **Ti** | 0,1176 | 4,505 | 47,88 | 3560 | 25,060 | 4,340 |
| **V** | 0,1409 | 5,960 | 50,94 | 3665 | 24,480 | 3,700 |
| **Cr** | 0,2310 | 7,200 | 51,96 | 2945 | 23,550 | 3,680 |
| **Nb** | 0,2323 | 8,570 | 92,90 | 5073 | 24,440 | 7,500 |
| **AI** | 0,2407 | 2,689 | 26,98 | 2793 | 24,350 | 3,260 |
| **Fe** | 0,3169 | 7,870 | 55,85 | 3145 | 24,980 | 4,150 |
| **Co** | 0,3786 | 8,900 | 58,93 | 3230 | 24,800 | 4,380 |
| **Mo** | 0,3837 | 10,220 | 95,94 | 4700 | 23,930 | 6,900 |
| **Ge** | 0,4355 | 5,323 | 72,59 | 3120 | 23,220 | 3,770 |
| **Ta** | 1,1587 | 16,650 | 180,94 | 5623 | 25,290 | 8,700 |
| **Pd** | 1,1706 | 12,200 | 106,42 | 3273 | 25,860 | 4,800 |
| **Mn** | 1,2719 | 7,320 | 54,93 | 2353 | 26,280 | 3,150 |
| **W** | 1,3408 | 19,340 | 183,85 | 5953 | 24,270 | 8,760 |
| **Pt** | 1,6581 | 21,450 | 195,08 | 4100 | 25,860 | 5,560 |
| **Au** | 2,3635 | 19,320 | 196,96 | 3150 | 25,400 | 3,920 |
| **Si** | 0,1172 | 2,300 | 28,08 | 3573 | 19,790 | 3,910 |
| **Cu** | 0,6566 | 8,960 | 63,54 | 2816 | 24,430 | 3,560 |
| **Ag** | 1,9415 | 10,500 | 107,86 | 2440 | 25,360 | 2,700 |
| **C** | 0,0068 | 2,300 | 12,00 | 4473 | 8,536 | 7,410 |
| **MAX** | 2,3635 | 21,450 | 196,96 | 5953 | 26,280 | 8,760 |
| **MCC** | 1,0000 | 0,810 | 0,813 | 0,005 | 0,464 | 0,021 |

A search was done with the help of COMPI software with additional determination over drift. The two variants of the model were obtained:

$$y = 0{,}3207 + 1{,}718 \cdot x_2 - 0{,}777 \cdot x_2^2 +$$
$$0{,}668 \cdot x_3x_4 - 1{,}388 \cdot x_3x_5 \qquad (3)$$

$$y = 1{,}4343 - 5{,}856 \cdot x_6 + 0{,}4302 \cdot x_2x_2 -$$
$$4{,}4347 \cdot x_2x_4 - 1{,}309 \cdot x_2x_5 + 7{,}819 \cdot x_2x_6 -$$
$$7{,}189 \cdot x_3x_4 + 4{,}781 \cdot x_3x_5 + 0{,}7226 \cdot x_4^2 -$$
$$0{,}58 \cdot x_4x_5 + 4{,}992 \cdot x_4x_6 \qquad (4)$$

The first model has root-mean-square error 40%, the second one – 20%. So, GMDH permits to forecast sputtering coefficients with relatively high accuracy (20—40%) for several elementary substances over its physical properties. May be such approach can be successfully used not only for sputtering coefficients, but also for other performances of interaction, such as accommodation coefficients and so on.

## BIBLIOGRAPHY

1. Ecshtain B. Computer simulation of particle interaction with solid body surface(in Russian)/ M.Mir, 1995, pp.321
2. Pleshivtsev N.B., Bazshin A.I. Physical process of ion beams interaction with materials (in Russian)/M.:Vusovskay kniga, 1998, pp.392
3. Inakhnenko A.G., Urachkovsky Y.P. Complex system simulation using experimental data (in Russian)/M.: Radio and Svias, 1987, pp.120
4. International Scientific and Educational Center of Information Technologies and Systems of National Academy of Science of Ukraine – developer's page http://www.gmdh.net/gmdh.htm.
5. Problems of Application physics. Sputtering of solid bodies by ion bombing: Physical sputtering of single-element solid bodies. Editor R.Berish - Mir, 1984, pp. 336.

# THE NANOLAERED FRAGMENTS IN AN AMORPHOUSED ALLOY $Ni_{82,3}Cr_{7,0}Si_{4,6}B_{3,1}Fe_{3,0}$

**Shpak A.P., Maiboroda V.P.,(1) Kunitskii Uy.A.,(2) Molchanovskaya G.M.,(1) Zuchina A.L. (1)**
G.V.Kurdyumov Institute of metallophizic of NASU,
Vernadskii Boulevard 36, Kiev, 03142, Ukraine
(1)I.Franzevich Institute of Materials Sciense Problems of NASU, Kiev, Ukraine
Krshishanovskii Street 3, Kiev, 03142, Ukraine, E-mail: maiborod@ipms.kiev.ua
(2)Technical center Pocrovskaya Street 13, Kiev, 04070, Ukraine

As is known materials obtained be the way of a high-speed spreading and cooling, for example, by the method of spining, are characterized by properties, distinguished from crystalline analogs. The amorphoused alloys are characterized by high hardness and durability (above at 5-10 of time), by large in 3-5 times a specific electrical resistance, smaller (on two order) magnetic anisotropy [1], and also have the best barrier properties at a diffusion [2].

Until recently researches of a structure were reduced in basic to use of a X-ray radiation. If the block coherent scattering corresponds to a size of a microgrouping and makes 3-5 nm, the obtained X-ray pattern contains broadened diffractional maximas. It as though testified to a unregulated disposition of atoms in space. Therefore also was considered, that their the atoms also are located disordered. But the further X-ray researches have shown, that the small impurities of crystalline substance begin to be exhibited as acute diffractional maximas, if their concentration exceeds 4-5%. This fact speaks that the amorphous substance at all is not amorphous in understanding of peratomic desordering. It is more correct to name such materials the X-ray-amorhous.

In work [3] is shown, that in melt saves about 96% of homoeopolar connections, which determine a force of connections and type of packing of atoms. Also the carried out researchs of a liquid condition [4] testify that the current of micrivalues of melt is accompanied by selection both loose of separate clusters [5], and thin films, on the surface of which sometimes place nanodrops or separate clusters. In this connection the spining reduces in stratifying of melt on structural polyfragments and freezing at high-speed cooling. So, for example, the researches of a structure of gasthermal covering from amorphoused alloy on base of Ni [6] show, that it consists from regularly ordered goffered stratified nanofragments, which contain crystalline and icosaedrick clusters. In this work the reasons of high hardness of a covering also are specified.

The purpose given work is the prolongation of the begun researches of a hereditary structure of amorphous materials, in particular, obtained by a method spining.

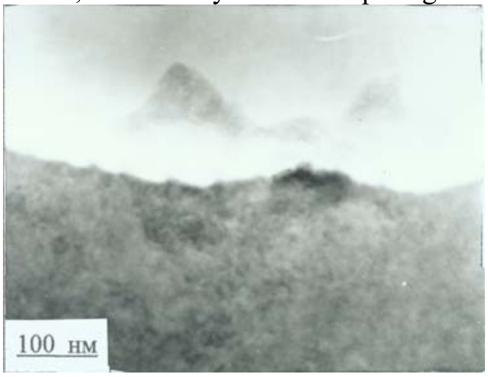

*a*

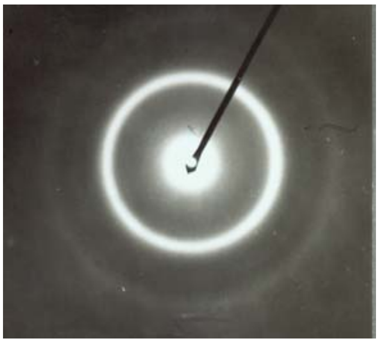

*в*

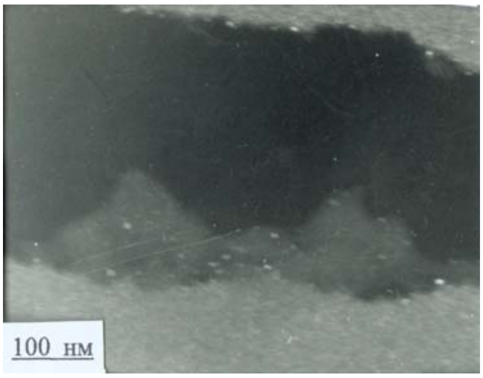

*c*

Fig.1.

On fig.1 *a,b,c* are reduced stratified nanofragments of alloy. That last belongs to a matrix sample testifies the luminescence on a darckfield image (fig. 1,*c*).

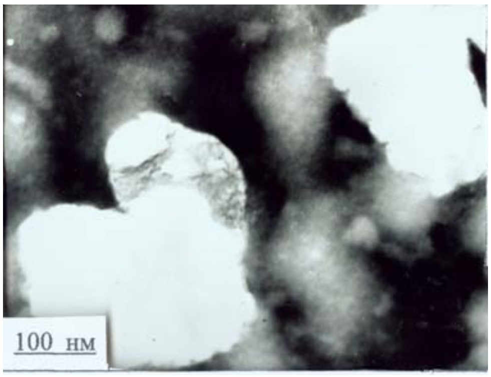

Fig.2

The labyrinth structure is typical for amorphous materials (fig.2), also contains nanolayers and clusters.

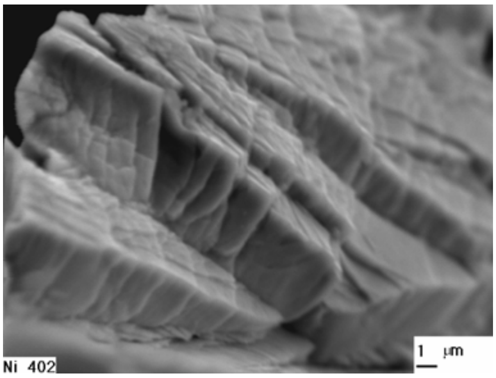

Fig.3.

Most brightly the nanolayered structure of researched alloy is exhibited on a surface of destruction after a rupture of a sample (fig.3).
However the morphological typical is a vien character of a surface of destruction (fig.4). As shown in work [7] it is connected with nanolayered structure of a material.

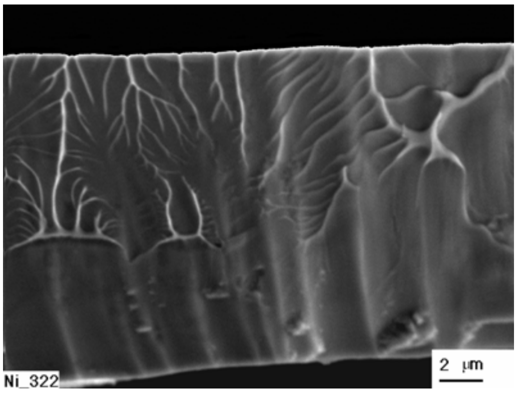

Fig.4.

The structure of X-ray-amorhous film obtained by a method of spining consists from nanolayered fragments containing embed of crystalline clusters. These films make packages. On our sight is anomalous high performances of hardness and the durabilities are connected just with the film structure of X-ray-amorhous fillet.

The list of the literature

1. I.V.Zolotuchin, Soros observ magazine, № 4: 73 (1997);
2. I.V.Zolotuchin, Yu.E.Kalinin Uspechi phis.nauk, v. 160 № 9:75 (1990);
3. V.P.Maiboroda, A.P.Shpak, Yu.A.Kunitskii. The structural aspects of the theory of melting and solidification, (Kiev: Academperiodika: 2002);
4. V.P.Maiboroda, A.P.Shpak, Yu.A.Kunitskii, Uspechi.phis.met., v.4, $^{1}$ 3 (2003);
5. V. P. Maiboroda, Thin Solid Films, 195, № 1/2: 357 (1991);
6. A.P.Shpak, V.P.Maiboroda, Yu.A.Kunitskii, S.L.Revo, A.L.Zuchina, Metallophizika. Noveishie technologii., v.25, № 12:1525 (2003);
7. A.P.Shpak, V.P.Maiboroda, Yu.A.Kunitskii, S.L.Revo. Nanosloistyi kompozity i pokrytiya. (Kiev. Academic periodicals 20003).

# CAST COMPOSITE SHS-MATERIALS ON TITANIUM AND CHROMIUM CARBIDES AND BORIDES BASIS

**Gorshkov V.A.** and **Yukhvid V.I.**
Institute of Structural Macrokinetics and Materials Science of RAS, Chernogolovka, Russia
ISMAN, Chernogolovka, Moscow Region, 142432, Russia, E-mail: yukh@ism.ac.ru

The carbides and borides of a titanium and chromium have high hardness and stability to aggressive medium at high temperatures.

Mixes of oxides of a chromium, titanium, nickel, ferrum etc. with aluminum, carbon and boron oxide were used for obtaining by Self-propagating high temperature synthesis of ingots of composite materials (CM) on the carbides and borides base

The combustion temperature of such mixes is 2500-3500 K therefore final products after combustion are in the liquid state. The "Metal" (Cr, Ti, C, B, N, AI, Mn, Fe) and oxide ($AI_2O_3$, $Cr_2O_3$, $Ti_2O_3$ etc.) phases of end-products have different specific weights, therefore gravitational separation take place. During cooling, the melt crystallizes, and the end-products are formed in two ingots: above - oxide, from below - "metal".

The results of studies are given in the report: regularities of SHS, properties of cast composite materials **(CCM)** on the titanium and chromium carbides and боридов bases with intermetallic binder, and the examples of their practical usage also.

## SHS of CCM on the Ti and Cr carbides and borides basis.

Synthesis was conducted in SHS-reactors in nitrogen medium at pressure of 4 МПа. The ratio of “hard” ($CrO_3$+Al+C(B) or $CrO_3$+$TiO_2$+Al+C(B)) and “matrix” (NiO + Al) component were varied in experiment.

The analysis of final products has shown that combustion products have the cast layered structures and are separated easily from each other by mechanical way.

The experimental study have shown that increasing of a “matrix” part (NiO+Al) in initial mixture go to decreasing of sputtering mass during combustion and the essential increasing of phase separation for studied systems. Increasing of initial mixture mass go to increasing of output of a metal components in ingot to estimated value. The mass of (NiO+Al) in initial mixtures essentially effect on chemical and phase composition micro- and macrostructure "of a “metal" ingots: the contents Ni and Al proportionally increases, and Cr, Ti, C decreases.

According the data local ч-ray analysis the ingots of target products represent composite materials in which carbide grain ($Cr_3C_2$,

TiC- $Cr_3C_2$ solution, $CrB_2$, $TiB_2$- $CrB_2$ solution) are distributed in a Ni-Almatrix.

## Practical usage CCM on the Ti and Cr carbides basis.

Composite materials on the Ti and Cr carbides basis have high hardness and wear-resistance and, therefore were used for obtaining protective coatings on a parts working in extreme conditions. As a rule, for hardfacing composite materials are used a powders of definite fractions. For obtaining powders the ingots of the synthesized materials are milled and classified. After milling each particle of a powder represents an aggregate, in which carbide grain is in intermetallic matrix.

The tests of SHS carbide powders with intermetallic bindle were conducted in ARC International (Hyderabad, India) and VNIITS (Moscow, Russia). For comparison of properties the industrial powders of the “METCO” corporation (USA), TULACHERMET(Tula, Russia) and TZNTS (Torez, Ukraine) plants were used. The coating were put on steel bases by both detonation and plasma methods.

The SHS coating have essential advantages before industrial: hardness and wear-resistance above - on 1,2—1,3 times and on adhesion with the basis in 1,5—1,6 times.

## Practical usage CCM on the Ti and Cr borides basis.

The tests of cast composite materials on Ti and Cr borides grains basis were conducted in VNIIST(Moscow). The special electrodes of diameters 3 and 4 mms for an electric arc surfacing were made of borides grains base.

Particles of borides not dissolved during surfacing, uniformly distributed in a matrix because of optimal size of grains and composition of binder.

A matrix after hardfacing, as a rule, have austenite structure.

The regularity of an abrasive wear in conditions of impact loads is studied.

The optimal sizes and quantity hard component in powder compositions are established.

Surfacing coatings have a wear resistance superior in 2—3 times higher then industrial coating of Sormait-1, EN - ITS - 02.

The high a wear resistance of coating is determined by high hardness of titanium – chromium borides. There hardness is 2000—3500 кг/мм$^2$. Surfacing coatings have shown good properties in conditions of abrasive-impact loads, including low (up to –50 °C) and high

(up to +75 °C) temperatures.

Practical usage of ore raw material for SHS CCM.

The important problem for the SHS is the replacement of initial chemically pure oxides on cheaper ore materials. Such change, on the one hand, make chipper an initial SHS mixtures and on the other hand, expands a source base. Earlier we pointed using of chemically pure components (oxides of a chromium, titanium, boron, nickel, ferrum and aluminium) in the SHS processes.Now we show using of two ore concentrates, rutil and manganese, for hardfacing the Cr—Ti- B—Ni—Fe—Mn—Al composite material.

From comparison of chemical compositions it may be seen that ore concentrates, used in experiments, include impurity of ferrum, silicon, aluminium, calcium, magnesium oxides.

The contents of other impurity (S, P etc.) does not exceed 1%. The impurity in ore concentrate, on the one hand, decrease heat release of initial mixtures and on the other hand, can result in appearance in CCM of undesirable impurity.

The visual analysis of CCM synthesized from “oxide” and “ore” mixtures has shown, that they look like two-layer ingots with clear separating of “metal" and oxide phases.

The studies of SHS parameters have shown, that the replacement of chemically pure oxides on ore raw material weakly changes technical characteristics.

The replacement of chemically pure reactants on ore raw material did not show essential effect on an elemental composition of CCM. The main impurity in it is the silicon. Calcium and magnesium in CCM it is not revealed.

From the conducted research we have the conclusion, that the replacement of chemically pure oxides of a titanium and manganese on ore concentrates does not hinder with obtaining of high-performance cast composite materials on the basis of carbides and боридов of a titanium and chromium.

The research has been supported by Russian Foundation of Fundamental Research (project № 03—03—32859).

# ALUMINUM CASTING ALLOYS FOR SERVICE AT CRYOGENIC TEMPERATURES

**Tikhonov A.A., Gavrilyuk V.V., Karpov V.N.**[(1)]
Public Joint Stock Company “KOMPOZIT”
ul. Pionerskaya 4, Korolev, Moscow Region, 141070, Russia, Kompozit.Mat@g23.relcom.ru
(1)Moscow State Aviation Technological University
ul. Orshanskaya 3, Moscow, 121552, Russia, E-mail: mati@implants.ru

Modern development of machine-building industry had demanded application of materials, including aluminum casting alloys, serviceable in conditions of ultra low temperatures.

It is known that at decreasing temperature up to temperature of liquid hydrogen or helium, metallic alloys increase their strength characteristics with falling pasticity; at that, the largest embrittlement was noticed for titanium alloys, certain grades of steel and aluminum alloys with high content of magnesium [1].

It was stated by investigations of mechanical properties of well-known and experimental aluminum casting alloys at cryogenic temperatures that alloys containing copper are remarkable for the best combination of strength and plasticity. However, well-known alloys did not assure required level of plasticity at these temperatures.

In the PJSC “KOMPOZIT”, casting alloys were developed AK8M3, AK8M1,5 and AM5 based on systems Al-Si-Cu and Al-Cu with addition of well-known and original elements with good strength and plasticity in a wide temperature range from 20K to 473K (Table 1).

These alloys differ from standard alloys by good plasticity and high strength at cryogenic temperatures. The alloys possess a good processability allowing to obtain high quality large-size and complex-shape castings.

Weldability of alloys is satisfactory and allows not only elimination of surface casting defects by welding-up, but also creation of complex welded constructions like “casting + semiproduct (sheet, pipe, profile, forging)”.

The alloys are not inclined to corrosion cracking in stressed state. The threshold stress, i.e. the maximal stress at which cracking does not occur in corrosive medium (3% solution of NaCl), for all alloys makes 0.9 of their yield point. The threshold stress for standard alloys like AK9ч, AK8M3ч is at a level of 0.75, and for AM4,5Кд alloy – only 0.2-0.3 of the yield point.

Table 1.

| Alloy grade, casting method, thermal treatment | Test temp., K | $\sigma_B$, MPa | $\sigma_{0.2}$, MPa | $\delta_5$, % |
|---|---|---|---|---|
| AK8M3 K, T5 | 20 | 472-530 | 350-384 | 3.3-5.8 |
| | 77 | 434-458 | 329-355 | 4.6-6.8 |
| | 293 | 354-380 | 252-271 | 7.4-10.3 |
| | 373 | 322-345 | 242-259 | 7.6-10.4 |
| | 473 | 243-271 | 209-231 | 8.5-11.2 |
| AK8M1,5 Д, no thermal treatment | 20 | 381-403 | 176-200 | 4.9-7.1 |
| | 77 | 294-328 | 162-183 | 5.3-7.7 |
| | 293 | 265-275 | 161-181 | 12.2-18.0 |
| | 473 | 171-183 | 134-152 | 17.6-25.0 |
| AM5 K. T5 | 20 | 609-680 | 450-531 | 4.6-8.6 |
| | 77 | 528-574 | 366-414 | 8.3-12.3 |
| | 293 | 420-467 | 270-328 | 10.4-17.4 |
| | 373 | 353-390 | 272-312 | 10.4-14.4 |
| | 473 | 300-330 | 213-249 | 9.4-13.0 |

The alloy AK8M3 represents a cuprous silumin. It is intended for obtaining by permanent-mould casting and liquid forging of such hermetic parts as casings, lids and such load-bearing parts as impellers, brackets, fittings for exploitation in a temperature range from 20K to 473K.

The alloy was used for manufacturing of hermetic enclosure and loaded impeller of an engine working on liquid hydrogen. In the other case, the alloy was used in a welded construction “cast (scroll casing) + cast (pipe)”.

Cuprous silumin AK8M1,5 is a high-tech alloy for pressure die casting. Large-size parts (the largest size from 300 to 600 mm) of various shape and complexity with wall thickness from 0.8 to 3 mm were manufactured from that alloy and used in diverse articles. Unlike the standard alloy AK12, this alloy can be poured at lower temperature (873-953K depending on type of casting). At permanent-mould casting, the alloy has good mechanical properties after thermal treatment by T5: $\sigma_B$=335-360 MPa, $\delta$=4-5 %.

The alloy AM5 was developed and applied as a substitute for the standard alloy AM4,5Кд, which is characterized by increased inclination to formation of hot cracks both at casting and welding as well as by very low corrosion resistance in stressed state. Thin-walled and complex shape molded pieces are manufactured from the alloy AM5 by lost-wax process or plaster-mould casting, middle size and complexity molded pieces are manufactured by permanent-mold casting, large size and complex molded pieces are manufactured by sand mold casting. The manufactured experimental welded unit “casting + sheet of 1201 alloy” in testing had demonstrated a high structural strength.

The developed alloys can be applied in manufacturing of molded pieces in rocket, aviation, automotive and cryogenic engineering for exploitation in extreme conditions, e.g. in conditions of low and ultra low temperatures (open space, far North, refrigerating plants, hydrogen engines, etc.) and corrosive media (sea water).

It is expedient to subject foundry goods from the alloys to hot isostatic pressing before thermal treatment to eliminate internal defects such as shrink cavities and pores. Such a treatment increases strength characteristics by 20-40% and plastic characteristics – by 1.5-3 times.

At that, hermiticity and structural strength of molded pieces grows up to 40-50%.

For all alloys proposed for application, specification certificates were completed and patents of the Russian Federation were taken out.

## REFERENCES

В.И. Старцев, В.Я. Ильичев, В.В. Пустовалов. Пластичность и прочность металлов и сплавов при низких температурах. Москва, Металлургия. 1975.

# STRUCTURE AND PROPERTIES OF THE WC–40%Co COMPOSITE PREPARED FROM AN ULTRAFINE POWDER, WITHIN A BROAD TEMPERATURE RANGE

**Laptev A., Tolochyn O., Golovkova M.**
Frantsevich Institute for Problems of Materials Science of UNAS,
3, Krzhyzhanovsky Str., 03142, Kiev, Ukraine, e-mail: shat@ipms.kiev.ua

Tungsten carbide (WC) and cobalt (Co) are in the base of commonly used hard metals. One of advantages of these tool materials is a high resistance to impact loading. To produce very strong effects, high cobalt hard metals are used, i.e. those with high content of ductile phase in the structure of a two-phase material. Industrial grades of hard metals to operate under impact conditions have a content of cobalt restricted to level of 25 wt% or 37 vol %. This limit is determined by the allowed level of the hardness decrease for hard metal products and their strengths. On the other hand, no well-defined relationship exists between the hardness of two-phase alloys and the volume fraction of the metallic binder as the hardness depends on the thickness of the cobalt interlayer between carbide grains rather than on the general content of cobalt, $HV=990\times L_{Co}^{-0,2}$ [1]. There is a theoretical possibility, therefore, to achieve a high hardness for two-phase composites in case of a very high content of ductile phase, ($V_{Co}$) but at very fine sizes of carbide particles, ($L_{WC}$), as $L_{Co}=L_{WC}[V_{Co}/(1-V_{Co})(1-C_{WC})]$, where $C_{WC}$ is the contiguity of carbide phase. Thus, mechanical properties of hard metals or composites with ultra fine structure and high content of ductile phase are very attractive in terms of science and practice. It is to be noted then that the possibilities of conventional technology in obtaining such composites are restricted, but the desired material can be prepared by means of other methods of powder consolidation that use the low-temperature pressure processing. Therefore, we aimed our researches at the density, structure and mechanical properties of composite WC-40 wt.% Co prepared of ultra fine WC и Co powders by high-energy pressing within the temperature range of 950-1250 °C. Sintering of preforms at low temperatures and in the presence of liquid phase was conducted for comparison. The effect of annealing at T=1190 °C for 8 hours on the structure and properties of specimens produced by pressing at 950-1150 °C was also studied. The oxygen content in the mixture under study was at the level of 4.0 wt.% , therefore, the optimum content of saccharose added to the mixture was identified, as needed for bonding and evacuating of the extra oxygen. The mixture under study was heated and densified under the vacuum of ~0.13 Pa. The effect of pressing temperature on the density of specimens, their electrical resistivity and coercivity was investigated. Moreover, mechanical properties, bendiing/compressing ultimate strength, fracture toughness, Vickers hardness, and also relative plastic deformation were determined on specimens pressed at various temperatures.

It was found that an essentially dense state for given composite was achievable at 1150 °C, Fig.1a. The specimens pressed at 1050 °C have a porosity of about 0.7 %. Annealing of porous specimens results in an increased density, reduced electrical resistivity and coercivity. The drop of coercivity after the solid state annealing is primarily due to the coarsening of structure, Fig.2 a, b. Visual inspection of the microstructure showed the tungsten carbide particle sizes were 0.2–0.4 μm of specimens pressed at 1050°C, and increased up to 0.6–0.8 μm i.e. nearly two times due to annealing.

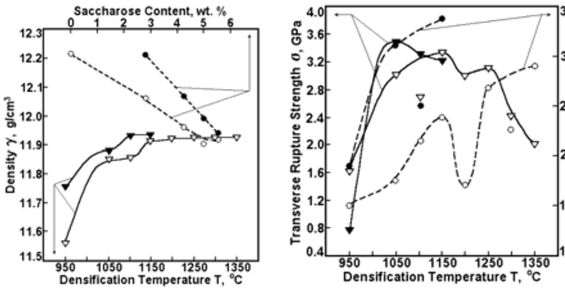

a b

Fig. 1 The effect of temperature on density (a), bending strength and crack resistance of (b) VK40 hard metal.

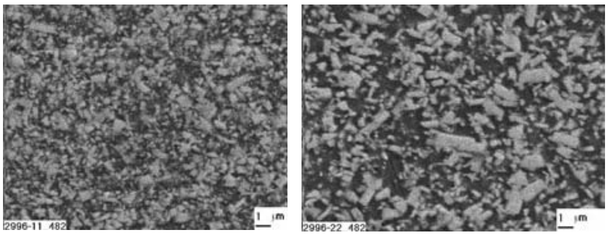

a b

Fig. 2 The structures of specimens pressed at T=1050°C (a) and annealed for eight hours at T=1190°C (b).

Mechanical properties of specimens pressed at various temperatures and also after annealing are of interest. The present composite revealed, in fact, an transverse rupture strength of 3000–3400 MPa, Fig.1b. The maximum bending strength was achieved on annealed specimens, which were pressed at a rather low as 1050 °C temperature. A substantial effect of annealing was produced also on the fracture toughness of specimen, Fig.1б. The fracture toughness values at the level of 31–33 MPa·m$^{1/2}$ were obtained after annealing of specimens pressed at 1050–1150°C. The specimens prepared by the liquid-phase sintering have $K_{1C}$=28 MPa·m$^{1/2}$, however, the level of crack resistance of a similar alloy sintered using conventional technology was considerably lower, i.e. 17.2 MPa·m$^{1/2}$ [2]. The Vickers hardness at 30 кg indentor load was at the 7.6–7.7 GPa level, which corresponded to that of conventional alloy, VK25KS [3] having the transverse rupture strength of 2180 MPa and compressive strength of 2690 MPa. The composite under study has as high as 2900 MPa compressive strength in spite of an increased binder content. In this case, the fine structure provides the increase of both the transverse rupture strength and compressive strength. It should be also noted that the composite under study showed the maximum plastic deformation for its «low temperature» specimens, i.e. specimens with a finer structure and thinner interlayers of binder. An opposite trend can be observed for conventional hard metals. An unusual behavior of this material is probably associated with the minimum degree of contact between carbide particles (contiguity $C_{WC}$), or with its absence.

In conclusion, the low temperature densification of ultra fine WC–Co powders with high content of plastic constituent is able to provide a material having a good combination of mechanical properties, i.e high strength and toughness characteristics while maintaining the desired level of hardness. Materials of such type are able to show an efficient operation under conditions of rather strong impact loads during stamping and upsetting of items.

## References.

1. Laugier M.T. Coercivity, hardness and microstructure in WC-Co composites // J. Mater. Science Lett., 1985. - 4. - p.211-216.
2. Ochkasov V.F. Determination of crack resistance of WC-Co hard metals // Study of hard metals. .Proceed.. VNIITC. - M.:Metallurgia, 1991. - p. 16-21. (In Russian).
3. Rigevanov V.C. Blinkov A.N., Abramov A.V. Livshitz T.A. etc. Evaluation of durability of sintered hard metals of WC-Co group under impact/cycling loading.// Study in the area of design and application of hard metals. Proceed. VNIITC. - M.:Metallurgia, 1987. - p. 114-118. (In Russian).

# DISCONTINUOUSLY REINFORCED ALUMINIUM COMPOSITES FABRICATED BY REACTION CASTING PROCESS

**Chernyshova T.A., Kobeleva L.I., Bolotova L.K., Panfilov A.A., Panfilov A.V.**
Baikov Institute of Metallurgy and Material Science RAS, Moscow, Russia
Leninsky prospect, 49, Moscow, 911991, Russia, e-mail: chern@imet.ac.ru
Vladimir State University, Vladimir, Gorkyi st., 87, 600000, Russia, e-mail: alexey@vpti.vladimir.ru

Particulate reinforced aluminium matrix composites (MMCs) have potential advantages such as high properties and low cost, which make them attractive materials for the production of structural machine components in modern engineering. However, the application of these MMCs for engine parts has been limited due to softening of Al matrix and interfacial reaction between matrix and reinforcement at the high temperature (more than 300 °C). In order to improve the high temperature strength, the new in-situ process (Reaction Casting) has been developed by which matrix is strengthened supplementary by disperced intermetallic compounds or new ceramic phases. The intermetallic compounds are formed by the exothermic reaction between aluminium melt and introducing metal powder (Ti, Ni, Fe) or the metal oxide powder $TiO_2$ (NiO):

$Ti+Al \rightarrow TiAl_3, TiAl, Ti_3Al + \Delta H,$ (1)
$TiO_2+Al \rightarrow Al_2O_3+TiAl_3, TiAl.$ (2)

The new ceramic phases can appear by exothermic interfacial reaction between hard particles and the elements from liquid solutions:

$Si(Al)+C \rightarrow SiC+ \Delta H,$ (3)
$Ti(Al)+B_4C \rightarrow TiB_2+TiC + \Delta H,$ (4)
$SiC+Ti(Al)+B \rightarrow TiB_2 + TiC + Ti_5Si_3 + \Delta H,$ (5)
$Al+B \rightarrow AlB_2+ \Delta H.$ (6)

It is known, that the wetting between ceramic particles and molten metal can be activated by exothermic reactions. Hence, in-situ process is a effective method for introducing a larger amount of ceramic reinforcement into an Al alloy melt without rejection. Moreover, MMCs fabricated by this process are characterized by: 1) high adhesion bound on the interface boundaries reinforcement/matrix due to a low lattice mismatch between intermetallic compounds and matrix; 2) thermal stability; 3) uniform distribution of the reinforcement in the matrix. These factors have direct influence on the working properties of materials.

The purpose of this work to study the structure, the composition of the interaction products and the mechanical properties of the new MMCs fabricated by reaction casting process. Reaction casting was carried out by three modes: 1) by infiltration the molten aluminium by 750-900 °C into the preheated preform placed in the mold; 2) by introduction the preform into the melt; 3) by the mechanical stirring of ceramic particles into a molten matrix with addition an Al-Ti master alloy.

The matrices were aluminium A99 and Al-alloy AK12 (12wt.%Si). As reinforcements α-SiC particles of the green type with an average diameter of 28μm and $B_4C$ particles of dimension less 63μm were used. Pure Ti powder and B powder of the amorphous type were mixed with ceramic reinforcements for manufacture the preforms. The preforms were heated to temperature 600—640 °C.

To find out the exothermic reaction characteristics, the differential thermal analysis of was performed (Fig.1). Microstructure of MMCs has been analyzes by an optical microscope and SEM – EDX and XRD. Mechanical properties such as bending strength, tensile strength, Brinel hardness, wear and elevated temperature properties were examined.

The phase chemical composition of the MMCs prepared in-siyu process is present in table.

The microstructure investigation show that the solidification of the composite melt contained Ti addition begins with the formation of intermetallic phases. The equiaxis rectangular crystals are identified as $Al_3Ti$ using x-ray diffraction microanalysis. The size of $Al_3Ti$ crystals increases with increase both temperature of molten Al-alloy and exposure duration until pouring. The crystals are nearly uniform distributed in the matrix.

The introduction both SiC-particles and Ti powder in matrix did not modify a shape of intermetallic compounds. SiC particles are pushed by growing dendrites into the interdendritic region. If composite melt is overheated the facetes of SiC particles become rough. When the preforms added to the Al melt consist of $B_4C$ particles or B powder, Ti powder and SiC particles, the layers of new phases appear on the surface of SiC particles. According EDX- and XRD – analyses these layers contain Ti, Al, Si, C, that form complicated compounds. A noticeable effect of B and $B_4C$ addition into the melt is change a rectangular shape of intermetallic phase $Al_3Ti$ into starlike or needles. The Brinel hardness of MMC samples were determined using a load 102,6 kg, a ball with a diameter of 2,5 mm, a load duration of 20 s. Samples of the MMCs containing a large amount of reinforcement (SiC, $B_4C$, $Al_3Ti$, $TiB_2$, TiC) have maximum hardness (table.). In Fig. 2 the results of mechanical tests samples of MMCs and AK12 alloy by elevated temperature are presented. The results indicate that the intermetallic compounds are very effective for improving both the high temperature strength and hardness. Tribological properties were investigated under dry sliding against 40X steel counterface using the test wear machine УМТ-1, by sliding speed of 0,2—1,85 m/s and load of 400—1500 H. The high wear resistance and stability against seizure of MMCs are correlated with the increased hardness, strength and matrix/particle bounding strength.

| material | The phase composition of MMCs | HB, MPa |
|---|---|---|
| Al + Ti | Al, $Al_3Ti$ | 270 |
| Al + [SiC+Ti]* | Al, $Al_3Ti$, AlTi, TiC, SiC, $Ti_5S_4$, $TiSi_2$, $SiO_2$ | 292 |
| Al + [$B_4C$+Ti] | Al, $Al_3Ti$, $TiB_2$, TiC, $B_4C$ | 320 |
| Al + [$B_4C$+Ti+SiC] | Al, $Al_3Ti$, $TiB_2$, $B_4C$, SiC, $TiSi_2$ | 540 |
| Al + [B+Ti] | Al, $Al_3Ti$, AlTi, $AlB_2$, $TiB_2$, TiB, TiO | 290 |
| Al + [B+Ti+SiC] | Al, $Al_3Ti$, AlTi, $AlB_2$, $TiB_2$, TiC, TiB, $B_4C$, SiC | 358 |
| AK12 (12%Si) | Al, Si | 624 |
| AK12 +SiC | Al, Si, SiC | 712 |
| AK12 - [Ti+B+SiC] | Al, Si, $Al_3Ti$, SiC | 688 |
| AK12– [Ti+$B_4C$+SiC] | Al, Si, $Al_3Ti$, $B_4C$, SiC | 624 |

* в скобках состав преформ

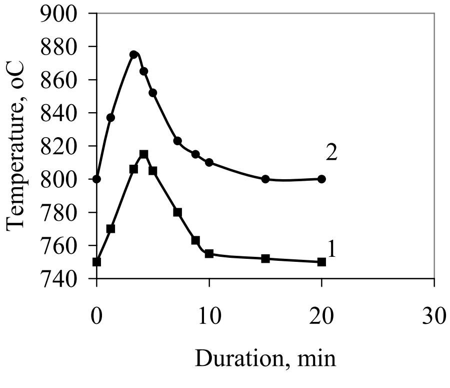

Fig.1 Temperature-Time curves of Al-melt by introduction Ti-powder (1) and the perform, contained Ti powder and SiC particles (2)

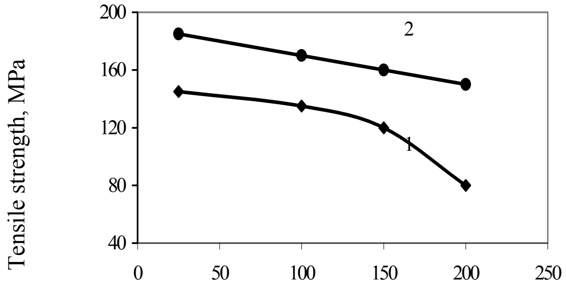

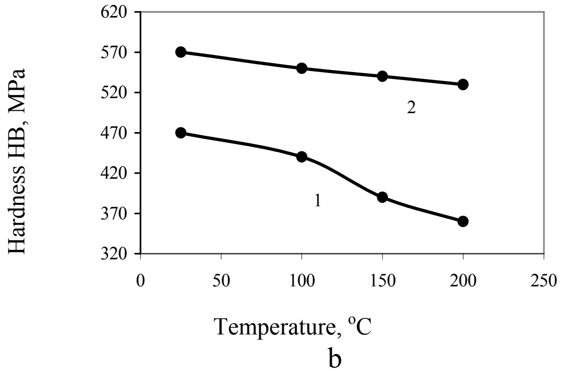

Fig.2. Tensile strength (a) and hardness (b) at elevated Temperatures of Al-alloy AK12 (1) and MMC AK12-10%Ti-5%SiC (2).

# REFLECTANCE AND EMITTANCE OF POLYMER COMPOSITE MATERIALS AT NONSTATIONARY HEATING BY LASER RADIATION

**Dlugunovich V.A., Zhdanovskij V.A., Snopko V.N.**
Institute of physics of NASB, Minsk, Belarus
68 F. Skarina Ave., Minsk, 220072, Belarus; e-mail: vdlug@dragon.bas-ney.by

Polymer composite materials are widely used in modern spacecraft and aviation engineering, in motor industry and shipbuilding [1, 2]. Basically, these materials are used in high temperature constructions under influence of intensive thermal fluxes, including radiation one. Therefore a lot of publications were devoted to investigation of spectral emittance and reflectance in the visible and IR regions of spectrum of polymer composites stationary heated at high temperatures. Results of these investigations are in part summarized in some reviews [3, 4].

Application of lasers for processing and not destroying control of polymer composites [5, 6], and also creating of lasers systems for detection, location and damage of the defence constructions created with use of polymer composites [7], has demanded the information on reflectance of polymer composites heated by laser radiation. For the first time in this publication was undertaken the attempt to summerized the existing information in reflectance and emmitance of polymer composites heated by laser radiation.

The most publications were devoted to investigation of directional-hemispherical reflectance ($R_\lambda(0;2\pi)$) of glass fiber reinforced plastics [8-13]. Reflectance of organic fiber reinforced plastics [9, 10, 14, 15] and carbon fiber reinforced plastics [11, 16] was less investigated. And practically there are no data on reflectance of carbon-carbon composite materials (CCCM) [17]. Reflectance at wavelength of Rb ($\lambda$=0,69 μm) [12], Nd (1,06 μm) [8, 12], He—Ne ($\lambda$=0,63; 1,15 and 3,39 μm) [9—11,14—16]; $O_2$I ($\lambda$=1,315 μm) [13], CO ($\lambda$=5,25 μm) [11] and $CO_2$ lasers ($\lambda$=10,6 μm) [9, 10, 14—17] was investigated.

It was established, that before laser heating of investigated polymer composites surface the $R_\lambda(0;2\pi)$ is depend, basically, on material type and laser radiation wavelength. Heating of glass-, organo- and carbon fiber reinforced composites up to the temperatures of pyrolysis of organic components caused carbonization of heating zone. Carbonization of glass and organic fiber reinforced plastics caused decrease of $R_\lambda(0;2\pi)$ in the visible and near IR regions of spectrum (0,63; 0,69; 1,06 and 1,15 μm) [8—15] and increase of $R_\lambda(0;2\pi)$ in the middle IR region (3,39; 5,52 and 10,6 μm) [9, 11, 14, 15]. Special feature of glass fiber reinforced plastics is burning out of carbonized layer and exposure of glass fibers during further heating that caused increase of $R_\lambda(0;2\pi)$ in visible and near IR regions of spectrum (0,63 and 1,15 μm) and decrease of $R_\lambda(0;2\pi)$ at wavelength 3,39 and 10,6 μm [9, 10].

Heating of phenolic carbon fiber reinforced plastic by CW $CO_2$ laser radiation up to the temperature 1500 K did not cause change of $R_\lambda(0;2\pi)$ at wavelength $\lambda$=0,63 μm but results to increase of $R_\lambda(0;2\pi)$ at wavelength 5,25 μm [11]. At the same time action of CW $CO_2$ laser radiation on unidirectional epoxy carbon fiber reinforced composite cause the increase of $R_\lambda(0;2\pi)$ not only at wavelength 0,63 μm but at 3,39 and 10.6 μm [16]. Thus reflectance $R_\lambda(0;2\pi)$ of unidirectional carbon fiber reinforced plastic depends on orientation of carbon fibers comparatively to the polarization plane of laser radiation. The maximal reflection is observed at concurrence of fiber direction with polarization plane, and minimum reflection is when fibers direction is orientated across a polarization plane of laser radiation [16]. Action of CW $CO_2$ laser radiation with energy densities $q$ up to 100 W/cm$^2$ on CCCM cause to increase of $R_\lambda(0;2\pi)$ at wavelength 10.6 μm, and with increasing $q$ above 200 W/cm$^2$ reflectance $R_\lambda(0;2\pi)$ begin to decrease [17].

Attempts to establish temperature dependence of reflectance of polymer composites heated by laser radiation, have shown that its reflectance is not unequivocal function of the heated surface temperature during pyrolysis of material organic components. The increase of heating rate of a polymer composite shifts its temperature dependence of reflectance to the higher temperature region. Thus the increase of reflectance at wave-length 3.39 и 10.6 μm of the glass and organic fibers reinforced plastics heated by laser radiation is cause not only by carbonization of their surfaces, but also amplifies by temperature dependence of $R_{\lambda}(0;2\pi)$ of formed charred layer [9,10,14–17]. The temperature of the beginning of burning out of carbonized layer and exposure of glass fibers on a surface of glass fiber reinforced composite heated by laser radiation also increases with increase of material heating rate [9,10]. Changing of reflectance at wavelength 10.6 μm of CCCM heated by CW $CO_2$ laser radiation with $q$ above 200 W/cm$^2$ depends not only on temperature, but also on material type and absorbed laser energy [17].

Changing of spectral normal emittance $\varepsilon_{\lambda n}$ (for opaque materials $\varepsilon_{\lambda n}=1-R_{\lambda}(0;2\pi)$) of organo- [18], glass- [11,18] and carbon fibers reinforced plastics [11,19] heated by CW $CO_2$ laser radiation with $q$ changes from 60 W/cm$^2$ [11] up to 1.2 kW/cm$^2$ [18] was investigated. It was shown that $\varepsilon_{\lambda n}$ at wavelength 2.2 μm of investigated glass and polymer fibers reinforced plastics increases from 0.30 up to 0.85 and from 0.4 up to 0.8 accordingly during material heating up to 1600 – 1800 K [18].

Emittance $\varepsilon_{\lambda n}$ at the wavelength 0.63 and 1.15 μm of glass fiber reinforced plastic quickly increases up to 0.8 at the first seconds of laser heating, but at that time at the wavelength 5.25 μm $\varepsilon_{\lambda n}$ decreases till 0.55 [11]. In the same conditions emittance $\varepsilon_{\lambda n}$ of phenolic carbon fiber reinforced plastic practically do not change despite on increase of surface temperature [11].

## REFERENCES

1. Полежаев Ю.В., Юревич Ф.Б. Тепловая защита. М.: Энергия, 1976.

2. Материалы и покрытия в экстремальных условиях. Взгляд в будущее: в 3т. / под ред. С.В.Резника. М.: Изд-во МГТУ им. Н.Э.Баумана, 2002.

3. Рубцов Н.А., Аверков Е.И. Промышленная теплотехника. 1983. Т.5, №5. С.75—87.

4. Hampartsoumian E., Hainsworth D., Taylor I.M. et. al. J. Inst.Energy. 2001. Vol.74, P.91—99.

5. Mathew I., Goswani G.L., Ramakrishnan N. et.al. J. Mater. Process. Techn. 1999. Vol.89—90, P.198—203.

6. Jung-Taek Oh , Seung-Woo Kim. Optics Express. 2003. Vol.11, №14. P.1669—1676.

7. Wilson I.R. Aerospace. America, 2001. Vol.39, №3. P.34—40.

8. Минько Л.Я., Гончаров В.К., Лопарёв А.Н. ФХОМ. 1979. №1. С.31—36.

9. Длугунович В.А., Снопко В.Н. ИФЖ. 1987. Т.53, №2. С.442—448.

10. Длугунович В.А., Ждановский В.А., Захаров Н.С. и др. Изв. АН СССР. Сер.физ. 1991. Т.55, №6. С.1227—1232.

11. Карпухин В.Т., Маликов М.М., Монахов Н.В. и др. ФХОМ. 1991. №3. С.38—43.

12. Минько Л.Н., Насонов В.И. Оптич. журн. 1996. Т.63, №2. С.65–68.

13. Freeman R.K., Rigby F.A., Morley N.I. Thermophys. Heat Transf. 2000. Vol. 14, №3. P.305—312.

14. Агафонов В.А., Геда Я.М., Длугунович В.А. и др. ЖПС. 1986. Т.45, №1. С.25—30.

15. Длугунович В.А., Ждановский В.А., Снопко В.Н. ТВТ.1998. Т.36, №6. С.959—965.

16. Длугунович В.А., Доброхотов И.Н., Ждановский В.А., и др. ТВТ. 1990. Т.28, №6. С.1131—1134.

17. Длугунович В.А., Ждановский В.А., Снопко В.Н. ФХОМ. 2003. №2. С.44—50.

18. Ерёмин В.И., Коваленко И.П., Левашенко Г.И. и др. Кв. электр. 1990. Т.17, №10. С.1317—1320.

19. Девитт Д.Т., Рондо Р.Э. Аэрокосмическая техника. 1991. №3. С.146—154.

# DEVICE AND SOME OUTCOMES OF DEFINITION HEAT CONDUCTION LOW HEAT CONDUCTIVITY OF MATERIALS

**Borovik V.G., Frolov G.A., Sitalo V.G.(1), Tykhyy V.G.(1), Borovik D.V.**
Frantsevich Institute for Problems of Materials Science of NASU,
3, Krzhizhanovsky St., 03142, Kiev, Ukraine, E-mail: frolov@alfacom.net
(1)YUZHNOIE State Design Office, 3, Krivorozhskaja str., Dnepropetrovsk, 49008, Ukraine,
E-mail: info@yuzhnoye.com

Broad usage of honeycomb structures and other low heat conductivity materials in space-rocket and an aeronautical engineering requires perfecting methods of their calculation, that it is impossible without knowledge of properties, including thermal characteristics. Specially it is important at maintenance of space vehicles in orbit. In this case it is necessary to supply a split-hair accuracy of calculations of a thermal status of a design as, at first sight, minor deviations of a computational thermal conditions from actual may result in an overheating or a supercooling of a design at its long-lived maintenance.

The installation is intended for measurement of heat conduction low heat conductivity materials (3 layer honeycomb panels, foam plasticses, thin-layer heat-shielding and heat-insulating materials etc.) in a temperature range from 400 $^0$C up to 300 $^0$C on the basis the computer-controlled recording system of measured temperatures and processing of the obtained outcomes. Thus the system allows to define probable effect of different laws of a temperature variation of a heated up surface on heat conduction of heat-insulating materials.

The Technique is based on registrations of increase of temperature of the heat receiver which is heated up with a heat flow, passing through tested the sample, on a surface which one the given temperature with the help of the main heater is supported. The heat receiver represents the copper chrome-plated cylinder(drum) a dia and an altitude of 100 mm. Surfaces of a heat receiver, not contacting with a sample, lagged from an environment. During experiment on surfaces of a heat receiver, which one are not abuted with a sample, the zero heat flow with the help of the compensatory heaters arranged inside a thermal insulation of a heat receiver is supported. It allows to supply(ensure) adequate accuracy at definition of heat conduction of materials with $\lambda \le 0{,}1 \cdot W/(m \cdot K)$.

The software of the computer-controlled measuring system works, as the routine DOS/Windows-application, enables to set modes of tests of models to process and store results of tests by the way datafiles. Electrical signals from sensors (thermocouples) continuously, in a real-time, go in a computer through a module of linking. After program processing outcomes are mapped on the display, for example, by the way diagrams of change of temperatures of units of a measuring cell during all experiment. Recording of the minutes of experiment allows to conduct computerized analysis of the obtained outcomes and to calculate thermal conductivity for each concrete temperature of a sample. The full telemetry of a sample registered during experiment, includes temperatures of the main and compensatory (base and lateral) heaters; temperatures top and bottom backs heat-absorbing element; a channel of measurement of an electrical noise of a system.

For calculation of thermal conductivity of λ expression will be used:

$$\lambda = -Cm(T_n - T_0)\delta / F(T_н - T_n)\tau, \qquad (1)$$

Where *C*, *m* - thermal capacity of a material of a heat receiver and his(its) weight, $T_0$, $T_n$ – initial and current temperatures of a heat receiver, *T¡* - temperature of the heater (for a case of tests at constant temperature of the heater), *δ*, *F* - the area and width of a sample, τ - time, during which one a temperature difference (*T¡* - *T»*)

It is saved by a constant.

During experiment the temperature of heat receiver $T_n$ is augmented, therefore for calculation of thermal conductivity have used expression (1) written to differentially - an incremental view:

$$\lambda_i = \frac{C\left(T_{n_i} - T_{n_{i-1}}\right)}{\dfrac{F}{\delta}\left(\dfrac{T_{н_i} + T_{н_{i-1}}}{2} - \dfrac{T_{n_i} + T_{n_{i-1}}}{2}\right)\left(\tau_i - \tau_{i-1}\right)}, \qquad (2)$$

Where indexes *i* and (*i* - 1) correspond to values, measured and definite in instants $\tau_i$ and $\tau_{i-1}$. Generally expression (2) may be used at any law of a temperature variation on a heated up surface of a sample.

For implementation of a described technique the installation is set up, in a structure which one enter: a test cell, inside which one the sample, heaters and a heat receiver, equipped are arranged by thermocouples; the supply unit of heaters; the computer; the interface plate of linking of a test cell and the supply unit with PECM (analog-to-digital converter); the software.

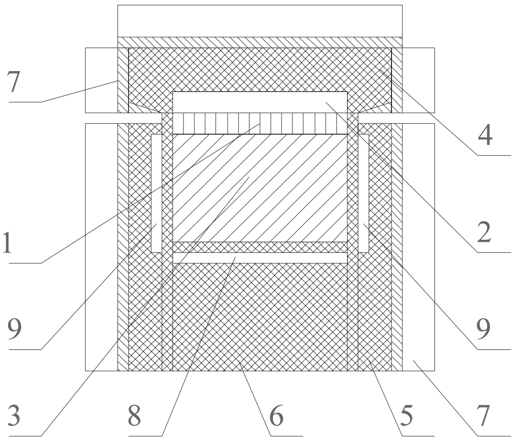

Fig.1

The sample **1** is set on a heat receiver **3** and прижат from above by the unit of the main heater **2**. The heat receiver **3** lies on the heat-shield basis **6,** inside which one the flat compensatory heater **8** is arranged. A sample **1** and a heat receiver **3** are placed inside of a heat-insulating tube **5**, inside which one the thin cylindrical compensatory heater **9** is located. A heat-insulating tube **5** and the basis of the heater **4** are arranged inside a chilled body **7**. The heater, a heat receiver and a chilled body **7** are made of a material with high heat conduction. The heater **2**, a heat receiver **3** and compensatory heaters **8** and **9** are supplied with thermocouples. On a heat receiver the upper temperature transmitter of a heat receiver (the circle of an electrosheet copper, on peripherals which one the thermocouple junction is fixed) is established. The lower temperature transmitter of a heat receiver is arranged on a heat insulator of the base compensatory heater. The temperature of a heat receiver is determined as mean arithmetic between indications of the top and bottom thermocouple. The temperature transmitter of the main heater (the circle of a copper nickel-plated metal paper, on peripherals which one the thermocouple junction is fixed) is pasted to a working surface of the heater, which one is abuted with a sample.

Experiments were conducted on samples of foam plastics ПС-1 a dia of 100 mm and width from 5 up to 30 mm. It was established, that average value of thermal conductivity of this material equally 0,035 ±0,002 W/m·K.

Below the relation of temperature of a heat receiver to time of experiment is adduced for it is model different width (fig. 2) and summary outcomes of definition of thermal conductivity of foam plastics ПС-1 on samples of miscellaneous width (fig. 3), from which one it is possible to draw following conclusions:

- the least dispersion of values of thermal conductivity is watched after 10000 seconds of heating;
- thermal conductivity of foam plastics ПС-1 does not depend on width of a sample and time of heating.

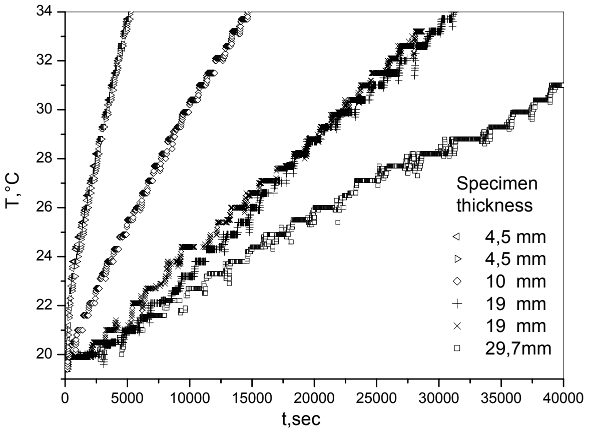

Fig.2

Fig.3

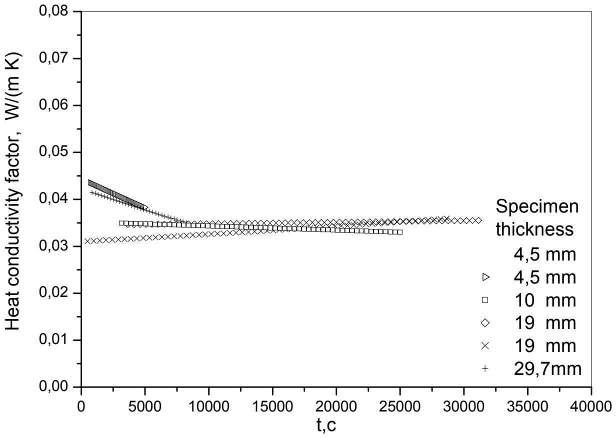

# STUDY OF STRUCTURE AND HIGH TEMPERATURE STRENGTH OF COMPOSITE MATERIALS BASED ON BORON NITRIDE.

**Vishnyakov L.R., Pereselenceva L.N., Sinayskyi B.M., Mazna O.V., Barschevska A.K.**
Frantsevich Institute for Problems of Materials Science, NASU,
3 Krzhizhanovsky str., Kyiv, 03142, Ukraine, e-mail: vish@i.com.ua

High refractoriness, thermal stability and thermal resistance, electrical and heat resistance of boron nitride, its chemical resistance in various aggressive media make it irreplaceable material for new important applications. However a low hardness, limited corrosion resistance to oxidative medium at 1000-1200 $^0$C reduce its application. Moreover, boron nitride belongs to hardly sintering materials and requires high energy consumption during hot pressing - high temperatures of up to 2000 $^0$C or above, and high pressure (of 30 to-35 MPa) - to achieve high density of bodies.

In this work, we succeeded in implementation of the conception of development of composite materials based on boron nitride and aluminum silicates, in which the synthesis of new phases (sialones or mullite respective of mixture composition) is performed during hot pressing. The synthesis of new phases in situ shall permit a considerable decrease of hot pressing parameters due to formation of a liquid phase during the low-temperature stages of pressing and reaction of formation of aluminum silicates at high-temperature stages, and to prepare essentially pore free materials based on boron nitride.

In this paper, a study of mechanical properties (bending and compression strength, modulus of elasticity) of composites as developed differing in structures, porosities, phase compositions, directions of hot pressing and testing temperatures was performed.

Scanning electron microscopy and X-ray diffraction methods were used for investigation of the structure and phase composition. The strength within 20 to 1200 $^0$C under vacuum was measured by three-point bending on rectangular beams of 3,0 x 4,0 x 30 mm in size, the compression strength was determined at room temperature, the electric tensiometer method was used to measure modulus of elasticity.

The effect of composite porosity on the ultimate bending strength was studied by analyzing a bulk of data obtained within the porosity range $\theta \cong 0–25\%$. Dependence of $\sigma_B(\theta)$ with a good degree of accuracy can be described following the model

$$\sigma_B = \sigma_{B0} \exp(-b\,\theta)$$

where $\sigma_B$ is the strength of the porous body,

$\sigma_{B0}$ is the strength of the dense body,

$b$ is the coefficient, which depends on the structure and testing conditions.

This model assumes that debonding effect of pores, $d\sigma$ is proportional to the integral porosity $\theta$ and does not directly account for the morphology of pores and their growth. The above processes take into consideration the coefficient of structure, b for a specific material. In our case, for boron nitride composites, the values of coefficient b fall into the interval of values proposed by E. Rishkevich [1] b = 0,04–0,07.

Table 1 gives a reduced phase composition of composites under study as resulted from X-ray diffraction data.

**Table 1**. Phase composition of boron nitride composites (volume fraction 0,75)

| Composite | Phase composition |
|---|---|
| 1 | $SiO_2$, amorph. |
| 2 | $Al_2O_3$, Corrundum |
| 3 | Mullite |
| 4 | Aluminum boron silicate |
| 5 | Sialon |

The typical mictrostructure of composites under study is presented in Fig. 1. The structure of composites under study features an expressed texture orientation governed by the morphology of crystals initional particles of hexagonal boron nitride: the particles when compacted place their developed surfaces each against other to form a morphological structure and being in no dependence on the composite phase composition.

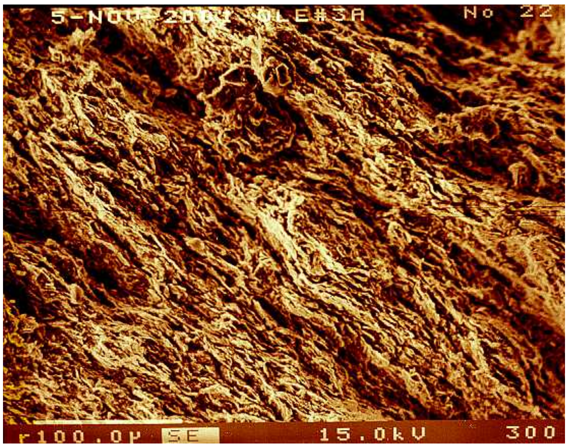

Fig. 1. Typical fracture surface of composites based on boron nitride or aluminum silicates (300)

Table 2 and Figs. 2 and 3 give the results of investigation of strength properties of boron nitride-Sialon/mullite composites as function of porosity, pressing direction and testing temperature. It follows from these data that the major factor influencing the strength values is porosity. The strength-porosity relationship is of exponential nature. The specimens having an insignificant porosity reveal high values of bending strength (100-120 MPa), at the 20-25 % porosity, the strength sharply drops showing 30-50 MPa. It should be noted that within the temperature range of 20-1200 $^0$C, the strength exhibits any noticeable change. A similar low dependence is also observed on the direction of hot pressing despite a pronounced texture microstructure of composites.

**Table 2.** Physical/Mechanical properties of BN-Sialon composites (specimens porosity is 18 to 25 %)

| | |
|---|---|
| Modulus of elasticity, GPa | 25,0 |
| Bending strength along pressing direction, MPa | 35-50 |
| Bending strength normally to pressing direction, MPa | 25-40 |
| Compression strength along pressing direction, MPa | 55-65 |
| Compression strength normally to pressing direction, MPa | 40-55 |

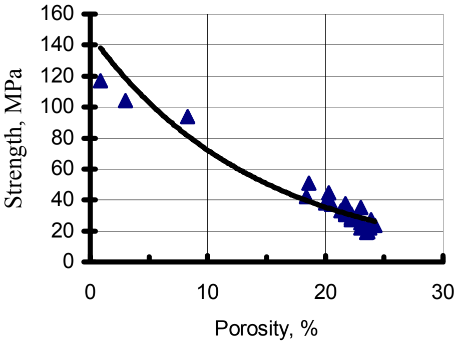

Fig. 2. Bending strength versus porosity of BN–Sialon composite

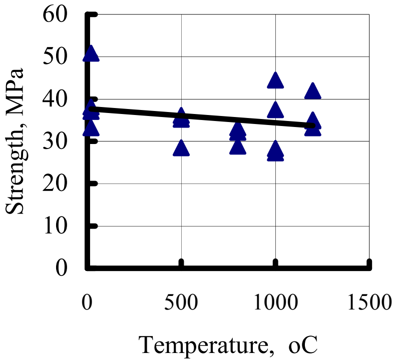

Fig. 3. Temperature-bending strength dependence of BN – Sialon composite (specimens porosity 18-25%)

It can be concluded from examination of composite deformation diagrams within 20-1200 $^0$C, and also fracture surfaces of specimens after the testing that the fracture mechanism varies with the testing temperature: at room temperature the fracture behavior is of brittle nature, while at high temperatures, plastic flow signs can be observed in a material.

In conclusion, composites based on boron nitride or aluminum silicates have been developed, which combine high density and strength, due to use of reaction of synthesis of new phases at hot pressing.

## References

1. Belov S.V. Porous materials in machine engineering. M. Machinostroyenie 1981. – P. 247. (In Russian).

# POLYMER COMPOSITES CONTAINING NATURAL ZEOLITES TO BE EXPLOITED UNDER EXTREME CONDITIONS*

**Okhlopkova A.A., Petrova P.N.**
Institute of Nonmetallic Materials SB RAS
20, Avtodorozhnaya St., 677007, Yakutsk, Russia, inm@ysn.ru

Polymer-based tribotechnical materials play an important role within the structure and the volume of the materials applied in the production of friction units. It can be explained by the fact that diverse urgent requirements of tribotechnique can be satisfied by application of special polymer materials, which do not demand lubrication, in deep vacuum and under other extreme conditions [1].

The present paper covers tribotechnical characteristics of PTFE modified by natural zeolites in the wide range of temperatures, loads and sliding velocities.

Tribotechnical tests at room temperature were carried out using Friction Machine I-47 at p=0.1 MPa, v=0.5 m/sec. during 3 hours. It was shown that wear velocity for the composites filled with natural zeolites is maximal at the initial testing stage and gradually reduces tending to zero. Actuation of the filler in the planetary mill AGO-2 causes significant reduction of the composite wear rate. Such considerable growth of wear resistance of PTFE after injecting small amounts of actuated fillers can be explained by the fact that unlike pure PTFE wear particles do not leave friction area, but participate in the wear processes and form a strong transient film on the friction surfaces of the contacting units [2].

Injection of actuated zeolites into PTFE 2-3 times raises the material wear resistance at high loads compared to that of the composites containing an inactuated filler in the same concentration.

Taking into account that the developed PCM compositions were designed for friction units of technique and technological equipment operating under the conditions of cold climate, we paid special attention to thermo-frictional properties of PCM at low temperatures using a tribometer with a removal unit and vertical rotation axis of a friction machine TL-A. (Scheme of friction – “finger-disk” (end-face friction), sample-bush with the diameter of 22x12 mm, at pressure – 0.7 MPa, rotation speed 2.24 rpm (2 mm/sec.)). Such small sliding speed excludes temperature changes on the friction surface at the expense of self-heating, which allows monotonous reducing of the working unit temperature.

Low-temperature investigations of friction coefficient of the composites based on PTFE and natural zeolites showed that the developed composition performed higher friction coefficient having values from 0.06-0.09 to 0.12-0.15 accompanying temperature lowering from +20°C to -70°C. This can be explained by “freezing” of PTFE structure followed by degradation of segmental mobility of the macromolecules, which results in slowing down relaxation processes and growing capacity to resist shear forces [3]. All studied anti-frictional compositions based on PTFE and natural zeolites preserve their operability at temperatures -40°C - -60°C under the conditions of low sliding velocity and modest loads.

One of the investigation tasks was to study tribotechnical properties of filled compositions under real friction conditions. In this connexion we have carried out experiments using a horizontal friction machine I-47 (p=0.1 MPa, v=0.5 m/sec.). The experiments allowed measuring the launching friction torque for cooled to -35°C material and PCM friction coefficient with temperature growing to +20°C. Experiments showed that actuation of zeolites causes lower launching (0.3 compared to 0.39) and stable dynamic friction coefficient, intense transfer of the composite material to the steel counterbody and low wear speed for PCM.

Influence of positive temperatures on the value of the friction coefficient was studied using horizontal friction machine I-47 at p=1 MPa, v=0.5 m/sec. Heating was made using outer ring heater.

---

* The investigation was supported by the Russian Fund of Fundamental Research “r2003arctic-a” (grant # 03-03-96019)

Investigation of thermo-frictional dependencies (temperature interval 0°C - 320°C) allowed registering stability of friction coefficient for pure PTFE within the whole temperature range. After PTFE filling with inactuated zeolites thermo-frictional dependencies change complicatedly. One can observe monotonous growth of friction coefficient to 300°C, after which it starts to decrease slightly.

Injection of 2-minute actuated zeolites causes reduction of launch coefficient of friction compared to pure PTFE and stable values within the temperature range 0…150°C followed by insignificant growth of its values. Deformation and orientation processes dominate within the temperature range from 20 to 150°C. These effects are accompanied by plastic deformations and orientation of PCM surface layers in the sliding direction, which causes stability in friction coefficient values [4]. Growth of friction coefficient of PCM at temperatures above 150°C can be explained by the activation of molecular interaction on the friction surfaces and reducing of the layer crystallinity at the expense of the crystal destruction and their transition into amorphous phase, as the temperature of the contact area can be close to that of the crystallite melting (~327°C) [5]. Temperature growing will cause increase in wear rate of unfilled PTFE, for filled materials this index decreases. Temperature growth conduces to growth of autohesion of wear particles and, evidently, to formation of monolith film of transfer, thus reducing wear rate. Besides, at elevated temperatures one can notice active tribo-chemical reactions in PCM, when filler particles play the role of catalysts of cross-linking for separate segments of the PTFE macromolecule tribo-destruction [2]. This leads to formation of wear resistant surface layer of PCM.

.

Estimated were the regularities of PTFE formation depending on contents, chemical nature and time of actuation of natural zeolites. It was shown that 2-minute actuation of zeolites causes radical reorganization of PTFE structure, which raises PCM wear resistance by 90-150 times, deformational characteristics by 20-25 per cent with strength being the same as that of unfilled one (20-22 MPa).

Therefore, one can see the efficiency of application of natural zeolites as PTFE fillers aiming at production of tribotechnical materials. Actuated zeolites are more applicable for the materials exploited under extreme conditions.

**References**

1. Friction and Wear of the Materials Based on Polymers / V.A.Bely, A.I.Sviridenok, M.I.Pokrovets, V.G.Savkin. – Minsk: Science and Technique, 1976. – 432 pp.
2. Okhlopkova A.A., Vinogradov A.V.> Pinchuk L.S. Plastics Filled with Ultradispersed Compositions. – Gomel: IMMS, BAS, 1999. – 164 pp.
3. Chersky I.N. Application of Fluoroplastic-4 for Sealing Units Working at Low Temperatures // Physical and technical problems of Transport in the North, 1971. – p. 103-107
4. Influence of Conditions of Structure Formation on Friction Properties of F-4 Containing Additives // Comp. Polym. Mater. – 1986. - # 30. – p. 25-28
5. Sviridenok A.I., Savkin V.G., Nevzorov V.V. Tomotribographic Investigations of Polymers // Structure and Properties of the Polymer Surface Layers. – Kiev: Naukova Dumka, 1972. – p. 106-110.

# THE STUDY OF THE ENVIRONMENT HIGH TEMPERATURE EFFECTS ON THE OPTICAL PARAMETERS OF SILICON AND TITANIUM OXIDE THIN FILMS

**Prosovskii O.F.,** **Kelina R.P.**
Obninsk Research and Production Enterprise (ORPE) "Technologiya", Obninsk, Russia
Obninsk, Kaluga Region, Russia, E-mail: onpptechn@kaluga.ru

The effects of extreme outer conditions (high temperature) on the optical properties of thin film condensates which are used in optical structures of precise interference light filters are studied in this paper. The method of determination of optical thickness of the selected interference pair - film-forming materials with high and low refraction indexes was used for the study. This method is based on the optical measurements of the reflection of a two-layer coating of quarter-wavelength films of the materials produced by the evaporation in vacuum. The optical thickness of a thin film is the product of the film refraction index n into the geometric thickness h. In order to determine the refraction index of a thin film coating and its geometric thickness a well-known method of reflectance spectrum measurement with the following calculation of n and h parameters with the help of a personal computer was used. The accuracy of measurements received much attention in the course of these investigations. For this purpose the data from a spectrophotometer controller were transferred through the serial port directly to a personal computer and were recorded on a hard disk for the following processing - constructing the plots and tables. Owing to this a human factor was eliminated and the measurement accuracy was maximized.

A pair of hard materials - silicon and titanium oxides was chosen for the study. These materials make it possible to create interference light filters of various optical structures and possess higher operating characteristics (mechanical action resistance) as compared to the characteristics of a pair of softer materials such as magnesium fluoride and zinc sulfide. The choice of hard materials is also defined by the factthat these materials (silicon and titanium oxides) correlate well from the viewpoint of the linear expansion coefficient and they make it possible to produce multy-layer (40 and more layers) interference light filters.

The investigations of high temperature (up to 500 °C) effects on thin-film vacuum of silicon and titanium condensates oxide produced by the electron-beam evaporation at various temperatures of substrate heating in the course of deposition of the films in vacuum were performed. The variation of thin films structure under high temperature heating of the specimens was evaluated. The method of evaluation is based on the measurement of open porosity of thin films produced.

The practical value of this work is the possibility to determine the ultimate levels of environmental temperatures at which the established optical parameters of interference coatings are retained, and the possibility to determine properly technological parameters of thin films deposition in order to produce light filters resistant to the effects of high temperature.

1. Pulker H.K., Gunter K.H. // Vacuum Technic / 1972/-Vol.21, No.8, P.202-207.
2. Ritter E., Hofman R. // J.Vac.Sci.Technol. – 1969.-Vol.6, No.4, p.733-73.
3. Prosovskii O.F.//Optical-mechanical industry.-1990., No.7, p.61-64.

# ABOUT NATURE OF POROSITY OF THE CAST REFRACTORY COMPOUNDS

**Stepanchuk A.N.**
National Technical University of Ukraine,”KPI”
030056, Prospect Pobedy, 39, Ukraine
Tel.(044) 2417617; E-mail: astepanchuk@iff-kpi.kiev.ua

Refractory compounds, in particular, the carbides of transitional metals of the periodic table and materials with their participation find wide application in different field of science and technique. At the same time, as shown in works [1-2], their specific properties will be more completely realized, when carbides are in the cast. Such materials have a 100% density, advanced abrasive ability, oxidation and corrosion resistance.

In addition, such materials, due to the high density and purity can be the obejct of researches in regard to get their physical-mechanical properties for more exact prognostication of application field of refractory compounds and materials with their participation. In this connection the study of conditions of making and forming of structure and properties of the cast refractory compounds in our view is a fully actual task.

Information about a production of the cast refractory compounds is limited and concerned, mainly, the study of their properties. Besides the vital importance has an influence of technological parameters on forming of properties of materials at conditions of their making. As it was already marked above, the porosity that occurs in the cast refractory compounds depending on the conditions of their making has the essential influence on properties of materials. In this connection the attempt of proving of nature of the porosity of the cast refractory compounds, that, in principle, is not characteristic for them, is done in this work.

The cast carbides of titan, zirconium, niobium, chrome, molybdenum and tungsten were explored. The cast carbides were prepared by method described in work [3]. Influence of cooling speed of fusion and gas pressure in a working chamber on the structure of the cast carbides was studied. Cooling of fusion was conducted on two variants. In the first variant a melt was cooled at a speed of 320—350 degree/min to the temperature 500 °C and then at a speed of 60—80 degree/min to the room temperature. Such regime of cooling took place in the case of melting without heating of fusion. On the second variant regulated speed of cooling was within the limits of 40—50 degree/min due to application of the indirect heating of melt.

The process of forming of structure and properties of carbides was examined based on suppositions that there is their dissociation with subsequent evaporation of products of dissociation and influence on this process of pressure of gas in a working chamber at melting of carbides [3].

The study of microstructure showed that for most explored carbides melted at low pressures, the presence of pores, which are located on the border of corns, is characteristic. At that an amount of pores and their size are diminished with the increase of gas pressure at melting. It should be noted that porosity of the carbides got without heating of the melt is higher, than at the carbides got with warming up of melt. It is also set that for the carbides of transitional metals of 1Уa and V groups of periodic system the size and amount of pores are diminished in a line TiC—ZrC—NbC. Microporosity is practically absent for the carbides of transitional metals of the У1a group.

The study of porosity of the cast carbides and its dependence on the conditions of their production allows to express some assumption about porosity nature. For example, it can be conditioned by the evolution of gaseous products of decomposition in the process of crystallization of melt, or can have the character of inclusion (carbon) and, finally, can constitute a shrinkage porosity, arising in the process of crystallization of melt with large range of crystallization. How is noted in work [4], important influence on the process of formation of shrinkage defects (porosity belongs to them) are provided by properties of matter in the interval of temperatures of its crystallization from melt $\Delta\tau_{kr}$ and intensity of the external cooling of cast which determines the value of temperature gradient $\delta\tau$, arising in the cast section.

Depending on the numeral value of relation [4]:

$$K=\frac{\Delta\tau_{кр.}}{\delta,\tau}$$

a few types of shrinkage defects are differentiated. If K considerably less unit, there is the well developed shrinkage cavity in the cast. This phenomenon is characteristic for crystallization of materials with narrow interval of temperatures of crystallization at cooling with large intensity. If K≈1, in this case the both concentrated shrinkage cavity and crystallization porosity are usually founded.

And, finally, the dissipated crystallization porosity is observed in the all volume of cast if K more than unit.

From the diagrams of the state of the Me-C systems for the transitional metals of the IV-a – V-a sub-groups, it is possible to do the conclusion, that the corresponding carbides in area of homogeneity possess the wide temperature range of crystallization, that is increased towards compositions with less contents of the bound carbon. Compositions, nearly stoichiometric, practically have no the temperature range of crystallization.

In connection with foregoing, calculating K at different $\Delta\tau_{kr}$, it is possible to define the type of shrinkage defects which can arise up in the process of crystallization of carbides, and consequently indirectly to judge about behavior of carbides during melting.

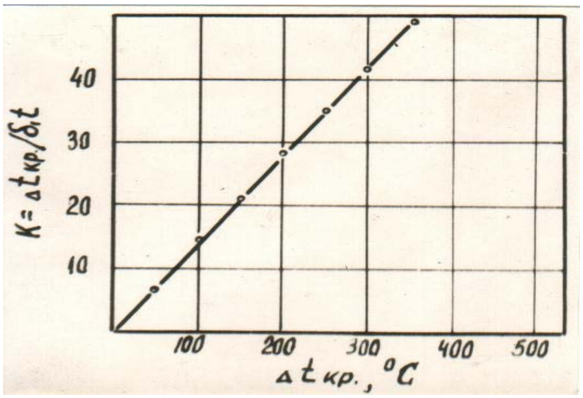

Fig 1- Dependence of parameter K on the temperature range of crystallization

The calculations conducted by us showed (fig.1), that the crystallization of nearly stoichiometrical carbides must be accompanied by formation of both shrinkage cavity and crystallizatio.n porosity. Probability of formation of the crystallization porosity grows with decrease of the C/Me relation due to the increase $\Delta\tau_{kr.}$

Thus it is possible to assume that during crystallization of carbides in the conditions of this work the porosity has the shrinkage character, although influence of components evaporation and also presence of free carbon is not eliminated.

Diminution of porosity with the increase of gas pressure at melting it is possible to explain by suppression of components evaporation at carbides decomposition, that leads to the carbide melt with higher contain of carbon and the narrow temperature range of crystallization.

On the other hand, the diminution of porosity could be explained by influence of gas pressure on the filling of intercrystal emptinesses appearing in the process of liquid phase crystallization during the process of ingot formation in the range of crystallization $\Delta\tau_{kr}$.

## Literature

1. Степанчук А.Н., Вдовиченко Н.С., Нечипоренко А.А. Применение композиционных материалов с участием тугоплавких соединений для нанесения газотермических покрытий. //Сб.НТ Киевского политехнического института. ч.П. - 1994. - С. 78 - 87.

2. Адамовский А.А., Степанчук А.Н. Особенности шлифования титановых изделий кругами из карбида ниобия. //Технология и организация производства. - 1978. - №4. - С.24 - 26.

3. Степанчук А.Н., Шлюко В.Я., Криворучко И.П. Технология получения отливок из карбидов титана, циркония и ниобия. //Технология и организация производства. -1971. №4. - С.93 - 95.

4. Усадочные процессы в металлах // Труды Ш-го совещания по теории литейных роцессов. - М.: Изд-во АН СССР. - 1960 . - С. 32.

# RESEARCH INTO PHYSICOTECHNICAL PROPERTIES OF BORON NITRIDE AT HIGH TEMPERATURES. EXPERIMENTAL EVALUATION OF SINTERED BORON NITRIDE SERVICEABILITY IN THE ARTICLES FOR HIGH-TEMPERATURE EQUIPMENT

**Rusanova L.N., Gorchakova L.I., Kulikova G.I., Alexeev M.K.**
Federal State Unitary Enterprise ORPE “Technologiya”, Obninsk, Russia

A high-pure isotropic material with satisfactory strength has been produced by reaction sintering of turbostratic boron nitride powders with an addition of amorphous boron. The boron nitride content in the material is up to 99 wt.%.

Of the dielectrics, boron nitride stands out because of its stability of operational characteristics over the temperature range of up to 2000 °C. It may be used in various products for rocket and airspace engineering. A high temperature threshold of stable state retention, resistance to thermal shock, weak dependence of physical properties on temperature and radio frequency make these materials by far very promising for the production of the most essential components and assembly units in rockets.

Over the investigated temperature range of up to 2000 °C, a temperature coefficient of dielectric permittivity does not exceed 3%. Absolute value of dielectric permittivity is within the range of 2,8—3,3 depending on ceramic density. Dielectric loss at 2000 °C is less than $10^{-2}$. Electrical resistance of reaction-sintered ceramics is $10^{12}$-$10^{14}$ Ohm·m at 20 °C and $10^{5}$-$10^{7}$ Ohm·m at 1000 °C.

Boron nitride falls within destructible thermal protection materials. When heated up to a destruction temperature, boron nitride transfers the heat easily from the heated surface due to its high thermal conductivity. High value of dissociation temperature and relatively high value of thermal capacity assure high efficiency of boron nitride as a thermal protection material.

At a temperature of around 3000 °C boron nitride sublimates with a considerable endothermic effect. Under sublimation conditions its thermal protection ability is the most efficient. At the same time boron nitride oxidation is accompanied by exothermal effect which somewhat impairs the thermal balance on the surface of the article operating in the oxidizing flow.

All over the investigated temperature range (above 3000 °C) at high powers of a plasma flow as well as when tested using a powerful laser plant, reaction-sintered boron nitride shows high resistance. It has superior thermal-erosion characteristics to those of all known kinds of thermal protection materials.

Dielectric windows 80 mm in diameter which are tested on a gas-dynamic bed have been manufactured from reaction-sintered boron nitride. Working life at 2400 °C is 20 sec., the rate of a rise in temperature – 500 °C/sec, the ablation on multifold cyclic heating does not exceed 0,2 kg/m$^2$, the efficient enthalpy measures 16,5 MJ/kg.

At present the successful testing of a number of pilot products intended for introduction in perspective high-temperature equipment has been conducted.

# INVESTIGATION OF THE DEPENDENCE OF OXYGEN-ION CONDUCTIVITY OF SOLID ELECTROLYTES OPERATING IN LIQUID-METAL MEDIA ON STRUCTURAL AND PHASE CERAMIC COMPOSITION

**Yakushkina V.S., Korablyova Ye.A., D'jachenko O.P., Vikulin V.V.**.
Federal State Unitary Enterprise
"Obninsk Research and Production Enterprise "TECHNOLOGIYA", Obninsk, Russia

Ceramic materials of the $ZrO_2$—$Y_2O_3$, $ZrO_2$—MgO systems find wide application in fabrication of solid electrolytes for the oxygen concentration sensors intended for use in different liquid-metal media at temperatures ranging from 300 to 1800 °C.

Stringent requirements are imposed upon solid electrolyte materials, i.e. together with ionic conductivity, chemical resistance to melt metals the material must have high thermomechanical properties. For instance, solid electrolyte used in sensors for the control of the oxidation level of liquid steel during the express analysis in metallurgy must be able to withstand a thermal shock and retain its serviceability for several seconds at a temperature of 1500—1800 °C. Solid electrolytes for oxygen activity sensors operating in liquid-metal heat carrier (Pb or Pb—Bi) at a temperature of 300—600 °C are subjected to cyclic thermal shocks and vibration and hydromechanical attacks.

The quality of solid electrolytes which provides for stability and accuracy of sensor readings depends on the type and nature of conductivity, density, thermal resistance which are considerably specified by the structure and ceramics phase composition.

The object of this research work is to study the dependence of the oxygen-ion conductivity of solid electrolytes on the phase content and structure of the ceramics and to specify the region of oxygen-ion conductivity only.

Chemically deposited powders and the process of thermoplastic injection molding were used for the preparation of solid electrolytes from ceramics of the $ZrO_2$—$Y_2O_3$, $ZrO_2$—MgO systems.

As a result of investigations provided, the dependence of oxygen-ion conductivity of solid electrolytes operating in liquid-metal media on the phase and chemical composition, structure and density of the ceramics has been established. The solid electrolytes from the $ZrO_2$+3mol %$Y_2O_3$ ceramics of a tetragonal modification have the best oxygen-ion conductivity in the temperature range from 360 to 500 °C and strength 550—750 MPa. The graphs of the dependence of the electromotive force of fast–acting sensors for the oxidation level control operating in liquid steel in the temperature range from 1500 to 1800 °C on the test time, phase composition and ceramic structure.

The results of the investigation have been applied to the fabrication of solid electrolytes for oxygen activity sensors intended for use in the experimental set-ups and test beds operating with liquid-metal heat carrier (Pb or Pb—Bi).

# SOLID-PHASE PROCESSES AND THERMAL DIFFUSIVITY OF HEAT-INSULATING CARBIDE MATERIALS

**Ulyanova T.M., Krut'ko N.P.**
Institute of General and Inorganic Chemistry of the NAS of Belarus,
220072 Minsk, 9 Surganov Str., E-mai:ulya@igic.bas-net.by

The thermophysical properties of individual substances and composites are the function of a number of parameters: structure, compositions, porosity and also external actions such as temperature, radiation, magnetic field, moisture content, etc. In turn, the thermophysical properties of heat-insulating materials: heat conduction, thermal diffusivity, heat capacity, and thermal expansion determine the thermal stability of ceramics and its operating conditions. The mechanism for heat transfer in solids is reasonably well studied theoretically. But up to now exact relations for calculation of thermal conductivity of heat-insulating materials and amorphous substances have not yet been succeeded. In this connection, the necessity exists of carrying out experimental investigations into the thermophysical properties as a function of physical-chemical characteristics of materials and their structure in effort to create purposeful heat insulators. The present work is devoted to studying the dependence of the effective thermal diffusivity of the heat-insulating composite material C-ZrC-HfC on its structure and on the physical-chemical processes that proceed in it over the temperature range 1000-2050$^0$C.

Heat-insulating samples were prepared by carefully mixing the powders and fibers of zirconia and hafnia with the binder of the mixture of epoxy and phenolformaldihyde resins. Zirconia and hafnia fibers were produced from hydrocellulose filaments impregnated with the appropriate salts of metals, followed by their heat treatment in the oxidizing atmosphere. The zirconia powder of high purity was used and powdered hafnium oxide was prepared by 1000$^0$C calcination of acetic hafnium. The prepared green bodies were subjected to helium heat treatment by smoothly increasing the temperature to 1000$^0$C. The samples were shaped as porous cylinders 26 mm in dia and 70 mm in length. The X-ray phase analysis revealed that the prepared heat-insulating material was composed of the individual monoclinic phases of zirconia and hafnia, and also of carbon of turbostrata structure. The content of oxides in the samples was varied from 0 to 89%, of nitrogen from 0.10 to 0.15, of carbon from 10.40 to 19.15%.

By varying the ratio of oxide fibrous and powdered components in the base mixtures we regulated the density and porosity of samples. The apparent density was varied from $1.54 \cdot 10^3$ to $2.14 \cdot 10^3$ kg/m$^3$, and the value of the total porosity was accordingly 68-43%. The thermal diffusivity responsible for the propagation velocity of the isothermal front in a solid under heating was chosen as an experimental thermophysical characteristic:

$$\mathbf{a = \lambda / c \cdot \rho} \quad \text{W/m·deg}$$

Here **a** is the thermal diffusivity, **λ** is the thermal conductivity, **c** is the heat capacity, and **ρ** is the density.

According to the heat conduction theory, in solid heat insulators heat is transferred due to the vibrations of atoms and molecules by the phonon mechanism.

Effective thermal conductivity was measured in a high-temperature resistance furnace equipped with a graphite heater. The inner diameter of the heater was equal to 30 mm, its wall thickness was 6 mm, and its length was 330 mm. Samples with different apparent density ($1.54 \cdot 10^3$ and $2.14 \cdot 10^3$ kg/m$^3$) were used and heated with a rate of 0.65-0.75 deg/s over the temperature range under continuous helium blowing-through of the furnace space to remove forming gaseous products. The sample temperature was measured by a reference optical pyrometer EOP-66 and by a chromel-alumel thermocouple. Thermal diffusivity was determined during entire monotonic heating of samples up to 2050$^0$C. The relative error of the quantity **a** was 9%. The initial temperature rise from 20 to 200$^0$C was not high (0.1 deg/s). This condition was necessary to remove the absorbed moisture from the porous samples not deforming them. A further temperature rise occurred with a higher rate since the samples had been preliminarily annealed at 1000$^0$C, and then the heating rate was again decreased to 0.5 deg/s.

The study showed that the thermal diffusivity varied a non-monotonic manner with increasing temperature, its values decreased over the ranges 1100-1200, 1300-1400 and 1600-1700$^0$C. The samples with different apparent density showed up this behavior. As a whole, the value of the parameter **a** was higher for the sample with a less density and a higher porosity. This agrees with the heat transfer theory.

Consider the reasons that initiated a decrease in the values of the thermal diffusivity of samples over certain temperature ranges. In heat insulators with phonon heat conduction, as the temperature elevates, the number of thermal vibrations increases and heat conduction enhances. At the same time the number of short-wave phonons that dissipate long-wave phonons transferring energy grows. The phonon dissipation is also affected by the crystal lattice imperfection, crystal defects, and foreign impurities. All this causes a thermal front to decelerate in solids. From the literature it is known and the results of the thermogravimetric and X-ray phase analyses of our experiments support that over the temperature range 1100-1200$^0$C in zirconia the monoclinic structure transforms into the tetragonal one, the crystal lattice is disordered, and a new phase is formed. Hence the structural changes in solids can also decrease the propagation velocity of the thermal from.

By the data of the thermogravimetric analysis the samples with metal oxides and carbon started to lose their mass at 1250$^0$C. The main mass loss occurred over the temperature range. 1300 – 1600$^o$C. From the data of the X-phase analysis it follows that at 1300$^0$C the phases of zirconium and hafnium carbides began forming. The reaction of carbide formation proceeded at a higher temperature for hafnium oxides as against zirconia. During these processes the tetragonal crystal lattices of metal oxides collapsed and the cubic ones of carbides were formed. Likely the latter initiated the dissipation of long-wave phonons and a decrease in thermally diffusivity. According to our data the minima on the curves for the thermal diffusivity **a** as a function of zirconium carbide within 1300-1500$^0$ and hafnium carbide over the range 1600-1700$^0$C.

When analyzing the results obtained, we took into account that the reactions of carbide formation proceeded with the release of gaseous products of CO and $CO_2$, whose values of effective thermal diffusivity were considerably higher than those of the sample material. Hence, heat transfer in solids would have to increase. However, the samples were heated by the helium flow that penetrated into pores, mixed with evolved gases. The latter were constantly removed by the inert gas flow. In addition, the thermal diffusivity of helium was by the order of magnitude higher than that of carbon monoxide, therefore, their contribution to the heat transfer process appeared to be inconsiderable in this experiment. Upon 2hr isothermal keeping of samples at 2050$^0$C the chemical processes ceased and the produced heat-insulating material contained metal carbides and carbon. The samples were cooled and thermal diffusivity was again determined over the temperature range 900-2050$^0$C. On heat treatment, the quantity **a** monotonically varied with elevating heating temperature, which was consistent with the heat conduction theory for heat insulators.

The formation of carbides in the considered systems was also markedly affected by the heating rate of samples. Under the non-isothermal temperature rise conditions the kinetic curves were obtained for the samples of the model systems with different heating rates from 0.11 to 0.37 deg/s. All the kinetic curves were S-shaped and governed by Arrhenius' equation. As the heating rate increased, the reaction of carbide formation moved up in higher temperatures by 100$^0$C, which was stipulated by the local reaction at the interface MeO-C. In the general case, zirconium and hafnium carbides were formed in the samples with fibrous oxides at the temperatures that were by 200-300$^0$C lower than those in the reactions with powdered components. The latter was bound up with the high-dispersed state of oxides in fibers and their enhanced reactivity.

The study of the effective thermal diffusivity of the samples of the model systems: metal oxide - carbon has shown that it is not only the heat-insulating characteristic of material but is also a high-sensitive parameter that correlates with phase changes, solid-phase reactions in composites and can be used for controlling physical-chemical processes in the development of high-temperature heat-insulating materials.

# THE USE OF AERO-GEL $AL_2O_3{\cdot}H_2O$ FOR THE PRODUCTION OF SILICON NITRIDE CERAMICS

**Kelina I.Yu., Martynov P.N.(1), Askhadullin R.Sh.(1), Chevykalova L.A., Pljasunkova L.A., Peshchenko D.V., Zakorzhevkij V.V.(2), Yudintsev P.A.(1).**
Federal State Unitary Enterprise “Obninsk Research and Production Enterprise “Technologiya”
15 Kiev Str., Obninsk, 249035, Kaluga Region, Russia, *onpptechn@kaluga.ru*
(1)Leipunsky State Research Center of Russian Federation - Institute of Physics and Power Engineering.1, Bondarenko sq., Obninsk, 249033, Russia.
(2)Institute of Structural Macrokinetics and Materials Science.
Chernogolovka, Moscow Region, 142432, Russia

Within the last few years a considerable progress in the improvement of a characteristics level of technical ceramics has been achieved and an insight about interrelation between its composition, properties, microstructure and production technology has been widened. One of the problems of the development of wear-resistant structural materials is to provide for their high-temperature strength properties at 1000-1300°C and high hardness and wear resistance.

A number of hot-pressed materials based on silicon nitride powders which were obtained by plasma-chemical and self-propagating high-temperature syntheses (PCS and SHS) has been prepared at FSUE “ORPE “Technologiya”. Typical sintering activators for these powders are yttrium and magnesium oxides. They are introduced into the powders just in the course of PCS and if the powders are prepared by SHS method, the mechanical way is used. The content of sintering activator for the powders with the particle size 0.01 μm used in plasma-chemical synthesis process varies within the range of 3 to 18 weight % ($Y_2O_3$) and 1.5-5 weight % (MgO). In the case of polydispersed powders with particle size 1-2 μm, used in self-propagating synthesis process, the high density of the ceramics is achieved when using the activator content 2-2.5 times as much as compared with ultrafine dispersed powders used for plasma-chemical synthesis.

It is known that $Al_2O_3$ is an efficient sintering activator for silicon nitride powders. In different researches carried out a content of the sintering activator varies from 2 to 15 weight % [1]. From the data given in paper [2] it is evident that the mechanical strength for the ceramics containing $Si_3N_4$ and 2-10 weight % $Al_2O_3$ is 640-710MPa at room temperature and 310-560 MPa at 1200°C.

Also it is known that the complex MgO (1-5 weight %) and $Al_2O_3$ (1-9 weight %) additive allows for obtaining silicon nitride ceramics with a high level of physical and mechanical properties including in addition high-temperature properties. Using these systems foreign companies have developed various high-temperature strength materials, for example, the grades SN-201, SN-205, “Kyocera”, Japan, HS-130, “Lucas”, USA, “Saint-Gobain/Norton”, USA [3].

In the paper presented here a possibility of obtaining dense heat-resistant ceramics based on $\alpha\text{–}Si_3N_4$ powders (SHS) with the use of small amounts of the sintering activator in the form of high-active aero-gel of alumina monohydrate $Al_2O_3{\cdot}H_2O$ has been investigated. This aero-gel possesses a high specific surface area up to $800 m^2/g$ and has a nanodimensionality of structural components (20-50 nm) and is produced from gallium-aluminium melt (Fig.1) subjected to selective oxidation process. Also, the possibility of increasing physical and mechanical ceramics properties when using an additional content of the aero-gel has been investigated.

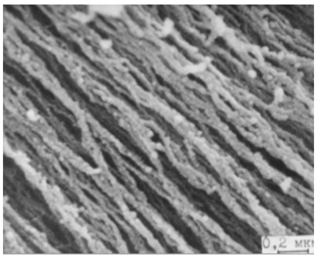

× 50000

**Fig.1.** The microstructure of $Al_2O_3{\cdot}H_2O$ material synthesized by a selective oxidizing of Ga-Al melt.

The silicon nitride powders with the average particle size of 0.7 and 0.5 μm produced by a method of self-propagating high-temperature synthesis at the SHS Research Center of Institute of Structural Macrokinetics and Materials Science have been chosen for investigations. Taking into consideration high aero-gel dispersivity, its content varied in the range of up to 2 weight %.

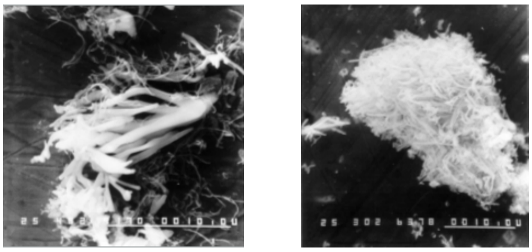

a) $d_{av}$ – 0.7 μm b) $d_{av}$ – 0.5 μm

**Fig.2.** Microstructure of initial powders α-$Si_3N_4$ (SHS) with different average particles size.

A mixing of portions of starting powder and sintering activator was carried out in benzine with the use of milling bodies made from alumina in cassette mixer for 50 hours followed by drying in air.

The ceramics specimens were made by hot pressing in graphite molds at 1750-1800°C under 15-20 MPa in nitrogen medium.

In the course of the research the physical/mechanical properties of the experimental specimens based on silicon nitride (SHS) and produced with the use of aero-gel as sintering activator were evaluated. This evaluation totally confirms the results of microstructural research concerning the optimum content of the sintering activator for the powder with dispersivity up to 1 micron (**Fig.3**). The following high characteristics are obtained when introducing 2 weight % aero-gel for the powders having particles with medium size equal to 0.5 micron: zero porosity, strength 600-700 MPa at room temperature and 400-420 MPa at 1300°C, microhardness up to 20 GPa.

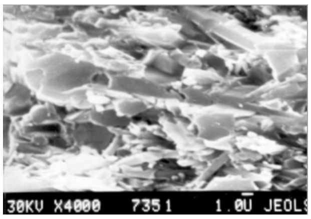

**Fig. 3.** The microstructure of ceramics in the system $Si_3N_4$ – 2 weight % $Al_2O_3 \cdot H_2O$

X-ray phase analysis shows that in X-rayograms of being researched specimens the peaks which are typical for α-$Si_3N_4$ and which are difficult to be determined quantitatively at this stage of the research are present along with the main peaks β-$Si_3N_4$, which are characteristic of previously developed hot-pressed materials.

The further improving of the high-temperature properties of the ceramics in this system should be ensured by minimization of α-phase at the expense of completion of α→β transformation.

On the basis of carried out analysis of composition and properties of the foreign and domestic materials in the system $Si_3N_4$-MgO-$Al_2O_3$ and previously obtained results concerning the use of aero-gel $Al_2O_3 \cdot H_2O$ as sintering additive it was recommended to introduce aero-gel into matrix powders $Si_3N_4$ (SHS) in amounts of no more than 1 weight % to obtain the ceramics in this system.

Microstructure analysis of the manufactured ceramics specimens showed good distribution of the aero-gel fibers over the whole volume in the course of specimens manufacture by developed technology even at aero-gel content of 0.5 weight %. The X-ray phase researches showed at this stage the presence of α-$Si_3N_4$ in the specimens, as well as in the system $Si_3N_4$-$Al_2O_3 \cdot H_2O$, which is not typical for ceramics in the system $Si_3N_4$-MgO.

The results of research into ceramics physical/mechanical characteristics in the system $Si_3N_4$-MgO-$Al_2O_3 \cdot H_2O$ showed that additional introduction of 0.5-1 weight % aero-gel into the system $Si_3N_4$-MgO (5 weight %) ensures the decrease in open porosity to 0,3%, increase in strength to 750 MPa at room temperature, broadening of working temperatures range to 1300°C, increase of hardness to 21GPa.

The achieved result, except for zero porosity, is also characteristic of ceramics having composition $Si_3N_4$-$Al_2O_3$ (aero-gel) but larger content of aero-gel which is ineffective due the high cost of aero-gel when introducing the results of the developments in industry.

## References

1. G.G. Gnesin, I.I. Osipova. Hot-pressed Materials Based on Silicon Nitride // Powder metallurgy. – 1981. - №4. – pages 32-45.

2. R.A.Andrievskii, I.I.Spivak. Silicon Nitride and Materials Based on It. – Moscow: Metallurgiya, 1984. – 102 p.

3. Progress in Ceramic Gas Turbine Development, Vol.2. Edited by Mark van Roode. – ASME PRESS. – 2003. – 856 p.

# FRICTION AND WEAR BEHAVIOUR OF MATERIALS AND COATINGS PROMISING FOR VACUUM AND LOW-TEMPERATURE CONDITIONS

**Vvedenskij Yu.V., Gavrylov R.V., Gamulya G.D., Ostrovskaya Ye.L.,**
**Yukhno T.P., Kostornov A.G. (1), Solntsev V.P. (1), Frolov G.A. (1)**
Special Research and Development Bureau for Cryogenic Technology
of Verkin Institute for Low Temperature Physics and Engineering of NASU
47, Lenin Ave., Kharkov, 61103, Ukraine, mail@cryocosmos.com
(1) Frantsevych Institute for Problems of Materials Science of NASU
3, Krzhyzhanivs'ky St., Kyiv, 03142, Ukraine, frolov@alfacom.net

In view of the growing demand for orbital space stations for long-term service the problem of providing failure-free performance of movable conjunctions in responsible units and mechanisms of space systems is of prime importance. Dependent on the working conditions the materials of friction units can suffer simultaneous action of the following space factors (SF): reduced environmental pressure; low molecule return coefficient; temperature drop from 4,2 to 400 K; variation of the conditions of heat exchange with the environment; exposure to the electromagnetic solar radiation and to the action of radiation belts of the Earth, etc.

Reliable data on the effect of SF on the friction and wear characteristics of materials are lacking, so it is necessary to carry out comprehensive investigations on the ground simulating the action of SF and also in the conditions of a real space flight, which would enable one to verify the adequacy of the friction-and-wear data obtained.

The present work presents the data on friction behaviour of some promising materials and coatings in laboratory ground conditions simulating the action of SF (pressure and temperature, low molecule return coefficient; variation of heat exchange with the environment). For studying friction and wear the cryogenic vacuum rig UTI TV has been employed [1]. Pressure in the rig was varied from the atmospheric to $2 \cdot 10^{-5}$ Pa, the initial temperature of samples - from 293 to 77 K. The temperature of cryogenic screens (77 K) guaranteed the coefficient of molecule return not to exceed 0,4.

The object of studies was a friction pair "ball (pin)-on-disc". The materials tested were light alloys, solid lubricant coatings (SLC) [2 - 4], self-lubricating composite antifriction materials (SCAM) and materials with the elements of self-organization [5, 6]. In all cases quenched bearing steel containing 15% chromium was chosen as a counterbody material.

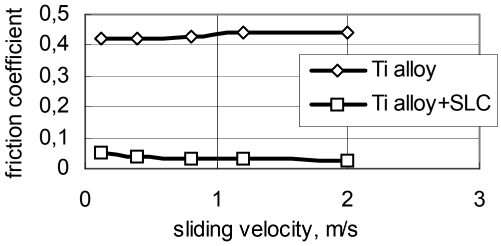

Fig. 1. Steady-state friction coefficient *vs* sliding velocity in vacuum for friction pairs "steel / titanium alloy" and "steel / SLC on titanium alloy"

The investigations performed proved the friction-and-wear characteristics of light alloys to be unsatisfactory in the extreme service conditions (Fig. 1). However, these characteristics can be improved by special contact surface treatment. Thus, deposition of SLC onto the surface of the titanium alloy BT23 permits one to reduce by the order (from f=0,4 to f=0,02) the friction losses in vacuum in a wide range of friction parameters changing. The light alloy substrate strengthening prior to SLC deposition results in the essential increase of a friction pair wear life.

With the testing temperatures in vacuum going down the friction wear life of a SLC deposited onto the laser strengthened surface of the titanium alloy BT23 increases (Fig. 2). The coefficient of friction in this case tends to increase not exceeding, however, the level of values typical of antifriction materials (Fig. 3).

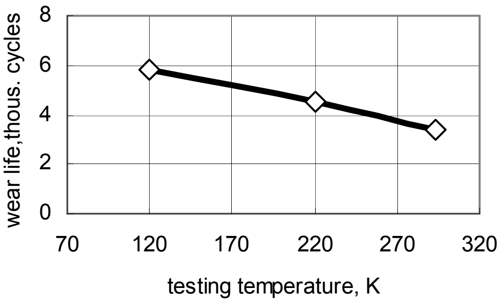

Fig. 2. Temperature dependence of the wear life of SLC on the laser strengthened surface of titanium alloy in vacuum

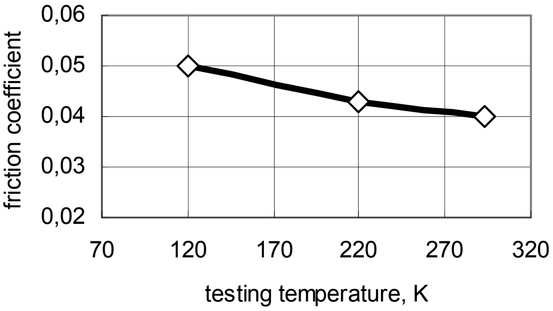

Fig. 3. Temperature dependence of the steady-state friction coefficient of friction pair "steel / SLC on the laser strengthened surface titanium alloy" in vacuum

With fixed friction parameters (sliding speed 0.1 m/s, normal load 25 N) the pairs of SCAM based on copper are characterized by a stable friction coefficient, changing in air depending on the material composition from f=0,2 to f=0,3. The environmental pressure drop down to 10 $^{-4}$ Pa leads to the coefficient of friction decreasing to 0,13—0,27. With the temperature decreasing in vacuum the coefficient of friction of such materials tends to decrease too.

Friction pairs of the material with self-organizing elements (based on highly alloyed tool steel) having the same friction parameters are characterized by high wear resistance both in air and in vacuum for a wide range of testing temperatures. In this case the coefficient of friction at a steady state period is f=0,48 and f=0,4 in air and in vacuum, respectively.

The investigations performed permit us to choose the materials prior to carrying out parallel full-scale studies of friction and wear characteristics in space and in simulating laboratory conditions. Final choice of material for verifying adequacy of the data obtained should be realized taking into account the criteria of wear resistance and ultimate allowed friction coefficient values for antifriction materials.

[1] Ostrovskaya Ye., Yukhno T., Gamulya G., Vvedenskij Yu.V., Kuleba V.I. // Tribology International – 2001, V.34, p. 265—276.

[2] Гамуля Г.Д., Островская Е.Л., Юхно Т.П. // Порошковая металлургия – 2001 - №3/4, с.47—57.

[3] Yukhno T.P., Vvedensky Yu.V, Sentyurikhina L.N. // Tribology International – 2001, V.34, p.293—298.

[4] Введенский Ю.В., Гаврилов Р.В., Гамуля Г.Д., Островская Е.Л., Юхно Т.П. // Сб. тез. Третьей украинской конф. по перспективным космическим исследованиям", 2003, Кацивели, Крым. Институт космических исследований НАНУ – НКАУ, с.55.

[5] Гамуля Г.Д., Скороход В.В., Солнцев В.П., Сурду М.Н., Фролов Г.А. // Космічна наука і технологія – 2002, т.8, №5/6 –С.28—34.

[6] Броновец М.А., Гамуля Г.Д., Еланский ЮА., Завгородный Л.Т., Скороход В.В., Солнцев В.П., Сурду М.Н., Тихий В.Г., Фролов Г.А. // Космічна наука і технологія – 2002, т.9, №5/6 –С.40—46.

# PERSPECTIVES OF THE DEVELOPMENT OF SILICON NITRIDE CERAMIC SHELLS

**Kelina R.P., Rusin M.Yu., Shkarupa I.L., Vikulin V.V.**
Federal State Unitary Enterprise “Obninsk Research and Production Enterprise “Technologiya”
15 Kiev Str., Obninsk, 249035, Kaluga Region, Russia, *onpptechn@kaluga.ru*

The materials based on silicon nitride and compositions from silicon and boron nitrides could become more appropriate and adequate for the development of radomes for defence missiles, which operate in severe aerodynamic conditions and at temperatures ranging from 800 to 1500 °C.

High-temperature ceramic materials based on silicon nitride and compositions of thereof, produced by reaction and compression sintering and hot pressing methods and intended for use in thermal strengthened structures, bearing static, dynamic and cycling loads have been developed at FSUE ORPE “Technologiya”. The materials with high-strength and thermal-stable properties may operate for a long time at temperatures of 1300–1600°C and for a short time at 1500-1600°C. Depending on the technology, the properties of silicon nitride materials vary within wide limits: density is from 2,35 to 3,45 g/cm$^3$; porosity from 16% to zero; strength from 200 to 1000 MPa; thermal-conductivity coefficient from 5 to 20 Wt/m; thermal resistance from 600 to 1200 °C and more.

Among the materials developed, the material based on reaction-bonded silicon nitride and ranking below only in mechanical strength properties, has considerable advantages in comparison with sintered and hot-pressed materials in the production of large-sized, thin-walled, complex-shaped articles. The material has stable strength characteristics at a level of 200—250 MPa in a temperature range from 20 to 1400 °C, a hot slip casting provides for a minimum linear shrinkage to 1% after the molding process and the absence of a linear shrinkage in the reaction sintering process. Reaction-bonded silicon nitride densified under elevated temperatures has a strength at a level of 450—500 MPa in the temperature range of 20—1300 °C, and stable dielectric properties in a wide temperature range of 20—1200 °C.

A set of ceramic material tests for thermal heating resistance have shown that all the materials withstand the heating rate 150grad/s up to the temperature of 900—1300 °C, and without any visible failure.

The temperatures and the resulting thermal stresses, which are peculiar to the article РПО-50 undergoing the action of heat exposure during the flight along the most tense trajectory have been calculated for the articles having wall thickness 6, 8, 10 mm. The investigations have shown that the strength in all cases is quite sufficient, because the greatest tensile stresses reach the value of 25 MPa and the greatest compression stresses do not exceed more than 60 MPa, that is quite allowable for any variant being considered. Nevertheless, it should be noted, that all the materials possess low thermal-protective properties during operation under the indicated operating conditions.

The investigations of dielectric properties of ceramic materials in a wide temperature range of 20—1320 °C have shown the stability of relative dielectric constant (no more than 10%). The dielectric constants presented here are shown for the materials which initially were not intended for use in radioparent radomes, and, therefore, they may be improved and stabilized by way of modification and improvement of the production technology of materials and articles.

Timeliness of the problem being set for the purpose of searching new solutions is confirmed by applications for foreign patents on radioparent radomes from silicon nitride, namely, the USA patent № 5.103.239 of 7.04.92 (Fig. 1) and by demonstration of silicon nitride radome shell by Honeywell Ceramic Components Corp. (Fig 2).

The analysis performed shows that high-temperature ceramic materials based on silicon nitride may be used for the designing of radomes for advanced avia– and naval-based missiles, the operating temperature of which can be up to 1500 °C.

Composite radome for the missile Patriot. (woven ceramic fiber and ceramic matrix).

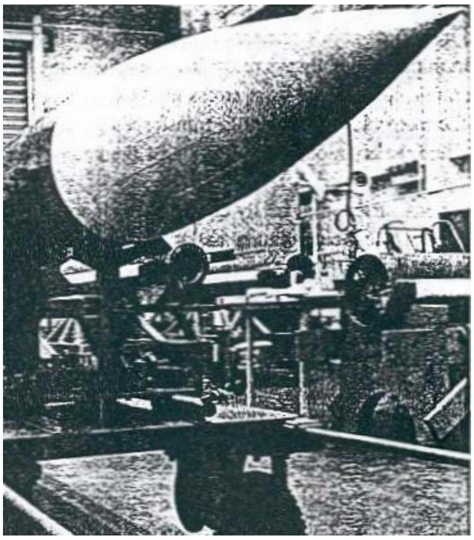

Fig. 1

Radioparent radome from silicon nitride produced by Honeywell Ceramic Components Corp

Fig. 2

# THE THIN-FILM TRANSDUCER OF LOW PRESSURE

**Karitskaya S.G.**
Buketov Karaganda State University
Universitetskaya, 28, Karaganda, 470074, Kazakstan, e-mail: ksg@kargu.krg.kz

The advance in technology bound with a development of the outer space, requires high-precision methods and stable, fast-response devices. In this connection creation of contactless means and instrumentation systems of major aero-hydrodynamic parameters permitting to receive the data about fields of pressure, temperatures, value of friction etc., and also to visualize them at computer processing to scale of real time is one of actual problems. The application of such measuring systems, according to the experts of the company McDonnell-Douglas, allows considerably reducing expenditures for the creation of new aircraft models at least ten times [1].

The successfully applied lately new measuring method of pressure in aerodynamics is based on using of luminescent pressure transducers or so-called the luminescent pressure-sensitive paints. They are usually a matrix with implanted in it phosphor molecules. Luminescence of these molecules depends on of oxygen concentration in air (than more oxygen concentration the less luminescence intensity).

It is known that the conditioned by random collisions between the luminophor and oxygen dynamical luminescence quenching is described by Stern-Folmer's equation [2]:

$$I_0 / I=1+k\ [O_2],$$

where $I_0$ and $I$ – the fluorescence intensity in the absence and presence of oxygen accordingly; $k$ - Stern-Folmer's constant of luminescence quenching ; $[O_2]$ – the oxygen concentration.

On the other hand, the concentration of the oxygen dissolved in the solution or in the matrix, according to Henry's law is directly proportional to its partial pressure on the solution surface:

$$[O_2]=q\cdot p,$$

where $q$ - Henry's constant or a solubility coefficient of oxygen in a solution (or in a matrix).

The systems on the basis of luminescent pressure-sensitive paints allow receiving the unique information on a field of pressure profile in real time that it is impossible to be provided by other methods.

The given conclusion is based on following advantages of the luminescent pressure measuring method:

- The non-sluggishness,
- The absence of a perturbation of explored flows,
- The high sensitivity, accuracy and the high spatial pressure resolving ability in view of the molecular device of the luminescent pressure-sensitive paints,
- The visualization, i.e. the obtaining in real time on the screen monitor of the spatial an pressure distribution pattern it stipulated by activity on the explored model of the subsonic and supersonic airflows,
- Capability of automation of measurements.

The outcomes of researches of the pressure with application of systems on the basis of the luminescent pressure-sensitive paints on airfoils with large curvature have shown good concurrence with the transducers data [3,4].

One of the ways of improvement of the optical measuring method of pressure is the improvement of the characteristics of the luminescent pressure transducer. Their main disadvantage is the temperature effect on oxygen diffusion in a matrix.

On our view the known luminescent pressure transducers can be divided into 2 classes. The first class: a polar matrix with the implanted polar luminophor. And the other class: a non-polar matrix with the implanted non-polar luminophor.

It is known, the polar luminophor has the intensive luminescence excited by stationary lighting. The polar luminophor has a sharp response to different physicochemical actions and a large life time of an excited state also. It is known, the non-polar matrix is chemically inertial and has a high diffusivity of gases. Therefore we offer the thin-film pressure transducer of a new type: the polar luminophor implanted into a non-polar matrix. The complex of ruthenium is selected as polar luminophor. Under the change of air pressure over the range 0—1 the atmosphere the luminescence of a ruthenium complex is quenched in 6-8 times (fig.1, 2). The given circumstance is important from the point of view of signal-to-noise ratio of the video camera used for obtaining of the information. The silicone rubber of the marks "сктн-а", having the diffusivity of gases ($3\cdot10^{-5}$ cm$^2$/c) was used as a matrix.

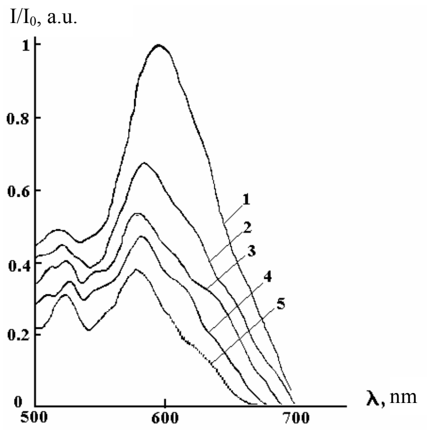

Fig. 1. Luminescence spectrum of the ruthenium complex at different values of pressure: 1 – 0 Pa , 2 – 0.25·$10^5$ Pa, 3 – 0.5·$10^5$ Pa, 4 – 0.75·$10^5$ Pa, 5 – $10^5$ Pa.

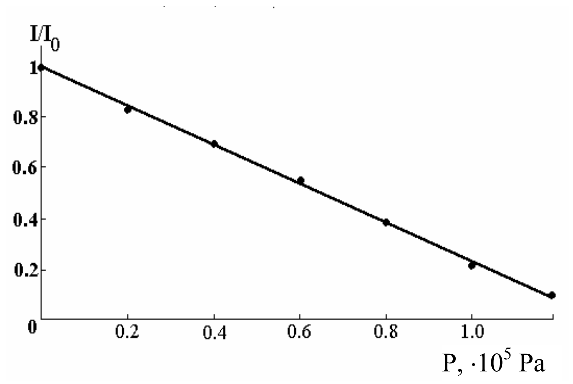

Fig.2. Dependence of the luminescence intensity of the ruthenium complex in rubber from pressure.

As the atmosphere temperature influences outcomes of pressure measurements, we offer to use a film consisting of several layers:

1) a layer reacting to the change of a temperature and a pressure,
2) a layer-filter not "feeling" of changes of a temperature and a pressure,
3) a layer reacting only to a temperature change,
4) a diffusive layer.

The "layer-filter" containing a luminophor, plays the important role. This luminophor absorb of light in that range, as molecule of luminophor of the first layer, but with luminescence in diverse spectral range. This layer is intended for recording of the "discontinuities" of an exciting light intensity and the vibration of model in a wind tunnel. It allows conducting researches of the motive bodies.

The diffusive layer act as light filters. The application of light filters before the video camera lens is not always justified so far as they have large transmission band. The diffusive layer is intended for prevention of ingress of irradiating light reflected from an object surface ("glares") into the video camera lens.

The technique of a graduation of the given piezometer was developed. At a graduation the environment pressure on the thin-film piezometer was read on the manometer "ОБВ1-1000".

The elaborated luminescent thin-film piezometer was applied in researches of process of subsonic flow about the airfoil of a swept wing established in a wind tunnel. The obtained experimental data are in good conformity with the literary data and outcomes obtained by the inclined tube micromanometer.

The elaborated luminescent fine-film polymeric piezometer is bonded on metal by special adhesives easily. The piezometer has sufficient long-time stability (rate of change of the characteristics no more than 0,1 % per day) and fits for visualization of pressure fields in air over the range 0-1,5·$10^5$ Pa at the temperature of 270- 310 °K and the air humidity over the range 0- 100%.

## References:

1. Gouterman M., Callis J., Burns D., etc. Luminescence Imaging for Aerodynamic Testing. Proceedings of the ONR/NASA Workshop on Quantitative Flow Visualization. Rev. Sci. Inst. 1990. Vol.61. N11. P. 3340-3347.
2. Joseph R. Lakowicz Principles of Fluorescence Spectroscopy. Plenum Press, New York, 1983. – 496 p.
3. Morris M.J., Donovan J.F., Kegelman J.T., Levy R.L., Schwab S.D. Aerodynamic Application of Pressure-Sensitive Paint // 30-th Aerospace Sciences Meeting and Exhibit, 1992. Reno, NV.
4. Borovoy V., Bukov A., Mosharov V., Orlov A., Radchenko V., Phonov S. Pressure Sensitive Paint Application in Shock Wind Tunnel // 16eme Congres ICIASF. Dayton (Ohio). 1995.

# FEATURES OF MECHANICAL AND MICROSTRUCTURAL BEHAVIOR OF ECA PRESSED AL—MG—LI—ZR ALLOY UNDER HIGH STRAIN RATE SUPERPLASTICITY

**Myshlyaev M.M.(1, 2), Mironov S.Yu.(3), Myshlyaeva M.M.,**
**Medvedev M.M., Zolotarev A.K., Isaev V.V., Travkin A.A.**
Institute of Solid State Physics, RAS
2 Institutskaya, Chernogolovka, 142432, Russia, myshlyae@issp.ac.ru
(2)Baikov Institute of Metallurgy and Material Science,
49 Leninsky Prospekt, Moscow, 119991, Russia, myshlyae@issp.ac.ru
(3)Institute of Metal Superplastisity Problems,
39 Khalturina str., Ufa, 450001, Russia, s-72@mail.ru

The structure of rods subjected to the equal-channel angular (ECA) pressing under different conditions have been studied by X-ray diffraction analysis, transmission electron microscopy, scanning electron microscopy, including back electron scattering diffraction and orientation image microscopy, technique. A fine-grained structure has been shown to form in the process of pressing, finer grains forming at lower pressing temperatures. A largest number of grains demonstrate the formation of a dislocation substructure involving subgrains bounded by dislocation boundaries. A most developed substructure forms under pressing at elevated temperatures when coarser grains form.

A mechanical behavior has been studied for ECA pressed samples having different structural states. Temperature and strain rate conditions to attain ultimate strains to failure have been defined for samples of each structural state. It has been shown that samples with a developed substructure are subject to a superplastic (SP) straining. Contrary to the expectations the ductility of finest-grained samples turned out low. It has been found that the ultimate SP straining to failure is characteristic of samples subjected to 10-pass ECA pressing at 370 °C. It complies with the strain rate of $10^{-2}$ $s^{-1}$ at 370 °C. Its greatest value was about 2000%.

Mechanical behaviour of the alloy has been studied in SP straining conditions. Multistage high strain rate of SP strain has been shown. Dependencies of the true strain rate on temperature, the true stress and true strain for the straining during hardening stage and softening stage have been established. The activation energies and the coefficients of strain rate sensitivity of stress (m), which characterize these stages, have been determined. It has been shown that the strain up to ~2000% corresponds to this alloy and m ≈0,45 for both stages. These parameters really correspond to SP flow.

It has been established that the hardening stage deformation has the strain rate $\sim 10^{-2}$ $s^{-1}$ and is controlled by volume self-diffusion. This is typical for SP deformation by intra-grain sliding. Dynamical recrystallization on sub-grain level corresponds to this stage. It has been established, that during the softening stage the strain rate is $\sim 10^{-3}$ $s^{-1}$ and is controlled by grain boundaries self-diffusion. This is typical for SP deformation of fine-grain materials, which is caused by grain boundary sliding. Structural behavior by SP straining conditions has been studied. The data showing intra-grain sliding during the hardening stage and dynamic recrystallization with participation of grain boundary sliding and migration during the softening stage have been obtained.

The support from the RFBR (Projects 04-02-16120, 04-02-97261) is appreciated.

# STRUCTURE AND PROPERTIES OF ALUMINUM-STEEL JOINTS PURPOSED FOR OPERATION IN EXTREME CONDITIONS

**Gulbin V.N.**
R & D Institute of Construction Technology
43, Altufievskoe sh., Moscow, 127410, Russia, E-mail: vngulbin@mtu-net.ru.

This report presents study of structure and properties of bi-metal of aluminum and AMг6 aluminum alloy joined with 12X18H10T corrosion-resistant steel by mean of explosive welding.. These joints are purposed for operation in extreme conditions (nuclear and cryogen-vacuum equipment).

Welding of aluminum alloys with steels meets a lot of difficulties because of significant differences of their physical and mechanical properties. One of important problems is to avoid forming of diffusion area featured by brittleness because of presence of various flaw-building structures. Explosive welding with properly selected parameters allows to obtain aluminum-steel joints without brittle zones.

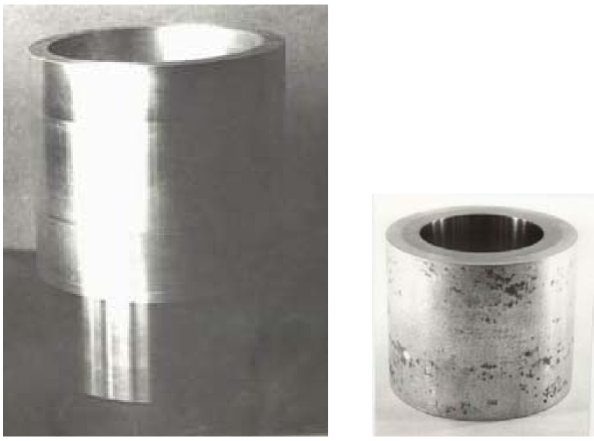
a b

Fig.1. Pictures of transitional parts made of AMг6(АД1)+12X18H10T: a – step-free transitional part, 180 mm diameter; b – tubular transitional part, 86 mm diameter.

In order to obtain step-free transitional parts made of AMг6+12X18H10T for nuclear components (Fig.1a), explosive welding was applied for obtaining of АД1 pure aluminum layer, 0,5-1,5 mm thickness. Then explosive welding was used for adding of AMг6 layer, that is application of aluminum sub-layer. Besides that, in order to obtain tubular joint of AMг6+12X18H10T, explosive welding was used for joining of 12X18H10T steel (Fig.1b) with tubular half-finished products made of AMг6 with pure aluminum cladding inside of them.

Metal-graphic analysis of joint area showed, that there is a wave-building in the contact area (Fig.2). Along the contact boundary AMг6+AD1 (Fig. 2a) there is a developed wave-building with distinct turbulence behind wave's top, but without inter-metallic admixtures. It confirms a deformation mechanism of explosive weld forming noted in work [1]. Along the junction boundary of AD1+12X18H10T there is a pure-developed wave-building with unsignificant admixtures (Fig.2b). Micro-roentgen-spectral analasys of these admixtures showed their main content of chemical compositions of $FeAl_3$ and $Fe_2Al_5$.

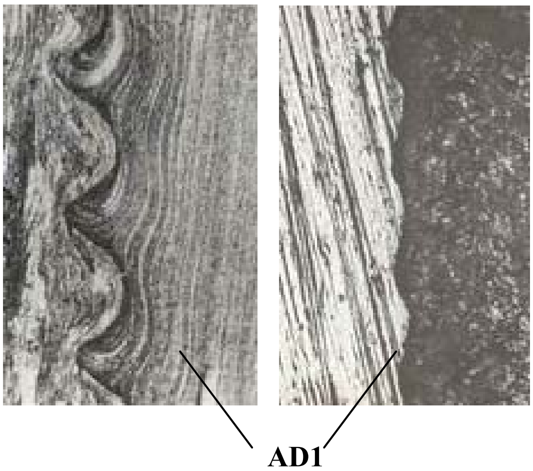

a b

Fig.2. The micro-structure of aluminum-steel joint (x100): a – AMг6+АД1 joint's transitionl area; b – АД1+12X18H10T joint's transitional area.

Mechanical tests of AMг6+AD1+12X18H10T three-layered joint (Fig.3) indicated its break by AD1 layer always, as the weakest one. However, compressing testing of ring specimens showed no layers separation (Fig.3b).

Special quality inspection methods were applied. Such as helium leak detection, thermal cycling (heating up to +200 $^0$C and cooling to room temperature), gamma-hard raying. Special tests showed good results; the transitional joint could withstand over 100 cycles by the thermal-cycling testing.

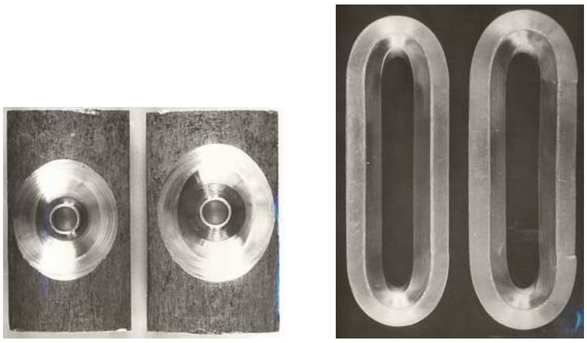

a b

Fig.3. Post-testing specimens pictures: a – tensile of layers ($\sigma_t$=22,0 and 19,6 kgf/mm$^2$);
b – compressing of ring specimens.

With use of these research results a technology of explosive welding was developed for bi-metal transitional joints of 12X18H10T steel +AMr6(AD1), 120-180 diameter and for stepped transitional parts, 75-120 mm diameter.
A pilot lot of such transitional parts was produced [2].

A stepless explosive-welded joint of AD0 with 12X18H10T corrosion-resistant steel was studied as a component of a cryogen-vacuum equipment purposed for super-conductors cooling in colliders facilities. Along AD0+12X18H10T joint boundary there is a featured wave-building with high mechanical properties ($\sigma_t \geq 20$ kgf/mm$^2$). Hundred percent quality inspection (ultrasonic flaw detection, helium leak detection) showed no continue flaw-building layers in the joint's transitional area.

Thermal-cycling tests (cooling in liquid nitrogen and heating up to room temperature) showed a high withstanding of this joint by cryogen conditions: the specumens could withstand over 100 cycles without of any loss of service characteristics. Using these research results a technology was developed for explosive welding of bi-metal stepless transitional parts of AD0 + 12X18H10T steel. A pilot industrial lot of such transitional parts passed real tests in the Serpukhov collider being erected, and showed high service properties.

References

1. Hammerschmiedt M., Kreie H. Microstructure and joint forming mechanism by explosive welding / Impact waves and phenomena of high-rate deformation of metals. Rev. By M.A. Meyers and L.E. Mourr. M.: Metallurgia, 1984. pp.447-456.
2. Application of explosive welding for bi-metal joints production / V.V. Roshchin, V.N. Goulbin, V.B. Nikolaev. Papers: Matters of nuclear science and technology. Series: Nuclear engineering and technology. 1989. Issue 5. pp.24-29.

# PLASMA SYNTHESIS OF METAL-CARBON CLUSTERS AND CAPABILITIES OF THEIR USAGE IN HAZARD CONDITIONS

**Churilov G.**
Kirenky Institute of Physics SB RAS, Krasnoyarsk, Russia, e-mail: churilov@iph.krasn.ru
Krasnoyarsk State Technical University, Krasnoyarsk, Russia

Since 1990 when firstly was shown that carbon has a new important allotrope – fullerite, intensive development of plasma methods of carbon based substances production had begun [1-2]. Injection of different metals into carbon-helium plasma on purpose to endohedral fullerene synthesis allowed to obtain carbon-coated metal clusters. We have investigated nickel clusters coated with carbon [3].

In electron microscopy studies of the carbon condensate, particles of nickel coated with a non-conducting material have been detected (Fig. 1). The fact that the particles were non-conducting has been established by an indirect method. The particles were placed under a microscope on a conducting (metallic) surface and irradiated with an electron beam. As a charge accumulated on the particles, a discharge via the substrate occurred. The discharge of the particles was accompanied by visually detected radiation.

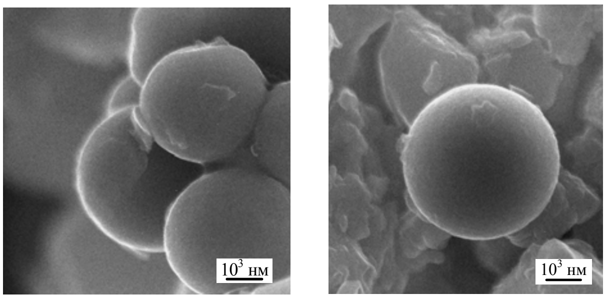

Fig. 1. TEM images of nickel particles in fullerene soot.

EPR spectroscopy detected a magnetic resonance of the metallic particles in the soot and the thermolysis residue (Fig. 2): $\Delta H^{Ni}$=80 mT and $g^{Ni}$=2,20. The large width of the electron paramagnetic resonance line in our experiments is explained by the fact that the particles of nickel in the soot have sizes amounting to a few millimeters. The g-factor value coincides with the data in [4].

In the fullerene extract, the content of nickel according to the analysis of the X-ray luminescence data was 0,02%. In Fig. 3 the magnetic resonance spectra of Ni-containing fullerene extract is shown. The observed spectrum is possibly associated with fine (~10 nm in diameter) crystalline particles of nickel that have anisotropic magnetic properties.

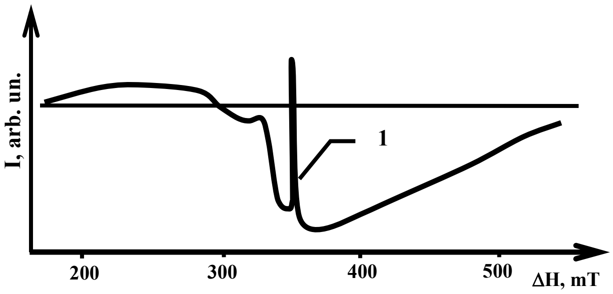

Fig.2. Ferromagnetic resonance of Ni-containing soot.

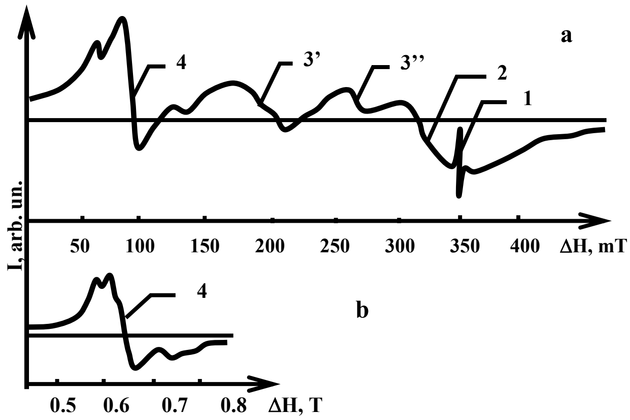

Fig.3. Magnetic resonance spectra of Ni-containing fullerene extract at frequencies (a) 9 and (b) 35 GHz at 293K; g=2,001 (1), 2,15 (2), 2,6 (3’), 3,6 (3’’), and 7,7 (4).

As electron microscopy indicates, nickel particles coated with non-conducting material were formed during fullerene synthesis with nickel. Electron paramagnetic resonance (EPR) analysis of the fullerene containing soot with nickel indicated the presence of fullerene and large-sized particles ($10^3$—$10^4$ nm), which exhibited skin effect and a domain structure without magnetic anisotropy, and some finer particles (~10 nm). In benzene extract of fullerene the ratio of coarse and fine particles changed in favor of the latter. Clusters of several (from two to four) atoms also was observed via an intermediate nonmagnetic atom or molecule, possibly fullerene. The behavior of the fullerene extracts with nickel in a magnetic field at 77 K bore resemblance to that of spin glasses.

It is known that nickel has a big value of magnetostriction constant. But ultrasonic sensors are manufactured from piezoceramics though it has a low limit of energy conversion. It is related with impossibility to use nickel slabs at high frequency because of eddy currents losses. Usage of nickel particles encapsulated in carbon coat will allow to create ultrasound radiators which will exceed up-to-date generators by order.

## References

[1] Kratschmer W., et al., Nature, 1990, **347**, 354.

[2] Churilov G.N. Instruments and Experimental Techniques, 2000, **43**(1) 1. Translated from Pribory i Tekhnika Eksperimenta, No. 1, 2000, pp. 5—15.

[3] Petrakovskaya E.A., Bulina N.V., Churilov G.N., Puzyr' A.P. A study of the synthesis products of fullerenes with nickel and cobalt. Tech. Phys., 2001, **46**, No.1, 42-46. Trans. from Zhurn. Tekh. Fiz., 2001, **71**, No.1, 44—48.

[4] Bagguley D.M.S. Proc. Phys. Soc. London, Ser.A, 1953, **66**, 765.

# ACOUSTIC RESEARCH IN MATERIALS WITH DEVELOPED MESOSTRUCTURE

**Bezimyanniy Y.G.**
Frantsevich Institute for Problems of Materials Science of NASU,
3 Krzhizhanovsky St., Kiev, 03142, Ukraine, E-mail: bezimyni@i.com.ua

Porous and composite materials are widely used in technique including their applications in extreme conditions [1]. The materials above are produced from different powders and fibers by routes of technology for dispersed systems through creation of developed mesostructure [2], which control is of great importance in refinement of this technology as well as in evaluation of hardware quality [3].

In solving these problem of control using acoustic methods one of the most important issue is correct acoustic interpretation of the challenge solved [4]. The interpretation consists in representing (within the framework of the chosen mechanical model using parameters of sound field existing or forming in material studied) the certain property that we want to control. The final product of such representation is the functional dependence of the characteristics for the property required on the sound field behavior as well as the choice of such sound field behavior which is the most effectively related to parameters of the material property studied and allows us to diagnose it. As this takes place, the criterion for truth of the obtained functional dependence may be the correlation dependence that can be attained empirically, and the basis for the choice of the mechanical model may be the structural model of the material at the mesolevel.

We have analyzed [5] possibility of applying the simplest biphase structural model at the mesolevel to reveal the functional relation between acoustic characteristics and porosity of powder materials distinguished by their properties. It has been shown that even for such a comparatively simple problem, a good numeral agreement between functional and correlation dependence is not observed in the most of cases. It has been concluded that changing to heterogeneous and heterophase models is expedient.

In this paper possibilities of acoustic modeling using heterogeneous and heterophase structural models at the mesolevel have been analyzed.

Two types heterogeneous and heterophase structures with the developed mesolevel may be distinguished: matrix and frame [2]. Let us consider their generalized structural models (Fig.) assuming that in both cases material is isotropic and has a regular structure.

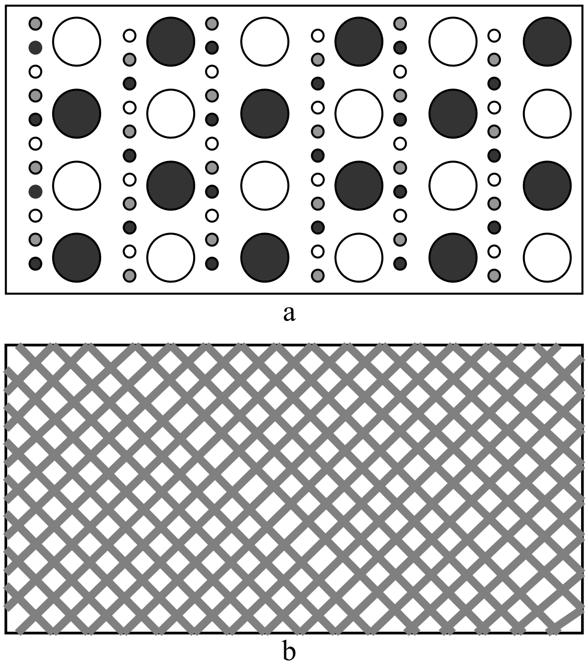

Fig. Matrix (a) and frame (b) models of mesostructure of material

The first model (Fig. a) is a homogeneous solid mono- or heterophase matrix in which other phases are uniformly distributed as homogeneous spherical inclusions of different size. According to this model, the material structure is described by such parameters as radii of phases and their volume. Any integral property of material may be considered as some effective value of this property. This value is a function of properties of submesostructural elements and connections between them. Besides the above factors, the wave size of the element is significant to obtain effective values of acoustic characteristics of material. The wave size is important to determine effect of one or another element on the resulting property [6]. The model is applied for comparatively low content of inclusions (up to 30%).

Mechanical behavior of isotropic solid body is completely determined by its four acoustic characteristics, for example, two different sound velocities and two corresponding effective attenuation coefficients of elastic wave [4]. Considering the above mentioned, the effective value of sound velocity for any elastic wave can be written as the functional dependence:

$$V=F(V_i, V_j, K_k, K_d), \qquad (1)$$

where $V_i$, $V_j$ - sound velocities of elastic wave within the materials forming matrix and materials of inclusions, respectively; $K_k$, $K_d$ - coefficients considering quality of contacts between individual elements in the mesostructure and defect of individual elements in the mesostructure, respectively.

To attain the effective attenuation coefficient of elastic wave this function should have the following form:

$$\alpha = \sum \alpha_i + \sum \alpha_r + \sum \alpha_k + \sum \alpha_d, \qquad (2)$$

where $\alpha_i$, $\alpha_r$, $\alpha_k$, $\alpha_d$ - attenuation coefficients of elastic wave resulting from absorption in matrix, scattering by inclusions, quality of contacts between particles, defects present in the mesostructural elements, respectively.

Thus, effective acoustic characteristics of material make allow us to establish functional relation between the effective values of sound velocity and the attenuation coefficient of elastic wave, on the one hand, and properties of components of matrix elements, inclusions, quality of contacts between mesostructural elements and defects present in them.

The structural model of the frame structure is a homogeneous solid mono- or heterophase frame of a regular shape. The frame is inside the mono- or heterophase filler (Fig. b). According to this model, the material structure is described by geometric size of the unit cell of the frame and the volume of phases. This model may be applied for high content of filler (up to 100%). Besides the above acoustic characteristics of elastic wave for the frame structure, resonance frequencies of elements of the frame cell may serve as diagnostic parameters [7]. The following functional dependence may be written for them:

$$f=(a_k, V_k, z, K_d), \qquad (3)$$

where $a_k$ - size of a resonance element of the frame; $V_k$ - sound velocity of elastic wave within the frame; z - acoustic resistance of loading (filler) on the resonance element.

The numeral values of functional relations (1)-(3) have meaning only in solving particular problems. Some of these problems we have considered and given in the reports at this conference and in the articles [7-9].

**REFERENCES:**

1. Международная конференция «Новейшие технологии в порошковой металлургии и керамике»: Тез. докл. – Киев, 2003. – 436 с.
2. Скороход В.В. Теория физических свойств пористых и композиционных материалов и принципы управления их микроструктурой в технологических процессах // Порошковая металлургия. - 1995. - № 1/2. – С.53–71.
3. Роман О.В., Скороход В.В., Фридман Г.Р. Ультразвуковой и резистометрический контроль в порошковой металлургии. – Минск: Вышэйш. шк., 1989. – 182 с.
4. Безымянный Ю.Г. Возможности акустических методов при контроле структуры и физико-механических свойств пористых материалов // Порошковая металлургия.- 2001.- № 5/6.– С.23–33.
5. Безымянный Ю.Г. Использование акустических характеристик для контроля структуры пористых материалов / Электронная микроскопия и прочность материалов. Сб. науч. тр. Киев, 1999. – С.93-105.
6. Безымянный Ю.Г. Особенности акустических измерений при тестировании материалов различных классов // Тез. докл. Международ. конф. "Новейшие технологии в порошковой металлургии и керамике", Киев, 2003.- С.369-370.
7. Bezimyanniy Y.G. Burlachenco Y.V. Relation of acoustics characteristics and structure parameters of Foam nichel // Second Int. Conf. “Materials and Coatings for Extreme Perfomances: Investigations, Applications, Ecologically Safe Technologies for Their Production and Utilization” Proceedings of Conferense. Katsiveli-town, Crimea, Ucraine, 2002, P.363-364.
8. Безымянный Ю.Г., Касимов М.А., Истомина Т.И., Райченко А.И. Использование акустических методов для оценки качества алмазных композитов с металлической матрицей // Тез. докл. Международ. конф. "Новейшие технологии в порошковой металлургии и керамике", К., 2003.- С.369-370.
9. Безимянний Ю.Г., Боровик В.Г., Степаненко А.В. Дослідження взаємозв’язку модуля пружності композиту алмаз + SiC з його структурним станом // Доповіді НАНУ. – 2003. - №2. –С.90-93.

# FORMATION OF DEFECTS DURING APPLYING COATINGS AND THEIR INFLUENCE ON PROPERTIES OF BORIDE LEYERS OF STRATUMS

**Spiridonova I.M., Fedash V.P., Saevich O.V.**
Dnepropetrovsk national university
Naukova str., 13, 49050, Dnipropetrovsk, Ukraine

In the work the research of formation of defects in boride coating obtained by a method of electrolysis is conducted. As defects formation of vacancies, linear and boundary dislocations and surface defects relating to the macroscopic category was accepted. The influence of defects farmed previously was investigated, during chemical-thermal treatment and consequent cooling. The study of defects in a structure of boride layer and their correlation with corrosion properties is conducted.

The formation of defects in anisotropic prismatic crystals of hemiboride of iron and isotropic dendrites of monoboride of iron is considered.

The equilibrium amount of vacancies formed in various conditions of formation of a diffuse zone is caluelated. The modes of boriding ensuring both the maximum amount of diffusion pores (groups of vacancies, dislocations), and the increased perfection, degree of phases are shown. It is shown that under influence of temperature the maximum amount of bivacancies is formed, the magnification of a degree of perfection of crystal is achieved during consequent annealing.

The preliminary accumulation of defects facilitates and intesifies mass transfer of boron and processes of a diffusion. Hereinafter during high-temperature soaking the annihilation of defects is observed. However crystalline structure of borides is characterized by large internal stresses, which in turn provokes formation of microcracks. The growth of the latter will be sped up both during sharp cooling, and during further warle of a material with formation of macrocracks.

Perfection of phases results in increase of corrosion resistance of materials, and the magnification of an amount of defects and pores causes its decrease.

# METHODOLOGY OF THE ANALYSIS OF CONSTRUCTION MATERIAL WITH MICRO- NANOCRYSTALLINE STRUCTURE

**Minakova A.V., Minakov V.N., Puchkova V.Y.**
Frantsevich Institute of Problems of Materials Science of NASU,
3, Krzhizhanovskogo St., 03142, Kiev, Ukraine, E-mail: altifer@ipms.kiev.ua

Structure transformation at large plastic deformation in the range of phase-structured instability taking place by the scheme: the grain – the dislocation timber – the dislocation tangles – cellular-polygonal structure - micro-nanocrystalline structure is accompanied by heterogeneous distribution of electron density. Fluctuations of electron density result in diffuse dissipation of X-rays at small angles. On account of very short wavelength of the characteristic X-ray radiation (~0,1÷0,2 nm), the size of "scattering volumes" must be from several tens to several thousands angstroms. Diffuse "corona" which appears at low angle dissipation does not depend on atom distribution in lattice of dispersed particles [1, 2]. The models for calculation of the angular distribution of X-ray quanta for diffuse dissipation at small angles, as well as formula for calculation of the minimum size of "scattering volumes" are adduced in mentioned above monographs

$$2\Theta^{*} = \frac{\lambda}{d}, \tag{1}$$

where 2Θ* is an angle on difractogram, by which diffuse dissipation merges with background of the x-ray radiograph according to Debay-Waller factor; d - the size of particles; λ - a wavelength of the characteristic radiation.

Distribution of X-ray quanta intensities within the angle range $2\Theta = 20 \div 142^{0}$ were set into computer. Processing of experimental data of intensities distribution was realized by means of program "Powder Cell 2.3". The silicon powder was used as standard: peak intensity, angular position of peaks is quite enough coincided with theoretically calculated values.

Researching of micro- nanocrystalline states created at the plastic deformation with great one-time reductions in the temperature range of phase-structure instability or during polymorphous transformations in technically pure titanium displays that diffuse "corona" is observed on debyegrams. This "corona" is an increasing of the X-ray background at reduction of the reflection angle during X-ray analysis in monochromatic X-ray radiation. Part of the difractograms within the angle range $2\theta = 20^{0} \div 45^{0}$ are represented on fig. 1. The value of the angle $2\theta^{*}$ allows to estimate the size of scattering volumes of "quasi-particles" of crystalline body" by the formula (1). This size is equal ~ 3 A and it is larger than interplanar spaces which are responsible for reflection under the law of Wulff-Bragg.

Determination of the areas of coherent scattering and microdistortions was carried out in assumption that total line spreading is a simple sum:

$$\beta = \beta_{grain\ size} + \beta_{lattice\ distortion}, \tag{2}$$

$$\beta = \frac{\lambda}{\varepsilon \cos\Theta} + \frac{4\overline{\sigma}}{E_{hkl}} tg\Theta, \tag{3}$$

where β - physical line spreading; λ - wavelength; E - modulus of elasticity; Θ - Wulff-Bragg angle; $\overline{\sigma}$ - elastic stresses (microdistortions, lattice distortions); ε - size of crystalline grains of the coherent reflection.

Expression (3) is converted to formula:

$$\frac{\beta\cos\Theta}{\lambda} = \frac{1}{\varepsilon} + \frac{4\overline{\sigma}}{\lambda E_{hkl}} \cdot \sin\Theta \tag{4}$$

The dependence $\frac{\beta\cos\Theta}{\lambda}$ from $\sin\Theta$ is a linear function. The experimental straight line cuts off the segment $\frac{1}{\varepsilon}$ on the axis of ordinates $\frac{\beta\cos\Theta}{\lambda}$, which is reciprocal to the linear size of crystalline grains, but the line slope determines the value of $\frac{4\overline{\sigma}}{E_{hkl}}$, which can be used for calculation of the average value σ [2].

The line slope is practically missing both for cold-shaped foils and for forged by 3 axes titanium in the temperature range of phase existence β → β+α → α. (fig.3). It shows that microdistortions are practically equal to zero. The size of coherent reflection areas are 0,18 and 0,1 mkm for foil and forged titanium accordingly. The essential difference in line width does not exist. By Taylor method it was organized the separation on lines when stacking defects caused line spreading H-K = 3N±1 and also on lines when stacking defects did not cause line spreading H-K = 3N, where H, K - indexes of reflecting planes α – titanium with hexagonal close packing, but N - whole numbers. The asymmetry of diffraction line profiles for researched materials and change of their intensities correlation in comparison with theoretically calculated values are observed. Probably this is specified by forming of stacking defects under great plastic deformation on plane of the prism and the pyramids. The TEM dark-field image of the cold-rolled titanium is represented on fig. 2. The dispersed "quasi-particles" of crystalline body with size 1,0 ÷ 10,0 nm are presented inside crystalline grains with size 0,15 ÷ 0,5 mkm.

Maximum accessible values of true fracture stress (which are equal ~ E/50 for micro-nanocrystalline states), true deformation before destruction, modulus of plasticity (the resistance to the large plastic deformation) are required for understanding the physical nature of large values of plasticity and strength of metal construction materials with micro- nanocrystalline structure.

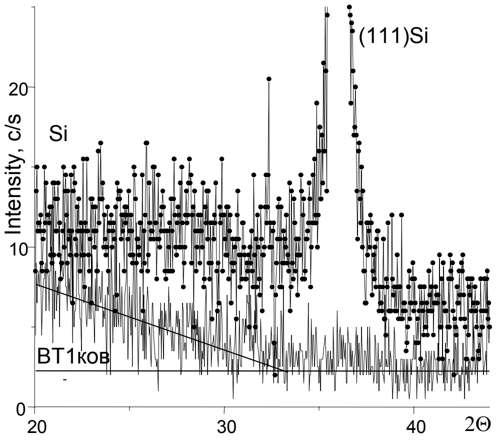

Figure 1. Diffuse dissipation of the forged Ti and powder Si (Fe $K\alpha_{1,}$, $\alpha_2$).

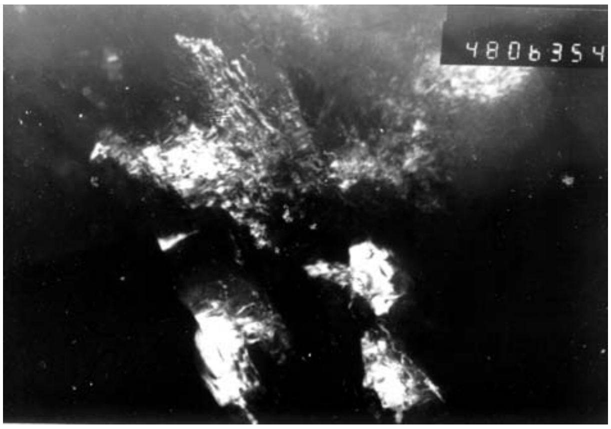

Figure 2. The TEM dark-field image of the cold-rolled titanium

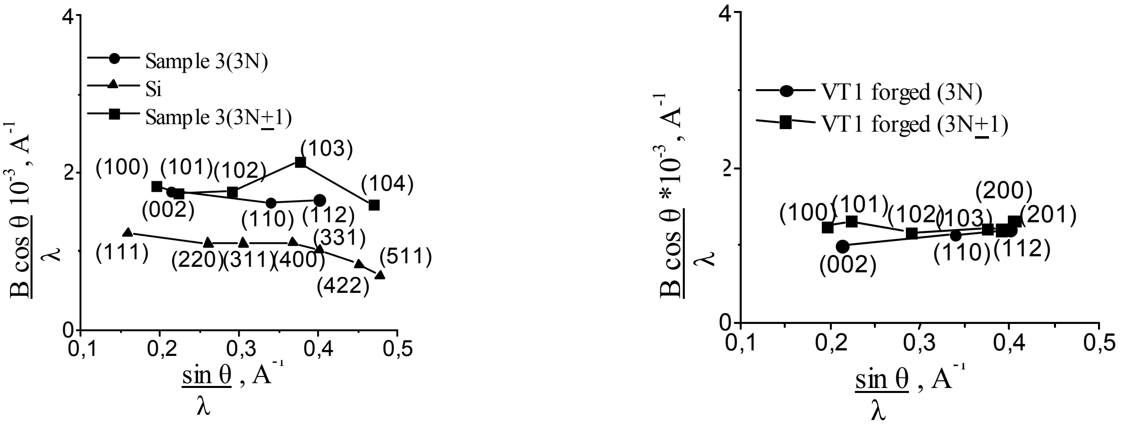

Figure 3. Dependence of line spreading from reflection angle: a - cold-rolled foil Ti;
b - forged by three axes Ti.

LITERATURE

1. Taylor A. X-ray Metallurgy. - M.: Metallurgy, 1965. – 663 p.
2. Pines B.Y. The Lectures on Structural Analysis. Kh.: Publishing House: Kharkovskiy university, 1967. – 476 p.

# INFLUENCE OF LOADING RATE AND LOAD VALUE ON CREEP OF TITANIUM-SILICEOUS CARBIDE $Ti_3SiC_2$ AT THE MICROINDENTATION

**Gorban' V.F., Pechkovsky E.P., Samelyuk A.V, Firstov S.O.**
Frantsevich Institute for Problems of Materials Science of NAS Ukraine
3 Krzhizhanovsky St., Kiev-142, 03680, Ukraine, E-mail: epp@ipms.kiev.ua

In connection with that after a stop of a loading at a microindentation the material continues continuously residually to be deformed during some time, the stage of exposure can be considered as creep of a material. Here two major parameters are: loading rate (rate of increasing of applied force, i.e. rate of a dynamic loading) and value of permanent load at the subsequent exposure. An indentation as the method of studying of creep characteristics is especially convenient and informative when it is accompanied by automatic record of indentation diagrams.

In this work ternary compound titanium-siliceous carbide $Ti_3SiC_2$ - one of the representatives of a new class of materials - nanolaminates [1], - single-phase, compact, made by sintering, the grain size $d$=5-15 microns is studied [2]. The main feature of hexagonal crystal structure of this compound is the ability of basic planes of silicon atoms easily to slide concerning titanium atomic layers. At a microlevel it is shown in intergranular and intragranular delamination of material at loading. At indentation around hardness indents the zones of destruction are observed which represent set of the bent, stratified, shattered grains of the various sizes and form [3, 4]. Such effect of energy dissipation, certainly, should bring in features in creep kinetics.

Microindentation carried out by a diamond Berkovich pyramid at room temperature at loading up to $P$=4 N with precision $10^{-3}$ N; displasement $h$ determined with precision ± 2,5 nm; the record of the loading, taking a load and unloading diagrams was made. All process of test, the records of the diagrams and significant part of processing of results were made automatically with use of computer programming.

For the analysis of creep characteristics behaviour it was used primary kinetic curves *h (t)*. Structural researches carried out by raster electronic microscopy method.

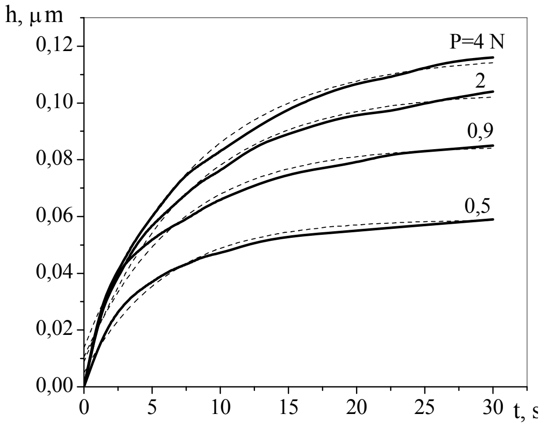

As the analysis of the creep diagrams $h_c(t)$ has shown these curves are quite satisfactorily described by exponential dependence such as $y=y_o+a*\exp(-x/b)$ for various meanings $V_P$ and $P$ (**Fig. 1**). Accordingly expression for displacement at creep ($h_c$) gets a form:

$$h_c = h_{max} * (1\text{-}\exp(-t/t_1)) \qquad (1)$$

Here $h_{max}$ - the displacement of indenter during taking load time $t$ (in ultimate case it is greatest possible displacement at given dynamic loading rate $V_P$ and load $P$); $t_1$ - the time during which indenter takes root on depth equal $h_1$=0,632*$h_{max}$.

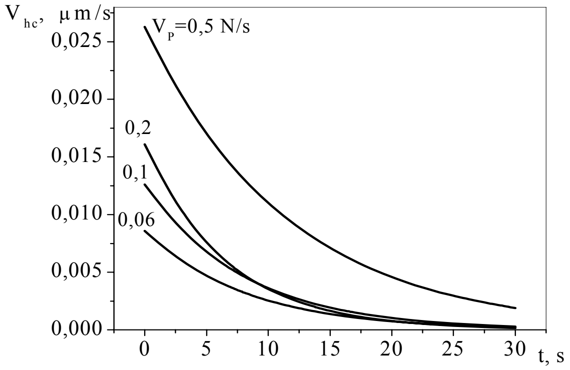

By the form creep curves are similar to that receive at a stage of the unsettled creep in tensile tests at a constant stress.

The differentiation of the relationship (1) on time gives expression for displasement rate at static loading $V_h$:

$$V_h = (h_{max} / t_1) * \exp(-t/t_1) \qquad (2)$$

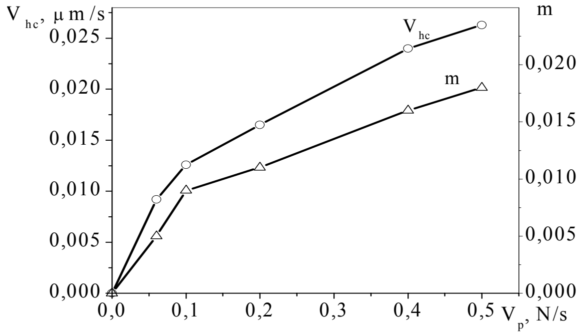

Kinetic curves for creep rate $V_h$, constructed on the equation (2) are shown in a **Fig. 2.** It is visible, that the significant fall of creep rate occurs already in first 5-10 s, and through 30 s the creep practically completely stops.

Here it is important to note that for the initial moment of creep the value of displasement rate $V_h$ grows with increase of loading rate $V_P$. In other words, the increase of dynamic loading rate results in increase of deformation rate at subsequent static loading of a material, and this dependence has a quite concrete kind (**Fig. 3**).

The increase of the sizes of an indent at taking load, which takes place at creep, means decrease of hardness. Received kinetic hardness curves have allowed to apply a technique rebuilding of dependence $H_c(t)$ in logarithmic coordinates [5] and to determine meanings of the decrease rate of hardness - parameter *m* [6] (Fig. 3):

$$H_c = a * t^{-m}, \qquad (3)$$

where *a* - constant of a material and conditions microindentation.

As well as it was necessary to expect, in complete conformity with experimental data about direct connection between speeds $V_P$ and $V_{hc}$ decrease rate of hardness at static loading, which is characterized by value *m*, also grows at increase of dynamic loading rate (Fig. 3).

Increase of dynamic loading rate intensifies destruction in area, which adjacent to indenter. The area of the destruction zone around indents accordingly grows, material fails on fineer fragments. The similar situation takes place and at increase of load. The influence of static loading it is shown in effect of formation of arbors around indents as swelling of areas with less broken sites.

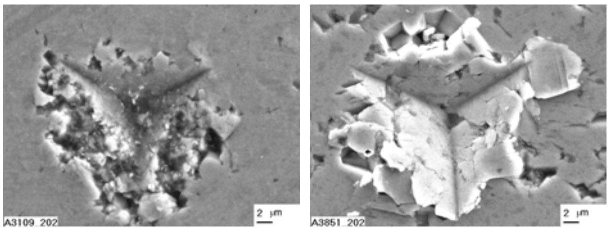

a b

**Fig. 4**. *a* - dynamic loading with $V_P$=0,4 N/s; *b* - $V_P$=0,5 N/s with the subsequent taking load 50 *s* at *P*=0,2 N.

Effect of increase of creep characteristics of titanium-siliceous carbide $Ti_3SiC_2$ at an indentation with raising rate at a dynamic loading and load values it is possible to explain by increase of the saved up elastic strains value (so, and stress concentration) which at the subsequent exposure under constant load (creep) in the greater degree can proceed in plastic deformation and lead to formation of microcracks.

1. M.W. Barsoum / Prog. Solid St. Chem. - 2000. - Vol. 28. - P. 201-281.
2. Н.П. Бродниковский, Э.П. Печковский, С.А. Фирстов и др./ Металлофиз. новейшие технол. 2003, т. 25, № 9, с. 1179-1200.
3. T. El-Raghy A. Zavaliangos, M.W. Barsoum, S.R. Kalidindi / J. Am. Ceram. Soc. - 1997. - Vol. 80, No.2. -P. 513-516.
4. В. Ф. Горбань, Э. П. Печковский, С. А. Фирстов и др.. Труды Межд. конф. «Новейшие технологии в порошковой металлургии и керамике», 2003, Киев, с. 416-417.
5. В. П. Шишокин, Журн. теорет. физики, 1938, **7**, вып. 18, с. 1613-1628.
6. Г. С. Писаренко, В. А. Борисенко, С. С. Городецкий и др., Прочность тугоплавких металлов. М., Металлургия, 1970.

# ELECTRONIC STRUCTURE OF RHOMBOHEDRAL PHASES ζ-$Ta_4C_{3-x}N_x$

**Khyzhun O.Yu., Kolyagin V.A.**(1)
Frantsevich Institute for Problems of Materials Science, National Academy of Sciences of Ukraine,
3 Krzhyzhanivsky st., Kyiv 03142 , Ukraine
(1)Institute of Physical Chemistry, Russian Academy of Sciences, 31 Leninsky st., Moscow 117915,
Russia

Carbides and nitrides based on refractory metals of groups IVB to VIB of the Periodic Table attract attention due to their ability to form intermediate phases in the composition range between the f.c.c. TX and h.c.p. $T_2X$ structures (T denotes transition metal atoms and X either carbon or nitrogen atoms). Crystal structures of the mentioned intermediate phases can be ascribed by a common formula of $(h_m c_n)_p$-type in Jagodzinski-Wyckoff symbols, where *h* and *c* are the hexagonal and cubic metal packing motifs, respectively. The intermediate phases of $(h_m c_n)_p$-type are characterized by large quantities of $c_h/a_h$ ratios, where $c_h$ and $a_h$ are the hexagonal lattice parameters [1,2].

Many of transition metal carbides and nitrides are capable of forming unlimited solid solutions with each other. Physical and chemical properties of such solid solutions depend greatly on their composition. Some properties of the carbonitrides, as a function of the TC/TN ratio, are nonmonotonous and can be understood by considering their electronic structure [3].

It is well known that conventional powder metallurgy methods do not allow to synthesize a continuous cubic single-phase TaC–TaN solid solution using the hexagonal form of tantalum mononitride with the structure of CoSn-type and cubic tantalum monocarbide with the structure of NaCl-type as precursors: samples containing less than 40 at.% of cubic TaC are two-phase materials [4]. A stoichiometric cubic $TaC_xN_y$ system, where $x + y \approx 1$, was first synthesized by authors [4] using high pressure–high temperature treatment.

Rhombohedral $Ta_4C_3$ and $TaC_{0.59}N_{0.15}$ specimens studied in the present work were synthesized using the method of high-temperature interaction of refractory metal interstitial alloys with their oxides [5]. The rhombohedral $Ta_4C_3$ carbide was a single-phase material with lattice parameters $a$=0.3120±0.0003 nm and $c$=3.005±0.004 nm. The rhombohedral $TaC_{0.59}N_{0.15}$ carbonitride studied, due to the data of XRD analysis of this specimen made in Ref. [5], consisted of about 90 wt.% of the rhombohedral $R\bar{3}m$ phase, ca. 5–7 wt.% of hexagonal $Ta_2C$ hemicarbide, and small impurities (ca. 3-4 wt.%) of a phase based on metallic tantalum. Lattice parameters of the rhombohedral (structure $R\bar{3}m$) $TaC_{0.59}N_{0.15}$ carbonitride were the following: $a$=0.3107±0.0006 nm and $c$=3.009±0.005 nm [5].

Results of XPS studies of the valence-bands in the rhombohedral $TaC_xN_y$ specimens, $Ta_4C_3$ and $TaC_{0.59}N_{0.15}$, are presented in Fig.1. The Ta 5*d*-like emission bands for the above compounds were investigated in Ref. [5].

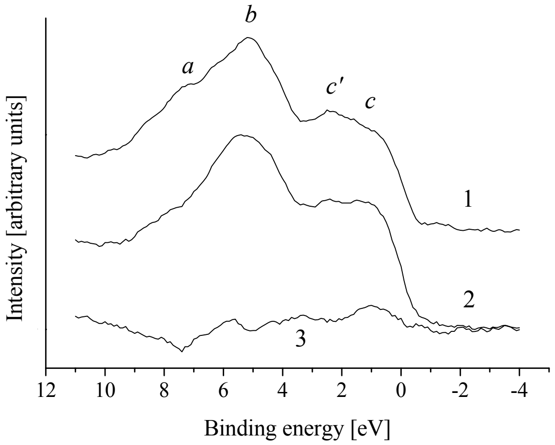

Fig.1. XPS valence-band spectra of rhombohedral (1) $Ta_4C_3$ and (2) $TaC_{0.59}N_{0.15}$ compounds and (3) the difference curve of the above spectra.

The XPS valence-band spectra presented in Fig.1 were normalized so that the intensities of their main peaks "*b*" are equal. It was shown in Refs. [6,7] that, the main maximum "*b*" of the XPS valence-band spectrum in tantalum carbides and nitrides is created due to Ta 5*d*-like and C(N) 2*p*-like states taking part in forming hybridized $d_{Ta}$–$p_{C(N)}$ bonds, but the sub-band "*c*" of the spectrum is created due to the contribution of the Ta 5*d*-like states forming Ta–Ta bonds in the compounds. Therefore, increasing intensity of the near-Fermi sub-band "*c*" of the XPS valence-band spectra in the sequence $Ta_4C_3 \rightarrow TaC_{0.59}N_{0.15}$

indicates that the metallic component of the chemical bonding increases somewhat when a portion of carbon atoms of the $Ta_4C_3$ compound has been substituted for nitrogen atoms. The difference curve of the XPS valence-band spectra of rhombohedral $TaC_{0.59}N_{0.15}$ and $Ta_4C_3$ compounds (curve 3, Fig.1) has its maximum in the near-Fermi region, around 1 eV below $E_F$. The half-width of the XPS valence-band spectrum increases by 0.3 eV when going from $Ta_4C_3$ to $TaC_{0.59}N_{0.15}$ mainly due to an increase of the relative intensity of the near-Fermi sub-band "*c*" of the spectrum.

It should be mentioned that, when studying the Ta 5*d*-like emission bands in the above compounds, it was observed [5] that the relative intensity of the near-Fermi feature "*c*" of the band increased somewhat in the sequence $Ta_4C_3 \rightarrow TaC_{0.59}N_{0.15}$ (from $I_c/I_b$=0.64±0.03 in $Ta_4C_3$ to $I_c/I_b$=0.68±0.03 in $TaC_{0.59}N_{0.15}$). The half-width of the band increases by 0.5 eV when going from $Ta_4C_3$ to $TaC_{0.59}N_{0.15}$ [5]. Therefore, changes of the XPS valence-band spectra (reflecting the energy distribution of the total density of states in the compounds investigated) are similar to those of the Ta 5*d*-like spectra. This is in agreement with the results of the band-structure calculations of tantalum carbides and nitrides [8,9].

Dependence of the XPS Ta $4f_{7/2}$ core-level binding energies upon content of carbon and nitrogen atoms in the rhombohedral tantalum carbonitrides studied is presented in Fig.2. For comparison, results of analogous studies of cubic $TaC_xN_{\sim0.8-x}$ system [5] is also shown in the figure. Fig.2 shows that substitution of carbon atoms for nitrogen atoms in the studied cubic $TaC_xN_{\sim0.8-x}$ and rhombohedral $Ta_4C_3$–$TaC_{0.59}N_{0.15}$ systems leads to increasing the Ta 4*f* core-level binding energies. This fact indicates that the positive charge on tantalum atoms increases somewhat in the sequences $TaC_{0.82} \rightarrow TaC_{0.05}N_{0.97}$ and $Ta_4C_3 \rightarrow TaC_{0.59}N_{0.15}$. Therefore, in the studied cubic and rhombohedral tantalum carbonitrides, substitution of a portion of carbon atoms for nitrogen atoms leads to increasing the ionic component of the chemical bonding.

Due to the fact that the relative content of nitrogen and carbon atoms in the studied cubic $TaC_xN_y$ system [(C+N)/Ta) ≈ 0.8] is higher as compared with that of the rhombohedral compounds investigated [(C+N)/Ta) ≈ 0.74], the ionic component of the chemical bonding in the rhombohedral samples is smaller as compared with that in the cubic $TaC_xN_{\sim0.8-x}$ system (see Fig.2).

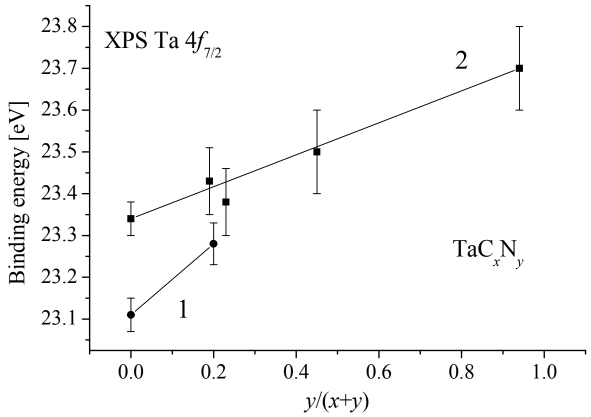

Fig.2. Dependence of the XPS Ta $4f_{7/2}$ core-level binding energies upon content of carbon and nitrogen atoms in the (1) rhombohedral and (2) cubic $TaC_xN_{\sim0.8-x}$ [5] tantalum carbonitrides studied.

[1] E. Parthé, K. Yvon, Acta Cryst. B, **26** (1970) 149.

[2] V.A. Kolyagin, S.G. Brailovsky, R.K. Chuzhko, Izv. AN SSSR: Neorgan. Materialy, **26** (1990) 1871 (in Russian).

[3] A. Neckel, Int. J. Quantum Chem., **23** (1983) 1317.

[4] E.M. Gololobov, N.I. Sedrenok, In: Nitrides: Manufacturing, Properties and Applications, Zinatne, Riga (1984), Vol. 1, p. 87 (in Russian).

[5] O.Yu. Khyzhun, V.A. Kolyagin, J. Alloys Compd., **363** (2004) 32.

[6] O.Yu. Khyzhun, E.A. Zhurakovsky, A.K. Sinelnichenko, V.A. Kolyagin, J. Electron Spectrosc. Related Phenom., **82** (1996) 179.

[7] O.Yu. Khyzhun, Ya.V. Zaulychny, Phys. Status Solidi (b), **207** (1998) 191.

[8] P. Weinberger, C.P. Mallett, R. Podloucky, A. Neckel, J. Phys. C, **13** (1980) 173.

[9] G.H. Schadler, A.M. Boring, P. Weinberger, A. Gonis, Phys. Rev. B, **38** (1988) 9538.

# STRUCTURE AND MECHANICAL PROPERTIES OF SURFACE LAYER ON IRON UNDER FRICTION HEATYING

**Yurkova A.I, Belots`ky A.V, Byakova A.V.**(1)
National Technical University of Ukraine “Kiev Polytechnic Institute”,
37 Prospect Peremohy, 04056, Kiev, Ukraine E-mail: yurkova@list.ru
(1) Institute for Problems of Materials Science, NANU,
3 Krzhyzhanivs'ky St., 03142, Kiev, Ukraine, e-mail: byakova @ vic.com.ua

***Introduction*** Severe plastic deformation is available process for substantial refinement of metallic grain structure up to nano-scaled structure e.g.100 nm and less. This structural refinement occurs at the surface under friction treatment, resulting in gradient of grain size in cross-section. Submicrostructured region and, then microstructured one follow nanostructured region placed at the top surface. From the point of view referred to forming nanostructured surface layer with excellent adhesion to matrix friction treatment has essential advantages compared to coating performed by PVD technique.

**Experimental** The cylindrical samples made of iron (0.064wt.%C) were heated by friction during rotation [1] at 773K for 1 hour. Ar-gas and $NH_3$-gas were employed in experimentation. The grain size of the annealed iron sample before treatment was about 100 μm.

X–ray diffraction (XRD) analysis and powerful optical microscopy (resolution ~0,4 μm) were used in course of experimentations. The average grain/block size was calculated from the broadening of bcc-Fe diffraction peaks by using the Scherrer method. Dislocation density was determined by XRD method when a physical broadening of the diffraction peaks is used.

The microhardness value was determined under loads $P \geq P_c$, ensuring outmost stable contribution of plastic component to total deformation and, so, actual stable numbers of Vickers hardness. The plasticity characteristic $\delta_H$ was obtained through microhardness measurement results. Plasticity characteristic $\delta_H$ was calculated on the modern approach [2].

***Results and discussion*** It was shown, that friction treatment causes the refinement of parent coarse-grained structure resulting in formation of gradient nanostructured surface layer. Microstructure morphology of the treated surface layer differs from that typical for matrix (Fig. 1). Severe friction deformation evidences are seen in surface layer, in which grain boundaries could not be identified compared to matrix. Both friction processes either in Ar-gas or in $NH_3$-gas causes to the refinement of surface layer grain structure, resulting in the increase of the grain boundaries extension. However, gas nature influences the thickness of refined surface layer. The thickness of refined layer that was performed by friction with $NH_3$-gas is 3 times greater then that obtained by friction with Ar-gas.

By using XRD-analysis indications were obtained that significant broadening of Bragg diffraction peaks occurs when friction with Ar-gas is employed. Generally, several reasons can cause the phenomenon above, i. e. decreasing the grain size, raising the dislocation density and increasing the structural microstrains. The averaged grain/block size, that was calculated using diffraction peaks broadening was assessed as great as 30-40nm. Dislocation density evaluated by calculations was believed to achieve $10^{11}$ cm$^{-2}$ whereas for annealed iron it was as great as $10^6$–$10^8$cm$^{-2}$.

By using XRD-analysis it was found that grain/block size increase gradually with increase of the distance to surface whilst opposite is true for dislocation density and microstrains.

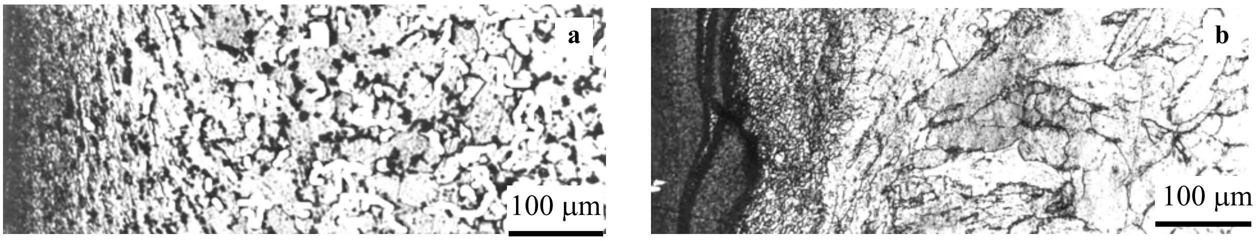

Figure 1 – Optical micrographs of structure observed in iron cross-section treated by friction:
a – Ar-gas; b – $NH_3$-gas

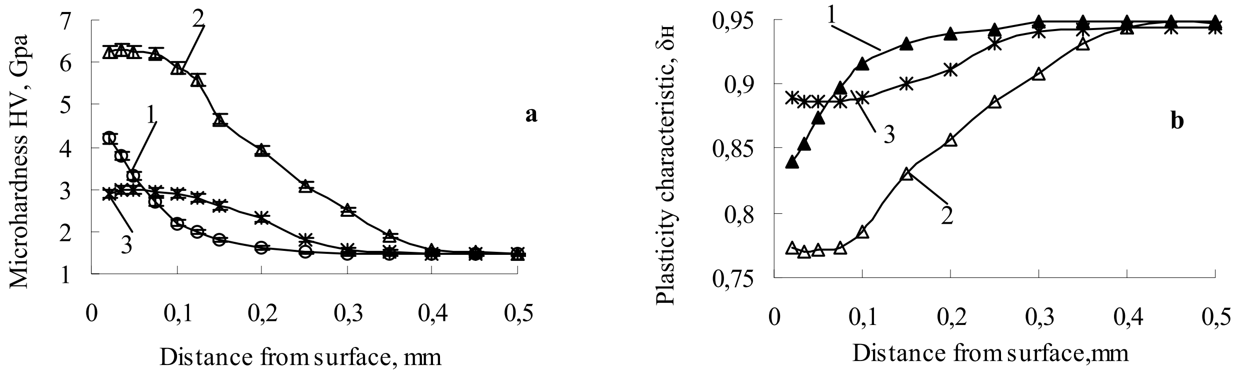

1 – friction with Ar; 2 – friction with $NH_3$; 3 – furnace nitriding, 3 hour
Figure 2 – Change in hardness (a) and plasticity characteristic $\delta_H$ (b) with the distance to treated surface

It was found from TEM analysis that grains/blocks sizes ranged from 100 to 300 nm are formed at the distance to surface about 0.05 mm [3].

The microhardness of nanostructured layer, obtained by friction treatment with Ar-gas, is 3 times higher than that found for original coarse-grained iron as shown in Fig. 2a. The thickness of hardening layer corresponds to that of refined one being recognized as great as 0.08 mm. The refinement of grain structure leads to increasing of hardness and, so, to decreasing the plasticity characteristic $\delta_{н}$ as shown in Fig. 2b. The hardness number decreases and, thus, plasticity $\delta_{н}$ increases as distance to surface increases. It is notable that plasticity characteristic $\delta_{н}$ for the refined structure is less then critical value 0.9 while opposite is true for matrix iron. It was shown that under tensile testing the samples are fractured in brittle manner when plasticity $\delta_H < 0.9$ [4]. However, we suspect that there is no danger of brittle fracture of thin surface layers, which demonstrate $\delta_H < 0.9$, since bending in elastic region deforms them.

The results, shown in Fig. 1 and 2 indicate that both layer thickness and hardness value obtained in the surface of iron by friction with $NH_3$-gas are greater compared to those performed by friction with Ar-gas. Apparently, nitrogen diffusion into iron surface occurred simultaneously with structural refinement by friction causes the phenomenon above. It is notable that the thickness of nitriding layer being obtained by friction with $NH_3$-gas is greatest and it cannot be achieved by currently available processes of nitriding [5].

According to XRD analysis very thin layer, consisted of $\varepsilon$–nitride and $\gamma$`-nitride, was formed on the top surface of iron treated by friction with $NH_3$-gas. Nitriding refined layer based on $\alpha_N$-phase (nitrous ferrite) follows the nitride layer. Interference peaks recorded in the region of $\alpha_N$-phase were found to be very broadening and removed to small angles. These results indicate that nitrogen content in $\alpha_N$-phase was anomalously high. Moreover, both the increase of dislocation density and extension of grain/block boundaries occur owing to grain refinement. Nitrogen content recorded in $\alpha_N$-phase at room temperature is higher by 3 times compared to that indicated by state diagram for system Fe–N even in the region of high temperature [5].

Nitriding refined layer obtained on iron by friction with $NH_3$-gas was believed to have the greatest values of Vickers hardness and, so, the smallest value of plasticity characteristic $\delta_H$ compared to those recorded for currently available nitriding layers as well as to those found for surface layer performed by friction with Ar-gas.

***Conclusion.*** It was found that surface friction treatment both with Ar-gas and $NH_3$-gas is favorable to form gradient nanostructured surface layers on iron. Cell size formed at the top surface of iron has found to be 40 nm and it increases gradually as the distance to surface increases. The greatest value of hardness for nitriding layer with ultra-fine grain structure causes additionally by anomalous high solubility of nitrogen in $\alpha_N$-Fe, refined under friction.

1. Bilots`ky A.V., Yurkova A.I. Technologiya i Organizatziya Proizvodstva , № 2: 40 (1988).
2. Galanov B.A., Milman Yu.V., Chugunova S.I., Goncharova I.V. Superhard Mater, **21** № 3: 23 (1998).
3. A.I. Yurkova , A.V. Bilots`ky , Yu.V. Milman, A.V. Byakova Met. Phys. Adv. Tech., 2004 (in press).
4. Milman Yu.V., Galanov B.A., Chugunova S.I Acta Metall. Mater., **41** № 9: 2523 (1993).
5. R. Chatterjee-Fischer, F.W.Eysel. Nitrierer und Nitrocarburienen (Expert vetag, 1990).

# CREEP OF TITANIUM-SILICEOUS $Ti_3SiC_2$, TITANIUM, SILICON, GRAPHITE AND TITANIUM CARBIDE AT MICROINDENTATION

**Gorban' V.F., Pechkovsky E.P., Firstov S.O.**
Frantsevich Institute for Problems of Materials Science of NAS Ukraine
3 Krzhizhanovsky St., Kiev-142, 03680, Ukraine, E-mail: epp@ipms.kiev.ua

At exposure under constant load of a pyramidal indenter , as it is known [1-4], the law of similarity of an indent is kept, therefore absolute increase in its sizes in time can characterize creep of a material. In other words, the indentation method allows to build and analyze primary creep curves - dependence of indent sizes (diagonal and depth) at time i.e. to supervise kinetics of an indenter indentation in a material under data conditions. Simultaneously occurring decrease in hardness can be used for the analysis of relaxation course of stresses in a material which is reflection of decrease in it of elastic strain level, increases in plastic deformation and also possible fracture. At data temperature key parameters determining creep kinetics are loading rate (rate of increasing of applied force, i.e. rate of a dynamic loading) and value of constant load at the subsequent exposure.

In this work ternary compound titanium-siliceous carbide $Ti_3SiC_2$ - one of the representatives of a new class of materials - nanolaminates [5], - single-phase, compact, made by sintering, the grain size $d$=5-15 microns [6, 7] is studied. In addition other materials representing various types of a crystalline lattice and interatomic bond were studied: the titanium iodide high-clean, silicon single-crystal (111), graphite pyrolitic (the direction of an indentation axis was perpendicular to sedimentation planes), hot-press titanium carbide.

Microindentation carried out by a diamond Bercovich pyramid at room temperature at load up to $P$=4 N with precision $10^{-3}$ N; depth of displacement $h$ determined with precision ± 2,5 nm; the record of the loading, taking a load and unloading diagrams was made. All process of test, the records of the diagrams and significant part of processing of results were made automatically with use of computer programming.

For the analysis of creep characteristics behavior it was used primary kinetic curves $h_c(t)$. Structural researches carried out by raster electronic microscopy method.

The analysis of diagrams has shown that creep of the investigated materials at a microindentation (depth of indenter indentation $h_c$) the above than its hardness achieved at a previous dynamic loading is lower. Titanium-siliceous carbide $Ti_3SiC_2$ occupies intermediate position between plastic and brittle materials (**Fig. 1**).

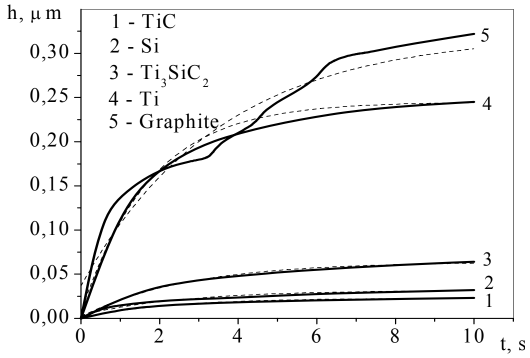

Character of dependence displacement-time $h_c(t)$, i. e. creep kinetics, for all investigated materials is described by exponential expression (dotted curves)

$$h_c = h_{max} * (1 - \exp(-t/t_1)) \qquad (1)$$

Here $h_{max}$ - the indenter displacement during taking load time $t$ (in ultimate case it is greatest possible displacement at given dynamic loading rate $V_P$ and load $P$); $t_1$ - the time during which indenter takes root on depth equal $h_1$=0,632*$h_{max}$.

By the form creep curves are similar to that received at a stage of the unsettled creep in tensile tests at a constant stress in the field of low temperatures.

The differentiation of expression (1) on time gives expression for creep rate at static loading $V_h$:

$$V_h = (h_{max}/t_1) * \exp(-t/t_1) \qquad (2)$$

For all investigated materials the increase of dynamic loading rate $V_P$ results in increase of displacement rate $V_h$ i. e. creep rate of a material at subsequent static load (**Fig. 2**).

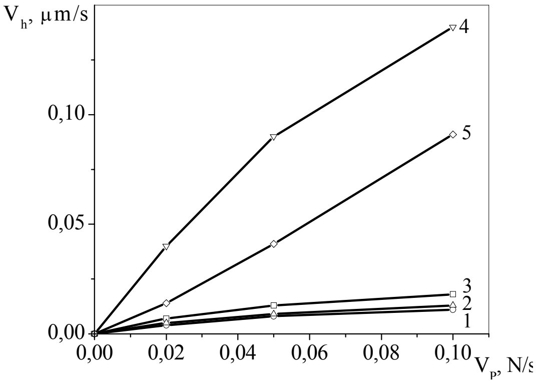

deformation at a dynamic loading (value $A_d$), it is more at the subsequent creep (value $A_c$) (**Fig. 3**).

On increase of creep characteristics materials settle down in the following sequence: titanium carbide TiC (a crystalline lattice such as NaCl, atomic bond - ionic with covalent component); silicium (a crystalline lattice such as diamond, interatomic with rising in rate of a dynamic loading and values of load is offered. At raising in dynamic loading

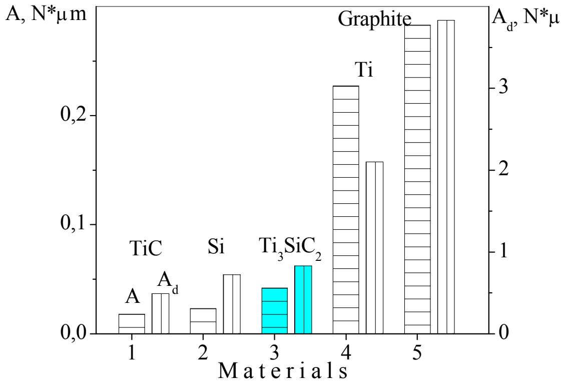

1. Yu.V. Milman, B.A. Galanov, S.I. Chugunova, Acta Mater. – 1993. – Vol. 41.– P. 2523-2532.
2. О.Н. Григорьев, Б.А. Галанов, Пробл. прочн. – 1985. - № 6. С. 31-35.
3. Григорович В.К. Твердость и микротвердость металлов. – М.: Наука, 1976.
4. B. J. Kooi, R .J. Poppen, N. J. M. Carvalho, J. Th. M. De Hosson, M. W. Barsoum, Acta Materialia, 2003, **51**, 2859.
5. M.W. Barsoum, Prog. Solid St. Chem. - 2000. - Vol. 28. - P. 201-281.

It is established that there is a correlation between dynamic loading characteristics and the subsequent creep. Most fully, conditions of an indentation and all features of deformation of a concrete material at all stages are taken into account with value of the fulfilled indentation work [8]. Results show that the more tendency of a material to

bond - covalent); $Ti_3SiC_2$ (a crystalline lattice - hexagonal, interatomic bond has three components - metal, ionic, covalent); titanium (a crystalline lattice – hexagonal close packed, interatomic bond - metal); graphite (the layered mineral, one of the carbon polymorphic modification, it has hexagonal crystalline lattice).

The following explanation of increase of creep characteristics for the investigated materials at an indentation

rate in a material the value of the accumulated elastic strains (so and stress concentration) grows which at the subsequent exposure under constant load in the greater degree can proceed in plastic deformation or lead to formation of microcracks, i.e. provide increase of creep of a material and a stress relaxation in it. The load increase leads not only in raising of the accumulated elastic strains by the moment of end of a dynamic loading but also to an intensification of its realization in the creep form.

6. В. Ф. Горбань, Э. П. Печковский, С. А. Фирстов и др. Труды Межд. конф. «Новейшие технологии в порошковой металлургии и керамике», 2003, Киев, с. 416-417.
7. Н.П. Бродниковский, Э.П. Печковский, С.А. Фирстов и др./ Металлофиз. новейшие технол. 2003, т. 25, № 9, с. 1179-1200.
8. В. Ф. Горбань, Э. П. Печковский, С. А. Фирстов и др. Труды Межд. конф. «Новейшие технологии в порошковой металлургии и керамике», 2003, Киев, с. 373-374.

# RSPECTIVE MATERIALS FOR ELECTRODES OF ELECTROCHEMICAL GAS SENSORS

**Afanasyeva V.P., Sylenko P.M.**(1)
Institute for Applied Problems in Physics and Biophysics of NASU,
3 Sluzhbova St., 03142, Kyiv, Ukraine, e-mail: vpa @ ukr.net
(1)Frantsevich Institute for Problems of Materials Science of NASU,
3 Krzhyzhanovsky St., 03142, Kyiv, Ukraine, e-mail: dep69@ipms.kiev.ua

## INTRODUCTION

The control of the contents of oxygen is very important for experimental and clinical medicine, in power and food processing industry, during the conduct of environmental evaluations.

Oxygen gas analyzers are widely used for oxygen determination. The operation of these devices is based on electrochemical analysis methods. They have superior metrological performance parameters and make it possible to determine oxygen in the sample being tested.

However, use of oxygen sensors in extreme requirements increasing some metrology performances. So, at long-lived definition of oxygen in the ecologically closed space it is necessary to apply sensors of oxygen with high stability of operation.

The miniaturization of oxygen sensors is necessary for its use in mountain medicine [1], and also in medical devices to provide safe, effective, and economical intermittent hypoxic training. The application of this instrument is based on novel methods for increasing non-specific body resistance to extreme environmental factors and pathogenic agentsвbasing [2].

The miniaturization of oxygen sensors and the increase of its stability operation can be reached using new materials for manufacture of electrodes.

The objective of this investigation is to create method for manufacturing metal-polymer materials for compact and stable anodes for oxygen sensors working in extreme requirements.

## RESULTS AND DISCUSSION

At development of electrochemical oxygen sensors as anodes usually are used lead, cadmium and zinc as punched plates or wire.

- PVA +Pb obtained at the current density 150A/ cmI. during 15 minutes;

The area of the anode should exceed the area of the cathode as a minimum 10 times for stable operation of the sensor that larges the sizes and mass of sensors [3]. These deficiencies can be eliminated at use of anodes for oxygen sensors made of metal–polymer materials.

We have developed the method of metal–polymer composite materials obtaining to make larger surface of lead, cadmium and zinc. The coats of such materials were formed as a result of two processes: deposition of a polymeric compound and electrochemical metal ions recovery.

Polyvinyl alcohol (PVA) coat was formed as a result of the cathode diffusion layer alkalizing at the hydrogen ions recovery. The ions of fumarole acid, which are a component of the electrolyte, interacted with hydroxyl ions and PVA, with transverse boundary creation between polymer molecules.

Eletctrodeposition of polymeric compound with metals is possible only at two simultaneous processes: hydrogen ions and metal ions recovery on the cathode, So, lead, cadmium and zinc can be eletctrodeposited with PVA at an exact choice of electrolytes compositions and deposition parameters.

Eelectrolytes for obtaining of all metal–polymer composite materials were prepared by immixing 10 % PVA water solution (molecular weight is 34000), containing 1 % of fumaroles acids, with 15 % water solution of $ZnSO_4$ or $CdSO_4$ or 2 % solution of $Pb(NH_2SO_3)_2$ in the ratio 1: 1 .

Eletctrodeposition of metal–polymer materials was conducted on metals of oxygen sensor's anodes at following optimum parameters of processes:

- PVA +Zn obtained at the current density 90A/cmI. during 3 minutes;

As it is visible from figure 1, the extremums of curves I and 2 determinate the germination of zinc

- PVA + Cd obtained at the current density 80A/ cmI. during 22 minutes.

Structure, composition and the properties of metal–polymer materials depend from relation of the rate of the metal ions reduction process and from the rate of polymeric compound filming.

At deposition of different metal-polymer coats two mechanisms of coats formation take place:
1-Rate both of a polymer deposition and rate of metal ions recovery are approximately identical,
2-Rate of metal ions recovery exceeds rate of polymer deposition.

As have shown our examinations, 1-st mechanism is implemented at obtaining of PVA + Pb coat. In this case coat of necessary thickness with uniform structure and composition is formed.

At realisation of the second deposition mechanism there is germinations of metal through a film of polymer and quality of coat is aggravated.

Such mechanism of metal-polymer coat forming take place at PVA + Zn and PVA+Cd deposition. The dependences of width and composition of PVA+Zn coat from deposition time are shown in fig. 1.

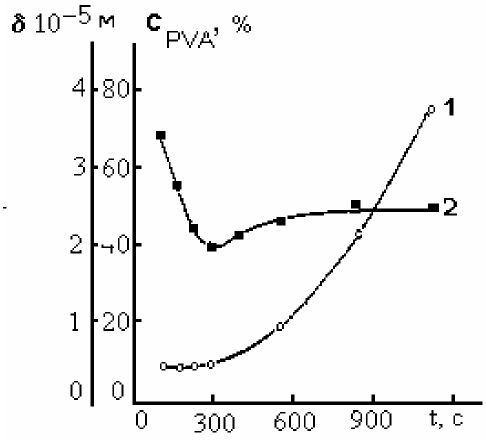

Fig. 1. Kinetics of change of width (1) and composition (2) of metal-polymer coat obtained from solution containing 5 % PVA and 7,5 % $ZnSO_4$ at a current density 90A/ cmI.

through a film of a polymer at time of a deposition more than 300 s.

Electronic-microscopic investigation of metal-polymer coats have shown presence of metal on the surface of coat, obtained during time of deposition more than 300 seconds.

The anodes for oxygen sensors containing PVA+Zn, PVA+Cd and PVA+Pb were manufactured and investigation of their polarizability were carried out. The obtained results have shown, that a polarizability, which determines stability of oxygen sensor operation, 10 times less in comparison with polarizability were carried out. The obtained results have shown, that a polarizability, which determines stability of oxygen sensor operation, 10 times less in comparison with conventional anodes

So, the most perspective material for anodes of oxygen sensor is metal-polymer PVA+Pb coat. The anodes manufactured of this materials. except high stability, can supply long-time operation of sensors, due to their thicker coats in comparison with PVA + Zn and PVA +Cd coats.

## CONCLUSIONS

1. The method for manufacturing metal-polymer coats of PVA+Pb, PVA+Zn and PVA+Cd was developed.
2. It is determinate that the most perspective material for high-stable anodes for oxygen sensors is the PVA+Pb coat

### ***references***

1. Bakaj E.A., Serebrovska T.V.,. Shylkevich T.P. at al. Equipment for partial oxygen pressure measurement during intermittent hypoxic training. High Altitude Medicine and Biology J., 2002.- (1):P-118.
2. Bernardi L., Passino C., Serebrovskaya Z., at al. Respiratory and cardiovascular adaptations to progressive hypoxia. Effect of interval hypoxic training, Eur. Heart J., 2001, (22):879-886.
3. Afanasyeva V.P, Mochkivska N.M. Roitman E.M. Electrochemical sensor for transcutaneous determination of oxygen partial pressure in blood. Patent of Ukraine №58119A, Publ. 15.07.2003.

# STRUCTURAL CHARACTERISTIC OF NANOCARBON MATERIALS

**Ovsiyenko I.V., Len T.A., Babich N.G., Kapitanchuk L.M.(1), Sharff P.(2)**
Shevchenko Kiev National University, ovsienko@univ.kiev.ua
(1)Paton Institute for Electric Welding of NASU, 3 Bozhenko st., 01006, Ukraine
(2)TU Ilmenau, Institute of Physics, D-95684, Ilmenau, Germany

Creation of novel functional composite materials based on nanocarbon is one of the directions of modern nanotechnology. That is why attestation and establishment of structural characteristics of nanocarbon materials obtained by different methods are very urgent task.

The paper presents the results of structural characteristics investigations of obtained by arc discharge method nanocarbon material. The samples obtained by arc discharge method on the surface of anode (Sample #1), on the top of cathode (Sample #2) and around of cathode (Sample #3) are investigated.

Obtained raw samples from electrode surface are the dark-gray powders. x-ray phase analysis shows presence in all samples catalyst particles – iron, nickel and cobalt and also copper particles. As it was expected the largest content of copper is in the sample #3, the smallest content of copper is in the sample #1. Such distribution also is observed for catalysts: the largest content of catalysts is in sample #3, and contain of catalyst in samples #1 and 2 is smaller.

The structural analysis of obtained samples was carried out by method of X-Ray diffractometry. The investigations were made with diffractometer ДРОН- 4 07 in filtered Co $K_{\alpha}$ radiation. The Fig.1 presents diffractograms for raw samples #2 and 3.

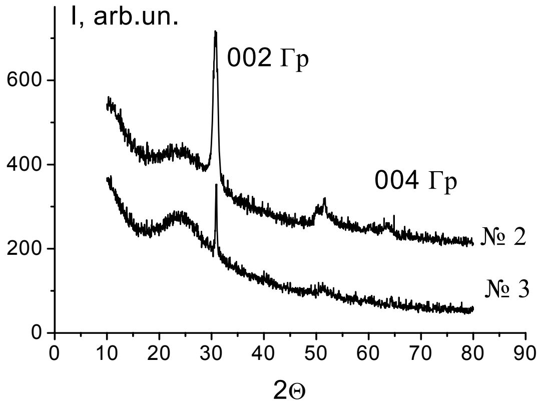

Fig. 1 Diffractograms for raw samples #2 and #3.

As it is shown on the figures for both samples besides lines of catalysts lines corresponding to 002 reflexes of graphite are observed. The angle position of these lines corresponds to the interlayer distances $d_{002}$=3,38A for sample №2 and $d_{002}$=3,36A for sample №3. These interlayer distances can be formed both nanocarbon or multiwall carbon nanotubes.

For more careful structure analyzes of obtained materials the investigations of samples particles surface were carried out by method of SEM (JSM–840, JEOL, Japan. The results of investigations are shown on the Figs. 2 –4.

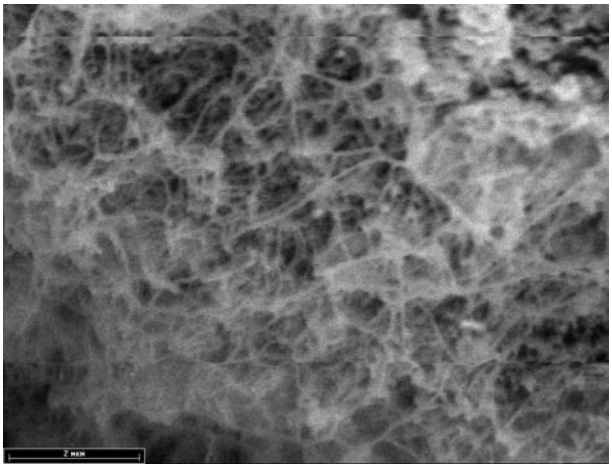

Fig.. 2. SEM imagine of surface of sample#1.

As it is shown on the figures the surface structures of samples obtained from different parts of electrodes are quite different. In the sample #1 it is neatly showing the filiformed structures, which are the bundles of carbon nanotubes.

The diameter of these nanotubes is in the range from 15nm to 60 nm, that is these nanotubes are multiwalls nanotubes. Besides with multiwall nanotubes in sample #1 the nanocarbon particles and the finest particles of catalysts are revealed.

Sample #2 is solid carbon mass with ingrained in it catalysts particles. At the back of carbon particles superfine “runners” are revealed. These “runners” are carbon nanotubes. The diameter of these nanotubes from date of SEM is up to 30 nm. Material obtained from the top of cathode is more “dirty” than materials obtained from anode surface and nanotubes concentration in it is smaller.

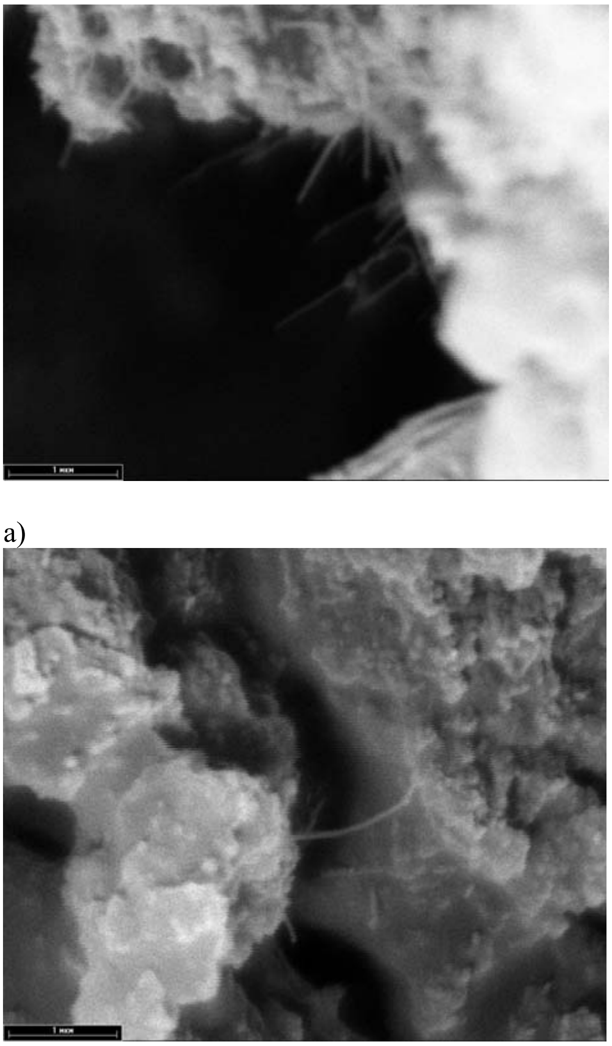

a)

б)

Fig.3. SEM images of surface of sample #2: a) and b) – different parts.

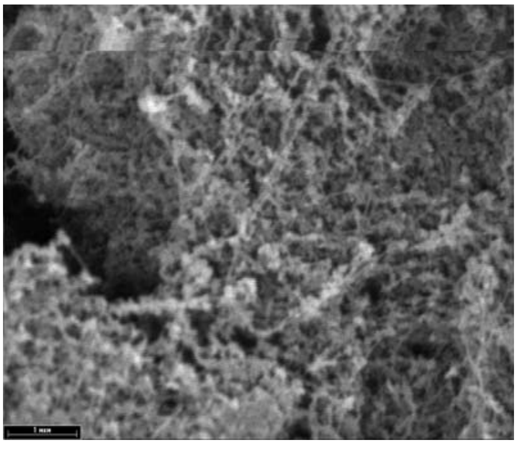

Fig.4. SEM image of surface of sample #3.

Sample #3 is porous dendritic structure. The SEM investigations wasn’t revealed carbon nanotubes ib this sample. There aren’t also catalysts particles on the SEM imagines. However more precise structure analysis of sample #3 by method TEM (Fig. 5) allows to reveal the typical “runners” with diameter up to 6 nm, which are evidently singlewall carbon nanotubes or multiwall nanotubes with small number of carbon layers.

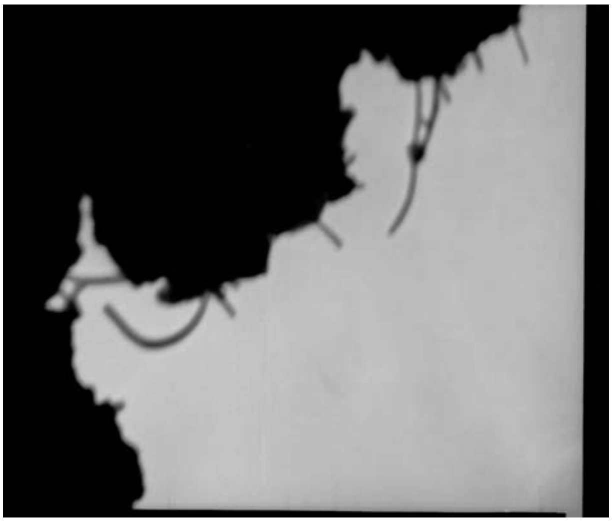

Fig. 5. Fragment of particle of sample #3 (TEM).

Consequently, carried out investigations obtained by arc discharge method nanocarbon materials have revealed, that composite and structural characteristics of these materials are essentially determined by one's position: material obtained with anode surface contains the greatest number of multiwall nanotubes and small number of nanocarbon. The material formed at the top of cathode contains mainly carbon deposition with penetrating nanotubes. The material made on the surface of cathode is dendritic structure with single nanotubes with size up to 6 nm.

# METALLMATRIX COMPOSITE ON $TIH_2$ BASE TO BE NOT DESTRUCTED DURING THE REVERSIBLE HYDROGENATION

**Bratanich T.I., Permyakova T.V., Skorokhod V.V.**
Frantsevich Institute for Problems of Material Science of NASU,
3 Krzizanovsky St, Kiev, 03142, Ukraine

It is know the numerous attempts to create the composites to be not destroyed during the hydrogenation which consist from the porous metallic matrix and uniformly placing in it insertions of the hydriding intermetallic compounds. The essential demerits of such composites are the volume increase of the intermetallic insertions during the hydrogenation and the considerable strains in the porous metallic matrix. It causes the appearance of the cracks in the matrix and the destruction of the composite on the whole during the cyclic hydrogenation. Moreover, their low mass and volume hydrogen capacity is the demerit of the known composites too. Firstly, it is connected with the utilization in the capacity of the hydriding insertions not base hydriding metals but intermetallic compounds. Secondly, the metallic matrix of the composite is usually porous and its porosity is equal near 50 %. It causes the lowering of the volume specific hydrogen capacity of the composite too.

The aim of the present work is the elaboration of the structure, composition and making method of the composite to be not destroyed during the hydrogenation with high mass and volume hydrogen capacity.

The proposing composite material is made from nickel and / or $Ni_3Al$ plastic matrix, in which the insertions of the titanium dihydride or titanium in the quantity of 42 - 46 % mass. are placed uniformly. In this time the matrix is not porous and titanium insertions are porous.

Ti - Ni ( $Ni_3Ti$ ) composite was manufactured from the nonporous intermetallic compound TiNi produced by the melting with the titanium concentration from 42 to 46 % mass. by means of its destructive hydrogenation. The composition of the initial Ti - Ni alloy was in the bounds of the TiNi homogenous field accordingly to Ti - Ni state diagram. During the destructive hydrogenation titanium was hydrogenated selectively from TiNi up to $TiH_2$ and the metallic nickel and / or $Ni_3Ti$ were formed. The composite $TiH_2$ - Ni was formed after the destructive hydrogenation under the conditions of our experiment. After dehydrogenation we had Ti - Ni composite. During the heating up to the temperature of the destructive hydrogenation the volume of the initial TiNi increased by 10 % because of the thermo elastic austenite - martensite transformation. During TiNi destructive hydrogenation up to $TiH_2$ and Ni the titanium volume increased by 25 % because of the hydrogen penetration to the titanium crystallic lattice. This volume increase of the titanium insertions was compensated by the preliminary TiNi volume increase during the martensite phase transformation. Thus, we have elaborated the composite material consisting from the nonporous nickel matrix and porous titanium dihydride or titanium insertions with 25 % of the porosity.

The manufactured material was investigated with the reference to hydrogen. Ti - Ni samples were heated in vacuum up to 773 K with the next hydrogen feed with 0,1 MPa of pressure and with exposure in this conditions up to maximum hydrogen absorption by titanium will be reached. The quantities of the absorbed hydrogen were calculated according to the pressure fall in the work volume and were controlled by the volume method during the dehydrogenation too. Nondestruction was controlled by the volume increase and was investigated by microscope.

The investigations have demonstrated that the samples of the elaborated material with mass compositions 42 Ti - 58 Ni, 44 Ti - 56 Ni and 46 Ti - 54 Ni had the specific mass hydrogen capacities being equal to 195, 206 and 217 ml $H_2$/ g comp. accordingly. With the calculation of the matrix nonporosity and 25 % porosity of the titanium insertions their specific volume hydrogen capacities are equal accordingly to 1077, 1120 and 1154 ml $H_2$ / $sm^3$ comp. In this time the samples increased in the volume by 8 % at the expense of nondestructing martensite transformation, had not cracks, didn't destruct during the hydriding - dehydriding. Such stability of Ti - Ni samples against the destruction during the hydrogenation was ensured by the fact that the porous titanium insertions didn't create the pressure on the nonporous nickel matrix in which the destructing strains didn't accumulate. It was reached at the expense of the preliminary thermo elastic austenite - martensite phase transformation of TiNi to be accompanied by the volume increase of the initial TiNi by 8 - 10 %.

Table
Properties of Ti - Ni composites

| Material composition % mass. | Specific mass hydrogen capacity, $mlH_2$/gcom | Specific volume hydrogen capacity, $mlH_2$ / $sm^3$ comp. | Relative volume increase, % |
|---|---|---|---|
| 38Ti - 62Ni | 176 | 1006 | 0,3, cracks |
| 42Ti - 58Ni | 195 | 1077 | 0,3 |
| 44Ti - 56Ni | 206 | 1120 | 7,8 |
| 46Ti - 54Ni | 217 | 1154 | 8,8 |
| 50Ti - 50Ni | 236 | 1211 | 15,2 cracks |
| 71Ti-29$Ni_3$Ti | 143 | 711 | 9,7 |

Out of the homogenous field at the titanium concentration less than 42 % mass. And more than 46 % mass. initial Ti - Ni alloy except TiNi intermetallic compound contains too the intermetallic compounds $Ti_2Ni$ and $Ni_3Ti$ accordingly in which the austenite - martensite transformations don't take place. These phases are ballast from the point of view of the compensation of the titanium insertions volume increase. That is why Ti - Ni samples with the mass titanium concentrations 38 and 50 % mass. increased in volume accordingly by 13,3 and 15,2 % during the hydrogenation, had the net of cracks, lost the durability partly, that is began to destroy.

Thus, the elaborated Ti - Ni composite with nonporous nickel matrix and porous titanium insertions in the quantity from 42 to 46 % mass. has the high specific mass and volume hydrogen capacity. This is reached at the expense of the increase of the insertions hydrogen capacity at the substitution of the intermetallic compound on the hydriding metal ( titanium ), and at the expense of the formation of the nonporous nickel matrix during TiNi destructive hydrogenation. In this case in the determined bounds of the mass titanium concentration the samples didn't destruct during the hydrogenation.

# INFLUENCE OF ELEMENTARY COMPOSITION ON PLASTICITY CHARACTERISTIC OF NANOSTRUCTURED $TIN_{1±X}$ COATINGS

**Byakova A.V., Milman Yu.V., Vlasov A.A.**$^{(1)}$
Institute for Problems of Materials Science, NANU,
3 Krzhyzhanivs'ky St., 03142, Kiev, Ukraine, e-mail: milman@materials.kiev.ua
$^{(1)}$ National Technical University of Ukraine “Kiev Polytechnic Institute”,
37 Prospect Peremohy, 04056, Kiev, Ukraine, e-mail: byakova@vic.com.ua

## Introduction

For many potential applications understanding mechanical behaviour of TiN like coatings via elementary composition in the range of homogeneity on nitrogen is essential. Unfortunately, mechanical properties of TiN like coatings are yet imperfectly characterised and limited usually to microhardness measurement results. That is why in practical use there is some confusion concerning judgment of mechanical behaviour of these coatings. Complete set of mechanical parameters including plasticity characteristics, $\delta_H$, [1, 2] seems to be helpful at the most to overcome this problem.

In the current paper mechanical properties of TiN like coatings are studied in details by using plasticity characteristics, $\delta_H$, besides microhardness value. Characterisation of mechanical properties for TiN like coatings via content of interstitial elements such as nitrogen, carbon, and oxygen is clarified also.

## Coating characterisation and testing by indentation technique

*Structural characterisation*: Titanium nitride coatings of submicro-and nano-scaled grain structure were performed by physical vapour deposition (PVD) techniques attributed to Ion Bond process. Typical conditions of coating application are listed in Table. Coating structure was examined by X-ray diffraction (XRD), optical microscopy, and scanning electron microscopy (SEM). Compositional depth profiles for $TiN_{1±x}$ coatings were measured by Auger-electron spectrum analysis (AES). Dimensions of the short and long axes of grain, $D_{min}$, and $D_{max}$, arranged respectively parallel and perpendicular to coating interface were used to define grain morphology (size and shape).

*Indentation experiments*: Microhardness value HV and plasticity characteristic $\delta_H$ were determined through microindentation measurement results. Indentation experiments were performed in coating cross section. Indentation loads ranged from 0.2 to 1.4 N were used in tests. To avoid responsibility as to inaccuracies, which can occur due to the influence of scale factor, coatings were tested under loads higher than critical, $P \geq P_c$, ensuring almost stable values of microhardness and plasticity characteristic $\delta_H$. Plasticity characteristic $\delta_H$ was determined according to modern approach [2]. Young’s modulus, $E$, and Poisson’s ratio, $\nu$, relevant to titanium nitrides were adopted over handbooks.

## Results and discussion

*Structural characterisation of coatings*: Structural parameters and composition of coatings are documented in Table. Coatings consisted of fibred grains with the dimension $D_{max}$ equal to coating thickness and dimension $D_{min}$ ranged from 100 to 1500 nm were formed as shown in Fig.1. Coatings obtained under low pressure of nitrogen-gas, $p < 1$ Pa, contained intermixture of two phases, $\varepsilon$-$Ti_2N$+$\delta$-TiN, whereas under high pressure of nitrogen-gas, $p>3$ Pa coatings were made of $\delta$-TiN single phase. Besides nitrogen some amount of carbon and oxygen being ranged totally from 5 to 8 at.% was found in composition of TiN like coatings, which are denoted in Table by numbers 1-8 whereas coatings marked in Table by numbers 9, 10 contained only small amount (less than 5 at.%) of carbon. Probably, foreign interstitial elements such as carbon and oxygen diffused in condensate from reactive gas atmosphere exploited by deposition technique. Thus, formation of titanium oxycarbonitride and titanium carbonitride is allowed by conditions of coating application. Attention should be drawn to the fact that over stoihiometric compositions with indices total more than 1 was found to be typical for submicro- and nano-structured coatings made of titanium nitride. The increase of element solubility in solid could be caused by nano-sized grain structure of coating. The results determined for oxycarbonitride coatings $Ti(NCO)_{1±x}$ (see Table, samples 1-8) indicate that Vickers hardness decreases and, so, Table. Conditions of application and coating characterisation

| № | Conditions of coating application | | | Thickness, μm | Elementary composition | Nitrogen content, at.% | Range of grain size $D_{min}$, μm |
|---|---|---|---|---|---|---|---|
| | Nitrogen partial pressure, Pa | Substrate | T, °C | | | | |
| 1 | 0.01 | Ti-alloy | 400 | 15 | $Ti(CNO)_{0.82}$ | 32 | 1.0 …1.5 |
| 2 | 0.03 | Ti-alloy | 400 | 15 | $Ti(CNO)_{0.91}$ | 33 | 0.8 …1.0 |
| 3 | 0.33 | Ti-alloy | 400 | 15 | $Ti(CNO)_{1.03}$ | 36 | 0.5 …1.0 |
| 4 | 3.83 | Ti-alloy | 400 | 15 | $Ti(CNO)_{1.13}$ | 40 | 0.4 … 0.6 |
| 5 | 4.47 | Stainless steel | 400 | 19 | $Ti(CNO)_{1.19}$ | 41 | 0.1 …0.2 |
| 6 | 6.30 | | 550 | 36 | $Ti(CNO)_{1.20}$ | 42 | 0.1 …0.2 |
| 7 | 8.00* | | 400 | 16 | $Ti(CNO)_{1.22}$ | 43 | 0.1 …0.2 |
| 8 | 10.00 | Ti-alloy | 400 | 15 | $Ti(CNO)_{1.22}$ | 44 | 0.1 …0.2 |
| 9 | 8.00 | Stainless steel | 550 | 20 | $Ti(CN)_{1.11}$ | 47 | 0.1 …0.2 |
| 10 | 8.00 | | 550 | 35 | $Ti(CN)_{1.03}$ | 48 | 0.1 …0.2 |

Notice: *- Inner Ti layer of 2 μm thickness is located at the interface of TiN like coating.

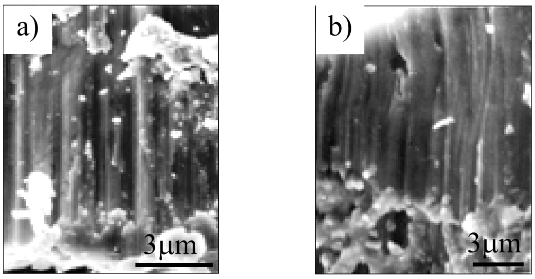

Fig.1. SEM images of coatings made of $TiN_{1+x}$, which are indicated in Table by samples (a) 1 and (b) 4.

plasticity characteristic $\delta_H$ increases continuously as content of interstitial elements increases as shown in Fig. 2.

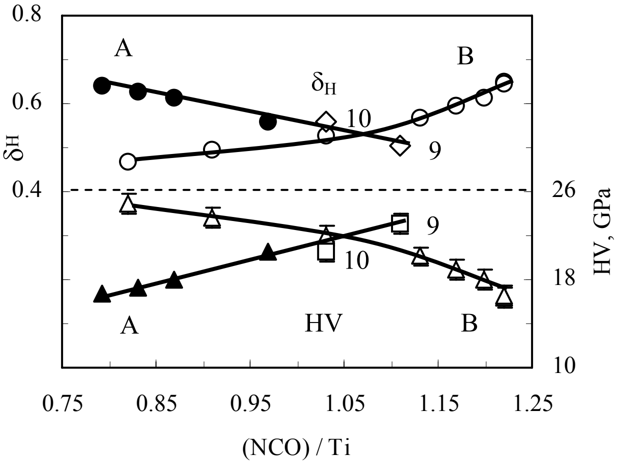

Fig.2. Mechanical parameters (A) for coatings (open symbols) and (B) for bulk TiN nitride (closed symbols) *vs*. content of interstitial elements. Numbers 9 and 10 at the plots indicate the data for samples of $Ti(NC)_{1\pm}x$-coatings (see Table) whilst no numbers at the plots specify the samples for $Ti(NCO)_{1\pm x}$-coatings.

However, the opposite is true for bulk titanium nitride for which plasticity characteristic $\delta_H$ was calculated using the tabulated data for Vickers hardness published in [3]. Unlike to oxycarbonitride coating, $Ti(NCO)_{1+x}$, the data for carbonitride coatings, $Ti(NC)_{1+x}$, (see Table, samples 9, 10) line up well on a single plot for bulk nitride when it is extrapolated to the region of over stoihiometric compositions. It is therefore believed that the difference between character for correlation of parameters HV and $\delta_H$ for $Ti(NC)_{1\pm x}$-coatings *vs.* content of interstitial elements and those revealed for bulk TiN-nitride and $Ti(NC)_{1+x}$ -coatings could be associated with the presence of oxygen as was reported originally for oxidized carbide and nitride compounds [4].

Thus, the results determined in the present study indicate that over stoihiometric compositions are typical for submicro- and nano-structured coatings made of TiN. Plasticity of TiN-like coatings is affected by the nature and content of additional interstitial elements. Compared to bulk titanium nitrides, TiN-like coatings alloyed by small amount of carbon and oxygen (less than 8at.% in total) exhibit smaller plasticity in the region of under stoihiometric compositions whereas the opposite is true in the region of over stoihiometric compositions.

## Acknowledgements

The research was supported partly by Science and Technology Centre in Ukraine (STCU), project No. 1997.

1. Yu.V. Milman, B. A.Galanov, and S.I. Chugunova// Acta Metall. Mater. –1993. – 41.N 9. –P. 2523-2532.
2. B. A.Galanov, Yu.V. Milman, S.I. Chugunova, and I.V. Goncharova// Superhard Mater. – 1999. – 21.N 3.– P.23-35.
3. G. V. Samsonov, I.M. Vinitzkiy, Refractory Compounds: Handbook. – Moscow: Metallurgiya, 1976. – 558 p.
4.R. F. Voytovich. Oxidising carbides and nitrides.- Kiev: Naukova dumka, 1981. – 192 p.

# COALESCENCE PHENOMENON IN $CrSi_2$ AMORPHOUS-CRYSTALLINE THIN FILMS

**Dvorina L.A., Dranenko A.S.**
Frantsevich Institute for materials Science Problems, Academy of science of Ukraine 3,
Krzizanovsky str. , Kiev, Ukraine E-mail: dvorina@materials.kiev.ua

Phenomenon of coalescence is the process of recrystallization at which the substance is transporting from more small crystals more large. In cause of Ostwald coalescence realized as recrystallization of "grain in grain". Lifshitz and Slyozov receive strictly solution for case of coalescence in solid solution. Effect of coalescence in island thin films where the process of mass transfer between the granules of A on substrate B is investigated too [1].

Thin films of chromium disilicide have attracted attention because of their unique combination of electrophysical properties, increased stability under temperature gradient, mechanical stresses, aggressive media. Thin films of chromium disilicide solid solutions have been intensively studied from both fundamental and applied points of view, due to their important application in very large integrated-circuit technology as metallic materials for gate electrodes, interconnection and surface resistors in hybrid integrated circuit, sensor and other. In this work we present the results of coalescence phenomenon of nanostructure in amorphous-crystalline films in thickness range 20-80 nm.

The films were prepared by the ion-plasma method sputtering chromium disilicide targets, produced by hot forming powder $CrSi_2$. The residual gas pressure was about $1x10^{-4}$ Pa, and the pressure of argon during deposition was $4x10^{-2}$ Pa. At a target voltage of 1 kV and a target current of 50 mA, the film thickness was 10-100 nm.

To investigate the structure by transmission electron microscopy, the films were condensed on (100) surface NaCl, from which they were separated by distilled water and supported by grids of copper or molybdenum. Resistivities were calculated from the sheet resistance. The sample composition was controlled by a standard Auge-sputter depth-profiling technique, which combined argon-ion milling technique with Auger electron spectroscopy (AES) and SIMS. Ellipsometric measurements were made with ellipsometor LEF-2.

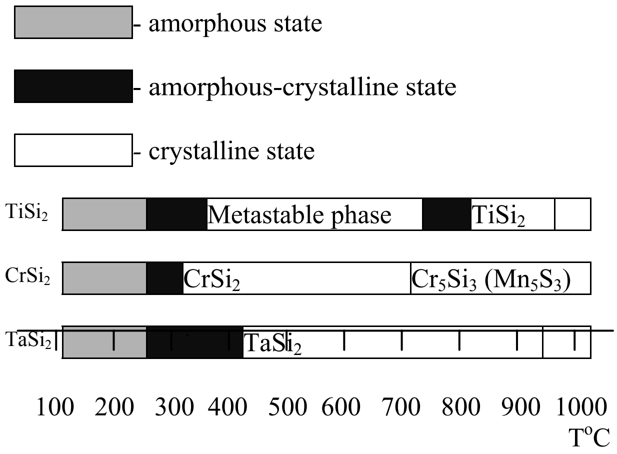

Fig.1. Diagram of phase transitions on crystallization of disilicides in thin films.

The light source was He-Ne laser (λ =632,8 nm).

Films deposited at $T_s$ = 333 K are amorphous. The transmission electron micrograph shows a fine – grained contrast which is typical of amorphous structures. It is shown, that films deposited on the substate at $T_s$ = 573 K have amorphous and crystalline phase. For annealing temperatures >973 K the amorphous films crystallized into polycrystalline hexagonal phase $CrSi_2$ type (C40). Transition from amorphous to crystalline phase take place on the narrow temperature range as shown in fig1. AES and SIMS depth profiles showed uniform distribution metal and silicon throughout the film thickness, and its ratio corresponded to target compositions. In all samples, carbon with some oxides (<1,5 nm) was detected on the surface, presumably in form of native silicon oxide. The oxygen concentration in the layer is normally not uniform in depth. No other contamination was found.

The studies of microstructure are an important stage of material research. The knowledge about the relationship between the parameters of structure and properties is necessary for the development of advanced ceramic thin films. For this purpose the quantitative analysis of structure is used as a significant research tool. This work aimed at the application of computer aided quantitative analysis for the description of microstructure of amorphous-crystalline thin films.

In the quantitative analysis of amorphous-crystalline thin films were determined such parameter as $D_f$ - Feret's diameter, which is average of particles projections for 64 directions πk/64, where k = 0…63, for this direction [2].

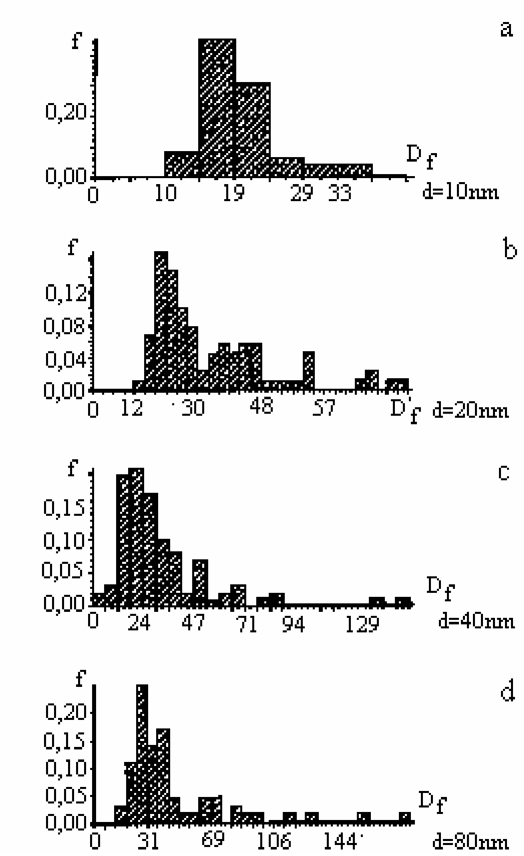

Fig.2. Histograms of Feret"s diameters for $CrSi_2$ amorphous-crystalline films for variety thinks: a - d=10 nm; b - d=20 nm; c - d=40 nm; d=80 nm.

In Fig.2 the examples of distribution of Feret"s diameter of crystalline phase are shown. It should be noticed that the histograms are stretched in right-hand. The calculation of relative number of particles $N_u / N_s$ in interval from 0 to u is absolutely the same as in paper [1]. So we present only working equation:

$$\frac{N_u}{N_s} = \int_s^u \varphi(u)du = 1 - e^{-\frac{3\psi}{4}}, \qquad (1)$$

where $u = R/\bar{R}$,

$$\varphi(u) = \frac{14}{9}\ln\left(1-\frac{3u}{4}\right) + \frac{2}{3}\left(1-\frac{3u}{4}\right)^{-1} + \qquad (2)$$

$$+\frac{11}{9}\ln\left[\left(\frac{3u}{4}+1\right)^2\right] + \frac{\sqrt{2}}{9}arctg\left(\frac{1+3u}{4}\right) - 2{,}1$$

An illustration to the calculation of the coalescence phenomenon in $CrSi_2$ amorphous-crystalline thin films is presented in Fig.3.

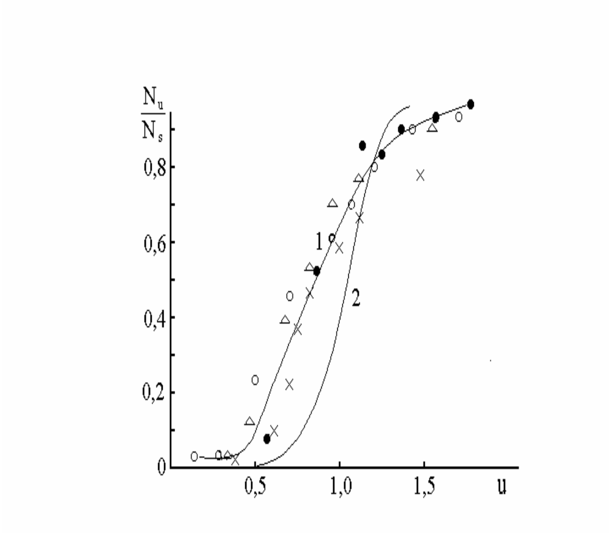

Fig.3. Experimental (1) and theoretical (2) curves correspondence formulae (1). Points on curve (1) ploted to histograms Fig.2.: ○- a; ● - b; Δ - c; × - d.

Thus, the results of the volume of the transported material, which enables the experimentally observable changes in the object geometry were calculated in tems of the kinetic diffusion coalescence theory for the regions films. It is shown the coalescence process, i.e. the growing of crystalines with the diminution of their number.

1. Ya. E. Geguzin, Yu. S. Kaganovsky and V.V. Slyozov Surface heterodiffusion coefficient by the vethod of mass transfer // J. Phys. Chem. Solids.-1969.-v.30.-P.1173-1180.
2. A.S.Dranenko, L.A.Dvorina, O.I.Gatman Thickness dependency of microstructure characteristiks of $CrSi_2$ thin films //Powder metallurgy -2001.-5/6.-P.112-116.

# PECULIARITIES OF SURFACE LAYER STRUCTURE FORMATION UNDER LAZER TREATMENT OF POWDERED COATINGS ON TITANIUM ALLOYS

**Bloschanevich A.M., Dan'ko S.V., Khomenko G.E., Popchuk R.I., Rogozinskaya A.A., Rudyk N.D.**
Frantsevich Institute of Problems of Materials Science of NASU,
3, Krzhizhanovskogo St., 03142, Kiev, Ukraine, E-mail: altifer@ipms.kiev.ua

The service conditions of surfaces and volume of the machine details often differ much. Existing methods of the surface treatment (hardening, surface thermal and chemical-thermal treatment, surfacing, cladding) allow to change the structure, composition, as well as to realize full replacement of surface material in order to change the surface layer's properties directly.

Laser alloying is one of the most efficient surface hardening method. Due to greater heating and cooling rates the physical-chemical processes in the zone of laser treatment greatly differ from traditional surface treatment. This allows obtaining the surface layers with unique mechanical and physical-chemical properties. Spending expensive and deficit components in thin layer determine an economical factor of this method.

This article deals with researches of the structure formation peculiarities and properties of the surface layers of low-alloying titanium alloy (OT-4) at pulsed laser alloying of powder coatings: TiC, TiN, B, BN, $ZrO_2$, (50% TiN+50% $B_4C$).

Microhardness measurements were carried out by means of device PMT-3 at mass load P = 40 grams. Optical microscopes MIM-8 and Neophot-3F were used for microstructure analysis, phase analysis of the surface layer after laser alloying in copper $K_\alpha$-radiation was carried out on the X-ray device DRON-3M. Phase X-ray diffraction analysis results are presented in the table 1.

The samples with powder coatings were laser treated by fuse method on pulse technological unit "Kvant-15" (diameter of the beam was ~ 0,15cm, pulse energy - 3 ÷ 4 joules and duration 5 microseconds). This treatment was realized with spot overlapping ~ 75 % and track overlapping ~ 50 %.

Results of thickness changing and maximal strengthening in depth of the laser alloying zones of powdered coatings are presented in the table 2. Maximal strengthening in the fuse zone was obtained for powdered coatings, consisted of B, $ZrO_2$ and composite 50% TiN+50% $B_4C$. Microhardness of the alloying zones increases 3,5 ÷ 4,5 times in comparison with source material. Formation of the porous surface layer with thickness up to ~ 15 mkm is typical for all coatings. This is probably caused by evaporation of the coating mixture used for fixing powdered coatings. The boride-alloying layer has extremely disperse structure of the strengthening phases with high microhardness, as well as the layer with columnar structure is present in bottom area of the fuse zone. Less disperse precipitations of the strengthening phase in the grain body and on the grain boundaries of the basic material are observed outside the fuse zones. Such spectrum of structure changing in the depth of the laser alloying zone results to microhardness changing in wide ranges. The treatment of the powdered coatings, consisting of $ZrO_2$ and composite TiN+50% $B_4C$ determines similar result. The most efficient strengthening is observed in narrow interval (table 2).

Short-term annealing ($\tau$ = 0,5 hour) at $400^0$ C results not only to microhardness increasing of powdered coatings $ZrO_2$, B and 50% TiN+50% $B_4C$, but also to extension of the strengthening layer zone that is obviously caused by the dissolution of the supersaturated solid solution. The exfoliation of the surface-alloying layer from the basic material was not observed at the bending test.

Thus $ZrO_2$, B and composite TiN+50% $B_4C$ are the most efficient materials for forming of high modular coatings at laser surface treatment stated above of the titanium alloy OT-4. This method can be recommended for details exploited at extremely wearing conditions and under percussive pulsed loads.

Table 1. Phase composition of the surface alloying layer after laser treatment.

| Composition/coating | Phases determined by X-ray analysis | |
|---|---|---|
| | Basis | tracks |
| OT-4 / source | α (HCP) | β (BCC) |
| OT-4 | α (HCP) | $Ti_2O$, TiO |
| OT-4 / B | α (HCP), $TiB_2$ | TiB, $B_7O$, TiO |
| OT-4 / BN | α (HCP), $B_7O$ | TiB, $TiB_2$, TiO |
| OT-4 / TiN | α (HCP) | TiN, $Ti_2O$, TiO |
| OT-4 / $ZrO_2$ | α (HCP), $ZrO_2$ (tetragonal) | $ZrO_2$ (cubic), $ZrO_2$ (monocrystallic), $Ti_2O$ |
| OT-4 / TiC | α (HCP), TiC | $Ti_2O$ |

Table 2. Size and microhardness of the laser treated zones.

| Composition/coating | Zone depth, mkm | | $H\mu^{max}$, GPa / depth, mkm | |
|---|---|---|---|---|
| | | Annealing at $400^0C$ | | Annealing at $400^0C$ |
| OT-4 / source | - | - | ~3,10 ÷ 2,6 / - | - |
| OT-4 | ~ 140 | ~ 220 | ~ 5,0 / surface | ~ 4,6 / ~ 80 |
| OT-4 / $ZrO_2$ | ~ 300 | ~ 320 | ~ 18,0 / ~ 15 | ~ 20,0 / surface |
| OT-4 / TiC | ~ 270 | ~ 240 | ~ 9,0 / ~30 | ~ 53,0 / ~ 30 ÷ 60 |
| OT-4 / B | ~ 310 | ~ 420 | ~ 18,0 / ~ 40 ÷ 75 | ~ 27,5 / ~ 160 |
| OT-4 / TiN | ~ 280 | ~ 240 | ~ 8,5 / ~15 ÷ 30 | ~ 19,0 / surface |
| OT-4 / BN | ~ 360 | ~ 540 | ~ 9,5 / surface | ~ 9,5 / surface |
| OT-4 / 50%TiN+50% $B_4C$ | ~ 240 | ~ 540 | ~ 14,0 / ~ 30 | ~ 37,7 / ~ 45 |

# RESEARCH INTO ANISOTROPY OF POWDER IRON PROPERTIES

**Bezimyanniy Y.G., Skorokhod V.V., Talko O.V., Glazkov E.E.(1), Frydman G.R.(2)**
Frantsevich Institute for Problems of Materials Science of NASU,
3 Krzhizhanovsky St., Kiev, 03142, Ukraine, E-mail: bezimyni@i.com.ua
(1)National Technical University of Ukraine «Kiev Polytechnic Institute»,
pr. Pobedy, 37, Kiev, 03056, Ukraine
(2)Haifa , Israel

Materials from iron powder and mixtures based on it are widely used in different fields of industry [1]. Powder materials are produced by cold pressing (molding) of powder followed by sintering. The consolidated body produced at this stage is isotropic on load. However, after relieving load, as a result of elastic aftereffect, the feeds show anisotropy in properties. Anisotropy of elastic aftereffect weakens the contact cross section of the feed in the direction perpendicular to the direction of elastic aftereffect and reduces tensile strength in the direction parallel to elastic aftereffect. At the sintering stage anisotropy in properties is increased [2]. Therefore, research and control of anisotropy in the material properties are of interest at different stages of the technological process.

Anisotropy has been studied by results on the measured sound velocity of the elastic wave. The powder iron samples of a prismatic form have been chosen as the subject of investigation. The samples have been cut off along and transverse to the load applied in pressing. After molding and sintering the samples have been subjected to additional afterpressing to obtain the target porosity. It has been supposed that as a result of the closest packing, material may gain cubic or hexagonal symmetry of structure [3].

To evaluate the extent of anisotropy in the material, sound velocities of longitudinal ($V_e$) and transverse ($V_t$) elastic waves have been measured in all possible directions. The sounding directions (1, 2, 3) in the samples and corresponding sound velocities of elastic waves are shown in Fig.1. Here, the first number of the index for sound velocity of elastic wave points to the sounding direction, and the second one (for transverse waves) points to the direction of particle oscillations. The obtained results have been verified for consistency with cubic and hexagonal macrosymmetry in the material properties. For this purpose, the sounding directions in the material have been analyzed from the viewpoint of their orientation relative to the axes of symmetry.

The hexagonal system of symmetry [4] (Fig.2a) is characterized by one 6-fold axis of symmetry. It has 12 components (different from zero) of tensor of elastic modules. Five of them are independent: $C_{11}$, $C_{12}$, $C_{13}$, $C_{33}$ and $C_{44}$. Correspondingly, sound velocities of elastic waves are independent in five characteristic directions. For this system in the (001) plane perpendicular to the 6-ford axis sound velocities of elastic waves do not depend on the propagation direction, i.e. there exists isotropy in properties. Relation between linear elastic modules and sound velocities of elastic waves for some directions are represented by relationships (1).

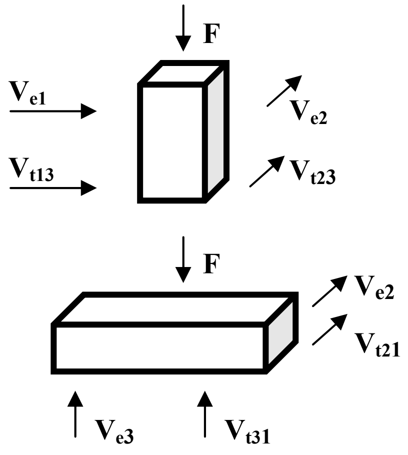

Fig.1. Scheme of sounding samples relative to the pressing direction F.

The cubic system of symmetry [4] (Fig.2b) is characterized by three 2-ford axes of symmetry and four 3-fold axes. It has 12 components (different from zero) of tensor of elastic modules. Three of them are independent: $C_{11}$, $C_{12}$, and $C_{44}$. Correspondingly, sound velocities of elastic waves independent in tree characteristic directions. Relation between linear elastic modules and sound velocities of elastic waves for some directions are represented by relationships (2).

Three types of elastic waves (quasi-longitudinal and two quasi-transverse) have been analyzed by their five independent values (assuming hexagonal symmetry of the material) and by three values (assuming cubic symmetry). The analysis above has allowed the calculation and the construction of the surface for reverse sound velocities of elastic waves. Examples of such surface for the hexagonal system are given in Fig.3.

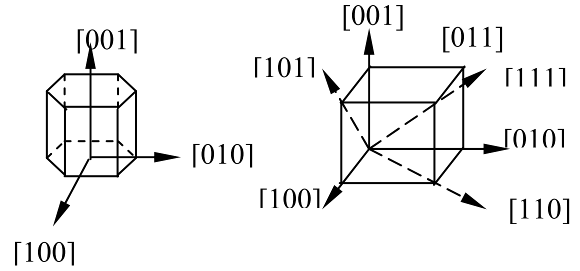

a b

Fig.2. Hexagonal (a) and cubic (b) systems of symmetry.

$$
\begin{aligned}
&\rho\cdot\left(V^{l}_{[001]}\right)^2 = C_{33}; \qquad \rho\cdot\left(V^{t}_{[001]}\right)^2 = C_{44};\\
&\rho\cdot\left(V^{l}_{[001]}\right)^2 = C_{11};\\
&\rho\cdot\left(V^{(001)}_{[100]}\right)^2 = (C_{11}-C_{12})/2;\\
&\rho\cdot\left(V^{l}_{[101]'}\right)^2 = \rho\cdot(V^{l}_{[011]})^2 = (C_{11}+C_{33}+2\cdot C_{44})/4+\\
&+\left[[(C_{11}-C_{33})/2]^2+(C_{33}+C_{44})^2\right]^{1/2}.
\end{aligned}
\qquad \mathbf{(1)}
$$

$$
\begin{aligned}
&\rho\cdot\left(V^{l}_{[100]}\right)^2 = \rho\cdot\left(V^{l}_{[010]}\right)^2 = \rho\cdot\left(V^{l}_{[001]}\right)^2 = C_{11};\\
&\rho\cdot\left(V^{l}_{[110]}\right)^2 = \rho\cdot\left(V^{l}_{[101]}\right)^2 = \rho\cdot\left(V^{l}_{[011]}\right)^2 =\\
&= (C_{11}+C_{12}+2C_{44})/2;\\
&\rho\cdot\left(V^{l}_{[111]}\right)^2 = (C_{11}+2\cdot C_{12}+4\cdot C_{44})/3;\\
&\rho\cdot\left(V^{t}_{[100]}\right)^2 = \rho\cdot\left(V^{t}_{[010]}\right)^2 = \rho\cdot\left(V^{t}_{[001]}\right)^2 = C_{44};\\
&\rho\cdot\left(V^{t}_{[111]}\right)^2 = (C_{11}-C_{12}+C_{44})/2;\\
&\rho\cdot\left(V^{[001]}_{[110]}\right)^2 = \rho\cdot\left(V^{[010]}_{[101]}\right)^2 = \rho\cdot\left(V^{[100]}_{[011]}\right)^2 = C_{44};\\
&\rho\cdot\left(V^{[1\bar{1}0]}_{[110]}\right)^2 = \rho\cdot\left(V^{[10\bar{1}]}_{[101]}\right)^2 = \rho\cdot\left(V^{[01\bar{1}]}_{[011]}\right)^2 = (C_{11}-C_{12})/2.
\end{aligned}
\qquad (2)
$$

Experimentally obtained sound velocities of elastic waves and calculations of cross-sections for reverse sound velocities of elastic waves characteristic of systems of symmetry considered have been analyzed. Analysis has shown that the result above do not contradict the assumption that the studied material demonstrates transversal isotropy in sound velocities of elastic waves. This is possible when the material shows hexagonal or cubic macrosymmetry in its structure. For the hexagonal macrosymmetry of structure, the 6-fold axis of symmetry is directed along the pressing direction. For the cubic macrosymmetry of structure, the 3-fold axis of symmetry is directed along the pressing direction.

a

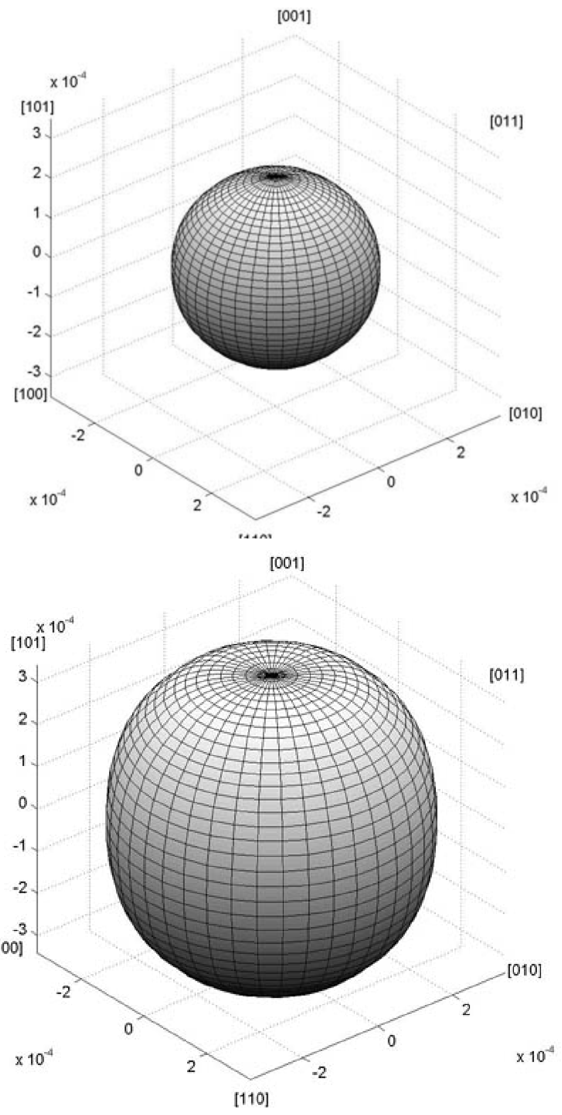

b

Fig.3. Surface for reverse velocities of quasi-longitudinal (a) and quasi-transverse (b) elastic waves.

**REFERENCES:**

1. Международная конференция «Новейшие технологии в порошковой металлургии и керамике»: Тез. докл. – Киев, 2003. – 436 с.

2. Бальшин М.Ю., Кипарисов С.С. Основы порошковой металлургии. М.: Металлургия, 1978. – 184 с.

3. Кингери У.Д. Введение в керамику. М.: Из-во лит. По строительству, 1967. – 500 с.

4. Дьелесан Э., Руайе Д. Упругие волны в твёрдых телах. – М.: Наука, 1982. – 424 с.

# HEAT CAPACITY AND ENTHALPY OF $Mg_2Ni$ IN TEMPERATURE RANGE 59.43 – 947 K

**Gorbachuk N.P., Muratov V.B., Zakharov V.V.**
Frantsevich Institute for Problems of Materials Science, National Academy of Science of Ukraine,
Krzhyzhanovsky Str., 3, 03680 Kiev, Ukraine, e-mail: bas@ipms.kiev.ua

Intermetallic compound $Mg_2Ni$ is widely known due to opportunities is convertible to absorb hydrogen in significant quantities (4 atoms per formula unit) at temperatures close to room [1]. Knowledge of the thermodynamic properties of substances is necessary for optimization of synthesis process and manufacturing of new materials with the previously predetermines properties. At the same time of items of information on thermodynamic properties of $Mg_2Ni$ in the literature are absent.

The purpose of the present work was the research heat capacity in the temperature range 59.43–300.54 K and enthalpy of $Mg_2Ni$ in the temperature range 558–947 K. The intermetallide under study were produced of magnesium and nickel (99.8 %) by arc melting with tungsten nonconsumable electrode in purified argon.

According to the X-ray phase analysis the preparation synthesized were singe-phased with lattice parameters: a = 0.5190 nm, b = 0.1322 nm.

Heat capacity at low temperatures were measured by adiabatic calorimetry method with periodic input of heat on low temperature standard thermophysical unit [1], and enthalpy - by drop calorimetry method on high-temperature differential calorimeter [2]. The error of the heat capacity measurement not to exceed 0.4 %, and of enthalpy - 1.5 %.

The experimental data of heat capacity smoothed out by a method of sliding approximation by the cubic multimembers with weight factors [1] (fig.1). To obtain main thermodynamic functions under standard conditions the experimental data on the low temperature heat capacity for the alloys studied were extrapolated to 0 K using equation of follows [2]:

$$C_p^0(T) = \gamma T + D\left(\frac{\theta_D}{T}\right) + \sum_{i=1}^{n-1} E_i\left(\frac{\theta_{E_i}}{T}\right), \qquad (1)$$

where $\gamma$ is coefficient of electron heat capacity, $D\left(\frac{\theta_D}{T}\right)$ and $E\left(\frac{\theta_{E_i}}{T}\right)$ is Debye and Einstein heat capacity, respectively, n is number of atoms in the substance formula.

The parameters of equation (1) is: $\gamma = 18 \cdot 10^{-3}$ $J \cdot mole^{-1} \cdot K^{-2}$, $\theta_D = 304$ K, $\theta_{E_1} = 461$ K, $\theta_{E_2} = 200$ K .

Fig.1. Smoothed data of low temperature heat capacity

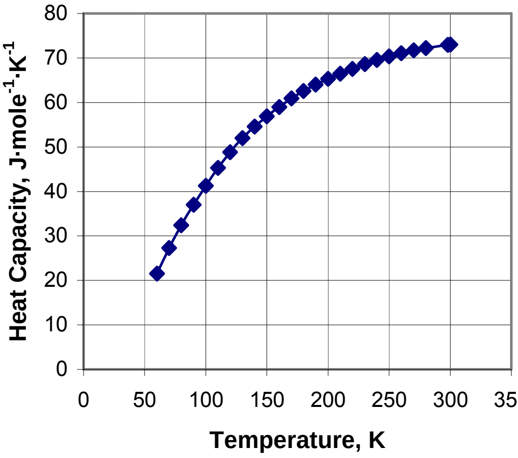

The main thermodynamic functions of the $Mg_2Ni$ at 298.15 K were obtained: $H^0(T) - H^0(0\,K) = 14107 \pm 71$ $J \cdot mole^{-1}$; $C_p^0(T) = 72.94 \pm 0{,}29$ $J \cdot mole^{-1} \cdot K^{-1}$; $S^0(T) = 90.6 \pm 0{,}7$ $J \cdot mole^{-1} \cdot K^{-1}$; $\Phi^0(T) = 43.2 \pm 0{,}7$ $J \cdot mole^{-1} \cdot K^{-1}$.

Experimental data (fig.2) of enthalpy ($J \cdot mole^{-1}$) in the temperature range of 298,15–947 K ($Mg_2Ni$) were approximation using Mayer – Kelly equation:

$$H^0(T) - H^0(298{,}15\,K) = AT^2 + BT + CT^{-1} + D \quad (2)$$

At confidential probably 0.95 values of enthalpy, designed on (2), are characterized by an average relative confidential interval not to exceed 1.35 %.

Proceeding from (2) the temperature dependencies of heat capacity, entropy and Gibbs's energy ($J \cdot mole^{-1} \cdot K^{-1}$) function are as follows:

$$C_p^0(T) = 2AT + B - CT^{-1} \qquad (3)$$

Fig.2. Experimental data for enthalpy of $Mg_2Ni$

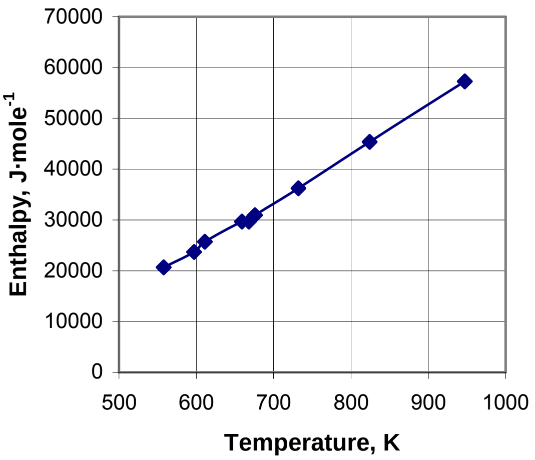

$$S^0(T) = 2AT + B\ln T + 0{,}5CT^{-2} + E \qquad (4)$$

$$\Phi'(T) = AT + B\ln T - DT^{-1} - 0{,}5CT^{-2} + (E - B) \quad (5)$$

Coefficients of temperature dependences (2–5) were calculated by the least square method using two boundary conditions, i.e. zero value of enthalpy at 298.15 K and standard value of allow heat capacity to provide agreement between high and low temperature heat capacity values. The parameters of the temperature dependencies (2–4) are equal: $A = 233.341\cdot10^{-3}$, $B = 59.60$, $C = 50968$, $D = -20014$, $E = -263.24$.

Monotonous increase of the heat capacity of $Mg_2Ni$ in temperature range 298.15–947 K to suppose that heat capacity at constant pressure is the sum of three contributions: lattice in harmonic approximation, electronic and anharmonic.

**References**

1. Antonova M.M. Hydrides of the intermetallics compounds (in Russian) – Kiev, 1997. – 46 p. – (Prep. / NAS Ukraine. Institute for Problems of materials Science; #10).
2. Bolgar A.S., Krykla A.I., Suodis A.P. / Low Temperature Heat Capacity of Praseodymium, Neodymium and Samarium Sesquicarbides (in Russian) // Zh. Fiz. Khim. – 1998. – 72 – #4 – P. 439-443.
3. Bolgar A.S, Gorbachuk N.P, Blinder A.V / Enthalpy of $Gd_5Si_3$, $Gd_5Si_4$, GdSi, $GdSi_{1.88}$ in Temperature Range 298.15 – 2200 K. Enthalpy of the Melting (in Russian) // Teplophiz. Visok. Temperatur. – 1996. – 34. – P. 541-545.
4. Litvinenko V.F., Bolgar A.S., Muratov V.B. and other. The Experimental Data Processing on enthalpy with Considerations (in Russian): Institute for Problems of materials Science AS USSR, Kiev (1984), dep v VINITI 19.09.84; #6300-V.

# OXIDATION BEHAVIOUR OF TITANIUM ALLOYS OF Ti-B SYSTEM

**Poryadchenko N.E., Oryshich I.V., Khmeljuk N.D., Kalashnikova L.A.,**
**Kulak L.D., Kuzmenko N.N., Golovkova M.E.**
Franchevich Institute for Problems of Material Science of NAS of Ukraine, Kyiv, Ukraine
E-mail: rapid@materials.kiev.ua

During last years a large attention is spared to alloys based in Ti-B system. The study of structure and mechanical properties both at room and at high temperature takes the principal place in these investigations. At the same time the oxidation behaviour of these alloys is not studied.

In present work the kinetics of high temperature oxidation in air at 800 °C, 20 h of titanium alloys based in Ti-B system, and also their structure and scale morphology, which is formed on the sample surface during oxidation, were investigated by the traditional mechanistic means, that is, thermobalance, metallography, electron microprobe, and X-ray analyses. The alloys were produced by plasma-arc smelting. 7 alloy compositions, obtained by alloying the base BT1-0 alloy with different amounts of the components (0,9-1,6 mas.% of boron, 2,5-3,5 mas.% of aluminium, 5-5,7 mas.% of zirconium, and 1,2 mas.% of silicium), were studied.

It is known [2, 3], that the resistance to oxidation of alloys is provided with a film (a scale), formed on a surface of samples during oxidation. As it was shown in the researches carried out, alloys behave themselves differently in the given oxidation conditions. After oxidation on a surface of samples is a scale, which has different quality and the protective properties depending on the alloy composition (Fig.1). On double alloys with 0,9 and 1,6 mas.% of boron and on an alloy with addition aluminium alloying the scale has bad adhesion and falls away. The scale morphology is similar to that on BT1-0 alloy by presence of lamination and bad adhesion (Fig. 2 *a*, *b* ) and has traces of evaporation process (Fig. 2c).

Complex alloys are oxidized with formation a protective film, but it is not dense and has the large share of crystals of the elongated form (Fig. 2 *d*). X-ray analysis has shown, that a scale consists mainly of titanium oxide ($TiO_2$, rutile). On alloys containing boron and aluminium it was found the small amounts of $B_2O_3$, $Al_2O_3$, and $Al_2O_3 \cdot B_2O_3$ oxides, which were formed under an outside layer of titanium oxide. It allows to consider, that the different form of the titanium oxide crystals is formed as a result of influence of the alloying elements on a speed and an orientation of the diffusion flows.

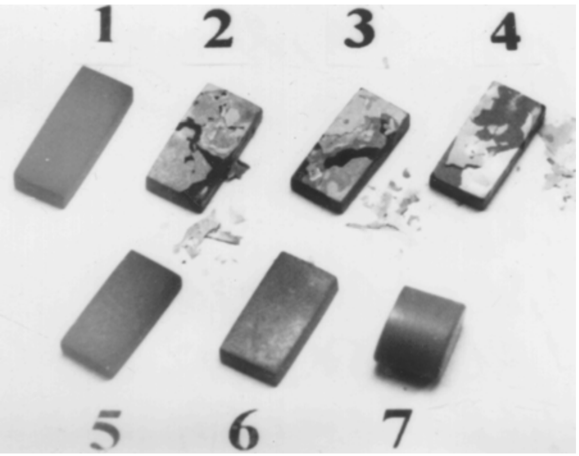

Fig. 1. Photograph of the titanium alloys samples after oxidation at 800 °C, 20 h:
1 – BT1-0; 2 – BT1-0+0,9B; 3 – BT1-0+1,6B;
4 – BT1-0+1,2B+3Al;
5 – BT1-0+1,2B+2,5Al+5Zr;
6 – BT1-0+1,3B+2,5Al+5,7Zr;
7 – BT1-0+1,2B+2,5Al+5Zr+1,2Si.

At the same time, the data of kinetic researches show, that the specific mass change for all alloys differs practically a little. The alloy, which contains silicium, has the least oxidation speed of 0,14 mg/(cm$^2$·h) in comparison with 0,17 mg/(cm$^2$·h) for BT1-0 alloy.

It is earlier established [4], that at 800 °C titanium is oxidized under the parabolic law with a primary role of titanium ions diffusion fnd formation of titanium oxide ($TiO_2$ ). After titanium transition in the scale the emptinesses are formed on border of titanium - scale. With occurrence of these emptinesses the flow of titanium ions stops and formation of the scale occurs by diffusion of oxygen and its dissolution in metal, and also formation of the many-layer scale and exfoliation of the separate layers, that provides a rather small level of heat resistance. Proceeding from the phase composition of alloys, morphology and phase structure of the scale, it is represented, that the oxidation resistance of BT1-0

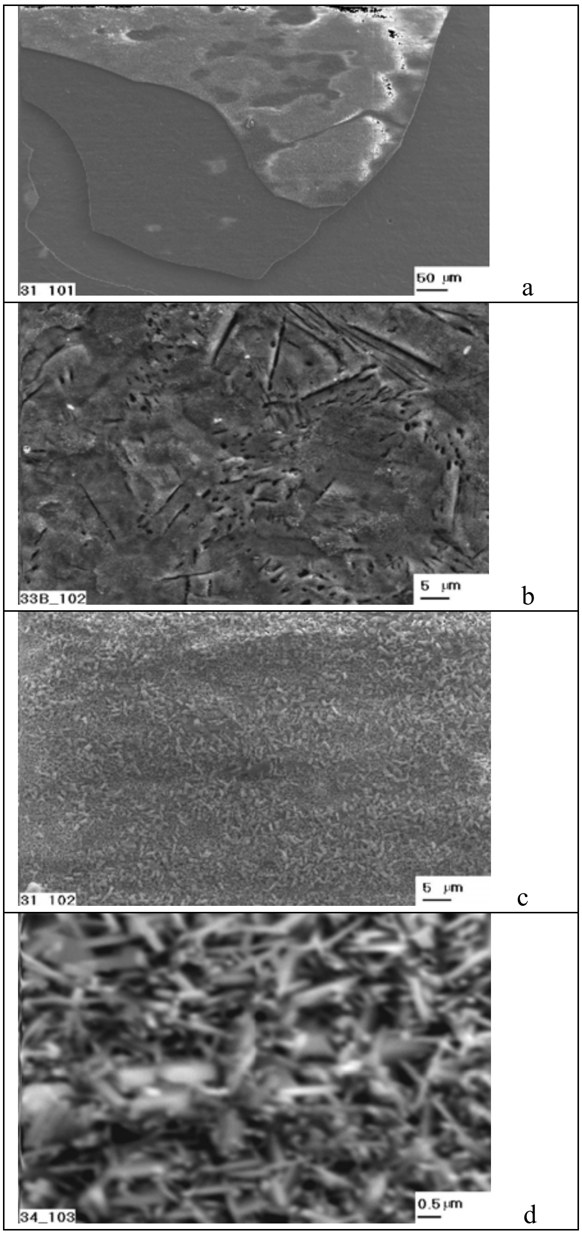

Fig. 2. Morphology of scale on the surface of titanium alloys after oxidation at 800 °C, 20 h:
*a* - general view of scale; *b* – surface of metal;
*c d* -external surface of scale ;
*a, b, c* - alloy with 0,9 %B;
*d* - 1,2B+2,5Al+5Zr+1,2Si alloy.

alloy alloyed by boron up to 1,6 mas.% is reduced, apparently, as a result of oxidation of boron, which is present in initial structure of an alloy, with formation of fusible oxide $B_2O_3$ (Tm≈ 290 °C) and its partial evaporation, that causes porosity of rutile scale and decrease of its protective properties and saturation of a metal surface by oxygen. Metallographic researches have shown presence of a surface layer with the raised hardness on depth up to 70 microns.

Additional alloying of an boron-containing alloy by 3 mas.% of aluminium, which, as it is known [3], raises heat resistance of titanium alloys, has appeared insufficient, as the heat resistance of an alloy was not improved. And only addition of 5 mas.% of zirconium, or 5 mas.% of zirconium and 1,2 mas.% of silicium raises it insignificantly. It is connected to formation of more dense $TiO_2$ oxide with zirconium dissolved in it (as phases with zirconium oxide do not reveal by the X-ray analysis), and also with deceleration of diffusion processes in the alloy connected to the slower oxidation of compounds (borides, silicides), included in composition of complex alloys. The increase of heat resistance of an BT1-0 alloy, associated with introduction of silicium, took place in alloys based in Ti-Si system without boron and was shown in work [4].

Thus, the investigated alloys based in Ti-B system have the heat resistance not above than that for ferrite and austenite alloys, which have the oxidation rate of 0,01-0,02 mg/(cm$^2$·h) under the same condition. We consider that the alloying of Ti-B system alloys by silicium it is necessary for increase of the heat resistance of this alloys.

REFERENCES

1. Kofstad P. High-temperature oxidation of metals.- M.: Mir.- 1969.- 390 p. (translation in Russian)
2. Kofstad P. High-temperature oxidation of titanium.- J. Less-Common Metals.- 1967, 12, N 6.- P. 1-9.
3. Voitovich R.F., Golovko E.I. High-temperature oxidation of titanium and its alloys .- M.: Nayk. Dymka.- 1984.- 256 p. (in Russian)
4. Kuzmenko N.N., Poryadchenko N.E., Oryshich I.V., Kulak L.D., Okun I.U. Reseach of Heat Resistance of Titanium Alloys with Silicon, Aluminium and Zirconium Received by Plasma-Arc Method in Proceeding of the Nato Advanced Reseach Workshop " Matallic Material Efficiency ", 07-13 September, 2003, Kyiv, Ukraine.- P. 56.

# NANOCOMPOSITES BASED ON THE POWDER (SiC-C)-$Si_3N_4$-$Si_2N_2O$, OBTAINED UNDER THE CONDITIONS SHS

**Davidchuk N.K., Gadzyra N.F., Gnesin G.G.**
Institute for Problems of Materials Science of NASU,
3, Krzhyzhanovsky st., Kiev-142, 03680, Ukraine, e-mail: gadzyra@gadzyra.kiev.ua

The purpose of the present work is to synthesize the powders in system (SiC-C)-$Si_3N_4$-$Si_2N_2O$, to obtain near fully dense materials on its basis by hot pressing without activators and with activators of sintering, to research of their phase content, microstructure and mechanical properties. It is necessary to note, that the phase (SiC-C) is a solid solution of carbon in silicon carbide which was studied earlier [1-3].

Composite powder was obtained by method self-propagating high-temperature synthesis (SHS) in disperse system silicon - carbon. Utilization, as a carbon component, of thermal expansive graphite (TEG) which formed during thermo-stroke the hydrolyzed components of carbon intercalation is the main feature of the developed SHS method. It has been earlier established, that the specific structure of particles TEG impede to instant distribution of exothermal reaction in all volume and results in development of " glowing" SHS process which characterized by a high level non-equilibrium due to chemical gasotransport reactions. [4].
Synthesis of powders carried out at temperature 1200°C on air. Clearing of the powder from non-reacted carbon and silicon has been carried out according to [5].

Sintering of the obtained powders was carried out using hot pressing in graphite die at pressure up to 30 МПa. The comparative investigation of ceramic composite (with or without activators) structure formation under hot pressure condition has been carried out. As additive were used X-ray amorphous oxide aluminum. It has been added via water solution of salt $Al(NO_3)_3 \cdot 9H_2O$ with the subsequent thermal dissociation in the environment of argon at the temperature 700 $^0$C.

Investigations of phase content and microstructure of the synthesized powders and sintered ceramics were carried out by standard techniques of X-ray and electronic-microscopic analyses.

It was established, that interaction TEG and Si on air form solid solution of carbon in silicon carbide and additionally nitride phases $Si_3N_4$ and $Si_2N_2O$ are formed.

By the data of X-ray analysis established, that during sintering of composite powder without activators formation of dense ceramics occurs due to decomposition of silicon nitride. The mechanisms of structure formation in investigated composites in dependence with initial powders phase content have been studied.

Structural state of SiC-C before and after sintering corresponds to solid solution of carbon in silicon carbide, because its lattice parameter is kept understated (a=0,4353 nm) in relation with lattice parameter of equilibrium в-SiC (a = 0,4359 nm).

By the results of electron-microscopic research established, that highly refined particles SiC-C (0,05 mkm) are distributed both in a body of crystal phases, and in an amorphous phase. These structural feature of a phase SiC-C plays the important role in hardening of obtained ceramics [6]. Whereas hot pressing was carried out without application of additives and the protective environment during sintering there observe formation of amorphous oxide phases which decrease hardness and crack resistance of sintered ceramics (HV10.0˜18 GPa, $K_{1c}$?6.0 MPa•$м^{1/2}$)

X-ray analysis show, that during hot pressing of composite powder with addition of the activator with reflections of phases (SiC-C) and $Si_3N_4$ peaks additionally phase of sialon $Si_3Al_6O_{12}N_2$ are fixed. Occurrence of sialon, obviously, is the result of interaction between phases в- $Si_3N_4$ and $Si_2N_2O$, and also activating additives $Al_2O_3$ which have not been found out in structure of sintered ceramics.

The analysis of sintered samples microstructure has shown, that the regions with highly refined structure (0,13-0,15 mkm) are dominating. Such condition of ceramics was realized due to addition of activator promoting occurrence of a liquid phase which homogeneously distributed between particles of initial components and prevent their oxidation during sintering. Stability of highly refined solid solution (SiC-C) and absence of structural - free $SiO_2$ results to increasing of mechanical properties of obtained materials (HV10.0 = 26,0 GPa, $К_{1c}$ ˜ 7.0 MPa $м^{1/2}$).

### *The literature*

1. Gadzyra N.F., Gnesin G.G., Andreev A.V., Kravets. V.G., Kasyanenko A.A. Silicon carbide with superstechiometric carbon // Inorganic materials. 1996. V.32. № 7. PP. 816-820.
2. Gadzira M., Gnesin G., Myкhaylyk O., Britun V., Andreyev O. Solid solution of carbon in в-SiC // Materials Letters. 1998. V 35. P. 297-305.
3. Gadzira M., Gnesin G., Myкhaylyk O., Andreyev O. Synthesis and structural peculiarities of nonstoichiometric в-SiC // Diamond and Related Materials. 1998. V. 7. P. 1466-1470.
4. N.F.Gadzyra., G.G.Gnesin., A.A.Mihajlik. The mechanism of formation of a solid solution of carbon in silicon carbide. // Powder metallurgy, 2001, №9/10, PP 90-97.
5. N.K.Davidchuk., N.F.Gadzyra., G.G.Gnesin. Some features of formation of ceramics on the basis of composite powders (SiC-C)-$Si_3N_4$-$Si_2N_2O$. // Powder metallurgy, 2001, №1\12, PP 65-70.
6. N.F.Gadzyra., G.G.Gnesin., A.A.Mihajlik. Nanocomposite ceramics on the basis of a powder of solid solution of carbon in silicon carbide. // Refractory and technical ceramics, №12, 2001, PP 4-9.

# THE ELECTRICAL RESISTIVITY AND HALL EFFECT OF $La_3Se_4$, $Pr_3Se_4$ AND $Nd_3Se_4$ AT CRYOGENIC TEMPERATURES

**Kopan' A.R.**, **Kopan' T.V.**(1), **Korablov D.S.**(2)
I. N. Frantsevich Institute for Problems of Materials Science, National Academy of Sciences of Ukraine, 3, Krzhyzhanivsky Str., 03680 Kyiv, Ukraine, bas@materials.kiev.ua
(1)Shevchenko Kyiv Nathional University, 58, Vladimirsky Str., 02033 Kyiv, Ukraine, kopa@alex-ua.com
(2)National Technical University of Ukraine "KPI", ave. Peremogy, 37, 03056 Kyiv, Ukraine, sergiy2@yahoo.com

A chalcogenides with $Th_3P_4$ type of the crystal lattice (the so-called γ-phase) are the most interesting among the rare-earth semi-conductors. Same structure type is kept within this phase, and the lattice spacing is little changed, but electrical properties are changed from insulator ($Ln_2^{3+}X_3$, Ln – lanthanoid, X – S, Se, Te) to metallic ($Ln_3^{3+}X_4$) [1].

The electrical resistivity (ρ) of $Pr_3Se_4$ is linearly increased 280-1320 K [2], while the electrical current carrier concentration remains a constant ($n=5\times10^{21}$ $cm^{-3}$) that is one order less than for usual metals [1]. It was shown [3] that n fixed from the Hall effect for $La_3Se_4$ is too big and equal $5{,}4\times10^{21}$ $cm^{-3}$ at the temperature 300 K. Therefore, the selenides of $Ln_3Se_4$ composition are singular semi-conductors at the temperature more than 250 K.

The purpose of this work is to study the degeneration phenomenon, if it is real and controlled by the temperature.

The $La_3Se_4$, $Pr_3Se_4$ and $Nd_3Se_4$ selenides were fabricated by the ampullaceous method from the high purity elements (Se –extra pure 22-4, rare earth metal (REM) content 99,8-99,9 %).

The samples 0.5x5x5 mm were used for electrical resistivity and Hall effect motive force measurements and were placed in the space (0.6 mm) between a poles of magnet with poles surface (7x7) $mm^2$.

An inaccuracy of electrical resistivity measurement composed 3-5% at the T>100K and 0.5-1% at the 150-300 K. The Hall electromotive force measurement error compiles 4-6% mainly due to accuracy of magnet field intensity measurement.

Data are shown in Figures 1-3. The electrical resistivity is decreased with temperature between 70 and 200 K. Activation energy of this process composes 540, 498 and 415 $J\cdot mol^{-1}$ respectively for $Pr_3Se_4$, $La_3Se_4$ and $Nd_3Se_4$. In this temperature range the concentration of electrical current carrier is increased (Fig. 2).

According to [4-6], at the temperature about 70K the $La_3Se_4$ has an anomaly of heat capacity caused by secondary phase transition. This is explained by close disposition of Fermi energy of conductivity electrons to zone structure anomaly [5].

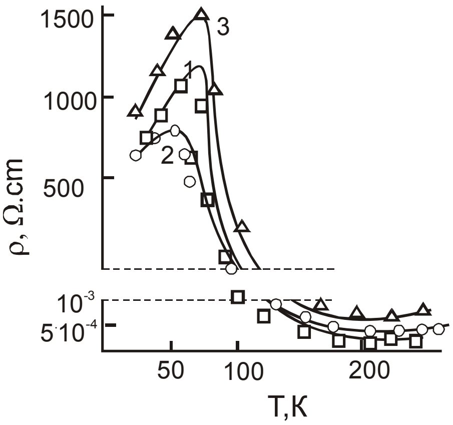

Fig.1 Dependence of the electrical resistivity on temperature: 1-$La_3Se_4$, 2-$Pr_3Se_4$ , 3-$Nd_3Se_4$.

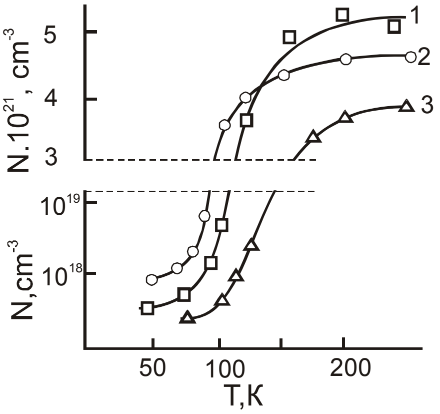

Fig.2 Dependence of the current carrier concentration on temperature: 1-$La_3Se_4$, 2-$Pr_3Se_4$, 3-$Nd_3Se_4$

There is not information on phase transition in the selenides of Pr and Nd at the T<300K.

Obviously, a peak of dependence ρ(T) at the range 65-70K for $La_3Se_4$ is caused by secondary phase transition. Above 70K a growth of current currier, perhaps, is explained through the change in the electronic subsystem.

For some rare earth metal a localized 4f levels in energy size can fall in the forbidden zone of semi-conductor and to be as impurity levels [7]. This is a unique fact because it is impossible to create such huge concentration ($\approx 10^{21}$ $cm^{-3}$) of impurity levels for the standard semi-conductor. Perhaps, when 4f levels of (REM) selenide are located inside of forbidden zone, then ones begin to determine the kinetic phenomena and to be responsible for varied phase transformation.

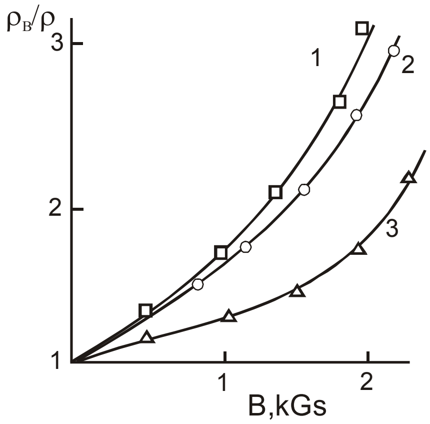

Fig.3 Dependence of the relative electrical resistivity on the magnetic field induction B (T=293K): 1-$La_3Se_4$, 2-$Pr_3Se_4$, 3-$Nd_3Se_4$

On the base of analysis of isobaric heat capacity components of compounds like $Ln_3Se_4$ (Ln-Pr, Nd) it follows [8] that in the range of 35-300K the 4f electrons could contribute to heat capacity by transition to high energy levels. These levels are appeared as a result of splitting of $Ln^{+3}$ main states in the field of the crystal lattice (Stark effect).

At the temperature T>200K an electric conductivity depends on a mobility of electron gas. Therefore, the electrical resistivity (ρ) is increased with the temperature rise because of the atoms oscillation while the number of the current carrier is not increased (Fig.2).

The electrical resistivity increase of $La_3Se_4$, $Pr_3Se_4$ and $Nd_3Se_4$ at the temperature interval 25-50K are to be observed that it is typical for strongly singular semi-conductors. There are superconductors among compounds of such composition. For example, the temperature of superconductive transition of $La_3Se_4$ is $T_c$=7,4 K [4].

It was found [1] the ferromagnetic behavior of metallic compounds corresponding to $Ln_3X_4$ such as $Ce_3Se_4$, $Nd_3Se_4$ and $Gd_3Se_4$. Since these materials have strong f-d exchange interaction of the current carrier with magnetic subsystem then it is possible to control the electrical properties of material by magnetic field, and vice versa to influence on magnetic system of crystal at the change of the current carrier concentration [7]. It is the main advantage of such materials.

The electrical resistivity of $Ln_3Se_4$ is increased to 1,5-3 times at the moderate induction of the magnetic field B (about 2 kGs). It follows from Fig.3. Thus, the materials on the base of $Ln_3Se_4$ can be used for the infra-red radiation detectors, the energy converter from the thermal to electric, the magnetic head to compare with information from hard disk [9].

## Reference

1. Physical properties of the rare earth chalcogenides / L.V. Golubkov, E.V. Goncharova, V.P. Guze, G.M. Loginov, V.M. Sergeeva, I.A. Smirnov / Ed. V.P. Guze. – L.: Nauka, 1973.-304 p.
2. Guze V.P., Sergeeva V.M., Golikova O.A.Kinetic processes in the rare earth chalcogenides of $Ln_3X_4$ composition // FTT– 1969. – T.11, №6. – C. 2568-2576.
3. Holtzberg F., Seiden P.E. and S von Molnar Superconductivity in the Lanthanum Selenide System // Physical Review. - 1968. – Vol.188, №2. – P.408-412.
4. Westeholt K. Bach H., Methfessel S. // Solid State Common - 1983. – Vol. 45, 2. – P.137.
5. Westeholt K. Bach H., Methfessel S // Ibid. – 1980. – Vol. 36, №5. – P.431.
6. Kriklya A.I., Bolgar A.S., Blinder A.V.. and others Thermodynamic characteristics of $Ln_3Se_4$ //Electronic structure and properties of the refractory compounds and alloys and their use in materials science Frantsevich IPM, NASU, Kiyv. P. 106 -111 (2000).
7. Smirnov I.A. Rare earth semi-conductors – the prospects of development and application. // Jurn. Vsesojuzn. Chim. obchestva im.D.I. Mendeleeva. – 1981. - №6. – C.602-611.
8. Bolgar A.S., Kopan A.R., Gorbachuk N.P. Thermodynamic properties of $Pr_3Se_4$ and $Nd_3Se_4$ at the low temperatures // Ukr. Him. Zurnal. – 2002. – T.68, №4. – C.87-91.
9. Kurc V., Zam P.R. The oriented crystallization of the electric materials M. Metallurgiya1980. – 272c.

# UTILIZATION OF CONCENTRATED SOLAR IRRADIATION FOR RECEIVING MODIFIED SPARK COATINGS OF TIN-CR MATERIAL

**Paustovsky A.V., Novikova V.I., Tsyganenko V.S., Mordovets N.M., Timofeyeva I.I., Isayeva L.P., Sheludko V.E., Lityuga I.V.**
Frantsevich Institute for Problems of Material Science, the Ukraine NASU, Krzhizhanovsky str.3, Kyiv 03142, Ukraine, E-mail: post@ipms.kiev.ua

Concentrated solar irradiation is one of materials treatment methods by different energy flows. Advantage of this method is non-contact heating in all media and vacuum and purity of heating.

In works [1, 2] the positive influence of solar treatment on properties of materials surface it is showed.

Spark treatment allows to produce surface layers with changed structure and composition. These coatings very firmly joined with material base. Lacks of this method are non-continuity and roughness of coatings as a consequence of discontinuous charge pulse.

The aim of this work is investigation of influence the solar energy on spark coatings for increasing their physical-mechanical properties.

In this work the electrospark coatings of materials next compositions: 20%TiN+80%Cr; 40%TiN+60%Cr; 90%TiN+10%Cr, pure nickel and titanium nitride are studied. The electrospark alloying carried out in EFI-46A unit a mode of I=1,5A, C=300μF. As the material for backing the steel of mark U8 have been used. The working of surface by solar radiation was carried out in SGU-2 unit, involving a mirror paraboloid concentrator of solar energy supplied with Sun tracking system and the monitoring-measuring equipment. The heating flow θ is equal to 400 wt/sm$^2$. The temperature of cool wall of specimens was not higher than 400°C.

It is known that according to composition and physical nature of coating material the radiant ability coefficient [3] (factor of blackness) of the surface, i.e. its ability to absorb or reflect the heating flow, may essentially change. The higher the blackness factor the higher the temperature of surface warming, the more intensive the specimen heating.

In this work the dependence of specimen warming temperature from working time is *studied. The heating curves of considering* compositions show that the maximal absorbing (the most intensive heating of steel) has the material with the composition 40% TiN+60%Cr (Fig.1,curve2).

For spark coatings that consists of material 20%TiN+80%Cr the value of warming temperature somewhat low than for material 40%TiN+60%Cr. The lower absorbing ability has the electrospark coating of the composition 90%TiN+10%Cr (Fig 1, curve 3). However this values are far higher than for spark coatings from titanium nitride (fig.1, curve 4). The warming rate of surfaces for specimens investigated distinguishes for different composition of coatings material. Thus the warming rate of the surface from material 90%TiN+10%Cr is higher than for coatings with the composition 40%TiN+60%Cr.

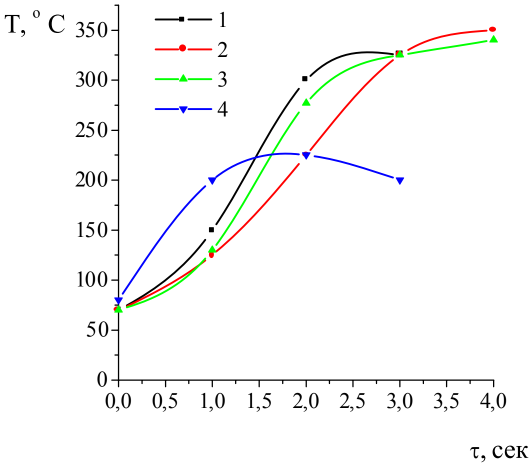

Fig.1. The dependence of warming temperature from treatment time for electrospark coatings of TiN-Cr system: 1- 20%TiN+80%Cr; 2- 40%TiN+60%Cr; 3- 90%TiN+10%Cr; 4- TiN.

The maximal warming temperature reaches in 2.5 s for the first composition and in 4 s for the second composition. The highest rate of warming (τ=1.5s) has the coating from titanium nitride.

With the help of X-ray investigation of the surfaces TiN-Cr materials the existence of such phases is established: the intermetallics $TiCr_2$, FeCr, $Fe_2Ti$ and the oxides $TiO_2$ and $Fe_2O_3$. It was found that under heating temperature more than 1000 °C of electrospark coatings the interaction of iron from steel backing with the elements of coating material take place following the formation of oxides $TiFeO_3$ and $FeCr_2O_4$.

It has been established by metallography that the increasing of chromium content in electrode material leads to increasing of layer depth from 10 to 100 μm (Fig. 2). This depth is equal 100 μm for 20%TiN+80%Cr material. Maximum hardness of alloyed layer is 18000 MPa for composition of 40%TiN+60%Cr (Fig. 3). Concentrated solar treatment leads to formation of the grey layer on surface with microhardness of 24000 MPa.

It is shown for all investigated materials the change of steel structure in heating zone. This connect with the formation of martensite, troostite and sorbite with hardness of 9000-6000 MPa.

## Conclusions.

It is determined that maximum warming temperature of spark coating after concentrated solar irradiation (350°C) have specimen with 40%TiN+60%Cr composition. The rate of surface warming for material 90%TiN+10%Cr in two times more than warming rate of specimen with the coating of 40%TiN+60%Cr. The maximum microhardness of the alloyed layer has 40%TiN+60%Cr coating (18000MPa).

It is established that heating leads to local hardening of steel surface following the increase of hardness to 6000-9000 MPa.

Fig. 2. Structure of the electrospark coating with composition 90%TiN+10%Cr and the steel U8 after CSR, x570.

Fig.3. Structure of the electrospark coating with the composition 40%TiN+60%Cr after CSR, x230.

## Literature

1. Podchernyaeva I.A., Shapoval G.A., Tsyganenko V.S. The formation and properties laser coatings on the base of oxide-nitride ceramics //Poroshkovaya Metallurgiya.- 1992.- №12.- P.29-33.
2. Podchernyaeva I.A., Lavrenko V.A., Frolov G.A., Dyubova L.D., Pasichny V.V. About laws of formation of a superficial layer in conditions of the concentrated solar and laser hardening // Poroshkovaya Metallurgiya.-1994.- №5/6.- P.60-64.
3. Latyshev L.I., Petrov V.A., Chehovsky V.Ya. and others. Emission properties of solids.- M.: Energya.-1974.- 471 p.

# HIGH-TEMPERATURE CREEP OF $Ti_3SiC_2$ – TiC COMPOSITES AT THE INDENTATION

**Burka M. P., Grigorjev O. N., Demidik A. N., Ivanova I. I., Kotenko V. A., Pechkovskii E. P., Firstov S. A.**
Frantsevich Institute for Problems of Materials Science of NAS Ukraine,
3 Krzhizhanovsky St., Kiev-142, 03680, Ukraine, E-mail: epp@ipms.kiev.ua

In work [1] it is investigated high-temperature (T=1000-1200 °C) creep of titanium-siliceous carbide $Ti_3SiC_2$ by single-axis tensile method at a constant stress (within the limits of 10-100 МПа); expression for region in which creep rate is constant with time is received.

Creep at an indentation has basic feature - it proceeds in conditions of a three-dimensional stress state of a material under action of the concentrated load. In connection with that at exposure at loading of a pyramidal indenter the law of similarity of an indent is kept [2], the absolute increase in its sizes in time is the characteristic of material creep. In other words, the indentation method allows to build and analyze primary creep curves - dependence of the sizes of an indents (a diagonal and depth of displacement) with time i.e. to control kinetics of an indenter displacement in a material under data conditions.

Simultaneously occurring decrease in hardness can be used for the analysis of stress relaxation course in a material. As a "hot hardness" method, it has found a wide extension at high-temperature tests as measure for the accelerated comparative estimation of hot-resistance of materials [2, 3].

In work it was studied ternary compound titanium-siliceous carbide $Ti_3SiC_2$ - one of representatives of a new class of materials - nanolaminates [1], - single-phase, compact, made by sintering, grain size $d$=5-15 microns [4]. Results of this research was compared to those received on composite materials $Ti_3SiC_2$ - TiC with contents TiC of 65 and 80 % volumetric and porosity of 6-8 %; composites were produced by hot pressing of powder mix TiC-SiC-C [5].

Indentation was carried out by diamond Vickers pyramid at load $P$=10 H at temperatures 1000 °C (0,49 $T_{decompose}$), 1100 (0,53), 1200 (0,57); time of exposure $t$=1-60 minutes. By results of measurement of diagonals on restored indents it was determined indenter displacement $h_c$. For the analysis of creep characteristics behavior it was used primary kinetic curves $h_c$ *(t)*.

As it has shown the analysis of creep curves, received at various temperatures, they are quite well described by exponent dependence such as $y=y_o+a*\exp(-x/b)$ (**Fig. 1**). Accordingly, expression for indenter displacement at creep $h_c$ of material gets a view (dotted curves):

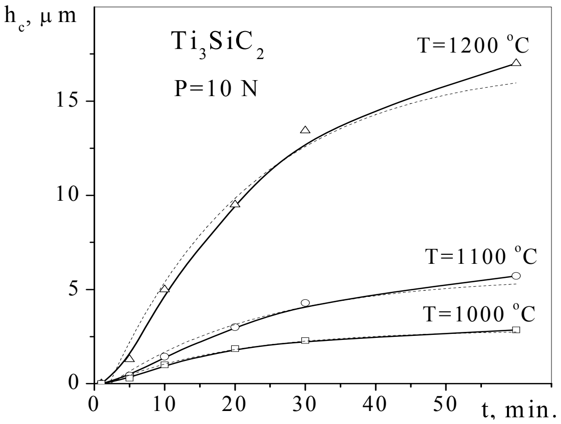

$$h_c = h_{max}*(1- \exp(-t/t_1)) \qquad (1)$$

Here $h_{max}$ - indenter displacement during exposure time $t$ (in a limiting case it is greatest possible displacement under data conditions of a loading and exposure); $t_1$ - time during which the indenter takes root on the depth equal $h_{1=}0,632*h_{max}$. The differentiation of relationship (1) on time gives expression for creep rate at indentation $V_{hc}$:

$$V_{hc} = (h_{max}/t_1) * \exp(-t/t_1) \qquad (2)$$

By the form creep curves (Fig. 1) are similar to what receive on tensile in case of high-temperature creep of metals [6]. Here stages of the unsteady creep (creep rate $V_{hc}$ continuously decreases) and the established creep ($V_{hc}$ it is practically constant) precisely become apparent. The boundary of these stages is in area of 30 minutes (Fig. 1).

The attention pays to sharp increase of creep $h_c$ and creep rate $V_{hc}$ of titanium-siliceous carbide $Ti_3SiC_2$ at rise in temperature from 1100 up to 1200 °C. Creep rate on the established stage at temperature 1000 °C makes 0,02 μm/min., 1100 -

0,05 and 1200 - 0,12. As it has been shown in [4], such effect can be connected to a sharp intensification of a dynamic weakening process, which is caused by decrease in integral dislocation density as a result its annihilation and dumping in formed microcracks.

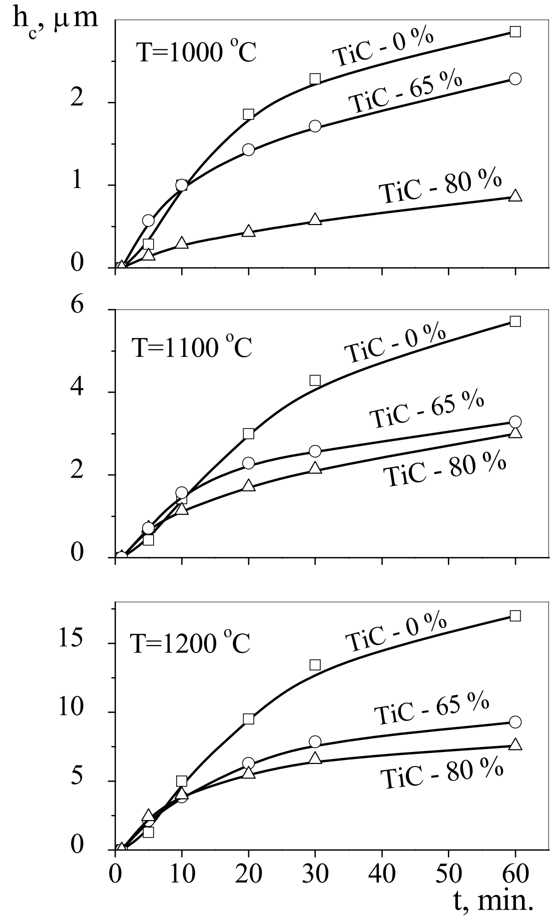

Creep $h_c$ and creep rate $V_{hc}$ of the composite materials that include a lot of titanium carbide TiC, as one would expect, is considerably reduced in comparison with titanium-siliceous carbide $Ti_3SiC_2$ which is not containing its (**Fig. 2**). In addition, at rise in temperature distinction between them grows.

In full conformity with a correlation of creep of the investigated materials, there is also their kinetic curve decreases in hardness (**Fig. 3**). The value and rate of decrease in hardness grow with rise in temperature, it is especial at 1200 °C. Composite materials have higher hardness level and are more stable, i.e. more heat-resistant.

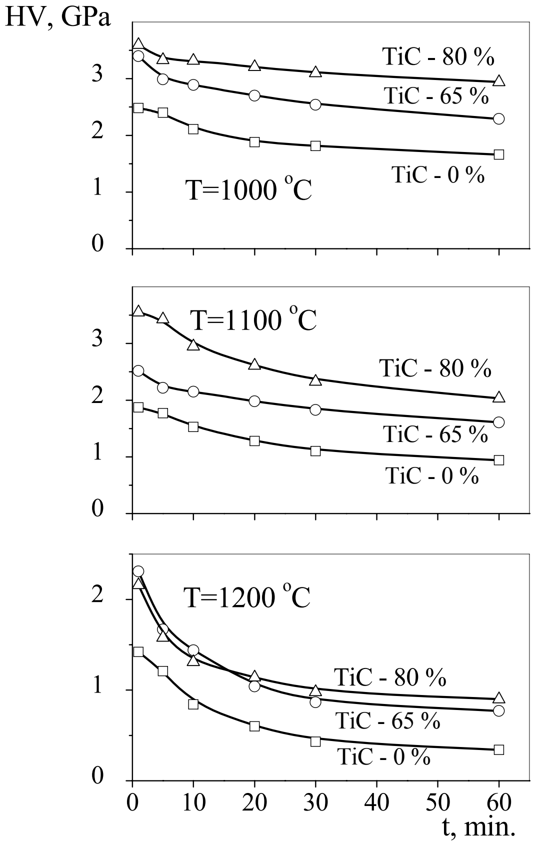

Results of this work make agree with data received on tensile tests [1].

1. M. W. Barsoum, Prog. Solid St. Chem., **28 :** 201 (2000).
2. V. K. Grigorovich, Hardness and microhardness of metals. (M.: Nauka: 1976).
3. V. A. Borisenko, Hardness and strength refractory materials at high temperatures. (Kiev: Nauk. dumka: 1984).
4. N. P. Brodnikovsky, E. P. Pechkovsky, S. A. Firstov, etc., Metallofiz. Noveishie Tekhnol., **25 :** 1179 (2003).
5. V. F. Gorban', E. P. Pechkovsky, S. A. Firstov, etc., Internat. conf. «The newest technologies in powder metallurgy and ceramics», 373 (Kiev: 2003).
6. Dj. Virtman, Dj. R. Virtman, Physical metallurgical science, 216 (M.: Mir: 1968).
6. Dj. Virtman, Dj. R. Virtman, Physical metallurgical science, 216 (M.: Mir: 1968).

# RESEARCHES OF CAST STRUCTURE FORMATION AND MECHANICAL CHARACTERISTICS IN A TEMPERATURES INTERVAL OF 20-1300 $^{O}$C OF ZRCR$_2$ INTERMETALLIC

**Pisarenko V.A., Kusnetzova T.L., Zubets Yu.E, Kalashnikova L.I., Sameluk A.V.**
Frantsevich Institute for Problems of Materials Science NAS of Ukraine,
03680 Kiev-142, st.Krzhizhanovskogo, 3, IPM NAS of Ukraine. E-mail: ipm@materials.kiev.ua

It is very important to exclude an interaction between the separate layers at elaboration of high-temperature composite materials (CM). It can be achieve by creation of antydiffused barriers preventing interaction between the separate layers of system.

Stable $TiCr_2$, $ZrCr_2$, $HfCr_2$ intermetallics are represented perspective for creation chromium layered compositions. High density packing of atoms and its regulation complicate a diffusion in these intermetallics and consequently these materials are perspective for use its at anty-diffused barriers at temperatures up to 1300 °C and above.

The purpose of the carried out researches was study of an opportunity to direct the cast structure formation $ZrCr_2$ intermetallic on specially developed conditions casting and crystallization of ingots, which ensure absence of crystalizated cracks and cast defects, and also to study of physic-mechanical and structural properties received cast in a wide temperatures interval.

The choice of this system for researches is caused by that the $ZrCr_2$ intermetallic is most diffusion proof in a temperatures interval of 1300 °C and above and because it is most perspective for dusting antydiffused layers. From the casting point of view, this system is most difficult for reception of defectless casting. Therefore, elaborated parameters of melting and casting can have unique importance for reception of qualitative cast ingot of all types of intermetallics chromium with other refractory metals with more simple cast technical characteristics.

It was carried out the researches of cast structure formation of $ZrCr_2$ intermetalide samples depending on heat -physical parameters of crystallization. It was established basic heat - physical parameters of crystallization of $ZrCr_2$ intermetalide with stoichiometrical composition and intermetalide with the surplus zirconium contents (up to 2-3 at. %). It was shown, that the structure of the intermetalide crystallized in crater crucible – crystalliser was coarse-dendrite with cracks on borders of grains and uniform one with the size of grains from 50 up to 150 microns without crystallizing cracks was get at casting of samples of different cross section in copper chill and ceramic form.

It was carried out X-ray structure analysis casts, received in various conditions of the crystallisation and cooling. The results of these researches are given in the table. The opportunities of occurrence "basking" structures at phase transformations in intermetalide are discussed. At high speeds of cooling it has not time to be fixed homogeneous structure at phase transformations in an ingot, that results in formation of structures such as mar aging, which were named "basking" structures. At reduction of cooling speed it is possible to receive metastable phase, which can pass in more stable structures, that at the end results in decrease of internal pressure and formation of more homogeneous structures. The above-stated situation obliges to search such cast technology, which would cause the minimal internal pressure and would not result to cracking of ingots.

It was established to receive homogeneous phase structure of cast samples probably can receive on 3 variants:
- to cast samples at superhigh speed of cooling - > $10^3$ grad/s ($\gamma$ - phase);
- to cast ingots at low speed of cooling on all perimeter cast samples- < $10^2$ grad/s ($\alpha$-phase);
- to carry out annealing of cast preparations at temperature 1400 - 1450 °C during 4-5 ч.

However the second and third variants of reception the homogeneous phase structure $ZrCr_2$ samples intermetallic can not acceptable for cast cathodes, as at casting samples of stechiometrical structure intermetallic at low speed of cooling, as well as at the annealing the received cast there will be cracks in connection with change crystal- chemical phase composition and the intermetallic fragility.

Therefore, if at casting of high-quality targets it is impossible to ensure superhigh speed of cooling intermetallic at crystallisation, necessary for fixing high-temperature γ-phase, it is necessary to use $ZrCr_2$ intermetallic with surflus contents of 2-3 % at Zr up stechiometrical composition, its eutectic can be as elasticised at crystallisation an ingot, interfering occurrence of cracks.

Thus, the introduction in an ingot of superfluous contents of 2-3 % at Zr up stechiometrical composition has allowed to receive ingots without crystallisation cracks and casting defects.

First it was possible to investigate the mechanical characteristics of the defectless cast preparations $ZrCr_2$ intermetallic in at interval temperatures to 1300 °C. The specimens were cut out from the casting storage for the compression strength test at the temperatures 1173-1573 K. The short-time high-temperature strength of intermetallide was $\sigma_b^{1373}$ = 665 MPa and $\sigma_b^{1573}$ =140 MPa. The destruction took place in the main on grains borders: to 1373 K - brittle, above it (1473-1573 K) – plastic deformation occurs. The plastic deformation was without hardening. At transcrystalline destruction the type of destruction most likely can be related to "venous", which is more characteristic for amorphous metal materials.

CONCLUSIONS

1. Introduction in composition $ZrCr_2$ intermetallic optimum superfluous contents of Zr to 2-3 % at. up stechiometrical composition, eutectic that can be as elasticised at crystallisation the ingot, and casting melt in copper chill ($V_{cool}$. ~$10^3$ grad/s) have secured to receive intermetallic cast samples without crystallisation cracks, with uniform small crystalline structure and of a grain size from 80 to 100 microns.
2. X-ray structure analysis of the received $ZrCr_2$ intermetallic cast samples has established, that the formation "basket" structures is connected to cooling speed of ingots and characterizes a degree of transformation of high-temperature γ - phase in low- temperature α-phase.
3. First the strength characteristics $ZrCr_2$+2%Zr intermetallic are investigated at temperatures 900-1300 °C. It was established, that cold brittleness temperature of a researched alloy is 1100 °C.
4. At the test temperatures of 1200 and 1300 °C the plastic deformation and bluntness of crack tops is observed. The destruction occurs basically on the grain borders. The weakest point at destruction is eutectic ("white") phase, which is enriched by the zirconium.
5. $ZrCr_2$ intermetallic destructs similarly to amorphous materials, at that so-called "venous" character of destruction is observed.

Table. The analysis of concurrence interplaner distances of intermetallic samples, cast at various speeds of cooling.

| Phase | Stechiometrical composition, $V_{cool.}=10^3$ grad/s | $ZrCr_2$+2%Zr, ceramical cast form, $V_{cool.}=10^2$ grad/s | $ZrCr_2$+2%Zr bottom, $V_{cool.}\geq10^3$grad/s | $ZrCr_2$+2%Zr, chill ∅12 mm, $V_{cool}=10^3$ grad/s |
|---|---|---|---|---|
| β-$ZrCr_2$ | good concurrence | some lines | some lines | good concurrence |
| α-$ZrCr_2$ | some lines | very good concurrence | good concurrence | some lines |
| Zr | not present | some lines it is possible to attribute to Zr | on the first lines most intensive is not present | the first 6-7 lines |
| Cr | not present | not present | not present | practically it is not present |

# ACOUSTIC IMAGING OF STRUCTURE OF CARBON COMPOSITES WITH A METAL MATRIX

**Bezymyanniy Y.G., Kasimov M. A.**
Frantsevich Institute for Problems of Material Science of NASU,
3 Krzhizhanovsky St., Kiev, 03142, Ukraine, E-mail: bezimyni@i.com.ua, mk500@pochta.ru

The materials manufactured with usage of diamond powders, represent heterogeneous systems, which have a stacked outline and variety of space allocation of inclusions. More often, by virtue of features of the technology, the anisotropy of properties is inherent in them. Space of inclusions, through imperfection of the process equipment, not always homogeneous on size. The defects as deviation of structure from norm can be present on various hierarchical levels in any structural unit of a material.

As the physico-mechanical properties of materials manufactured with usage of diamond powders, in many respects are defined by space allocation of inclusions, which has idiosyncrasies for each sort of inclusions and varies during its manufacture, the models of their structure are expedient for building of a position of mesolevel and to distinguish depending on sort of inclusions and stage of the technological process.

For example, after a stage of pressing, material manufactured with usage of diamond powders is possible to consider as discrete heterophase the transversally -isotropic hard environment, which alternate corpuscle connected by the unsufficiently generated contacts at presence pores. Physico-mechanical properties of such material stipulated by physical properties, sizes and configuration of alternate corpuscles of materials of bunch and inclusions, quality of contacts between them, and also percentage, sort, form and allocation on size of pores. After a stage of sintering the contacts between alternate corpuscles of bunch already generated and material can be considered as the environment, continuous and enveloping inclusion, and unsoundness of structure of porous space is caused by presence of incomplete contacts between materials of bunch and inclusions, and also presence of porosity.

For an effective valuation of quality of diamond composites with a metal matrix within the framework of theoretical model some simplifications are accepted. The alternate corpuscles of diamond inclusion have the spherical form, evenly distributed on size, the metal matrix represents the continuous isotropic environment.

The accepted model represented in a figure 1 [7].

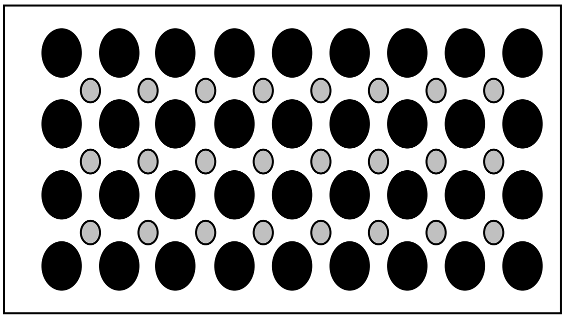

Figure 1. Model representation of a diamond composite with a metal matrix.
In a figure the white color represents a metal matrix, black — diamond inclusion, gray — pores.

The technique is developed on the basis of usage of the acoustic characteristics for definition of quality of diamond composites with a metal matrix manufactured by methods of powder metallurgy. The acoustic characteristics " are understood the term " speed of diffusion and damping factor of an elastic wave.

The designed dependences of speed diffusion of an elastic wave both damping factor from porosity and percentage diamond stuff are defined by simulation of real heterophase system by the geometrically defined units of microstructure [2]. The scalar values settle up by a rule of additivity:

$$A_{еф} = \sum_i A_i * \theta_i ,$$

where Aеф effective value of scalar property; θi accordingly value of property of i- phase.

For non-scalar properties a fairly following inequality:

$$K > K_{еф} > \overline{K}^{-1} ,$$

where

$$K = \sum_i k_i * \theta_i \equiv K_V \quad ,$$

$$\overline{K}^{-1} = \sum_i \frac{\theta_i}{k_i} \equiv K_R$$

- average on Voigt and Reuss.

The complexity of definition of quality of contacts of diamond inclusion with a metal matrix consists in presence of porous space, is inhomogeneous distributed on size.

There is a number of models circumscribing correlation of physico-mechanical properties of materials with porosity [1].
In a figure 2 the results of theoretical accounts represented in view of a used technique and experimental researches.

To avoid influence of porosity on physico-mechanical properties of diamond composites it is possible, evaluating the ratio of values obtained by an experimental way, to theoretical within the framework of used model.

The designed formula looks like this:

$$\delta = \frac{C \exp}{Ctheor \quad (\theta \ , k \ )} \quad ,$$

where
θ - porosity, k - density of diamond inclusion.

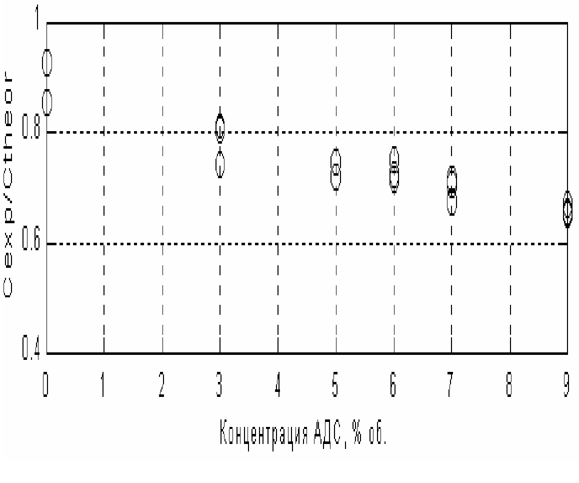

Fig. 2

# $TiSi_2$ OXIDATION UNDER NONISOTHERMAL CONDITION

**Koshelev M.V., Dranenko A.S., Dvorina L.A.**
Frantsevich Institute for Problems of Materials Science of NASU,
3,Krzhizhanovsky St., 03142, Kiev, Ukraine, E-mail: dvorina@ipms.kiev.ua

High-temperature oxidation of silicides of transition metals of the IV group of the periodic system was stadied by izothermal weigth determination in the air atmosphere at the temperature range 800-1500 K [1-3]. It is shoun, that the best resistant to haige-temperature oxidation is titanium disilicide [3]. However, cannot be investigated oxidation of $TiSi_2$ with thermogravimetry (TG) and differential thermal analysis (DTA) techniques with aim of determination of kinetic and thermodynamic parameters of oxidation reaction.

The derivatograms for $TiSi_2$ powder (Ti-46,0%, Si-52,6%, C-0,3%, Fe-0,1%, Al-0,03%, Ni-0,05%, Cr-0,01%, Ca-0,01%) were obtained with a MOM Typ Q-1500 D Derivatograph in the temperature range 300-1250 K. The particle size of the sample taken was below 240 mesh sieves. Specimen weights were 350 mg, and all experiments were performed in static air at heating rate of 10 K/min. The temperature difference $\Delta T$ was indicated with sensitiviti of 1 μV/mm. The referense material was precalcined $Al_2O_3$ at 1500 K. Thermocoople were calibrated with the NBS-ICTA recommended DTA temperature standards $KNO_3$, $SiO_2$, $SrCO_3$ [4].

Fig. 1 shows the derivatogram of $TiSi_2$ powder. It is seen that the temperature at which oxidation process is initiated is 693 K (Fig. 1 TG curve).

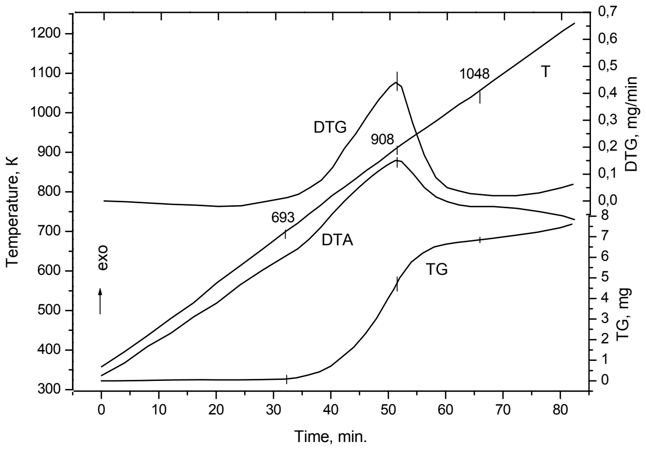

Fig. 1. Derivatogram for $TiSi_2$ powder.

A wide exotermal DTA peak was observered in temperature range 693-1048 K. The oxidation rate attained a maximum (DTA, DTG) at about 908 K and decreased thereafter. The mass gain and oxidation rate is discontinue at the temperature 1033 K. At subequent heating small increase weight gain at temperature above 1173 K is displayed. After probe cooling with the furnace to 300 K at second test we have observed substantially smaller wright gain (a 10-12 times) at the temperature range 693-1048 K (Fig. 2). This testify to formation a protective layers on the surface of $TiSi_2$ grains.

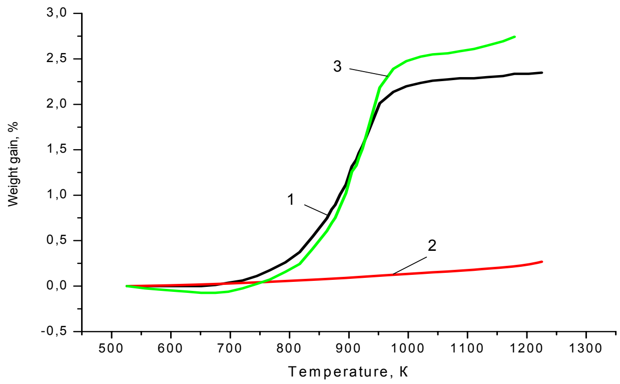

Fig. 2. TG curves of $TiSi_2$ powder:
1 - initial test; 2 - second test after cooldown inside the furnace; 3 - follow-up heating of coolling probe after regrate in porselain mortar.

After regrate in porselain mortar preliminary oxidized $TiSi_2$, the process of oxydation at the temperature rang 693-1048 K was renewed. In this case weiht gain and oxidation rate are higher than of the initial test of powder.

The activation energy can be obtained on the basis of the method of Horwitz and Metzger using the equation [4, 5]:

$$\ln\ln\left[\left(W_i - W_f\right)/\left(W - W_f\right)\right] = {E\theta}\Big/{RT_s^2} \qquad (1)$$

were $\mathbf{W_i}$, $\mathbf{W}$ and $\mathbf{W_f}$ - are the initial, actual and final sample weights respectively; **E** – actiation energy, J/mol; **R** – gas constant, J/(mol·К); **Θ=T-T$_s$**, **T$_s$** - temperature at the point of inflexion of reaction, К.

A plot of $\ln\ln\left[\left(W_i - W_f\right)/\left(W - W_f\right)\right]$ versus Θ should then be a straignt line of slop $E/\left(2.303RT_s^2\right)$ (Fig. 3).

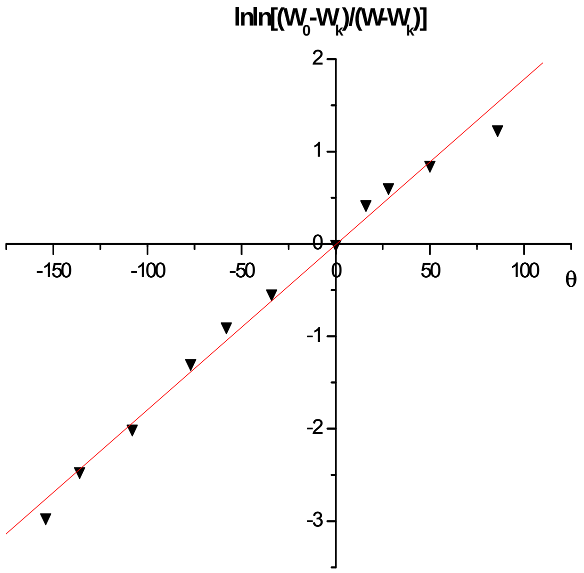

Fig. 3. A plot of $\ln\ln\left[\left(W_i - W_f\right)/\left(W - W_f\right)\right]$ versus Θ for TiSi$_2$ powder.

The pre-exponential factor **A** can be obtained using the equation [4]:

$$A = f'\left(\alpha_s\right)\cdot\frac{E\cdot q}{R\cdot T_s^2}\cdot\exp\left(\frac{E}{R\cdot T_s}\right),$$

(2)

were q - heating rate; $f'\left(\alpha_s\right)\approx 1, \alpha_s$ - fractional conversion at the point of inflexion of reaction.

The thermodynamic parameters i.e. the entropy of activation S, the free energy of activation G, and the enthalpy of activation H were calculated starting from [6]:

$$S = 2.303\cdot\log\left(A\cdot\frac{h}{k\cdot T_s}\right), \qquad (3)$$

were h and k are Planck`s and Bolthzmann`s constants respectively.

As the reaction rate mainly depends on the free energy of activation, the entropy of activation S should decide the magnitude of G acccoding to:

$$G = E - T_s\cdot S \qquad (4)$$

The enthalpy of activation was calculated using:

$$H = E - R\cdot T_s$$

(5)

Values: E = 127,03 кJ/mol; A = 42714,17 s$^{-1}$; S = -19,92 J/(mol·К); G = 142107,3 J/mol and H=119472,5 J/mol were found of the oxidation process of TiSi$_2$ powder.

**References**

1. G.V. Samsonov, L.A. Dvorina, B.M. Rud` Silicides // -M. -Metallurgy. -1979.
2. R.F. Voitovich, E.I. Golovko, O.A. Frenkel Peculiarity oxidation of disilicides of transition metals of the IV-VI group in air // -Silicides and their application in technics // -IPM. -Kiev. -1990. - P.66-72.
3. R.F. Voitovich, E.A. Pugach. Oxidation of refractory compounds. 1. Silicides of transition metals of the IV group // Powder metallurgy. -1974. -N 1. -P.63-70.
4. J. Šesták Theory of Thermal Analysis: Physico-chemistry properties of solids // - M. -Mir. -1987.
5. H. Horwitz and G. Metzer // Anal. Chem. -1963. - v.35. -P.1464.
6. S. Glasstone A Textbook of Phisical Chemistry // -Macmillan. -Bombay. -India. -2nd edn. -1974.

# STRUCTURE AND PHASE COMPOSITION OF QUASICRYSTALLINE SYNTHESIZED COVERINGS OF AN AL-CU-FE ALLOY

**Maiboroda V.P. Buzhenets E.I., Oliker V.E., Terentyev A.E., Frolov G.A., Golovkova M.E.**
I.Franzevich Institute of Materials Sciense Problems of NASU, Kiev, Ukraine
Krshishanovskii Street 3, Kiev, 03142, Ukraine, E-mail:maiborod@ipms.kiev.ua

The series of traditional of deriving of quasicrystalline materials recently has replenished with a new mode basing methods of powder metallurgy [1]. As show researches of the authors, pressing and sintering of powder mixtures consisting of a mixture of ikosaedric i-phase and a cubic β-phase, with magnification of a content of i-phase is at a loss.

The use at plasma-sprayed coating the powder mixture consisting on 80% from a i-phase nor allows to receive a qualitative covering on substrates, for example, from stainless steel, titanium or molybdenum.

With decreasing of an amount of i-phase the adhesion of a covering raises, but thus hardness of a covering disastrously is reduced also.

With the purpose of deriving satisfactory adhesion of a quasicrystalline covering and raise in it of a content of the i-phases up to 70-80 of % the researches of influence of conditions of plotting and relation of i - and β-phases in coating powder mixture on a structure and phase composition of covering are carried out.

As a substrate the stainless steel of a austenite class was used. As in a researched alloy the β-phase at 973 K turns in i-phase, so for plotting a covering was used a mixture consisting in basic a β-phase and residual i-phase.

During researching of a modification of phase composition of coverings in relation to an initial powder mixture it was established, that with a content of i-phase in a powder mixture less ~20% (on volume) the structure of a covering is practically constant. With a raise of a content of i-phase in a mixture up to ~ 30% the variation by conditions of plasma-sprayed coating allows essentially to increase a content of i-phase (up to 60% and more) owing to it synthesizing during plotting on a substrate. For study of a nature of this appearance the structural researches of coverings containing i-phase in an amount 30% and 60% from volume were carried out.

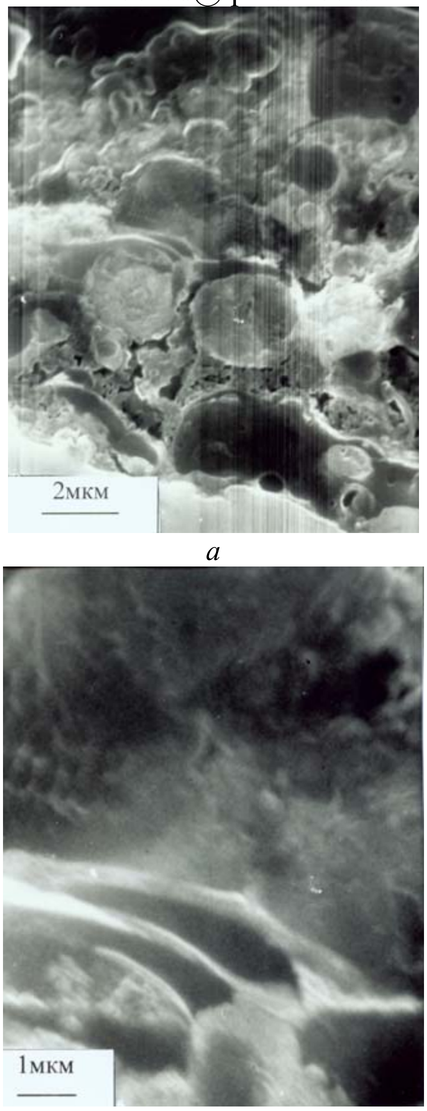

*a*

*b*

Fig.1

As shown on fig.1, and typical structural fragments of a structure of a covering with a smaller content of i-phase is the presence of spherical grains and in a smaller degree of the plate-like elements (fig.1, б).

The reduced structure testifies to a lack of flattening of microdrops and spreading on a substrate.
The structure of coverings containing up to 70% of i-phases (fig.2, *a*) consists from prolated cellular and threadlike (vein) fragments, and also from microplate elements (fig.2*, b*).

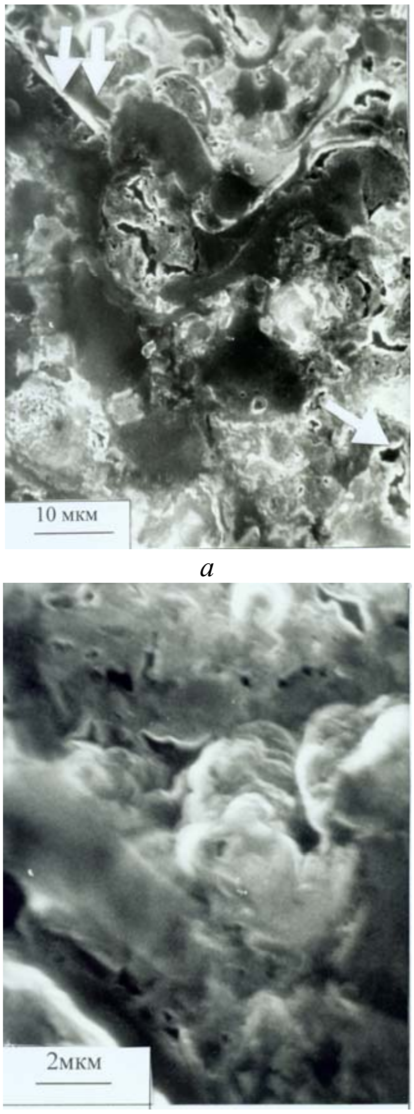

*a*

*b*

Fig.2

In some grains the inclusions of the pentagonal forms (.fig.2,*a*; 3) are observed.

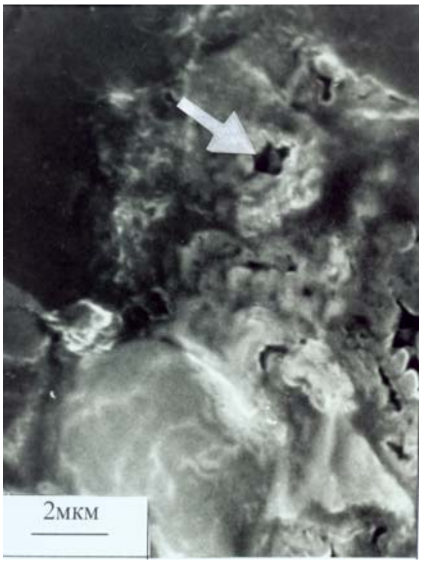

Fig.3

The comparison of outcomes of structural researches testifies, that the increased synthesizing of i-phase happens during flattening (spreading) of drops on a substrate and is connected with more intensive, masstransfer of components in a mixture.

The vein morphology of fragments (fig.1, *a* ↓↓) reminds a surface of breaks of amorphousing alloys [2] and of nanolayered metal aggregates [3], and is connected with nanolammellar structure by last. Therefore there is a foundation to suppose, that threadlike fragments derivated also in quasicrystalline coverings (fig.1, *a* ↓↓) at some conditions of their plotting.

The list of the literature

1. Maiboroda V.P., Demidik A.N., Stegniy A.I., Frolov G.A., Scholniy B.K., Pinchuk N.D. Н.Д. The declaration patent of UkraineUA № 47658, 15.07.2002. Bul. № 7 2002.
2. S.V. Pan ,V.Milman and A.A. Malyshenko Segregation effect as a possible mechanism for strengthening sn metallic glasses/ Materials Science and Engineering. A145 –1991.-C.27-132
3. A.P.Shpak, V.P.Maiboroda, Yu.A.Kunitskii, S.L.Revo. Nanosloistyi kompozity i pokrytiya. (Kiev. Academic periodicals 20003).

# FORMATION OF NANO-CRYSTALLINE CARBON DURING THE SYNTHESIS PROCESS OF SiC FIBERS

**Vyshnyakova K.L., Oleinik G.S., Pereselentseva L.M.**
Frantsevich Institute for Problems of Materials Science of NASU,
3 Krzhizhanovsky st., Kyiv,03142, Ukraine, vish@i.co.ua

This paper presents a methodological study for the structural transformation during the process of silicon carbide fibers synthesis by the method of thermal treatment of hydrate cellulose preliminarily impregnated with silica.

Characterization was performed by methods of IR-spectroscopy, XRD, SEM, TEM combined with microdiffraction.

It was found the pyrolysis of hydrate cellulose in the presence of silica passes through interaction in the system leading to produce intermediary compounds within 200-600 ºC. The IR-spectroscopy study confirms the presence of Si-C and Si-O-C bonds in these intermediary compounds, that at 700-800 ºC according to the x-ray and microdiffraction analyses transform into amorphous (glassy) product of silicon oxycarbide of variable composition $Si_xC_yO_z$ which is characterized by the presence of Si-O, Si-C and Si-O-C bonds. The elements ratio in this compound depends on silicon dioxide amount absorbed by hydrate cellulose fibers during their impregnation with silicate-containing solutions. The silicon oxycarbide phase maintains its amorphous state when heated up to 1000 ºC. Above this temperature the decomposition of silicon oxycarbide starts, and it produces crystalline $SiO_2$ (cristobalite) as well as crystalline graphite-like carbon. As it was shown by the TEM study, the silicon oxycarbide decomposition at 1100 ºC results in nucleation of onion-like carbon of the size within 10-50 nm. The electron diffraction pattern represents very broad rings of carbon (002) and (100). Then, at 1200-1300 ºC the enlargement of the onions up to 100-300 nm takes place. Starting from 1300 ºC nanofibers and nanotubes of carbon are forming, the onions are being destroyed and nanocrystalline silicon carbide with a grain size of 20-50 nm is produced. At the temperatures higher than 1500 ºC there is a recrystallization process of the SiC grains growth. In the range of 1450-1500 ºC the process started from silicon oxycarbide destruction is wholly completed by the cubic β-SiC synthesis in correspondence with the final equation of $SiO_2+3C=SiC+2CO$. Figure demonstrates the steps of structural evolution of the fibers of silicon oxycarbide when heated in the temperature range of 1000-1500 ºC.

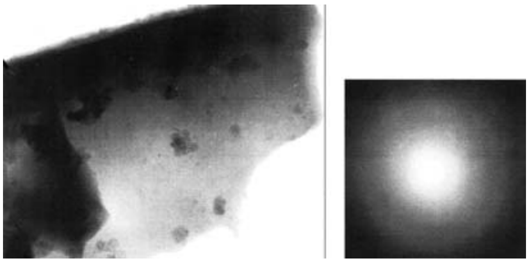

Silicon oxycarbide

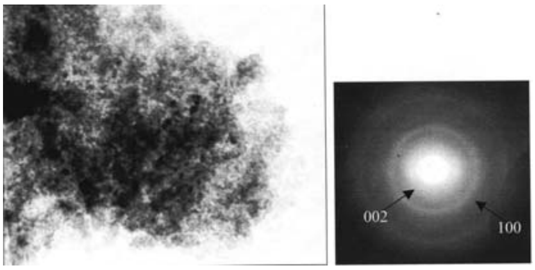

C onions formation

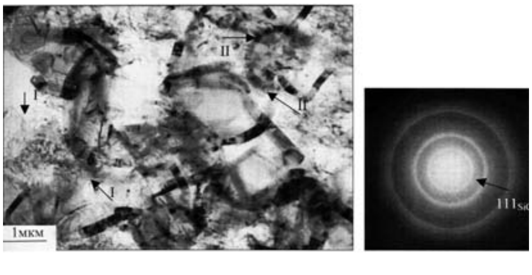

Carbon nanofibers and nanotubes and nanocrystalline SiC formation

Figure. Structural evolution of SiOC fiber heated at 1000-1500 ºC.

# RESEARCHES OF HEAT RESISTANCE STEEL 45 BY ELECTRIC SPARK ALLOYING WITH FERROCHROMIUM

**Paustovsky A.V., Brodnikovsky N.P., Kuznetsova T.L., Alfintseva R.A., Oryshich I.V., Rokitska E.A**
Frantsevich Institute for Problems of Material Science of NAS of Ukraine,
Krzhuzhanovsky str.3, Kyiv, Ukraine, 03164, E-mail: dep53@ipms.kiev.ua

One of the basic tasks of a modern science and engineering is an improvement of technologies for increase of physical-mechanical properties of constructional materials with using of relatively accessible and cheap materials for these purposes.

Nowadays there is a number of methods of superficial hardening and restoration of the worn-out details. An electric spark alloying (ESA) by a compact electrode in a gas atmosphere is most effective of them. ESA method permits to decide the basic task - to improve physic-chemical properties of materials on the basis of iron, titanium and others by coating refractory metals, its alloys and compositions on their surface. The basic material, which is applied in present time as electrodes for hardening a surface by ESA method is the harden alloys on the basis of tungsten carbide. However thickness of its coatings does not exceed 20-30 microns. Use the electrodes on the basis of metals (nickel, chromium etc.) permits to increase a layer thickness to 500 microns and more. It is especially important for restoration of the worn-out details. However, these materials are expensive and scarce for Ukraine and not always provide a complex of the necessary exploitation characteristics.

Researches of phase structure of electric-spark coatings with the high pure and small alloying chromium on steel 45 carried out previously [1] have shown, that the hardening of a superficial layer is caused by formation of carbide phases and of increasing defects density because of thermal impact. It has caused the high wear and heat resistance characteristics of an electric-spark coating.

Researches of last years, which have been carried out in IPM NASU [2] have shown that complex purified ferrochromium with the chromium contents 40-60% can successfully be used instead of high pure chromium with the purpose to receive of the heat resistant coatings.

In this work the task of research of opportunity of application concerning cheap ferrochromium, which is made in Ukraine, for heat resisting coatings has posed. For this purpose it was studied influence of an alloy content, which is used for ESA, on density and smooth of a coating. The development of technological parameters of getting the surface layers from ferrochromium with thickness from 0,3 up to 1,0 mm is carried out, that is very important for getting of a unbroken heat resistant layers at the reparation of worn-out details. The change of heat-resistance of steel, speed of formation, the composition and the structure of scale were investigated.

It is established, that the including of the deoxidizing agents - RGM or aluminum in electrodes - promotes to increase of fluidity of surface alloying layer at ESA process. Therefore a coating defects decreases and its density increases.

The comparison of heat resistance of steel 45 without a coating and this one after ESA with the purified ferrochromium containing to 2% aluminum was carried out. It was researched the samples annealed in the chamber furnace of resistance at temperature 800°C during 2, 4, 10 and 20 h. Samples had the form of a cube with the side size 10 mm. The coating of the composition mentioned above was coated on all sides of samples. The thickness of a coating was about 100-120 microns. The samples were insert into the corundum crucible. The heat resistance was evaluated as increase of samples mass by a method of weighing with analytical weights with 0.0005 g accuracy. Character kinetic curves, that describe the oxidation process is different (fig. 1). Last one for steel with a coating is close to parabolic dependence, that testifies about density of scale layer and diffusive character of its thickness increase. For steel without a coating the dependence of mass change and time is close to linear. It testifies about friable character of a scale layer and its protective action absence. The increase of mass for the unprotected steel 45 is higher in 30-40 times, than for steel with a coating.

It is established also, that the thickness of a scale on an steel 45 after oxidation during 4 hours was 0,18-0,20 mm and increased up to 0.80-0.90 mm for 20 hours, while on an alloy Fe-60Cr-2Al for the same period such thickness was changed from ~0.001 up to 0.002 mm.

Besides, on steel 45 layer, that was placed under the scale, was very impoverished by carbon up to pure ferrite formation. At ESA with the purified ferrochromium the thin layer protective scale is formed on a surface. It keeps strongly on a surface of a sample and protects against intensive oxidation as a coating as basis metal.

The structure of steel protected by ferrochromium coating practically has not changed (fig. 2). The dark-gray protective scale is formed both on purified ferrochromium cast and on a coating during oxidation. At consideration of the scale structure it was established that morphology a film, which was formed on borders and in a body of a grain differs appreciable. The fine crystalline film is formed on borders. This fact is usually connected with a segregation of impurity and power condition of grains borders.

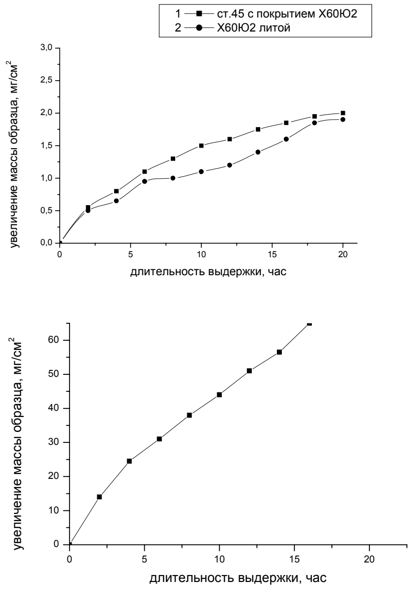

Figure 1 – Kinetic curve of samples oxidations at 800$^0$C, for 20h: a) 1-steel 45 with ESA with ferrochromium coating; 2- cast ferrochromium; b) steel 45

The results X-ray structure analysis testify about formation complex oxides of iron, chromium and aluminum of during oxidation (table 1).

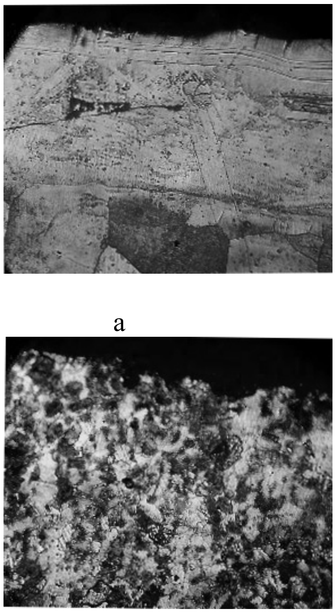
a

Fig. 2. - Structure of steel 45 samples with a coating (a) and without this one (b) after oxidation at 800 $^o$C, for 4 h.

The table 1 - Phase composition of samples scale after oxidation.

| Material | Phase scale composition |
|---|---|
| Steel 45 without a coating | $Fe_3O_4$, FeO, $Fe_2N$, $Fe_4N$ |
| Steel 45 with a coating | $Cr_2O_3$, $CrO_3$,<br>FeO ($Cr_2O_3$, $Al_2O_3$),<br>$Fe_3O_4$, FeO, $Fe_2N$, $Fe_4N$, $Cr_2N$ |

Thus, it is established that electric-spark coatings on steel 45 with purified ferrochromium containing 60 %Cr and up to 2 % of aluminum have high heat resistance (up to 900 $^o$C) that will allow to increase working temperature for the steel details on 100-200 $^o$C.

REFERENCES

1.Н.Д. Бега, В.Ф. Горбань, А.В. Паустовский и др. Электроискровые покрытия из сплавов на основе хрома // Порошковая металлургия. 1994.-№ - С.85-95.
2.А.М. Ракицкий, Т.Л. Кузнецова, Н.Е. Порядченко, Н.И. Панарина. Исследование свойств высокохромистых сплавов системы железо-хром-алюминий // Металлофизика и новейшие технологии.-1997.- N6.-С. 736-739.

# STRAIN SENSITIVITY IN $BaB_6$ – $LaB_6$ AND $SnO_2$ – Sb THICK FILM RESISTORS

**Paustovsky A. V., Rud B. M., Sheludko V. E., Gonchar A. G., Telnikov E. Ya.**
Frantsevich Institute for Problems of Material Science of NASU, 3 Krzhizhanovsky St., Kiev, 03142, Ukraine, E–mail: dep65@ipms.kiev.ua

The structure of thick film resistors (TFR) is glassy matrix with distributed conducting phase particles and electrical conduction of such films is determined by the mechanism of charge transport between conducting particles through the dielectrical interlayers. The magnitude of TFR resistivity is known to be changing while deforming [1,2]. Though TFR resistivity sensitivity to deformation is less than discontinuous thin films and a number of semiconductors have, but because of low TCR values, properties stability, high mechanical strength and rather low cost the films have found their application as the sensors in the manufacture of the strain gauges. It is seen from the analysis of literature that ruthenium compounds are used, in overwhelming majority, as conducting phase when manufactured the strain gauges [2]. The data on the use of $BaB_6$ – $LaB_6$ and $SnO_2$ – Sb systems are completely lacking.

The aim of this work is to investigate the strain sensitivity of $BaB_6$ – $LaB_6$ and $SnO_2$ – Sb TFRs by means of 3–points bending method.

The magnitude known as the gauge factor (γ) is taken to be a measure of strain sensitivity. It`s determined according to the formula:

$$\gamma = \frac{\Delta R}{R\varepsilon}, \qquad (1)$$

In the formula $\frac{\Delta R}{R} = \frac{R - R_0}{R_0}$; $\varepsilon = \frac{6ht}{L^2}$

Symbols: $R_0$ – TFR resistance without strain, Ohм; $R$ – TFR resistance in the stressed state, Ohм; ε – deformation; $h$ – deflection, mm; $t$ – substrate thickness, ($t$ = 1,2 mm); $L$ – the distance between knife–edges, ($L$ = 40 mm).

Gauge factor γ was measured by means of the method shown in Fig. 1 in longitudinal ($\gamma_l$) and transverse ($\gamma_t$) directions relating to current lines. Since $\gamma_l$ is a bit higher (~ 20–30%) than $\gamma_t$ [2] at all times, sensing element of the strain gauge is settled in longitudinal orientation.

The compositions $BaB_6$ + glass–binder (30 wt. %), $Ba_{0,76}La_{0.24}B_6$ + glass–binder (40 wt. %), $LaB_6$ + glass–binder (40 wt. %), $Sn_{0.9}Sb_{0.1}O_2$ + glass–binder (50 wt. %) were adopted as the objects of investigation. The making of TFRs was realized with the method of paste mask printing on the dielectric ВК–94 substrate followed by the heat processing in the travelling ПЭК–8 oven [3]. The thickness of TFR makes up 25–30 μm. Resistivity was measured with Щ–302 combined digital instrument.

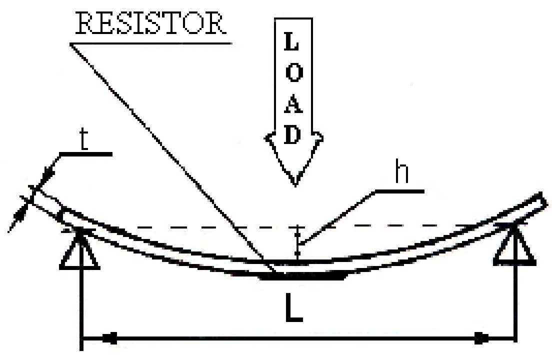

Fig. 1. The method of strain sensitivity measuring.

Shown in Fig. 2 are the resistivity – deformation relationships for $BaB_6$ – $LaB_6$ — based TFRs. Calculated with the formula (1) γ values are listed in the Table.

The distinguishing feature of all the samples in study is high reproducibility of results over the whole measuring range. For $Sn_{0.9}Sb_{0.1}O_2$ – based films we obtained analogous plot but resistivity decreasing, when loaded, was noted.

Table

| COMPOSITION | GAUGE FACTOR | |
|---|---|---|
| | $\gamma_l$ | $\gamma_t$ |
| $BaB_6$ + 30 % glassy | 3,0 | 2,7 |
| $Ba_{0,76}La_{0.24}B_6$ + 40 % glassy | 2,6 | 2,4 |
| $LaB_6$ + 40 % glassy | 2,4 | 2,2 |
| $Sn_{0.9}Sb_{0.1}O_2$ + 50 % glassy | -12,8 | -9,6 |

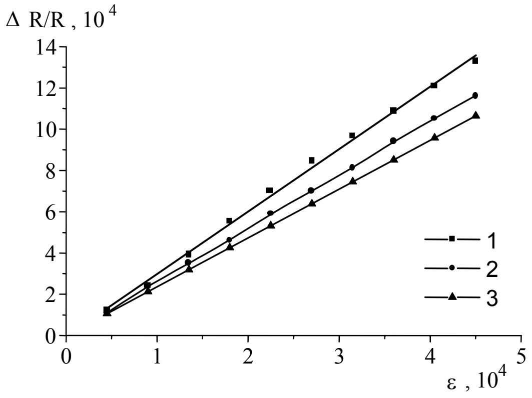

Fig. 2. Change in resistivity as a function of deformation: 1 – $BaB_6$, 2 – $Ba_{0,76}La_{0.24}B_6$, 3 –$LaB_6$.

As may be seen from the data depicted, $\gamma_l$ is more than $\gamma_t$ (in absolute value) for all the films. The values of gauge factor for Ru–containing TFRs are known to lie within the range 3 to 20 [1,2]. For $BaB_6$ – $LaB_6$ films $\gamma$ value does not exceed 3. So small sensitivity of resistivity to deformation is important when used the films as resistors.

High strain sensitivity is representative of the films in which the conduction mechanism between conducting particles is due to tunneling. The average thickness of the dielectric interlayer for $BaB_6$ – $LaB_6$ system is within the range 50–200 nm [4]. The magnitudes are big for effective tunneling and Mott transition mechanism prevails in the present case. So small $\gamma_l$ and $\gamma_t$ values can be explained by this fact.

The average thickness of the dielectric interlayer for $Sn_{0.9}Sb_{0.1}O_2$ films comes to ~ 10 nm and the tunneling mechanism of charge transfer prevails. This should lead to high $\gamma$ values. Earlier [5] we have investigated the same $Sn_{0.9}Sb_{0.1}O_2$ samples with the method of uniaxial strain and $\gamma$ value has come to 60.

Negative $\gamma$ values obtained while measuring by means of 3–points bending method, from our viewpoint, are associated with the fact that structural features of $SnO_2$ – Sb films make them sensible to complex–strained state taking place in the present case.

In this way, for the first time the longitudinal $\gamma_l$ and transverse $\gamma_t$ gauge factors of $BaB_6$ – $LaB_6$ and $SnO_2$ – Sb TFRs were defined. Despite the fact of resistivity decreasing $\gamma$ values of $SnO_2$ – Sb films are high (in absolute value) and it makes these films long–term materials for sensitive elements of the strain gauges.

## References

1. Prudenziati M. Thick film Sensors. – N–Y.: Elsevier, 1994.– 464p.
2. Belavic D., Pavlin M., Gramc S. et all. Some Applications of Thick – Film Strain Gauge.– Proc. of 24th Intern. Conf. and Exhib., IMAPS., Poland.– 2000.– P. 199 – 202
3. Dyshel` D., Tel`nikov E. Ya. Rud` B. M. Compositions without noble metals for thick film gas sensor heater fabrication // Sensors and Actuators.– 1996.– B. 35–36.– P. 244-246.
4. Рудь Б. М., Виницкий И. М. Влияние структурных факторов на электрические свойства толстоплёночных резисторов // Новые материалы для толстоплёночной технологии в микроэлектронике: Сб. науч. тр.– К.: ИПМ им. И. Н. Францевича АН УССР, 1991.– С. 8–14
5. Гончар А. Г., Виницкий И. М., Рудь Б. М. Механізм впливу залишкових термічних напружень на електрофізичні властивості композиційних плівок на основі $SnO_2$ – Sb // УФЖ.–2002.– 47, № 1.– С. 61–64.

# THE NEW SELF–LUBRICATING COMPOSITION MATERIALS FOR JOINTS OF FRICTION IN SPACE EQUIPMET

**Kostornov A.G., Fusshich O.I., Chevichelova T.M., Simeonova Yu.(1), Sotirov G (1).**
Frantsevitch Institute for Problems of Materials Sciences, National Academy of Science,
3, Krzhizhanovsky St., 242142, Kiev, Ukraine, e-mail: dir@ipms.kiev.ua
(1)Sapse Research Institute at Bulgarian Academy of Sciences, 6, Moskovska St.,1000, Sofia,
Bulgaria, e-mail: office@space.bas.bg

Space studies have shown the complex and non-traditional character of the tribological processes in vacuum, where the medium is extremely rarefied, with lack of oxygen and humidity, without convectional cooling and without the traditional in contact. As a result, contact interactions are realised at elevated temperature, increased plastic deformation, destruction of oxides and secondary surface structures, at strongly increasing adhesive activity of the frictional surfaces, leading to intensive wear and often stickslip effect, as well as to appearance of seizure center in contact. The specific of triboprocess in space requires searching and usage of new antifrictional materials fulfilling the requirement for work in space environment. Our experience in material research and their use in Space have shown that self- lubricant copper based composite materials are suitable for space application. These materials have high stability and reliability by continuous (about 5 years) usage under dry friction vacuum conditions.

The material IPM-301 has been applied in the tribojunctions of the scanning antenna of the space radiometric system “R-400” which operated trouble-free in space on the “MIR” Orbital Station for about 5 years (fig.1).

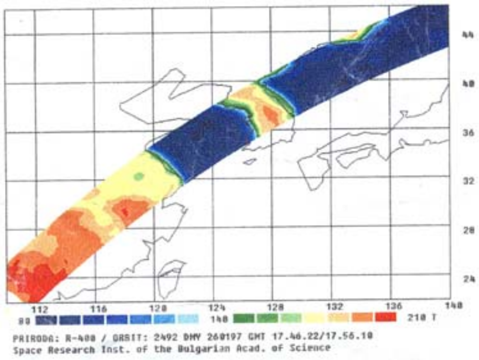
44
40
36
32
28
24
112
116
120
124
128
132
136
140
80
140
210 T
PRIRODA: R-400 / ORBIT: 2492 DMY 260197 GMT 17.46.22/17.56.10
Space Research Inst. of the Bulgarian Acad. of Science

Fig. 1. Radiothermal emission of the Earth’s surface. The signal was measured of “R-400” system in the friction joints of which IPM-301 material was studied.

Compositional materials IPM-304, IPM-305 are the subjects of research. A little amount of special additives introduced into the materials allowed us to obtain the original microstructure of the component carrying the load. The antifriction component of self-lubricating composite materials has been chosen. Its composition has been optimized what provides required and optimum antifriction characteristics of materials – wear and friction coefficient.

Samples from materials of IPM mark have been subjected to the complex test at IPM, ISR and European Major Technology, Testhouse (Austria).

Austria with the cooperation of the specialist in tribology from ISR has carried out the test using modern vacuum and tiybotechnical equipment and according to the international technique “EUROPEAN ROUND ROBIN TEST”.

The study of friction coefficient and wear of materials has been carried out at friction in vacuum ($1*10^{-5}$mbar) at load 2N and 10N and friction velocities 0,2m/s and 1m/s by the systems:
- Pin (IPM) – disk [steel AISI52100(100Cr6)];
- Ball [steel AISI52100(100Cr6)] – disk(IPM).

Tribological study has been realised by means of equipment and devices of Aerospace Materials Technology Testhouse – AMTT. UHV-tribometer has been used.

This facility enables the investigation of materials and coatings with respect to friction and wear properties. It enables on-line measurement of friction force and linear wear during unidirectional or oscillatory sliding according to standardised pin-on-disk or ball-on-disk geometric. Measurement of total wear is done by profilometry, SEM or microbalance, investigation of surface structure or material transfer by SEM/EDX. Reproducibility and repeatability of test results are proven by European Round Robin Test.

By SEM are investigated structural – morphological particularities of friction surface, and by X-ray analysis are obtained data of the spectrum f the elemental composition of the surface layer after dry friction in vacuum.

An interesting fact is that by increasing 5 times load (from 2N to 10N) at velocity 0,2m/s the friction in vacuum does not increase by wear $6*10^{-6}$ $mm^3/Nm$.With their triboparameters there materials are comparable to the material LB9 Glacier BS 1400 LB4-6).

Because of the distinct of triboprocesses in vacuum and especially due to the increasing of adhesion, it should be expected an increment of the values of triboparameters at dry friction in vacuum. In our case appears the opposite result, well expressed at all regimes of friction in vacuum. This result could be explained by the presence of the effect of self-lubrication.

Our previous studies have shown that under dry friction in vacuum by this type of material appears certainly self-lubricant effect, pressing out of solid lubrication on the friction surface is observed (fig.2).

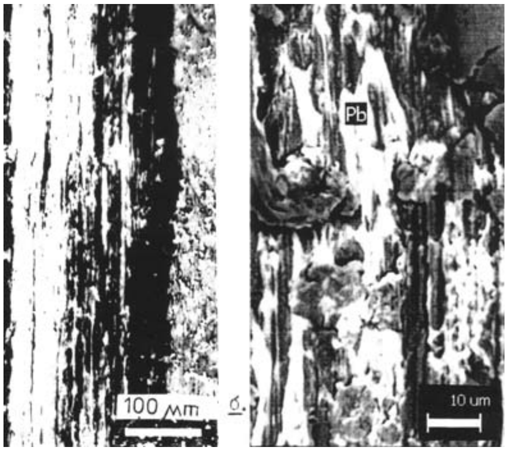

Fig. 2. Formation of separating lubricant.

With the increasing of velocity and load, the power of friction increases, temperature in contact grows and the surface enriches with solid – lubricating component (fig.3), i.e. the material is adapting to various regimes of loading, that provides stable tribotechnical characteristics with confinions exploitation in vacuum (load 20N; velocity 0,2m/s; distance 50000m).

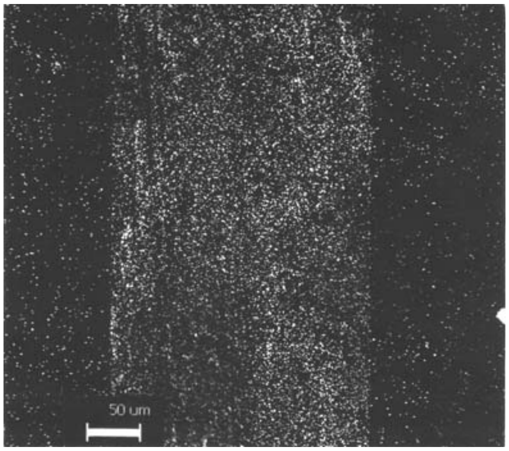

Fig. 3. Enrichment of friction surface with solid lubricant.

The results from the all complex study of self-lubricant composite materials are of interest for space material science and technologies and set plenty of actual questions related to their application in space.

# STRUCTURE AND PHASE STATE OF COATINGS WHICH DEPOSITED BY SPARK TREATMENT OF HARD ALLOYS

**Paustovsky A.V., Gubin Yu.V.**
Frantsevich Institute for Problems of Materials Science of National Academy of Science of Ukraine, 3 Krzhizhanovsky str., 03142, Kiev, Ukraine, e-mail: dep65@ipms.kiev.ua

In this work carry out investigation of phase state in coatings which deposite by spark treatment method of hard alloys on steel surface.
Spark treatment were work out in air atmosphere on “Elitron-22” equipment on regimes: work current 0,8 1,8 and 2,8 A; treatment time 2,5 and 10 minutes.

Base surface were У8 steel which treated by heating for disappearance of residual stresses. Heating work out by 3 hours in protective atmosphere on temperature 750°C.

Spark treatment work out by electrodes on base of hard alloys of titanium carbide and tungsten carbide base with additions of carbon. Phase composition of spark coatings were determined by X-ray method. Difractogrammes were investigated on ДРОН-2.0 equipment in irradience of iron anode with manganees filter on regime voltage 14 kV, current 16μA and irradiation of cobalt anode on regime voltage 40 kV, current 30 μA.

X-ray analysis of spark coatings surface show that phase content of coating sufficiently dependence on energy of treatment. In structure of coating which deposite by T15K6 electrode on regime with current 2,8A with treatment time 2 minutes to find reflexes of titanium carbonitride TiCN, tungsten carbide TiC, α-cobalt and α-ferrum.

In coatings which deposited by same electrode on more light energy regimes with current 0,8 and 1,8 A difraction reflexes of TiCN don′t observed. In this coatings observed reflexes of titanium carbide TiC, tungsten carbide WC, α-cobalt and α-ferrum.
Formation of titanium carbonitride TiCN on more strong energy regime of spark treatment can be explained by absopbtion of atmosphere nitrogen on more high temperatures in contact point “electrode-treated surface”/
Relative intensity of reflexes is different for coatings which deposite on different energy regimes. Difractogrammes of coatings which deposited on light energy regimes have more intensity of α-ferrum lines and small intensity of lines of other phase compounds.

This difference can be explained that more light energy regimes of spark treatment leads to formation of small coating depth and difraction reflexes of X-ray formed in coating, transitional layer and specimen base. In structure of coatings which deposite by same electrode on same energy regimes by treatment time 5 and 10 minutes. discovered same phases. It is observe difference in relative intensityes of lines of different phase compounds of coatings. Decreasing of α-ferrum phase intensityes and increasing of intensityes of other phases can be explained by increasing of spark coating depth on more treatment time.

In structure of coatings which deposite by electrodeT15K6 with 0,4% carbon addition observe same phases such by treatment by T15K6 electrode. It is exist sufficient difference in reflexes relative intensityes. Intensityes of reflexes except α-ferrum is more that can be explained by more mass transfer. Thid data confirm advisability utilisation of electrodes of hard alloys with carbon addition. Maximum mass transfer occur by alloying on regime with current 2,8A. Mass transfer is sufficiently much by treatment on regime with current 1,8 A. Mass transfer is nonsufficient by treatment regime with current 0,8A. This evidence by small intensity of TiC, WC and α-Co reflexes and much intensity of α-ferrum reflexes of specimen base.

Increasing of treatment time to 5 and 10 minutes no leads to change of quality phase content. Spark treatment on this regimes leads to decreasing of α-ferrum reflexes relative intensity and increasing of reflexes intensity of other phases. This can be explained by increasing of coating depth.
In structure of coatings which deposite by spark treatment of hard alloys BK20 and BK3 with 0,4% carbon addition it is observe phase reflexes of α-Fe, α-Co and tungsten carbide WC. On difractogrammes of coatings which deposite on more strong regimes with current 1,8 and 2,8A it is observe more relative intensity of phases except

α-ferrum. This difference can be explained by increasing of coating depth. Increasing of treatment time to 5 and 10 minutes leads to decreasing of α-ferrum reflexes intensityes and increasing of other phase intensityes.

.

Copmaring of difractogrammes of coatings which deposite by BK20+0,4%C and BK3+0,4%C electrodes show that same treatment regimes leads to formation of same phase content.

It is established regularityes of change of phase content of coatings which deposited by spark treatmeny by hard alloys

# RESEARCH OF 3d-METAL ATOMS CHARGE STATES IN ARC-MELTED ELECTROCONDUCTING OXIDE MATERIALS

**Zyrin A.V, Bondarenko T.N.**
Frantsevich Institute for Problems of Materials Science of NASU,
3 Krzhizhanovsky St.,Kiev, 03142, Ukraine, E-mail:zyrin@ipms.kiev.ua; rs@ipms.kiev.ua

## INTRODUCTION

Electroconducting oxide materials, capable longly to work at high temperatures in gas media with high oxygen partial pressure and having mainly electronic (hole) conductivity, consist, generally, of transitional metals based oxide compounds. The heterovalency doping of them is forming the current carriers concentration increase. This doping causes charge states change of variable valency atoms.

The electroconductive lithium doped nickel and cobalt oxides, perovkitelike manganites, cobaltites or chromites of rare earth elements were in such a way obtained. In three last the 3d-metals atoms valency regulation was realized by substitution of a 3-valency rare-earth atoms part by 2-valency alkaline earth atoms, that resulted in 3d-metals atoms valency increase. That was equivalent to hole current carriers concentration increase.

The similar electroconductive oxide materials are used in fuel cells electrodes and other current sources, in gas sensors, heating elements, thermistors etc.

These materials were obtained by standard ceramic methods. In this work the examples was synthesized by use of the mixtures of initial substances melting in an dc electrical arc. The patent IPMS-made equipment was used. It assured magnitude of an interelectrode distance automatically to support during of melting.

3d-metals atoms charge states were evaluated on a displacement of X-ray absorbtion K-edge spectra. The spectra were obtained with standard X-ray difractometer by in [1] described technique.

## RESULTS AND DISCUSSION

By the electric arc melting method were fabricated lithium doped nickel and cobalt oxides, including monocrystals from them, these were grown by the socalled arc-transfer method; lanthanum manganites and cobaltites with quasichemical formula $Me^{3+}_{1-x}Me^{4+}_{x}La_{1-x}Ca_{x}O_{3}$ (Me=Mn, Co) and lanthanum nickelites $Ni^{3+}_{1-x}Ni^{4+}_{x}La_{2-x}Ca_{x}O_{4}$.

The absorption spectra of the materials were obtained on X-ray difractometer ДРОН-1.5 with use of a X-ray tube with the copper anode brake radiation.

A quartz singlecrystal with 2d = 0.236013 nm (310)-face was used as crystal-analyzer. It was installed instead example for XRD-analysis on a goniometer table. Instead of a $K_{\beta}$ radiation cutting filter the lamina of a researched material are located. The reflected by crystal - analyzer and past through an absorber X-radiation intensity was registred by a counter during standard rotation of a table with crystal-analyzer and counter.

The absorption K-edge position of 3d-metals atoms in researched materials were compared in pure metals and their individual oxides, in which the metal had various valence states.

## REFERENCES

1. The use of standard X-ray diffractometer for a rapid research of atoms charge states and qualitative analysis of powder materials on their absorption X-ray spectra. Zyrin A.V, Bondarenko T.N.-in: Тез. докладов международной конференции «Новейшие технологии в порошковой металлургии и керамике».-Киев, 2003.- с.399.

# PROPERTIES OF MATERIALS OF THE BN-$B_4C$ SYSTEM

**Grigorev O.N., Kotenko V.A., Lyashenko V.I., Rogozinskaya A.A., Dubovik T.V., Chernenko L.I., Panashenko V.M.**
Frantsevich Institute for Problems of Materials Science of the NAS of Ukraine
3 Krzhyzhanovsky St., Kyiv, 03142, Ukraine, e-mail: panavic@ukr.net

With the aim of investigating the structural features and properties of materials of the BN-$B_4C$ system, specimens on the base of boron nitride with additives of boron carbide in a mass ratio 1:1 were pressed and sintered at a temperature of 1800 ºC in a nitrogen atmosphere. As initial materials, boron nitride powders with different defect contents synthesized by three methods, namely the carbamide method (compositions 1 and 2), nitriding of amorphous boron (composition 3), and the solution method (compositions 4-6), and boron nitride powder of commercial grade (composition 7) were used. As an additive, milled $B_4C$ powder with an average particle size 5-8 μm was introduced.

In previous investigations [1], it has been established that the indicator of sintering intensity of the above-listed materials is the rate of formation of the *r*-BN phase as a result of the nitriding of boron carbide, whose content during sintering of specimens significantly decreases. A preliminary thermodynamic calculation performed using the «Astra» program in the temperature range 100-2000 °C (a step of 100 °C) also has shown that $B_4C$ is thermodynamically unstable in a nitrogen atmosphere and interacts with nitrogen by the reaction $B_4C + 2N_2 = 4BN + C$.

In the present work, the Meyer hardness, the electric resistivity, and thermal stability under the action of a focused solar radiant energy were determined on sintered specimens of the BN-$B_4C$ system.

In the Meyer hardness test, a preliminary selection of the indenter sphere and the test load was performed. The test load was 43.03 N (5 kgf) and the diameter of the steel ball was 2.5 mm. The sizes of indentations were determined with an accuracy of ±0.05 mm. The hardness was calculated as a ratio of the applied load to the area of the indentation projection by the formula $HM = 4P/\pi d^2$, where HM - the Meyer hardness, P - the applied load, and d - the diameter of the indentation. In each case, the average value of the hardness and the sample standard deviation (for each specimen, the number of measurements was equal to 7) were computed.

The contact compression strengths of specimens were calculated from their values of the Meyer hardness and of the modulus of normal elasticity [2] (Table 1). From the data presented in Table it is evident that specimens on the base of BN powders obtained by the carbamide method at 1500 °C possess the highest hardness and contact compression strength. The values of the electric resistivity of all tested specimens were larger than $10^{10}$ Ohm·cm.

An investigation of the thermoerosion mass losses of specimens of the BN-$B_4C$ system under the action of focused solar radiant energy was performed on a SGU unit in the Heliocenter of the IPMS of the NAS of Ukraine. Specimens 10 mm in diameter and 12 mm in length were weighted and measured before and after tests in solar radiation. A focused solar energy flow was directed to the free ends of specimens fixed in clamps. The solar radiation was equal to 150 units. The angle of opening of shutters was varied from 58 to 84 °, the exposure time under radiation was 60-90 sec, the test temperature was 2500-2700 °C. After the tests, an X-ray analysis of the radiated surfaces of specimens and Meyer hardness tests were performed (Table 2).

The data presented in Table 2 indicate that the specimens of the BN-$B_4C$ system have high thermal stabilities under radiation by focused solar energy for 60-90 min, retain their shape and appearance. The X-ray analysis data show that, after the test, the surface layer contains only *h*-BN and traces of $B_2O_3$, while $B_4C$ burns up.

A comparison of the values of the Meyer hardness before and after tests in solar radiation suggests that they decreased after radiation (Table 1 and 2). This is associated with the burning up of the hardening $B_4C$ additive from the surfaces of the specimens. The electric resistivity of the specimens did not change after radiation and was above $10^{10}$ Ohm·cm.

The investigation of the materials of BN-$B_4C$ system will be continued.

Table 1. Properties of sintered specimens of the BN-$B_4C$ system on the base of BN powders with different defect contents

| Composition No. | Method and temperature of preparation of BN | Meyer hardness | | | Porosity, % | Contact compression strength, MPa |
|---|---|---|---|---|---|---|
| | | HM, MPa | Standard deviation, MPa | Probability factor, % | | |
| 1 | carbamide, 1500 °C | 85,7 | 7,2 | 8,3 | 25 | 66,0 |
| 2 | – ″ – 1300 °C | 55,6 | 2,5 | 4,6 | 30 | 51,5 |
| 3 | nitrid. $B_{amorph.}$, 1300 °C | 43,2 | 1,6 | 3,6 | 32 | 43,6 |
| 4 | solution, 1650 °C | 25,6 | 1,1 | 4,5 | 30 | 23,9 |
| 5 | – ″ – 1650 °C | 53,4 | 3,1 | 5,8 | 30 | 50,0 |
| 6 | – ″– 1500 °C | 84,0 | 4,7 | 5,6 | 15 | 41,6 |
| 7 | commercial, 1600 °C | 58,0 | 4,2 | 7,2 | 20 | 52,3 |

Table 2. Characteristics of specimens of the BN-$B_4C$ system under conditions of solar heating (solar radiation of 150 W/$cm^2$)

| Composition No.* | Weight, g | | Angle of opening of shutters, deg. | Exposure time, sec | Phase composition of the surface | Meyer hardness, HM | | |
|---|---|---|---|---|---|---|---|---|
| | before test | after test | | | | HM, MPa | Stand. deviation | Probability factor, % |
| 1 | 0,930 | 0,927 | 65 | 90 | *h*-BN, $B_2O_3$ - traces | 30,6 | 1,3 | 4,4 |
| 2 | 0,901 | 0,900 | 58 | 60 | – ″ – | 38,6 | 2,1 | 5,3 |
| 3 | 0,871 | 0,866 | 58 | 60 | – ″ – | 29,5 | 1,5 | 5,1 |
| 5 | 0,903 | 0,883 | 49 | 60 | – ″ – | 25,6 | 1,5 | 5,8 |

- Note: see table 1.

**References**

1. Григорьев О.Н., Бега Н.Д., Ляшенко В.И., Дубовик Т.В., Котенко В.А., Панашенко В.М. Зависимость структуры спеченного карбонитрида бора от степени дефектности исходного порошка BN // Порошковая металлургия (в печати).
2. Галанов Б.А., Григорьев О.Н., Трунова Е.Г. Статистические характеристики контактной прочности керамики // Сб. науч. трудов «Электронная микроскопия и прочность материалов». - К.: ИПМ НАН Украины, - 2001. - с. 125-135.

# HEAT-RESISTANT TWO-PHASE EUTECTIC ($L1_2+\beta$) ALLOY OF Al-Ti-Cr SYSTEM

**Mordovets N.M., PoryadchenkoN.E., Korzhova N.P., Legkaya T.N.(1), Vojnash V.Z.(1) , Chmeljuk N.D.**
Frantsevich Institute for Problems of Material Science, Ukraine NASU,
Krzhizhanovsky str.3, 03680, Kyiv-142, Ukraine, E-mail: korzhova@ipms.kiev.ua
Kurdumov Institute of Metal Physics, Ukraine NASU,
(1)Vernadskogo str. 36, 03680, Kyiv-142, Ukraine, E-mail: barabash@imp.kiev.ua

The development of aircraft industry requires of creation the new materials with high specific strength and heat resistance. As such materials classified alloys on the base of $Al_3Ti$ and TiAl intermetallics.

We developed the compositions of new high-temperature strength alloys on the base of alloyed by Cr $Al_3Ti$ intermetallic [1, 2]. The structure of this alloys is formed by two cubic phases as a result of univariant eutectic reaction $L \rightleftarrows L1_2+\beta$, where $L1_2$ - intermetallic $Al_3Ti_{1-x}Cr_x$, β - solid solution on the base of chromium (Fig. 1)

Fig.1. Microstructure of $L1_2+\beta$ eutectic alloy of ternary Al-Ti-Cr system.

This alloys has extremely high and stable strength properties: yield strength in a temperature interval 20-750 °C equals 650 - 800 MPa and at 1000 °C (0.8 $T_{melt}$) - 145 MPa.

There is information in literature that the intermetallic $L1_2$ alloyed by Cr has high heat resistance [3, 4]. The aim of this work is to investigate the heat resistance of developed by us eutectic ($L1_2+\beta$) composites in comparison with TiAl intermetallic that shown a good performance as a constructive material for production of aircraft engines details [3].

The alloys for investigations were prepared by arc-melting method with a nonconsumable tungsten electrode on a water-cooled copper hearth in a gettered-argon atmosphere. The chemical composition of alloys are (at. %): 55Al-22Ti-23Cr, 52Ti-48Al.

The investigation of heat resistance was carried out on "Derivatograph" device with continuous recording of mass change for the specimens with sizes 10x5x3 mm. The tests with duration to 7 hours were carried out at 800 and 1000 °C in the still air medium. The heat resistance of alloys was estimated by mean value of mass change on unit of specimen surface ($\Delta m/s$, $mg/sm^2$). The comparison of oxidation resistance was carried out also by oxidation rate ($V$, $mg/sm^2 \cdot h$). The investigation of the phase composition of the surface films was fulfilled by X-ray method.

The results of investigation of the oxidation kinetics of studied alloys are given in Fig. 2.

Fig. 2. Mass change of the alloys during oxidation in air at the temperatures of 800 and 1000 °C.

At 800 °C the heat resistance of eutectic ($L1_2+\beta$) alloy some higher than the heat resistance of $Al_{48}Ti_{52}$ alloy. An increase of tests temperature leads to acceleration the oxidation process of the $Al_{48}Ti_{52}$ alloy: at 1000 °C its heat resistance approximately in considerably below than the eutectic alloy which mass change does not higher than 0.17 $mg/sm^2$.

From the character of kinetic curves (Fig 2) it may be assumed that the eutectic ($L1_2+\beta$) alloy oxidize in parabolic manner at both test temperatures. The process of TiAl alloy oxidation follows the parabolic law only at 800 °C, and at 1000 °C the alloy oxidize in linear manner.

Such difference in oxidation mechanisms of this alloys reflects on the character of oxidation rate change: in period of heating the oxidation rate increase, but afterwards, for $(L1_2+\beta)$ alloy practically not change at the both test temperatures (Fig. 3).

Fig. 3. The oxidation rate change of the alloys at oxidation in air at the temperatures of 800 and 1000 $^{o}$C.

The oxidation rate of eutectic $(L1_2+\beta)$ alloy at temperature of 1000 $^{o}$C is not high and equals not higher than 0.024 $mg/sm^2 \cdot h$ (at a complete oxidation time to 7 hours) (Fig. 3). The results obtained is in correspondence with the dependence of high-temperature strength and heat resistance from the composition and the structure of material that determined by R.F.Voitovich [5] (at investigation temperature the yield strength of eutectic alloy is in 1.5 times higher than the yield strength of TiAl alloy).

On the surface of specimen of eutectic alloy that oxidized at 1000 $^{o}$C the thin (~10-15 μm) film forms that consists (in agreement with X-ray data) mainly of aluminum oxide $Al_2O_3$. On the specimen of $Al_{48}Ti_{52}$ alloy oxidized in the same conditions the oxide film (>30 μm) of titanium oxide $TiO_2$ forms.

The investigations carried out showed that the eutectic $(L1_2+\beta)$ alloy 55Al-22Ti-23Cr has high heat resistance up to 1000 $^{o}$C and considerably exceeds the heat resistance of TiAl alloy. It testifies to undoubted perspective of use the new eutectic $(L1_2+\beta)$ alloy of ternary system Al-Ti-Cr as a heat-resistant material. In view of the high thermal stability of the structure and mechanical properties of eutectic composite and also the good compatibility of its chemical composition with $Al_{48}Ti_{52}$, it might be recommended for use as material for coatings of alloys on the TiAl base and for practical application in conditions of elevated temperatures usage.

## ACKNOWLEDGEMENTS

The authors would like to thank Dr. M. Karpets help in performing of X-ray investigations.

## REFERENCES

1.Barabash O.M., Milman Yu.V., Miracle D.B., Karpets M.V., Korzhova N.P., Legkaya T.N., Mordovets N.M., et.al. // Intermetallics 11 (2003) 953-962.

2. Podrezov Y.N., Barabash O.M., Milman Yu.V., Korzhova N.P.,. Legkaya T N., et.al. // Proc.of NATO Advanced Research Workshop “Metallic Materials with High Structural Efficiency”, Kyiv, September 7-13, 2003, p. 63.

3. Lee J.K., Oh M.N., Wee D.M. // Intermetallics 10 (2002) 347-352.

4. Parfitt L.J., Smialek J.L., Nic J.P., Mikkola D.E.//Acta Metallurgica et Materialia, **25** (1991) 727-731.

5. Войтович Р. Ф., Головко Э.И. Высокотемпературное окисление титана и его сплавов. - Киев, Наукова думка, 1984, 256с.

# ELASTIC AND DAMPING PROPERTIES OF MICROSCALE MULTILAMINATED Cu(Y)/Mo COMPOSITES

**Vdovychenko O.V.**
Frantsevich Institute for Problems of Materials Science of NASU,
3 Krzhizhanovsky St., Kiev, 03142, Ukraine, E-mail: ovdovych@uninet.kiev.ua

Recently, there has been renewed interest in metallic microscale multilaminated composites (MMC) in an attempt to exploit them in extreme performance applications. That was motivated by the increased mechanical properties of MMC that exceed the rule-of-mixture (ROM) value calculated based on the average of the parent materials [1]. The MMC of the Cu/Mo family prepared by evaporation and alternate vapor deposition in vacuum are promised [2]. Taking into account the fact, that machinery made from MMC usually used under cyclic loading, the elastic and damping properties are important merits. Optimal combination of thermal and mechanical characteristics can be obtained by choice of the appropriate structure [3].

This paper is concerned with the effect of structure of the Cu–(0,01…0,3)%Y/Mo MMC, manufactured in Paton's Electric Welding Institute of NASU [2], on their elasticity and energy dissipation. The materials consisted of alternate layers of copper and molybdenum (Fig.1), obtaining by electron beam physical vapor deposition on substrate at 973 K. Fabrication technique details and the static strength characteristics of the MMC are given in [2]. The thickness of all microlayers were fixed for each material and ranged from 1 to 10 $\mu m$ for different batches according to the Table.

| Batch # | $V_{Mo}$ | $h_{Cu}$ | $h_{Mo}$ |
|---|---|---|---|
| 1. | 0,36 | 2,0 | 1,0…1,3 |
| 2. | 0,19 | 5,0 | 1,0…1,3 |
| 3. | 0,33 | 5,0 | 2,5 |
| 4. | 0,37 | 5,0 | 3,0 |
| 5. | 0,44 | 5,0 | 4,0 |
| 6. | 0,14 | 7,0 | 1,0…1,3 |
| 7. | 0,22 | 7,0 | 2,0 |
| 8. | 0,15 | 10,0 | 1,7 |

Specimen dimensions were 50x5x1 mm. Young's modulus *E* was measured along the layer direction (Fig.1) by longitudinal resonance oscillation of the bar specimen technique. Logarithmic decrement $\delta$ was determined under alternating bending oscillation of cantilever beam with frequency 1 to 2 kHz. The Young's modulus was calculated with assumption, that specimen is macroscopically homogeneous since wavelength essentially exceeded the characteristic dimensions of the structure elements.

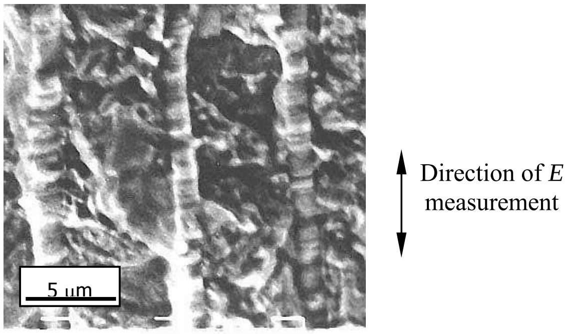

Fig.1. Micrograph of Cu(Y)/Mo MMC.

Young's modulus and decrement determination results under maximum cyclic stress of 150 MPa, are shown in Fig.2.

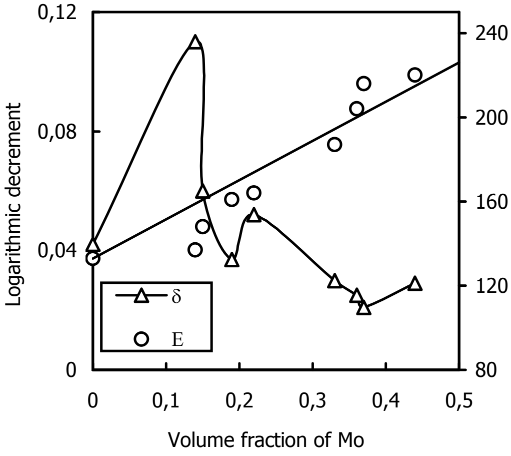

Fig.2. Dependence of E and $\delta$ of Cu(Y)/Mo MMC on molybdenum volume fraction.

The line conforming to the "rule-of-mixture" according Voigt model under the assumption that strains in each of the phases are equal: $E_{MMC} = E_{Mo}V_{Mo} + E_{Cu}V_{Cu}$ and $E_{Mo}$=320 GPa, also depict in Fig.2.

As it can be seen in Fig.2, the materials damping property change is nonmonotonic when Mo volume fraction increase. Therefore it could be suggested that interfaces between layers act as sources of energy dissipation in the MMC. This circumstance could explain the rise of $\delta$ value in comparison with monolithic copper (Fig.2). Fig. 3 shows dependence of decrement on inverse bilayer thickness connected with number of the interfaces in the composites as $n = 2 \cdot \left( \dfrac{H}{h_{Cu} + h_{Mo}} \right) - 1$, where $H$ - is the specimen thickness. Fig. 3 indicates that there is no unique dependence between *n* and $\delta$ and hence there is another factor of energy dissipation change.

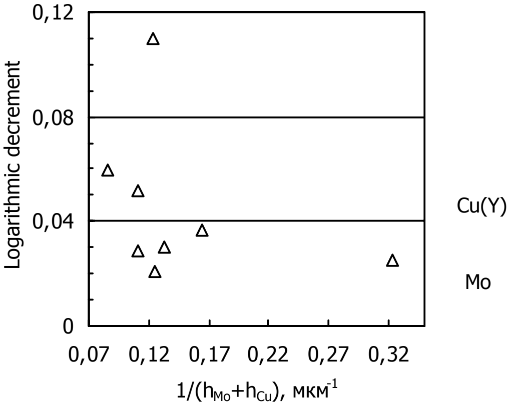

Fig.3. Logarithmic decrement as a function of inverse bilayer thickness.

The author supposes that internal thermal stresses appeared during the MMC cooling are such a factor. These stresses are the functions with argument of ($h_{Cu} / h_{Mo}$) and its can be estimated as

$$\sigma_{Mo} = -\int_{T_i}^{T_f} \frac{\dfrac{E_{Mo}(T)}{1-\nu_{Mo}}(\alpha_{Mo}(T) - \alpha_{Cu}(T))}{1 + \dfrac{h_{Mo}}{h_{Cu}}\dfrac{E_{Mo}(T)}{E_{Cu}(T)}\dfrac{1-\nu_{Cu}}{1-\nu_{Mo}}} dT$$

$$\sigma_{Cu} = -\int_{T_i}^{T_f} \frac{\dfrac{E_{Cu}(T)}{1-\nu_{Cu}}(\alpha_{Cu}(T) - \alpha_{Mo}(T))}{1 + \dfrac{h_{Cu}}{h_{Mo}}\dfrac{E_{Cu}(T)}{E_{Mo}(T)}\dfrac{1-\nu_{Mo}}{1-\nu_{Cu}}} dT ,$$

where $E$, $\nu$ and $\alpha$ with relevant subscripts are Young's modulus, Poisson ratio and linear expansion factor of copper and molybdenum respectively, $T_i$ and $T_f$ are initial and final temperatures respectively.

Fig.4 shows dependence of the calculated residual thermal stresses (tensile) on the quotient $h_{Mo}/h_{Cu}$. Actual stress level depends on relaxation processes connected with mechanical interaction of constituents in the interface zones. Also, Fig. 4 presents influence of $h_{Mo}/h_{Cu}$ on experimentally measured mechanical quality $Q = \pi / \delta$.

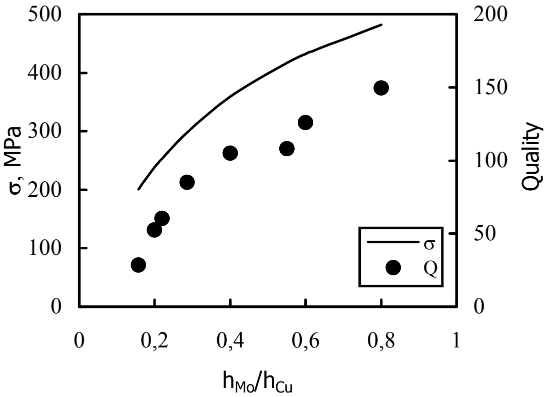

Fig.4. Mechanical quality of the MMC and residual stress in Cu(Y) layers versus $h_{Mo}/h_{Cu}$.

Parabolic rise of Q can come out from strain hardening of Cu layers under thermal stresses. Presence of twins also indicates these layers hardening.

1. F. Kavarana, K. Ravichandran, and S. Sahay *Scripta Mat.,* **42**, 10, 2000, 947-954.
2. N. Grechanuk and V. Osokin *Probl. Spets. Electrometall.*, 4, 1993, 35-39 (in Russian).
3. V. Kuzmenko, Yu. Lugovskoi, N. Grechanuk V. Osokin and O. Vdovychenko Abstr. 2$^{nd}$ All-Union Symp. "Synergetics", Moskow, 1991, 84 (in Russian).

# IMPACT OF THE HIGH-SPEED HEATING ON SHAPE MEMORY EFFECT IN ZrIr

**Kudryavtsev Yu.V., Semenova E. L.(1)**
G.V. Kurdyumov Institute of Metal Physics, National Academy of Science of Ukraine, Vernadsky Str. 36, 03142, Kiev, Ukraine, kudra@imp.kiev.ua
(1)Frantsevich Institute for Problems of Material Science of NASU,
Krzhyzhanovsky Str. 3, 03680, Kiev, Ukraine, selena@materials.kiev.ua

This study presents new findings in the field covering alloys that possess high-temperature shape memory effect. Now the ZrIr equiatomic alloy with the temperature of martensitic transformation about 1000 °C can be added to the known previously ZrRh, TiRh, TiPd equiatomic compounds that have the highest temperature shape recovery about 680 $^{o}$C.

As starting materials for synthesis of the ZrIr alloy iridium rod and iodized zirconium with a nominal purity of 99.9 wt. % were used. The alloy containing 50 at. % Ir was melted in an arc furnace under an argon gas atmosphere. In order to ensure a complete melt the ingot was remelted four times and then was cast in mould. The weight losses on preparation did not exceed 0,05 wt. %. For the further investigation specimens have been prepared by spark-cutting slices with the parameters 0,8mm×1,5mm×20mm. Electrical resistivity analysis method and thermomechanical test, performed by a three-point bending scheme were used in the study.

Investigation of the ZrIr alloy capability to restore its shape on heating after preliminary deformation on cooling was carried out by using the installation applied earlier [1] but with somewhat modified electric furnace. The sequence of the ZrIr thermomechanical test was the following: heating of specimen in unloaded state up to the temperature known to be higher than $A_f$, loading of specimen, its cooling under the load down to temperature lower than $M_f$, undoading, heating of the unloaded specimen deformed plastically in the range of temperatures of direct transformation up to the temperature higher than $A_f$. The heating rate was about 10$^{o}$/min. Five cycles were carried out with the same ZrIr specimen. In each cycle the ZrIr specimen underwent deformation on about ~0.5 mm. The total accumlated deformation (size of the bend) was more than 2,5 mm in five cycles. The reverse transformation sequence B19'→B2 in ZrIr was not registered at the bend-temperature curves. Nevertheless it seemed to take place, as it was be demonstrated by curves of the electrical resistance recorded repeatedly with the same specimen and data of the high-temperature X-ray diffraction analysis [1, 2].

The increasing of diffusive mobility of atoms in ZrIr may influence reverse transformation and therefore it also may influence the process of shape restoration by changing the transformation kinetics from martensitic to diffusive one. It is also possible that the reverse transformation in ZrIr likely ZrRh runs according to martensitic kinetics, however upon slow heating up to $A_s$ the relaxation of elastic stresses arised on direct transformation.

We assumed that there was a good probability that activization of diffusive processes could have an impact on the character of the B19'→B2 reverse transformation in ZrIr whose transformation temperatures are higher than those in ZrRh. For the purpose of suppressing of diffusive processes the rate of heating of specimen was decided to increase substantially. To do this, the special device was constructed (Figure 1b). It involved two thin-walled metallic coaxal tubes. One of them was used for loading of specimen, the other one served as a support for specimen. The specimen was set into the device. The device along with the specimen was inserted in vertical shaft furnace, heated up to 1080$^{o}$C, the temperature known to be higher than $A_f$ for ZrIr. Then the specimen was loaded by P=600 gr and cooled under the load down to 20 $^{o}$C by removal of the device from the furnace. The amount of the bend of the specimen was measured by micrometer (it came to 0.7 mm) and then the specimen was sharply inserted in hot sharf furnace again using thin wire made from chromel and was allowed to stay there to its heating up to 1080 $^{o}$C (the temperature was estimated by the specimen colour). For the small masses of both the specimen and the wire the heating occured rapidly. Then the specimen was pulled out from the furnace and cooled to 20°C. The bending measured 0.2 mm. So the restoration of shape added up to about 71%.

The many times repeated experiment with different specimens of the ZrIr alloy under different amounts of initial deformation revealed that the restoration of bend is in the range 70-75%. In this experiment the alloy was heated with rate about 100°C/sec whereas in the first experiment it was heated with rate more than 100 times less.

So as it was expected in the light of isostructurality of both original ZrRh and ZrIr phases and their transformation products the equiatomic ZrIr alloy having been deformed on cooling happened to be capable to restore its shape on heating under specific conditions.

Undoubtedly, the mechanism of influence of diffusive processes on the reverse transformation in ZrIr accompaning by SME requires further study.

We think that multicomponent alloys based on the equiatomic ZrIr alloy may get the full shape restoration at the temperatures close to 1000°C. The alloys based on equiatomic compounds formed by transition metals of IV group (Ti, Zr, Hf) with platinum group metals are considered to be with good prospects as the materials possessing high-temperature SME.

## References

1.E.L.Semenova, Yu.V.Kudriavtsev “Structural Phase Transformation and SME in ZrRh and ZrIr”, Metallophysica, 1991, 13 No7, c. 118-122.

2.V.N. Yeremenko, E.L. Semenova, T.D. Shtepa, Yu.V. Kudryavtsev "X-Ray Study of the ZrRh- and ZrIr- based phases at high temperatures", Dopov. Akad. Nauk Ukr. RSR, 10(A) (1978), 945-947.

3.E.L. Semenova, Yu.V. Kudryavtsev, "Structural Phase Transformation and Shape Memory Effect in ZrRh and ZrIr", J. Alloys and Compounds, 203(1994), 165-168.

# STUDY HEAT RESISTANCE SINTERED TITANIUM ALLOY Ti – Cr – TiC

**Petrova A. M.**
Frantsevich Institute for Problems of Materials Science of NASU,
3 Krzhizhanovsky St., Kiev, 03142, Ukraine,
E – mail : serdyuk@materials Kiev. ua

The purpose of the given work is to research the influence of chromium and carbide of titanium on heat resistance of sintered titanium alloy Ti – Cr – TiC. The titanium alloy is used in the nodes of friction both under room and raised temperature. The investisation of its heat resistance is an actual problem.

The research was conducted on sintered samples of unalloyed titanium and titanium alloy of the composition Ti – Cr – TiC, made on the base of powder of electrolytic titanium by method of the cool pressing and the following caking in vacuum 0,13 Steps under alike technological mode.

The test on toughness of sintered samples was conducted on the machine PRV – 302 with sprain and bend at velocity of lo ading $0{,}11 \cdot 10^{-5}$ m/c, in vacuum 0,133 Steps, in interval of the temperature 20 – $1000^0$ C.

The structure of sintered materials os explored, the results of the comparative test of toughness on bend and sprain in interval of the temperature 20 – $1000^0$ C are received, the diagrams of sprain of titanium materials depending on loads and the temperature of the test are built, the dependency of the relative lengthening of materials depending on the temperature of the test is installed, the fractographical research of the surface of the dog – leg materials is conducted.

It is shown that toughness on bend of unalloyed titanium forms 1000 MPa under room temperature, it sharply falls with inereasing of the temperature and it decreases in two times under $250^0$C, but it forms 10 MPa under $1000^0$C. Toughness of the alloy Ti – Cr – TiC forms 750 MPa under room temperature and it saves on this level betore the temperature $250^0$C, but then it falls sailledly, remaining on 10 – 300 MPa above that unalloyed titanium. Toughness of the alloy exceeds toughness of unalloyed titanium, as from the temperature $100^0$C. Dependency of toughness at sprain from the temperature carries such regularity, as under bend However, according to its value toughness at sprain is lower in two times than under bend. The Samples of unalloyed titanium suffer significant plastic deformation at sprain in all interval of investigated temperature, then the area of plastic deformation on diagrams of the sprain exists for titanium alloy at the temperature $\geq 500^0$C. Relative lengthening of the samples of unalloyed titanium remains constant value before the temperature $500^0$C and forms 10 %, then it sharply grows, reaching under $1000^0$C 85%.Relative lengthening forms 2 – 5 % for titanium alloy before the temperature $700^0$ C, then it slowly grows and forms 17 % under $1000^0$C . Consequently, the turning of the material from frail condition in plastic exists for titanium alloy with increasing of the temperature. Conditionally it is possible to consider, that transition in plastic condition occurs at the temperature ~ $700^0$C, above which the relative lengthening exceeds 5%, but toughness practically falls before the value of unalloyed titanium.

Thereby, unalloyed titanim suffer significant plastic deformation in all investigated warm – up interval that is particularly expressed at the temperature $\geq 500^0$C increasing of the temperature of the test is also accompanied by significant softening of titanium. The alloying of titanium base by chromium, as well as presence of hard enabling of the carbide of titanium on border grain of titanium base, reduces the plasticity of titanium greatly and promotes the conservation under raised temperature of toughness of alloy Ti – Cr – TiC is higher on 10 – 300 MPa in interval of the temperature 100 – $1000^0$C, in contrast with unalloyed titanium.

# CONSTITUTION OF THE AS–CAST ALLOYS OF THE Al–Cr–Fe SYSTEM IN THE RANGE OF COMPOSITIONS 50–100 at. % Al

**Khoruzhaya V.G., Pavlyuchkov D.V., Korniyenko K. Ye., Martsenyuk P.S., Velikanova T.Ya.**
Frantsevych Institute for Problems of Materials Science, NASU,
Krzhizhanovskogo, 3, 03680, Kyiv–142, Ukraine, dimpav@ipms.kiev.ua

The wide usage of aluminium alloys, due to their low densities, is known well. Doping of aluminium by iron and other d-transition elements opens new opportunities for use of these alloys. So, for example, these elements serve as ligature for modifying of aluminium with the purpose of high-strength alloys creation. Recently the aluminium systems became very interesting for scientists because the probability of quasicrystalls formation in these systems. The quasicrystalls have characteristic properties like as corrosion stability, high hardness, low constant of friction etc. They are already known for application as dispersers for high-strength steels and as components of new type of aluminium composites; as high-temperature resistant coverings, as absorbents of sun energy, hydrogen accumulators, thermo-elements, catalysts etc.

The Al-Cr-Fe system that is studying by us, is insufficiently investigated in the range of compositions 50-100 at.% Al. Literature data contain particular information of the elements of isothermal sections in the temperature range 600–1150 °C [1-3]. However, information on phase equilibria in the range of compositions 75-90 at.% Al is absent.

According to the data of [4], the ternary compound $Al_{81}Cr_{11}Fe_8$ had been defined at examined range of compositions. In [5] formation of the quasicrystal phase with icosahedral symmetry being present in the alloy of composition 75 ± 0,5 at.% Al, 12 ± 1 at.% Cr, 12 ± 1at.% Fe is reported.

In present work the investigation of constitution of as-cast Al-Cr-Fe alloys containing 50 to 100 at. % Al with the purpose of ternary compounds search and character of the formation establishment, is carried out. On the basis of obtained data the liquidus surface projection of the investigated system is plotted (Fig.1).

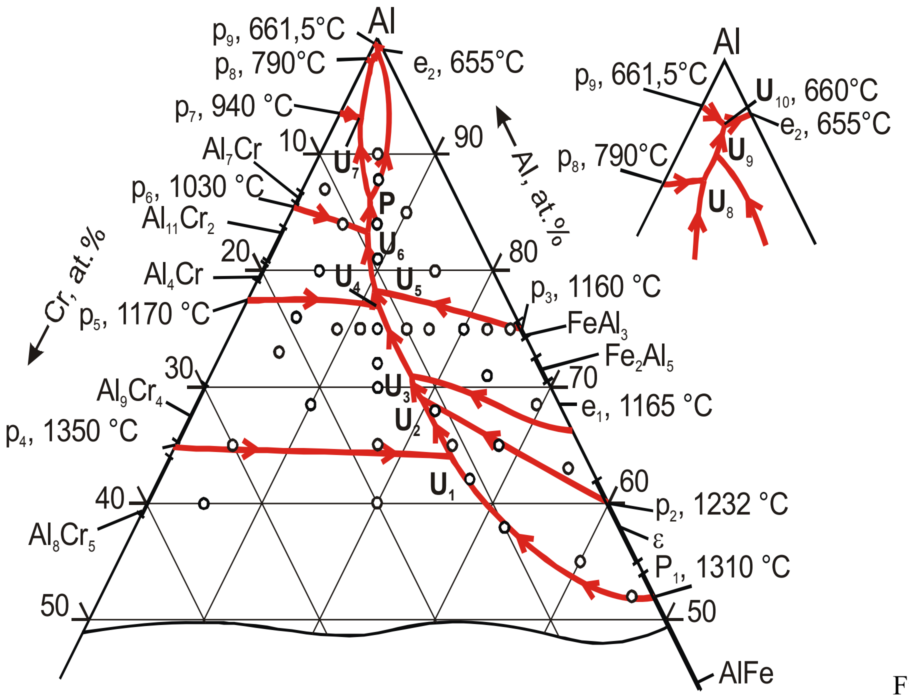
p9, 661,5°C
Al
p8, 790°C
e2, 655°C
p7, 940 °C
Al7Cr
10
90
Al, at.%
U7
p6, 1030 °C
P
Al11Cr2
U6
20
80
Cr, at.%
Al4Cr
U4
U5
p3, 1160 °C
p5, 1170 °C
FeAl3
Fe2Al5
30
70
Al9Cr4
U3
e1, 1165 °C
U2
p4, 1350 °C
U1
60
40
p2, 1232 °C
Al8Cr5
ε
P1, 1310 °C
50
50
AlFe
Al
p9, 661,5°C
U10, 660°C
e2, 655°C
p8, 790°C
U9
U8

Fig. 1. Liquidus surface projection of the Al-Cr-Fe system

38 alloys were melted with the purpose of investigation of the ternary system. For it's preparation aluminium A-995 (purity 99.995 wt.%), metallic purified chromium and carbonyl especially pure iron were used. The melting was carried out in the laboratory arc furnace with a nonconsumable tungsten electrode under an argon atmosphere (pressure 50-80 kPa) that had previously been gettered by melting of titanium. The research of samples in as-cast state was carried out by LOM, XRD, EMPA and DTA methods.

On the basis of EMPA data, which were confirmed by XRD, for the first time it was shown that the field of primary crystallization of a phase based on the iron – chromium's solid solution stretches in the ternary system up to 64 at.% Al, similarly to the forming binary system Al-Cr, at the contents of iron close to 25 at.%, being narrowed by aluminium up to 52 at.% with increase of the contents of iron down to the forming Al-Fe system. During transition to ternary system the peritectic character of crystallizations of the five intermediate phases, which formed in the Al-Cr system ($Al_8Cr_5$, $Al_9Cr_4$, $Al_4Cr$, $Al_{11}Cr_2$ and $Al_{13}Cr_2$) is remaining. The as-cast ternary alloy's microstructures testify about that and illustrate the structure typical for the peritectic reactions. The liquidus temperatures of alloys containing 50 to 12 at.% Cr determined by DTA decrease by iron content increasing, i.e. liquidus surfaces of the phases on the basis of Al-Cr compounds fall deep into the ternary system.

The lower liquidus temperatures of ternary alloys in comparison with alloys of the Al-Fe system, by increase of Cr content in them also testify to fall of liquidus surfaces of the phases, which are formed in the system Al-Fe (AlFe, ε, $Al_5Fe_2$, $Al_3Fe$), deep into the ternary system. Such fall of liquidus surfaces deep into the ternary system from forming binaries results that in the ternary system the processes proceeding by monovariant curves, which correspond to joint crystallization of phases on the basis of forming binary compounds, are carried out at lower temperatures, than invariant processes with participation of the corresponding phases in forming binary systems. Thus the change of crystallization's way of phases AlFe and $Al_5Fe_2$ was observed.

In the alloys containing more than 85 at.% Al, with an approximately equal ratio of Fe and Cr, in ternary system position of the field of primarily crystallization of ternary compound $Al_{81}Cr_{11}Fe_8$ (ν) founded before, was established for the first time. It was shown, that it formed by twice peritectic reaction $L+Al_3Fe+Al_{13}Cr_2 \leftrightarrow \nu$. The extension of the field of primarily crystallization reaches 98 at.% Al, and the temperature interval is 1010-740°C.

In the range of compositions rich in aluminium by comparative DTA results for the alloys Al98-Cr1-Fe1 and Al98-Fe2 it was shown first, that the lowest liquidus temperature of alloys is the temperature 655°C corresponding to the binary eutectic $L \leftrightarrow \langle Al \rangle + Al_3Fe$ in the Al-Fe system.

## References

1. Kornilov I.I., Mikheyev V.S., Kornyenko-Gracheva O.K., "Phase diagram of the ternary system Fe-Cr-Al", "Stal'", **5/6**, 57-59 (1940).
2. Chabb W., Alfant S., Bauer A.A., Jablonowski E.J., Schober F.R., Dickenson R.F., „Constitution, Metallurgy and Oxidation Resistens of Fe-Cr-Al Alloys", Battelle Memorial Institut, Columbus, (1958).
3. Palm J., "The Al-Cr-Fe System - Phases and Phase Equilibria in the Al-rich Corner", *J. Alloys Compd.*, **252**, 192-200 (1997).
4. Sui H.X., Li X.Z., Kuo K.H., „Hexagonal $Al_{81}Fe_8Cr_{11}$ with $a$=4.00 nm and $c$=1.24 nm", *Philos. Mag. Let.*, **79**(4), 181-185 (1999).
5. Ziani A., Michot G., Pianelli A., Redjaimia A., Zahra C.Y., Zahra A.M., "Transformation of the Quasicrystalline Phase Al-Cr-Fe Induced By Rapid Solidification", J. Mater. Sci., 30, 2921-2929 (1995).

# CREATION OF THE REGULAR MACROSTRUCTURE OF THE LAMINATE CERAMIC FOR THE HEAT RESISTANCE INCREASE

**Frolov A.A.**
Frantsevich Institute for Problems of Materials Science, of NASU, 3 Krzhizhanovsky St.,Kiev, 03142, Ukraine, E-mail: ipms(g),alfacom.net.

The laminate ceramic materials with double-sided protective coatings are used for the production of the chemical devices and containers components implying in the processes of thermo-chemical treatment of chemical compounds, [I], The heat resistance is the cardinal property determining the efficiency of the material in such conditions. It is depends on the sizes and shape of articles and on the heat exchange with the environment. More then 20 heat resistance criterions of the various ceramics and the different service conditions were developed [2]. The determination of the heat resistance of laminate ceramic materials is more complicated than that is for one-layer ceramics. The problem of the thermal expansion coefficient co-ordination exists.

It was proposed to use the coefficient of the shape and size for the heat resistance description of laminate ceramic material [3] (the parameter has inverse magnitude of the factor of the shape and size of article [2]). The corresponding formula of the laminate ceramic samples is:

A $T_{dexL}$ = *R/Sf*

(1),

where: A $T_{desl\_}$ is temperature drop leading to for standard sample destruction;

*R* is heat resistance criterion.

*Sf* is a coefficient of the shape and size of samples (or articles);

*Sj* is a coefficient depending on tensions between the ceramic layers. The *Sj* equation may be written in the general case [3]:

•V $^=$ *jfofiub.. '^front. 'Sfbound '^ hound fai*

(2),

where: S/^. is shape and size coefficient of substrate;

*Sfcoat* is shape and size coefficient of coating; *Sfbound* is shape coefficient of the boundary between the substrate and coating; *Shmmtifai)* is the size coefficient of the boundary between the substrate and coating. It is a function of tensions, o\.

All coefficients $S_{fsilh}$, $S_{fcoah}$ $S_{fboimil}$, $S_{hmin}$*d(^* and *Sf* are more than 1, if samples or articles have the size more than the standard sample. *Sf* must be increase if any *S* coefficient increases.

One can compare two laminate ceramic samples which have equal form and size, but different ceramic materials. It may be written, according to (l)and(2):

(3),

where: AT^,,.,/, AT^,/, *S,* $^2$ and *S,*- are destroying temperature drop and form and size coefficients of compare samples.

The form and size of compared samples may be defined as standard. Then *S/* (in (I)) mast be equal to 1.

If the substrate of laminate ceramic sample is made of the fragments being fasten together by the outer layer material (coating material) then the coefficients >$/«,,,, and $S$^$_{OJm}$/ will be remain equal to 1 as the form and size of coating and the form of boundary between substrate and coating will not have modification. The fragments have smaller size and simple form as compared with whole substrate and the boundary size between fragment and coating is smaller as compared with the whole boundary between substrate and coating. Therefore the coefficients *S/xuf,* and $Sh_{nutt}$*d.(oJ* will be decreasing. The coefficient *S,.,/,*$^2$ must be < S,,,,// and $S_{hmmd}$*(0T)* $^2$ must be < $S_{hmi},_d$*(a^'* and we have:

*S*

*<S*

(4) and

(5)

So the heat resistance of the laminate ceramic samples which have the fragment substrate structure must be more than heat resistance of samples which have equal form and size and the whole substrate. We neglected the influence of additional boundaries between materials of substrate and coating on the joint areas in our foregoing inferences. We neglected the modification of coating material form at the joint area correspondingly.

It was produced a layer ceramic sample substrate of a quartz ceramic. A quartz ceramic have the unique high heat resistance due to the porosity and very small thermal expansion coefficient. Experiment samples was not destroyed by the maximum heat influence in the focal zone of light energy concentrator, where the power density of •) T light energy was 9,193-10 KW/M (with reflection account-3,5-$10^3{}_K$W/M$^2$) [4].

It was produced double-sided protective coatings of niobium pentaoxide. The heat expansion of $Nb_2O_5$ ceramic have the negative value area of thermal expansion coefficient in temperature interval up to 650 °C [5]. The melted $Nb_2O_5$ ceramic have unique high heat resistance. It melts in the focal zone of light energy concentrator and the destruction of samples is absent.

The heat resistance increase model by the substrate ceramic parting was tested on the following way: Quartz ceramic substrate was made of fragments being fasten together by the $Nb_2O_5$ solder [3]. Obtained fragment rings and the whole substrate rings have equal form and size. Dish substrates were produced having similar form and size, but one of them had substrate of large plate, the second one had the fragment plate substrate. The double-sided protective coatings of Nb2O$_5$ was melted on the substrates of the rings and dishes in the focal zone of optical furnace.

The tests of 4 litre capacity dishs were carried in the manufacturing conditions in the prosess of thermochemical treatment of high purity niobium hydrate. Acoustical emission was observed without special apparatuses application at the time of cooling of the dish with large plate substrate. It is indicative of the crack generation exist in the article. At the same time the acoustical emission was absent in the cooling processes of dish which had fragment plate ceramic substrate. The fragment substrate dishes too had 1500 thermocycles [1] and had no destruction traces.

The heat resistance of rings with fragment and whole substrates were compared at the coating melting processes in the focal zone of optical furnace. The quartz ceramic rings were not destroyed by the maximum heat influence. Scanning in the focal zone lead only to melting of the ring surfaces. However through crack was generated in the ceramic substrate by the coating fusing processes. The double-sided coating fusing processes on the fragment substrate rings was carried out without destruction.

The coefficients S$^1$^,/, and *Shounci.foi)* in (2) of layer ceramic samples with the fragment substrate must be smaller then those of ceramic samples with whole substrate. It is possible to writ the heat resistance layer ceramic comparing:

*rag /*$(S_f'')_W$*hoie* < A and according to (5):

(6),

where the subscripts *(frag.)* and *(whole)* signify that the coefficient *Sf"* and temperature drop AT^tf. are correspond to the layer ceramic samples with fragment or whole substrate. In other words the ceramic samples with fragment substrate must have higher heat resistance than the samples with whole substrate.

**Conclusions**

It was used the heat resistance criterion for the heat resistance description of the laminate ceramic materials. It was demonstrated that the boundary area between substrate and coating laminate would be decreasing and the boundary stresses would be decreasing too during manufacturing the substrate of the laminate ceramic of fragments fasten with the soldering joints of coating material. The heat resistance of laminate ceramic materials must increase.

The testing of the laminate ceramic samples showed that the heat resistance of the samples with the fasten fragment substrate of the quartz ceramic and the double-sided protective coatings of Nb2Os would be greater than the heat resistance of the laminate samples with the whole substrate.

References

1.Фролов А.А. Керамические материалы для получения высокочистых соединений ниобия и тантала // Стекло и керамика, 1992, №7, стр. 14-15.

2.Стрелов К.К. / Структура и свойства огнеупоров.-М.: Металлургия, 1982.-215с.

3.Фролов А.А. О возможности повышиния термостойкости контейнерных изделий из керамики с двухсторонним защитным покрытием // Международная конференция "Новейшие технологии в порошковой металлургии и керамике" Тезисы докладов, 8-12 сентября 2003г. Киев Украина.-с. 349-350.

4.Ливийский, Ю.Е., Ромашин А.Г. Кварцевая керамика.- М.: Металлургия, 1974. -264с.

5.Кржижановский Р.Е., Штерн З.Ю. / Тепло физические свойства неметаллических материалов: Справочник. - Л.: Энергия. — 1978.-333с.

# WEAR- AND OXIDATION RESISTANCE SPRAY COATINGS BASED ON ALUMINIDE TITANIUM AND TIALITE

**Oliker V. E., Sirovatka V.L., Hrechyshkin Y.F., Timofeeva I.I., Gridasova T.Y[(1)].**
Frantsevich Institute for Problems of Materials Science of NASU,
3 Krzhizhanovsky St., Kiev, 03142, Ukraine, E-mail: olik@materials.kiev.ua
[(1)]National Technical University of Ukraine ,, KPI ", Kiev,03056, Ukraine

One of the attractive directions for protective of aerospace structural parts from Ti - alloys including alloys based on γ-TiAl from the friction and oxidative wear is the development of spray coatings from the elements included in these alloys. The chemical affinity between compositions of coating and substrate leads to high adhesion and durability. The phase formation of the detonation coatings from the powders Ti-50Al was investigated. The powders of alloy were prepared by crushing of ingot and mechanical alloying of the elementary powders Ti and Al. The application of the polyphase nanostructure powder materials which were activated by the mechanical alloying did the phase formation process of coatings more universal and guided, due to more active and sensitive reaction of material with a gas environment. It is shown that from the mechanically alloyed powder Ti-50Al it is possible to consolidate by the detonation-gas spray method the coating based on the tialite $AL_2TiO_5$ at oxidizing influence of working gas environment on the powder and the coating based on the titanium aluminides with inclusions TiN at nitriding influence of working gas environment on the powder. At the use of the cast microstructure powder γ-TiAl it is inherited his phase composition by coating. The work in the friction pairs of the developed detonation coatings ( based on γ-TiAl and on titanium aluminides with dispersed inclusions TiN, and from tialite), and also alloys based on cobalt, nickel and titanium were envestigated. The tialite coating was the best for work in the conditions of dry friction in a pair with the stainless steel 12X18H10T (minimum friction coefficient and minimum wear of contacting surfaces). The stable work with a minimum wear in the friction pair with a polyethylene of the mark Chirulen provide coatings based on γ-TiAl and on titanium aluminides with dispersed inclusions TiN, and from tialite. Side by side with high wear resistance the tialite coatings can protect the parts from oxidation in air up to 700 $^0$C. The development of the oxidation-resistant coatings based on Cr-containing gamma titanium aluminides. It is shown, that the Sc-microalloing of these alloys may result: the raising their oxidation-resistant (as little as 1000 $^0$C in air), refining, modification and formation of oxide dispersed strenghened structure with coherent binding between phases for achievement of increased fatique characteristics for the expansed temperature range.

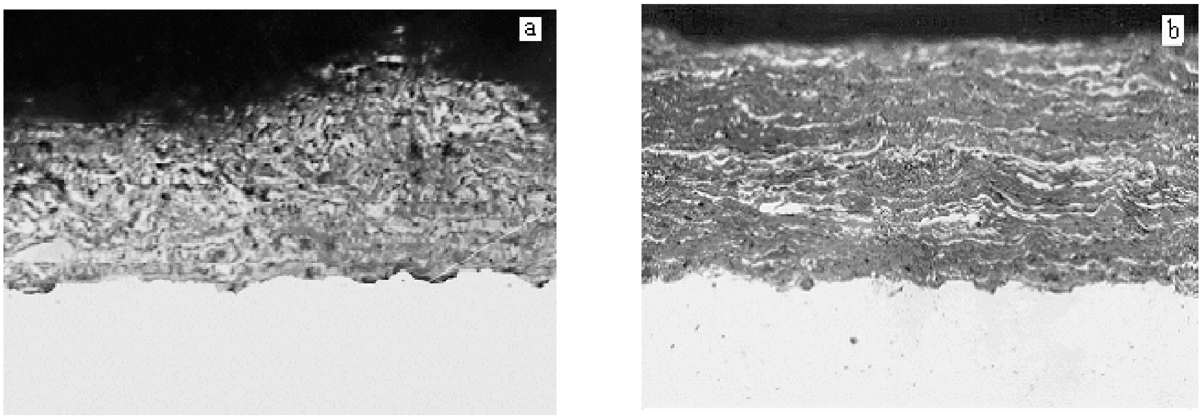

Figure 1. The optical image of the structure coatings: a- γ-TiAl; b - on basis $Al_2TiO_5$

# PHOSPHORUS DETERMINATION IN ALUMINUM-PHOSPHATE GAS-THERMAL COATINGS

**Kravchenko L.P.**, **Kurochkin V.D.**, **Kolomytcev M.V.**(1), **Romanenko O.M.**, **Derenovska N.A.**
Institute for Problems of Material Science, NAS of Ukraine, Krzhizhanovsky str. 3, Kyiv, 03142, Ukraine, vkur@ipms.kiev.ua
(1)Paton institute for electric welding, NAS of Ukraine, Bozhenko str.,11, Kyiv, 03680, Ukraine, kozjakov@ukr.net

Plasma gas-dynamic coatings of aluminum-phosphates with high heat- and wear resistance have find application in chemical industry as material for the die holes, strickle boards and other devices where such properties are used.

The powder for coating was prepared by compound of aluminum phosphate and alumina with $TiO_2$ additions (so called emery powder). Compound was drying and then pulping through the fore screen, then was baked at 850 - 900°C and finally was grinded in a ball crusher to obtain particle size of 60 - 40 μm. In result of thermal processing on the surface of aluminum oxide a particles of $Al(PO_3)_3$, $AlPO_4$ are formed with great specific surface [1]. Coating was made by supersonic air-plasmatron “Kyiv-C” and by detonation method. During coating and surface melting it loses $P_2O_5$ and a layer consisting of phases $Al_2O_3$ and $AlPO_4$ is formed.

The aim of this work is phosphorus determination that remains in a coating after air plasma spraying and design of nondestructive methods of its testing. In elaboration of analytical methods of analysis of new materials a complex of methods were used to obtain reliable results. Every method used has its advantages and weak points.

Quantitative phosphorus determination in coatings and basic powders was carried out by four methods - chemical, atom emission spectrometry (AES), X-ray fluorescence (XRF) and glow discharge mass-spectrometry (GDMS). Chemical method was used as independent test of host powder. Results of this method were used for correction of structure effects in instrumental analytical methods. This method hardly may be used for analysis of coatings because of tedious procedure of separation of coating from underlying surface.

Most efficient for this task is considered X-ray fluorescence method. Its advantage is a possibility of nondestructive analysis of nonconductive samples. This method allows also to analyze new type of materials without standard reference materials for calibration of instrument. Absorption- and secondary excitation correction was done by means of developed by authors software and data base which used method of fundamental parameters. This method allows to use any material containing elements to be analyzed. In analysis of light elements an emitting layer is several μm, thus it is necessary to take into account possible influence of a surface structure on the line intensity. Thin emitting layer allows depth profiling study of phosphorus distribution. Analysis was carried out by means of X-ray spectrometer VRA-30, excitation by W-tube, voltage 30 kV, current - 25 mA, crystal-analyzer was PE, $K_\alpha$ - line of phosphorus.

AE analysis was performed with the use of quartz spectrometer ISP-30. A sample to be analyzed was introduced into an anode crate and evaporation kinetic of phosphorus into direct current arc was measured. Hydroxilappatyte (GAP) was used as standard reference material since phosphorus concentration in it is well known. In the Fig.1 is presented kinetic of changes of spectral line PI- 253.40 nm, which is proportional to the average concentration of phosphorus atoms in the arc.

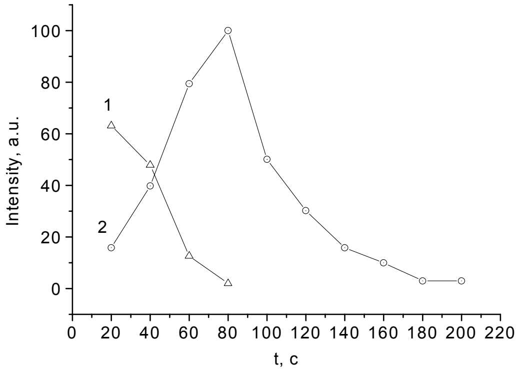

Fig.1. Kinetic of phosphorus evaporation from an anode crate in a direct current arc. 1- aluminum-phosphate; 2 - GAP.

Phosphorus concentration was measured from ratio of integrals of kinetic curves. As shows comparison, relative discrepancy of chemical and AE analyses is about 10 – 15 %.

GDMS with use of VG9000 mass-spectrometer allows to analyze all elements and isotopes of periodical system from $^{1}H$ to $^{238}U$ in concentration range 100 – $10^{-7}$ % [2]. Test specimen serves as a cathode and is sputtered by argon ions. Atoms are subsequently ionized in glow discharge and extracted for mass analysis. Discharge initiation was made by scratching a coating that results in excitation of discharge between underlying and discharge cell. As the substrate is sputtered the surface become conducting that is sufficient to sputter the sample by argon ions. Sputtering rate is of 0.2 – 0.5 μm/min and allows to conduct depth profiling study of thin layers. Quantitative analysis in this method is based on measurements of relative sensitivity factors (RSF) with standard reference materials. Distinctive feature of this method is week dependence of RSFs of the sample matrix. This allows to use reference materials containing measured elements with different matrix. However, in analysis of nonconductivity samples it is desirable to make RSFs correction to obtain reliable results.

Element concentration is found from equation:

$$[P] = RSF(^{31}P)^{*} (I\,(^{31}P^{)}/ ab) / I\,(^{27}Al),$$

where I ($^{31}P$), I ($^{27}Al$) are ion currents of isotope $^{31}P$ and $^{27}Al$ respectively; ab - abundance of isotope measured.

RSF correction was made on the base of chemical analysis and AES. As it follows from experiments, X-ray method and GDMS give overstated results compared with chemical and AES methods. This effect is a result of difference in structure of phosphate powders and HAP powder used for instruments calibration. Phosphates form a coating on the surface of aluminum oxide particles that is the reason of the effect observed. Thus XRF and GDMS methods may be used for nondestructive analysis with appropriate correction.

Results show that phosphorus concentration in deposits depends on technology of powder preparation and conditions of coatings formation. It varies from 0.5 to 16 mas. %. Measurements show that basic powders loose approximately half of phosphorus content during thermal spraying. This corresponds to the conversion of aluminum meta- to orthophosphates. Methods developed allows express and precise analysis of phosphorus content in aluminum-phosphate coatings and conduct fine depth profiling study of phosphorus distribution.

## REFERNCES

1. Будников П.П., Хорошавин Л.Б. Огнеупорные бетоны на фосфатных связках. – М.: Металлургия, 1971. – 192 с.
2. Курочкін В.Д. Дослідження молекулярних інтерференцій у плазмі жевріючого розряду при мас-спектрометричному аналізі вуглецевих матеріалів // Український хімічний журнал. – 2002. – Т.68. – №10. – С.108 – 112.

# OPTICAL PROPERTIES OF InN FILMS - BASIC MATERIAL FOR SOLAR CELLS

**Goryachev Yu. M., Malakhov V. Ya., Rud B. M.**
Frantsevich Institute for Problems of Materials Science, NASU, 3,
Krzhizhanovsky st., 03680, Kiev-142, Ukraine, E-mail: vlad.malakhov@ipms.kiev.ua

Last ten years indium nitride has focused a growing interest as III-V semiconductor material with direct band gap of about 2.0 eV and being simultaneously rather steady against excited environments and radiation. That is why it possesses potential applications in photonic devices such as LEDs, lasers, full color displays, especially high efficiency solar cells both for terrestrial and space energy sources [1-3].

The development of low temperature growth methods has resulted in remarkable improvements in the structural, electrical and optical properties of group III nitride compounds. Recently it has been revealed that the true band gap of hexagonal InN is about 0.7 eV [4-5], in a sharp contrast to a nearly 2.0 eV widely accepted and cited as a reference value in the periodical literature [6-8]. Thus the band gaps of the $In_xGa_{1-x}N$ ternary alloys system could extend over a very wide energy range (0.7 eV to 3.4 eV) that accordingly expands frameworks of practical application of these materials in PV area. In this connection the present authors report their arguments based own experimental data regarding a possible revision of the fundamental gap value of indium nitride.

From the analysis of the crystalline structure of textured InN films (AFM, SEM and RHEED data), absorption spectra and Raman spectra, the direct band gap value $E_g$~2.0 eV follows [9]. Any experimental proof of presence of oxide phase in researched films has not been received [10]. At the same time a revealed deviation from stoichiometry (nitrogen vacancies) in the nitride layers explains sharp increase in absorption spectra close 0.7 eV, connected with point defects. A measured value of 0.11 for the effective mass ratio in InN films [11] removes existing discrepancy between a narrow band gap value and wide one for the benefit of the last, i.e. that the band gap of InN is about 2.0 eV and not 0.7 eV. Potential application of InN/Si heterojunctions in PV devices, including high efficiency and radiation stable solar cells for terrestrial and space destination are also discussed.

X-ray diffraction patterns of $\alpha$-InN (wurtzite) layers deposited by low temperature plasma enhanced reactionary sputtered (LTPERS) on ceramic substrates demonstrate a very strong diffraction peak corresponding to the InN (002) plane [9]. The same result was obtained from study of the RHEED pattern of InN film on ceramics. These results show that no outsider phases except InN one were presented in the films. Some off-stoichiometric In/N ratio, with an abundance of indium inside nitride films was caused by nitrogen vacancies. A perceptible oxygen concentration was revealed in the films by Auger-investigation, probably leads to amorphous indium oxide partially forming (bound oxygen). Moreover, other inactive oxygen molecules are incorporated in voids between InN grains [9, 12].

Further, both transmittance and reflectance spectra in visible spectral range were taken to determine the band gap energy of InN thin films on $CaF_2$ (fluorite) substrates. At this procedure the band gap energy of InN layer was derived from absorption coefficient $\alpha$ and yielded $\mathbf{E_g} \cong 2.03$ eV, which is very close to value reported earlier [11].

In addition the photothermal deflection spectroscopy (PDS) technique was used to explore some peculiarities in free carriers absorption spectra for InN polycrystalline films deposited on different substrates (Fig. 1).

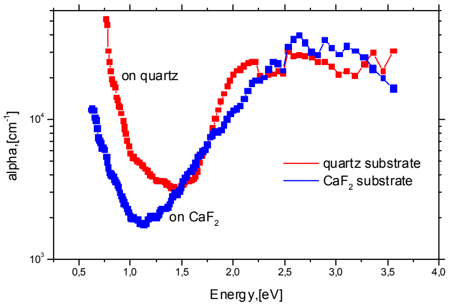

***Figure 1.*** Absorption spectra of InN polycrystalline films deposited on fluorite and quartz substrates.

As the absorption coefficient increases deeply in the range of 0.5-1.0 eV that is connected to absorption of light on free carriers (electrons), therefore inconveniently to define the contribution of point defects close 0.7 eV to absorption [13] .

The analysis of linear dependence of electron effective mass **m*** from **E**$_g$ value for different direct band gap II-VI and III-V semiconductor compounds directly specifies very enormous discrepancy (~ 200 %) in **m*** value for "narrow" bandgap (< 1.0 eV) and direct bandgap (~2.0 eV) of InN film material [14].

Therefore earlier proclaimed "narrow" band gap (0.7 eV) for pure InN increases while strong doubts. The alternate suggestion that it is defect-related will be more acceptable [15].

In order to estimate the potential possibilities of InN film material for solar cells fabrication, some theoretical and practical considerations were used. To achieve an optimum power conversion efficiency $\eta$ for solar cells based on an InN n-layer (emitter) and p-Si (base), large $\alpha$(E), minority carrier lifetime $\tau$, diffusion length **L** (at least $\alpha$**L**>3 for front side illumination) and surface recombination velocity **S** have to be combined. This can be achieved under compromise condition of optimum band gaps **E**$_g$ (~1.0 and 2.0 eV) for an efficient tandem system consisting of several stacked single cells between a large $\mathbf{I_{sc}}$ or $\mathbf{V_{oc}}$ [1].

Summarizing, an appropriate solar cell base material should exhibit a proper energy gap and a strong absorption ($\alpha_{InN} > 10^4$ cm$^{-1}$) adjusted to the solar spectrum, a dopability by carriers featuring high mobilities and long lifetimes [16]. Another important advantage of an InN/Si heterojunction in future solar cells is a protective function including protection from radiation using the absorptive InN layer as a top coating. Besides InN layers inert to influence of aggressive chemical environments are characterized by long-term stability of the electric and optical parameters.

The existing problem of heteroepitaxy of InN films on Si will be resolved by research into an appropriate buffer layer (e.g. AlN thin layer) on InN-Si interface, to match the lattice periods and improve of heterojunction operating parameters (Fig. 2).

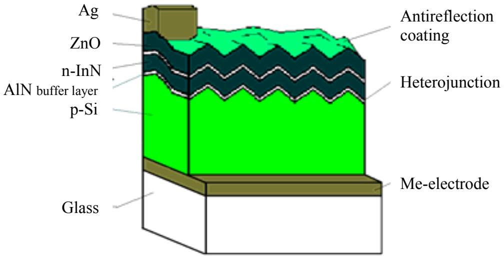

***Figure 2.*** Layer structure of InN/Si solar cell.

The fabrication of high quality InN/Si heterojunctions and its further characterization are also of great importance for manufacturing of high efficiency solar cells both for terrestrial and space applications.

## References

1. Yamamoto A. et al., *Sol. Energy Mater. and Sol. Cells*, **35**, 53-60 (1994).
2. Ambacher O., *J. Phys. D: Appl. Phys*. **31**, 2653-2710 (1998).
3. Xu Y-N., Ching W.Y., *Phys. Rev. B***48**, 4335-4350 (1993).
4. Wu J., Walukiewicz W., Yu K.M., Arger III J.W., Haller E.E., Lu H., Schaff W.J., Saito Y., and Nanishi Y., *Appl. Phys. Lett.* 80, 3967 (2002a).
5. Davydov V.Yu., Klochikhin A.A., Seisyan R.P., Emtsev V.V., Ivanov S.V., Bechstedt F., Furthmuller J., Harima H., Mudryi A.V., Aderhold, J., Semchinova, O., Graul, J., *Phys. Stat. Solidi* (b) 229, R1 (2002a).
6. Malakhov V.Ya. and Chenakin S.P., *Proc. of the ONTI IPMS*, Kiev, 119 (1977).
7. Tansley T. L. and Foley C. P., *J. Appl. Phys.* 59, 3241 (1986).
8. Westra K. L., Lawson R. P., and Brett M. J., *J. Vac. Sci. Technol.* A 6, 1730 (1988).
9. Malakhov V. Ya., *Proc. of the Euromat’99*, **9**, 75-79 (1999).
10. **Malakhov V.Ya., *Proc. of the TATF’2000*,** Extended Abstract Booklet, 351-353 (2000).
11. Tyagai V., Malakhov V. et al., *J. Sov. Phys. Semicond. (USA)*, **11**, 1257-1261 (1977).
12. Tansley T., Egan R. and Horrigan E., *Thin Solid Films*, **164,** 441-448 (1988).
13. Butcher K. S., NCSR Discussion Forum (3/22/02) *Mater. Res. Symp. Proc.* 693 (2002).
14. Nag B. R., *Phys. Stat. Solidi* (b) 233, No. 3, R8-R9 (2002).
15. Nag B. R., *Phys. Stat. Solidi* (b) 237, No. 2, R1-R2 (2003).
16. Malakhov V. Ya., *Solar Energy Materials & Solar Cells* 76 (4) 637 (2003).

# EMISSION PROPERTIES OF SCANDATE CATHODES WITH OS-IR-AL TOP-FILMS

**Getman O.I., Panichkina V.V.**
Frantsevich Institute for Problems of Material Science, NASU,
3 Krzhyzhanovski str., Kiev, 03142, Ukraine, e-mail:vv@pani.kiev.ua

The thermoionic cathodes with high current density, high stability to poisoning of residual gases and small vaporability are necessary for modern electronic devices (ED) such as display tube, television tube, travelling-wave tube. The oxide cathodes being used in electronic devices have lifetime about tens of thousands of hours but their current density are 0.1-0.15 A/cm$^2$. When the current density is rised up to 1 A/cm$^2$ their long life is decreases.

When the high current density up to 10 A/cm$^2$ during streaming operation is required for powerful ED the tungsten-barium impregnated cathodes (IC) are used. But their working brightness temperature are very high, - 1000-1100$^0$C. In that case the lot of the active matter is evaporating and is precipitating on the electrodes. Since the leakage of various kinds being appeared the tube characteristics are changed. In order to increase the reliability of ED the working temperature must be decreased.

The working temperature may be decreased on 100-150$^0$C by the thin Os-Ir-Al films, which are evaporated on the emission surface of impregnated cathodes. Also the working temperature may be decreased on 100-150$^0$C when the $Sc_2O_3$ was added to the impregnant [1, 2]. There are so-called the scandate cathodes.

The emission mechanism of the scandate cathodes is not known completely now. At the same time the emission properties of thermoemitters may be improved due to the field-emission part [3]. It is based on the analysis of current/voltage (I/U) characteristics of scandate cathodes.

The influence of Os-Ir-Al thin film on the emission properties of scandate cathodes are investigated. Three types of cathodes were selected for studies:

- IC-1 – the scandate IC with the $2,4*BaO*0,6CaO*0,1Sc_2O_3*0,9Al_2O_3$ as impregnant;
- IC-2 – - the scandate IC with the $2,4*BaO*0,6CaO*0,1Sc_2O_3*0,9Al_2O_3$ as impregnant and with the Os-Ir-Al film of about 0.5 μm thickness on the emission surface;
- IC-3 - the standard IC cathodes with $2,4*BaO*0,6CaO*Al_2O_3$ as impregnant.

Emission tests are carried-out in close-space experimental diode with the molybdenum anode in vacuum not less 1x10$^{-7}$ mm Hg in impact behavior. The cathode diameter was 4 mm, the anode-cathode distance was 1 mm. The porosity of tungsten skeleton of IC was 22%. The impulse duration was 5 μs, the relative pulse relation was 5000, the amplitude of saw-shape voltage was 1.5-3.5 kV. Current-voltage characteristics were measured as a function of temperature. The temperatures in the range 900-1200$^0$C are determined with the optical micropyrometer on the top of Mo-cap of the cathode units. In the following text temperatures are given as brightness temparetures. The I/U characteristics were measured as a function of temperature under 5 and 10 A/cm$^2$ current density.

In the fig.1-3 the I/U characteristics of the cathodes are shown. As shown from fig. 1, the anode current density of the scandate cathode (IC-1) is not rising proportionately the temperature in the Schottky region. This implies that the I/U characteristics are deviating from the "3/2 law" in the region where the anode current is limited by the volume charge. Contrary to IC-1 the I/U characteristics of IC-2 with the Os-Ir-Al film have not any features in the region of volume charge and are comfurmed to "3/2 law" (fig.2).

As shown from Fig.3, the scandate cathodes with film have smaller the anode currents under equal meanings of temperature and of anode voltage.
Under emission current density to 5 and 10 A/cm$^2$ the characteristic temperatures of IC-2 with surface film are more than 55 and 120$^0$ higher as the same are for IC-1 (see Table).

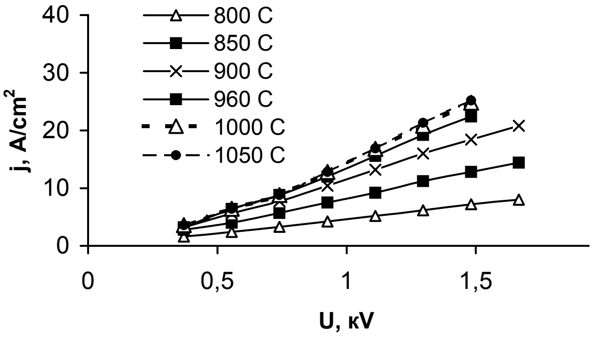

Fig.1. The current-voltage characteristics of IC-1

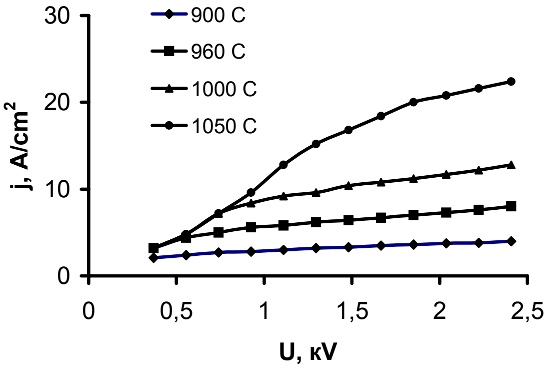

Fig.2. The current-voltage characteristics of IC-2

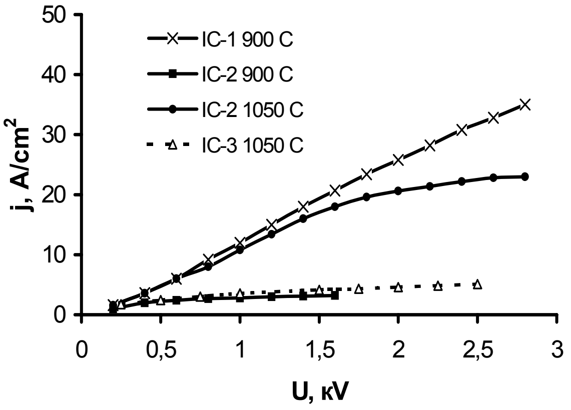

Fig.3. The current-voltage characteristics of IC-1, IC-2, IC-3 at 900 and 1050$^0$C.

The characteristic temperatures of the tungsten-barium cathodes (IC-3) are higher more than 115 and 175$^0$ in comparison with the scandate catrhodes (IC-1) (see Table).

Table - The characteristic temperatures of cathodes ($T_{ch}$)

| Cathode | $T_{ch}$, °C | |
|---|---|---|
| | 5 A/cm$^2$ | 10 A/cm$^2$ |
| IC-1 | 880 | 985 |
| IC-2 | 985 | 1050 |
| IC-3 | 1095 | 1150 |

From the results it is shown that the Os-Ir-Al film eliminates the positive effect of $Sc_2O_3$ on emission properties of tungsten-barium IC. It can be explained that the electric field would not penetrate through the metal film to the near-surface layer of the emission surface. As a result the I/U characteristics of IC-2 did not contained the field-emission part of anode current. When on the cathode surface the metal film is absent the electric field can penetrate due to $Sc_2O_3$ deep into the cathode surface and the autoemitters will be formed.

These experiments confirm the hypothesis about the thermoautoelectron character of emission of scandate cathodes.

Literature

1. Гетьман О.И., Ракитин С.П.,Шнюков В.Ф. и др. Влияние скандия на свойства МПК // Известия РАН, сер. физическая, 1994, т.58, №10.
2. Гетьман О.И., Ракитин С.П., Паничкина В.В. и др. Влияние фазового состава барий-кальциевых алюмоскандатов на эмиссионные характеристики импрегнированных катодов // Порошковая металлургия, 2000, №11/12.
3. Бех І.І., Ільченко В.В.Костюкевич О.М., Лушкин О.Є. Вплив скандію на емісійні властивості металевопористих катодів // Вісник Київського університету. Сер. фіз.-мат. науки, 2003, №2.

# ELECTRICAL CONDUCTIVITY OF POROUS MATERIALS FROM DISCRETE METAL FIBERS

**Kostornov A.G., Klimenko V.N.**
Frantsevich Institute for Problems of Materials Science of NASU,
3 Krzhizhanovsky St., Kiev, 03142, Ukraine, E-mail: v.klimenko@gala.net

High porous metal fibrous materials are applied in modern technical equipment as filters of gases and liquids, porous cooling materials, damping, capillary structures of thermal pipes, etc. Often these materials work in extreme conditions of high temperatures and mechanical loadings that demands to raise their properties. At the same time it is known, a condition of interparticle contacts substantially influences on properties of powder or fibres materials. In the present research a influence of imperfection of interparticle contacts and the sizes of particles on property electrical conductivity of porous fibrous materials is considered.

For powder materials this problem is solved and between electrical conductivity and the size of contacts directly proportional dependence [1] is established:

$$\lambda = \xi\lambda_0(1-\Theta)^{1,5}, \qquad (1)$$

where λ - electrical conductivity of porous material; ξ - the relative size of interparticle contacts; $\lambda_0$ - electrical conductivity of substance of particle; Θ - porosity. The member $\lambda_0(1-\Theta)^{1,5}$ is theoretical electrical conductivity of material.

At the same time, numerous experimental researches [2] shows, that electrical conductivity of real fibers materials have nearly theoretical values irrespective of a condition of interparticle contacts. For the decision of this problem it is necessary to establish quantitative dependence between electrical conductivity of fibers materials and the size of interparticle contacts.

The analysis which has been carried out with use of the theory of electric properties of single contact [3] has shown, that for fibous materials the resistance R and the size of contact are connected as follows:

$$R=\frac{2\rho_0}{\pi d}\left(\frac{1}{\xi}arctg\frac{\sqrt{1-\xi^2}}{\xi}-1.2\sqrt{1-\xi^2}\right), \qquad (2)$$

where $\rho_0$ - electrical resistance of substance of fibers.

The single fibrous particle of length *l* and diameter d with the regularly distributed circular interparticle contacts of diameter ξd has been considered. Two contact members with resistance R/2 form one contact [3]. The number of the contact members of fibrous particle Z is large. The first half of the fibrous particle constitute the inlet of the current and second – outlet was suppoused. At numbering the branches of a current from center of particle, resistance of branch is equal r·i + R/2, i - changes from 0 up to Z/2. For conductivity of the branches of a current take into account of distance from the center of a fibre up to the center of contact it is possible to write down:

$$\lambda_i=\frac{1}{r\cdot i+R/2}\cdot\frac{L_1 i}{l}, \qquad (3)$$

where $L_1$ - length of an intercontact site.

Total conductivity of all branches for considered model:

$$\lambda_\Sigma=\frac{L_1}{l}2\int_0^{Z/2}\frac{i}{r\cdot i+R/2}di, \qquad (4)$$

After integration of the expression (4):

$$\lambda_\Sigma=\frac{L_1}{lr}\left(Z+\frac{R}{r}\ln\frac{R}{R+r\cdot Z}\right). \qquad (5)$$

For transition from conductivity of single fibrous particle in the considered model to conductivity of a fibrous material:

$$\lambda/\lambda_0 = \lambda_\Sigma/\lambda_\Sigma(0)\cdot \lambda_\Theta/\lambda_0, \qquad (6)$$

or $$\lambda/\lambda_0 = \left(1+\frac{R}{r\cdot Z}\ln\frac{R}{R+r\cdot Z}\right)\lambda_\Theta/\lambda_0, \qquad (7)$$

where $\lambda/\lambda_0$ - relative electrical conductivity of fibrous material; - $\lambda_\Theta/\lambda_0$ relative electrical conductivity of fibrous material with perfect interparticle contacts versus porosity by the Skorokhod's model [4].

Resistance of an intercontact sites:

$$r = \rho_0\frac{L_1}{\pi d^2/4} = \frac{\rho_0 l}{Z\pi d^2/4}\ . \qquad (8)$$

After substitution (2) and (8) in (7) finally it turns out:

$$\lambda/\lambda_0 = \left[1-\frac{A}{2l/d}\ln\left(\frac{2l/d}{A}+1\right)\right]\lambda_\Theta/\lambda_0\,, \qquad (9)$$

where $A = \frac{1}{\xi}arctg\,\frac{\sqrt{1-\xi^2}}{\xi} - 1.2\sqrt{1-\xi^2}$.

The calculated electrical conductivity dependences from the relative size of interpartial contacts and length of fibers by (9) are shown in fig. 1. Dependence 1 for powder materials also is shown in fig.1. From fig. 1 it is visible that the increase of the relative length of particles *(l/d)* results to the considerable increase of the electrical conductivity of material which comes nearer to theoretical value even for small sizes of contacts.

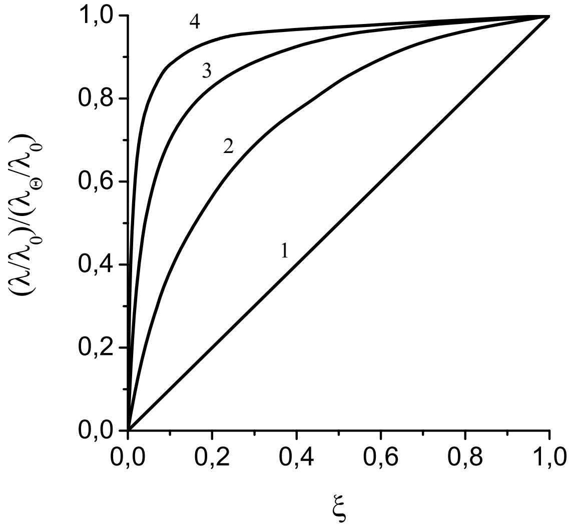

Fig. 1 The calculated electrical conductivity dependences porous powder (1) and fibrous (2, 3, 4) materials versus relative size of interparticle contacts. Relative length of fibrous particles *l/d*: 2 - 10; 3 - 50; 4 - 200

1 Роман О.В., Скороход В.В., Фридман Г.Р. Ультразвуковой и резистометрический контроль в порошковой металлургии. - Минск: Вышэйшая школа, 1989. - 182 с.

2 Косторнов А.Г. Проницаемые металлические волокновые материалы. - Киев: Техніка, 1983. - 128 с.

3 Holm R. Electric Contacts. - Berlin / Heidelberg / New York: Springer-Verlag, 1967. - 482 p.

4 Скороход В.В. Некоторые физические свойства высокопористых тел // Порошковая металлургия. - 1967. - № 6. - С. 33-38.

# METASTABLE AMORPHOUS METALLIC MATERIALS

**Hertsyk O.M., Kovbuz M.O., Bednarska L.M., Yezerska O.A.(1), Nosenko V.K.(2)**
Franko Lviv National University
6 Kyryla and Mefodiya Str., Lviv, UA - 79005, Ukraine: L_Bednarska@franko.lviv.ua
(1)Fraunhofer IFAM, Wiener Strasse 12, Bremen, Germany
(2) Kurdumov Institut of Metal Physics of NASU
Vernadskiy av., 36, 252142, Kiyv, Ukraine

The new material search in connection with medium miniturization are intensified, for example, materials that composed from crystals by dimension of 1-15 nm in the amorphous matrix [1]. It is known, that the high dispersion of crystalline phase brings to the increasing of surface energy, which has a significant influence on various physical and chemical material characterictics. Ability of amorphous metallic alloys (AMA) to controlled recrystalisation successfully applies for the aim of receiving of nanocrystal materials with the high mechanical durability, with improved m-metal properties, and also with specific catalytic ability.

Thus, research of physical and chemical properties of $Fe_{78,5}Ni_{1,0}Mo_{0,5}Si_{6,0}B_{14.0}$, $Co_{66,5}Fe_{4,0}Mo_{1,5}Si_{16,0}B_{12,0}$ AMA under conditions of low and high temperatures ((77÷773) K)) represents the high interest because of their destination application [2, 3].

Under influence of various external factors, in particular heat treatment, undergoes the changes not only the surface composition, but also the alloy structure. For example, in alloy $Fe_{78,5}Ni_{1,0}Mo_{0,5}Si_{6,0}B_{14.0\ 0}$ the content of Fe, Ni and Mo changes till 78,32; 1,11; 0,37 (atomic %), respectively, and after heat treatment 77K and 78,14; 1,15; 0,35 (atomic %) – at 673K. At temperatures above 293K the volatile molybdenum oxides $MoO_3$, have been created, and the next bonds between Fe-Si and Mo-Si substitute in the Fe-O, Mo-O and Si-O bonds.

With temperature increasing of heat treatment from 77 to 773 K the alloy structuring intensifies. Consequently the local geterogenety of energy distribution arises, that leads to intensification of its chemical activity and reflects on changes of electrochemical corrosion parameters AMA. The values of corrosion currents increase from $3{,}3\cdot10^{-5}$ A/cm$^2$ (77 K) till $16{,}7\cdot10^{-5}$ A/cm$^2$ (773 K).

As is known [4], that the process of low temperature crystallization of amorphous alloys has step character. Under heat treatment in the range of 370-450 K the reversible and irreversible changes of structural characteristics of AMA occur. In the Fe-based alloys at the initial crystallization stage has been creates the phase, which respects to typical δ-intermetallitic phase according to its structure.

The X-ray results of $Fe_{78,5}Ni_{1,0}Mo_{0,5}Si_{6,0}B_{14.0}$ surface testify about a small decreasing of interatomic distances and an increasing of dimensions of well-ordered areas in consequence of annealing under 473-673 K, that provokes the cristallization process of alloy based on iron. The new crystalline phase has been appeared at temperature of 773 K that is caused by forming of grain-oriented structure.

The analogous researches of corrosion resistance changes of amorphous alloy on cobalt base $Co_{66,5}Fe_{4,0}Mo_{1,5}Si_{16,0}B_{12,0}$, which was previously heat treated at ((77÷673) K), ), indicate on its higher stability in comparison with alloys on iron base. At the heat treatment of above >293 K it was observed the minor increasing of corrosion currents and the potential shifts in anodic direction.

1. Zolotuchin I.V. Nanocrystalline metallic materials // Physics. 1998. №1. C.103-105. (in Russian)
2. The formation of intermetallic phases upon crystallization of amorphous alloys $Co_{67,2}Fe_{3,8}Cr_{3,0}Si_{14,0}B_{12,0}$ and $Co_{66,5}Fe_{4,0}Mo_{1,5}Si_{16,0}B_{12,0}$ / Mudry S., Kotur B., Bednarska L. et al.// Journal of Alloys and Compounds. 2004. Vol.367. P.274-276.
3. Influence of annealing on the physical and chemical properties of Fe-Si-B-(Me) amorphous alloys / Bednarska L., Galadzhun Ya., Gorelenko Yu. et al.// Journal of Alloys and Compounds. 2004. Vol.367. P.270-273.
4. Alechin V.P., Honik V.A. Diffraction researches of high temperature alloys. - Moscow: Science, 1980.-pp.189 (in Russian).

# CAST INVAR AND SUPERINVAR ALLOYS FOR ELEVATED TEMPERATURES

**Rabinovitch S. V., Kharchuk M. D., Chermensky V. I., Rusin M. J.**$^{(1)}$
The Urals State technical University – UPI
Mira str., Ekaterinburg, 620002, Russia
Tel. (3432) 745961, fax (3432) 502838; E-mail: emb-ustu@mail.ru
The Urals State technical University – UPI
Kiev road, 15, Obninsk, Kaluga region, 249035, Russia
Tel. (08439) 67210; E-mail: onpptechn@Kaluga.ru

Cast superinvar alloys are the most perspective construction materials for the production of complex-profiled,-large-sized,- and co-ordinated by their thermal extension with the quartz ceramics-parts for the articles, designed for high tech. apparatus.

In the Chair of Electronic Machine-building of the Urals State Technical University (UGTU–UPI) there have been developed over twenty five novel cast alloys with a pre-set thermal extension linear coefficient (TELC). In the process of developing the alloys we have solved such essential problems as the influence of intra-crystalline liquation of components on the TELC value [1—3 a.o.], elimination of hot shortness [4, 5], introduction of the melting technologies as well as various casting methods for the alloys [6—8].

Among the alloys developed, the superinvar 32НКБЛ [7] is specific for its application in high precision articles.

Profound research for the improvement of this alloy to make it possible to use it as a material for some special parts, operating under elevated temperatures has been conducted lately together with the Obninsk Research-and Production Enterprise “Technology”.

The modern state of knowledge on the thermal extension of invar and superinvar alloys for the construction purpose is evidence to the fact that their close agreement by TELC values with quartz ceramics under temperatures over 373 K (100 °C) is not practically possible. Thus, one can speak only about an acceptable approximation to the thermal extension values of quartz in some of the temperature ranges.

One of the main demands to the thermal stability characteristics of any metallic parts, agreed by their TELC values with quartz ceramics at temp. over 373 K is that the materials for these parts should have mean TELC values in the range of room temperature to 573K (300 °C) 1,5—2 times lower than those of the superinvar 32НКБЛ. This corresponds to achieving TELC values at the level of $1,5\cdot10^{-6}K^{-1}$ in the temp. range of 20—200 °C and about $3,0\cdot10^{-6}K^{-1}$ in the range of 20—300 °C.

You can reduce the TELC of the 32НКБЛ alloys within the temperature ranges, stated above , by increasing the Co contents in it up to 6—8%, while retaining the Ni contents within 31,5—33,0%. We affirm, however, that the Co increase such as that, results in lowering the crack-resistance of the alloy.

The Ni increase beyond 33% results in increasing the TELC of the alloy in the temperature ranges of 20—200 and 20—300 °C. To make the Ni content lower than 31,5% can lead to the rise of the martensite transition point, as well as to significant TELC increase as a result of martensite formation. This is connected with the invar alloys tendency to liquate nickel to the boundaries of the structural elements (cells, dendrites). In concordance with the results of our former researches [2] the difference between the Ni content on the boundaries and in the center of the structural elements in the real conditions of cooling may achieve as much as 5% in weight. In the central parts of cells and dendrites, depleted of Ni, the zones, in which under minus temperatures the $\alpha$-phase (martensite) precipitates out, may possibly occur.

To prevent the martensite occurrence while increasing the crack-resistance in increasing the Co content, we added chrome in the prototype alloy. This alloying component lowers the martensite transition point [9, p. 219], and, for all that, as we established, increases the crack-resistance of the investigated cast alloys.

In the alloys investigated we also changed the niobium content. Niobium was introduced into the basic alloy in quantities less than its solubility limit. For all that, the electronic explore showed, that in liquating to the boundaries of the elements, Nb can concentrate there in quantities higher than its solubility limit. We thus lowered the Nb content to 0,3—0,5% in weight, to minimize the second phases occurrence.

Chemical contents of the investigated alloys, as well as their TELC-values are included in the patent description [10]. In the temperature ranges of 20—200 and 20—300 °C the mean TELC values (1,20—1,58)$\cdot 10^{-6}K^{-1}$ and (2,65—3,30)$\cdot 10^{-6}K^{-1}$, respectively have been achieved, which is significantly lower than the corresponding TELCs of the prototype alloy 32НКБЛ, which make (2,0—2,6)$\cdot 10^{-6}K^{-1}$ and (5,1—6,0)$\cdot 10^{-6}K^{-1}$, respectively.

On the base of the results obtained we selected two rated compositions of the required alloys. The first its suggested tradename is 32НКХБЛ – designed for use in the temperature range of 20—200 °C, and the second, the suggested tradename is 32НКХБЛ-1 – for use with higher temperatures 20—300 °C. The 32НКХБЛ-1 alloy differs from the 32НКХБЛ alloy only by its higher Co content, which ensures the shift of the higher temperature limit of the invar effect to the range of still higher temperatures.

Tests of the required physical, chemical and technological first of all, of the casting properties of the alloys created, have been conducted. As to the physical and mechanical properties, the novel alloys are on the whole like the basic superinvar 32НКБЛ [7]. They possess, however the necessary advantage as to their mean TELC in the temperature ranges of 20—200 °C (32НКХБЛ) and 20—300 °C (32НКХБЛ-1). This testifies to the achievement of the aim, set for the research – to develop novel alloys having mean TELC values under higher temperatures 1,5—2 times lower than the superinvar 32НКБЛ.

The alloys created have been used for the production of parts for airspace apparatus, their TELC values being coordinated with those of quartz ceramics. During the research we have worked out the methods of melting, casting and thermal treatment which provide the required combination of TELC values with the technological properties of the alloys. In the scientific respect the carried out work confirms the perspectivness of a complex alloying approach in the creation of novel cast invar alloys, which is able to provide simultaneously the required invar effect as well as the set casting properties, required for the production of shaped (complex-profiled and large-sized) castings.

The experimental part of the work, including melting, casting and thermal treatment of the alloys has been carried out in the foundry conditions with the participance and financial provision of the enterprise “RPC LINVAR”.

## References.

1. R. A. Sidorenko, S. V. Rabinovitch, M. D. Kharchuk. The research of crystallization peculiarities of the alloy 32НКД // Izvestiya vuzov. Chornaya Metallurgija. 1978. № 10. p. 144—147.
2. S. V. Rabinovitch, M. D. Kharchuk, V. I. Chermensky. Influence of microliquation of nickel on the thermal extension of cast ferronickel alloys // Izvestiya vuzov. Chornaya Metallurgija. 1994. № 10. p. 29—32.
3. O. M. Ogorodnickova, E. V. Chermenskaya, S. V. Rabinovitch, S. V. Grachev. The thermal extension linear coefficient of the cast Fe-Ni alloys and superinvars Fe-Ni-Co // Phizika Metallov i Metallovedenje. 1999. V.88. № 4. p. 46—50.
4. Patent of RF № 1.096.956. The alloy on the basis of ferrum. / S.V.Rabinovitch, M.D.Kharchuk, R.A.Sidorenko etc.
5. Rabinovitch S.V., Sidorenko R.A., Kharchuk M.D., Joffe A.Y. Cast parts from superinvar for optic devices // Optico-mekhanicheskaya Promishlennost. 1978. № 11. p. 49—51.
6. S. V. Rabinovitch, M. D. Kharchuk, V. I. Chermensky, R. A. Sidorenko. New precision cast alloys with the pre-set Thermal extension linear coefficient // Liteynoje proizvodstvo. 1994. № 1. p. 15—16.
7. ТУ В3-27-85. Castings from the precision alloy 32НКБЛ. Specifications.
8. ТУ В3-28-85. Castings from the precision alloy 36НБЛ. Specifications.
9. Precision Alloys. The directory edited by B. V. Molotilov. M.: Metallurgy, 1983. 439 p.
10. Patent of RF № 2.183228. Cast alloy on the basis of ferrum / S. V. Rabinovitch, M. D. Kharchuk, V. I. Chermensky etc. // Pablished 10.06.2002. Bull. № 16.

# PRESSURE AND SCALE DEPENDENCES OF RESISTIVE PROPERTIES OF CERAMICS

**Goryachev Yu.M., Dekhteruk V.I., Rud B.M., Siman M.I., Fiyalka L.I.**
Frantsevich Institute for Problems of Material Science of NASU
3, Krzhyzhanovsky str., Kyiv, 03142, Ukraine. E-mail: phil02@ukr.net

Pressure is known to effect both kinetic and thermodynamic properties of solids in a complex way [1,2], which is especially complex in case of multiphased and ceramic materials. The work deals with one of such problems, namely with the influence of high pressure on electron transfer in ceramics.

We have established that the main factors determining the mechanism of influence of pressure on resistive properties of ceramics are the following: the surface energy of contacting particles, friction coefficient, and breaking point of particles.

To develop a physical model for these ideas, we took the following mathematical model for the relationship between the ceramics electrical resistance $R_{cer}$ and local resistivities $R_o(x,y,z)$:

$$R_{cer} = \iiint\limits_{x,y,z} R_o(x,y,z)/(x^2y^2)\cdot dxdydz. \qquad (1)$$

Further elaboration of the model yielded the following expressions which bound the average resistivity of ceramics $R_o$ with the resistance of unit contact R, average resistance $R_c$ and radius $r_o$ of particles "A", the contact thickness δ, the contact radius $r_1$ and the average size of particles "B" ($d_o$), which here play the role of a binder forming the contact:

$$R_o=\pi/2\cdot(R+R_c)\cdot(r_o+\delta/2), \qquad (2)$$

$$R=R_B\cdot\delta/(\pi\cdot r_1^2), \qquad (3)$$

$$R_c=R_A\cdot LOG(4\cdot r_o/\delta-1)/(\pi\cdot r_o), \qquad (4)$$

$$\delta=2\cdot(Y-r_o), \qquad (5)$$

$$r_1=r_o\cdot(P\cdot(1-K_{tr})/(\tau+\sigma/d_o))^{0.5} \qquad (6)$$

Here:

$Y=((r_o+d_o/2)^2-(P\cdot r_o^2-D_{op})\cdot(1-K_{tr})/\tau),^{0.5}$
$do=2\cdot C\cdot r_o/(3\cdot(1-C)),$
$D_{op}=(P\cdot r_o^2-r_1^2\cdot\sigma/d_o)\,\sigma/(d_o\tau).$

The following characteristics of materials under study were taken as input ones:
$K_{tr}$ - the interphase friction coefficient, τ - the yield point, σ - the surface tension coefficient, $R_B$ - the electrical resistivity of the "B" phase, $R_A$ - the electrical resistivity of the "A" phase, P - the pressure, C - the volume fraction of the "B" phase. The calculations performed showed that baric-resistive properties of ceramics substantially depend on the dispersity of constituent phases.

The pressure and scale dependences of electron transfer parameters and electric resistivity of ceramics composed of two main phases (semiconductor higher manganese silicide $MnSi_{1.73}$ and dielectric boron oxide $B_2O_3$) are presented in Fig. 1-2.

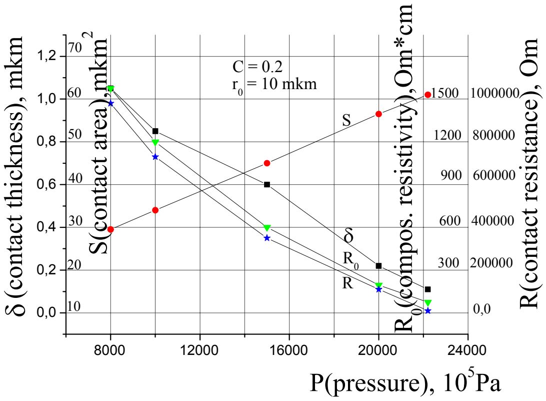

Fig. 1. The influence of pressure on electron transfer parameters in the (1-c)A+cB composite, where A - conducting phase, B - dielectric binder. For a size of "A" particles of 10 μm, c=0.2 at the resistivity of binder "B" and particles "A" 2000 and 0.1, respectively; intercontact tension 1 j/m$^2$, binder yield breaking point 0,8 GPa and the coefficient of friction between the binder and particles 0.4.

Input data for the calculations were taken from [3] and listed in the Table. They correspond to two temperatures: room temperature Tc and 1200 K (Tx). High-temperature characteristics (Yx) were determined with the functional of their temperature dependence which is linear in the frame of the used model:

$$Y_x=(Y_o-Y_{np})\cdot(T_{np}-T_x)/(T_{np}-T_o) \qquad (7)$$

Here $Y_O$, $Y_{np}$ - characteristics at room and maximal (a priori known) temperatures. In the case of interphase energy, the maximal temperature is the critical temperature, whereas for the friction coefficient and yield point it is the melting point. At these temperatures the values of the characteristics above are negligible.

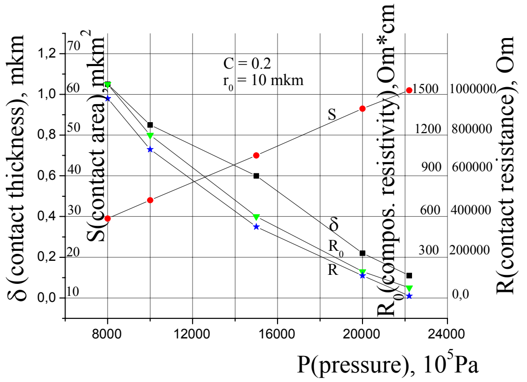

Fig. 2. The influence of the particle size of the conducting "A" phase on the electron transfer parameters in the (1-c)A+cB composite, the other conditions being equal to those in Fig. 1.

Table. Physicochemical properties of conducting ($MSi_{1,73}$ ad $CrSi_2$) and binding ($B_2O_3$ ad $Ni_3B$) phases in ceramics studied

| Фаза | T, K | σ,J/m$^2$ | Ktr | τ, GPa | Тпл, K | Ткр, K |
|---|---|---|---|---|---|---|
| $MnSi_{1.7}$ | 300 | 2 | 0.4 | 1.3 | 1440 | 6000 |
| | 1200 | 1.7 | 0.084 | 0.28 | | |
| $CrSi_2$ | 300 | 5 | 0.5 | 1.7 | 1775 | 7400 |
| | 1200 | 4 | 0.19 | 0.67 | | |
| $B_2O_3$ | 300 | 1 | 0.4 | 0.8 | 600 | 2500 |
| | 1200 | 0.6 | 0 | 0 | | |
| $Ni_3B$ | 300 | 1.5 | 0.3 | 0.7 | 1450 | 6050 |
| | 1200 | 1.3 | 0.065 | 0.15 | | |

As can be seen, the following internal parameters markedly effect the pressure and scale dependences of the resistive properties of ceramics under study: the area, thickness, and electrical resistance of interparticle contacts. Influence of particle size on resistivity was not observed. With a increasing the particle size the contact resistance decreases. In this case, however, the contact thickness increases , thus, the number of contacts in the specimen cross section, which results in compensating the influence of the contact resistance decrease.

The results obtained permit the following conclusions to be drawn: High pressure is an effective means aimed at reaching high thermoelectric effectiveness and high thermoelectric figure of merit of ceramics. An increase in pressure up to 25 kbar was shown to markedly decrease the resistance of ceramics. However, a further pressure increase causes an increase of resistance, perhaps, due to breaking ceramic particles, which results in increasing the resistance between particle pieces.

Replacement of high-resistance $B_2O_3$ binder with low-resistance one (for example, based on boron) leads to a substantial decrease in resistance of ceramics. In particular, using manganese boron (having the same conductance type with the highest manganese silicide) as a binder increases the thermoelectric figure of merit and effectiveness of ceramics.

## References

1. Тонков Е.Ю. Фазовые диаграммы элементов при высоком давлении. - М.: Наука. 1976. - 190 с.
2. Горячев Ю.М., Дехтярук В.И., Симан Н.И., Шварцман Е.И. Термические и барические зависимомти электрофизических свойств халькогенидов. // Сб. Теория и моделирование электронного строения и свойств тугоплавких соединений и металлов. - Киев, ИПМ НАНУ. 1997. - С.108-111.

Самсонов Г.В Тугоплавкие соединения М.: Металлургия. 1976. - 558 с.

# SUPERCONDUCTING THICK FILMS AND POSSIBILITIES OF THEIR APPLICATIONS IN CRYOGENIC TECHNICS AS SENSOR MATERIALS

**Shulishova O.I.**
Frantsevich Institute for Problems of Materials Science, NASU,
3, Krzhyzhanivs'ky St., Kyiv, 03142, Ukraine, e-mail: raitch@ipms.kiev.ua

The high temperature superconductivity discovery that evoked incredible expectations concerning the possibility of room temperature superconductivity achievement caused a significant decrease in public interest to conventional “low-temperature superconductors” that hardly reached hydrogen temperatures over the past decades.

However, even if these expectations come true the demands for facilities and materials that are necessary for the operation at helium level of cooling will not disappear or diminish. Electronics, e.g., remains such a field where the need for helium level of cooling will always exist. Any electronic circuit consists of passive elements – resistors and conductors – 60-80 %. These elements determine the whole circuit operation in many respects. The thermal noise electromotive force of resistor that is determined by the production of its resistance and temperature limits the threshold power of the useful signal. It is impossible to increase the sensitivity of receiver decreasing its input resistance, and the only radical measure of noise reduction is the decreasing of devices operating temperature. Circuit cryostatting in the liquid helium allows to decrease resistors thermal noise level by two orders of magnitude that will allow to decrease the threshold power of the signal received in the same times. It is especially important for the long distant Earth’s and space communications.

The thick film production process initial materials are paste-like compounds. The thick film production process is widely used in nowadays electronics to fabricate passive elements. This techniques offers some advantages over the thin film one among which there are the simplicity and lower cost of equipment, less sensitivity to contamination, the lower surface finishing class of substrates applied, higher reliability and reproduction of operating characteristics.

The thick film production process initial materials are compounds that comprise a conductive phase powder suspension mixed with glass powder in organic solvent. The necessary configuration and-thickness films are deposited mechanically through the mask on the ceramic substrate, an organic is removed by drying, and after wards films are subjected to heat treatment. The films obtained in such a manner comprise not uniform disordered structure of three-dimensional chains of randomly oriented contacts that are formed by the conductive phase particles in the glass matrix.

The quantity of conductors in large-scale integrated circuits may be so big that their total input in the resistance becomes comparable with the good resistor input. As thick films comprise disorder media in which a substantial resistance growth is observed with the temperature drop, it is clear that at the circuit cryostatting aimed to improve resistors operation conductors become a source of substantial additional power losses and circuit operation parameters degradation. Thus, the problem of such thick conductor films creation that would not degrade circuit operation at the cryostatting but would fulfil their role as ideal as possible reducing the electrical loss to zero at all, arises. We have solved this problem by means of pastes based on superconductive niobium carbides, nitrides and carbonitrides having $T_c$ 11.1 K, 16,3 K and 17,9 K respectively.

Carbides, nitrides and carbonitrides have a simple crystal structure B1 (of NaCl-type) and form a wide class of superconductive compounds having unlimited mutual solvability and wide areas of homogeneity. It allow to obtain superconductive materials and, correspondingly, superconductive thick films with virtually and desirable superconductive temperature $T_c$ from the lowest one to 18 K.

Superconductive thick films properties do not depend only on chemical composition, but on the superconductive component grading composition as well as the superconductive and dielectric paste components quantitative relation.

Thus, changing the chemical and grading composition of the superconductive component and its quantitative part in a paste, it is possible to obtain superconductive thick films varying slightly their properties combination in superconductive and normal state:

- $T_c$ from the lowest one to 18 K,
- superconductive width $\Delta T_c$ from the part of one degree to 18 K,
- film resistance in the normal state, $\rho_n$, from the tenth parts to tens Ohm/□ ,
- temperature coefficient of resistance TCR in the normal state positive, negative, or practically equals zero.

Superconductive thick films critical fields $H_c$ are several orders greater than those of the initial components in solid state, their critical currents $I_c$ depend on phase ratio and comprise $10^2$ - $10^4$ A/cm$^2$ at 4,2 K.

It is known that superconductive metals and compounds possess much lower conductivity in the normal state that normal metals such as copper and silver. Introducing normal metal with high conductivity, e.g., silver, in the paste compound one can obtain unique films having such a high conductivity at temperature higher than $T_c$ that cannot be achieved for any superconductors and having zero resistance at temperatures lower than $T_c$.

Thick films based on niobium carbides, nitrides and carbonitrides properties allow to apply them as:

- conductive elements with zero electric losses in integrated circuits of helium level of cooling;
- conductivity elements having superconductivity at $T<T_c$ and extremely high conductivity at $T>T_c$ (compounds with silver);
- thermal switches, switches that are converted in the normal state by the current passed;
- resistance cryogenic thermometers with the linear dependence (transition to the superconductive state with wide $\Delta T_c$ );
- sensors for liquid helium level gauges having reliable potting automatization (high, small TCR, $T_c$=4,2 K);
- materials for superconductive screens having any dimension and form deposited by the paste spraying technique.

Apart from practical application in cryogenic electronics, instrument engineering, and cryogenic engineering superconductive thick films may be used in scientific researches as model systems for phase transition investigations, for superconductivity and localization competition, for laws of percolation theory study as well as for the investigation of charge effects role in systems having Josefson's junctions.

# THE FEATURES OF NONEQUILIBRIUM STATE AND PROPERTIES OF W-NI-CU CONTACT WORKING LAYER UNDER COMMUTATION OF CURRENT IN THE OIL

**Minakova R.V., Golovkova M.E., Gorban' V.F., Popov S.M., Kizimenko F.A.(1)**
Francevich Institute for Problem of Materials Science of NASU, Kyiv,
Krzhyzhanovsky Str., 3, Kyiv-142, 03680, Ukraine, e-mail: 29min@ipms.kiev.ua
(1)OAO «Ukrainian Transformerbuildings Institute» (VIT),
Dnepropetrovsky Str., 11, Zaporozh'e, 69069, Ukraine, e-mail: postmaster@vit.zp.ua

The composite materials on base of refractory W, Mo, Cr, C and electric conductional Cu, Ag and their alloys hold a firm place among the electrical contact materials on account of their high level of resistance to erosion in the extremal condition of are discharge influence.

The support spot of arc is the place, where under influence of power heat stream the assemblage of physical-chemical process occurs. Gessinger and Melton [1] have stated that the evaporation of formed liquid is the basic mechanism of erosion for this kind of contacts operating in air and $SF_6$. In the work [2,3] an evidences were received of contact material carry-over in the liquid and solid phases. The fact was stated too, that brittle cracks develop as effect of thermal stresses gave rise to high velocity of heating and cooling of contact material within the are foot area. It was showed that single cracks could be merged in the net and go deeper into contact work layer under influence of surrounding. These facts and brittle explosion-similar fracture under influence of voltage-break-down confirmed of hard phase take part in electrical erosion. However it is necessary to take into consideration that secondary structure (not source) is failing, what is forming at the contact work layer during the first commutation cycle. In such case for ascertain of secondary structure role under of current commutation if is necessary to collect of date about its formation and failure as a result of influence different interior and exterior conditions. In this paper an attempt to analyze of feature of formation and properties of secondary structure in the working layer of W-Ni-Cu contacts under arc discharge influence in the oil (as the most of destructive medium [2, 4]) is presented.

In the work W-Ni-Cu contacts of mark КМК-Б20 (Ni – 1,5-3%; Cu – 41-47%; W – residue), were investigated. They were received by method of powder metallurgy according to scheme: simultaneously reduction of W-Ni powder – mixing of source charge – compacting – sintering – impregnation – control of properties. The method of working layer structure and some properties analysis: optical and scanning electron microscopy, local X-ray micro-analysis, method of micro-hardness. The contacts were tested in the contactor of switching device PHTA-III-35/1250. The testing on electrical wear resistance was carried out in volume 25-50 th of switches under follow regime: current – 1190-1250 A; rebuilding voltage – 662,5-1262 B; time of arcing – 10-19 ms.

Macrostructure analysis of contacts surfaces showed its enriching by easy-melted component, cover by soot and forming coarse relief. The bubbles in refractory component (at the different stages of them evolution up to explosion) are another feature of surface relief. Microstructure analysis of cross section evidences about presence in the contacts working layer of discharge heat influence region. It is shown that zone, what adjacent to source structure, depleted of copper, but remains valid of composite and W-Ni geterogeneous agglomerates structure feature. At the zone, what adjacent to surface the segregation of structure components, formation of extended fields of refractory and light fusible components with pores and cavities are observed. The fields of refractory component are formed as result of compacting, sintering and following joining by sintering of agglomerates to these fields in the presence of liquid phase. In the source station geterogeneous agglomerates are shown by exterior W-layer and interior volume from alloy on the Ni-base (or inter-metallic in W-Ni system). The process of sintering and joining by sintering of agglomerates is accompanied by disintegration of them and redistribution of composing element. The following action of heat stream causes of refractory component melting and equalization of Ni and Cu content in it. The proof of this fact was visualized by X-ray microanalysis in X-rays of these elements. Practically uniform Ni and Cu distribution in the refractory component and its dispersing evidence about growth interaction of elements in the system W-Ni-Cu under influence of arc discharge power heat stream. Carbon from product of oil distraction falling mithin the secondary structure under its formation distributes in this structure non-homogeneous. It concentrates under surface of secondary structure, in the wall of bubbles and pores. This distribution of carbon was verified by measurements of working layer micro-hardness. It is established, that layers under surface show: hardness 12-35GPa, modulus of elasticity 280-420GPa; coefficient of ductility 0,74-0,85, what is a salient feature of tungsten carbide (for source material these parameters correlatively equal to 2,1-3,6GPa; 135-210GPa; 0,92-0,94). These distinctions of contact working layer under high velocity of heating and cooling encourage to advent of cracks, which can be filled with melting copper, containing nickel, reducing of angle wetting (fig. 1).

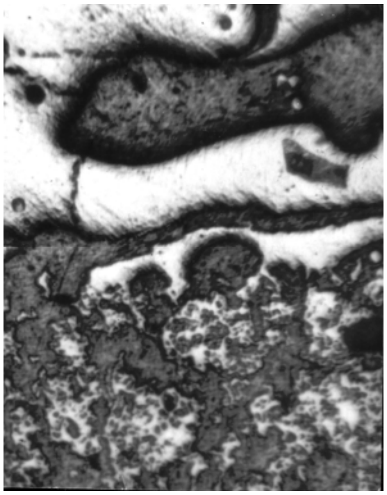

Fig. 1 – Failure secondary structure, x120

Local explosion-similar failure of bubbles and spalling (fig. 2) of undersurface layers of refractory component are bounded up with enrichment in carbon.

Carried out analysis confirms that structural changes in working layer of W-Ni-Cu contacts are connected with features of self-organization of second structure forming and its failure in the space of the discharge thermal influence. The self-organization takes place in the non-equilibrium conditions of high temperature, velocity of heating and cooling influence under current commutations. The point of view about absence of mutual solubility W and Cu in the wide range of temperature (as the base of composite materials of creation) is not in agrement with all of assemblage processes in the working layer, but reflects of present-day level of knowledge about systems Me VIa gr. – Cu – (additions-impurities in the high temperature range).

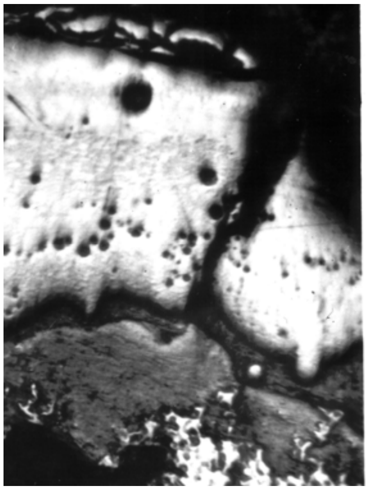

Fig. 2 – Spalling of the secondary structure, x120

## References

1. Gessinger G.N., Melton K.N. Burn-off of W-Cu contact materials in an electrical arc // Powder Metallurgy Intern., 1977. – 9. – N2. – P. 67–72.

2. Жаворонков М.А., Лавриненко И.А., Левченко Г.В., Минакова Р.В. Сравнительное исследование электроэрозионного разрушения металлокерамических контактов под воздействием дуги в трансформаторном масле и на воздухе // Сильноточные электрические контакты и электроды. – К.: Наук. думка, 1977. – С.247–258.

3. Игнатко В.П., Кухтиков В.А., Кресанова А.П., Минакова Р.В. Сравнительное исследование эрозионных процессов на медных и металлокерамических электродах в сильноточной квазистационарной дуге // Электрические контакты (теория и применение). – М.: Наука, 1972. – С.71–84.

4. Slade P.G. Arc erosion of tungsten Based contact Materials. A review // Int.j.of Refractory & Hard Metals . – 1986. – V.5. – N4. – P.208–214.

# ELECTRO- AND TRIBOTRCHNICAL PROPERTIES OF THE SILVER-BASED SLIDING CONTACTS IN VACUUM

**Zatovsky V.G., Kriachko L.A.**
Frantsevich Institute for Problems of Materials Science of NASU, Kyiv
Krzhyzhanovsky Str., 3, Kyiv-142, 03680, Ukraine, E-mail: 29min@ipms.kiev.ua

Work of sliding electrical contacts (SEC) in vacuum like any pair of friction is complicated with the limitation of process of the separating oxide layer formation and desorption of the surface gas layer. These phenomena lead to gripping of the contacting juvenile surfaces, and, as a result, to their increased wear, and sometimes also to a breakdown of the contact unit. Since one of the most important requirements for SEC is the low and stable contact resistance value $R_c$, the use of classical vacuum lubricants as the separating medium is in this case unacceptable because of the presence of a low electric conduction layer in the intercontact gap, which decreases the reliability of the electrical signal transfer. This leads to the release of additional energy in the contact zone, and to an increase of the surface temperature of contact elements, the lubricant destruction, to the oxidation of the activated work layers, and, as a result, to the contact unit work failures. As the optimum method of eliminating such deficiencies of the SEC can be the dosed introduction of the lubricating elements into the friction zone directly from the contact material volume, achieved with the use of the self-lubricated composite materials.

In the present work it have been given the results of investigating the tribotechnical properties under normal conditions and in vacuum to $10^{-4}$ SEC from silver and compositions on its basis, including reinforced by the manganese oxide $MnO_2$, the iron (Ni, Co) group metals, and containing as hard lubricating fillers $MoS_2$ or ZnS .

SEC of the 2 mm diameter cylinder forms were obtained by methods of rolling and wire drawing of the sintered powder mixtures. Rings from the bronze БрАЖ-9-4 were the counterface. Friction of the sliding pairs was accomplished according to the end diagram under the contact load $N_c$ = 0,3 N at sliding rate 0.2 m/s, resources L = 4 km., direct current I = 2 A, the voltage dead SEC before closing U = 24 V.

Tabl gives the values of the SEC specific wear ($\Delta m/L$), coefficient of friction ($\mu$) and contact resistance ($R_c$) of contact pairs after work under normal conditions and in vacuum at the environmental temperature.

According to the table, the introduction of solid lubricating fillers into the contact material composition has a positive influence on the SEC characteristics being investigated: their wear resistance in the friction process in vacuum more than twenty times higher than of contacts made of cast silver.

Sufficiently high level of the optimum content of the lubricating fillers in the contact materials (7,5 % vol. $MoS_2$ and 5 - 10 % vol. ZnS) leads to the weakening of a silver matrix of the compositions and limits the resource of the SEC work. Additional strengthening of the compositions by the metals of the group of iron (Ni, Co) and, especially, in their combination with the oxide of manganese $MnO_2$ makes it possible to considerably decrease the coefficient of friction and the wear of composition contacts at the friction both under normal conditions and in vacuum (see the Table).

In the general case, such changes of the controlled characteristics give us the right to assume that under the conditions of high rarefaction the presence even of this acknowledged lubricant as $MoS_2$ in the SEC composition does not exclude entirely the appearance of the local centers of gripping of the friction pairs materials. A small increase of the intensity of their wear and friction coefficient at simultaneous reduction of the contact resistance value observed under these conditions for all materials, testifies about this. It is result of degassing in vacuum of the SEC surfaces, which causes, as a rule, decrease of the friction characteristics, but at the same time conductivity in the contact area is improved.

Is actuel, the results of investigating has confirmed the essentuel influence of the air rarefaction degree on the friction coefficient of the contact pairs. Dependence $\mu$ versus the vacuum degree has the minimum, which does correspond to residual air pressure about 100 - 0,1 Pa. This effect is the result of a change of the chemically and physically adsorbed layers under the vacuum conditions of variable value. At the air rarefaction up to 100 Pa molecules of the physically adsorbed layers due to a decrease of environmental kinetic pressure are obtained large mobility. These layers are separated from those chemically adsorbed, improving the materials deformation processes in the friction zone, which leads to the decrease of the friction coefficient.

At a pressure under 0,1 Pa the layer of chemical adsorption (oxide dissociation) is destroyed, and it is not restored because of the practically absent gaseous medium. The oxide layer removal occurs due to the mechanical abrasion of contact materials. Under these conditions the probability of the formation of the centers of gripping is increased, the process of friction is hindered, which is seen of the values μ increase.

Dependence of $R_c$ on the rarefaction degree the range from the normal pressure to 10 Pa takes the form of the falling curve. The contact resistance is stabilized at lower residual pressures and its values are 0,6 - 0,7 of its test values in the air medium.

An increase of the contact load from 0,3 N to 1 N leads to the 1 decrease of the $R_c$ values level without a change of the general direction of its dependence on the rarefaction degree of air. This is caused by an increase of the real contact area as a result of the plastic deformation of micro-protrusions on the contacting surfaces, the mechanical destruction of the nonconducting films, etc.

Thus, the obtained results lead to the conclusion about the prospect of the SEC application on the basis of hardening silver, which contain 7,5 % vol. $MoS_2$ or 5 - 10 % vol. ZnS respectively, in the revolving current collecting devices, which work in vacuum. As additional resource for an improvement in their workability, apparently, can serve the introduction of the lubricating fillers also into the composition of counterface.

Wear intensity (Δm/L), friction coefficient (μ) and contact resistance ($R_c$) SEC from Ag and based composites

| №№ | Material SEC* | Δm/L, mg/km | | μ | | $R_c$, mOh** | |
|---|---|---|---|---|---|---|---|
| | | air | vacuum | air | vacuum | air | vacuum |
| 1. | Ag | 0,7 | 22,6 | 0,5 - 0,6 | 0,8 - 1,0 | 16 ±3,5 | 14 ±5,0 |
| 2. | Ag-7,5$MoS_2$ | 4,3 | 6,5 | 0,13 - 0,15 | 0,18 - 0,20 | 31 ±4,0 | 30 ±3,0 |
| 3. | Ag-Ni-7,5$MoS_2$ | 0,23 | 0,7 | 0,28 - 0,30 | 0,33 - 0,35 | 30 ±2,5 | 24 ±2,0 |
| 4. | Ag-Ni-$MnO_2$-7,5$MoS_2$ | 0,20 | 0,35 | 0,27 - 0,30 | 0,31 - 0,32 | 30 ±2,0 | 24 ±1,5 |
| 5. | Ag-Co-$MnO_2$ | - | 0,40 | - | 0,22 - 0,25 | - | 25 ±1,5 |
| 6. | Ag-10ZnS | 0,65 | 0,78 | 0,36 - 0,40 | 0,40 - 0,42 | 36 ±3,0 | 25 ±2,5 |
| 7. | Ag-Ni-10ZnS | 0,50 | 0,62 | 0,35 - 0,37 | 0,42 - 0,45 | 38 ±2,0 | 28 ±2,0 |
| 8. | Ag-Ni-$MnO_2$-5ZnS | - | 0,25 | - | 0,30 - 0,32 | - | 23 ±2,0 |
| 9. | Ag-Co-$MnO_2$-5ZnS | - | 0,47 | - | 0,30 - 0,32 | - | 23 ±2,0 |

* - Solid lubrication showed in % vol.
** - Value $R_c$ achived after L = 4 km.

# PYROLYTIC GRAPHITE, ITS STRUCTURE, PROPERTIES AND PRODUCTION PARAMETERS

**Skachcov V.A., Karpenko V.D.(1), Ivanov V.I.**
Zaporozhye State Engineering Academy
Lenin Avenue, 226, Zaporozhye, 69006, Ukraine, E-mail: colourmet@zgia.zp.ua
(1)State plant «Uglecompozit»,
GSP-982, Northern highway, Zaporozhye, 69600, Ukraine, E-mail: kvd@vuglecomp.zp.ua

Pyrolytic graphite is rather chemically pure material, which finds wide application in special branches of technology. It is obtained by carbon vapor deposition on a heated substrate at temperatures above 1800 °C.

The basic problem in obtaining thick plates of pyrolytic graphite consists in compensation of residual thermochemical tensions, which cause deformation of plates when they cool down.

Residual thermochemical tensions in pyrolytic graphite depend on the temperature and the rate of decomposition of hydrocarbons in a flow reactor, the rates of reaction gas flow along the deposition surfaces.

For the assessment of the rates of the reaction gas flow along the deposition surfaces physical modeling of gas flow distribution in a cold multi-tier reactor has been carried out. The rates of gas currents along the tiers of the reactor have been determined, stagnant areas in special areas of the reactor have been revealed. The availability of stagnant areas causes formation of commercial carbon, whose microparticles deposit on the surface of pyrolytic graphite to be formed and disturb its crystal structure.

The methods of mathematical modeling were used for creating the reaction gas rate distribution fields along the tiers of the reactor, which correlate with test values obtained with a model reactor.

The mathematical modeling also makes it possible to evaluate the reaction gas concentration change along the tiers of the reactor taking into account its decomposition on the heated surfaces and also to determine the rates of chemical reaction of hydrocarbon decomposition. The mathematical model of thermochemical decomposition of pyrolytic graphite from hydrocarbons in the gas phase has been presented. During hydrocarbon decomposition the processes of homogeneous and heterogeneous type are involved which are described by a closed system of kinetic equations, which contain components of convection and diffusion transfer of reaction gases.

Kinetic equations are registered relative to the degrees of decomposition of initial gas and products being formed as a result of thermochemical process in the reactor. The simplification of the solution of the equation system is ensured by application of double-flow method of equally accessible surfaces developed for flow reactors with porous permeable walls.

X-ray diffraction analyses have been carried out for pyrolytic graphite being formed with the results obtained in various zones of each tier of the reactor.

The dependences of the interplanar distance $d_{002}$ and the dimensions of pyrolytic graphite crystallites on the rate of reaction gas current and the rates of their decomposition have been established. The residual thermochemical tensions in pyrolytic graphite samples have been assessed and their connection with sizes of crystallites and technological parameters of pyrolytic graphite deposition has been established.

The procedure for the assessment of commercial carbon formation parameters has been developed which makes it possible to evaluate the volume and the rate of its formation.

The application of the proposed approach in practical processes of pyrolytic graphite deposition makes it possible to determine parameters of commercial carbon formation dependent on the duration of the process and to establish its influence on the structure of the deposited pyrolytic carbon.

The preformed analyses for the processes of pyrolytic graphite formation and its structural and mechanical parameters reveals physical and chemical peculiarities of formation of the above material and makes it possible to develop the production process on the scientifically grounded basis.

# THE INFLUENCE OF THERMAL STRESSES ON STRENGTH OF CARBON MATERIALS AT HIGH TEMPERATURES

**Gracheva L. I.**
Pisarenko Institute for Problems of Strength of NASU
2 Timiryazevskaya Str., Kiev, 01014, Ukraine, e-mail: mila@vol.kiev.ua

Carbon-carbon composite materials (CCCM) are successfully operated at temperatures above 1000 C. Creation of CCCMs, as is known, involves repeated heating up to temperatures above 1000 C. A degrading polymeric composite in the course of heating develops thermal stresses, which is mainly caused by the anisotropy of thermal shrinkage deformation of the initial carbon-filled plastic.

The object of the present investigation was to determine the magnitudes of thermal manufacturing stresses and their effect on the strength of CCCMs at high temperatures.

To study the physical and mechanical properties of high-temperature composite materials, the scientists of the G.S. Pisarenko Institute for Problems of Strength, National Ac. Sci. of Ukraine, developed special techniques and created unique setups which allow obtaining the material parameters under simulated service conditions: variation of heating rate and change of composition and pressure of gaseous medium in a temperature range from 20 °C to 3000 °C.

In heating of polymeric composite materials, physical and chemical transformations take place: polymeric thermosetting binder is transformed into a porous coke composition reinforced by various fibers.

This new material differs radically from the initial one and the transition from one state to another takes place gradually. Since the temperature and rate of heating specimens are certain averaged values not reflecting their local variations in some components of the composition, they cannot be used to describe the regularities of the process.

The temperature dependences of thermal strains in carbon-filled plastics (CFP) based on phenol-formaldehyde matrix are illustrated in Fig. 1. From these curves we can see that at high temperatures expansion occurs along the warp (in the plane of fabric filler), whereas shrinkage takes place along the filling. This means that the thermal strain coefficient in two mutually orthogonal directions differs not only in value, but also in sign. From the preceding gives us grounds to assume that heating produces shear strains in the material, which change their magnitude and sign with increasing temperature.

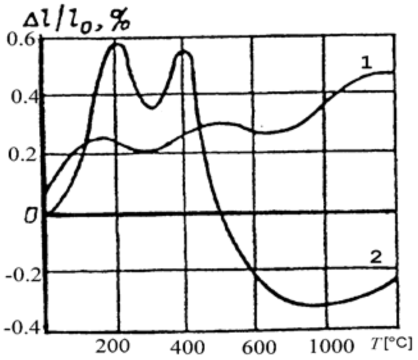

Fig. 1. Temperature dependence of thermal strains in CFP along the warp (1) and filling (2).

The shear strains inevitably give rise to shear stresses τ, which are given by

$$\tau = 2G\varepsilon = \frac{E(\varepsilon_w - \varepsilon_f)}{1+\mu},$$

where $G$ is the shear modulus, μ is Poisson's ratio, $\varepsilon_w$ and $\varepsilon_f$ are the strains along the warp and filling, respectively.

Tangential stresses in the carbon-filled plastic shown in Fig. 2 are due to the thermal strains caused by the thermal degradation of the polymer. Both the dilatograms (Fig. 1) and thermal shear stresses vary depending on the heating rate (Fig. 2). In the course of repeated heating, shear stresses cause the acceleration of the fracture process which proceeds as a result of the thermal degradation with no external forces applied.

The dilatometry results showed that the relative values of thermal strains in carbon composites are less than those in the initial material by a factor of 100 and higher.

The investigation into the physical and mechanical properties of CCCMs at high temperatures revealed that in the temperature range from 20 to 1000 °C softening of composites occurs, e.g., in compression their ultimate strength $\sigma_{uc}$ decreases by almost 30% and the elasticity modulus $E_c$ by 14—15%.

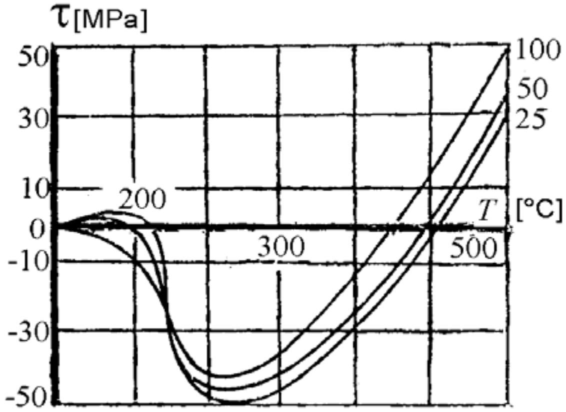

Fig. 2. Temperature dependence of shear stresses in carbon-filled plastics at different heating rates (numbers near curves)

Further rise of temperature results in the increase of the ultimate strength values reaching their maximum at 2000 C. In this case, the values of $\sigma_{uc}$ exceed its initial value at room temperature more than twice.

Similar results were obtained in studying the strength of CCCMs in torsion in the plane of the composite reinforcement. The magnitudes of shear stresses $\tau_{zx}$ and $\tau_{zy}$, as well as the elasticity moduli $G_{zx}$ and $G_{zy}$, decrease at temperatures from 300 °C to 700 °C, then increase reaching their maximum at $T$=1000 °C, and then gradually decrease.

The performed investigations of the structure aid in establishing the relationship between the strength characteristics and stress-strain behavior of the composite material.

In the course of formation of the material in the temperature range from 20 to 500 °C, thermal deformation results in the development of orthogonal cracks in the carbon-filled plastics. Mechanical tensile loading combined with the action of shear stresses occurred in the composite due to thermal deformation under the above temperature conditions results in the brittle fracture of CCCMs.

## Conclusions

It was shown that at the same temperature the thermal strains in carbon-filled plastics (CFP) in two mutually perpendicular directions in the plane of the reinforcement differ both in the magnitude and sign.

The thermal shear stresses occurring in carbon-filled plastics on the basis of phenol-formaldehyde matrix due to thermal shrinkage deformation in the first technological heating in the temperature range from 20 to 1000 °C were calculated. It was demonstrated that these stresses are retained and cause softening of CCCMs in strength tests within the same temperature range.

The performed investigations of the CCCM microstructure confirmed that the increase in shear strains due to thermal deformation of the initial material, carbon-filled plastic, results in a drop of their strength and elasticity modulus in the temperature range from 20 to 1000 °C.

# HEAT RESISTANCE AND THERMAL STABILITY OF COMPLEX COATINGS ON COMPOSITE CARBON MATERIALS UNDER HIGH-TEMPERATURE AND CORROSION MEDIA ACTION

**Zmij V.I., Kartmazov G.N., Kartsev N.F., Kovtun N.V.**
National Science Center “Kharkov Institute of Physics and Technology”,
1, Akademicheskaya St., Kharkov, 61108, Ukraine, e-mail: kartmazov@kipt.kharkov.ua

Carbon-carbon composite materials (CCCM) possess a series of advantageous properties due to which they are widely used in many branches of science and engineering, in particular, missile technology, aerospace engineering, atomic-power industry etc. [1]. However, these materials have a low corrosion resistance that restrains their application in oxygen-containing media at temperatures exceeding 500 °C because of forming the gaseous volatile oxides $CO+CO_2$.

In this connection, to enlarge considerably the field of CCCM application in many branches of national economy it is necessary to solve a problem of their corrosion resistance improvement. The problem of protection of carbon composites from oxidation, by deposition on them corrosion-resistant coatings, is related with overcoming some difficulties. The cause is their rather high porosity and oxide volatility, structural nonuniformity and low coefficient of linear thermal expansion, as well as, the anisotropy of physical-chemical and mechanical characteristics.

At present, there are many different methods of CCCM production. In any particular case a number of pores, their sizes and distribution in the whole volume of the specimen, and, consequently, their properties are essentially dependent on the structure of carbon material, which in turn is determined by the process parameters of CCCM production. According to [2], the majority of carbon composite materials are produced by the liquid technology of CCCM(*l*). The minor part is obtained by the gas-phase, isothermal, thermogradient and combined methods of CCCM(g).

The literature contains sufficient publications in which discussed are different problems including the formation of protective coatings on graphite and carbon composites, as well as, the study of their operating characteristics. Chiefly, the works are devoted to the development and investigation of protective coatings on carbon materials in the temperature range from 1200 °C to 1700 °C. The problem of CCCM protection from oxidation in the temperature range from 1700 °C to 2000 °C now is not yet solved. Mainly, it is related with difficulties in overcoming the above-mentioned factors, first of all, with the high volatility of carbon oxides, as well with their comparatively low coefficient of linear thermal expansion leading to the problem of coating adhesion with the base.

In this connection the present work is devoted to research of protective coatings and methods of their formation providing the heat resistance of CCCM in the temperature range from 1700 °C to 2000 °C with a satisfactory thermal stability. As multicomponent and multilayer protective coatings we have tested, in main, high-melting carbon-boron silicides, which were formed on CCCM. The used methods were: gas-phase deposition, activated vacuum diffusion saturation, including, through the liquid phase, as well as, partial melting in vacuum. To clarify the influence of methods used for formation of initial carbon composites on their heat resistance and thermal stability, CCCM(*l*) and CCCM(g) were chosen as samples.

Taking into account the requirements to structural materials based on CCCM under conditions of high temperatures, thermal cycling and oxidizing-reducing media, to solve the problems of protection of composite carbon we have carried out research on development of complex multicomponent materials and the multilayer coatings every of which should perform proper functions.

The first layer, in our opinion, should provide a significant decrease of the surface porosity, should have well adhesion with the carbon substrate. Besides, for smoothing thermal stresses, it should possess the coefficient of linear thermal expansion as close as possible to that of CCCM. As the second layer, the composites should be chosen which have barrier properties reducing the diffusion penetration of carbon from the substrate and oxygen from the environment onto the corresponding interfaces. The external layer composed, for the most part, of heat-resistant compositions, should carry out protective functions and have self-healing properties.

In total, we have performed a great quantity of experiments, tested much compositions of protective coatings formed on CCCM with the use of different above-mentioned technologies. The most characteristic results of performed investigations are given in the table. The heat resistance was determined by the averaged time to final failure at corresponding temperatures; the thermal stability was specified by the number of thermal changes in the cycle: heating to 1800°C – 60 s, cooling – 30 s.

Table

| Carbon-carbon material mark | Composition of protective coatings | Heat resistance - thermal stability | | |
|---|---|---|---|---|
| | | Temperature of testing, °C | Time to failure, hours | Number of thermal cycles |
| CCCM(g) | $SiC-ZrB_2-CrB_2-HfSi_2-WSi_2$ | 1800 | 5,0 | 52 |
| CCCM(g) | $SiC-ZrB_2-HfB_2-WSi_2$ | 1900 | 1,6 | |
| CCCM(g) | $SiC-B_4C-HfB_2-WSi_2-HfO_2-ZrO_2-Al_2O_3-SiO_2$ | 2000 | 0,5 | |
| CCCM(*l*) | $SiC-ZrB_2-HfB_2-WSi_2$ | 1800 | 3,5 | 48 |
| CCCM(*l*) | $SiC-B_4C-HfB_2-WSi_2$ | 1800 | 5,2 | 57 |
| CCCM(*l*) | $SiC-ZRB_2-HfB_2-WSi2$ | 1900 | 0,4 | |
| CCCM(*l*) | $SiC-B_4C-HfB_2-WSi_2-HfO_2-ZrO_2-Al_2O_3-SiO_2$ | 2000 | 0,15 | |

Accomplished investigations evidence that the heat resistance and thermal stability of coatings on carbon-carbon composite materials depend not only on the composition and method of their formation but also on the type of initial material. It is shown that heat resistance and thermal stability of single-type coatings on CCCM(g) is slightly higher than on CCCM(*l*).

## References

1. F.P.Sanin, L.D.Kuchma, Ye.O.Djur. A.F.Sanin. Solid-propellant rocket engines. Materials and technologies. Published in Dnipropetrovs’k University Publishers, 1999, 320 p.
2. V.A.Gurin,V.F.Zelensky. Gas-phase methods of making carbon and carbon-carbon materials. // Problems of atomic science and engineering (VANT), Kharkov, 1999, No 4 (76), p.13-31.

# TRIBOTECHNICAL PROPERTY OF SUBSTRUCTURE FROM ALLOYS VT3-1 AND SAP-2 WITH TI—AL—N, MO—AL—N COATS

**Beresnev V.M., Tolok V.T., Gritsenko V.I., Chunadra A.G.**
Karazin Kharkov National University
Svobody sq., 4, Kharkov, 61077, Ukraine, kirdin@pht.univer.kharkov.ua.

The development of modern technique requires engineering of new composition materials (coats), which could supply high use reliability of machines (aggregates of fuel automatics), and also increase term of their service in extreme conditions. The serviceability and longevity of machines is determined by properties of materials from which the knots of friction manufactured. The constructional materials, used in aggregates, do not allow realizing in kinematical couples a necessary level antifriction: the friction coefficient is in limits from 0,1 up to 0,15. The lowering of a friction coefficient up to 0,05…0,08 would allow considerably to increase precision of work pieces regulation, and, hence, their reliability and profitability.

In the present work the results of examinations tribotechnical properties of composition coats are submitted on the basis of nitrides of transition metals doped by aluminum.

Deposition of coats Ti—Al—N, Mo—Al—N was carried out on technology, reduced in operation [1]. Materials served samples from an alloy VT3-1 and SAP-2 (8x8x30 *mm*). The friction machine carried out trials on friction under the plan “plane-cylinder” in medium of aviation fuel. In quality rider the rollers manufactured from wrought high carbon chromic steel of the mark 95X18 were applied. Temperature during trials made 70 °C.

The adhesion of coats to substrates was estimated on the relative area chip at a share local plastic deformation of a substrate and coat by introduction indenter of a Rockwell hardness gauge at a loading on indenter 980 *N* [2]. The obtained coats having chopped off have no and by this measure are satisfactory.

The width of coats was accepted 1,5...2,5 microns. The trials were carried out at small (29...166 *N*) and major (235...1960 *N*) loadings. A loading up to a given loading is model was carried out by degrees, the duration of each trial made 6 hour. During these trials were measured: friction coefficient, volumetric breakup of a carrier socket and weight breakup of a roller. The explored coats well work up to the peak loading, and the volumetric breakup at magnification of a loading varies incidentally (fig.1).

Table 1.

Results of friction coefficient measuring.

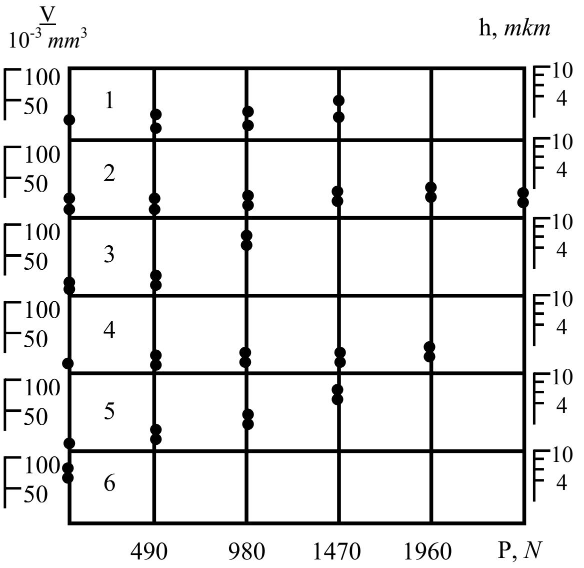

Fig.1. A breakup of coats at different loadings put on an alloy VT3-1.
1 – Ti-Al-N (Al 5% mass), 2 – Ti-Al-N (Al 10% mass),
3 – Ti-Al-N (Al 20% mass) 4 – Mo-Al-

| Composition of a pair of a coat (Alloying element % mass) | Medial value $f_{\text{fr}}$ | | |
|---|---|---|---|
| | Small loadings | Major loadings | Blanket |
| VT3-1+TiAlN (Al5%) | 0,04 | 0,07 | 0,055 |
| VT3-1+TiAlN (Al10%) | 0,04 | 0,05 | 0,045 |
| VT3-1+TiAlN (Al20%) | 0,07 | 0,09 | 0,08 |
| B1(98X18) | 0,158 | 0,149 | 0,155 |
| SAP-2+TiAlN (Al5%) | 0,07 | 0,09 | 0,08 |
| SAP-2+TiAlN (Al10%) | 0,05 | 0,06 | 0,055 |
| SAP-2+TiAlN (Al20%) | 0,09 | 0,12 | 0,105 |
| B2(AD33+Ti+anode) | 0,218 | 0,11 | 0,161 |

The breakup of rollers working in a pair with explored coats, approximately in 2 times is less, than without a coat. These results testify to low outwearing ability of experimental coats. In tab.1 the results of average values of a friction coefficient of explored pairs are submitted at different loadings. Depending on the content of concentration of doping devices in coats the friction coefficient varies.

Comparing tribotechnical performances of explored friction pairs should be marked, that coverings Ti—Al—N with the content of aluminum from 10 up to 15% (mass) raise a wear hardness of carrier sockets from an alloy VT3-1 from 4 up to 8 times depending on a loading, differ by low outwearing ability in relation to rider (steel 98X18), and also ensures values of a friction coefficient 0,07...0,08 for the accepted test specifications. As to coats Mo-Al-N, concentration of aluminum 8...15% (mass) also renders influence on a wear hardness (outwearing ability them in 2...10 times are less), friction coefficient 0,05...0,06.

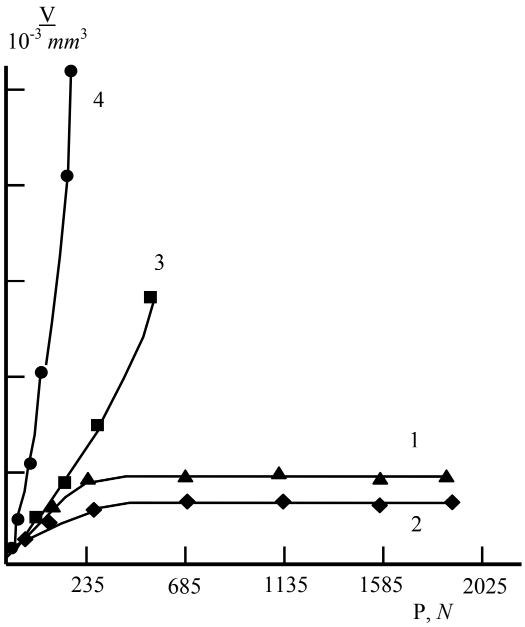

Fig.2. A volumetric breakup of coats Ti-Al-N, put on an alloy SAP-2 depending on a loading.
1 – Al 5% mass, 2 – Al 10% mass, 3 – Al 20% mass, 4 – B2 (AD33-Ti+anodization) base var.

Trials for friction and the breakup are model from an alloy SAP-2 with coats Ti—Al—N was carried out on a circumscribed above procedure. As a result of trials were estimated: a volumetric breakup of a carrier socket, weight breakup of a roller and medial friction coefficient in comparison with base variant. In a fig.2 the results of influence of a loading on a breakup of carrier sockets are given.

As contrasted to by base variant (B1) of a coat Ti-Al-N is characterized by low outwearing ability. At small loadings of a coat have advantage before (B1): its outwearing ability is less in 2…15 times, and at the major outwearing ability is less in 2…5 times. The friction coefficient both at small, and at major loadings is at a level 0,05…0,06.

Thus, the carried out analysis testifies to embodying with the help coats Ti—Al—N and Mo-Al-N rather high tribotechnical performances, which exceed tribotechnical performance of base variants. By the basic properties of attrition-resistant coats, as it was scored in operations [2, 3], is its low adhesiveness activity in relation to rider. By a purposeful doping it is possible to regulate adhesiveness activity of a material (coat).

## References

1. Beresnev V.M., Perlov D.L., Fedorenko A.I. Ecologically safe vacuum-plasma inventory and technologies of drawing of coats. Kharkov. — ChICIPI — 2003. — P. 211—212.
2. Beresnev V.M., Fedorenko A.I., Gritsenko V.I. et all. Examination of frictional properties of composition coats obtained by a vacuum - arc method // Physical engineering of surface. - 2003. — V.1, №2. — P. 180—183.
3. Matsevitij V.M., Kazak I.B., Spolnikov A.I. et all. Some aspects of adhesiveness interaction of a solid body // Rep. NASU — 2002 — №9. — P. 99—105.

# STRUCTURE AND FEATURES OF COMBINED COATINGS ON HEATRESISTANT ALLOYS

**Abrahimov N.V., Shkretov Y.P.(1), Terekhin A.M. (1), Loukina V.V. (1), Borstch E.V. (1).**
Zhoukovsky Air Force Engineering Academy,
Planetnaya street, 3, Moscow, 125190, Russia, OGMet@ salut.ru
(1)Federal State Unitary Enterprise, Moscow Machinbuilding Production Plant "Saluit"
Budienovsky avenue, 16, Moscow, 105118, Russia, OGMet @salut.ru

Producing demand of heat resistant aluminum coatings with improved mechanical performances like viscosity, plastic, crack resistance led researchers to structures in NiAl system content intermediate phases with lowering aluminum content. The most practical interest are represented coatings that content alongside primary phase β-NiAl for heat resistance responsible more hard, viscose, but less heat resistant phase γ'-Ni3Al. Combined coating on ZhS6U and ZhS32 alloys got by vacuum plasma spraying of nickel based alloys with aluminum, tantalum, wolfram, Gaffney, silicon, chromium and yttrium doping followed by calorizing with gas circulation method [1].

Combined coating structure consist of to layers: one outer mostly of β-NiAl phase of 24-26% AL content and inner is reached by chromium, tantalum and wolfram with comparatively low Al concentration of 8-12%. Under comparatively low Al storage in correspondent coating thickness of 40-50 μm a combined coating protects reliably ZhS6U and ZhS32 alloys on more than 1000 hours under temperature1050° C, has good thickness stability due inserting tantalum and wolfram at the first stage of processing. Disintegration speed of β-phase is lowering in 1.6 times under an open air oxidation with 1050ºC temperature. Residual compression stresses are formed in the coating that positively influence on fatigue strength of alloys. Hot iso-static compacting of combined coating ensured substantial growing thermal fatigue strength of parts.

For solving reparability problem the method is drawn up for local surface part protection which are not a subject of saturation under gas processing aluminizing or chromo-aluminizing ensured adsorption of halogenated molecules and binding deposition Al- atoms into high-melting compounds. This drawn up method of protection from aluminizing does not influenced on structure, composition and performances as deposited coating and surface layers of alloy protected as well.

Parts repairing with coatings recovering is conducted with usage of electrolyte [2]. It includes in weight %%:
HNO3 25-40; HF 0.5- 4; Fe (powder) 0.2 – 1.0; CrO3 0.3- 1.5; water up to 100%.
Parts are hold under 18ºC temperature (not less) in 2 minutes or more period of time. The method allows to conserve area of diffusion coating under etching and provides coating recovering in passages and cavities of such parts as turbine cooled blades.

References:
1. RF Patent # 2213801, 2003.
2. RF Patent # 2200211, 2003.

# STRUCTURAL EVOLUTION OF Ti/TiC MULTILAYERED COATINGS

**Dahan I., Frage N., Frumin N., Goldberg M., Dariel M.**
Department of Materials Engineering, Ben-Gurion University of the Negev,
Beer-Sheva, Israel, nfrage@bgumail.bgu.ac.il

Recently, films with a gradually changing composition, incorporating metal and ceramic components have been reported as wear protective coatings [1]. The production of such coatings is a logical development of the multilayer concept as discussed, for example in [2, 3] The sharp interfaces between the layers may give rise to film failure by interface crack growth], but the potential of a multilayer coating in the framework of the functionally graded materials FGM concept is well established. One approach for utilizing this approach consists of depositing a multilayer in a FG architecture, followed by heat-treatment aimed at eliminating the sharp interfaces. Such an approach allows generating an interface-free graded coating. Clearly the evolution of the microstructure of the initial multilayer as a function of the subsequent heat-treatment is of paramount importance in evaluating the merit and the viability of such approach.

The evolution of the microstructure is governed to a large extent by the nature and density of interfaces within the multilayer. Reactions that occur at material interfaces alter the local structure and chemistry and, consequently, affect the physical properties. Reactions are likely to occur at the interface between the metallic and the ceramic components of cermets, since these composites often have to undergo high-temperature treatments. Multilayered materials, on account of their large and well defined interface area, are suitable systems for a systematic study of the reactions that take place at the interface. Multilayers, deposited by physical deposition methods, i.e., evaporation or sputtering, offer the additional advantage of providing an easy approach for a systematic variation of some of the important parameters, such as the absolute and relative thickness of the individual layers that determine the outcome of the interface reactions.

Numerous studies have dealt with the stability and the structural and compositional evolution of metallic multilayers. Much more limited is the available information regarding metal–ceramic multilayers, specifically multilayers formed by a metal and carbide. The present work is concerned with the compositional and the structural evolution of a Ti–TiC multilayer system in the course of different heat treatments. Titanium carbide is stable over of a wide range of compositions that extends at 1000 °C from $TiC_{0.5}$ to TiC. Over this range, the concentration of structural carbon vacancies increases from 0% to 50% in $TiC_{0.5}$

Two kinds of multilayers consisting of 30 equi-thick ~40 nm TiC layers and 20 and 60 nm thick Ti layers, respectively, were sputter deposited on Mo substrates. The structural and the compositional evolution of these multilayers were examined by x-ray diffraction, transition electron microscopy (TEM), high-resolution TEM, Auger electron microscopy spectroscopy and differential thermal analysis (DTA), in the as-deposited state and after various heat treatments up to 500 °C. Initially, the Ti layers had a crystalline columnar grain structure displaying a (002) texture. The TiC layers displayed weak crystallinity with a pronounced (111) texture, (Fig.1).

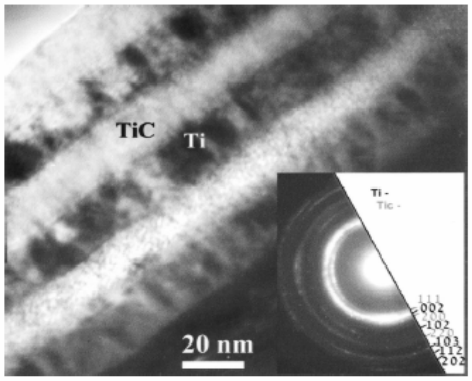

Fig. 1. Bright-field TEM image from the as-deposited multilayer (thin Ti layers).

In the course of the heat treatments, carbon diffused from the carbide layer into the adjacent Ti layers transforming the latter into off-stoichiometric $TiC_x$ with $x>0.5$ and simultaneously depleting the carbon content of the initial carbide layer. The formed $TiC_x$ layers maintained the textural relationship with the neighboring TiC layers, consistent with a transformation that involved only a ABAB to ABC stacking change of the Ti sublattice.

In a Ti—TiC multilayer system, the final microstructure depends, in principle, on the relative thickness of the two constitutive layers. Relatively thin initial Ti layers, intercalated within thicker carbide layers, are transformed progressively by the influx of carbon atoms diffusing across the $TiC_x/Ti$ boundary into additional carbide, until their eventual disappearance. If the Ti layer is thick enough, the carbon in excess of the low carbon composition limit of the adjacent carbide layer is not sufficient to cause the complete transformation of the metal into carbide. Such a Ti layer will endure, albeit with reduced thickness, intercalated within carbide layers with reduced carbon content.

X-ray diffraction from the two types of as-deposited multilayers, before and after annealing, revealed strong (111) and (002) textures for TiC and Ti layers, respectively. After diffusion annealing, two features are noteworthy in both multilayer types: (a) the TiC layers maintain their initial (111) texture, and (b), in the multilayers with thin Ti layers, the TiC (111) peak after the disappearance of the Ti layer appears to be split into two peaks: One narrow and well defined peak corresponding to a low carbon concentration ($x \sim 0.5$) and a second broad TiC (111) peak similar to that of the original as-deposited TiC. This last observation suggests that even after the disappearance of the Ti layer, the TiC layer is not yet fully crystallized.

After annealing the multilayer with thick Ti layers at 350 °C for 24 h, the appearance of a 9–11 nm thick layer is observed at each Ti and TiC boundary .This layer consists partly of well crystallized formed $TiC_x$ , with a carbon content corresponding to the Ti/TiC phase boundary and that was generated by the influx of carbon from the original stoichiometric TiC layer into the adjacent Ti layer and, partly of a crystallized fraction of the original TiC layer following its decreased carbon content.

Figure 2 shows the results of DTA scans after a heat treatment. The presence of exothermic peaks is clearly discernable above 400 °C for both types of multilayers. The low temperature peak was attributed to the exothermic reaction between theTi layer and the influxing carbon. The second peak was attributed to the crystallization of the original nanostructured TiC. XRD diffraction results had shown that in a multi-layer, with thin Ti layers, the latter disappeared completely after the heat treatment. According to the TEM results, the initial TiC layers underwent complete crystallization after the heat treatment of multilayers with thick Ti layers.

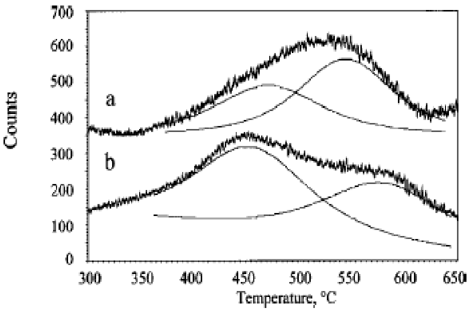

Fig. 2. DTA graph from self-standing coating before and after annealing: (a) Thick Ti layers and (b) Thin Ti layers. The two curves were normalized with respect to the sample weight and are shifted with respect to the ordinate, given in arbitrary units.

The structural evolution of the Ti/TiC multilayer system, in particular, the crystallization of only a part of the TiC layers multilayers with thin Ti layers and the presence of two different exothermic heat peaks in the DTA runs were accounted for in terms of two intrinsically different mechanisms. The first mechanism involves the flux of carbon atoms from the TiC into the adjacent Ti layers; it takes place exclusively via the diffusion of the high mobility carbon atoms and as a result of the steep carbon concentration gradients in the vicinity of the interface between the layers. The second mechanism involves also involves crystallization and grain growth that occur within the TiC layers. These mass transport-related effects involve the mobility of both the C and the Ti species. These phenomena in strongly bonded materials, such as TiC, are determined by the diffusivity of the slower, i.e. Ti species.

A model based on the local environment of the Ti atoms at low carbon concentration, i.e., a high probability of vacant carbon neighboring sites, accounts for the increased mobility of the Ti atoms [4]. Thus, in $TiC_x$ carbide at $x \approx 0.65$, the diffusivity of Ti starts to increase substantially and, thereby also, the ambipolar diffusivity that determines mass transport in this compound. The increased mobility of the Ti component allows crystallization of the initially amorphous TiC layer to occur, at least partly, in the vicinity of its initial interface with the adjacent Ti layer.

[1] A.A.Voevodin. C.Rebholz, J.M. Schneider, A.Mattews, Surf.Coat.Technol. 73 (1995) 185.

[2] H.Holleck, M.Lahres, P. Wall, Surf.Coat.Technol. 41 (1990) 179.

[3] A.A.Voevodin, A.L.Erokin, V.V.Lyubimov, Phys. Stat. Solidi A,145 (1994) 565.

# THE FEATURES OF COLLISION OF DEFORMABLE PARTICLE WITH A SURFACE OF DUCTILE SOLID BODY

**Uryukov B., Kadyrov V., Tkachenko G.**
Frantsevich Institute for Problems of Materials Science, NAS of Ukraine,
3, Krzhyzhanovsky Str., 03142, Kyiv, Ukraine, E-mail: cosmos@ ipms.kiev.ua

Dynamics of collision of particles with a target plays the determining role in spraying of coatings, therefore a lot of attention in researches of this process is given to it. The interaction of liquid drop with solid basis is considered as the basic physical model of this process, because the best adhesion of coating with a basis take place at the temperature of sprayed particles nearby the melting temperature. At that usually it is considered, that the basis is not deformed at all [1, 2]. In the process of abrasive erosion of ductile materials, when the solid particle collide the solid target both materials can be deformed. Thus the shock-wave process consists of two stages. First, "the stage of closed wave" [2], schematically shown on the Fig.1.

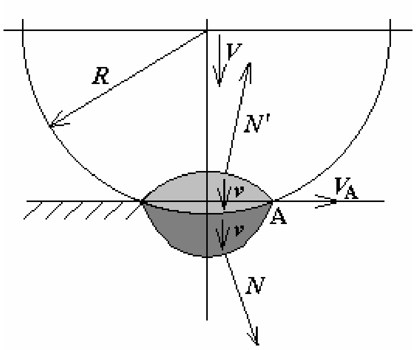

Fig.1. The stage of closed wave at impact of a particle against a target. $V$ – the speed of particle; $v$ – the speed of material in compression zone; $N$ and $N'$ – the speeds of shock waves in target and particle; $V_A$ – the speed of boundary of contact area.

It is characterized by that the shock waves in the particle and in the mass of target are isolates on the boundary of the contact zone and do not leave on free surface. Its duration $t_1$ determined by condition: $V_A = \min(N, N')$. If the impact speed is smaller in comparison with the speeds of sound in materials, the speeds of shock waves are close to the speeds of sound: $N \approx a$, $N' \approx a'$. Then $t_1 \approx VR/2a_*^2$, where $a_* = \min(a, a')$, usually $a < a'$. The total duration of contact determined by the time of the shock wave passage through the particle from contact area up to dome of the particle and reverse (as a wave of unloading). It is equal to $t_c = 4R/a'$. The ratio of characteristic times $t_1/t_c$ has the order $(M/8)\cdot(a'/a)$, where $M = V/a$, and is small at $M \ll 1$. Nevertheless, the stage of the closed wave plays the important role in the formation of stressed state of a target because of high dynamic loads, which realized during this time. The second stage is accompanied by the spreading of unloading waves and reduction of pressure on contact up to forced pressure level ($p \sim \rho V^2/2$). The complete analysis of shock-wave processes even at the stage of the closed wave is impossible without application of numerical methods (examples are given in [1]). Nevertheless, some characteristic patterns can be revealed analytically at investigation of dynamics of a small vicinity of the point A – the boundary of contact zone (Fig.2). It is supposed that the impact velocity is so great, that the arising pressure exceeds the yield point of target material [3, 4].Similarly to [2] one can consider the coordinates system rigidly connected to the point A. Then dynamics of material in its vicinity can be represented as shown on Fig.2.

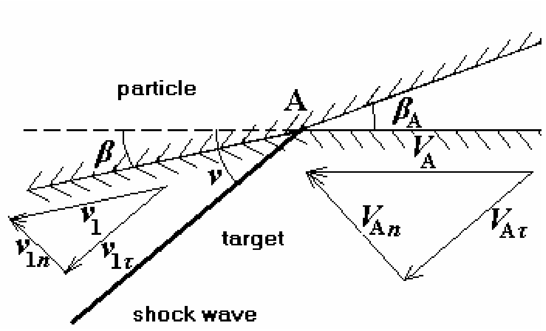

Fig.2. The scheme of interaction of the particle with the target in movable coordinate system.

The target material runs on particle surface with the speed $V_A$. As both materials can be deformed, the contact surface in compression zone is directed in relation to undisturbed surface of the target under the corner $\beta$, instead of $\beta_A$, if the particle surface was not deformed.

The corner $\beta_A$ determined, as $tg\beta_A = V/V_A$, and corner $\beta$ – from the ratio $tg\beta = v/V_A$, where $v$ is the speed of material in the compression zone in the direction of particle speed of movement $V$. In approach of a weak shock wave ($N \approx a$) we shall have:

$$tg\beta = \gamma V/V_A,$$

$\gamma = \omega'/(\omega + \omega')$, $\omega = \rho_0\, a_0$, $\omega' = \rho'_0\, a'_0$ – acoustic impedance of materials (the index 0 corresponds to the normal conditions).

The following equation of state [4] was used:

$$p = \frac{\rho_0 a_0^2}{n}\left[\left(\frac{\rho}{\rho_0}\right)^n - 1\right] + \Gamma c_v \rho T$$

Where $n = 4$ for solids, $n = 7 - 8$ for liquids, $\Gamma$ – Grunaisen coefficient, equal to $(4n-1)/6$.

Together with the “compatibility” equations on shock wave [5], one can receive the analytical solutions for all characteristics of the process.

The results of calculation of their distributions on radius of the contact zone, related to maximal radius in the stage of the closed wave $r_{A\max}$,

$$\frac{r_{A\max}}{R} = \frac{M}{\sqrt{1+M^2}}$$

are shown on Fig. 3 – 5.

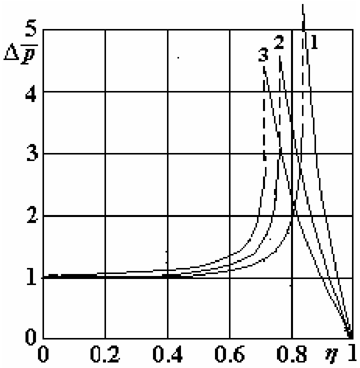

Fig.3. Distribution of pressure on the radius of contact zone. 1 – 3: $M$ = 0,1; 0,2; 0,3.

The pressure is related to pressure in an initial contact point $p = \gamma\rho a V$; the temperature – to initial temperature, the speed of the target material, parallel to the target surface, – to speed of impact. In the calculations it was assumed $\gamma$ = 0,3, that corresponds to collision of quartz particle with the target from steel 10. It is seen that the maximal values of parameters are observed at the time moment, a little bit smaller the duration of the «stage of closed wave». The pressure can in 4,5 – 5,5 times exceeds the pressure in a weak shock wave, temperature can rise in 30 – 40 times more normal, and speed of movement of the target material – in 3 – 4.5 times more the impact speed. The analysis of these effects allows better understand a nature of destruction of plastic materials at particle impact.

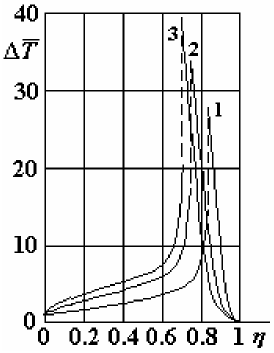

Fig.4. Distribution of temperature on the radius of contact zone. 1 – 3: $M$ = 0,1; 0,2; 0,3.

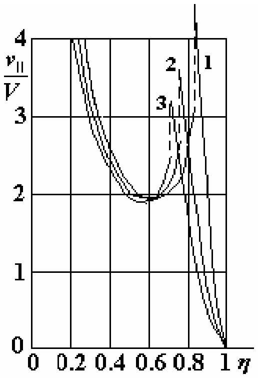

Fig.5. Distribution of speed of environment on radius of contact zone. 1 – 3: $M$ = 0,1; 0,2; 0,3.

1 Эрозия: Под ред. К. Прис. М., Мир, 1982, 464с.

2. Б.А. Лебедев А.Д., Урюков Импульсные ускорители плазмы высокого давления. – Новосибирск, ИТФ СО АН СССР, 1990, 290с.

3. Uryukov B. at al. Similarity Criteria of Powder Spraying of Plastic Materials. MEE 2002, pp. 396..

4. Зельдович Я.Б., Райзер Ю.П. Физика ударных волн и высокотемпературных гидродинамических явлений. М., Наука, 1966, 686 с.

Кочин Н.Е. и др. Теоретическая гидромеханика. Т.2, – М. – Л., Гостехиздат, 1948, 612с.

# DEVELOPMENT AND EXPLORATION OF OVERLAYING WELDING MATERIAL PROOF IN REQUIREMENTS OF ABRASIVE OUTWEARING

**Marchenko S.V.**
Sumy State University
2, R.-Korsakov Str., Sumy, Ukraine, s_marko@ukr.net

Used now abrasive-proof materials contain in makeup rare land metals Cr, B, W, that not always meets technological and operational requirements.

The purpose of work is development and exploration of overlaying welding material for protection of the parts of mechanisms and machines subject to an attrition. One of the base requirements showed by us to a material, was its high efficiency to action of abrasive environment together with use of widespread and inexpensive components for its reception.

The electroarc overlaying welding by a powder wire is the most comprehensible expedient of hardening and reduction of parts of machines.

The wearing quality of overlaying welding metal depends on structure. It has been fixed, that the optimum molding box is the martensite-austenitic lower die with solid pluggings - the martensite resists to a wear well - , and austenite is a viscous component and interferes with a spalling of pluggings.

For work in requirements of abrasive outwearing we designed a self-protective powder wire with system of alloy building C—Ti—Si—Mn—N.

One of the primary goals was finding out of an optimum carbon content, titanium and nitrogen in a complex with other elements in mix material and their transition in overlaying welding metal. The complete factorial experiment for definition of necessary amount of elements was used, where abrasive determination of overlaying welding metal acted as parameter of optimization.

The following builders enter into a charge makeup of a wire: graphite of 13,6—15,5%, ferrotitanium of 70,5—77,0%, a ferromanganese of 3,7—3,8%, silicium-calcium 2,4—2,5%, a carbamide 0,9—1,1, a ballast (an iron powder) 0,1—8,9%.

Thus the block coefficient of a powder wire makes 34—38%.

The boosted contents of titanium in a complex with carbon and nitrogen creates requirements for interlinking titanium - formation of carbides of titanium, titanium - enough solid and strong bridgings.

Carried out by us metallographic, the X-ray diffraction analysis and gaugings of a microhardness allows to conclude, that the structure of overlaying welding metal consists of carbides of iron doped by titanium, a martensite, a retained austenite, carbides and titanium carbide-nitrites.

The chemical analysis of overlaying metal has shown the boosted contents of titanium (more than 4,1%) and nitrogen (about 0,04%). Hardness of overlaying welding metal makes 63—65 HRC.

Laboratory researches of resistance of overlaying welding metal to abrasive outwearing by a fixed abrasive, a free abrasive and in a stream of abrasive particles were carried out. The relative wearing quality in comparison with the etalon (chromic pig-iron ЧХ-28) is 1,8—1,9.

It is possible to subject overlaying welding metal to a heat treatment with the purpose of pinch of its technological properties at use of metal-cutting inventory. Hardness after annealing makes 30—35 HRC. The hardening allows to receive hardness 65—67 HRC.

Precomputation of economic efficiency has shown, that the cost price of materials for manufacture of the given powder wire is more than twice below than builders of piece electrodes Æ-590,620.

Technological, operational effects of testings of overlaying welding metal allow to use a designed powder wire for overlaying welding and reductions of parts of agricultural machinery, pulp pumps, etc.

# FIRE PROTECTIVE COATINGS THERMOPHYSICAL PROPERTIES DETERMINATION BY FIRE TEST EXPERIMENTAL DATA

**Krukovsky P., Novak S. (1), Cvirkun S. (2)**
Institute of EngeneeringThermophysics
2a, Zhelyabova Str., Kiev, 03057, Ukraine, E-mail: kruk@i.kiev.ua
(1) Ukrainian Fire Safety Institute,
Rubalska, Str. 18, Kiev, 01011, Ukraine, E-mail: ukrndipb@uni.net.ua
(2) Cherkasy Fire Safety Institute
Onoprienko Str., 8, Cherkasy, 18034, Ukraine, E-mail: fire@ck.ukrpach.net

Introduction. One of the way of maintenance of building constructions and equipment fire resistance of premises and industrial objects is the covering the constructions and equipment with fire resistance coatings from fireproof materials. For designing optimum parameters of these materials, which work in a wide range of temperatures (up to 1200C), are necessary knowledge of them thermophysical properties (TFP).

Such properties, first of all, are heat conductivity and thermal capacity coefficients. For the majority of the fire resistance materials used for maintenance of set fire resistance of building constructions and the equipment, their thermophysical properties, as a rule, essentially depend on temperature due to physical and chemical processes proceeding in materials during heating. Therefore, speaking about these materials TFP, as a rule, mean not their true characteristics, and the so-called effective, taking into account mentioned above physical and chemical processes.

Existing traditional methods as a rule do not allow to find TFP of fire protective materials as a functions of temperature under conditions of heating close to real conditions of a fire while the methods based on the heat conduction inverse problems solution [1-3], allow to find these functions under heating conditions close to standard fire conditions, - to fire tests conditions.

The purpose of work is temperature dependences of effective heat conductivity and thermal capacity of fireproof materials method presentation. The method based on the heat conduction inverse problems solution with experimental data of material samples heating in fire furnace under heating conditions close to standard conditions. The method application for fire protective gypsum plates TFP determination by thickness 2 sm in a range of temperatures from room up to 1000 C was presented as well.

Experiment. In the furnace three square bars of a fireproof material in the size 15 x 15 x 2 sm have been subjected to unilateral heating. From them two samples have been prepared for tests with different thickness of coverings, namely one bar thickness of 20 mm, pasted to a metal plate thickness of 6 mm. (a sample № 1) and two bars with thickness of 20 mm the everyone which attached to a metal plate by thickness of 6 mm and have been stuck together among themselves with the help alumosilicat glue (a sample № 2).

Behind a metal plate two layers of heat insulators thickness of 30 and 50 mm (fig. 1) settle down.

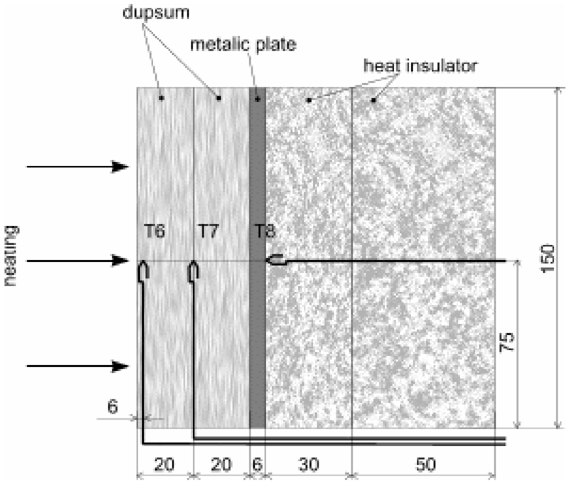

Fig. 1 The sample № 2 scheme with two gypsum bars

In Fig. 2 an experimental values of temperatures in installation sites of thermocouples for a sample № 2 are resulted. The temperature in fire furnaces changed on a known temperature curve of a standard fire.

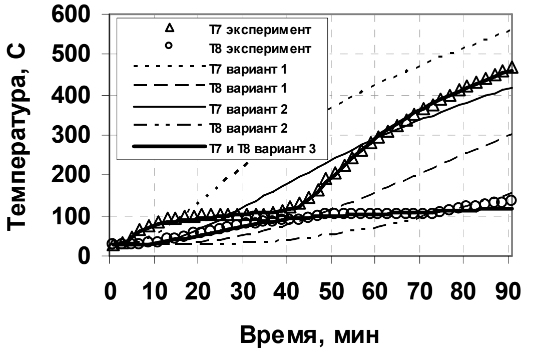

Fig. 2 Calculational and experimental values of temperatures in installation sites of thermocouples for a sample № 2 (see the table).

The TFP determination technique uses the so-called theoretical and experimental approach based the inverse problems solution [1-3]. Mathematically the technique concludes in search of such temperature functions desired λ and Cρ for which criterion

$$\phi = \sqrt{\frac{1}{n}\sum_{i=1}^{n}\left[T_i^{\text{Э}} - T_i^{P}(\lambda, C)\right]^2} \rightarrow \min$$

rreaches a minimum [1-3], where $T^{\text{Э}}_i$ - experimental values of temperatures, $T^{P}_i$ - calculation values of temperatures in points of an arrangement of thermocouples, n - total points of temperature measurements in space and in time.

Results. Desired effective heat conductivity λ and a specific volumetric heat capacity Cρ coefficients as a function of temperature are showed in fig. 3 and 4. The gypsum density was measured. Before tests it was Cρ=980 kg/m$^3$, after tests - Cρ=750 kg/m$^3$.

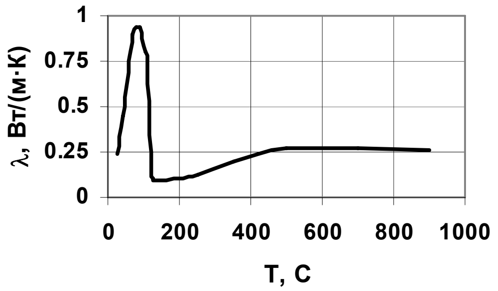

Fig. 3 Dependence of effective heat conductivity of gypsum on temperature.

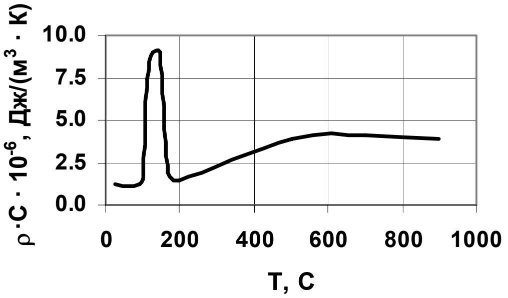

Fig. 4 Dependence of effective ($C_v$ = Cρ) heat capacity of gypsum on temperature

Presence of horizontal sites in area 100 C on curves of temperatures measurement explains degidratation and evaporation of water containing in gypsum, therefore dependence of thermal capacity Cρ from temperature (fig. 4) has in area 100 C "splash" which after 150 C is reduced. The peak of heat conductivity in area 100 C (fig. 3) explains by water vapour movement from places where occurs degidratation.

| Var. № | λ, Wt/(m K) | Cρ, J/(m3 K) | $\phi$, K |
|---|---|---|---|
| 1 | 0,24 | $1{,}7 \cdot 10^6$ | 105 |
| 2 | 0,207 | $2{,}8 \cdot 10^6$ | 34 |
| 3 | Fig.2 | Fig. 3 | 6,3 |

In tab.1 var.1- the literary data for gypsum TFP, var.2 - the constants obtained by inverse problems solution, var.2 - the functions obtained by inverse problems solution (see fig.3 and fig.4).

The conclusion. The stated technique allows to determine temperature dependences effective heat conductivity and a thermal capacity of fire protective materials with experimental data of several samples heating of materials in fire furnaces simultaneously. Application of the technique illustrates in the report by TFP determination for vermikulit and reactive fire protective materials.

Literature

1. Kozdoba L.A., Krukovsky P.G. Heat transfer inverse problem solution metods. Kiev, Naukova dumka, 1982, 360 p. (In Russian).
2. Alifanov O.M., Zantsev V.K., Pankratov B.M., Artjuhin E.A., Mishin V.P., Guk V.I., Golosov A.S. Algorithm's for diagnostics of thermal loadings of flying devices / Editor V.P.Mishin. Moscow.: Mashinostroenie, 1983, 168 h.
3. Krukovsky P. G. Heat and mass transfer inverse problems (general engineering approach). Kiev, Institute of Engineering Thermophysics NAS of Ukraine, 1998, 224 p.

# LIFE TIME AND OPERATION TEMPERATURE ESTIMATION FOR MCrAlY COATINGS FOR GAS TURBINE BLADES

**P.Krukovsky, K. Tadlya, O. Tadlya,**
**A.Rybnikov(1), I.Kryukov(1), N. Mojaiskaya(1), V. Kolarik(2), W. Stamm(3)**
Institute of EngeneeringThermophysics, 2a, Zhelyabova str., 03057 Kiev, Ukraine,
E-mail: kruk@i.kiev.ua
(1) Polsunov Central Boiler and Turbine Institute, Politechnicheskaya, 24, 194021 St. Petersburg, Russia. E-mail: rybnicov@online.ru
(2) Fraunhofer-Institut für Chemische Technologie, Joseph-von-Fraunhofer Str. 7, 76327 Pfinztal, Germany, e-mail: vk@ict.fhg.de
(3) Siemens AG Power Generation, Mellinghofer Str. 55, 45473 Mülheim an der Ruhr
Germany, e-mail: werner.stamm@siemens.com

Vanes and blades of modern gas turbine exposed to high temperature oxidation. It protective by MCrAlY coatings, where M – metal (Ni - nickel and/or Co - cobalt), Cr – chromium, Al – aluminium, Y – yttrium is base coating alloy component. Life time of these coatings is about 30000 hours (3-4 years) and more. It is determined by time of Al diffusion from protective coating which initial concentration in coating is composed from 6 to 12 %wt. Experimental approach to life time determination is practically not possible due to long terms and expensive cost. It is often difficult or not possible practical application of present models, which describe high temperature oxidation and diffusion processes, due to absence reliable values of models initial parameters, for example diffusion coefficients. In literature presents information about diffusion coefficients for simple compounds alloys only (double or triple alloys) although used in practice is more complicated.

In this work models coefficients (effective diffusion coefficients of Al, coefficient of Al activity appearance in interdiffusion zone and anthers) is proposed determine using solution of diffusion inverse problem with use experimental data of Al concentration profile across the coating at different temperatures for various exposures of samples in furnaces.

Physical model of diffusion Al distribution in “oxide-coating-base alloy” system have following description (Fig. 1). It is obtained by analysis of experimental investigation of NiCoCrAlY coatings.

The protection against oxidation is achieved by the formation of a thin $Al_2O_3$ layer on the coating surface ($x_1$-$x_0$). The oxygen absorbed from the gas medium diffuses to the $x_1$ direction across the oxide scale and reacts with the Al to form $Al_2O_3$. Al diffuses from the coating in two directions:

- towards the oxide – coating interface $x_1$;
- towards the coating – base alloy interface $x_4$;

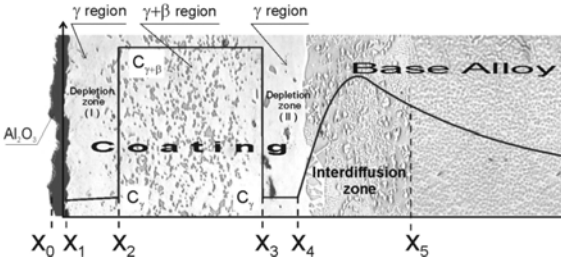

Fig. 1. The typical concentration profile of the Al at MCrAlY coating and base alloy.

Due to Al diffuses from γ+β - two-phase region at coating occur formation two aluminum depletion zones (γ- phase) that increase with time and temperature (Depletion zone I and II, Fig. 1). Al diffuses from γ+β - two-phase region only due to β- phase disappearance. Al concentration profile has stepped form in coating and form with maximum in interdiffusion zone. Al from interdiffusion zone diffuses partially to the base alloy and partially back to the coating.

Boundaries $x_2$ and $x_3$ move towards each other due to β- phase content decrease in γ+β - two-phase region of coating $x_2<x<x_3$. Al concentration $C$ and β- phase concentration $C_\beta$ in γ+β - two-phase region decrease with time.

A mathematical model with describing above stated processes is presented in detail at [1].

Experiment.

Polished samples of a 200 μm thick NiCoCrAlY coating with 10 % Al forming a γ-(Ni/Co,Cr) / β-NiAl – structure were exposed at 900 and 950°C in air for currently 20000 hours. The coating was deposited on IN738 by Low Pressure Plasma Spraying (LPPS). The samples were characterised metallographically in cross section before exposure and after 100, 300, 1000, 10000 and 20000 hours. After each time interval the concentration profiles of Al across the coating thickness were determined by electron microprobe performing the analysis every 2 to 10 µm and up to 100 µm into the base material. The window size for the element analysis was 400 µm parallel to the surface and 3 µm perpendicular to the coating surface.

Results.

Parameters identification with technique described in [1] carry out with use 300, 1000 hours exposures (Fig. 2). The time of β- phase disappearance is accepted as life time criterion. Calculation results were compared with experimental data for 10000 and 20000 hours exposures (Fig. 3).

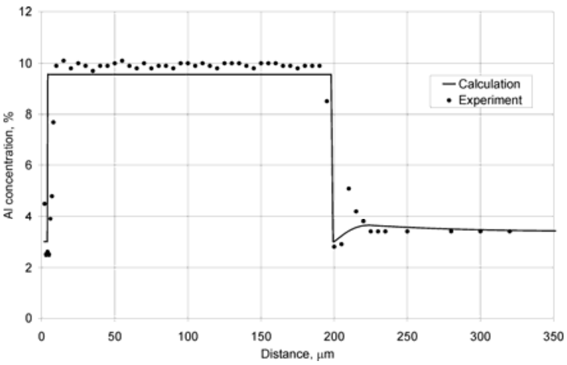

Fig. 2. Measured and calculated Al concentration profile across the coating and across the first 150 µm of the base material for 1000 h at 900 °C.

The average operation temperature of coating across the blade estimation is carried out by method the same described in [1]. Preliminary experimental investigation gas turbine coating is carried out at position show at Fig. 4. As results was obtained data about residual Al content at coating. Average operation temperature of coating was found by solution of inverse problem (Fig. 4). This methodic the same described in [1].

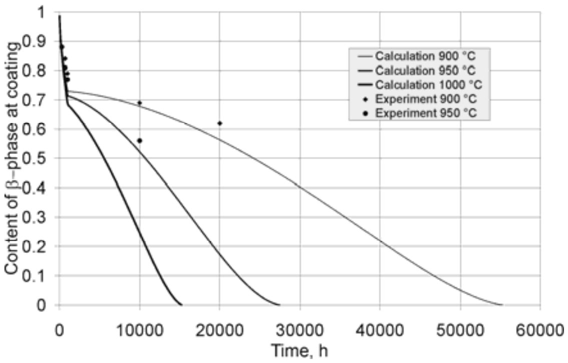

Fig. 3 The predicted and measured β-phase content at coating during oxidation for coating thickness 200 micron at 900, 950 and 1000 °C .

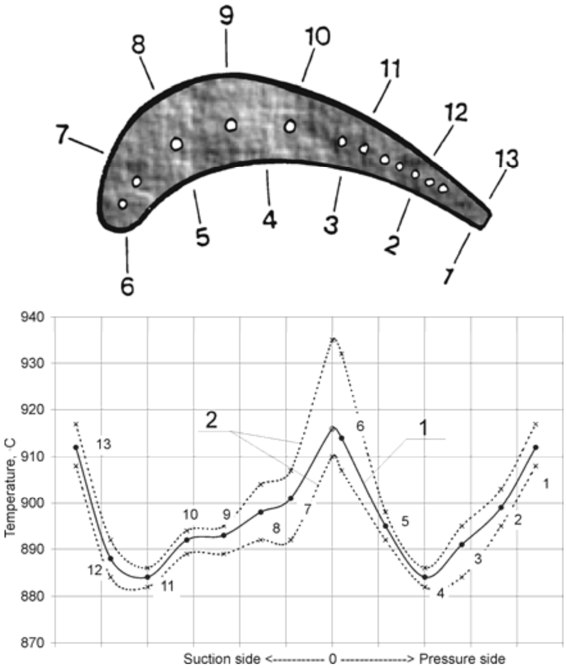

Fig. 4 Operation temperature profile across the blade after operating time 26400 h in turbine flowing channels. The numbers points are corresponded to numbers of position at blade. 1- calculation; 2 – range of measurements error.

So models and methods briefly described display their effectiveness for life time estimation for NiCoCrAlY coating for gas turbine blades and average operation temperature estimation for these coatings based on experimental data of Al content.

**Reference**

1. Krukovsky P.G., Tadlya K.A. Calculation and Experimental approach for Life Time and Temperature Analysis for Gas Turbine Blades Protective coatings// Industrial heating engineering 2003 v. 23 №4 pp. 41-50. (In Russian).

# THE EXAMINATION AND SELECTION OF ORGANIC COATINGS FOR THE PROTECTION OF THE ABOVEGROUND STORAGE TANKS FROM CORROSION

**Groysman A.**
Oil Refineries Ltd., P.O.Box4, Haifa, 31000, Israel, GALEC@ORL.CO.IL

Aboveground storage tanks (AST) for crude oil and fuels suffer from various types of corrosion. The presence of water, salts, hydrogen sulfide and microorganisms are the main factors in AST corrosion. Corrosion can result in uncontrolled leakage, loss of fuels, safety problems, and environmental damage. On the other hand, corrosion products may contaminate fuels and decrease their quality. Corrosion mechanism, types of corrosion and corrosion zones in AST are discussed. Organic coatings remain the most prevalent technique for the anticorrosion protection of aboveground storage tanks.

The API RP 652 recommends using coating systems based on the two generic types, epoxy and polyesters. This standard does not relate to coating systems based on zinc silicate, silicone epoxy, phenolic epoxy, novolac epoxy, polysiloxane, polyurethane and polyvinyl chloride materials, and does not relate to fuels containing oxygenates (for example, MTBE – methyl-tert-butyl-ether) or aromatic solvents (toluene, benzene and xylene) added to gasoline for increasing its octane number.

In order to make up these deficiencies, more than 50 industrial paint and coating systems from 30 manufacturers were examined under laboratory conditions in a three phase medium: 3% NaCl+0,2% $NaBO_3$ aqueous solution, gasoline with 60% vol. toluene or 15% vol. MTBE added (organic phase), and vapor phase. The panels with coatings were placed in the beakers containing the aggressive solution in such a manner as to enable examination of the resistance of coatings in the three phases: aqueous, organic and vapor. Visual examination was made every 7—10 days according to the standards. The experiments lasted 3 to 9 months. The solutions were refreshed every month. A paint specification standard was developed for selection of lining systems for inner surfaces of AST. Some of them are being introduced into practice for the protection of inner surfaces of AST which are currently in service.

# TEMPERATURE DEPENDENCE STRENGTH OF ADHESION BOND EPOXY CAUCHUK GLUES WITH STEELS

**Kuksenko V.S., Vettegren V.I. Bashkarev A.Ja.(1), Sitov V.A.(2)**
Ioffe Physico – Technical institute of RAS
26, Polytechnical Str., Saint Petersburg, 194021, Russia, Victor.Vettegren@mail.ioffe.ru
(1)Saint Petersburg State polytechnic university
29, Polytechnic Str., Saint Petersburg, 195251, Russia, bashkarev@stu.neva.ru/
(2)Federal State unitary enterprise "Central scientific institute of materials"
8, Parade str. Saint Petersburg, 191014, Russia

The special glues began used wide for glue of construction steels last time. Because it is important the task of prognoses the glue bonds in wide range of temperature. To do it the temperature dependencies of strength the adhesion bonds of epoxy rubber glues with steels 45 at constant velocity of loading was studied. The temperature range is 20—450 K. The characteristic temperature dependence strength of glue bond with steel for glue K-300 (silicon organic resin strengthen by low molecular weight polymer) show on figure 1.

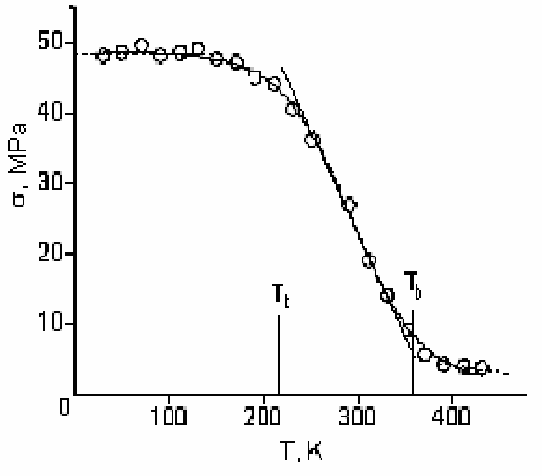

Figure 1. Temperature dependence strength of adhesion bonds glue K-300 with steel 45.

It was found that the strength decrease proportional temperature between two characteristic temperature $T_t$ and Tb. The strength is not depend on temperature at $T<T_t$, but it depend on speed of loading. The incline of temperature dependence strength decreases at $T>T_b$.

Values of temperatures $T_t$ and $T_b$ are shown in table.

The vibrations of molecules glues are "frozen" low $T_t$. They are described by Bose statistic. Because it thermal fluctuation are not format and fracture cause by tunnel transitions [2, 3]. One mode of thermal molecular vibration (twisting mode) un froze (vibration of this mode is described by Boltzman statistic) at $T_t$.

Характеристические температуры $T_t$ и$T_b$.

| Клей | $T_t$ | $T_b$ | $U_{0t}$ | $\gamma_t$ |
|---|---|---|---|---|
| | K | | кДж/моль | nm$^3$ |
| К-300 | 220 | 360 | 110 | 1,8 |
| KVS-31 | 220 | 295 | 150 | 1,7 |
| Kriosil | 265 | >400 | 105 | 1,7 |
| КDS-19 | 195 | 315 | 125 | 2,8 |
| КG-1м | 155 | 400 | 115 | |

Origin of thermal energy for thermal fluctuation appear. Because the glue molecules rupture by thermal fluctuations and tunnel transitions at $T_t<T<T_b$. Because the strength σ decreases proportional temperature T according Zhurkov equation [1]:

$$\sigma = U_{0t}/\gamma_t - (k_B T/\gamma_t)\ln(\tau/\tau_0) \qquad (1)$$

where $U_{0t}$ is activation energy of fracture, $\gamma_t$ is empirical parameter, τ is time to fracture, and $\tau_0 = 10^{-13}$ sec. The effective values of activation energy and parameter $\gamma_t$ in this temperature range are shown in table.

Bending mode of the molecular vibration an froze at $T>T_b$. Because the segmental movement appear and fracture deformation of glues increase in tens times Because of the parameter γ in Zhurkov's equation depend on deformation, it change during to fracture process. In this case the temperature dependence change as:

$$\ln\sigma = A - (3T_b/T) \qquad (2)$$

where A is parameter depending on strength at $T=T_b$, activation energy of fracture and time to fracture.

The values $T_t$ and $T_b$ can be determined by for example from thermal dependencies of capacity, relaxation spectroscopy and so on. That is why if the values of strength are determined at 3 or 4 temperatures at range $T_t<T< T_b$ one can calculate the strength and time to fracture the glue bond with steels in any temperature range [3].

## References

[1] Zhurkov S.N .// J. Fracture Mech.. 1965. V 1. N 1, P. 311—316.

[2] Slutsker A.I., Idarov Ch. // Polymer Science (A).

1984. Vol. 26, B. 9, P. 1823 -1829.

[3] Bronnikov S.V., Vettegren V.I., Frenkel S.Y. // Adv. Polymer Sci. 1998. V. 125, P. 103—148.

Supported by Federal program "Integration 2002", Grants № Б 0012 and И 0189

# THE TEMPERATURE SENSITIVE COATING

**Akylbaev Gh. S., Kusainov K.K., Karitskaya S.G.**
Karaganda State University named after E.A. Buketov
Universitetskaya, 28, Karaganda, 470074, Kazakstan, e-mail: ksg@kargu.krg.kz

Requirement in different sensors precipitately increases in connection with progress of the automated monitoring and control systems, with intrusion of new manufacturing processes, with transition to floppy computeraided productions, in particular in modern aero- and space naval architecture. The sensors, founded on optical visualization methods are the most perspective sensors

Optoelectronic systems, based on application as optical sensitive elements of crystalline phosphors [1] and liquid crystals [2] are widely used for getting information of temperature fields on the surface of objects of a compound geometrical form. The principle of operation of the indicated systems is based on a temperature luminescence quenching. The intensity of afterglow of the irradiated samples decreases as a result of the given process. The main drawbacks in the application of such sensitive elements with the purpose of measuring fields of temperatures are the insolubility of crystal phosphors in a polymeric binder [1], or rather narrow interval of temperatures (2—3 $^{o}$K), measured by liquid crystals with high sensitiveness to temperature and dependence of optical characteristics on other factors, for example, pressure [2].

With the purpose of correction of the indicated trouble, the temperature sensitive coating on the basis of arilmethane dyestuffs permitting with sufficient reliability to measure distribution of temperatures fields on objects of a compound geometrical form in extreme conditions (a temperature cycling, a vacuum) in a temperature over the range 253÷375 °K, is developed by us. It is provided measurement accuracy in the indicated range with an error ±1 °K.

The temperature sensitive coating (a width 4—8 microns) is represented by a molecular dyestuffs solution in polyvinyl butyral. The luminescence of the molecular dyestuffs at an intrusion them in a polymer matrix depends on temperature. The intensity of the dyestuffs luminescence changes several times within the temperature change from 273 to 375 K. A wavelength of a maximum of absorption by molecules of this dyestuffs implanted in a polymer matrix is 445 nm; a maximums of a luminescence of the dyestuffs molecules and their associates are 560 (for monomers) nm and 580 (for associates) nm.

We have studied the mechanism of temperature influence on luminescence of arilmethane dyestuffs in polymeric matrixes experimentally. The realization of experimental researches permitting to find out a capability of decreasing of the lower value of a temperature band is planned. The earlier given fact was not investigated in view of technical difficulties.

The automation of research process of the spectral and temperature characteristics of the obtained films was conducted in our lab. With this purpose the role of the chart recording device of the fluorescent plant constructed on a preferred circuit, was assigned to the personal computer. The computer was a part of a structure of the analogue and discrete input-output controller. The analogue and discrete input-output controller is intended for registration and digital conversion of analogue electrical signals of thermocouples and photo sensors, and also for the monitoring and control of actuating devices of the experimental plant, such as, limit switches, step-by-step motors of monochromators and to that similar. The control and programming of the controller implements the computer on a bit-serial interface [3]. The personal computer executes general control of the plant on a bit-serial interface. The controller is exchanged by the data with the computer, operates process of analog-to-digital conversion of a signal from a multiplier phototube and treats reference signals from the sensor of a monochromator. The observed data are mapped in a graphic presentation on the screen monitor.

The computations of integral values $I_{ti}$ of a luminescence were performed on the obtained experimental luminescent spectrums for each value of temperature. The integral values $I_{ti}$ of a luminescence were used at construction of a plot of relative integral values $I_{t_i}/I_{t_0}$ of a luminescence of the sample from temperature:

$$I_{ti}/I_{t_0}=f\,(t_i),$$

where $I_{ti}$ - integral value of luminescence of the sample for any value of temperature $T_i$,

$I_{t_0}$ - integral value of luminescence of the sample for the temperature $T_0$=253 K.

The designed temperature sensitive coating has been used in researching temperature fields on the surface of a diametrically streamlined circular cylinder. The researches were conducted on the plant including a hydrodynamic channel of a selfcontained type, which is described in [4]. The argon laser "ЛГН-502" with a general radiated power 1 W was as an irradiation source. The irradiation of a sample was conducted by a full spectrum ($\lambda$=457б9÷514б5 nm). The ray, passing through rotary lenses and electromechanical shutter, enters a diverging lens. Then the ray illuminated a surface of the located in a hydrodynamic channel the cylinder with the temperature sensitive coating. The intensity of a laser radiation was checked with the photodiode. At processing of experiments results the normalization of the intensity of a laser radiation in relation to an emission power at the moment of a photographing of support exposure was conducted. The distribution of a luminous emittance of temperature sensitive coating of an irradiated surface of the cylinder was recorded on a photographic film. The processing of the obtained experimental data was made by scanning of the photographic image in computer storage with treatment of this image with application of the special application packages.

Temperature in each treated point was determined on a plot of the dependence of the relative integral values $I_{ti}/I_{t_0}$ of a luminescence of temperature sensitive coating from temperature. Definite thus temperatures of the cylinder surface in each point of its image were correlated to a scale of gray tones and halftones selected arbitrarily with the purpose of obtaining of the most contrast image of a field of temperatures.

Measuring of an instantaneous picture of the temperature field conducted with the temperature sensitive coating fixes changes of hydrodynamical characteristics of the flow well matched with the theory.

As have shown outcomes of check measurements, value of temperatures obtained copper- constantan by thermocouples fixed in different points of the cylinder and by the temperature sensitive coating, coincide within the limits of experimental error (≅4%) and differ, on the average, on ±1°K. The comparative analysis of experimental results conducted for determination of temperature of a circular cylinder in a hydrodynamical channel by the luminescent method with experimental data received by the method of holographic interferometry [4] with the analogical hydrodynamic regimes has shown that the absolute value of differences of experimental data for the two curves lie within the limits of the experimental error.

The obtained outcomes testify about a feasibility of a luminescent method with application the temperature sensitive coating on the basis of aril methane dyestuffs as the molecular sensor for research of temperature fields on a surface of objects of the compound geometrical form. Application of modern means of recording, such as the digital photographic camera or digital video camera will allow completely to automate process of visualization and diagnostic of temperature fields of bodies, passing stage of processing of the photo images. It will promote a decrease of an error of measurements essentially.

## References:

1. Gouterman M., Callis J., Burns D., etc. Luminescence Imaging for Aerodynamic Testing. Proceedings of the ONR // NASA Workshop on Quantitative Flow Visualization, Purdue University. 1990.
2. Fibre-optical sensors. / under edition T. Okosi: translation from the Japanese language. Leningrad, 1990. – In Russian.
3. Stashin V.V. etc. Designing of digital devices on single-chip micro controllers. - Moscow, 1990. - In Russian.
4. Akylbaev Gh. S. The new optical research methods of a heat-mass transfer. – Almaty, 1995. – In Russian.

# THE ANALYSIS OF DYNAMICS OF INCLUSIONS IN VISCOUS MEDIA UNDER THE THERMOCAPILLARITY EXERTION

**Raychenko O.I., Byakova A.V., Nakamura T.(1), Derev'yanko O.V., Gnyloskurenko S.V. (2)**
Frantsevich Institute for Problems of Materials Science, Ukrainian National Academy of Sciences,
3, Krzhyzhanivs'ky St., Kyiv, 03142, Ukraine, e-mail: raitch@ipms.kiev.ua
(1)Institute of Multidisciplinary Research for Advanced Materials, Tohoku University,
2-1-1 Katahira, Aoba-ku, Sendai 980-8577, Japan, e-mail: ntakashi@tagen.tohoku.ac.jp
(2)IIS Materials, Tokyo University, Tokyo City Build., 1-33-6 Komaba Megaro-ku Tokyo,
153-0041, Japan, e-mail: slava@iis.u-tokyo.ac.jp

## Introduction

The behavior of emulsions, foamed liquids, suspensions in a non-uniform temperature field is very essential for most important scientific fields and technological branches (for example, the motion of bubbles, particles of refractory materials or slag drops in metal melts). Although the theory of bubbles and drops motion is developed and published it cannot be applied to the solid particles thermocapillary motion. So, careful verification of the fundamental equations describing dynamics of foreign inclusions in a viscous medium with a temperature gradient is of great importance.

The present paper aims to give a more precise definition to the above-mentioned problem.

## Model and theoretical study

We use here the well-known conventional model as follow: an inclusion (bubble) is immersed in a viscous unlimited fluid (Fig.1a). The temperature field in a medium (without influence of inclusion) has a constant gradient. Such conditions were adopted elsewhere [1-9]. In [10] the model considered the motion in the infinite medium under joint thermocapillary/gravity influence and the thermocapillary part of the theory took into account the dependency of the surface (interfacial) energy on the particle location. The author [11] performed the comparative analysis of the theories of thermocapillary motion of inclusion under zero-gravity condition. In the present model the gravity is not considered also. The air bubble in aluminium melt serves as the example here (Fig. 1).

These scaled velocities here are the modified capillarity criteria in essence.

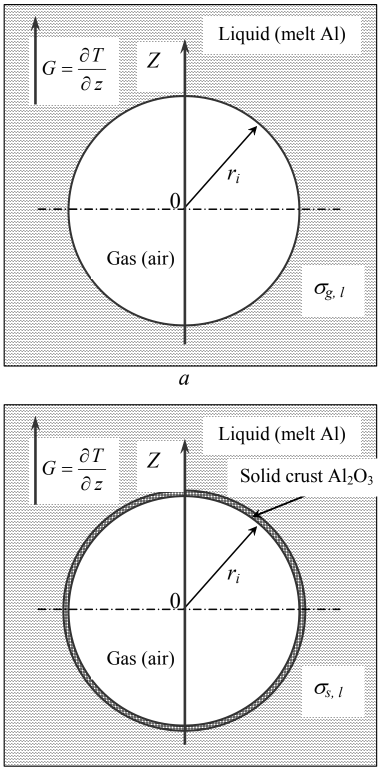

*a*

*b*

**Fig. 1**. Model used in the present theory. *a*- an air gas bubble in aluminium melt; *b*- bubble with solid crust. $G = \partial T/\partial z$ is the temperature gradient; $r_i$ is the bubble radius; $\sigma_{g,\,l}$ is the surface tension on gas (air) – liquid (Al) interface; $\sigma_{s,\,l}$ is the surface tension on solid ($Al_2O_3$) - liquid (Al) interface.

The equations for the scaled velocities of the various inclusions are obtained:

$$Ca_b = \frac{u_b\,\eta}{2\sigma_{T;g,l}\,G\,r_i} = 1 \text{ (bubble)},$$

$$Ca_d = \frac{u_d \eta}{2\sigma_{T;ld,l} G r_i} = \frac{4+3\alpha}{(2+3\alpha)(2+\beta)} \text{ (drop)},$$

$$Ca_s = \frac{u_s \eta}{2\sigma_{T;s,l} G r_i} = \frac{1}{2+\beta} \text{ (solid particle)}$$

where the indices $g$, $l$, $s$ concern gas, liquid and solid, respectively; $u_{b,\ d,\ s}$ are the velocities of inclusions; $\eta$ is the viscosity of a liquid medium; $\alpha = \eta_i / \eta$ is the reduced viscosity; $\eta_i$ is the viscosity of an inclusion; $\beta = k_i / k$ is the reduced conductivity; $k_i$ and $k$ are the thermal conductivities of an inclusion and a medium, respectively; $\sigma_{T;\ g,l}$, $\sigma_{T;\ ld,\ l}$, $\sigma_{T;\ s,l}$ are the interfacial tension temperature coefficients, the double indicies ($g$, $l$), ($ld$, $l$), ($s$, $l$) concern bubble, drop, solid inclusion in liquid medium, respectively.

## Conclusions

The present theory might be the scientific basis of the research method ought to be further developed more rigorously. Many essential elucidations to understand interaction between foreign inclusions (mainly, solid particles) and surrounding fluids could be obtained from the proper space-experiments.

At analysis of the dynamics of a bubble at orifice submerged in a liquid with temperature gradient, it is necessary to consider few stages of bubble formation ("under critical growth", "critical growth" and "necking") [12, 13].

The chemical content of gas (air) in a bubble can be of great importance [9], in particular, for an inclusion/medium contact layer (zone). For example, if a bubble submerged in Al melt contains oxygen then on its surface a thin layer of alumina might appear. Thus a contact between an inclusion and a medium will transform from the gas/liquid type to the solid/liquid type (namely, $Al_2O_3$ (sol.)/Al(liq.)) (Fig. 1b).

The proper mathematical and computer analysis is given.

## References

1. N.O. Young, J.S. Goldstein, and M.J. Block, *Journal of Fluid Mechanics,* **6**, p.350-356, (1959).
2. V.M. Kuznetsov, B.A. Lugovskoy, and E.I. Sher, *Zhurn. Prikl. Mekh. Tekhn. Fiz.,* No.1, p.124-126, (1966). (In russian). [Engl. ed.: *NASA Technical Translation* F-16569, Sept. 1975].
3. A.S. Povitskiy and L.Ya. Lyubin, *Fundamentals of Dynamics and Thermo-Mass-Exchange of Liquids and Gases at Zero-g Condition,* Mashinostroyeniye, Moskva, 1972. (In russian).
4. Yu. Yalamov and A.S. Sanasaryan, *Inzhenerno-Fizicheskjy Zhurnal,* **28**, p.1061-1064, (1975). (In russian).
5. W.R. Wilcox and R.S. Subramanian, *AIAA Journal*, **17**, p.1022-1024, (1979).
6. G. Wozniak G., J. Siekmann, and J. Srulijes, *Zeitschrift für Flugwissenschaften und Weltraumforschung,* **12**, p.137-144, (1988).
7. B.N. Antar and V.S. Nuotio-Antar, *Fundamentals of Low Gravity Fluid Dynamics and Heat Transfer,* CRC Press, Boca Raton, Ann Arbor, London, Tokyo, 1993.
8. S.S. Sadhal, P.S. Ayyaswamy, and J.N. Chung, *Transport Phenomena with Drops and Bubbles,* Springer-Verlag, New York, 1997.
9. R.S. Subramanian and R. Balasubramaniam, *The Motion of Bubbles and Drops in Reduced Gravity,* Cambridge University Press, Cambridge, 2001.
10. O.I. Raychenko, *Reports of the National Academy of Sciences of Ukraine*, No.3, p.92-96, (2003). (In russian).
11. O.I. Raychenko. *High Temperature Materials and Processes*, (to be published).
12. S.V. Gnyloskurenko, A.V. Byakova, O.I. Raychenko, and T. Nakamura, *Colloids and Surfaces A: Physicochem. Eng. Aspects*, **218**, p.73-87, (2003).
13. A.V. Byakova, S.V. Gnyloskurenko, T. Nakamura, and O.I. Raychenko, *ibid.*, **229**, p.19-32, (2003).

# THE EFFECT OF STRUCTURE-TOPOLOGICAL TRANSFORMATIONS ON DYNAMIC CONSTANTS AND OPTICAL DAMAGES OF $AS_2S_3$ CHALCOGENIDE GLASSES AND FILMS

**May K.V., Fekeshgazi I.V., Кlimenko A.P. (1), Mitsa V.M. (2)**
Lashkaryov Institute of Semiconductor Physics of NASU
41, pr. Nauki, Kyiv, 03028, Ukraine, E-mail: http: // www.isp.kiev.ua
(1)Kiev national university of technologies and design
2, str. Nemirovicha Danchenko, Kyiv, 01011, Ukraine
(2)Uzhgorod national university.
46, str. Pidhirna, Uzhgorod, 88000, Ukraine, E-mail: admin@univ.uzhgorod.ua

It is known, that different structure-topological complexes are formed depending on technological conditions of synthesis of the chalcogenide glasses and films, which determine their optical properties. The analysis of the effect of structure-topological transformations on refraction coefficient, constants of linear and two-photon absorption, Raman scattering, dynamic constants and optical damages of $As_2S_3$ chalcogenide glasses and films was carried out.

Fast quenching of the melt of the given substance is the most widespread way for the fabrication of massive glasses. With the purpose to evaluate the effect of structure-topological transformations on opto-physical parameters of glassy $As_2S_3$ on the conditions of synthesis the samples were used which were synthesized from an elementary As and S components of the purity OSCh-5 at different temperatures $T_i$ of melt treatment and quenching rates $V_i$. Temperature $T_1$=870 K - is the minimal temperature, at which the interaction As with S occurs in real time scales (150 hours), $T_2$=1120 K – is the temperature, at which glassy $As_2S_3$ is usually synthesized, temperature $T_3$=1370 K – is the maximal temperature, at which of $As_2S_3$ molecule do not yet dissociates on elementary components. The rates $V_1=10^{-2}$ K/sec and $V_{13}=10^2$ K/sec are restricted by possible experimental conditions, while $V_2$=1 K/sec is optimal for synthesis of glassy $As_2S_3$.

The electronic microscope EMB-100B and standard criteria for the gradation of micro-dispersion and microheterogeneity levels, which were determined by the ratio of quantity of precisely contoured boundaries to quantity of pseudo-granules in the region of 0,1 μm size was used for an establishment of microstructure of glasses.The values of linear losses coefficient and two-photon absorption constants were determined from the experimentally measured dependences of transmitted light intensity I on intensity $I_0$ of incident light. They have sublinear character, while dependences of the reverse transmission $I_0/I$ are in direct proportion to $I_O$. This linearity indicated that two-quantum transitions specifies the dominant contribution in the process of nonlinear light absorption. The threshold optical damage $I_d$ was determined as minimal power density of laser radiation, which results in occurrence of bright flare on a surface of a sample and, as a consequence, to the sharp reduction of intensity of transmitted ruby laser beam.

The formation of the different structural - topological elements was carried out by the selection of different $T_iV_i$ . The basic set of possible structural groups is realized which can be divided into two basic types: A type - homogeneous, where main motive is bipyramidal $AsS_{3/2}$ structural units, inherent to glasses with microdispersion structure of different degree of connectivity and continuous structural network; and B type which is formed by heteroatomic pseudo-molecular units $As_2S_{4/2}$, $As_3S_3$, $As_2S_5$ and homogeneous aggregations of sulfur $S_8$. The same results are received also from the comparative analysis of Raman spectra of arsenic trisulfide glasses in the region of valence vibrations. The realization of the first type take place at the minimal values of and second type - at maximal ones. Thus, the band gap width increase is observed under the decrease of density, refraction index from 2,71 up to 2,48 and two-photon absorption coefficient from 0,37 up to 0,15 cm/MW, at respective increase of the value of the threshold optical damage.

On the basis of the comparative analysis of Raman spectra of trisulfide glasses in the region of valence vibrations it was shown, that with increase of melt temperature and cooling rate the concentration of s.u $As_2S_{4/2}$, As $_{3/3}$, $S_8$, $S_n$ in a matrix of a-$As_2S_3$ structure is increased.. At such increase a dilatation degree of a matrix of a-$As_2S_3$

structure, density and speed of ultrasound in glass are decreased and, respectively, dynamic strength of a glass expressed by elastic modules is decreased.

By the results of low-frequency Raman spectra of a-$As_2S_3$ investigations it was confirmed, that low-frequency Raman spectroscopy in the region of boson maximum together with the data of ultrasonic study is the effective method of evaluation of the sizes of structural correlation in glasses in different approximations of their structure. Resolution capability of LF spectra is higher that the resolution capability neutron diffraction analysis studies of glasses in that spectral region. At variation of physico-technological conditions of a-$As_2S_3$ synthesis with the growth of melt temperature and cooling rate (except $T_1v_2$ conditions) the low-frequency shift LF "boson" maximum from 26 a-$As_2S_3$ ($T_1v_1$) up to 20 $cm^{-1}$ a-$As_2S_3$ ($T_3v_3$) is observed, which is accompanied by increase of radius of structural correlation $R_c$ in homogenic approximation of the glasses structure and of the length L of structural correlations - in the chain approximation. For all cases ratio L/Rc ˜ 2. In binary $As_yS_{1-y}$ glasses it was revealed, that with the increase of average coordination z=3y+2 (1-y) the LF shift of a maximum towards the high-frequency area of a spectrum from 19 $см^{-1}$ (z=2,1) up to 26 $cm^{-1}$ (z=2,4) is observed, which is accompanied by the intensity lowering of LF maximum, non-monotonic size L decrease of chains from 1,5 up to 1,4 nm, respectively. The minimum L=1,42 nm at z=2,4 corresponds to the maximum of dynamic strength. These coordination changes and the respective growth of elastic modules of $As_yS_{1-y}$ glasses from z = 2,1 up to z=2,4 agrees with the predictions of the topological-cluster (TC) concept about increase of dynamic strength of a matrix of glass structure due to the increase of interchain interaction and lacing of the one-dimensional clustersкластеров into layer-chained at approach to $As_{40}S_{60}$ structure, z=2,4, (1D-2D transition). The change of $As_{40}S_{60}$ structure to the side of As enrichment ($As_{42}S_{58}$) results in growth of intensity LF vibrations and to the increase of the cluster sizes. Simultaneously with L growth the decrease of dynamic strength of the glasses is observed at z>2,4 and deviation from theoretically predicted by the TC concept of the elastic modules growth according to $(z-2,4)^{3/2}$ law. The revealed dilatation of a glass matric structure at z>2,4 is accompanied by the formation of new $As_2S_{4/2}$ and $As_{3/3}$ s.u.

The decrease of the two-photon absorption coefficient with the growth of $T_i$ or $V_i$ is caused by increase of band gap width. The theoretical estimations of the optical strength of a-$As_2S_3$ which were carried out in adiabatic approximation have shown, that theoretical and the experimental data differ almost by three orders. At the same time, according to the theory the values of the optical threshold increases, because the values of the coefficients of linear and non-linear losses are decreased, and the size of width of the band gap - increases.

The results of investigations of the films Raman spectra, obtained from the vapor phase of a-$As_2S_3$, in which the multinuclear кластеры $(As_2S_3)$ n (n=1-10) are present, have shown, that the structure of the short order in obtained films, mainly is formed by $As_{3/2}$, $As_{4/2}$, $As_{3/3}$, $S_8$, $S_n$ s.u.

The possibility of the depletion of the film by the high volatile component at the initial stage of the films growth foresees the theoretical analysis of the discrete deposition process. However non-heterogeneity of a condensate on composition structure here was observed within several monolayers. The influence of boat temperature on the dissociation processes of a material during discrete thermal evaporation is confirmed by results of the analysis of a-$As_2S_3$ film structure. It was shown, that the sizes of transitional area at discrete and commonly used thermal deposition from open boat are not bigger than 3,0 nm. However the structure of the films, which are received by thermal deposition from open boat, is micro-nonuniform. Optical strength of the micro-non-uniform films on the glass substrates P=30 $MW/cm^2$. For a-$As_2S_3$ films, obtained by the discrete thermal evaporation, mean value of P=60 $MW/cm^2$, and vibrational spectra of such films are similar to the spectra of volume glasses obtained at intermediate cooling rates.

¤This work was carried out with the partial financial support from the State Foundation of fundamental investigations of Ministry of education and science, Ukraine.

# INVESTIGATION OF EFFECTIVE THERMAL CONDUCTIVITY OF THERMAL PROTECTION MATERIALS AT EXTREMUM TEMPERATURES

**Paderin L.Ya., FischerW.P.P.** (1)
Central Aero-Hydrodynamic Institute (TSAGI),
Zhukovsky, 140180, Moscow Region, Russia Email:Pader@inbox.ru
(1)European Agency on Defence and Space (EADS), Bremen, Germany

The specific and the basic difficulties, arising at the thermal conductivity investigations of the porous semi-transparent insulation materials, are caused, in the main, by combination of three types of heat transfer in these materials. These are heat conduction through the solid fraction (the fibber skeleton and contacts between ones) of material, radiant heat transfer and molecularly-convective heat transfer in gas-solid fraction systems within material. The relative part of each heat transfer type in the total heat transfer depends of concrete chemical composition, physical structure of material, value and gradients of temperature within material and environmental gas pressure. Nevertheless, at present time in the design and engineering calculation practice the study of heat transfer in these materials is evaluated by means of numerical calculations of non-linear heat conduction equation with using effective thermal conductivity, in which each of three heat transfer components is taking into account.

By present time the great volume various both theoretical and experimental investigations, concerned to evaluation of heat transfer and effective thermal conductivity as well as its separate component, of porous semi-transparent materials is performed. However, because of material structure and studied physical processes complexity, simplifying assumption are made, when the above both theoretical model is developed and the calculations are performed. That is reducing significantly the adequacy of theoretical models and calculation results obtained to real physical processes, taking place within materials and, in connection with this, limiting the possibilities of practical using above model and results. For example, at present time there are no the adequate theoretical models, permitting to identify the fibber skeletons and the thermal contact resistance between the fibbers, that do not permits the objective theoretical evaluating the total heat transfer, especially conductive and molecular- convective heat transfer parts within considering materials as well as their effective thermal conductivities and separate components of ones.

In practice, when the thermal design problems are solved, the information about the effective thermal conductivity of the thermal protection materials, is obtained by means of experimental thermo physical investigations.

At present time the effective thermal conductivity measurements of thermal insulation materials are performed by means of the steady state method of heated plate (test sample) with compensation of heat leakage from the plate and its heater under study (Hot Guard Plate Method), in the main. In present work the new version of the method and facility for the experimental and numerical-experimental evaluating effective thermal conductivity of thermal insulation materials in the ranges of temperature $T = 400 \div 2000$ K and ambient pressure $P = 10^0 \div 10^5$ Pa are suggested. According to this method two test samples, puts up symmetrically concerning to the adjustable electric resistance heater and one-dimensional heat flux is provided in the test samples between their heating and cooling sides under test conditions. The effective thermal conductivity $\lambda_{eff}$ is evaluated on the base of the measuring of electrical power of the heater (N), temperatures of heated ($T_h$) and cooled ($T_c$) sides of the samples, its thickness (h) and cross-section area (S) from the relationship

$$\lambda_{eff} = N \cdot h / 2\,(T_h - T_c)S$$

The effective thermal conductivity measurement errors in above ranges of temperatures and gas pressure for steady state measurements are decreased until 5 % in comparison with known analogues. At that the facilities will be available for creating both steady state and transient thermal regimes, providing the wide ranges of spatial and time temperature gradients in the test samples, that permits by means of joint experimental and calculation investigations to evaluate:

- the effective thermal conductivity by means of steady state method,

- -gas conductivity component in effective thermal conductivity of materials in dependency of gas pressure,
- -applicability ranges of effective thermal conductivity obtained by means of steady state method for transient thermal regimes; to consider the possibilities for correction of thermal conductivity values as applied to concrete transient thermal regimes,
- effective thermal conductivity, using the results of the temperature measurements in the test sample under transient thermal regime of one, by means of the inverse thermal conduction task solution method as well as to verify the similar data obtained by other authors on other facility,
- influence of radiant, geometrical, thermo physical parameters (emissivity of external sides, thickness, spatial and time gradients...) of a sample on its effective thermal conductivity,
- accuracy of new theoretical or empirical approaches for evaluating effective thermal conductivity as well as the separate components of these coefficients for concrete materials.

As example the test results, obtained for series of flexible fibber materials, are presented.

The work was funded by INTAS in the frame of Project № 00 – 652.

# BORON POWDERS GAS-THERMAL TREATMENT AND DEPOSITIONS

**Gabunia D.L., Tsagareishvili O.A., Darchiashvili M.D., Gabunia L.D., Darsavelidze G.Sh.**
Institute of Metallurgy and Material Sciences of the AS of Georgia 15 Al.Kazbegi ave., 0160
Tbilisi, Georgia, E-mail: root@metall.acnet.ge

Boron possessing a number of the specific physical-mechanical and chemical properties, having two isotopes -$^{IO}$B and "B - distinguishing by the value of seizing section of thermal neutrons (3990 and 0,05 Barn respectively), is a prospective material for protective coatings on different details and designs [1]. It is know a number of technological mode of production of protective coatings by use of elementary boron or its compound [2]. A gas- thermal deposit of coatings is one of the perspective methods possessing a number of advantages over other methods. A powder yield is of importance for carrying out of coating deposition by gas-thermal. Industrial amorphous and "fine-crystalline" boron powders have a small volume weight (0,2 g/cm$^3$) and a relatively lower density. They are oxidated, aggregated and practically no yielded.

As it is known, powders with spehrical form of partides successfully solve the yield problem. The most acceptable process of powder spheroidization is their plasma-treatment, that thanks to the high-intensive heat source has the profitable thermal end gas-dynamic characters for spheroidization processes. However, as for as our information goes, production data for spheroizided boron particles are partially absent.

In the present work we attempted to determine possibilities for application industrial production boron powders in order to their spheroidization and deposition of gas-thermal coatings.

As the initial material was used "fine crystalline" boron powder of industrial production. It is a polydispersion system with the predominant fraction of particles less than 10 um. In accordance with x-raying a crystalline p -rhombohedral phase and a amorphous boron phase both observe in the initial powder. The presence of great amount of fine-dispersed particles as well as the amorphous phase in the powder are good reasons for aggregation of particles and powder crumpling. This has made it impossible to passage the powder through a bunker-feeding. In order for facilitating the main powder transportation it is necessary to add a high- yield powder-carrier promoting the mixture yield. As a powder-carrier utilized spheroizided aluminium powder AC.H-4 with mean value of particles no more than 40 um. Correlation of the boron powder amount to the powder-carrier one was 1:1 in the mixture.

Gas-thermal treatment of boron powder as well as coatings deposition carried out on the installation UPU -3 of plasma dusting. For the plasma making gas use made of argon. The powder mixture let pass through the plasma stream and then cooled down in a water bath. Thus it has been produced powders consisted of boron, aluminum and products of their interaction . X-ray analysis of the powder mixture of boron and aluminum showed that after gas-thermal treatment there were side by side - p-rhombohedral boron phase as well pure aluminum and dodecaboride of aluminium - A1B$_{12}$.

It has been of interest to trace the possible alterations in the structure of boron powder after their gas-thermal treatment. The powder cleaned off aluminum in dilute HC1 (1:4) by chemical treatment and following washing down in distilled water. X-raying and x-ray electron probe analysis showed the pure aluminum contend did not exceed 0,1 wt.% in the purifying powders. However , diffraction lines of the second phase are observed by the side of p -boron diffraction pattern. The second phase is identified as dodecaboride of aluminium -A1B$_{12}$. The observed delicate intensity of A1B$_{12}$ diffraction lines is apparently conditioned by low content of the indicated phase. Investigations of forms and surface conditions of boron powder subjected to gas-thermal treatment permitted a number of morphological to be revealed. The most often following types of boron particles are observed:

- spherical particles having diameter to 1,0 um with comparatively smooth surface and feebly-expressed micro relief;
- spherical particles having diameter to 40 um with rather developed surface containing pores or cavities;
- particles with rounder (smelting) borders.

It has been stated that particles from one to several microns form the most portion in total mass of the material.

The portion of spheroidized boron particles of 50 - 100 um sized does not exceed 30% in the final product. Micro spheres of 10-20 um sizes considerably more than larger particles. It is necessary to note the presence of no subjected to gas-thermal treatment particles of the initial boron powder in the processing product that seems can be explained by their location on the outlying area.

The structure of boron micro spheres is formed under enough great cooling ($10^3$ - $10^4$ degree.$s^{-1}$). So crystallization of boron particles is getting unstable in this condition and appearance of metastable of amorphous phases is likely to take place. The presence of heavy temperature gradients under crystallization because of low heat-conductivity of boron leads to considerable thermal stresses and in consequence, to plastically deformation of boron by twinning as well as to cracking. There are twinning zones and micro cracks on the surfaces of micro spheres.

Electron diffraction analysis showed the presence of boron suboxide - $Bi_2O_2$ m the products of gas-thermal treatment both in crystalline and amorphous states, as well as in a -tetragonal modification of crystalline boron.

For deposition of the coating on aluminum substrate as initial was tested both an industrial powder and boron powders with different granulometric compositions subjected to gas-thermal treatment. Coatings that were produced on the base of 20-100 u,m dispersion powders, characterized by satisfactory adhesiona properties.

**References**

1. Glukhov V.P. Boride coatings on Iron and Steels. Kiev: Naukova Dumka. 1970, p.26-66.
2. Zverev A.N., Sharivker S.Yu., Astakhov E.A. Detonation Dusting of Coatings. Leningrad. Sudostroenie, 1977.
3. Gabunia D.L., Tavadze F.N., Tsagareishvili G.B., Crushing of Crystalline boron and Investigation of its Fractionation Powders. In Proceedings: The Technological Combustion Problem. Moscow., Chernogolovka. p.79-82.

# PROPERTIES OF MATERIALS ON THE BASE OF ALUMINUM OXIDE AND ALUMINUM NITRIDE

**Tsyganenko V.S., Lityuga N.V., Dubovik T.V., Rogozinskaya A.A., and Panashenko V.M.**
Frantsevich Institute for Problems of Materials Science of the NAS of Ukraine
3, Krzhyzhanovsky St., Kiev, 03142, Ukraine, e-mail: panavic@ukr.net

With the aim of increasing the mechanical strength, oxidation resistance, and heat resistance, aluminum oxide additives in amounts of 10—50 mass % were introduced into aluminum nitride. Specimens of the indicated compositions were prepared by pressing and further sintering at 1800 °C in a nitrogen atmosphere. The electrophysical, chemical, and thermomechanical properties, including thermal decomposition under heating by solar radiation, were investigated on sintered specimens (Table 1 and 2).

The properties of the materials presented in Table 1, were determined by standard procedures. An investigation of the effect of a focused solar radiation flux on specimens was performed using a SGU-4 heliounit (Table 2). As characteristics of thermal decomposition, the following parameters were taken:

- the rate of mass loss

$$V_m = \Delta m/(F\cdot\tau),\ \mathrm{kg/(m^2\cdot sec)},$$

where Δm is the decrease in the mass, kg,

τ is the test time, sec;

F is the surface area of the specimen, $m^2$;

- the spectral radiating capacity;
- the true surface temperature, °C.

The two last characteristics were determined by procedures described in [1, 2]. Using an actinometer, a galvanometer, and a water-cooled calorimeter, simulating a model of a perfect radiator, the direct solar radiation and the heat flux per unit area ($kW/m^2$) were determined (Table 2).

From data presented in Table 1 it follows that the addition of aluminum oxide to aluminum nitride increases the mechanical strength, heat resistance, and oxidation resistance, with dielectric characteristics being retained. According to the X-ray analysis data, the materials on the base of aluminum nitride and aluminum oxide are mixtures of the following phases: AlN with the lattice constants a = 3.114 A, c = 4.986 A, α-corundum, $\gamma$-$Al_2O_3$, and oxynitride with the composition $5Al_2O_3\cdot AlN$. The performed investigations indicated that the materials of the AlN—$Al_2O_3$ system were not wetted with molten aluminum at 1100 °C and with a carbon steel at 1450 °C.

The data given in Table 2 show that the rate of mass loss for specimens of the AlN-$Al_2O_3$-based materials under conditions of unilateral radiant heating in the temperature range 2440—2495 °C for 60 sec was 0.083-0.183 $kg/(m^2\cdot sec)$. That is, at the indicated temperatures, the materials can be in operation under conditions of intensive heating for a short period of time. The true surface temperature and spectral radiating capacity, that determine the heat balance on the surface of a specimen, are important characteristics.

Taking into account that $Al_2O_3$ melts at a temperature above 2040 °C and dissociates at a temperature above 3000 °C [3] and that AlN begins to dissociate at 2200 °C [4], it can be assumed that under solar heating at 2440—2495 °C, the melting of $Al_2O_3$ and the active dissociation of AlN proceed. This is confirmed by the X-ray analysis data, which indicate that after radiation, in the surface layers of specimens, the following phases are present: $\alpha$-$Al_2O_3$, $\gamma$-$Al_2O_3$, and traces of AlN.

## CONCLUSIONS

The complex of the investigated properties (high dielectric characteristics, mechanical strength, and thermal stability) shows that the materials of the AlN—$Al_2O_3$ system can be used in high temperature engineering as electrical insulating and refractory materials and in rocketry and astronautics as radioparent materials for protection of antenna systems of air-borne equipment for operation in dense atmospheric layers.

Table 2. Test results for materials of the $AlN-Al_2O_3$ system under solar heating on a SGU-4 heliounit

| Composition, mass % | Test conditions | | Test results | | |
|---|---|---|---|---|---|
| | Heat flux per unit area, $kW/m^2$ | Duration, sec | Spectral radiating capacity | True surface temperature, °C | Rate of mass loss, $kg/(m^2 \cdot sec)$ |
| AlN | 6850 | 63 | 0.73 | 2460 | 0.083 |
| AlN—5 $Al_2O_3$ | 6900 | 60 | 0.79 | 2450 | 0.098 |
| AlN—10 $Al_2O_3$ | 6850 | 60 | 0.81 | 2465 | 0.161 |
| AlN—20 $Al_2O_3$ | 6850 | 58 | 0.85 | 2440 | 0.155 |
| AlN—30 $Al_2O_3$ | 6850 | 60 | 0.80 | 2450 | 0.134 |
| AlN—40 $Al_2O_3$ | 6900 | 59 | 0.80 | 2440 | 0.183 |
| AlN—50 $Al_2O_3$ | 7200 | 62 | 0.85 | 2495 | 0.148 |

Table 1. Properties of materials of the $AlN—Al_2O_3$ system

| Property | Amount of the $Al_2O_3$ additive to AlN, mass % | | | | | | |
|---|---|---|---|---|---|---|---|
| | 0 | 5 | 10 | 20 | 30 | 40 | 50 |
| Electric resistivity, Ω·cm: 20 °C | $10^{13}$ | $10^{13}$ | $5.6 \cdot 10^{12}$ | $6.2 \cdot 10^{11}$ | $6.0 \cdot 10^{11}$ | $3.5 \cdot 10^{10}$ | $1.5 \cdot 10^{10}$ |
| 500 °C | $8.2 \cdot 10^{8}$ | $3.4 \cdot 10^{9}$ | $2.1 \cdot 10^{9}$ | $9.3 \cdot 10^{9}$ | $5.0 \cdot 10^{8}$ | $1.5 \cdot 10^{8}$ | $8.0 \cdot 10^{7}$ |
| 1000 °C | $4.1 \cdot 10^{5}$ | $6.8 \cdot 10^{6}$ | $1.0 \cdot 10^{6}$ | $1.0 \cdot 10^{6}$ | $1.2 \cdot 10^{6}$ | $6.2 \cdot 10^{5}$ | $1.2 \cdot 10^{5}$ |
| Coeff. of thermal expansion, $deg^{-1}$: 20-1000 °C | $4.5 \cdot 10^{-6}$ | $4.5 \cdot 10^{-6}$ | $4.2 \cdot 10^{-6}$ | $4.3 \cdot 10^{-6}$ | $4.6 \cdot 10^{-6}$ | $5.0 \cdot 10^{-6}$ | $4.8 \cdot 10^{-6}$ |
| Compression strength, MPa | 126 | 145 | 174 | 189 | 192 | 190 | 195 |
| Thermal stability, the number of thermocycles, 1200-20 °C, air | 32 | 38 | 45 | 42 | 51 | 58 | 64 |
| Temperature of the onset of oxidation, °C | 1320 | — | — | — | — | — | 1560 |
| Dielectric permittivity, at $10^5$ Hz: 20 °C | 5.5 | 5.0 | — | — | — | — | — |
| 500 °C | 10.5 | 7.0 | | | | | |
| Dielectric loss angle, at $10^5$ Hz: 20 °C | 0.0015 | 0.0012 | — | — | — | — | — |
| 500 °C | 0.0040 | 0.0029 | | | | | |

**References**

1. Стегний А.И., Шевченко А.В., Лопато Л.М. и др. Термический анализ окислов с использованием солнечного нагрева // Докл. АН УССР. Серия А. — 1979, №6. — С. 484-487.

2. Францевич И.Н., Дверняков В.С., Пасичный В.В. Определение тепловых параметров специальной гелиоустановки, предназначенной для исследования тугоплавких веществ // Доповіді Академії наук УРСР. — Киев: Наук. дум., 1966, №5.

3. Тугоплавкие материалы в машиностроении. Справочник - М.: Машиностроение, 1967, 302 с.

4. Косолапова Т.Я., Андреева Т.В., Бартницкая Т.С. и др. Неметаллические тугоплавкие соединения. - М.: Металлургия, 1985, 224 с.

# FORMATION OF INTERMETALLIDES DURING ANNEALING CHROMIUM WITH EVAPORATED LAYER OF Nb AND Zr

**Brodnikovsky N.P., Dubicovsky L.F., Zykova E.V., Sameluk A.V.**
Franchevich Institute for Problems of Material Science of NAS of Ukraine,
Krzhyzhanovski str.,3, 03680, Kiev-142, Ukraine. E-mail:dep53@ipms.kiev.ua

It is known, that use layers from Lawes phases as diffusion barriers raises of properties stability of composite materials at high temperature [1]. In this work connection between condition evaporation of Zr and Nb layers on chromium, the layers structure, and kinetics of chromium intermetallides forming during high temperature annealing was studied by means of metallography, scanning electronic microscopy, X-ray phase and micro X-ray spectral analyses.

Layers of Nb and Zr obtained by method of electron-beam evaporation in vacuum $4\cdot10^{-4}$ Pa on heated chromium (99% Cr) backing according technique described in [2]. The annealing for formation of the intermetallide layers were carried out in vacuum ($P=3\cdot10^{-3}$ Pa) and argon in an interval of temperatures 1000-1300 °C.

The niobium films by thickness 6-8 microns were received at condensation temperature 700 and 980 °C with speed of condensation v = 0,11-0,2 μm / min. After annealing the films had small grain structure with the size of a grain 0,3-0,5 microns (Fig. 1, a), which practically remained constant at annealing in vacuum at temperature 1200 °C during 5-10 hours. At annealing in argon at T=1300 °C within 2 hours the insignificant increase of grains was observed. The grain size them became 0,5 -1 microns and the separate grains ran up to 2 microns. The borders of grains had clear facets. Column structure with the crystallite size of 1-2 microns on cross-cut section of the Nb – film was showed as a result of thermal etching during further annealing in argon within 2 hours. The microhardness of niobium films in as obtained condition was H = 3 GPa.

The zirconium films were received at condensation temperature of $T_c$=700 and 850 °C and condensation speed of v=0,11and 0,5 μm / min. Structure of films, obtained at temperature 850 °C was small crystallic with the sizes of grains 4-6 microns (Fig. 1, b). At low temperature of condensation (700 °C) the structure with the clear facets grains having size from 10 up to 120 μm was formed. On a surface of evaporated film the stepped microrelief was

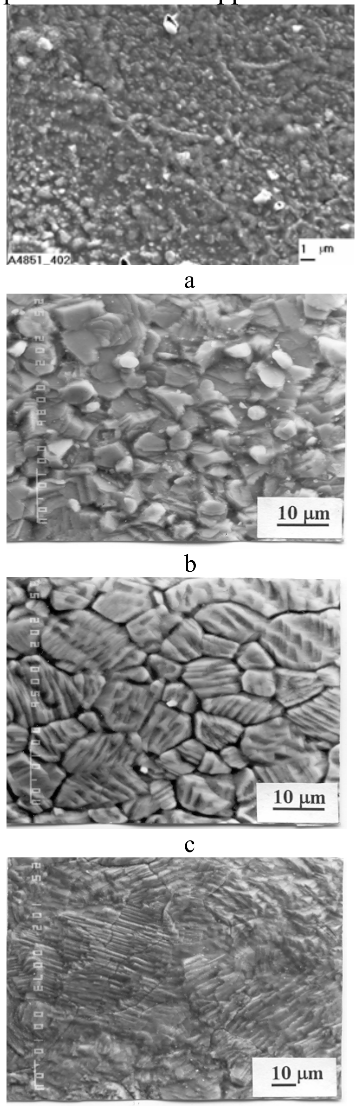

a

b

c

d

Fig. 1. Microstructure of Nb and Zr films surface after evaporation on chromium with different procedures: film of Nb-a:$T_c$=980°C, v=0,11 μm/min.; film of Zr- b: $T_c$ =850°C, v=0.11 μm /min.;
c: $T_c$=700 °C , v=0.12 μm /min.;
d: $T_c$=700 °C, v=0.5 μm /min.

observed. Density of steps and size of a grain grew with increase of speed of condensation (Fig. 1, c, d). The increase of the relief complication with growing of condensation speed results in increase of area of free grain surface on which Zr atom can setting. Us result formation of crystal structure remains possible at growing of condensation speed up to high values , although quantity of defects may grows.

X-ray phase analysis has shown, that after annealing at temperature of 1100 $^{o}$C or higher the cubic $NbCr_2$ and hexogonal $ZrCr_2$ were formed. The microhardness were H = 10,8 GPa and H=12,9 GPa for niobium and zirconium intermetallides, accordingly.

It was shown with help of the microspectral analysis, that the process of formation of intermetallides compounds at annealing chromium with Nb or Zr layers had identical features. Both boundaries of forming intermetalide layer was flat, without protuberance, which were observed in case of annealing of chromium with Ti layer [2]. The thickness of the niobium intermetalide layer after anneaaling in vacuum at temperature T =1200 $^{o}$C during 5 hours was 3 micron and 4 micron after anneaaling in Ar at T=1300 $^{o}$C during 2 hours. Prolongation of annealing in Ar within of 2 hours did not result in increase of thickness of the $NbCr_2$ layer.

Dependence of thickness of $ZrCr_2$ layer on annealing time and conditions of Zr layer obtaining is showing on fig. 2. The experimental data are described by parabolitic low with power equal to 0.5. It correlates with literature data [3] and is evidence of diffusion character of intermetalide layers forming. The velocity of $ZrCr_2$ layer growing is bigger if evaporation velocity of Zr layer on chromium is bigger (fig. 2). The reason of the increasing of the intermetalide layer growing may be activation of diffusion formation of $ZrCr_2$ layer by excess of point defects , which forms at higher velocity of evaporation Zr layer.

So, velocity of intermetalide layers growing may be controlled by changing of evaporation conditions of

metal layers. Intermetalides layers will be thinner, if evaporated metal layer will be dense.

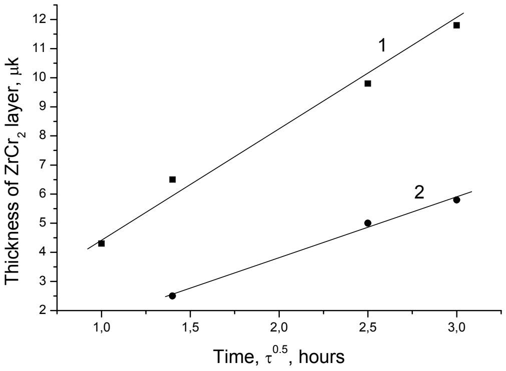

Fig. 2. Dependence of thickness of $ZrCr_2$ layer on annealing time in vacuum at T=1200 $^{o}$C for different conditions of Zr layer obtaining.

1-Тк=700 $^{o}$C, v=0,5 μm/ min.

2-Тк=850 $^{o}$C, v=0.11 μm / min.

### References

1. Змий В.И., Руденький С.Г., Ковтун Н.В.Вакуумное активированное диффузионное насыщение как способ получения антикоррозионных и эрозионно-стойких покрытий для материалов ядерных и термоядерных реакторов // Вопросы атомной науки и техники.2001, №2, с. 131-134.

2. Zykova E/V/. Dubikovsky L.F., Brodnikovsky N.P. Features of forming of intermetallic compounds in a zone of contact chromium-coating from metal of IV group.-Interrnational conference: " Science for Materials in the Frontier of Centuries:Advantages and Challenges ". Proceedings of Conference. 4-8 November 2002. Kyiv. Ukraine.-P.539-540.

3. Гегузин Я.Е. Диффузионная зона.-М.: Наука.-1979.-343 с.

# KINETIC OF FORMATION OF SPARK COATINGS ON THE BASE OF Ni–Cr ALLOYS IN DEPENDENCE OF THEIR STRUCTURE

**Paustovsky A.V., Alfintseva R.A., Kurinnaya T.V., Pyatachuk S.A.**
Frantsevich Institute for Problems of Materials Science of Ukraine,
3 Krzhizhanovsky St., 03142, Kyiv, Ukraine, e-mail: dep65@ipms.kiev.ua

There exist very much methods of strength increasing and restoring of weared detail surfaces with necessary physic-chemical and exploatation properties.

Spark treatment is more effective method of restoring and increasing surface strength method. This method allows to economy of high price materials. The electric-spark coating (“white layer”) structure formation under localisation of high pressures ($2 \cdot 10^6$ to $7 \cdot 10^6$ MPa), temperatures ($10^5$ to $10^6$deg/s) defines its high physical and mechanical properties.

Sufficient cooling of electric alloys leads to formation of phase conglomerates due to crystallisation [1]. Binary Ni-Cr alloy of eutectic composition (1A), ternary Ni-Cr-Al eutectic alloy (4A) and Ni-Cr-Al-Y alloy (6A) that is analogous to the ternary eutectic composition but alloyed by 2 mass% of yttrium were used as anodes for spark alloying (SA). Chemical composition (mass %) of the alloys is given in the Table.

**Table**

| № alloy | Ni | Cr | Al | Y |
|---|---|---|---|---|
| 1A | 50,5 | 49,5 | – | – |
| 4A | 50 | 41 | 9 | – |
| 6A | 50,7 | 38,3 | 9 | 2 |

Electrodes for SA were made by two methods, namely, melting in an arc furnace with a noncousumable tungsten electrode in a protective atmosphere and high-energy hot pressing in vacuum (HEHP) elaborated at Frantsevich Institute for Materials Science Problems National Academy of Science of Ukraine [2].

Structure of cast alloy 1A represented stratum-thunk eutectic, consisting with α (Cr-based) and (Ni-based) solid solutions. In the alloy 4A the ternary eutectic structure consisting of γ, α and β (NiAl) intermetal based solid solution is observed. In the cast alloy 6A along the boundaries of the ternary eutectic (α+γ+β) colonies, the binary eutectic consisting of γ Ni-based solution and $Y_2Ni_{17}$ intermetal phase was found. As determined by differential thermal analysis, the melting point of the binary eutectic is 1175 °C, that of the ternary one, 1267 °C.

The phase composition of hot-pressed alloys is formed during sintering of powder mixture of nickel, chrome, aluminium and yttrium hydride. Under heating there occurs the formation of α, γ and β–phases of solid solution with grain structure 5-10 mkm in size. The micro-X-ray analysis has shown that in the cast alloy, yttrium is distributed non-homogeneously as large conglomerates forming the eutectic (Fig1a).

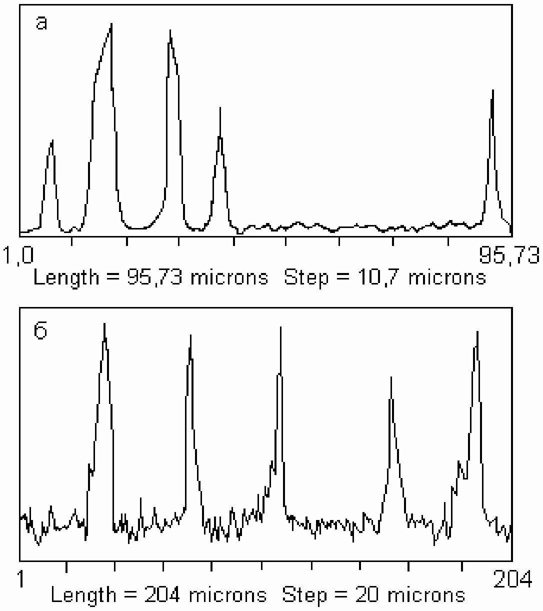

Fig. 1.Yttrium distribution in cast (a) and hot-pressed (b) Ni–Cr–Al–Y alloy.

In the HEHP alloy, oxides, oxynitrides and intermetallic phases containing yttrium distribute homogeneously over the whole sample volume and form a dispersion-hardened structure (Fig. 1b).

The 45 steel was subjected to electric spark alloying using cast and hot-pressed electrodes made of the alloys mentioned above. To that end, an EFI-46A unit was used in the following mode: the vibrator frequency 100 Hz, the short-circuit current 1,5 A, the processing duration for 1 $cm^2$ area 10 min.

The main parameters of electric-spark alloying process were determined from the time dependences of the anode erosion and the cathode mass gain. They include: the specific anode erosion Δa, and the specific cathode mass gain Δk measured at each minute of the 1 $cm^2$ area treatment: the total anode erosion and the total cathode mass gain measured over 10 min of the 1 $cm^2$ area processing; and the mean material transfer coefficient $k' = \Sigma\Delta k / \Sigma\Delta a$. Kinetic curves of the anode erosion, the cathode mass gain, as well as values of the mean material transfer coefficient for cast and hot-pressed electrodes 6A are shown in Fig.2.

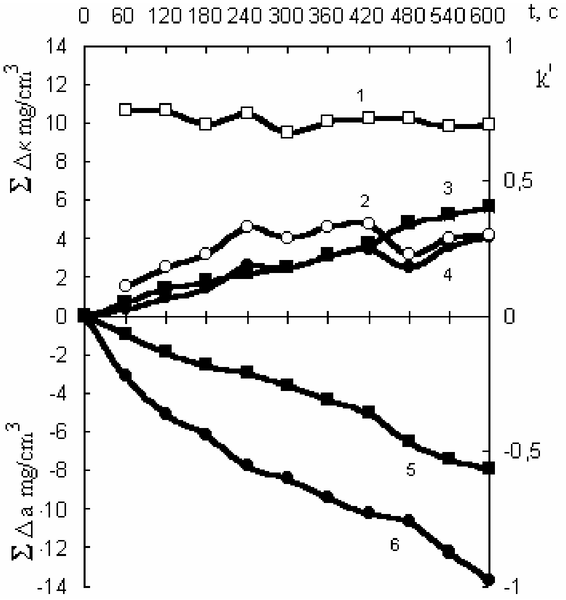

Fig. 2. Kinetic curves of the total cathode mass gain ∑Δk (3,4), total anode erosion ∑Δa (5,6) and mean mass transfer $k^{`}$ at electric–spark alloying of 1 $cm^2$ of the Steel 45 with Ni–Cr–Al–Y alloy at the specific alloying duration $t$ = 600 s/$cm^2$ (1,2). (1,3,5) for hot–pressed alloy, 2,4,6 for cast one

The cast anode erosion attains a maximum value of $13{,}6 \cdot 10^{-3}$ mg/$cm^3$. It is lower for the HEHP anode. The presence of ternary and binary eutectics containing intermetallide pases as large colonies (conglomerates) favors the brittle destruction of the anode by the spark pulse.

As a consequence, the erosion products contain the solid phase along with liquid and vapor ones. The solid phase has no time enough to melt within the short pulse action period. The solid destruction products are no fixed on the cathode, thus causing the material loss. The mean materials transfer coefficient for the alloying with HEHP electrodes exceeds that for the cast electrodes (k′ is 0,7 to 0,8 and 0,3 to 0,5 respectively).

## References

1. Таран Ю.Н., Мазур Р.С. Структура эвтектических сплавов.–М.: Металлургия, 1978.– 312 с.

2. Лаптев А. В. Возможности метода высокоэнергетического горячего прессования в вакууме для создания материалов с ультратонкой структурой и высокой прочностью // Порошковая металлургия.– 2000.– №3/4.– С.8-19.

3. Городецкий Г. П. Исследование сплавов двойных эвтектик α+γ и α+β системы Ni–Cr–Al // Металлы 5, 199 (1992).

# WEAR RESISTANCE OF THE COMPOSITE ELECTROCHEMICAL COATINGS WITH FILLER OUT OF FINEDISPERSED OXIDOCERAMIC

**Barykin N.P., Valeeva A.Kh., Valeev I.Sh.**
Institute for Metals Super plasticity Problems RAS,
39 St. Khalturina str., Ufa, 450001, Russia, E-mail: aigirsh@rambler.ru

## Introduction

At present composite materials displaying high operating properties is widely used in fundamental research and industry. The composite electrochemical coatings have properties of metals (electro- and thermo-conductivity, plasticity and others) and nonmetals (ovenproofens, chemical stability, high hardness and others). The composite electrochemical coatings applied provides an opportunity to increase supporting capacity of articles, sliding bearings for example.

The aim of this work was to electrodeposite composite electrochemical coatings (CEC) on the babbit (Sb(10—12)wt.%, Cu(5—6)wt.%, Sn-rest), widely used in antifriction material for producing sliding bearings bushes in machine building and power engineering. This method allows producing compact, non-porous coatings with given thickness on the article surface and provides minimal expenses of materials and energy.

## Experimental

The composite electrochemical coatings (CEC) with aluminosilicochromium powder (ASCP) as the second phase substance were obtained on the babbit (Sb(10—12)wt.%, Cu(5—6)wt.%, Sn-rest). ASCP consists of disperse particles with sizes from 1 to 4 μm (20% have spherical form and 80% have irregular form with rounded edges). Disperse particles have developed contact surface with specific value 4500 $m^2$/kg. The chemical composition of the powder is as follows: aluminum oxides - 60±2%, silicon oxides - 18±2%, chromium oxides - 15±2%, potassium oxides – 2%. All listed chemical components attend in each disperse particle and in either weight.

The chloridefluoric electrolyte with the following composition (g/l), was used: tin chloride $SnCl_2{*}2H_2O$ – 40—60; sodium chloride NaCl – 5-10; sodium fluoride NaF –40—60 [1]. The second phase content was 200, 300, 400 g/l. Ethylendiaminetetraacetic acid disodium salt was used for stimulate CEC precipitation.

The electrolysis was performed at pH 1,6 – 4,4; temperature 18—25 °C, current density A/$dm^2$ and mechanical mixing. The coating out of pure tin was used for comparison

Determination of the coatings chemical composition was achieved by means of micro x-ray analysis by using a JXA-6400 analyzer (Japan).

Optical (“Axiovert 100A” Carl Zeiss Jena GmbH, Germany) microscope with “KS Lite 3.0” image analyzing system was used to study the structure of the coating. Microhardness was determined by means of a special device MHT-10 to “Axiovert 100A” microscope, under a load of 2 g.

The samples were tested for wear at dry friction and in conditions of boundary lubrication using a disc-on-shoe test machine at room temperature (20±2)$^o$C in the air with a relative humidity of 40-50% under the following conditions: sliding velocity 0.79 $ms^{-1}$, pressure 7 – 20 MPa and sliding distance to 25 km. Discs were made of hardened steel (C—0,4wt.%, Cr—1,0wt.%, Al—1,0wt.%) with a hardness of 52-55HRC. Shoes were made of babbit (Sb(10—12)wt.%, Cu(5—6)wt.%, Sn-rest) with coating.

The roughness of the shoes and the disk was in the range of 0,1 to 0,2μm.

The samples were weighed before and after the testing with an accuracy of $10^{-4}$ g to determine the wear loss. The wear intensity was calculated using the formula:

$$I=\Delta m/LS \qquad (1)$$

Where Δm is the weight loss, S is the area of contact, L is the sliding distance.

Results and discussion

The dependence of second phase substance quantity in the coating, microhardness and wear intensity at dry friction (sliding distance 50 m) on the ASCP content in the electrolyte is shown in fig.1.

One can see that CEC obtained from electolyte contains 200 g/l ASCP provides microhardness higher by two times than coating from pure tin.

CEC obtained from electrolyte contains 300 g/l ASCP shows the lowest microhardness value and provides minimal value of the wear intensity under dry friction conditions.

The wear intensity of CEC in conditions of boundary lubrication is shown in fig.2.

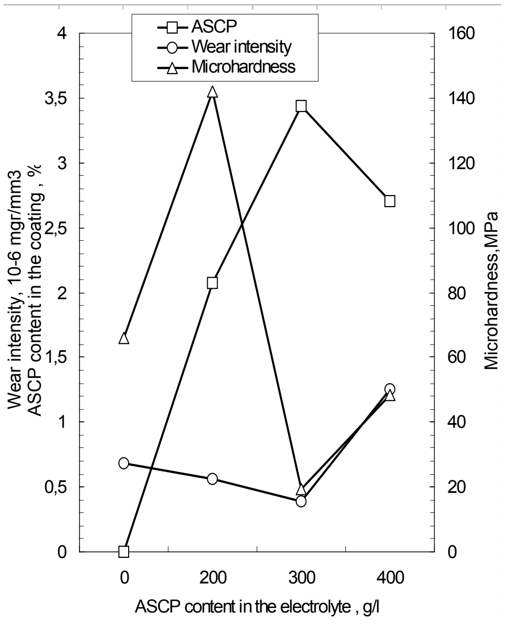

Fig. 1. Dependence of the ASCP content in coating, microhardness and wear intensity at dry friction (sliding distance 50 m) on ASCP content in the electrolyte.

It is seen that the process of wear of the babbit without coating, with coating from pure tin and with coating obtained from the electrolyte with 200g/l ASCP described by curves like to fading sinusoid. A similar type of the wear was observed in work [2].

CEC obtained from electrolyte with 300 g/l ASCP shows a different type of the wear. At the beginning of the sliding distance the wear intensity increases insignificantly, at sliding distance 800 m it reduces and stays constant for a long time. The fact that particles of finedispersed ceramic (3,5% weight mass) attend in the obtained coating explains this type of wear.

## Conclusion

CEC obtained from stannic electrolyte with 300g/l ASCP provides the absence of a stage of wear-in and decreases wear of babbit (Sb(10—12)wt.%, Cu(5—6)wt.%, Sn-rest) by 40 %.

## References

1. Saifullin R.S. Composite coatings and materials. M.: Chemistry, 1977, 272 p. (in Russian).
2. Khrushev M.M., Kuritsyna A.D. // Friction and wear in machines. M.-L.: AS USSR, 1950, V.5, pp.76—82. (In Russian).

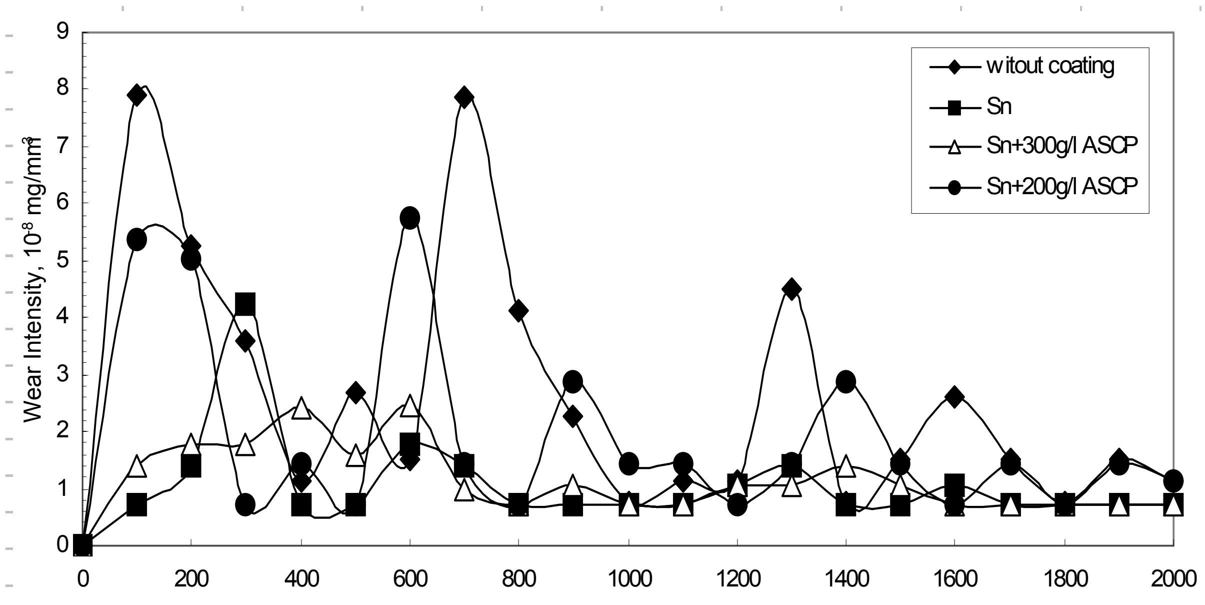

Fig .2. Dependence of wear intensity on sliding distance.

# CALCULATION OF OSCILLATORY SPECTRA DEUTERATING cis-1,4-POLYISOPRENES

**Egamov M.Kh., Karimov S.N.**
Khujand centre of science AS of Republik of Tajikistan, Khujand, Tajikistan
Syrdar`inskaya street – 26, Khujand town, 735714, Tajikistan E-mail: muchtor@khj.tajik.net

The method isotropic replacements is represented by the powerful tool of research of a microstructure of polymers as considerably facilitates identification of strips of the absorption caused by local fluctuations. Isotroping replacement of atoms in molecules and polymeric circuits is used also for reception of the additional data on frequencies of normal fluctuations. Thus it is supposed, that potential energy and geometry of a molecule (or a polymeric circuit), at such replacement remains constant. Only modelling isotropic replacements with an oscillatory spectrum of polymers can be found out influences, whether there corresponds this assumption of the validity. Comparison of the designed frequencies of normal fluctuations deuterate polymers with their experimental values shows, as far as adequately describe the chosen power constants a real frequency spectrum of polymer.

For reception of more reliable reference of strips of absorption cis-1,4-polyisoprene (PI) and researches of correlation between spectra various deuterating PI earlier authors of works [1] have been received deuterating PI which structures are resulted in tab. 1. Received in this work IR–spectra PI are very valuable to the theory fluctuation of polymers as enable to check up efficiency of the developed computing methods.

In the present work the theoretical analysis of oscillatory spectra cis-1,4-polyisoprene and lines deuterating PI with the big length of periodic part N=100, where N-number of repeating elements of a circuit is lead. As model for calculation the model of an one-dimensional crystal has been accepted, geometrical parameters of repeating which link are identical to an elementary part of a macromolecule crystal cis-1,4-polyisoprene.

Table 1.
Structures deuterating cis-1,4-polyisoprenes

| Polymer | Structure |
|---|---|
| PI | (-$CH_2$-C ($CH_3$) =CH-$CH_2$-) n |
| PI-D | (-$CH_2$-C ($CH_3$) =CD-$CH_2$-) n |
| PI-D3 | (-$CH_2$-C ($CH_3$) =CD-$CD_2$-) n |
| PI-D4 | (-$CD_2$-C ($CH_3$) =CH-$CD_2$-) n |
| PI-D5 | (-$CD_2$-C ($CD_3$) =CH-$CH_2$-) n |
| PI-D8 | (-$CD_2$-C ($CD_3$) =CD-$CD_2$-) n |

The power constants accepted for calculation of oscillatory spectra, are taken from the same work [1], but modified according to the improved values of power constant molecules of propylene and cis-butene – 2.

Theoretical calculation of oscillatory spectra is lead by Gribova L.A.'s stated in known technique. At carrying out of calculations of frequencies of normal fluctuations deutering cis-1,4-PI weights of atoms H are replaced with weights of atoms D in corresponding places it agrees tab. 1. Results of calculation and reference of frequencies are resulted in tab. 2. The comparative analysis of the data shows, that experimental and the designed frequencies very well coincide. It can testify to reliability of the used field and an admissibility of the assumption of an invariance of potential energy and geometry of polymer at deutering. It is interesting to note, that in most cases the references made on the basis of the analysis of experimental data, coincide with the references made on the basis of calculation. The analysis of the received results show, that deutering will result not only in displacement of frequencies of fluctuations, but influences on forms of fluctuations, and it affects on references of strips. In other areas of displacement of frequencies insignificantly. The received data can be used at the decision more challenges of IRS.

REFERENCE

1. Abdulov H.S., Gribov L.A., Nelson K.V. Calculation of spectral curves of IR-absorption cis-1,4-polyisoprene different conformation // JPS, 1998, v.58, № 4.- p.621-625.

Table 2.

### Comparison of the experimental and designed frequencies (см$^{-1}$) fluctuations cis-1,4-PI and deutering cis-1,4-PI

| PI | | PI - D | | PI-D 3 | | PI-D4 | | PI-D5 | | PI-D8 | | **Referring** |
|---|---|---|---|---|---|---|---|---|---|---|---|---|
| Exp | Calc | Exp | Calc | Exp | Calc | Exp | Calc | Exp | Calc | Exp | Calc | |
| 1 | 2 | 3 | 4 | 5 | 6 | 7 | 8 | 9 | 10 | 11 | 12 | 13 |
| 1670 | 1659 | 1660 | 1659 | 1650 | 1657 | 1660 | 1669 | 1660 | 1653 | 1650 | 1650 | $Q_{c=c}$ |
| | 1643 | | 1643 | | 1641 | | 1656 | | 1638 | | 1636 | |
| 1320 | 1315 | 1345 | 1313 | | | | | | | | | $\alpha_{cн2}$ |
| | | | | 1315 | 1279 | | | | | | | $\alpha_c D_{2,}$ $\beta cD_2$ |
| | | | | | | 1312 | | | | | | $\beta cH_2$, $Q_{c-c}$ |
| | | | | | | | | | | 1305 | 1298 | $\gamma_{c=c-c}$, $Q_{c-c}$ |
| 1290 | 1289 | 1290 | 1289 | | | | | | | | | $\beta cH$,$Q_{c-c}$ |
| | | | | | | 1300 | 1299 | 1290 | 1293 | | | $\alpha cH_2$, $\beta_{ch2}$ |
| | 1274 | 1275 | 1271 | | | | | | 1266 | | | $\alpha cH_2$, $\beta_{ch2}$ |
| 1140 | 1162 | | 1155 | 1155 | 1144 | | | | | | | $\alpha cd_2$, $\beta_{cd2,\chi}$ |
| | | | | | | 1165 | 1191 | | | | | $\alpha cH_2$, $\alpha cD_2$, $\beta_{cH}$ |
| | 1118 | | 1122 | 1125 | 1134 | 1120 | 1129 | 1120 | 1122 | | | $\alpha cH_2$, $Q_{c-c}$ |
| 990 | 966 | | | | | | | | | | | $\beta_{cD,}$ $\alpha cH_3$, |
| | | 990 | 975 | | | | | | | | | $\alpha_{cD2,}$ $\alpha_{cD3,}$ $\beta_{cD2,}$ |
| | | | | | | 960 | 958 | 970 | 965 | 960 | 965 | $_\chi$, $\alpha_{cD2,}$ |
| 940 | 943 | 910 | 933 | 940 | 933 | 925 | 931 | 940 | 953 | | 927 | $\beta cD$ |
| | | | | 915 | 911 | | 910 | 915 | 931 | | 926 | $\beta cD$, $\alpha_{cD2}$ |
| | | | | | | 900 | 903 | 895 | 905 | 900 | 914 | $\alpha_{cH3,}$ $\alpha_{cH2,}$ $\alpha_{cD2}$ |
| 840 | 811 | 835 | 817 | | 839 | | 847 | | | | | $\alpha_{cD2,}$ $\beta_{cH3,}$ $\alpha_{cH3}$ |
| | | | | | 820 | 815 | 831 | 806 | 824 | | 817 | $\alpha_{cH3,}$ $\beta_{cD3,}$ $\alpha_{cD2}$ |
| | 784 | 770 | 774 | | | | 786 | 770 | 791 | 780 | 777 | $\gamma_{c=c-c}$ |
| 575 | 540 | 565 | 535 | | 556 | | | | | | | $\beta cD_2$, $\beta cD_3$, |

# INVESTIGATION OF THE MANUFACTURE PROCESS OF HEAT RESISTANT KAOLIN MATERIAL BY PLASMA METHOD

**Brinkiene K., Cesniene J., Kezelis R., Mecius V.**
Lithuanian Energy Institute
Breslaujos 3, LT-44403 Kaunas, Lithuania, cesniene@isag.lei.lt

The quest for improvement of series of working properties of materials used in extreme conditions leads to, among other processes, the development of production of high alumina ceramics. As raw material for production of $Al_2O_3$ based articles usually various natural minerals – bauxites, kaolin clays and others are utilized.

Manufacture processes of refractory materials and high temperature thermal insulation materials are linked to labor-consuming, preliminary mechanical processing of source raw material and to great energy consumption for their thermal treatment. On-stream technological process is required for these purposes.

In connection with the rising demand of high quality thermal insulation materials working at high temperatures the new methods of their manufacture are sought. One of such methods at present time is plasma technology having good prospects. This technology enables joining together the processes of melting of raw material and manufacture of material required (high temperature insulation fiber, nano-dispersed particles or spherical ceramic granules) and so forming a single process, using kinetic energy of high temperature flow generated by the plasma generator [1, 2].

The deciding factor determining efficient use of the plasma technology for manufacture of materials above mentioned is determination of optimal parameters of high temperature flows and geometry of plasma chemical reactor.

Taking into account above-mentioned problems, the main points linked to the plasma method of production of high temperature fiber and spherical kaolin granules using for this purpose a plasma chemical reactor with linear DC plasma torche are investigated in this work. The main quality characteristics of kaolin wool and of the products on its basis are high heat resistance and low thermal conductivity [3].

The plasma chemical reactor consists of three straight sections having length of 0.2 m and two other sections, each 0.15 m long positioned at 90° angle to each other. To minimize heat losses the inner reactor surface is lined with zirconium oxide 0.02 m thick. All sections are made of stainless steel and are cooled by water. The internal diameter of the reactor is equal to 0.04 m and the total length is one meter. Such design enables to change the length of the reactor, if needed, as well as the flow direction and the duration of exposure of material processed. The kaolin with particle size <100 micrometers was chosen as source raw material. Operational parameters of the device are given in the Table.

Table. Working parameters of the plasma device

| | |
|---|---|
| Capacity of the plasma generator | 93 kW |
| Gas flow rate | 19,5 g/s |
| Temperature of gas entering reactor | 2580 K |
| Temperature of gas leaving reactor | 1740 K |
| Powder consumption | 1,4 g/s |
| Natural gas consumption | 0,2 g/s |
| Gas velocity in the inlet section | 89 m/s |
| Gas velocity in the outlet section | 105 m/s |

On evidence of data by scanning electronic microscopy disperse particles introduced into the reactor are heated up completely and fully melted. The kaolin particles sized <100 µm melt then forming depending on flow parameters and its kinetic energy either spherical particles or fibers. Melted kaolin granules obtained by the plasma method are shown in Fig. 1.

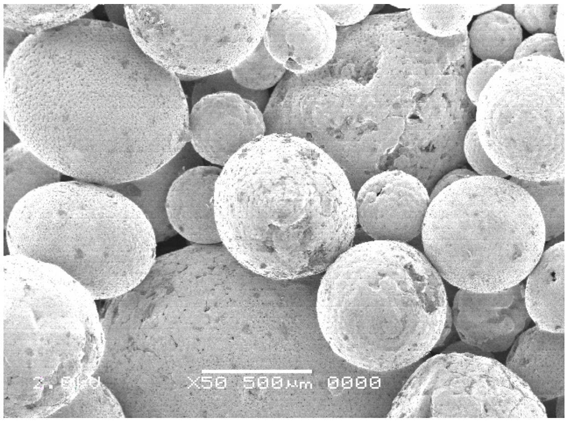

Fig. 1. Granules of melted kaolin

The product obtained can be used as high temperature insulation material with special properties.

With the aim of intensification of heat exchange between the high temperature flow and the injected particles in order to obtain the fiber products a small amount of propane butane gas was added. Gas combustion products (vapors $H_2O$ and $CO_2$) increase radiation heat transfer between the high temperature flow and particles considerably. As a result melting process was intensified [4, 5].

Morphology of fiber, obtained by plasma melting of kaolin raw material is shown in Fig. 2.

Morphology of fiber, obtained by plasma melting of kaolin raw material is shown in Fig.2.

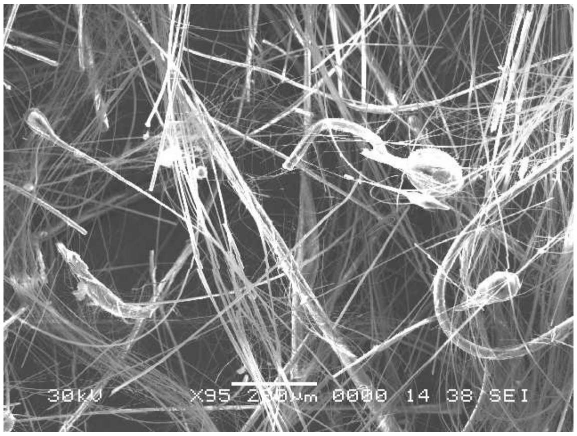

a)

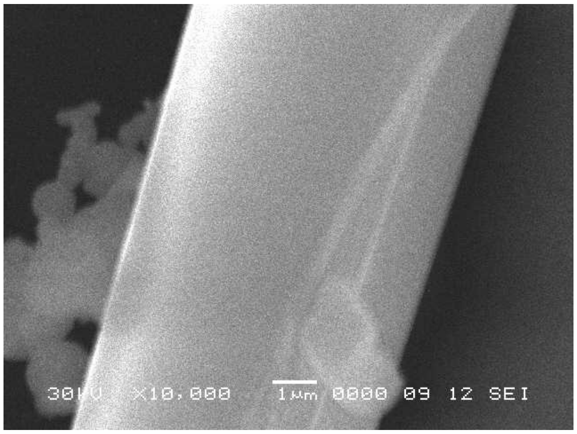

b)

Fig 2. Morphology of kaolin fibers: *a* - general view; *b* – enlarged view

The main characteristics of fiber material including diameter and length of fibers, the amount and the form of non-fiber inclusions were studied using scanning microscopy.

The average fiber thickness was 5 to 8 μ. On evidence of structure analysis data the formation of non-fiber inclusions having shapes of beads with various diameters is not inherent in fiber material obtained during plasma melting of kaolin (Fig. 2).

The average size of granules melted of kaolin is 500 μm.

According to the data of X-ray difractometry analysis the product material obtained is amorphous glassy material with some amount of crystal phases. In main peaks of low intensity are observed in the X-ray diffraction pattern. The reflections were indexed on mulite, corundum and quartz.

By the data obtained, the plasma method of processing of given raw material can be successfully applied for production of high temperature heat insulation materials of various types.

## References

1. Mose A., Burov I. Processing of dispersed materials in plasma reactors. Minsk: Nauka i technika. 1980, 208 p. (*in Russian*).
2. R. Kezelis, V. Balkevicius, A. Kaminskas. Regularities of glass fiber manufacturing by means of plasma technology // Power engineering. 2000. N 4, p.110-116.
3. Strelov K.K. Fundamentals of refractory materials technology. M.: Metalurgija, 1985, 480 p. (*in Russian*).
4. Ambrazevicius A., Zukauskas A., Valatkevicius P., Kezelis R. Plasma heat transfer during turbulent gas flow in the entrance region of a circular tube //AIAA Paper N 74-718, ASME Paper N 74-HT-38. Boston, 1974, p.4.
5. Huang Chen, Yi Zeng, Chuanxian Ding. Microstructural characterization of plasma-sprayed nano structured zirconia powders and coatings. Journal of the European Ceramic Society. Vol. 27. N 1 (2001), p. 57-63.

# HIGH TEMPERATURE OXIDATION OF THE CONNECTION POINT OF THIN THERMOELEMENTS

**Kriukiene R., Cesniene J.**
Lithuanian Energy Institute
Breslaujos 3, LT-3035, Kaunas, Lithuania, cesniene@isag.lei.lt

Thermal conductivity is one of the most important properties of heat resistant materials. The ho-wire (cross-array) method is used to determine thermal conductivity of refractory materials under investigation. For this reason, junctions of thermal electrodes of thermocouples deserve particular attention, because a junction point during exploitation is affected more than other parts of the thermocouple by the temperature and by ambient medium including also other factors. Even slight metal surface defects in the junction part can considerably increase oxidation rate [1]. The connection point of thermal electrodes must be able to carry considerable mechanical loads without showing any traces of fragility, as it may be broken later during repeated measurements.

Connection of thermal electrodes may be carried out in several ways: by welding, by soldering or by twisting them together [2]. The most often applied one is welding as it provides the best contact between electrodes for various temperatures and work conditions. At temperatures over 600°C only welding of chromel and alumel and others are used. Usually, welding is carried out in air or argon medium by the electric arc [3]. The main drawback of this method is bead formation invariably occurring during welding process, where beads are large enough (exceeding electrode diameter even 3 to 4 times) and porous. Large and porous junction points allow significant measurement errors if used in transient temperature fields.

For welding thin electrodes (∅ 0,2-0,5 mm) laser pulse and powerful diode devices were introduced recently [3]. Laser welding enables to obtain small welding points. However, formation of pores in the welding point cannot be avoided.

In comparison with pulse devices powerful diode laser devices are distinguished by their efficiency and cost-effectiveness [3]. Argon gas protects thermal electrode materials against air oxygen and contamination elements.

Although laser welding is advantageous one, the further development is desirable, primarily, with the aim to reduce welding point porosity of thin electrodes. There is also another way of solving this problem – to choose or to find other method able to produce better welding points of thermal electrodes and of measuring elements of thermal properties of materials. On the other hand the welding method for thermoelements mustn't be a complex one because for defining thermal properties of material and temperature differences measurement sensors are fabricated from several and even several tens of various thermoelement materials [2].

Porosity of the joining point as the result of welding by procedures described is caused directly by the approach used itself, that is, spot heating by outer heat source: electric arc or laser ray. First of all, an outer heat source heats and welds together outer layers of metals, while internal layers remain unwelded. Further heating seals the pores in the welded seam, so air or other gases are unable to escape. Welding process in a vacuum vessel can diminish porosity, but it is too costly and complicated procedure.

After studies of various methods of welding of thermocouples and metals we chose the electrical point welding method [4]. In the course of this welding process due to the electric current the metal temperature commences to rise and later metal begins to melt in the contact point only but not in the entire spot. The thin wires first touch each other by very small contact area and only at a melt stage this area begins to grow. In this way the thermal electrode welding point without porosity is obtained.

Using the same method we designed and produced thermal property measurement elements. Thermal property measurement sensors can be connected by two (differential couples), or by tens (heat flow measurement devices), connected cross- like (heat conductivity measurement sensors) and so on. In order to obtain the high quality welding points of thermocouples and thermal measurement sensors we had to create and to implement technology of welding thermal electrodes having diameters of 0,2-0,3 mm and the complete quality checking control system, based on contact resistance measurement [5].

Connection points were welded for chromel-alumel wires (∅ 0,3 mm) and nichrome wires (∅

0,5 mm). Welding quality was controlled by measuring contact point resistance [5]. The samples prepared at the 900°C in oxidizing medium were held with different exposure durations. Pictures of these microstructures are presented in Fig. 1 and Fig. 2.

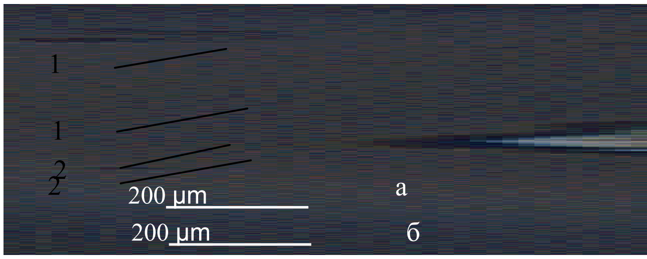

Fig.1.Microstructure of the chromel-alumel thermocouple welding point, which was held at 900°C: a – for 4 h, b – for 36 h, 1 – alumel, 2 – chromel

Oxidation of the thermocouple welding points takes its course in the same way as oxidation of the thermoelements. In case of alumel it occurs homogenously throughout its surface, while in case of chromel it takes the form of separate, growing oxidation centres. Oxidation intensity was slightly greater at the welding seam. In the microstructure cleared with reagent (Fig.1b) alumel structure changes, which have occurred during welding, are seen. However, their influence on welding itself is insignificant.

Oxidation of the welding point of the thermal conductivity measurement cross wire device depends on arrangement of wires welded and can occur in various, dissimilar ways. The thermocouple can be welded best to nichrome when contacting chromel (Fig. 2a). However, in this case the alumel electrode is more damageable. In the case of nichrome welded to the alumel electrode, sides of the welding seam are more likely to be damaged by oxidation. Such welding seam damage may influence accuracy of measurements and must be accounted for during design.

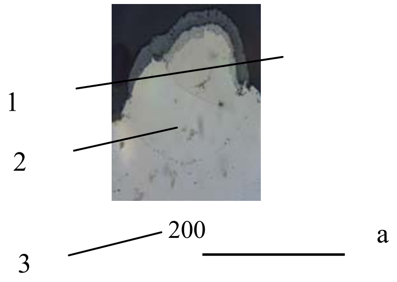

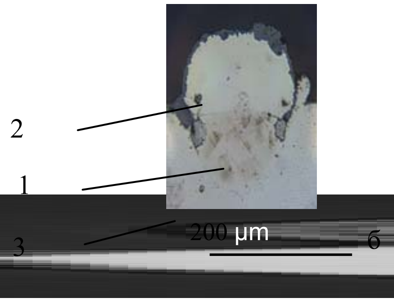

Fig.2. Microstructure of the chromel-alumel-nichrome thermocouple welding point, which was held at 900°C for 50 h. 1 – alumel, 2 – chromel, 3 – nichrome.

It was established that oxidation in welding points of thermocouples and thermal measurement sensors used in high temperature medium goes on with considerably greater intensity in comparison with oxidation of remaining parts. It is not main factor determining service life of a sensor because at the same time thermoelements themselves are oxidized. Welding using the electrical point method enables to obtain small and non-porous connection points allowing greater measurement accuracy.

## References

1. Huntz A.M., Lefevre B., Cassino F. Roughness and oxidation: apllication to NiO growth on Ni at 800°C. J. Materials Science and Engineering, 2000, A290, p. 190-197.
2. Childs P.R.N. Practical temperature measurement. Oxford, Butterworth. 2001. P. 372.
3. Triantafyllidis D., Schmidt M.J.J. Li L. Comparison of high power diode laser and Nd: YAG laser microwelding of K-type thermocouples. J. of Materials Processing Technology, 2003, v. 138, p. 102-108.
4. Орлов Б.Д., Чакаев А.А.., Дмитриев Ю.В и др. Технология и оборудование контактной сварки. М.: Машиностроение, 1986, с. 352.
5. Левинскас Р., Крюкене Р. Контроль качества сварки измерительного креста установки для определения теплопроводн. материалов. Рига, 1999, 3 Международная конференция МЕТ - 99, с. 68 – 72.

# FORMING DIFFUSIONE COVERINGS ON THE BASIS OF TITAN ON WOLFRAMLESS HARD ALLOY TH20

**Khyzhnyak V.G., Dolgykh V.Y.(1), Sygova V.I.(1)**
National Technical University of Ukraine «KPI»
Victories av. 37, 03056 Kiev,
(1)Sumy State University,
St. Rimskogo-Korsakova, 2, 40007 Sumy

Last time wide distribution was got by wearproof coverings on a hard alloy cut instrument [1, 2]. The basic advantages of coverings are increases of firmness of instrument, diminishment of force of cutting, improvement of quality of processed, increase of labour productivity [1, 3]. Unlike of coverings on the basis of TiC and TiN, which oxidize on air at the temperature of 500 °C, multi-layers coverings on the basis of carbides and nitride titan, oxide of aluminum are stable against oxidization to 800 °C [2, 4].

In article [5], was shown possibility of applying on the surface of wolframless hard alloy TH20 by the method of diffusive metallization of multi-layer coverings on the basis of carbide of the titan TiC and intermetallics $Ni_3Ti$ and NiTi.

Thus, the purpose of work was to study influence of multi-layer coverings on firmness in the conditions of friction of sliding without grease of the hard alloy TH20.

Coverings inflicted at temperatures 950 °, 1000 °C, time 1,5—2 hours, in the closed reactionary space at the reduced pressure. As initial components was used powder of titan, $CCl_4$, carbonaceous additive, [4].

Phase composition and thickness of coverings, specified in a table determined by the X-ray diffraction and metallographic analyses. Microhardness was determined on the device ПМТ-3.

The wearproof in the conditions of friction of sliding was determined on methods [6]. Influence of parameters of cutting on wearproof was estimated on the size of relative wear which was determined as attitude of sizes of small hole of wear toward the way of cutting. The index of relative wearproof was determined as relationship of time of work of wolframless instrument with covering to the set wear to the proper time of work of instrument without covering.

Table Phase composition and some descriptions of coverings on the basis of titan

| Temperature (°C) and time of satiation (ours) | Phase composition of coverings (from a surface to basis) | Thickness of coverings, mkm | Microhardness, GPa |
|---|---|---|---|
| 1000,2 | $NiTi/Ni_3Ti/TiC$ | 6,0/9,0/1,5 | 11,5/14,0/- |
| 950,1 | $NiTi/Ni_3Ti/TiC$ | 4,5/8,0/2,5 | 11,5/13,5/- |

It is shown that the wearproof in the conditions of friction of sliding without grease of the alloy TH20 with coverage on the basis of titan in 6 – 8 times is higher, than initial.

### Literature:

1. Третьяков В.И. „ Основы металловедения и технология производства спеченных твёрдых сплавов” – М.: Металлургия, 1976. – 527 с.
2. Верещака А.С. , Третьяков И.П. „Режущие инструменты с износостойкими покрытиями” – М.: Машиностроение, 1986. -192 с.
3. Крючков В.Я. „Исследование стойкости пластин из безвольфрамового твёрдого сплава ТН20.- станки и инструменты”. - 1987, №7. –С. 25 – 26.
4. Лоскутов В.Ф., Хижняк В.Г., Куницкий Ю.А., и др. „Диффузионные карбидные покрытия” – К.: техника, 1991. -168 с.
5. Hizhnjak V.G., Dolgykh, Carpets M. V. Structure and properties of diffusion coatings on wolframless firm alloys // Second international conference “Materials and coatings for extreme performance: investigations, applications, ecologically safe technologies for their production and utilization” / Katsiveli-town, crimea, Ukraine, 2002, p. 446 – 447
6. Долгих В.Ю., Криворучко Д.В. „Исследование влияния покрытия на основе Ti на износостойкость твёрдого сплава ТН20” – Вісник Сумського державного університету. Технічні науки. - 2003, №2 – С. 44 – 49

# THE WETTABILITY OF DIMOND-LIKE CARBON FILMS BY SOLUTION OF DIFFERENT PHYSICO-CHEMICAL NATURE

**Kaplunenko O.I., Kutsay O.M., Loginova O.B., Perevertailo V.M., Gontar A.G.**
Institute for Superhard Materials of NASU
2, Avtozavodskaya Str., Kiev, 04074, Ukraine, E-mail: pol@ism.kiev.ua

In the present work, a wettability of dimond-like carbon films by the solution of different physico-chemical nature (distilled water, biosolution, glycerol) has been studied. The structure, morphological peculiarities and chemical conditions of surface influence upon the contact interaction. The treatment by vacuum drying increase the mean values of wetting angles. Glycerol (apolar liquid) have not a sensibility for chemical state change of the surface films.

Wetting angles in the film-liquid system were assessed by the sessile drop method under normal conditions.

The results are discussed in comparison with the previously reported studies of a-C:H and diamond film wettability [1, 2]. Unlike that works which prefab preparation of samples surface were not taken into enough consideration, our results fill up this blank.

1. N.V.Novikov, S.I.Khandozhko, V.M.Perevertailo, L.Yu.Ostrovskaya, A.G.Gontar, O.B.Loginova. The wettability of a-C:H films by solution of different physico-chemical composition // Diamond Relat. Mater. 9 (1998) 1263.
2. L.Ostrovskaya, V.Perevertailo, V.Ralchenko, A.Dementjev, O.Loginova. Wettability and surface energy of oxidized and hydrogen plasma-treated diamond films // Diamond Relat. Mater. 11 (2002) 845

Contact angle (θ, degrees) ta-C films with biosolution, distilled water and glycerol

| Biosolution, ðÍ 7,4 | Distilled water, ðÍ 7 | Glycerol | Surface of film |
|---|---|---|---|
| 53 | 61 | 47 | as deposited |
| 66 | 63 | 49 | implanted |

# OBTAINING OF DIAMONDLIKE a-C:N COATINGS UNDER EL.-M. IRRADIATION

**Shalaev R.V., Prudnikov A.M., Varyukhin V.N.**
Donetsk Physical&Technical Institute of NASU
72 R. Luxembourg St., Donetsk, 83114, Ukraine, sharos@mail.ru

Diamondlike nanocrystalline films are the perspective material and attract significant interest, due to unique “diamond” properties - high hardness, wear resistance, chemical inertness, biocompatibility and so on. Research of properties such films depending of conditions of their growth represents the important technological problem.

Influence of electromagnetic radiation on the gas phase near the surface of growth, and on growing surface may render extremely large influence on passing of processes of the growth and quality of obtained materials. Influence of radiation on structure diamond and diamondlike thin films directly during their growth is investigated in an insufficient measure [1—3]. Similar researches are useful to understanding photostimulated growing processes in the films, that allows to operate by structure growth effectively.

In the present work influence UV- and visible radiation on structure and property of diamondlike nitride carbon films [4] during their growth was investigated. For obtaining of films was used standard magnetron attachment of vacuum universal post VUP-5M. The heater was designed which provided an opportunity of simultaneous irradiation of the surface of substrate with electromagnetic radiation. The α-C:N films were grown by the method of magnetron sputtering of the graphitic target in an atmosphere of pure nitrogen, on substrates from a quartz glass. Growing surface of the film was irradiated with the focused radiation of mercury lamp DRSH-250 with power density about 1 W/cm$^2$, with use of UV-filters. The temperature of a substrate was changed in limits 150—450 °C. Pressure of gas in the chamber was controlled by devices of the vacuum post and was about 0,2 Torr. Time of films growth was 120 minutes.

Amorphous diamondlike carbon nitride films (series K and series KT) were obtained which properties substantially depend from spectral structure of used radiation, that has allowed to speak about photostructural processes in the formed film. The morphology and thickness of the films were determined by parameters of the discharge (pressure of a gas mix, a magnetron current), temperature of a substrate, and energy of the electromagnetic radiation falling on the substrate. Film’s color varied from dark brown up to light brown and orange.

Spectroscopic researches of diamondlike films α-C:N in a visible and near IR-range (range of wavelength 690—1700 nm) of a spectrum were carried out on ZMR-3MD spectrophotometer. The films of series K are grown at 200 °C, irradiated with full spectral range of lamp, irradiated only with the UV-component and not irradiated (fig. 1) were investigated.

Fig.1. – Absorption spectra of α-C:N films under various conditions of an irradiation (series K).

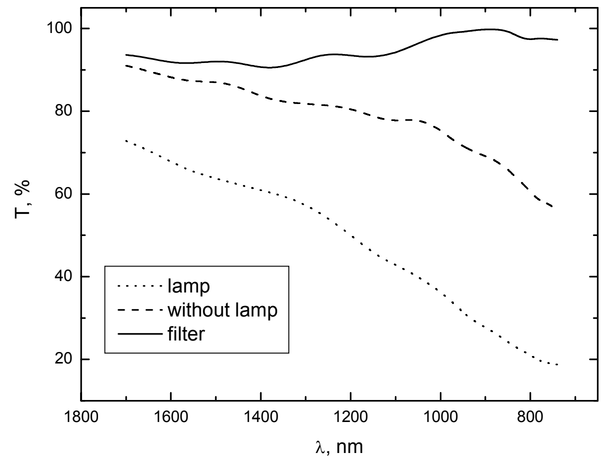

Spectra of the films, grown without an irradiation, are typical for usual diamondlike amorphous carbon films [5]. The film irradiated with full spectral range of lamp is characterized by a smaller transparency both in IR-, and in visible area. In this case the light stream makes additional heating of growing surface (together with resistive heating) that results in darkening of the films owing to thermal graphitization. At an irradiation only by UV-component of the spectrum (with use of the filter) the film differs the high transparency

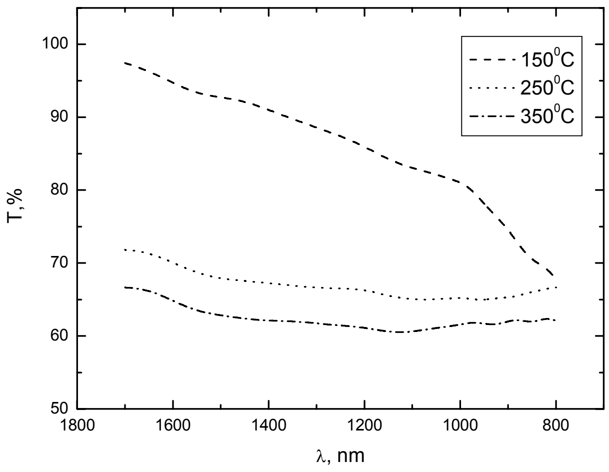

Fig. 2. – Absorption spectra of α-C:N films grown at various temperatures of a substrate (series KT).

both in visible and in IR-areas of a spectrum and has a characteristic light brown (orange) shade.

We assume, that UV-radiation additionally stimulates the growing surface of the film, increases mobility of growing radicals on the surface, increases efficiency of etching of the graphitic phase. All this increases a ratio of $sp^3/sp^2$ – hybridizated sites and results in growth of more ordered and qualitative structures [2].

Spectra of the films series KT, obtained at various substrate temperatures and irradiated only by UV-component of the lamp spectrum are shown on Figure 2. Apparently, at increase of the substrate temperature the films transparency considerably decreases in the IR-field of the spectrum. Probably it is related with formation of current-carrying clusters in structure of film at increase of temperature.

Results of the work allow to make a conclusion, that the UV-irradiation of the growing surface of the films is effective for increase of mobility (excitation) of radicals, responsible for the growth of film and as results increases efficiency of etching of graphitic phase; results to growth of structural orderliness, improves quality of the films without significant complication of technology of its obtaining.

## Literature

1. R.W.Lamberton, S.M.Morley, P.D.Maguire et al., Thin Solid Films, **333**, 114 (1998).
2. V.N.Varyukhin, R.V.Shalaev, S.-C.Yu et al., Jpn.J.Appl.Phys., **41**, L1393 (2002).
3. Г.М.Гуро, Г.А.Калюжная, Т.М.Мамедов и др., ЖЭТФ, **77**, 6 (12), 2366 (1979).
4. Y.-S.Jin, T.Shibata, Y.Matsuta et al., Thin Solid Films, **345**, 18 (1999).
5. B.Dischler, A.Bubenzer, P.Koidl, Appl.Phys.Lett., **42(8)**, 636 (1983).

# EFFECT OF HIGH-TEMPERATURE ANNEALING AND ULTRAVIOLET IRRADIATION ON CAPILLARY AND MECHANICAL PROPERTIES OF NANOSTRUCTURED TITANIA COATINGS

**Ostrovskaya L.Yu., Perevertailo V.M.(1), Dub S. N.(1), Matveeva L.A.(2), Milani P. (3), Kholmanov I. N.(3), Shmegera R.S. (1)**
Institute for Superhard Materials of NASU
2, Avtozavodskaya Street, Kiev, 04074,Ukraine, ostrovska@ism.kiev.ua
(1)Institute for Superhard Materials of NASU
2, Avtozavodskaya Street, Kiev, 04074,Ukraine, pol@ism.kiev.ua
(2) Institute of Semiconductor Physics of NASU
42, Nauki Prospekt, Kiev, 03028,Ukraine, matveeva@isp.kiev.ua
(3)University of Milan, 16, via Celoria, Milan, 20133, Italy, Paolo.Milani@mi.infn.it

Nanostructured coatings with controlled wettability and high mechanical properties are of interest for many applications, such as biocompatible coatings for medical implants, chemical and biosensors, high-capacity condensers in electrochemistry. In this connection, it is very important to determine the conditions of the variations in the coating wettability and mechanical characteristics.

Here we discuss a significant influence of high-temperature annealing and UV-illumination on wettability and mechanical properties of a special class of nanostructured coatings: cluster-assembled titania (ns-$TiO_2$) thin films, obtained on different substrate materials (Si, Al, polyethylene) by a supersonic cluster beam deposition (SCBD) technique [1]. This method allows the tailoring of the film surface morphology and roughness by tuning the primary cluster size (from few tens of atoms per cluster up to several hundred atoms).

The contact angles on the coatings for the liquids of different polarities (water, glycerine) were measured by a sessile drop technique under normal conditions as a function of the film thickness (from 100 nm to 15 μm), roughness (from 25 to 750 nm) and morphology. The accuracy of the measurement was ±1—2°. The nanohardness tests have been carried out using a Nano Indenter-II nanohardness tester (MTS Systems, Oak Ridge, USA) with Berkovich indenter under the peak load of 1 mN. During the test the load dependence of indenter displacement was measured. A load-displacement curve was received in result. Hardness and elastic modulus were calculated according to Oliver and Pharr technique [2]. The accuracy of measurements of the indent depth and of indentation load were ±0,04 nm and±75 nN, respectively. $TiO_2$ coatings were annealed in air in the temperature range from 100 to 800 °C with holding time of 3 hours at each temperature. For UV radiation treatment (3 hours), we used the 365 nm wave-length radiation.

Our results show that the wettability of nanostructured films can be efficently tailored by the film roughness and morphology. The contact angle is found to increase from 66º to 80º with increasing surface roughness from 25 to 750 nm (Fig. 1, curve 1). This might be caused by properties inherent in nanostructured materials (generally, according to Wenzel's equation for rough surfaces, wetting angle decreases with increasing surface roughness). The unannealed ns-$TiO_2$ coatings exhibited the high stability to oxidation: the contact angles did not change after being hold in dark for 3 months (Fig. 1, curve 2).

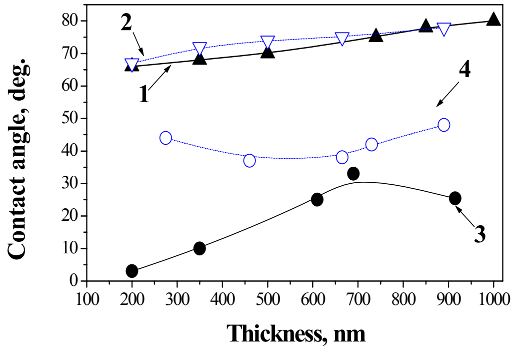

Fig.1. Variation of wettability of $TiO_2$ films caused by annealing: 1— as-prepared film; 2—after holding in dark for 3 months; 3—annealed at 800 °C during 4 hours; 4—annealed and held in dark for 3 months.

Annealing the ns-$TiO_2$ film in air (800 °C, 3 h) decreases the contact angle from 80° even to zero (Fig. 1, curve 3) because of the changes in structure, surface morphology and chemistry (Fig. 2).

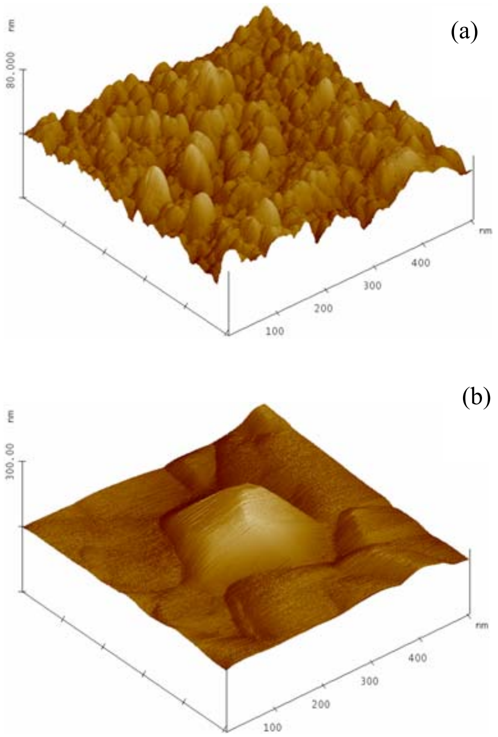

Fig. 2. Variation of surface topography of the 8.3- nm thick ns-$TiO_2$ coating on the annealing: (*a*) —as-deposited film; (*b*) — annealed at 800°C for 3 hours.

Micro-Raman spectra of the heat-treated $TiO_2$ sample show the evolution of the $TiO_2$ phases. The phase transformation (rutile→anatase) takes place on annealing above 600 °C [1], which leads to changes in structure, morphology and chemistry of the sample surface. The $Ti^{4+} \rightarrow Ti^{3+}$ transformation gives rise to the formation of $Ti^{3+}(H_2O)_6$ complex on the film surface, which impart high hydrophilic properties to the surface[3]. After the ns-$TiO_2$ sample was stored in dark for 3 months, the contact angle increased slowly (Fig. 1, curve 4). Irreversible structure change prevents the recovering of contact angles to their original values.

The UV illumination causes the same change of hydrophobic-hydrophilic properties, but it might be attributable to a radical change in the surface chemistry only. As opposed to the annealed coatings, the UV-illuminated coatings completely restore their hydrophobic properties after being hold in the dark for about 2 –5 h.

Mechanical tests have shown that a hardness of as-deposited ns-$TiO_2$ film (rutile) is about 4.3 GPa and elastic modulus is about 109 GPa, which is much lower than should be expected for oxides.

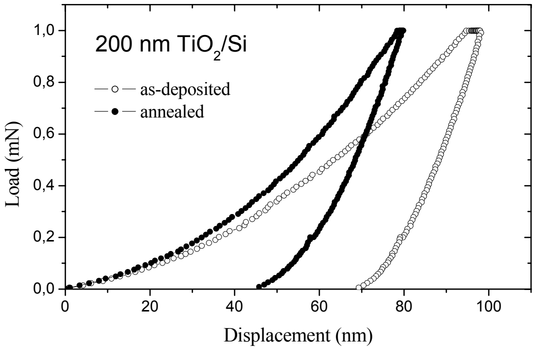

Fig. 3. Load-displacement curve for a ns-$TiO_2$ coating

Reduced hardness and elastic modulus is caused by the specific (hierarchical) structure of ns-$TiO_2$ coatings (Fig. 2, a). It was found, that for as-deposited film, a region containing fine grains is of a higher hardness than that containing coarse grains. High-temperature annealing increases the hardness to 7,3 GPa, especially, for the fine-grained films (Fig. 3). UV-illumination did not affect mechanical characteristics.

Our results are of great importance not only for determination of the temperature range, in which the wettability of ns-$TiO_2$ coatings does not change, but also as a demonstration of the possibilities of tuning the wettability and improvement of the mechanical characteristics of nanostructured coatings by different surface treatments (high-temperature annealing or UV-irradiation).

1. E. Barborini, I. N. Kholmanov, P. Piseri et al., *Appl. Phys. Lett.*, 81, No 16 (2002) 3052.

2. W.C. Oliver and G.M. Pharr., *J. Mater. Res.*, 7, No 6 (1992) 1564.

# THE FORMATION OF CRYSTALLINE PHASES UNDER HIGH-TEMPERATURE TREATMENT OF RAPIDLY QUENCHED CoSiB ALLOYS

**Zakharenko M.I., Babich M.G., Yeremenko G.V., Semen'ko M.P., Speka M.V.**
Shevchenko Kiev National University
64, Volodymyrska Str., Kyiv, 01033, Ukraine, zakharenko@univ.kiev.ua

Rapidly quenched alloys (RQA) of Co—Si—B system attract much attention from the point of their industrial application in different elements of magnetic circuits (magnetic cores, sensors and precise current transformers) due to extremal level of their soft magnetic properties. For example, $Co_{58}Fe_5Ni_{10}(Si,B)_{27}$ has a coercivity $H_c$=8—10 mA/cm and a maximal magnetic permeability $\mu_{max}=2\cdot10^5$ [1]. Co-base RQA (developed by Vacuumschmelze GmBH) has $\mu_{ma}=9\cdot10^5$ [2]. Meanwhile, the properties of Co-based RQA are strongly affected by their time and temperature instability, which is determined both by the atomic structure of the as-quenched alloys and by the atomic rearrangement occurring while heat treatment. That is why, the investigations of temperature-temporal stability and structural phase transformations occurring upon heating of such alloys are of high interest from the point of view of their industrial applications.

Co-rich rapidly solidified alloys of CoSiB system (general composition $(Co, Me)_{72}(Si, B)_{28}$, Me=Fe, Cr) have been prepared in a form of ribbons 10 mm wide and 20-30 μm thick by single-roll quenching technique using the source materials of high purity. The speed of a quenching disk was equal to 820—850 $min^{-1}$. The contents of RQAs have been controlled by the X-ray fluorescent method. In total 7 alloys differing by the content of metal admixtures (Fe and Cr) have been investigated.

The studies we have performed earlier [3] proved the existence of different types of magnetic inhomogeneities in the CoSiB- based RQAs. These inhomogeneities exist in a wide temperature range, however their amount, type and dimension could vary upon heating that exerts an essential influence, in particular, on the temperature dependences of magnetic susceptibility and electric resistivity.

In order to reveal the phase transformations occurring upon heat treatment of the studied RQAs and to control their phase composition the appropriate diffraction patterns have been analyzed. The latter were collected with DRON-4-07 automatic diffractometer (Co Kα radiation) in a discrete mode. The scanning parameters were the following: step scan $0.05^0$, counting time per step 5 s. The peak positions and integral intensities of the observed reflections were determined using full profile analysis. The unit cells were refined by the least-square method. The fragments of the X-ray diffraction patterns for one of the investigated RQAs annealed for 10 min at different temperatures $T_a$ are presented, as an illustration, at Fig. 1.

It is clearly seen that even at sufficiently low values of $T_a$ the parameters of the X-ray diffraction pattern vary, though RQAs remain still roentgen-amorphous (curves 1—4). The detected changes indicate the evolution ribbons' structure within the stability of amorphous state. This also manifests in essential variation of the alloys' physical properties (electrical and magnetic, in particular). Thorough analysis of the experimental data we have obtained earlier showed the complex multi-stage character of the RQAs' structural relaxation occurring just in this temperature range.

Starting from the temperature of 840 K one can observe sufficiently narrow peaks of crystalline phases emerging over diffuse halo. The X-ray diffraction patterns obtained for the specimens annealed at $T_a$=840—850 K (curves 5, 6) testify the presence of the sole crystalline phase along with the relaxed amorphous matrix. This phase has been successfully identified (reliability factor *R*=0,04) as high-temperature β - modification of $(Co, Me)_2Si$ (structure type $Ni_2In$, space group $P6_3/mmc$, *a*=0,3881 nm and *c*=0,4850 nm; 2(Co, Me): 2(a) 0 0 0; 2(Co, Me): 2(d) 1/3 2/3 3/4; 2Si: 2(c) 1/3 2/3 1/4). The regularities of the temperature dependencies of electric resistivity evidence the validity of the known Rayleigh law in this case. Hence, a matrix structure containing fine crystalline inclusions is formed in the heat-treated RQAs, the resistivity of these inclusions being essentially higher that for the as-prepared RQAs.

The alloys annealed at the temperature range $T_a$>900 K were shown to be two-phase. The analysis of the X-ray diffraction spectra for these specimens showed the presence of the low-temperature α - modification of $Co_2Si$ (space group *Pnmm, a*=0,49255 nm, *b*=0,37445 nm, *c*=0,71082 nm) and $Co_3B$ (space group *Pmmm*),

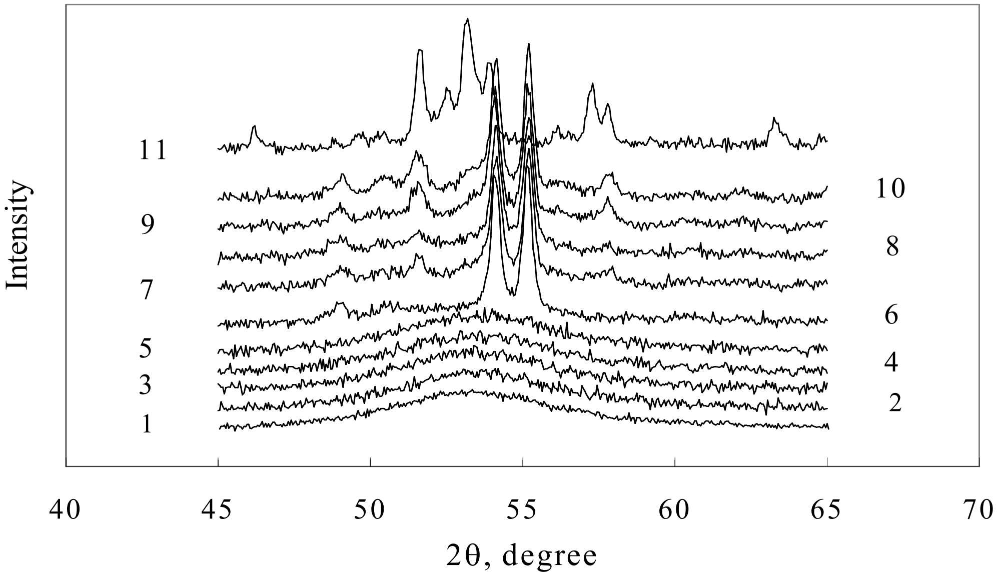

Fig. 1. Fragments of the X-ray diffraction patterns for RQA annealed at different temperatures: 1 - as-prepared, 2 – 800 K, 3 – 810 K, 4 – 825 K, 5 – 840 K, 6 –850 K, 7 – 860 K, 8 – 870 K, 9 – 880 K 10 – 895 K and 11 – 920 K.

the lattice spacings of the latter one depend on the composition of the source RQA and differ from those listed in ASTM database (12—0443). In our opinion, this is caused by the influence of Fe and Cr dopants, which form the solid solution on the base of $Co_3B$ lattice.

An additional argument in favor of this statement follows from data of magnetometric studies of the crystallized specimens. Reasoning from the cooling branch of thermomagnetic curves, at least two ferromagnetic phases with different Curie points $T_C$ are formed in crystallized samples. One of them is characterized by the Curie temperature $T_C \approx 860$ K that is in a fairly good agreement with the reference value for $\alpha$ - modification $Co_2Si$ [4]. The reference value $T_c$=647 K for the binary $Co_3B$ pase essentially differs from the experimental values. This could be caused by the influence of doping Me atoms dissolved just in the lattice of this phase.

The alloys subjected to heat treatment at $T_a$=850 900 K (curves 7—10) were shown to be three-pase and contain $\alpha$-$Co_2Si$, $\beta$-$(Co, Me)_2Si$ and $Co_3B$.

It should be also noted that the phase composition of the investigated RQAs even after annealing at $T_a$=950 K differs from that available in literature for the crystalline alloys of Co—Si—B system.

The authors gratefully acknowledged Dr.V.G.Nosenko (Institute for Metal Physics NASU) for supplying the specimens of rapidly quenched alloys.

1. Boll R., Warlimont H., IEEE Trans. Magn. **MAG-17**, (1981), p. 3053.
2. Konczos G., Tompa K., Varga L., *Preprint KFKI 1982 – 22* (KFKI, Budapest, Hungary, 1982).
3. Babich M.G., Yeremenko G.V., Maslov V.V., et al. Abstr. SMM16, September 9—12 2003, Dusseldorf, Germany. - P.T4-57.
4. T.B. Massalski (Ed.), *Binary Alloy Phase Diagrams*, ASM International, Materials Park, Ohio, USA, 2nd edition plus updates on CD-ROM, 1996.

# DEFORMATION AND FRACTURE OF CARBON-CARBON COMPOSITE MATERIALS AT HIGH TEMPERATURES

**Dzyuba V. S., Kravchuk L. V., Kuriat R. I., Oksiyuk S. V., Tokarsky V. A.**
Pisarenko Institute for Problems of Strength, NASU
2 Timiryazevskaya Str., Kiev, 01014, Ukraine, sergio@ipp.kiev.ua

In manufacturing structural elements operated under high-temperature (~3300K) conditions, extensive use is made of carbon-carbon composite materials (CCCM). Today's topical problem is studying their thermomechanical properties under conditions as close as possible to the operating ones. The challenge of solving this problem is to ensure accurate measurement of load and strain, provide fast heating of specimens at a rate of about 1000 deg/s, and maintain a uniform temperature field along the gauge length.

Resolving of these difficulties was one of the main concerns in upgrading test equipment, as well as in modifying the methods developed earlier and creating new ones, which would provide taking into account the peculiarities and specifics of conducting high-temperature tensile, compressive, and torsion tests of CCCM. Many of these methods were patented [1—2].

To solve the above problems, we employed a setup for testing CCCM at temperatures from 293 to 3300K in vacuum, air or inert medium, which was created at the G. S. Pisarenko Institute for Problems of Strength, National Ac. Sci. of Ukraine on the basis of a 1958U 10—1 test machine. To completely automate testing, the setup is equipped with modern control and measurement facilities operated by a PC. The setup incorporates a system for program heating of specimens, which makes it possible to realize conditions close to those experienced by materials in operation. The present setup is also distinguished by unique experimental techniques of multichannel measurement of specimen strains with strain gauges touching the specimen sections not subjected to direct heating and the possibility of conducting tests in vacuum, as well as neutral and hostile environments.

Taking into account the need for high rates of heating, it is performed by sending an electric current. To this end, devices combining the functions of grips with those of current leads and equipped with water-cooling elements were developed considering the type of tests (tension, compression, torsion) for which they will be used. To create a uniform temperature field along the specimen gauge length, a unique method of additional heating of its boundary sections was devised. The thermal loading conditions are governed via three power supply units not connected to each other and controlled by a single heating control system. The temperature of the specimen gauge length is measured with thermocouples and/or an infrared pyrometer depending on the temperature range. This method of heating makes it possible to conduct tests at heating rates up to 1000 deg/s and create a uniform temperature field with a temperature scatter of ±25 K along the specimen gauge length within the whole temperature range.

To study the deformation behavior of degrading composite materials at temperatures up to 3300K, we used an ingenious method of determining strains from the results of contact measurements of displacements of the specimen sections adjacent to the specimen gauge length, which are not subjected to direct heating. The scheme of conducting measurements by this method is given in Fig. 1.

On either side of the tested specimen 1 there are projections 2 arranged in pairs, which are adjacent to the gauge length. Strains along the specimen axis are determined from the measurement data on the displacements of projections relatively to each other.

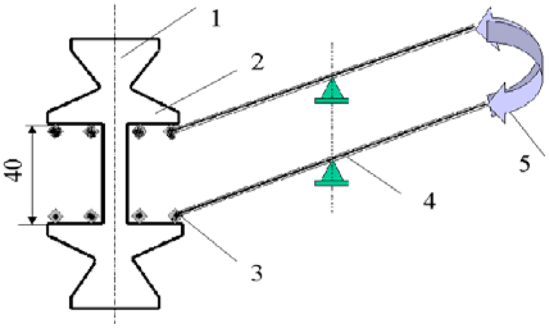

Fig. 1. Scheme of strain measurements in tension.

Measurements are made at four points at different distance from the specimen axis using strain gauges. The strain measurement device consists of eight arms 4 fastened on horizontal axes. Measuring prisms 3 from heat-resistant ceramics, which touch the specimen, are fastened on one end of the arms. The other ends placed in pairs are connected with glued strain gauges by elastic clamps 5.

One of essential advantages of this method is a possibility to rule out skewing or misalignment of the specimen and grips in the course of preparation of the experiment, minimize its effect, and take it into account in subsequent calculations. The accuracy of strain measurement was ~0.5 μ.

The paper presents the results of investigations into the influence of temperature from 293 to 3300K on the tensile strength of CCCM (Fig. 2).

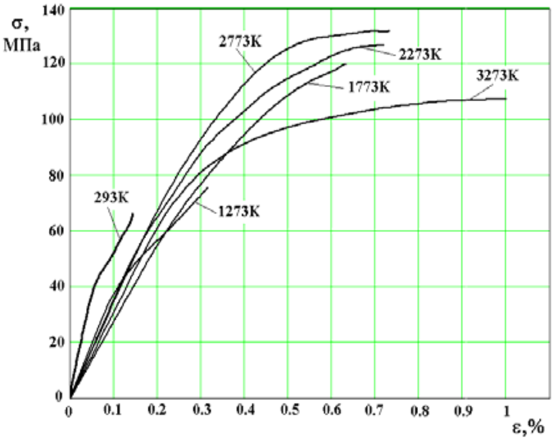

Fig. 2. Influence of temperature on averaged σ–ε curves in tension.

Analysis of this influence is given and the mechanism of specimen fracture is studied in the whole range of the test temperatures.

The strength properties remain almost unchanged up to the temperature 1273K. In the range from 1273 to 2773K, hardening of the material due to structural changes is observed. At higher temperatures (up to 3300K) a decrease in strength is observed while the deformation behaviour is somewhat different. In the range from 293 to 1773K fracture strain increases 4—5 times as compared to that at room temperature. As the temperature increases up to 2773K, changes in the deformation behavior are insignificant. A temperature rise up to 3300 K leads to an 8-10-fold increase in fracture strains.

A method to predict CCCM strength at high temperatures is outlined and comparison of calculation data with experimental ones is given. Thus, the above techniques and test facilities provide not only obtaining reliable data on the CCCM strength, but also predicting their strength under thermal and mechanical loading.

1. Patent 2003098506, Ukraine, I.Kl. 7 G01N1/00. “Plane specimen for tensile strength tests of composite materials under high-temperature conditions,” V. S. Dzyuba, L. V. Kravchuk, V. A. Tokarskiy, and S. V. Oksiyuk (Ukraine), No. 2003098506; applied for on 15.09.2003.
2. Patent 2003087440, Ukraine, I.Kl. 7 G01N1/00. “Specimens for tests of nonmetallic materials under axial loading,” V. S. Dzyuba, L. V. Kravchuk, V. A. Tokarskiy, and S. V. Oksiyuk (Ukraine), No. 2003098506; applied for on 24.09.2003.

# RESEARCH OF A REACTIONARY SINTERING OF A SYSTEM AL-CR

**Romanov G.N.**, **Tarasov P.P.**(1), **Dyachkovskii P.K.**(1)
Tomsk State University, Tomsk, Russia
Lenin pr.36, 634050, Tomsk,Russia, romgeorg@mail.ru
(1)Yakut state university,
Belinskii st. 58, 677016, Yakutsk, Russia

The aluminum has such extremely important properties, as small specific weight and corrosion resistance. The development of a powder metallurgy of aluminum allows to make from aluminum of an work pieces as for mass series production in different industries, and specialized assigning, including for aerospace engineering.
For obtaining easy, strong and corrosion-resistant materials with given properties perspective technology is the reaction sintering of alloys in vacuum. The basis of technology of a reactionary sintering of powder bodies is the problem on a genesis of intermetallic compounds at interaction of a solid phase with liquid. The given problem leaves far for frameworks of concerns of physics of a sintering and is diffused to many other physical phenomena and technologies, concerns of processes which are flowing past on interphase boundary.

The conducted earlier dilatometric researches have shown, that as a result of attachment to a dust of aluminum of some of brass, titanium, nickel, ferrum due to a heat of a exothermic reaction is possible to conduct a liquid-phase sintering of such mix at temperature of board below than temperature of formation of a fluid phase [1, 2]. Such volumetric changes are possible are to defined as a feature of a sintering of systems "aluminum - transient metal ". The researches of volumetric changes of a system aluminum - chromium are prolongation of such activities.

The advantage of a dilatometric method in research of process of a sintering of the pressed metallic powders in that also consists, that it enables continuously to record changes of linear dimensions of a powder body and its temperatures during all time of a sintering. The obtaining of such data specially is important for finding-out of the nature of fast flowing past processes, in particular, at an exothermic sintering, when due to reactionary interaction of components of a powder mixture changes not only volume of pressed body, but also its temperature, though thus temperature of board is supported by a constant. In work the dilatometer of an own design [2] is utilised.

In work the in-depth dilatometric researches of process of an exothermal sintering of a system Al-Cr are conducted. The contents of a dust of a chromium in a mixture made 2,5; 5; 7,5; 10; 12,5; 15; 17,5; 20 at.%. Cylindrical pressed bodies of all mixtures by an altitude 10 and dia of 10 mms had an initial porosity 20%. The sintering was made in a vacuum dilatometer. The handset with a sample was placed in board, preheated up to 700°C. The selection of given temperature is conditioned by that the appearance of a fluid phase in a system Al-Cr takes place at lower temperature as a result of a melting of aluminum (660 °C).

As is established in [3] compulsory condition of obtaining of the new class of aluminium two-phase alloys is gas loosing an annealing, precursor to a liquid-phase sintering, pressed bodies in vacuum at temperatures component 0,7—0,9 from melting points a matrixes. In this connection in work the mode was used, when samples and in case of a sintering in board and at dilatometric researches were previously subjected to an annealing at temperature 500°C within one hour.

The analysis of sintering dilatogramm of alloy with the contents 2,5 at. of % has shown, that after achievement 660 °C approximately 6 minutes, while the aluminum is melted, temperature of a sample remains to a constant, and only then it reaches 700 °C, temperature in a handset of a dilatometer. The curve of a changing sizes to considerable value of shrinkage and its subsequent crumpling because of exuberant quantity of a fluid phase. At a sintering of a mixture with the contents of a chromium 5 at. of % in a start by the begining of shrinkage the short-lived growth of a sample is watched, which one then again is replaced by shrinkage. The appearance of this growth can be called by increase at a sizes of fragments of a chromium owing to preferential diffusion in them of atoms of aluminum with formation of intermetallic compounds. After shrinkage of a sample takes place as a result of a re-grouping of fragments of a solid phase in liquid under effect of capillary forces. Thus to a solid phase it is necessary to relate not only derivated intermetallic compounds, but also oxide fragments of aluminum and, probably, chromium. In this case temperature site has appeared less, than for alloy with 2,5 at. of %, that is possible connected that a lot of a chromium gives a lot of a heat, which one is selected at formation of intermetallic compounds on its basis and is spent for a melting of aluminum. The value of growth of a sample with 7,5 at. of % of a chromium at the moment of originating exoeffect, is higher as contrasted to by sample inclusive 5 at. of % of a chromium, because of higher concentration of a chromium. Thus the final value of an aftershrinkage appears minor. At a sintering pressed bodies with the contents of a chromium 10 at. of % of a chromium samples grow at once, as soon as there is a fluid phase, without any preliminary shrinkage. It testifies to presence steady solid phase of a skeleton of a sample during all period of a sintering. After short-lived, but vigorous growth the shrinkage of a sample conditioned by a re-grouping of fragments of a solid phase is watched. However value of shrinkage does not surpass value of preliminary growth, therefore as a result of a sintering samples are augmented at a rate of, becoming more porous, than initial pressed body. The allocation of a heat as contrasted to by samples with the smaller contents of a chromium is more significant, and temperature of a sample grows spasmodically.

Dilatogramm of a sintering of a powder sample with 12,5 at. of % of a chromium testifies that during a melting of aluminum arise discontinuous temperature climb of a sample and its sharp volumetric growth, which one on any moment is interrupted by shrinkage. That fact, that begun growth of a sample on stage of temperature climb is very fast replaced by shrinkage, can indicate that the generatrix most fusible intermetallic compounds could at once melted, causing partial destruction solid phase of a skeleton and re-grouping of fragments. The general growth of a sample including short-lived shrinkage, is prolonged approximately so long as its temperature will not fall up to temperature in a handset of a dilatometer (700 °C). The increasing of a sample which is were synchronized to its self-heating, can be explained by growth of intermetallic grains by diffusion of atoms of aluminum in fragments of a chromium. The prolongation of growth pressed body at stage of a temperature drop of a sample up to 700°C, probably, is connected to a crystallization intermetallic of a phase from a melt.

Metallurgical researches is model were conducted on optical and on an electronic scanning microscope Philips XL-20. For alloys inclusive 2,5; 5 and 7,5 % of a chromium, the value of shrinkage during a sintering surpasses growth. Therefore initial porosity is model of these alloys, in the final accounting, decreases. Their pattern after a sintering represents an aluminium matrix inclusive actuations of intermetallic compounds. With increase of the contents of a chromium samples become more porous, and the volumetric contents intermetallic of actuations increases, though their size remains approximately identical. Apparently, it can be connected with the higher contents of a chromium and with a higher jump of temperature is model at exoeffect. Probably, these factors cause growth of grains intermetallic of a phase owing to crystalline modification through a melt.

The conducted researches have shown, that in a system the aluminum - chromium can be received as porous (up to 50 % of pores for alloy with 15 at. of % Cr), and dense material (with ultimate tensile strength up to 350 МПа for alloy with 10 at. of % Cr).

## The literature

1. Savitskii A.P., Martsunova N.R., Jdanov V.V. A contact melting in systems with intermetallic compounds, Adhesion of melts and soldering of materials, 1977, № 2, pp.55—57.
2. Savitskii A.P. Liquid phase sintering of the systems with interacting components. Novosibirsk; Nauka, 1991,184 p.
3. Rusin N.M. Regularity of a sintering and property of alloys on the basis of aluminum with the components of transient metals. Abstract candidate dissertation.- Tomsk, 1996, 15 p.

# INCREASE OF CORROSION STABILITY OF STEEL DETAILS BY DRAWING CHROMOSILICIDE COATINGS

**Iantsevitch C. V.**
National Technical University of Ukraine "KPI", Kiev, Ukraine

## INTODUCTION

The result of drawing diffusion silicide coatings is marked increase of rust resistance, fire resistances and wear resistances of carbon steels [1]. Details of machines thus, fabricated from medium-carbon steels with silicide coatings. Such coatings can be subjected to the further heat treatment without appreciable change of their rust resistance in acid conditions. Nevertheless, such way of hardening of details of machines has not found wide practical application in a domestic industry at corrosion protection of steels in aggressive environments because of high porosity this coatings. To improve quality silicided of beds and to raise their rust resistance in aggressive environments it is possible for score of padding alloyed by their chromium [2, 3, 4]. In National Technical University of Ukraine "Kiev Polytechnic Institution" the new ways and compositions of initial reagents for complex saturation of carbon steels by silicium and chromium are developed. In the present paper was investigated the influence doped by chromosilicide coatings on corrosion and electrochemical behaviour of carbon steels in concentrated solutions of acids. The opportunity of a heightening of rust resistance of such diffusion layers is shown by oxidation.

The purpose of the carried out work is the development of new high-performance and technologically simple ways of saturation of a surface of steel by a silicium and chromium, and study a phase, chemical makeup, structure and properties of a diffusive layers, corrosion stability in different aggressive medium.

## EXPERIMENT

The applying process of the chomosilicide coatings onto the carbon steel* (20, 45) surface has been performed at a temperature of $1050^0$C for 6 h. The compositions containing an expedient amount of the ferrosilicon powders and chromium have been used as the saturating steels, whereas ammonium fluoride has been used as an activating agent.

The corrosive stability of the steel with coating and its electrochemical behavior in the solution under study depend on the 10% solution solution sulphuric, chlorine, phosphoric, acetic and nitric acids the exposition term of samples in a solution. The exposition term of samples in a solution has been changed in limits from 24 up to 576 h. The testings carried out on samples without seen defects (having chopped off, cracks).

A microstructural analysis of the chromosilicide coatings on steels was performed with a raster microscope - microanalyser "CAMECA". Microhardness and thickness was measured on the equipment PMT-3. The phase compositeon was studied wing an - X-ray diffractometer of "DRON-YM1"-type. In quality monohromator have utillized a single crystal of graphite established on a diffracted bunch. The difractograms from samples removed in an interval of angles 2θ 25 - 85° by a method of step-by-step scanning. The step of scanning made 0,05°, exposure time in point – 5—7 s. The diffraction profiles registered from a surface of initial samples and from a surface of samples after sequential removal by grinding of bed of coating by width 10 nm.

## RESULTS AND DISCUSSION

The results of phase X-ray crystal analysis show, that on steel 20 and 45 diffusive beds consist of carbides of chrome $Cr_{23}C_6$, $Cr_7C_3$, doped by silicium and $\alpha$ - solid solution of silicium and chromium in iron. Under taken over conditions on a surface of steels 20, 45 the diffusive beds by thickness 100 … 120 μm, accordingly are formed.

Metallographicly chromosilicide coatings 3% $HNO_3$ in ethanol, beds with the advanced external border come to light as light not pickled. The typical microstructure of steel 45 after complex saturation by silicium and chromium is presented in Figure 1.

The layers located immediately at border was undressed by coatings - steel, will match $\alpha$ - solid solution of silicium and chromium in iron.

At s of chr

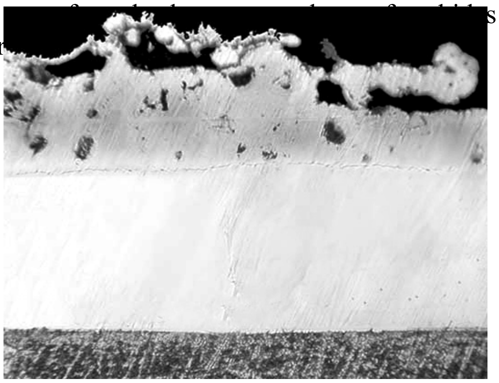

Figure 1.Microstructure CrSi coatings on steel 45, x500.

The microhardness of coatings makes 19,5GPa. The porosity chromosilicide coatings made 47—52 pores e/sm$^2$, that in 2—3 times there isless this characteristic silicide coatings.

The study in the present work and received early [5] corrosion tests have shown, that on all researched marks of steels (steel 20, 45) chromosilicide coatings least resistant in 10% solution chlorine, both sulphuric acid and most resistant - in a solution nitric acid. In 10% solution sulphuric, chlorine, phosphoric, acetic and nitric acids of a coatings brake speed staining of steel 45, accordingly in 4; 4,5; 8; 17 and 9000 times. The protective properties chromosilicide coatings depend on a surface condition of researched samples - presence on it of defects (having chopped off, of cracks) and oxide layers. The long endurance coatings on air and their heat treatment in a muffle result in increase of protective properties of diffusive beds and their propensity to passivation.

The coatings by oxidizing in a soaking drum results in formation of more dense oxide layers. Shaping on a surface of complex diffusion coatings on a base of silicium and chromium of oxide layers result in increase of rust resistance in various aggressive environments. So, in 10% solution sulphuric acid coatings brake speed staining of steel 45 in 1500 times. Thus their stability depends on carbon content in steel of a base, that is explained by distinction in composition and structure of diffusion layers on the investigated steels.

The chromosilicide coatings can be recommended for protection of details of machines working in aggressive medium.

## CONCLUSIONS

1. It is established, that the drawing chromosilicide coatings on a detail of machines from carbon steels considerably rise their corrosion stability in solutes of acids.
2. The corrosion stability of samples with chromosilicide coatings in various aggressive environments is much higher, in comparison with samples with silicide coatings. It is connected to formation on a surface of simple steels of coatings on a base of carbides chromium such as $Cr_7C_3$, $Cr_{23}C_6$, by shaping is immediate on a surface dense $\alpha$ - solid solution of silicium in iron and practically of pore-free protecting film on a base of a oxide silicium alloyed chromium.

## REFERENCE

[1]. V.I Ydovitsky Antifriksionnoe poristoe silicirovanie yglerodistuh staley – M, Maschinostroenie, (1977), p.132 (in Russian)

[2]. H.P. Liahovitch, L.G. Voroschnin, G.G. Panich Polycomponent coating – Minsk, Nauka i technika, (1974), p. 140, (in Russian)

[3]. Kasparova O.V., Zorin A.A., Koloturkin Y.M., Zays O.V., Orlov U.V., Butko A.A. // Zaschita metallov, V.25, **2**, (1989), P.191-195 (in Russian)

[4]. Shapovalov E.T., Stetsovsky L.L., Schvarsman L.A. // Zaschita metallov, V.25, **3**, (1989), P. 378-380 (in Russian)

[5] I.S. Pogrebova, C.V. Iantsevitch, V.M. Garbyz, V.V. Kornienko // Fiziko-khimicheskaya mekhanika materialov, V.2, (2001), P. 108 (in Ukraine).

---

* Steel 20: C=0,22%, Mn=00,62%, Si=0,35%, S less 0,04%, P less 0,035%
Steel 45: C=0,40%, Mn=0,80%, Si=0,37%, S less 0,04%, P less 0,035%

# INFLUENCE OF ANNEALING ON STRUCTURE AND PROPERTIES OF COATINGS OF CARBIDES CHROME

**Khyzhniak V.G., Korol V.I.**
National Technical University of Ukraine "KPI", Kiev, Ukraine

The precipitation of coatings on a base of carbides of transition metals IV - VI of groups of a periodic system allows considerably to increase production characteristics of machines details at work in conditions of high unit loads and elevated temperatures [1].

In a given work with the purpose of study of processes, which run in coatings under operation of high temperatures annealing samples with diffusive coatings on a base of carbides chromium was executed.

The carbides coatings on a surface of steel 40 precipitations at temperature 1323K and dwell time 4 hours in self-contained reactionary space at underpressure. As initial reagents have used a powder of chrome, perchloromethane, carboncontent additive [2]. Annealing carried out at temperature 1323K and dwell time 6 hours at underpressure in a reducing atmosphere.

A microstructural analysis of carbide coatings on steels was performed with a raster microscope - microanalyser "Camebax SX50". Makeup of diffusive courses defined on raised by an electronic bunch Kα - radiation in a spectrum of the appropriate element has been studied. Microhardness and thickness was measured on the equipment PMT-3. The phase compositeon was studied wing an - X-ray diffractometer of "DRON-YM1"-type.

The explorations of structure of diffusive courses carried out on an optical microscope «Neophot 21». For revealing structure of a diffusive course samples subjected to pickling treatment in reagents Murakami [10 g $K_3(FeCN)_6$, 10 g NaOH, 100 ml $H_2O$] and 3—5% $HNO_3$ solution in ethanol. Microhardness and thickness of diffusion layers of carbide phases defined on microsections on the device PMT – 3 has been studied.

The consideration of the received data has shown (table 1), that as a result of the lead annealing the change of phase makeup of coatings was not observed. Some decrease of a lattice constant of carbides is marked.

Marked after annealing increase a layers depth of a chromium carbide $Cr_7C_3$ and decrease of thickness $Cr_{23}C_6$ are caused by features of diffusion processes proceeding at annealing on border the steel base (diffusion of atoms of carbon from an alloy of a base in a carbide layer undressed a coatings and chromium in transition zone) [3, 4].

Metallographicly carbide layer on a surface of the investigated steels is displaid as light, not pickled 3-5% $HNO_3$ solution in ethanol zone, blanket thickness 12,0 - 14,0 μm. In carbide coatings two courses are visible.

Table 1. Phase, structure and thickness of diffusive layers on a base of chromium carbides an initial and annealed condition on steel 40*

| Condition of a sample | Phase of a carbide zone | The parameter of the lattice, $10^{-9}$ m | Thickness, μm | Microhardness $H_m$, GPa |
|---|---|---|---|---|
| Without treatment | $Cr_{23}C_6$ | a = 1,0691(2) | 10,0 | 14,6 |
| | $Cr_7C_3$ | a = 0,7009(3)<br>b = 1,2172(6)<br>c = 0,4538(2) | 3,6 | 17,2 |
| Bakeout | $Cr_{23}C_6$ | a = 1,0684(3) | 7,6 | 14,0 |
| | $Cr_7C_3$ | a = 0,7003(3)<br>b = 1,2139(7)<br>c = 0,4533(3) | 6,0 | 16,8 |

Table 2. The contents of elements in coatings on a base chromium carbides on steel 40

| Point of gauging | Condition of a sample | Contents of elements, % | | |
|---|---|---|---|---|
| | | Cr | C | Fe |
| The external boundary of a coating (2-3 µm from a surface of a coating) | Without treatment | 69,0 | 13,7 | 8,9 |
| | Bakeout | 69,7 | 16,6 | 12,9 |
| The central coating zone (6-8 µm from a surface of a coating) | Without treatment | 60,0 | 17,0 | 18,0 |
| | Bakeout | 62,6 | 18,0 | 21,0 |
| The internal boundary of a coating (2-3 µm from a surface of a coating) | Without treatment | 52,3 | 18,4 | 29,2 |
| | Bakeout | 45,8 | 17,7 | 36,4 |

Course located immediately at a base is a carbide $Cr_7C_3$ and consists of needles. The surface layer was expressed a structure with the extended crystals and will match to a carbide $Cr_{23}C_6$.

The axis of crystals of a carbide $Cr_{23}C_6$ is located perpendicularly to front of a diffusion, cross aggregate size 0,5 - 1,5 µm. After holding annealing in structure of coatings the insignificant reduction of the grains sizes of a carbide $Cr_{23}C_6$ (up to 0,3 -1,0 µm) and increase of the sizes of needles of a carbide $Cr_7C_3$ was observed.

Some decrease of a microhardness of courses $Cr_{23}C_6$ and $Cr_7C_3$ after annealing apparently is connected that at annealing the atoms of iron under influence of a gradient of thermodynamic activity are redistributed from an alloy of a base, collect in a diffusive course and substitute from one up to four atoms of a chrome in a crystal lattice of carbides of a chromium [5, 6].

Thus in coatings after performance of annealing the decrease of a layers depth $Cr_{23}C_6$, propagation of a bed depth $Cr_7C_3$ is marked which is accompanied by reduction of aggregate size and some decrease of a microhardness of carbide phases.

The results of explorations stated in work, can be useful at modeling the phenomena proceeding in a diffusive course at details of machines from steels at elevated temperatures.

## Reference

[1]. Himiko – termicheskaja obrabotka metallov i splavov. Spravochnik: pod red. Boriseniuk G.V., Vasiliev L.A., Voronin L.G. M.:Metallurgiya, 1981, p 424. (in Russian)

[2]. Loskutov V.F., Khyzhniak V.G., Kunickij J.A., Kindrachuk M.V.Difuzionnye karbidnye pokrytiya. K.: Tehnika, 1991, p.168 (in Russian)

[3] Arzamasov B.N. Hhimiko – termicheskaja obrabotka v aktivirovanyh sredah. M.:Metallurgiya, 1979, p. 212 (in Russian)

[4] Dumchenko V.V., Griboedov Y.N., Bogaturev Y.M. // Zaschitnue pokrutiy na metallah, V.10, (1976), P.27-29 (in Russian)

[5] Tod L. Karbide i nitride perehodnuh metallov - M.: Mir, 1974, p. 294 (in Russian)

[6] Metalovedenie I termichesky obrabotka stali V.1 Spravochnik // Bernschtayn M.L., Rahschadta A.G. :M., (1961), p. 747 (in Russian).

---

* Steel 40: C=0,43%, Mn=0,50-0,80%, Si=0,17-0,37%, S less than 0,04%, P less than 0,035%

# MECHANOSYNTHESIS, STRUCTURE AND PROPERTIES OF TERNARY CARBIDE $TI_3SIC_2$

**Antsiferov V. N., Smetkin A. A., Kachenyuk M. N.**
Center of Powder Material Science
Ul. Professora Pozdeyeva 6, 614013, Perm, Russia solid@pm.pstu.ac.ru

Production of dense heat-resistant materials with high strength and wear-resistance at high temperatures is an important and pressing problem nowadays. The polycrystalline ternary carbide $Ti_3SiC_2$ is one of these materials. Layered disposition of refractory carbides in $Ti_3SiC_2$ provides for unique mechanical characteristics of this material, which are unusual for ceramic materials: plasticity at high temperatures, high strength in both brittle and plastic state, and high crack-resistance.

There are various methods of titanium silicide and carbosilicide production. The latest paper presents results of research of $Ti_3SiC_2$ production using method of mechanosynthesis in vacuum.

Mechanosynthesis was done in "Sand" vacuumized planetary grinding mill during 3, 6 and 10 hours at grinding bodies-charge ratio of 30:1 and rotation speed of 360 rpm. Initial composition of charge in mole ratio of components was 3:1:2.

Particle-size analysis of synthesized powder after 3 and 6 hours of processing shown that quota of particles with average size of 2,5 µm amounts to ~50% (Fig. 1).

Increase of mechanical alloying duration to 10 hours results in increase of particle size, i.e., their conglomeration occurs. On the basis of X-ray analysis of the powders synthesized, it was determined that the most optimum time of powder compound mechanic activation is 3 hours, as further processing does not result in qualitatively different effect. According to X-ray analysis, the compound corresponds to $Ti_3SiC_2$—$Ti_xC$—TiSi composition without lines of pure titanium and carbon.

Then, the powder was pressed at P=300 MPa and sintered in argon in temperature range of 1150—1600 °C. At 1250 °C, porous specimens with volume fraction of pores of 40% were obtained, and pore size range amounts to 0,1—1,0 µm. Figure 2 shows porogram of sintered specimen.

Sintering of synthesized powder pressings in temperature range of 1400—1500 °C in argon atmosphere allows obtaining titanium carbosilicide $Ti_3SiC_2$—$Ti_xC$. At that, relative density of the sintered material is 85%.

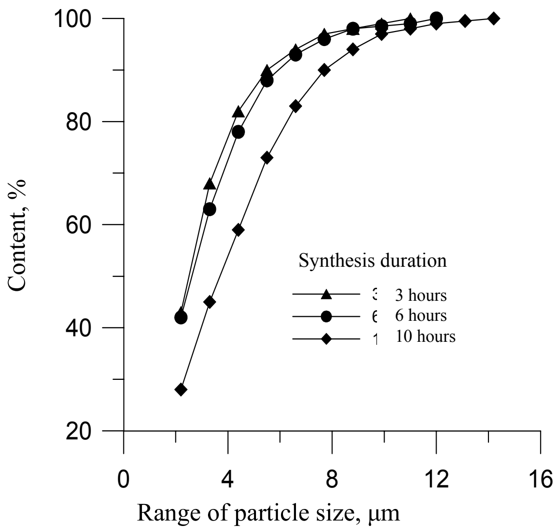

Figure 1 – Distribution of particles in synthesized compound of Ti—SiC—C

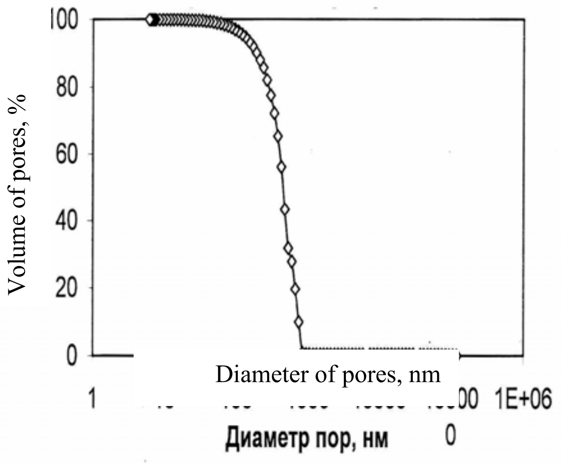

Figure 2 – Porogram of $Ti_3SiC_2$ sintered at 1250 °C

To increase density of the sintered titanium carbosilicide, methods of hot plastic deformation are used. Hot compaction of specimens at 1000—1300 °C allowed obtaining relative density of up to 92%.

Metallographic analysis of the specimens sintered shown that structure of material is microcrystalline, and average grain size is 1 μm. Vickers hardness of maximum dense specimens based on synthesized compounds is determined at loads of 49,3 и 98,1 N, the results are shown in Table 1. Data presented demonstrate that increase of load results in decrease of specimens hardness. Review of scientific literature shown that Vickers microhardness of $Ti_3SiC_2$ decreases with increase of load, stabilizes at higher loads and amounts to 7.4 GPa for specimens with inclusions of titanium carbide; 4 GPa for more pure specimens and 6 GPa for the specimens obtained using CVD method. These values indicate that $Ti_3SiC_2$ is abnormally soft comparing to other carbides.

Table 1 – Hardness of $Ti_3SiC_2$ at various loads

| Load, N | Vickers hardness, GPa |
|---|---|
| 49,3 | 11,5 |
| 98,1 | 4,37 |

It should be noted that after indentation at high loads (98,1 N) the imprint does not have diagonal microcracks, which are typical for brittle materials; this fact denotes quasiplastic nature of destruction. Decrease of microhardness in polycrystalline specimens with increase of load may be explained by the fact that at higher values of load, when area of contact with the specimen is larger, probability of capturing a grain with orientation for deformation increases. Critical stress intensity factor under conditions of plane deformation $K_{IC}$ (according to data from scientific literature) takes on values 6 MPa·m$^{1/2}$ to 9,4 MPa·m$^{1/2}$, depending on method of specimen preparation, average grain size and test procedure. Study of crack-resistance of $Ti_3SiC_2$ based on mechanically alloyed compound shown that at specimen relative density of 82—85% $K_{IC}$=4,69 MPa·m$^{1/2}$, and at 92% of density $K_{IC}$=6,33 MPa·m$^{1/2}$. Crack-resistance increases due to formation of great number of bonding bridges in the path of crack development, and to peculiarities of destruction of $Ti_3SiC_2$ grains, which is accompanied by grain splitting along the basal plane and microplastic deformation.

# MAGNETIC PROPERTIES OF AMORPHOUS ALLOYS Fe—Si—B IN A WIDE INTERVAL OF TEMPERATURES

**Hryhoryeva O.V., Belous M.V., Sidorenko S.I.**
National Technical University of Ukraine “KPI”
Peremohy Ave. 37, Kyiv, 03056, Ukraine, e-mail: grigoks@mail.ru

The investigation of magnetic properties of amorphous alloys is one of the most actual problems of the today’s physics of the solid state. This problem is actual as from the point of view of physical representation and also in the plane of possible practical applications.

The changes of magnetization during the heating of amorphous alloy $Fe_{82}Si_2B_{16}$ were studied in this work. We were going to get the information on the processes of crystallization and on the magnetic properties in a wide interval of temperatures.

The method of the differential thermomagnetic analysis with use of two etalon of armko-iron was applied [1]. The method of so-called internal etalon was applied also, in which a graduation of registered changes of magnetization was carried out using the well-known magnetic effect in the Curie point of carbide of iron θ-$Fe_3C$ (fig. 1).

We hoped that the information about the magnetization of amorphous foils $Fe_{82}Si_2B_{16}$ and about their Curie points might be obtained by using the differential thermomagnetic analysis in the combination with X-ray study. The X-ray researches were carried out using standard diffractometry (Fe-anode).

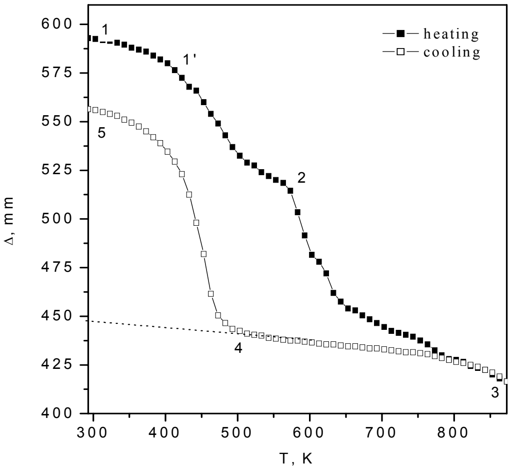

Fig.1. Magnetic effect in the Curie point of the θ-$Fe_3C$ carbide.

The thermomagnetic curve of heating and cooling of amorphous alloy $Fe_{82}Si_2B_{16}$ is shown on fig. 2. The principal feature of the thermomagnetic curve is that this curve has the reversible character in the temperature interval from room temperature up to approximately 395°C (668 K). This reversible character of thermomagnetic curve says on our opinion that the changes of magnetization, which are observed, are caused by the nearing to the Curie temperature of the amorphous alloy $Fe_{82}Si_2B_{16}$.

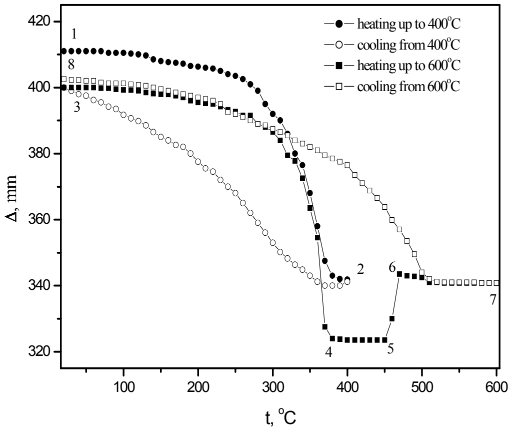

Fig.2. The thermomagnetic curve of cyclic heating of alloy $Fe_{82}Si_2B_{16}$.

The well-known relations of the thermodynamical theory of the temperature dependence of the spontaneous magnetization of a ferromagnetic near Curie point permit to estimate approximately the value of Curie temperature of amorphous alloy $Fe_{82}Si_2B_{16}$. In this case we to use the concrete value of the corresponding thermodynamic coefficient. This value is unknown for the amorphous alloys. We calculated the principal thermodynamic coefficient for pure ferromagnetics Fe, Ni, co and for phases θ-$Fe_3C$,

$Fe_3B$, $Fe_4N$. The middle value this coefficient was used for estimating Curie temperature of amorphous alloy $Fe_{82}Si_2B_{16}$. The value we got (390 °C, 663 K) is according to data published [2] very reasonable.

The second typical feature of all thermomagnetic curves we got is the fact that the curves have the irreversible character in the temperature interval 425—490 °C (698—763 K) during the heating the irreversible increase of magnetization is observed. This process is accompanied by the appearing of X-ray patterns the sharp lines of α-Fe and boride phase $Fe_3B$ and FeB (fig. 3). Also weak interferentions of phases $Fe_3Si$ were observed. These data permit to content that the increase of magnetization saying about is the result of the crystallization of the amorphous alloy:

$(Fe_{82}Si_2B_{16})_{am} \rightarrow (Fe+FeB)+Fe_3Si+Fe$ (1)

We used the common principles of quantitative analysis of additive properties of alloys developed in work [3].The following equation that describes the magnetic effect during the crystallization of the amorphous alloy $Fe_{82}Si_2B_{16}$ was got:

$$\frac{\Delta_{cr}}{\Delta_{\theta}} = \frac{\sigma_{Fe}^{(773)}}{\sigma_{\theta}^{(293)}} \cdot \frac{M'(1-0,24-0,36)}{15C \cdot 10^{-2} M_0}, \quad (2)$$

$\Delta_{cr}$ and $\Delta_{\theta}$ are the corresponding magnetic effects in units of the scale of magnetometer.

In the same way the equation for the determination of the specific magnetization of boride $Fe_3B$ was obtained. This phase is formed during the crystallization amorphous alloy $Fe_{82}Si_2B_{16}$. As we found the specific magnetization of boride $Fe_3B$ is 192 $Tl \cdot 10^{-4}$ $cm^3/m$. This value is in 1,5 times greater then the specific magnetization of cementite θ-$Fe_3C$ and 1,1 times lower then the specific magnetization of α-iron.

According to experimental data, which we obtained the specific magnetization of alloy $Fe_{82}Si_2B_{16}$ after it's crystallization measured at room temperature, does not differ of the magnetization of this alloy in amorphous state. The calculation shows that the numerical value of the specific magnetization σ ($Fe_{82}Si_2B_{16}$) is 159 $Tl \cdot 10^{-4}$ $cm^3/g$. This value is close to the values in references [4].

The calculation of measured in our experiments changes of magnetization in the temperature interval of phase transformation permit to determine the specific magnetization of the amorphous alloy $Fe_{82}Si_2B_{16}$ at 470 °C (743 K, this is the middle temperature of narrow interval of crystallization).

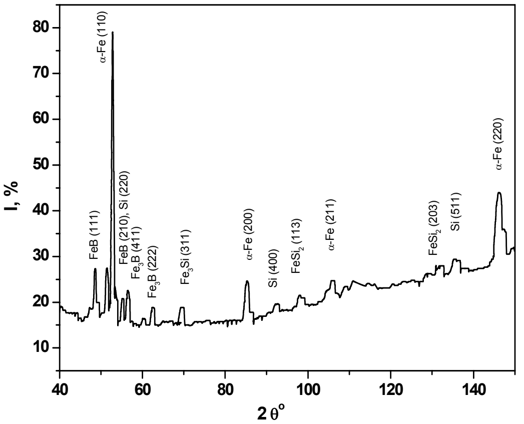

Fig.3. The diffractogramme of $Fe_{82}Si_2B_{16}$ alloy after crystallization.

The method of study of magnetic properties that is described above could be used in the investigation of diffusion layers, coatings of different nature; zones are obtained by laser treatment etc.

## References

[1] Belous M.V., Hryhoryeva O.V., Lakhnik A.M., Moskalenko Yu.N., Sidorenko S.I., “Thermomagnetic analysis of amorphous alloys Fe-B”, Met. Phys. Adv. Tech., Vol. 23(12), (2001) p.1639-1650.

[2] Luborsky F.E., et al. “ Magnetic properties of metals and alloys”, Eds. Kahn, R.U. and Haasen, P., Metallurgy, Moscow, Vol. 3(29), (1987) p. 624.

[3] Belous M.V., Cherepin V.T., Vasiliev M.A., “Transformations during the tempering of the steels”, Metallurgy, Moscow, (1973) p. 232.

[4] Zolotukhin I.V., ”Physical properties of amorphous metallic alloys”, Metallurgy, Moscow, (1986) p. 176.

# ELECTRIC PROPERTIES OF NANOCOMPOSITE MATERIALS GRAPHITE-COBALT

**Matzui L., Vovchenko L., Stelmakh O., Kapitanchuk L.**
Shevchenko Kyiv National University
Volodymyrska Str., 64, Kyiv, 01033, Ukraine, matzui@univ.kiev.ua

The electric and magneto-resistance of graphite-Co composites have been investigated in the temperature range 77—300K and magnetic fields 1500kA/m by four-probe method. Graphite-Co powders were obtained by Co reduction in $CoCl_2$ compound by $C_8K$ intercalation compound:

$$C+K \rightarrow C_8K \qquad (1)$$
$$C_8K+CoCl_2 \rightarrow C\text{-}Co+KCl$$

$C_8K$ compounds have been prepared on the basis of various types of graphite: natural disperse graphite (Gr) (size of flakes is 50μm) and thermoexfoliated graphite (TEG) [1].

Phase composition, stage of intercalation compound, the character of Co particles distribution on the graphite particles surface have been analyzed using the X-ray diffraction, electron scanning microscopy and Auger-spectroscopy.

The investigations were performed on the DRON-4-07 X-ray diffractometer (filtered $CoK_\alpha$ irradiation), LAS-2000 Auger spectrometer ("Riber", France), JSM-840 electron microscope (JEOL, Japan).

The X-ray studies of obtained Gr-Co composites have shown that they are the compounds of the third stage with the identity period of intercalant layers $I_c$=13,7Å. The distance between graphite layers that contain the layer of intercalant $d_i$ had been found equal to 6,9Å. We suppose that the intercalant layer consist predominantly of Co atoms. A few amount of K atoms also can be present in intercalant layer. According to the investigations of others authors [2, 3] in such composite materials when the metal insertion was performed via intercalation of graphite metal particles are situated both on the surface and in the bulk of graphite support.

The samples of compacted CM graphite-Co for measuring of electric and magneto-resistance were prepared in press moulds by using hydraulic press: the density of compacted TEG—Co was 1,94g/cm$^3$, while the density of compacted Gr—Co with polyvinylacetate (PVA) as binder was 1,3g/cm$^3$ . The content of PVA in Gr—Co composite was 15—20wt.%.

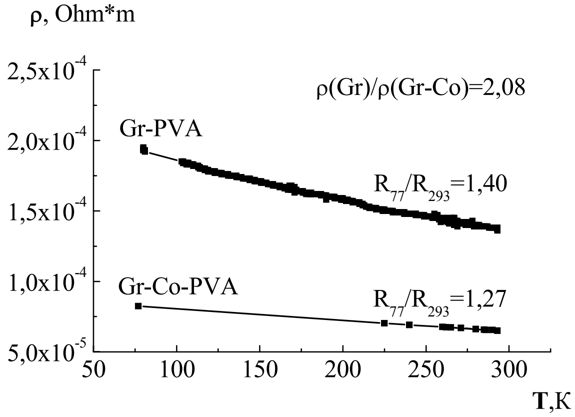

Figs. 1, 2 present the dependence of electrical resistivity of composite materials TEG—Co, Gr—Co on temperature T.

Fig. 1. Temperature dependence of electrical resistivity for pure Gr and Gr—Co.

As it is seen from figures the electrical resistivity of compacted Gr—Co and TEG—Co samples decreases under Co insertion approximately on 2 times in comparison with pure Gr and TEG.

The electric resistance of TEG-Co and Gr-Co decreases under heating from 77 to 300K. Ratio $R_{77}/R_{300}$ for compacted TEG—Co samples is equal to 1,3 that is smaller in comparison with pure compacted TEG ($R_{77}/R_{300}$=1,60). In the case of Gr-Co sample the ratio $R_{77}/R_{300}$ also decreases from 1,4 (for pure Gr-PVA) to 1,27 (for Gr—Co—PVA).

The decrease of electrical resistivity ρ of Gr and TEG under adding of Co via graphite K intercalation and subsequent reduction of Co in $CoCl_2$ may be explained by intercalation of graphite with Co and increase of charge carriers total concentrations n:

$$\rho \sim \frac{1}{en\mu} \qquad (2)$$

where μ - the charge carrier mobility.

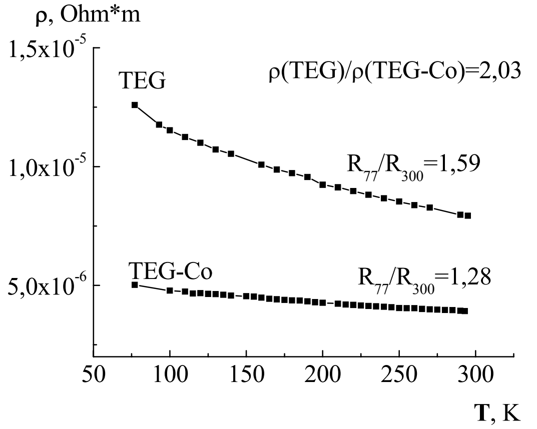

Fig. 2. Temperature dependence of electrical resistivity for pure TEG and TEG—Co.

Insertion of Co in TEG or Gr via intercalation leads to decrease of magneto-resistance in TEG—Co, Gr—Co and changes its temperature dependence. Fig. 3 presents the dependence of magneto-resistance on magnetic fields for initial graphites Gr and TEG and Gr—Co, TEG—Co.

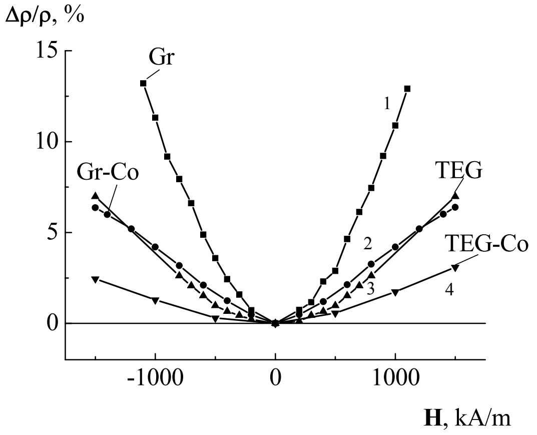

Fig. 3. The dependence of magnetoresistance on magnetic field for pure Gr, TEG and CM Gr—Co, TEG—Co.

The decrease of magneto-resistance of Gr—Co and TEG—Co in comparison with pure Gr and TEG may be satisfactory explained by decrease of charge carrier mobility under charge carrier concentration increase. For classic case the dependence of magneto-resistance for pure graphite on carrier mobility $\mu$ and magnetic field H may be described by following expression:

$$\frac{\Delta\rho}{\rho} \sim \mu^2 H^2$$

(3)

It was found that $\Delta\rho/\rho$ does not obey to $H^2$ (for both TEG—Co and Gr—Co $\Delta\rho/\rho \sim H^{1,6}$). This fact may me explained by the influence of magnetic particles Co on the transport of charge carriers under action of electric and magnetic fields.

References

[1]. E.Kharkov, V.Lysov, L.Matsui, L.Vovchenko, M.Tsurule, N.Morozovskaya. Patent of Ukraine N 33777A, 15.02.2001, bul.1.

[2]. A. Furstner, F. Hofer, H. Weidmann. Carbon, 1991, 29, No. 7, P.915—919.

[3]. A. Mastalir, Z. Kiraly, I. Dekany. Colloids and Surfaces. A: Physico-chemical and Engineering Aspects, 1998, 141, P.397—403.

# ANISOTROPY OF ELASTIC PROPERTIES OF COMPACTED SAMPLES BASED ON THERMOEXFOLIATED GRAPHITE

**Vovchenko L., Zhuravkov A., Samchuk A., Matzui V.**
Shevchenko Kyiv National University
Volodymyrska Str., 64, Kyiv, 01033, Ukraine, vovch@univ.kiev.ua

The anisotropy of elastic properties of compacted composite materials (CM) based on thermoexfoliated graphite (TEG) [1] and TEG-Ni (Co) have been investigated. The samples have been compressed along *a*- and c-axis (*a*-axis is perpendicular to pressing *c*-axis under sample's compacting). It was shown that elastic characteristics of CM based on TEG at compression along *a*-axis essentially differ from elastic characteristics under *c*-axis compression.

Fig. 1 presents the dependence of loading on deformations $\sigma=f(\varepsilon)$ for pure compacted TEG at compression along *a*-axis. As it is seen from figure for the all cycles of increasing loading $\sigma_i \rightarrow \sigma_{i+1}$ *(where i=1, 2, 3...;* $\sigma_1$=20MPa, $\sigma_2=\sigma_1$+15MPa etc.) the irreversible deformations occur in the sample. These deformations are the plastic deformations that leads to increase of the sample's density.

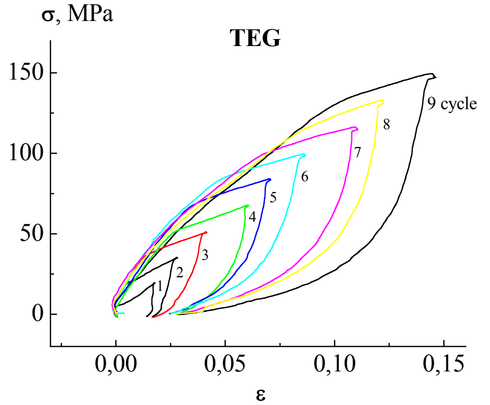

Fig.1. Diagrams «relative deformation-loading» for compacted TEG at compression along *a*-axis (d=1,89 g/cm$^3$).

It must be noted that the samples carry the large loading along *a*-axis (up to 150MPa). At the compression of the samples along *c*-axis the destruction was observed at 40—50MPa [2].

The effective Yung module along *a*-axis $E_{eff}$ for compacted TEG is equal to ~1,5GPa that is in 3 times higher than $E_{eff}$ along *c*-axis [2, 3].

This difference in $E_{eff}$ for two directions (*c*-axis and *a*-axis) is clearly illustrated by Fig.2.

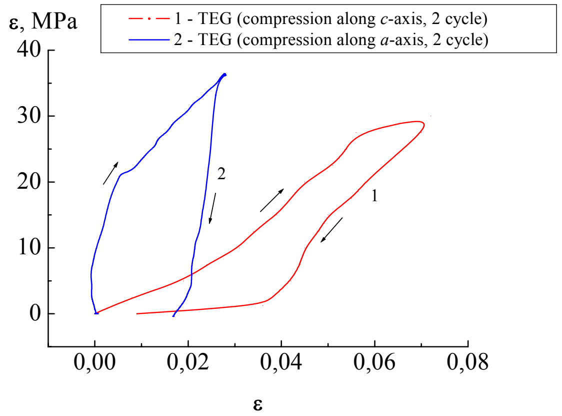

Fig. 2. Diagrams «relative deformation-loading» for compacted TEG at compression along *c*-axis (curve 1) and *a*-axis (curve 2) (d=1,89 g/cm$^3$).

For the all cycles "loading-unloading" along *a*-axis the large plastic and elastic deformations are observed. Plastic deformations occur due to stripping and slipping of graphite "macroplans". Under threshold loading we observed the destruction of the sample due to macrocracks arising during stripping of graphite macroplans and their destruction.

In the case of compression of CM based on TEG along pressing axis (*c*-axis) the sample's destruction occurs due to increase of intrinsic pressure in closed pores under external loading and increasing of temperature [3].

The fixing of metal on TEG particles leads to decrease of elastic and strength characteristics along *a*-axis. The largest plastic deformations of TEG-Co, TEG-Ni were observed under the first "loading-unloading" cycle. The dependence $\sigma=f(\varepsilon)$ for TEG-Co, TEG-Ni significantly differs from such dependence for pure TEG: the concaves on $\sigma = f(\varepsilon)$ dependence for TEG-Co, TEG-Ni samples at the first cycles "loading-unloading" may be explained by fact, that partial sample's destruction and their pressing occurs. Fig.3 presents the diagrams for pure TEG and TEG-Co, TEG-Ni.

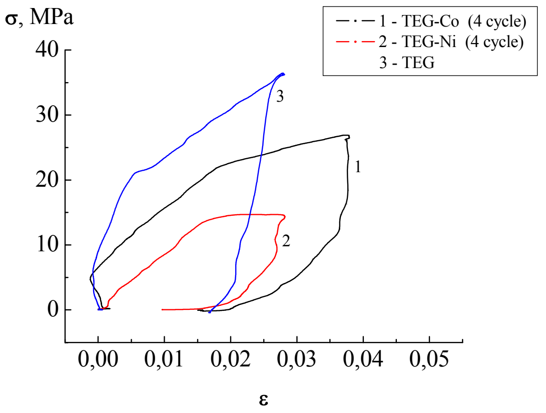

Fig. 3. Diagrams «relative deformation-loading» for compacted TEG-Co (curve 1), ТРГ-Ni (curve 2) and TEG (curve 3) at compression along *a*-axis.

It was found that compacted TEG-Co and TEG-Ni samples are characterized by approximately equal values of strength (50—60 MPa) at compression along a-axis in comparison with strength at compression along pressing axis *c*. $E_{eff}$ for the samples TEG-Co, TEG-Ni is equal to 0,8GPa.

The investigations of electrical resistivity $\rho$ of compacted TEG under compression along *a*-axis have shown that $\rho$ increases proportionally to value of loading. For the example, the increase of electrical resistivity was about 25% at mechanical loading ~15MPa for compacted TEG. The irreversible change in the value of $\rho$ is caused by plastic deformations and arising of microcracks in the samples.

Thus, the elastic characteristics of CM based on TEG at compression along *a*-axis (perpendicular to pressing axis) differ significantly from elastic characteristics under compression along pressing axis *c*. The effective Yung module along *a*-axis $E_{eff}$ for compacted TEG increases in 3 times in comparison with $E_{eff}$ along *c*-axis.

Deposition of nickel or cobalt on TEG particles leads to decrease of elastic and strength characteristics of compacted CM based on TEG under compression along a-axis: effective Yung module decreases in 2 times; the strength of CM TEG-Ni, TEG-Co under compression does not depend on direction of external loading action.

## REFERENCES

[1] E.Kharkov, V.Lysov, L.Matsui, L.Vovchenko, M.Tsurule, N.Morozovskaya. Patent of Ukraine N 33777A, 15.02.2001, bul.1.

[2] L. Matzui, A. Zhuravkov, E. Kharkov. Abstract of ISIC11, Moscow, Russia, (2001) 114.

[3] L.Yu. Matzui, L.L.Vovchenko, A.V.Zhuravkov. Metalofiz. I novejsh. teknologij, 2001, V. 23, №12, P.1677-1686 [in Russian].

# STRUCTURE AND THERMOMAGNETIC BEHAVIOR OF TEG-Co NANOCOMPOSITE MATERIALS SYNTHESIZED BY CHEMICAL DEPOSITION TECHNIQUE

**Babich M.G., Len' T.A., Matzui L.Yu., Semen'ko M.P., Zakharenko M.I.**
Shevchenko Kiev National University
64, Volodymyrska st., Kiev, 01033, Ukraine, zakharenko@univ.kiev.ua

In recent years nanostructured materials have attracted an increasingly interest due to the possibilities of their industrial applications in the integrated and magnetoelectronic devices such as sensors, spin valves, high-density magnetic recording media [1, 2] as well as in development of highly effective catalysts [3]. An important feature of such systems as "carbon – nanostructured Co", which have been intensively studied recently [1, 4], is the increasing of the effective distance of neighboring magnetic particles. Besides, in a case of formation of the carbon-encapsulated structures the protection against surface oxidation of metallic grains increases that is an important factor from the application point of view. The latter is conditioned by the fact that even the lowest amounts of oxides could make a dramatic influence on operational properties of nanostructured composite materials. The natural solubility of C in Co is extremely low and metastable cobalt carbides decompose even at low-temperature annealing. So, Co-C system is a good candidate to produce composite materials (CMs). Such materials have already been prepared using a set of different methods. But the common problem for all cases is the necessity to provide sufficiently high parameters of the material's stability, especially, under the action of different external actions.

In this work we report the regularities of thermomagnetic behavior of Co— CMs prepared through the chemical deposition of Co on the surface of thermoexfoliated graphite (TEG) depending on the type of utilized Co salt and conditions of their synthesis.

The CMs of Co— system were prepared by chemical deposition of cobalt on the surface of TEG [5] through salt thermolysis and Co reduction. The surface of TEG has been preliminary treated by the oxidant to form the active centers fixing the particles of modifier The deposition of modifier has been performed using either Co acetate or Co nitrate. The specimens have been prepared in three differing procedures:

1. thermal shock at 800 °C for 12 s and subsequent reduction of oxides at 350 °C in a hydrogen flow;
2. heat-treatment at 350 °C in a hydrogen flow;
3. thermal shock in vacuum.

In a result cobalt modifier particles were deposited on the surface of TEG through several successive chemical reactions The powders of modified TEG produced by this method had the density ranging from 0,03g/cm$^3$ to 0,07g/cm$^3$ that considerably exceeds the density of initial TEG.

The phase composition of the prepared composites was determined by the X-ray phase analysis (DRON-4 diffractometer, filtered CoK$_\alpha$-radiation). Scanning electron microscopy (JSM-840 microscope) was used to study morphology, shape and distribution of Co particles on the TEG surface. The microprobe X-ray spectroscopy method was used to determine the element composition of the obtained CMs.

The X-ray diffraction patterns for all the synthesized CMs contain only the relatively weak peaks of graphite, the width of these peaks was found to be as higher as more non-equilibrium are the conditions of CNs synthesis. No Co or Co-containing phases were detected regardless of the fact that sufficiently high content of Co was expected for all specimens. This could be considered as an evidence for nanocrystalline state of the Co modifier. Co modifier particles are distinctly observed and almost uniformly distributed on TEG surface according to the SEM data for the CMs prepared through heat-treatment at 350 °C in a hydrogen flow using both Co acetate and Co nitrate. Besides, a tendency to the particles' segregation was observed for CMs synthesized from the nitrate salt. In a case of CMs synthesized using thermal shock Co particles were found to be almost unobservable that is caused, to our mind, by the higher dispersity of modifier. Moreover, it has been turned out that Co content in CMs being synthesized through the thermolysis on the nitrate salt is almost independent on the synthesis conditions. At the same time, Co content in a case of CMs synthesized cobalt acetate being used through thermal shock was found to be some lower as compare to prepared through the heat-treatment at 350 °C in a hydrogen flow.

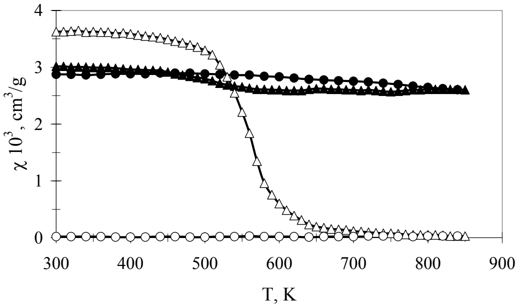

Fig. 1. $\chi$(T) dependences for TEG—Co CMs prepared from nitrate through procedure 1 (open markers) and 2 (filled markers): triangles – heating, circles – cooling.

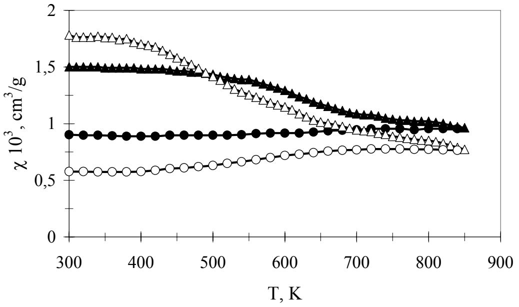

Fig. 2. $\chi$(T) dependences for TEG-Co CMs prepared from acetate through procedure 1 (open markers) and 2 (filled markers): triangles – heating, circles – cooling.

The pointed differences in the size and morphology of modifier particles, their concentration and distribution character on TEG surface in different CMs are clearly displayed in the peculiarities of thermomagnetic behaviour. Figs. 1, 2 present the temperature dependences of magnetic susceptibility $\chi$(T) for some of the synthesized CMs. These dependences in the temperature range 300—900 K have been obtained by the Faraday technique using automated magnetometer.

It is necessary to note that CMs synthesized through technology 1 are characterized by higher susceptibility value independently on salt type. However, more pronounced degradation of $\chi$ (down to total disappearance of ferromagnetism in a case of nitrate CMs) is observed during heating as compare to the specimens synthesized through technology 2. The stated regularities in $\chi$ behavior, as it is follows from the performed analysis, are conditioned by the process of metal particles interaction with the oxygen containing in the composites. The modeling of this process showed the character of the susceptibility reducing within the experimental temperature range to be determined predominantly by the size distribution of metal particles. Furthermore, the state of the surface of modifier particles, or in more exact terms, the state of oxide layer being formed on their surface upon synthesis is an important factor with respect to the stability of the developed composite materials.

It was also found that the character of susceptibility changing essentially depends on the type of the salt-precursor. CMs synthesized according to the technology 1 using Co acetate was found to possess higher resistance to oxidation as compare to those synthesized using Co nitrate. Presumably, such behavior could be related with the influence of products of salt thermolysis and its kinetics.

The influence of thermal cycling and isochronal annealing on the magnitude of magnetic susceptibility of the synthesized materials are also under consideration.

This work is supported by the Science and Technology Center in Ukraine (STCU) through Grant no. 1618.

1. Yu M., Liu Y., Sellmyer D.J., J. Appl. Phys., **85** (1999) 4319.
2. McHenry M.E., Majetich S.A., Artman J.O., et al., Phys. Rev. **B49** (1994) 11358.
3. Ischenko E., Gayday S., Babich N., et al., Abstr. CARBON-2003, Oviedo, Spain, p.189.
4. Tomita S., Fuji M., Hayashi S., et al., J. Appl. Phys, **88** (2000) 5452.
5. Babich M.G., Matzui L.Yu., Nakonechna O.I., et al., Mater.Sci.Forum, **373—376** (2001), p.241.

# INFLUENCE OF IRRADIATION ON ELECTRICAL RESISTIVITY OF COMPOSITE MATERIAL THERMAL EXPANDED GRAPHITE - FLUOROPLASTIC

**Kopan V. S., Revo S. L., Karaman D. Yu., Ivanenko Ye. A., Sementssov Yu. I.**(1)
Shevchenko Kiev National University
Academic Glushkov ave. 2, build. 1, Kiev, 03022, Ukraine, revo@univ.kiev.ua.
(1)Institute of Surface Chemistry of NASU
General Naumov str., Kiev, 03164, Ukraine

The electrical resistance of materials depends from series of factors, the most important of which are phase and structural state, impurity contents, stress, etc. For practical purposes and for stable working of electronic equipment in different irradiation conditions particularly it is important so that electrophysical parameters of the equipment node materials do not changes under irradiation influence. So, it is necessary that devices, which consist function materials, survive during working in several radioactive contamination conditions and possible change of structure state exposed irradiation materials accordingly. It is concerning of stability working of resistors particularly.

The electrical resistance of metallic materials can changes on 2÷20 % under γ-quanta, electrons, neutrons irradiation, depend from the radiation dose is known [1]. Carbonic composite materials change their parameters less after equal radiation dose influence. Small unit weight, better stability in corrosive mediums and smaller than analogs prime cost are distinctive features of carbonic materials furthermore.

The purpose of the work was research of kinetics of electrical resistance changing of resistors from composite material (CM) on the base of different matrix of fluoroplastic (FP) with thermal expanded graphite (TEG) stuff (TEG—FP).

It is possible to control the electrical resistance *(R)* parameters of both modified TEG and CM on the base of polymer matrix with conductivity TEG stuff in a wide range as previous researches shown [2, 3].

Under changing of the pure or modified by Ni, NiFe blend, Co, Fe TEG density only is possible to get resistors with adjusted specific resistance in range from $10^{-5}$ Ω*m till $10^{-4}$ Ω*m particularly.

To change electrical resistance of CM of percolation system TEG-FP specimens for several orders is possible. For the system [2] the depending $\rho(\theta)$ has threshold view under TEG concentration $\theta > 7$ vol. %. Under increase of critical concentration $\theta_C$ electrical resistance of the CM decrease sharply from $\rho=10$ till $\rho=10^{-5}$ Ω*m. In case, when stuff concentration rather below than $\theta_C$ the electrical resistance of the CM define by supports of charge tunneling from one electrical conductivity particle to an another through dielectric gap between them. Possibility of the tunneling realization define by work function value of an electron from a TEG particle in gaps mainly. It does not depend practically from radiation dose in one's turn. And so, consequently, value of $\rho$ of the CM does not depend from radiation dose in contrast to pure TEG.

The CM specimens were made from fluoroplastic 3-V matrix and stuff from TEG with bulk density 1.8÷2 kg/m$^3$ and vermiform particles length 1÷4) mm. Irradiation of the specimens with $\theta=5\div20$ vol. % was made by electron bunch in the EMV-100AK microscope, as well as in X-Ray diffractometer DRON-4. The electrical resistance was measured after a regular dose radiation receiving by the specimens directly. It used the specimens with size 3*1*0,001 mm$^3$.

There are dependents value of the relative electrical resistance from radiation dose *D* which was define by current strength value (150 μA), accelerating voltage value and time of exposure for different concentrations of the stuff on figures 1, 2. The value $\frac{\Delta R}{R} = \frac{R - R_0}{R_0}$ describes on the ordinate axes. Here $R_0$ – starting (till the irradiation) electrical resistance value, *R* - electrical resistance value after irradiation with radiation dose *D*. The volume concentration of TEG denotes by digits.

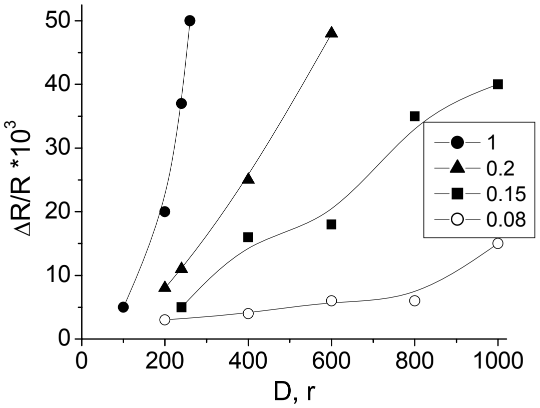

**Fig. 1.** The dependents of relative electrical resistance value *ΔR/R* from radiation dose by electrons *D* for the CM TEG—FP for different TEG concentrations.

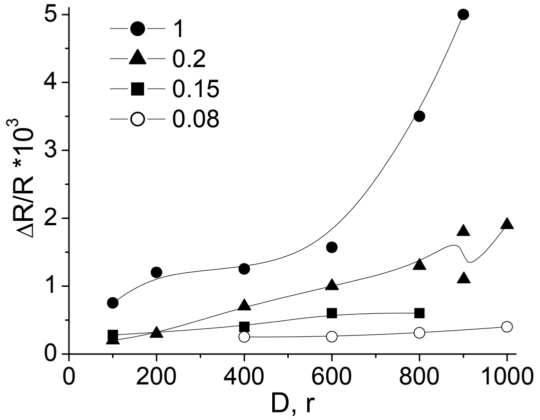

**Fig. 1.** The dependents of the relative electrical resistance value *ΔR/R* from radiation dose by X-Ray quanta (anode – Fe, accelerating voltage – 40 kV) for CM TEG – FP for different TEG concentrations.

From analyses of the figures it may be concluded next points:

1. The rate of electrical resistance value changing $v_\rho = (\frac{\Delta R}{R\Delta D})$ for TEG under irradiation by electrons exceed $v_\rho$ for the CMs for one order. It confirm the model approximations to the effect that electrical resistance of the CM TEG – FP under $\theta \le \theta_C$ controlled by gaps between particles of the electrical resistance stuff.

2. Under irradiation by X-Ray γ-quanta $\frac{\Delta R}{R}$ smaller for one order than under irradiation by electrons. It conditioned by small X-Ray irradiation absorbtance comparably electrons. So, the TEG - FP system decrease on 50% (absorb) X-Ray irradiation under a targer thickness 10 mm, and electron rays under the thickness 1 μm.

3. $v_\rho$ increases under increasing of TEG concentration $\theta > \theta_C$ because the gap between particles role decreases in the electrical resistance formation.

4. To made stabile to irradiation resistors from percolation CMs from dielectric and electrical conductivity components is advisably. To select the concentration of the components from correlation $\theta \le \theta_C$. is necessary.

## References.

1. H. G. Van Buren. Defects in Crystals. Moscow: 1962. 584 p. (Russian).
2. S. L. Revo, D. Yu. Karaman, I. P. Shevchenko, K. O. Ivanenko, Yu. I. Sementsov. Electrical resistance and thermo-e.m.f. of the composite material thermal expended graphite – phluoroplastic. Scientific noutes of NPU of Dragomanov. – Kiev, NPU, 2002, N3. P 169—174. (Ukrainian).
3. L. Yu. Matsuy, L. Yu. Ovsienko, S. L. Revo, K. O. Ivanenko, G. P. Grinevich. Researche of the electrical resistance of thermal expanded fraphite modefied by Ni, NiFe, Co and Fe. Scientific noutes of NPU of Dragomanov. – Kiev, NPU, 2001, N2. P 89—94. (Ukrainian).

# INFLUENCE OF ANNEALING ON STRUCTURE AND COMPLEX OF MECHANICAL CHARACTERISTICS RIBBON SAMPLES OF METALLIC GLASSES 82К3ХСР

**Feodorov V.A., Permyakova I.J., Ushakov I.V.**
Department of general physics, Derzhavin Tambov State University
Internatsionalnaya Str. 33, Tambov, 392622, Russia, E-mail: feodorov@tsu.tmb.ru

## INTRODUCTION

The metal glasses (MG) play the important role among perspective materials, having the complex of unique properties, on which level they exceed conventional metal materials in many respects.

The broad application MG till now is at loss for their rather low thermal stability. In this connection the purpose of the present work is: investigation influence of annealing on the mechanical characteristics MG (microhardness, Young's modulus, and plasticity), learning of features of their structural transformations at annealing, installation of composition and structure of selected phases during crystallization.

## EXPERIMENTAL TECHNIQUE

We studied an 82K3XCP (in Russian) metallic glass of the composition (wt %) 75,4%Co+3,5%Fe+3,3%Cr+17,8%Si in the form of a ribbon 30 μm thick. Prior to experiments, samples were annealed in a furnace $T_{an}$=373-823 K and held at a specified temperature for $t$=10 min.

Curves of expansion were obtained by the explosive machine of a string type. The rigidity of the test computer makes >$4\times10^7$ H/m.

Indentation of the contact party of ribbon annealed MG was carried out by microhardness gauge PMT-3.

In $U$-method we estimated the deformation of bend $\varepsilon_f$ at which take place brittle fracture of the MG: $\varepsilon_f = h/(D-h)$, where $h$ is the thickness of the sample, $d$ is the distance between two parallel plate of the specific designed measuring tool at the moment of fracture. Temperature of transition in the brittle state ($T_f$) was estimated as average temperature from $T_1$ and $T_2$, where $T_1$ - greatest temperature of an annealing, at which else $\varepsilon_f$ =1, $T_2$ - lowest fixed temperature of an annealing, at which was observed a sharp abatement of a plasticity ($\varepsilon_f$<<1)

The amorphism MG was controlled by X-ray diffraction analysis on a DRON-2 diffractometer. It was found by DSC (Rigaku-8230) temperature of crystallization of researched MG is ≈ 829 K.

## EXPERIMENTAL RESULTS AND DISCUSSION

The characteristics of mechanical characteristics MG depend on temperature, at which the test is carried out. Results of investigations of dependence $\sigma$ – $\varepsilon$, detected at expansion and simultaneous excitement of bend oscillations in samples are a bright illustration of such behaviour [1].

The analysis of curves stress - deformation was made at different temperatures of annealing (fig. 1). The application of tests of expansion with the purpose to install behaviour of a tensile yield point MG $\sigma_T$ from temperature of annealing was complicated. The strong embrittlement of samples occurs at reaching particular temperature and the material was brittlly destroyed, not having achieved a tensile yield point.

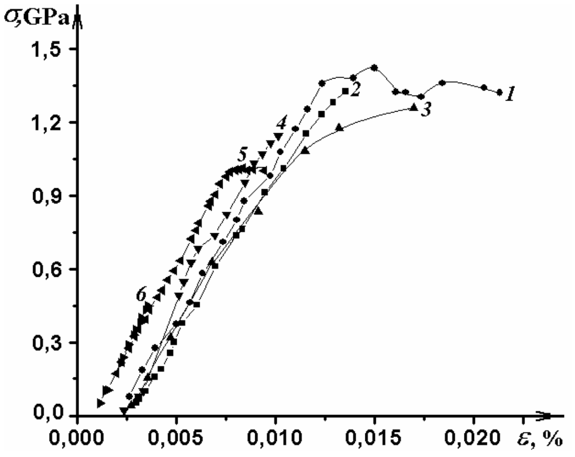

Fig. 1 Curves stress - deformation: *1* – without annealing, *2* – 373 K, *3* – 453 K, *4* – 543 K, *5* – 613 K, *6* – 723 K.

The calculation of angles of inclination of linear plots of a curve expansion $\sigma$ – $\varepsilon$ was carried out at each temperature of annealing for definition of Young's moduluses. Thus, it was possible to found the influence of thermal treatment on character of behaviour of the elastic characteristic *E*.

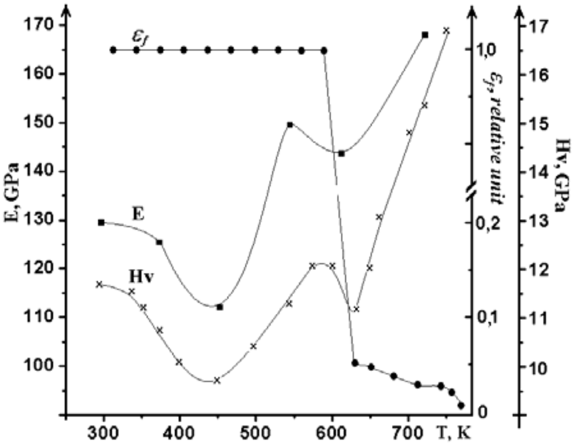

Fig. 2 Temperature dependence of a Young's modulus (*E*) of a microhardness (*Hv*) and plasticity ($\varepsilon_f$) annealed MG

The comparison of values changes of Young's modulus, microhardness and plasticity of MG from temperature was represented in a fig. 2. It was found by *U* - method, at $T_{an} \leq 593$ K the fracture of MG is not observed, down to a state $\varepsilon_f = 1$. It was happened thanks to the plastic deformation, which is displayed in the form of numerous glide bands. There is a derivation of arterial cracks at $T_{an} > 628$K, during bend and the samples are destroyed. Temperature of temper embrittlement ($T_f$) is ≈613 K.

Within of «relaxational» model of an phenomena, the transition in a friable state after temperature effect is higher $T_f$ was stipulated by growth micrononcontinuity (micropores) in an amorphous matrix owing to annihilation and reallocation of areas of superfluous free volume. Micropores (since critical size and depending on composition of alloy) are effective sources of quasi-friable crack, promoting catastrophic fracture at an affixed external loading.

Minimum plasticity conforms to temperature of an annealing $T_{an} \approx 829$ K and connects with transition of samples in a dispersible submicrocrystalline state. This value of temperature coincides with data of DSC, at which there is a crystallisation.

The legible correlation between a Young's modulus and microhardness (fig. 2) is observed. The first minimum *E* and *Hv* falls to area of temperatures near to a glass transition. The second minimum corresponds to area near to temperature of temper embrittlement of a material. The low-temperature annealing reduces *E*, *Hv* because the structural discontinuity calls appearance of local concentrators of stress. The thermal treatment at higher temperatures results in stabilization of structure and nonmonotone increase these investigated mechanical characteristics.

The morphology of surface layers and character of growth crystals from an amorphous phase is investigated. After an annealing at 688 K$<T<T_{crys}$ the amorphous state is saved under the data of a X-ray structural analysis. Nevertheless the dendritical crystallisation, not spreading in a depth of amorphous foils and also discharge of cubic crystals is observed on a surface.

The local reduction of temperature of crystallisation on a surface is called by origin of concentration gradients which was caused by electoral oxidation and segregation of alloying elements in surface layers of ribbon MG.

Annealing at $T_{an}$=533—653 K does not reduce to violation X-ray amorphism of MG. There is increase of width amorphous halo during the increase $T_{an}$ only. This growth corresponds to structural modifications, connected, apparently, with changes of a degree of regularity of the short-range order of MG. Annealing at $T_{an}$=688 K leads to derivation the first crystals in an amorphous matrix, determined as $\beta$-Co phase with face-centered cubic crystal lattice. Accompanying the increase of heat treatment temperature up to 723 K the growth of number of diffraction lines is marked on diffractogramms. Except for $\beta$-Co phase, crystalline phases $\alpha$-Co (hexagonal close packing crystal lattice) and combination CoSi and $Co_2Si$ was appeared. The intensity of X-ray lines of $\alpha$- and $\beta$-Co is even more increased, that indicates on the growth of a volumetric fate of these phases in MG at approximation of annealing temperature to temperature of crystallization ($T_{an}$=823 K). Crystallization of all size of a researched alloy takes play at $T_{an}$=823 K.

[1] Bobrov O.P., Laptev S.N., Khonik V.A. Relaxation of stresses in metallic glasses $Zr_{52,5}Ti_5Cu_{17,9}Ni_{14,6}Al_{10}$ // Herald of Tambov State University. Ser. Natural and technical science. 2003. V. 8. No. 4. P. 525—527.

This work was supported by the Grant of RBFR (project No. 01-01-00403).

# HEALING OF MICROCRACKS IN ALKALI–HALIDE CRYSTALS AT INFLUENCE OF ULTRA-VIOLET RADIATION

**Fedorov V.A., Plushnikova T.N., Tjalin Yu.I., Chivanov A.V., Chemerkina M.V.**
Derzhavin Tambov State University
International str., 33, Tambov, 392622, Russia, feodorov@tsu.tmb.ru

Characteristic feature for alkali–halide crystals is observably in them spontaneous healing noncontinuity, an event in top of cracks cleavage. This phenomenon was described by M.P. Shaskol'skoj in 1961 at first [1]. However, till now there are only individual attempts of its explanation, the mechanism of healing of cracks (restoration continuity) to pay attention of researchers [2] till now.

In work [3] possible mechanisms of spontaneous healing of cracks in alkali–halide are offered. It is shown, that heating and radiation of a seen range influences on development of microplastic shifts in top of a crack. Is established exponential character of dependences of change of density of dispositions at tops of cracks from temperature and time of an exposition of radiation.

The purpose of work: to define influence of electromagnetic radiation of a ultra-violet range on process of healing of the cracks, received at asymmetric cleavage, in alkali–halide crystals.

Researches carried out on optical transparent monocrystals LiF, NaCl, KCl with the quantitative content of impurity from $10^{-2}$ up to $10^{-3}$ weight. %. The size of samples 10x20x2 mm. Cleavage a crystal of a sample carried out asymmetrically, that it is extremely convenient for studying processes of spontaneous healing cracks, as at lateral cleavage narrower part of a crystal, practically always there is a stop and healing of top of the basic crack. A asymmetrical degree cleavage ≈ 0,65÷0,75 [3].

For irradiation of monocrystals applied mercury-quartz lamp PRK-2, from which spectrum of radiation them used a strip in area $\lambda$=250—300 нм (energy E~4,15—4,95 эВ). The temperature of samples during experiences was supervised by the thermocouple and remained constant T~293 K. Time of influence varied from 10 minutes to 3 hours.

During influence on crystals UV – radiations a kind of the healed site and dislocation picture, revealed by etching at top of a crack appreciablly varies. The effect is kept up to the certain value of influence time.

It is revealed, that in the beginning with increase of time of influence UV - radiations there is a reduction of scalar density of dispositions at tops of cracks, the length of the healed site is increased, and the length of dislocation beams sockets in top of a crack decreases.

It is marked, that at absence « dislocation sockets » and presence of a line of dislocation on continuation of a trajectory of a crack (the site of spontaneously healed crack at asymmetric cleavage [3]) also the additional healing a crack essentially time-dependent irradiations is observed.

The length of dislocation beams can be reduced for LiF on (5÷500) microns, for NaCl on (5÷700) microns, and can achieve 100% from initial length. The length of the healed site can achieve values for LiF at 10 to 90 microns, for NaCl at 20 to 650 microns.

Thus, at influence UV – radiation the restoration of continuity a crystal is taken place. On plastic crystals (NaCl) formation of more extended healed sites is observed.

Movement of dispositions in beams dislocation sockets is investigated. By a method of double etching it is revealed, that dispositions can move as to area of top of a crack, that conducts to reduction of length of beams in dislocations sockets, and to form the new strips of sliding. Movement of dispositions in a plane of a plane of spontaneously healed crack being continuation is revealed also.

The mechanism of cracks healing is represented by the following:

In the conditions, appropriate to experiment, movement of dispositions carries thermal–activationly character and is defined by frequency and energy of formation of pair excesses on dispositions [4]. At action of some tangential stress – $\tau$ in a plane of pattern disposition thermal–activationly movement by last will occur in a direction of action $\tau$. Thus the increase of number of formed pair excesses, in particular, and in a direction of action of tangents stresses will bring in increase of mobility of a disposition.

At irradiation alkali–halide quantums of electromagnetic radiation small energy ($h\nu < E_3$, where $E_3$-energy of the forbidden zone) in them arise, located on defects, electronic excitation and low-energy excitons, i.e. elementary excitation of a crystal as pair hole-electron [4]. When the exciton achieves nucleates on a disposition of the double excess representing in the beginning a pair of charged vacancies one of exciton components, for example, electron is grasped nucleate by vacant unit of a negative ion, that results in occurrence of the F-centre. Thus located beside the vacant unit of a positive ion makes a repulsion and diffuses as a vacancy, and alongside with nucleate the F-centre is formed new nucleate vacant unit of a negative ion. The F-centre grasps remaining hole and again becomes vacant unit. In the result there is an expansion of a double excess or movement dispositions jogs at which the disposition creeps in next Paerls valley takes place. Formation of congestions of vacancies at such mechanism of interaction exciton and the dislocation, offered Zeyts, observed at temperatures of liquid nitrogen [4].

At rooms temperatures they quickly resolve. Exciton ecombination on a disposition it is accompanied by allocation of the energy, observably as luminescence alkali–halide, and the formed F-centers result in colouring. Considered processes also are thermal–activationly and with rise the temperature of the irradiated crystal intensity of a luminescence and colouring decrease on exponential law. The exciton interaction, received at UV–irradiation, with nucleate pair excesses on a dislocation in a field of tangents stress $\tau$ should increase mobility of dislocations. It convertible movement of dispositions in area of top of the crack, resulting to healing and also reduction of integrated density of dislocations in a zone of top of a crack speaks due to tightening dislocations loops.

The dislocation congestion in beams dislocations the sockets formed in top of a crack, is in a field of own tangents stress, aspiring to move apart dislocations. Thus the part from them inevitably will fall down in top of a crack, reducing size of its plastic opening $\delta$. And, if $\delta$ will make size < 40 нм [3] restoration not only optical contact between surfaces of a crack, but also restoration continuousity i.e. curing is possible, stimulused UV – radiation.

Process of healing of cracks can be intensified, if simultaneously with UV–irradiation to raise temperature of a crystal [3].

Apparently, disintegration and formation of these defects it is possible to explain change of mobility of dispositions in alkali–halide, resulting on initial stages of irradiation to curing noncontinuousity such as cracks cleavage.

Process of disintegration of radiating defects is accompanied by a luminescence of crystals which spectral structure is close to structure of radiation UV source used in work.

Thus influence of electromagnetic radiation UV range, causing a relaxation of mechanical stresses in top of cracks due to convertible movement of dislocation, results in their partial healing.

The healing degree and relaxation of stresses depends on plastic properties of alkali–halide and time exposition.

*This work supported by the grant of RFBR (project 02-01-01173).*

## REFERENCES

1. Shaskol'skaja M.P., Van Yan-Ven, Gu Shu-Chao. About occurrence of dispositions at distribution and merge of cracks to ionic crystals // Crystallography, 1961. V. 6, N 4, p. 605—613.
2. Betehtin V.I., Petrov A.I., Kadomtzev A.G. Influence of hydrostatic pressure upon curing micropore and high-temperature creep // FMM, 1990. V. 5. p. 176—184.
3. Fedorov V.A., Plushnikova T.N., Tjalin Yu. I. Healing of the cracks stopped at asymmetrical cleavage in alkali-halide crystals and calcite // FTT, 2000. V. 42, N 4, p. 685—687.
4. Van Buren. Defects in crystals. M., 1962. 584 p

# ZYRCONOLITE MATRIXES FOR HIGH-LEVEL WASTE ($CAZRTI_2O_7$) IMMOBILISATION

**Shabalin B.G.**
Institute of Environmental geochemistry of NAS and MES of Ukraine,
$34^A$ Palladin Ave., Kyiv-142, Ukraine, E-mail: CENTER@radgeo.freenet.kiev.ua

In the last few years a new long-term strategy on high-level waste (HLW) underground disposal is under elaboration. The strategy is grounded on two new technologies, which can radically alter the general strategy of underground disposal [1]. The first of them is a fractionation technology for all kinds of liquid HLW. The second one is a synthesis technology for ultra-durable mineral-like matrix (immobilisators) aiming for the most dangerous long-lived radioisotopes to be embodied in its crystal lattice on the basis of isomorphic substantiation mechanism. Choice of optimum matrixes is of key factors in assurance of safe management with long-lived HLW of nuclear fuel cycle and yet it remains actual problem. Zyrconolite (ideal formulae $CaZrTi_2O_7$) [2] is one among the most perspective mineral matrixes for actinide and lanthanoide immobilisation. Matrixes based on zyrconolite have been received from mixture of mechanically activated oxides [3] at 1450 °C by cold pressing and sintering method (CPS) and by method of hot isostatical moulding of calcinated powders. These powders were produced from alkoxides at 1280 °C and 150 MPa [4]. By now the topicality of matrix production with minimum of material and energy costs still persists.

The results from study of synthesis optimum conditions and dynamics of phase formation are presented in thesis along with something of the features of zyrconolite matrixes produced from the mixture of coprecipitated hydroxocarbonates (method CPC). This method makes possible to produce polycrystalline samples with a high degree of homogeneity and more active when sintering for production of ceramic immobilising materials. The Sr, $Ce^{4+}$ и Th, which served as HLW elements-imitators were inserted into zyrconolite crystal lattice so that the experimental procedure on interaction of zyrconolite with cations existing in HLW could be carried out.

As initial salts for solutions to be prepared the nitrates of calcium and strontium, tetrachlorated titanium, zyrconile nitrates, cerium chloride and thorium nitrate were used. Water was put to use as a solvent for all salts. Solutions were analysed by complex of chemical methods. Ammonium carbonated buffer solution was chosen as a precipitating agent. The production of thorium-bearing material mixture has been performed in the presence of hydrogen peroxide. Precipitation was infiltrated (filtrate was checked by qualitative reactions for completeness of precipitation), eluted, dried up and subjected to thermal processing. Powder mixtures were pressed under 200—400 MPa with the purpose to form tablets 10—12 mm in diameter and 3 mm in height. These tablets were subjected to calcination in the open air at 900—1400 °C during 1—5 hours. The products are formed as homogeneous, clear isotropic grains 1—3 μk in size, with no certain habit during the process of mixture heat treatment. The grains are condensed to aggregates as big as 100—300 μk. The resulting ceramic tablets were of stabilised density and satisfactory appearance (chips, cracks, form curvatures are absent). Homogeneity and very fine porosity (1—3 μk) distributed uniformly throughout the section area are characteristic for the microstructure of section sintered tablets.

Study of zyrconolite synthesis conditions has demonstrated the fact of matrix material phase composition dependence from synthesis conditions and overall chemical composition of mixture. The formation of pure zyrconolite ($CaZrTi_2O_7$), as well as Sr, $Ce^{4+}$, Th-bearing zyrconolite is followed by crystallisation of intermediate oxide phases - perovskite, rutile and baddeleyite. Amount of zyrconolite phase is growing as the mixture thermal processing temperature increases up to 1400 °C, calcination duration (1200 °C, 4 hours), or in a case if there is a stoichiometric deficiency of divalent cations (Ca, Sr) and some excess of quadrivalent (Zr, Ti, Ce, Th) in the initial mixture content. It was determined that exceeding of Sr zyrconolite content more than 1.2 weight % (by SrO) within the mixture composition can lead to zyrconolite crystallisation accompanied by Sr-enriched perovskite, which quantity is growing with Sr content increased. Study of $Ce^{4+}$ и $Th^{4+}$ -

bearing zyrconolite affirmed isomorphic $Ce^{4+}$-entering predominatingly Zr positions, and $Th^{4+}$-entering predominatingly Ca positions. Radioactive γ-rays irradiation of ceramic samples by brake radiation on the linear electron accelerator till $2,3 \cdot 10^7$ Gy doesn't lead to essential volume change of samples; their density and colour do not vary, they hold the integrity, cracks are absent. Radiographs of initial and γ-rays irradiated samples do not vary practically. That is to say, the processes of radiation amorphisation within the ceramic materials under such radiation loads were not observed. This fact is verified by analysis of structural changes of natural zyrconolites of different ages with various Th and U content. According to the analysis zyrconolite crystalline state is held at total exposure till $2\cdot 10^{16}$ α-decay/mg, adequate $10^6$ years of age [5]. Leaching rate of elements from synthetic zyrconolite produced by CPC method at 90 °C is close to rate for samples produced by CPS and forms ($g/cm^2 \cdot day$): Ca ($10^{-3}$), Ti ($10^{-6}$), and Zr ($10^{-7}$). It is found that the rate of element transport to solution is reduced quickly with increased leaching time. This fact testifies of secondary phases' protective layer formation on the sample surface.

1. Gabaraev B.A., Ganev I.Kh., Lopatkin A.V. et. al. Irradiated fuel of РБМК-1000 and ВВЭР-1000 management under development of nuclear energetic // Atomic energy, 2001, v. 90, issue 2, p. 121-132 (in Russian).
2. Sombret G.S. Waste forms for conditioning high level radioactive solutions // Geol. Disp. High Level Rad. Wastes. Athens: Teoph. Publ., 1987. P. 69-160.
3. Vance E.R., Begg B.D., Day R.A., Ball C.J. Zirconolite-rich ceramics for actinide wastes. Scientific basis for nuclear waste // Management XIX. Materials Research Society Symposium Proceedings. November 27-December 1, 1995. Boston, Massachusetts. U.S.A. Pittsburgh, 1995, v. 353, p.767—774.
4. Ringwood A.E. Disposal of high-level nuclear wastes: a geological perspective // Mineralogical magazine, 1985, v. 49, p. 159—176.
5. Lumpkin G.R., Smith K.L., Blackford M.G. et al. The Crystalline-Amorphous Transformation in Natural Zirconolite: Evidence for Long-Term Annealing. MRS'97, Switzerland, p. 56—57.

# EFFECT OF MECHANICAL DEFORMATION ON HYDROGEN TRANSPORT IN AL

**Lunarska E., Ryumshyna T.A.$^{(1)}$, Chernyayeva O.**
Institute of Physical Chemistry of Polish Academy of Sciences
Kasprzaka 44/52, 01-224 Warsaw, Polande, e-mail: ellina@ichf.edu.pl
$^{(1)}$Physical and Technical Institute of NASU
Luxemburg 72, Donetsk, 83114, Ukraine, e-mail: Tatjana@konstant.fti.ac.donetsk.ua

The improvement of detail utilization under deformation in corrosive medium is an important problem of the material science. The hydrogen permeation is one of responsible factors for failure of material functioned in salt, acid, alkalis and others solutions. Aluminium and Al-alloys production have a large application in the aircraft construction, shipbuilding, and chemical industry because of a favourable union of properties (low specific gravity, high strength and plasticity, high heat and electric conductivity). Hydrogen doesn't interact chemically with Al, but one is dissolved well. An oxide film formed in the corrosive environment protects the AL from hydrogen permeation, but an appearance of electric fields and charges tends to distract the protection. Although hydrogen transport in Al affects susceptibility to hydrogen embitterment and stress corrosion cracking, the data concerning hydrogen diffusivity in Al established in electrochemical measurements of hydrogen permeation tests [1] are quite scarce and scattered.

A mechanical deformation of materials under hydrogen permeation has two main aspects. First, there are stress and strain fields caused by an external deformation. These fields are changed in the presence of hydrogen saturation. Second, there are the hydrogen induced stress and strain fields ("concentration" fields) [2], which are changed at a mechanical deformation of materials. Concentration strains and stresses have self-influence on hydrogen flux and create unusual phenomena. So, the transition minimum of hydrogen permeation has been observed at measurement of hydrogen pressure within the Pd tubes at increase in hydrogen pressure outside the tube [3], which has been associated with the effect of metal straining on hydrogen transport (Lewis effect - self induced "uphill" diffusion).

Hydrogen permeation tests were done in the present work for Al membranes using electrochemical Devanathan-Stachurski method [1]. Specimens were cut from 25μm, to 1mm thick, 99.99 Al foils. 0.01N NaOH was used as the base test solution.

Hydrogen permeation tests [4] were done using the specially modified double cell enabled the Pd coating of the egress side of a membrane (Figure 1). Special attention have been paid at the membrane preparation and mounting to avoid the formation of oxide and hydroxide films on Al surface. At application of polarization ($J_c$), to the ingress side, the build up hydrogen permeation transients $J_0$ were recorded in the egress cell until the steady state value ($J_\infty$) was reached. At cessation of polarization of the ingress side, the decay permeation transients were recorded.

In the course of the measurements, the unusual permeation transients J(t) were observed, revealing the transition decrease $J_m$, in hydrogen permeation current in the egress cell at application of cathodic polarization at the ingress side of a membrane (figure 2). The effects of membrane thickness, scheme of application and cessation of cathodic polarization of the ingress surface were checked for the extreme parameters ($J_{m,}$, $t_m$).

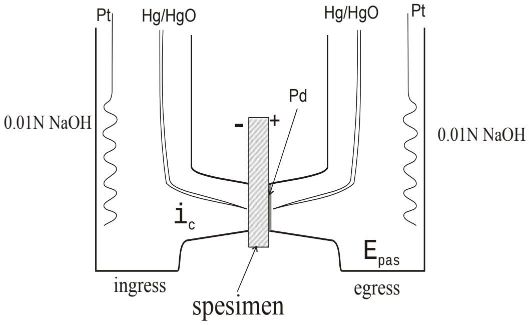

Figure 1
Scheme of the modified double cell for hydrogen permeation measurements.

Anode current extremes were caused by counter "self-induced" hydrogen flux, stipulated by the hydrogen redistribution in the heterogeneous deformed plate.

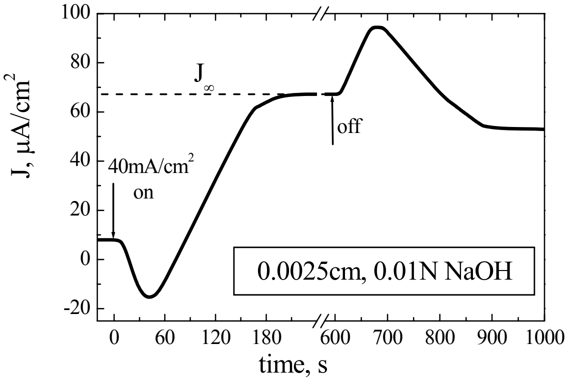

Figure 2
Change of the hydrogen permeation current as recorded in the egress cell after application and cessation of the cathodic polarization in the ingress cell.

At the cathode polarizations the hydrogen concentration increases hardly on input surfaces a membrane. Because of a concentration expansion the ingress side is mechanically deformed and the dissolved hydrogen atoms moved to the expanded region producing a counter hydrogen flux (Gorsky effect). The inward hydrogen flux causing by gradient of hydrogen concentration summarized with the outward hydrogen flux causing by gradient of hydrogen induced strain produced the minimum of hydrogen permeation [3, 5].

The mechanical deforming of material under a hydrogen absorption also influents on diffusion. It is possible to describe the influence of stress state in a material on the diffusion by inserting the amendment into the diffusion coefficient. One takes into account the geometry of external forces [6]. So, at the compression of material diffusion is slowed, but at the sprain - increases. The diffusion process depends on the mutual location of the deformation direction to a concentration gradient. At complex tense conditions (for instance, at two - axes strain of plates) with shear stress component, additional hydrogen fluxes appear in the plate.

If the plate is deformed and at the same time the permeation conditions are changed (for example, at application of a cathodic polarization) then the decreasing of deforming stress is observed and an additional deformation appears in the elastic stage of deforming (fig. 3). The cessation of hydrogen entrance practically returns the deforming stress to the level, corresponding to deforming in usual conditions.

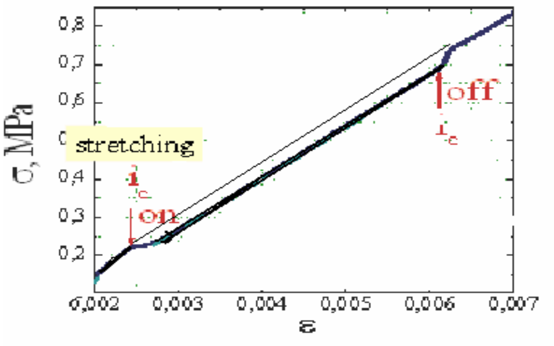

Figure 3.
Change of the deforming stress at after application and cessation of the cathodic polarization $i_c$=40mA/cm$^2$ .

Thereby, the joint action of an external and hydrogen induced "concentration" internal stresses leads to an appearance of new effects in the material, which change behaviour of material. The concrete nature of these changes (strengthening or weakening) depends on the type mechanical loading, gradients of hydrogen fluxes, their mutual influences and others.

1. V.M.A. Devanathan, Z. Stachurski, 'The Mechanism of Hydrogen Evolution on Iron in Acid Solutions by Determination of Permeation Rates', *J.Electrochem.Soc.,*1964, **111**, 619—623.
2. T.A.Ryumshina, S.P.Illyashenko. Study of stress and strain fields in an infinite plate at hydrogen. Int.J. Hydrogen Energy, 1999, **24**, N 9, 825—828.
3. F.A. Lewis, J.P. Magennis, S.G. McKee, P.J.M. Sebuwufu, 'Hydrogen chemical potentials and diffusion coefficients in hydrogen diffusion membranes', *Nature*, 1983, **306** (15), 673—675.
4. E.Lunarska, O.Chernyayeva, T.Ryumshyna. "Peculiarities of hydrogen transport in Al", Proc. of Second International Conference, "Environmental Degradation of Engineering Materials "EDEM 2003", Bordeaux, France, 29.06—02.07.2003, CD #PL1-1.
5. E.Lunarska, T.A.Ruymshyna, O.Chernyayeva. Influence of concentration deformation on the hydrogen transport in Al. *Izvestiya RAN*, *Physics*, **67,** N 10, 1417—1420.
6. T.A.Ruymshyna. Peculiarities of hydrogen diffusion in stressed medium. *Fizika I technika vusokich davleniy* 1999, **9**, № 2, 87—91.

# INFLUENCE OF PHASE COMPOSITION ON DEFORMATION MECHANISMS IN Ti—5Al—5Mo—5V ALLOY

**Konsantinova T.E., Ryumshyna T.A., Volkova G.K.**
Physical and Technical Institute of NASU
Luxemburg 72, Donetsk, 83114, Ukraine e-mail: Tatjana@konstant.fti.ac.donetsk.ua

Titanium alloys are broadly used in industry and attracts the increasing interest. In recently the tendency to replace many aircraft steels and aluminum alloys on titanium alloys has appeared that stipulated more good combination of mechanical and high-temperature strength [1]. Possibilities of creation of greatly efficient structures not realized yet despite a number of studies, devoted to Ti and its alloys. Investigations in this direction are actively developed in present time, and corresponding problem has got a name "structured minimization" [2]. A nanosize structure and their influence upon properties of material have the particular interest.

In the present work:

- an influence of a structured state (phase composition) on deformation mechanisms in the titanium alloy (Ti—5Al—5Mo—5V);
- deformation mechanisms in the alloy and forecasting on their base of methods of getting the nanostructures were studied.

The titanium alloy Ti—5Al—5Mo—5V is two-phase α+β - alloy, in which the variety of phase states is realized by quenching from different temperatures. Three initial phase composition with the different phase ratio were explored:

- single - β- phase – state (received after annealing 900 °C, 1 hour, water-quenching);
- two-phase 85%β+15% α (850 °C, 1,5 hour, water-quenching);
- two-phase 45% β+55 % α (850 °C, 1,5 hour+750 °C, 3 hours, air cooling).

Samples were deformed with high pressures (HP) (hydroextrusion) before 50%. Structure of samples was studied by optical and electron microscopy and x- rays. Mechanical characteristics ($\sigma_{0.2}$, $\sigma_{в}$, $\psi$, $\delta$) were checked at straining of standard samples before destroying with the speed of 20 mm/min.

It was installed that mechanisms of plastic deformation in the alloy Ti—5Al—5Mg—5V are different for single-phase and two-phase states.

For 100% β – composition the deforming with HP before=5—15%, causes the appearance of big amount of narrow layers, which consist of orthorhombic α′′- martensite orientationally connected with a source β -matrix, as was set up by X-ray [3] (fig. 1).

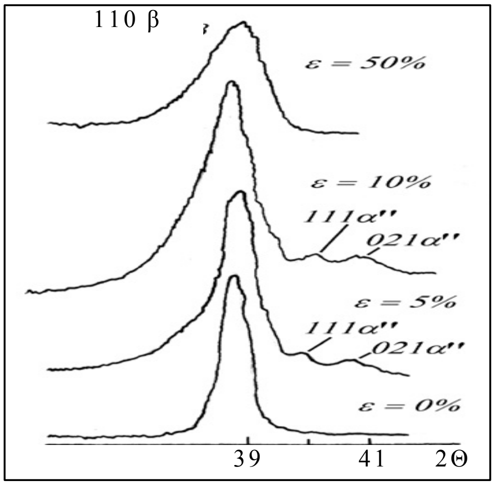

Fig.1. The appearance of deformation martensite at HP-deforming.

As TEM studying showed, the martensite is observed as laminated one. As a rule, the martensite plate have a complex "packet" structure with internal enclosure of smaller packages, the least of which reaches 20 nm. Orientations of nested plate boundaries for the most parts are equal and were ~70 ° to boundaries of external plates. When the deformation increases up to more than 30%, x-rays do not observe the martensite already. Probably, a formation α′′- martensite occurs also under developed plastic deformation (>30%), but then a quick inverse α′′→ β conversion takes place. At the inverse conversion α′′→ β, the source structure of β - phase is restored completely, but boundaries of martensite plates and packages are saved, and as a result, β -grain is greatly fragmented. The martensite transformation is one of the manifestations of the ***rotary mode***.

Formation of big amount of areas on the place of former martensite layers containing grains of nanocristalline size with big disorientation contributes to the 50% growing of breaking point, 20% growing of yield point at some reduction of plasticity (fig. 2). A plateau presence under ε < 30% confirms an inclusion of martensite deformation mechanism at the point.

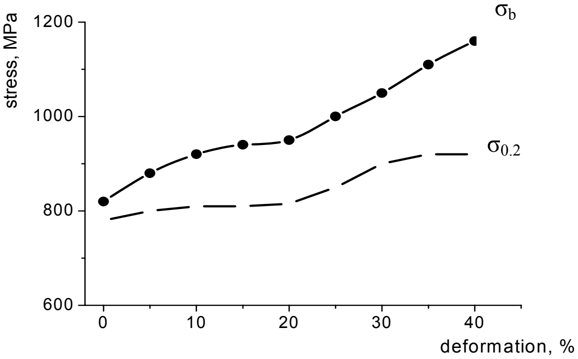

Fig.2. The influence HP-deforming on strength in single – β – composition.

An usual dislocation sliding occurs on the initial deformation stages of two-phase 45% β+55% α – alloy. Then, the growing disordered orientation within grains is observed at the achievement of high dislocation density (ε ~30%) confirmed by TEM. The mechanical strength ($\sigma_в$, $\sigma_{0.2}$) increase (fig. 3). However, deformation reveals itself in continuous change an disorientation within a grain, unlike discrete change of the orientation at deformation of a single-phase alloy. So the rotational mode of deformation in single-phase alloy is replaced with the ***bended mode*** in two phase 45%β+55% α- alloy.

Analysis of the structure evolutions and its influence upon mechanical properties allows to reveal deformation mechanisms of and to predict ways of a creation sub micro- and nanostructure.

For single-phase alloy a decrease of grains pulverizing occurs by the reversible martensite transformation. For the two-phase alloy step-like annealing in combination with a intermediate deformation and a following aging. Deformation ensures conditions for bended mechanism and allows to form a structure with continuously changing orientation and high dislocation density. After the aging, a precipitating α-phase has high dispersion (~20 nm). That has allowed raising the strength limit of alloy on 35—40% at the conservation of plasticity. Changing a rotary mode, shown in formation deformation martensite for the single-phase alloy on the bended mode for the two-phase alloy connected with change degrees of doping hard dissolve.

New possibilities of governing structure of alloy were opened by knowledge of mechanisms of deformation. The combination of annealing and following deforming provides conditions for bend deformation mechanism and allows forming a structure with continuously changing disorientation and high dislocation density.

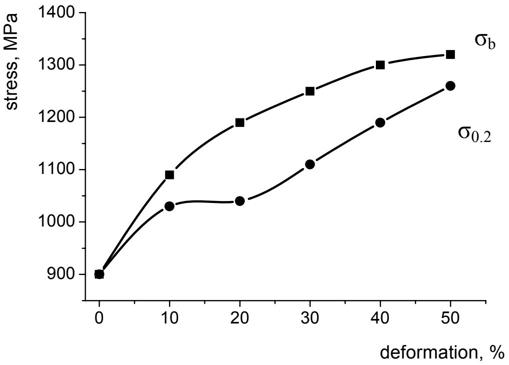

Fig.3. The influence HP-deformation on strength in two-phase 45%β+55% α alloy.

The intensive plastic deformation is a necessary stage for creation of nanostructure. Decreasing of structure element sizes causes to rise of strength.

1. B.A.Kolachev, V.A.Livanov, A.A.Buchanova. Mechanical properties of Ti and its alloys. M.,Metallurgy, 1974, 544 p.
2. D.B.Miracle. *NATO ARW, Metallic Materials with Structural Efficiency,* Abstracts, Kyiv-2003, (2003), p.9.
3. T.E.Konstantinova. *Mesostructure of deformed metals.* Donetsk, DonFTI of NASU, 1997.
4. T.E.Konstantinova, G.K.Volkova, A.A.Adamets. *Proceedings of the Conf .on Martensite Transformations in Solids* (Kiev, IPM NASU, 1992, p.294.

# OVERHEATING EFFECT ON STRUCTURE AND MECHANICAL PROPERTIES OF NICKEL-BASE HIGH-TEMPERATURE CASTING ALLOY ZHS6K

**Dashunin N,V., Manilova E.P., Masaleva E.N., Rybnikov A.I.**
Polzunov Central Boiler & Turbine Institute (CBTI)
Politehnicheskaya str, 24, Saint-Petersburg, Russia, rybnicov@online.ru

Nickel-base casting alloy ZhS6K is widely used as a material for gas turbine components. The maximum metal service temperature of components manufactured from ZhS6K alloy is in the range from 700 to 900 °C. However, unforeseen metal temperature rises over normal service values may occur during gas turbine operation.

In order to find out the mechanism of short-term overheating and its affect on the ZhS6K metal structure and properties, one melt of exact-sized cast specimens with the best level of mechanical properties after standard heat treatment at 1210 °C for 4 hrs and air-cooling was studied (Table 1). In this state, the γ'-phase in ZhS6K alloy is uniformly distributed as globular particles while a separate fine dispersion (2—4 μm) of MC carbide particles can be found on the grain boundaries (Fig. 1).

Short-term (10—20 min) and longer-term (up to 24 hrs) alloy exposures at 950 °C after heat treatment under standard conditions caused no changes in alloy structure or mechanical properties. Heating up to 1000 °C may produce some γ'-phase coagulation while the particle shape remained unchanged; however, there was an increase in $M_6C$ carbide particle size (4—6 μm) on grain boundaries. These structural changes lead to a slight degradation in the alloy's ductility. An increase in overheating temperature up to 1050 °C produce a more significant γ'-phase coagulation and $M_6C$ particle growth on the grain boundaries, which decreased the percentage of tensile extension to about one-fourth that of the initial state.

More distinct structural changes may be observed during overheating at temperatures between 1100 and 1180 °C with exposures for even 10 min. In addition to $M_6C$ globular particle size growth (up to 10 μm and above), a needle-like shape modification of this carbide was observed to form (Fig. 2). The γ' alloy-strengthening phase was found to have two configurations. The normal finely dispersed fraction (0,1—0,3 μm) was found to precipitate only within the grains, while coarse particles (up to 10—15 μm) were observed along grain boundaries and as separate particles within the grains.

Table 1. Mechanical properties of ZhS6K alloy cast specimens after different heat treatment procedures.

| Heat treatment procedure | Tests at 20 °C | | | |
|---|---|---|---|---|
| | $\sigma_{0.,2}$, MPa | $\sigma_B$, MPa | δ, % | ψ, % |
| No heat treatment | 881,3 | 1004,5 | 4,3 | 5,8 |
| 1210 °C, 4 h. | 934,9 | 1077,0 | 7,8 | 8,2 |
| 1210 °C, 4 h.+<br>950 °C, 24 h. | 915,6 | 1020,8 | 5,7 | 6,9 |
| 1210 °C, 4 h.+<br>1000 °C, 24 h. | 901,6 | 998,6 | 4,2 | 5.3 |
| 1210 °C, 4 h.+<br>1050 °C, 24 h. | 885,0 | 943,2 | 2,7 | 3,8 |
| 1210 °C, 4 h. +<br>1100 °C, 24 h. | 852,1 | 888,9 | 2,0 | 4,3 |
| 1210 °C, 4 h. +<br>1130 °C, 24 h. | 807,5 | 834,0 | 1,2 | 1,9 |
| 1180 °C, 4 h. | 779,1 | 794,8 | 1,2 | 1,0 |
| 1210 °C, 4 h. +<br>1130 °C, 24 h.+<br>1220 °C, 4 h. | 942,8 | 1059,0 | 7,0 | 8,8 |

For structural components analysis the microstructure was examined by the methods of EPMA [1]. Sizes and morphology of γ'-phase were estimated by the method of extraction carbon replicas.

Structural changes in the alloy had a great effect on alloy ductility. The percentage extension is reduced to 0,8—2,0% instead of 5—8% in the initial state after heat treatment. The strength properties remain at almost the same level (Table 1).

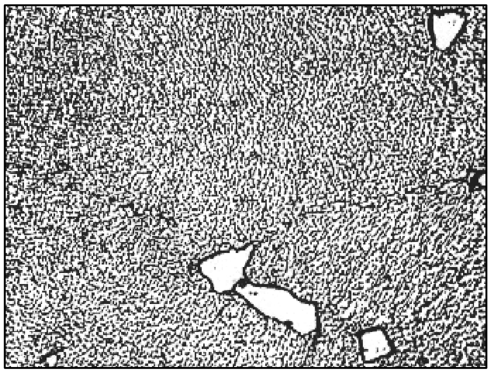

Fig. 1. ZhS6K alloy microstructure after heat treatment 1210 °C, 4 h., air cooling, 1000X.

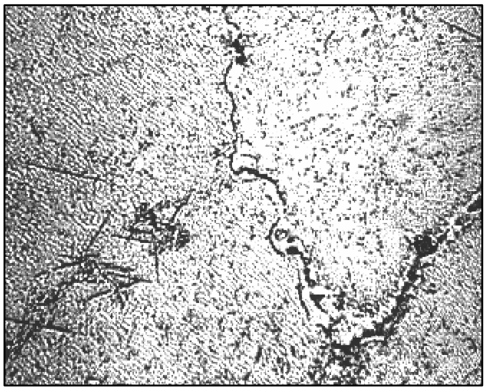

Fig. 2. ZhS6K alloy microstructure after heat treatment 1210 °C, 4 h.+1130 °C, 24 h. air cooling, 1000X.

It should be noted, that a similar structure of the alloy is also observed when heating ZhS6K during the standard solution heat treatment is performed below the temperature for the completion of γ'-phase solutioning (e.g., below 1190—1200 °C), which is sometimes the case in industrial heat-treatments of casts. The experiment showed that heating the “raw” (non-heat-treated) as-cast specimens up to 1180 °C for 4 hrs lead to the above structure formation and consequently, to mechanical property degradation. This suggests that under-heating during heat treatment degraded the metal properties more significantly to a level below that of the non-heat-treated as-cast state. To this structural state of the alloy, there corresponds also a low level of plastic properties. It is significant that the lower level of ductility detected in tests at room temperatures is confirmed by testes of specimens at constant strain rate [2] $\upsilon$=0,1% /h at 800 °C . The metal deformability in the initial state after standard heat treatment is quite satisfactory (3,0—4,5%), while in the defective metal structure it is reduced to 0,3—0,6%.

Thus, the above results suggest that ZhS6K alloy overheating in the range of 1050—1180 °C leads to considerable changes in alloy structure and mechanical properties. A similar metal microstructure that promotes embrittlement is also formed by under-heating during solution heat treatment. These results should be taken into account when protective high-temperature coatings are applied to ZhS6K alloy components, because it is well known that the process heating used to produce thermal diffusion and electron-beam coatings is carried out at 1050—1150 °C for 4—24 hrs. According to the results given in this work, heating at such temperatures may lead to an extremely low level of alloy ductility.

It should be noted that an additional heat treatment of metal with the defective structure at 1290 °C for 4 hrs entirely recovered its microstructure and mechanical properties to the initial level after heat treatment .

## REFERENCES

[1] Rybnikov A.I. et al., Trudy CKTI, Vol. 177, 1980, pp.29—49.

[2] Stanjukovich A.V., Highh-temperature material brittleness and plastisity. Metallurgy, 1967, p.199.

# FEATURES OF STRUCTURE AND EVOLUTION OF PROPERTIES AMORPHOUS METALLIC ALLOY 82K3XCP AFTER IMPULSE LASER RADIATION

**Ushakov I.V., Feodorov V.A., Permyakova I.J.**
Derzhavin Tambov State University,
Internatsionalnaya Str., 33, Tambov, 392622, Russia, ushakoviv@mail.ru

## INTRODUCTION

Metallic glasses are important perspective materials. They use in practice widely now [1, 2]. It is explained by complex of their physical properties. Growth of their practice usage is an important reason of fundamental and applied investigations. Amorphous metallic alloys have low thermal stability [3]. As a result, problems of both macro- and micro- treatment are very important.

The research is devoted to investigation of evolution of structure and mechanical properties of amorphous metallic glass 82K3XCP subjected to local treatment by focused laser radiation.

## MATERIALS AND EXPERIMENTAL TECHNIQUE

The material used in the present work was metallic glass 82K3XCP, of the composition (wt %) 83,7Co+3,7Fe+3,2Cr+9,4Si in the form of a ribbon 30 μm thick. Used laser "KVANT-15". The wavelength was 1064 nm. The energy of a pulse was 4 – 8 J. The samples were irradiated according to two methods. According to the first method, samples with sizes 10x20 mm were irradiated by laser pulses. After laser treatment the samples were situated on substrate (the method is thoroughly described in [4]) and mechanically tested. According to the second method samples with sizes 10x20 mm situated on substrates. Different thermostable materials used for preparation of the substrate. The substrates situated on metallic base. After the preparation the samples were irradiated by laser pulses.

Mechanical testing was carried out on a PMT-3 microhardness gauge. The achieved results were compared with results obtained on sample subjected to thermal treatment in furnace.

## EXPERIMENTAL RESULTS AND DISCUSSION

It was established, that on samples, after irradiation by impulse with energy 4 – 8 J., areas of annealed material with diameter from 300 μm to 2 mm were appeared. In case of small area and much energy of laser impulse in the center of the area appeared melted zone. The size of zones of melting and annealing depends from energy of pulse and sizes of irradiated area (pic. 1). In circumstances of bigger irradiated area and more equal distribution energy, the melted zone didn't appear, the material in irradiated zone amorphous or partly crystallized.

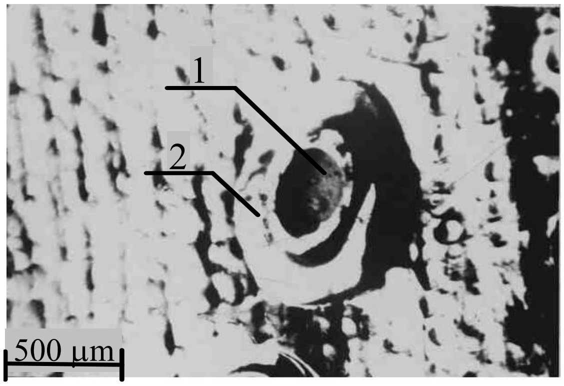

**Pic. 1.** Laser irradiated area on MG situated on a substrate. 1 – zone of melting and burning, 2 – thermally treated zone

After microindentation of the irradiated area, characteristical micropictures of destruction might be observed: the offprint from pyramid of Vichers is situated in the center of squares with lines parallel to planes of the pyramid. Analogous micropictures were observed on samples annealed in furnace and subjected to local loading by pyramid of Vichers.

Experimentally determined some statistical characteristics of destruction. Testing was made at constant distance from centre of irradiated areas, all irradiated areas were formed by pulses with equal energy, duration and other characteristics.

The relationship of cracks initiation from value of load was determined.

Experimental data were approximated by linear dependence N=aP+b (pic. 2), after calculations the next coefficients were obtained: a=0,1; b=-4,71; R=0,92.

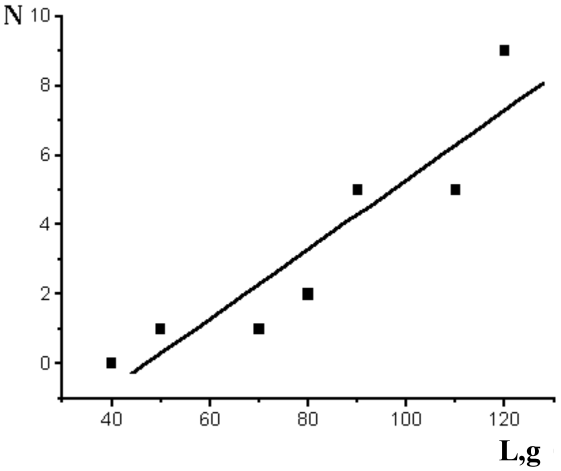

Pic. 2. The dependence of number loading, at which cracks formation took place, from value of load. N – number of such actions after ten experiments.

It is established, that reproduction of experimental data was worse than in case of usage of samples after furnace annealing. It is explained by changing of mechanical properties of material according to distance from the centre of irradiated area. On the base of analysing of data obtained on samples treated to laser annealing and annealing in furnaqce [5,6] the structure condition of material in laser irradiated area was evaluated.

## CONCLUSIONS

1. The parameters of laser impulses required for reproduction formation of laser annealed areas are determined.
2. It is established, that at indentation of laser annealing metallic glass situated on polymer substrate, the regularities of destruction are analogue to ones obtained on metallic glass annealed by tradition techniques.
3. On the base of analysing data obtained by X – ray analysis and differentially – scanning calorimetry, on samples subjected to laser radiation and ones subjected to traditional methods of annealing were determined probable structural evolution in areas of laser irradiation.

## ACKNOWLEDGEMENTS

This work was supported by the Grant of RBFR (project no. 01-01-00403).

## REFERENCES

1 *I.B. Kekalo* Amorphous magnetic materials. Moscow, MISiS. 2001. 276 p.

2 *A.I. Mmanohin, B.S. Mitin, V.A. Vasil'ev, A.V. Revjakin* Amorphous alloys. Moscow, Metallurgy. 1984. 160 p.

3 *I.B. Zolotukhin* Physical properties of amorphous metallic materials. Moscow. Metallurgy. 1986. 176 p.

4 *V.A. Feodorov, I.V. Ushakov, E.I. Klimacheva* // Proceedings of the second internatsional conference "Micromechanisms of plasticity, fracture and ayttendent phenomena", Vestnik of Tambov State University. 2000. Vol 5, №. 2—3., p. 370—374.

5 *V.A. Feodorov, I.V. Ushakov. Journal of technical physics*. 2001. Vol. 46, № 6. p. 637—676.

6 *V.A. Feodorov, I.V. Ushakov,* V.M. Polikarpov, E.I. Klimacheva // Proceedings of the XXXVI internatsional conference "Physcs of processes of deformation and destruction, calculation of mechanical condition of material. Actual problems of strength". Republic Belarus, Vitebsk. 2000. Part II., p.. 385—390.

# HEAT RESISTANCE OF DETONATION COATINGS OF POWDERS PRODUCED BY THE SHS METHOD

**Borisova A.L., Borisov Yu.S., Astakhov E.A., Kaplina G.S., Mits I.V.**
Paton Electric Welding Institute
11 Bozhenko Str., Kiev, 03150, Ukraine, e-mail borisov@pwi.ru.kiev.ua

Application of temperature-stable protective coatings to extend life and improve reliability of parts operating within a temperature range of 600-1400 °C is a topical problem for different tubes of heat exchangers, torch and heater nozzles, components and units of thermal and melting furnaces, glass dies, components of pumps for transportation of molten metals, etc.

This study was conducted to investigate air heat resistance of detonation coatings sprayed from new compositions of composite powders of the cermet, oxysilicide and oxy-carbosilicide types produced by using the SHS technologies.

Analysis of thermograms of composite powders based on processing the curves of oxidation of these powders during heating in air at temperatures ranging from room one to 1000 °C showed that powders of compositions 4, 5 and 6 (Fig. 1) possess the highest heat resistance.

The above powders were used for detonation spraying of coatings on stainless steel samples for subsequent testing in air within a temperature range from 600 to 900 °C. Studies were conducted to investigate the effect of different technological factors (powder particle size, detonation spraying conditions) on structure, phase composition and heat resistance of the coatings, as well as the effect of the composite powder "nichrome – aluminium alloy" (grades PT-NkhAS-05 and PT-NkhAS-10) added to a mechanical mixture with the SHS powder and used as a sub-layer.

When using for spraying the powder with a particle size of 10-20 μm, density of the coatings and degree of their oxidation are higher than those of the coatings produced by using powders with a particle size of 20-40 μm.

The spraying process is accompanied by phase transformations, as a result of which composition of a coating substantially differs from that of a powder. In particular, the following transformations occur: $\alpha$-$Al_2O_3 \rightarrow \gamma$-$Al_2O_3$, $NiAl \rightarrow Ni_2Al_{18}O_{29}$ and $Cr_3C_2 \rightarrow Cr_7C_3 \rightarrow Cr_{23}C_6$, and formation of ternary compounds takes place.

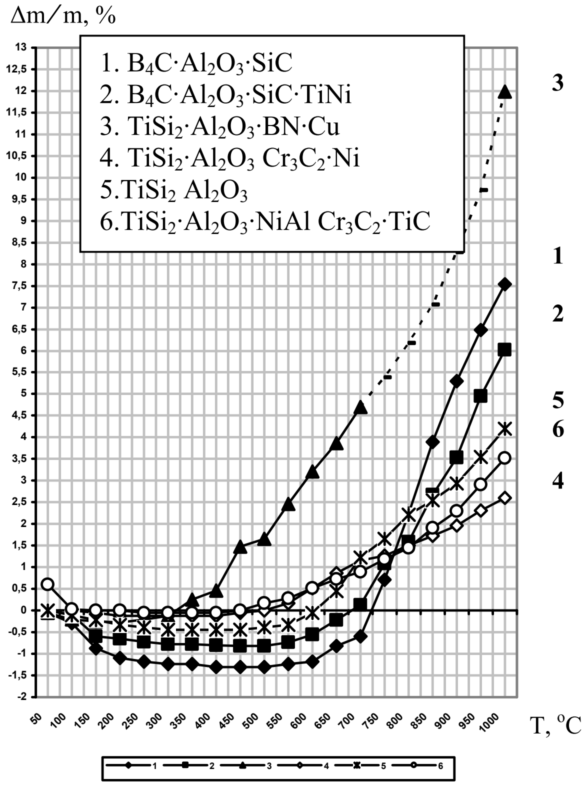

Fig. 1. Thermograms of powders produced by the SHS method

The oxidation process induces changes in composition of the coatings. X-ray phase analysis of the oxidised coatings showed that their main components undergo the following transformations:

1. NiCr is partially oxidised to form $NiCr_2O_4$.
2. Allotropic transformation $\alpha$-$Al_2O_3 \rightarrow \gamma$-$Al_2O_3$ takes place in testing to heat resistance, as well as in spraying, leading to increase in the $\gamma$-$Al_2O_3$ content of a coating.
3. $TiSi_2$ is subjected to oxidation to form $SiO_2$, which results in formation of lower silicides TiSi and $Ti_5Si_3$.

4. $Cr_3C_2$ is oxidised to form $Cr_2O_5$ and formation $Cr_7C_3$ and $Cr_{23}C_6$.

Tables 1 and 2 give some test results on heat resistance of the coatings.

Table 1.

Results of testing the SHS powder coatings to heat resistance

| Test conditions | | Specific gain in weight, mg/cm$^2$ | | | |
|---|---|---|---|---|---|
| T, $^0$C | Time, h | $TiSi_2 \cdot Al_2O_3 \cdot Cr_3C_2 \cdot Ni$ | $TiSi_2 \cdot Al_2O_3 \cdot$ | $TiSi_2 \cdot Al_2O_3 \cdot$ NiCrBSi | $TiSi_2 \cdot Al_2O_3 \cdot NiAl \cdot Cr_3C_2 \cdot TiC \cdot$ |
| 600 | 1 | 0,270 | - | 0,045 | 0,134 |
| | 2 | 0,325 | | 0,178 | 0,262 |
| | 3 | 0,325 | | 0,197 | 0,344 |
| | 4 | 0,325 | | 0,197 | 0,433 |
| 800 | 1 | 0,115 | 0,140 | 0,236 | 0,115 |
| | 2 | 0,223 | 0,178 | 0,459 | 0,159 |
| | 3 | 0,255 | 0,210 | 0,599 | 0,210 |
| | 4 | 0,376 | 0,248 | 0,662 | 0,217 |
| 900 | 1 | | 0,160 | | |
| | 2 | | 0,242 | | |
| | 3 | | 0,318 | | |
| | 4 | | 0,369 | | |
| 1000 | 1 | | 0,287 | | |
| | 2 | | 0,427 | | |
| | 3 | | 0,481 | | |
| | 4 | | 0,678 | | |

Table 2.

Results of testing coatings of mechanical mixture $75(TiSi_2 \cdot Cr_3C_2 \cdot Al_2O_3 \cdot Ni)+25$(PT-NkhAS05) on a sub-layer of PT-NkhAS05 to heat resistance

| Test conditions | | Specific gain in weight, |
|---|---|---|
| T, $^0$C | Time, h | mg/cm$^2$ |
| 600 | 1 | 0,019 |
| | 2 | 0,025 |
| | 3 | 0,045 |
| | 4 | 0,070 |
| 900 | 1 | 0,038 |
| | 2 | 0,051 |
| | 3 | 0,064 |
| | 4 | 0,178 |

Analysis of the test results made it possible to find the following:

1. Coatings sprayed from mechanical mixture $75(TiSi_2 \cdot Cr_3C_2 \cdot Al_2O_3 \cdot Ni)+25$(PT-NkhAS-05) on a sub-layer of PT-NkhAS-05 have the highest heat resistance both at 600 and 900 $^o$C
2. The highest heat resistance of the SHS powder coatings at 800 $^o$C was exhibited by coatings of $TiSi_2 \cdot Al_2O_3$ and $TiSi_2 \cdot Al_2O_3 \cdot NiAl \cdot Cr_3C_2 \cdot TiC$.
3. Heat resistance of a coating sprayed from the $TiSi_2 \cdot Al_2O_3 \cdot NiAl \cdot Cr_3C_2 \cdot TiC$ powder is much higher at 800 $^o$C than at 600 $^o$C.
4. Heat resistance of coating of the SHS $TiSi_2 \cdot Al_2O_3$ powder decreases with increase in the test temperature. Adding NiCrBSi to the composition of this powder leads to high values of heat resistance at 600 $^o$C and their dramatic decrease at 800 $^o$C, compared with the $TiSi_2 \cdot Al_2O_3$ composition (Table 2).

The authors would like to thank the Science and Technology Center in Ukraine for the financial support it rendered to perform this work (Project G046).

# EFFECT OF HEAT TREATMENT ON STRUCTURAL TRANSFORMATIONS OF AMORPHOUS DETONATION COATINGS

**Astakhov E.A., Kaplina G.S., Adeeva L.I., Mits I.V., Golnik V.F.**
Paton Electric Welding Institute
11 Bozhenko Street, Kiev, 03150, Ukraine, e-mail borisov@pwi.ru.kiev.ua

Growing requirements to properties of coatings make it necessary to look for new ways of producing surface layers of materials characterised by increased hardness, wear and corrosion resistance. One of such possibilities can be realised by depositing thermal spray coatings with nanocrystalline structure. Scientific articles dedicated to this issue contain a sufficient amount of evidence that thermal spray coatings with nanocrystalline structure have higher values of hardness, wear and corrosion resistance than coatings of the identical composition but having a conventional crystalline structure [1-3].

As a rule, thermal spray coatings with nanocrystalline structure are produced by two ways:

1) by using nanocrystalline powder materials for spraying;

2) by subsequent heat treatment (HT) of coatings produced from amorphising materials at heating temperatures and rates that provide crystallisation of the amorphous structure to form the microcrystalline (nanocrystalline) one.

Of practical interest for producing nanocoatings by using initial nanocrystalline powders is detonation (DS), plasma (PS) and HVOF spraying technologies. Relatively low temperatures and a short time during which the powder particles dwell in the spraying process in the case of using the above technologies help to preserve the nanocrystalline structure in a finished coating. The decisive factor that ensures high properties of nanocoatings in thermal spraying is optimisation of properties of nanopowders intended to meet the following requirements:

- production of particles with a narrow range of sizes;
- low porosity of particles;
- high strength of particles.

Requirements imposed on the nanopowders for TS are higher than those imposed on powders of conventional sizes, and special equipment and investigation procedures are needed to produce them. Coatings sprayed from the nanopowders often contain a substantial amount of the amorphous phase. So, the coatings should be subjected to heat treatment to transform it into the nanocrystalline one.

In this study we tried out the second way of producing coatings, i.e. DS and PS performed under conditions that provide the amorphous structure and its transformation during subsequent HT.

DS and PS were performed using the amorphising alloy PG-Zh5: Fe-20 at. % B. Table 1 gives thickness and the amorphous phase (AP) content of the layers produced by spraying, according to the X-ray phase analysis data.

Table 1.
Thickness and amorphous phase content of coatings immediately after spraying using alloy PG-Zh5

| Coating characteristics<br>Spraying method and parameters | Thickness, μm | Amorphous phase content, % |
|---|---|---|
| DS, particle sizes –40 μm | 300-330 | 32 |
| DS, particle sizes –63+40 μm | 300-320 | 57 |
| PS | 300-400 | 74 |

The choice of parameters for HT of the coatings containing AP was based on the following:

- results of differential thermal analysis (DTA) of separated coatings;
- results of X-ray phase analysis;
- analysis of data available in literature on crystallisation of amorphous coatings and strips of an identical composition.

Analysis of literature data on crystallisation of amorphous strips with a composition of Fe-20 at. % B, produced by melt spinning [4], and massive layers produced by TS [5] allows distinguishing the following basic peculiarities:

1. As the heating rate increases, the crystallisation temperature grows from 360 °C at $V = 2\cdot10^{-2}$ °/s to 740 °C at $V = 10^{6}$ °/s.

2. Temperature ranges of crystallisation in massive layers are wider by 100 °C than in amorphous strips.

3. Crystallisation leads to pronounced changes in properties.

4. Presence of crystalline inclusions in amorphised TS coatings does not decrease their thermal stability.

Results of DTA of a separated coating with a composition of Fe-20 at. % B allowed us to determine the crystallisation ranges:

- temperature of the beginning of crystallisation – 670 K;
- temperature of maximal crystallisation – 770 K;
- temperature of the end of crystallisation – 870 K.

The rate of heating in DTA was 80 °/min.

We selected heating within a temperature range of 300-500 °C for HT of thermal spray coatings. Samples with coatings were placed in a stainless steel muffle preliminarily purged with high-purity argon. The argon flow rate was set at 20-30 ml/min. Then the muffle was installed in a work space of a shaft heating furnace and heated to the HT temperature at a rate of 20-22 °/min. Holding at the HT temperature was 30 min. Table 2 gives the X-ray phase analysis data on variations in the AP content caused by HT.

Table 2.

Variations in AP content of coatings caused by HT

| AP, % TS type | Heating temperature, °C | | | | | |
|---|---|---|---|---|---|---|
| | Without TS | 300 | 330 | 360 | 450 | 500 |
| DS, particle size –40 μm | 32 | 32 | 28 | 21 | 18 | 0 |
| DS, particle sizes +63-10μm | 57 | 57 | 54 | 27 | 15 | 0 |
| PS | 74 | 74 | 72 | 51 | 10 | 0 |

According to the X-ray phase analysis data, the intensity of lines of metastable borides $Fe_3B$ (tetragonal and orthorhombic) decreases with increase in the annealing temperature.

Together with the samples for metallographic examinations and X-ray phase analysis, also the samples for abrasive wear tests were subjected to HT.

As shown by comparison of hardness and abrasive wear of the detonation coatings with a structure formed as a result of HT of the amorphised coatings to those of the coatings deposited under conditions providing the traditional crystalline structure, hardness of the coatings subjected to HT at 450 °C is 25-30 % higher than that of the coatings with the crystalline structure, and their wear resistance is 2 times as high, which seems to be associated with change in the wear mechanism, rather than with increased in hardness.

## References

1. H.G.Jiang, M.L.Lau, E.J.Lavemia. Synthesis of Nanostructured Engineering Coatings by High Velocity Oxygen Fuel (HVOF) Thermal Spraying. Journal of Thermal Spray Technology. Vol. 7 (3). Sept. 1998. P. 412-413.
2. D.A.Stewart, P.H.Shipway and D.G.McCartney. Influence of Heat Treatment on the Abrasive Wear Behaviour of HVOF Sprayed WC-Co Coatings. Surf. Coat. Technol. In press.
3. S.Usmani, S.Simpath, D.Houck, and D.Lee. Effect of Carbide Grain Size on the Sliding and Abrasive Wear Behaviour of Thermally Sprayed WC-Co Coatings. Trib. Trans., Vol. 401 (No. 3). 1997. P. 470-478.
4. Kinetics of crystallisation of amorphous alloy $Fe_{80}B_{20}$ in a wide range of heating rates. V.I.Krysov, A.I.Limanovsky, V.I.Naberezhnykh. In book of abstracts, 3rd All-Union Meeting "Physics-Chemistry of Amorphous (Vitreous) Metal Glasses". M. A.A.Baikov IMEET, 1998, P. 128.
5. Yu.A.Kunitsky, V.N.Korzhyk, Yu.S.Borisov. Non-crystalline metallic materials and coatings in engineering. Kiev, Tekhnika, 1998, 200 p

# GAS-ABRASIVE WEAR OF DETONATION COATINGS OF COMPOSITE POWDERS AT INCREASED TEMPERATURES

**Borisov Yu.S., Revo S.L.(1), Kostyuchenko A.I.(1), Borisova A.L., Astakhov E.A.**
Paton Electric Welding Institute
11 Bozhenko Street, Kiev, 03150, Ukraine, e-mail borisov@pwi.ru.kiev.ua
(1)Shevchenco Kiev State University,
Glushkova str.,2, b.1, Kiev, Ukraine, revo@univ.kiev.ua

One of characteristics of materials and coatings operating under extreme conditions is their resistance to erosion wear [1]. Surfaces of flying vehicles, power generating plants and other types of modern engineering items are subjected to this effect.

Gas-abrasive wear is one of the types of erosion wear. It occurs when a high-velocity gas flow containing abrasive particles impacts the surface. The special device and test procedure were developed to determine resistance to gas-abrasive wear of detonation coatings at increased temperatures. Figure 1 shows block diagram of the developed device. This device allows formation of a heated air jet with a maximum heating temperature of 600 °C. The jet contains abrasive particles (corundum with a particle size of 0,6-0,8 mm) and is ejected at a velocity of up to 140 m/s. The gas-abrasive jet was directed to the surface of a test piece measuring 20x20x3 mm at an angle of 90°. Time of each test was 15 min. Weight of the abrasive transported by the jet during this time was 1 kg. Detonation coatings were deposited using the "Perun-S" machine. Composite powders produced by the SHS technology were used for the deposition. Compositions of the spray powders and their particle sizes, as well as hardness of the detonation coatings are given in Table 1.

Resistance of the steel substrate and coatings to the impact of a high-velocity air flow at 600 °C on their surface was estimated at the first stage of the tests. Weight loss of the steel 45 sample after 4 min was 40 mg/cm$^2$, whereas weight of the sample with the detonation coating of the $TiSi_2$-$Al_2O_3$-$Cr_3C_2$-NiCrBSi composite powder decreased after 60 min only by 0,43±0,05 mg/cm$^2$. This shows that the coating under such conditions has high resistance to oxidation wear.

Characteristics of gas-abrasive wear is change in sample weight as result of gas-abrasive jet action expressed in mg·cm$^{-2}$ (sample surface) ·kg$^{-1}$ (abrasive rate). Results of the test are shown in Table 2.

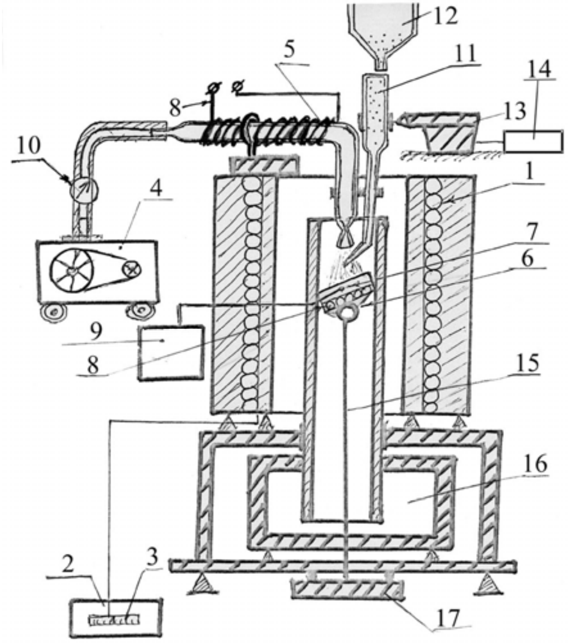

Fig.1. Block diagram of device for gas-abrasive wear test.

1 – furnace
2, 3 – power unit
4 – compressor
5 – piping
6 – turning platform with a specimen
7 – thermocouple
8– additional heaters
9 – measurement unit
10 – cock
11 – ejector pipe
12 – funnel
13 – vibrator
14 – power unit
15 – rod
16 – abrasive collector
17 – base

Table 1.
Characteristics of spray SHS-powders and detonation coatings.

| № | Spray Powder Composition, wt.% | Particle size, μm | Detonation coating hardness, HV $_{0.05}$ |
|---|---|---|---|
| 1a | 99NiAl-1$Y_2O_3$ | 10-20 | - |
| 1b | -“- | 20-40 | 590±90 |
| 2a | 30,5$TiSi_2$-17$Al_2O_3$-32,1$Cr_3C_2$-42,5Ni | 10-20 | - |
| 2b | -"- | 20-40 | 820±100 |
| 3a | 35$TiSi_2$-20$Al_2O_3$-45NiCrBSi | 5-10 | - |
| 3b | -"- | 20-40 | 750±300 |
| 4a | 30$TiSi_2$-16$Al_2O_3$-30NiAl-10$Cr_3C_2$-14TiC | 10-20 | - |
| 4b | -"- | 20-40 | 736±300 |

Influence of gas-abrasive wear on surface profile of detonation coating produced from SHS-powder $TiSi_2$-$Al_2O_3$-NiCrBSi is shown at Fig.2.

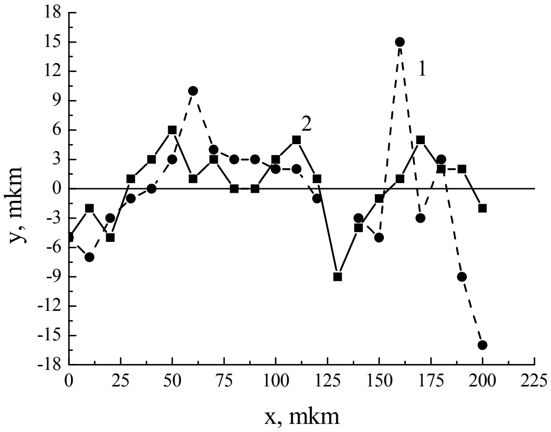

Fig.2. Surface profile detonation coating from powder $TiSi_2$-$Al_2O_3$-NiCrBSi, 5-10 μm before (1) and after (2) gas-abrasive test.

Table 2.

| Spray Powder Composition | Powder Particle size, μm | Gas-abrasive wear, mg/cm$^2$·kg |
|---|---|---|
| NiAl-$Y_2O_3$ | 10…20 | 3,1 ± 0,1 |
| NiAl-$Y_2O_3$ | 20…40 | 1,5 ± 0,1 |
| $TiSi_2$-$Al_2O_3$-NiCrBSi | 5…10 | 6,0 ± 0,15 |
| $TiSi_2$-$Al_2O_3$-NiCrBSi | 20…40 | 2,6 ± 0,1 |
| $TiSi_2$-$Al_2O_3$-NiAl-$Cr_3C_2$-TiC | 10…20 | 3,5 ± 0,15 |
| $TiSi_2$-$Al_2O_3$-NiAl-$Cr_3C_2$-TiC | 20…40 | 7,0 ± 0,3 |

Comparison of the data obtained with the results of evaluation of gas-abrasive wear resistance of thermal spray coatings obtained by other investigators [2] shows that the developed composite detonation coatings are superior in resistance to both plasma coatings of self-fluxing nickel alloys with hardness of 55-60 Rc (1,97-2,71 mg/cm$^2$·kg) and extensively used coatings from a mechanical mixture of NiCr and $Cr_3C_2$ (75:25) (4,02 mg/cm$^2$·kg). Gas-abrasive wear resistance of these coatings produced by the HVOF method is comparable with the data generated by this study and amounts to 0,93-1,47 mg/cm$^2$·kg [2]. It should be noted at this point that the said coatings were tested at a lower temperature (400 °C) and at a velocity of abrasive particles equal to 30 m/s [2].

## Acknowledgments

The authors would like to thank the Science and Technology Center in Ukraine for the financial support it rendered to perform this work (Project G046).

## Literature

1. Erosion, M.Mir, 1982-464 p.
2. S.Ch.Cha, P.Wölpert, High-Temperature Erosion and Corrosion Measurement of Thermally Sprayed Materials, Adv.Engineering Materials, 2003, 5, N4, 213-217.

# INFLUENCE OF PLASMA COATINGS ON MECHANICAL PROPERTIES OF COBALT-CROMIUM ALLOYS

**Besov A.V., Dolgov N.A.**(1)
National Technical University of Ukraine «KPI»
37, Pobedy Ave., Kiev, 03056, Ukraine, E-mail: donika@inbox.ru
(1)Pisarenko Institute for Problems of Strength of NASU
2, Timiryazevskaya str., Kiev, 01014, Ukraine, E-mail: coating@ipp.kiev.ua

Mechanical properties of substrate-coating system are different from uncoated substrate properties. Now influence of coatings on mechanical properties of the substrate is studied insufficiently. Strength properties of a coated substrate depends on coating structure [i], processing technique [ii], coating thickness [iii], etc.

This study aimed to provide understanding influence of plasma coatings on mechanical properties of metal alloys.

Mechanical properties of substrate-coating system are necessary for strength analysis of constructional elements with coatings both analytical and numerical methods. Also mechanical properties are necessary for optimisation spraying processing technique by strength condition, maximal productivity of spaying equipment as well as minimal power expenses.

Now mechanical properties of coatings could be defined by many different testing methods. Specimen shape and dimensions have been developed for each method. Different measurement methods might lead to different mechanical property values.

Therefore the method for determining of mechanical properties both substrate and coating was developed. Static tensile testing of coated specimens as well as uncoated specimens are used in the method. Metal substrate was made according to standards for a mechanical property definition of metals without coatings. Tests were performed by standard tensile-testing machine. Such approach provides continuity of tests, comparability of results and an opportunity of development of a standard method for coating testing. The basic advantage of such approach is reception of mechanical properties of coatings during tensile test of standard specimens. The offered approach allows receiving from experiment a number of mechanical properties of the substrate-coating system.

Strains are measured during loading by strain gauges, which were attached to the specimens. Also stretching force corresponding to these strains are measured. Acoustic emission (AE) analysis is used to monitor cracking and delamination. Strains of cohesive failure $\varepsilon_{cr}$ are determined according to AE activities.

Then a number of mechanical properties of substrate-coating system are calculated.

1. Elastic modulus of substrate $E_S$ and that of coating $E_C$ are calculated. The elastic modulus of coating $E_C$ is calculated by composite section method [iv]. The difference of stress-strain curves of specimens with coatings and specimens without a coating take into account at calculation.

2. Ultimate tensile strength $\sigma_u$ is determined. Cohesion strength of the coating is calculated from equation $\sigma_{u\_(coat)} = \varepsilon_{cr} \cdot E_C$.

3. Yield strength $\sigma_y$ for specimen with coating and specimen without coating are determined.

Cobalt-chromium alloy powder [v] was used for a spraying of coatings. Spraying of coatings was carried out on specially created "PLAST" microplasma equipment [vi]. Spraying parameters are given in Table 1. The coating was symmetrically sprayed on the both side of the substrate. The coating of 100 μm thickness was plasma sprayed. The substrate was to sand blasting for improvement of adhesion strength. Cobalt-chromium alloy (61-65 wt.% Co, 25-28 wt.% Cr, 3-3.75 wt.% Ni, 4.5-5.0 wt.% Mo) was used as the substrate.

The uncoated substrates were tested for

determining mechanical properties of cobalt-chromium alloy. The coated specimens also were tested to stretching. Stress-strain curves of two types of specimens are recorded. Strains to fracture of coating $\varepsilon_{cr}$ are measured. Stress-strain curves of the tested specimens are shown on Figure 1.

**Table 1. Spraying parameters**

| Current<br>(A) | Stand off distance (mm) | Particle size distribution (μm) |
|---|---|---|
| 5.0-5.8 | 28-42 | 40-100 |

Mechanical properties of coated specimens and uncoated specimens are given in Table 2.

Table 2. Mechanical properties of coating-substrate system

| | Tensile Strength $\sigma_u$ (MPa) | Yield Strength $\sigma_y$ (MPa) | Elastic modulus $E$ (GPa) |
|---|---|---|---|
| Substrate | 500 | 310 | 180 |
| Coating | 301 | - | 70 |
| System | 448 | 275 | - |

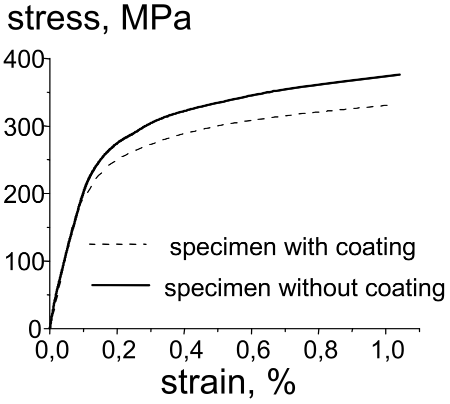

Fig.1. Stress-strain curves of uncoated and coated specimens

In this study, the elastic modulus of plasma coating has been determined. It is concluded that unique microstructure and inhomogeneity of the plasma coating leads to decrease in elastic modulus as compared to the metal substrate. An irregular network of cracks can be seen. The stretch deformation induced increase in the crack density in the loading direction. Upon further straining small pieces of the coating were detached. The coating receives a part of loading applied to the specimen and reduces a stress level in the coating-substrate system. In view of that the coating elastic modulus is lower compared to substrate elastic modulus then the stress in the coating is lower essentially. However weak part of the tested substrate-coating system is the coating.

References

---

i. J.G.Veksler, V.P.Lesnikov, V.P.Kuznetsov, and S.J.Paleeva. Influence of heat resisting coatings on thermal stability of nickel alloys in corrosive gas streams [In Russian], pp.15-20 in *Temperature resistance coatings*, Science, Leningrad (1985).

ii. E.V.Izvolenskii, A.N.Krasnov, N.V.Matveev, I.V.Miloserdov, and Yu.V.Oreshchenkov. "Effect of coatings or chemical (electrochemical) treatment on the strength characteristics of steels," *Strength of Materials (A translation of Problemy Prochnosti).*, **-16** [10] 1387-1390 (1984).

iii. G.Cholvy and J.M.Cuntz . "Evaluation of aluminium alloys for protection against corrosion on aluminium alloys and steel used in aeronautical industry," *Vide. Couches mines.*, **48** [260] 17-24 (1992).

iv. L.A.Yaroshevskaya, B.A.Lyashenko, R.V. Tolstopyatov, and O.P.Smishchenko. "Evaluating the composite section method of determining the elastic properties of enamel coatings," Strength of Materials (A translation of Problemy Prochnosti)., **4** [5] 634-636 (1972).

v. A.V.Besov, V.A.Maslyuk, and A.M. Stepanchyuk. "Manner of production of cobalt-chromium alloys powders of for thermal spraying of coatings on medical manufactures [in Ukrainian]," Patent No. 48648A (2002).

vi. A.V.Besov and V.V.Morozov. "Opportunities of use of plasma technology in medicine [in Ukrainian]," Metal Science and Treatment of Metal., [3] 62—66 (2002).

# STRUCTURE AND MECHANICAL PROPERTIES OF Al—Cu—Fe QUASICRYSTALLINE ALLOYS

**Sidorenko S.I., Demchenko L.D., Makogon Yu.N., Pavlova E.P., Zakharov S.M.**(1)
National Technical University of Ukraine "Kiev Polytechnic Institute"
37 Peremogy prospect, Kiev 03056, Ukraine, sidorenko@uap.ntu-kpi.kiev.ua, demles@yahoo.com
(1)The G.V.Kurdumov Institute for Metal Physics of National Academy of Sciences of the Ukraine
36 Vernadsky Avenue, Kiev 03680, Ukraine

*Nowadays* the creating of wear resistance hard coatings with high fracture toughness on aluminium alloys is one of the main problems of searching of many scientists from the well-known firms worldwide, the solution of which would allow to increase the details lifetime of the aircraft and automobile machines.

The great interest has been generated in recent years in new *quasicrystalline* materials as a result of substantial progress in the technology of stable quasicrystalline phase production, theoretical and experimental achievements and very interesting industrial applications.

The attention is paid to the creation of the alloys with *nano-* and *quasicrystalline* structures under the particular conditions and that could be used for the strengthening of wear resistive coatings for the details of mechanical engineering. One of the methods is the obtaining of the quasicrystalline coatings from the aluminides.

Quasicrystals were discovered in 1984 by D.Shechtman [1] and coworkers, who published electron diffraction patterns from rapidly quenched, metastable samples of $Al_6Mn$ that exhibited relatively sharp diffraction peaks arranged in a pattern with icosahedral point group symmetry.

The quasicrystalline state is an intermediate state between crystals and amorphous solids [2]. The quasicrystals display medium to *long-range atomic order, while lacking the periodicity of crystals* It is well known that periodic structures cannot exhibit crystallographically forbidden rotational symmetries, e.g.; fivefold, eightfold, tenfold and twelve-fold rotation axes).

The positional order in the icosahedral phase alloys is *aperiodic* rather than periodic. Tiling geometry [3, 4] is used to describe the quasicrystalline structure. Recently a new theory becomes more accepted, namely it is proposed that quasicrystals could be described as an assembly of *clusters which can simulate different atoms in the periodic table* [5, 6].

The physical properties of quasicrystals differ from the properties of metal and insulators. These materials display a unique combination of physical properties: low electrical and heat conductivity, a semiconductor dependence of conductivity on *T*, unusual optical and magnetic properties, exhibit a low friction coefficient and surface energy, high strength, hardness, wear and corrosion resistance, high stability under radiation, and so on [7-9].

The *purpose* of this work is to investigate the structure and mechanical properties (microhardness) of quasicrystalline Al-Cu-Fe alloys, serving for preparation of the cathodes for ion-plasma deposition coatings on a basis of the Al-Cu-Fe system, to estimate percentage of phases with different hardness in Al-Cu-Fe alloys of the various compositions, and to find the optimal compositions of such alloys for the ion-plasma deposition of the coatings.

The Al-Cu-Fe alloys of various chemical compositions: $Al_{91}Cu_5Fe_4$, $Al_{65}Cu_{20}Fe_{15}$, and $Al_{58}Cu_{26}Fe_{14}Ti_4$, with different amount of quasi-crystalline phase were melted. The $Al_{91}Cu_5Fe_4$ alloy was also made in form of foil. The alloys were investigated by means of X-ray diffractometry, optical metallography and microhardness tests to compare their structure and properties.

The results of X-ray diffractometry given in table 1 showed that *i*-phase mainly formed in $Al_{65}Cu_{20}Fe_{15}$ and formed 80 wt.% of specimen, the occurrence of intermetallic compounds (*β*-phase; $CuAl_2$) was small (20 wt.%).

Table 1. The phase composition of the Al-Cu-Fe alloys (the estimated quantities of the phases are given in wt%)

| Phases | Alloys | | |
|---|---|---|---|
| | $Al_{91}Cu_5Fe_4$ | $Al_{65}Cu_{20}Fe_{15}$ | $Al_{58}Cu_{26}Fe_{14}Ti_4$ |
| i-phase (icosahedral) $Al_{65}Cu_{20}Fe_{15}$ | - | 80% | 50% |
| β-phase (cubic solid solution) Al(Cu,Fe) | - | 10% | 20% |
| $Al_4Cu_9$ (cubic) | - | - | 15% |
| $CuAl_2$ (tetragonal) | 15% | 10% | 10% |
| AlCu (monoclinic) | 15% | - | 5% |
| Al (fcc) | 70% | - | - |

The $Al_{58}Cu_{26}Fe_{14}Ti_4$ alloy consists of 50 wt.% of *i*-phase and 50 wt.% of intermetallids (*β*-phase; $CuAl_2$; $Al_4Cu_9$; AlCu). In $Al_{91}Cu_5Fe_4$ the *i*-phase is not revealed by means of XRD, the alloy is mainly presented by *fcc*-solid solution of Cu and Fe in Al (70 wt.%).

The Vickers microhardness (*HV*) of these alloys was measured on standard procedure by microindentation. The results of microhardness tests are given in table 2.

Table 2. The percentage of phases with the different hardness in Al-Cu-Fe alloys (given in %)

| Alloys | The interval of microhardness values, GPa | | | | |
|---|---|---|---|---|---|
| | Super High HV 6,7 – 8,5 | High HV 5.2 – 6.6 | Medium HV 3.6 - 5.1 | Low HV 2.0 - 3.5 | Super Low HV 0.5 - 1.9 |
| $Al_{91}Cu_5Fe_4$ | - | 5% | 15% | 10% | 70% |
| $Al_{65}Cu_{20}Fe_{15}$ | 32% | 38% | 20% | 10% | - |
| $Al_{58}Cu_{26}Fe_{14}Ti_4$ | 8% | 20% | 65% | 7% | - |

The high microhardness is observed in $Al_{65}Cu_{20}Fe_{15}$ alloy containing the maximum of *i*-phase (fig 1). The average *HV* of $Al_{65}Cu_{20}Fe_{15}$ alloy is 4.9-6.9 GPa. The composition of this alloy approaches the stoichiometric one. The microhardness of *i*-phase measured by microindentation approximates 6–8 GPa.

With the decrease of *i*-phase quantity in alloy the microhardness falls. The *HV* of $Al_{58}Cu_{26}Fe_{14}Ti_4$ alloy lies in the range 4.6-5.1 GPa. The high content of intemetallic compounds in $Al_{58}Cu_{26}Fe_{14}Ti_4$ alloy doesn't result in the micro-hardness increase.

The lowest hardness exhibits the $Al_{91}Cu_5Fe_4$ where the formation of *i*-phase is not fixed by XRD. The *HV* of $Al_{91}Cu_5Fe_4$ averages 1.4-2.4 GPa.

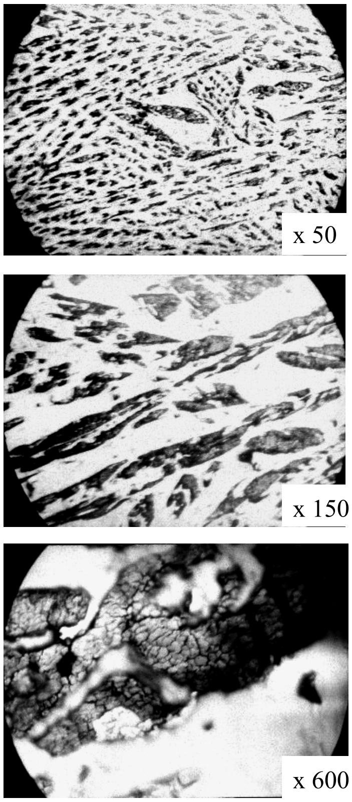

Fig. 2 The microstructure of quasicrystalline $Al_{65}Cu_{20}Fe_{15}$ alloy.

The fig. 2 demonstrates the microstructure of $Al_{65}Cu_{20}Fe_{15}$ alloy where the content of quasicrystalline phase is maximal. The light structural component of the alloy possessing maximal HV (6–8 GPa) belongs to the icosahedral phase, the dark one is presented by different intermetallic compounds. The dark precipitations are oriented along the certain crystallographic directions.

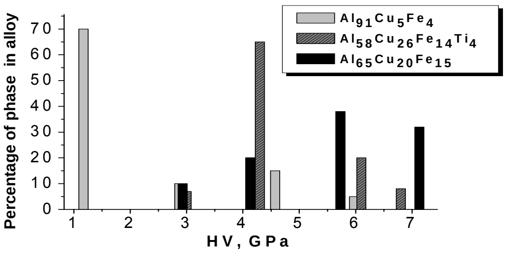

Fig. 1 The percentage of phases with the different hardness in Al-Cu-Fe alloys.

The researches were supported by Science and Technology Centre in Ukraine (Project No 2469).

## References

[1] D. Shechtman, I. Blech, D. Gratias, and J.W. Cahn, Phys. Rev. Lett. 53 (1984) 1951-1953

[2] Ю. Векилов, Сорос. образ. журнал 1 (1997) 87-91

[3] M. Baake, arXiv:math.HO/0203252 v1 (2002)

[4] B. Grunbaum and G.C. Shephard, Tilings and Patterns, W.H. Freeman, New York (1987)

[5] В. Крапошин, Кристаллография 41 (1996) 395-404

[6] В. Крапошин, Кристаллография 44 (1999)995-1006

[7] J-M.Dubois, Mater Science Eng A294-296 (2000) 1

[8] M.Feuerbacher, M.Bartsch, B.Grushko, U.Messerschmidt, K.Urban, Philos. Mag. Lett. 76 (1997) 369-76

[9] J.M. Dubois, P. Weinland, European Patent EP 0356287 A1 and US Patent 5204191 (1993).

# OPERABILITY OF INORGANIC COMPOSITE MATERIAL UNDER EXTREME CONDITIONS

**Podobeda L.G., Vasilenko V.V., Rusin M.Yu.**
Federal State Unitary Enterprise “Obninsk Scientific Industrial Enterprise “Technologiya”
Obninsk, Kaluga Region, 249035,Russia, onpptechn@kaluga.ru, http://www.technologiya.ru

The ФОСТ inorganic composite material based on glass fabric and aluminophosphate binder is intended for manufacturing the structural and radio technical articles and units which, operate for a long time at 873-1073K when warmed up totally.

The special research is needed to use the ФОСТ material at higher temperature under increased thermal and mechanical loads and also to gain the information about the material behavior when it operates under the complicated climatic conditions.

Such works on the whole complex of the material physical/technical characteristics were carried out with the binder content that was the optimum one with respect to bending strength, tensile strength, shear strength, impact resistance, linear expansion coefficient, stability of thermo physical and dielectric properties.

The problems of ensuring the structural and service reliability under conditions close to the actual ones were considered separately.

One of the research lines was concerned with determination of the material high-temperature characteristics at the level of ultimate capabilities of measuring plants -1073 K. The limits of the material resistance to destructive loads under bending, tension and compression (taking into account the anisotropy) were in the range of 50 to 130 MPa at an impact resistance of 15000 J/m$^2$.

The second line of the research was concerned with the complex of the problems connected with the possibility of the material characteristics change under the action of climatic factors and under long-term storage. The tests in humidity chamber under the action of sea fog have shown that the material without moisture-proof coatings demonstrated the same dielectric characteristics as those of the specimens having both organosilicon and fluorineplastic coatings.

The changes of the material dielectric properties are insignificant and they do not affect the articles operability under thermo cycling from 213 to 393K during 10-20-50 cycles. However, when using the fluorineplastic coatings no changes of dielectric properties take place. In so doing the material strength does not change, either.

The third line of the works was concerned with the determination of the articles operability under heat flow and bending load which act simultaneously. The article out of the ФОСТ material withstood two-fold bending load at about 1500K.

In order to evaluate the interaction of the ФОСТ material with the connection material (alloy 32НКД) in humid environment, the special research has been carried out under conditions, which simulate the long-term storage. This research has shown that the interaction of the ФОСТ material (fastened to connection material-alloy 32НКД through the heat resistant sealant "Viksin") does not cause the alloy corrosion. In so doing the strength remains unchanged in the interlaminar shear in the material.

Since the ФОСТ material possesses the excessive acidity (PH<7), further research has been carried out into upgrading the ФОСТ material by means of inner and outer alkali neutralizing in order to eliminate casual effects of interaction of contacting materials in connection zone during penetration of water. Thus the structural reliability of the article has been increased additionally.

By and large the ФОСТ material has demonstrated the necessary level of operability in thermo stressed state at a temperature up to 1500K and under long-term storage.

# SPECIAL FEATURES OF THE THERMAL AND THERMOMECHANICAL BEHAVIOUR OF TiNi UNDER FORMATION OF MONOCLINIC AND RHOMBOHEDRAL MARTENSITES

**Koval Yu.N., Kudryavtsev Yu.V.(1), Semenova E. L.(1)**
Kurdyumov Institute of Metal Physics, NASU
Vernadsky Str. 36, 03142, Kiev, Ukraine, koval@imp.kiev.ua, kudra@imp.kiev.ua
(1)Frantsevich Institute for Problems of Material Science, NASU
Krzhyzhanovsky Str. 3, 03680, Kiev, Ukraine, selena@materials.kiev.ua

Dilatometry, resistometry and X-ray studies as well as thermomechanical tests of TiNi with the compositon close to equiatomic one have been carried out.

The specimens for the investigation were prepared from the alloys taken from different melting series and underwent various thermomechanical processings in a particular wiredrawing.

All the main characteristics of the martensitic transformations in TiNi known previously such as the critical temperatures of martensitic transformations, their decrease after thermocycling via temperature range of the martensitic transformations, availability of SME and the premartensitic distortions of the crystal structure of the high-temperature B2 phase, forming of rhombohedral and monoclinic martensites have been confirmed.

The dilatometric curves of the specimens was found at first time to demonstrate sign-variable coefficient of the thermal linear expansion unlikely the behaviour of the monoclinic martensite, its coefficient of the linear expansion being always negative in the temperature range related to the formation of rhombohedral martensite.

Rate of the contribution of monoclinic and rhombohedral martensites in the thermal expansion (contraction) and bent (restoration of the shape) depends on previous thermomechanical processings and conditions of dilatometric and thermomechanical tests (value of load, cycling on temperature and load, materials of holder, so on) and can change substantially. As a result the summing dilatometric effect can be both positive and negative.

In the thermomechanical bending tests the increase of load brings to multiple increasing of the share of rhombohedral martensite in the products of the phase transformation. It is evident that in this case the bending occurs at the expence of rhombohedral martensite.

However the thermomechanical cycling (heating-cooling, loading-unloading) can lead to a reverse process, when no bending takes place but a restoration of the shape on formation of the rhombohedral martensite, while the formation of the monoclinic martensite provokes only bending as usual.

# THE INCREASING OF MECHANICAL PROPERTIES OF SILICICON NITRIDE BASED CERAMICS DURING HIGH TEMPERATURE DEFORRMATION

**Gnylytsya.I.D., Kryl Ya.A.**
Ivano-Frankivsk National Technical University of Oil and Gas
Karpatska Str., 15, Ivano-Frankivsk, Ukraine, igorgn@nung.edu.ua, kryl@nung.edu.ua

Silicon nitride due to low coefficient of the warm-up expansion, high hardness, strenght under high temperature, heat steady finds using as material for details gas-turbine engines, in friction elements, working under high temperature, without lubrificant, in aggressive environment. The silicon nitride based materials have not yet exhausted its potential as constructional material. The possibility of structured strenghtening such materials opens the new prospects for their use.

Deforming processing under high temperature is one of the directions of the improvement properties of silicon nitride based materials.

The materials, containing as activation additives $Y_2O_3$ and $Al_2O_3$, which form the eutektic, under 1760 $^0$C were chose for undertaking the investigations. The materials of following composition: $Si_3N_4$-5mass.%$Y_2O_3$-2mass.%$Al_2O_3$ and $Si_3N_4$-5mass.%$Y_2O_3$-5mass.%$Al_2O_3$ were used.

By X-ray difraction studies is determined that the source sintered samples of both composition were two-phase: β-$Si_3N_4$ and ligament of the composition Al-Y-N-O.

The intensity of difractional peaks source sample correspond theoretically calculated to importances that is indicative of absence in this material texture (the coefficient of the texture T=1).

The source sample had 5-6 % porosity, 10-25 volume % elongated grains of β-phase was present in microstructure.

The hardness of sintered materials was at a range 15,0-15,5 GPa, the coefficient of fracture toughness $K_{1C}$10 was 5,5 - 6,0 MPa·m$^{1/2}$.

The direct scheme of extrusion was chose for deformation coming from possibility of the regulation of the tense condition (Pic.1).

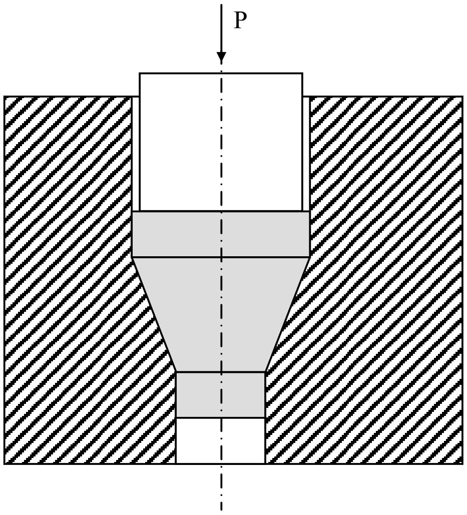

Pic. 1 The scheme of deformation

High temperature deformation was conducted with degree of press out 40 - 80 % under specific pressure 20-30 MPa within the range of the temperature 1750-1850 $^0$C. Deformed with degree of press out 55 % sample is shown on picture 2.

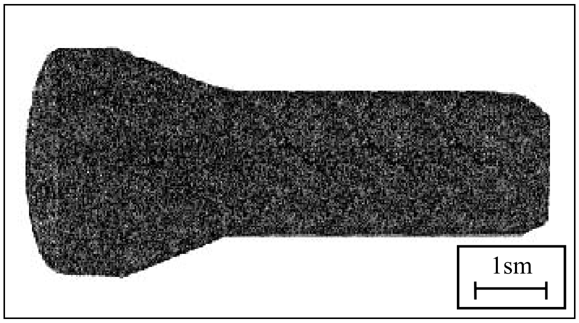

Pic.2 Deformed sample

As a result of X-ray difraction studies are determined that after high temperature extrusion in deformed material except β-$Si_3N_4$ phase is registered beside 30 volume % of rhombic phase $Si_2N_2O$. For determinations of the possibility of existence directed structure in deformed material was realized scan in directions parallel and perpendicular to direction of extrusion. The difraction from planes parallel and perpendicular to direction of extrusion show presence of the texture in deformed sample. So for planes parallel to direction of extrusion for $\beta$ - $Si_3N_4$ coefficient of the texture $T_{101}$=1,34 that there is sign that much elongated grains $\beta$-$Si_3N_4$ are oriented along direction of deformation.

X-ray difraction results about presence of the anisotropic structure were confirmed by electronic microscope studies (Pic. 3).

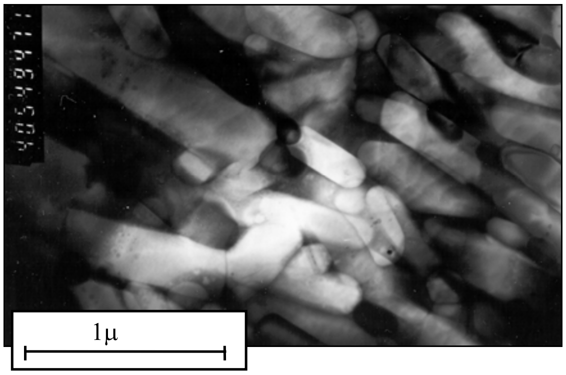

Pic. 3 The directed structure
of the deformed material

By microstructural studies was determined that in process direct extrusion at the temperature range 1750-1850 $^0$C amount of anisotropic grains in structure goes up to 45-60 volume %.

Measured density of the got material nearly equal theoretical importances that is indicative of practical absence of remaining porosity.

According to anisotropy of the got structure material after high temperature deformation had the properties, which greatly differ depending on that in what planes (parallel or perpendicular to direction of extrusion) they were measured (Pic. 4).

Under room temperature material in planes perpendicular to direction of extrusion possesses the increased fracture toughness: $K_{1C}10$=11,5-12,0 MPa·m$^{1/2}$. In planes parallel to direction of extrusion importance of the fracture toughness coefficient is within the range 7,5-7,8 MPa·m$^{1/2}$.

After deformation hardness of the material in perpendicular to direction of extrusion planes little above and forms order 16 GPa.

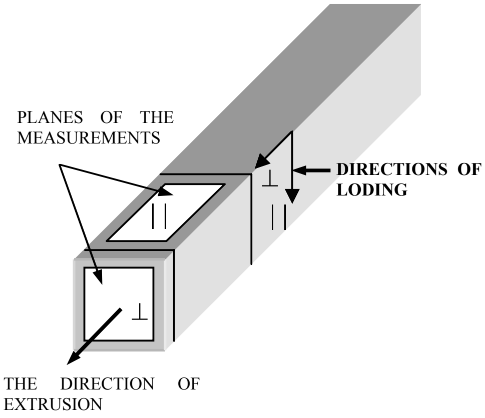

Pic. 4 The scheme of loading

The increasing of fracture toughness of silicon nitride based materials, containing in structure anisotropic grain $\beta$-$Si_3N_4$ is caused action of two factors: the first - a deflection of the crack (the pass-by by crack such grain), the second - a branching the crack.

If crack is held up on elongated grain, that she tries curly and this raises the resistance to spreading the crack. When increase the way spread-thread of the crack increases value of surface energy of the destruction and signifies $K_{1C}$.

Increase of hardness after high temperature deformation is due to intensive displacement of intergranular phase and shaping more density structure with small insulated pores.

Therefore use silicon nitride based products with anisotropic structure, designed with provision for schemes of loading and got by high temperature deformation, can provide increasing field-performance characteristic of such materials and increase the area of their using.

# PROPERTIES OF TITANIUM – FULLERENE COATINGS

**Shpilevsky M.E., Shpilevsky E.M., Matveeva L.A.** (1)
Luikov Heat and Mass Transfer Institute of the NASB,
Str. P.Brovki, 15, Minsk, 220072, Belarus, E-mail: shpilevsky@itmo.by
(1)Institute of physics of semiconductors of NASU
pr. Nauki, 45, Kiev, 03028, Ukraine, E-mail: matveeva@class.Semicond.kiev.ua

**Introduction.**

At last years a number of the materials consisting of structural elements of nanometric sizes (so-called, nanomaterials) with unique combination of properties was received. The special place among nanomaterials is occupied with materials on the basis of fullerenes and carbon nanotubes (CNT) which are unique carbon nanoparticles. Fullerene molecules $C_{60}$ owing to their high symmetry and isolation of all σ -bonds have high temperature stability (in the inert atmosphere they keep stability up to 1700 K). Fullerenes are capable to attach up to six free electrons, and besides of formation of chemical compounds at external interaction, it is possible the introduction of atoms of other chemical elements into a cavity of fullerene molecule (creation of endoedral complexes).

In the present work the structure, adhesive and tribological properties, corrosion stability in acid and alkaline medium of composite titanium – fullerene coatings were investigated.

**Technique.**

Coatings were obtained by a method of vacuum simultaneous evaporation and condensation of the titanium and fullerenes $C_{60}$ on usual thin-film technology. As the evaporation temperature of titanium and sublimation temperature of fullerite differ essentially, it was used two evaporators wich were located close by. Coatings were piled up on substrates of glass, table salt, titanium alloy Ti—6Al—4V.

The structure of materials was investigated by methods of the roentgenography, the electronography, the transmission electron microscopy, the atomic-power microscopy. X-ray structure analysis of samples was carried out on diffractometer DRON- 3. As standards films of pure titanium and fullerite were used. Electronographic and electrono-microscopic researches were carried out on microscope TEM-100. The atomic-power microscopy was carried out on microscope Nanoscope III. The sizes of structural elements and a roughness of a surface were determined on received images. The friction coefficient of coverings as the function of the number of cycles and as the function of the coordinate was determined under the scheme ”coating – point” on original tribometer [1].

Chemical stability of coatings in acid and alkaline medium was investigated by methods of resistoromerty and optical interferometry. Thickness of coatings was determined on Linniks interferometer MII-4 and was within the limits of 800—1000 nm in dependence the made series.

For measurement of adhesive durability of layers the method of normal taking off was used. For the application of the force necessary for taking off the films from a substrate the cylindrical cores (from stainless steel) of different diameter with the help of epoxide resin were attached to these films. Adhesive durability and the limit of strength were determined from dependences of taking off force from the taking off coating area from the substrate and from the length of the break perimeter of the coating at the tests.

**Results.**

X-ray diffraction (X-ray structure and roentgenophase) the analysis has allowed to establish, that the titanium-fullerene coatings consist of several phases: titanium, fullerite, $Ti_xO_yC_{60}$. The size of structural elements of layers Ti-$C_{60}$ depends on fullerite concentration in an alloy and makes 10 ÷100 нм. Diminution of the sizes of structural elements with increase of fullerene concentration is explained by small mobility of $C_{60}$ molecules and restriction by them of the titanium atoms mobility. Changing of the sizes of structural elements of metal – fullerene coatings from density of atom-molecular stream and temperature of a substrate qualitatively confirms the typical dependences for metal films. The surface of Ti-$C_{60}$ layers is enough smooth.

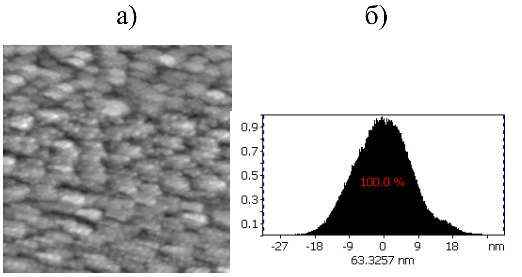

***Fig.*** *A surface of Ti-$C_{60}$ film.*

*a) The image of a surface received with the help of a atomic-power microscope, the size of a field - 2 microns x 2 microns;*

*б) The histogram of distribution of heights.*

Titanium-fullerene coatings have a low friction coefficient, which has unlinear dependence on concentration and high enough adhesive durability. Friction coefficient of coverings (at speed of sliding 0,12 m/s and at loading on an edge equal 5,0 $\cdot 10^6$ Nm$^2$) on a glass substrate have made 0,16—0,17, on a titanium substrate - 0,11—0,12, and adhesive durability of the titanium-fullerene coatings on these substrates is equal 0,62 ГPa and 0,84 ГPa, accordingly. Strength of coatings makes 8,9 ГPa, and Jung module - 91 ГPa.

Low values of friction coefficient are explained of probable changing of the friction mechanism. Fullerenes owing to isolation of all σ -bonds may show the properties of the molecular bearing [2]. So, not looking on the scheme "point-coating" used at tribological tests, which provide the displaing of the mechanism of a sliding friction, the presence of fullerene molecules provide the action of the mechanism of rolling friction.

High durability of coatings on our opinion is explained by two reasons: a) the nanosize structure, б) the formation of chemical compound $Ti_xO_yC_{60}$. High strength and tribological characteristics of coatings provide their advantage in comparison with pure layers of the titanium and fullerite. Comparison strength characteristics of coatings with strength characteristics human bone (durability on a stretching 120—175 MPa, and Jung module 17-27 MPa), and also with characteristics of some ceramic biomaterials [3] shows the advantage of the investigated coatings. The last is show the opportunity of use the titanium -fullerene coatings at manufacturing of various kinds of mobile and motionless implantes (endoprosthesis): total femoral prosthesis, femoral-head prosthesis, condylar prosthesis, humeral, spacer prosthesis, etc.

The received coatings have shown high chemical stability in the diluted acids and alkalis 3 % solutions HCl, NaOH, KOH). Appreciable changes on a surface of coatings it was not observed at testing of samples in acid and alkaline medium within 2400 hours.

**Conclusion.**

The titanium-fullerene coatings have important mechanical, tribological, corrosion properties, combining hardly combined properties (for example, small density with high durability, high adhesion and low friction coefficient, high durability and high plasticity) in one material. The combination of the named properties allows to come to a conclusion on perspectivity of application the titanium –fullerene coatings in extreme conditions (biomedicine, shipbuilding, aviation and space engineering).

**References**

1 Vasilev I.I., Prokoshin V.I., Shplevskij E.M. Installation with Holl device of small movings for measurement tribological parameters of the fullerene containing films //Fullerenes and Fullerene- Lice Structures. - Minsk: BSU, 2000. - P. 195-200.

2. Shpilevskij M.E., Shpilevskij E.M., Stel'makh V.F. Fullerenes and Fullerene- Lice Structures: The Basis for Promising Materials //Journal of Engineering Physics and Thermophysics. 2001. Vol. 74. №o 6. P. 106-112.

# STRUCTURAL DISTORTIONS IN $ZrB_{12}$ AND $LuB_{12}$ SINGLE CRYSTALS

**Werheit H., Paderno Yu.(1), Filippov V.(1), Paderno V.(1), Schwarz U.(2), Pietraszko A.(3)**
Institute of Physics, University Duisburg-Essen, Campus Duisburg,
D-47048 Duisburg, Germany, h.werheit@netcologne.de
(1) Frantsevich Institute for Problems of Materials Science of NASU,
3 Krzhyzhanovsky str., Kiev, 03142Ukraine, paderno@ipms.kiev.ua
(2) Max Plank Institute of Solid State Chemistry, Noethnitzer Str. 40,
D-01187 Dresden, Germany, schwarz@cpfs.mpg.de
(3) Institute of Low Temperatures and Structure research PAS,
Box 1410, 50-950 Wroclaw, Poland, adam@int.pan.wroc.pl

Due to their unique combination of outstanding properties like high melting points and hardness, extraordinary thermal and chemical stability, metal-boron refractory compounds are widely used in modern techniques [1, 2] are particularly favored for being used under extreme conditions. Structural imperfections resulting from intrinsic characteristics, preparation technology or exploitation conditions are known to influence their material properties essentially.

While in solids with simple periodic structures defects usually occur as weak deviations from the ideal structures, for some complex boron structures (β-rhombohedral boron and boron carbide), was proved that ignoring the intrinsic structural defects leads to serious mistakes in the theoretical determination of electronic properties, for boron carbide even metallic instead of semiconducting character [3, 4]. At present, it cannot be excluded that in other complex boron systems like metal borides such far-reaching effects of structural imperfections, defects or distortions on the electronic and other properties occur as well.

Raman spectroscopy is a very sensitive method for indicating structural distortions in crystals and hence for yielding information on structural peculiarities.

We studied the Raman spectra of two members of the $MeB_{12}$ family, $LuB_{12}$ and $ZrB_{12}$. Single crystals were obtained using crucible-less induction zone melting; X-ray epigrams obtained from both end of the large crystalline rods confirmed that they are entirely single crystalline.

The crystal structure ($UB_{12}$ type) can be described in terms of a modified fcc unit cell with the metal atom in the center of regular $B_{24}$ cubo-octahedra with B atoms at each of their 24 vertices. An alternative description is a modified NaCl type structure formed by metal atoms and $B_{12}$ cubo-octahedra (see [5] and references therein). This is a clathrate-type structure composed of two sublattices, boron clusters and RE atoms respectively.

The comparison of cell parameters and density measurements already indicate the existance of vacancies within the boron sublattice, certainly generating structural distortions. As a possible further source of structural distortions the relatively large mass difference of the $^{10}B$ and $^{11}B$ isotopes leading to a considerable difference of the zero-point energies must not be ignored.

The Raman spectra were obtained at room temperature with a Jobin Yvon Labram spectrometer using a HeNe laser of 15 mW power for excitation and a 600 g/mm grating. The spectral resolution is about 1 $cm^{-1}$. The detection range on the sample surface was about 10 μm in diameter. The notch filter of the spectrometer excluded the range $\wedge$ 100 $cm^{-1}$ from detection.

In Fig. 1 the Raman spectra of $Zr^{nat}B_{12}$, $Lu^{nat}B_{12}$ and $Lu^{11}B_{12}$ are displayed. The natural isotope distribution (~ 19 % $^{10}B$ and ~ 81% $^{11}B$) is responsible for the broadening of the Raman lines of the respective samples towards higher frequencies. For a single vibrating boron atom this shift can be estimated according to the factor

$$\omega_1/\omega_2=(m_2/m_1)^{1/2}=$$
$$(m(B_{11})/m(B_{10}))^{1/2}=1.0488.$$

In the spectra of $Lu^{nat}B_{12}$ and $Lu^{11}B_{12}$ with the average boron atomic mass relation 11/10.811 the corresponding factor is determined to 1.0174. The factors obtained from the strongest Raman lines of $Lu^{nat}B_{12}$ and $Lu^{11}B_{12}$ are somewhat smaller (1,009- 1,015), indicating that other bonding conditions like atomic distances and bonding forces also depend on the boron isotope and therefore influence the vibration frequencies as well.

The Raman spectra of $Lu^{nat}B_{12}$ and $Lu^{11}B_{12}$ prove that the different boron isotopes distributed in the $B_{12}$ cubo-octahedra evoke sufficiently strong imperfections to lift the selection rules. The distinct broad Raman signal at wave numbers below about 600 cm$^{-1}$ occurs in Lu$^{nat}$B$_{12}$ only and is missing in Lu$^{11}$B$_{12}$. Several of the weak modes of the material with natural isotope distribution are missing in the isotope-enriched material.

Irrespective of this effect of isotopes, the investigated ZrB$_{12}$ and LuB$_{12}$ single crystals obviously contain structural imperfections sufficiently strong for lifting the phonon selection rules. This can be concluded from the numerous Raman peaks detected in spectral ranges, where only Raman-inactive vibrations are expected.

Further investigations are required to correlate such Raman peaks with specific distortions. The structure refinements by X-ray investigations yield first important results. While in the idealized structures the metal atoms are accomodated exactly in the center of the cubo-octahedra, in the real structures of both borides investigated, they are systematically shifted towards the squared surfaces of the cubo-octahedra. This result is immediately correlated with the occurrence of the rather strong Raman lines in the low frequency sprectral range, where the lattice vibrations related to the movement of the metal atoms are expected.

The estimation of the influence of the structural imperfections in the dodecaborides on their electronic properties is highly desired for a real understanding of the electronic properties of compounds with complex crystal structures.

This work was partly supported by the INTAS (No 01-0617 and No 03-51-3036

References

1. T.Serebriakova, V.Neronov, P.Peshev, Refractory borides. Metalurgia, M., 1991 (in Russian).
2. Boron and Refractory Borides. Ed. V.I.Matkovich, Springer, Berlin-Heidelberg- New York. 1977.
3. R. Schmechel, H. Werheit, J. Phys.: Condens. Matter **11** (1999) 6803.
4. R. Schmechel, H. Werheit, J. Solid State Chem. **154** (2000) 61.
5. H. Werheit, Boron compounds, in: O.Madelung (ed.), Landolt-Boernstein, Numerical Data and Functional Relationships in Science and Technology, New Series, Group III, Vol. 17g, Springer, Berlin, 2000, pp. 1 – 491.

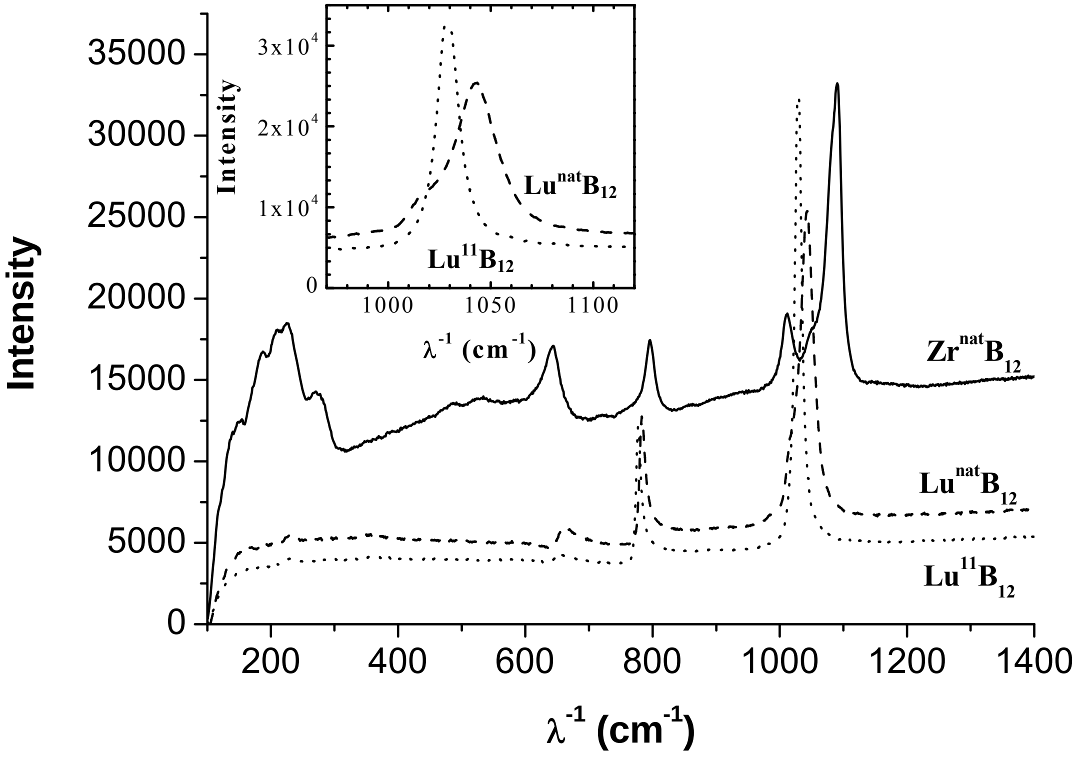

Fig. 1. Raman spectra of Lu$^{nat}$B$_{12}$, Lu$^{11}$B$_{12}$ and Zr$^{nat}$B$_{12}$

# EUTECTIC COMPOSITE MATERIALS BASED ON $B_4C$ - $Me^{V\text{-}VI}B_2$ SYSTEMS

**Paderno Yu.B., Liashchenko A.B., Paderno V.N., Filippov V.B., Martynenko A.N.**
Frantsevich Institute for Problems of Materials Science of NASU,
3 Krzhyzhanovsky str., 03142 Kiev, Ukraine, paderno@ipms.kiev.ua

Boron carbide based eutectics in systems with some metal borides due their high hardness and wear resistance simultaneously with high stability in aggressive agents attracted the attention both scientists and technicians from the point of view of creation of new kind of composite ceramic materials. Such composites are prepared usually by means of common powder metallurgy methods – pressing of powders, sintering or hot pressing.

It is known that the directional solidification of eutectic alloys by optimization of their composition and technological parameters permits to control the formation of specific plate- or fiber-like structure. Such structures provide unidirectional strengthening of obtained composites in compare with individual components.

The eutectic systems with boron carbide $B_4C$ as a matrix phase are very promised, as due its complicate crystal structure and some specific physical properties it may be supposed that such composites should keep its main characteristics and gain new useful ones.

It may be expected that the high brittleness of individual boron carbide will be compensate by the second boride phase and interfaces boundaries and consequently the whole composite material will have higher mechanical properties.

The most constitutional diagrams of $B_4C$ – $MeB_2$ systems have eutectic character with negligible small mutual solubility of components [1, 2]. It provides the stability of structure and phase composition of composites in wide temperature limits and, consequently, the reliability of materials in working conditions.

The alloys having composition close to the quasi-binary $B_4C$ – $ZrB_2$, $B_4C$ – $NbB_2$ and $B_4C$ – $MoB_2$ eutectics were investigated. It was studied the influence of the metal boride phase and technology solidification parameters onto the composite structure formation, particularly the possibility to obtain fiber-like or plate-like configuration of the strengthening diboride phase.

The high-frequency equipment "Crystal 111" for directional crystallization permitted to change the crystallization rate, inert gas pressure, homogenization of the melted zone.

The X-ray diffractometer HZG-4a and electron microscopes Stereoscan S4-10, Electron probe analyzer CX-50 permits to study formed structure of composites, particularly the configuration of the strengthening diboride phase.

The preliminary evaluation of possible eutectic structure formation during crystallization was done by quenching of arc-melted drop of the studied composites. In all experiments the big grains of boron carbide and plates (in $MoB_2$ alloy) or needles (in $ZrB_2$ and $NbB_2$ alloys) of the diboride phase were seen. It was shown also that these plates or needles are situated not only between, but also sometimes penetrate the boron carbide grains. This result is important from the point of view of possibility to strengthen the main boron carbide grains.

The investigation of the influence of the composition onto the regularity of the eutectic structures formed by directional crystallization permitted to evaluate the eutectic compositions in studied systems. They are in limits 23-25 %vol. of $ZrB_2$, 33-35 %vol. of $NbB_2$ and 61-63 %vol. $MoB_2$ in their alloys with $B_4C$.

The structure researches of longitude and cross sections of obtained samples showed that by the directional crystallization of $B_4C$-$ZrB_2$ and $B_4C$-$NbB_2$ systems there are formed self-strengthened composites with regular needle-like eutectic structure. The $B_4C$-$MoB_2$ system is characterized by homogenous fine grain eutectic structure, reminding both plate-like and called "Chinese hieroglyphs" (Fig.1). The matrix phase in all alloys is represented by the boron carbide phase.

This result correlates with presentations about the role of volume parts relation of the constituent phases in the eutectic structure formation – fiber-like or plate-like or more complex - of composites [3].

It was shown for $B_4C$-$NbB_2$ system that the eutectic structure configuration practically was not changed by variation of the solidification rate in limits 3 – 8 mm/min, the whiskers diameter was near I μm, similarly to the $B_4C$-$ZrB_2$ system.

The $MoB_2$ plates in its eutectics have near 0.5 μm thickness.

It is worth to mention that during last years this system cold attention both from the point of view of its constitutional diagram and as possibility to obtain new kind of interesting for modern technology materials.

Usually to obtain the boron carbide based materials there are used sintering or hot pressing, particularly isostatic hot pressing methods. The resulting structure has not any directional preference of mechanical properties, the grains of both phases are equal-axis, strengthening of composite is realized due the interface effects.

In the case of directional crystallization the structure picture is changed, diboride grains have unidirectional configuration, boron carbide grains are penetrated by diboride ones. Due such structure rupture mechanism is changed, is more complicate which results in higher strength.

The fracture toughness ($K_{1c}$) of $B_4C$-$MoB_2$ composite according indenting method is in limits 7…13 MPa/m$^{1/2}$ in compare with source components (2,5-3.5 MPa/m$^{1/2}$) [4].

Apparently due some mutual solubility the hardness of both phases slightly increased up to 55…60 GPa and 32…34 GPa for $B_4C$ and $MoB_2$ based accordingly.

It should be mentioned that boron carbide – molybdenum diboride composite ceramic material successfully combine comparatively high strength with micro-plasticity, by micro-hardness measurements any cracks were not seen for 150 gr loading.

These results suggest the outlook of directional crystallization technology application to obtain on the boron carbide based new ceramic materials for extreme conditions.

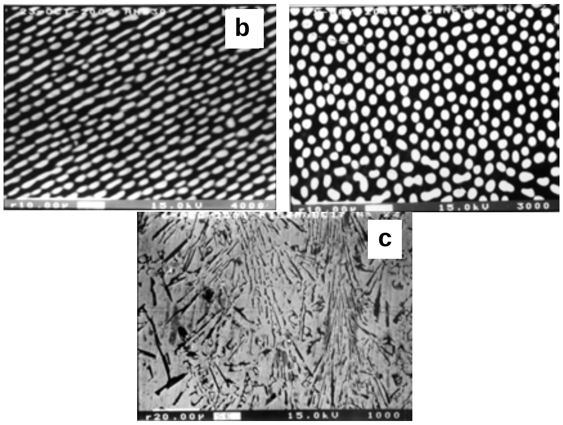

Fig. Cross-section structure of directionally solidified $B_4C$ – Me $^{IY-YI}B_2$ eutectic compositions: a) $B_4C$-$ZrB_2$, b) $B_4C$-$NbB_2$, c) $B_4C$-$MoB_2$

References.

1. Ordanian S.S., Dmitriev A.I., Bizhev K.T., Stepanenko E.K. //Powder Metallurgy (1987) #10, 66-69 (in Russian)
2. Ordanian S.S. //Ogneupory (1989) #1, 15-17 (in Russian)
3. Ashbrook R. //J.Am.Cer.Soc. (1977) 60, #9-10, 428-435
4. Kisly P.S., Kusenkova M.A., Bondaruk N.I., Grabchuk B.L., //Boron carbide. –Naukova Dumka.-Kiev.-1988.-215 P. (in Russian)

# DIRECTIONAL SOLIDIFICATION OF WC – $MeB_2$ ALLOYS

**Paderno V.N., Liashchenko A.B., Paderno Yu.B., Filippov V.B.**
Frantsevich Institute for Problems of Materials Science of NASU
3 Krzhyzhanovsky Str., Kiev, 03142 Ukraine, paderno@ipms.kiev.ua

There exist a numerous tungsten carbide based alloys, which are used mostly for cutting instruments, in heavy alloys etc. The tungsten carbide is a main component in the hard alloys, it is used in wear resistant fused covers, in fused and crushed form as abrasive materials etc.

In spite of the tungsten carbide is any plastic in compare with other hard refractory compounds, nevertheless the task of reduction of its brittleness, especially in fused form, is very important.

The possibility to increase the resistance to the brittle rupture of the melted tungsten carbide by means of creation of composites with participation of some other refractory non-oxygen ceramic compounds was studied in the presented work.

The conception of the work was in the possibility to strength the melted tungsten carbide matrix, which usually consists from the mixture of two carbides – WC and $W_2C$, by formation inside the matrix of the thread – like whiskers or plates of any other sufficiently strong phase.

It is known, for instance, that during the co-crystallization of the eutectic mixtures of some boride phases, for instance $MeB_6$ and $MeB_2$, the transition metal diboride phase $MeB_2$ due its crystal chemistry peculiarities is crystallized in the plate- or more often in the needle – like configuration, which results in a raise of strength and decreasing of brittleness of obtained composites [1].

Unfortunately the sufficient information about constitutional diagrams of pseudo-binary systems of tungsten carbide with transition metal diborides is absent.

In [2, 3] it is mentioned that in the W – C – B system the ternary phases are absent and that boron does not solve in the WC. Then it may be supposed the absence of solubility and the constancy of the tungsten carbide in the WC – $MeB_2$ systems. It may be supposed also that similarly to some other carbide - boride systems in this case by the co-crystallization of such kinds of composites it may be achieved the formation of eutectic composite structure.

The structure and some properties of some pseudo-binary alloys WC – $MeB_2$ (Me – Ti, Zr, Cr, W) having different compositions were investigated. The samples were obtained both by arc melting and by means of induction zone melting with directional solidification.

The Stereoscan S 4-10 and Electron Probe Analyzer CX-50, X-Ray diffractometer HZG -4A were used for the structure researches.

The electron microscopy research of samples in the WC – $TiB_2$ system revealed the existence of the eutectic structure (Fig.1).

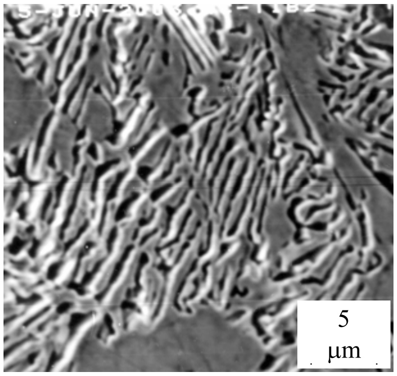

Fig. 1. Microstructure of the WC-$TiB_2$ composite (13 mol % $TiB_2$)

In the WC – $ZrB_2$ system is confirmed the formation of the eutectic structure, which is sufficiently close to the whisker – like structure. There are seen parts of cross-section of the solidified drop having uniform distributed diboride phase (Fig.2).

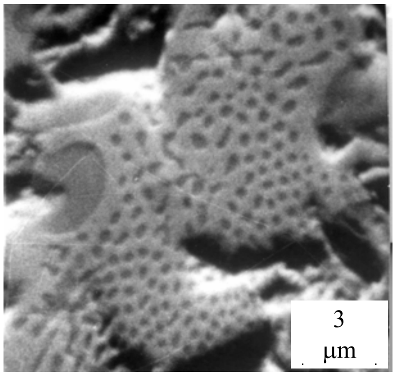

Fig. 2. Microstructure of the WC-$ZrB_2$ composite (20 mol % $ZrB_2$)

The structure of the solidified drops in the WC – $CrB_2$ and WC – $WB_2$ systems also showed the existence of the eutectics simultaneously with carbide phase grains.

Some properties of obtained composites, particularly Vickers hardness ($H_V$, using 1 kg load), micro-hardness ($H_\mu$, using 100g load) were measured, by indentation method were evaluated the values of the fracture toughness ($K_{1c}$).

The micro-hardness of alloys in the WC – $TiB_2$ system (26…30 GPa) is any higher than for the individual WC (18…24 GPa); the more is the part of $TiB_2$, the more is the hardness of the composite. The micro-hardness of the WC – $ZrB_2$ (20…22 GPa) and WC – $CrB_2$ (16…19 GPa) alloys is very close to the WC data.

The Vickers hardness for WC – $TiB_2$ and WC – $ZrB_2$ alloys is about 19 GPa, for WC – $CrB_2$ about 15 GPa.

For $K_{1c}$ there were obtained values in limits of 7…10 $MPa.m^{1/2}$ for the WC – $TiB_2$ system, 5…7 $MPa.m^{1/2}$ for the WC – $ZrB_2$ system, 3…5 $MPa.m^{1/2}$ for WC – $CrB_2$ system.

Obtained values of the mechanical properties are comparatively high and suggest that the continuation of these works may have both scientific and practical interest.

References

1. Yu. Paderno, V. Paderno, V. Filippov, Some peculiarities of structure formation in eutectic d- and f-transition metals boride alloys//Boron-rich solids AIP Conference Proceedings, (1991`),# 231, NY, p.561-569
2. G.V.Samsonov, L.Ya. Markovski, A.F.Zhigach, M.G.Valiashko, Bor, ego soedinenia i splavy, AS USSR Ed., Kiev, 1960, 590 p. (in Russian).
3. Handbook of Ternary alloy Phase Diagrams, (P.Villars, A.Prince, H.Okamoto ets.), 1998, ASM, USA, vol.5, p.5384

# THE STRUCTURE AND PROPERTIES OF THE COMPOSITES BASED ON IRON ALLOYS CONTAINING BORON AND CARBON DESIGNATED FOR SERVICE IN AGGRESSIVE MEDIA

**Spiridonova I.M., Sukhovaya E.V., Vashchenko A.P.**(1)
Dnepropetrovsk National University
13 Nauchny Lane, Dnepropetrovsk, 49050 Ukraine, odm@ff.dsu.dp.ua
(1)Machinery of Supreme Soviet of Ukraine
6-8 Bankovskaya St, Kiev, 01009 Ukraine, vashchen@rada.gov.ua

Iron alloys containing boron and carbon depending on the content of the alloying elements possess a wide range of the properties that make it possible to use these alloys both as the binders and the fillers of the composites, Thus, the alloys containing up to 3,0 pct, of boron and up to 1,0 pct, of carbon wet W—C and Cr—Ti—C hard alloys better than brass, And, the increase in boron content of the alloys above 5,0 pct, ensures their high wettability with brass, Therefore, taking into consideration the requirements for the composites, their high resistance to corrosion in various aggressive media can be assured by means of choosing the relevant compositions of fillers and binders.

The influence of the structure of the fillers and the binders made of Fe—C, Fe—C—B, and Fe—B—C alloys on the resistance of the composites to corrosive attack has been investigated using samples of which compositions are given in Table 1, The aggressive media have been chosen with a view to studying corrosion processes proceeding with oxygen and hydrogen depolarization.

The fillers (particulate) made of iron alloys containing boron and carbon which have eutectic (E), eutectic and peritectic (E—P), peritectic and eutectic (P—E), or peritectic (P) structures have been infiltrated by brass binder (samples No,1 to No,6), And, the composites reinforced with 60 to 70 vol, pct, W—C (samples No,7 to No,9) or Cr—Ti—C (sample No,10) particulate have eutectic Fe—B—C binder, The results of the determination of a corrosion rate are given in Table 2.

In all the investigated solutions corrosion resistance of the composites having the brass binder and the fillers made of Fe—C, Fe—C—B, and Fe-B—C particulate (samples No, 1 to No, 6) is lower than that of the initial alloys used as the fillers, This result is connected with comparatively low anticorrosive properties of the brass a volumetric content of which in the composites is in the range of 30 to 40 pct.

Despite the total decrease in the corrosion resistance of the composites, they, nevertheless, are characterized by a sufficiently low corrosion rate comparable to that of the standard sample made of Ст3 (S), especially, in 3-pct solution of NaCl and solution $2N \cdot CH_3COOH$ (Table 2), The corrosion rate of the composites reinforced with Fe—C—B filler is higher than that characteristic of the composites with Fe—B—C filler.

Table 1

Chemical composition and structural type of the investigated binders and fillers made of Fe-C, Fe-C-B, and Fe-B-C

| Sample | Filler, wt, pct, | | | | | | | Binder, wt, pct, | | | | | |
|---|---|---|---|---|---|---|---|---|---|---|---|---|---|
| | B | C | Fe | W | Cr | Ti | Type* | B | C | Fe | Cu | Zn | Type* |
| 1 | | | | — | — | — | E | — | — | — | bal, | 38 | S,S, |
| 2 | — | 4,0 | bal, | — | — | — | E | — | — | — | bal, | 38 | S,S, |
| 3 | 4,7 | 1,5 | bal, | — | — | — | E—P | — | — | — | bal, | 38 | S,S, |
| 4 | 5,0 | 0,2 | bal, | — | — | — | E | — | — | — | bal, | 38 | S,S, |
| 5 | 9,0 | 0,2 | bal, | — | — | — | P | — | — | — | bal, | 38 | S,S, |
| 6 | 9,0 | 2,0 | bal, | — | — | — | P—E | — | — | — | bal, | 38 | S,S, |
| 7 | — | 3,5 | — | bal, | — | — | E | 1,2 | 0,9 | bal, | — | — | E |
| 8 | — | 3,5 | — | bal, | — | — | E | 2,0 | 1,2 | bal, | — | — | E |
| 9 | — | 3,5 | — | bal, | — | — | E | 3,0 | 1,0 | bal, | — | — | E |
| 10 | — | 10,0 | — | — | bal, | 20,0 | P | 3,0 | 1,0 | bal, | — | — | E |

* - eutectic (E), eutectic and peritectic (E—P), peritectic and eutectic (P—E), peritectic (P), solid solution (S,S,)

Table 2

The results of the determination of a corrosion rate (g/sg m·hr) of the composites in acid and neutral media

| No, | $0,5N\cdot H_2SO_4$ | $5N\cdot H_3PO_4$ | $5\%HNO_3$ | $1N\cdot HCl$ | $2N\cdot CH_3COOH$ | $3N\cdot NaCl$ | $3\%Na_2SO_4$ |
|---|---|---|---|---|---|---|---|
| 1 | 163,93±0,42 | 133,91±0,08 | 150,64±0,32 | 6,03±0,18 | 4,60±0,41 | 0,1±0,11 | 0,36±0,01 |
| 2 | 120,72±0,12 | 92,12±0,03 | 128,40±0,16 | 2,92±0,43 | 2,82±0,14 | 0,05±0,03 | 0,21±0,12 |
| 3 | 272,96±0,29 | 140,24±0,05 | 132,31±0,14 | 15,2±0,25 | 14,83±0,15 | 0,1±0,01 | 0,72±0,21 |
| 4 | 68,73±0,1 | 32,53±0,3 | 103,67±0,41 | 4,68±0,23 | 1,92±0,31 | 0,03±0,00 | 0,23±0,07 |
| 5 | 6,24±0,09 | 2,86±0,23 | 64,32±0,22 | 2,80±0,12 | 1,42±0,2 | 0,12±0,04 | 0,18±0,02 |
| 6 | 3,18±0,03 | 1,97±0,03 | 64,74±0,3 | 2,21±0,33 | 0,91±0,07 | 0,09±0,07 | 0,12±0,06 |
| 7 | 0,31±0,03 | 0,29±0,06 | 1,23±0,42 | 0,29±0,1 | 0,05±0,01 | 0,01±0,00 | 0,03±0,00 |
| 8 | 0,82±0,04 | 0,74±0,08 | 3,14±0,16 | 0,09±0,08 | 0,04±0,02 | 0,01±0,01 | 0,02±0,01 |
| 9 | 1,36±0,05 | 1,05±0,1 | 5,43±0,28 | 0,18±0,08 | 0,11±0,09 | 0,03±0,01 | 0,04±0,00 |
| 10 | 1,43±0,02 | 1,08±0,09 | 6,03±0,1 | 0,22±0,03 | 0,16±0,05 | 0,02±0,00 | 0,05±0,01 |
| S | 140,5±0,14 | 151,4±0,1 | 172,9±0,2 | 18,9±0,3 | 5,0±0,2 | 0,12±0,05 | 0,38±0,03 |

The composites having eutectic Fe—B—C binder and the fillers made of W—C (samples No,7 to No, 9) or Cr—Ti—C (sample No, 10) particulate are characterized by high corrosion stability, At that, the samples having the same binder reinforced with Cr—Ti—C filler corrode heavier than the samples with W—C filler, The alteration in the contents of boron and carbon of the iron-base binder of the composites reinforced with W—C particulate, mainly, results in the change of the corrosion rate the values of which correlate with those for Fe-B-C binder, i,e, the decrease in the corrosion rate of the composites coincides with the decrease in the corrosion rate of the initial binder when a volumetric percentage of Fe—$Fe_3$(C, B) eutectics in its structure diminishes, The corrosion rate of (W—C)-reinforced samples decreases almost 250 times and more than 110 times in the solutions of sulphuric and phosphoric acids, correspondingly, in comparison with that characteristic of the initial Fe—B—C binder, The increase in corrosion stability of the composites is observed in 5-pct solution of $HNO_3$ as well (up to 75 times), which is connected, mainly, with a high resistance to corrosion of tungsten carbides in the solutions of nitric acid of different concentrations, With increase in the boron content of the Fe—B—C binder from 1,2 (sample No, 7) to 3,0 wt, pct (sample No, 9) the corrosion rate increases in most of the investigated solutions, but the maximal corrosion stability has sample No,8 the binder of which contains 2,0 pct, B; 1,2 pct, C; Fe - balance, The metallographic analysis of the surface of the samples after corrosion tests confirms the results of the determination of corrosion stability of the composites, Due to different corrosion stability of the filler and the matrix the relief formed by the particulate raising above the matrix is observed on the surface of brass-matrix composites No,1 to No, 6 reinforced with Fe—C, Fe—C—B, or Fe—B—C fillers, The boundaries around the particles of the fillers corrode heavier than surrounding areas, This phenomena results in the subsequent spalling of the particulate from the matrix, Therefore, samples No, 5 and No,6 that feature interfaces of the smallest width are characterized by the minimal corrosion rate.

The investigation of samples No, 7 to No, 10 having eutectic Fe—B—C binder and W—C or Cr—Ti—C fillers shows that no explicit relief appears after corrosion tests, The particles of the filler do not almost tower above the surface of the matrix, Due to high corrosion stability of both the filler and the matrix the surface of the samples is destroyed in the aggressive media more evenly comparable to samples No, 1 to No, 6, The particulate does not practically break off despite the formation of relatively wide interfaces in the composites, This result can be explained by high corrosion stability of the phases formed at the interfaces of the composites No, 7 to No, 10, As a result, the primary corrosion of the interfaces between the filler and the matrix which gives rise to spalling of the particulate is not observed, And, corrosion stability of the composites with eutectic Fe—B—C binder and W—C or Cr—Ti—C fillers changes because of a different contents of Fe—$Fe_3$(C, B) eutectics and primary austenite in the structure of the Fe-B-C binders increasing with the decrease in the volume of the eutectics, Therefore, these composites boast the maximal corrosion stability in acid and neutral media.

# MECHANICAL CHARACTERISTICS SOLAR CELL BATTERIES OF MAJOR STRUCTURE COMPONENTS

**Pokhil Yu.A., Gavrilov R.V., Yacovenko L.F., Alexenko E.N.,**
**Tarasov G.V.(1), Rassamakin B.M.(2)**
Special Research and Development Bureau for Cryogenic Technologies of Institute for Low Temperature Physics and Engineering of NASU,
47, Lenin ave., Kharkov, 61103, Ukraine, mail@cryocosmos.com
(1)State Design Bureau "Yuzhnoe", 3 Cryvorozhsky str., Dniepropetrovsk, 49008, Ukraine
(2)National Technical University of Ukraine"KPI" 37, Peremoga ave., Kyev, Ukraine

In order to create reliable and durable structures of Space vehicles, researchers need a knowledge about influence of the outer Space environment factors (such, in particular, as temperature) on physical and mechanical properties of materials to be employed in structures of Space vehicles.

Purpose of this paper are investigations for influence of temperature, within interval of 373-77K (which in fact are typical operational temperatures for Space vehicles on near- Earth and geo- stationary orbits) on static and dynamic mechanical properties of a range of materials (used in manufacturing of Solar cell batteries' panels for Space vehicles), such as:

- epoxy- carbon plastics – i.e., a "skin" - material intended to cover the honeycomb- panel carcass of Space vehicles' solar cell batteries;
- bonding glues;
- the Silicon single- crystal , which is a material of photo-electric converters of Space vehicles' solar cell batteries;
- the protection quartz- glass.

Mechanical characteristics being measured: elastic (Young) modulus (E), ultimate strength ($\sigma_B$) and parameter of cyclic durability ( fatigue-resistance curves). Materials have been tested under static deformation, whereby epoxy- carbon plastics and bonding glues were subjected to tension deformation, while silicon and quartz-glass were tested by bending deformation. Testing of epoxy- carbon plastics and bonding glues on fatigue- resistance was carried out at alternating tension, with coefficient of cycle- asymmetry R = 0.1, and at frequency of 10Hz. Fatigue testing of silicon and quartz- glass was carried out at: ideally symmetric bending loading and console-symmetric bending loading, at frequency of 10Hz.

Factor of testing temperature influence on parameters of ultimate strength and resistance to fatigue of all materials under study is represented by relevant graphs in Figures 1 through 6. It is notable that static, elastic and dynamic characteristics of all materials tend to grow with drop of temperature. Thereby, influence of temperature on fatigue resistance of materials is generally in good correlation with temperature-influence on parameter of ultimate strength, under similar loading conditions.

It has been found that parameters of ultimate strength ($\sigma_B$) and Young modulus (E) of epoxy-carbon plastics, tested in lengthwise and transverse directions, at cooling from 373K down to 77K, are growing up by almost 2 times, depending on orientation of filler- fibers vs. direction of tension loading. For lengthwise samples, these parameters are mainly defined by properties of carbon fibers, and for transverse samples, these parameters are defined by properties of fiber- bonding material. Thereby, values of strength and rigidity for lengthwise samples exceed those of transverse samples by more than 10 to 20 times.

Is has been stated that under conditions of single- axial tension, bonding glue behaves in the following manner: at 153K and 373K it shows elastic deformation; and at 287, it occupies a highly plastic state. Under conditions of tension, values of $\sigma_B$ and E of bonding glue are growing up by 50 and 77 times, with temperature decrease from 373K to 150K, correspondingly.

Under bending, the single- crystal Silicon shows a essential dependence of ultimate strength ($\sigma_B$) – parameter on crystallographic orientation. Depending on orientation of samples relatively to axis of loading, values of ultimate strength ($\sigma_B$) either remain irrelevant of temperature factor, or tend to grow up with temperature drop. Destruction of all types of Silicon test samples, under bending within entire range of test-temperatures, is always characterized as a brittle fracture.

Concerning the protection quartz- glass, is has been shown that $\sigma_B$ – parameter under bending, at temperatures of 373K and 293K, differs but slightly; whereas, under temperature drop down to 77K, ultimate strength of the glass grows by almost 2 times. Failure of of quartz- glass samples , within 373K … 77K range of test- temperatures, has always the brittle character.

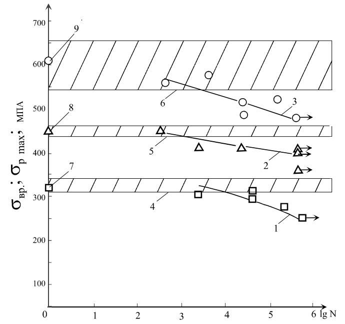

Fig. 1 Characteristic curves of fatigue resistance for carbon- plastics (lengthwise orientation) at alternating tension: curve 1- at 373K; curve 2 - at 293K; curve 3 - at 77K; 4 through 6 – fields of dissipation for values of parameter ($\sigma_B$), at 373K, 293K and 77K, correspondingly; 7 through 9 - $\sigma_B$average values obtained at 373K, 293K and 77K, correspondingly; ($\sigma_{Pmax}$) - maximal tension stress within a cycle

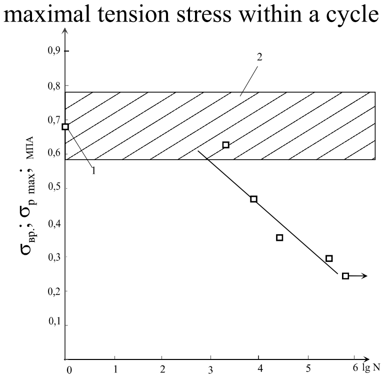

Fig. 2 Characteristic curve of fatigue resistance for bonding glue under alternating stretching at 293K:

1- average value of ultimate tension ; 2 - field of dissipation for values of ultimate strength

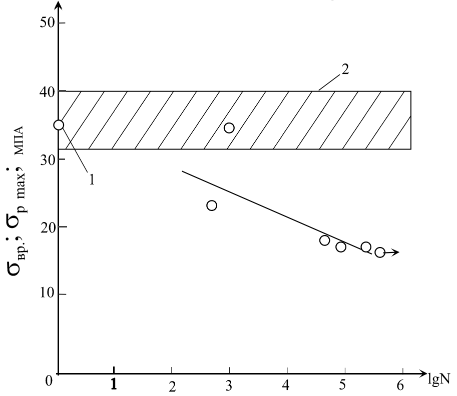

Fig. 3 Characteristic curves of fatigue resistance for bonding glue under alternating stretching, at 150K:

1- average value of ultimate strength , 2 - field of dissipation for values of ultimate strength

Thus measured experimentally mechanical characteristics of materials have been used for analysis of stress- strain state under thermal gradient loading, of Solar cell batteries' panels intended for Space vehicles' applications.

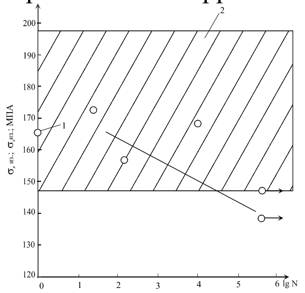

Fig. 4 Characteristic curve of fatigue resistance for Silicon crystal (type 1-a test- samples) under symmetric bending, at 77K: 1- average value of ultimate strength of Silicon, 2 - field of dissipation for values of ultimate strength of Silicon

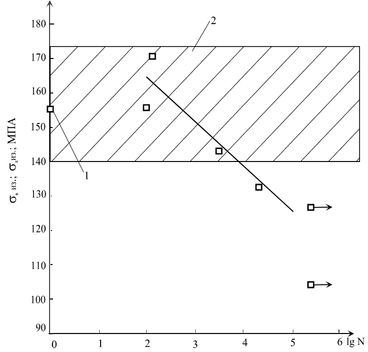

Fig. 5 Characteristic curve of fatigue resistance for quartz- glass, under symmetric bending, at 373K:

1- average value of ultimate strength of quartz- glass; 2 - field of dissipation for values of ultimate strength of quartz- glass

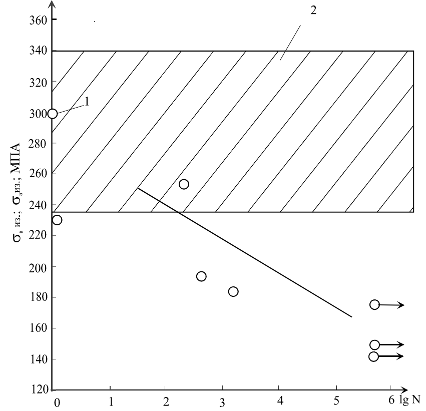

Fig. 6 Characteristic curve of fatigue resistance for quartz- glass, under symmetric bending, at 77K:

average value of ultimate strength of quartz- glass, 2 - field of dissipation for values of ultimate strength of quartz- glass.

# STUDY OF NANOSCALE HETEROSTRUCTURE MATERIALS BY DENSITY FUNCTIONAL TB AND PATH PROBABILITY METHODS

**Masuda-Jindo K., Kikuchi R.**$^{(1)}$
Department of Materials Science and Engineering, Tokyo Institute of Technology, Nagatsuta,
Midori-ku, Yokohama 226-8503, Japan
$^{(1)}$Materials Science and Mineral Engineering, University of California,
Berkeley, CA 94720-1760, USA

Self-assembled semiconductor quantum dots and nanocrystals are now being widely fabricated for applications as optoelectronic devices, biological labels and for other purposes. For quantum dots, epitaxial growth in the Stranski-Krastanow mode has emerged as one of the promising fabrication techniques. Similarly, wet chemical techniques have been utilized to produce semiconductor nanocrystals, e.g., CdTe, CdSe, and CdS systems and also quantum-dot-quantum- well nanocrystals. The importance of diffusion as a tool for post-growth tuning of the energy levels has been realized for a long time and, using rapid thermal annealing techniques, has been successfully demonstrated in semiconductor quantum-well structures. The present paper aims at extending the interdiffusion studies of nanoscale heterostructures theoretically. The energy levels and exciton energies in quantum dots and nanocrystals are investigated using the ab initio TMBD and path probability methods (PPM) including the many-body effects, the Coulomb interaction, strain, interface mixing are taken into account. The finite differences method in the framework of the effective-mass and envelope function approximation is also employed for comparison to calculate the single-particle energies and the Coulomb interaction energy of the exciton. Here, the generalized tight-binding molecular dynamics (TBMD) method is used to study the optimized atomic structures and electronic properties of the nanoscale materials. We also report that the thermodynamic and mechanical properties of the nanoscale materials are quite different from those of the corresponding bulk materials. The critical layer thickness for generating the misfit dislocations are investigated for the semiconductor heterostructures with interface disorder [1—2].

[1] K. Masuda-Jindo and R. Kikuchi, Int. J. of Nanoscience, **1**, (2002) 357—371
[2] K. Masuda-Jindo, V. V. Hung and P. D. Tam, Phys. Rev., **B67** (2003) 094301—1.

# INVESTIGATION OF BORID COATING STRUCTURE AND PROPERTIES ON THE BORON-CHROMIUM-PLATED CARBON STEEL

**Spiridonova I.M., Pilyaeva S.B., Zdorovets N.A., Fedorenkova L.I.**
Dniepropetrovsk National University,
per. Nauchniy 13, Dniepropetrovsk, 49050 odm@ff.dsu.dp.ua

During borated in powder medium the boride layers with high hardness and wear-resistant are formed on steel parts. However their use have been limited because of brittleness and heat-resistant.

The increase of physic-chemical characteristics of the boride coating is provided by diffusion saturation of steel surface with boron and chrome (boron-chromium-plated).

Therefore the investigation results of boron content coating structure and properties formed during treatment in the powder medium consisted of boron carbide and activator $CrF_3$ have been realized in this work.

The boride layer structure and properties was investigated by metallography, X-ray structural and durametric analyses. Crack resistant (critical coefficient of strain intensity $K_{1C}$) was determined according method [1] with formula:

$$K_{1C}=(0{,}016\pm0{,}004)(E/H)^{1/2}P/C^{3/2}$$

where E – Young's modulus, H – microhardness, P – indenter load, C – radial crack dimensions.

Surface roughness after boron-chromium-plated was determined by the profile recorder M201.

Diffusion saturation was realized on steel parts of steel 45, in the steel containers in powder medium. In this powder medium a boron carbide fraction of total mass changed from 65 to 80%, a chrome three-fluoric was within limits of 20—35%.

The saturation process was carried out in pressurize container with fusible seal under the temperature 950±10 °C and time of stand in furnace over the 2—6 hours.

The powder medium compositions were given in tabl.1. Table 1

| Components | Components content, fraction of total mass, % | | | |
|---|---|---|---|---|
| | 1 | 2 | 3 | 4 |
| Boron carbide | 65 | 70 | 75 | 80 |
| Chrome three-fluoric | 35 | 30 | 25 | 20 |

Dependence of coatings thickness on saturation time to the different temperatures and compositions were shown in Fig.1.

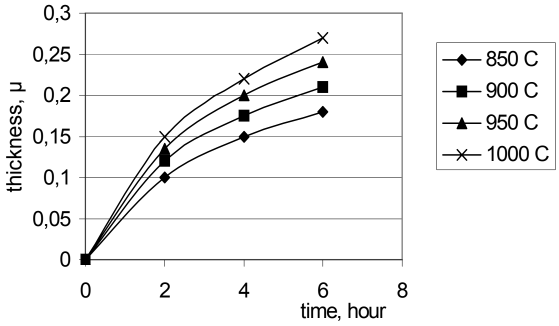

*Fig.1 Influence of temperature and treatment duration to thickness of boron-chromium-plated layer*

The thickness of boron-chromium-plated layer, microhardness of structural components, crack resisting (critical coefficient of strain intensity $K_{1C}$) and surface roughness of steel 45 depending on composition of mixture after treatment under temperature 950±10 °C and treatment duration 4 hour were shown in table 2.

Table 2

| Component | Thickness of layer, µ | | Micro hardness $H_\mu$, MPa | | $K_{1C}$, MPa·$m^{1/2}$ | | Sur face rough ness $R_a$, µ |
|---|---|---|---|---|---|---|---|
| | (Cr,Fe)B | Total | (Cr,Fe)B | $(Cr, Fe)_2B$ | (Cr, Fe)B | $(Cr, Fe)_2B$ | |
| 1 | 30-50 | 130-150 | 23770 | 19740 | 1,79 | 2,95 | 1,5-1,7 |
| 2 | 40-50 | 200-220 | 22660 | 18600 | 1,81 | 3,1 | 1,1-1,2 |
| 3 | 40-45 | 220-250 | 22750 | 18539 | 1,83 | 3,22 | 1,2-1,3 |
| 4 | 30-40 | 180-200 | 20900 | 17940 | 1,8 | 3,0 | 1,5-2,1 |

The chemical reactions with forming of boron haloids compounds and chrome ions take place in the heating process of steel parts in the powder medium consisted of boron carbide and chrome three-fluoric. Increase of boron and chrome diffusion velocity is observed in these conditions.

According to X-ray structural and metallography analyses the diffusion zone consist of (CrFe)B layer with addition $(CrFe)_5B_3$ and $(CrFe)_2B$ phases.

Microstructure of boron-chromium-plated layer was shown in Fig. 2.

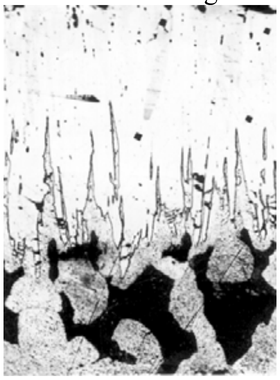

*Fig .2 Microstructure of diffusion zone after boron-chromium-plated, X300*

Addition of alloy components in the powder medium based on boron carbide usually is accompanied by decreasing of saturation velocity and diffusion zone thickness [2]. In the given powder medium an alloy component includes in activator composition. These make the boron-chromium-plated layers are more thickness for short treatment duration. This layers have more microhardness and crack resistant in comparison with those, which were formed in medium, consisted of boron carbide and activator NaF [3]. The given composition allows to increase a saturation velocity by boron and chrome, to decrease a brittleness and crack resistant of the boride layers, as well as to receive a less surface roughness after diffusion saturation.

Heat resistant and abrasive resistant of the boron-chromium-plated layers allow their using under condition of the gas corrosion and corrosion-abrasive wear.

Conclusions: The presence of activator $CrF_3$ in the composition of powder medium provides a high velocity of diffusion saturation, allows receiving the boride coatings alloying by chrome with high microhardness and crack resistant.

## References

1. N.V. Novikov, S.N. Dub, S.I. Buluichev. Methods of microtests on the crack resistant. Plant laboratory. 1988 г. №7. P.60—67.
2. Y.V. Dzyaduikevich, N.I. Zabolotskaya. Influence of additions on diffusion saturation process for refractory metal and alloys. – Protective coating on metals. 1989. 23. P. 64—67.
3. Chemical-heat treatment of metal and alloys. M. – “Metallurgy”, 1981, 424 p.

# ANALYSIS OF INFLUATION RULE OF CRACK WITH SUBSTRUCTURE IN DEFORMATION ORIGIN NANOMATERIALS

**Borysovska K. M., Podrezov Yu. N., Verbylo D. G.**
Institute for Problems of Material Sciences of NASU
3, Krzhizhanovsky Str, Kiev, 03142, Ukraine, kmb@materials.kiev.ua

Nanocrystalline materials is one of the perspective directions of material science. Their high properties could be used for work in extremely conditions with high mechanical and vibration loading. The requirement for this materials are high strength, hardness and fracture toughness. All these properties are connected with structure of a material.

Research of quasicleavage fracture of nanoiron created using EACP method, have shown, that the nanostructure creation results in repeated increase of fracture toughness for a crack propogating in planes perpendicular to the plane of deformation. At the same time it is revealed, that at crack propagation in a plane of deformation, nanomaterial exhibits heightened predilection to a exfoliation, which one is accompanied by a decrease of power inputs on material fracture.

It is possible to explain this effect by abrupt increase of crack tip shielding when the edge of a plastic zone becomes close to grain boundary. The grain boundary is a reliable barrier to dislocations so then the edge of plastic zone reach the grain boundary, the sharp increase of dislocation density takes place on the plastic zone edge near to the crack tip. This leads to a substantial increase of fracture toughness.

The sharp increase of a shielding effect of a crack tip at nearing of edge of a plastic zone to grain boundary can result in full compensation of external stress and closing of a crack.

In this case the source of destruction appear in the head or in nearby boundary of a pile-up with a further confluence with a main crack. Thus, when the grain size is comparable to or less then that the size of a plastic zone, the mechanism of destruction change from direct to counter, which result in a sharp increase of fracture toughness.

We have modelled interaction of a crack and dislocations, emitted from its tip with a dislocation wall located near to tip of a crack. The image force as well as interaction between dislocations in a wall and emitted dislocations was taken into account. The change of a stress field near crack tip without dislocations emitted and under different conditions of a dislocation multiplication from a zone, near to crack tip was analyzed. The model allows to observe the evolution of dislocation structure near to tip of a crack and to estimate the influence of a size effect (spacing interval up to a dislocation wall) on a stress field in the region of crack propagation.

The calculation results allow to estimate the influence of the shielding effect of dislocation wall on the fracture toughness and J-integral. It was shown that the wall leads the substantial growth of the dislocation crowd near the crack tip, that in turn leads to increase of fracture toughness.

Within the framework of proposed model we have analyzed the possible reasons of the fracture of material along the nanograin boundaries. The role of effects of segregation and fields of elastic stresses in an energy balance of destruction is reviewed. The role of a size effect in an energy balance of destruction is considered.

# INVESTIGATION OF TOTAL EMISSIVITY OF TERMAL INSULATION MATERIALS AND COATINGS AT EXTREMAL TEMPERATURES

**Paderin L.**
Central Aero-Hydrodynamic Institute (TSAGI), Zhukovsky, Russia
Zhukovsky, 140180, Moscow Region, Russia, E – mail: pader@inbox.ru

The knowledge of total hemispherical emissivity of materials and coatings is of basic interest for the design and development of high temperature structures. Taking into account, that at high temperatures the radiant properties including total emissivity of materials and coatings are often most sensitive to the specific environments, first of all gaseous components, it is desirable to perform the investigations of above properties in simulated operating conditions. By present time in the most degree base of data, provided the total emissivity temperature relations, have created for high conductive materials, first of all for metals. Investigation of thermal insulation materials and coatings on ones is more complicated problem. Therefore these materials have studied in significantly smaller degree. In the main, it is caused by the methodical difficulties, connected with heating and measuring temperature of test sample examined surface. Because of low heat conductivity the total emissivity measurements on these materials at high temperatures (T>1000K) require that the radiation heater and the radiation detector are to be located on the same side of the test sample. In this case, the measurement of the radiation flux emitted from the sample surface is complicated by the heater radiation, which is reflected from the sample simultaneously. Therefore, total hemispherical emissivity measurements are most complicated because the radiation detector is to be located at a relatively short distance from the test sample surface. This causes intensive radiant heat exchange between sample and radiation detector and, by it possible significant measurement errors in addition. The measurement of sample examined surface temperature create serious problem since the traditional contact and optical methods of temperature measurements are practically not applicable. Especially, it is related to hemispherical emissivity investigation of sample, which examined surfaces should be isothermal. Therefore, a new special method is to be created to measure sample surface temperatures taking into account the particularities of emissivity measurement method and facility.

In literature the methods and facilities for normal emissivity measurements (total and spectral) of thermal insulation materials under vacuum conditions are presented above all. Information about measurements of the total hemispherical emissivity as well as directional emissivity of these materials at high temperature is not discussed.

In proposed paper some modifications of method and facility for measurements of total hemispherical and normal emissivities are presented. Total emissivity is evaluated from the measurement of the heat flux radiated from the examined surface of a test sample, which rotates in an isothermal heating zone of controllable temperature, and comparing radiation fluxes from test samples and blackbody model at the same temperature. Facility comprises the following basic units: vacuum chamber, mechanism for rotating of a sample with adjustable speed, radiant heater, calorimeter type radiation detector, temperature sensors and thermal insulation outlined the heating zone. Unlike to known methods the radiation detector is placed inside of chamber immediately in heating zone, that permits to measure hemispherical radiant flux from a test sample. A test sample is either a disk of 120÷200 mm diameter or a square plate of 120 to 150 mm length. The sample thickness ranges from 0.1 to 50 mm. In particular, samples of up to some millimeters in thickness are to be manufactured of high conductive material. If the sample thickness is less than50 mm, an extra insulation corresponding differential thickness is arranged between the sample and its support. Concrete peculiarities and parameters of method and facility variants depend of emissivity type, operating conditions, temperature range of measurements and test sample parameters. The test facility is optimized to get the sample surface as isothermal as possible, so that the potential systematic error caused by speed of rotating sample as well as by reflection of the heater radiation from the test sample surface are negligible. Prior to the measurements the radiation detector is calibrated under operating conditions in the setup by means a spherical model of a black body under vacuum conditions (P<10 Pa). If the measurements are to be performed at gas pressure (P>10Pa), additional calibration of the detector is carried out for the prescribed pressure/temperature range using a reference sample of known and stable temperature dependent emissivity. At present time the existing methods and facilities enable the following measurements: 1) hemispherical and normal emissivities under vacuum conditions in temperature range 150K≥T≤2000K and at adjustable air pressure, simulating operating conditions, in temperature range 500K≥T≤1600K. Absence of intermediate absorptive and reflective medium and elements between a test sample and radiation detector, contactless method for evaluating test sample temperature as well as calibration of radiant detector in operating conditions provide the high accuracy of measurement. The uncertainties are assessed for measurements of hemispherical and normal emissivities to be lower than 5%. The developed methods and facilities in the following enable the investigations practically on any types materials, structure rigid and flexible components as tiles, honeycomb, blankets and other flat sample as well as of thermal control coating on ones. The test results of different materials and coatings are presented.

The work was performed at financial support of INTAS in the frame of project № 00 – 652.

# THE ROLE OF DISPERSED “QUASI-PARTICLES” OF CRYSTALLINE BODY IN STRENGTHENING OF TITANIUM AND HIGH-STRENGTH ALLOY VT-22

**Minakov V.N., Minakov N.V., Puchkova V.Y.**
Frantsevich Institute of Problems of Materials Science of NASU,
3, Krzhizhanovskogo St., 03142, Kiev, Ukraine, E-mail: altifer@ipms.kiev.ua

The TEM dark-field images of alloy VT-22 (Ti - 5Al - 5V - 5Mo) show that dispersed quasi-particles with size 50 ÷ 100 A are present inside α- and β-phases, fig. 1. The additional reflexes were not detected on the electron-diffractions. Also the additional diffraction maximums were not discovered on diffractograms in monochromatic Fe $K\alpha_{1,2}$ X-ray within the angle range of $2\theta = 20^0 \div 142^0$.

The results of interference lines width processing (according to [1]) are represented on fig. 2. The segments intercepted on axis of abscissas correspond to the areas of the coherent reflection and are equal to ~ 0,1 mkm for β-phase and to average value 0,1-0,15 mkm for α-phase. The line slope (fig. 2) displays change of stresses: in forged state they are equal for α- and β-phases, but annealing of alloy at $750^0$ $\tau$=1 hour reduces stresses.

An increasing of the X-ray background (fig.3) was established during research of titanium and alloy VT-22. It occurs at the reduction of the reflection angle $2\theta$ from $45^0$ to $20^0$. Increase of the X-ray background at small angles depends on electron density change. Variation of electron density and formation of small-angle dissipation X-ray quanta is already described for initial stages of the decay supersaturated solid solutions of the Guinier zones [2], in case of colloidal and dispersed low-bounded particles and others [1, 2, 3]. The crystalline structure of the particles is unessential. The size of particles is a determining factor. Increasing of the background is observed for the size of particles less than 1000 A. Maximum size of particles is defined by formula

$$d = \frac{\lambda}{2\Theta^*},$$

where $2\Theta^*$ is an angle on difractogram, by which diffuse dissipation merges with X-ray background according to Debay-Waller factor; d - the size of particles; λ - a wavelength of the characteristic radiation.

The X-rays diffractograms within the angle range $2\theta = 20\text{-}45^0$ are shown on fig.3. Increasing of the background was observed for filings, cold-rolled titanium foil, titanium forged by 3 axes, alloy VT-22 both after forging by 3 axes and with the subsequent annealing at $750^0$C, $\tau$ = 1 hour. The size of dispersed “quasi-particles” is ~ 3A. Data of X-ray diffraction analysis and transmission electron microscopy indicates the difference in size of dispersed “quasi-particles” in crystalline body that probably can be explained by moiré effect related to the superposition of reflections from curved planes. The curve of planes was observed by the method of high resolution electron microscopy of γ-phase in premartensite state and α-phase after martensite transformation in Ni-Al intermetallide [4] and ferrous alloys [5, 6, 7].

Data represented on fig. 4 show that modulus of plasticity increases at reduction of the test temperature (tangent of the line slope angle). The modulus of plasticity increases and true deformation before destruction decreases at the strength increasing. Strength (yield true fracture stress) increasing is caused by the strengthening by both the forming of the crystal boundaries (of cells, nanocrystalls) and formation of the dispersed “quasi-particles” of crystalline body. Forming of the dispersed “quasi-particles” of crystalline body is accompanied by increasing of the strength parameters at conservation of large values of plasticity. It is possible to state that deformation of micro- and nanocrystalline titanium and alloy VT-22 with dispersed “quasi-particles” occurs self-similarly.

## LITERATURE

1. Taylor A. X-ray Metallurgy. - M.: Metallurgy, 1965. – 663 p.
2. Pines B.Y. The Lectures on Structural Analysis. Kh.: Publ. House: Kh. university, 1967. – 476 p.
3. Guinier A. The Radiography of Crystals. - M.: St. Publ. House of phys.-mat. lit-re, 1961. – 604 p.
4. Tanner L.E., Schryvers D., Shapiro S.M. Electron microscopy and neutron scattering studies of premartensitic behavior in ordered Ni-Al β-phase //Mater.Sci.Eng., A127. – 1990. -205-213p.
5. Fujita F.E. A statistical thermodynamic theory of pre-martensitic tweed structure // Mater.Sci.Eng. A127. – 1990. - 246-248p.

6. Researching of Lattice Dynamics and Fine Structure of Face-centered Alloys of ferrous-nickel system . // PMM. -T. 66, 4. - 1988.

7. Taylor K.A., Chang L., Olson G. Spinodal decomposition during aging of Fe-Ni-C Martensites // Metal.Trans., 20A, №12. –1989. - 2717-2737p.

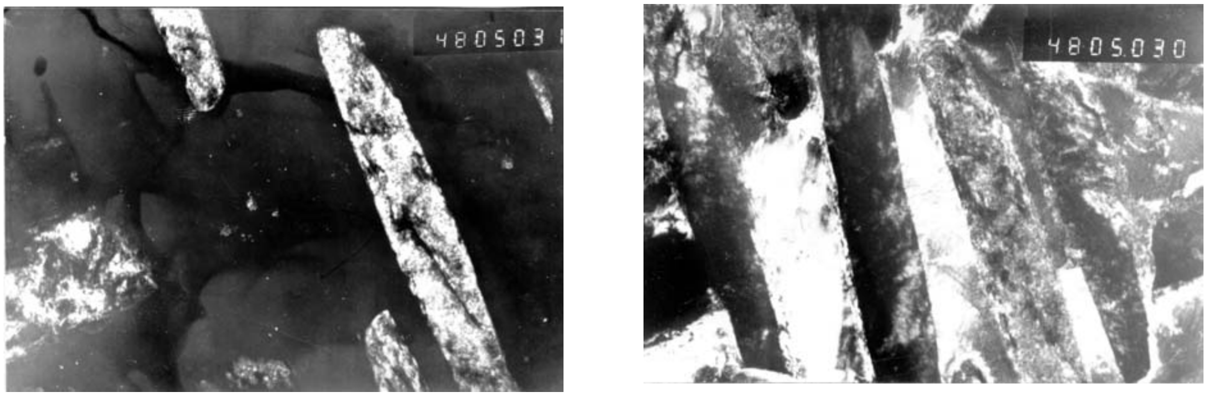

Figure 1. TEM dark-field images of: a - α-phase of the alloy VT-22; b - β-phase of the alloy VT-22.

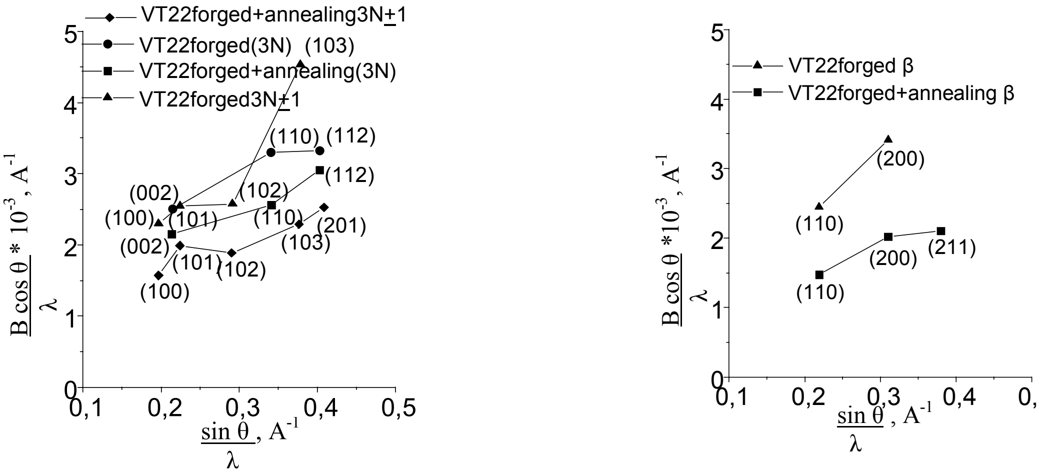

Figure 2. Dependence of line spreading from reflection angle: a - α-phase of the alloy VT-22; b - β-phase of the alloy VT-22.

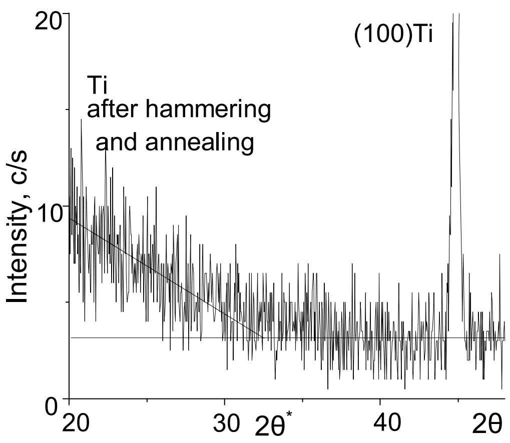

Figure 3. Diffuse dissipation of the forged alloy VT-22.

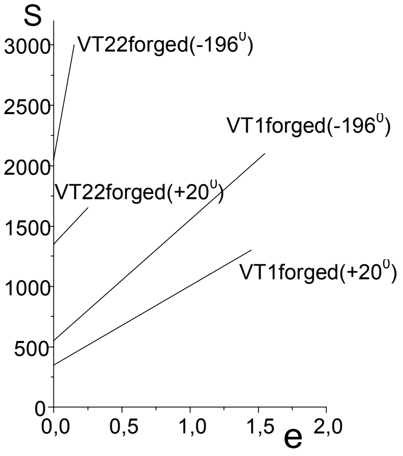

Figure 4. True values of stresses and plasticity at single-axis strain.

# MECHANICAL PROPERTIES OF HIGH POROUS METALLIC MATERIALS WITH POROUS SPACE STRUCTURE CORRELATION

**Boitsov O., Chernyshev L.(1), Solonin S.(1)**
Kurdyumov Institute of Metal Physics of NASU
36 Vernadsky Str., Kiev, 03142, Ukraine
(1)Frantsevich Institute for Problems of Materials Science of NASU
3 Krzhyzhanovsky Str., Kiev, 03142, Ukraine

High porous metallic materials could be used for the operations at high temperatures, inetrelectrode mountings in plasma oscillators of high capacity for cutting or joining of metallic details, for example.

Such materials with porosity of 60-80% could be obtained from metallic powders using removal of pore-formed substance while sintering, for example, urea or ammonium bicarbonate. This technology allows to vary widely the characteristics of porous material space – pore sizes, various porosity kinds.

One of the most important operational characteristics of porous materials is the mechanical strength. Well-known researches of these characteristics usually connect them with the values of general porosity, paying less attention to the theoretical description of porous structure elements influence on mechanical characteristics of porous materials.

In this connexion main task of the work is the research of correlation of mechanical strength of porous powder materials, obtained by pore-forming, and their pore space. The materials of such a class were selected because their porous structure and the structure of usual powder materials differs by vaulted character in porosities more than 46%. In one's capacity of investigated materials were used the samples of porous nickel. Data about their mechanical characteristics are shown on fig.

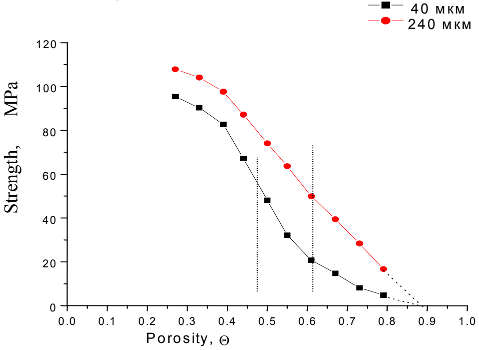

Obtained results certify about more high values of materials' porosity, while obtaining of which was used more massive pore-forming powder. Besides, the calculations show that obtained dependencies are described most sufficiently by S-like curve, the equation of which could be presented as:

$$\sigma = \frac{\sigma_{\max} - \sigma_{\min}}{1 + \exp\left(\frac{\theta - \theta_c}{\delta}\right)} + \sigma_{\min} \quad (1)$$

where $\sigma_{max}$, $\sigma_{min}$ - the highest and the lowest value of strength, $\theta_c$ – porosity, at which the greatest strength change occurs, $\delta$ - parameter that shows speed of strength alteration at $\theta_c$, $\theta_c$ – current strength.

The metallic phase of our porous material is an object of extremely developed surface that allows to attribute it to fractal objects, and consequently in the S-like curve extreme at $\theta_c$ porosity the strength should change greatly.

In the result of electroconductivity of porous samples measurement on alternating current and application of enlarging nets method in separate images of microstructure there was determined that at $\theta_c$ porosity area the alteration of metallic phase fractal degree was observed, which corresponds to the geometrical change of phase from quasi-three-dimensional to quasi-bidimensional structure of metallic phase.

According to M. Balshin [1] work the material situated between pores represents critical zone or locus which transmits load. This critical zone could be shown as the value proportional to the square of interphase surface S that could be accordingly to the work[2] evaluated in such way:

$$S=\frac{3\left[G\theta^{2}+\theta(1-\theta)\right]}{D_{p}},\qquad (2)$$

where G – matrixity [2] of the material, $\theta$ - porosity, $D_p$ – pore size.

Besides, assuming that the geometrical transition point $\boldsymbol{\theta_c^*}$ is an analogue to percolation threshold, it could be defined as:

$$\boldsymbol{\theta_c^*=\theta_c(1-G_{0,5})+G_{0,5}},\qquad (3)$$

where $\theta_c$ – geometrical transition point in the system with pore-former pore size that equals metallic phase powder by particle size.

Subject to that strength of investigated porous material in our case has minimal and maximum values at porosities 10 and 80%, we substitute $S_{max}$ and $S_{min}$ in the equation(1).

$$\sigma=\frac{\sigma_0}{D_p}\left[\frac{1,92G_{0,8}-0,03G_{0,1}+0,21}{1+\exp\left[\left(\theta-0,5+1,5G_{0,5}\right)\right]/\delta}+D_p-1,92G_{0,8}-0,48\right]$$

The analysis of this equation shows that one of the most important factors, which define the mechanical strength of porous material, is matrixity of porous space. The higher it is (i.e. larger pore size), the higher strength is.

1. Bal'shin M., Kiparisov S. // Principals of Powder Metallurgy (Rus.). — M.: Metallurgiya, 1978. — 177 p.
2. Skorokhod V. // Theory of porous and composite materials physical properties and principals of microstructure management in technological processes // Powder Metallurgy (Rus.). — 1995. — #1/2, P. 53—71.
3. Skorokhod V. // Structure-percolation effects in theory of general conductivity of ceramics and ceramic composites (Rus.) // Ceramics 47. Polish ceramics bulletin. – 1995. — # 9. — P. 39—46.

# TRIBOTECHNICAL PROPERTIES OF NANOCOMPOSITES AL-SIC, AL-SIC-MNS

**Antsiferov V.N., Gilev** V.G.(!), **Rabinovich** A.I.(i)
Research Center of Powder Materials Science, Perm, Russia, patent@pm.pstu.ru (1)ZAO «Novomet-Perm», Perm, Russia, Gilev@novomet.ru

Nanoporous silicon carbide ceramics is used for reception of Al-SiC and Al-SiC-MnS nanocomposttes. The combination of nanopores and greater channel pores in ceramic performs allows to receive the composites incorporating extensive nan o structured Al-SiC sites with inclusions of firm greasing of manganese sulfide. Tribotechnica! tests were carried out in conditions of a sliding friction in pair with steel without greasing and at greasing by water have. The high density, hardness and nanostructured condition of a part of volume of a material provides increased wear resistance and in some cases a low friction factor.

The purpose of the search is reception of nanostructural composites both abrasive stable and simultaneously possessing antifriction properties.

Nanocrystal metal materials have high strength, hardness and passive hardness. Transition to nanostructures frequently ensures simultaneously raise of passive hardness and decrease of friction coefficient.

Composite materials such as Al-SiC, and Al-SiC-MnS where Al is an alloy on .the basis of aluminium AK5M2U.2 are received by the method of impregnation of nanoporous SiC-ceramics by metal alloys under pressure.

Ceramics on basis SiC with pore size about 10-100 nanometers and porosity of 45-60 % which was gained from the ultradisperse reaction mixtures of silicium and blacklead with a specific surface area of 120 m2 / g reactionary sintering with the negative volumetric effects was used [1]. The given ceramics is characterized by the high strength caused by nanocrystal state of a carcase [1], and also - low temperature of a synthesis that allows to induct into an initial intermixture for reception ceramic perform, rather low-melting additives of solid lubrications. In the capacity of solid lubrication additives of a powder of sulphide of manganese are used.

Application of performs with the composite hierarchy of the porous structure with micro and nanopores along with the grid of larger channel pores has allowed to receive the dense samples of the composites incorporating extensive nanostructural areas by pressure injection.

Tribotechnic properties of KM at a slip in a pair with a steel at a dry friction and at a greasing water are defined. The friction coefficient of composites Al-SiC at a dry slip on steel X12M with velocity of 3 km/s oscillates in limits 0,4-0,9.

Injection of manganese sulphide in composites Al-SiC 25-40 % insignificantly reduces friction coefficient at a dry friction on steel, but essentially raises passive hardness at heightened pressures, increments maximum permissible pressure at a dry friction up to 0.8 MPa. The magnification of passive hardness is more essential at injection MnS during greasing water, the phenomena reminding effect of unabrasiveness are observed in this case.

1. Gilev V.G. Synthesis of micro and nanoporous materials from silicium carbide in the ultradisperse reactionary systems // The Magazine of Applied Chemistry. 2004. T.77, K«4. pp. 538-543.

# SOME ASPECTS OF APPLICATION OF COMPOSITE MATERIALS IN UNITS OF FRICTION SUBMERGED ELECTRIC MOTORS (SEM) WORKING IN EXTREME CONDITIONS

**Kurilov G.V., Kurilov A.G.** (1)
Research-and-production corporation "Technology - 2000"Ltd, Kharkov, Ukraine
pr. Moskovsky, 140/1, Kharkov, 61120, Ukraine, kt_2000@ukr.net
(1)Research-and-production corporation "Technology - 2000"Ltd, Kharkov, Ukraine
pr. Moskovsky, 140/1, Kharkov, 61120, Ukraine

Conditions of operation and mechanical intensity of separate units, in particular bearings of sliding, and details SEM results in necessity to apply to their manufacturing new progressive composite materials, more modern technology of processing; constantly to improve their design; precisely to define geometrical parameters and mechanical characteristics due to the improved methods of calculation and bench tests.

Use of methods of powder metallurgy allows to solve a number of the important scientific and technical problems. Powder composite materials distinguish valuable advantages, namely an opportunity of reception and regulation of various characteristics: durabilities, thermal stabilities, corrosic stability porosity, hardness, damping and antifrictional properties due to introduction of various additives, changes of manufacturing techniques. [1]

One of basic units SEM are: the basic (radial) bearing of sliding, which case works in a variable magnetic field and should possess high specific electroresistance as much as possible to weaken currents of Foucault directed in the bearing and heating; the persistent bearing, the taking up weight parts of rotors of SEM, and also condensation face relit a rotating shaft which basic purpose is protection against penetration stratum liquids in cavity SEM.

In connection with the high requirements showed to characteristics SEM, actual there is the questions connected to definition of physicomechanical properties, such as durability, pliability, wear resistance of the composite materials used in units of friction. The pliability of bearing support determines a line of important dynamic properties SEM, including resonant sites of a spectrum of vibrations and the dynamic forces working on the part of a rotor on bearing unit.

The problem of increase of reliability and durability of machines is closely connected to the decision of questions of application of lubricants for units of friction and as a whole with the decision of the questions concerning the theory of friction, greasing and deterioration which now takes rather important place in aspect of problems of mechanical engineering. One of the effective means protecting rubed surfaces from dripping and subsequent deep pull out, creation between them of special layers of greasing is: easily deformable, maintaining the repeated mechanical influence, having strong connection with the basic material, keeping the properties in the set range of temperatures. For these purposes firm lubricants to which number the layered firm substances possessing owing to the crystal structure in low factor of friction concern have found wide application: graphite, $MoS_2$, $WS_2$, $MoSe_2$, WC, BN, mica, talc, etc. These materials are applied as a powder rendered on working surfaces by a method of rub in, as firm coverings with use as binding various organic and inorganic pitches, and also as filled of ftoroplast , have received a wide circulation and have won a strong place at the decision of the problems connected to decrease of friction and deterioration [2, 3].

The essential role in deterioration of the tool at cutting steel is played with the abrasive-mechanical wear process caused by friction of the tool about firm particles, contained in a matrix of a processable detail. Changing a chemical compound of steel, alloying it separately or in combinations with sulfur, lead, selenium or phosphorus, it is possible to render essential influence on structure and morphology of superfluous metal and nonmetallic phases (sulfides, selenids) and, as investigation, on machining of steel. [2]

Experience of last years on application HLM of the connected pairs friction has shown, that for the units working at insufficient greasing, the most perspective from the point of view of maintenance of reliable work are materials on a basis ftoroplast, possessing good antifrictional and antiwear the characteristics, having low factor of friction and stable antifrictional properties at rise in temperature. However application of ftoroplast is limited, that is connected to its mechanical and physical and chemical properties. Besides factor, friction and wear resistance of ftoroplast temperature, loading substantially depend on such factors, as speed of sliding, conditions of greasing, hardness and a roughness of the material working with it in pair.

Way of improvement of physicomechanical characteristics and effective utilization of ftoroplast in units of friction is application as a material for bearings of compositions of ftoroplast with fillers or ftoroplast introduction in a metal porous skeleton.

Lead before research on application of metalftoroplast bearings of sliding in submerged electric motors (SEM) used for an oil recovery, have allowed to draw a conclusion about them enough high reliability in operation. Measurement of the moments of friction on researched bearings (steel - bronze and steel-metalftoroplast) in a range of temperatures of oil 40—160 °C at constant speed of sliding $\upsilon$=and on bearing N=150N has shown 4,71 km/s to loading, that the best antifrictional properties the pair friction steel - metalftoroplast possesses.

Are conducted theoretical and experimental researches of a feasibility of parts SEM, made a powder metallurgical technique, the powdered materials for them are selected, the methods of manufacturing of parts and conduct SEM, under operating conditions on crafts are studied.

The researches have shown, that parts made a powder metallurgical technique for SEM (turbine and a bore protector of a material ЖГр1, bearing case from a material ПТХ4-2 and support from a material ДО4Ц4Гр2Мс3Б [3, 4]) answer presented requests and are recommended to operation.

The perspective application of items made of the set forth above materials, has allowed to save raw material, semifinished items and specially, that is very important, to lower the costs of manufacturing of parts SEM at simultaneous preservation of the main figure of merits and reliability of electric motors.

1. Курилов Г.В. Трение и износ, 1983, т. 4, № 3, с. 499.
2. Резников В.Д., Курилов Г.В., Ходос Л.С., Панфилова Л.М., Богомолов С.И. Проблемы прочности, 1985, № 2, с. 60.
3. Гребень А.М. и др. А. с. 1455743 (СССР) от 01.10.1988 г. Спеченный антифрикционный материал на основе меди и способ его получения.
4. Курилов Г.В. А. с. 1521948 (СССР) от 15.07.1989 г. Подпятник для машин с вертикально вращающимся валом.

# STUDY ON FRICTION AND WEAR BEHAVIOR OF PARTICLES REINFORCED ALUMINUM ALLOY MATRIX COMPOSITES UNDER DRY SLIDING CONDITIONS

**Chernyshova T.A., Kobeleva L.I., Lemesheva T.V.**
A.A. Baikov Institute of Metallurgy and Materials Science
of Russian Academy of Science (RAS), Leninskiy pr-t, 49, 119991 Moscow, Russia

Metal matrix composites (MMCs) based on aluminum alloys reinforced by high modules, high stronger particles characterize attractive properties, such as: high specific stiffness and strength, fracture toughness, electro conduction and heat conduction, wear resistance etc., that make it perspective for wide application in various fields of mechanical engineering. Various examples are known of successful application such MMCs in composition friction pair in lubricated sliding condition. Moreover wear resistance is significantly higher than it bearing bronze or Al-alloys [1, 2].

The data of tribological properties in dry sliding condition are contradictional: coefficient of friction and wear resistance turn out to be higher or lower than its matrix [3, 4]. The reasons of this are considered to be difference in techniques and composition of MMCs, and also in conditions of friction tests.

Therefore, the aim of the present work is to investigate behavior under dry sliding condition and evolution structure of surface layers specimens of unreinforced silumin AK12 and MMCs based on it, reinforced by particles of silicon carbide or polyreinforced by both particles of silicon carbide and graphite. According to patent [5] in specimens of MMCs with polyreinforcements, ceramics particles provide the carrier capacity and wear resistance of MMCs; graphite filler is added to MMCs to create a protective coating on contact surface, i.e. plays the role of lubricate.

Dry sliding wear tests were performed using the test wear machine УМТ-1 in scheme axial loading of ring specimens (GOST23.210-80). Specimens of MMCs for tribological examinations were produced by stir casting route by adding SiC particles with an average size of <3 and 28μm and graphite particles (average size of 63-100 and <400μm) simultaneously to melt of AK12.

Worn surface and wear debris were analyzed by optical and scanning electron microscopes (SEM) and X-ray diffraction. Tribological examinations showed that SiC particles reinforced composites are characterized by higher wear and seizure resistance than binary Al—Si alloy. The addition of graphite particles to Al—Si—SiC MMCs increases wear resistance (Fig. 1) and seizure resistance (Table 1), reduce friction coefficient (Fig. 2).

Microstructural investigations showed that already at low relative translation rates of friction bodies (0,38m/s) and low loads (400N) grooves of plastic deformation towards sliding are formed on friction surfaces of bushes. These grooves are more visible on unreinforced specimens (depth of grooves are more 10μm with spacing between ridges to 0,5μm) and less evident on MMCs specimens, when ceramic particles act as padding elements. At average loading regime on the steady state wear rates in stripes of plastic deformation of MMCs specimens are emerged the signs of structure self-organization in the form of cells with an average size 5—10μm contouring of SiC particles with size ~1μm. The letter can be attributed to decohesion and destruction of particles with following charging they to matrix. The forming of such dissipative or fractal structures on friction surface may define as steady intermediate state providing high wear resistance of MMCs specimens. With increasing of parameters and duration of tests, the width of stripes, where dissipative structures are formed, and size of their fragments are reduced. Simultaneously the zone of plastic shear and rotation are dilated from surface to deep into specimens (Fig. 3). The width of this zone reaches 100—150μm in depending on composition MMCs. The SEM micrographs of worn surfaces of specimens after seizure showed that the reinforcing of matrix AK12 lead to change of seizure site microrelief. In presence of SiC particles seize sites are more fragmentize than that of unreinforced specimens, likely, it's because increasing of alternations frequency of processes of seizing and breaking adhesive bonds. The addition of graphite particles to MMCs improves seizure resistance, in seizure sites increases fraction of area relative slipping of friction bodies.

Thus, carried out investigations testify about high tribological properties of particles reinforced composites based on aluminum alloy AK12. The reinforcing of relatively soft matrix with high hard SiC particles allows to obtain the high value of wear resistance. The polyreinforcing of silicon carbide and graphite provides a low friction coefficient and seizure resistance.

Table 1.
Seizure conditions of AK12 alloy and specimens of MMCs based on it.

| № | Combination of specimens | Seizure parameters | | |
|---|---|---|---|---|
| | | Load P, N | Number of revolutions per minute n | Time before seizure t, min |
| 1 | AK12 | 400 | 600 | 11 |
| 2 | AK12 – 6,5% $SiC_3$ *) | 400 | 600 | 6; 0,75 |
| 3 | AK12 – 5% $SiC_{28}$ | 400 | 1500 | 1,6 |
| 4 | AK12 – 2,5% $SiC_{28}$ – 1,25% $C_{<400}$ | 750 | 1500 | 12 |
| 5 | AK12 – 5% $SiC_{28}$ – 5% $C_{63-100}$ | 750 | 1500 | 8 |
| 6 | AK12 – 10% $SiC_{28}$ – 5% $C_{63-100}$ | 1150 | 1000 | 8 |

*) – here and in the following text, digits near symbols of reinforced particles means an average size of filling.

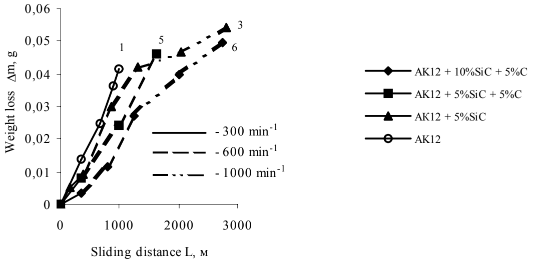

Fig. 1 Weight loss Δm at load P=400H and different sliding rates.

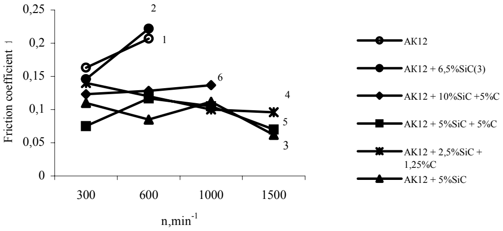

Fig. 2 The relationship between average value of friction coefficient f and number of revolutions per minute n (P=400N).

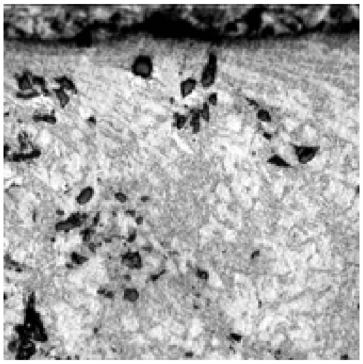

Fig.3 Optical microstructure of MMC №5 AK12 – 5%$SiC_{28}$ –5%$C_{63-100}$ in perpendicular plate of friction surface, after seizure, x350.

## References:

1.*Hosking F.M., Portillo F., Wunderlin R., Mehrabian R.* // J. Mater. Sci., 1982, V.17, №2, p. 477—498.

2.*Chernyshova T.A., Kobeleva L.I., Plishkin D.N.* Trans. IWRI (2001), vol.30. Special Issue: HTC – 2000, p. 529—534.

3.*Sannino A.P., Rack H.J.* Wear, 1995, V.189, №1, p. 1—19.

4.*Pramila Bai B.N., Ramasesh B.S., Surappa M.K.* Wear, 1992,V.157, №2, p. 295—304.

5.*Chernyshova T.A., Panfilov A.V., Kobeleva L.I. et al.* Patent №2171307 "Composite material antifriction purpose for working under semi-dry condition". Reg. 27.07.2001.

# INVESTIGATION OF STRENGTH CAPACITY OF CERAMIC SHELLS UNDER HIGH-TEMPERATURE HEATING

**Lipovtsev Yu.V., Rusin M.Yu.(1), Khamitsaev A.S.(1), Rabinovitch S.V.(2),
Khartchuk M.D.(2), Chermenski V.I.(2), Golementsev L.M.(3)**
Obninsk State Technical University of Nuclear-Power Engineering, Obninsk, Russia
(1)Federal State Unitary Enterprise
"Obninsk Research and Production Enterprise "Technologiya", Obninsk, Russia
(2)Ural State Technical University, Ekaterinburg, Russia
(3)Experimental-Design Bureau "Novator", Ekaterinburg, Russia

In the paper consideration is given to a wide range of problems arising on designing one class of engineering structures whose design model can be presented as a composition of two basic elements: a thin-walled shell of revolution and a thin-walled lap-jointed ring under the action of external pressure and heating. Experience of forming an adhesive-bonded lap joint between a shell and a thin-walled ring has proved itself in the development of many structures with the shells made from brittle materials.

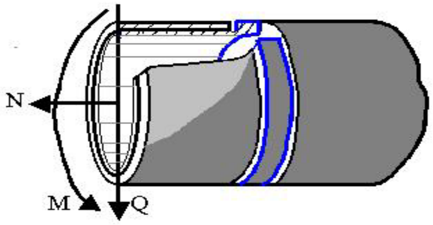

Fig.1. Zone of a ceramic shell-to-metal ring joint

When joining a ceramic shell to a ring it is necessary to provide the stressed-strained state of the shell close to zero-moment and for that to match thermal strains and displacements of the shell and the ring as well as the stains caused by external mechanical effects. Only when thorough studies are carried out at all the stages of the development work: from the development of the new materials with predetermined physical-mechanical properties and the methods of forming large-sized and complex-shaped shells to the final strength tests of the developed structure, one can achieve positive results and complete the entire cycle of the development work with putting the article into full-scale production.

In the thermostressed state of the shell's major part and zone of the shell-to-ring joint, the governing factors are not only external thermal and mechanical effects but also many other factors relating to the interaction between the shell and the ring.

By all the examples of the thermostressed state of the shell and the elements of the shell-to-ring joint we were trying to show consistently that it is essential to start the studies not with provision of a complicated design model but with provision of a sequential system of models the simplest one of which takes account of fewer factors and yet it enables one to have sufficiently simple design equations and to determine the necessary relationships. Then one can use more complicated models and refine numerical results.

For the shells from alumina ceramics having high strength characteristics (elasticity modulus of 70—100 MPa) and high values of linear thermal expansion coefficient in the order of $9 \cdot 10^{-6}$ $K^{-1}$ the problem of joining the elements is solved by means of solders retaining high strength at a temperature as high as 773 K and above and through hard hot-setting adhesives. In this case it is possible to use the rings from composite materials.

For the shells from sitall having strength limits smaller by a factor of 2-3 and a linear thermal expansion coefficient smaller by a factor of 3-5 as those of alumina ceramics, adhesive bonds have been applied using high-resilient sealants with the ring in an outer or internal position.

For the shells from quarts ceramics showing attractive properties with respect to thermal resistance and stability of physical-mechanical characteristics over a wide temperature range, an adhesive bond structure has been developed using a resilient sealant with the ring made from the precision invar alloy 32 NKD [1—3]. The linear thermal expansion coefficient of this alloy varies from $0{,}5 \cdot 10^{-6}$ $K^{-1}$ to $2 \cdot 10^{-6}$ $K^{-1}$ over the temperature range up to 473 K, and the strength capacity of the ceramic shell is fully provided in many structures.

Considerable problems with matching the thermal strains arose on joining an invar ring from the 32 NKD alloy to a glass-ceramic shell. Hence, we have developed new alloys of the super-invar type [2].

As an initial composition for the new alloys, traditional super-invar of the 32 NK type was used. This alloy made from pure industrial materials upon induction melting exhibits linear thermal expansion coefficient of about $8 \cdot 10^{-6}$ $K^{-1}$ over the temperature range of 20—400 °C. However, it has unsatisfactory narrow temperature range for invar effect: its lower limit – martensite transformation temperature is above -60 °C while the higher limit determined by Curie point is at a level of 200°C. That is why we have alloyed by carbon and adjusted the composition for the content of nickel and cobalt.

It is significant to note that the use of Fe—Ni—Co—C carbonic invar alloys is caused by the possibility of achieving improved casting properties, which from the point of view of making complex-shaped and large-sized rings for ceramic shells makes these alloys most preferable among all casting invar and super-invar alloys. Carbonic alloys have increased crack resistance and fluidity. In the case of low content of carbon these properties are similar to those of the well-known casting steels 50L, 55L. At a large content of carbon it is possible to achieve the casting properties typical of high-nickel types of austenitic cast irons - Ni-resist cast irons. Inoculation of the smelt by a rare-earth metal, special alloying, optimization of temperature-time conditions for smelting and casting of these invar alloys have afforded quality castings using different casting techniques. Besides, welding and cutting technologies are suitable for carbonic invar alloys.

Our experimental data and calculations made on their basis for minimization of the linear thermal expansion coefficient allowed us to assume that good results can be achieved through a sufficiently moderate alloying by cobalt. The laboratory experiments with the use of pure initial materials have confirmed this assumption.

As a result of a purposeful work package carried out the new materials have been developed which can be suitable for manufacturing the rings to be connected to the ceramic shells. They include the 32 NKBL, 32 NKMBL and 32 NKHBL alloys.

To justify the application of these materials instead of the 32 NKD alloy for manufacturing the rings, the paper presents the results of calculations of temperature fields and thermal stresses in the elements of an adhesive bond between a ceramic shell and a ring which arise at a different time of exposure to environmental thermal and mechanical effects. Comparative analysis of the use of different materials for the ring has been made for the shells from quartz ceramics and glass-ceramics. The procedure and calculation algorithms used are described in the reference paper [3].

## REFERENCES

1. Romashin A.G., Rusin M.Yu., Tumanov A.I., Khora A.N., Shmatchenko A.P., Lipovtsev Yu.V. Author's Certificate No. 98165 of 5 Sep. 1976, Appl. No.1595213 of 20 Oct.1975.

2. Tchermensky V.I., Rabinovitch S.V., Khartchuk M.D., Maksimova E.V., Rusin M.Yu., Khamitsaev A.S. New materials of the super-invar type ensuring minimization of stresses in metal-to-quartz ceramics joints in aerospace engineering. Proceedings of 16 Scientific and Technical Conference "Structures and technologies for manufacturing products from non-metal materials", Obninsk, 2001.

3. Lipovtsev Ju.V. The statement and algorithms of solving transient axisymmetric boundary-value problems of thermoelasticity for shells. // Pr.MatM.2003. V.67, No.6. P.954-964.

# PHASE OPTICAL AND PROTECTIV SILICON CARBIDE FILMS

**Krupa M.M., Andreeva A.F.(1), Bondar Yu.V.(2), Skirta Yu.B.**
Institute of Magnetism NAS of Ukraine,
36-B, Vernadsry st., Kiev - 142, 03680, Ukraine, krupa@imag.kiev.ua
(1)Frantsevich Institute of Material Scienes NAS of Ukraine,
3, Kryzchanovsky st., Kiev-142, 03680, Ukraine, andreeva@ipms.kiev.ua
(2)Institute of geochemistry of environment NAS of Ukraine,
34-a, Palladina, ,Kiev - 142, 03680, Ukraine, juliavad@yahoo.com

Films of silicon carbide are characterized by high mechanical strength and chemical resistance. Silicon carbide is transparent in visible region of a spectrum; it has high value of refractive index and it is well-known material for production of photoelectric transformers and light-emitting diodes. Thus, mentioned testifies of good prospects for the use of SiC films as the optical and protective layers.

The investigation of some appropriate technological regimes to obtain thin films of silicon carbide (40-20 nm) has been carried out. Their properties as clarifying layers have been explored. We have done also a phase structure having submicron size of some structural elements and studied the protective properties of the resultant SiC films. SiC films were produced by two methods: by electron-beam dusting and magnetron sputtering. Pure polycrystalline silicon carbide was used as a target. Sometimes the targets were pressed from very thin (~0,5 micron) SiC powder with the overabundant content of the silicon. The formation process of some figures with phase contrast in SiC films under a laser cut was investigated by using a special station, which worked on the basis of a precision knot with aerostatics guiding with management from an interferometer on a Doppler effect [1]. The radiation of single-mode argon laser was used.

By optimization of technological parameters the regular submicron structure with the minimum size of the element ( *d=0,1-0,2* micron ) was obtained in thin SiC films with *h<0,06* microns. It is possible to reach more small size of the element in the thinner films (*h= 20 nm)*, however at these conditions a value of phase contrast will deteriorate. When using more thick films (h=0,1-0,3 micron) a cut line becomes more non-uniform and the size of the figure element is increased. However at these conditions a value of phase contrast of formed structure rises. A small size of the line of laser cut is connected with the fact, that silicon carbide evaporates without the melt stage under the laser treatment.

A large value of the a refractive index of SiC films allows to obtain some submicron structure with a high value of phase contrast on the surface of an optical detail. Figure 1 demonstrates the picture of a phase contrast of the plane surface, which was covered by SiC film. The latter was cut by laser beam.

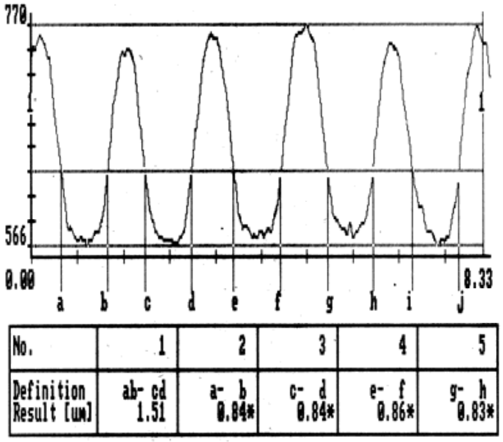

| No. | 1 | 2 | 3 | 4 | 5 |
|---|---|---|---|---|---|
| Definition<br>Result [um] | ab- cd<br>1.51 | a- b<br>0.84* | c- d<br>0.84* | e- f<br>0.86* | g- h<br>0.83* |

Fig. 1. The phase contrast obtained at the cut of some SiC film by argon laser

A set of measurements has been carried out on the reflections on the part of air. It is clear, that under the measurements on the part of a glass and under a gear transmission the value of the contrast will increased 2.5 times as large.

The large values of a refractive index allow also to use them for making dielectric polarization and clarifying coats. For example, when using 5-layer coatings of SiC and $SiO_2$ the effective film polarizer (more than 92 %) has been received.

Considered technology allows to utilize the regime of the control over the required characteristics during the manufacturing, that leads to the raising of the operation reliability.

Protective properties of SiC film have been investigated also. For this purpose the degradation of TbFe films was studied. Mentioned films strongly suffer from the oxidation and their magnetic characteristics sharply change. For the measurements we used a method of the accelerated degradation under a high temperature, and checked the changes of the value of the coercive force at air.

Figure 2 demonstrates the change in the characteristic of $Tb_{21}Fe_{70}Co_9$ film, covered by different protective layers. Obtained results testify of the high efficiency of silicon carbide films of 0.1 micron thickness.

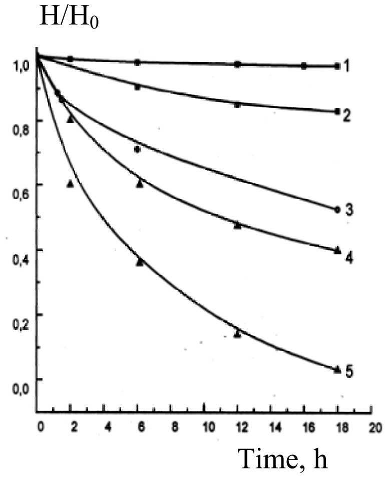

Fig. 2. Change of the coercive force of the studied films heated at different temperatures: 1- film with protective layer of SiC, T=100° C; 2 - films with protective layer of SiC, T=200 ° C; 3 film with protective layer of $SiO_2$, T=150°C; 4 film with protective layer of $SiO_2$, T=100°C; 5 - film without protective layer, T=22 °C.

Degradation time at room temperature was determined from the corresponding results carried out at high temperature according to the following:

$$H(t,T) = H(T)e^{-\frac{t}{\tau_H}}$$

$$H(T) = H_0 e^{-\left(\frac{kT}{W_H}\right)^l} \text{, (1)}$$

Where H - coercive force of the film at temperature T=0 K; $W_H$ -potential of activation of degradation process; l –is a numerical coefficient close to unity.The calculated time of the degradation at room temperature exceeds 50 years. Increasing of the protective SiC layer thickness leads to the growth of the protective efficiency of the SiC films. At these conditions the mechanical strength of the coat also grows.

Thus, obtained results testify, that it is possible to create plane optical devices, which can operate within a wide spectral diapason and have high mechanical strength, thermal, and chemical resistance by using method of laser cutting.

## Reference

1. Krupa M.M. Formation of phase nanostructure by methods laser cutting of silicon carbide films // JOT. - 1998. - Vol. 65, #3, - P. 80-82

# STUDY OF FRICTION-AND-WEAR CHARACTERISTICS OF STRUCTURAL MATERIALS IN TECHNOLOGICAL CRYOGENIC ENVIRONMENT

**Vvedenskij Yu.V., Volobuev F.I, Gamulya G.D., Ostrovskaya Ye.L., Yukhno T.P.**
Special Research and Development Bureau for Cryogenic Technology of
Verkin Institute for Low Temperature Physics and Engineering of NASU
47, Lenin Ave., Kharkov, 61103, Ukraine, mail@cryocosmos.com

Development of ecologically pure cryogenic technologies of processing of various kinds of materials (food products, medicinal raw materials, industrial scrap, etc.) caused the necessity of providing high serviceability of materials in different units and element of equipment used in the extreme working conditions including liquid nitrogen and cool nitrogen vapour.

The most difficult problem is to provide good performance characteristics for movable conjunctions of cryogenic equipment. However, for the time being the friction-and-wear data on structural materials for the conditions simulating the work of cryogenic production equipment are lacking.

The present work presents the trobological analysis of movable conjunctions of the equipment intended for fast freezing of food products (first of all, berries and fruits) by liquid nitrogen, It is shown that in the most difficult conditions the elements of the roller conveyor are employed which supply the processed products to the cooling and freezing zones of a fast-freezing tunnel. The results of friction tests for the shaft-bush pair simulating operation of the bush-roller of the conveyor are also presented.

The tests have been carried out in various technological media (in liquid nitrogen at 77 K, in gaseous nitrogen under lowered temperature (down to 210 K) and in air at room temperature) for a wide range of changing the normal load and shaft rotation frequency.

Friction in gaseous nitrogen under lowered temperature is found to be characterized by the highest friction coefficients compared to the case of friction in liquid nitrogen and in air (Figure 1).

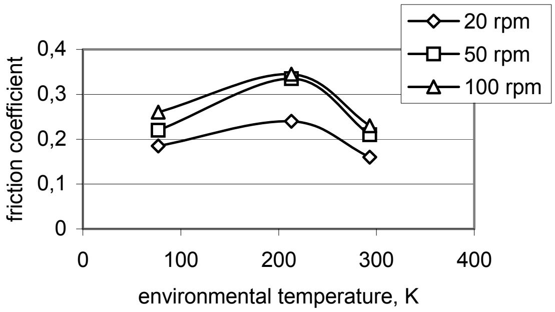

Figure 1. Friction coefficient *vs* temperature for shaft-bush pair (steel 12Cr18Ni9Ti – PTFE). Normal load is 2,5 N.

Higher coefficients of friction in cold nitrogen vapour can be the result of both the change of the conditions of heat removal from the contact zone and possible moisture condensation on the contact surfaces.

Long-duration tests of shaft-bush pair in gaseous nitrogen showed the high wear life of both mating elements.

The studies performed discovered the extreme character of friction coefficient-temperature dependence. It can be the result of both the changes of the material properties under temperature lowering and the change of the state of aggregation of the cooling environment.

The work was supported by the Science and Technology Center in Ukraine.

# NEW WC-Co HARDMETALS WITH REINFORCED Co-BASED BINDER FOR MINING AND CONSTRUCTION

**Konyashin I., Cooper R, Ries B.**
Boart Longyear Technical Development Centre
Staedeweg 18-24, D-36151 Burghaun, Germany
ikonyashin@boartlongyear-eu.com

The need for improved hard materials for mining and construction is rapidly growing. Wear and failures of hardmetal buttons and inserts in drilling bits, road-planing and coal picks, etc. are the major factors determining the effectiveness of mining and construction tools. Such tools work usually under extremely harsh operating conditions including temperatures of nearly 1000 °C, high impact loads, thermal shock, intensive abrasive wear and severe fatigue.

In many applications, particularly in mining and construction, one has to employ ultra-coarse WC—Co grades with a WC mean grain size of 3 to 10 μm. In the microstructure of such hardmetal grades the Co-based binder is present in form of relatively thick interlayers of up to several microns in size. In this case, the hardmetal lifetime is restricted by the low hardness, wear-resistance and limited fracture toughness of the binder making the possibility of the binder reinforcement extremely important.

New WC—Co grades consisting of rounded WC grains, and a reinforced Co-based binder have been developed, examined and tested. The new hardmetal grades have an improved combination of hardness/wear-resistance and transverse rupture strength/fracture toughness due to their special microstructure and the binder reinforcement. As a result, the lifetime of coal and road-planing picks with the new grades is considerably enhanced compared to conventional WC—Co hardmetals. Results on physico-mechanical properties of the new grades and their numerous laboratory and field tests and microstructure studies by means of optical and scanning and transmission electron microscopy will be presented.

# INFLUENCE OF ENVIRONMENTAL FACTORS ON OUTGASSING OF SPACECRAFT COATINGS

**Khassanchine R.H., Grigorevskiy A.V., Timofeev A.N., Rasskazov P.V.(1), Ivanova I.V. (1)**
Joint-Stock Company “Kompozit”
4, Pionerskay str., 141070, Korolev, Moscow region, Russia e-mail: angaln@mail.ru
(1) State Scientific-and-production Rocket-Space Center “TsSKB-Progress”,
18, Pskovskaya str., Samara, 443009, Russia

*Mathematical models describing influence of environmental factors on outgassing of spacecraft coatings and condensation of originated volatile products are presented. Numerical analyses of the processes were carried out to compare qualitatively result deviations obtained under the exposure to individual factors. Experimental results confirming importance of the effect of material temperature, UV and electron radiations on polymeric composites are given.*

The polymeric composites have a number of features allowing them to be used as external coatings on spacecraft. For these materials outgassing in operating conditions is the major source of volatile products that are able to condense on contamination-sensitive surfaces of spacecraft equipment such as optical control systems, members of solar arrays, telescopes, etc. This, in turn, is one of the factors that restricts potentially serviceability and lifetime of the equipment alone and a space vehicle as a whole. With further extension of spacecraft service life, development of prediction models describing outgassing processes of coatings and deposition of volatile products on contamination-sensitive surfaces becomes the issue of the day.

The article presents the mathematical models built under the assumption that outgassing process in polymeric composites in operating conditions consists mainly of the following processes:

1) desorption of volatile products adsorbed by surface or originated onto it under the exposure to environmental factors;

2) diffusion and desorption of volatile products absorbed or originated in it as a result of the thermal decomposition or due to action of the electromagnetic or ionizing radiation;

3) evaporation (sublimation) of a solid substance under the exposure to environment.

The molecular binding energy in the polymeric materials being comparable in value or less then the energy of certain electromagnetic quanta, their action as well as the action of ionizing radiation on materials in vacuum can intensify the sublimation.

The basic provisions of the mathematical models are confirmed by the experimental results of influence of environmental factors on outgassing kinetics of polymeric composites.

# DEVELOPMENT ANTIFRICTION COMPOSITION MATERIAL FOR OPERATION IN TETROXIDE OF NITROGEN

**Slys I.G., Brakhnov N.V., Berezanskaya V.I.**
Frantsevich Institute for Problems of Materials Science NAS of Ukraine,
03680, Kiev - 142, street. Krzyzanovskogo 3, E-mail: slys@materials.kiev.ua

It is known, that in 80 years of the twentieth century in USSR were developed and new more productive and costeffective atomic-power settings working on fast neutrons with use as the heat-transfer medium and a working body of nitrogen tetroxide ($N_2O_4$) were designed.

There was an acute necessity of security of serviceability of clusters of abrasion (bearings and face seals) equipment of mobile and stationary atomic power plants. The turbine and the pumps are aggregates atomic power-station(APS), the steams of which abrasion are greased and are cooled by a solution phase of nitrogen tetroxide. In face seal abrasion sami-fluid, and in the bearing fluid.

Relative speed of slipping 100m/s, temperature of a working body 1000C, specific pressure: for face seal 15kg/cm2, for the bearing 20kg/cm2. A resource of operation till 10000 hours.

To ensure serviceability at such rigid conditions a stressing with abrasion, it was necessary to create a composition antifriction material, which successfully stood up to resisted to destroying effect not only abrasion, but also aggressive heat-transfer medium ($N_2O_4$) in pool or vapor phase, radiation and temperature originating in conjugate steams at a high-speed stressing by abrasion, erosive shattering of a pool or gas actuation medium.

The scientific school generated in Institute of problems of materials technology by the academician Academy of Sciences of USSR Fedorchenko I.M. has undertaken the decision such complex matereals technologeof a task [1].

As a material - fundamentals for creation of antifriction materials capable to work in contact to gas or pool hostile environments, the stainless strips were selected which have high durability and corrosion stability in many hostile environments. However owing to high viscosity they have the large propensity to setting, even at abrasion with lubrication.

We have assumed, that rational use of powder metallurgical techniques will allow to save a high corrosion stability of a stainless strip and, in too time, cardinally to increase its resistance to setting at a stressing by abrasion. By us is established, that such effect can be reached by the following paths:

a) By introduction in makeup of a material reactive of substances, capable to interact during a stressing by abrasion with a material of conjugate surfaces and formation on them of protective antifriction films (stratums) [2-3];

b) By creation of heterogeneous structure at the expense of a doping by hardening elements (carbon, boron), that ensures resistance against setting, of chemical and abrasive effect [4];

c) By overlapping a doping by hardening elements and introduction reactive of substances [5-7].

Resting on the specified scientific and technical reachings in IPM AS of USSR, the new composite of the brand Cr23N18MsC was developed [8].

The designed technique of its deriving allows at one-time cold pressing and sintering in an autonomous gas environment [9] at temperature $1100^0$C to receive large-sized (up to 16kg) articles with residual porosity 3-7 %.

The mechanical characteristics sulftd-cementation of a material of the brand CrX23N18MsC are investigated at 20, 200 and $400^0$C, the Designed material a little bit loses durability at a heightening of test temperature. It also successfully has passed a hydraulic test at an air pressure 100ат. and fire resistance at $600^0$C. The radiation stability (under an operation of an integrated stream 2x1017-2x1019 a neutron / $см^2$) not much more yields stainless strips of the same brand.

The corrosion stability of a material Cr23N18MsC in $N_20_4$ is much higher, than pure sintering of a stainless strip Cr23N18 (see tabl. 1). It, on seen, is connected to better quality of sintering and reduction of a reactionary surface chamical-thermal processes, stipulated by passing, activating conduction of a mass to contact surfaces between particles and formation of complex non-corrodible sulphides and carbon-sulphides of a chrome and molybdenum.

From sulhid-cementation of a material Cr23N18MsC the large-sized preforms 103x54 in diameters and height 90 mm manufactured. The bearings for trials on pump the stand CH-1 of

Institute of kernel power engineering AS BSSR, flowing through dissociating heat-transfer medium $N_2O_4$ manufactured of these preforms. Contr-solid the steel 20Cr13, azotized on depth of 0,2-0,3 mm, hardness of a surface 56 served. HRC. After 50 hours of trials of guide bearings of traces of a wear are not fixed. Contr-solid too without traces of a wear. A friction surface without scratch marks and scores.

During trials the pilot plant a Curl - 2 equipped with bearings from a material Cr23N18MsC, for the first time has typed a design amount of turnovers, (peripheral speed > 50м/s). Traces of a wear and centers of burning on a surface of a material Cr23N18MsC it is not revealed.

The technique of deriving of large-sized preforms from a material Cr23N18MsC on the equipment Brovary of a factory of a powder metallurgy is successfully tested. Is established, that the prismatic workpieces by a mass up to 4кг are well pressed on 2000т squeezer and 3% are sintered in containers with a meltable shutter up to porosity.

By trials on serviceability in INE AS BSSR is established, that the material Cr23n18MsC has good antiweld properties, stability against ignition, can be applied in steams of abrasion, where high reliability is necessary from the point of view of jamming in emergency operation. Also, his application in лабиринтных or slotted seals turbogenerations working on the dissociating heat-transfer medium is possible.

The table 1

Corrosion stability спеченной of steel Cr23N18 and antifriction material Cr23N18MsC in $N_2O_4$. Duration of a trial 360 hours.

| The brand of a material | $200^0$C, 50atm. | | $400^0$C, 50atm. | |
|---|---|---|---|---|
| | Speed of staining of $g/m^2h$ | A surface condition | Speed of staining of $g/m^2h$ | A surface condition |
| Cr23N18 | +0,104 | In sepparate places of a stain and smudges | +0,215 | Of brownish tone of blueing |
| Cr23N18MsC | -0,006 | Grey brilliant | -0,003 | Dark grey brilliant |

The literature

1. I.M.Fedorcehnko. The bibliography of the scientists Ukrainian SSR. Kiev, Наукова думка, 1984
2. Slys I.G., Pugyna L.I. Certifucate of invention USSR N194321, N7.
3. Fedorchenko I.M., Slys I.G., Pugyna L.I., Etc. Certifucate of invention USSR N276425, 1970, N23.
4. Fedorchenko I.M., Slys I.G., Pugyna L.I., Etc Certifucate of invention USSR N286413, 1970, N34.
5. Fedorchenko I.M., Slys I.G., Pugyna L.I., Etc Certifucate of invention USSR N224085, 1968, N25.
6. Fedorchenko I.M., Slys I.G., Pugyna L.I., Et Certifucate of invention USSR N331976, 1972, N25.
7. Fedorchenko I.M., Slys I.G., Pugyna L.I., Etc. Certifucate of invention USSR N339196, 1972, N33.
8. Fedorchenko I.M., Slys I.G., Pugyna L.I., Etc. Certifucate of invention USSR N449970, 1974, N42
9. Fedorchenko I.M., Slys I.G., Sosyovsky L.A. PM, N5, 1972, 15-19.

# PLANNING TEMPERATURE MEASURMENTS AT EXPLORING THERMOPHYSICAL PROPERTIES OF ANISOTROPIC MATERIALS

**Prosuntsov P.V.**
FGUP “VIAM”, Radio Street, 17, Moscow, 105005, Russia

High-porous fibrous heat insulation materials (such as LI-900 and TZMK-10) have found usage in heat insulation systems of Reusable Launch Vehicles. Nowadays this class of material is developing in the direction of more refractory fiber use and switching to soft materials. Among the distinguishing features of high-porous heat-insulation materials one can name the difficult, combined nature of the radiative and conductive heat transfer running in the volume of the material. Besides, most fibrous heat insulation materials possess a considerable anisotropy of thermophysical properties, connected with the peculiarities of the technological productions.

The present paper offers the statement and the algorithm of the two-dimensional radiative and conductive heat transfer inverse problem solution, used for parametrical identification of thermophysical properties (volumetric heat capacity and thermal conductivity coefficient) of semi-transparent scattering materials. The results of mathematical modeling, held for analyzing accuracy and stability of two-dimensional radiative and conductive heat transfer inverse problem solution, showed that empirical treatment of choosing the setting place and number of temperature sensors may lead to great errors in the posterior inverse problem solution.

That’s why a problem of temperature changes optimal planning while defining the thermophysical properties of anisotropic material from a two-dimensional inverse problem solution was set and solved.

General approach to the problem of planning temperature changes while defining the thermal conductivity coefficient is considered in the works by O.M. Alifanov and E.A. Artyukhin [1, 2].

Under the measurement plan $\Lambda=\{N_t,(x_1,ó_1),(x_2,ó_2),(x_3,ó_3)\,...(x_{N_t},ó_{N_t})\}$ we understand the totality of $N_t$ number and the places of setting temperature sensors $d=\{(x_1,ó_1),(x_2,ó_2),(x_3,ó_3)\,...(x_{N_t},ó_{N_t})\}$. According to [2] we consider the measurement plan at which the maximum of normalized Fisher-matrix determinant to be optimal: $\det(F(\Lambda))=\max$.

Fisher-matrix elements are calculated as follows: $F(\Lambda)=\dfrac{1}{N_t}\Phi_{jk}$, $j,k=\overline{1,K}$, where $K$ is a total number of parameters used at presenting unknown temperature dependences of thermophysical properties and $\Phi_{jk}=\sum\limits_{n=1}^{N_t}\int\limits_0^{\tau_m}\theta_j(x_n,ó_n,\tau)\cdot\theta_k(x_n,ó_n,\tau)\,d\tau$. Values $\theta_k(x,ó,\tau)$ represent sensitivity functions of the temperature field in the point of the sensor set which are determined from the accompanying boundary problem.

For searching Fisher-matrix determinant maximum this work presents a rather simple, still a high-performance flexible non-gradient method that is a variant of the well-known Nelder-Meed method.

The problem of temperature changes optimal planning for the experiment scheme in figure 1 was solved.

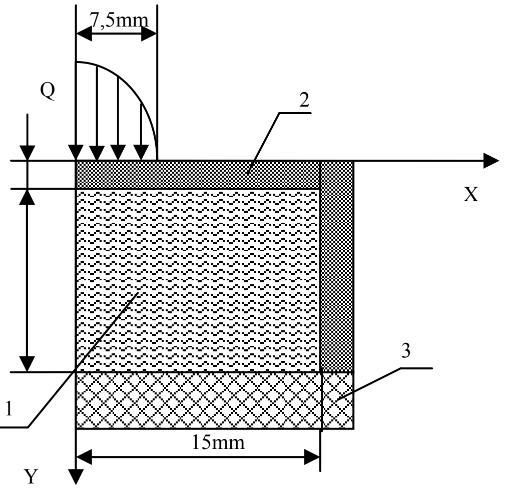

Fig.1 Experiment scheme 1 – specimen; 2 – shield;
3 – heat-insulating layer.

The peculiarity of the given scheme is the presence of a side highly heat-conducting shield which strengthens heat transfer in the radial direction. Thus the commensurability of the axial and the radial flows is achieved and good evenness of the two-dimensional inverse problem convergence for the $\lambda_x(T)$ and $\lambda_y(T)$ dependences is ensured.

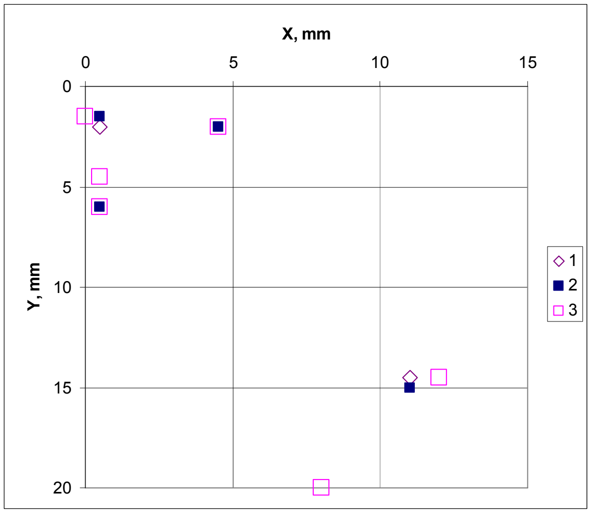

Fig.2 Solution results of the optimal planning problem for different numbers of temperature sensors

1 – 2 sensors; 2 – 4 sensors; 3 –6 sensors.

Figure 2 provides the optimal changes plan for different numbers of temperature sensors.

The dependence of optimal temperature sensor setting coordinates from the specimen diameter and thickness was investigated (fig. 3 and 4).

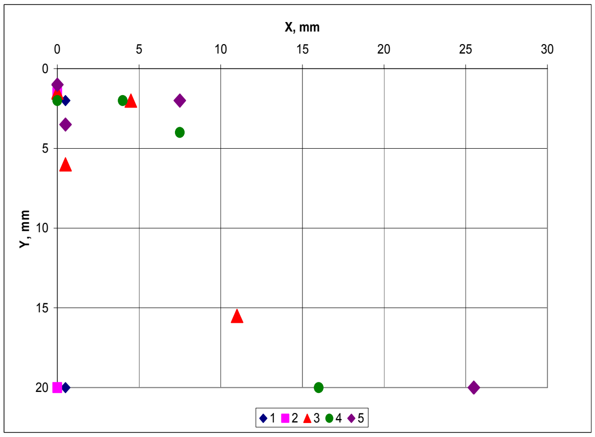

Fig.3 Solution results of optimal planning problem experiment at different specimen diameter. 1 – specimen diameter 10 mm; 2 – 20 mm; 3 – 30 mm; 4 – 40 mm; 5 – 60 mm.

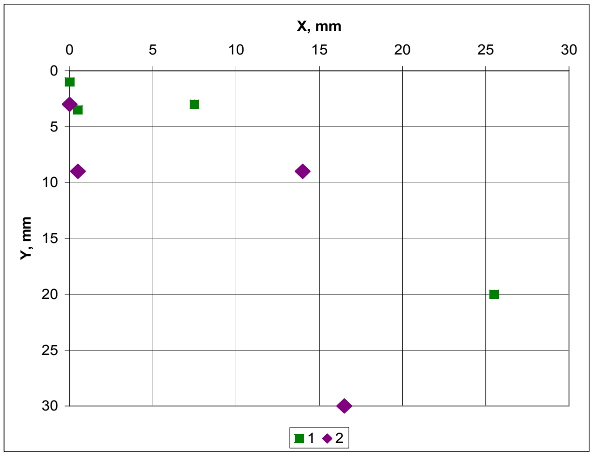

Fig.4 Solution results of optimal planning problem experiment at different specimen thickness. 1 – specimen thickness 20 mm; 2 – 30 mm.

The results of the optimal planning problem solution are used while holding thermophysical investigations while performing INTAS project (grant № 00-0652).

## Literature

1. O.M. Alifanov. Inverse Heat Transfer Problems. – Moscow: Mashinostroenie, 1988. – 279c. (In Russian)
2. O.M.Alifanov, E.A. Artyukhin, S.V.Rumyantsev Extermal methods of solving ill-posed problems and their applying to inverse problems.– Moscow.: Nauka, 1988. – 343c. (In Russian)

# ESTIMATION OF METAL COVERING INFLUENCE ON RESISTANCE TO DESTRUCTION OF SILICON CARBID IN A BEND AND COMPRESSION CONDITIONS

**Dubikovsky L., Ochrimenko G.**
Frantsevich Institute for Problems of Material Science of NASU,
Krzhizhanovsky str.3, 03680, Kyiv-142, Ukraine, E-mail: chern@materials.kiev.ua

Is established, that a number of not metal materials, for example boron and silicon carbide created in a National academy of sciences of Ukraine, due to high and stable durability on compression, can be used as constructional for high-tensed and responsible products [1 … 4].

However, the increase of the operational characteristics of many ceramic materials, for example, boron and silicon carbide, is limited to absence in laboratories accessible and convenient in circulation hydraulic press, effort (0,01 … 1,00) $\times 10^{10}$ N.

Earlier created greatest in the world of hydraulic press by effort (0,065 … 0,075) $\times 10^{10}$ N for this task are not suitable because of large weight - up to 20 thousand T and significant height of a design - up to 35 thousand mm [5].

Is known hydraulic press for work at external hydrostatic pressure [6, 7] with design effort (0,1 … 1,0) $\times 10^{10}$ N, to make which it is possible on the process equipment of the Ukrainian enterprises from known constructional materials.

Its feature - cylindrical tubular base by a diameter D = (0,4 … 1,0) $\times 10^{4}$ and length (0,5 … 1,5) xD mm can be made from high-strength of not metal constructional materials according to [8].

Feature of technology - cylinder make type-setting in an axial direction of rings. At absence of sheets necessary dimension, the rings of the required sizes make of connected sectors [8].

In the present message with reference to the decision of the mentioned task Brovary's factory silicon carbide SiC was investigated [1 … 4]. SiC possess a little bit large relation of strength at a bend $\sigma_И$ and compression $\sigma_C$ in comparison with those date at technical glasses and sytal [1,8]. As the enterprise makes plates by the size up to 20 × 300 × 400 mm, the rings of the necessary sizes can be made from sectors. Thus there is a problem - way of connection of sectors and modular rings should ensure tightness, durability and reliable.

Perspective connection of preparations from SiC can be the soldering, for which performance it is necessary to put metal coverings. In the literature contain limited date about influence of similar processing SiC on its characteristics $\sigma_И$ and $\sigma_C$ [9].

By the purpose of the present message was to estimate influence on $\sigma_И$ and $\sigma_C$ of samples SiC, made by the diamond tool up to a roughness $Ra \le 1{,}25$ a micron (with the sizes 3,5 × 7 × 48 and 3,5 × 7 × 12 mm), metal coverings from TiN, Al, Ni and Cu. Before drawing of a covering samples were processed waterless fluorine - hydrogen without flare with allocation of gas under the circuit: SiC+HF > $H_2SiF_6$ + $C_xH_yF_z$ [9].

The listed coverings rendered on samples by the following ways: TiN - at vacuum installation {with size of vacuum $(10^{-2}...10^{-1})\times 1{,}3$ Pa} by a method plasma-ion deposition, including condensation with ion bombardment (general duration of process - 90 min); Al type AD-by condensation from the heated up surface in vacuum; Ni and Cu - electrochemical depositing at density of a current 0,3... 0,7 A/dm$^2$, electrolyte temperatures 293 … 298 K during 10 … 20 min in sour and neutral electrolyte.

The characteristics of coverings are given in tab. 1,

The table 1. The characteristics of coverings

| Π | $\delta$, mm | $\eta$, μm | $\rho$, % | $\chi$, % | Φ, % |
|---|---|---|---|---|---|
| TiN | 0,01 | 0,12 | 1,0 | 98 | 90 |
| Al | 0,01 | 0,10 | 0,5 | 99 | 94 |
| Ni | 0,03 | - | 20 | 16 | 94 |
| Cu | 0,02 | 0,10 | 3 | 30 | 98 |

where the designations are accepted: П – covering; $\delta$ - its thickness; $\eta$ - size of a grain; $\rho$ - porous; $\chi$ - durability of coupling; Ф - reflective ability. The test of samples was carried out on a technique described in [1, 8]. The results of tests are submitted in tab. 2.

The factors $\gamma_{П_И}$ and $\gamma_{П_C}$ are equal to the relation $\sigma_И$, and also $\sigma_C$ after etching a surface or drawing of coverings to durability of initial samples - with a roughness $Ra \leq 1{,}25$ micron.

The table 2. Influence of etching in HF and metal coverings on durability SiC

| The characteristics of surface | $\sigma_И$, MPa | $\gamma_{П_И}$ | $\sigma_C$, MPa | $\gamma_{П_C}$ |
|---|---|---|---|---|
| Polish. $Ra \leq 1{,}25$ μm | 161 | 1,00 | 2486 | 1,00 |
| Etching in HF | 167 | 1,04 | 2500 | 1,00 |
| Covering Al | 186 | 1,16 | 2389 | 0,96 |
| Covering Cu | 182 | 1,13 | 2421 | 0,97 |
| Covering Ni | 175 | 1,09 | 2442 | 0,98 |
| Covering TiN | 169 | 1,06 | 2516 | 1,01 |

The influence of metal coverings on $\sigma_И$ And $\sigma_C$ for SiC is shown in figure, where on an axis abscissa is specified atomic or molecular mass of a covering M, a.m.u., on axes of ordinates - $\gamma_{П_И}$ (at the left) and $\gamma_{П_C}$ (on the right).

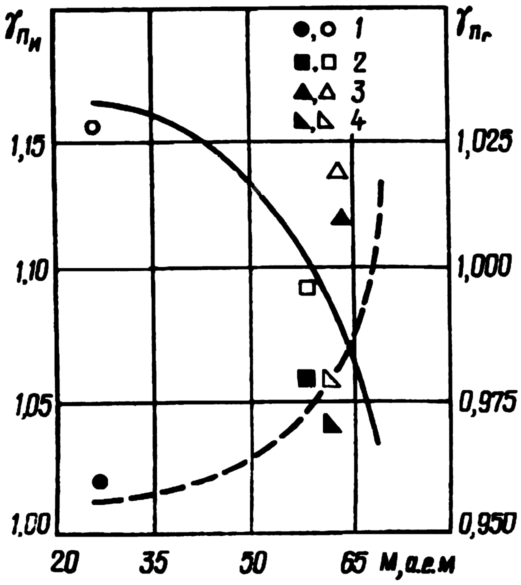

Figure. Dependence of factors $\gamma_{П_И}$ at a bend (dark points, shaped line) and $\gamma_{П_C}$ at compression (light points, continuous line) samples SiC after drawing coverings from Al (1), Ni (2), Cu (3) and TiN (4) from weight of atom or molecule of a covering M.

From the submitted results the durability of samples SiC after drawing the investigated coverings follows, that at a bend – without changing and reducing $\sigma_C$ does not exceed 5 %. Hence, researched Brovary's factory SiC can be applied together with examined metal coverings for manufacturing both sectors and rings, and all modular of compound rings of base perspective press [1, 2].

## REFERENCES

1. Конструкционная прочность стекол и ситаллов/Г.С.Писаренко, К.К.Амельянович, И.Козуб и др. – Киев: Наук. думка, 1979. – 284 с.

2. Дубиківський Л.Ф., Охріменко Г.М. Вироби із конструкційної кераміки в умовах стиску. – В кн.: Ceram-2001. Международная конференция "Передовая керамика – третьему тысячелетию. Тезисы докладов". – Киев: Украина, 5 – 9 ноября 2001 года. - С. 166.

3. L.Dubikovsky, G.Okhrimenko. Research of technological factors on strength of materials on the basis of silicon oxide. – Second International Conference "Materials and Coatings for Extreme Performances: Investigations, Applications, Ecologically Safe Technologies for Their Production and Utilization". Proceedings of Conference. 16 –20 September 2002. - Katsiveli-town-Crimea, Ukraine. - S. 340 – 341.

4. Дубиковский Л.Ф., Охрименко Г.М. Тестирование прочности керамических материалов. – В кн.: «Международная конференция «Новейшие технологии в порошковой металлургии и керамике». Тезисы докладов. 8 – 12 сентября 2003 г.». – Киев, Украина. – С. 412 – 413.

5. Кузнецов Н. Советский "король станков" в Иссуари. –"За рубежем". – 1977. - №3 (864).

6. Охрименко Г.М. Гидравлический пресс. А.С. СССР, № 641711 с приоритетом от 9 декабря 1974 года. Зарегистрировано в Государственном реестре изобретений Союза ССР 14.09.78 года.

7. Охріменко Г.М. Преси для роботи при зовнішньому гідростатичному тиску. – Київ: Київська організація Шевченкового Братства України, 7511 (2003). – 21с.

8. Прочные оболочки из силикатных материалов//Г.С.Писаренко, К.К.Амельянович, И.Козуб и др. – Киев: Наук. думка, 1989. – 224 с.

9. Оценка влияния фторидной обработки и последующего нанесения покрытий на прочность керамики из карбида кремния/ Бушлов В.А., Дашевская О.Б., Уминский А.А. и др. – В кн.: VIII Всесоюзный симпозиум по химии неорганических фторидов. Тезисы докладов. Полевской, 25 августа 1989. – Москва: Наука, 1987. - С. 79.

# THE PROBLEMS OF MATERIALS AND COVERINGS USED IN HIGH PRESSURE AND TEMPERATURE AUTOCLAVES

**Denbsky G., Schmidt C.**(1)**, Shtefan E.V.**(2)**, Mikhailov O.V.**(3)
P:T-Procedures GmbH, Ganghoferstr. 2, 85375 Neufahrn, Germany,
e-мail: pbyt.procedures@gmx.net
(1)P:T-Procedures GmbH, Ganghoferstr. 2, 85375 Neufahrn, Germany,
e-мail: sinetempore@gmx.net
(2)National universities of food technologies, 01033, Kiev, Vladimir, 68,
Ukraine, e-мail: shtefan@visti.com
(3)Frantsevitch Institute for Problems of Materials Science, NASU
3, Krzhyzhanovsky St., Kyiv, 03142, Ukraine, E-mail: olmi@alfacom.net

The results of development and experimental research of the process equipment for fast and complete mineralization of resistant organic matrices by adjustable and complete disintegration of hydrogen peroxide in the high pressure and high temperatures autoclaves are presented. The technology in question is intended for the quantitative analysis of low concentrations of heavy metals and radionuclides in samples like foodstuff, biological and toxicological materials.

The high concentrated hydrogen peroxide (70 %) is disintegrated by flare when heated to the boiling point. It is suggested to use this exothermically reaction for the complete decomposition of organic substances inside the autoclave with the subsequent analysis of inorganic components. As a result of the reaction, the pressure and the temperature achieve during several milliseconds 80 mpa and $1000^0$C. For realization of the given technology the special autoclaves with volumes of working cavity from 20 ml up to 600 ml were developed.

When choosing the material for the autoclaves, alongside with the demand for the complete decomposition of the organic matrix, there was a focus on reducing of mineralization time. Thus, the material of the autoclave should provide: 1) durability on long time of operation at fast changes of pressure and temperature; 2) high heat conduction parameters; 3) indifference to poorly sour environment at high temperatures. The material steel 1.4980 (high-heat resisting austenite X5NiCrTi26 15) [1] meets best these requirements.

The autoclave design should provide: 1) fast loading and unloading of technological components; 2) uniform high-speed heating with minimal power expenses; 3) autoclave fast moving from the heating block to the cooling bath; 4) simplicity of manufacturing, reliable and long-term operation. For the solution of this problems information technologies of designing are used [2]. The substantiation of the constructive decisions was executed by taking into account the non-stationary warming up of the autoclave and the stress – strain state of the autoclave elements.

To ensure the absence of steel components in the solution resulting from the extreme conditions during the mineralization, the cavity of the autoclave must be covered by a layer of a chemically inert and heat resisting material. The long-term experience in using autoclaves of this type for chemical reactions which were accompanied by extreme pressures and temperatures [3], corroborates the suitableness of tantalum as material for coverings. However, high costs of such covering limit its application. Less expensive cover by a 2μm-gold layer is not fit for short heating to temperatures above 1000°C.

Extensive series of experiments, which were carried out, demonstrate the main shortcomings and advantages of these types of autoclaves.

## Literature

1. Denbsky G., Fischer H.-J., Chem.-Ing.-Tech. 58 (1986) Nr. 3, S.218-220
2. Shtefan E.V. Modelling of the disperse systems behaviour in the non-equilibrium processes of food manufactures: NUFT Science Works, №8, Kiev, 2000. – p.p. 63-66
3. Denbsky G., Lebensm.-Chem. Gerichtl. Chem. 39 (1985) Nr. 5, S. 108

# INVESTIGATION OF HIGH-TEMPERATURE CORROSION RESISTENCE OF STRUCTURUL STEEL ALUMINAZED WITH THE USE OF HIGH-SPEED FUEL-AIR SPRAYING

**Kotlyar A., Buchakov S., Kisil V., Yevdokimenko Yu., Kolotilo A.**
Francevich Institut for Problems of Materials Sciens NAS of Ukrane,
3, Krzhyzhanovsky str., Kiev 03142, Ukraine, E-mail: yevd@ua.fm

The protection of large-sized steel structures being operated under higher temperatures against high-temperature corrosion is an actual problem which requires economically expedient ways of its solutions.

One of the ways to raise high-temperature corrosion resistance of steels is an aluminizing.
The tests of steel aluminized parts under industrial conditions have shown that their operational life increases 5-15 times depending upon temperature for parts manufactured out of low-carbon steel and more than 10 times for the parts manufactured out of high-temperature steel under the operational temperature 1150°C [1].

But traditional technology of aluminizing is characterized by some following deficiencies limiting its application: the necessity of expensive coverings, shielding gases, additional equipment, the complexity of the aluminizing of large-sized structures [2; 3]. The applications of coverings is connected with low density and adhesion of aluminium coatings applied usually by the method of electroarc metallization or flame spraying method. The improvement of these characteristics would permit to decline some stages of aluminizing process. High density of aluminium coatings under the higher adhesion permits can be obtained by the method of high-speed fuel-air spraying.

The burner of installation of fuel-air spraying "Струмінь" was used for the applying of coatings [4]. The plates manufactured out of low-carbon and alloy steel were used as the samples. The samples with aluminium powder coatings were subjected to homogenizing under temperature 700°C in air, argon medium or vacuum. The obtained results demonstrate that aluminizing both low-carbon and alloy steel is realized successfully from the layer sprayed by the method of high-speed fuel-air spraying without using special coverings. Aluminized samples were subjected to thermocyclic tests. The structure of aluminized samples made out of steel 10 after 10 cycles of heating and up to 1000 and 800°C and cooling in air is given in the Fig. 1a and 1b. The depth of aluminized layer is 80 и 150 mµ accordingly.

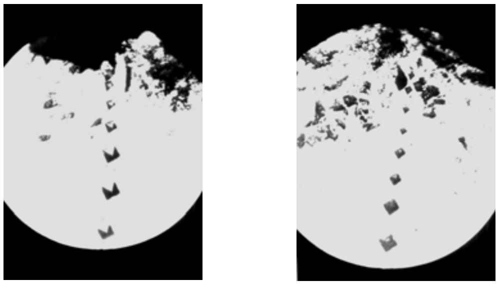

Fig.1a Fig. 1b

Fig. 1Strucrure of aluminized samples after thermocycling(a – under 1000°C; б – under 800°C)

The investigation of the dependence of the mass change upon the number of cycles for aluminized samples made out of steel 10 under their heating up to 1000°C in air have being carried out. Some results of these investigation are given in the Fig. 2.

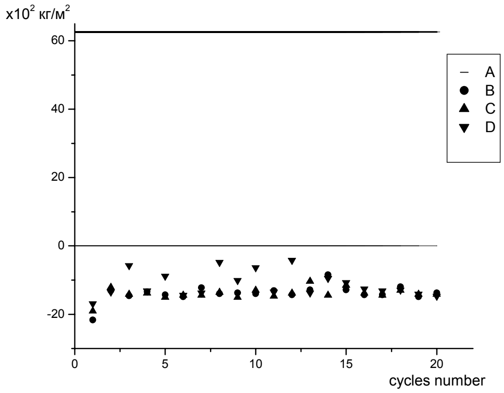

Fig. 2. Dependence of mass change reduced to coating area unit upon cycles number for aluminized samples under 1000°C thermocycling (A – sample for comparison, B;C;D – aluminized samples)

As it is obvious from the Fig.2 the sample for comparison purpose lost 0.6 g/mm$^2$ on the average during the cycle. At the same time for aluminized samples some mass increase was observed due to aluminium oxidation.

The experiments have been carried out for the determination of the dependence of aluminized samples mass change upon heating cycle duration. The cycles duration was 1 hour and 10 hours. It is established that the destruction of aluminized samples depends in greater degree upon the number of heating cycles than total cycles duration.

It is shown that high-temperature corrosion resistance of aluminized sample annealed in air does not differ practically from the resistance of samples annealed in shielding medium or vacuum (not more than 20% as to mass increase).

The application of the method of high-speed fuel-air spraying permits to obtain a coating of small thickness with low porosity and high adhesion strength. Due to high adhesion strength after spraying the coating remains on samples surface and protects in addition the surface of main metal on account of the continuation of the process of aluminium diffusion. Lesser porosity of the coating (under 1.5%) in comparison with other methods of spraying also increases shielding properties of the coating because it keeps oxigen out of main metal surface. High coating density permits to carry out aluminizing from the layer of lesser thickness which prevents melted aluminium draining off the surface during annealing process and in that way decreases aluminium expenditures.

So, carried out experiments confirm the possibility of using high-speed spraying for aluminizing large-sized structures under industrial conditions without applying auxiliary equipment. In this case their heat resistance turns out to be comparable wholly with the resistance of the structures aluminized in vacuum or shielding medium and exceeds the heat resistance obtained by aluminizing with the use of coverings. It is connected with high quality of aluminium coatings obtained by the method of high-speed fuel-air spraying, first of all with their low porosity and high adhesion strength. It makes it possible to:

- Decrease the cost of the process because the expense for shielding gases, coverings and aluminizing equipment are excepted;
- Carry out objects aluminizing directly at the place of their use and also the aluminizing of large-sized objects and structures;
- Carry out the annealing of structures operating under high-temperature conditions immediately in the process of their operation;
- Carry out the recovery of damaged intermetalloid layer at the place of object use.

## References

1. Гордонов П.Т. Повышение жаростойкости стальных изделий методом алитирования 1962г.
2. Диффузионное насыщение и покрытия на металлах. Сбор. науч. тр. – Киев. ИПМ АН УССР «Научная мысль» 1983г – 144с.
3. Алитирование деталей методом металлизации распылением 1966г.
4. Ю.И. Евдокименко, В.М. Кисель, В.Х. Кадыров, А.А. Король, О.И. Гетьман. Высокоскоростное газопламенное напыление порошковых алюминиевых покрытий // Порошковая металлургия. – 2001. - №3/4. – С.30-37

# EXPERIMENTAL INVESTIGATION OF MATERIAL DAMAGES INDUCED BY HOT XENON PLASMA

**Hassanein A., Burtseva T.A., Minakova R.V(1)., Golovkova M.E.(1), Popov S.M.(1)**
Argonne National Laboratory,
9700 South Cass Avenue, Argonne, IL 60439-4838, e-mail: burtseva@anl.gov
(1) Francevich Institute for Problem of Materials Science of NASU,
Krzhyzhanovsky Str., 3, Kyiv-142, 03680,Ukraine, e-mail: 29min@ipms.kiev.ua

Dense plasma focus devices operating with a frequency 2-5 kHz, pulse energy of the order of 1-100 J, and a gas mixture of Xe and He are very promising as the sources of Extreme Ultraviolet (EUV) radiation for microlithography. A serious problem in the design of such EUV sources concerns erosion of the pinch plasma facing components under action of electric currents, hot plasma particles, and photon radiation [1]. Material erosion limits lifetime of pinch facing components thereby reducing a practical feasibility of the EUV sources. Investigation of the erosion mechanism and their dependencies on the operational parameters is quite important for the development of commercial EUV devices.

This study deals with experimental investigation of material erosion caused by hot Xe plasma. The pinched Xe plasma temperature is about 40 to 50 eV. Such temperatures are required for the tenfold ionization of xenon and production of $Xe^{+10}$ ions emitting the spectral lines at the wavelength near 13.5 nm. The electrodes made of the composite materials (CM) in systems W-Ni-Cu-$LaB_6$ and Mo-Cu-$LaB_6$, also known as electric heavy current contact materials were compared to the electrodes made of pure copper. Manufactured by the methods of powder metallurgy, these CM materials had a matrix structure with grain-colonies in which W-particles and W-grains were distributed. Initial and secondary electrode structures were investigated by various methods, such as optical and scanning electron microscopy, local X-ray and microanalysis, mass-spectral and micro hardness methods.

The macrostructure analysis of the electrode appearance after the tests allows to detect the influxes of melted material for all investigated samples. Such influxes were clearly observed on the side surface, but practically absent near the butt-end of the hot plasma interacting electrodes. In accordance with the frequency of the energy pulses, the melt portions layer one another at melting and further crystallization and form the fish flake like relief. The repetitive action of the heat source on the electrode was determined to favor the thermal fatigue damage of such a sandwich, fig. 1.

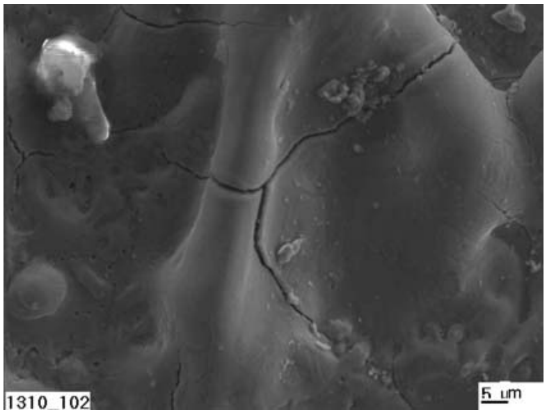

Figure 1. Thermal fatigue failure of the electrode secondary structure

The analysis of electrode sections of the crystallized melt area testifies the intensified interaction of the main elements W(Mo) and Cu under the influence of temperature, additions and impurities. Accordingly to the mass-spectroscopy, such impurities could be O, H, Li, Be and others. In W and Cu based materials with Ni presence, the fragmentation of W-agglomerates and dissolving of W-grains appeared. At that, the shape and the distribution of new particles in each layer determine the anisotropy of a secondary structure formation. The structure and the distribution of W in the melt after crystallization are shown in fig. 2 a, b. The increase of W-dissolving in the Cu with Ni presence in the zone of thermal plasma influence also increases the micro hardness of the material (3.02 GPa for the initial material; 3.38 GPa for the boundary layer; 3.7 GPa for secondary structure).

Despite Mo and Cu are practically insoluble in each other, the peculiarities of the secondary structure and Mo-distribution features are evidance of Mo-solubility in Cu increasing, as shown in fig.

2 c, d. This could be caused by the observed impurities, such as oxygen first of all. It is known [2], that the oxides, triple compounds, eutectic and pseudo-eutectic are formed in equilibrium Cu-Mo-O system.

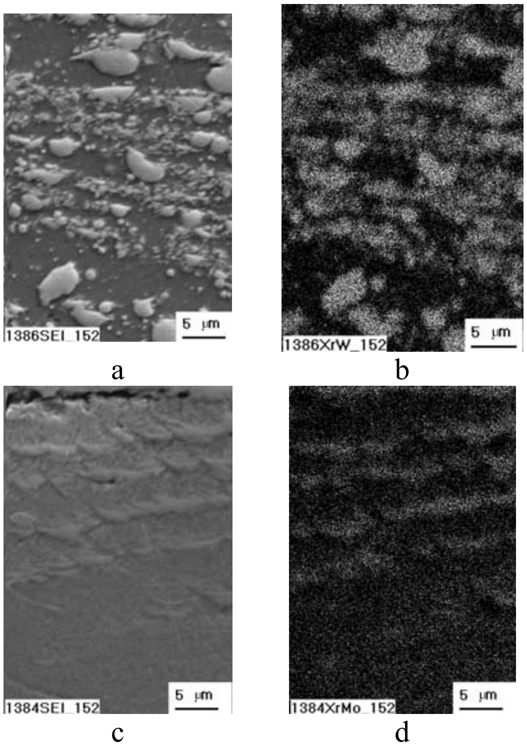

Figure 2. W(a,b) and Mo(c,d) distribution in the secondary structure of the copper-made electrode

The presence of oxygen in the melt and the increase of Mo-solubility facilitate the particle growth of the refractory component, and at the crystallization of the melt layers improve the anisotropy formation of the particles in each layer of the secondary structure. The micro hardness of the powder Mo-Cu electrodes structure is changed as follows: initial material has 1.69 GPa; for boundary lawyer has 1.69 GPa; and the secondary structure – 1.9 GPa. Shown in fig. 3, the structural erosion properties of pure copper made electrode also confirm the impurities influence: grain-boundary failure of the area of plasma-material interaction is caused, as well known [3], by the joint hydrogen and oxygen effect. The following conclusions were made after the analysis of structure and composition of electrode CM subject to the hot plasma influence:

1. In the presence of impurities and additions under the test conditions, the temperature of the melt formation is decreased, and the solubility of the refractory component is increased. These change the morphology and dispersion of the secondary structure, and favor the thermal fatigue damage.
2. Within the area of plasma-electrode material interaction, the irreversible structure changes are not accumulated, and the secondary structure is not preserved because the electrode material is carried over by the vapor and condensates.
3. In utilizing copper-containing CM, the increased solubility of the impurities at high temperatures requires to decrease their content in the initial material and in the plasma environment.

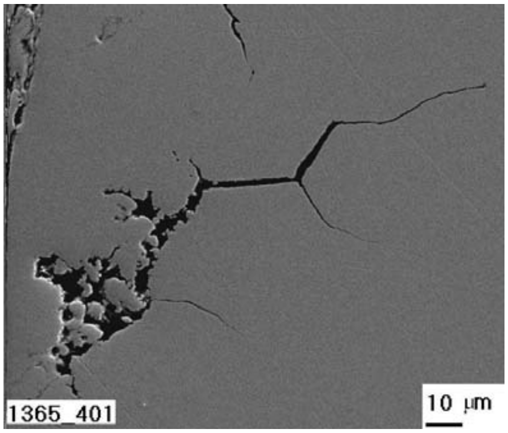

Figure 3. The thermal impact area damage of the pure copper electrode

References

1. Hassanein A., Burtseva T., Brooks J.N. et al. Candidate Plasma-Facing Materials for EUV Lithography Source Components// Emerging Lithographic Technologies VII. Feb. 25-27, Santa Clara, USA, Proceedings of SPIE v. 5037. 2003. p. 358-369.

2. Nassau K., Shiver J.W. Cupric-Molybdenum oxide phase diagram in the air and in the oxygen // J.Amer.Cer.Soc. - 1969. - 52. -N1. - P.36-40.

3. Черноусова К.Т., Новиков А.В., Фридман Л.П. О причинах охрупчивания бескислородной меди / В сб. «Свойства меди и ее сплавов». – Алма-Ата: Наука, 1969. – С. 3-5.

# INFLUENCE OF METHODS OF RECEIVING AND TECHNOLOGY OF SURFACING ON STRENGTH PROPERTIES OF SELICON CARBIDE CERAMICS

**Savorovskiy F. G., Maslov V. P.**
STDO with PP ISP NASU, 4, Lysogorskaya str., Kiev, Ukraine
Phone/fax: +380 (44) 2651957, E-mail: sctb@ln.ua
Phone/fax: +380 (44) 2650555, E-mail: maslov@isp.kiev.ua

Among frail nonmetallic materials the silicon carbide distinguishes by its unique physical properties. If in the first half of XX century it was used in an abrasive industry, in the end of XX century first of all silicon carbide showed itself as a unique material in semiconductors devices, and its strength properties allowed to refer silicon carbide as a perspective material for laser systems and space telescopes mirrors.

In industry there are several ways of silicon carbide receiving, from which most technologic and most used in production is the technology of so-called self-bound silicon carbide. In this process, at sintering in protective atmosphere at the temperature of 1800—2000 °C again formed from components, silicon carbide (secondary) binds initial (primary) grains of silicon carbide. Resulting from such process, the continuous framework of silicon carbide will be formed. However, in this material there is a residual porosity, residual graphite and silicon. Total value of such pores and additives can reach 5%. This technology was used on Brovarskiy plant of powder metallurgy for receiving items up to 500 mm in diameter.

To receive more dense and qualitative silicon carbide ceramics the way of deposition of silicon carbide from a vapour phase is used. The method develops abroad under a title CVD (chemical vapor deposition) - chemical deposition from a vapour phase. Process is conducted under the temperatures of 1200—1600 °C as a rule in hydrogen environment. The most simple way of chemical reactants supply lies in usage of organometallic compounds with silicon and carbon in stoichiometric proportion in its structure. The sediments of CVD process are pore-free, polycrystallic and practically do not contain additives.

The strength properties of silicon carbide ceramics essentially depend on a way of receiving, presence of additives, porosity. The self-bound silicon carbide has 1,5—2 times smaller strength, than samples received by a method of a chemical or physical deposition from a vapour phase.

During the scientific researches the technological modes of machining (grinding and polishing) of silicon carbide ceramics with the purpose of receiving a surface with optical quality were studied. Optimum process is the milling cutting of a plane or orb by a diamond tool on metal bundle with diamonds graining of 315/250 on type 3Б machines. The following grinding was also made by diamond tool on metal bundle with graining of 125/100 on the typical optical effecting equipment, thin grinding with diamond (“tablet”) tool on metal bundle with graining of 40/28 or 28/20. Polishing was made on type ШП machines, using pitch polisher and diamond micro powder 1/0 as the water suspension.

The silicon carbide ceramics strength properties essentially depend on surface quality. So, for example, the polishing in sliding ion beams allows to achieve on micro samples strength level of 3500—4000 Mpa.

# OPTICAL METHODS FOR NON-DESTRUCTIVE CONTROL OF STRENGTH CHARACTERISTICS OF DETAILS MADE OF BRITTLE NON-METALLIC MATERIALS

**Maslov V. P., Rodichev Yu. M.[1], Sarsembaeva A. Z.**
Lashkarev Institute of semiconductor physics NASU,
41, Prospect Nauki, Kiev, Ukraine
Tel/Fax: +380 (44) 265 05 55, E-mail: maslov@isp.kiev.ua
[1]Pisarenko Institute for Problems of Strength NASU
2, Timiryazevskaya Street, Kiev, Ukraine,
Tel/Fax: +380 (44) 296 52 57, E-mail: rym@ipp.kiev.ua

In optical-electronic sensory devices for production of functional precision details the brittle non-metallic materials with different strength and thermal properties (glass, crystals, ceramics, glassceramic) are used. However, at climatic temperatures and external mechanical effects the essential details can be damaged, that leads to failure in activity of all device. The analysis of the possible reasons of destruction has shown, that the locus (beginning) of destruction is determined by defects of the polished surface layers and also defects on peripheral auxiliary surfaces.

There are different optical methods that permit to conduct non-destructive control of strength characteristics of details made of friable non-metallic materials.

## 1. Microscopic method

Microscopic method permit analysing of Griffith cracks, that enlarges at loading, presence on the detail surfaces. Details strength is determined by presence of such defects. The new method was proposed. It lies in that brittle non-metallic details are loaded in the elasticity area, are standed at this loading and surface condition is examined, especial attention is paid to the peripheral surfaces. For instance, sheet of hardened float-glass, several meters length and 0,5 meters width, was curved at transverse efforts effect at its own weight. After several hours of loading microscopic splinters appearance was find out. Long-time strength of such glass could be valued at investigation of planer formation intensity. Investigations were conducted with the help of microscope MBS-4 at 70—100 time magnifications. Such method permits appreciation of strength and reliability of sheet glass at building constructions glazing with hardened glass.

Microscopic method could be used for the examination of defect presence at detail surface during step-by-step grinding and polishing. In this case it is appropriate to use metallographycal microscope MMR-2R that permit investigation of samples up to 20 kg weight.

## 2. Polarization methods

Polarization methods permit with the help of polariser and analyser to analyse stresses in the sample by investigation the detail on gleam. With the help of such method one could investigate complex construction models made of organic glass.

We have investigated different honeycombs constructions by this method. Honeycombs were fulfilled in the shape of hexahedrons, circles and triangles. Stresses presence at loading was examined by polarization method. It was established that hexahedron and circle honeycombs had the least stresses and triangle honeycombs had the greatest stresses.

This method is also effectively used at the control of glazing of aircrafts cabins, at electron-beam tube frames and other products made of brittle non-metallic materials manufacturing.

## 3. Ellipsometric method

The ellipsometry (reflective polarimetry) is an optical method of measurement. It is based on the analysis of beam polarisation changes of polarised light after its reflection from the studied surface. As strength of processed details depends on damaged surface layer depth, for the criteria of quality it was selected the minimum ellipticity tgρ that is the most sensitive to the quality of polished surface, as it was shown in [1—3].

Realized investigations have shown that the residual ellipticity value decreases with the damaged layer removing from the surface till the value that remain constant, however for the deep polished glassceramic samples it has value that is different from zero [4]. Value of minimal ellipticity is determent by the material structure and stresses in the surface layer. Result of parallel roentgen investigations of crystal constituents' state have shown that half-width value for Cu—Kα radiation changes accordingly to the minimum ellipticity tgρ at damaged layer removing. Could be supposed that residual values of tgρ and half-width of diffraction line of Cu-Kα radiation are conditioned by deformations in the surface layer of polished samples.

Offered ellipsometric method of control has allowed optimisation of the technological process of diamond grinding and polishing of different brittle non-metallic materials, including sensitive details made of optical ceramics KO1, KO12. It was established, that after diamond processing the depth of the damaged layer was 1,2÷1,5 times less, than at processing by a free abrasive of the same stippling.

4. Method of IR thermometry

Method of IR thermometry is the remote investigation of temperature distribution by own investigated objects IR radiation registration. Thermography is based on the thermal images analyses that were obtained with the help of registration device called IR camera [5].

During the investigations samples made of brittle non-metallic materials were heated or cooled for creation of temperature difference between samples and environment where they were. Thermograms were obtained with the help of IR camera. They have shown vacuums (defects and other incompactness) in the samples cause they had temperature that differs from the temperature of the whole sample.

Use of IR camera permit increasing of production, informatively and clearness of control without any damaging of investigated objects. Results of investigations are saved in computer for document and further comparison of results in time.

IR methods use permits defect determination in opaque in visible area of spectrum optical details made of different friable non-metallic materials.

In such a way methods of non-destructive control of strength characteristics of details made of brittle non-metallic materials that are presented in this work are effective for using as for investigations so for the industrial control.

1. T. V. Vladimirova, N. Ya. Gorban, V. P. Maslov, T. S. Melnik, V. A. Odarich, The research of the optical proper ties and building of sitall**, 9**, p.31-330, MP, 1979;
2. Fundamentals of an ellipsometry, under edition of A. V. Rzhanov, Novosibirsk, Nauka, 1979;
3. T. V. Andreeva, V. A. Tolmachev, Methodological aspects of ellipsometric experiment on optical materials, **10**, p. 36—39, OMP, 1986;
4. A. I. Belyaeva, A. A. Galuza, T. G. Grebennik, V. Pyuriyev, Optical constants of surface layer on gadolinium gallium garnet: ellipsometric study, Semiconductor Physics, Quantum Electronics and Optoelectronics, 1999, V. 2, № 4, p. 61—65;
5. V. P. Maslov et. al., Eye that see everything, Investigation of remote undamaged control opportunities, ESTA in the innovation epicentre, №40, p. 20—21, 2003.

# CORROSION RESICTANCE OF Ti AND ITS ALLOYS IN SEA WATER

**Vyazovikina N.V., Kus'menko H.H., Kulak L.D., Vyazovikin I.V.** [(1)]
NASU Institute for Problems of Materials Science
03142, 3 Krzhizhanovsky st., Kiev, Ukraine; e-mail: NVyazovikina02@yandex.ru
[(1)]Voronezh Technological Institute, Voronezh, Russia

The basic industries widely using titan and its alloys, the aircraft and technical equipment of an outer space exploration, sea shipbuilding, and chemical and the food-processing industry, nonferrous metallurgy [1] now are. For wide using of Ti and its alloys in sea shipbuilding their increased corrosion resistance in environments containing $Cl^-$- ions is especially important. Therefore studying of corrosion behavior of Ti alloys in natural sea conditions has the important practical value.

New alloys on the basis of Ti-Si system alloyed with Al, Zr and Nb that show high physical and mechanical characteristics in the Institute for Problems of Materials Science of NASU are developed. The influence of these alloying additives on corrosion resistance of Ti and its alloys in water solutions containing $Cl^-$ions till now are insufficiently investigated. In this connection the purpose of the present work is to study corrosion behavior of Ti alloys alloyed with additives of Si, Al, Zr and Nb, in natural sea conditions.

Corrosion behavior of alloyed alloys with silicon strengthing as cast and deformed by gravimetric method at temperature 295 K in sea water (Black sea, Crime, Ukraine) have been studied. The specimens were deformed up to 90%. Titanium VT1-0 (technical titanium) was used as etalon. All specimens under study were sandpapered, washed in ethyl alcohol and distilled water. Then they were weighed and immersed into sea water. They stayed in sea for 40 days. After that the specimens were took out from sea, washed and weighed again. Corrosion rates $V_{cor.}$ of Ti and its alloys were calculated in g $m^{-2}$ $day^{-1}$.

The results of carried out investigations showed that all alloys under study were stable in sea water. Total corrosion rates $V_{cor.}$ of investigated specimens changed within the limits of 0.010-0.100 g $m^{-2}$ $day^{-1}$ and depended on chemical composition and structure of alloys. According to [1] when the corrosion rates of investigated alloys $V_{cor.} \leq 0.100$ g $m^{-2}$ $day^{-1}$ these alloys get in the group "stable". It was established that $V_{cor.}$ of Ti-Si alloys containing 1-4 % Si coincide with $V_{cor.}$ of VT1-0 practically (0.020 g $m^{-2}$ $day^{-1}$) but $V_{cor.}$ of the alloy Ti-6%Si is higher. Additives of Al into alloys of Ti-Si system decrease their corrosion rates in 10 times and alloying of alloys Ti-Si-Al with Zr and Nb does not influence on their corrosion resistance in sea water. Deformation of Ti-Si-Al-Zr and Ti-Si-Al-Nb alloys also decrease their corrosion rates in 10-20 times in comparison with $V_{corr.}$ of alloys of the same chemical composition as cast.

High concentration of active centers on the surface of deformed alloys influence positively on their passivation in sea water. Increase of connection strength of Ti atoms with oxygen of water because of improvement of active centers forming on the surface of deformed alloys resulted in producing of close passive films that protect deformed alloys better then passive films forming on the alloys of the same chemical composition as cast.

Thus, carried out stand investigations showed that $V_{cor.}$ of VT1-0 and alloys of Ti-Si system as cast coincide practically, Al decreases $V_{cor.}$ of Ti-Si alloys in 10 times but Zr and Nb does not influence on corrosion resistance of Ti-Si-Al alloys in sea water. Deformation decreases $V_{cor.}$ of Ti-Si-Al-Zr and Ti-Si-Al-Nb alloys in 10-20 times in sea water in comparison with $V_{cor.}$ of alloys of the same chemical composition as cast.

Developed Ti alloys can be used as corrosion resistant materials for making of ship that work in extreme naval conditions.

1.I.L. Rozenfeld, K.A. Zhigalova.- Uskorennie metodi kopozionnich ispitanii metallov (Teoriya i Praktika). Izdatelstvo: "Metallurgiya", Moskva, 1966.

# TECHNOLOGICAL SUPPORT OF OPTICAL - ELECTRONIC SENSOR DEVICES FUNCTIONABILITY UNDER EXTREME CONDITIONS

**Maslov V. P.**
Lashkarev Institute of semiconductor physics of NASU
41, Prospect Nauki, Kiev, Ukraine
Tel/Fax: +380 (44) 265 05 55, E-mail: maslov@isp.kiev.ua

In optical-electronic sensor devices for functional precision parts manufacturing frail nonmetallic materials with different strength and thermal properties are used (glass, crystals, ceramics, glass-ceramics). At the measuring (sensor) channel clusters collecting rigid glues are widely applied, which provide a high-precision mutual position of parts of different materials. However, at climatic and external mechanical effects the essential parts can be destructed, which results in device failure.

The analysis of possible causes of destruction has shown, that the locus (beginning) of destruction is determined by surface defects on auxiliary surfaces of circumferential areas, for example, grinded bevels and grinded surfaces for pasting.

The researches of general rules of destruction of parts of different frail nonmetallic materials have shown, that the mechanical strength of a machined part $\sigma_L$ depends on depth of the disturbed surface layer **L**: $\sigma_L = \sigma_0 \exp(-BL)$, where $\sigma_0$ - strength of parts with high-performance polished surfaces.

To guarantee the functionability of responsibility of parts of frail nonmetallic materials and clusters collected on their basis, it is recommended:

1. To make machining of the parts auxiliary surfaces with the minimum disturbed layer.

As a result of the conducted researches the new engineering solutions about structures of the LSS (СОЖ), structures of abrasive suspensions, structures of a working section of diamond tools and operational sequences of machining operations were worked-out, which allow to guarantee the disturbed layer of minimum value and to eliminate the appearance of defects such as scratches and points on a working surface of parts.

2. To remove the disturbed layer by etching.

The principles of formation of pickling solutions were designed, which allow to improve roughness on 1 class and to reduce the danger of aggressive acids usage.

3. To conduct auxiliary special low-temperature annealing.

The conducted researches have shown, what the residual disturbed layer, which remains even after polishing, can be reduced at annealing at temperatures of 200—300 °C less, than used for an annealing massive samples.

4. To apply original ways of pasting parts and clusters.

Now there are some new approaches, in which compositions from several different in properties glues are used, new special filling materials and new methods of preparing of surface for pasting. Besides, the methods of unglue bonding were worked-out.

5. To apply mechanical parts, which guarantee damping and relaxation of external influences, for example, alloys with "memory" effect.

The possibilities of using of parts such as flanges or fasteners such as bolt connections with special gaskets were studied, which guarantee vibration damping on high frequencies 2 and more times.

The recommendations designed during scientific researches had been realized in manufacturing of devices of IR-engineering, laser gyroscopes and mirror - prism optical systems.

# FORMATION OF FIRM SCALE ON HEAT-TRANSPORT SURFACES UNDER EXTREME WORKING CONDITIONS AND PRACTICE OF TAKING IT OFF

**Kusaiynov K., Sakipova S.E., Nusupbekov B.R.**
Buketov Karaganda State University
University, 28, Str., Karaganda, 470074, Kazakhstan, E-mail: iph@kargu.krg.kz

It is known, that irrespective of quality of water treatment, during long exploitation on inner surfaces of heat exchange tubes firm scale is formed, which completely covers those surfaces and is remarkable for its strong hardness. The strength of the firm scale is due tj the fact that it is under extreme conditions: the temperature of heat carrier (water stream) is about 500÷700°C, the exerted pressure is ~150bar.

The increase of a bed depth of the firm scale in addition to a natural surface roughness results in such undesirable consequences, as increase of thermal resistance of a wall, decrease of convective heat transfer of a heat carrier, increase of hydraulic losses etc.

The analysis of properties demonstrates, that the heat conduction of firm coatings on an inner side of a tube almost in 40 times as low as the heat conduction of the metal of tube, therefore formation even of a small layer by depth $\delta_H$ $\sim 1,5\cdot 10^{-3}$m results in temperature rise of metal and its overburning, i.e. the heat-transport characteristics of the equipment gets worse considerably.

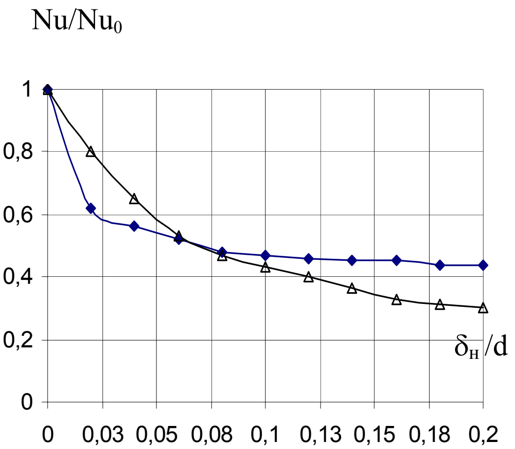

Fig. 1. Relation of heat transfer to depth of deposits:
Δ- for boiler tube with a dia $18,8\cdot 10^{-3}$m, ♦ - for boiler tube with a dia $51\cdot 10^{-3}$ m.

In fig.1 the experimental relation of relative convective heat transfer of a tube to relative thickness of the firm scale $\delta_H/d$ is adduced, where d is diameter of a tube. As it is seen in the chart the intensity of convective heat transfer sharply decreases at small depth of the firm scale, and the further increase of the latter doesn't influence considerably the value of the convective heat transfer.

It is established, that depending on the depth of scale the heat exchange properties of boiler tubes are reduced to 50-60%. Therefore, in order to intensify by the process of thermo exchange it is necessary to remove firm scale from surfaces.

The removal of firm scale in customary mechanical or chemical ways is not effective and harmful in ecological aspect.

The proposed in this paper method of removal firm deposits, founded on the electrohydraulic effect, is most worth-while and effective, as it supposes direct transformation of energy of electric discharge in water in mechanical energy of pressure surge.

Theoretical fundamentals of electrohydraulic effect and its some practical applications are well known. The industrial version of the of the installation for destruction of extra-hard surfacing, covering the inner surfaces of tubes is developed and built in laboratory of hydrodynamics and heat exchange of our university. The equipment tests were conducted on samples of tubes with the diameters d $=51\cdot 10^{-3}$m taken from spent boiler (marks E1/9, DKVR).

During the tests the relation of discharge voltage to the value of inter electrode spacing interval in the discharger and relation of length of a zone of destruction of scale to a stored energy on the store was investigated.

The relation of length of a zone of destruction *L* to the value of energy *W* is adduced in a fig. 2. The investigation has shown, that depending on a degree of hardness of coatings, the minimum value of energy, at which they starts their destruction, varies within the limits 55÷65 J.

Depending on the value of stored energy of discharge W and the depth of coating *d*, the length of cleaned segments of a tube *L* can reach up to 1÷1,5 diameters of a tube *d*.

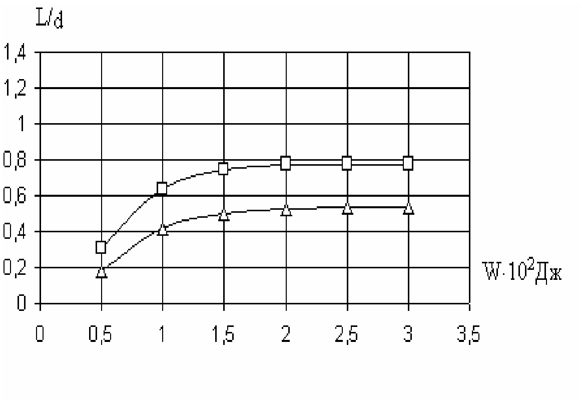

Fig. 2. Relation of length of a zone of destruction at different values of energy of discharge: d = $51\cdot10^{-3}$m; $\delta_н$ =: □ - $(7\div9)\cdot10^{-3}$m; Δ- $(12\div16)\cdot10^{-3}$m.

The geometrical sizes of the broken off pieces (spalls) can reach up to the diameter of a tube *d*. At the same time, as it is seen in fig.2, the optimum length of a zone of destruction tends to equal with the increase of value of energy of discharge. Under the same conditions the further increase of stored energy does not result in increase of length of a zone of destruction. All this allows to establish some best value of energy on the condenser, the further increase which is not expedient, the more so that excessively large geometrical sizes of the broken off deposits make their taking out from the cleaned zone difficult.

The experiments demonstrate, that the cleaning the heat exchange surfaces off firm scale with the application of the installation, the operation of which is based on the use of the underwater electric discharge, as a source of powerful pulse pressure is completely warranted.

However, more delicate hydrodynamic effects of electric discharge in water, apparently, are connected with the influence of heterogeneity of the working medium itself, i.e. the presense of firm and gaseous phases in it, which when sligthly changing density, essentially influence the hydrodynamics of distribution of shockwaves.

The influencing of a gas phase on dynamics of a shockwave is studied well enough, whereas the influence of firm fragments in a working medium on the purification process is not done enough. The influence of the sizes of firm dispersed fragments and their concentrations on dynamics of pulse pressure is not investigated either.

In this connection, the experiments on analysis of influence of concentration and sizes of a dispersed solid phase on dynamics of pressure at the front shockwaves accompanying electric discharge were conducted.

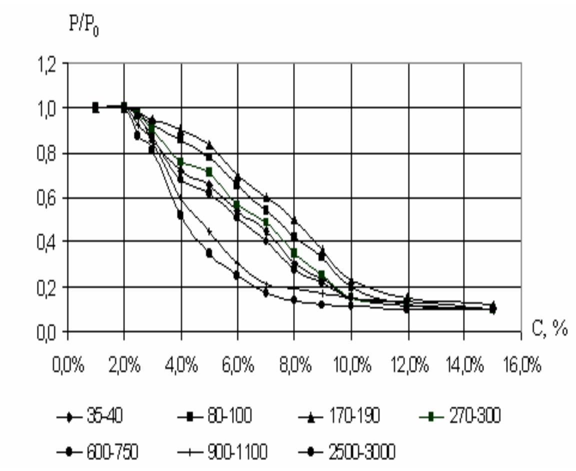

Fig. 3. Relation $P/P_0$ to the concentration of a dispersed solid phase (the sizes of fragments are adduced in microns).

In experiments the relation $P/P_0$ to the concentration and sizes of firm dispersed fragments was studied, where P is an amplitude of pulse pressure of electric discharge in an investigated dispersed phase, $P_0$ is pressure in a clean liquid. In a fig. 3 the plots of dimensionless pulse pressure $P/P_0$ tj the concentration C for the different sizes of a disperse phase at the pressure $P_0$=10bar are adduced.

As it is seen in the graph, the pressure for all sizes of all fragments is continuously decreases beginning the concentration of fragments about two percents and practically becomes minor at values from ~ C ~12÷14 %.

At the definite sizes of dispersed fragments the non-linear dependence is observed. At the same concentration the amplitude of pulse pressure at electric discharge depends on the sizes of dispersed fragments. This effect is apparently connected with the formation of firm structural clusters of a disperse phase, which under certain conditions offer minimum resistance to a wave propagation of pressure.

On the base of results of the researches the effective technology of an electrohydraulic method of removal of firm scal, forming inside heat exchange tubes during long exploitation under extreme conditions, has been developed.

# INVESTIGATION OF INFLUENCE OF OIL MEDIUM ON THE PROPERTIES OF FROST RESISTANT SEALING RUBBERS UNDER NATURAL EXTREME CONDITIONS

**Petrova N.N., Fyodorova A.F.**
Institute of Nonmetallic Materials SB RAS
20, Avtodorozhnaya St., 677007, Yakutsk, Russia, inm@ysn.ru

In winter time machines and mechanisms perform premature failures under the conditions of the North. About 30 per cent of these failures (automobile transport, mining technique, technological pipelines) are due to complete or partial destruction of rubber sealing units. The main reason of that is unsatisfactory frost resistance of the units due to incorrect choice of the elastomer base or degradation of its low-temperature properties under combined impact of climatic factors.

It is very difficult to model behavior of the elastomer materials under combined influence of climate and aggressive media in the laboratory, so, in order to evaluate the materials one has to carry out field tests.

There is a system of complex evaluation of sealing rubbers operability under combined impact of oil media and ambient temperatures characteristic of the North, which includes investigation of basic operational properties and the rubber composition (physical and mechanical indices, oil- and frost resistance, residual deformation of compression, plasticizer contents) before and after the impact.

Investigation of rubbers based on butadiene-nitrile caoutchouc B-14, 7130, 77455 showed that before exposing in oil they performed satisfactory level of fhysical-mechanical and low-temperature properties. However, their contact with the medium at room temperature caused degradation of the sample mass at the initial exposition stage (1 week) due to the plasticizer washing-out, which leads to decrease of frost resistance and sizes of the units produced of these rubbers.

To slow down washing out of the plasticizer from the elastomer matrix B-14 rubber was modified by 15 wt. parts of preliminarily actuated (crushed in AGO-5 planetary mill) natural zeolites having high adsorption capacity. With this it becomes possible to reduce oscillations of values of swelling rate at the expense of densification of the vulcanization network (molecular weight of a chain section of the vulcanization network between neighboring interlaces decreases from 2294 to 1912 conventional units), as well as possible adsorption of the plasticizer by the zeolites.

Rubber based on new propylene-oxide caoutchouc (SCPO), which is serially produced at Sterlitamaksk plant of synthetic caoutchoucs performs high level of frost resistance, strength and elasticity.To decrease swelling degree and residual compression deformations this rubber was also modified by actuated zeolites. Application of zeolites after different actuation time (3, 5 and 10 minutes) and injection of different amounts (5, 10, 15, 20 wt. parts) showed that injection of 20 wt. parts of zeolites actuated for 3 minutes reduces swelling of rubbers based on SCPO by 20 per cent, the rest of the properties being unchanged. Injection of 15 wt. parts of natural zeolites actuated for 10 minutes into the recipe reduces residual compression deformation by 25 per cent.

To evaluate operability of rubbers we have carried out investigations of oil impact under the conditions of field exposition. Studied were the properties of the following serial rubbers: B-14, modified and unmodified by zeolites, 7455, 7130, as well as the rubber based on propylene-oxide caoutchouc before and after their contact with oil at ambient temperatures under the conditions of Yakutsk.

It was shown that interaction of the rubbers with oil media at cyclic temperature oscillations causes intensification of diffusion processes, such as penetration of oil into the rubber and washing out of plasticizers. Temperature regime in the conditions of field exposition (seasonal and annual temperature alternations) destabilizes basic operational properties of the rubbers. With this, strength characteristics and residual compression deformation do not change marginally, their values do not exceed allowable ones. Basic negative impact diffusion exerts on such operation parameters as swelling degree and frost resistance coefficients. Coefficient of frost resistance for all investigated rubbers reduces marginally and irreversibly after 2 months of exposition at extreme temperatures (-45°C to -55°C).

Necessity to take into account diffusion processes, which occur at contacting of rubber and oil while designing rubber units and investigating their operability under real operation conditions determined the following: detailed study and modeling of rubber swelling process in oil at room temperature. While performing swelling experiments one can observe an initial stage of swelling, which occurs during the first day of exposition in oil. More likely it is conditioned by quick penetration of light hydrocarbons from the oil. Mathematic processing of the results shows that it is absorbed fraction that initiates the process of the plasticizer (dibutylphtalate) washing out of the rubber after its contacting with oil. Simultaneously swelling of the material takes place, which is due to diffusion of heavier oil fractions into the elastomer. In order to describe kinetics of the rubber swelling in oil we applied the equation obtained as a result of solving Fix's diffusion problem for the multi-component system allowing for the plasticizer washing out.

There is a correlation between computed values of diffusion coefficients at room temperature and basic operational properties of rubbers after field exposition.
The correlation allowed determining new approaches to optimize rubber recipes at the stage of their designing. Injection of adsorbents into the material – natural zeolites, application of mixtures of elastomers, one of which has higher oil and benzene stability, provides slowing down oil diffusion and plasticizer washing out of the polymer matrix.

Hereby the results of investigations of combined impact of oil and ambient temperatures on the basic operational properties of sealing rubbers allowed developing recommendations on their application. B-14 rubber did not satisfy the requirements for rubbers to be exploited in hydrocarbon media, as its contact with oil causes irreversible decay in low-temperature properties in critical operation areas. 7130 rubber, whose polymer base consists of a mixture of two rubbers, i.e. BNKS-18 and BNKS-40, is a rubber with reduced frost resistance, but it is applicable to produce the units, which don't have to satisfy high frost resistance requirements but they must perform high stability in hydrocarbon media. The material based on propylene-oxide rubber performed the highest stability of properties as its low-temperature ones in the critical area of operation are determined by the polymer base ($T_s$=-74 °C) and hardly depend on the plasticizer contents.

# WEAR RESISTANCE OF DIFFERENT MATERIALS IN BODY SIMULATED FLUID (BSF)

**Lashneva V.V., Dubok V.A., Tkachenko Ju.G., Matveeva L.A.**(1)
Frantsetich Institutre for Problems of Material Science of NASU
Krzhyzhanovsky St. 3, Kiev, 03142, Ukraine, dubok@imps.kiev.ua
(1) Institute of Semiconductors Physics of NASU
Science Pr.,115, Kiev, 03150 Ukraine, matveeva@isp.kiev.ua

Wear resistance is a major characteristic of the movable joint of surgical implants, in particular, hip endoprosthesis. Hip endoprosthesis is the precise technical device, implanted into human body to replace partially or totally the injured hip joint with the purpose to restore its lost functions.

Now surgeries with total hip endoprosthesis are the most widespread operations on hip joint due to traumas and degenerate-dystrophy diseases. Quantity of such operations in the whole world is about 1 million per year. Only a few achievement of modern medicine can be compared with total hih prosthesis surgery by efficiency and improvement of quality of patient's life. However despite of development of a lot of different designs of total hip prosthesis, all existing hip prosthesis can not meet the users' demands on long service life of the hip prosthesis and after several years the necessity to replace some components of the prosthesis increases.

The technical resource of hip endoprosthesis is limited mainly by wear resistance of the tribological pair of the hip joint. In the majority of hip prosthesis designs, produced worldwide, the friction pair consisits of metal alloy and polyethylene with a super-high molecular mass.

In particular, in domestic hip prosthesis the titanium alloy BT is utillized and polyethylene Chirulen, produced by the German corporation Hoechst AG. Wearing of such pair makes about 0,1 mm per one year, that guarantees service life of the endoprosthesis not less than 10 years.

With the purpose to prolong the service life of domestic hip prosthesis, increase its reliability and working stability, the comparative tests were held to compare wear resistance of polyethylene Chirulen in pair with other domestic materials, allowed for application in medicine, namely with CoCrMo alloy, high pure $Al_2O_3$ ceramics and 13X18H10T stainless steel.

The wear tests were made with the help of the rod-to-disk device in following conditions: constant load -5 H/mm$^2$; speed of slip - 0,1 m\s; the environment - Ringer solution; temperature - 37 °C; duration of tests - 20 hours.

The results of the wear measurements (decreasing of the polyethylene volume in contact with studied materials) are listed in table.

Table Polyethylene wear in different friction pairs

| Hours | Wearing polyethylene, cm$^{-3}$ | | | |
|---|---|---|---|---|
| | BT6 | CoCrMo | 12X18H10T | $Al_2O_3$ |
| 5 | 0,0160 | 0,0017 | 0,00315 | 0,0003 |
| 10 | 0,0260 | 0,0020 | 0,0069 | 0,0013 |
| 15 | 0,0320 | 0,0022 | 0,01015 | 0,0021 |
| 20 | 0,0390 | 0,0027 | 0,01245 | 0,0026 |

It is visible, that the greatest change of the polyethylene volume (greatest wearing) was found in pair with titanium alloy BT 6. The polyethylene wearing in pairs with other studied materials CoCrMo alloy and ceramics Al2O3- is much lower - approximately in 8 - 10 times. Thus, CoCrMo alloy, $Al_2O_3$ ceramics Al2O3 and 12X18H10T steel can be recommended for replacement of BT6 alloy in friction joints of hip endoprosthesis.

# PECULIARITIES OF WELDING TOOL OPERATION MADE OF OXIDE AND CARBIDE/CARBON DISPERSION STRENGTHENED MATERIALS OF DISCOM® TRADE MARK IN RIGID WELDING MODE

**Shalunov E.P., Dovydenkov V.A.(1), Simonov V.S.(2)**
United Scientific and Technological Laboratory of the
Composite Materials of the Chuvash State University,
Moskovsky av.15, Cheboksary, 428015, Russia, e-mail: shalunov2003@mail.ru
(1)Mechanical Alloyed Materials Plant DISCOM Co., Ltd,
Panfilof St. 41,Yoshkar-Ola, 424003 Russia, e-mail: discom@yoshkar-ola.ru
(2)STRAZH-VE Co., Ltd, Krylov St. 53A,Yoshkar-Ola, 424007 Russia, e-mail: strazh@mari-el.ru

Welding modes are characterized by the combination of their parameters and also by the shape and size of the contact surface of the welding tool.

The basic parameters of the resistance spot welding are welding current $I_w$, welding time $\tau_w$, electrode compression force $P_w$.

At electric arc welding by a consumable wire electrode in the shielding gas environment (MIG/MAG welding) the basic parameters of welding are the following: $I_w$, arc voltage U and feed speed of the wire electrode to the welding zone V.

Rigid modes of welding are understood to be characterized mainly by big values of the welding current $I_w$ and small values of $\tau_w$ [1]. The influence of the compression force of electrodes $P_w$ or feed speed of the wire electrode V and the shape and size of the contact surface of the welding tool on the intensity of the welding process is not taken into consideration, though in most cases they are of essential importance to assess stress loading of the welding tool and its life time.

The paper [2] presents design equations to define the so-called energetic tension of the welding tool which takes into account the combined influence not only of electric parameters ($I_w$, $\tau_w$, U) but also mechanical parameters ($P_w$, V) and also the shape and size of the contact surface of the welding tool and the properties of its material on the welding tool.

In particular, energetic tension of the electrode of the resistance spot welding is generally the following:

$$E_{\text{Å}} = \frac{W_{\text{Å}}}{\text{À}_{\text{Å}}} = \text{Ò}_{\text{Å}} \frac{\tilde{n}_{\text{Å}} \cdot \gamma_{\text{Å}}}{1 + \beta \cdot \text{Ò}_{\text{Å}}} \cdot \ell_E, \qquad (1)$$

where $W_E$ – the total energy (electrical, mechanical, thermal) influencing the electrode, J;
$A_E$ – the electrode contact surface area, $mm^2$;
$c_E$ – specific heat of the electrode material at constant pressure and the electrode heat temperature $T_E$, J/kg · °C;
$\gamma_E$ – absolute density of the electrode material at normal temperature, $kg/m^3$;
$\beta$ – coefficient of volume expansion of the electrode material, 1/°C;
$\ell_E$ – the distance from the contact surface of the electrode up to the bottom of its cooling groove, mm.

Energetic tension of the current contact tip for MIG/MAG welding in general is calculated on the equation:

$$E_{\text{Ò}} = \frac{W_{\text{Ò}}}{\text{À}_{\text{Ò}}} = \frac{I_W \cdot U}{\pi \cdot d_T \cdot V}, \qquad (2)$$

where $W_T$ – electric power fed to the tip, J;
$A_T$ – the surface area of the operation hole of the tip, $mm^2$;
$d_T$ – diameter of the operation hole of the tip, mm.

The analysis of the modes of resistance spot welding and MIG/MAG welding applied in most Russian plants (ОАО «АвтоВАЗ», ОАО «ГАЗ», ОАО «УАЗ» ОАО «КАМАЗ» and etc.) and foreign plants (FORD, OPEL, ŠKODA, General Motors and etc.) using welding tool made of CuCrZr (БрХЦр) showed that such a tool works trouble free it its energetic tension does not exceed 9…10 $J/mm^2$. At larger values of energetic tension, and consequently, at more rigid modes of welding in bronze material of the welding tool the process of weakening starts to develop (mainly of dynamic recrystallization) resulting in intensive wear of the contact surface of the welding tool.

Application of Oxide and Carbide/Carbon Dispersion Strengthened Copper (OCDS-Copper) of DISCOM® trade mark having mainly high recrystallization temperatures (850… 950 °C) in the welding tool enables the consumer to use such a welding tool effectively at energetic tension up to 30 $J/mm^2$.

The fact that welding tool made of OCDS-Copper of DISCOM® trade mark endures higher values of energetic tension results in longer life time as compared with the life time of a analogical tool made of chrom zircon bronze and more over made of chromium bronze. So, at resistance spot welding of steel sheets (08KP), the total gage making up 1,6 mm (energetic tension of electrodes is equal to 11 J/mm$^2$), the life time of electrodes made of C16.106 OCDS-Copper of DISCOM® trade mark is nearly 1,8 times higher than that of the electrodes made of chrom zircon bronze and at resistance spot welding of steel sheets , the total gage making up 2,8 mm (energetic tension of electrodes is equal to 23 J/mm$^2$) the life time of electrodes made of this OCDS-Copper is 3,6 times higher [3].

When using the wire electrode of 1,0 mm in diameter at MIG/MAG welding (energetic tension of electrodes is equal to 10…13 J/mm$^2$) the life time of the contact tips made of C16.106 OCDS-Copper of DISCOM® trade mark is 1,9…2,0 times higher than that of the electrodes made of chrome zircon bronze and using the wire of 1,6 mm in diameter (energetic tension of electrodes is equal to 23…26 J/mm$^2$) the life time of the contact tips made of this OCDS-Copper is 2,5 times higher [2].

The availability in OCDS-Copper of microfibrous structure oriented in the direction of the current going through the welding tool reduces the loss of the supplied electric power at rigid mode welding by 13…15% [2].

Thanks to high recrystallization temperature and availability of residual carbon in most types of OCDS-Copper of DISCOM® the welding tool made of these materials also possesses high antiadhesive properties that is especially important with rigid modes of resistant spot welding of galvanized steel, aluminium, magnesium and other alloys and also at welding by means of steel wire electrode coated with copper, aluminium or copper wire [4].

As it has been already mentioned above, the availability of microfibrous structure with OCDS-Copper of DISCOM® trade mark imparts strong wear resistance to the welding tool made of these materials, especially under rigid welding conditions. For instance, electrodes for resistance spot welding show the effect of “self-sharpening” [2] of their contact surface after a definite number of welded spots, and the hole of current-carrying tips for MIG/MAG welding is increased by 20…30% less than the hole of the similar tips made of bronze CuCrZr (БрХЦр) [5].

The peculiar features of the welding tool made of OCDS-Copper of DISCOM® trade mark mentioned above, apart from the absence of the necessity of the additional thermal mechanical processing that is a must for dispersion hardening chrome zircon bronze CuCrZr (БрХЦр), have provided widely spread use within a short period of time since the moment of these materials introduction [5, 6] in welding fabrication of many Russian (over 200) and foreign plants producing automobiles, buses, tractors, locomotives, carriages, vessels, electric apparatus and other machinery.

## Reference

1. Оборудование для контактной сварки: Справочное пособие/ Под ред. В.В. Смирнова. – СПб.: Энергоатомиздат. 2000. – 848 с.
2. Шалунов Е.П. Высокоресурсный сварочный инструмент из дисперсно-упрочненных композиционных материалов на основе порошковой меди. – Чебоксары: ИНТЦ «ДИСКОМ», 2003. – 257 с.
3. Шалунов Е.П., Равицкий Г., Берент В.Я. Высокоресурсные электроды контактной сварки из медных дисперсно-упрочненных композиционных материалов: разработка, производство, применение // Электрические контакты и электроды: Тез. докл. Междунар. конф. «ЭК-2003», Кацивели, Крым, 15 – 21 сент. 2003 г. / ИПМ НАН Украины, Киев, 2003. – С. 89 – 92.
4. Shalunov E.P., Lipatov J.M., Golubyatnikov D.A. Experience of producing semi-finished items and ready-mady articles made of oxide and carbide dispersion strengthened powder copper in Russia // Deformation and fracture in structural PM-materials: Proc. of the Int. conf. «DF PM-99», Piešťany, Slovak Republic, Sept. 19 – 22, 1999. – Vol. 1. – P. 365 – 373.
5. Шалунов Е.П., Матросов А.Л. Высокоэффективные электродные материалы из порошковых композиций на основе меди // Современные технологические процессы получения изделий из металлических порошков: Материалы Республ. межотрасл. научно-практ. конф. / ЦНТИ, Чебоксары, 1987. – С. 45 – 46.
6. ÖP 400.580. Kupferwerkstoff für elektrisch leitende Verschleissteile / E. Schalunov, G.Jangg, H. Walther, A. Matrosov ua. OÄ 1341/93 von 08.07.1993.

# USE OF THE SOLAR BATTERY IN AUTONOMOUS REQUIREMENTS OF MAINTENANCE

**Tarasov V.K., Murzin L.M.**
Sevastopol National Engineering University
Gogol 14, Str., Sevastopol, mash sevgtu 14

The solar battery on semi-conductors is used in different requirements as a generator of electrical energy. As a rule, it is extreme requirements of maintenance, such as: in a near space for energy-ensuring of board users of energy of different power on space plants; on the Earth as engine installations of automobiles etc. Use of solar batteries as power sources in earth requirements pursues first of all ecological purposes. In the present operation the results of an experimental research of operation of the solar battery in a technological system autonomous apiary are submitted by long-lived operation it in requirements of a steppe band of the south of Ukraine and northern Crimea. The ecological aspect of use of an ecologically clean power source by operation apiary in an agricultural band has the special value both for a surrounding medium, and for itself apiary, ensuring comfortable conditions of life for the personnel apiary and for family of bees during the tax of honey. Important the simplification of apiarymen buizness and heightening of productivity of process of manufacture of honey in requirements of an independent farm is also.

In an introduced material the technological system moved apiary, installed on the automobile ZIL-130 with the trailer surveyed. The solar battery (photoelectric transformer-FET) by power 2x20W is firmware in a circuitry and ensures recharging of the power secondary generator of the automobile 6ST-90 in a self-acting condition. The duration of operation of a technological system apiary makes 180 - 210 days and envelops a period since April till October. Thus, the requirements of maintenance are rather manifold and power up as cold (temperature up to 3—5 °C), and hot (temperature up to 45—50 °C) periods of year. Autonomous moved apiary works in variable weather requirements (rain, dust). If to take into account, that the duration of solar periods and solar activity in different seasons and different seasons can rather considerably vary, the opportunity recharging of the power secondary generator during all time in use apiary is rather problematic. So, in explored seasons 2002—2003 years during the intensive tax of honey and, accordingly, peak of energy-ensuring, duration of periods of low solar activity (cloudy sky, rains) made of 5 -10 days. At a maximum level of a power consumption 10—20 Amp-hrs /day of capacity of a storage battery 90 A/h suffice for 4—7 days (under condition of maximum discharge 40—50% from an aggregate capacitance of the battery) Thus requirement of maintenance of an electrical engine installation in a technological system autonomous moved apiary it is possible to refer to extreme.

The technological system moved apiary consists of the following devices and blocks:
The 1-block of management, 2-cutout switch network, 3-sockets, 4-voltmeter, 5-ammeter charging of the secondary generator, 6-solar batteries (2 pieces till 20 W, I—2 A), 7-power generator 6ST-90, 8-ammeter of a load, 9-block of fuses, 10-time element, 11-electromotor of honey - extractor, 12-lighting gears, 13- transport - loading device, 14-other domestic consumers. Block – sheme of equipment of apiary are makes on figure1.

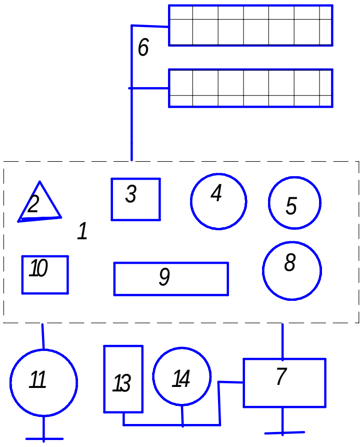

Figure 1. Block –sheme of equipment of apiary

The basic user of the electric power in field requirements is an electromotor honey-extractor. At acceleration honey-extractor starting currents the magnitudes 15 A achieve. At a voltage rating 12 V the power consumption makes 180 W. The duration of a period of starting makes 1 minute. The amount of startings within a working day achieves 30—40. Total of energies consumed in the starting periods of operation of installation are made by 5—7 Amp-hrs / day in a power consumption.

In a stationary period a pumping out (at a current 4A and duration of a cycle 3-5 minutes) make 10—12 Amp-hrs / day. Thus, the common daily power consumption in an intensive period a pumping out of honey makes 15—19 Amp-hrs / day. The estimation of intensity charging of the secondary generator from the solar battery is manufactured at the following dispatchings (current charging 2—4 And, daily duration charging 8—10 ч). The energy, generated by the solar battery, makes 16—40 Amp-hrs / day. Hence, the solar battery consisting of two panel, within light day ensures a day time power consumption apiary during the intensive tax and pumping out of honey. The maximum period of the intensive tax of honey and its pumping out makes of 5—10 days of a continuous cycle. Hence, the common expenditures of the electric power for security of function honey-extractor make 150—190 A/h, that in some times exceeds capacity of the secondary generator.

Hence, it is required constantly to manufacture for normal operation of the secondary generator during an intensive pumping out of honey charging of the secondary generator in a self-acting condition.

The load of the solar battery by power 40 W thus makes 90-100 %.

Using as test of an estimation of functional performances of installation an index of a reliability - it is necessary to mark probability of a fault-free operation p(t), that the circumscribed installation can normally and effectively work during a long-lived season only under condition of p(t)=1. Experience of maintenance of the solar battery as an engine installation independent apiary and the absence of refusals proves 100% of a reliability of such battery. Besides distinctive feature of a construction of the solar battery in domestic performance is the simplicity of maintenance and absence of necessity of its service and repair.

By other way of the solution of a problem of a reliability are the redundancy of low- reliabilities devices can by making be parallel - sequential schemes of installations. For example, it can be insert of the spare secondary generator in a web, however such path is not optimum from a point of view of economic indexes of the tax of honey and in view of additional cares of a drift of the additional secondary generator.

The materials of the present operation allow to make the positive forecast concerning a perspective of use of solar batteries for energy-ensuring apiaries and other plants requiring ecologically clean power sources. The transition to such systems creates new opportunities of architecture of work in farms distinguished from nowadays existing high efficiency of work, nowadays existing by high efficiencies, for production.

# GAS DETONATION COATINGS TO PREVENT “SELFBONDING” OF MACHINERY PARTS

**Kadyrov V., Remeslo V.**
Frantsevich Institute for Problems of Materials Science NAS of Ukraine,
03142, Kyiv-142, 3, Krzhyzhanovsky Str., Ukraine, E-mail: valkad@alfacom.net

All metals and alloys have ability of “selfbonding” in the surface contacts at the distances no longer then distance of interatomic action forces [1]. To create highly-developed bonding it is necessary to obtain of high contact pressure, which helps to increase plastic deformation of metals, or heating, which increase activity of lattice. In case of high pressure and high temperature, the further contact surfaces approachment and physical contact forming will be developing due to the creep. The following factors are influence on the bonding processes: temperature and contact time exposure, specific pressure and working environment, surface condition and contact materials combination, their mutual solubility in solid state. Besides, are very important the physic-chemical properties of the materials such as a lattice type, ductility, hardness, modulus of elasticity, melting temperature, atomic radius, surface energy and so on [2]. Bonding of many machinery parts, for example parts of atomic power equipment, which are working at high temperature and pressure in the pure helium environment is very complicated scientific and technical problem. It is known, that at the influence of temperatures below of 1000 $^{O}$C and insignificant loads the bond strength of contacting pair reaches a great deal, commensurable with the strength of the contacting metal. In order to limit volume interaction of materials, disposed to mutual solubility, it is necessary to insert between them a barrier layer/coating, which can prevent forming of solid solutions of contacting materials. Protective coats for such purpose should have sufficient strength and adhesion to the metal. Such coats can be deposited on the contacting materials surfaces by thermal spraying methods. One of most promising methods for such application is gas detonation spray method providing high strength of sprayed coats and high adhesion to the substrate. Detonation spray particles velocity can reach 700-900 m/s, particles temperature –1000- 1500 $^{O}$C, which provides higher density and adhesion of sprayed coats, than in the case of flame and plasma spraying. Detonation coatings can be obtained by gas-detonation installations [3,4]. Promising materials to spray coatings to prevent selfbonding are aluminum oxide, electrocorundum zirconia, notable by high refractoriness, hardness and strength, stability in vacuum, in inert gases environment and in the reduction atmosphere up to the temperature of 1800-1900 $^{O}$C [5]. Thermal stability and selfbonding test was done on ring samples made of Х18Н9Т steel and ХН55МВЦ alloy installed on special stand. Samples to check selfbonding were tested in helium atmosphere at the temperature of 950 $^{O}$C. Working pressure on the ring samples was created considering the sample material long-term strength at the temperature of 950 $^{O}$C during 1000 hours and was equal to (0,2-0.35) σд.п.. Contact surface of ring samples was equal to 10 square centimeters. Evaluation of selfbonding test results of different contacting pairs was done visually by registering of bonding zones on the samples surfaces. The minimal temperature and pressure which caused initial selfbonding were determined, i.e. was determined “threshold of selfbonding”, at the same time the surface conditions were evaluated (bonding area, actual contact surface). Increasing of working load have cause changes of surface contact area, deformation degree and destruction of the coating. The bonding strength was determined as rings tensile load divided on nominal contact area. In the process of samples spraying the temperature in the detonation zone and particles on flight velocity have varied in vide range by changing of volume ratio of detonating gas mixture components ($O_2:C_2H_2$ was changed in the range of 1.15-2.5), by changing of combustion chamber infill degree of detonating mixture (in range 0.3-1.0 of combustion chamber volume). Stand off distance and firing frequency were invariable and were equal to 170 mm. and 3Hz., accordingly. Samples coated by aluminum oxide, electrocorundum zirconia, nickel alloyed by aluminum and silicon, nickel mechanically blended with 15, 30 and 45% of aluminum oxide, nichrome, nichrome alloyed by boron and aluminum, nichrome mechanically blended with 25, 50 and 75% of electrocorundum zirconia were tested. Test results evaluation of samples without coating has demonstrated their considerable adhesion and their adhesion strength has reached values of 30-70 MPa for X18H9T steel and 10-18 MPa for XH55MBЦ alloy. Coatings having in their composition nickel, molybdenum have demonstrated considerable tendency to the bonding even at the moderate test parameters. Growing velocity of selfbonding increases sharply in case of raising of temperature from 700 $^{O}$C to the 900 $^{O}$C approaching to the strength of the substrate material. Adhesion strength with substrate, number of thermocycles prior the destruction of aluminum oxide and electrocorundum zirconia coats was 26-32 MPa, 12-30 cycles and 28-45 MPa and 30-35 cycles, accordingly. Samples with the aluminum oxide and electrocorundum zirconia coatings didn't bond with each other, however take place their spalling, delamination and exfoliation with the substrate during the disassembling of samples package, which is probably caused by tremendous gradient of residual stresses on the boundary metal-coating because of big difference in the coefficients of thermal expansion. In such conditions the optimal variant of the coating, which prevent bonding at the elevated temperatures and contact loads can be lamellar coating with damping underlayer and oxide outer layer. Damping layers should to provide sufficient level of strength and thermal cycle resistance, and outer oxide layer should prevent selfbonding. In such conditions is very important the choice of composition of sprayed damping layers, providing smooth fluent transfer from metal to ceramic with smoothing negative influence of coefficients of thermal expansion gradient of contacting pair. As such kind of coatings were investigated multi-layer coatings of the following composition: nichrome alloyed (X20H80, aluminum, boron), mechanical mixture of alloyed nichrome with 25, 50 and 75 % of electrocorundum zirconia and electrocorundum zirconia. To determine coatings thermal resistance the thermal cycling of the samples was done at the following parameters: heating up to 950 $^{O}$C with velocity of 200 $^{O}$C/h, exposure for 4 hours and cooling with the furnace to 200 $^{O}$C followed by new cycles. The samples were assembled to the package, after put into the helium environment and were loaded by force of 3,5 MPa. It was determined that application of a damping multi-layer coatings of material nichrome alloyed (NiCr-Al-B) mixed with electrocorundum zirconia, concentration of alloyed nichrome in which changes from 100% on the substrate to 0% on the surface, and the concentration of electrocorundum zirconia increases in opposite manner has permitted to increase thermal cycle resistance of oxide coatings on the X18H9T and XH55MBЦ steels up to 150 cycles without visible signs of selfbonding.

Refrences.

1. Казаков Н.Ф. Диффузионная сварка материалов. М. , “Машиностроение”, 1976г.
2. Боровский и др., Процессы взаимной диффу-зии в сплавах, М., Наука, 1973, 360с.
3. Kadyrov V., Nevgod V., Garda A., Detonation-Gas Apparatus for Applying Coatings, United States Patent # 4,687,135.
4. Kadyrov E., Kadyrov V. , Advanced gas detonation coating process DEMETON, Proceedings of the 14th Inter. Thermal Spray Conf. ITSC'95, Kobe, (May,1995) pp. 417-425
5. Ремесло В.В., Федоренко В.К., Кадыров В.Х. и др., Структурно-фазовое состояние и термостойкость детонационных покрытий из оксида алюминия, Порошковая металлургия, 1985. №5,сс.32-38.

# STRUCTURAL ASPECTS OF HIGH-ENERGY INFLUENCE ON TITANIUM ALLOYS

**Dan'ko S.V., Minakov N. V., Popchuk R.I., Rudyk N.D.**
Frantsevich Institute of Problems of Materials Science of NASU,
3, Krzhizhanovskogo St., 03142, Kiev, Ukraine, E-mail: altifer@ipms.kiev.ua

This article describes the peculiarities of phase and structural state of titanium alloy under pulsed influence of explosive detonation waves. The thermodynamic parameters are following: detonation speed - 8,3 km/second, exothermicity of reaction - 5500 kilojoules/kg, the temperature of the blast - 3850 $^0$C [1].

The chemical composition of investigated titanium alloys is demonstrated in the table 1.

Accumulated influence of detonation wave energy on sample surface causes not only the fuse of material, but also its evaporation. In addition a channel is formed in the depth of the sample. The depth, geometrical form and dimensions of this channel are defined by physical and mechanical properties and phase and structural state of the source material. Forming channels under given thermo-mechanical parameters of detonation wave for different alloys are characterized by common features: forming of a small lune at the direct interaction with sample surface, creation of the direct channel, widening zones and channel ending (if the sample was not destroyed). Sizes of the separate channel elements of researched alloys are shown in the table 2.

The microhardness measurement was carried out in the cross-section from sample surface to channel surface to estimate the structure homogeneity and strength of initial samples. The alloys VT-22 (I), VT-22 (II) have the largest values of microhardness – 4800 ÷ 4600 MPa. These values remain the same for the whole cross-section with dispersion interval ± 250 MPa. The alloy VT3-1 is characterized by the more complex character of microhardness change, the average value is 4500 ÷ 5000 MPa with dispersion interval ± 500 MPa. The reduction of the average microhardness was observed for alloy VT-3M from sample surface 3200 ± 200 up to 2800 ± 200 MPa in surface layer of the channel up to 2 ÷ 2,5 mm thick. The average microhardness for the alloy VT-22 (II) along the channel in the lune zone and area of the "direct" channel remains at the level of the cross-section values, however dispersion interval increases up to ± 700 MPA, and microhardness increases up to 5500 MPa in the zone of channel widening and ending. Such microhardness change is also observed along the channel for alloy VT-22 (I) except for widening zone where microhardness reduction to 4200 Mpa is observed. Microhardness did not change along channel for alloys VT3-1 and VT-3M on comparison with cross-section though the dispersion interval of microhardness increases up to ± 500 MPa.

The deformation in materials occurs dissimilarly and is concentrated in narrow adiabatic displacement bands under conditions of high-energy pulsed influence. Displacement bands are observed at metallographic analysis in the form of light bands spreading from channel surface into the depth of the sample. The beginning of the adiabatic bands forming in the zone of the direct channel is typical for all materials, but distribution of these bands along the channel length has essential differences. So, adiabatic bands are extremely narrow (~ 1,0 mkm) for alloys VT-22 (II), VT3-1. In general they are linear with internal breakups, their density decreases in the widening zone (the alloy VT-22 (II)), where the destruction of the material occurs along the grain boundaries.

At the same time the density of the adiabatic bands on the whole channel length increases in the alloys VT-22 (I), VT-3M, but internal breakups are observed only in the widening zone. The bands in the form of the web have a curvilinear character and spread into the sample depth up to 80 ÷ 90 mkm from channel surface.

Thereby, the deformation under high-energy pulsed influence occurs unevenly and is localized in adiabatic displacement bands in researched alloys. The parameters and distribution character of these bands along the channel depend on physical and mechanical properties and phase and structural state of the source material.

Table 1. Chemical compositions of titanium alloys.

| | Ti | Al | Mo | Fe | Cr | V | Si |
|---|---|---|---|---|---|---|---|
| VT-3M | base | 3,79 | - | 0,1 | - | 0,26 | - |
| VT3-1 | base | 5,5-7,0 | 2,0-3,0 | 0,2-0,7 | 1,0-2,5 | - | 0,5-0,4 |
| VT-22 | base | 4,0-5,7 | 4,5-5,0 | 0,5-1,0 | 0,5-2,0 | 4,0-5,5 | - |

Table 2. Sizes of the channel zones.

| | The lune | | The direct channel | | The widening zone | | The general depth, mm |
|---|---|---|---|---|---|---|---|
| | diameter, mm | depth, mm | diameter, mm | length, mm | max diameter, mm | length, mm | |
| VT-3M | 10 | 8 | 6 | 13 | - | - | 37 |
| VT3-1 | 12 | 4 | 8 | 20 | 8 | ~ 32 | 35 (destroyed) |
| VT-22 (I) | 8 | 3 | 4 | 13 | 7 | ~ 21 | 34 |
| VT-22 (II) | 10 | 7 | 4 | 15 | 8 | ~ 55 | ~55 (destroyed) |

The note. The alloy VT-22 (I) was heat-treated after forging in addition.

# INFLUENCE OF CORROSION IN SEA WATER ENVIRONMENT ON PHYSICO – MECHANICAL PROPERTIES OF GREEN BODIES FABRICATED FROM A COPPER BASED HETEROGENEOUS MATERIAL

**Epifantseva T. A., Martiukhin I. D., Scherbakova L. N., Kayuk V. G., Mikhailov O. V.**
Frantsevich Institute for Problems of Materials Science of NAS of Ukraine,
Krzhizhanovskogo st. 3, Kiev 03142, Ukraine, e-mail: TANYA14@kv.ukrtel.net

Copper based heterogeneous powder materials are considered among the most promising ones for hydrodynamic blast formation under conditions of detonation [1]. Among a number of powder compositions materials of Cu-Pb-C and Cu-W formulations due to their physico-mechanical properties are of special interest for fabrication of cumulative charge facings used for shelf deposits drilling. Development of composite powder materials for such applications must include investigations of structural changes and physico-mechanical properties evolution under conditions of corrosive environment impact. The choice of corrosive environment in this case is governed by the necessity of prolonged contact of the materials in question with sea environment and sea water. Until now such data is not available in the literature.

In the present work corrosion and its influence on mechanical properties of green bodies fabricated from copper based heterogeneous composites in interrelation with their structure and composition have been investigated.

Electrolytic copper powder of the PMS grade ($\rho$=8.96 g/cm$^3$) with dendritic particle shape and mean particle size 100 μm, lead powder with mean particle size 50 μm, ($\rho$=11.3 g/cm$^3$), and tungsten-based alloy with mean particle size 10 μm ($\rho$=17.1 g/cm$^3$) were used as the starting materials. The tungsten-based alloy W-7%Ni-3%Fe is produced by mechanically mixed oxides joint reduction.

Prismatic samples (4.36 x 43.6 x 6.3 mm) were cold pressed under pressure of P=10 T/cm$^2$. Green density and residual porosity of the produced samples were compositionally dependent and were measured for Cu-20%W formulation as $\rho$=9.1 g/cm$^3$, $\theta$=10%, for Cu-50%W as $\rho$=8.2 g/cm$^3$, $\theta$=30%, and for Cu-18%Pb-2%C as $\rho$=8.78 g/cm$^3$, $\theta$=10%, respectively. Since there is no mutual solubility of components under conditions of cold pressing it is possible to produce green heterogeneous powder bodies with specific microstructure and certain mechanical strength.

Microstructural investigations of the green bodies revealed that regardless of the heavy component properties (particle size and picnometric density) its particles are inhomogeneously distributed in the copper matrix. Moreover, the tungsten alloy particles are located in the interparticle areas while the lead ones are located inside the pores. It was established that corrosion resistance of the investigated materials is determined in sea water is determined by their microstructure and by the tungsten-based alloy content in the compositions 1 and 2.

Corrosion tests in sea water revealed that the samples containing 20 wt.% W-based alloy show weight gain (K=$1.1\cdot10^{-4}$ g/cm$^2\cdot$day) while the ones with the higher w-based alloy content show weight loss due to dissolution (K=-2.0 $10^{-4}$ g/cm$^2\cdot$day). Dissolution in this case is irregular, the main dissolving component being Fe that is present in the W-based phase. Dissolution products are distributed between the surface of the sample and the electrolyte. The corrosion potential ($E_{corr.}$) changes of the Cu-W-Fe materials in sea water indicate that the corrosion process is uniform and its rate is constant for compositions with 50 wt% W-based phase while materials with low W-based phase content oxidize from the surface similar to the pure copper bodies.

Influence of corrosion in sea water on the phisico-mechanical properties of all compositions has been investigated. Young's modulus, flexural strength and ultimate strain as well as microdeformation curves for all materials were obtained. Regardless of the composition of the copper-based heterogeneous powder materials their strength properties improved by a factor of 2 to 3 after corrosion due to exposure to sea water. Such strengthening can have negative influence on the hydrodynamic blast formation under conditions of detonation [3]. Therefore in order to preserve the phisico-mechanical and functional capabilities of the copper-based heterogeneous materials of the investigated composition it is necessary to form a protective layer on their surface. Such layer can be formed from Styrofoam which will not hinder the hydrodynamic blast formation in sea water environment [4].

## Literature

1. Bikov Yu. N., Vorkina T. E., Gorohov V. M., Efimov A. M. Development of powder compositions for cumulative charges facings production for oil and gas wells perforation // Poroshkovaya Metallurgiya. Minsk., 1995, v. 17, p. 36-46.
2. Serdiuk G.G., Epifantseva T. A., Derzhavets L. I. Application of a powder material for oil and gas wells perforation // Poroshkovaya Metallurgiya. 1990. N4. p. 38-42.
3. Epifantseva T. A., Serdiuk G. G., Derzhavets L. I. Influence of strength of a powder material on the piercing properties of charge facings // In books: “Physics of Explosion”. – Ministry of Machine Building. – 1988. – p. 37-40.
4. Hand-book for Sappers. Ed. by Kolibernov E.S., Ministry of Defense Publishing, Moscow. 1989. 235p.

# RADIATION RESISTANCE MAGNETO-RESISTIVE PERMALLOY FILMS

**Krupa M.M., Lezhnenko I.V., Matvienko A.I.,Skirta Yu.B.**
Institute of magnetism NASU
36-b, Vernadsky str, Kiev,03142, Ukraine, krupa@imag.kiev.ua

The radiation-hardened sensors are widely applied in a nuclear industry, space examinations, to a science. Operations on making radiation-resistant sensor are conducted in many countries: USA, Japan, England and others. One of the important problems is pinch of radiation stability of sensing devices of data units, as which, in basic, the semiconductor materials are applied. Data units recently are made on the basis of semiconductors with radiation stability up to 1015н/см2. The sensor controls on the basis of alloys, apparently, would allow considerably lifting a threshold of radiation stability.

The perm alloy films NiFe are one of the best materials for building of high-sensitivity, miniature sensor for measurement of loose magnetic fields. On the basis of such films it is possible to receive magneto-resistive sensor with sensitivity $10^{-4}$-$10^{-5}$ A/m, and more sensitive modulation ferroresonance sensor of a magnetic field, magneto-resistive sensor on a basis permalloy films have a low level of own noise and low in comparison with semiconductor materials factor of temperature drift of the magnetic and electrical characteristics.

These sensors can work in wide area of frequencies (from zero up to same megahertz). All this allows using perm alloy films for manufacture magnetic heads of record and reading of the information, for measurement of electromagnetic signals, for measurement of variations of a magnetic field of earth, and also for monitoring systems behind work of the executive mechanisms in space and in atomic engineering. At practical use of such gauges there is a question of radiating stability permalloy films.

The experiments that have been carried out in 70-years have shown, that under activity of an irradiation (gamma, neutron, a-particle) the properties permalloy films, which define the characteristics of sensor controls, change. In the given message we want to state results of our development on making radiation resistance magneto-resistive permalloy films. On the basis of these films experimental samples magneto-resistive sensors with good characteristics on sensitivity and angular selectivity to a magnetic field are created.

Already first our researches have shown, that selecting modes sputtering of films with imposing of a constant magnetic field it is possible to receive magneto-resistive films with very small dispersion of anisotropy of magnetization. On the basis of these films it is possible to make magneto-resistive sensors of a magnetic field with sensitivity by best than 10° A/in and selectivity on a direction of action of a magnetic field no more than 1 degree. However these of a film have smaller radiating stability.

The radiating stability received films depends not only on a mode sputtering and thickness received films, but it strongly is influenced by a material and condition of a surface of a substrate, on which the film is put.

We have lead a cycle of works on selection of technological modes of reception permalloy films with high radiating stability. We have lead a cycle of operations on selection of technological modes of reception films NiFe with high radiation stability. Optimization of parameters of reception films on substrates from polished fused quartz, and also subsequent their processing's (annealing and laser processing) have enabled to receive permalloy films with high stability to rapid neutrons (higher $10^{19}$ $\text{см}^{-2}$) and to gamma irradiation at $2x10^{9}$ rad. The carried out researches have shown, that the increase of radiating stability perm alloy films can be connected by change of their crystal structure.

On the basis of these permalloy films experimental samples of magneto-resistive and modulation ferroresonance sensors of a magnetic field such as were made and their characteristics are measured. The sensitivity of such sensor has fallen in comparison with similar sensors on a basis permalloy films with smaller radiating stability on the order. Has increased also in some times and angular width of the diagram of selectivity on a direction of action of a magnetic field.

Thus, the received effects (results) show, that on a bottom (basis) permalloy films it is possible to make small-sized, sensors, which sensitivity does not yield to sensitivity of semiconductor sensors, and the radiation stability is higher above than at semiconductor.

# THE GETTING OF FLEXIBLE POWDER CORDS FOR DEPOSITION OF COMPOSITE COATINGS

**Stepanchuk A.M., Vdovichenko H.S., Polegeshko O.B.**
National Technical University "KPI"
Prospect Pobedy, 39, Kiev, 030056, Ukraine
Ph. 241-76-17, E-mail: astepanchuk@iff-kpi.kiev.ua

Now one of problems in engineering is the improvement in quality of parts of machines and mechanisms, their productivity and reliability.

One high-performance way of a decision of these problems is applying of protective coatings with refractory compounds, which are deposited by gas-thermal methods [1-3].

At the deposition of composite coatings with involvement of refractory compounds it is necessary to provide requirements, which could promote a complete smelting-down of sprayed coating components and cast state of refractory compounds or its recrystallization through easily melted component. That also promotes a formation of strong linkage between component of coatings and obtaining of higher operating performances. The works are known, in which the conditions of the coatings getting from powder of refractory compounds or their mixes with other materials were investigatesed. However, in our opinion, the opportunities of the quality coatings getting are not completely implemented through these ways. It is bound with deficiencies, which are inherent to powder materials feed in the spraying zone. In this respect the flexible powder (FPC) is the perspective material for a spraying of composite coatings [1, 3, 4]. The development and research of conditions of the flexible powder cord getting from the composite materials, and also the investigation of coating deposition processes with using of FPC is an actual problem in the field of multifunction coatings fabricated now.

In this connection the requirements of flexible powder cord forming with predetermined properties were studied. The cord consists of the refractory compounds powders and the self-fluxing alloys powders. The rheological characteristics of the plasticized mixes (plastic durability, plastic viscosity, conditional dynamic yield stress, character of outflow curves) were investigated depending on a composition and the amounts of a plasticizer. The plasticizer was a 20% solution of a co-polyamide. The best values of these magnitudes were defined, and in further utilized at the study of influence of the different factors on FPC properties forming. A density, ultimate tensile strength, angle of bend and elastic after-effect are the most relevant characteristics of FPC. In this connection the influence of the particle size of powders, their specific surface, contents of the plasticizer and reduction ratio of the plasticized mixture were estimated during the forming process.

The analysis of the obtained results was conducted and the mechanism of forming of the cord properties was proposed. Thus, the process of compacting occurs as a result of a structural deformation process – namely more dense packing of powder particles at the expense of their relative displacement. The plastic deformation of powder particles or their brittle failure is not observed. In this connection the size of powders particles, their size distribution and specific surface affect the main influence on process of compacting. The plasticizer executes a role of lubrication at the formation and ensures the strength properties of FPC and its flexibility. At that the highest values of durability and the optimal values of flexibility are reached, when a binder forms a uniform framework and interlayers between powder particles (see figure 1).

It is obvious that properties of the powder cord depend on many factors. With the purpose of optimization of manufacture requirements of FPC with given properties the mathematical treatment of experiment data was conducted with the use of experiment scheduling.

The equations of a regression, which establish the dependences of relative density, elastic aftereffect and angle of bend from the plasticizer content, average size of particles, reduction ratio and plasticizer concentration were obtained:

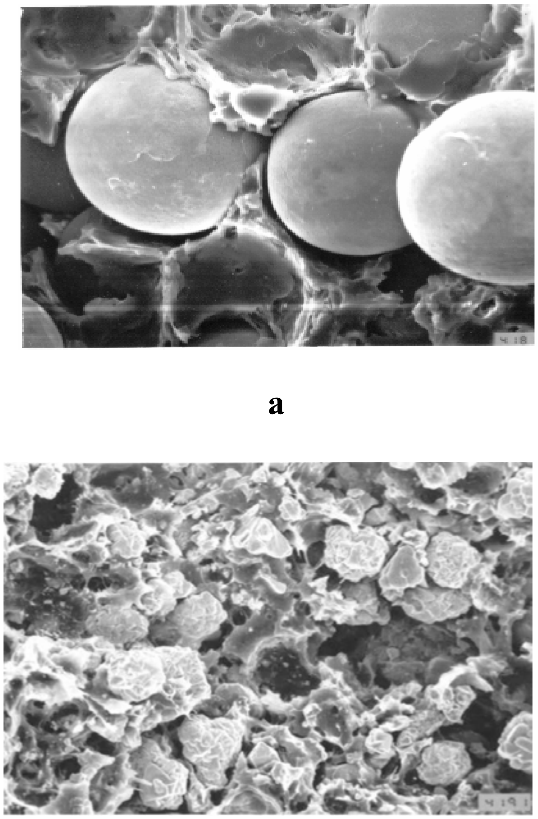

**a**

**b**

a - spherical powder particles;
б - powder particles of irregular shape

Figure 1 - Structure of fracture of the flexible powder cord

$$\delta = -37{,}052 + 0{,}035\,V - 0.0063d + + 0.396k + +0.169C - 0.00123\,VC$$

$$\gamma = -4.833 + 4.139V + 0.504d - 0.04V^2 + 0.001d^2 + +4.857 \cdot 10^{-5} Vd^2 - 5.703 \cdot 10^{-4} V^3 - 7.284 \cdot 10^{-6} d^3 -$$

$$\theta = -3870.4 + 716.5V - 147.1\mathrm{d} - 57.7V^2 - 6.9d^2 + 0.004V^2 d + 2.3\mathrm{V}^3 + 0.05d^3 - -2.9 \cdot 10^{-6} V^2 d^2 - -3.2 \cdot 10^{-5} V^3 d - 0.05V^4 + +0005d^4 + 0.0003V^5 - -3.9 \cdot 10^{-6} d^5$$

Where $\gamma$ - density, g / cm$^3$; $\delta$ - elastic aftereffect, %; $\theta$ - angle of bend, degree; $V$ - volumetric content of plasticizer, %; $C$ - concentration of plasticizer, %; $d$ - average size of particles, micron; $k$ - reduction ratio, %.

The obtained mathematical models adequately describe the experimental data (regression coefficients

$R^{\gamma} = 0{,}9552$; $R^{\delta} = 0{,}9988$; $R^{\theta} = 0{,}9870$) and can be utilized for optimization of processes of FPC forming with given properties. For indispensable calculations the computer program in the Visual Basic with the use of a Microsoft Exel 9.0 package were designed, which allows to calculate the demanded requirements of FPC formation with 95 % probability.

Literature

1. Вдовиченко М.С., Данильчук М.П., Степанчук А.М. Структура и свойства композиционных газотермических покрытий , полученных с помощью гибкого порошкового шнура // Вісник ЖІТІ, Житомир; -1999. -№9. - С..35-38.
2. Степанчук А.М., Вдовиченко М.С.. Перспективи використання композиційних газотермічних покриттів у хімічній промисловості // Хімічна промисловість України. - 2001. - №4.- С. 4-8
3. Степанчук А.Н., Вдовиченко Н.С. Нечипоренко А.А. Применение композиционных материалов с участием тугоплавих соединений для нанесения газотермических покрытий //В сб. НТТ Киевского политехнического института, ч.П, Киев; КПИ, -1994. - С.78-87.
4. Степанчук А.Н., Скорин Г.Т., Вдовиченко Н.С. Структура и свойства газотермических покрытий из композиций, полученных с помощью ГПШ. // Труды ГИХС "Исследование свойств порошковых материалов и термонапыления деталей горнообогатительного оборудования. Люберцы: ГИХС, **76,** - 1988. - С..36-41.

# APPLICATION OF COMPOSITE SELFLUBRICATING MATERIALS FOR OPERATION AT INCREASED TEMPERATURES

**Shevchuk U.F., Roik T.A.** (1)
Frantsevich Institute for Problems of Material Science, NAS of Ukraine,
3, Krzhyzhanovsky st., 03680, Kiev-142, Ukraine, e-mail: chern@materials.kiev.ua
(1) State Scientific and Technical Centre of Arms of Ministry of Industrial Policy of Ukraine,
6, Industrial, 03057, Kiev-57, Ukraine, e-mail: kba@kba.kiev.ua

In the friction units of gas-turbine motors, in the constructions of modern gas-transfering equipments there are critical matings, which operate at increased temperatures, loads in the conditions of corrosive environment. As a support bearings of vanes costly special bearings of swinging and sliding are traditionally used in such units of friction. They are manufactured of high-alloyed alloys. However, in stringent operating conditions (loads up to 5 MPa, temperatures up to 500-650 °C, wastes of fuel burning) after 200-250 h of operation defects are appeared on the bearings: increased wear on the races in a mode of hollows. This causes the instable operation of reversing gear, increased backlashes, gain in loads and breaking levers.

Investigations in design of composite selflubricating materials on the base of iron and nickel for sliding bearings instead of swinging bearings have been carried out for increasing of serviceability such friction units. Physic mechanical, antifrictional properties have been researched and introduction of bearings from new materials into production has been carried out.

Materials of 3 groups have been researched: on the base of Fe (composition 1), on the base of Ni (composition 2) and on the base of Ni-Mo composite (composition 3) in all cases with addition 10-12 mas.% of high-temperature solid lubricant $CaF_2$ [1].

Optimal technological parameters of mixing, pressing and sintering of materials have been experimentally determined. They ensure (by data of metallographical and X-ray structural analysis) forming of structure as a homogeneous solid solution of metal matrix with uniformly distributed inclusions of $CaF_2$.

Physic mechanical and antifrictional properties of the materials have been presented in tab.1, 2.

Table 1

Physic mechanical properties of materials

| Material grade | Porosity, % | HB, MPa | $a_k$, J/m$^2$ | $\sigma_{ben}$ MPa |
|---|---|---|---|---|
| Compos.1 | 8-12 | 1100-1200 | 500-600 | 450-550 |
| Compos.2 | 9-12 | 1200-1400 | 700-800 | 600-650 |
| Compos.3 | 8-12 | 1500-1800 | 800-900 | 650-700 |

Table 2

Antifrictional properties of materials

| Material grade | Friction coefficient | Wear, mkm/km | Limiting load, MPa |
|---|---|---|---|
| Compos.1 | 0.18 | 140 | 5 |
| Compos.2 | 0.18 | 185 | 5 |
| Compos.3 | 0.14-0.18 | 100 | 7 |

Antifrictional properties of composite materials were determined by high-temperature friction machine “BMT-1” on air at the temperature 600 °C, load 5 MPa, sliding speed 1m/s in pair with specimen of alloy “BT-14” with nitrided surface (for composition 1, 2) and with specimen of “ЭИ961” steel (for composition 3).

Friction process of materials was accompanied by formation of stable separative scoring-preventive films on mating surfaces, which completely coat operative surfaces [1, 2].

Experimental investigations of composite selflubricating materials of compositions 1-3 scale-resistance have been carried out. Specimens were heated on air at the temperature 600 °C during 30 h. The results of experiments have been presented in tab. 3.

Table 3

Research results of scale-resistance.

| Material grade | Absolute up-weight, g | ΔP/S, mg/cm$^2$ |
|---|---|---|
| Compos.1 | 0.0403 | 8.1 |
| Compos.2 | 0.0156 | 5.5 |
| Compos.3 | 0.0074 | 2.6 |

Visual check up has shown surfaces of oxidated specimens from all compositions were coated of dense oxide film of dark colour, which is firmly coupled with metal matrix. Metallographical analysis of oxidated specimens didn't show the development of volume oxidation processes that proves good protect properties of oxide films.

Experimental batch of sintered sliding bearings workpieces from materials of composition 1 and 2 has been manufactured for carrying out the industrial testing in friction units of blading in gas-turbine motors.

Composite bearings were tested during 790 h. at 560-630 °C in wastes of fuel burning. During this time 1450 complete reverses have been carried out at load 5 MPa on friction pair.

After testing and knocking down of motor the technical check up and measurements showed that on 2 vanes (of 20) with bearings from material of composition 1 seizing of friction unit took place along external spherical surfaces. On another 18 vanes a state of operative surfaces was sufficient.

Maximal (absolute) wear of bearings along internal surfaces has accounted 0,156 mm for material of composition 1, 0,055 mm - for material of composition 2.

Composite materials of composition 3 were successfully tested in the industrial friction units of gas-transfering equipments “ГТН-25” during more than 1400 h. During this time 380 starts were carried out. The inspection of friction units has shown the bearings have not damages and fit for further service. On the base of received data the decision on use the bearings from material of composition 3 into lot production was made.

Using of bearings bushes from material on the base of Ni-Mo alloy has offered to turn the blading of high pressure compressor in gas-transfering equipment.

It has increased its efficiency by 0,5% and reliable operation of equipment generally.

Industrial making technology of sliding bearings has been developed and introduced into production. Engineering specification has been developed and issued (TC, TI).

## Literature

1. Shevchuk U.F., Roik T.A. Composite materials for high-temperature units of friction /Abstracts, International Conference “Advanced materials”, Symposium A: Engineering of composites, investigations, technologies and perspectives, Kiev. - 1999. - P. 280.
2. Shevchuk U.F., Roik T.A. Powder antifrictional materials for operation at increased temperatures // Powder metallurgy, №1-2. - 2001.- P. 53-58.

# IMPROVED HIGH TEMPERATURE SUPERCONDUCTOR MATERIAL FOR POWER APPLICATIONS

**Gawalek. W., Habisreuther, T., Zeisberger, M., Litzkendorf, D., Kracunovska, S., Prikhna, T.A.(1), Oswald, B.(2), Kovalev, L.K.(3)**
Institut fuer Physikalische Hochtechnologie e.V.
Winzerlaer Strasse 10, 07745 Jena, Germany
(1)Institute for Superhard Materials of NASU
2, Avtozavodskaya Str., Kiev, 254074, Ukraine
(2)OSWALD Elektromotoren GmbH, Benzstr. 12, 63897 Miltenberg, Germany
(3)Moscow State Aviation Institute, Volokolamskoe shosse, 125871 Moscow, Russia

Because of its unique magnetic properties melt textured especially single domain $YBa_2Cu_3O_{7-d}$ (YBCO) bulk HTS (High Temperature Superconductor) material has a large potential for MAGLEV and energy technique applications. Its material quality is meeting commercial demands in the superconductor industry. $YBa_2Cu_3O_{7-d}$ bulk HTS was tested successful in circular and linear superconducting magnetic bearings (fly wheels for the energy technique and MAGLEV transportation) as well as in electric motors and generators (hysteresis machines, reluctance machines and trapped field machines).

The magnetic material quality is given by the ability to store magnetic energy in supercurrent loops. It is measured by the current load as product of critical current density $j_c$ and smallest diameter of superconducting current loop d in a single domain. In a type II superconductor, the total magnetic moment is given by $m=VAj_cd$ (V: superconducting volume fraction, A: geometrical factor) Because the perovskite lattice of the $YBa_2Cu_3O_{7-d}$ material is strong anisotropic, we have to look on the current flow in the ab-planes. Beside this we have a growth induced sector structure in the single domains. The levitation force depends on the gradient of the magnetic field imposed by the lecitated magnet and the total magnetic moment m of the superconductor. However, it is important to note, that between trapped field mapping results and levitation force results exists no simple relation in macroscopic disturbed material domains.

In small samples critical current densities up to $10^5$ A/cm$^2$ @ 77 K are measured by vibration sample magnetometry. But there are indications of reduced critical current densities over full sample dimension also in single domain samples, caused by macroscopic inhomogeneities in thickness, as well as subgrain boundaries and cracks in lateral direction.

Nevertheless we reached in a (38x38x17)mm$^3$ block with 1,445 T a record value of trapped field @ 77 K and between two blocks 2,5 T @ 77 K.

Because the critical current density seems to be limited to about $10^4$ A/cm$^2$ for YBCO @ 77 K, the size of weak link and crack free regions (perfect domains) should be increased in order to increase the energy product. There are three ways to solve this problem:

1. better understanding and control of the melt textured growth process, in order to avoid small angle grain boundaries acting as weak links.
2. multi seeding in the top seeded process, and
3. superconducting joining of single domains in ab-direction.

In general the macroscopic growth sector structure of melt textured blocks has to be considered by using the material for magnetic applications. Growth structure related magnetic hard and soft regions influence the penetration of magnetic flux.

We produce YBCO material blocks in different shape in a batch process and compose cryomagnetic function elements for bearings.

High power density electric reluctance motors with output power up to 200 kW are constructed and successful tested in OSWALD Electromotors Company Miltenberg/Germany and MAI Moscow.

For practical application the in comparison with conventional machines 8 times increased dynamic is important.
A 2 MW power fly wheel for local energy tuning has been constructed in the DYNASTORE project in Germany..

In Moscow a people moving MAGLEV system with 6 m rail lenght, loading about 300 kg was constructed with our material (40 kg YBCO) by the SPETSREMONT Company and MAI.

For MAGLEV large scale application the economic permanent magnetic rail construction is an open problem. Also effective cryocoolers for MAGLEV and energy technique applications have to be developed.

# GOVERNING PARAMETERS THERMO-EROSION DESTRUCTION OF A MATERIALS IN A SUPERSONIC HETEROGENEOUS FLOW

**Ershova T.V., Mikhatulin D.S., Polezhaev Yu.V.**
Institute for High Temperature RAS,
13/19, Izhorskaya St., Moscow, 125412, Russia E-mail: mikhatulin@ihed.ras.ru

Paper view the capabilities of the simulation of thermal-erosion impact of the dusty atmosphere on units of nose faces of a rockets on gasdynamic ground-stands and the requirements to modes are considered, which one are necessary for playing back in experimental researches.

The model of thermal-erosion destruction of materials is offered, at which one the total mass entrainment is divided on thermal, erosive, and gasdynamic components, each of which is studied separately. The conditions are studied, when these component do not depend from each other, and when this relation cannot be neglected.

The parameters of the research task of relation of an erosion resistance of materials from temperature of a warm-up of surface layer (size and particle concentration in a flow, speed of their shock and quantity of heat, absorbed streamlined wall), governing both transition between mechanisms of destruction, and temperature of a warm-up of surface layer are formulated. Are tendered numerical and engineering methods of definition of this temperature. The examples of experimental research of an erosion resistance of different classes materials (metals, glass- and carbon plastics, carbon-carbon compositions) are resulted depending on temperature of surface layer, sizes of particles and stagnation pressure.

By comparing the values that characterize a rate of destruction ($\delta_{er}/\tau_{er}$) and a velocity of propagation of the thermal wave in the material ($\delta_T/\tau_T$) we can obtain a relation that can be interpreted as a new criterion of thermal similarity for the case of the stationary impact of heterogeneous flow:

$$\mathrm{E} = \frac{\delta_{er}}{\delta_T}\frac{\tau_T}{\tau_{er}} = \left[\frac{G_p V_{pw}^2}{2q_\Sigma}\right]^2 \cdot$$

$$\cdot\left[\frac{c_M\left(T_w - T_{1-s}\right) + \Delta Q_w + \Gamma\gamma\left(H_e - h_w\right)}{H_{er}}\right]^2 \cdot \left[\frac{G_T}{G_{er}} + 1\right],$$

or in the case of the absence of the thermochemical entrainment by mass

$$\mathbf{E} = \left[\frac{G_p V_{pw}^2}{2q_\Sigma}\right]^2 \cdot \left[\frac{c_M\left(T_w - T_{1-s}\right)}{H_{er}}\right]^2 = \left[\frac{G_{er} c_M\left(T_w - T_{1-s}\right)}{q_\Sigma}\right]^2$$

Here, the first term is the ratio of two input gas flow parameters, namely erosion parameter (the density of the kinetic energy of particles) and the thermal parameter (the heat absorbed by the wall).

The second term is the ratio of the material characteristics responsible for the acquired energy distribution: the erosion characteristics (effective enthalpy of erosion destruction) and the thermal one (effective enthalpy of thermochemical destruction). These ratios include all the above governing parameters. Therefore, the number E is the ratio of the thermal energy dispersed due to erosion destruction of the surface layer of the thickness $\delta_{er}$ to the thermal energy accumulated by the heated layer of the thickness $\delta_T$.

In Fig.1 numerous experimental data processed numerically method are generalized as a single dependence of the dimensionless mean-integral temperature $\theta_s$ on the parameter E. Metals have low value of E. Respectively, high erosion resistance (small crater depths) is characteristic for them as well as high heat conductivity $\lambda_M$ and diffusivity $a_M$ and deep heating, that is $\delta_{er} << \delta_T$. As a consequence, the mean temperature of the entrained layer is close to the surface temperature $T_w \approx T_s$. Fiberglass plastics have different dependences of $T_s$(E) и $T_w$(E). Here, the surface temperature $T_w$ is equal to the temperature $T_m$ of thermochemical destruction up to the critical value $\mathrm{E}^* \approx 1$. This critical value of E divides the drawing into two areas: the zone of the thermal-erosion mechanism of destruction ($\mathrm{E} < \mathrm{E}^*$) and that of the erosion mechanism $\left(\mathrm{E} \geq \mathrm{E}^*\right)$. With E=0 we have the zone of the thermochemical mechanism of destruction.

On the whole, to estimate the temperatures $T_s$ and $T_w$ in a wide range of the parameter E, the following semi empirical expression can be used :

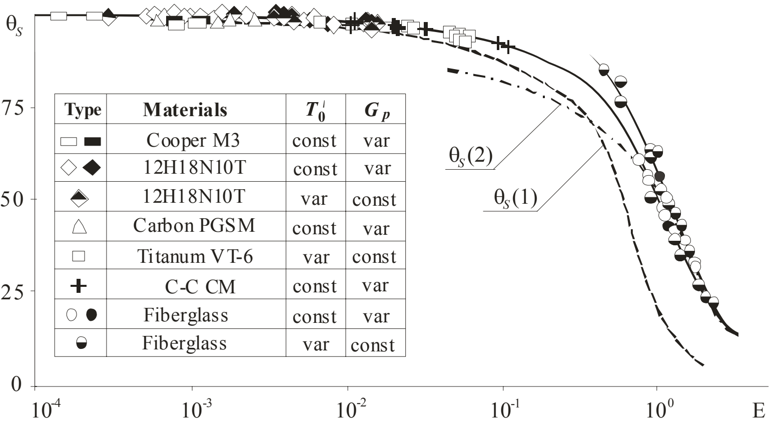

**Рис. 1.**

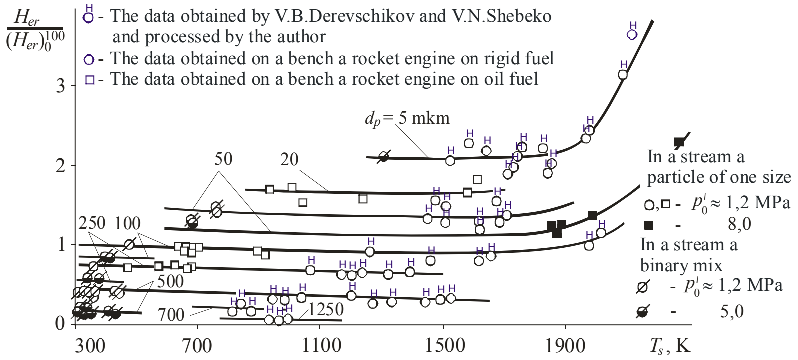

**Рис. 2.**

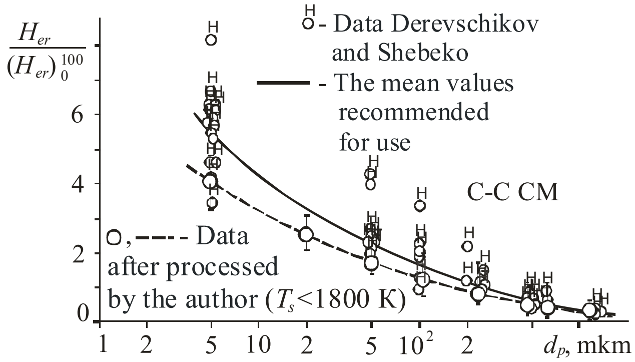

**Рис.3.**

$$\theta_s = \frac{T_s - T_0}{T_w - T_0} = \exp\left[-\left(0{,}1342\mathrm{E} + 1{,}2787\mathrm{E}^2 - 0{,}906\mathrm{E}^3 + 0{,}2\mathrm{E}^4\right)\right]$$ t

ogether with the energy balance in destructed layer

$$\left(\alpha/c_p\right)_\Sigma \left(H_e - h_w\right) + \eta G_p \frac{V_{pw}^2}{2} =$$

$$= \varepsilon\sigma T_w^4 + G_\Sigma c_м \left(T_w - T_0\right) + G_T\left[\Delta Q_w + \Gamma\gamma\left(H_e - h_w\right)\right].$$

In Fig. 2, the results of the experimental research erosion of the carbon - carbon composite material (C-CCM) in a hyperthermal heterogeneous flow are given in dependence from the whole complex of the parameters – mean-integral temperature $T_s$, size of particles $d_p$, stagnation pressure $p_0'$. It is draw attention to itself that as against conventional materials for C-CCM the relation of an effective enthalpy of erosive destruction is weakly varies in a significant temperature range (from room temperatures up to approximately 1800-1900 K), and then is augmented in several times. Here, the analogy with the temperature dependence of strength properties of carbon materials is clearly seen. The matching of these data with the erosion characteristics of a heat-shielding material with conventional properties (fiberglass plastics) determines operational niches for each of them.

The data of the present researches and the V.B. Derevschikov researches [1] after processing on a designed technique satisfactorily coincide. Derevschikov V.B. studies relation $H_{er}(d_p)$, which one shown in a Fig. 3. His these data is processed in relation $H_{er}(T_s)$. We see that taking into account of temperature effect $T_s$ this relation manages to be updated, and dispersion of the data is the essential less.

The researches on carry of the results of analysis thermal-erosion resistance of a heat-shielding materials on conditions of supersonic flight (M=8) in dusty atmosphere in depended on altitude function and speeds of flight, size and density of the particles in a dust cloud, radius of bluntness of a forward point of a vehicle are carried out. The conversion from thermochemical destruction of a wall at flight of the vehicle in a clear air to thermal-erosion destruction at its going into a dust cloud is studied.

## Литература

1. V.B. Derevschikov, D.S. Mikhatulin, Yu.V. Polezhaev, V.N. Shebeko. Capabilities of a simulation and ground-based stands for the thermal-erosion researches. – M., 1994. – (Preprint IVTAN, № 2-363). – 62 p. (in Russian).

Supported by the Russian Foundation of Basic Research (grant N 03-02-16329) and by program of supporting leading scientific schools of RF (grant N1141.2003.8).

# THE INVESTIGATION OF PROTECTIVE COATING INFLUENCE ON CORROSION RESISTANCE OF WELDED ZIRCONIUM COMPOUNDS

**Bushmin B.V., Gorchakov A.A., Dubinin G.V. (1), Dubrovsky Y.V., Nickitin I.A. (1), Plishevsky M.I. (1), Semenov A.N. (1), Tjurin V.N. (1), Hazov I.A.**
SPC «INTEKO» FSUE «Red Star»
Electrolitnij pr-d, 1a, 115230, Moscow, Russia, e-mail: serbin@dol.ru
(1)FSUE NIKIET, Russia, 101000, Moscow, ab. 788

Zirconium alloys, mostly with 1 and 2,5% Nb, which are used in atomic (nuclear) energetic besides active interaction with atmospheric gases under 400 °C are structure-sensitive. Welded interconnections of these alloys are characterized as structure-phase heterogeneity and function properties heterogeneity. In particular, structure-phase heterogeneity causes reduced corrosion resistance of welded interconnections in water and high parameters steam.

In order to improve the corrosions resistance in such welded interconnections we can use the low-temperature annealing (520—580 °C) of major duration (more than 50 hours) in vacuum.

The most effective is thermo-mechanical and mechanico-thermal process which includes plastic strain and following low-temperature annealing during 10—15 hours.

However such process requires special rolling and vacuum equipment for its realization and be-sides such process can’t be always used because of items’ constructive peculiarities.
The possibility of improving the corrosion resistance of welded interconnections in zirconium alloys is investigated in this work, which was done by electron-beam welding in vacuum by applying special protective coatings using plasma-ion method.

As protective coatings, the coating of titanium (Ti), titanium nitrite (TiN), zirconium nitrite (ZrN), chromium (Cr) and coatings of mixed components Ti—Cr, Zr—Cr (Ti—Cr)N, (Zr—Cr)N, (Ti—Zr)N and multi-layer coatings such as Ti—TiN—Ti—TiN were tested.

Corrosion tests were carried out in autoclaves with water with electrical-resistance not more than 1,0 mksm/sm and pH=6,5—7,0. The temperature in tests was t=280 °C, the pressure p=9,8 MPa, with oxygen concentration [$O_2$]=0,1—0,3 mg/kg.

Maximum test duration is 4000 hours. The best result were shown by protective coatings of thickness of TiN, Cr and Zr-Cr and multi-layer coatings Ti—TiN—Ti—TiN with 5—10 μm thickness.

# INVESTIGATION OF HEAT RESISTANCE OF THIN LAYER COVERINGS

**Gladkov V.E., Kusainov K.K., Gladkova V.K.**
Buketov Karaganda State University
Universitetskaya st., 28, Karaganda, 470028, Kazakhstan, iph@rargu.krg.kz

An important practical task is measuring of heat resistance of thin layer covering (HRTC), measuring of total heat resistance of separate layers of poly layer plate. Example of such kind of task may be the investigation of heat resistance of protective varnish colored covering, investigation of heat exchange in one of glue connections, measuring of total heat resistance of layers of receiving element of absolute radiometer [1]. The last task touches the problem of measuring solar constant and it is necessary to give effect to its decision by the method of nondestructive inspection based directly on receiving element of radiometer [2].

In spite of success in the development of theory and practice of measuring of heat resistance of thin layers [3], there is no devised (worked out) methods, permitting satisfactorily solving the task of measuring of heat resistance of separate layers of multilayer plate.

Suggested methods of measuring HRTS by the temperature of surroundings permit, on the one hand, to heighten the accuracy of measuring of energy illumination, and, on the other hand, to examine the principles of measuring HRTS by the temperature of surrounds [4,5] suggested methods of measuring HRTS differ from familiar on conditions heat exchange of the model with surroundings. That is why in the basis of classification of examined methods we put the condition of equality of temperature of one of the surfaces of investigated model and temperature of surroundings. So, there are two methods of measuring HRTS: 1) By equality of temperatures of lower surface of model and surroundings, 2) By the equality of temperatures of higher surface of model and surroundings. Methods are realized with the help of elaborated devices.

The basis of heat block of all appliances forms receiving block of absolute radiometer, including receiving element, consisting of heater 2, pilled up on it absorbing radiation of covering 2, thermo battery 3 and thermoelectric refrigerator 4 (picture 1).

Analyzing model is the part of this multilayer receiving element. Its example may be absorbed covering together with adjoining layers of glue and isolation or thin dielectric layer, settled down under absorbed covering. For the heat of model except heater 1, one can use the key of radiation 8.

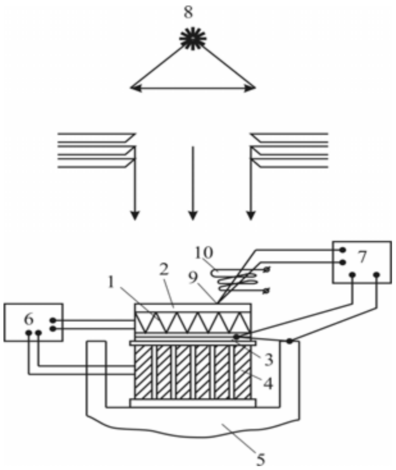

Picture 1

Heat of receiving element is put into effect alternately by the current of radiation or by capacity, selected in heater, on putting the electric current through it and on simultaneous cooling till the temperature of medium on one of the surfaces of received element.

Appliances differ by the methods of task of bordered conditions on the surfaces of received element, by the methods of control of equality of temperatures one of the surfaces of received element and surroundings, by discharge parameter through which unknown heat resistances are defined.

For substantiation of methods of measuring of heat resistances of thin layer covering adopted the method of electroheat analogy. Received elements of appliances in normal directions are tick layer systems. For the analyses of heat process in received element seven equivalent layers are distinguished: absorbed covering, varnish, glue, heater, two layers of electroisolation, glue with the consideration of heat resistances, sources, flow of heat, conditions of heat exchange of every layer the scheme of substitution is formed (made) with intense parameters.

On the basis of scheme of substitution expressions were received, defining heat resistances of thin layer covering by two methods:

$$\sum_{i=1}^{3} R_i + \frac{R_4}{2} = \frac{\varepsilon_{\ddot{e}1} - \varepsilon_{\acute{y}1}}{\mathring{a}W} \qquad (1)$$

$$\sum_{i=1}^{3} R_i + \frac{R_4}{2} = \frac{\varepsilon_{\acute{y}} - \varepsilon_{\ddot{e}}}{\hat{A}\mathring{a}WN} \qquad (2)$$

where $\varepsilon_{л1}$ and $\varepsilon_{л2}$ – discharge signal of term element in measuring the temperature of surface of received element in two phase of the heat; $\varepsilon_{э}$ and $\varepsilon_{л}$ – discharge signal of thermo battery in two phase of the heat; e – coefficient of thermoEDS; N – number of thermosteams in thermo battery.

In the basis of working formulas defining heat resistances there is nonequivalence of heat of received element by the current of radiation and by electric current of radiation and by electric current.

Quantitative by nonequivalence of the heat is defined by the relation of capacities of radiant and electric heat which permit, by researched coefficients, to carry out measuring only in the capacity of electric heat.

The research was carried out by total heat resistance of thin layers of received element of cool radiometer from density of covering. The method of measuring was used on the temperature of surroundings the models were prepared with various absorbed coverings, used in precision radiometry (1-soot; 2-AK-243; 3-AK-243, GGO; 4-enamel ПФ-115; 5-soot-and-varnish compose). Measuring was carried out in the range of capacity $(1{,}5\text{-}10)\cdot 10^{-2}$ Volt.

Total heat resistance of layers of received element of absolute radiometer cause one of the basic systematical defects of absolute radiometers [6].

Picture 2

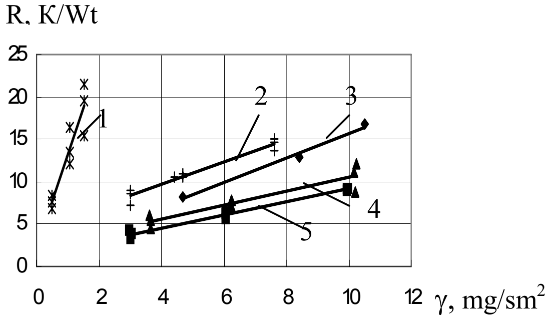

Much work is devoted to the research of this defect of nonequivalence. Measuring forming the defect of energetic lighting caused by heat resistance, for absolute radiometer has maximum size 0,2 % (percent). Suggested methods of measuring heat resistance of thin layer covering permit to choose correctly absorbed covering, to account the defects of its measuring decrease forming defects measuring of energetic illumination, causing by heat resistance.

Literatures:

1. Platunov E.S., Buravoy S.e., Kurepin V.V., Petrov G.S. Thermophysical measurings and instruments (devices), Leningrad, 1986, Page 256.
2. Skljarov U.A., Brichkov U.I., Kotuma A.I.and others. Radiometric measurings with ISZ. «Resurs-01» № 4// Research of the earth from the cosmos 2000, № 3, Page 58-62.
3. Aliphanjv O.M., Vabischevich P.N., Mihaylov V.V. and others. Bases of identification and designing of heat processes and systems, Moscow, 2001, Page 400.
4. A.S. № 1312462. USSR. Method of measuring of thermal resistance of thinlylayer coverings Registered 22.01.1987.
5. Title № 8710. Device of measuring of heat resistance of thinly layer covering. Decision about the issue of title 15.03.2000.
6. Kmito A.A., Skljarov U.A. Pyrgeliometryja. Leningrad, 1981, Page 232.

# NEW MATERIALS IN SPACE-ROCKET SYSTEMS OF AN UNLIMITED DISCRETIZATION

**Nerus M.**
SSRDC "Vektor"of the NAS of Ukraine
3, Krzhizhanovski St., Kiev, 03680, Ukraine, E-mail: nerus@ukrpost.net

Selection of a material for space-rocket systems of an unlimited discretization has the nuances. Heats, the strong pressure, activity of medium, high-speed gas streams, changing loads are present operation conditions of materials in new space-rocket systems. In the capacity of softening operation conditions of rocket systems can appear: small volumes of combustion chambers, short duration of running processes, a self-sufficiency of reactive load-bearing elements - RLBE.

The Principle of an Unlimited Discretization of Rocket Systems has been offered by the author to attention of specialists in the Second Ukrainian Conference of Perspective Space Explorations, September 21-26, 2002, Katcivelly-town, Crimea, Ukraine [1].

Perspective space-rocket systems of new capabilities can be created using a new Principle:

- The Discrete Garland Rocket System DiGRSN (fig. 1);
- The Discrete Pyramidal Rocket System DiPRSN (fig. 2).

## The Discrete Garland Rocket System - DiGRSN

Traction of power unit of the DiGRSN:

$$P = P_1 + P_2,$$

where $P_1$ - traction from combustion of main fuel;
$P_2$ - traction from high-speed removal (throws away) the bodies of completing RLBE.

$$P = U_0 m + U_1 m_K,$$

where $m$ - mass of main fuel;
$m_K$ - mass of the bodies of RLBE;
$U_0$ - outflow velocity of a working medium;
$U_1$ - speed of irradiation of completing bodies.

## The Discrete Pyramidal Rocket System - DiPRSN

Traction of power unit of the DiPRSN:

$$P = P_1 + P_2,$$

where $P_1$ - traction from combustion of main fuel;
$P_2$ - traction from combustion of an overload fuel – the bodies of completing RLBE.

$$P = U_0 m + U_0 m_K,$$

where $m$ - mass of main fuel;
$m_K$ - mass of the bodies of RLBE;
$U_0$ - outflow velocity of a working medium.
-

Growth of traction and permanent removal of spurious freights allow increasing carrying capacity of the discrete space-rocket systems in 2…4 times as contrasted to all known space-rocket systems [2].

Design features of new space-rocket systems demand also new constructional and energy materials.

Usage in constructions of discrete space-rocket systems of nano-laminated composite materials is represented perspective [3].

### LIST OF LITERATURE

1. Energy and material authority problems of the ascent in space and descent to ground of the vehicle with small overloads. // Space science and techniques, Appendix, volume 9, №2, 2003.
2. Alemasov V.E. Theories of rocket motors. – M.: Oborngiz, 1962
3. Shpak A.P., Mayboroda V.P. and others. Nano-laminated composite materials and covers. – K.: Akademperiodika, 2003

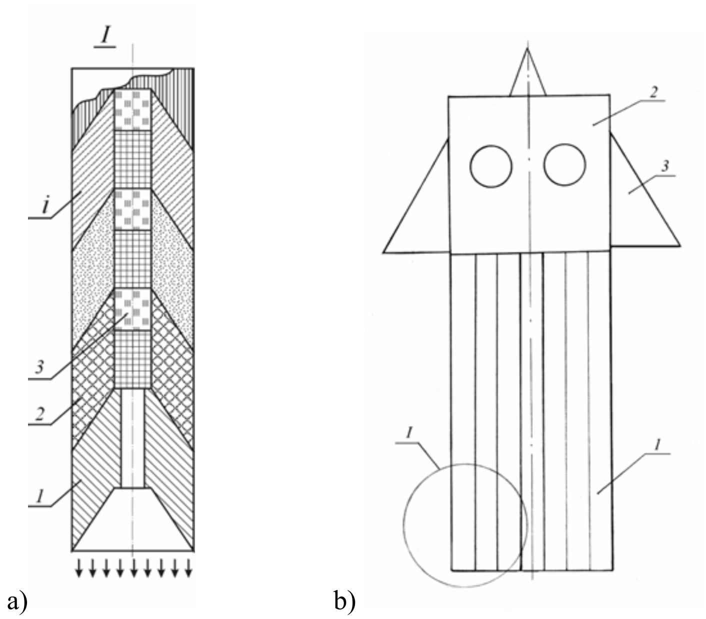

Figure 1. The Nerus's Discrete Garland Rocket System - DiGRSN.
a) Garland-chain of reactive load-bearing elements RLBE;
b) Garland packets the carrier rocket.

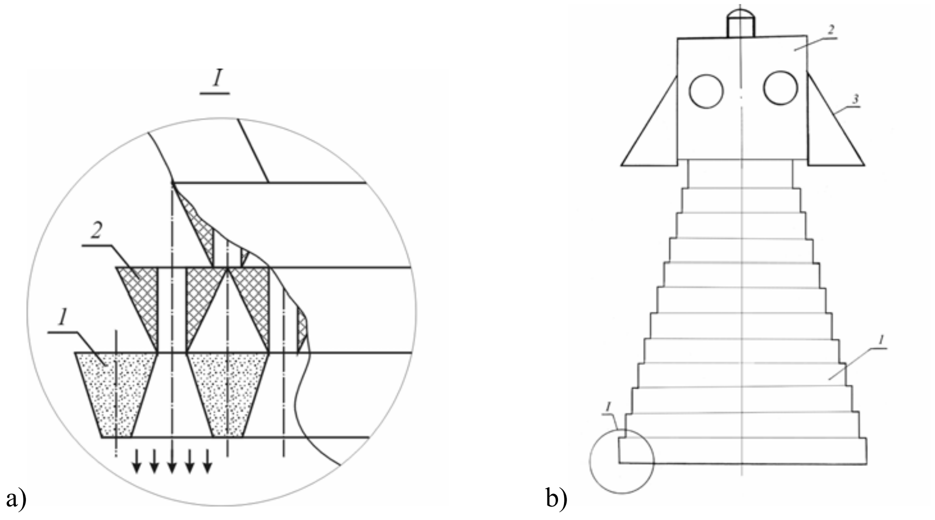

Figure 2. The Nerus's Discrete Pyramidal Rocket System – DiPRSN.
a) Discrete pyramidal power unit;
b) Pyramidal packets the carrier rocket.

# ELABORATION AND OPERATION OF THERMAL CONCRETE «BRAB30И15*» LINING ELEMENTS AND OXIDE-CERAMIC «M-1*» IN EXTREME CONDITIONS

**Tropinov A., Tropinova I., Vladimirov V.(1)**
Private scientific company «Alineka»
13 Kavkazskaya str., suite 45, Kiev, 03035, Ukraine, E–mail: alineka@kiev-page.com.ua
(1)Scientific- productive commercial company «MaVR»,
2 Gagarina str., suite 218, Zhukovskiy, 140180, Russia, E–mail:mavr@pt.comcor.ru

The introduction of energysaving techologies into heat and power engineering, such as, the traditional fuel [(gas, mazut) substitution for bio – fuel (gas and mazut and bio–fuel (seeds of sunflower, buckwheat, etc.)] changes the regimen in a fire – chamber from the standard into extreme one. The temperature in the fire- chamber has been raised up to t=1500 $^{0}$C, the speed and gas-air basic mixture have been raised too, including, non-burnt particles. The first up to v=40 m/sec, the second the continents of $R_2O=K_2O+Na_2O$, up to 51%, including thermal shifts = shifts per 24 hours. The use of pressed refractories, such as: chamotte, magnesite, magnesito chrome, as well as, oxid ceramics materials irrational, as the given items don't meet above mentioned extreme conditions in complex, including difficulties of «complicated geometry» lining production or increased price. Hence, with the purpose of resources operation raising and for the solution of the above given problem two technologies have been used – in a way of «matrix», perceiving thermal shifts, increased temperature, and allowing to receive items of «complicates geometry» - dry shakes of refractory concretes of PSC «Alineka», and for alkali corrosion protection under high temperature – oxide – ceramic covering (technology SVS) «M-1*» SPCF «MaVR». The choice of the technologies is grounded on, first, - BRAB30И15 refractory concrete [1] possesses the ability to produce items of «complicated geometry», characterized by the high residual strength, solidity and thermal durability [2], and consequently, it can perceive extreme conditions for the exception of alkali corrosion, from which it must protect. For the second, oxide-ceramic covering «M-1*» [3], which is characterized in its turn, by the high temperature of use, increased erosion strength to the action of chemical active and aggressive gases and high – speed gas flows, as well as, increased adhesive to aluminium-silicate refractories.

Table 1.Physico – technical properties of refractory concretes and protective covering «M – 1*»

| Some physico-thechnical properties | Chamotte brick «Sha» | Refractory concrete BRAB30И15 | Refractory concrete BRAB30И15k* | Oxide-ceramic covering «M–1*» |
|---|---|---|---|---|
| 1.Middle density, kg/m$^3$ | 2200 | 2400 | 2450-2500 | 1800–2000 |
| 2.Strength under pressure, MPa, | | | | |
| after: t=20$^0$C | 20–25 | 42,3–76,8 | 36,8–44,7 | 15–25 |
| t=1100$^0$C | 16–21 | 34,4–42,3 | 28,7–31,4 | -- |
| t=1350$^0$C | 9,1–9,9 | 9,3–19,1 | 21,4–23,4 | -- |
| 3.Maximum permissible temperature of application, $^0$C | 1400 | 1500 | 1600 | 1800 |
| 4.Thermal stability, 800 $^0$C – $H_2O$ | 10 | 42–47 | 54 | -- |
| 5.Coefficient of linear thermal broadening x10$^{-6}$x $^0$C$^{-1}$ | 7,8 | 7,6–7,4 | 4,8–7,6 | 7,4–7,6 |
| 6.Hardness after Moss | 6,0 | 8,0 | 8,5–9,0 | 9,0 |

At the same time, the above given problem solution is possible only in case, the linear expansion of refractory concrete and oxide-ceramic coverings are equivalent to and coordinated with each ofter. The diagram of the first heating must be coordinated too. Adhesia to refractory concrete must be high to perceive thermal cycles and mechanical loading from high speed flow of gas medium and particles of non-burnt fuel. The worked out composition of oxide-ceramic covering «M-1*» proved compatibility of linear thermal broadening of the concrete and covering. The production of a boiler hatch 400x450 mm for «Vinnitskiy MZHK» and following operation during 2 months proved effectiveness of the covering. Resources of the concrete have been increased in 1,5 times but some concrete and covering oxfoliation have been determined. This is possible because of alkali corrosion condition where the beginning of concrete softening reduces. That is why, the concrete composition has been elaborated in the frames of thermal-mechanical used qualities increasement by the use of some aggregate with higher temperature of the softening beginning.The covering has been strengthened by the high temperature resistance filling, which is more stable to alkali corrosion conditions. The linear broadening of the concrete and the covering are equal under the heating (tabl. 1).Samples cubes not revealed the exfoliation of concrete and covering. To find out the operational endurance,3 boilers hatches 400x450 mm have been produced refractory concrete BRAB30И15к* as well as oxide-ceramic covering «M-1*» and installed at «Vinnitskiy MZHK» boiler. After 6 months of operation the concrete and covering are in satisfactory condition (see draw. 2). Thus, one can state the following: concrete without cove-ring is being destroyed during 2 months (see dr. 1), and with covering «M – 1*» resources are being increased in 3 times and its being operated at present.

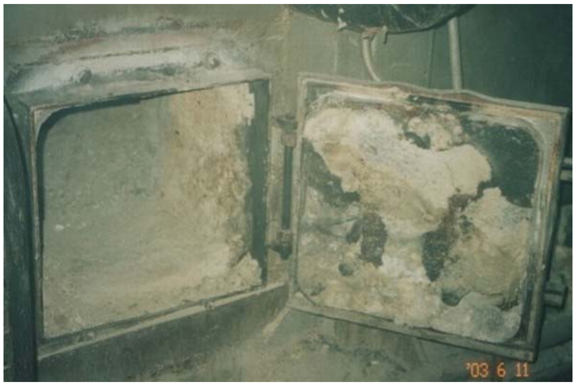

Dr. 1. Refractory concrete BRAB30И15 boilers hatch without protective covering after 2 months of operation, june 2003.

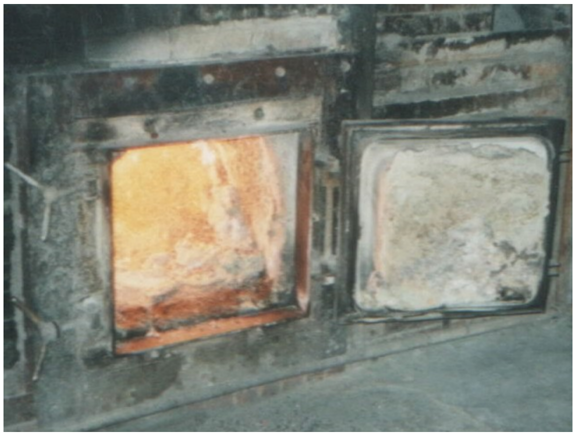

Dr. 2. Refractory concrete BRAB30И15к*with oxide-ceramic covering «M-1*» after 6 months of operation, february 2004.

1. Tropinova I, Tropinov A. Refractory concrete for a shaft furnace // Concrete and reinforced concrete in Ukraine. - 2000. - № 3. - P. 15–19.
2. Tropinov A.,Tropinova I The experience of application of thermal refractory concretes in boilers furnace on biofuel // New refractories. 2003 - №11. - P. 24–26.
3. Vladimirov V.,Galagan A., Illyuhin, etc. New refractories and thermal insulation materials and technologies of their producttion // New refractories. - 2002. - № 1. - P. 81–88.

# ENERGY CONSTANTS DETERMINING WARM-UP AND ABLATION OF HEAT-PROTECTIVE MATERIALS

**Frolov G., Baranov V.(1), Solntsev V.**
Frantsevich Institute for Problems of Materials Science, of NASU
3 Krzhizhanovsky St., Kiev, 03142, Ukraine, E-mail: frolov@alfacom.net
(1)G.E.Pukhov's Institute of Simulation Problems in Power Engineering of NAS of Ukraine

Such concepts as fluctuations, dissipative structures and self-organization play an essential role in the real revolution happening now in materials science [1]. Any dissipative system, initially in a homogeneous stationary status, being influenced by stationary streams, including thermal, which intensity exceeds the critical value, should originate ordered heterogeneous states - dissipative structures.

We may also consider the process of stationary ablation of a material as a result of a dissipative structure formation. In this case under a dissipative structure we understand a warmed layer that moves with a stationary rate under effect of continuous heat intake to the surface being heated. The foundation for this assumption is that the macrokinetics of heat destruction is a result of common interaction of several processes: thermal conductions, heat - mass transfer, radiation, changes of phase and other interior transmutations caused by an exterior energy flow. The system's behavior is rather composite: non-equilibrium, open and meeting all requirements of initiation and existence of dissipative structures.

Fibonacci number φ [2] has been lately receiving an increasing attention. Number 1.618 or 0.618 is known as the "golden ratio" or the "golden section". It is established that interactions close to the "golden ratio" are very frequently met in the nature. The "golden ratio" is also successfully used for determining similarity between structures of different materials [3]. However, such approach does not often allow us to explain occurrence of some properties of a material. In our opinion, it happens due to loss of understanding of a physical essence of investigated phenomena. At the heart of all physical processes, including those of acquiring another aggregate status, lays the energy conservation law. Therefore consideration of only geometrical characteristics of structures cannot give us a complete understanding of the nature of their origin.

In this respect an emphasis is laid on finding possible correlation between the different energy constants used in models of a warm-up and ablation of material, with number of Fibonacci.

In proceedings [4] the role of heat destruction constant ($K_{T_p} \approx 0.74$) is substantiated during a warm-up and ablation of a material. It determines dependence of the surface temperature during its heating on the temperature of destruction (fusion) up to the steady state, and regularities of a mass ablation rate change and warm-up of a material in a non-stationary mode. In the same place it is shown that the full amount of heat which is necessary for a gasification of mass unit of a material equals:

$$2(\Delta Q_w)_{\max} \approx \frac{\sqrt{\pi}}{1-K_{T_p}} H(T_к) \approx 6.8H(T_к). \qquad (1)$$

Here $(\Delta Q_w)_{\max}$ is maximum thermal effect of physical and chemical transformations on the surface; $H(T_к)$ is enthalpy of a material at the boiling temperature. Since for vaporization heat ($\Delta Q_и$) for the majority of prime substances and silicon dioxide the relation

$$\Delta Q_и \approx (\Delta Q_w)_{\max} \approx 3.4H(T_к) \qquad (2)$$

is proved, enthalpy of a gasified material makes it possible to write:

$$(\Delta Q_w)_{\max} + H(T_к) \approx 4.4H(T_к). \qquad (3)$$

The amount of energy expended on blowing effect in a boundary layer (plus radiation) $\Delta Q_{вн}$ is equal to the difference of the total material heat destruction (1) and the enthalpy of a gasified material (3):

$$\Delta Q_{вн} \approx 2.4H(T_к). \qquad (4)$$

For rating enthalpy of a warmed layer $H(\overline{T})$, we shall use an expression resulting from the equation for allocation of temperatures in a stationary warm layer:

$$\frac{H(\bar{T})}{H(\bar{T}_w)} \approx \frac{4}{K^2}\left[1-\exp\left(-\frac{K^2}{4}\right)\right]. \qquad (5)$$

From (5) for coefficient $K \approx 3.83$, determining with $\theta^* = 0.005$ practically all the warmed layer, we shall receive that the ration $H(\bar{T})$ to material enthalpy at the surface temperature at $H(\bar{T}_w)$ is equal to ~0.27. As $\bar{T}_w$, as a rule, considerably exceeds the fusion temperature, the enthalpy of the warmed layer should also include the heat of melting. The melting heat of silicon dioxide is equal to ~160 kJ/kg and makes ~0.07 of enthalpy of the molten silicon dioxide at temperature 1996 K.

The destruction of material surface practically begins immediately in steady conditions at dimensionless rate of ablation $\bar{G}_\Sigma > 0.5$ and stagnation enthalpy more than 20000 kJ/kg. Thus almost all ablative material is installed gas. In this case the complete amount of heat necessary for gasification of a mass unit of material can be recorded as follows:

$$2(\Delta Q_w)_{\max} = \left\{\left([H(\bar{T})]_{\text{тв}} + \Delta Q_{\text{пл}}\right)_{\text{жид}} + \right. \\ \left. + (\Delta Q_w)_{\max}\right\}_{\text{газ}} + \Delta Q_{\text{вн}}. \qquad (6)$$

From here we can observe that components of a heat balance (6) may be conventionally divided into two groups of factors of a heat absorption. A heat of melting $\Delta Q_{\text{пл}}$ and $(\Delta Q_w)_{\max}$, including a heat of vaporization, though make in combination a considerable proportion in a heat balance, are spent for a change of an aggregate state of a material and cannot be treated as fissile processes of heat absorption without a change of its shape. At the same time enthalpy of a solid warm layer which makes ~0.2 of heat content of ablative material in a liquid or solid status, and $\Delta Q_{\text{вн}}$, exceeding this magnitude by the order, should be referred to the factors that provide direct protection of a material shape from heat destruction.

Using expressions (1) - (4), we shall receive the classical "golden ratio" between heat energies of material destruction, which displays that the whole relates to the greater as the greater relates to the smaller:

$$\frac{2(\Delta Q_w)_{\max}}{[(\Delta Q_w)_{\max} + H(T_{\text{к}})] - [H(\bar{T})]_{\text{тв}}} =$$

$$= \frac{[(\Delta Q_w)_{\max} + H(T_{\text{к}})] - [H(\bar{T})]_{\text{тв}}}{\Delta Q_{\text{вн}} + [H(\bar{T})]_{\text{тв}}} \approx 1.62. \qquad (7)$$

The ratio of a total energy of heat destruction of a material to the amount of heat ablated from the surface by its destruction products is equal to the ratio of this amount of heat to the total of heat energies (blowing effect, radiation and enthalpy warm layer without a heat of melting), which are spent for protection of the material shape from heat destruction, and is in compliance with the "golden ratio".

The obtained dependences establish communication between the energy coefficients describing exterior streams and an interior dissipation of energy, being eventually reduced to correlation of the known dimensionless constants and the heat destruction constant. The ratio (7) displays that in the composite systems dimensionless parameters, anyhow, can be bound by relations which value is close to the "golden ratio".

It is a matter of a future concern to show how universal is this connection and how far we may go in using it for analysis and search of requirements for initiation of dissipative structures with nonlinear adaptation mechanisms pertaining to them.

## References

1. Prigozhin I., Kondepudy D. Current thermodynamics. From Thermal Engines Up To Dissipative Structures. Tr. with English. M.: the World, 2002.
2. Vorob'ev N.N. Number of Fibonacci. M.: Science, 1992.
3. Ivanova V.S., Balankin A.S., Bunin I.Z., Oksogoev A.A. Synergetrics and Fractals in Materials Science. M.: Science, 1994.
4. Frolov G.A. Heat Destruction Constant and Its Role in Processes of Warm-up and Ablation of Material Mass // IFJ 2004. Vol. 77, № 2.

# HEAT TRANSFER IN RINGER CHANNAL BETWEEN INTERNAL HEATED AND EXTERNAL COOLED POROUS CILINDERS

**Karimova A.G., Dezider'yev S.G., Zubarev V.M.(1), Sattarov I.Kh.(1), Khabibullin M.G.(1)**
Tupolev Kazan State Technical University
K. Marx str., 10, 420111, Kazan, Russia, E-mail ud@ud.kstu-kai.ru
(1)OAS Kazan Motorbuilding Industrial Assosiation
Dement'ev str., 420036, Kazan, Russia, E-mail ogpa@kmpo.ru

Porous effusion protect cooling is most effectiveness of known methods of air cooling with date mass flow of cooler [1, 2].

Effusion cooling method create on a hot porous wall (near to warm source) restrictive boundary layer of cool air against warm flow to cooled wall. There is three important thermodynamic function, which cooling air carry out: it cool an external surface of porous wall (from cool side) with permanent boundary layer suction and intensify cooling process on this side ($\alpha_{air}$); take away mostly warm in a porous hot wall ($\alpha_v$); create a cold boundary layer on a hot internal side of porous wall ($\alpha_g$).

Technical literature contains description in detail cases use of porous cooling at main hot flow along porous wall, but practically absent data without it.

This work is dedicated for research of heat transfer process and temperature condition in channals, formed by coaxial cilinders: warmed internal, cooled middle porous, external once.

It was created model plant for realizing expeiences in broad diapason of main parameters changing: mass flow of cooling air and temperature factor.

It was fulfils some measurements during experiments: mass flow of cooling air, pressure and temperature in the entrance, internal and external temperature of porous wall, external cilindre and air temperature distribution inside between hot and porous cilindres.

The results of experiments was processed correctively with thermodynamics lows.

As result of some experiments there was received formulas, wich observe influence of mass air flow (as Reynolds number) and temperature factor to heat transfer:

$$Nu_{av}=0{,}059Re_{av}^{1{,}05}(T_g/T_{por}) \qquad (1)$$

$$Nu_x=0{,}065\ Re_x^{1{,}05}(T_g/T_{por}) \qquad (2)$$

This formulas may be used as boundary condition for calculation temperature condition of porous wall. Future experiments will exact some influence factors for this formulas.

## Literature list

1. Manushin E.A., Baryishnicova E.S. Results of science and technics, series "Turbobuilding" Moscow publishing house VINITI, 1980, T. 2, 280 p.p.
2. Lokai V.I., Dezider'ev S.G. Calculation of turbine blades temperature for effusion cooling "Works of KAI", collection 101, 1968, Kazan, p.p.15-20.

# MATERIALS FOR THE RELATIVE CONJUGATIONS OF SPACE ENGINEERING

**Bronovets M., Kostornov A., Skorokhod V.,**
**Solntsev V., Frolov G., Futshich O., Yarosh V.M.(2), Tsvelev V.M.(2)**
Frantsevich Institute for Problems of Materials Science, of NAS of Ukraine, Kiev
E-mail: frolov@alfacom.net
(1)Interdepartmental Scientific Council on Tribology at the Russian Academy of Science,
MinIndScientific Russia and Union NIO, Moscow, Russia, E-mail: brnovets@ipmnet.ru
(2)Lavochkin NPO, Moscow, Russia

In environment of space vacuum routine gears which provide increase of a wear resistance of materials in process triboactivation, are not implemented in connection with absence of atmosphere of the fissile gases (oxygen, nitrogen and carbon dioxidal). At dry friction in vacuum as a result of plastic deformation accumulation and, as consequence, defects of structure, processes of gripping intensively develop. Application of solid lubricants and other coatings not always allows to calculate on continuous serviceable lifes, in particular, in extreme situations when exposures essentially may exceed physical-mechanical properties and functionalities of coatings.

Capabilities of improvement of functional properties of equilibrium materials are practically exhausted. Their further increase may be provided at the expense of application of materials with non-linear gears of adaptation which non-equilibrium physicochemical systems with element of self-organization have.

Use of materials on the basis of self-organizing inorganic systems for friction units represents special interest. These wear-resistant materials are capable to disperse an external flow of energy and improve the functional properties at friction in extreme conditions. The space vacuum, medium of Mars and Venus planets are extreme for activity of friction units of space vehicles (SV). In these conditions effect of external power flows on materials is most intensively developed. It is necessary to expect, that compositions on the basis of self-organizing systems may show a maximum level of the functional properties.

Comparison testings of materials with self-organization elements and their equilibrium analogs have shown, that introduction up to 1 vol. percent of thermodynamic instability element in a high-strength titanium alloy which may be used for friction units of SV, reduces its wearing by some orders. This in essence new generation of materials also may be recommended for manufacturing of bearings and cog-wheels, friction connections and brake shoes, the multilayer armour, blades of turbines and other heat-stressed details with increase of fire resistance on 200 - 500$^0$C.

New antifriction selflubricating materials (SKAM) are designed for activity in open Space. In these materials the idea of high use reliability and durability is implemented by a differentiated functionality of structural components. One of them efficiently precludes with destruction at the considerable pinch efforts and sliding speeds (a carrier part), and another – solid lubricant provides formation on a working surface of shield screening film which precludes a gripping of the conjugate surfaces and reduces a friction coefficient.

The material of such class was applied in friction units "Lunokhod-2" and a radiometric system "P-400" on orbital station "MIR". Materials such as SKAM-IPM on tests in the Austrian center of aerospace and space materials technology and techniques at change of load in range 2 □ 10H have shown values of a friction coefficient at level 0,12 □ 0,15. Thus wearing was in 2 □ 3 times less wearing of LB9 (Glacier) best material used now.

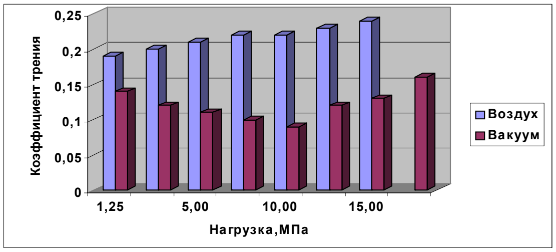

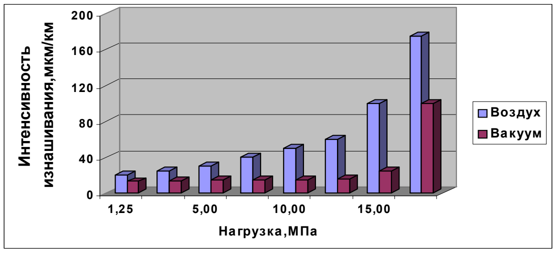

Tribotechnical properties SKAM-IPM at tests for air and vacuum are shown in figure. It is visible, that the characteristic of such material is much better in vacuum than by activity on air.

Large interest for use in friction units of SV also represent the solid lubricant coatings. For example, INTA, INASMET, and ESTL (European Space Tribology Laboratory) have offered European Space Agency to create tribotechnical laboratory (TriboLAB) on ISS (J. Serrano, J. Cómez-Elvira and etc. “Tribolab. A Facility Trobological Tests in the International Space Station”) where research of solid lubricant coatings is scheduled alongside with other antifriction materials

Lavochkin Association created complex of the ground testing equipment and autonomous friction simulator (FS), that should be installed on the “LUNA-22”. In device are using two schemes of the friction testing: "shaft-bush" and disc-indenter”. Taking into account, that the device should work in a fine vacuum large attention conversioned on researches solid lubricant coatings based on $MoS_2$.

The first activation of the FS instrument was expressly done through 32 days of staying at the Moon orbit. The measurement during the first minute showed the same high friction coefficient of the hard lubrication coating on the basis of $MoS_2$, which was recorded in the air atmosphere at the launch pad of the "LUNA-22". This could be explained by the fact that "input" surface layer of the lubricant coating didn't change during 32 days under the open space factors action.

Throw 1,5 - 2,0 min test friction coefficient have value for scheme "shaft-bush" 0,24-0,22 and for scheme "disc-indenter" 0,16-0,15. Friction coefficient to the end of the first communication contact decrease for "shaft-bush" to 0,14-0,10 and for "disc-indenter" to 0,10-0,09.

The tests on the Moon orbit established a tendency of reducing of the friction coefficient to some limit value after the beginning of work of the joints, which keeps independently on the number of activation's of the instrument and duration of non-movable contact. The starting friction factor increased depending on the duration of the FS instrument being in the switched off state. This argues that $MoS_2$ has the so-called "stop-effect".

When comparing the test result of HLC in space and in the laboratory facility, it is necessary to note that vacuum and weightlessness of far space represent more favorable conditions for $MoS_2$ in comparison with results of technological vacuum. The correct utilization for the friction units of the lubrication coating, tested in the vacuum facilities, will provide the operation of the SV mechanisms in the conditions of outer Space.

By analyzing the results of tests of samples of friction pair, acquired in the ground-based laboratory facility and with the help of FS instrument on the Moon orbit it is possible to implicate their satisfactory correlation. This argues that the developed complex of ground-based equipment, including vacuum facilities, measuring devices, means and methods of preparation for the tests, as well as the methodology developments allow to carry out the correct ground tests of the'friction units of the separate mechanical assemblies of the SV and units as the whole, and with sufficient reliability to prognoses functional characteristics and working ability of these assemblies in the exploitation environment in close and deep space.

On the basis of acquired results of ground and flight tests of samples of pairs of friction it is implied to develop the guideline/technical documentation (GTD) necessary for provision of tests and certification of antifriction materials on the endurance under affect of factors of the outer space and the bringing of GTD in accordance with the international requirements.

# NEW TECHNICAL BRANCHES OF IRON POWDERS

**Mironov V.**
Riga Technical University,
Azenes 20-331, Riga, LV-1048, Latvia, e-mail: mironovs@bf.rtu.lv

*There is known broad application of iron powder for purposes of powder metallurgy, metal welding and cutting. Relatively new areas of application are chemistry and metallurgy. Some of them are discussed below.*

### *I. Application of Iron Powder for Metal Extraction from Solutions*

The process is most effective in case of positive electrochemical potential (see Table 1). The most effective is application of iron powder for adding Cu, Ni, Hg, and Cr at purification of sewage water coming from galvanization and other processes. The greater is electrode potential of metal in comparison with iron, the faster is reaction of adding.

It is required 0.88 kg of Fe iron for production of 1 kg of cupper. Usually Cu: Fe ratio is 1: 1.1 or 1: 1.5. For metal extraction there is known application of iron of 45-100 mkm grain sizes. This production method is used in electronic industry where many printed circuit boards are produced. Sludge after electro-erosion is processed as well. Purification of galvanization sewage with inclusions of silver, nickel, chromium is currently central as well.

Table 1. Comparison of electrochemical potentials of some metals.

| No., | Metal, | Value of potential, V |
|---|---|---|
| 1. | Gold | +1,42 |
| 2. | Platinum | +1,2 |
| 3. | Silver | +0,80 |
| 4. | Cupper | +0,34 |
| 5. | Lead | -0,13 |
| 6. | Nickel | -0,23 |
| 7. | Cobalt | -0,28 |
| 8. | Cadmium | -0,40 |
| 9. | Iron | -0,44 |
| 10. | Chromium | -0,56 |
| 11. | Zinc | -0,76 |
| 12. | Manganese | -1,03 |
| 13. | Aluminum | -1,71 |
| 14. | Magnesium | -2,38 |

In accordance with production process to solutions containing the abovementioned metals, cupper, for example, iron powder is added and chlorine gas is introduced ($Cl_2$). The following reaction takes place:

$$Fe + CuCl_2 \rightarrow FeCl_2 + Cu$$

$$2\,FeCl_2 + Cl_2 \rightarrow 2\,FeCl_3$$

Usually steel scrap is used for this purpose. However, it is more useful to make adding of metals operations using metal powder, because it is possible to use high-speed propeller powder dusting devices. For small volumes, e.g. silver collection in photographic darkrooms, there may be used special cartridges containing iron powder.

Some of powders, suitable for metal extraction from sewage water, are presented in Table 2.

Table 2. Main types of iron powders manufactured by Höganäs Company. [1]

| Grade of powder | Chemical analysis % | | | Grain size, µm |
|---|---|---|---|---|
| | Fe | C | S | |
| M 40 | 95.0 | 0.25 | 0.015 | 150-180 |
| M 80 | 95.0 | 0.25 | 0.015 | 75-150 |
| M 100 | 95.0 | 0.25 | 0.012 | 45-100 |
| W 120 | 95.0 | 0.30 | 0.015 | 20-35 |
| W 00.25 | 96.5 | 0.01 | 0.005 | 45-120 |
| CMS | 94.7 | 0.29 | 0.019 | 69% < 45 µm |
| CMS 95 | 97.0 | 0.04 | 0.015 | 52% < 45 µm |

## II. Application of Fe-powders in Aluminum Metallurgy

Alloying of aluminum with the aid of iron is well known. Usually there is used metal scrap. However, in recent time there have considerable promise application of pure iron powder, Fe-Al briquettes, and iron flakes. For aluminium alloying, for example, there is well known Al-10%, Al-20%Si, and Al-10%Mn compositions. These ready mixed compositions solute faster and at lower temperature than scrap. However, cost of these compositions is higher.

In recent years there is developed iron introduction in melt using injection method and application of pre-bribriquei and pre-compressed powder materials. At thin foil production iron content is about 1-1.5%. In this case there is especially undesirable application of steel scrap due to relatively big grain size. In addition, scrap sorting and transportation is very complicated. Higher temperature is required for melting. Injection method of iron powder introduction is not expensive, at may be easy automate. However, there is necessary significant preparation of production connected with caking devices for injection purchase and installation [2,3].

Tablet method (usually tablets contain up to 80% of Fe) is very useful for production supply. Therewith, precise dosing is provided. Disadvantages of this method are: presence of bonding materials, special packing requirements [3].

Pressed materials, Ferrosol *100* and *"Melting Flakes",* for example, are very good for use in semi-automated and automated modes. High purity of end product is provided. *LSM/Bostlan*, *Hoesch* Companies (Germany), which use M40, AT 40.29, and AT 500 powders are the most known. The production method developed by *Höganäs AB* Company [3]. The best dissolving is provided at temperature of 750˚C. Dissolving takes 4-5 minutes. The best are powders produced using reducibility method, because they have higher specific area of grains. For tablet and briquettes production there may be used less expensive dusted powders.

## III. Application of ferromagnetic powder for mill scale removal

New area of steel and cast iron powder application is magnetic-abrasive removal of scale from rolled stock. Due to high hardness of scale, the hardness of powder grains shall be not less than 600-800 HV. Application of cast iron powder of 300-400 mkm grains size was discussed in [5]. Maximum size of surface roughness after magnetic-abrasive cleaning was less than Ra 4.5. Powder consumption is of 0.1-0.6 kg per 1 ton of rolled stock.

## Literature

1. http://www.hoganas.com
2. T. Pedersen, E. Mybostad, "Alloying in Aluminium By Injection", Ardal og Sunndal Verk A/S, Metallurgical R&D Center (1985)
3. Olof Andersson, "Jämpulver I Aluminiumindustrin" Lägesrapport 1989-01-17, Höganäs AB.
4. http://www.luftek.no/Powder/inj-data.htm, Webpage, Lufitek A/S, Norway

Л.Г. Делюсто. Абразивно-порошковая очистка проката от окалины. М.Машиностроение. 2002, 460 с.

# PERFORMANCE OF VARIOUS MATERIAL COATINGS IN AUTOMOTIVE 42 VDC SWITCHES

**Nouri H., Driscoll P. B., Miedziński(1), Ciric R**
*University of the West of England, Frenchay Campus*
*Coldharbour Lane, Bristol BS16 1QY, UK*
(1)Wrocław University of Technology, Wrocław, Poland

The performance of coated silver sintered materials such as AgCdO, AgNi and $AgSnO_2$ are investigated for currents ranging from 5-30A, opening speeds of 100mm/s-300mm/s for a gap-length of 5mm at 42 volts. Results suggest that the rate of erosion for AgCdO under resistive loads is greater than for inductive loads and the situation is reversed for AgSnO2 and AgNi. It is also found that for AgCdO the crossover of the anodic and cathodic arc occurs at a current of 10A. Further, for AgSnO2 and AgNi materials as speed increases, the rate of erosion increases at lower current.

Ecological requirements to reduce fuel consumption, together with increasing power demand of automotive systems has led manufacturers to increase system voltage from 14 Vdc to 42 Vdc. The higher voltage level dictates further understanding of the reliability and electrical safety of these coated materials.

The preference of Silver sintered coated materials in automobile contacts is mainly due to its properties of low material transfer in inductive circuits[1-3]. Numerous researches have investigated the performance of these materials at 14 and 42 volts dc[1-5]. In this paper attempts are being made to investigate the influence of current (5-30A), speed (100 - 300 mm/s) and load (L=0 to 10 mH) on arc duration and material transfer.

The test rig shown in figure 1 is designed and constructed to simulate the operation of contacts in automobile switches and relays. To avoid the make arc, a timing device and a contactor are used to isolate the power supply on contact closure. Contact holding force is provided by a spring that fits over the anode shaft. The cathode contact is mounted to a fixed stainless steel shaft and the contact gap is adjusted via a micrometer. The anode electrode is also fixed to a steel rod which in turn is connected to a solenoid plunger. A LVDT – Linear Variable Differential Transformer measures the displacement.

Experiments are conducted using two types of loads: resistive (5 - 30A) and inductive (10mH) with time constants ranging 1.19 – 7.14 ms. Each test is conducted at 100, 200 and 300mm/s breaking speeds, with 1000 operations per test. The frequency of one 'make and break' operation is kept to 0.25Hz per operation.

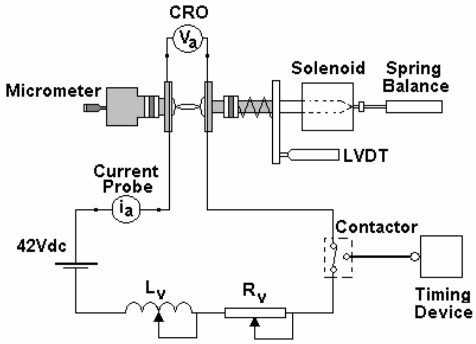

Figure 1 –Schematic diagram of test

Erosion is measured by weighing the contacts after 1000 operations using a micro-balance (±2µg accuracy) to obtain mass losses, $\Delta m_a$ and $\Delta m_c$. Table 1 shows the test conditions.

| Parameter | Value |
|---|---|
| Voltage (Vdc) | 42 |
| Current (A) | 5 – 30 |
| Series Inductance (mH) | 10 |
| Series Resistance (Ω) | 8.4 – 1.4 |
| Breaking Speed (mm/s) | 100 – 300 |
| Fixed Gap Length (mm) | 5 |
| Contact Holding Force (N) | ≈15 |
| No. of operations (break only) | 1000 |

Table 1 – Parameters used during

Table 2 shows the mechanical composition and melting points of coated materials under investigation. The contacts are Ø4mm solid rivets; the anode being of the button type variety and the cathode of the convex category.

| Material | Composition (%) | Melting Point $(^0C)$ |
|---|---|---|
| Ag/Ni | 90 Ag, 10 Ni | 960 |
| Ag/CdO | 90 Ag, 10 CdO | 960 |
| $Ag/SnO_2$ | 92 Ag, 8 Me0 (EMB 8) | 960 |

Table 2 – Contact material

Figure 2 illustrates the measured arc duration for various contact materials and loads at a breaking speed of 200 mm/s. A closer examination of the results obtained suggest that generally, as breaking speed increases from 100 to 300mm/s the arc duration for all contact materials decreases.

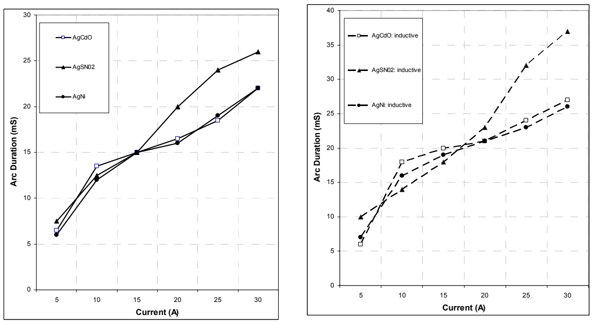

(a) (b)

*Figure 2 - Arc duration vs. current at a breaking speed of 200mm/s for various materials after 1000 operations, under: (a) resistive loads; (b) inductive loads (10mH).*

Furthermore under resistive loads the arc duration is higher and this is reflected on the erosion rate of contact materials.

Mass variation of AgCdO, AgSnO$_2$ and AgNi for resistive and inductive loads at breaking speeds of 100 and 300mm/s are shown in Figures 3, 4 and 5, respectively.

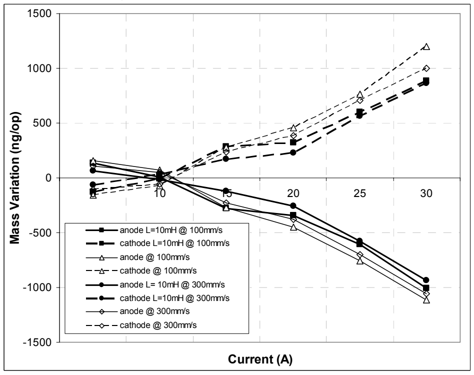

Figure 3 - Mass variation of AgCdO contacts vs. current in resistive and inductive loads, at breaking speeds of 100 and 300mm/s.

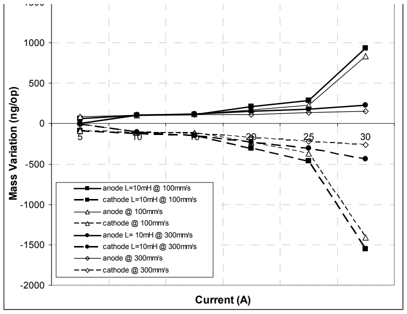

Figure 4 - Mass variation of AgSnO$_2$ contacts vs. current in resistive and inductive loads, at breaking speeds of 100 and 300mm/s.

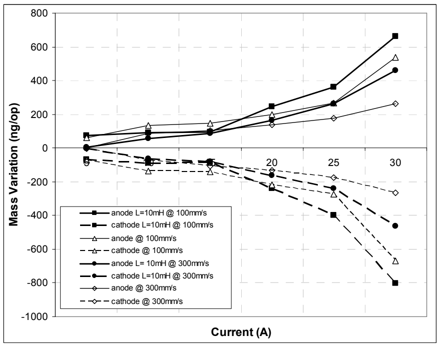

Figure 5 - Mass variation of AgNi contacts vs. current in resistive and inductive loads, at breaking speeds of 100 and 300mm/s.

## CONCLUSION

*The performance of AgCdO, AgSnO$_2$ and AgNi for typical 42 Vdc automotive systems are studied. The findings are summarized as:*

- *AgCdO contacts suffer from anodic erosion up to currents of 10A, regardless of breaking speeds of between 100-300mm/s, and inductive loads of 10mH. This is caused by the well known cathodic arc and explains why erosion at high currents is less with AgCdO than AgSnO$_2$ contacts. AgCdO have a long anodic phase which supports the accumulation of a large amount of mass upon the electrode during early stages of the arc.*
- *AgSnO$_2$ shows little signs of erosion below 15A, suggesting the results of the short anodic phase. Unlike AgCdO, AgNi shows a transition in the net zero point as breaking speed is increased. This implies that the duration of the long anodic phase is delayed with increasing breaking speed, from 100 to 300mm/s.*
- *AgSnO$_2$ shows a significant reduction in erosion as breaking speed is increased from 100 to 300mm/s and therefore would be suitable in the use of switches with controlled speed. AgCdO would be suitable for switches with uncontrolled speeds, between 100 and 300mm/s under the conditions tested. Metallurgical modification would influence the effect of these erosion rates at specific loads and speeds.*

## REFERENCES

[1] *N. Ben Jemaa et al*, 'Break Arc Study for the New Electrical Level of 42V in Automotive Applications.' *IEEE Transactions on CaPT, Vol 25, No. 3, Sept 2002, PP 420 – 426.*

[2] *V. Behrens et al*, 'Switching behaviour of Silver Based Contacts Materials in 42V DC Applications', *Proceedings ICEC 2002, PP 69 – 74.*

[3] *L. Morin et al*, 'Contact Materials Performances under Break Arc in Automotive Applications', IEEE Transactions on CaPT, Vol 23, No. 2, June 2000, PP 367 – 375.

[4] *N. Ben Jemaa,* 'Effects of parameters on the transistion from Anodic to Cathodic Arc', *Proceedings ICEC 1999, PP 173--179.*

[5] *L. Doublet*, 'Erosion and Material Transfer Under 42 Volts Direct Current', *Proceedings ICEC 2002, PP 62--68.*

# LIGHT-WEIGHT SEAMLESS BOTTLES OF HIGH-STRENGTH STEEL FOR AUTOMOBILE TRANSPORT

**Sergeyev V, Ivanov A., Litvinsky I., Makatyora V., Jarko.V., Yelansky Y.**[(1)]
Osada State Tube Institute
1[a], Pisarzhevsky str., Dnepropetrovsk, 49600, Ukraine, E-mail: Postmaster@vniti.dp.ua,
[(1)]Yuzhnoye State Design Office
3, Krivorozhskaja str., Dnepropetrovsk, 49008, Ukraine, E-mail: info@yuzhnoye.com

According to last data of OPEK and some International organizations, oil deposits of our planet, with such consumption level of liquid motor fuel as for the present day, can be exhausted through 20-30 years.

Among other alternative types of a motor fuel for vehicles is a compressed natural gas (CNG) as the most promising one, and its reserves in the world are estimated at more optimistic level.

Solution of the problem to transfer the vehicles to CNG is especially urgent one in connection with a need to save a high-expensive liquid fuel and improve ecological environment of large cities.

One of the most important completing elements of automobiles using CNG, are the high-pressure bottles (19,6 MPa and more), which are used as fuel tanks.

Operating conditions of vehicle bottles are characterized frequently by such extreme facts as shock, vibration and alternating loads, atmospheric and thermal effects. Therefore basic parameters of such bottle should provide a high operational reliability with minimum possible reduction of its specific mass m (bottle mass M, kg, falling at 1 liter of volume V, i.e., m=M/V, kg/l).

In order to reduce a mass for production of bottles of some types, including vehicle bottles, composite materials are used, mainly, the fiberglass-reinforced plastics. Specific mass of such bottles, depending on a design version, is 0,7…0,5 kg/l. However, a lifetime of such bottles is limited by time (to 10 years), and it is caused by a formation of shell flaws under effect of factors mentioned above as well as by aging of composite materials.

The seamless mono-metal bottles have great advantages in real operating conditions, which are made of steel of different types, both carbon and alloyed ones. Their service life is from 20 to 30 years and more, with that a cost level is less by several times than this index of bottles made from composite materials. Main disadvantage of steel bottles is their high specific mass, accounting about 1,8…1,2 kg/l.

Therefore the task to be achieved for a maximum reduction of a bottle mass with maintenance of its operating reliability during use with the vehicles can be solved at the expense of employment of a mark of steel with the more high strength properties.

Experience of the Ya.E.Osada State Tube Institute in development of the seamless steel and metal-composite bottles for the defense industry, aviation and space hardware, including to support a man’s vital activity in space, made possible to offer the 20ХН4ФА-grade high-strength steel for vehicle bottles. Mechanical properties of steel mentioned make possible to ensure a specific mass of bottles (m) at level 0,8…0,75 kg/l with a safety factor on ultimate strength 2,6.

The best bottles of the same purpose and produced by the Italian Faber company have an index m=0,9 kg/l, with that it is achieved at the expense of a safety factor reduction on material ultimate strength from 2,6 to 2,25, and it reduces substantially the structural strength and operating reliability.

The Ya.E.Osada STI has offered several developments of the type-size bottles with capacity from 20 to 50 liters, designed for different vehicle types. Prototypes have successfully passed such special tests as hydraulic ones for ultimate strength, cyclic tests up to a moment of a leak proof-ness loss as well as for penetration by shooting through.

The seamless cold-worked tubes are proposed to use as an incoming billet for production of the vehicle bottles. Manufacturing technology of such bottles provides to use a high-production single-action method for seaming bottoms and fillers, as well as a hardening thermal treatment. In combination with a number of tests and quality control during all technological processes these operations make possible to master a production of vehicle bottles with high indices of the structural strength and operating reliability. A seaming process of the bottle bottoms and fillers made from thin-walled tubular billets may be stable mainly at the expense of optimum strain purpose the limiting reducing conditions are required to be defined primarily; these conditions should provide a high-production seaming without the loss of a billet stability in tangential direction.

A linear dependence between stresses and strains related to a mid-surface is taken as an assumption in analyzing the billet strain process. With that the modulus of plasticity module is used instead of the Young modulus, and it is well substantiated with account of insignificant strains during one billet cycling .

This problem can be simplified using the Saint Venant semi-inverse method, when separate parameters in form-changing are defined experimentally, revealing the fundamental laws and neglecting secondary ones.

In order to obtain a wall thickening required for tapping the qualitative thread in a cylindrical section of the bottle fillers, in a number of cases an axial supporting lockup of a filler butt end is needed to be used during strain process. This condition can cause the loss of a billet stability in axial direction.

Therefore for a calibration development of a forming tool the main conditions should be defined, which provide the filler seaming process stability. Using the law of definite volume of metal under strain and with account that a billet elongation in axial direction is absent practically, the expression is obtained, which defines a wall thickness value, whereby a required thickening in a cylindrical filler section may be obtained without an axial supporting lockup:

$$S_0 = \frac{S_T (R_1 + r_г)(2R - S_г)}{4R^2 (R_1 + R)}$$

where $R$, $r_г$ –radius of a billet and cylindrical filler section; $R_1$ – transfer radius of a spherical section into a cylindrical one; $S_о$, $S_г$ - thickness of a billet wall and cylindrical filler section.

A wall thickness value, defined according the formula mentioned, is a limiting condition in the need for a respective supporting lockup section on the forming tool.

In the case, when we use an axial supporting lockup, an axial force should be defined, which provides a required metal set, excluding the loss of a billet stability in an axial direction. For this purpose, the experimental researches were conducted, when forces, shifted with respect to an axis in the same manner as it takes place during seaming process, were applied conditions. For this to the specially manufactured filler specimens; with that the values of forces and stresses were defined, under those a beginning of a filler plastic strain takes place (stresses were defined by means of the strain gauges placed in axial and tangential directions).

Solution of the problems defining the optimum strain conditions of the thin-walled billets made from the 20ХН4ФА-grade high-strength steel during a single-action seaming process in combination with a hardening heat treatment of the bottles, set of tests and their quality control during all processes make possible to master an industrial production of the light-weight vehicle bottles with high indices of the structural strength and operating reliability.

# PERSPECTIVE REFRACTORY AND HEAT-INSULATED MATERIALS AND COATINGS FOR EXTREMAL OPERATION CONDITIONS

**Vladimirov V.S.**, **Karpuhin I.A.** (1), **Iluhin M.A.**(1), **Moyzis S.Y.** (1), **Moyzis Y.S.** (1)
Bauman, MSTU Moscow, Russia
Vtoraya Baumanskaya str., 5; E-mail: bauman@bmstu.ru
(1) ZAO NPKF «MaVR», Zhukovsky, Russia
M.R. Gagarina str., 2, E-mail: mavr@pt.comcor.ru

Development of new refractory and heat-insulated materials and coatings, operated under extreme conditions (high temperatures and 2-phase flow blower speeds, aggressive conditions, complex and alternating loadings and etc.) is one of the most important modern problem, being actual not only for aero-space engineering, but also for any civil branches of national economy.

During last six years ZAO NPKF «MaVR» with participation of collaborators of MSTU n/a N.E. Bauman, TsAGI, FRI
develops and introduce new types of refractory and heat-insulated materials and coatings, having more higher operational features and characteristics in comparison with traditional features and characteristics into different branches of national economy. For receiving of the same materials base special technological processes, using perspective technology of self-extending high-temperature synthesis (SHS), cold swelling and its joint application are developed.

**SHS-technology** is based on the principles of combustion without gas of systems oxidizer-fuel, going in condensed phase. Opportunity of the same combustion without gas is conditioned by above all high values of heat-evolution under chemical interaction and thermal stability of combustion products. In particular these factors determines formation of the same chemical structures of final products, capable to stand the high thermal, mechanical and chemical loadings without changing of main characteristics in wide range of influences. High speeds of SHS-processes determine its high productivity, impenetrable for traditional methods on development of materials with increased operational characteristics.

**Method of cold swelling** for non-organic compositions are executed under room temperature without any heating and forming of special conditions. Swelling effect is as usual based on reactions of chemical interactions of two or more components of compound with formation of gasiform products of reaction. Effectiveness of this method depends on the right selection of components.

On the basis of mentioned and other modern technologies ZAO NPKF «MaVR» developed the series of new non-molded refractory and heat-insulated materials and coatings and at the present time deliver them to any Customers.

At the present time production is organized for the following types of non-molded materials:

- dry technological compounds for receiving of thin (0,5…2,5 mm) ceramic SHS-coatings with the specified operational features (more than 15 kinds of compositions);
- SHS-mortars for «welding» by ceramic joint into monolith for different kinds of refractory products (more than 5 kinds);
- dry technological compounds for formation on the working surfaces of piece-goods and refractory concretes of thick-wall (4…10 mm) ceramic plasters (more than 10 kinds);
- dry technological compounds for receiving of gunite-masses and repair-restoration solutions (more than 5 kinds);
- dry technological compounds for receiving of refractory light ($\rho$=500….1200 kg/m$^3$) and particularly light (200 ….500 kg/m$^3$) cellular concretes (more than 15 kinds) by the cold swelling method;
- dry compounds and liquid components for receiving metal-phosphate refractory coatings and plasters (more than 5 kinds);
- dry technological compounds for production of glue compositions and mastics for gluing of heat-insulated porous strong-formed and fibrous materials;
- dry technological compounds for production of coatings, plasters, concretes and anti-burnt-on paints for aluminium productions.

Application of these mentioned non-formed materials allows:

- to form on the working surfaces of some wide-used refractory materials: piece refractors (of alumino-silicate, alumina, silica, periclaz-spinellide and other classes), refractory concretes and also mullite-siliceous and corundum fibrous materials – protective-strengthening coatings and plasters with the specified operational features;

- to combine into monolith using specially selected compositions of mortars (SHS-masonry solutions) piece refractors of alumino-silicate, alumina, silica, periclaz-spinellide and other classes, at that the oxide-ceramic material formed in the region of joint is substantially more strong, more erosion- and corrosion-stable in comparison with the rest laying;
- to execute of extreme and plan repair and repair-restoration works for linings of high-temperature thermal aggregates (metallurgical aggregates, heating furnaces, boilers, chemical reactors, columns, scrubbers and others) due to application of gunite-masses, repair-restoration solutions, glue compositions, concretes, coatings and plasters, mentioned above;
- to form all the necessary heat-protective elements for structures of high-temperature thermal aggregates at the place of execution of lining and repair works with the usage of casting technology (on the base of application of technological admixtures for receiving of light and particularly light refractory cellular concretes).

Dry technological compounds are also widely used at the experimental production shop of «MaVR» during the production of numerous nomenclature of ready products: blocks, bricks, plates, bars, shells and etc.

Developed non-formed refractory materials are successfully approved and demonstrated their high effectiveness in the real conditions of operation at more than 60 enterprises, plants and industrial complexes of different branches of industries; and at the present time some of them (SHS-mortars, dry compounds for receiving of coatings, plasters and repair-restoration compositions) are widely used during operation of high-temperature thermal aggregates and during execution of lining works at the enterprises of ferrous and non-ferrous metallurgy, machine-building, chemical and petrochemical industry, heat-and-power engineering, municipal economy and etc.

At the enterprises mentioned above non-formed refractory and heat-insulated materials of «MaVR» firm were effectively used during execution of repair and repair-restoration works for linings of the following types of high-temperature thermal aggregates and elements of their structures:

- metallurgical furnaces (open-hearth, electric arc steel-smelting, inductive for smelting of cast iron and non-ferrous metals, catoptrical for smelting of non-ferrous metals, cupolas and furnaces-scoops for smelting of steel);
- scoops (steel-pouring, intermediate scoops for pouring of steel, scoops for pouring of cast iron, small filling scoops for conveyer filling of cast iron into forms, vacuum and filling scoops for smelted aluminium and its alloys and so on);
- steam and water-heated boilers, recuperators, burner blocks, protective cocks, gas flues and smoke-stacks;
- chemical reactors, high-temperature columns, pyrolysis furnaces, baths and scrubbers;
- heating furnaces of press-forging, instrumental and rolling productions;
- burning and heating furnaces for productions of construction industry;
- cremation installations and furnaces for burning of different kinds of waste products.

At the present time works on expansion of nomenclature for output products, and also on development of new types of refractory composite concretes, plasters, coatings and gunite-masses are successfully carried out.

# TO THE PROBLEM OF REFUSE RECLAMATION OF MACHINE MANUFACTURING

**Rud V. D., Halchuk T. N.**(1)
Frantsevich Institute for Problems of Material Science of NASU,
3 Krzhyzhanovsky St., Kiev 03142, Ukraine. E-mail: stern@materials.kiev.ua
(1)Lutsk State Technical University
75 Lvovska St., Lutsk 43018, Ukraine, E-mail: dekan@rud. lutsk. ua

The problem of recycling of machine-building complex waste is constantly in sight of both scientists of different scientific orientations and production workers. The improvement of technology of reclamation of grinding slurries of bearing production is one of such urgent directions. Scientific schools of academic institutes and higher educational institutions of Belarus, Russia and Ukraine have made a valuable contribution to this problem. Original technologies of primary recycling of grinding slurries are offered. Powders obtained with application of these technical solutions are used for friction and antifriction materials. They are also used for structural members manufacturing. It, first of all, is caused by rather low physico mechanical and technological properties of powders, which are determined by grading structure and axes variation of powder particles of steel ШХ15. An original technology of finishing treatment of steel ШХ15 powders obtained from grinding slurries ОАО ЛПЗ has been developed in Lutsk State technical University [1].

The novelty of this technology lies in additional deforming of powders and milling them in ball mills and in subsequent reducing roasting for surface cold working removal. The quality of powders, duration and labour imput of operations depends on technology of obtaining, on method of storage and transportation of slurries after grinding of hardened parts. Powder particles of steel ШХ15 oxidire less in the process of storing and transportation and after magnetic separation they have more regular structure as compared with analogical powders after grinding of unhardened parts. Theoretical and experimental investigations resulted in determination of kinetic curves of milling and optimum modes of all stages of additional processing. Metallographic research and mesh analysis showed that the shape of particles approximates to spherical one, the sizes of particles settle down in a narrow frictional range. It, in its turn, improved technological properties of powders: the bulk density of powders has increased, the angle of natural tilt has decreased for 30—50%, and their packing properties have improved. Powders of steel ШХ15 obtained by developed technology have been used for manufacturing such machine parts as, auger, union, cylindrical porous filter elements for lubricating and cooling liquid. Compaction of blanks was carried out by means of vibration technologies [2] or with the help of dry radial isostatic compaction method [3]. Strength tests showed that the strength of materials of steel ШХ15 powders obtained by new technology increases for 150—200%.

References

1. Спосіб отримання металевого порошку зі шламових відходів підшипникового виробництва: Деклараційний патент 63558. Україна. – 06.05.2003. 7В22F9/04 / В.Д.Рудь, Т.Н.Гальчук, О.Ю. Повстяний
2. Пристрій для вібраційного формування виробів з металевих порошків. Патент на винахід №18095А. Україна-17.06.97.В 22F3/02 / Ю.Я. Ткачук, В.О. Кузьмін, В.Д. Рудь, О.О. Сергеєв.
3. Заболотний О.В., Рудь В.Д., Богінский Л.С. Виготовлення фільтруючих матеріалів із застосуванням сухого радіально-ізостатичного пресування. // Наукові нотатки. – Луцьк: ЛДТУ, 2003. –Випуск 12. – С. 106-123.

# UTILIZATION OF NICKEL-CADMIUM STORAGE BATTERIES WITH OBTAINING OF CHARGES FOR PRODUCTION OF CERMET CONTACTS

**Olynets V.(1), Sribniy V., Tsupko F.(1), Skydanovych N.**
State enterprise “Argentum”, Lviv, Ukraine
(1)National University “Lvivska Polytechnika”, Lviv, Ukraine

Use of second raw materials in the processes of the production of the mixtures of powdered metal (charges) for the extrusion of electrical contacts gives the possibility to decrease the prime cost of production, to organize ecologically clean production technology, in this case having minimally changed or rearranged the basic stages of technological process. It was shown [1], that the argentiferous charges, prepared with the use of second raw material, in their properties do not differ from the charges, prepared with the use of pure metals as source material.

The purpose of this work was investigation of the possibility of using the active mass of the electrodes of the alkaline nickel-cadmium storage batteries as the raw material for production of the argentiferous charges СН30м, СН29Г2м and СОК15м, and also the determination of the optimum technological parameters of process.

Research was conducted on the industrial equipment at SE "Argentum", and the obtained production (charges and the prepared of them electrical contacts) were subjected to tests for the purpose of checking their correspondences to the advanced technological requirements.

The simplified scheme of the process of extraction of nickel and cadmium from the storage batteries is given in Fig. 1.

The active mass, extracted from the plates of storage batteries, was rinsed in the deionized water for the purpose of the washing out the remains of electrolyte. The rinsed mass was loaded into the reactors, where they lixiviated the basic components (nickel or cadmium) by the solution of nitric acid. Preheating of reaction medium to 70-80 $^{O}$C is necessary for the complete extraction of nickel from the solid phase into the solution, the leaching of cadmium was carried out without the preheating. Mother liquors with pH 4-4,5, and also water after the rinsing of solid residue in the reactors, were given into the reactors-sedimentators, where with the aid of $H_2O_2$ admixtures, mainly iron, were precipitated. After settling the solutions of metals nitrates were filtered and directed to the synthesis of the salt mixtures for obtaining the charges. The charges СН30м and СН29Г2м were obtained by the thermal decomposition of the mixture of coprecipitated oxalates of nickel and silver in the protective atmosphere. Precipitation was conducted from the diluted heated solution of metals nitrates by the solution of ammonium oxalate. For obtaining the charge СОК15м precipitation was conducted by the solution of sodium bicarbonate, and the thermal decomposition of the mixture of precipitated salts was conducted without the protective atmosphere. Before the thermal decomposition the saggings were repeatedly washed in the deionized water and dried with tempereture 80$^{O}$C.

The obtained charges for the technological parameters and impurity content correspond to the advanced requirements and were successfully used for the production of electrical contacts.

Thus, it is developed and successfully inculcated in the industrial production technology of the utilization of the alkaline nickel-cadmium storage batteries with obtaining of the high quality charges for the extrusion of cermet electrical contacts.

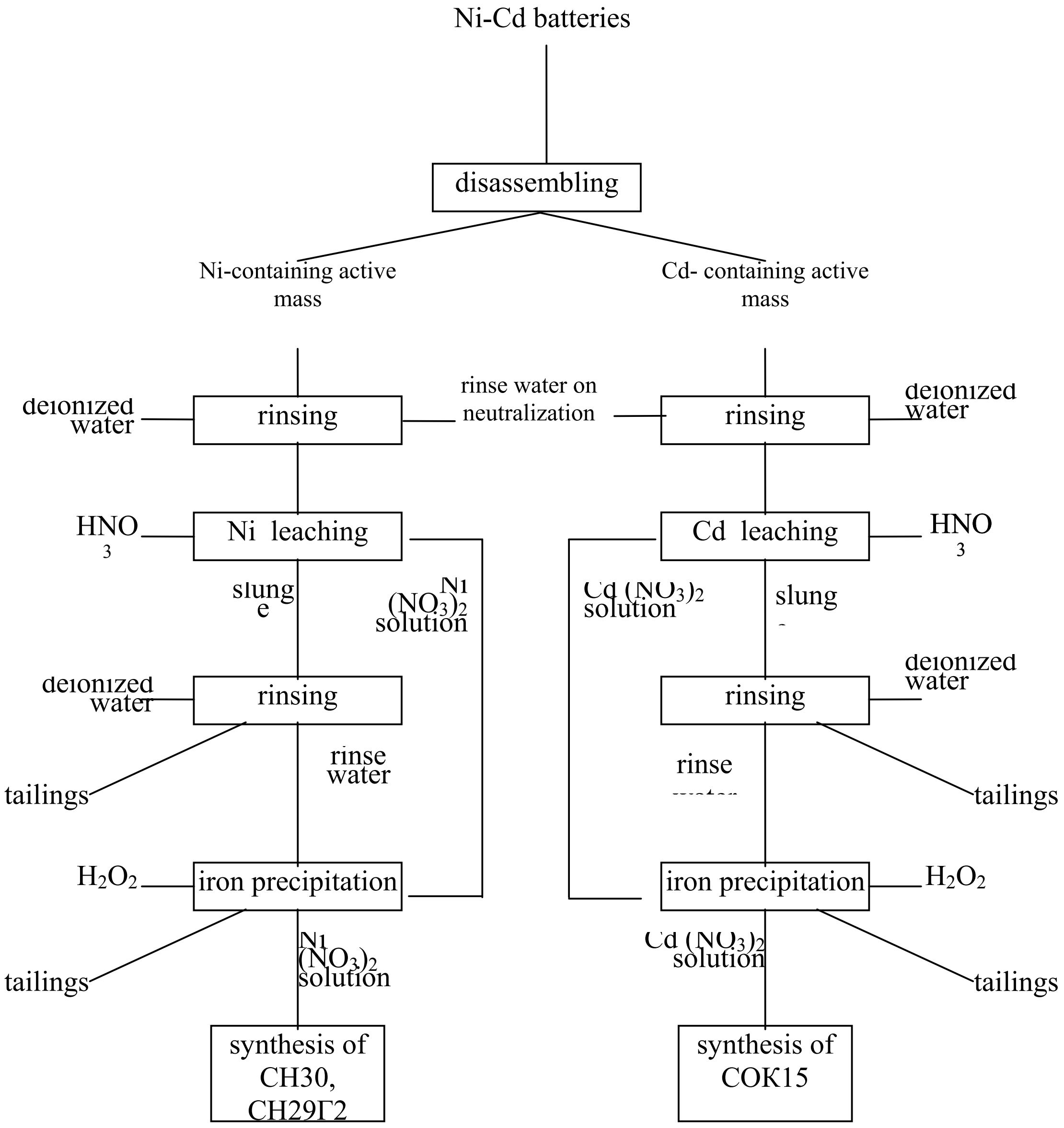
Ni-Cd batteries
disassembling
Ni-containing active mass
Cd- containing active mass
deionized water
rinsing
rinse water on neutralization
rinsing
deionized water
HNO3
Ni leaching
Cd leaching
HNO3
slunge
Ni (NO3)2 solution
Cd (NO3)2 solution
slung
deionized water
rinsing
rinsing
deionized water
tailings
rinse water
rinse
tailings
H2O2
iron precipitation
iron precipitation
H2O2
tailings
Ni (NO3)2 solution
Cd (NO3)2 solution
tailings
synthesis of CH30, CH29Г2
synthesis of COK15

Fig. 1. The scheme of reprocessing of nickel-cadmium storage batteries

**Literature sources:**

1. Срібний В.М., Цюпко Ф.І., Скиданович Н.І., Олинець В.Т. Отримання порошків металів з вторинної сировини // Материалы международной конференциии “Электрические контакты и электроды - 2003”, Украина, Крым, Кацивели, 15-21 сентября 2003 г.

# ELECTROCHEMICAL PRODUCTION OF THE NICKEL POWDERS FROM AMMONIUM SOLUTIONS OF THE LEACHING OF SECOND RAW MATERIALS AND THEIR MORPHOLOGY

**Kunty O.I.**
National university “Lviv politechnik”, Lviv, Ukraine
E-mail: kunty@polynet.lviv.ua

Processing the second raw material of the metals, especially colored and precious is one of the directions of metallurgy, which is intensively developed in the last decade. In this case the accent is done on obtaining of not simply commodity metal, but specific production on its basis (foil, powder) [1]. Taking into account the forecasts of the prospect for the development of powder metallurgy [2], or commercial interest, it is expedient to develop the technologies of dispersed materials, using second raw material.

This communication is the continuation of the work of authors [3, 4] on the complex processing of secondary metal with obtaining of powdered metal, using electrochemical processes. The possibility of the realization of the given below functional diagram, when the leaching of the nickel-containing raw metal is carried out by ammonium solutions, is studied. This gives the possibility to practically completely extract nickel from the lamellas of the electrodes of storage batteries [5].

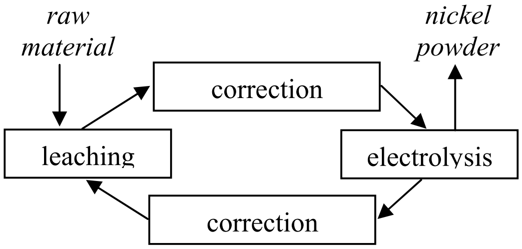

Electrolysis with the use of the undissolved anodes assumes the extraction of nickel from the leaching solutions of the system $NiSO_4(NiCl_2) - (NH_4)_2SO_4 - NH_3 \cdot H_2O$ and using a recycling of technological solutions. Cathode precipitation under certain conditions makess possible to obtain dispersed metal with assigned physico-mechanical properties.

With the high concentrations of nickel in the electrolyte (0,3-0,5 M) on the cathode precipitates compact metal. However, sediment is characterized by high intemal stress, which is shown in cracks formation (fig.1). Such sediments easily yield to grinding with obtaining of nickel powder. The conditions of electrolysis are characterized by high current outputs (~80%).

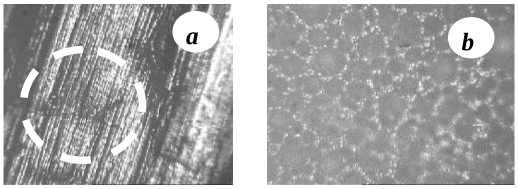

Fig. 1.Nikel, obtained in the electrolyte: 0,5M $(NH_4)_2SO_4$, $NH_3 \cdot H_2O$ (до pH = 8,5), 0,5M $NiSO_4$. t = 30 $^oC$, $i_{cat}$ (A/dm$^2$) = 5(*a*), 10 (*b*)

In the ammonium electrolytes, combined cathodic reactions occur:

$$[Ni(NH_3)_n]^{2+} + 2e \rightarrow Ni + nNH_3 \qquad (1)$$

$$[NH_4]^+ + e \rightarrow [NH_4] \rightarrow NH_3 + ½H_2 \qquad (2)$$

$$2H_2O + 2e \rightarrow H_2 + 2OH^- \qquad (3)$$

With the decrease of nickel concentration in the electrolyte and increase $i_{cat}$ the part of reactions (2, 3) increases, which leads to the decrease of the nickel current output. The changes in the conditions of electrolysis indicated, significantly affect also the morphology of cathodic sediment. Cathodic reactions (1—3) occur with the liberation of gas and it is the more intensive, the higher is the value of $i_{kat}$. The decrease of nickel concentration leads to the diffusion limitations. Summary the factors indicated create conditions for the formation of porous and dispersed sediment. The special feature of its morphology is the presence of spherical elemental particles (fig.2). Ball-shaped form, obviously, is caused by cathodic reaction (1). Under the conditions of the formation of dispersed sediment this reaction occurs more rapidly, where the higher values of $i_{cat}$, i.e., on the protrusions of dispersed particles. On the protrusions, as a result of reactions (1, 2) is created the increased concentration of molecules $NH_3$, which leads to the higher local cathodic polarization. Thus, crystal nucleus grows under the conditions of the smoothing effect.

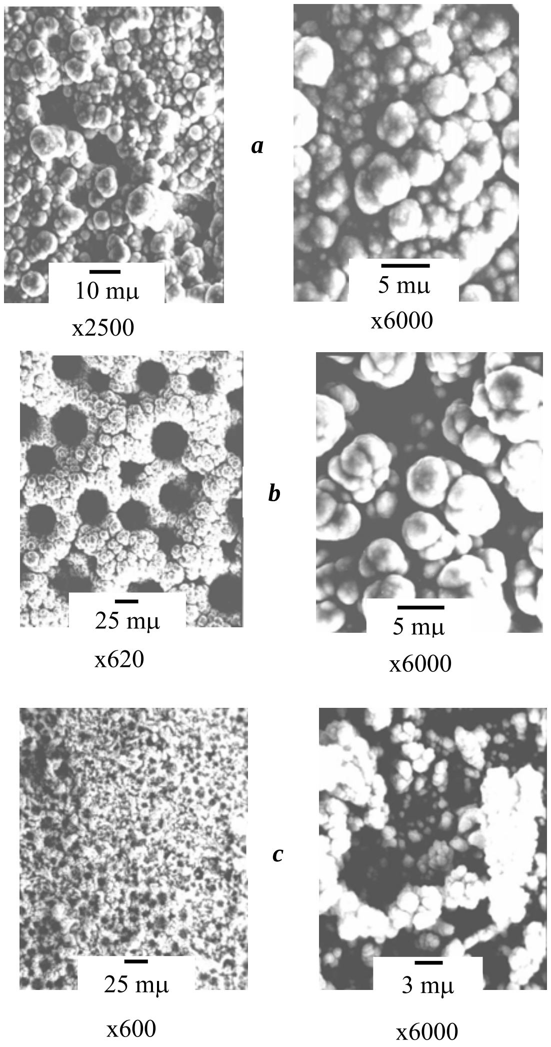

Fig.2.Microstructure of cathodic sediment of nickel, obtained in electrolyte: 0,5M $(NH_4)_2SO_4$, $NH_3{\cdot}H_2O$ (to pH = 8,5), t = 30 $^oC$: *a)* – 0,5M $NiSO_4$, $i_{cat}$ = 20 A/dm$^2$; *b, c)* – 0,1M $NiSO_4$, $i_{cat}$ = 50 (*b*), 100 (*c*) A/dm$^2$

The sizes of spherical particles somewhat decrease with increase in the cathodic current density and reduction in nickel concentration in the solution. As the elements of the first level of the structure of dispersed nickel sediment, spherical particles formate associates (second level of structure). The formation of the latter depends on the conditions of electrolysis. With an increase in ion concentration of nickel and by reduction $i_{cat}$ is observed the tendency toward the inosculation of associates with the formation of open formation (third level of structure) (fig.2). The craters and the voids, which are formed as a result of the gas generation (reactions 1-3), incorporates into the relatively integral open structure, loosening it. With very high values of $i_{cat}$, the third level structure is unstable, and cathodic sediment, which consists of the associates predominantly of the second level of structure (fig.2), easily crumbles.

In the mode of the electrolysis, when a constant concentration of nickel ions is supported, and the real value of $i_{cat}$ = const, the precipitable spherical particles close ones in the sizes. With processing of the solutions of leaching according to the diagram given above the first condition is reached by the hydrodynamic mode of electrolysis, the second – by use of the revolving disk or drum cathodes. Dispersed sediment is constantly removed from the cathodes. Thus, the sizes of dispersed particles are the function of the following basic and interconnected with the electrolysis technological parameters: 1) cathodic current density; 2) the feed rate of concentrate into the electrolyzer; 3) the speed of rotation of cathode-drum or disk; 4) temperature.

1. Худяков И.Ф., Кляйн С.Е., Агеев Н.Г. Металлургия меди, никля, сопутствующих элементов и проектирование цехов. – М.: Металлургия, 1993. – 432 с.

2. Левина Д.А., Чернышев Л.И. Западные специалисты прогнозируют дальнейшее развитие порошковой металлургии в мире // Порошковая металлургия. – 2001. – №3/4. – С. 124-126.

3. Кунтый О.И., Знак З.О., Дюг И.В. Контактное осаждение медных порошков на цинке в растворах $H_2SO_4$–$CuSO_4$, $H_2SO_4$–$CuSO_4$–$ZnSO_4$ и их морфология // ЖПХ. – 2003. – №12. – С.1992-1994.

4. Цементація нікелю на магнії / О.І.Кунтий, О.Б.Масик, М.С.Хома, Р.М.Камінський // Вопросы химии и химической технологии. – 2003. – №4. – С.116-119.

5. Демидов А.И., Красовицкая О.А. Извлечение никеля из отработанных електродов никель-железных аккумуляторов в аммиачных растворах // ЖПХ. – 2000. – №10. – С.1656-1660.

# GAS GENERATOR AS A MEANS OF SOLID ORGANIC WASTE UTILIZATION

**Gavrylov R.V., Gladkiy V.V., Bescorsiy A.P.**
The Special Research and Development Bureau for Cryogenic Technologies of Institute for Low Temperature Physics and Engineering of NASU
47, Lenin Ave., Kharkov, 61103, UKRAINE; E-mail: mail@cryocosmos.com

Engineers of SRDB - CT - ILTPh&E – NAS of Ukraine have developed equipment and technologies of obtaining combustible gas, generated from various kinds of organic waste, including home- junk waste.

As an example, there is an industrial gas generator which is put in operation at a oil- extraction factory, and which utilizes 25 tons of sunflower- shell a day. As another example, there is an industrial gas generator, which is put in operation at a timber- milling plant, and which utilizes 25 tons of wood- saw waste a day.

There has also been developed, fabricated and tested a miniature gas- generator, intended to utilize about 2,5 tons of various organic industrial and agricultural waste, as well as home- junk waste, a day. This miniature gas- generator is equipped with auxiliary raw- material grinding machine. In terms of humidity, the raw material should be pre- conditioned to maximum 40%, i.e., it should subsequently undergo compaction and drying. This miniature plant can be employed anywhere, to obtain either heat- supply, or electric energy. With purpose to obtain heat- supply, the organic fuel should be burnt in a water- steam boiler facility, whereas obtaining of electric power is feasible through feeding the gas (obtained from the organic fuel) into internal combustion- engine of autonomous electric generator.

There has also been developed a further project of another plant, oriented at obtaining of heat- supply, electric power and commercial- quality solidified carbonic acid. These ideas can be realized by aid of a relevant complex system. It would include: an internal combustion-engine as a generator of compressed gas; two thermal exchangers and; a turbo- detander.

Within gas generator, organic waste matter undergoes decomposition, which is accompanied by emission of combustible gas. With purpose of cleaning this gas from solid particles, the gas is normally fed into filter unit. Upon cleaning, the combustible gas is subjected to burning inside the gas generator, whereby thus compressed gas will be transformed into carbonic acid, which process results in elevation of temperature and pressure.

Within the high temperature heat exchanger, mixture of gases will undergo a cool- down to ambient/ room temperature. By aid of pneumatic system, heat supply is fed either to drying chamber filled with raw organic waste, or to other technological facilities. With purpose to separate the gas from moisture, gas is fed to a relevant de-humidifier.

The mixture of cooled and dried matter, which also contains the gaseous carbonic acid, will be fed to low- temperature heat exchanger and to turbo- detander; whereby, under influence of high pressure of this mixture, there occurs its temperature- drop, down to minus (90—100 °C). As a result, the carbonic acid will turn into solid particles, to be accumulated in a relevant collector. Cold gas- mixture (being mainly the nitrogen gas) will be fed to chilled heat exchanger, with purpose to refrigerate every new portion of incoming gas mixture, which contains carbonic acid.

Now, the exhausted component of the gas- mixture will be evacuated to ambient atmosphere, whereas solid carbonic acid thus obtained, will be reloaded into refrigerated special- purpose transport containers and, further, shipped to its market and consumers.

Organic waste raw material processing plants can be manufactured in stationary and mobile versions, depending on final task. Whereas mobile plants are intended to yield thermal and electric power, stationary facilities produce both and, moreover, the solid carbonic acid as well. There are also known some technologies of transforming the waste- generated gas into traditional kinds of motor fuel, such as methanol, for example. Residual solid stuffs that remain after gasification, such as slag and ashes, can further be utilized as road- coating components.

# CERAMIC MATERIALS BASED ON INDUSTRIAL WASTES

**Suzdaltsev E.I, Tsvetkova M.M.**
Federal State Unitary Enterprise “Obninsk Research and Production Enterprise “Technologiya”
15, Kiev Str., Obninsk 249035, Kaluga region, Russia, onpptechn@kaluga.ru

The problem of wastes recovery is a very important one for the industries that use ceramic and glass products.

Among these wastes are chamotte brick scrap occurring on disassembling various furnaces with the expired service life, spent chamotte boxes, glass-melting pots, rejected products from quartz ceramics, sheet glass scrap, glass bottle scrap, etc. Large quantities of these valuable materials are dumped affecting adversely the environment while they are valuable raw materials for the production of ceramics.

Studies have been made and a number of ceramic materials have been developed in which up to 70% of ceramic and glass wastes is used.

The materials developed can be divided into two groups depending on their properties and wastes used in their production:

- materials with an unattractive body containing up to 35% of chamotte wastes, up to 35% of glass wastes (including glass bottle scrap) and a clay additive as a plasticizer;
- materials characterized by a high level of body whiteness and translucency and containing up to 30% of quartz ceramics wastes, up to 40% of sheet glass wastes; kaolin and clay additives as plasticizers (kaolin improves the product quality increasing whiteness and translucency level).

The materials of the first group are produced using chamotte and glass wastes without sorting them for the colour and removal of impurities as these technological operations increase the cost several times and require additional equipment.

The process for the production of articles from these materials consists of the following operations:

- grinding of starting components in the grinder;
- preparation of slip by wet grinding in ball mills;
- product molding by casting into plaster molds;
- engobing or glazing;
- drying;
- firing.

The materials based on chamotte and glass wastes are sintered at 1000°C until the water absorption level of the body is 0.5-12% (depending on the composition).

These materials with an unattractive body are from yellow to grey in colour, often have dark inclusions caused by impurities in wastes and by impurities entering during grinding.

Coloured engobes with 70% of ceramic and glass wastes and low-melting unfritted glazes of different colour with 50% of glass wastes have been developed to mask body imperfections.

The process for the production of the materials with a high level of whiteness and translucency (the second group) is analogous to the previous one but it includes the operation of magnetic enrichment of slip, which is necessary for the removal of iron impurities entering on grinding starting components.

A low-melding clear unfritted glaze with 55% of sheet glass wastes has been developed for these materials. The use of unfritted glaze saves energy for fritting.

These materials are sintered at 1000 °C until the water absorption level of the body is no more than 1.5%. The translucency of the products with a 2,5 mm thick body exceeds 15%.

The materials developed are used for the production of decorative goods (vases, ornamental flower-ports, lamp components, sculpture).

# HIGH TEMPERATURE PROCESSING OF SOLID DOMESTIC AND INDUSTRIAL WASTES

**Tovarovskiy I. G., Tovarovskaya G. I.**
Iron and Steel Institute of NASU
Academic Starodubov square, 1, Dnepropetrovsk, 49050, Ukraine, iosif@tig.dp.ua

The problems of domestic and industrial waste utilization are effectively solved through thermal methods, among which the high temperature methods are the most universal as regards the range of the wastes being processed, energy utilization and elimination of deleterious substances. A study of the characteristic features of the most advanced methods (high temperature gasification by VOEST-ALPINE, and processing in a slag melt – by SPA "ALGON" and MISIS) allowed to develop the fundamentals of a more effective technology that synthesizes the advantages of the cyclone-type gasifiers, molten-state processes and in-shaft countercurrent processes in order to achieve the goal of the full utilization of wastes of variable composition, and to obtain such ultimate products as electric power, construction engineering materials, metals and other by-products while fully eliminating harmful emissions.

The task of the project includes creation of a universal unit and technology that provide for high temperature processing of wastes of varying composition with different properties while using of any available fuel with full utilization of all the processing products and elimination of deleterious substances. These conditions could be met by the discussed high temperature technologies "ALGON"- MISIS and "VOEST-ALPINE" in case of removal of their limitations stated above. To solve this task, this project, together with the advantages of the known technologies, uses a combination of cyclone gasifyers with a melt bubbling bath. The proposed technology and unit are schematically shown in Fig. 1.

The unit includes a round or oval in plan melt bath with tuyeres for periodic tapping of metal and slag. Above the bath there is a dome that passes in the central part in a shaft. Along the dome periphery around the shaft there are fuel gasifiers (powdered coal, liquid, gaseous fuel). Concentrically thereto screw conveyors are installed to feed the furnace with unsorted domestic garbage, industrial and other wastes, as well as readily available iron ore materials, such as lean iron ores (up to 30 % iron), slag-contaminated residues of metal working and casting, residues of other industries containing iron and its oxides.

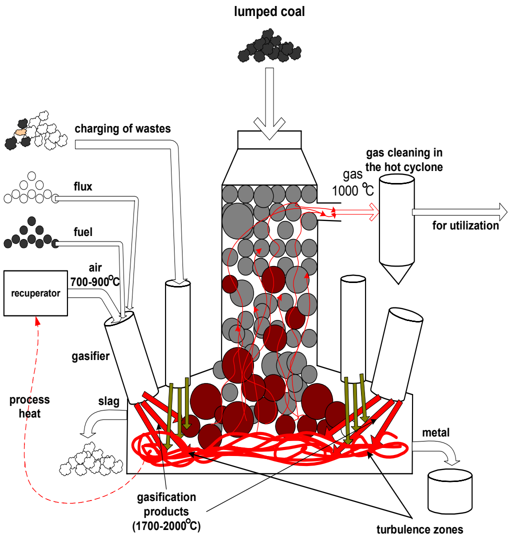

Fig. 1. Schematic diagram of the technology and unit for high temperature processing of wastes

The cyclone gasifiers are tangentially fed with the heated in the recuperator atmospheric blast (700-900° C) and fuel (powdered coal, fuel oil, natural gas, fuel residues, etc.), as well as partially milled fluxes (limestone, etc.) and iron containing materials.

The gas is tangentially taken out of the gasifier together with the liquefied mineral components at the temperature of 1600-2000 °C and led to the slag bath where bubbling is created. A mix of the wastes is fed by a screw feeder into the bubbling zone close to the gasifiers. To make the screw feeding more effective, heavy lumped materials (limestone, construction garbage, metal, etc.) are added to the soft and light-weight materials (paper, carton, polymers, food residues, herbs, etc.).

In the bath the carbon and hydrocarbons of the wastes react with $CO_2$, $H_2O$ and redundant oxygen ($O_2$) of the hot gas forming CO, $CO_2$, $H_2$, $H_2O$. The solid components pass into the melt (1400-1500° C), while some part of the oxides (including iron) are reduced to metals and precipitate.

The formed hot gas is flown to the shaft that is continuously charged with lumped coal and other lumped carbon containing materials (such as broken electric furnace electrodes). The oxidizing gas components during their filtration through the coal layer react with the carbon according to the reactions: $CO_2 + C = 2\ CO$; $H_2O + C = H_2 + CO$ with an endothermic effect, therefore their temperature gets down during the filtration while the calorific value increases (due to the formation of $CO + H_2$). Besides, partial gas cleaning takes place that is then finalized during gas removal from the shaft in the hot cyclone. The latter is a cyclone unit with a refractory lining. The dust-laden gas is tangentially fed therein on the top and removed centrally. The dust particles are pressed to the cyclone wall by the centrifugal force of the gas and are decelerated, settling down in the lower portion (in the dust collector) from where it is pneumatically transferred to the main process, for instance, to the gasifier.

The produced gas at a temperature of about $1000^{o}$ C is used for energy utilization according to the conventional electric power generation schemes using either steam turbine or gas turbine units. The latter allow, even with low calorific value wastes, to achieve > 25 % efficiency (the usual efficiency during processing of wastes is < 20 %). Some part of the energy of the produced gas is used for blast heating in the recuperator.

Along the dome perimeter around the shaft at least 4 cyclone type gasifiers (CG) of 2-3 mt/h fuel capacity can be installed. The total fuel capacity with 4 CG will approximately equal 10 mt/h; with 8 CG – about 20 mt/h, etc. The waste charging screw conveyors (SC) are installed according to the number of CG, and their capacity is calculated according to the fuel/waste (f/w) ratio that is usually > 0.03 kg/kg. The proposed technology features a higher value of that ratio which provides a stable operation of the energy scheme, while melting all the mineral components and eliminating deleterious substances. With the f/w value = 0.3, i.e. by an order higher, the waste capacity equals: for a 4 CG unit (and correspondingly 4 SC) ~ 35 mt/h; for a 8 CG unit (and correspondingly 8 SC) ~ 70 mt/h, etc.

The heat volume introduced by the gas and its temperature is adjusted by adjusting the volume of the fuel being burned and the oxidizer consumption ratio within the 0.5-2.0 range (mole $O_2$/mole C). The first is required to compensate for the heat unbalance resulting from charging of materials with varying heat requirement, the second is required to upgrade the temperature potential of the gases when refractory materials (with a higher melting temperature) are charged.

With the change of value $\alpha$ the consumption of the lumped carbon in the shaft and the rate of its descend to the bath change, thus allowing to modify the lumped coal consumption and the gas permeability of the bed. When the gas permeability gets lower it is possible to increase the coal bed exchange rate by increasing ($\alpha$) and, correspondingly, the oxidation level of the gas leaving the CG.

During the processing of wastes fluxes and other components are added thereto to produce slag of the composition that is required for its subsequent utilization in the construction engineering industry (cement production), road building and other fields. The problems of producing such slag are conceptually feasible.

The technology synthesizes the advantages of the cyclone gasifiers, in-melt processes and in-shaft countercurrent for solving the task of complete utilization of variable composition wastes to obtain electric energy, construction materials, metals and other by-products while fully eliminating deleterious emissions.

The technology employs, along with the wastes, low grade materials and fuel, and atmospheric air as an oxidizer (without any oxygen addition).

The proposed technology setup features flexible control and self-regulation of the processes (due to the combination of the melt bath and a coal bed). This makes it adaptable to any conditions.

According to the preliminary estimates a facility of minimum production capacity with 4 CG and 4 SC at 10 mt/h fuel consumption and 35 mt/h domestic waste consumption allows to produce 122 thousand $m^3$/h of gas with a calorific value of 5.4 MJ/$m^3$ that will operate a 72 MW electric generator. Iron and slag (for construction engineering) will be produced when processing substantial quantities of industrial wastes with metal containing components.

# ECOLOGICAL PURE PRESSED MATERIALS BASED ON OF SCRAPS OF BIORAW MATERIAL AND NEW ORGANIC-INORGANIC CONNECTING

**Ishchenko S.S., Budzinska V.L., Lebedev E.V.**
Institute of Macromolecular Chemistry of NASU
Kharkov Shausece, 48, Kyiv, 02160, Ukraine, E-mail: ihvs@ukrpack.net

The problem of creation of ecologically safe polymer composites with the high physical-mechanical characteristics presents recently the first places in researches, which are dedicated to polymeric systems. There are materials based on polymer and stuff of the miscellaneous chemical nature. The development of scientific ground to obtain such materials is the actual scientific task.

Synthesis of hybrid organic-inorganic polymer blends based on various chemical compositions of inorganic oligomers (silicates, polyphosphates) and organic compounds – isocyanates, polyurethanes, oligoetheracrylate, epoxides, plasticizers, and catalysts, surface-active agents is perspective direction for a national economy in the field of creation of such materials.

The aim of the present research consists in development of new organic-inorganic compounds as procure sores for ecological pure constructional and coating materials by a method of a molding of miscellaneous scraps of bioraw material: scraps woodworking (sawdust, shavings), processing of agricultures (straw, grape vine, stalks flax, peel sunflower, millet, buckwheat) with the purpose of their salvaging.

The replacement of urea-formaldehyde resin (UFR) by new organic-inorganic binder to receive pressed ecological safe construction materials, high toughness, water proof, frost-proof, and also fire resistat, that will allow: widely utilization such materials in the human environment (house, school, office); utilization miscellaneous scraps of bioraw material; to save natural timber; to expand export possibilities of Ukraine; to improve an ecology of the human environment.

In present research the waterborne silicate organic-inorganic binders (OIB), isocyanate containing compounds, plasticizers and additives: regulators of hardening; ground-wood-glutinous compositions (GGC) and presswork on their basis were analyzed.

Scientific analysis of processes of creation of organic-inorganic polymeric blends has proceeded to statement of the problem.

The concept was formulated of organic-silicate polymeric system genesis, which one is grounded on conception of the anionic mechanism of processes of polymerization and sequentially explains effect of miscellaneous components - modifiers on organic-silicate blend evolution. Physic-chemical transformations of the system were studied using author's method that includes IR spectroscopy, differential thermal analysis (DTA), and dynamic mechanical spectroscopy.

Analysis of experimental results allows concluding, that the polymerization comes accordingly anionic mechanism. The condensation of Si-A in an alkaline media is catalyzed by $OH^-$-ions:

$$\equiv SiOH^+ + OH^- \rightarrow \equiv SiO^- + H_2O \rightarrow \equiv SiO^- + HO\text{–}Si\equiv \rightarrow \equiv Si\text{–}O\text{–}Si\equiv + OH^- \qquad (1)$$

The initiation of polymerization of isocyanates takes place due to they attachment to a silicate fragment:

$$R\text{–}NCO + XO\text{–}Si\equiv \rightarrow \underset{(I)}{R\text{–}NX\text{–}COOSi\equiv} \qquad (2)$$

The compound (I) is extremely reactive with further transformations due to hydrolysis first of all:

$$R\text{–}NX\text{–}COOSi\equiv + H_2O \rightarrow$$

$$\underset{(II)}{R\text{–}NH\text{–}COOSi\equiv} + XOH \rightarrow \underset{(III)}{R\text{–}NH\text{–}COOX} +$$

$$+HO\text{–}Si\equiv + H_2O \rightarrow \underset{(IV)}{RNH_2{:}HOCOOX} \rightarrow$$

$$\rightarrow RNH_2 + XHCO_3 \qquad (3)$$

The formed amine reacts with isocyanate to form diureas. Hydrocarbonate partially is accumulated in an organic phase, and partially diffuses inside of dispersious particles promoting further polycondensation of silicate. Under certain conditions compound (I) can form with isocyanate isocyanurate.

It was shown that during organic-inorganic polymeric blend creation the reactions path (carbamide-, isocyanurate-, silica urethane formation homo- and copolymerization, polycondensation of liquid silica glasses) is determined by a size of a cation, and both by anion or water mobility in the initial silicate solutions [1].

It was established, that during collateral solidification of silicates with epoxy, isocyanate oligomer, oligoetheracrilate are obtained organic-mineral products with grafted silicate and organic polymer matrixes.

Depending on a type of functionality and the lengths of organic unit in organic-inorganic polymer blend the products can be obtained of miscellaneous phase composition. That is mapped on viscoelasticity properties of organic-mineral composite [2] and was proved by method of a dynamic mechanical spectroscopy.

Grounding on developed scientific principles of synthesis organic-silicate polymers, new functional composite for particular application is obtained - concrete sealing compounds, protective covering, which one have chemical, atmospheric and radiation (more than 2000 megarad) stability [3].

The obtained scientific and practical outcomes allow to contour paths of creation of new organic-inorganic binders and pressed materials on their basis.

Molded samples from scraps of bioraw materials: woodworkings, processing of agriculturals (straw, grape vine, stalks flax, peel sunflower, millet, buckwheat) were prepared based on OIB. Main properties of the materials was studied: strength at static bending ($\sigma_{st.}$), clay swelling in cold water on width ($\Delta l$) depending on the nature and humidity of an filler, amount and composition OIB, technological parameters of molded samples manufacturing. It was shown that parameters $\sigma_{st.}$, $\Delta l$ of samples analyzed essentially exceed the parameters of the samples on the basis of 15 % UFR (table).

It was proved, that presswork based on new OIB is ecologically safe.

It was determined that regulation properties of materials with new OIB it is possible in a wide range: by change of a ration between inorganic and organic components, amount of binder in GGC, change of composition of the organic component and parameters of a molding. The life capacity of GGC is not less than 8 hours.

Table.
Properties of molded sample on a basis OIB and different scraps of bioraw material.

| Amount OIB, % | The filler | $\sigma_{st.}$, MPa | $\Delta l$, % |
|---|---|---|---|
| 15 | straw | 38,5 | 11,3 |
| 15 | stalks flax | 44,7 | 6,5 |
| 15 | peel sabadilla sunflower | 37,5 | 5,7 |
| 15 | pounded wood | 45,0 | 8,5 |
| 15 UFR | pounded wood | 25,0 | 45,0 |

Thus, it is possible to gain presswork with a wide set of operating characteristic and with attractive decorative look (peel sunflower, millet, buckwheat, granulated straw) in addition. This presswork does not require veneer sheet and painting. Such hardware products can be utilized for an internal lining of habitation, industrial locations, various transport.

1. Ishchenko S.S., Prydatko A.B., Novikova T.I., Lebedev E.V. / Macromolecular compound, series A, 1996, V.38, №5, P.786—791.
2. Ishchenko S.S., Rosovickiy V.F., Prydatko A.B., Babkina N.V., Lebedev E.V./ ЖПС, 1998, №11, P.1929—1933.
3. Ishchenko S.S., Lebedev E.V. / Ukr. Chem. magazine, 2001, V.67, №8, P.116–119.

# AFFINAGE OF LAYERED MATERIALS

**Gulbin V.N.**
R & D Institute of Construction Technology
43, Altufievskoe sh., Moscow, 127410, Russia, E-mail: vngulbin@mtu-net.ru.

For recycling of non-similar metals joints there is necessity to separate layers of multi-layered material. One of advantage method is affinage of non-similar layered materials by mean of explosive separation of layers. Explosive impact on layered material causes separating forces in it as result of reflection of impact wave from layers boudaries. Deformation process leads to separation of layers.

This report presents research results of explosive affinage of layered materials with use of a method to create continuous defected sub-layers along boudaries of layered products.

Analysis of process of bi-metals explosive separation showed, that in process of explosive loading a bi-metal's wall became bent, which reached a maximum value by maximum pressure of detonation products. The experimental results cinfirm presence of residual deformation in bi-metal layers. That means the deformation ocurrs in elastic-plastic area. As result of bending displacement of layers ocurrs causing a complex stress-deformation condition of metal in deformation area and appearance of separating forces. Such separating forces appear by impact of refracted and reflected wave on the layers boundary. In by-contact areas normal compressing and tensile stresses ± $\sigma_{y,}$ as well as tangential shear stresses $\tau_{xy}$ appear (see Fig.1). By maximum pressure $P_{max}$ these stresses are also maximum, that causes start of separation process.

At initial moment of impact wave loading, the bi-metal is in a hightly compressed condition and the layers boundaries are under prevealing compressing stresses. Deformation leads to appearance of tangential stresses. After that, due to intensive unloading the compressing stresses decrease sharply; when detonation products' pressure achieves $P_{max}$ , tensile stresses become prevealing influence. Tangential stresses made the work of the layers shear begin to disappear. In the contact area due to micro-cracks opening, metallic joints are deteriorated and bi-metals layers are separated. So there are two stages of layered materials separation: comperssing and layers separation.

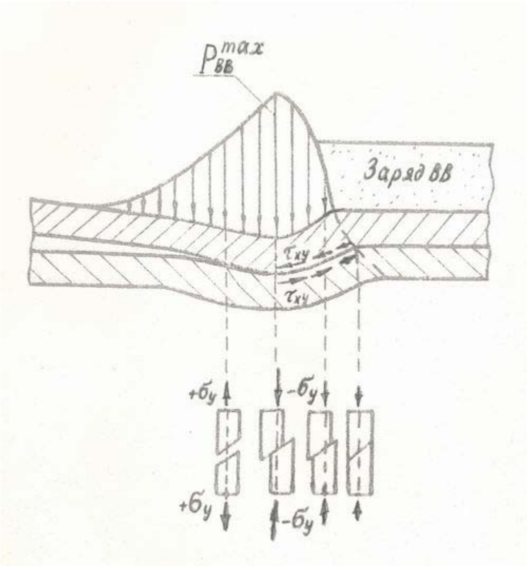

Fig.1. Scematic image of layers separation process and stresses distribution in seformation area [1].

It is possible to use two ways of explosive affinage. Application of explosive charges can be used for separation of flat layered materials. In this case the the following ratio can be used for calcuation of necessary thickness of stressed layer to be sufficient for separation of bi-metal's layers:

$\delta = P_{max} \cdot D \cdot \tau_s / r \cdot \sigma_p$,

here: $P_{max}$ - maximum pressure of impact wave's front; D - charge's detonation rate; $\tau_s$ - duration of impact wave's pulse; $\sigma_p$ - average fastness of bi-metal's layers joint; $r = \rho_0\delta_0/(\rho_1\delta_1+\rho_2\delta_2)$ - mass ratio of explosive charge and bi-metal; $\rho_0$, $\rho_1$ and $\rho_2$ - density of explosive substance and bi-metal's layers.

Inflat bi-metal also can be separated by mean of applied charge, however, in this case quality of separation is much worse and process productivity is lower. Thus it is better to perform affinage of shaped bi-metal in a pool through a liquis media. It is possible to use the following ratio for rough calculation of stressed layer thickness with use of intermediate liquid for separation of bi-metal:

$\delta = (P_{вв} \cdot V_{деф} \cdot \tau_s / r \cdot \sigma_s) \cdot (R_0/R)$,

here: $V_{деф}$ - bi-metal's deformation rate; $R_0$ - nearest distance from charge to boundary between layers to be separated; R - charge's effective radius, that is a sphere's radius for placing of required explosive charge.

It is known [2-4], that for production of non-similar layered materials from metals with limited solubility (for example: titanium + chrom-nickel steels and alloys, niobium + chrom-nickel steels and alloys, etc.), various brittle phases are formed on the boundary of layers. They serve as stress concentrators and as generators of a continue brittle layer. In order to obtain continue brittle sub-layer along the layers boundary, a thermal treatment is provided before explosive treatment. For bi-metals, which components form chemical compositions stable in range from forming- to room temperature, advance annealing is provided. During the annealing a continue inter-metallic sub-layer forms along the layers boundary. By explosive impact it is deteriorated with complete separation of the layers.

In the case when no chemical compositions form in a bi-metal, another thermal treatment process can be applied [5]. It privides thermal tretment in a media with a chemical element, which forms a solid solution with one of metals or stable compositions with another metal by saturation temperature. After such treatment, under explosive impact separation of layered materials ocurrs. There are also layered materials, whose metals have polymorphic transformation in result of diffusion saturation. In this case laured materials must be hardened after diffusion saturation, which leads to significant decrease of boundary's fastness due to residual stresses appearance. Explosive impact causes separation of such bi-metals.

Thus using of explosive impact on brittle phases or defects formed due to advance thermal treatment of layers boundary, it is possible to perform affinage of layered materials. Using of the pool method for explosive impact application ensures very high productivity of the affinage process and allows to use it in the affinage industry. In this case ecological conditions of explosive affinage are much better then by chemical affinage.

References

1. V.N. Gulbin. Explosive affinage of multi-layered materials. Vol.: Matters of atomic science and engineering. Ser.: Nuclear engineering and technology. 1990. Iss.5. p.32-35.
2. Krupin A.V., Solovjov V.Y., Kobelev A.G. a.o. Explosive deformation of metals. M.: Metallurgia, 1975.
3. Gulbin V.N., Rjabchikov E.A. Diffusion by explosive welding of titanum with steel / Vol.: Matters of atomic science and engineering. Ser.: Nuclear engineering and technology. 1988. Iss. 1(20). p.25-28.
4. Linetsky B.L., Gulbin V.N., Ivanov Y.D., Roshchupkin V.G. Study of structure and properties of niobium-steeel joints / Vol.: Matters of atomic science and engineering. Ser.: Nuclear engineering and technology. 1989. Iss.5. p.33-36.
5. V.N. Gulbin, B.L. Linetsky, Y.D. Ivanov a.o. The way to separate layers of multi-layered material. S.A. No. 1524278. Priority of 30.05.1988.

# INVESTIGATION OF POSSIBILITY TO USE CONCENTRATED SOLAR RADIATION FOR REDUCTION OF TUNGSTEN OXIDE OBTAINED BY INDUSTRIAL WASTE REPROCESSING

**Pasichny V.V., Ostapenko V.S., Ostapenko S.A., Babutina T.E.**
Frantsevich Institute for Problems of Materials Science of NASU,
3 Krzhizhanovsky St., Kiev, 03142, Ukraine, E-mail: pasich@ipms.kiev.ua.

Under the conditions of noticeable decrease of natural power resources and raw materials for producing expensive metals and alloys secondary use of industrial waste and development of energy saving technological processes become more and more actual. Tungsten is one of the most valuable metals for modern technology. Its world consumption is more then 30000 t per year [1]. There are some methods for regeneration of the waste containing this metal including the method based on their oxidation and the following reduction of obtained oxides. All the known methods are connected with great energy expenditures and based on the use of traditional power sources. In the IPMS NANU the exploratory research of the possibility of industrial waste reprocessing in the form of tungsten wire, hard alloys of BK type and other materials by their oxidation in solar furnaces i.e. when renewable ecologically pure solar energy is used [2]. Taking into account positive character of these works results it seemed to be expedient to investigate the possibility of the reduction of obtained oxide in a solar furnace which could be a final process of waste regeneration.

The purpose of this works is a study of the possibility of tungsten oxides reduction in a solar furnace for substituting traditional power source for ecologically pure solar radiation.

The powder of tungsten trioxide was used as a subject of inquiry. It had been obtained by oxidizing tangled tungsten wire in a solar furnace. The solar furnace SGU-6 with metal paraboloid of Ø 2.8 m has been selected for the experiments. The selection of the given furnace was considered with regard for the prospect of industrial realization of the technological process. This furnace is cheaper considerably than others and ensures necessary heating temperature. The experiments on the oxidation of tungsten industrial waste were carried out on the SGU-6 installation also [2]. It should be noted that in the IPMS NANU the analytic method for the selection of plane mirror facets of optimum sizes depending upon given energy characteristics of the concentrator and the technology of their applying onto antenna metal basis were developed [3].

The selection of cheap enough and available substance forming reducing medium was one of the given work problems. Two series of experiments have been carried out on tungsten trioxide reduction: with the use of solid hydrocarbons and solid phase reduction with the use of carbon black.

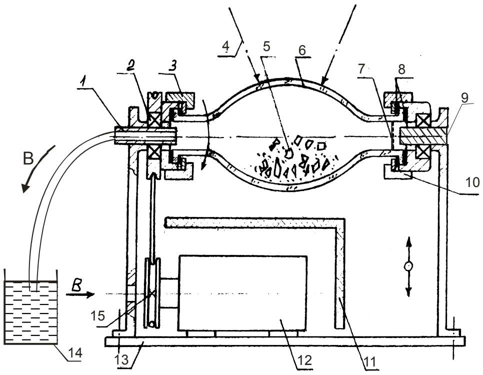

1- hollow shaft; 2- bearing; 3,10- coupling nut; 4- solar radiation; 5- substance being heated; 6- quartz reactor; 7- stopper; 8- gasket; 9- axis; 11- heat insulating screen; 12- electric motor; 12- plane basis; 14- volume with water; 15- drive pulley.
Fig.1.- Scheme of quartz rotary reactor.

Working mixture was located into specially developed rotary quartz reactor (Fig.1) in which the processes of oxidation and reduction of a product being heated run considerably faster then under stationary conditions due to mixing by rotation. For the process investigation the reactor has been sealed additionally and supplied with water seal through which the depressurization is realized.

During the first series of the experiments the mixture of tungsten trioxide with solid hydrocarbon as reducing component was selected. At the beginning stage of the experiment under temperature influence solid hydrocarbons change to gas phase creating hydrocarbon atmosphere which is favorable for reduction processes running. The gas atmosphere composition was defined by the following reactions running:

$MeO + H_2 \rightarrow Me + H_2O$, (1)
$CH_4 + H_2O \rightarrow CO + 3H_2$, (2)
$CO + H_2O \rightarrow CO_2 + H_{2,}$ (3)
$CH_4 + CO_2 \rightarrow 2C + 2H_2O$, (4)
$C + H_2O \rightarrow CO + H_2$, (5)

This version of the process carrying out differs by maximum simplicity and does not need to use gas utility systems or cylinders in contrast to the use of methane-hydrogen gaseous medium. The experiments of different duration of heating ( from 5 up to 120 min) have been carried out under the temperatures 800-850°C. The measurements were carried out by the thermocouple (chromel-alumel, Ø0.2 mm) the bead of which were located into working mixture under fixed reactor position. As X-ray phase analysis has demonstrated the degree of tungsten reduction under these conditions is not above 55-60%. As far as the explicit dependence upon heating duration in this case was not observed it became obvious that the gases being formed as a result of solid carbons thermal decomposition left the reactor too rapidly without the influence on the process later.

The second series of the experiments on reduction-carbidizing of tungsten differed from the previous one by the mixture composition. In this case the mixture was prepared in which solid carbon (carbon black) was added. Amount of carbon black was determined on the basis of the carried out calculations according to the reactions of tungsten reduction:

$2WO_3 + 3C \rightarrow 2W + 3CO_2$ (6)
$WO_3 + 3C \rightarrow W + 3CO$ (7)

In the case of reduction-carbidizing by solid carbon the transformation of $WO_3$ into WC is possible even under 600°C. Under this temperature the forming of WC is possible in the presence of free residual carbon. Under 700°C the achievement of stoichiometric WC and the relaxation to equilibrium in gaseous system $CO+CO_2$ are possible. Under the following temperature increase the partial pressure in the gaseous mixture removes in the direction of CO forming by the reaction (5). It causes so-called carbon burnout from WC. Under 1400°C obtaining practically pure tungsten with the additions of lower carbide is possible [4].

The duration of the mixture heating in the installation focal spot under the temperatures 850-950°C was from 30 up to 180 min in the second series of the experiments. In this case the reduction degree was up to 75%.

The cause of incomplete oxide reduction first of all was the imperfection of the construction of rotary quartz reactor. It demonstrated excellent qualities during the experiments on waste oxidation but in this case air access into the reactor was not excluded through the rotary units under the heating during the experiment. Besides, there were stagnant zones with lowered temperature where the reaction did not run well. When the working mixture was being unloaded its composition was averaged.

The conclusion was drawn in the work about the possibility of principle to realize the processes of the reduction and reduction-carbidizing of tungsten trioxide in solar furnaces as finishing stage of waste reprocessing. But in contrast to the oxidation the process of the reduction requires considerably more thoroughness during its engineering and technological organization.

1 Sampath A., Sudarshan T.S. Recycling of WC-C from scrap materials// Powder Metallurgy.- 2002.- Vol. 45.- № 1.- P. 21-24.
2 Pasichny V.V., Uvarova I.V., Babutina T.E. Investigation for remaking of primary solid alloy and tungsten wire wastes in solar furnace// Proceed. of 2-d Int. Conf. "Materials and Coatings for Extreme Performances…" (16-20 Sept. 2002, Katsiveli-town, Crimea, Ukraine).- P. 597-598.
3 Pasichny V.V. and Uryukov B.A. Theoretical aspect for optimization of solar radiation concentrators with plane facets// Solar Energy.- 2002.- Vol. 73, No. 4.- pp. 293-301.
4 Васкевич Н.К., Сенчихин В.К., Третьяков В.И. Некоторые вопросы термодинамики карбидизации вольфрама// Порошковая металлургия.-1985.- № 6 - С. 69-73.

# CALORIMETRATION OF SOLAR FURNACES

**Loudanov K.I.**
Frantsevich Institute for Problems of Materials Science, of NASU,
3 Krzhizhanovsky St., Kiev, 03142, Ukraine, E-mail: ipms@alfacom.net.

Solar furnace is not on instrument only for materials and coatings investigation under extremal conditions (high temperatures and powerful radiation fluxes) but it permits to realize ecologically pure technologies of production and utilization of technologies of production and utilization of various unique items for space equipment in particular.

As it has been determined by R.Aparisi in 1955 [1] any solar furnace is characterized by normal irradiancy distribution E(r) over focal spot plane which is described by the “error function” (Gaussian curve):

$$E(r)=\mathbf{E}(0)\exp(-\,\mathbf{C}r^2) \qquad (1)$$

where $\mathbf{E}(0)$ – maximum irradiancy (kW/sm$^2$) in solar furnace focus ($r = 0$);
E(r) – irradiancy at a distance r from the focus in focal spot plane;
**C**–measure of Gaussian “bell” width it characterizes the accuracy of concentrator mirror (sm$^{-2}$).

The knowledge of the irradiancy in solar furnace focal spot is necessary and sufficient for the calculation of temperature fields over samples surface and dept in solar furnace focus. Besides it permits to realize given conditions of investigation and technological processes parameters under extremal conditions[2].

Exactly for the determination of the parameters of irradiancy distribution over focal spot i.e. the couple of values **E**(0) and **C** the determination of solar furnaces energy characteristics is carried out. It is a laborious and continuable enough process requiring sunny summer weather certain equipment and first of all the availability of a calorimeter. The following various types of calorimeter are known: stationary calorimeter (flow calorimeter) in which the absorption of concentrated solar radiation takes place within a model of absorbute blackbody under stationary conditions and nonstationary calorimeters in which concentrated solar radiation is absorbed as a rule on a surface during short period. In addition, calorimeters can be subdivided into microcalorimeters with a detector of Φ 1-2 mm for detailed scanning all focal spot surface and “great” calorimeters (measuring integral characteristics) with the set of diaphragms the diameter of an inlet of which can be compared with the diameter of solar furnace focal spot.

Absolute flow calorimeters are the most used because they ensure the highest accuracy and reliability of the obtained result. But in contrast to microcalorimeters measuring point irradiancy values E(r) “great” calorimeters measure energy Q (kW) of incident concentrated solar radiation through diaphragm of radius $r_i$ (sm):

$$Q(r_i) = \pi\mathbf{E}(0)[1 - \exp(-\,\mathbf{C}r^2_i)]/\mathbf{C} \qquad (2)$$

This expression has been obtained by integrating point irradiancy distribution in focal spot plane $E(r)=\mathbf{E}(0)\exp(-\,\mathbf{C}r^2)$ over diaphragm area $F=\pi r^2$. It makes it possible to interpret experimental date obtained by “great” calorimeters with different diaphragms. The method for the measuring of solar furnaces energy characteristics mentioned in the [4,5] includes the measuring of the Q(r) by absolute flow-calorimeter with the use of superimposed diaphragms in number from one (Φ4 mm) up to four (Φ3; 6; 10 and 16,2 mm).

The analysis shows that statistic model of irradiancy distribution in focal plane (equations (1) and (2) mentioned above) include two unknown quantities **E**(0) and **C**. For their determination it is necessary and sufficient to solve the system of two equations with different coefficient values ($r_1$ and $Q_1$). For these coefficients determination it is necessary to carry out only to experiments with the use of two diaphragms with different inlets $r_1$:

$$\begin{cases} Q_1 = \pi\mathbf{E}(0)[1 - \exp(-\,\mathbf{C}r_1^2)]/\mathbf{C} \\ Q_2 = \pi\mathbf{E}(0)[1 - \exp(-\,\mathbf{C}r_2^2)]/\mathbf{C} \end{cases} \qquad (3)$$

The system of transcendental equations (3) in general case has no analytic solution i.e. it is impossible to obtain neither **E**(0) nor **C** in explicit form. Practically by the interpretation of the results of solar furnaces energy characteristics determination the step-figure $\overline{E}_i=f(r_i)$ is plotted on the basis of some measurements. Then by its approximation the certain estimation for the **E**(0) is determined graphically the accuracy of which is disputed enough. The value **C** in the [4,5] in this case they do not try even to determine although its knowledge also is necessary [2].

The detailed analysis of the system of equations (3) has shown that although in general case it analytically can not be solved correctly but for the $r_2 = r_1\sqrt{2}$ this system has correct particular solution:

$$\begin{aligned}&\mathbf{C} = r_1^{-2}\ln[Q_1/(Q_2 - Q_1)],\\ &\mathbf{E}(0) = Q_1^2C/[\pi(2Q_1 - Q_2)] \qquad (4)\end{aligned}$$

But precisely this relation of diaphragm openings practically was not used previously and in the published works the diaphragms set with arbitrary relation of inlets diameters was used. So the author has attempted to solve the system (3) approximately but in general case i.e. for any arbitrary relation of the diameters $r_1$ and $r_2$. On the basis of this solution obtained in analytic form the new method for the determination of solar furnaces energy characteristics has been developed and inventor's application "method of two calorimeters" has been submitted. Positive decision of the "Ukrpatent" is already received.

The patented method permits to find correctly enough the pair of the unknowns **E**(0) and **C** by the determination of solar furnace energy characteristics being carried out for any relation of the inlets of two calorimeter diaphragms. Moreover the obtained solution permits to calculate the unknown solar furnace parameters by long ago published experimental data. As an example it is possible to use the results of the measurements of solar furnace energy characteristics ($\mathbf{E}(0) \approx 4300$ kcal/m$^2$s) carried out of the SGY characteristics we shall use the experimental data obtained with the diaphragms of Φ6 and 10 mm ( $\overline{E}_i$ is 3930 and 2590 kcal/m$^2$s correspondingly). The calculation data are the following: **C**= 6,26sm$^{-2}$, **E**(0)= 5140 kcal/m$^2$s. So, the error of graphical approximation here is about 20% and it is unacceptable.

On the basis of the result for the **E**(0) obtained by the graphical approximation of step-figure the authors [4] have attempted to estimate integral reflection coefficient of the SGY concentrator ($A_3$) by the formula of P.Duves [6] (obtained within the limits of determinated model) and have obtained the value $R_3 = 0{,}682$. Analogous characteristic but within the limits of statistic model can be obtained by expressing the **C** and **E**(0) in terms of the mirror characteristics:

$$\begin{cases}\mathbf{C} = (180/\pi)^2(1 + \cos U)^2(h/p)^2\\ \mathbf{E}(0) = (180/\pi)^2E_oR\,h^2\sin^2U\end{cases} \qquad (5)$$

By solving this system we can express the values of integral reflection coefficient of the mirror $R_3$ and of the accuracy parameter of the concentrator h (grad$^{-1}$) in term of values **C** and **E**(0):

$$\begin{aligned}&R_3 = [(1 + \cos U)/\sin U]^2\mathbf{E}(0)/\mathbf{C}E_op^2,\\ &h = (\pi/180)p\sqrt{\mathbf{C}}/(1 + \cos U). \qquad (6)\end{aligned}$$

Substituting the values of the **C** and **E**(0) obtained above into the mentioned formulae we shall obtain the following values: $R_3 = 0{,}920$ and $h = 3{,}78$. In this case the $R_3$ distinguishes considerably from the value obtained by the formula of P.Duves. And the value h is close to the value obtained by R.Aparisi (h = 4) [6].

So in the given work the elements of solar furnaces theory, the methods of their energy parameters determination and also the questions of the determination of concentrators mirrors characteristics.

## REFERENCE:

1. Р.Р.Априси. Концентрация солнечной энергии в гелиотехнических сооружениях. Автореферат кагд. дисс. ЭНИН, М., 1955.
2. В.И.Зискин, В.В.Пасичный, А.В.Чоба. Аналитическое определение параметров термической обработки поверхности материала концентрированной солнечной энергией // Гелиотехника, 1986, №6, , с.34-37.
3. Р.А.Захидов и др. Технология и испытания гелиотехнических концентрирующих систем. Изд. «ФАН» Узб. ССР, Ташкент, 1978.
4. В.С.Дверняков и В.В.Пасичный. Определение паваметров специальной гелиоустановки (СГУ), предназначенной для исследований тугоплавких материалов//Доклады АН УССР, Киев, 1966, №6, с. 762-766.
5. В.В.Пасичный, В.С.Дверняков и др. Исследование характеристик теплового разрушения материалов при интенсивном радиационном нагреве// ИФЖ, 1977, с.65-69.
6. Солнечные высокотемпературные печи// Сб. под ред. В.А.Баума, ИЛ, М., 1960.

# DIELECTRIC COMPOSITES FOR APPLICATION UNDER CONDITIONS OF GLOWING DISCHARGE

**Zdolnik S.N., Petrovsky V.Ya.**
Fransevech Institute for Problems of Materials Science of National Academy of Science of Ukraine,
3 Krzhyzhanovsky St., Kiev, 03142, Ukraine,E-mail: Petrovsk@materials.kiev.ua

The up-to day lasers are able to produce pulsating and continuous flows differing in intensities and wave lengths. This opens a high opportunity for use of lasers in various applications of human activity including technologic ones.

The difference in pumping mode of lasers is due to a great variety of requirements to be met by the laser characteristics to suit specific applications.

To solve such problems of processing like cutting and welding of thick steel sheets, surface hardening, melting and alloying of large-shaped parts, gas discharging lasers are used, which produce the utmost power in the beam. Nevertheless, just the gas-discharging laser operates under the mostly severe-duties in respect to its constituting material because of a simultaneous effect of several factors, i.e. ablation, high electrical field and temperature exposure.

The cathode of a $CO_2$ laser gas-discharging camera is a functional component, emitting electrode of which is inserted into a casing of corrosion-resistance heat conductive electrical insulation.

While operating, a cold mixture is fed and a glow discharge is igniting over the cathode region during the mixture passing, and the temperature then rises up to 500 °C upon the cathode surface. An important role is given to the insulation, which should allow any electrical contact between two rows of neighboring cathodes, and to ensure operation of the electric unit under the following extreme conditions.

1. Mechanical loading effect induced by stressing during thermal cycling.
2. Electrical glow discharge (high voltage of 5-7 kV)
3. Current of near 100 mA/cm$^2$.

Silicon nitride proved to be the most useful material among a lot of materials able to function under these conditions, such as MgO, $Al_2O_3$, $Si_3N_4$, $ZrO_2$, BN, AlN, BeO. Hot pressed ceramics based on silicon nitride features a good combination of properties [1].

However, the arc resistance of silicon nitride based materials is not investigated and its thermal conductivity may vary within a broad range of 2 to 128 W/(m.K) [2].

Earlier [3], the effect of pressing temperature on the properties of hot-pressed silicon nitride dielectric materials was studied and the loss factor at the 1 kHz frequency may be used as criterion for qualifying silicon nitride-based dielectric materials.

In this work, we study the change in the microstructure of dielectric composites in relation to their mechanical and electrical properties.

The results of investigations are summarized in Table.

We found three structural states of the materials under study:

| № | Content, % | | | $T_{fl}$, °C | $T_{sl}$, °C | ΔΘ,° | λ, W/m K | $K_{1c}$, MN/m$^{1/2}$ | $H_v$, GPa | F=1 kHz | |
|---|---|---|---|---|---|---|---|---|---|---|---|
| | $Si_3N_4$ | $Al_2O_3$ | $TiO_2$ | | | | | | | ε | tgδ*10$^2$ |
| 1 | 91,53 | 5,43 | 3,04 | 1650 | 1660 | -5 | 50 | 6,5 | 13,8 | 11,15 | 1 |
| 2 | 84,39 | 12,57 | 3,04 | 1715 | 1725 | 10 | 53 | 6,1 | 14,9 | 11,2 | 2 |
| 3 | 82,61 | 5,43 | 11,96 | 1660 | 1660 | 0 | 47 | 6,4 | 14,3 | 14 | 2 |
| 4 | 75,47 | 12,57 | 11,96 | 1665 | 1665 | 0 | 50 | 6,4 | 12,5 | 20 | 2 |

1. At a certain temperature, a grain-boundary liquid is formed, which begins immediately to solidify with a rather great wetting angle (35°) of the main substance by the liquid, and this angle reduces during the time this liquid exists (Fig. 1a).

2. The liquid formed at high temperature exists for some time period, and the wetting angle increases (Fig. 1b).

3. The liquid when formed chemically reacts with the main phase to end immediately in solidification (Fig. 1c).

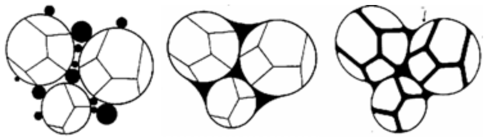
a b c

Fig. 1. Schematic representation of the microstructures of the materials under study

The first state characterizes by the formation of $SiO_2$-$TiO_2$ eutectics, the melting temperature of which is 1540 °C on the neutral substrate. As to our opinion, in a low-reduction medium proper for hot pressing, the melting temperature of this eutectics shifts to the high-temperature direction by near 100 ° on the $Si_3N_4$ crystal surface.

For the second state, the formation of $Al_2O_3 – TiO_2$ eutectics is rather probable, which melts at 1720 ° C on the neutral substrate.

The last state features formation of the $SiO_2$ melt, which solidifies immediately because of high-melting components dissolved in it.

All these processes are directly associated with pressure and temperature. In the first case, when the pressure and temperature show the same rate of rising, the particles were in the state of coagulation contact in the moment of liquid formation, and if the system solidifies in this moment, the fine-grained state retains, which shall feature a low hardness and heat conductivity, but a high value of crack resistance (Table, Spec.1). The value of loss factor is minimal within the whole frequency range (Fig. 2).

In case there is no liquid at first of compaction and then the processes of dissolution-precipitation occur at a constant temperature and pressure, followed with the hardening of crystallization contact, this results in an increasing of hardness and heat conductivity, but crack resistance decreased (Table, Spec. 2). The value of the lossd factor increases at the frequency of 1 kHz.

Specimens sintered without the liquid use (Table, Specs 3,4) exhibit low mechanical properties and low heat conductivity. The loss factor is high all over the frequency range.

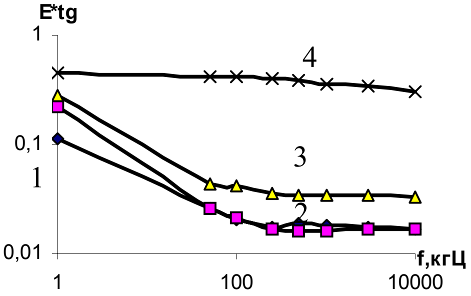

Fig. 2. Loss factor as function of frequency (the number of curves correspond to the numbers of specimens given in Table)

The tests of arc-resistance of dielectric materials showed that the first arcs appeared at the current of 70 mA/cm$^2$ (Specs 3, 4). Maximum currents of 220 mA/cm$^2$ are possible (Spec.1), however, the durability of items reduces at these currents. Therefore, the current of 100 mA/cm$^2$ shall be working current for the modules of given type, demonstrating a durable glowing discharge (Spec. 2).

In conclusion, the work done yielded a high performance dielectric composite able for operation under glowing discharge conditions, which used $Al_2O_3$ as activator and $TiO_2$ as modifying agent at the 4:1 ratio.

1. L.G. Podobeda - Powder metallurgy, 1979, № 1, p. 75-80.

2. V.Ya. Petrovsky, A.A.Kasiyanenko, L.I. Molochaeva - In collection of the scientific works. New powder materials and technologies in machine-building. - Kiev: IPM NASU, 1988, p.129-134.

3. G.G.Gnesin, V.M.Kirilenko, V.Ya. Petrovsky. - Powder metallurgy 1982, № 3, p. 53 - 59.

# INVESTIGATION OF POSSIBILITY TO USE THE CONCENTRATED SOLAR RADIATION FOR SURFACE AND SOLID PARTIAL MELTING OF BASALT, OBTAINING FIBRES AND CUTTING ARTICLES OF THEM

**Pasichny V.V., Sergeev V.P., Lykhodid S.I., Yastchenko O.M.**
Frantsevich's Institute for Problems of Materials Science (IPMS), National Academy of Science
3, str. Krzhizhanovsky, 03142, Kyiv, Ukraine; e-mail: pasich@ipms.kiev.ua

The problem of saving and using new renewable energy sources year after year becomes to be more and more actual. One of the promising ways to use solar radiation is its concentration and the following realization of various technological processes without intermediate transformation of solar energy into electricity. This way can be especially efficient in the regions, which are remote from traditional energy sources but have great solar potential and are abundant in row materials being fit for useful utilization. So, for example in some equatorial countries there are many islands of volcanic origin with rich reserves of basalt and other mineral raw materials fit for manufacturing products and articles of them by melting or thermal treatment.

In the IPMS during many years both integral developments of the processes for obtaining various basalt fibres and articles of them and the investigations of the possibility to use concentrated solar radiation (solar furnaces) for realizing high-temperature technological processes.

In the given work some preliminary results are represented which concern the investigation of the possibility to use solar furnace for surface melting of monolithic basalt , its remelting, fibres stretching out of a melt, thermal cutting articles made of basalt fibres.

Earlier some results of investigations had been published which concern surface melting of monolithic basalt in a solar furnace. It had been shown that grey plain surface of basalt gained fine colour of black glaze [1]. It makes it possible to recommend tiles and blocks of partially melted basalt as a facing construction material for walls of houses, monuments, mosaic panels and so on. The possibility is studied to manufacture glazed tiles made out of basalt aggregates. In contrast to monolithic basalt of high thermal stability the tiles made of aggregates containing 30-40% of melted product require gradual cooling at final stage as overwhelming majority of glass articles do [1].

The technology for obtaining basalt fibres in solar furnaces would be of practical interest. Preliminary experiments have been carried out on the installation SGU-4 with the concentrator of ∅2,0 m. The crucible made of the alloy based on chromium had the hole simulating a die in lower part. It was located in the concentrator focal zone in the way when its bottom and body were irradiated by light flux i.e. with the defocusing in the mirror direction. After basalt aggregates melting in the crucible which was demonstrated by the appearance of melt drop in the die hole the fibre was stretched with small glass stick by hand. The obtained fibres length was not above 1,5-2,0 m their diameter changed depending upon stretching rate from 30 up to 250 mkm. The experiments were carried out with the use of any available raw material without the analysis and some kind of extra blending. In this case high quality of continuous fibres is out of the question although the possibility of their obtaining in solar furnaces is proved in principle. The necessity of strict control of the stability of the melt given working temperature will cause very serious complication of production technique. In the same time the possibility of preliminary (preparatory) melt of raw basalt is quit possible close enough to place of its mining with purifying from low-melting and evaporable contaminating admixtures and extra blending initial mixture if necessary and manufacturing blanks being suitable for following transportation and use under industrial conditions. The process being more profitable economically is not excepted when the melt prepared in solar furnace is poured into additional reservoir the temperature in which is stabilized at necessary level by separate electric system. The reservoir volume can be small relatively which makes it possible to minimize the expenditures of traditional energy sources.

In the given work the possibility of cutting articles made of basalt fibres by concentrated radiation was investigated also. The necessity of such technology is in the possibility to avoid the destruction of cutting edges due to their partial melting and also article deformation being observed by mechanical cutting. Diminishing of hard alloy cutting tools consumption could be another advantage of cutting by concentrated radiation.

The following kinds of articles have been selected as subjects of inquiry:

1) The tight pack sheet of 3 mm thickness;
2) The cotton type lightweight sheet of 10 mm in free state and about 1 mm - in compression;
3) The ply of 4-5 mm thickness.

The experiments were carried out on the installation YCC-1 as solar furnace simulator. It's based on arc Xe-lamp of 3 KW and ellipsoidal mirror concentrator. Heating of samples was carried out directly in the concentrator focal plane by irradiancy 240 W/cm$^2$. Cutting was realized by moving samples over focal spot as the through cut was forming. Sample transport was manual. Duration of the experiments $\boldsymbol{t}$ was fixed by a stopwatch. Cutting rate $\boldsymbol{V_c}$ was calculated by the formula: $\boldsymbol{V_c = L_c \cdot t}$ , where $\boldsymbol{L_c}$ - length of a cut. Not less than three samples of every type of materials were tested.

The articles of all the three types were easily cut instantly after radiant heating start. In this case the drops black glasslike melt was formed on cut surface. Their size and number increased as material density increased. Cut surface changed its colouring for darker one (the samples 1 and 3) or light brown one (the sample 2). For all the samples the zone of thermal influence (ZTI) became apparent clearly in the form of temper colours on the side being heated mainly. The cut cross-sections has wedge-shaped profile. It is caused first of all by irradiancy distribution in focal zone, angle aperture of mirror concentrator and in certain degree by the nature of thermal processes and phase transformations within a material. The process of the samples № 3 heating and cutting besides basalt fibres melting was accompanied by slight burning and smoke generation obviously due to the burnout of an organic component. The experiments main results are represented in the Table.

TABLE. Results of experiments on cutting.

| Sample № | Irradiancy W/cm$^2$ | Cutting rate, mm/s | Width of cut, mm | ZTI, Mm |
|---|---|---|---|---|
| 1 | 240 | 4,4±0,1 | 2,5±1 | 7,0 |
| 2 | 240 | 5,6±0,4 | 3,0±0,5 | 7,0 |
| 3 | 240 | 5,2±0,5 | 3,0±1,5 | 7,0 |

The obtained experimental data confirm the possibility of principle to cut sheet articles made of basalt fibres by concentrated radiation. Cutting rate of tested samples was within the limits of 15-20 m/h. It can be increased essentially because the weakest operating conditions of the arc lamp were used in the experiments.

The carried out experiments and their results do not claim to information completeness concerning the affected problems but make it possible, on the authors opinion, to draw a conclusion, that there are rather potentialities to realize high-temperature technological processes connected with basalt on the basis of using renewable ecologically pure solar energy.

1. Pasichny V.V., Berezhetskaya V.Ya. Surface thermotreatment of facing and other materials by concentrated solar energy// Journal of Engineering Physics and Thermophysics.- 2001.- Vol. 74, № 6.- P. 143-145.

# PERFORATED STEEL PROFILES ON THE BASE OF INDUSTRIAL WASTES

**Mironov V., Serdjuk D., Muktepavela F.(1)**
Riga Technical University, Azenes 20-331, Riga, LV10-48, Latvia, e-mail: mironovs@bf.rtu.lv
(1)Institute of Solid State Physics, University of Latvia
Kengaraga 8, Riga, LV-1063, Latvia,
e-mail: famuk@latnet.lv

Full scale utilization of structural materials is one of the most significant problems in the modern building. There are few ways to solve the problem. Repeated using of industrial wastes is one of the possible ways to increase the effectiveness of structural materials applications.

There are a number of industrial enterprises in Latvia and neighbouring states, which consider industrial wastes as the potential objects for recycling. Currently only Daugavpils driving chain factory (Latvia) has approximately 100 tons of perforated steel band each months. [1] In the given work are shown examples of use of these waste products.

The perforated steel bands, which are industrial wastes of the driving chain manufacturing process of the Daugavpils driving chain factory, differ by their widths, shapes and dimensions of the holes, so as the grades of steel. Main geometrical characteristics for all types of perforated steel band are given in the table 1.

Main geometrical characteristics of perforated steel band

Table 1.

| Type of perforated steel band | Grade of steel | Thickness x widths, mm |
|---|---|---|
| 1 | Ст 08 пс,GOST 503-81 | 1,25 x 93 |
| 2 | Ст 08 пс,GOST 503-81 | 1,05 x 83 |
| 3 | Ст 08 пс,GOST 503-81 | 1,5 x 80 |
| 4 | Ст 08 пс,GOST 503-81 | 1,7 x 80 |
| 5 | Ст 08 пс,GOST 503-81 | 1,9 x 73 |
| 6 | Ст 50 пс,GOST 2284-79 | 1,05 x 110 |
| 7 | Ст 50 пс,GOST 2284-79 | 1,3 x 80 |
| 8 | Ст 50 пс,GOST 2284-79 | 1,6 x 90 |
| 9 | Ст 50 пс,GOST 2284-79 | 1,75 x 75 |
| 10 | Ст 50 пс,GOST 2284-79 | 1,9 x 83 |
| 11 | Ст 50 пс,GOST 2284-79 | 2,4 x 50 |
| 12 | Ст 50 пс,GOST 2284-79 | 3,1 x 42 |
| 13 | Ст 50 пс,GOST 2284-79 | 3,5 x 52 |

Samples different types of bands were tested for tension and hardness using standard Brinell method at loads of 50 N and 300 N. Test results demonstrated, that ultimate strength is from 830 to 1030 MPa and Brinell hardness is from 830MPa to 3030 MPa.

One sample was zinc plated. Plating thickness was of h=30-40 mkm. Testing of hardness on many areas and at different loads demonstrated retaining of initial hardness of HB=1060-1200 MPa.

Measurements of micro-hardness were made using micro hardness meter of ПМТ-3 type with precise loading device allowing application of loads within the range from 0,3g to 200 g. [2] Such layer-by-layer plting control provides not only plating micro hardness evaluation, but quality of plating bonding with the base, as well (Fig. 1).

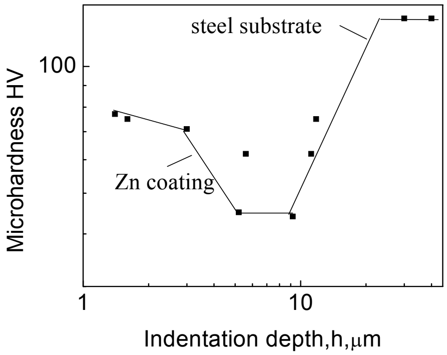

Fig.1. Microhardness as a function of indentation depth for Zn coating on steel substrate.

Several types of perforated steel profiles, which are considered as structural elements, are shown on Fig. 2. The perforated steel profiles are produced by the technology, which is described in the work [3].

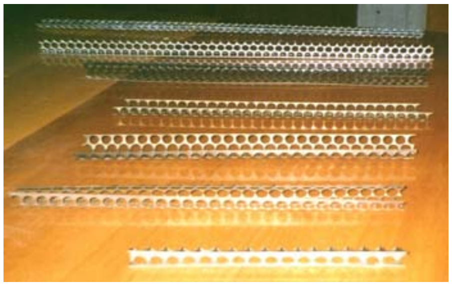

Fig.2. Profiles for finishing works on the base of perforated steel band

Perforated angle, channel and double-T profiles have the best opportunities for vast application.

Angle profiles using for plastering works is one of them. Big strength and rigidity of the profiles add increased resistance for separate layer. Joint of ceiling strengthening, which enables to carry heating installation in the design position is other example of angle profiles using (Fig. 3).

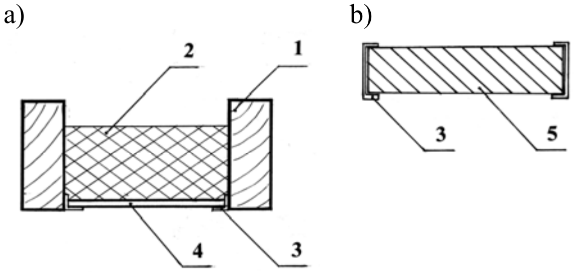
a)
b)

Fig.3 Probable ways of perforated steel profiles application:
a) - for ceiling structures, b) - for partitions; 1 - timber beam, 2 - heating instolation, 3 - perforated steel profile, 4 - plywood sheet, 5 - partition structure.

Perforated steel band could also be used as load bearing elements of several types of structures. Profiling and welding enables to obtain C, U, Z, T and double-T shape profiles, which could be utilized as elements of moulds for producing of reinforced concrete elements (Fig. 4), fences and other light weight structures.

Several types of perforated steel band also are suitable as reinforcement for reinforced concrete panels and beams [4]. Probability of perforated steel band using as reinforcing elements was checked by the practice.

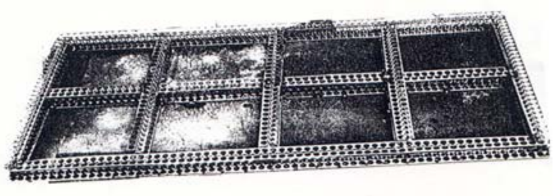

Fig.4. Element of mould for producing of reinforced concrete elements.

Reinforcement of masonry is simple and effective application of perforated steel band (Fig. 5).

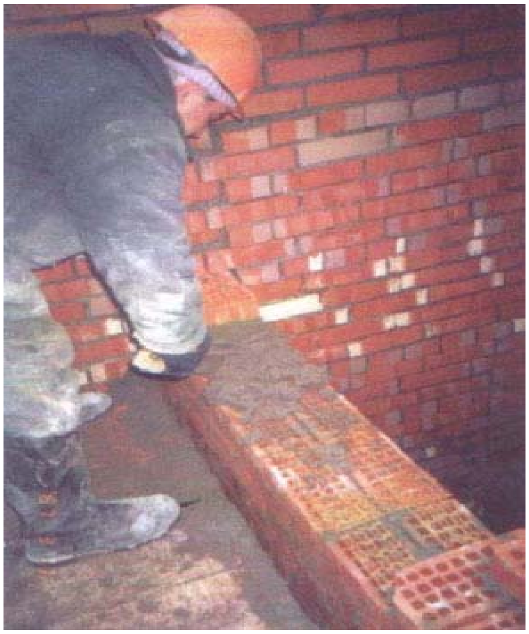

Fig. 5. Using of perforated steel band as reinforcement:

Profiles with the C and U shape on the base of perforated steel band also could be used as channels for the power cables.

## References

1. Mironov V., Serdjuk D. "Perforated Steel Band as a Constructional Material" // In: Proc. of Riga Technical University: Architecture and constructional science, 2003 p.157 – 162.
2. Manika, F. Muktepavela. Microhardness and adhesion of TiN/AlN multilayer coatings. // Surface&Coatings Technology, 1998, 100-101,p. 333-337.
3. K. Bogojavlenskij, A. Neubauer, V.W. Ris. Technologie der Fertigung von Leichtbau-profilen. / VEB Deutcher Verlag für Grund toffindustrie, Leipzig.-1978.
4. V. Mironov, I. Legalov, F. Kadysh, Working reinforcement. Russian pat. N9459, 16.03.1999

# SURFACE STRUCTURE OF COPPER ELECTRODEPOSITED IN MAGNETIC FIELD

**Silantiev V.I., Bondar E.A., Bondarkova G.V.**
Institute of Magnetism NAS of Ukraine,
36-b Vernadsky blvd., Kyiv, 03142, Ukraine; e-mail: atc@usuft.kiev.ua

The application of an external magnetic field during electrodeposition causes the variations of the process and so affects the morphology of the obtained depositions.

A study of the structure of electrodeposits depending on magnetic fields of relatively low values is of particular interest because of the opportunity to control the morphology of deposits.

In the work a thermostatically controlled electrolytic quartz cell with dimensions 30 sm in diameter and 30 sm in height was used. It was placed in the gap of the electromagnet, which produced a magnetic field strength up to 0.35 T. Constant-voltage power supply was used for the electromagnet. An electrolyte contains 150 g/l cupric sulfate and 50 g/l sulfuric acid.

The cathodic conditions were measured with regard to a chlorine-silver electrode. Polarization curves were taken in the voltage-dynamic mode and recorded with X-Y plotter. The rate of electrode potential change was about 0.2 V/c. The observations of the electrolyte flows were carried out with an optical microscope.

The structure of electrodeposits was studied with scanning electron (SEM) and scanning tunneling (STM) microscopes combined in РЭМТ-100 device.

In the absence of a magnetic field polarization curves were typical with well-defined regions of electrochemical, combined and diffusion kinetics. An application of a magnetic field of relatively low values (0.03 T) results in development of electrochemical and combined kinetics regions along with increasing of limiting currents [1]. The further increasing of a magnetic field flux density causes the more essential shift of polarization curves especially in the case of the perpendicular orientation of the magnetic field with respect to the electrodes (Fig.1). The effect arises from the thinning of the diffusion layer at the cathode due to the strong flows in electrolytic cell. The flow velocity increases with increase in magnetic field strength.

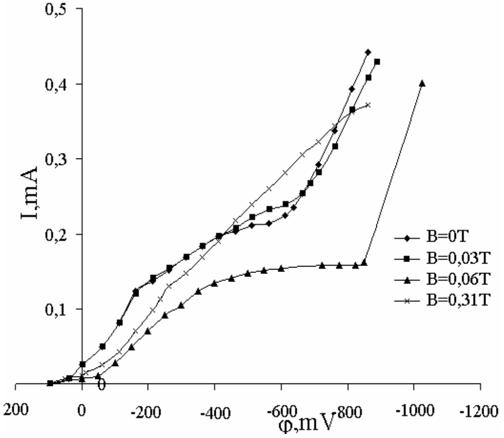

Fig.1.

The structures of electrodeposits for three typical regions of the cathode polarization curves (electrochemical, combined and diffusion kinetics) have been studied. The most distinctions in the structures were observed in the regions of diffusion kinetics with the high cathodic conditions. Thus, in the absence of a magnetic field the structures of electrodeposits was bush-shaped with branches made of dendrites (Fig.2), which grew in all directions from the cathode with equal probability. In the magnetic field of 0.13 T with the parallel orientation to the cathode faces (Fig.3) the deposits were formed by the compact complicated in shape particles uniformly distributed on the surface with branched dendrites preferentially directed along the surface of the cathode. In accordance with the present conceptions one could tell about the predominance of metal ions delivery rate along the longitudinal direction as compared with transverse one. In other words, it is expected magnetohydrodynamic flows directed along the cathode surface arise in electrolyte and set the direction of dendrite growth.

Increase of the magnetic field flux density up to 0.25 T causes the essential change of the deposit structure (Fig.4). Unlike two previous cases here "bushes" of dendrites are formed from unions of round-shaped particles with fairly compact packing. These peculiarities can be explained by the change of the surface cathodic condition during the electrodeposition. Thus, at the beginning of the process the value of the surface potential was 800 mV, in 20 seconds – 630 mV, and in the following 20 seconds it decreased to 600 mV. That indicates the process moving to the region of combined kinetics, i.e. to the uniform growth in all directions and as the result the formation of the spherical particles on branch fringes.

As a magnetic field of 0.25 T applied transversely to the electrode faces dendrite structure of deposits was observed (Fig.5), but the number of "bushes" per unit area was substantially smaller than in the first three cases. Dendrites had anisotropic structure. The branches of dendrites were formed by needle-shaped particles just as in the case of the absence of a magnetic field, but the number of "bush" branches was noticeably smaller.

So, the structure of copper deposits at the constant composition (concentration) of electrolyte is different depending on the value and configuration of a magnetic field. It can be explained by the concentration change of electrolyte at the electrodes under the action of magnetohydrodynamic forces. The obtained results can be used in a powder metallurgy for producing powders of different bulk weigh, dispersity and microstructure.

References

1. Gorobets Yu.I., Bondar E.A., Silantiev V.I., Bondarkova G.V. // Magnetic field on micro- and nanostracture of copper electrodeposits. ICFM-2003, Crimea.
2. Левин А.И. Электрохимия цветных металлов / М.:Металлургия, 1982, 256 с.

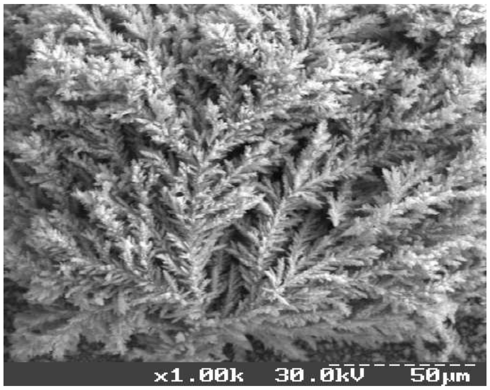

Fig.2.

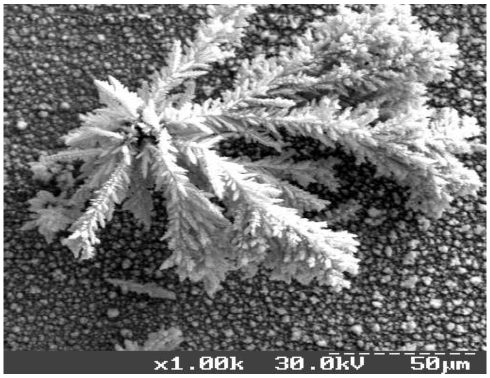

**Fig.3.**

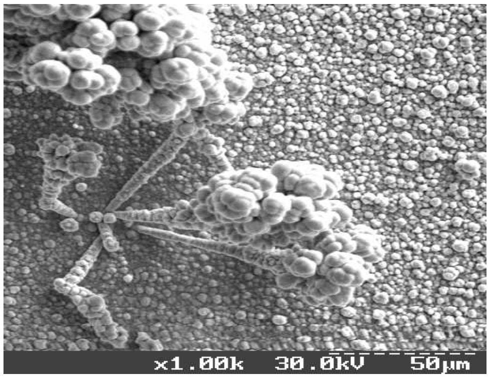

**Fig.4.**

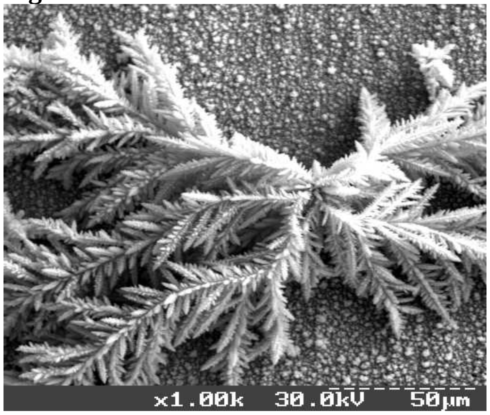

**Fig.5.**

# CREATION SYSTEMS OF TECHNOLOGY-ECOLOGICAL MONITORING OF RECYCLING OF INDUSTRIAL WASTES

**Bezruk Z.D., Viznuk A.A., Primisky V.F.**
State Department of Ecology and Natural Resources,. Kiev, street. Turovskaya, 28.
Ukrainian SRI of Analytical Instrument Making - "Ukranalyt"
Kiev, street. Tverskaja, 6, Email: ukr@analit.relc.com

By basis functioning of many industrial and power technologies, including the recycling (burning) of industrial wastes, are material and thermal balances, which underlie on the basis of industrial process, which transform raw material into ready production. In another turn algorithm of transformation is defined by technical characteristics of process by: temperature, pressure, quality of raw material, duration of process, which at realisation of a work cycle are adjusted by the operator or automatically. Because between parameters of technological process and completeness of processing (combustion) of raw material in a final product, there is a complex interrelation, which is defined by theoretical laws[1].

Smoke (industrial) gases, which arise in a consequence of passages of technological processes on processing raw material, also are a product, and thus there are laws of their formation. Having defined these laws for each concrete production process, we shall have an opportunity to calculate emissions of smoke gases on the current technological parameters of work of the industrial enterprise. Such parametrical ecological systems of monitoring (PESM) have appeared at the beginning, when there were problems of the control pollution of an atmosphere by industrial gases. Basis work of PESM are the mathematical models of sources of emissions, which calculate the concentration of smoke gases and their levels of emissions depending on parameters of technological processes, which is controlled by the appropriate sensor controls of technological process (pressure, expense, temperature). Thus mathematical model represents virtual replacement of real measuring process of level of emissions of smoke gases. The data, necessary for accounts, get out of existing control systems of production. Effective work of (PESM) is possible only at presence of the appropriate software. For work of PESM calculated thermal and material balances, which underlie functioning a production cycle.

Such calculation PSEM function on the majority of the enterprises of Ukraine. On the basis of their work at the industrial enterprises there were items of information on extreme allowable emissions (EAE) of toxic gases and are made the appropriate ecological payments.

However in course of time, particular last years, the deterioration of the basic industrial infrastructure has resulted that the majority of technological processes have those or other deviations from designed value. Often change of raw base, the different kinds of energy resources, idle time, absence duly regulate and repair work also influence of technological processes. All this results that the calculate mathematical models of productions can not already adequately display work cycles and the application results them for account of emissions of industrial gases in significant errors, which in turn results in a unreasonable level of ecological payments for the enterprises.

Legislator in 2000 year has brought in respective alterations to the basic nature protection laws « About protection of an environment » and « About protection of atmospheric air », in which is precisely stipulated, that the levels of emissions are defined by results of measurement « of actual emissions ».

Thus on replacement of parametrical model of ecological monitoring there comes gas analytical system of ecological monitoring (GSEM).

Most typical (GSEM) consists of a complete set automatic stationary gas analyzers for measurement of concentration (Ci) of smoke gases (CO, $SO_2$, NOx,, CH, dust) with system of selection and preparation of test, sensor-measuring of temperature, pressure and other parameters of smoke flow.

Important compound of GSEM is outlay meter of smoke flow , fig. 1.

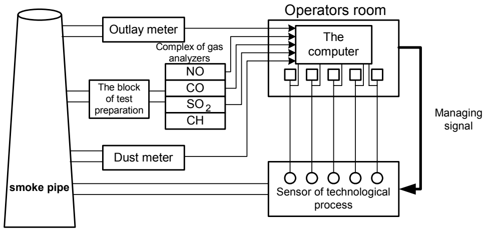

Fig. 1 Gas analytical system of ecological monitoring.

Such systems have found the greatest distribution in Western Europe, USA and Japan (western classification of such systems - CEMS).

It is necessary to notice, that in the majority of the countries is regulated not concentration of smoke gases, but mass emissions of these gases. Therefore presence in structure of GSEM outlay meter is necessary, as well as presence of the appropriate software to computers.

The application of GSEM only for ecological monitoring of emissions of smoke gases results in additional financial expenses of the enterprises and deterioration of their economic condition.

Therefore urgent there is a question of development and creation such GSEM, which have the extended functionality's, for example at the expense of creation of two-level hierarchy functioning.

To a level of ecological monitoring the level of technological monitoring of smoke gases increases which arise during technological processes and appropriate management of these processes by results of technological monitoring.

Thus the technological process is optimized, the consumption of raw material and energy resources is reduced, the economic parameters of the enterprises are improved. Joint-stock company «Ukranalyt » has developed and introduced in commercial operation for power objects multistage system of ecological and technological monitoring and optimization of processes of burning with application newest gas analytical sensor and computer processing of the information. [2,3,4].

The first level consists of system of technological monitoring (STM), automatically measures the concentration of CO (0-10 %), $CO_2$ (0-20 %), $CH_4$ (0-1 %),
$O_2$ (0-20 %) in a technological cycle. The measurement of oxygen is carried out by the high-temperature gauge on $ZiO_2$ in a zone of burning, and for measurement CO,$CO_2$, $CH_4$ is used multichannel infra-red gas analyzer.

The next level consists of system of ecological monitoring (SEM ), measures concentration of smole gas in out pipe, after a filtration and clearing. With the help specialized multichannel gas analyzer is measured the concentration CO (0-0,4g/$m^3$), NO (0-5g/$m^3$), $SO_2$ (0-0,5g/$m^3$), $NO_2$ (0-0,6g/$m^3$).

All measuring information with (SEM) and (STM) is processed with the help of the microprocessor device.

The system has passed state meteorological certification and has allowed to improve technological and ecological parameters.

**The list of used literature:**

1.Приміський В.П. Багатоканальний газоаналітичний комплекс для оптимізації процесу горіння і екологічного моніторингу сміттєспалювального виробництва. Вісник НТУУ "КПІ" Приладобудування № 24, 2002.-с. 93-98.

2.Патент України 65505А Газоаналітичний технологічний комплекс з мікропроцесорною системою /Безрук З.Д., Дашковський О.А.,Приміський В.П., і інші. Опубл. 2004. Бюл. № 3

3.Патент України 64586 А Еколого-технологічний газоаналітичний комплекс /Бородавка В.П., Дашковський О.А., Приміський В.П. і інші-2004 -Бюл.№2.

4.Патент України 58419А Багатоканальний газоаналітичний технологічний комплекс /Дашковський О.А., Воробйов С.С., Приміський В.П., і інші-2003-Бюл.№7.

# LIST OF PARTICIPANTS

**A**

Abraimov N.V. —145, 354
Adeeva L.I. —435
Afanasyeva V.P. —270
Akylbaev Gh.S. —367
Alexeev M.K. —240
Alexenko E.N. —458
Alfintseva R.A. —305, 381
Andreeva A.F. —152, 177, 479
Andrievskaya E. R. —11, 125
Antsiferov V.N. —165, 407, 470
Apininskaya L.M. —154
Apuhtin V.V. —84
Arinkin S.M. —135, 159
Artamonov I. —76
Artemyev V.P. —70
Askhadullin R.Sh. —244
Astakhov E.A. —433 435, 437

**B**

Babich M.G. —397, 415
Babich N.G. —272
Babutina T.E. —560
Bakulin V.N. —16
Baranov V. —10, 532
Baranova T.F. —197
Barmak K. —94, 98
Barschevskya A.K. —233
Barykin N.P. —383
Bashkarev A.Ja. —365
Bednarska L.M. —336
Belots`ky A.V. —266
Belotserkovets I.S. —14
Belous M.V. —409
Belous V.A. —167, 186
Belyanin A. —133
Beresnev V.M. —352
Berezanskaya V.I. —484
Bescorsiy A.P. —552
Besov A.V. —439
Bespalyy A.A. —84
Bezimyanniy Y.G. —257, 282
Bezruk Z.D. —572
Bezymyanniy Y.G.—298
Bieloborodova E.A. —44
Bilousov M.M. 190
Bloschanevich A.M. —47, 280
Bogatchev E.A. —146
Bogdanov M.V. —78, 80, 122
Bogomol Yu.I. —34
Boitsov O. —468
Bolotova L.K. —227
Bondar E.A. —570
Bondar Yu.V. —479
Bondarenko N.A. —36, 61
Bondarenko T.N. —313
Bondarkova G.V. —570
Borisov Yu.S. —21, 433, 437
Borisova A.L. —21, 433, 437
Borovik D.V. —231
Borovik V.G. —231
Borovinskaya I.P. —180, 182, 188
Borsch E.B. —354
Borysovska K.M. —463
Brakhnov N.V. —484
Bratanich T.I. —274
Brinkiene K. —387
Brodnikovsky N.P. —305, 379
Bronovets M. —535
Brusilovets A. —201
Buchakov S. —491
Budzinska V.L. —556
Bunchuk Y.P. —169
Burka M. P. —294
Burtseva T.A. —493
Burya A.L. —49
Bushmin B.V. —525
Buzhenets E.I. —302
Byakova A.V. —266, 276, 369
Bykov A.I. —207
Bykov Yu.G. —137

**C**

Cesniene J. —387, 389
Ciric R. —539
Chalov A.A. —70
Chemerkina M.V. —421
Chemerys V.T. —96
Chermensky V.I. —337, 477
Cherneko N.M. —9
Chernenko L.I. —314
Chernigovtsev E.P. —192
Chernyayeva O. —425
Chernyshev L. —468
Chernyshov G. —166
Chernyshova T.A. —166, 227, 475
Chevichelova T.M. —309
Chevykalova L.A. —180, 244
Chivanov A.V. —421
Chmeljuk N.D. —316
Chunadra A.G. —352
Churilov G. —255
Cooper R. —482
Cvirkun S. —360

**D**

D'jachenko O.P. —197, 241
Dahan I. —355
Dan'ko S.V. —280, 512
Daniel Leo —65
DarchiashviliM.D. —375
Dariel M. —355
Darsavelidze G.Sh. —375
Dashunin N.V. —429
Davidchuk N.K. —288
Deev B.B. —187
Dekhteruk V.I. —339
Dellith Jh. —140
Demchenko L.D. —441
Demechev V. —205
Demichev V. —209
Demidik A.N. —294
Demina S.E. —80
Denbsky Yu.V. —490
Derenovska N.A. —328
Derev'yanko O.V. —369
Derinovskaya N.A. —174
Dezider'yev S.G. —534
Dlugunovich V.A. —229
Dolgov N.A. —439
Dolgykh V.Y. —391
Dotsenko N.M. —21
Dovydenkov V.A. —505
Dranenko A.S. —278, 300
Driscoll P.B. —539
Dub S.N. —140, 163, 395
Dubicovsky L.F. —379, 488
Dubinin G.V. —525
Dubok V.A. —504
Dubovik T.V. —314, 377
Dubrovsky Y.V. —525
Dvorina L.A. —31, 278, 300
Dvornik M.I. —56
Dyachkovskii P.K. —401
Dybkov V.I. —94, 98
Dzyuba V.S. —399

**E**

Egamov M.Kh. —385
Egorova O. I. —165
Epifantseva T.A. —514
Eremeichenkova Yu.V. —103
Ershova T.B. —56
Ershova T.V. —523

**F**

Fadejev V.S. —54, 56
Fedash V.P. —259
Fedorenkova L.I. —461
Fedorov V.A. —419, 421, 431
Fedorova A.F. —502
Fekeshgazi I.V. —371
Filippov V. —450, 452, 454
Firstov S. A. —262, 268, 294
Fisher W.P.P. —7, 373
Fiyalka L.I. —339
Frage N. —355
Freik D.M. —89
Frolov A.A. —325
Frolov G. —10
Frolov G.A. —47, 231, 246, 302, 532, 535
Frolov V.S. —137
Frolova E.G. —124
Frumin N. —355
Frydman G.R. —282
Fushich O. —535
Fusshich O.I. —309

**G**

Gab A.I. —117
Gab I.I. —192
Gabunia D.L. —375
Gabunia L.D. —375
Gadzyra N.F. —288
Galinsky V.P. —14
Galkin A.F. —39
Galuschak M.A. —89
Galygin A.N. —5
Gamulya G.D. —246, 481
Gavrylov R.V. —46, 246, 458, 552
Gavrilyuk V.V. —223
Gawalek W. —140, 521
Gayduchenko A.K. —148
Gerasimyk G.I. —125
German M.L. —7
Getman O.I. —332
Gida V.M. —33
Gilev V.G. —470
Gladkiy V.V. —552
Gladkov V.E. —526
Gladkova V.K. —526
Glazkov E.E. —282
Globus M. —19
Glushakov V.G. —117
Gnesin G.G. —288
Gnyloskurenko S.V. —369
Gnylytsya.I.D. —446
Goldberg M. —355
Golementsev L.M. —477
Golnik V.F. —435
Golovanov V.I. —137
Golovkova M. —225, 286, 302, 343, 493
Gonchar A. G. —307
Gontar A.G. —392
Gorbachuk N.P. —284
Gorban' V.F. —262, 268, 343
Gorchakov A.A. —525
Gorchakova L.I. —240
Gorshkov V.A. —221
Goryachev Yu.M. —330, 339
Gracheva L.I. —348
Gridasova T.Y. —327
Gridneva I.V. —207
Grigorev O.N. —314
Grigorevskiy A.V. —5, 483
Grigorjev O.N. —294
Grinchuk P.S. —7, 82
Grinyov B. —19
Grishchishyna L.N. —108
Gritsenko V.I. —352
Groysman A. —364
Gubenko S.I. —169
Gubin Yu.V. —311
Gul'bin V. —113, 253, 558
Gusev E.L. —16

**H**

Habisreuther T. —140, 521
Halchuk T.N. —547
Hassanein A. —493
Hazov I.A. —525
Hertsyk O.M. —336
Holomeev M.G. —186
Hrechyshkin Y.F. —327
Hryhoryeva O.V. —409

**I**

Iantsevitch C.V. —403
Ilyukhin M. —543
Isaev V.V. —252
Isayev K.B. —12
Isayeva L.P. —292
Ishchenko S.S. —556
Ivakhnenko A.G. —217
Ivakhnenko G.A. —217
Ivanchenko L.A. —194
Ivanchev S.S. —29, 33
Ivanenko A.A. —105
Ivanenko Ye.A. —417
Ivanov A. —541
Ivanov V.I. —347
Ivanova A. —76
Ivanova I.I. —294
Ivanova I.V. —483
Ivashchenko L.A. —163
Ivashchenko V.I. —163
Izhevskyi V.A. —143

**J**

Jarko.V. —541
Jmajlov B. —76

**K**

Kachenyuk M.N. —407
Kadyrov V. —357, 509
Kadyrzhanov K.K. —68
Kalashnikova L.A. —286
Kalashnikova L.I . —296
Kalinin D.S. —80
Kapitanchuk L. —201, 272, 411
Kaplina G.S. —433, 435
Kaplunenko O.I. —392
Karaman D. Yu. —417
Karimov S.N. —385
Karimova A.G. —534
Karitskaya S.G. —250, 367
Karpenko A.V. —64
Karpenko V.D. —347
Karpov V.N. —223
Karpukhin I. —543
Kartmazov G.N. —350
Kartsev N.F. —350
Kasimov M.A. —298
Kasumov A.M. —177
Kayuk V. G. —514
Kazo I.F. —212
Kazymyrenko Y.A. —213
Kelina I.Yu. —180, 197, 244
Kelina R.P. —237, 248
Kezelis R. —387
Khabibullin M.G. —534
Khamitsaev A.S. —477
Kharchuk M.D. —337
Kharitonov D.V. —199
Khartchuk M.D. —477
Khassanchine R.H. —483
Khmeljuk N.D. —286
Kholmanov I. N. —395
Khomenko G.E. —280
Khorolsky M.S. —18
Khoruzha V. G. —94, 323

Khyzhniak V.G. —391, 405
Khyzhun O.Yu. —264
Kikuchi R. —460
Kisil V. —491
Kizimenko F.A. —343
Klimenko A.P. —371
Klimenko V.N. —334
Klochkov L.A. —207
Kobelev A. —113
Kobeleva L.I. —227, 475
Kogutyk P.P. —212
Kokhana I.M. —196
Kokhaniy V.O. —196
Kolarik V. —362
Kolesnikov F. —113
Kolomytcev M.V. —328
Kolotilo A. —491
Kolyagin V.A. —264
Konovalenko V.V. —29
Konsantinova T.E. —247
Konyashin I. —482
Kopan V. —201, 417
Kopan’ A.R. —290
Kopan’ T.V. —290
Korablov D.S. —290
Korablyova Ye.A. —241
Korniyenko K.Ye. —323
Korol A.A. —196
Korol V.I. —405
Korotin M.A. —115
Korzhova N.P. —316
Koshelev M.V. —300
Kossko T.G. —23
Kostenko A.D. —47
Kostikov V.I. —9
Kostornov A.G. —246, 309, 334, 535
Kostyuchenko A.I. —437
Kotenko V.A. —294, 314
Kotlyar A. —491
Kotova N.V. —42, 44
Koval K.V. —46
Koval Yu.N. —445
Kovalchenko M.S. —143
Kovalev L.K. —521
Kovbuz M.O. —336
Kovtun N.V. —350
Kozlov G.V. —49
Kozyakov I.A. —21
Kracunovska S. —521
Kravchenko L.P. —85, 328
Kravchuk L.V. —399
Kriachko L.A. —345
Kriukiene R. —389
Krokhmal S.A. —184
Krukovsky P. —360, 362
Krupa M.M. —479, 516
Krut’ko N.P. —242
Kryl Ya.A. —446
Kryukov I. —32
Kudin V.G. —74
Kudryavtsev Yu.V. —320, 445
Kuksenko V.S. —365
Kulak L.D. —286, 498
Kulik A.V. —80, 78, 118, 122
Kulik V.I. —78, 118, 122
Kulikova G.I. —240
Kunitskii Yu.A. —219
Kunty O.I. —550
Kurakin V. —30, 72
Kuriat R.I. —399
Kurilov A.G —473
Kurilov G.V. —473
Kurinnaya T.V. —381
Kurkova D.I. —192
Kurochkin V.D. —85, 328
Kurskaja I.N. —197
Kus’menko H.H. —498
Kusainov K.K. —367, 500, 526
Kuschevskaya N.F.— 198
Kuschevsky A.Ye. — 198
Kusnetsov V.P. —52
Kusnetzova T.L. —296
Kutsay O.M. —392
Kutusov V.L. —129
Kutusov A.V. —129
Kuzmenko L.N. —194
Kuzmenko N.N. —286
Kuzmov A.V. —124
Kuznetsova T.L. —305

L

Lakhin A.V. —146
Laptev A. —225
Lashneva V.V. —504
Lebedev E.V. —556
Legkaya T.N. —316
Lemesheva T.V. —475
Len T. —201, 272, 415
Lesnevsky L.N. —131
Lesnikov V.P. —52
Levshanov V. —72
Lezhnenko I.V. —516
Liashchenko A.B. —452, 454
Lijudvinskaya T.A. —174
Lipovtsev Yu.V. —477
Litvinsky I. —541
Lityuga I.V. —292
Lityuga N.V. —377
Litzkendorf D. —521
Loboda P.I. —34
Loginova O.B. —392
Logunov A.V. —137
Lopato L. —90, 111, 125
Loudanov K.I. —562
Lubinskiy V. —19
Luchka M. —178
Lukina V.V. —354
Lunarska E. —425
Lyashenko V.I. —314
Lykhodid S.I. —566
Lyulko V. —76

M

Maiboroda V.P. —219, 302
Maizis E. —543
Maizis S. —543
Makara V.A. —74, 212
Makarov Yu.N. —80
Makatyora V. —541
Makogon Yu.N. —441
Malakhov V.Ya. —330
Malyshev V.V. —117
Manilova E.P. —429
Manukhin A.V. —146
Marchenko S.V. —259
Marinin S.F. —137
Markov V.G. —16
Martiukhin I.D. —514
Martsenyuk P.S. —323
Martynenko A.N. —452
Martynov P.N. —244
Masaleva E.N. —429
Maslov V. P. —495, 496, 499
Maslyuk V.A. —148, 154
Masuda-Jindo K. —460
Matukov I.D. —80
Matveeva L.A. —395, 448, 504
Matvienko A.I. —516
Matzui L. —201, 411, 415
Matzui V. —413
May K.V. —371
Mayboroda V.P. —175
Maydanyuk A.P. —87
Mazna O.V. —233
Mechnik V.A. —36, 61
Mecius V. —387

Medvedev M.M. —252
Meleshevich K.A. —94
Meleshko A. —205, 209
Melnikov V.S. —140
Mezhylovska L.Y. —89
Miedziński —539
Mikhailov O.V. —92, 490, 514
Mikhalev A.M. —7
Mikhatulin D.S. —523
Milani P. —395
Milman Yu.V. —276
Minakov N.V. —466, 512
Minakov V.N. —260, 466
Minakova A.V. —260
Minakova R.V. —85, 343, 493
Minitsky A.V. —148, 154
Mironov S.Yu. —252
Mironov V. —537, 568
Mits I.V. —433, 435
Mitsa V.M. —371
Mojaiskaya N. —362
Molchanovskaya G.M. —219
Molyar A.G. —108
Mordovets N.M. —292, 316
Morozov A.F. —103
Moshchil V.E. —140
Mosina T.V. —174
Movchan B.A. —25
Mukhin I.A. —105
Muktepavela F. —568
Muratov V.B. —284
Murzin L.M. —507
Muzhanova L.P. —211
Myshlyaev M.M. —252

**N**

Nadiradze A.B. —217
Nagorny P.A. —140
Naidich Yu.V —192
Nakamura T. —369
Neklyudov I.M. —186
Nerus M. —528
Neshpor I.P. —110, 174
Neshpor O.V. —196
Nesterenko T.N. —64
Nikitin I. —113
Nikitin I.A. —525
NiloA.S. —118
Nosachev L.V. —142
Nosenko V.K. —336
Nosov G.I. —167
Nouri H. —539
Novak S. —360
Novikov N.V. —36, 61
Novikova V.I. —292
Nusupbekov B. —500

**O**

Okhlopkova A.A. —235
Okhrimenko G. —488
Oksiyuk S. V. —399
Oleinik G.S. —304
Oleshko A.I. —198
Oliker V.E. —302, 327
Oltra Roland —65
Olynets V. —548
Ordaniyan S.S. —110
Oryshich I.V. —286, 305
Ospennikova O.G. —182, 187
Ostapenko S.A. —560
Ostapenko V.S. —560
Ostrovskaya L.Yu. —395
Ostrovskaya Ye.L. —246, 481
Oswald B. —521
Oushakov A.M. —131
Ovsiannickov M.U. —129
Ovsienko I. —201, 272
Oznobishin A.N. —7

**P**

Paderin L. —373, 464
Paderno V. —450, 452, 454
Paderno Yu. —450, 452, 454
Panashenko V.M. —314, 377
Panasyuk A.D. —47, 174
Panasyuk O.A. —154
Panfilov A.A. —227
Panichkina V.V. —87, 332
Pashutina T.A —211
Pasichny V. —90, 560, 566
Paustovsky A.V. —152, 292, 305, 307, 311, 381
Pavlova E.P —441
Pavlygo T. —150
Pavlyuchkov D.V. —323
Pavlyukevich N.V. —7, 82
Pazdersky Yu.A. —33
Pechkovsky E.P. —262, 268, 294
Perelman V. —203
Pereselenceva L.N. —233
Pereselentseva L.M. —304
Perevertailo V.M. —392, 395
Permyakova I.J. —419, 431
Permyakova T.V. —274
Peshchenko D.V. —244
Petrova A.M. —322
Petrova N.N. —502
Petrova P.N. —235
Petrovsky V.Ya. —564
Pietraszko A. —450
Pilyaeva S.B. —461
Pinchuk N.D. —194
Pisarenko V.A. —296
Plaksin D.A. —68
Plishevsky M.I. —525
Pljasunkova L.A. —244
Plomodyalo L. —150
Plomodyalo R. —150
Plushnikova T.N. —421
Podchernyaeva I.A. —47, 54
Podcherniayeva I.A. —174
Podobeda L.G. —444
Podrezov Yu.N. —463
Pokhyl Yu.A. —46, 458
Poklad V.A. —137, 145
Polegeshko O.B. —517
Polezhaev Yu.V. —523
Polezhayev Yu.V. —12
Polozov B.V. —29
Popchuk R.I. —280, 512
Popov S.M. —343, 493
Porada O.K. —163
Poryadchenko N.E. —286, 316
Prikhna T.A. —140, 521
Primisky V.F. —572
Prosovskii O.F. —237
Prosuntsov P.V. —7, 120, 486
Prudnikov A.M., —393
Pryadko L.F. —54
Puchkova V.Y. —260, 466
Pyatachuk S.A. —381

**R**

Rabinovich A.I. —470
Rabinovich O.S. —82
Rabinovitch S.V. —337, 477
Ragulya A.V. —207
Ramm M.S. —78, 80, 118, 122
Rassamakin B.M. —458
Rasskazov P.V. —483
Ratner M. —19
Raychenko O.I. —100, 369
Razumovsky I.M. — 137
Red'ko V. —90, 125
Remeslo V. —509
Revo S. L. —417, 437
Reznik S.V. —7, 120

Ries B. —482
Rodichev Yu.M. —496
Rogozinskaya A.A. —280, 314, 377
Roik T.A. —519
Rokitska E.A. —305
Romanenko O.M. —328
Romanov G.N. —401
Rud B. M. —307, 330, 339
Rud V.D. —547
Rudyk N.D. —280, 512
Rula L.V. —49
Rusakov G.V. —163
Rusakov V.S. —68
Rusanova L.N. —240
Rusin M. —30, 72, 120, 211, 248, 444, 477, 337
Ruvinsky M.A. —89
Rybnikov A. —362, 429
Ryumshyna T.A. —247, 425

**S**

Safronov A.V. —40
Saigin V.V. —40
Sakipova S. —500
Samchuk A. —413
Samelyuk A. V. —98, 296, 262, 379
Sanin V.N. —187
Sarsembaeva A.Z. —496
Sattarov I.Kh. —534
Savchenko E.A. —217
Savchuk Y.A. —140
Savorovskiy F.G. —495
Savyak M.P. —155
Scherbakova L.N. —514
Schmidt Ch. —140, 490
Schwarz U. —450
Semen’ko M.P. —397, 415
Semenov A. —133, 525
Semenova E.L. —320, 445
Semenova I. —133
Sementssov Yu.I. —417
Serdjuk D. —568
Serdyuk G.G. —92
Sereda G.N. —120
Sergeyev V. —541, 566
Sergienko N.V. —140
Shabalin B.G. —423
Shalaev R.V. —393
Shalunov E.P. —172, 505
Sharff P. —201, 272
Shcheretsky A.A. — 84
Sheludko V.E. —152, 292, 307
Shevchenko A. —90
Shevchenko O.M. —175
Shevchuk U.M. —519
Shiljaev B.A. —186
Shkarupa I.L. —248
Shkretov Yu. —145, 354
Shmegera R.S. —395
Shpak A.P. —219
Shpilevsky E.M. —448
Shpilevsky M.E. —448
Shtefan E.V. —490
Shtern M.B. —87, 124
Shulakovsky A.V. —7
Shulishova O.I. —341
Shumikhin V.S. —84
Shurov N.I. —115
Shvagirev V.M. —5
Sidorenko S.I. —409, 441
Sidorko V.R. —98
Sidorov I.I. —9
Silantiev V.I. —570
Siman M.I. —339
Simeonova Yu. —309
Simonov V.S. —505
Sinayskyi B.M. —233
Sirovatka V.L. —327
Sitalo V.G. —169, 231
Sizonenko O.N. —157
Skachkov V.A. —64, 347
Skirta Yu.B. —479, 516
Skorokhod V.V. —3, 10, 274, 282, 535
Skydanovych N. —548
Slys I.G. —484
Smetkin A.A. —407
Smirnov K.L. —182
Snopko V.N. —229
Sokolov E.G. —70
Soldatov A. —209
Solntsev V. —246, 532, 535
Solonin S. —468
Sosnovsky L.A. —148
Sotirov G. —309
Speka M.V. —397
Spiridonova I.M. —259, 456, 461
Sribniy V. —548
Stamm W. —362
Stelmakh O. —411
Stepanchuk A.N. —238
Stepanchuk A.M. —517
Stetsyuk T.V. —192
Sudavtsova V.S. —42, 44
Sukhovaya E.V. —456
Suzdeltsev E. —72, 553
Suzdaltsev Ye.I —199
Svistun L. —150
Sygova V.I. —391
Sylenko P.M. —270
Sytov V.A. —365

**T**

Tadlya K. —362
Tadlya O. —362
Talko O.V. —282
Tarasov G.V. —458
Tarasov P.P. —401
Tarasov V.K. —507
Tchernovsky M.N. —131
Telnikov E.Ya. —307
Teplyakov V.V. —188
Terentyev A.E. —302
Tereokhina A.M. —354
Tikhonov A.A. —137, 223
Timofeev A.N. —5, 146, 483
Timofeyeva I.I. —163, 207, 292, 327
Timoshenko V.I. —14
Tjalin Yu.I., —421
Tkachenko G. —357
Tkachenko Ju.G. —504
Tkachenko L.N. —87, 92
Tokarsky V.A. —399
Tolochyn O. —225
Tolok V.T. —352
Toropov V.V. —7
Tovarovskaya G.I.— 554
Tovarovskiy I.G. —554
Travkin A.A. —252
Tretiak M.S. —7
Tropinov A. —530
Tropinova I. —530
Troshin A.E. —131
Trushkovskaja L.M. —212
Tsagarcishvili O.A. —375
Tsareva I.N. —129
Tsodikov. M.V. —188
Tsupko F. —548
Tsvelev V.M. —535
Tsvetkova M.M. —553
Tsyganenko V.S. —292, 377
Turkebaev T.E. —68
Tykhyy V.G. —231
Tyurin V.N. —131, 525

**U**

Udalov Yu.P. —110
Ulyanova T.M. —242
Unrod V.I. —110
Uryukov B. —357
Usenko N.I. —44
Ushakov I.V. —419, 431
Usherenko S.M. —169
Uskova N.N. —117
Uskova N.A. —108
Ustinov A.I. —25
Uvarov V.I. —188
Uvarova I.V. —155, 174

**V**

Vajs E. —178
Valeev I.Sh. —383
Valeeva A.Kh. —383
Varyukhin V.N. —393
Vashchenko A.P. —456
Vasilenko V.V. —211, 444
Vdovichenko H.S. —517
Vdovychenko O.V.— 318
Velikanova T.Ya. —323
Verbylo D.G. —463
Vergeles N.M. —154
Verhoturov A.D. —54, 56
Verkhovluk A. M. —84
Vettegren V.I. —365
Vikulin V.V. —197, 241, 248
Vishnyakov L.R. —196, 233
Vladimirov V. —530, 543
Vlasov A.A. —276
Voevodin V.P. —40
Vojnash V.Z. —316
Volkova G.K. —247
Volobuev F.I. —481
Vovchenko L. —411, 413
Vovkotrub N. E., —42
Vvedenskij Yu.V. —246, 481
Vyazovikin I.V. —498
Vyazovikina N.V. —498
Vyshnyakova K.L. —304

**W**

Wendt M. —140
Werheit H. —450

**Y**

Yacovenko L.F. —458
Yakushkina V.S. —241
Yamrozek J. —178
Yarosh V.M. —535
Yastchenko O.M. —566
Yelansky Y. —541
Yeremenko G.V. —397
Yevdokimenko Yu. — 491
Yezerska O.A. —336
Yudintsev P.A. —244
Yukhno T.P. —246, 481
Yukhvid V.I. —187, 221
Yurchuk E. —205
Yurechko D.V. —47
Yurkova A.I. —266

**Z**

Zaikov Yu.P. —115
Zainullina V.M. —115
Zakharenko M.I. —397, 415
Zakharov S.M. —441
Zakharov V.V. —284
Zakorzhevsky V.V. —180, 244
Zamaletdinov I. I. —165
Zarubova N.I. —40
Zatovsky V.G. —345
Zdolnik S.N. —564
Zdorovets N.A. —461
Zeisberger M. —521
Zenkov V.S. —161
Zhankadamova A.M. —68
Zhdanovskij V.A. —229
Zhukovskiy A.N. —36, 61
Zhuravkov A. —413
Zhuravlev V.S. —192
Zinevich T.N. —44
Zmij V.I. —350
Zolotarev A.K. —252
Zubarev V.M. —534
Zubets Yu.E. —296
Zubro S. —203
Zueva T.N. —184
Zukhina A.L —219
Zykova E.V. —379
Zyrin A.V. —194, 313